

MEDICAL PHYSICS *International*

EDITORIAL FROM CO-EDITORS-IN-CHIEF

MESSAGE FROM IOMP PRESIDENT

ENHANCING THE VALUE OF DIGITAL VISUALS FOR TEACHING MEDICAL PHYSICS

MEDICAL PHYSICS AND RADIOGRAPHY TRAINING MODEL TAILORED FOR RESOURCE LIMITED SETTINGS

Prof. HABIB ZAIDI HONORED WITH IOMP'S JOHN MALLARD AWARD

26th INTERNATIONAL CONFERENCE ON MEDICAL PHYSICS (ICMP-2023): IN RETROSPECT

*AN INITIAL QUANTITATIVE COMPARATIVE STUDY OF THE AXIAL AND LATERAL SPATIAL RESOLUTIONS OF DIFFERENT
ULTRASOUND TRANSDUCERS*

*BRAIN TEMPERATURE MEASUREMENT BY MAGNETIC RESONANCE SPECTROSCOPY THERMOMETRY USING REGRESSION
ANALYSIS*

*PROPOSAL FOR ANNUAL QA ASSESSMENT OF SAFETY AND CONSISTENCY OF OARS DOSES IN TREATMENT OF
CANCER BY BRACHYTHERAPY*

*QUALITY ASSURANCE OF PATIENT SETUP USING MEGAVOLTAGE PORTAL IMAGING AND DIGITALLY RECONSTRUCTED
RADIOGRAPH IN RADIOTHERAPY FACILITY WITHOUT KILOVOLTAGE IMAGING*

IndoQCT: A PLATFORM FOR AUTOMATED CT IMAGE QUALITY ASSESSMENT

TRUE TALES OF MEDICAL PHYSICS: INSIGHTS INTO A LIFE-SAVING SPECIALTY – by JACOB VAN DYK

BOOK OF ABSTRACTS OF THE 26th INTERNATIONAL CONFERENCE ON MEDICAL PHYSICS (ICMP-2023)

BOOK OF ABSTRACTS OF THE ICTP MASTER OF MEDICAL PHYSICS (MMP) THESES



The Journal of the International Organization for Medical Physics

Volume 11, Number 2, December 2023

MPI

MEDICAL PHYSICS INTERNATIONAL

**THE JOURNAL OF
THE INTERNATIONAL ORGANIZATION FOR MEDICAL PHYSICS**



MEDICAL PHYSICS INTERNATIONAL

The Journal of the International Organization for Medical Physics

Aims and Coverage:

Medical Physics International (MPI) is the official IOMP journal. It provides a platform for medical physicists to share their experience, ideas and new information generated from their work of scientific, educational and professional nature. The e-journal is available free of charge to IOMP members. MPI- History Edition is dedicated to History of Medical Physics.

MPI Co-Editors in Chief

Francis Hasford (Ghana) and Sameer Tipnis (USA)

MPI Editorial Board

John Damilakis, IOMP President (2022-2025), EFOMP Past-President, Greece

Eva Bezak, IOMP Vice-President (2022-2025), AFOMP President, Australia

Magdalena Stoeva, IOMP Secretary General (2022-2025)

Ibrahim Duhaini, IOMP Treasurer (2022-2025), MEFOMP Past-President, Lebanon

Mahadevappa Mahesh, IOMP Scientific Comm. Chair (2022-2025); AAPM President-Elect, USA

Simone Kodlulovich Renha, IOMP Professional Relations Comm Chair (2022-2025), ALFIM Past-President, Brazil

Arun Chougule, IOMP Education & Training Comm Chair (2022-2025), AFOMP Past-President, India

Kwan Ng, IOMP Awards and Honours Committee Chair (2022-2025), SEAFOMP Past President, Malaysia

Chai Hong Yeong, IOMP Medical Physics World Board Chair (2022-2025), Malaysia

Hassan Kharita, IOMP Publications Committee Vice Chair (2022-2025), MEFOMP Vice-President, Syria

Chris Trauernicht, President (2021-2023), FAMPO, South Africa

KY Cheung, IOMP Past-President, Hong Kong, China

Taofeeq Ige, FAMPO Past-President, Nigeria

Marco Brambilla, EFOMP Past-President, Italy

Anchali Krisanachinda, SEAFOMP Past-President, Thailand

Renato Padovani, EFOMP Past Secretary General, ICTP, Italy

Colin Orton, IOMP Past-President; AAPM Past-President, USA

MPI Founding Editors in Chief: Slavik Tabakov (IOMP Past-President) and Perry Sprawls

MPI History Edition Editors: Slavik Tabakov, Perry Sprawls, Geoffrey Ibbott

Technical Editors: Magdalena Stoeva & Asen Cvetkov, Bulgaria

Editorial Assistant: Vassilka Tabakova, UK

MPI web address: www.mpijournal.org

Published by: The International Organization for Medical Physics (IOMP); Web address: www.iomp.org ; Post address: IOMP c/o IPEM, 230 Tadcaster Road, York YO24 1ES, UK.

Copyright ©2013 International Organisation Medical Physics. All rights reserved. No part of this publication may be reproduced, stored, transmitted or disseminated in any form, or by any means, without prior permission from the Editors-in-Chief of the Journal, to whom all request to reproduce copyright material should be directed in writing. All opinions expressed in the Medical Physics International Journal are those of the respective authors and not the Publisher. The Editorial Board makes every effort to ensure the information and data contained in this Journal are as accurate as possible at the time of going to press. However, IOMP makes no warranties as to the accuracy, completeness or suitability for any purpose of the content and disclaim all such representations and warranties whether expressed or implied.

ISSN 2306 – 4609

CONTENTS

EDITORIALS	281
EDITORIAL FROM CO-EDITORS-IN-CHIEF <i>Francis Hasford, Sameer Tipnis</i>	282
MESSAGE FROM IOMP PRESIDENT <i>John Damilakis</i>	283
EDUCATIONAL TOPICS	285
ENHANCING THE VALUE OF DIGITAL VISUALS FOR TEACHING MEDICAL PHYSICS <i>P. Sprawls</i>	286
MEDICAL PHYSICS AND RADIOGRAPHY TRAINING MODEL TAILORED FOR RESOURCE LIMITED SETTINGS <i>A.N. Mumuni</i>	292
INVITED PAPERS	297
Prof. HABIB ZAIDI HONORED WITH IOMP'S JOHN MALLARD AWARD <i>F. Hasford, S. Tipnis</i>	298
26 th INTERNATIONAL CONFERENCE ON MEDICAL PHYSICS (ICMP-2023): IN RETROSPECT <i>S.D. Sharma</i>	300
15 YEARS IOMP HISTORY SUB-COMMITTEE <i>Slavik Tabakov</i>	302
HOW TO	303
AN INITIAL QUANTITATIVE COMPARATIVE STUDY OF THE AXIAL AND LATERAL SPATIAL RESOLUTIONS OF DIFFERENT ULTRASOUND TRANSDUCERS <i>K. Cilia, M.L. Camilleri</i>	304
BRAIN TEMPERATURE MEASUREMENT BY MAGNETIC RESONANCE SPECTROSCOPY THERMOMETRY USING REGRESSION ANALYSIS <i>A.N. Mumuni, M.M. Salifu, M.N. Abubakari</i>	311
PROPOSAL FOR ANNUAL QA ASSESSMENT OF SAFETY AND CONSISTENCY OF OARS DOSES IN TREATMENT OF CANCER BY BRACHYTHERAPY <i>P.K. Ndonye, S.N.A. Tagoe</i>	316
QUALITY ASSURANCE OF PATIENT SETUP USING MEGAVOLTAGE PORTAL IMAGING AND DIGITALLY RECONSTRUCTED RADIOGRAPH IN RADIOTHERAPY FACILITY WITHOUT KILOVOLTAGE IMAGING <i>M.T. Schandorf, E.C.D. Addison, T.B. Dery, A.A. Yorke</i>	323
IndoQCT: A PLATFORM FOR AUTOMATED CT IMAGE QUALITY ASSESSMENT <i>C. Anam, A. Naufal, W.S. Budi, H. Sutanto, F. Haryanto, G. Dougherty</i>	328
BOOK REVIEW	337
TRUE TALES OF MEDICAL PHYSICS: INSIGHTS INTO A LIFE-SAVING SPECIALTY – by JACOB VAN DYK <i>G.S. Ibbott</i>	338
INFORMATION FOR AUTHORS	341
BOOK OF ABSTRACTS	344
ANNEX 1	345
BOOK OF ABSTRACTS OF THE 26 th INTERNATIONAL CONFERENCE ON MEDICAL PHYSICS (ICMP-2023)	346
ANNEX 2	835
BOOK OF ABSTRACTS OF THE ICTP MASTER OF MEDICAL PHYSICS (MMP) THESES	836

EDITORIALS

EDITORIAL FROM CO-EDITORS-IN-CHIEF

As the new team of Co-Editors-in-Chief (EiCs) of Medical Physics International (MPI) journal, we took over from the founding co-EiCs, Slavik Tabakov and Perry Sprawls, in January 2023. Through guidance from the latter, we worked to produce the July Issue of the MPI publication (Vol. 11 No.1, 2023) which received very wide readership. The Issue had 280 pages, comprising full journal articles and Book of Abstracts from the First Regional Conference of the Federation of African Medical Physics Organizations (FAMPO) held in Marrakech, Morocco, from 10 – 12 November 2022, and Book of Abstracts from the Conference of the Middle East Federation of Organizations of Medical Physics (MEFOMP) held in Muscat, Oman, from 19 – 22 May 2023.

This current Issue of MPI (Vol. 11 No. 2, 2023) features full journal articles and books of abstracts. It focuses on publication of the Book of Abstracts of the 26th International Conference on Medical Physics (ICMP 2023) held in Mumbai, India, from 06 – 09 December 2023. The conference had 233 oral and 359 poster presentations. The conference was jointly organized by the Association of Medical Physicists of India (AMPI), International Organization for Medical Physics (IOMP), the Asia-Oceania Federation of Organizations for Medical Physics (AFOMP) and the South-East Asian Federation of Organizations for Medical Physics (SEAFOMP), on the theme Innovations in Radiation Technology and Medical Physics for Better Healthcare. Topics covered in the Book of Abstract cover artificial intelligence in medical physics, technology and techniques of radiation oncology, treatment planning, emerging and newer techniques of radiation therapy, imaging in radiation oncology, advanced technologies and techniques of medical imaging, emerging and newer techniques of medical imaging, radiation dosimetry and radiation safety, targeted therapy, radiation biology, modelling and simulation, translational research, education/training and certification in medical physics.

This Issue also features abstracts of theses from 51 students of the 8th and 9th cycles of the International Centre for theoretical Physics (ICTP) Master of Medical Physics (MMP) programme. The MMP programme is accredited by the International Organization for Medical Physics (IOMP). The MMP is a two-year advanced training programme run jointly by the ICTP and the University of Trieste (UniT). The programme is co-sponsored by the IAEA, and is supported by IOMP, the European Federation of Organizations in Medical Physics (EFOMP), the Italian Association of Medical Physics (AIFM), in collaboration with Trieste University Hospital.

Visit www.mpijournal.org/index.aspx for latest MPI publications and enjoy reading the exciting articles.

	<p>Francis Hasford, PhD. Editor-in-Chief Radiological and Medical Sciences Research Institute, Ghana Atomic Energy Commission, Accra, Ghana. haspee@yahoo.co.uk</p>		<p>Sameer Tipnis, PhD. Editor-in-Chief Department of Radiology and Radiological Sciences, Medical University of South Carolina, Charleston, USA. tipnis@musc.edu</p>
---	--	--	--

MESSAGE FROM IOMP PRESIDENT



Over the past six months, the IOMP has experienced a period of remarkable productivity. This report highlights a few key accomplishments. Our revamped website, which debuted a few weeks ago, is a testament to IOMP's dedication to embracing modern technology and adapting to the changing demands of our audience. Its user-friendly interface ensures smooth navigation, allowing visitors to easily access and find the desired information. We are excited to invite you to visit the new IOMP website at www.iomp.org and explore its features. Your feedback is incredibly valuable to us, as it guides our ongoing efforts to refine our online presence to better serve the needs and interests of our members.

The International Day of Medical Physics (IDMP), celebrated every year on November 7th, is a significant event that highlights the vital contributions of medical physicists to healthcare. This year, we organized a special webinar titled "The 60th Anniversary of IOMP – Personal Memories and Some Thoughts on the Future of Medical Physics." Speakers for the event included Azam Niroomand-Rad, Colin G. Orton, and Fridtjof Nüsslin, whose remarkable contributions and leadership have profoundly influenced the field of Medical Physics. This webinar was not just an educational event; it was also a celebration marking the 60th anniversary of the IOMP. It offered a unique opportunity to reflect on the organization's history, the personal experiences of its influential figures, and to ponder the future trajectory of Medical Physics. You can view the recording on our [YouTube Channel](#).

On behalf of the organizing committee, I extend our sincere appreciation for your enthusiastic participation in the International Conference on Medical Physics (ICMP-2023), held from December 6th to 9th in Mumbai, India. The conference was a success, drawing approximately 1400 colleagues from around the world. Your active engagement created an environment of rich learning and networking. It was indeed a rewarding experience for everyone involved, and we are grateful for your contributions.

We also acknowledge the challenges encountered, particularly the visa issues that unfortunately prevented some of our colleagues from attending the Conference. These situations have offered valuable lessons and highlighted areas needing improvement for future conferences. We highly value your feedback and insights, as they are integral to the continuous improvement of our conferences. We encourage you to share any thoughts or suggestions you may have, as they will be instrumental in shaping the success of future events.

IOMP accreditation is recognized as a mark of quality, ensuring that these events adhere to the highest benchmarks in educational excellence. During the last months, the IOMP Accreditation Board received several applications for accreditation of medical physics events. These activities reflect the IOMP's ongoing commitment to endorsing and promoting high-quality educational programs that contribute to the advancement and dissemination of knowledge in medical physics. For more information on IOMP's accreditation process and standards, as well as accredited programs, please visit the '[accreditation](#)' section of IOMP's website.

IOMP plays a pivotal role in enhancing the quality of medical physics globally by endorsing and sponsoring educational and training events organized by its national member organizations. These initiatives are instrumental in ensuring that medical physicists are well-trained and updated, which is crucial for the safe and accurate treatment of patients. In recent months, IOMP has sponsored and endorsed several significant events. I have kept you updated on these events through my messages in IOMP's e-newsletter. These endorsements by the IOMP highlight its commitment to advancing the field of medical physics through continuous education and professional development, thereby contributing to the enhancement of patient care worldwide.

To support and empower medical physicists in low- and middle-income countries, the IOMP recently issued a call for expressions of interest to receive free copies of medical physics books. This initiative has received an enthusiastic response, with over 300 applications from interested colleagues. Currently, the publication committee is engaged in the selection process to determine the recipients of these books. This step is crucial in ensuring that the resources are distributed effectively and reach those who can benefit most from them. This initiative not only

aids in the dissemination of knowledge but also aligns with the IOMP's commitment to advancing the field of medical physics globally, especially in regions where access to such resources may be limited.

I would like to express my sincere gratitude to all of you. This year, our collective efforts have led to exceptional progress. As we look ahead, let's continue to combine our strengths and aspirations for the benefit of our profession.

Wishing you a Happy New Year 2024 and a joyful holiday season!

Prof. John Damilakis

IOMP President

University of Crete, School of Medicine, Crete, Greece

john.damilakis@med.uoc.gr

EDUCATIONAL TOPICS

ENHANCING THE VALUE OF DIGITAL VISUALS FOR TEACHING MEDICAL PHYSICS

P. Sprawls

Emory University, Department of Radiology and Imaging Sciences, Atlanta, USA
Sprawls Educational Foundation, www.sprawls.org

Abstract— The development and availability of digital image technology and methods, including the internet, adds several significant values for the teaching and learning of medical physics. It addresses and provides solutions to several long-standing challenges relating to both the *effectiveness* and *efficiency* of classroom teaching. Medical physics educators, teachers, can provide *effective* classroom and conference learning experiences by using their knowledge and experience along with visuals (images, diagrams, illustrations, etc.) to enhance the formation of useful knowledge structures within the student's minds. The values provided by using visuals in the classroom include multimodality (audio and visual) teaching, enhanced comprehension and understanding of complex concepts, ability to physically engage (with sight) with the physical universe, memory enhancement, (we remember what we see better than what we are told), encourages critical thinking, and visuals are a universal language especially valuable for international medical physics education. The specific value of digital image technology is providing all medical physics classrooms and teachers, in every country of the world, with access to highly effective visuals contributing to the formation (learning) of conceptual knowledge that is required for many medical physics activities. This is through the process of Collaborative Teaching between *visual creators* and *classroom presenters*, each "teaching" and helping students learn. Digital image repositories provide the link and availability of visuals for all to use.

Keywords— concepts, digital, effective, efficient, teaching.

I. INTRODUCTION

Learning physics is the process of developing knowledge structures or mental representations of segments of the physical universe. It is a natural human function and process that begins at a very early age as we interact with the objects and conditions around us through sensory interactions, especially sight, sound, and touch. The development of our physics knowledge of water is an example illustrated here.

This knowledge is a complex network of sensory concepts developed through interactions with physical water. It is the type of knowledge that is especially valuable for guiding future interactions with and applications of water.

Formal learning of physics comes later in academic courses and classrooms where the learning process is organized, directed, and provided by teachers. Traditional classroom teaching generally provides abstract

representations of the physical universe in the form of verbal (word) and mathematical symbol representations.

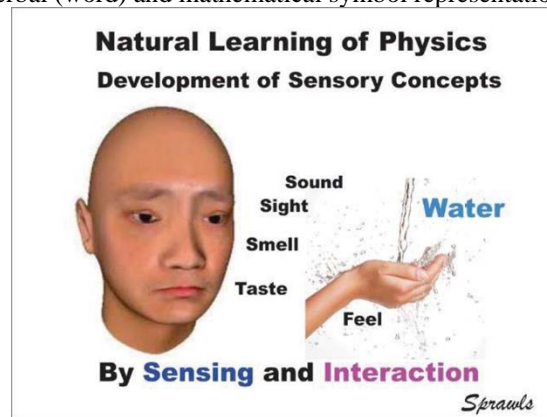


Figure 1. Learning the physics of water through sensory interactions.

While this type of knowledge is important, especially preparing learners for tests and examinations, it does not provide the type of knowledge that will be most useful for many future applications, especially applications that involve direct interactions with components and systems of the physical universe, ranging from preparing a cup of hot tea to optimizing a computed tomography imaging procedure. Both require conceptual knowledge, and not symbolic knowledge of words and mathematical symbols. This is especially true for both medical physicists and physicians practicing diagnostic and therapeutic radiology procedures [1. 2. 3.].

The physics classroom, including the medical physics classroom, has evolved over the years driven by the development and availability of technology [4.].

Teaching medical physics in the class or conference room has several significant challenges. First, the medical physics universe is outside of the classroom located in the hospital and clinics, and not always accessible for teaching. Student laboratory sessions and practical exercises in clinics do contribute to the development of conceptual knowledge but is often limited to the physical equipment and not the invisible radiations, interactions, etc. that is the major component of medical physics.

This significant limitation of the traditional class and conference room can be overcome with visuals that provide for a sensory (visual) interaction with the medical physics universe, both visible and invisible.

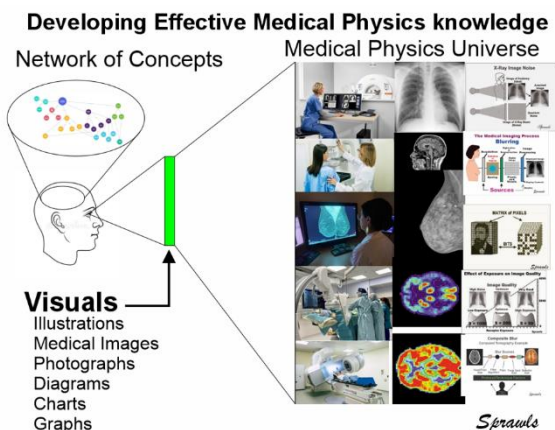


Figure 2. Visuals enable students to develop useful knowledge, or mental representations of the physical universe with a network of sensory concepts.

II. EFFECTIVE TEACHING

Teaching is the process of helping someone learn and can occur in many forms. Lecturing and telling others what we know, for example, “Roentgen discovered X-radiation” conveys facts that can be memorized and is good to know. The ability to make calculations and solve mathematical problems is a critical requirement for the practice of medical physics, a quantitative science. These symbolic (words and mathematical symbols) do not contribute to the formation of significant conceptual knowledge that is necessary for applied physics applications, especially relating to clinical procedures. Teachers can provide highly effective learning opportunities, that is *effective teaching*, by combining their knowledge and experience with visuals that provide visual connections with the clinical procedures or other real-world applications.

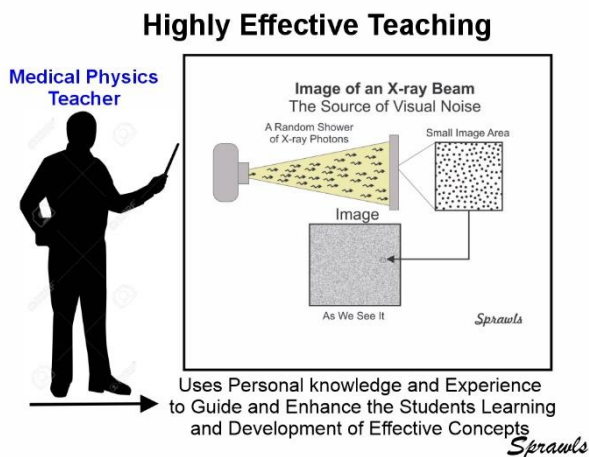


Figure 3. Effective teaching resulting from the combination of visuals in the classroom and discussions by an experienced medical physicist.

III. ENHANCED COMPREHENSION

A major value of visuals used in teaching is that of enhancing the understanding and comprehension of complex ideas, for example “image quality”, systems, procedures, interactions, etc. Recalling the old phrase, “a picture is worth a thousand words”. A visual can create immediate interest and interaction with the subject that leads to a more comprehensive understanding. The visual shown here contributes to the understanding of the very complex issue of blurring in medical imaging, including its effects, sources, and control.

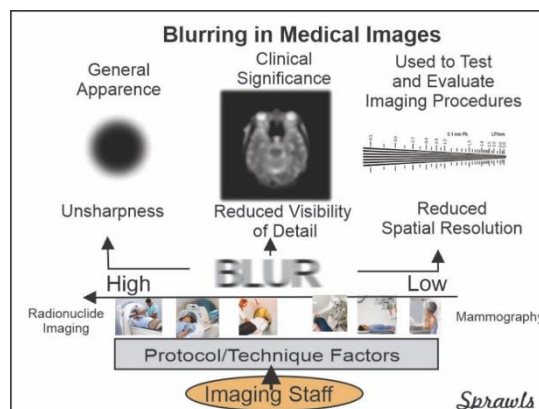


Figure 4. A visual to help students understand and develop conceptual knowledge of the many aspects of image blurring.

IV. MEMORY ENHANCEMENT

We remember what we have seen much better than words we have heard or were told. Visual memory is a significant function of our mental process and scientists have classified it into three distinct categories: iconic memory, visual short-term memory, and visual long-term memory. For medical physics education long-term visual memory contributes to the formation of “visible” mental representations of items and conditions in the physical universe, for example what an image with specific artifacts looks like. This is the type of knowledge needed to evaluate images. Teaching with visuals provides students with knowledge that will be remembered and useful in future work. An example is shown here.

With this visual representation of the Inverse Square Relationship, often referred to as a “Law”, students develop a concept, or understanding that is useful knowledge for the future. It will be remembered much longer than verbal definitions and equations. With this conceptual knowledge and understanding the quantitative relations, equations can be added for making calculations of actual values if needed

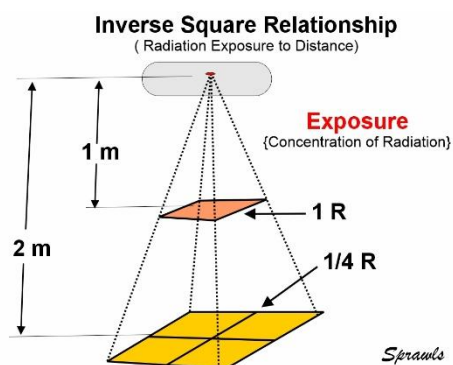


Figure 5. A visual representation of the inverse-square relation that is easier to remember and understand than definitions and equations.

V. MULTI-MODALITY TEACHING AND LEARNING

Using visuals along with a vocal lecture presentation or discussion combines two sensory “channels” of information (vision and sound) that can enhance each other. Each has specific characteristics. Visuals provide access to information in the form of objects with characteristics and relationships distributed in space throughout the area of the visual. This is especially significant when it is a representation of actual physical objects, relationships, events, and activities. The viewer, typically the student, can get the “big picture” and explore, concentrate on, and study details throughout the image. Vocal lectures are in the form of a continuing series of words, usually organized in sentences that often express facts. Especially in teaching physics, facts are presented as true and verified descriptions of some physical phenomena, observable condition, or event. An example of a vocally expressed fact is, “aluminum filters are used to modify the spectrum of an X-ray beam”. Students can memorize this and correctly answer examination questions but can have no understanding or concept of what it means in relationship to an x-ray system. The vocal process is very different from the information provided with visuals. It has its value when used together with visuals as illustrated here.

Highly Effective Multi-Modality Teaching

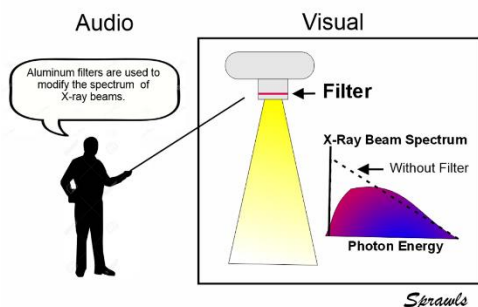


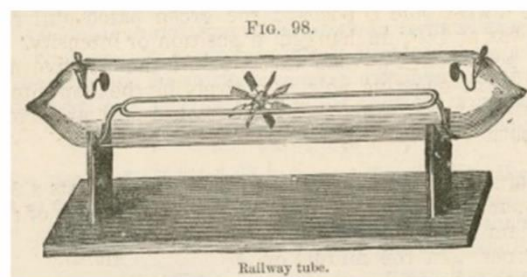
Figure 6. The value of a visual along with a spoken description in developing useful knowledge about the use of filters.

VI. VISUALS FOR TEACHING PHYSICS THROUGHOUT HISTORY

Throughout the history of teaching physics, one of the major challenges has been the availability of visuals to use in classes, usually limited to sketches on a blackboard during each class, erasing, and doing it again for the next illustration. This resulted in low quality illustrations requiring time to produce, and not permanent for use in other classes. This was a major factor that limited the use of visuals in physics classes and encouraged the use of symbolic representation, words, and mathematical equations, which were much easier to do.

Fortunately, textbooks often provided high-quality visuals along with discussion for “multi-modality” teaching. The early physics textbooks often contained high quality and detailed illustrations produced by skilled illustrators or “artists”, as shown here.

Hand Drawn Visual in Early Medical Physics Textbook



The apparatus shown in Fig. 98 was used by Professor Crookes to demonstrate that radiant matter could exert forces and games this the Railway Tube. It consists of a track running between the two electrodes at the ends of the tube. A small lite-weight paddle wheel is placed on the track so that the paddles in the upper position are in line between the two electrodes. When the electrodes are connected to an electrical source the paddle wheel rotates and moves along the track away.

Figure 7. An example of high-quality visuals, produced by skilled artists and illustrators, used in some medical physics textbooks in the past.

Textbooks continue to be a major source of visuals for physics education but have transitioned from hand-drawn to computer-graphics creations.

With the development of copy machines that produce images on transparent sheets, “transparencies”, and overhead projectors, illustrations copied from textbooks and other sources, provided classrooms and conferences with high quality visuals that were permanent and could be used many times.

The next major step was the development of 35mm photography and projectors, especially the Carousel projector. It became the practical method for copying and projecting clinical images, photographs of equipment and procedures, and copied from textbooks, and other printed sources...and in color. Most radiology and medical physics programs had cameras mounted on copy stands to photograph and produce slides that could be projected.

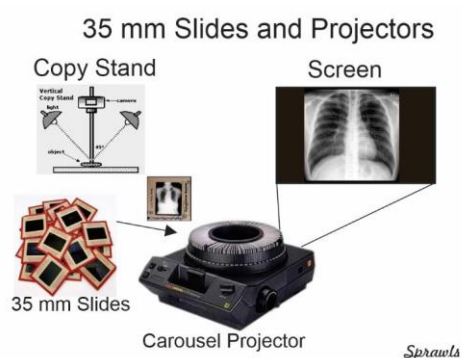


Figure 8. The photographic 35mm slides and projectors were a major advancement in providing high-quality visuals for both classrooms and conferences.

Along with the many values this provided, especially the ability to display high-quality images on large screens from permanent records, the slides, remained one limitation. The slides were physical objects that had to be organized and stored for potential future use, often occupying valuable office space. Even though slides could be duplicated for others to use, this was a limited activity.

VII. DIGITAL IMAGING

A revolutionary and continuing advancement in teaching medical physics is the development of digital imaging methods and techniques with technology for both the creation and sharing of high-quality visuals.

Digital photography, that everyone now has on their phones, can be used to produce high-quality images of clinical images, equipment, procedures, and anything else that is physically visible.

A variety of computer graphics programs are used to create visual representations of much of the invisible world of medical physics, including radiation, interactions, relationships, systems, and much more.

Both methods are valuable, especially when used together, to create visuals for teaching as illustrated here.

Visuals for Teaching the Physics of Mammography

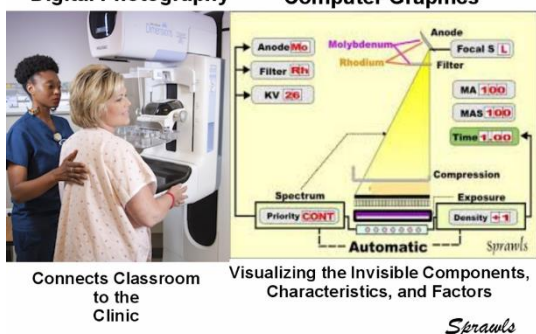


Figure 9. The combined value in using digital photography and computer-generated graphics for teaching medical physics.

The medical physicist who creates and shares visuals is a teacher with the potential of “teaching” many students in classrooms all over the world. A visual creator is like a textbook author with contributions to medical physics education, doing it with individual visuals.

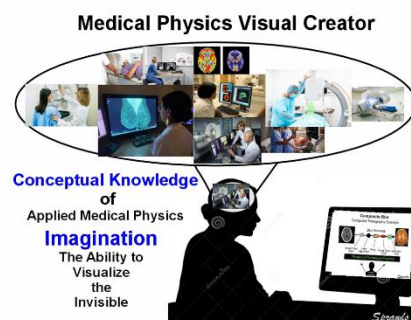


Figure 10. The requirements to be a successful visual creator.

The two requirements to be a successful visual creator is to have a comprehensive understanding and conceptual knowledge of applied medical physics and clinical procedures and a good imagination...the ability to visualize the invisible. While visuals, including diagrams of physical systems and circuits along with charts and graphs are useful in the classroom, that is for teaching the quantitative and mathematics of medical physics, it is the visuals of the invisible that contribute to effective learning and the development of conceptual knowledge networks in the mind.

VIII. COLLABORATIVE TEACHING AND SHARED VISUALS

There are two factors contributing to the ultimate value of visuals for teaching. One is the quality of the content that helps students learn and build appropriate and useful knowledge structures and the other is the number of students that have access to the visual. The value of visuals in textbooks is that they are viewed and studied by many students. The value of digital images is that they can be shared and used in classrooms around the world.

Collaborative Teaching is an established educational process that exists in several different forms or models. The common characteristic is that several individuals are involved together in providing a good learning experience for students. Generally, everyone brings specific knowledge, experiences, or resources to enhance the learning process. sometimes known as team teaching.

The interest here is in a specific model of Collaborative Teaching in which visuals are shared to enhance medical physics classroom and conference presentations and

discussions and the collaborators are the classroom teacher and the visual creator.

The general process for sharing visuals over the internet is illustrated here.

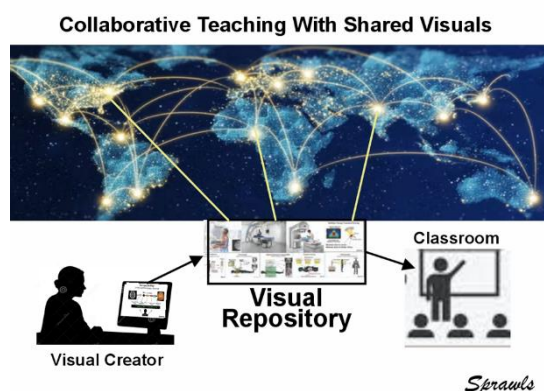


Figure 11. The purpose of a visual repository for collaborative teaching and enhancing medical physics education around the world.

In this context, a *visual repository* is any website that publishes visuals that are available for medical physics educators to download and use in their teaching. These include universities, medical physics organizations, and industry that post images for other purposes but are available for teaching. Of special value are websites that provide for the publication of visuals created by individuals to share with other educators and teachers.

There are two general methods for finding visuals on the web. One is to search the entire internet (World Wide Web) by a specific topic for a visual and the other is to go to designated repositories where visuals are organized and indexed.

A. Searching Throughout the Internet

There are several internet search programs, sometimes referred to as “search engines”, that can be used. Google Image Search is illustrated here for searching by several specific topics. Go to <http://www.images.google.com> and insert a subject to search for. Examples are shown here.

x-ray spectrum: [x-ray spectrum - Google Search](#)

x-ray tube: [x-ray tubes - Google Search](#)

Mammography Procedure: [mammography procedure - Google Search](#)

B. Searching Specific Repositories

These are repositories with visuals that are organized by subject and can be viewed before selecting.

- *The e-Encyclopaedia of Medical Physics*

An extensive text with visuals covering all areas of medical physics on the web at:

<http://www.emitel2.eu/emitwwsql/encyclopedia.aspx> .

- *The Sprawls Visuals*

Visuals for teaching the physics of medical imaging for medical physics students and physicians, especially Radiology Residents in training.

On the web at: www.sprawls.org/SprawlsVisuals .

IX. CONCLUSIONS

Teaching medical physics in the classroom has both advantages and disadvantages. A major advantage is the efficiency of getting classes together as a group for presentations and discussions led by a knowledgeable and experienced teacher. A major limitation and disadvantage is that the traditional classroom separates the students from real-world physics, especially in the medical clinics that they should be learning about. Classrooms are adequate for teaching the mathematical representation of physics relationships and interactions along with verbal descriptions but does not provide sensory, especially visual interactions that are critical for developing the conceptual knowledge that is necessary for many medical physics activities, evaluating the quality characteristics of an image is an example. This requires visuals (images, diagrams, etc.) in the classroom to provide a sensory interaction with the physics applications.

There is now the opportunity to enhance the value of visuals for teaching medical physics with more individuals becoming “teachers” by using their knowledge and experience to create and share visuals for all to use.

X. REFERENCES

1. Sprawls, P. Historical Evolution Of Physics Classroom Learning And Teaching. A Personal Perspective and Journey Perry Sprawls. Medical Physics International Journal, Special Issue, History of Medical Physics 8, 2022 968 <http://www.mpijournal.org/pdf/2022-SI-08/MPI-2022-SI-08-p968.pdf>
2. Sprawls, P. Developing Effective Mental Knowledge Structures For Medical Physics Applications. Medical Physics International Journal, vol.6, No.1, 2018 <http://www.mpijournal.org/pdf/2018-01/MPI-2018-01-p128.pdf>
3. Sprawls, P. Effective Physics Knowledge For Diagnostic Radiologists. Medical Physics International Journal, vol.7, No.3, 2019. Search <http://www.mpijournal.org/pdf/2019-03/MPI-2019-03-p257.pdf>
4. Sprawls, P. Maps For Developing Medical Physics Concept Networks in The Mind. Medical Physics International Journal, vol.10, No.1, 2022 <http://www.mpijournal.org/pdf/2022-01/MPI-2022-01-p019.pdf>
5. Sprawls, P. Enhancing Medical Physics Teaching with Image Repositories And Shared Resources Medical Physics International Journal, vol.8, No.3, 2020 <http://www.mpijournal.org/pdf/2020-03/MPI-2020-03-p479.pdf>

ABOUT THE AUTHOR



The long career of Perry Sprawls combines two activities, that of a clinical medical physicist in medical imaging and as an innovative educator. His work along with radiologists and technologists in the clinic provides an understanding of the *physics*

knowledge they needed to conduct imaging procedures (mammography, CT, MRI, etc.) that were adjusted and optimized to produce images with the necessary diagnostic information with managed risk to patients. These are the specific educational needs that he addresses in his educational activities, including textbooks, courses, and especially visuals that he creates and makes available to medical physics educators around the world to enhance their classroom presentations and discussions, in the spirit of Collaborative Teaching. Throughout his career he has recognized the limitations of the traditional classroom as

an effective learning environment for medical physics, especially clinically applied physics, and has applied a series of innovations to address this, using the technology available at the time. [Ref. 1]. The development of digital technology (especially computer graphics and the internet) now provides the opportunity to collaborate with other medical physics educators/teachers by creating and sharing high-quality and effective visuals for their use in classrooms, anywhere in the world: www.sprawls.org/SprawlsVisuals .

Contact of the corresponding author:
Author: Perry Sprawls, Ph.D.
Institute: Sprawls Educational Foundation
www.sprawls.org
Email: sprawls@emory.edu
Country: USA

MEDICAL PHYSICS AND RADIOGRAPHY TRAINING MODEL TAILORED FOR RESOURCE LIMITED SETTINGS

A.N. Mumuni

Department of Medical Imaging, University for Development Studies, Tamale, Ghana

Abstract— Medical Physics and Radiography training require a tailored, practical-focused curriculum deployed in well-resourced facilities. However, resource limited settings in low- and middle- income countries are faced with challenges of low expertise, brain drain, and lack of adequate medical equipment to optimize healthcare services in these regions. Various training models have been implemented for specific professionals, which can be modified to develop a framework for a structured practical training for Medical Physicists and Radiographers practicing in these regions. This paper presents a modified Teach-Try-Use approach to training of Medical Physicists and Radiographers in resource limited settings. The aim of such a program is to optimize the limited resources, both human and equipment, to meet the training needs of professionals in resource limited settings. Recommendations are made on how the model can be sustained and strengthened over time. It is expected that there will be challenges in the initial stages of its implementation, but these challenges should present opportunities to even make it better in future rounds of the implementation process.

Keywords— Medial Physics, Radiography, low- and middle- income countries, curriculum, education

I. INTRODUCTION

Medical Physics and Radiography services have become the core of healthcare systems in developed nations. In many of such jurisdictions, there are even healthcare personnel specialized in sub-disciplines of Medical Physics and Radiography. The situation of low- and middle- income countries (LMICs) is very different in terms of the availability of equipment, expertise and support systems [1,2] to enable full implementation of Medical Physics and Radiography practice. The consequence of this situation is often brain drain of the few experts to the developed settings, poor maintenance of equipment due to lack of effective quality control programs in most health facilities, and overall high cost of Medical Physics and Radiography services to the general population, where such services are available.

Pragmatic steps are therefore needed to adequately train, retain and equip the current cadre of professionals and yet-to-be inducted professionals of Medical Physics and Radiography in such resource limited settings. This would not only strengthen the practice of these very critical healthcare professions, but would ensure equitable provision of adequate and quality healthcare services in these regions.

The broader effect would then be a significant step toward achieving universal health coverage by 2030/2035.

The ideal order of steps to narrow the yawning gap in Medical Physics and Radiography services between the developed and developing nations would involve training of professionals, establishment of active professional networks of these professionals across borders, and provision of the relevant equipment in health facilities to support their practice. The nature and burden of diseases are becoming complex and, in some cases, could become global pandemics such as COVID. Preventive measures therefore are crucial in curbing the impacts of such pandemics. Medical Physicists and Radiographers have important roles to play in this regard.

Based on a number of existing models in other specialties (such as Radiology [3], MRI technology [4], Artificial Intelligence [5], and Medicine [6]), this paper proposes a structured model within which various curricular could be harmonized to train and upskill the expertise of Medical Physicists and Radiographers practicing in LMICs where most healthcare facilities are resource limited in terms of both expertise and equipment. The training model is relevant for all specialties of Medical Physics and Radiography and could be curated for any setting.

II. IMPLEMENTATION OF THE MODEL

A. NEEDS ASSESSMENT SURVEY

There is clearly a need for a structured, tailored, and sustainable Medical Physics and Radiography training in regions such as Africa, Latin America and South-East Asia. However, rather than using a one-size-fits-all approach to this, there should be a needs assessment using the same tool in all regions. This will provide information about the nature and scope of the needs of practitioners in these regions as well as available training resources, so that the appropriate training methods and content can be tailored to the needs of the experts in each region. Where necessary, steps should be taken to identify training facilities to support the practical components of the training.

Leadership of regional Medical Physics and Radiography professional bodies should collaborate in this in order to coordinate the process through targeting their members. Experts in the design and analysis of appropriate

tools for needs assessment could be engaged to assist the professional bodies in this regard. Not less than a response rate of 70 % to the needs assessment questionnaire should be targeted in each region. This would ensure that the multiplicity of challenges and professional needs of their members are well captured to influence the content of the training curriculum.

B. CURRICULUM DESIGN STRATEGY

Based on the needs assessment, a call should be made to invite curriculum design and educational content development experts to participate in the curriculum design process. All of them do not necessarily need to be Medical Physicists and Radiographers, particularly when there is the need for the group to work on developing the content and deploying them through various media platforms.

Generally, the curriculum for both professionals must have both theoretical and practical components, specific to each specialization. The theoretical component should cover all the basics required in the subspecialty of each field. For example, Medical Physicists in Radiation Protection do not need to go through the basics of Diagnostic Imaging Physics, if those topics are not relevant to their practice. Of course, specific imaging modalities that are based on ionizing radiation (such as computed tomographic and X-ray imaging) could be covered, but not in much detail as would be covered for those in Diagnostic Imaging Physics. Radiography professionals, on the hand, will be taken through all imaging modalities, but with limited physics content. Such fine adjustments will enable the content to be tailored to all professionals, regardless of their levels in the profession.

There should be more focus on the practical components of the curriculum. The needs assessment should have elements to enable the creation of a database of possible (private and public) training facilities at universities, hospitals, medical equipment vending companies, and research units. Both local and international experts (researchers, clinicians, equipment vendors, etc.) willing to form the faculty to provide training should be contacted both directly and indirectly by invitations. There should be minimum practical training hours to be achieved by all participants which would ensure that they acquire the requisite skillset for their specific practice.

The curriculum design phase should include pooling all these expertise and equipment together in readiness to implement all aspects of the training. An example of this strategy is currently being implemented by the Scottish Imaging Network: A Platform for Scientific Excellence (SINAPSE) [7]. SINAPSE is a collaboration of experts with medical imaging resources pooled from seven universities in partnership with the National Health Service and industry within Scotland, to support research and training in Imaging

Sciences. The goal of the consortium is to develop novel imaging methodologies and the next generation of scientists to apply these methodologies in addressing healthcare needs of the population in Scotland.

C. THE TRAINING MODEL

The tailored curriculum in the respective regions can be delivered using a modified approach of the Teach-Try-Use model previously implemented in Artificial Intelligence training [8,9]. The specific modifications of the model, incorporating other models, for Medical Physics and Radiography training are described as follows.

The *Instructive* component of the model will involve teaching participants the basics about the relevant themes related to their practice over a planned period of time. This can be a combination of live virtual and recorded lectures delivered by experts in various fields. In some cases, face-to-face or virtual tutorial sessions and seminars can be planned at the local sites of the training to provide further opportunities for participants to properly understand the concepts. Short quizzes could be used to assess the depth of their appreciation of the content delivered, whereas the interactive tutorial sessions will offer them an opportunity to have their challenging questions answered.

The *Try* component of the model will involve practical demonstrations of concepts by experts to participants either in face-to-face sessions (for those with access to the equipment) or in live video demonstrations, recorded versions of which can be accessed online by participants any time after the sessions. This component of the training should immediately follow each specific instructional session on the practical topic so that participants can easily relate the two for better appreciation of the concepts.

The *Use* component of the model will involve participants using the theoretical and practical knowledge gained to solve a number of practical real-life problems in their respective disciplines. Well-planned problems will be presented to them in teams, so that in a peer-to-peer interaction [3], they share knowledge and experiences in a problem-based learning fashion [6]. The topics to be considered here could range from optimization of quality control protocols, imaging techniques, patient safety issues, acceptance tests, etc. Solutions could be simulated with the aid of various simulation/virtual software and platforms and reports presented as project seminars to be assessed. The team leaders here will later become permanent facilitators for the program in their respective countries, whereas the team members will be added into a database to create an academy of trained experts who can always be contacted at any time as experts to train their peers.

Figure 1 shows the summary of the model, Figure 2 shows the organogram of the model implementation team and Table 1 shows the roles of the team members.

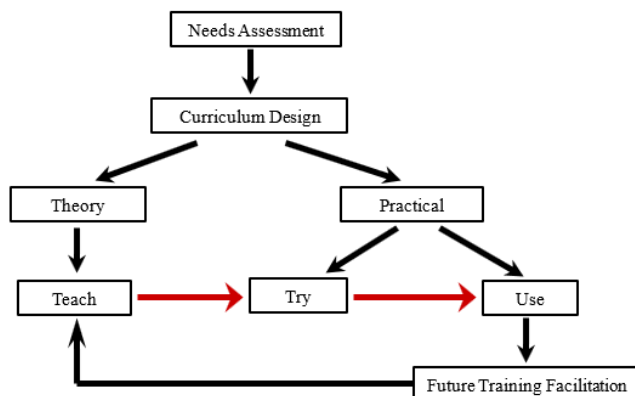


Fig 1 Structure of the training model

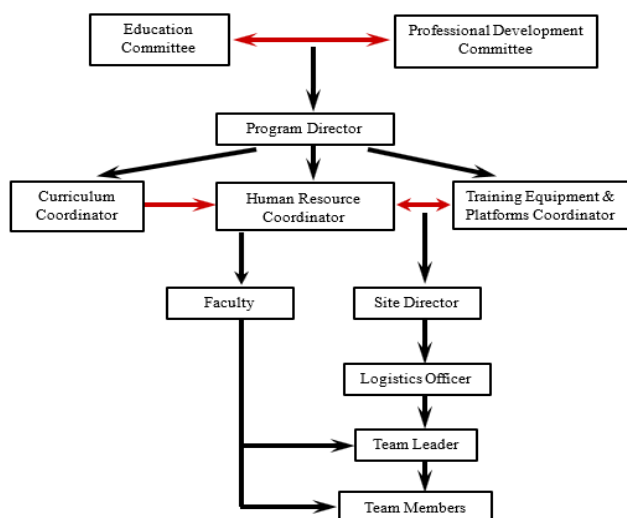


Fig 2 Organogram of the team to implement the training model

Table 1 Functions of the various team members to implement the training model

Team Member	Function in the model
Education Committee	Develops and revises the needs assessment tools and presents a synopsis of the curriculum to the Curriculum Coordinator to develop it further. Oversees the effective implementation of all aspects of the program
Professional Development Committee	Develops and maintains a database of accredited training facilities and available equipment for the practical component of the training. Responsible for continuous professional development program planning, and providing avenues for inter-regional interactions through conferences, seminars, summer schools, etc.
Program Director	Collaborates with the Education and Professional Development Committees to recruit and coordinate the functions of the Curriculum, Human Resource, and Training Equipment and Platforms Coordinators.

Curriculum Coordinator	Puts a team together through the support of the Education Committee to develop a tailored curriculum based on needs assessment outcomes. Reports to the Human Resource Coordinator the list of expertise or specialties of faculty required to teach various aspects of the curriculum
Human Resource Coordinator	Identifies, contacts, recruits and maintains a database of all experts who will serve as faculty or trainers in the program. In addition, provides and monitors the code of conduct of all stakeholders in the program. Responsible for coordinating a team to select applicants for the program based on established eligibility criteria.
Training Equipment and Platforms Coordinator	Coordinates with the Human Resource Coordinator to identify and recommend platforms, software and general resources needed by the faculty to teach. At the same time, sends a list of required resources to the Site Director.
Site Director	Recruits a Logistics Officer at their site to assist them with making arrangements for logistics support for the training at their local site. Ensures that an effective platform and environment are available for the smooth interaction between faculty and trainees
Logistics Officer	Ensures availability of functional equipment and other resources to support a smooth deployment of the training content to trainees
Faculty	Various experts including researchers, university teachers, clinicians, equipment vendors, etc. who will be teaching various aspects of the program content
Team Leader	This usually will be the seniormost member (in rank and expertise) of the team of trainees who will conduct tutorials for the team, and at the same time will receive mentorship on aspects of the training curriculum. Evolves to become a permanent facilitator to train others in their region.
Team Members	Each team will comprise of a maximum of ten members, excluding the Team Leader. They will receive the training over a planned period, and are therefore the target beneficiaries of the program. They later become academy members as team of experts to rely on as trainers of their peers in the future.

D. PROGRAM SUSTAINABILITY

The training model can be established and maintained if the following recommendations are taken into consideration:

- *Education Committee*

Each regional professional body must have an education committee whose membership should take on the roles discussed in Table 1. The function of this committee will, among others, include taking steps to revise the training curriculum as frequently as necessary to include new and emerging themes/topics and best practices for the respective specialties; they will also conduct participant satisfaction

and skillset upgrade surveys in respect of whether their expectations and needs were met after every round of completion of training session. The outcomes of such surveys will inform the revisions to the curriculum.

- *Professional Development Committee*

There must also be a professional development committee (Figure 2) in each regional society. Their function will be to identify and create a database of accredited facilities that will be ready and willing to support the practical component of the training. The committee should engage international societies they are affiliated to, in order to gain access to a wider scope of facilities and equipment vending companies. Involvement of vendors in this aspect of the training could offer such facilities firsthand access to the vending companies for support in areas of appropriate contract terms, equipment upgrades and troubleshooting, and site-specific training opportunities. In addition, the committee must design a structured credit scoring system to award professionals points toward their annual professional PIN renewal. Lastly, in collaboration with the education committee, the professional committee should organize inter-regional seminars, summer schools, and establish collaborations to enable exchange of ideas, networking, and offer platforms for presentation of common challenges and progress under the training program.

- *Center of Excellence*

Steps should be taken to either use the SINAPSE model of resource pooling [7] or establish regional centers of excellence for Medical Physics and Radiography training. Exchange programs, internships, and visiting lectureship arrangements could be made among such centers in the training process. The centers should be ultimately resourced and accredited over time to provide structured academic and continuous professional training toward certification. At the centers of excellence, steps should be taken to eliminate language barrier in the deployment of the curriculum by engaging other trainers who can speak the languages of trainers, where applicable.

- *Training College*

There should be an established collaboration between academic institutions, industry and the managers of the program in such a way that the relationship could evolve into an established training college with both virtual and physical space coverage within each region. Mounting the training model in such an establishment could make it easier to consider structured and accredited postgraduate training as well, to eliminate the barriers to postgraduate scholarships and opportunities for Medical Physicists and Researchers who may wish to join academic institutions. There are limited opportunities for postgraduate education in these two areas in most LMICs; this program could therefore evolve to provide such opportunities.

- *Funding*

A funding scheme for the program can be established and sustained through contributions of participating universities in terms of teaching, supervision, fee waivers, and equipment. The regional bodies could as well provide some funding support, through annual dues, to supplement other sources of funding for the program. Partnerships with vending companies and global healthcare bodies could offer opportunities to access funds to sustain the budget for the program. Indeed, academic training toward postgraduate certification should be charged to raise funds for the program, but significant fee waivers should be considered for applicants from LMICs.

- *Motivated Trainees*

Finally, participants must willingly apply to participate in the program and must show evidence of a need and motivation to engage in the program. Participants must have specific compulsory deliverables at every stage of the training, before they progress to the next stage. This is to ensure their active participation throughout the training process. Continuous professional training programs should be free, subject to trainees being in good standing with their professional societies. Postgraduate training on the other hand should be charged at high rates of fee waivers.

III. CONCLUSIONS

Medical Physics and Radiography training require the deployment of a tailored curriculum in well-resourced facilities. In the absence of such facilities, there is a need to develop and deploy innovative curriculum in a way that should meet the needs and expectations of all trainees. The refined Teach-Try-Use model is one effective means of meeting this requirement in resource limited settings. Challenges to be encountered in its implementation could provide avenues to perfecting the model in specific settings.

IV. REFERENCES

1. Trauernicht C, Hasford F, Khelassi-Toutaoui N, Bentouhami I, Knoll P, Tsapaki V (2022). Medical physics services in radiology and nuclear medicine in Africa: Challenges and opportunities identified through workforce and infrastructure surveys. *Health and Technology* 12(4): 729–37. DOI <https://doi.org/10.1007/s12553-022-00663-w>.
2. Hasford F, Mumuni AN, Trauernicht C et al. (2022). A review of MRI studies in Africa with special focus on quantitative MRI: Historical development, current status and the role of medical physicists. *Physica Medica* 103: 46-58. DOI <https://doi.org/10.1016/j.ejmp.2022.09.016>
3. Chetlen AL, Petscavage-Thomas J, Cherian RA et al. (2020). Collaborative learning in radiology: from peer review to peer learning and peer coaching. *Academic radiology* 27(9): 1261-1267.
4. Scan With Me (SWiM), training platform. <https://event.fourwaves.com/swim>

5. The **Sprint AI Training for African Medical Imaging Knowledge Translation (SPARK) Academy**, An annual CAMERA capacity building program in deep learning and medical imaging. <https://event.fourwaves.com/spark>
6. Mogre V, Amalba A (2015). Approaches to learning among Ghanaian students following a pbl-based medical curriculum. *Education in Medicine Journal* 7(1): 38-44.
7. Scottish Imaging Network: A Platform for Scientific Excellence (SINAPSE), <https://www.sinapse.ac.uk/>
8. Elahi A, Dako F, Surratt S, Schweitzer A (2022). RAD-AID's Teach-Try-Use Model to Implement AI in Low-and-Middle-Income Countries. Society for Imaging Informatics in Medicine 2022 Annual Meeting, Kissimmee, Florida, June 2022. Also, here <https://rad-aid.org/programs/informatics/>
9. SPARK Academy, <https://event.fourwaves.com/spark/pages>

Contacts of the corresponding author:

Author: Abdul Nashirudeen Mumuni
Institute: Medical Imaging, SAHS-UDS
Street: Dungu-Tamale Campus
City: Tamale
Country: Ghana
Email: mnashiru@uds.edu.gh

INVITED PAPERS

Prof. HABIB ZAIDI HONORED WITH IOMP'S JOHN MALLARD AWARD

F. Hasford¹, S. Tipnis²

¹ Radiological and Medical Sciences Research Institute, Ghana Atomic Energy Commission, Accra, Ghana.

² Department of Radiology and Radiological Sciences, Medical University of South Carolina, Charleston, USA.

I. SHORT BIOGRAPHY

Habib Zaidi was born and grew up in Algeria. He studied graduated in Electrical Engineering in 1990 from the University of Setif in Algeria and then was attracted to the fascinating world of medical physics and started his postgraduate program with extensive research training in Lund University under the supervision of Prof. Sören Mattsson, ending-up with a Ph.D. awarded by the University Geneva in 2000 followed by habilitation (Privat-docent) in 2004 [1].



Fig. 1 Prof. Habib Zaidi, photo taken in 2023.

Habib Zaidi (Fig. 1) is Chief physicist and head of the PET Instrumentation & Neuroimaging Laboratory at Geneva University Hospital and full Professor at the medical school of Geneva University. He is also a Professor of Medical Physics at the University of Groningen (Netherlands), Adjunct Professor of Medical Physics and Molecular Imaging at the University of Southern Denmark (Denmark), Adjunct Professor of Medical Physics at Shahid Beheshti University visiting Professor at Tehran University of Medical Sciences and Distinguished Professor at Óbuda University (Hungary). He is actively involved in developing imaging solutions for cutting-edge interdisciplinary biomedical research and clinical diagnosis. His research is supported by the EEC, Swiss National Foundation, EEC, private foundations and industry (Total >10M+ US\$) and centres on hybrid imaging instrumentation (PET/CT and PET/MRI), deep learning for various imaging applications, modelling medical imaging systems using the Monte Carlo method, development of computational anatomical models and radiation dosimetry, image reconstruction, quantification and kinetic modelling techniques in emission tomography as well as statistical image analysis, and more recently on novel

design of dedicated PET and PET/MRI scanners. He was guest editor for 14 special issues of peer-reviewed journals dedicated to *Medical Image Segmentation*, *PET Instrumentation and Novel Quantitative Techniques*, *Computational Anthropomorphic Anatomical Models*, *Respiratory and Cardiac Gating in PET Imaging*, *Evolving medical imaging techniques*, *Trends in PET quantification (2 parts)*, *PET/MRI Instrumentation and Quantitative Procedures and Clinical Applications*, *Nuclear Medicine Physics & Instrumentation*, and *Artificial Intelligence* and serves as founding Editor-in-Chief (scientific) of the *British Journal of Radiology (BJR)|Open*, Deputy Editor for *Medical Physics*, and Associate Editor or member of the editorial board of the *Journal of Nuclear Cardiology*, *Clinical Nuclear Medicine*, *Physica Medica*, *International Journal of Imaging Systems and Technology*, *Clinical and Translational Imaging*, *American Journal of Nuclear Medicine and Molecular Imaging*, *Brain Imaging Methods (Frontiers in Neuroscience & Neurology)*, *Cancer Translational Medicine* and the *IAEA AMPLE Platform in Medical Physics*. He has been elevated to the grade of fellow of the IEEE, AIMBE, AAPM, IOMP, AAIA and the BIR and was elected liaison representative of the *International Organization for Medical Physics (IOMP)* to the World Health Organization (WHO) and Chair of Subcommittee on Part 1 Examination of the International Medical Physics Certification Board (IMPCB) and the Imaging Physics Committee of the *AAPM* in addition to being affiliated to several International medical physics and nuclear medicine organisations. He is developer of physics web-based instructional modules for the RSNA and Editor of IPEM's Nuclear Medicine web-based instructional modules. He is involved in the evaluation of research proposals for European and International granting organisations and participates in the organisation of International symposia and conferences. His academic accomplishments in the area of quantitative PET imaging have been well recognized by his peers and by the medical imaging community at large since he is a recipient of many awards and distinctions among which the prestigious *2003 Bruce Hasegawa Young Investigator Medical Imaging Science Award* given by the *Nuclear Medical and Imaging Sciences Technical Committee of the IEEE*, the *2004 Mark Tetalman Memorial Award* given by the *Society of Nuclear Medicine*, the *2007 Young Scientist Prize in Biological Physics* given by the *International Union of Pure and Applied Physics (IUPAP)*, the prestigious (100'000\$) *2010 Kuwait Prize of Applied sciences* (known as the *Middle Eastern Nobel Prize*) given by the *Kuwait Foundation for the Advancement of Sciences (KFAS)* for "outstanding accomplishments in Biomedical technology", the *2013 John*

S. Laughlin Young Scientist Award given by the AAPM, the 2013 *Vikram Sarabhai Oration Award* given by the Society of Nuclear Medicine, India (SNMI), the 2015 *Sir Godfrey Hounsfield Award* given by the British Institute of Radiology (BIR), the 2017 *IBA-Europhysics Prize* given by the European Physical Society (EPS), the 2019 *Khwarizmi International Award* given by the Iranian Research Organization for Science and Technology (IROST) and the 2023 *John Mallard Award* given by the IOMP for innovative developments of high scientific quality. Prof. Zaidi has been an invited speaker of over 160 keynote lectures and talks at an International level, has authored over 900+ publications (he is the senior or first author in a majority of these publications), including 395 peer-reviewed journal articles in high ranking journals, most of them in Q1/D1 of their categories (h-index=76, >20'550+ citations | Google scholar as of 15 December 2023), 475 conference proceedings and 42 book chapters and is the editor of four textbooks on *Therapeutic Applications of Monte Carlo Calculations in Nuclear Medicine (2 Editions)*, *Quantitative Analysis in Nuclear Medicine Imaging*, *Molecular Imaging of Small Animals and Computational anatomical animal models*.

II. AWARDEE OF IOMP'S JOHN MALLARD AWARD

The **IOMP John Mallard Award** honours a medical physicist who has developed an innovation of high scientific quality and who has successfully translated this innovation in clinical practice.

Amongst several very high calibre nominations from all over the world, the Awards and Honours Committee of the IOMP considered **Prof. Habib Zaidi** as an outstanding medical physicist, with impressive capacity to innovate, develop and translate to clinical setting technological advances in the field of multimodality medical imaging and its application in clinical practice [2]. He has made valuable and seminal contributions in academia, education and mentoring and tutoring of many highly qualified medical physicists. His academic accomplishments in the area of quantitative PET imaging have been well recognized by his peers and by the medical imaging community at large since he is a recipient of many awards and distinctions. He has also been elevated to the grade of fellow of the IEEE, AIMBE, AAPM, IOMP, AAIA and the BIR.

Some main achievements:

- He developed versatile PET and CT Monte Carlo simulation packages that have been used extensively in imaging physics research.

- Zaidi is highly recognized for pioneering MRI-guided attenuation correction, carried out in 2002 prior to the advent of hybrid PET/MRI systems, demonstrating his visionary and futuristic outlook and paving the way for a new class of algorithms.
- In collaboration with some colleagues, he developed methodologies for metal artifact reduction in CT and correction of oral contrast medium for artifact-free CT and PET/CT imaging that have been applied in clinical setting.
- In collaboration with some colleagues, he developed a large number of advanced human, primate and small-animal computational models suitable for radiation dosimetry research.
- In collaboration with some colleagues, he developed innovative deep learning-powered algorithms for various multimodality medical image analysis applications, including imaging instrumentation design, image denoising (PET and CT), quantitative image reconstruction, image segmentation, artifact-free imaging, radiation dosimetry and computer-aided diagnosis, prognosis, and outcome prediction. Many of these developments have high potential for clinical translation.
- In addition to being a researcher with more than \$10 million in research grants, 400 peer-reviewed publications, he supervised 29 PhD theses and mentored and trained over 22 senior scientists and postdoc fellows.

In recognition of the extraordinary definite impact that Prof. Habib Zaidi had over the entire field of medical physics, the IOMP has decided to award him the **2023 John Mallard Award**.

Congratulations, Prof. Habib Zaidi.

III. REFERENCES

1. Habib Zaidi web site at <https://pinlab.ch/Habib/>
2. Announcement of the Award on IOMP web site <https://www.iomp.org/announcement-of-2023-john-mallard-awardee-habib-zaidi/>

Contacts of the corresponding author:

Author: F. Hasford
 Institute: Radiological and Medical Sciences Research Institute,
 Ghana Atomic Energy Commission
 Street: Atomic Street
 City: Accra
 Country: Ghana
 Email: haspee@yahoo.co.uk

26th INTERNATIONAL CONFERENCE ON MEDICAL PHYSICS (ICMP-2023): IN RETROSPECT

Sunil Dutt Sharma

¹ President, Association of Medical Physicists of India (AMPI)

² Co-Chair, Conference Organizing Committee & Scientific Committee, ICMP-2023

I. INTRODUCTION

The 26th International Conference of the IOMP namely the “International Conference on Medical Physics 2023” (ICMP-2023) was jointly organized by Association of Medical Physicists of India (AMPI), International Organization for Medical Physics (IOMP), Asia-Oceania Federation of Organizations for Medical Physics (AFOMP) and South-East Asian Federation of Organizations for Medical Physics (SEAFOMP) during 6 to 9 December 2023 at DAE Convention Centre, Anushaktinagar, Mumbai, India. The theme of the conference was Innovations in Radiation Technology & Medical Physics for Better Healthcare.

II. OPENING CEREMONY

The opening ceremony of the conference presented the mixture of Indian tradition (lamp lighting, welcome to dignitaries by flower bouquets, felicitation of guests) and global scientific culture. Dr. Sudeep Gupta, a renowned medical oncologist who is currently the Director of Tata Memorial Centre (a premier cancer institution of India), was the chief guest for this function. Figure 1 is the photograph of the opening ceremony of ICMP-2023 showing release of souvenir and book of abstracts of the conference.

III. PARTICIPATION

ICMP-2023 brought together experts, researchers, and professionals from around the world to discuss the latest advancements and breakthroughs in the field of medical physics and associated disciplines. This conference was well attended by more than 1300 participants from 33 countries including 134 delegates/invitees/experts from outside India. The participation of more than 325 medical physics students and about 200 medical physics senior citizens was the testimony of the larger medical physics community of India. We can proudly state that the ICMP-2023 has brought together the medical physics professionals of four generations (4G). Thus, ICMP-2023 was indeed the 4G conference. Figure 2 is a section of the participants.

IV. SCIENTIFIC PROGRAM

The scientific program of the conference was very comprehensive and it included almost all the topics of recent

interests for deliberations such as artificial intelligence in medical physics, technology and techniques of radiation oncology, treatment planning, emerging and newer techniques of radiation therapy, imaging in radiation oncology, advanced technologies and techniques of medical imaging, emerging and newer techniques of medical imaging, radiation dosimetry and radiation safety, targeted therapy, radiation biology, modeling and simulation, translational research, education/training and certification in medical physics.

The scientific schedule included 4 plenary sessions (6 talks), 2 joint sessions (IOMP-IAEA and IOMP-IRPA with 4 talks), 6 IOMP schools (including 2 CMPI teaching sessions), 14 special symposiums (46 talks), 36 scientific sessions (36 invited talks plus 102 oral paper presentations), 2 technical sessions (11 technical talks from the exhibitors), 359 poster presentations, 4 poster rapporteur sessions (15 reporters briefing on the poster presented at the conference), and one evening lecture. Scintillating debates (2 sessions), namely “Will AI replace clinical medical physicists?” and “Whether harmonization in certification of medical physicists is required?” and medical physics quiz competition (2 sessions) were the special attractions for many participants. Live telecast of the scientific deliberations was made through YouTube and links for all the deliberations are made available at the conference website www.icmp2023.org. In addition, links of all the presentations have also been communicated to IOMP, AMPI, AFOMP, and SEAFOMP for uploading at their websites.

V. SPECIAL INTERESTS

The inclusion of YOGA session (special thanks to Prof M. Mahesh for the proposal) on the mornings of 2nd, 3rd and 4th day of the conference was of special interests to many and it has been well appreciated. I am hopeful the Yoga session started from ICMP-2023 will be part of many other conferences in the world. The social aspects of the conference were equally attractive and have received wide appreciation from all. Cultural program in the evening of first day and complimentary dinners in the evenings of 1st, 2nd, and 3rd days, along with the arrangements for music and dancing was refreshing for all.



Figure 1: Photograph of the opening ceremony of ICMP-2023 [From left to right: V Subramani, Sunil Dutt Sharma, Eva Bezak, Dinesh Kumar Aswal, Sudeep Gupta, John Damilakis, Balvinder Kaur Sapra, Chai Hong Yeong, Rajesh Kumar]



Figure 2: Section of participants at the ICMP-2023

VI. SUMMARY

The total deliberations of the conference included 233 oral presentations and 359 poster presentations. To cover such a large number of oral presentations, it was inevitable to conduct three parallel sessions (please see the scientific program available at www.icmp2023.org). It is worth mentioning here that IOMP introduced four cash prizes (two for best oral presentations and two for best poster presentations) to encourage and enhance the quality of presentations in addition to quality of scientific work. Thanks to the panel of judges who evaluated the proffered oral and poster presentations which was indeed a herculean task.

VII. ACKNOWLEDGEMENT

I take this opportunity to thank IOMP, AMPI, AFOMP, SEAFOMP, trade exhibitors/supporters, invitees, experts, delegates, members/chairs/co-chairs of all the committees

of ICMP-2023 including members of local organizing committee and all those who have supported me directly/indirectly in making the biggest ever international conference on medical physics (ICMP) of IOMP a satisfying and successful event. In fact, ICMP-2023 was the mega event of medical physics which has created a few records to serve as reference for organizers of future ICMPs.

VIII. REFERENCE

1. <https://icmp2023.org/>
2. <https://www.iomp.org/icmp-2023-report/>

Contacts of the corresponding author:

Author: S.D. Sharma
 Institute: Association of Medical Physicists of India
 Country: India
 Email: sdsbarc@gmail.com

15 YEARS IOMP HISTORY SUB-COMMITTEE

Slavik Tabakov^{1,2,3}

¹ King's College London, UK, ² Past President IOMP, ³ Chair IOMP History Sub-Com

The IOMP History Sub-Committee (HSC) was established during the IOMP office 2006-2009. It was an activity led by the IOMP Past-President A Niroomand-Rad, who became the first Chair of HSC in 2008. The HSC was placed under the IOMP Publication Committee with the charge to keep information about the history of the organization, its active members and related data.

The members of the HSC so far include:
 2008-2012 Azam Niroomand-Rad, Chair (USA)
 Colin Orton (USA)
 Slavik Tabakov (UK)
 Robert Gould (USA)
 2012-2015 Azam Niroomand-Rad, Chair (USA)
 Colin Orton (USA)
 Peter Smith (UK)
 KY Cheung (Ex-Officio)
 2015-2018 KY Cheung, Chair (Hong Kong, PR China)
 Colin Orton (USA)
 Peter Smith (UK)
 Slavik Tabakov (Ex-Officio)
 2018-2022 Slavik Tabakov, Chair (UK)
 KY Cheung (Hong Kong, PR China)
 Colin Orton (USA)
 Madan Rehani (Ex-Officio)
 John Damilakis (Ex-Officio)
 Paolo Russo (Ex-Officio)
 2022-2025 Slavik Tabakov, Chair (UK)
 Azam Niroomand-Rad, USA
 Geoffrey Ibbott, USA
 KY Cheung, Hong Kong
 Perry Sprawls, USA
 John Damilakis, Greece (Ex-Officio)
 Eva Bezak, Australia (Ex-Officio)
 Francis Hasford, Ghana (Ex-Officio)

The first activities of HSC were at the WC2009 in Munich when a number of past IOMP Presidents, Chairs and active members were interviewed. The videos of these interviews were arranged by S Tabakov and M Stoeva as a free-access web activity. These interviews are now being re-established.

During the period 2010-2015 HSC collected information and published the full History Tables of the IOMP, listing various activities and each individual member of each Committee from the establishment of IOMP in 1963. These were published at the IOMP web site

and are updated by HSC during by each IOMP term of office.

During 2017 a long-term project was initiated "History of Medical Physics", which initially began its publications as Special Issues of the IOMP Journal Medical Physics International. The first issue related to the history of the profession was published in 2018 with Founding Editors Slavik Tabakov and Perry Sprawls. In 2019 Geoff Ibbott join the Editorial team and the three Co-Editors in Chief continue to produce 1 or 2 history-related issue each year. In 2022 the history editions were separated as an independent part of the MPI Journal family – MPI History Editions.

In the period 2019-2022 the MPI regular issues included topical papers tracing the professional development within each of the IOMP Regional Organisations (Federations). In 2023 the MPI History Editions (MPI-HE) issue was dedicated to the women-pioneers in medical physics.

In June 2022 MPI-HE published a full issue dedicated to the 60th Anniversary of IOMP, including as an Annex all 35 IOMP History Tables (with lots of information and all IOMP Committee members – over 1000 during these 60 years). This issue (230 pages) has thousands of downloads.

HSC express special gratitude to all its members and to the MPI-HE contributors over these 15 years. We encourage authors to contribute to the IOMP history-related activities for keeping a good track of the development of the profession and its contributions to contemporary medicine.

Specific history-related links and issues:

1. IOMP History Tables:
<https://www.iomp.org/history-sub-committee-activities/>
2. History of Medical Physics – project description:
<http://www.mpijournal.org/pdf/2017-01/MPI-2017-01-p068.pdf>
3. MPI-History Edition listing the history of the IOMP and all 35 History Tables:
<http://www.mpijournal.org/pdf/2022-SI-07/MPI-2022-SI-07.pdf>
4. MPI-HE web address with all history issues:
<http://www.mpijournal.org/history.aspx>

Corresponding author email: slavik.tabakov@emerald2.co.uk

HOW TO

AN INITIAL QUANTITATIVE COMPARATIVE STUDY OF THE AXIAL AND LATERAL SPATIAL RESOLUTIONS OF DIFFERENT ULTRASOUND TRANSDUCERS

K. Cilia, M.L. Camilleri

University of Malta, Msida, Malta

Abstract –

Accurate measurement of the spatial resolution of ultrasound transducers is critical for medical imaging. Spatial resolution places a limit on the amount of detail that can be retrieved in an image and impacts the range of clinical diagnosis errors. High spatial resolution allows precise and clear visualization of anatomical microstructures as well as pathological conditions. It also allows radiologists to detect small abnormalities and deformities. This article compares the spatial resolution of different ultrasound transducers, investigates the effect of spatial resolution with depth for different transducers, as well as the effect of spatial resolution with different frequencies for different type of transducers. The spatial resolution results are from acceptance tests performed between February 2019 and March 2023 for 14 ultrasound scanners equipped with 51 transducers: 22-linear, 23-curvilinear, and 6-sector. An ultrasound phantom was also used (CIRS model 040GSE). In addition, ImageJ was used to calculate the spatial resolution of the different ultrasound transducers at different depths within the phantom quantitatively.

Keywords –

Ultrasound, transducers, spatial resolution, Full-Width-Half-Maximum, ImageJ, phantom

I. INTRODUCTION

Over the decades, the use of ultrasound in medical diagnostics has constantly developed and improved. Nowadays, several people are familiar with ultrasound images from personal experience and prenatal examinations. However, current ultrasound systems are much more complex than before. Modern ultrasound systems can acquire precise measurements and dimensions of blood movement, as well as generate three-dimensional images of moving objects. These images are produced by a transducer, a device that generates sound waves and receives returning echoes from tissue interfaces. The collection of returned echoes are sampled and computed to produce an image. Post-processing is generated to improve the overall image according to the clinical protocol.

To ensure that the image obtained is of sufficient quality, a quality control (QC) programme is carried out on various types of transducers. This provides verification that the equipment can be put for clinical use. The QC tests

evaluate the performance of several clinical imaging parameters; one of which is 'spatial resolution'. Spatial resolution is the ability of an ultrasound system to differentiate between two objects that are relatively close in space [1]. Appropriate tests must be performed for each transducer type, frequency, and depth to analyse the performance and measurements of spatial resolution of ultrasound systems.

A. AXIAL SPATIAL RESOLUTION

The axial resolution is defined as the smallest separation between two closely spaced objects along the direction of the beam axis that can be displayed as two separate objects. The length of the pulse of an ultrasound beam is a contributing element that affects axial resolution. This is recognized as the spatial pulse length (SPL). The shorter the pulse length, the better the axial resolution. In theory, the smallest object spacing that can be determined is 1/2 of the SPL [2]. Conclusively, transducers with higher frequencies offer better image resolution, since the axial resolution is determined by the pulse length [3].

B. LATERAL SPATIAL RESOLUTION

Lateral resolution is defined as the ability of the system to distinguish between two separate points that are perpendicular to the ultrasound's beam axis. Lateral resolution is mainly related to the width of the ultrasound beam. That is the wider the beam, the poorer the lateral resolution, resulting in structures being unresolved. Therefore, the best lateral resolution is achieved at the focus [1]. As the ultrasound beam diverges above a certain depth, the lateral resolution becomes poor.

C. DIFFERENT TYPES OF ULTRASOUND TRANSDUCERS

Linear array transducers provide a rectangular field of view (FOV) that maintains its width near the surface of the transducer, and hence, they become notably appropriate when the region of interest broadens to the surface. Additionally, a linear array transducer appears from the outside as a shaped block that fits comfortably in the operator's hands, along with a rubber lens on the surface that comes into contact with the patient's skin. There is also a matching layer behind the lens, followed by a linear array

that ranges from 128 to 512 regularly spaced, thin, rectangular transducer elements separated by narrow barriers [2]. They are particularly suitable for superficial examinations, such as the neck, veins, and arteries of the limbs.

Curvilinear arrays, on the other hand, are characterized by the fact that the arrangement of PZT elements ahead of the front is curved or bent rather than following a straight line. Nonetheless, the maximum useful size of the active element group of a curvilinear array is smaller than that of a linear array with elements of the same size. As a result, the width of the beam in the focal zone is larger providing poorer performance lateral resolution than the linear array transducer. This is mainly due to the fact that as the number of active elements increases, the outermost elements move further and further away from the centerline of the array until they can no longer transmit or receive any data at all in that direction [2]. In addition, curvilinear arrays have the advantage that the FOV becomes wider with increasing depth inside the patient. Therefore, they are often used for abdominal applications [2].

Finally, a sector (or phased array) transducer produces a cone-shaped image or fan-like FOV arrangement, where the sound waves emerge from a small vertex. Cardiac imaging is the most common application of sector transducers [2]. The different transducers are shown in Fig. 1.

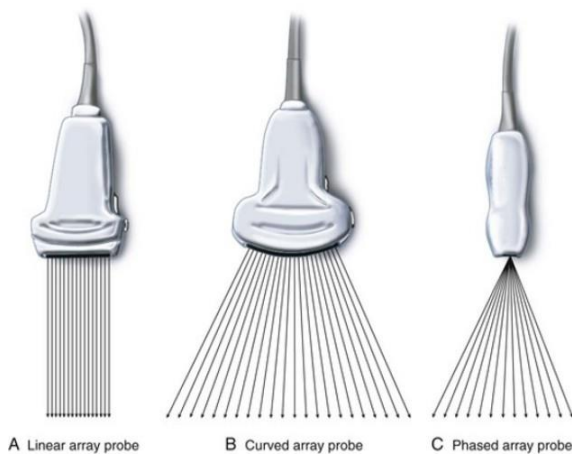


Fig. 1: Different transducer types

D. AAPM AND IPFM 102 STANDARDS

According to AAPM ultrasound Task Group No.1, the preferred way to quantify the spatial resolution is by measuring the FWHM. AAPM has suggested several performance criteria values for axial and lateral spatial resolution. It stated that the axial resolution should generally be 1 mm or less for transducers with central frequencies over

4 MHz and 2 mm or less for those with central frequencies under 4 MHz. However, when measuring the spatial resolution using the FWHM method, AAPM suggests that the FWHM of the axial resolution should be less than 0.45 mm for transducers having central frequencies higher than 4 MHz, and an FWHM of less than 0.9 mm for transducers having central frequencies lower than 4 MHz. The lateral resolution can be evaluated by measuring the width of a filament target at different depths; near, mid, and far-field zones of the transducer [4]. The recommended tolerances for the lateral resolution are shown below in Figure 2. It was noted that IPFM 102 does not have any specific tolerances for spatial resolution during acceptance testing, except for routine QA.

Depth (cm)	Transducer frequency (f) (MHz)	Lateral resolution		
		Response width or spacing between targets (mm)	FWHM (mm)	FWTM (mm)
>10	<3.5	≤4	≤2	≤4
<10	3.5 ≤ f < 5	<3	<1.5	<3
<10	≥5	<1.5	<0.8	<1.5

Table 1: AAPM recommended lateral resolution requirements

II. MATERIALS AND METHODS

In this study, multiple ultrasound scanners from various manufacturers that were accepted in the last four years were used. The scanners used were equipped with different transducers; linear, curvilinear, and sectors of various shapes, including hockey stick and endocavity/endovaginal probes. Also, a dedicated ultrasound phantom with appropriate features was used for testing spatial resolution. Furthermore, standard operation procedures (SOPs) documents authorized by the Medical Physics Department were utilized to perform acceptance QA physics tests on ultrasound systems and to conduct data analysis. These documents have operating instructions on how to perform several tests, as well as to analyse the ultrasound images quantitatively.

A. ACQUIRING PHANTOM IMAGES FOR DIFFERENT TRANSDUCERS

In the first part of the test, ultrasound images were acquired using a dedicated ultrasound phantom. The images were acquired following the IPFM 102 method to test the spatial resolution for Ultrasound Systems' [5]. An example of the obtained ultrasound image is shown in Fig. 2.



Fig. 2: An ultrasound image using a linear transducer on the *Canon Aplio i8000*

B. DATA COLLECTION TOOL

An evaluation of the axial and lateral spatial resolution was carried out between February 2019 and March 2023 for 13 ultrasound scanners equipped with 51 transducers; 22 were linear, 23 were curvilinear, and 6 were sector. Moreover, one phantom: CIRS Model 040GSE, and one software package: Image J, were also used in this study. Subsequently, all transducers utilized were broadband, with 5– 20 MHz frequencies for linear transducers, 3–9 MHz for curvilinear transducers, and 3-5 MHz for sector transducers. A list of all the tested ultrasound scanners is presented below in Table 2.

C. CIRS MODEL 040GSE

A Multi-Purpose, Multi-Tissue Ultrasound Phantom model 040GSE manufactured by CIRS was utilized during acceptance testing. The Model 040GSE is equipped with features enabling it to operate with diagnostic ultrasound devices. The phantom is filled with Zerdineâ, a gel material miming soft human tissue's acoustic properties. A wide range of transducer sizes and frequencies may be used with the phantom [6].

The phantom is split into two sections of different attenuation coefficient: each 0.5 dB/(cmMHz) and 0.7 dB/(cmMHz). Several small targets are positioned at known intervals in horizontal and vertical directions to check the precision and accuracy of the distance measurements and spatial resolution. The CIRS Model is certified to ISO 9001:2008 standards and backed with a certificate of compliance [6]. This phantom was chosen since it was the one used in acceptance testing, and it was the one readily available at that time. Other commercial phantoms that could have been used are; ‘*GAMMEX Sono 410 SCG*’, ‘*ATS 539*’, and ‘*GAMMEX 405GSX*’.

Table 2: A list of evaluated ultrasound systems and transducers

Manufacturer	Model	Linear	Curvilinear	Sector
Canon	<i>Aplio i800</i> (2)	i18LX5 (2)	6MC1 (2)	-
		L24LX8 (2)	i8CX1 (2)	-
	<i>Aplio a550</i>	11L3	8C1	-
		-	11C3	-
	<i>a450</i>	-	11C3 (2)	-
Hitachi	<i>Arietta 65</i>	L64	C251	-
Toshiba	<i>Aplio a400</i>	-	6C1	-
Philips Healthcare	<i>Sparq</i> (3)	L12-4 (3)	C5-1 (3)	S5-1
		-	-	S5-2 (2)
	<i>Lumify SMT-T590</i> (6)	L12-4 (3)	C5-2	S4-1 (2)
	<i>EIPQ Elite 5G</i>	L12-3	C5-1	-
		Hockey Stick L15-7io	-	-
	<i>CX50 POC</i>	L12-3	C5-1 (2)	-
		-	-	-
GE Healthcare	<i>Voluson S10</i>	-	C1-5RS (3)	-
		-	Endocavity IC9-RS	-
	<i>Vivid iQ</i>	12L-RS (2)	-	M5Sc-RS
		Hockey Stick L8-18i-RS	-	-
Esatote	<i>MyLAB X7</i>	SL3116	-	-
		L4-15	-	-
		Hockey Stick IH6-18	-	-
BK Medical	<i>bk3000-01</i>	Hockey Stick IH6-18	6C2	-
			Endocavity E14C4t	-

D. IMAGEJ

ImageJ is a free, open-source software built specifically for processing radiological images. ImageJ has the capacity to provide statistical information and data from line profiles. Therefore, this software tool was used in this project to measure the spatial resolution in the axial and lateral directions by implementing the FWHM method. This software tool was chosen since it is flexible, easily accessible, and preferred by medical physicists at that time. Other software tools that could have been used are; ‘*MATLAB*’, ‘*Python*’, and ‘*UltraIQ*’.

E. DATA ANALYSIS TECHNIQUE: OBTAINING THE FWHM FROM A LINE PROFILE

In order to obtain the spatial resolution in the axial and lateral directions using the FWHM method, a line profile was drawn across the nylon filaments on the ultrasound. Then, a dedicated Image J plug-in tool for FWHM was used to calculate the FWHM for each depth.

III. RESULTS

The data collected was presented in a series of scatter plots using Microsoft Excel to analyse the performance of each ultrasound transducer's axial and lateral spatial resolution. These graphs were investigated and related to the objectives of the study. Both of spatial resolution FWHM results were plotted against depth. These plots made evaluating and assessing various variables easier. However, the graphs plotted were based on the limited number of probes available.

A. RESULTS FOR AXIAL RESOLUTION

A graph of the axial resolution against depth was plotted for the three different transducers at different frequencies. The FWHM results of the transducer with the same frequency were averaged to obtain the most accurate and precise analysis as possible.

Linear transducers operating at frequencies 5 to 8 MHz showed the highest axial resolution (~0.54 mm) at the shallowest depth (10 mm). The axial resolution continued to increase with depth (Figure 5). Transducers with 9 and 10 MHz frequencies showed better axial resolution (~0.4 mm) than those with lower frequencies. The poorest axial resolution was measured at a depth of 90 mm for the 10 MHz transducer (~0.57 mm). Conversely, linear transducers with higher frequencies (15 to 20 MHz) had the best axial resolution at lower depths than other frequency ranges. Moreover, it was noted that the resolution of the 20-MHz transducer was worse than that of the 9- and 19-MHz transducers, especially at 40 mm depth (Fig.3).

On the other hand, for curvilinear probes, the axial resolution was broader for transducers operating at frequencies from 3 to 6 MHz. Moreover, the axial resolution decreased rapidly at 120 mm depth in this frequency range. However, even with increasing depth, transducers operating at higher frequencies (8.5 and 9 MHz) showed better overall axial resolution. The best resolution (~0.54 mm) was observed for the 8.5 MHz probe at 10 mm depth (Fig.4).

Finally, the best axial resolution for the sector transducers was observed for the 5 MHz transducers, especially at depths above 100 mm. However, the 3 MHz probe also had the poorest resolution, with increasing depths (Fig.5).

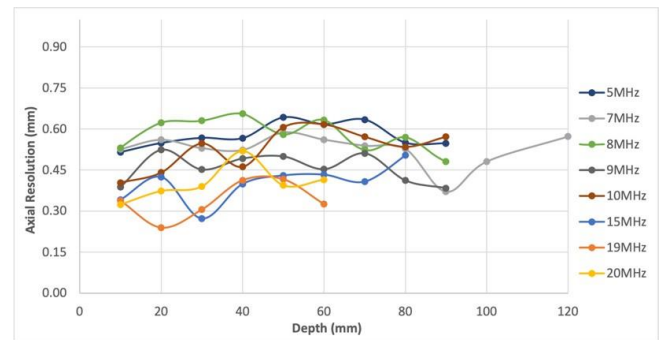


Fig. 3: Axial resolution (mm) against depth (mm) for linear transducers with different frequencies

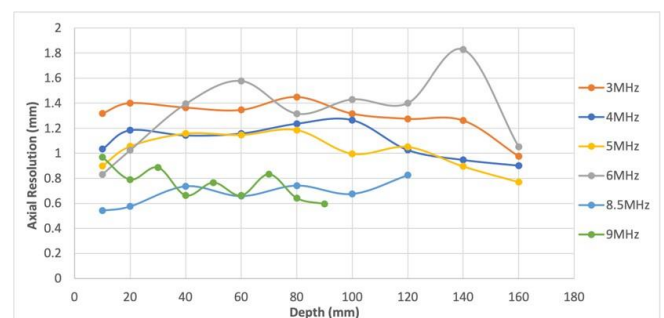


Fig. 4: Axial resolution (mm) against depth (mm) for curvilinear transducers with different frequencies

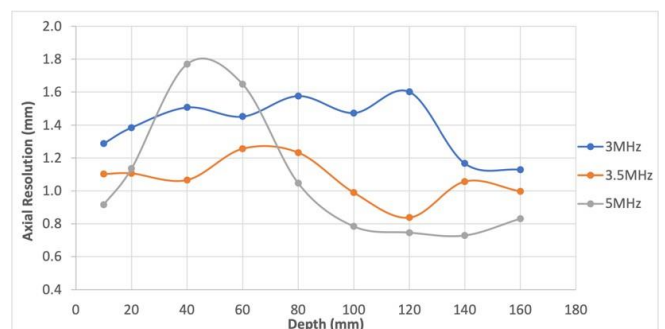


Fig. 5: Axial resolution (mm) against depth (mm) for sector transducers with different frequencies

B. RESULTS FOR LATERAL RESOLUTION

The linear transducers with 5-8 MHz frequencies showed worse lateral resolution, especially at depths of 50-70 mm and 100 mm, as shown in Fig.6. For transducers operating at 7 MHz, the lateral resolution deteriorated rapidly at 40-60 mm depths. Since only two transducers were tested at this frequency and different protocols were used, it might have impacted the final result. However, the 9 and 20 MHz transducers had the best lateral resolution, at most 1.19 mm. On the other hand, curvilinear probes with low frequencies (3-5 MHz) had the worst lateral resolution on average, even with increasing frequencies, even with increasing depth. However, the best lateral resolution was exhibited by the transducers operating at frequencies of 6 and 8.5 MHz (Fig.7) Finally, as expected, sector transducers at higher frequencies experienced a better lateral resolution than the lower frequencies, even with increasing depth. It was also found that the lateral resolution at 10 mm for 3 MHz sector probes was better than that of 3.5 MHz probes. The lack of limited 3.5 MHz transducers may have influenced this observation (Fig.8).

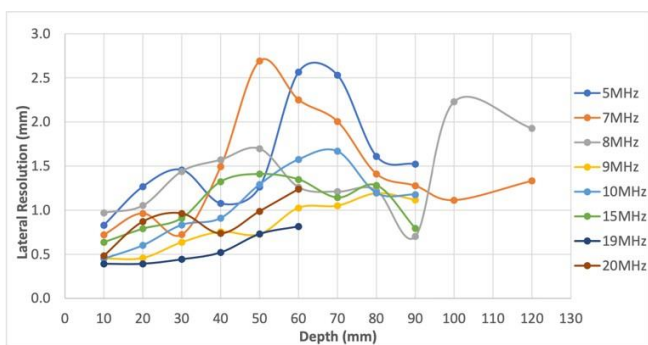


Fig. 6: Lateral resolution (mm) against depth (mm) for linear transducers with different frequencies

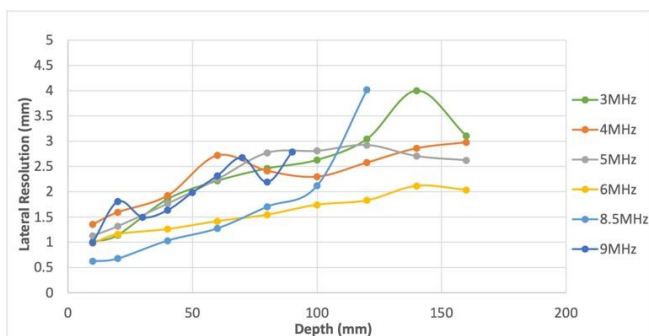


Fig. 7: Lateral resolution (mm) against depth (mm) for curvilinear transducers with different frequencies

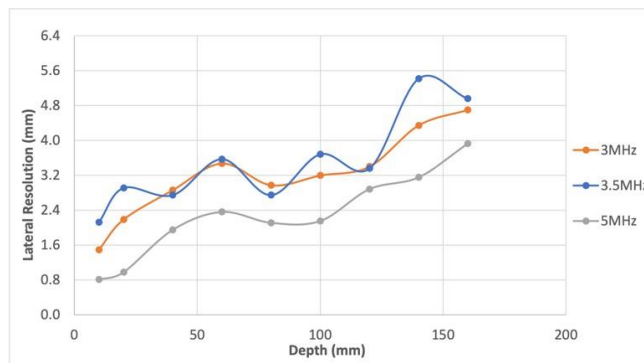


Fig. 8: Lateral resolution (mm) against depth (mm) for sector transducers with different frequencies

IV. DISCUSSION

This study evaluated and compared the axial and lateral spatial resolution of the linear, curvilinear, and sector array transducers. The effect of spatial resolution with depth was also investigated. This was done with the equipment previously, and conclusions were drawn from the scanners and transducers considered in this study. It is interesting to note that the results from previous literature are consistent with some key findings from this study. This is essential as it confirms and strengthens the reliability of the study's results.

Firstly, it was concluded that linear transducers provide better axial and lateral spatial resolution than curvilinear and sector array transducers. The axial resolution of linear transducers at 5 and 9 MHz did not exceed 0.64 and 0.52 mm, respectively, while the lateral resolution did not exceed 2.56 and 1.05 mm on average. On the other hand, the worse axial and lateral resolution was observed for curvilinear (C) and sector (S) probes, with a maximum axial resolution of 1.19 mm (C) and 1.77 mm (S) and a maximum lateral resolution of 2.71 mm for curvilinear and 3.92 mm for sector probes.

Linear transducers provide better axial and lateral spatial resolution due to their shape and design. Linear transducers theoretically have a narrow beam and provide a rectangular field of view, which allows them to produce a thin, highly focused beam that can be guided precisely to the area of interest in the patient. This concentrated beam improves axial resolution by minimizing the distance between the two scanned objects or structures, resulting in better distinction between them. In addition, the design of a linear transducer allows the beam to be focused in a specific direction, which helps to decrease the scattering of the ultrasound beam. As a result, the ultrasound image becomes more accurate and focused, providing better differentiation between adjacent

structures. Subsequently, better lateral resolution is achieved, thus agreeing with this study's first objective.

Secondly, the relationship between spatial resolution and depth was also examined. Theoretically, the axial resolution is determined by the SPL of the ultrasound waves. The SPL of an ultrasound wave is governed by the period of the electrical pulse used to generate the wave and not by the distance travelled. Therefore, SPL is independent of depth, so the axial resolution should remain constant at any depth. In this study, it was noted that the maximum deviation of the FWHM measurement of the axial resolution was less than 1 mm along the depth. The linear transducers experiencing less deviation than the curvilinear and sector transducers.

On the other hand, lateral resolution was found to deteriorate with increasing depth. Theoretically, the ultrasound beam initially converges, reaches the focal zone and then diverges as it penetrates deeper into the tissue. This causes the ultrasound beam to widen at the far field, making it more difficult to identify two adjacent structures. Thus, the lateral resolution is poorer with depth. This could also be observed visually from the acquired ultrasound image, where the first few nylon filaments are well resolved, while the others became increasingly blurred with depth. This may happen because the beam's intensity decreases due to partial waves being reflected and attenuated across the tissues. In this way, the second objective of this study was addressed.

Moreover, it was concluded that the axial and lateral spatial resolution improved at higher ultrasound frequencies. Theoretically, a higher frequency leads to a shorter wavelength and, thus, a shorter spatial pulse length. A shorter pulse length results in a better axial resolution. In addition, at higher frequencies, the beam width at the focus is narrower, resulting in better lateral resolution. Hence, the third and final objective was addressed. To determine if the current standards are still applicable or need to be revised, comparing the study's results with the existing standards is essential. As previously mentioned, there are still no corresponding FWHM standard values for axial resolution. However, the results were compared with the recommendations found in AAPM (Table 1). From the results obtained, the axial resolution for frequencies greater than 4 MHz for linear transducers exceeds an FWHM of 0.45 mm for most transducers. The highest value was obtained for the 8 MHz transducer. This was also observed for curvilinear and sector probes, where the largest FWHM was 1.82 and 1.77 mm for the 6- and 5- MHz transducers respectively. In contrast, for frequencies below 4 MHz, the FWHM values met the recommended AAPM standards. Thus, although some values were within the standards, most results differed widely. Note that the AAPM did not specify the depth at which the FWHM values correspond (for axial resolution), so this assessment is general and hence, it must be more accurate.

When comparing the lateral spatial resolution results with the AAPM standards, it was noted that the lateral resolution at frequencies below 3.5 MHz does not comply with the existing standards. The FWHM exceeded the recommended tolerance of 2 mm for curvilinear and sector transducers operating at 3 MHz, especially after 40 cm (for curvilinear transducers) and 15 cm (for sector transducers) depth. It is good to note that the AAPM does not indicate the FWHM values for lateral resolution for transducers with frequencies greater than 3.5 MHz having depths greater than 10 cm. Since spatial resolution was measured at depths greater than 10 cm, the comparison with the relevant standards (for lateral resolution) was very limited.

The following results imply that the current AAPM standards and recommendations need to be revised and improved accordingly. Both axial and lateral FWHM standards for spatial resolution should be increased, especially for those already mentioned. The medical physics profession needs to recognize these discrepancies and highlight that the current standards need strengthening. Technology constantly evolves, and ultrasound scanner manufacturers continually improve and upgrade their products to achieve optimal spatial resolution.

V. CONULUSSION

The main conclusions of the study were:

- a) Linear array transducers exhibited the best axial spatial resolution.
- b) Linear array transducers provided better lateral spatial resolution.
- c) Axial resolution remained constant with depth across all transducers.
- d) Lateral resolution deteriorated with depth for all transducers.
- e) Transducers with higher frequencies provided better axial and lateral spatial resolution.

Suggestions for further research are:

- a) Repetition of the study with a larger number of ultrasound scanners/transducers as well as using a broader frequency spectrum. This study considered QC images obtained from acceptance testing on all available ultrasound transducers. This can be extended by testing ultrasound scanners/transducers in all private clinics in Malta as well as in health centres.
- b) Replication of the study by comparing different protocols used by different manufacturers. This is a very interesting recommendation for the future because one can compare, for instance, a thyroid protocol with a breast protocol and assess the behaviour of frequency and/or spatial resolution.

- c) For a more comprehensive study, this study can be repeated by adjusting the focus to each nylon filament across the depth of the phantom. Since only the results of the acceptance tests were considered, the focus was set at a specific depth. Obtaining images with a focus at each depth can help determine the depth at which the spatial resolution improves or deteriorates.
- d) This study can be extended by examining how spatial resolution varies among different manufacturers. In this study, the spatial resolution for some ultrasound transducers varied depending on the manufacturer and model of the probe used. As technology is continually developing, manufacturers are striving to improve ultrasound scanners' spatial resolution through image processing techniques and reconstruction.

The research study's stated objectives were achieved and answered in depth. A quantitative measurement protocol and software analysis for evaluating the spatial resolution performance of ultrasound equipment is the way ahead for quality assurance programmes. Optimized spatial resolution leads to precise localization and identification of microstructures in the imaged region, which is critical for physicians to make an accurate diagnosis and ultimately locate the malignancy or any deformity. It could additionally reduce the need for unnecessary imaging procedures or invasive treatments, which can be expensive, time-consuming, and potentially harmful to the patient. Therefore, ultrasound images with high spatial resolution can improve and enhance patient treatment outcomes.

VI. REFERENCES

- [1] Ng, A., & Swanevelder, J. (2011). Resolution in ultrasound imaging. *Continuing Education in Anaesthesia Critical Care & Pain*, 11(5), 186–192. <https://doi.org/10.1093/bjaceaccp/mkr030>.
- [2] Hoskins, P. R., Martin, K., & Thrush, A. (2019). *Diagnostic Ultrasound: Physics and Equipment*. CRC Press/Taylor & Francis Group. ISBN 978-0-521-75710-2
- [3] Lomas, B. (2009). *SUMMARY OF KEY POINTS*. Crimson Business Ltd.
- [4] Goodsitt, M. M., Carson, P. L., Witt, S., Hykes, D. L., & Kofler, J. M. (1998). Real-time B-mode ultrasound quality control test procedures. report of AAPM Ultrasound Task Group No. 1. *Medical Physics*, 25(8), 1385–1406. <https://doi.org/10.1118/1.598404>.
- [5] Institute of Physics and Medicine in Engineering (IPEM). (2010). Report No 102 Quality Assurance of Ultrasound Imaging Systems. York: IPEM.
- [6] *Multi-purpose multi-tissue ultrasound Phantom MODEL 040GSE*. SUN NUCLEAR. (2022). Retrieved March 21, 2023, from <https://www.cirsinc.com/products/ultrasound/zerdine-hydrogel/multi-purpose-multi-tissue-ultrasound-phantom/>

Contacts of the corresponding author:

Author: Kyle Cilia
 Institute: University of Malta.
 City: Msida
 Country: Malta
 Email: kyle.cilia.19@um.edu.mt

BRAIN TEMPERATURE MEASUREMENT BY MAGNETIC RESONANCE SPECTROSCOPY THERMOMETRY USING REGRESSION ANALYSIS

A.N. Mumuni¹, M.M. Salifu², M.N. Abubakari¹

¹ Department of Medical Imaging, University for Development Studies, Tamale, Ghana

² Department of Medical Physics, University of Ghana, Accra, Ghana

Abstract— Information about core brain temperature is relevant for monitoring the physiological state of the body under both healthy and pathological conditions. Apart from standard clinical methods, various techniques have been proposed specifically for brain temperature measurement using magnetic resonance spectroscopy (MRS) thermometry. The commonest method is the calibration of the water frequency shift relative to the N-acetyl aspartate metabolite peak. This technique is based on temperature-dependent displacement of the water peak from its normal frequency position. Existing MRS thermometry methods are often associated with challenges of direct clinical utility, particularly where additional information about brain metabolism is required. This study deduced standard calibration equations using regression analysis for brain MRS thermometry. Clinically measured brain temperature (T_{brain}) using a temperature gun was used as the dependent variable and the water frequency shift from the NAA, creatine and choline peaks were each used as independent variables in separate regression analyses to yield equations of the form: Brain temperature (T_{brain}) = $k_1(\Delta H_2O - \delta_{\text{met}}) + k_2$, where k_1 is the gradient of the regression fit, k_2 is the intercept of the regression fit on the T_{brain} axis, ΔH_2O is the new water frequency after temperature-dependent shift, and δ_{met} is the normal frequency of the particular reference peak on the ppm axis (2.01, 3.03, and 3.20 ppm for NAA, creatine, and choline, respectively). The equations were validated in a separate group of healthy subjects and were found to provide accurate temperature estimates, with reproducibility better than 2.0 %. Future studies are required to assess the utility of the equations in study participants with a wide range of physiological characteristics.

Keywords— brain, magnetic resonance spectroscopy, temperature, thermometry, regression

I. INTRODUCTION

Proton magnetic resonance spectroscopy (¹H-MRS) is a nuclear magnetic resonance (NMR) technique that is capable of measuring brain metabolism noninvasively and *in vivo*. Normal brain function or pathology can be inferred from the biochemical profile obtained from a typical ¹H-MRS data [1,2]. In addition to the biochemical information, subtle changes in core brain temperature associated with physiological activities in the body can also be probed by ¹H-MRS [3]. Temperature variation causes a slight displacement of the water peak from its normal frequency position in the ¹H-MR spectrum. The N-acetyl aspartate (NAA) peak,

unaffected by the temperature variation, is mostly used as the reference peak relative to which the water peak displacement is measured, and this frequency difference can be converted to temperature estimate [4,5]. This procedure is often called MRS thermometry.

The balance between heat produced by cerebral metabolism and heat dissipated by cerebral blood flow determines the temperature of the brain in healthy individuals at rest [6-8]. The need for early biomarkers of brain swelling is crucial because decompressive surgery performed before clinical deterioration can improve treatment outcomes [9]. Pathologies are associated with subtle biochemical changes in the body which often do not show in anatomical imaging, but can be probed by ¹H-MRS. In pathologies where core body temperature is elevated, the MRS data may require some adjustments or corrections to be optimized before it can be used to estimate absolute metabolite concentrations. The ¹H-MRS method allows for a reasonably precise measurement of brain temperature noninvasively and *in vivo* [10] by comparing the chemical changes of water protons to an abundant internal reference, such as NAA [4,5,11], creatine [12], or choline [3]. Indirect brain temperature measurements, such as MRS thermometry, often require some sort of calibration techniques to estimate temperature [13]. This therefore makes them unsuitable for routine clinical application due to associated patient compliance issues and inaccuracies in the estimates.

This paper provides a procedure for the establishment of a standard procedure to deduce calibration equations that can be used for brain temperature estimation using MRS thermometry. The technique is applicable to clinical ¹H-MRS acquisition, as long as the water peak frequency can be obtained from the acquired data.

II. MATERIALS AND METHODS

A. STUDY PARTICIPANTS

Following the approval of the study protocol by the University of Ghana Ethics Committee for Basic and Applied Sciences (ECBAS) and the University of Ghana Medical Centre (UGMC) Institutional Review Board, seven (7) healthy volunteers (5 males/2 females, aged 22-43 years) participated in the study. No study participant had any

magnetic resonance imaging (MRI) contraindication or neurological condition.

B. MRI/MRS ACQUISITION

Data was acquired on a 1.5 T Philips Ingenia MRI/MRS System, equipped with a quadrature radiofrequency head coil.

Prior to going into the MRI bore, brain temperature of each study participant was taken at their forehead using an infrared (IR) temperature gun, and recorded as T_{IR} .

Structural MRI of the brain was acquired using the T_1 -weighted 3-dimensional turbo field echo sequence. Using the acquired MRI, voxel sizes were varied to fit the head size of each participant, typically ensuring a longer anterior-posterior dimension and positioning above the corpus callosum (Figure 1). Outer volume shimming for B_0 inhomogeneity was performed using both linear and second-order shims. 1H -MRS acquisition was performed using the standard Point RESolved Spectroscopy (PRESS) pulse sequence ($TE/TR = 144$ ms/2000 ms), which yielded the dominant spectral peaks of NAA, creatine, choline and water (not shown in Figure 2).



Figure 1: Voxel position in the brain MRI of a participant

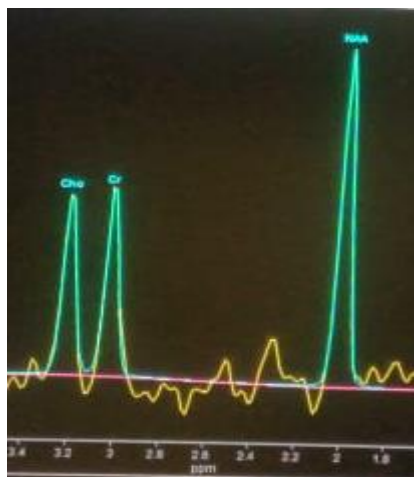


Figure 2: Spectral peaks of NAA, creatine, and choline at 2.01 ppm, 3.03 ppm and 3.20 ppm respectively

C. TEMPERATURE EQUATION

The raw spectral data were Fourier transformed to the frequency domain, and corrected for baseline and phase distortions in the jMRUI software (version 6.0). The NAA, creatine, and choline resonant frequencies visually were inspected to ensure that they were at their expected positions. Each 1H -MRS data was zoomed on the water peak (Figure 3) to observe the frequency variations in its position which were then recorded from the jMRUI analysis. Using each one of the spectral peak frequencies of NAA, creatine and choline (denoted by δ_{met}) as the reference, the frequency shift of the water peak from each reference peak was calculated as $(\Delta H_2O - \delta_{met})$.

A regression fit to the scatter plot of T_{IR} versus $(\Delta H_2O - \delta_{met})$ yielded an equation of the form:

$$T_{brain} = T_{IR} = k_1(\Delta H_2O - \delta_{met}) + k_2 \quad (1)$$

where k_1 is the gradient of the regression fit, k_2 is the intercept of the regression fit on the T_{brain} or T_{IR} axis, ΔH_2O is the new water frequency after temperature-dependent shift on the ppm axis of the frequency-domain spectra, and δ_{met} is the normal frequency of the particular reference peak on the ppm axis.

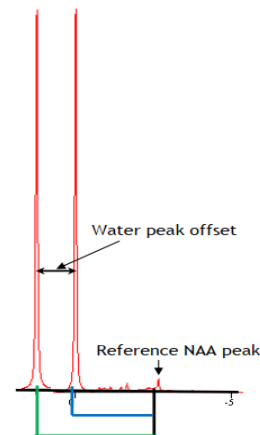


Figure 3: Temperature-dependent water frequency shift from its normal position, away from the reference NAA metabolite spectral peak

D. STATISTICAL ANALYSIS

The calibration equations were validated in a separate group of healthy volunteers whose temperature measurements were previously taken using the infrared temperature gun. Reproducibility of the measured MRS thermometric brain temperature using each equation was assessed by the coefficient of variation (CoV) for repeated measures, calculated as:

$$CoV = (standard\ deviation/mean) \times 100\% \quad (2)$$

The thermometer and MRS thermometry temperature measurements were compared for differences using the paired t-test, assuming normality of the data.

III. RESULTS

Tables 1-3 show the infrared temperature gun measurements (T_{IR}) and their corresponding calculated frequency displacements ($\Delta H_2O - \delta_{met}$) of the water peak (ΔH_2O) from the respective reference metabolite spectral peaks (δ_{met}). T_{IR} was used as the dependent variable while ($\Delta H_2O - \delta_{met}$) was used as the independent variable in the regression analysis.

Table 1 Water frequency shift from the NAA reference peak

T_{IR} (°C)	ΔH_2O (ppm)	δ_{NAA} (ppm)	$\Delta H_2O - \delta_{NAA}$ (ppm)
36.2	4.65	2.01	2.64
35.7	4.32	2.01	2.31
36.0	4.65	2.01	2.64
36.1	4.63	2.01	2.62
36.2	4.66	2.01	2.65
36.0	4.58	2.01	2.57
35.8	4.40	2.01	2.39

Table 2 Water frequency shift from the creatine reference peak

T_{IR} (°C)	ΔH_2O (ppm)	δ_{Cre} (ppm)	$\Delta H_2O - \delta_{Cre}$ (ppm)
36.2	4.65	3.03	1.62
35.7	4.32	3.03	1.29
36.0	4.65	3.03	1.62
36.1	4.63	3.03	1.60
36.2	4.66	3.03	1.63
36.0	4.55	3.03	1.52
35.8	4.40	3.03	1.37

Table 3 Water frequency shift from the choline reference peak

T_{IR} (°C)	ΔH_2O (ppm)	δ_{Cho} (ppm)	$\Delta H_2O - \delta_{Cho}$ (ppm)
36.2	4.65	3.2	1.45
35.7	4.32	3.2	1.12
36.0	4.65	3.2	1.45
36.1	4.63	3.2	1.43
36.2	4.66	3.2	1.46
36.0	4.55	3.2	1.35
35.8	4.40	3.2	1.20

Table 4 shows the deduced regression equations calibrated for *in vivo* MRS thermometry.

Table 4 Calibrated regression equations for brain MRS thermometry

Reference peak	Regression equation	R^2
NAA	$T_{brain} = 1.3280(\Delta H_2O - 2.01) + 32.626$	0.8909
Cr	$T_{brain} = 1.3275(\Delta H_2O - 3.03) + 33.987$	0.8843
Cho	$T_{brain} = 1.3275(\Delta H_2O - 3.20) + 34.213$	0.8843

The equations were validated using single-voxel 1H -MRS data previously acquired from the frontal brain region of six healthy volunteers. This data was not included in the regression analysis, but was strictly used for the validation of the calibration equations. The averages (\pm standard errors) of the estimated brain temperatures using the three reference metabolite peaks are shown in Figure 4.

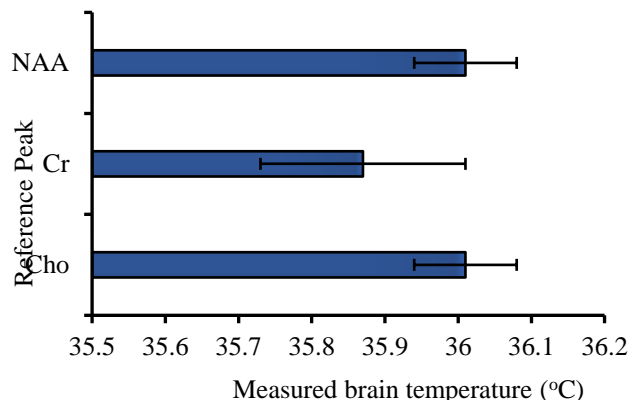


Fig 4 Average brain temperature estimates from MRS thermometry using the derived calibration equations

IV. DISCUSSION

The observed water frequency shifts have been reported to be independent of magnetic susceptibility [14,15]. Even though the NAA peak has been the most preferred reference choice due to its prominence in the MR spectrum and general utility in quantitative 1H -MRS studies, the methods of calibration presented here could be applicable to the creatine and choline peaks as well. The deduced temperature equations are valid for temperature prediction interval of between 35.5 °C and 37.5 °C. Therefore, future *in vivo* brain MRS thermometry studies could directly substitute the measured water frequency shift value into any of the respective calibration regression equations (Table 4) to estimate brain temperature with over 80% accuracy.

The calibration equations were validated using previously acquired clinical 1H -MRS data with accompanying brain temperature measurements. There were no significant differences between the 1H -MRS thermometric estimates from each of the derived equations (Table 4) and the previous clinical thermometer temperature measurements by paired t-test ($p > 0.05$). It was noted that the NAA and choline derived equations yielded slightly higher brain temperature values than the creatine derived equation (Figure 4). The reproducibility of the measurements across the validation group, as measured by the CoV, was better than 2.0 % for all the reference peaks.

MRS thermometry studies generally use the NAA peak as a reference, and have used phantoms [16], pH controlled aqueous solutions [3] or MR spectroscopy imaging methods [12] in brain temperature measurements. These methods are largely challenging for direct clinical applications due to the multiple steps and assumptions involved in the brain temperature measurement process. One study [3] used all the three reference peaks as used in this study, and then estimated brain temperature from the average of the measured temperatures from the three reference peak equations. Others have also implemented similar brain temperature

measurement techniques with the NAA reference peak in studies of brain activation during visual stimulation [4,11].

Our proposed method is both straightforward and clinically applicable without patient compliance issues, and yet provides accurate brain temperature estimates as observed in our validation estimates.

Our study and those reported in the literature [3-5,11,12,16] have been consistent in the observation of a linear relationship between the water frequency shift and brain temperature. According to Table 4, for every frequency shift in the water peak away from any of the reference peaks (in ppm), the measured brain temperature will show an increase of about 1.33 °C. In addition, in the absence of a temperature-associated frequency shift in the water peak, the equations predict a minimum brain temperature within the range of about 33-34 °C (Table 4). Therefore, our finding of a positive association between the water peak frequency shift and measured temperature is consistent with the findings reported previously. The range of temperatures (35.5-37.5 °C) used to derive the calibration equations are well within the normal physiological range of human temperature.

It is expected that in pathologies associated with elevated core body temperature, the water peak should drift significantly from its expected frequency position than the observed shifts reported here. This should then scale well with the expected temperature rise in the study subjects. However, such a group of subjects were not included in this study to verify this. Further validation studies of the calibration equations under different study participant conditions (both normal and pathological) are therefore needed to assess their accuracy, reproducibility and wider clinical applicability.

The accuracy of the regression fits and predictions can be enhanced ($R^2 > 0.89$) by a bigger sample size of study participants than used in the current study. The procedure for the establishment and validation of the regression equations should however be reproducible among different studies.

V. CONCLUSIONS

¹H-MRS thermometry technique tailored for clinical implementation to measure both brain metabolism and temperature is presented in this paper. Temperature gun measured brain temperature was used to calibrate cerebral water temperature-dependent frequency shift into a temperature measurement through regression analysis. The deduced models were validated and have been found to be accurate for brain temperature measurement within the normal human brain physiological temperature range.

ACKNOWLEDGMENTS

We wish to acknowledge Mr. George Nunoo of the University of Ghana Medical Centre, Accra, Ghana, for his assistance with the MRS data collection. The dedication of all the study participants is very much appreciated.

REFERENCES

1. Mumuni AN, Krishnadas R, Cavanagh J (2023). Peripheral inflammation is associated with alterations in brain biochemistry and mood: evidence from in vivo proton magnetic resonance spectroscopy study. *Pure and Applied Chemistry* 95(3): 289-300.
2. Hennig J, Speck O, Deuschl G, Feifel E (1994). Detection of brain activation using oxygenation sensitive functional spectroscopy. *Magnetic resonance in medicine* 31(1): 85-90.
3. Covaciu L, Rubertsson S, Ortiz-Nieto F, Ahlström H, Weis J (2010). Human brain MR spectroscopy thermometry using metabolite aqueous-solution calibrations. *Journal of Magnetic Resonance Imaging: An Official Journal of the International Society for Magnetic Resonance in Medicine* 31(4): 807-814.
4. Rango M, Bonifati C, Bresolin N (2015). Post-activation brain warming: a 1-H MRS thermometry study. *PLoS One* 10(5): e0127314.
5. Cady EB, D'Souza PC, Penrice J, Lorek A (1995). The estimation of local brain temperature by in vivo 1H magnetic resonance spectroscopy. *Magnetic resonance in medicine* 33(6): 862-867.
6. Ishigaki D, Ogasawara K, Yoshioka Y et al. (2009). Brain temperature measured using proton MR spectroscopy detects cerebral hemodynamic impairment in patients with unilateral chronic major cerebral artery steno-occlusive disease: comparison with positron emission tomography. *Stroke* 40(9): 3012-3016.
7. Nybo L, Secher NH, Nielsen B (2002). Inadequate heat release from the human brain during prolonged exercise with hyperthermia. *The Journal of physiology* 545(2): 697-704.
8. Sukstanskii AL, Yablonskiy DA (2006). Theoretical model of temperature regulation in the brain during changes in functional activity. *Proceedings of the National Academy of Sciences* 103(32): 12144-12149.
9. Schwab S, Steiner T, Aschoff A, Schwarz S, Steiner HH, Jansen O, Hacke W (1998). Early hemicraniectomy in patients with complete middle cerebral artery infarction. *Stroke* 29(9): 1888-1893.
10. Vescovo E, Levick A, Childs C, Machin G, Zhao S, Williams SR (2013). High-precision calibration of MRS thermometry using validated temperature standards: effects of ionic strength and protein content on the calibration. *NMR in Biomedicine* 26(2): 213-223.
11. Katz-Brull R, Alsop DC, Marquis RP, Lenkinski RE (2006). Limits on activation-induced temperature and metabolic changes in the human primary visual cortex. *Magnetic Resonance in Medicine: An Official Journal of the International Society for Magnetic Resonance in Medicine* 56(2): 348-355.
12. Sharma A A, Nenert R, Mueller C, Maudsley AA, Younger JW, Szaflarski JP (2020). Repeatability and reproducibility of in-vivo brain temperature measurements. *Frontiers in human neuroscience* 14: 598435.
13. Verius M, Frank F, Gizewski E, Broessner G (2019). Magnetic resonance spectroscopy thermometry at 3 tesla: importance of calibration measurements. *Therapeutic Hypothermia and Temperature Management* 9(2): 146-155.
14. Hashimoto T, Tayaina M, Miyazaki M et al. (1995). Developmental brain changes investigated with proton magnetic resonance spectroscopy. *Developmental Medicine & Child Neurology* 37(5): 398-405.

15. Poorter JD (1995). Noninvasive MRI thermometry with the proton resonance frequency method: study of susceptibility effects. *Magnetic resonance in medicine* 34(3): 359-367.
16. Corbett RJ, Lipton AR, Tollefsbol G, Kim B (1995). Validation of a noninvasive method to measure brain temperature in vivo using ¹H NMR spectroscopy. *Journal of neurochemistry* 64(3): 1224-1230.

Contacts of the corresponding author:

Author: Abdul Nashirudeen Mumuni
Institute: Medical Imaging, SAHS-UDS
Street: Dungu-Tamale Campus
City: Tamale
Country: Ghana
Email: mnashiru@uds.edu.gh

PROPOSAL FOR ANNUAL QA ASSESSMENT OF SAFETY AND CONSISTENCY OF OARS DOSES IN TREATMENT OF CANCER BY BRACHYTHERAPY

P.K. Ndonge¹, S.N.A. Tagoe²

¹ The Nairobi Hospital, Cancer Treatment Center, Nairobi, Kenya.

² University of Ghana, School of Biomedical & Allied Sciences, Accra, Ghana.

Abstract

The aim of the study was to assess the safety and consistency of organs at risk (OARs) doses received by the rectum, bladder and urethra during cervical and prostate cancer treatments by brachytherapy and thereafter propose the procedure for annual QA assessment of all radiotherapy treatments in an institution. The cervical cancer patients considered in the study received both EBRT and brachytherapy treatment in 2017 and were assessed for their bladder and rectal OARs doses received during the treatment. Only prostate cancer patients who received I-125 permanent seed implants brachytherapy doses alone were assessed for their rectal and urethra doses. The same study was again repeated in 2022 for consistency comparison with the 2017 results. The combined OARs doses for cervical cancer treatment by both EBRT and brachytherapy were below the recommended maximum doses for the respective OARs. Rectum and urethra doses in prostate brachytherapy treatment indicated doses below the target prostate dose, D90%, and thus received safe doses within acceptable limits. A similar safety assessment repeated in 2022 after five years did not reflect significant difference from those for 2017, a confirmation of consistency in the treatment practice at the hospital. The study results revealed that for all the cervical and prostate cancer brachytherapy treatments considered in 2017 and 2022, the OARs doses were below the recommended maximum dose limits for the respective OARs, and thus safe. There was no significant difference in the safety results realized in the repeat study after five years, a confirmation that the brachytherapy treatment practice at the institution was consistent. The safety and consistency assessment demonstrated in the study was thus proposed as an annual QA procedure in brachytherapy treatment of cancer and can be extended to cover all radiotherapy treatment modalities in an institution.

Keywords

Brachytherapy, Organs at risk, Safety, consistency, Cancer

I. INTRODUCTION

Brachytherapy is applicable for the treatment of tumors where applicators and radioactive sources can be placed within a body cavity (intra-cavitary, e.g., the uterine canal or vagina), into a lumen (trans-luminal, e.g. bronchus or esophagus), into an artery (intravascular e.g. Coronary or peripheral arteries, prevention of restenosis) and also where the tumor is accessible to needle or catheter sources being

placed within or directly into tissue, interstitial, intra-cavitary or surface application. A major advantage of this mode of treatment, as opposed to EBRT, is because a high radiation dose can be delivered locally to the tumor with rapid dose fall-off in the surrounding normal tissues.

Currently, artificially produced radionuclides such as Cs-137, Ir-192, Au-198, I-125, Pd-103 and Co-60 are used. Radionuclide sources for brachytherapy are now available with many radionuclides and in various shapes and sizes. Different sources have different applications depending on their emission type, radiation energy and how they are constructed. Below is a table of the most common radionuclides applicable in brachytherapy treatment.

Treatment of cervical cancer by brachytherapy can be done by application of high dose-rate (HDR) treatment equipment which use Iridium-192 sources, and of low, Cobalt-60 sources. Low dose-rate (LDR) equipment that use Caesium-137 source or a similar applicable LDR radioisotope are also applicable, although the HDR equipment are the most common now and currently recommendable due to their advantages of use. [1].

Brachytherapy treatment of prostate cancer can use LDR radioactive permanent seed implants for the treatment. The current commonly used LDR radioisotope seeds in this case are I-125 and Pd-103 isotopes; which are also recommended by the American Brachytherapy Society, since they have demonstrated excellent long-term outcomes [2].

HDR treatments normally take a few minutes, depending on the activity of the source at the time of treatment; while those for LDR can take several hours. HDR brachytherapy for cervical cancer is currently more preferable to LDR. This part of the study was done at a selected hospital in Kenya where there is a Varian GammaMedplus HDR system. The system uses an Iridium-192 source, with a half-life of 73.831 days. The source would be used for three months (90 days) and then changed for a new one with an initial activity of about 10Ci.

The cervical cancer treatment itself by HDR brachytherapy would take a few minutes, but the whole process from applicator insertion, CT imaging, treatment planning, treatment delivery, and applicator removal may take about two hours per patient.

The external beam radiation therapy (EBRT) treatment planning system was a Varian Eclipse and compatible to CT or MRI-based images for treatment planning. The applicators are platinum made Ring and Tandem or Tandem and ovoids, with variety of Tandem lengths, example 2, 4, and 6cm. The ovoids can be small or medium size. Another type of applicator is in the form of a Cylinder, of different diameters (1.4cm, 2.1cm, 2.3cm, 2.6cm, 3.0cm and 3.5cm).

The Clinical Oncologist performing a brachytherapy treatment would physically examine the patient first. Then choose a type of applicator for a particular patient depending on the patient's body anatomy and extent of the disease. The applicators would then be inserted after simple premedication of the patient. CT scan of the pelvic area of the patient would then be done for treatment planning purpose. Treatment planning Guidelines are available for planning cervical cancer treatment by different types of applicators.

The dose prescription protocol for the delivery of the brachytherapy dose was a boost dose of 16Gy delivered in two fractions of 8Gy a week apart.

As opposed to EBRT where the treatment dose is delivered externally and can be verified before entering into the patient, brachytherapy treatments are normally executed internally and verification using a diode for EBRT purpose may not be possible.

The approach for verification of cervical or prostate cancer brachytherapy treatment was attained by use of the treatment plan dose volume histogram (DVH). European Society for Therapeutic Radiology and Oncology (GEC Estro), in 2006, gave the recommended dose calculations based on three-dimensional image of the patient obtained from dose volume histogram (DVH) and the volume histogram connecting organ with the radiation dose received [3]. So, the DVH has now become a common tool to express the dose that is delivered to targets and OARs. It contains information about the doses delivered to partial volumes (either absolute or relative) of targets or OARs. So, the dose to OARs for each patient considered for the study was acquired from the patient's treatment plans and the data for the cervical cancer brachytherapy treatments compiled and presented in graphical form.

Radiation can be harmful to health if not used properly and all radiation administration to humans for treatment purposes need to be done by qualified professionals and the dose delivery verified for safety purpose.

Our study was in a selected hospital and assessed safety and consistency in OARs doses realized during cervical and prostate cancer brachytherapy treatment in comparison to the delivered tumor dose and the maximum recommended dose limits to the OARs. If the results are within the recommended values, the procedure would be recommended as an annual QA in radiotherapy treatments.

II. MATERIALS AND METHODS

A. Cervical cancer brachytherapy data

The study involved a total of 41 cervical cancer patients who received brachytherapy treatment at the hospital in both 2017 and 2022. The treatment applicators used for the patients were either a 'Tandem and Ovoids', 'Ring and Tandem' or a 'Vaginal Cylinder'. The applicator selection for a particular patient would depend on the clinical condition of the patient.

After insertion of the applicators in the brachytherapy theatre, the patient would then have CT scans of the pelvis for the purpose of treatment planning on the TPS. During treatment planning, the doses to the target volume, the rectum or bladder would be altered appropriately so that doses would not exceeded the maximum limits on the protocols. The final treatment plan would then be exported to the HDR Treatment system for execution of the treatment.

The doses received by the bladder and rectum during the cervical cancer treatment were taken from the treatment planning TPS 'dose statistics' and also through the TPS protocols for the OARs (D20, Gy); and the results presented graphically. Another graph plotted involved the brachytherapy OARs data with the EBRT OARs doses received previously before the brachytherapy boost dose.

The average dose for the bladder and rectum of all the 41 patients assessed were also determined and the results presented on a table.

B. Combined EBRT and brachytherapy treatment of cervical cancer

Bladder and rectum were targeted as the main organs at risk in cervical cancer treatment in both EBRT and brachytherapy.

We investigated the total bladder and rectum doses for the 41 cervical cancer patients treated at the hospital by both EBRT linac photon energies (6 MV and 15 MV) and Ir-192 HDR brachytherapy. Recommended EBRT 3D-CRT prescription total tumor dose is 45-50 Gy to be delivered in 25 daily fractions while brachytherapy need to be delivered as 6-8 Gy fraction dose weekly, 2-3 times depending on the patient's clinical condition. At the hospital, EBRT doses were delivered as 50 Gy in 25 fractions of 2 Gy daily while the protocol used for the delivery of the brachytherapy dose was a total boost dose of 16 Gy delivered in two fractions of 8 Gy a week apart.

C. Prostate brachytherapy treatment and data

Forty-two prostate cancer patients treated by LDR brachytherapy using I-125 permanent seed implants were also assessed. The treatment applies trans-rectal ultrasound-guided permanent prostate brachytherapy technique which is

an outpatient procedure associated with a rapid recovery and return to normal activity.

The Ultrasound equipment is a ‘bk Medical flexFocus 400’ model, used together with a C-Arm X-Ray Image Intensifier. A Treatment Planning System (TPS) is also available and linked to both the Ultrasound Guidance and the Image Intensifier.

The procedure is acknowledged by many brachytherapy institutions, including the National Cancer Institute [4], American Cancer Society [5], American Urological Association [6] and many others.

In Kenya, about 70% of cancer patients are diagnosed at late stages due to a combination of many diverse reasons.

Thus, majority of our prostate cancer patients are of ‘High-Risk’ classification and thus recommended to receive combined treatment with EBRT ‘boost dose’ in 6-12 weeks after receiving the LDR brachytherapy treatment [7], [8].

In our study, we only assessed the OARS doses resulting from the brachytherapy treatment by LDR I-125 permanent seed implants only.

III. RESULTS AND DISCUSSION

A. OARs doses in cervical cancer brachytherapy treatment

Table 1 below shows the protocols implemented on the Varian HDR brachytherapy TPS for treatment planning control of the doses to OARs.

Table 1. Varian TPS Protocols used for control of doses to the major OAR during HDR brachytherapy treatment planning of cervical cancer.

Results of the OARs doses (two fractions) realized by the 41 cervical cancer patients during the brachytherapy treatment in 2017 were presented in Figure 1A and 1B below. The maximum dose limit of 8 and 10 Gy for the D20 rectum and bladder OARs two fraction treatments were also plotted with 16 Gy for the two-fraction total tumor dose.

Structure	Index		Target Value	Actual Value
Bladder	D0.10cc (% of dose)	Is less than	125	
Bladder	D2.0CC (% of dose)	is less than	75	
Bladder	D20.0 (Gy)	is less than	5	
Rectum	D0.10cc (% of dose)	is less than	125	
Rectum	D2.0cc (% of dose)	is less than	75	
Rectum	D20.0 (Gy)	is less than	4	
Rectum	D1.0cc (% of dose)	is less than	95	
Rectum	D1.0cc (% of dose)	is less than	95	

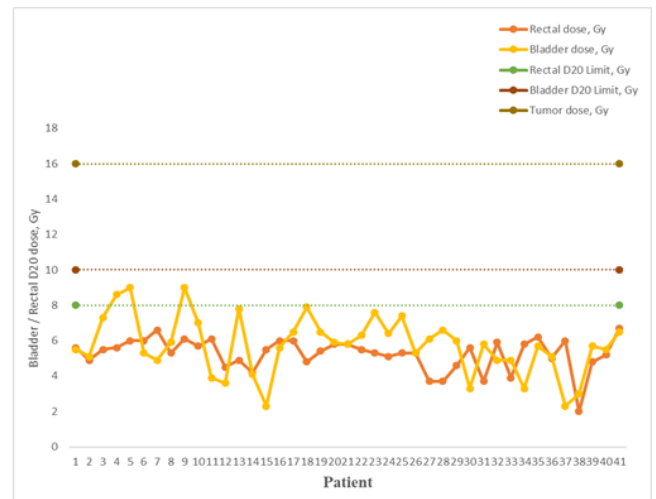


Figure 1A. Graph of D20 (Gy) bladder, rectum and total tumor dose for the 41 cervical cancer patients treated at the hospital in two fractions by I-192 HDR brachytherapy in 2017.

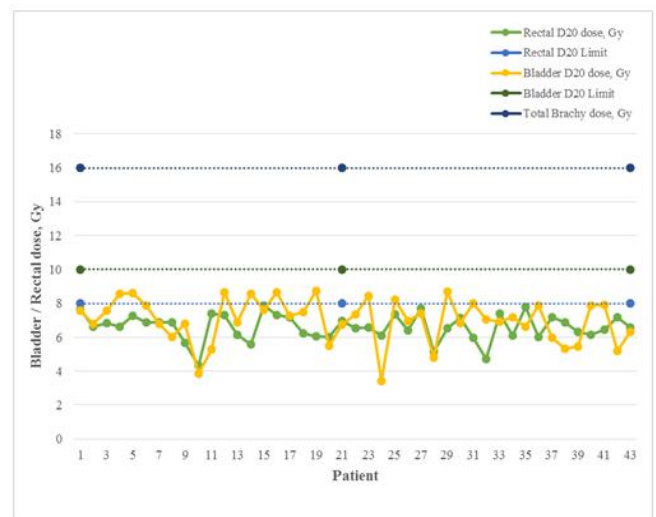


Figure 1B. Graph of D20 (Gy) bladder, rectum and total tumor dose for 43 cervical cancer patients treated (two fractions) by I-192 HDR brachytherapy in 2022.

For both assessments done in 2017 and 2022 for the brachytherapy treatment of cervical cancer, a mean dose of the bladder and rectum doses received were determined and a summary of the results presented on Table 2, below. All the treatments in the institution were based on 3-dimensional (3D) CT imaging and also 3D treatment planning and treatment.

The mean dose to both OARs for the 2017 and 2022 assessments were below the recommended maximum limits for the bladder (5 Gy) and rectum ((4 Gy) in a single fraction treatment. Also in accordance with the American

Brachytherapy Society (ABS) recommendation, [2], the dose to the bladder and rectum must be below 80% of the prescribed dose to the cervix. For a prescribed dose of 8 Gy per fraction to the cervix in our case, the bladder and rectum must not receive doses above 6.4 Gy. This means that our brachytherapy cervical cancer treatments are not only not harmful to the patients but also that the treatment practice has been consistent. These results were also in agreement with other related published results, [9].

Table 2. Two fraction mean doses to OARs in cervical cancer brachytherapy treatment in both 2017 and 2022 assessments.

OAR	Mean Dose, Gy, (2017)	Mean D20 Dose, Gy, (2022)	Max Dose Limit, Gy
Bladder	5.8	7.0	10
Rectum	5.2	6.6	8

B. Demonstration of combined OARs doses in cervical cancer treatment

Late-stage treatment of cervical cancer by radiotherapy at the hospital is normally a combination of EBRT and brachytherapy. First, an EBRT dose of 50 Gy in 25 fractions is administered, followed by a boost dose of brachytherapy, given in two fractions of 8 Gy, a week apart.

Since the two brachytherapy fraction doses applied during the treatment of cervical cancer by both EBRT (2 Gy) and brachytherapy (8 Gy) are different from the EBRT dose, the brachytherapy dose needs to be converted to match that of EBRT. The brachytherapy fraction dose of 8 Gy will need to be converted to equivalent dose to that EBRT fraction dose of 2Gy. The conversion will utilize α/β ratio which is dependent on the type of tumor. For cervical cancer, a ratio of $\alpha/\beta = 10$, [10], [11], [12], has been used and the following equations applied to determine the brachytherapy fraction dose.

$$BE D = [nxd(1 + d/(\alpha/\beta))] \dots\dots\dots(1)$$

Where n = number of treatment fractions,

d = dose per fraction, in Gy,

α/β = dose at which the linear and quadratic components of cell kill are equal.

Also, α is the linear dose damage response, and β the quadratic dose response in tissue.

BED is the biologically effective dose and is a measure of the true biological dose delivered by a particular combination of dose per fraction and total dose to a particular tissue, in this case, the cervix.

The biologically equivalent dose (EQD₂) is the dose delivered in 2Gy fractions that biologically equivalent to a total dose.

$$So, EQD_2 = BED / [1 + 2/(\alpha/\beta)] \dots\dots\dots(2)$$

So, the cervical cancer brachytherapy dose to be added to the 50 Gy dose delivered by EBRT will be 12Gy per fraction as determined from Equation 2. The total EBRT and brachytherapy (two fractions) treatment dose in our case was 74 Gy.

Below (Figure 2) is the graphical presentation of the OARs dose data for the 41 patient treatments by EBRT. The maximum limit for the rectum, which is more sensitive to radiation than the bladder, is also plotted at 50Gy.

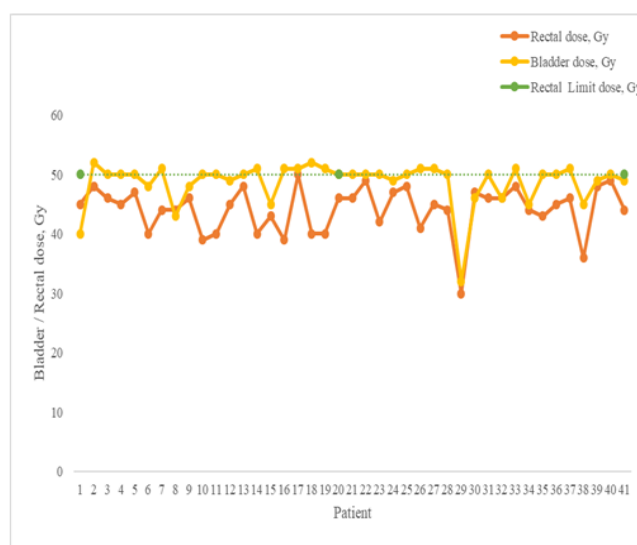


Figure 2. EBRT dose to the bladder, rectum and maximum rectal dose limit for the 41 cervical cancer patients treated at the hospital in 2017.

The maximum limit dose to OARs in both EBRT and brachytherapy treatments are normally controlled by the quality assurance (QA) process during the treatment planning stage. From the data of the 41 cervical cancer patients treated then on Figure 3 below, the mean total dose to OARs were below the maximum limit dose of 62 Gy for the rectum and 65 Gy for the bladder. Also reflected on the graph is the total tumor dose received for the combined EBRT and two fractions of brachytherapy treatment of 74 Gy. The recommended total dose for both EBRT and brachytherapy in high-risk cervical cancer treatment is 80-90 Gy, received in 50 Gy of EBRT plus three fractions of equivalent brachytherapy total dose of 36 Gy. For 50 Gy of EBRT combined with two fractions of HDR brachytherapy treatment, a total of 70-80 Gy tumor dose was recommended.

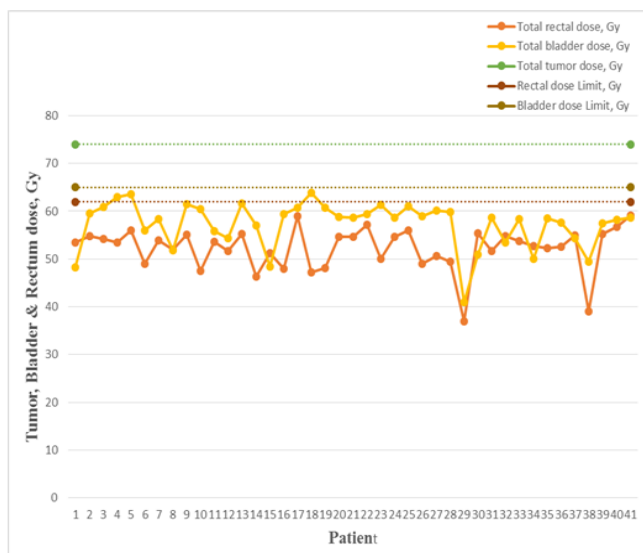


Figure 3. Combined EBRT and brachytherapy doses to the target tumor and OARs (bladder and rectum) for the 41 cervical cancer patients treated in 2017. The maximum dose limits realized in both treatments to the OARs are also plotted.

C. OARs doses in prostate cancer brachytherapy treatment

Brachytherapy DVH has now become a common tool to express the dose that is delivered to targets and OARs and contains information about the doses delivered to partial volumes of targets or OARs. So, the dose to OARs for each patient considered for the study was acquired from the patient’s treatment plan.

Analysis of rectal and urethra (OARs) doses from the plans DVH data of the 42 prostate cancer patients treated by I-125 permanent seed brachytherapy implants in 2017-2018 was done.

With a prescribed dose of 110 Gy, the protocol used for the LDR brachytherapy treatment with I-125 permanent seed implants recommends that the target dose to the prostate should be above 140 Gy [2]. The mean/average ‘Day zero’ dose, D90%, (dose that covers 90% of the prostate volume) for the 42 patients treated was 139 Gy. D90, also described as the dose that covers 90% volume of the CTV and would be larger than the prescription dose, $D90 > 100\%$ of prescription dose [13], [14]. The mean prostate dose realized in our study was 139 Gy and was within the acceptable $\pm 5\%$ uncertainty for radiotherapy dose delivery of 140 Gy. The mean urethra and mean rectal dose were 89.9 Gy and 56.3 Gy respectively. The urethra appears to be more resistant to radiation, compared to the rectum, since no significant radiation-related issues have been reported for the urethra. Also, being central to the prostate gland, restricting the urethra to low OAR dose would prevent the targeted prostate volume from getting the required tumor dose. The maximum dose received by the two major OARs, rectum and urethra,

during prostate brachytherapy treatment with I-125 is recommended to be below the target prostate tumor dose (140 Gy). So the mean dose received by the rectum and urethra in our case, were within the acceptable limits.

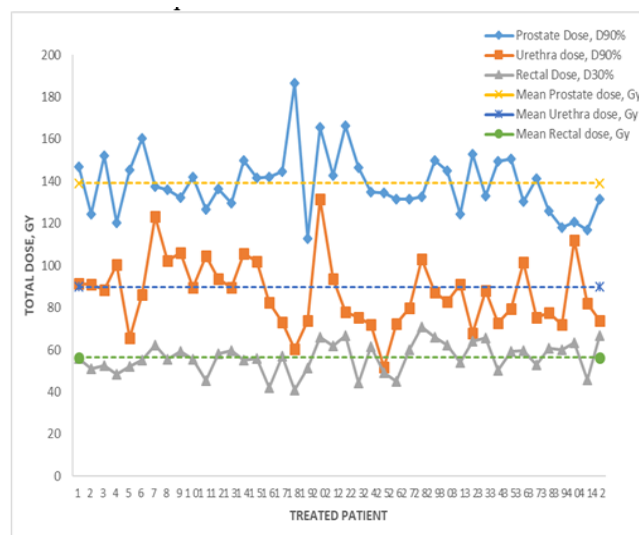


Figure 4A. Target and OARs doses for 42 prostate cancer patients treated at the hospital by brachytherapy using I-125 permanent seed implants in 2017-2018.

A ‘learning curve’ plot of the Day zero prostate dose, D90%, against the respective patients treated had a mean prostate dose of 139 ± 15 Gy as reflected on Figure 4A. Based on published literature, an acceptable dose range for post-implant D90% for I-125 may be 130-180 Gy as long as normal structures are not overdosed [2]. This confirms that our treatment results were within acceptable limits and similarly confirmation that the quality of our past treatments were satisfactory.

A repeat study of 31 prostate cancer patients treated by I-125 permanent seed implants in 2021-2022 was done to assess the consistency of the treatment practice. The results were presented graphically on Figure 4B for comparison with those for 2017-2018 on Figure 4A

Table 3 below gives a summary of results for the prostate brachytherapy treatment by trans-perineal I-125 permanent seed implants.

Table 3. Results of prostate cancer brachytherapy treatment by I-125 permanent seed implants in 2017 and 2022, showing the prostate target and OARs doses.

Organ	Mean dose, Gy, (2017)	Mean dose, Gy, (2022)	Max dose limit, Gy
Prostate (Target)	139	137	130-180
Rectum (OAR)	56	62	<140
Urethra (OAR)	90	116	<140

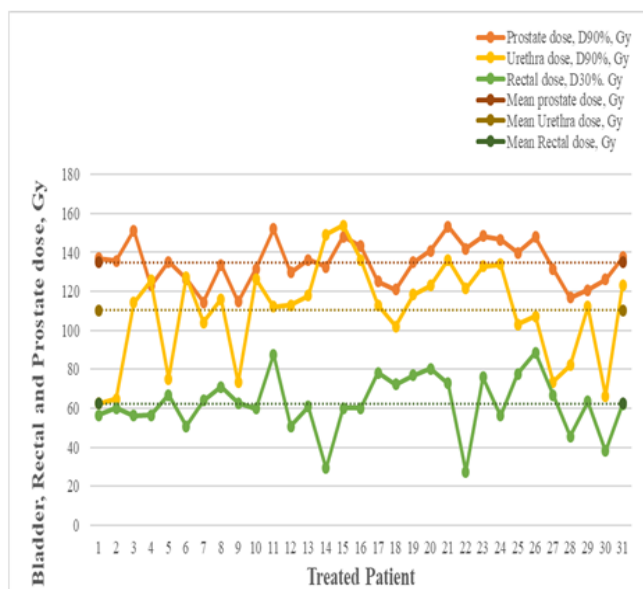


Figure 4B. Target and OARs doses for 31 prostate cancer patients treated by brachytherapy using I-125 permanent seed implants in 2021-2022.

IV. CONCLUSION

OARs doses in both EBRT and brachytherapy treatment of cervical cancer were assessed, while rectal and urethra (OARs) doses in prostate cancer treated by I-125 permanent seed implants were assessed from the DVH of the treatment plans.

The mean dose to both bladder and rectum in brachytherapy treatment of cervical cancer in 2017 and 2022 assessments were below the recommended maximum limits for the bladder (5 Gy) and rectum (4 Gy) in a single fraction treatment. Also in accordance with the American Brachytherapy Society (ABS) recommendation, [2], the dose to the bladder and rectum must be below 80% of the prescribed dose to the cervix. For a prescribed dose of 8 Gy per fraction to the cervix in our case, the bladder and rectum must not receive doses above 6.4 Gy. Our means single fraction doses to the bladder and rectum for 2017 and 2022 were below 6.4 Gy (Table 2), a confirmation that the doses to the OARs in brachytherapy treatment of cervical cancer were safe and consistent. These results were also in agreement with other related published results, [9].

In a combined treatment of EBRT and brachytherapy in treatment of cervical cancer, the combined doses to the OARs were also demonstrated as below the recommended maximum limits and safe.

A plot of the ‘Day zero’ prostate dose, D90%, against the respective patients treated had a mean prostate target dose of 139 Gy and 137 Gy, in the respective years of assessment,

2017 and 2022. The doses to the OARs as summarized on Table 3 are below the recommended target prostate dose. Based on published literature, an acceptable dose range for post-implant D90% for I-125 may be 130-180Gy as long as normal structures are not overdosed [2]. The maximum dose received by the two major OARs, rectum and urethra, during prostate brachytherapy treatment with I-125 is recommended to be below the target prostate tumor dose (140 Gy). So the mean dose received by the rectum and urethra in our case, were within the safe and acceptable limits.

The repeat similar study after five years produced results that were similarly safe and a confirmative demonstration of a consistent radiotherapy practice for treatment of cervical and prostate cancer by brachytherapy at the referred hospital.

The safety and consistency assessment demonstrated in the study is thus proposed as an annual QA procedure in brachytherapy treatment of cancer and can be extended to cover all radiotherapy treatments in an institution.

VI. ACKNOWLEDGEMENTS

I acknowledge my Institutions’ Ethics and Research Committee (Kenyatta National Hospital, University of Nairobi, and The Nairobi Hospital) for accepting and allowing me to do my PhD research project at the institutions.

CONFLICT OF INTEREST

No conflict of interest

REFERENCES

1. Khan F.M. (2003). The physics of radiation therapy. Third Edition. Philadelphia, USA.
2. Davis B.J, Horwitz E.M., Robert Lee W, et al, (2012). American Brachytherapy Society consensus guidelines for trans-rectal ultrasound-guided permanent prostate brachytherapy. *Brachytherapy*.11: 6-19.
3. Pötter R, Haie-Meder C, Limbergen E.V. et al. (2006). Recommendations from gynecological (GYN) GEC Estro working group (II) Concepts and terms in 3D image-based treatment planning in cervix cancer brachytherapy-3D dose volume parameters and aspects of 3D image-based anatomy, radiation physics, radiobiology *Rad and Oncology* 78: 67-77
4. NCI (2011). Prostate cancer treatment, --treatment option overview. National Cancer Institute. Available at: <http://www.cancer.gov/cancertopics/pdg/treatment/prostate/patient/pa g4>
5. American Cancer Society. (2011). Initial treatment of prostate cancer. American Cancer Society. Available at: <http://www.cancer.org/cancer/prostate Cancer/Detailedguide/prostate-cancer-treatment-by-stage>.
6. Thompson I, Thasher J.B, Aus G, et al. (2007). Guideline for the management of clinically localized prostate cancer. *J Urol*: 177: 2106-2131.
7. Horwitz E.M, Bae K, Hanks G.E, et al. (2008). Ten-year follow-up of radiation therapy oncology group protocol 92-02: A phase III trial of the duration elective androgen deprivation in localized advanced prostate cancer. *J Clin Oncol*: 26: 2497-2504.

8. Bolla M., Van Tienhoven G, Warde P, et al. (2010). External irradiation with or without long-term androgen suppression for prostate cancer with high metastatic risk: 10 year results of an AORTC randomized study. *The Lancet Oncology*; 11: 1066-1073.
9. Wibowo A, Haris B, and Islamiyah D.I, (2017). Dose evaluation of organs at risk (OAR) cervical cancer using dose volume histogram (DVH) on brachytherapy. *J. Phys.:Conf. Serv.* 853012013.
10. Fowler J.F, (1989). The linear quadratic formula and progress in fractionated radiotherapy. *Br j Radiol*; 62(740): 679-894.
11. Jones B., Dale R.G. Deehan C, et al. (2001). The role of biologically effective dose (BED) in clinical oncology. *Clin Oncol (RollRadiol)*: 13(2): 71-81.
12. Fowler J.F. (2010). 21 years of biologically effective dose. *Br J Radiol*: 83 (991): 554-568.
13. Crook J.M, Potters L., Stock R.G. and Zelfsky M.J. (2005). Critical organ dosimetry in permanent seed prostate brachytherapy: Defining the organs at risk. *Brachytherapy*; 4: 186-194.
14. Nath R, Bice W.S, Butler W.M, et al. (2009) AAPM recommendations on dose prescription and reporting methods for permanent interstitial brachytherapy for prostate cancer: Report of Task Group 137; *Medical Physics*; 36: 11, 5310-5322.

Contacts of the corresponding author:

Philip Kioko Ndonge,
Oncology & Cancer Treatment Centre,
The Nairobi Hospital,
P.O Box 30026, Code-00100,
Tel. +254 020 2845000,
Cell phone +254 711150081,
NAIROBI, KENYA.
Email: pkndonyeh@gmail.com

QUALITY ASSURANCE OF PATIENT SETUP USING MEGAVOLTAGE PORTAL IMAGING AND DIGITALLY RECONSTRUCTED RADIOGRAPH IN RADIOTHERAPY FACILITY WITHOUT KILOVOLTAGE IMAGING

M.T. Schandorf^{1,2}, E.C.D. Addison^{1,2}, T.B. Dery², A.A. Yorke³

¹ Oncology Directorate, Komfo Anokye Teaching Hospital, Kumasi, Ghana

² School of Nuclear and Allied Sciences, University of Ghana, Accra, Ghana.

³ Department of Radiation Oncology, University of Washington School of Medicine, Washington, USA.

Abstract

The purpose of this study is to assess the quality assurance (QA) of patient treatment setup using megavoltage (MV) images and digitally reconstructed radiographs (DRRs). Thirty anonymized image pairs (30) of DRR and MV images of patients treated on Varian Medical System Clinac IX were used. Identical landmarks were selected by experts on both images using an in-house MATLAB program called the Assisted Expert Manual Point Selection Application (ASEMPA). The differential translations were calculated using the combinatorial rigid registration optimization (CORRO) for both Anterior Posterior (AP) and Lateral (Lat) images to get the 3D shifts from two orthogonal 2D-images. The anatomical sites used were prostate and head/neck. The systematic error for Prostate cases ranged from 0.46cm – 18.62cm, while that for Head and Neck cases ranged from 1.57cm – 11.56cm. The study revealed significant variances and aided in evaluating the facility's setup accuracy. The results proved that our institution needs to do periodic quality assurance on the patient setup process given we currently do not have three-dimensional imaging capabilities for cone beam. Periodic quality assurance will be a guiding tool in correcting any discrepancies that may show up in the clinical workflow as well as periodic education and training on how to properly set up patients.

Keywords

Patient Setup, CORRO, Image Registration, Quality Assurance

I. INTRODUCTION

The main goal of radiotherapy is to deliver an optimal dose to the target volume while minimizing the dose to adjacent normal tissues. External Beam Radiation Therapy (EBRT) typically accomplishes this goal by employing multiple beams to ensure an even distribution of doses within the target volume. External beam radiotherapy techniques require positioning and the use of immobilization devices to ensure accurate tumour localization and treatment setup reproducibility. Accurate and reproducible patient setup

using Image Guided Radiation Therapy (IGRT) requires registering the daily images to the reference image set mostly from the planning computed tomography (CT) [4]. A digitally reconstructed radiograph (DRR), which is used to verify treatment in CT simulation, is one of the critical images that can be transmitted via radiotherapy communication [5]. To confirm patient positioning, digitally reconstructed radiographs (DRR) from the planning CT, or the planning CT itself are from compared to 2D electronic portal images obtained on the treatment, or 3D cone beam computed tomography (CBCT) images respectively.

The digital formats are communicated and managed using Digital Imaging and Communications in Medicine (DICOM). DICOM is the de facto standard in the industry for an image file format for radiological hardware [2]. For proper utilization, consistent portal image quality and a stable radiation response are required, which necessitates routine quality assurance (QA).

There are four widely used techniques for evaluating the integrity of image registration: visual inspection, fiducials, landmark point sets, and mutual information [5]. The patient position deviation can be calculated using the landmark point method to assess the images. Before beam delivery, the correction is used to align the patient nearly perfectly with the reference image position. Over the years, physicians visually verified registered images by comparing portal and diagnostic quality images to a digitally reconstructed radiograph (DRR). The accuracy with which this method of evaluating the quality of image registration is applied has been reported to be between 5 to 10 mm [4]. However, this method of registration is subjective and therefore unsuitable for large amounts of data.

The motivation for this study in our institution was to perform a quality assurance and management procedure on our newly installed Clinac IX to make sure patients set-up was being performed properly and find any gaps in the process that needed to be addressed.

Currently, our institution uses visual inspection for patient set up prior to beam delivery, fiducial, and landmark point methods to verify the patient's alignment, and these methods are subjective. The facility does not have the means to quantify the deviation occurring in the setup. Therefore, there

is a need to input a system that will quantify the deviations for optimal patient alignment and reduce the unevaluated incidences of exposure organs at risk. Figure 1 shows an image retrieved from the treatment offline review of the setup done for a patient during treatment.

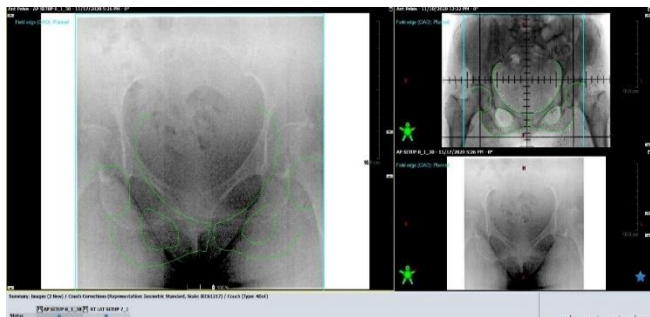


Figure 1: A Treatment Offline Review of Patient Setup from the Linear Accelerator (LINAC) Machine

Using an in-house developed tool, that employs the mathematics of combination without replacement, combinatorial rigid registration optimization (CORRO) we demonstrate the optimal alignment of clinical image pairs in our institution as a way to perform a rigorous post patient set-up quality assurance to inform future workflow.

II. MATERIALS AND METHODS

This study was a retrospective study using a quantitative research approach carried out at the Radiotherapy department at the Oncology Directorate of Komfo Anokye Teaching Hospital (KATH), Kumasi, Ghana after seeking ethical clearance from the Institutional Review Board (IRB) of the hospital. The sampling was done using the simple random method from the data provided by the hospital with a sample size of thirty (30); twenty (20) head and neck and ten (10) prostate cases. These images were from patients who had completed their full treatment.

This study was a quality control (QC) measure to improve radiotherapy patient setup in the radiation beam and to achieve set up reproducibility. In our facility we currently do not have a kilovoltage (kV) imager. We currently use MV portal imaging with a 2D digitally reconstructed radiograph for patient's set-up. Since transitioning from our Co-60 to a conventional linear accelerator (Clinac IX) we haven't performed any quality assurance measures to check the performance of the patient setup process. For an institution like ours it was very important to go through this retrospective study to inform and improve our current practice and workflow.

The centre treats majority of all cancers, with over 1,200 patients treated yearly. Using an independent MATLAB-based user interface assisted expert manual point selection algorithm (ASEMPA) corresponding landmark points were

selected on the MV portal images and the DRRs for both image sets (Anterior-Posterior view and Lateral view) for a single case by medical physics experts and the image registration between the corresponding image pairs are calculated using in-house MATLAB based algorithm combinatorial rigid registration optimization (CORRO) landmark point algorithm. Given the image quality of the MV images, corners and angles and pointed anatomy were the regions of focus. The output translation was applied to the MV image to match the DRR. The output translation Tx, Ty, Tz, were used to adjust the patient in three dimensions.

III. RESULTS AND DISCUSSION

The results were obtained after loading the image pairs to run an analysis on each image pair by picking corner points on the image pairs for Anterior-Posterior and Lateral views simultaneously. This analysis was done to compare the outcome with that which was done clinically. The tx and ty values gotten after running the registration in the in-house MATLAB algorithm were pixel values. The values were then multiplied by the ratio of the MV and kV image spacing since they did not have the same values. The ratio between MV and kV Image Spacing was achieved by equation (1):

The ratio between MV and kV image spacing

$$\frac{MV \text{ Image Spacing}}{kV \text{ Image Spacing}} \quad (1)$$

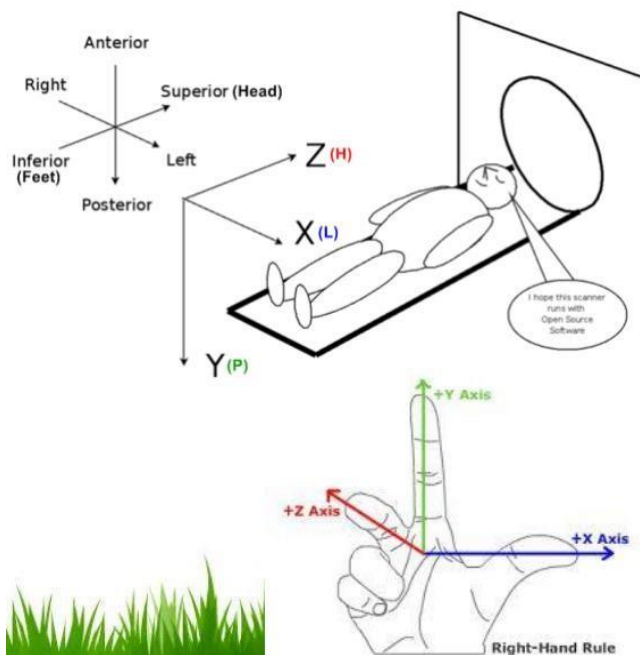
The values were changed to centimetres (cm) because the standard (clinical shifts) are in centimetres.

To convert the pixel values to shifts in centimetres using equations (2) and (3):

$$Tx \text{ (cm)} = \frac{tx \text{ (pixel)} \times \text{Ratio}}{10} \quad (2)$$

$$Ty \text{ (cm)} = \frac{ty \text{ (pixel)} \times \text{Ratio}}{10} \quad (3)$$

Based on Fig. 2 in the information provided, the 2D plane images for the anterior-posterior plane and the 2D lateral plane were translated to provide us with the x, y and z values. For the Anterior-Posterior view, as stated before, the x and z values were gotten, and for the lateral view, x and y values were gotten. The two x values were added and divided by 2 to find the average.



Source: http://mrl.cs.uh.edu/FMI_Fall_2013.html

Figure 2: DICOM Geometry Information

$$x = \frac{x_{AP} + x_{LAT}}{2} \tag{4}$$

The minimum root mean square distance between the Image pairs (i.e. MV_{AP} and kV_{AP} , MV_{LAT} and kV_{LAT}) was found using CORRO computation using equation 5. The results were compared to what was reported clinically by the therapists.

$$\sqrt{(\text{Lat}_{\text{Corro}} - \text{Lat}_{\text{Clinical}})^2 + (\text{Lng}_{\text{Corro}} - \text{Lng}_{\text{Clinical}})^2 + (\text{Vrt}_{\text{Corro}} - \text{Vrt}_{\text{Clinical}})^2} \tag{5}$$

Calculating the shifts

Sample results are shown in Table 1 for Prostate and head and neck cases. The ratio between MV and kV Image Spacing was calculated to be 0.401 mm.

Table 1 represents the differences between the CORRO and Clinical Lateral, Longitudinal and Vertical shifts as well as the root mean deviation. The table shows large variations between the two registrations. This is as a result of a lack of accuracy when it comes to patient setup reproducibility and these were because of the poor patient positioning, as could be seen in the offline review images. These were of much concern because they indicated the lack of precision and accuracy in the setup, and hence this led to the toxicity of healthy tissues, which goes against the aim of radiotherapy.

Table 1: A table showing the shifts calculated from the CORRO algorithm, shifts from the Eclipse Treatment Planning System (TPS) and the Calculated Root Mean Square Deviation for ten (10) Prostate cases and Head and Neck cases respectively.

PROSTATE							
Study ID	Lat _{Corro} (cm)	Lng _{Corro} (cm)	Vrt _{Corro} (cm)	Lat _{Clinical} (cm)	Lng _{Clinical} (cm)	Vrt _{Clinical} (cm)	Root Mean Square
MS001	0.6	18.6	-0.1	0.0	0.0	-0.6	18.616
MS002	-0.6	15.9	-0.4	-0.8	0.4	-1.3	15.527
MS003	2.5	7.1	8.4	1.6	-3.0	0.8	12.672
MS004	1.8	-2.9	-3.5	0.1	1.6	1.7	7.084
MS005	0.8	-4.6	1.2	1.1	0.2	-0.2	5.009
MS006	-1.0	-0.4	-0.9	-0.4	0.1	-0.9	0.781
MS007	-0.6	0.5	0.4	0.6	-4.1	-1.7	18.038
MS008	-2.2	-2.9	4.9	0.0	-0.3	-3.3	8.879
MS009	-0.7	2.0	-0.3	0.0	-0.4	0.2	2.550
MS012	0.0	1.0	1.3	-1.3	-2.3	0.0	3.778
HEAD AND NECK							
Study ID	Lat _{Corro} (cm)	Lng _{Corro} (cm)	Vrt _{Corro} (cm)	Lat _{Clinical} (cm)	Lng _{Clinical} (cm)	Vrt _{Clinical} (cm)	Root Mean Square
HMS010	-4.7	-8.4	0.2	-0.2	0.3	0.4	9.7969
HMS011	0.7	-2.7	1.0	-0.2	0.4	-0.2	3.4438
HMS017	-0.6	-0.4	1.4	0.0	0.0	0.0	1.5748
HMS022	-1.6	3.3	7.3	0.0	0.0	2.3	6.2008
HMS023	-0.1	-1.5	0.9	0.0	0.0	0.0	1.7521
HMS025	0.6	1.8	11.2	-0.4	0.2	-0.2	11.5551
HMS047	0.2	0.3	5.3	0.0	0.6	-0.1	5.4120
HMS048	-0.5	-0.2	0.8	1.0	-0.2	0.1	1.6553
HMS049	-0.6	-2.9	1.9	0.0	-0.4	0.6	2.8810
HMS050	-1.1	0.6	2.2	-2.9	-3.6	-1.8	6.0729

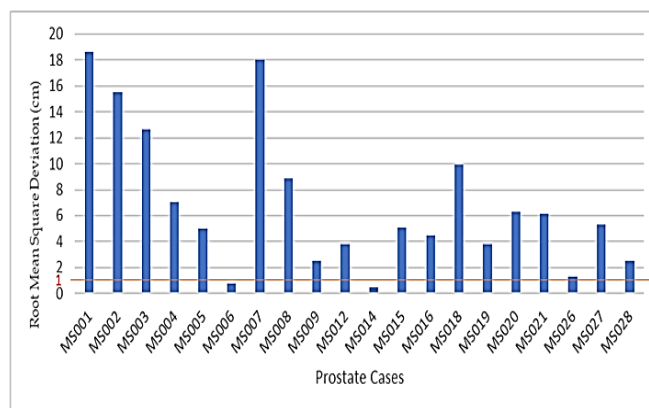


Figure 3: Graphical View of the Deviations Occurring in the Setup for Prostate cases.

Figure 3 is a graphical representation of the root mean square deviation that was calculated to find the deviation occurring between the two registrations. It was found that the root mean square deviations occurring in the shifts between that of the CORRO algorithm and that of the Clinical standard for the Prostate cases was found to be in the range of 0.46 cm – 18.62 cm. The range buttresses the lack of patient setup accuracy in the facility. The cases whose bar are below the red line in the graph are the cases that passed the facility's accuracy protocol of at most 1cm deviation.

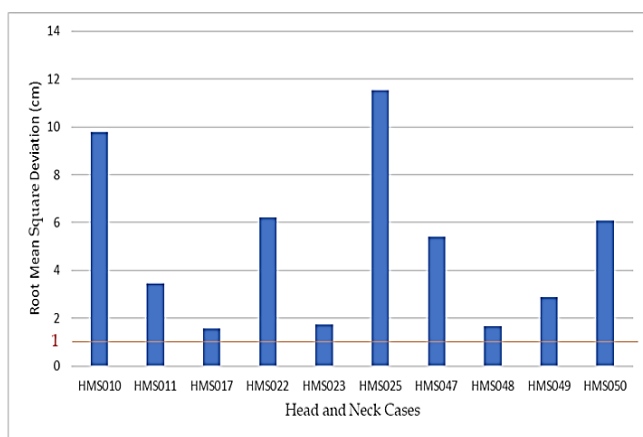


Figure 4: A Graphical View of the Deviations Occurring in the Setup for Head and Neck cases.

Figure 4 represents the graphical view of the root mean square deviation calculated for the CORRO and Clinical shifts for each head and neck case. The root mean square deviations occurring in the shifts between that of the CORRO algorithm and that of the Clinical standard of the Head and Neck was found to be between 1.57 cm – 11.56 cm. This represents the systematic error for both cases. The deviations occurring shows that there are large shift differences between that gotten from CORRO, which is being used for the quality assurance of the setup and that of which is done clinically. This proves that there is a gap that needs to be filled when it comes to the patient setup at the study location. The bars below the red line in Figure 4 represent the cases that passed the accuracy standard of at most 1cm deviation, of the facility, all others failed.

IV. CONCLUSION

It is well documented that patient setup plays a very vital role in delivering the prescribed dose to the target. Any misalignment will be detrimental to the patient. For a radiotherapy centre in the process of transitioning from Co-60 to modern linear accelerators without kV imaging capabilities as a guidance in the patient set up process, it is important to go through periodic quality assurance of this process to come up with mitigation strategies or update the workflow based on the findings. From our study, the results

showed large discrepancies from the expected results and as such the large deviations observed between the set-up shifts recorded versus the results obtained from our CORRO algorithm in three dimensions. The poor accuracy in the setup can be attributed to the patients getting their simulation CT from outside the institution which does not necessarily match the treatment coordinates. Also, it is recommended that the radiation therapists perform the CT simulation and record the treatment positions and any anatomical position the patient might be in at the time of simulation so that this could be reproducible at the time of treatment. However, given the current workflow at our institution this aspect is missing and puts a dent in the current workflow. As a result, the therapist must rely on information given to them by the medical physicists or the diagnostic radiographers the outside institution who took the images. Hence their exclusion from this crucial step makes it very difficult to reproduce the patient's set-up positioning and this might have contributed to the large discrepancies. We recommend that clinics with this current type of workflow must include radiation therapists or train them to perform patient CT simulation because such large deviations could be detrimental to the patient.

VI. ABBREVIATIONS

2D: two dimensional; 3D: three dimensional; AP: anterior – posterior; ASEMPA: assisted expert manual point selection application; cm: centimetre; CT: computed tomography; CORRO: combinatorial rigid registration optimization; DICOM: digital imaging and communications in medicine; DRR: digitally reconstructed radiographs; EBRT: external beam radiation therapy; EPI: electronic portal images; IGRT: image-guided radiation therapy; IRB: institutional review board; KATH: Komfo Anokye Teaching Hospital; kV: kilovoltage; Lat: lateral; LINAC: linear accelerator; mm: millimetre; MV: megavoltage; TPS: treatment planning system; QA: quality assurance.

CONFLICT OF INTEREST

The authors have declared that no competing interest exists with publication of the study.

REFERENCES

1. Clippe S, Sarrut D, Malet C, Miguet S, Ginestet C, Carrie C. Patient setup error measurement using 3D intensity-based image registration techniques. *Int J Radiat Oncol Biol Phys*. 2003; 56:259–265
2. Graham, R. N., Perriss, R. W., & Scarsbrook, A. F. (2005). DICOM demystified: a review of digital file formats and their use in radiological practice. *Clinical radiology*, 60(11), 1133-1140

3. Hashimoto, S., Shirato, H., Nishioka, T., Kagei, K., Shimizu, S., Fujita, K., ... & Miyasaka, K. (2001). Remote verification in radiotherapy using digitally reconstructed radiography (DRR) and portal images: a pilot study. *International Journal of Radiation Oncology* Biology* Physics*, 50(2), 579-585.
4. Verellen D, Ridder MD & Storme GA. (2008). A (short) history of image-guided radiotherapy. *Radiotherapy Oncology*; 86(1):4-13. doi: 10.1016/j.radonc.2007.11.023
5. Yorke AA, Solis DJ & Guerrero T. (2020). A feasibility study to estimate optimal rigid-body registration using combinatorial rigid registration optimization (CORRO). *Journal of Applied Clinical Medical Physics*;1-9. doi: 10.1002/acm2.12965
6. http://mrl.cs.uh.edu/FMI_Fall_2013.html

Contacts of the corresponding author:

Mercy Torshie Schandorf
Oncology Directorate,
Komfo Anokye Teaching Hospital,
P.O Box OS 312, Accra, Ghana.
Tel. +233 554 250 163,
Email; torshieschandorf@gmail.com

IndoQCT: A PLATFORM FOR AUTOMATED CT IMAGE QUALITY ASSESSMENT

Choirul Anam¹, Ariij Naufal¹, Wahyu S. Budi¹, Heri Sutanto¹, Freddy Haryanto², Geoff Dougherty³

¹Department of Physics, Faculty of Sciences and Mathematics, Diponegoro University, Jl. Prof. Soedarto SH, Tembalang, Semarang 50275, Central Java, Indonesia

²Department of Physics, Faculty of Mathematics and Natural Sciences, Bandung Institute of Technology, Bandung, West Java, Indonesia

³Department of Applied Physics and Medical Imaging, California State University Channel Islands, Camarillo, CA 93012, USA

Abstract— The quality control (QC) procedure of computed tomography (CT) is an important task to be regularly performed. It consists of daily, monthly, and annual tasks. Each procedure can be time-consuming. Manual QC can take many hours. Manual measurement of image quality parameters can also lead to a bias due to the subjectivity of examiners. IndoQCT answers these challenges by being automatic, fast, objective, and accurate. Unlike some existing software that can only be used on one type of phantom and with limited parameters, IndoQCT can be used to evaluate CT image quality using various phantoms and numerous parameters. In this report, the basic workflow of IndoQCT to automatically evaluate CT image quality on the American College of Radiology (ACR) phantom was assessed. IndoQCT provides a total of 9 main tabs, covering various image quality parameters, namely: CT number (water), CT number of multiple objects, noise, spatial resolution, low contrast, slice thickness, laser alignment, distance accuracy, and gantry tilt. As a tool for productive QC procedures in health facilities, IndoQCT can increase the efficiency of QC.

Keywords— computed tomography, QC, image quality, automatic

IV. INTRODUCTION

Quality control (QC) procedures on X-ray machines, especially computed tomography (CT) scanners, are essential to maintain the performance of the machine over time in order to achieve an accurate diagnosis and to deliver best treatment for patients. Medical personnel carry out routine QC procedures covering the mechanical aspects, output dose, and image quality [1]. Scanner performance is evaluated using a series of specific procedures using dedicated phantoms.

Evaluation of CT image quality can be carried out using manual methods. They mostly involve placing regions of interest (ROI) on target objects to measure certain parameters. The manual method is mainly for basic parameters that do not require complicated mathematical operations. Unfortunately, it can give rise to variability between users, and it is time-consuming [2]. Several automatic tools have been introduced to overcome this problem, especially for measuring advanced Fourier-based image quality parameters, such as the modulation transfer

function (MTF) and the noise power spectrum (NPS) [2-5].

With automated QC software, two main problems can arise, namely transparency and comprehensiveness. Paid software generally does not include complete and transparent documentation, and the algorithm for the automated procedures is proprietary. You are not purchasing the software but only paying to use it. The user is not able to configure/modify the measurement parameters to fit the specific image conditions. It is highly preferable to be able to create an optimal user-customized framework that can be configured in a user-friendly manner according to the specific conditions. With regard to comprehensiveness, although some open-source software provides documentation transparency, the software are limited and can only be applied to one dedicated phantom type, such as the Catphan (The Phantom Laboratory, Salem, USA) or ACR (Gammex Inc, Middleton, WI, USA) [2,6]. Since there are many types of QC phantoms on the market, especially built-in phantoms, the limited coverage of this software will limit easy access for many CT centers having different types of phantoms. Therefore, availability of a software that can be used on different types of phantom is important.

Based on these problems, we developed a software platform called IndoQCT. IndoQCT attempts to address these issues by integrating automated methods for CT image quality evaluation for the many types of phantoms available on the market. In this report, however, we will only demonstrate the basic workflow for common image quality parameters on the ACR 464 phantom.

V. METHODS

2.1 ACR 464 phantom

The ACR 464 phantom consists of 4 modules for measurement of various image quality parameters. The appearance of each module is shown in Figure 1. Table 1 shows the details of the modules and their roles in measuring image quality parameters along with their tolerance limits.

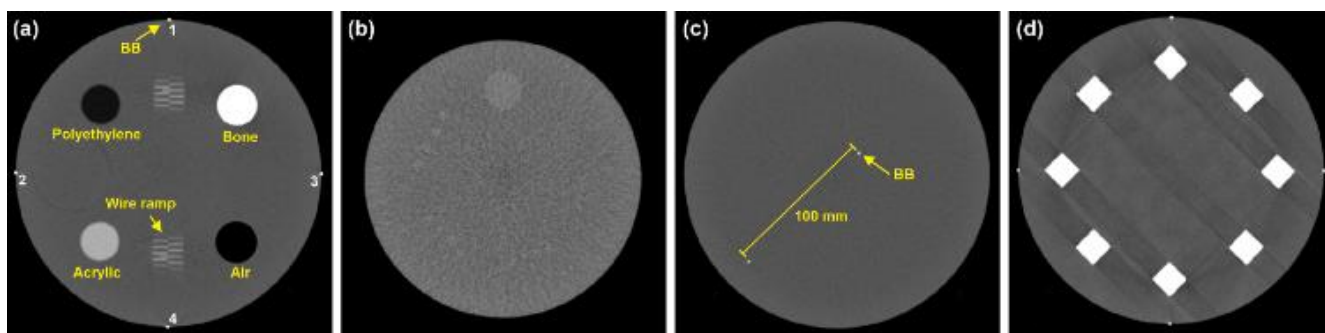


Fig. 1 Images of ACR phantom module (a) #1, (b) #2, (c) #3, and (d) #4.

Table 1 Image quality parameters on each module of ACR phantom

Module	Parameter	Tolerance limit
#1	CT number of multiple objects	<ul style="list-style-type: none"> • Air (-970 to -1005 HU) • Polyethylene (-107 to -84) • Solid water (-7 to +7 HU) • Acrylic (110 to 135 HU) • Bone (850 to 970 HU)
	CT number linearity	-
	Alignment	$\Delta \text{ laser} \leq \text{minimum slice thickness}$
	Slice thickness	$\Delta \text{ slice thickness} \leq 0.5 \text{ mm}$
#2	TTF*	-
	Low contrast (visual)	Minimum size $\leq 6 \text{ mm}$
#3	CNR**	$\text{CNR} \geq 1$
	CT number (water)	$-7 \text{ HU} \leq \text{CT number} \leq 7 \text{ HU}$
	CT number uniformity	$\leq 5 \text{ HU}$
	Noise	-
	Noise uniformity	Uniformity $\leq 2 \text{ HU}$
	NPS***	-
	Distance accuracy	-
	Gantry tilt	-
#4	Point MTF****	$10\% \text{ MTF} \geq 0.5 \text{ mm}^{-1}$
	Edge MTF	$10\% \text{ MTF} \geq 0.5 \text{ mm}^{-1}$
#4	Spatial resolution (visual)	Line pair $\geq 0.5 \text{ lp/mm}$

*) TTF is task transfer function

**) CNR is contrast to noise ratio

***) NPS is noise power spectrum

****) MTF is modulation transfer function

2.2 IndoQCT main architecture

2.2.1 Backend structure

IndoQCT was built using Python 2.7.9 with the PyQt5 Graphical User Interface (GUI) platform. To read and access Digital Imaging and Communications in Medicine (DICOM) images, IndoQCT used the Pydicom library [7]. Through the interface, the user can execute the automatic methods provided. The main matrix operation implemented is Numpy [8]. For the backend process, IndoQCT employed image processing modules, such as scikit-image [9], scipy [10], and Open-CV. For each parameter measurement, IndoQCT processes different functions, based conditionally on the type of phantom that can be selected.

2.2.2 Frontend structure

The IndoQCT GUI has a similar layout to many DICOM viewer software. Figure 2 shows the layout of the GUI components of IndoQCT. The main features for image quality measurement were embedded into the main tabs on the right side of the main viewer. The 9 tabs are based on their parameter categories, from top to bottom, namely CT number (water), CT number of multiple objects, noise, spatial resolution, low contrast detectability, slice thickness, alignment, distance accuracy, and gantry tilt. The tabs were sorted based on the frequency of their use in field scenarios. In each tab, it can be divided into sub-tabs according to its specific parameters, such as the CT number tab consisting of accuracy, uniformity, homogeneity, histogram, profile, and patient sub-tabs. However, in this report, we will only briefly elaborate on the parameters that are commonly assessed in QC procedures.

In each tab, the components were carefully organized so that both input parameters and results can be understood intuitively. Input parameters are useful for configuring the measurement parameters according to the image conditions to be evaluated. By default, the input parameters are set to ideal values that work for most images. The "Calculate" button is provided to trigger the automatic algorithm on each tab. After the automatic algorithm is activated, the results are printed in the results column on the right side. More in-depth details for each automatic measurement will be discussed in the image quality parameters section.

For each image quality measurement, the results are compared to the standards provided (Table 1). The evaluation according to the standard is automatically accomplished in the standards section (PASSED/FAILED). Several sets of configurations were included according to guidelines from regulatory agencies, such as Nuclear Energy Regulatory Agency of Indonesia (BAPETEN) [11], International Atomic Energy Agency (IAEA) [12], American College of Radiology (ACR), American Association of Physicists in Medicine (AAPM), and user baseline.

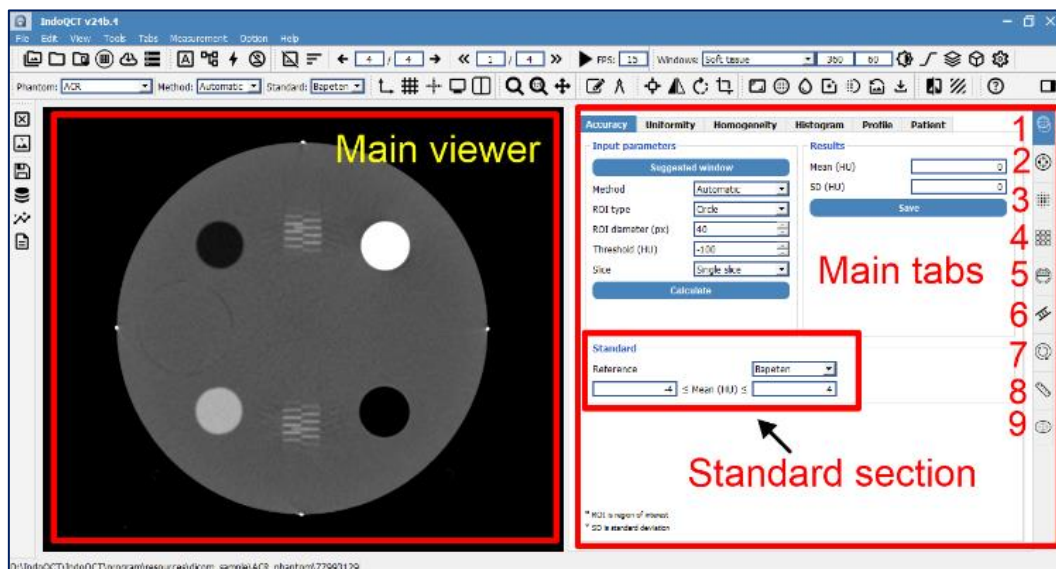


Fig. 2 The graphical user interface of IndoQCT. It consists of a main viewer, main tabs, and standard sections. A total of 9 main tabs for the measurement of different image quality parameters is provided: (1) CT number of water, (2) CT number of multiple objects, (3) Noise, (4) Spatial resolution, (5) Low contrast detectability, (6) Slice thickness, (7) Laser alignment, (8) Distance accuracy, and (9) Gantry tilt

2.3 Image quality parameters

2.3.1 CT number of water

In the tab of CT number of water, sub-tabs of CT number accuracy and CT number uniformity can be chosen. IndoQCT segments the phantom and determines its centroid coordinates. A circular ROI of 2 cm in diameter is placed at the centroid. Figure 3a shows the ROI positioning for CT number of water measurement on the ACR phantom. CT number accuracy is measured by averaging the pixel intensities in Hounsfield units (HU) of the ROI. For measuring CT number uniformity, IndoQCT places 5 ROIs, namely in the center of the phantom and at the periphery (3, 6, 9, 12 o'clock). Figure 3b shows the placement of each ROI in the CT number uniformity measurement. The peripheral ROIs were 3 cm away from the edge of the phantom. CT number uniformity is measured as the largest difference between the peripheral ROI and the central ROI, as defined by equation (1).

$$U_{CT} = \max (ROI_p - ROI_c) \quad (1)$$

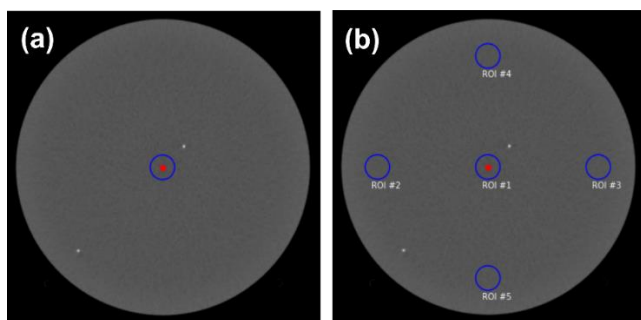


Fig. 3 Automatic measurements of CT number of water on ACR phantom. (a) CT number accuracy, and (b) CT number uniformity.

2.3.2 CT number of multiple objects

In the tab of the CT number of multiple objects, a feature for automatically measuring the CT number of objects with different densities was provided. The CT number of multiple objects is automatically obtained by detecting objects with varying CT numbers, as listed in the phantom manual book. ROIs are automatically drawn on the target objects to obtain the average CT number of each material (Figure 4a). The measurement results for each material are then displayed in the result column, along with its density and reference. As an extension of this measurement, the linearity of the CT number of multiple objects can be calculated by determining the regression coefficient between the CT number and the density of each material (Figure 4b) [13-15].

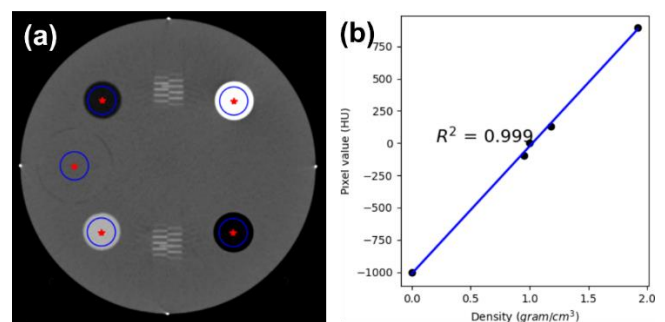


Fig. 4 Measurement of CT number of multiple objects on ACR phantom. (a) ROI placement on 5 different materials, (b) Determining the linearity.

2.3.3 Noise

In the tab of noise, noise accuracy is measured using a process similar to CT number accuracy (Figure 3a), by

placing the ROI in the center of the phantom. Noise is measured by calculating the standard deviation of the pixels within the ROI [16]. In addition to noise accuracy, noise uniformity is also evaluated to ensure that noise levels are uniform across regions. Noise uniformity is measured using a process similar to CT number uniformity (Figure 3b), by placing 5 ROIs at the center and at the periphery (3, 6, 9, 12 o'clock). Noise uniformity is defined as the maximum difference between maximum noise in one ROI and minimum noise in the one of the remaining ROIs, shown by equation (2).

$$U_{\sigma} = \max(\sigma) - \min(\sigma) \quad (2)$$

Noise texture characterized by NPS is also available in a specific sub-tab. NPS measurement is performed by drawing a number of square ROIs (i.e., 1, 3, or 5) on a homogeneous region in the phantom (Figure 5a). Then, the two-dimensional (2D) NPS is obtained using equation (3).

$$NPS_{(u,v)} = \frac{d_x d_y}{N_x N_y} \cdot |\mathcal{F}[I(x,y) - P(x,y)]|^2 \quad (3)$$

where u and v are the spatial frequencies in the X- and Y-axes. d_x and d_y are the pixel sizes, and N_x and N_y are the number of pixels in the X- and Y-axes in the ROI. F represents the Fourier transform, I represents the pixel value, and P is the polynomial fit of I .

One-dimensional (1D) NPS ($NPS(f)$) is obtained by radially averaging the two-dimensional (2D) NPS. The peak and average frequencies are determined from the 1D NPS [17,18]. Figure 5b shows an example of 1D NPS obtained on an ACR phantom image. An option for a polynomial fit of the 1D NPS with a maximum of 11-th order is provided, as proposed by [19,20].

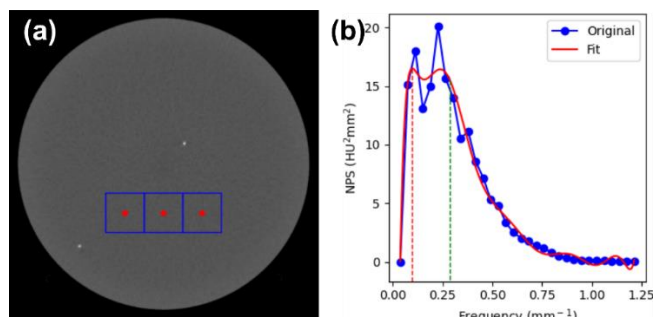


Fig. 5 Automatic measurements of NPS on ACR phantom. (a) ROI placement on homogeneous area, and (b) Example of 1D NPS with 11th order polynomial fit.

2.3.4 Spatial resolution

In the tab of the spatial resolution, several sub-tabs for various methods of measuring spatial resolution are provided. Spatial resolution can be determined using visual observation. The phantom images used generally display

line pairs. Figure 1d shows an image of the line pairs displayed at a window width of 100 and window level of 1100, as recommended by ACR. To minimize user variability in visual observation, IndoQCT provides an automated method. The ACR phantom image is processed to obtain a standard deviation (SD) map. The objects for a specific SD criteria are identified above the threshold to determine the resolvable objects (Figure 6a).

In addition to using line pairs, spatial resolution can also be measured through the modulation transfer function (MTF). In IndoQCT, Point MTF is one of the options to characterize spatial resolution [21-23]. In the ACR phantom module #3, there are 2 point objects that can be used for Point MTF measurement. One of the point objects is detected using simple segmentation to obtain its coordinates. A ROI is drawn at the coordinates of the point object (Figure 6b). The resulting array is summed according to the selected option (e.g. X-axis or Y-axis, depending on the desired resolution dimension), to generate a point spread function (PSF). The PSF is automatically zeroed and normalized (Figure 6c). A Fourier transform is performed on the PSF to generate an MTF curve (Figure 6d). The 10% and 50% MTFs are displayed in IndoQCT.

In many cases, Point MTF produces fluctuating curves due to high noise. Edge MTF provides a reliable alternative option [24,25]. In the ACR phantom, Edge MTF is obtained by collecting the phantom edge response (edge spread function, ESF), which is differentiated to generate a line spread function (LSF). The LSF is then Fourier transformed to generate the MTF curve. Figure 6e shows the ROI placement for edge MTF measurement. Since the edge response was obtained from the phantom edge, the potential for fluctuation is always present. To anticipate disturbances, several options to correct the ESF, such as tail replacement, homogenization, mirroring, and single logistic fit are provided. Users can select these options according to their needs.

TTF is an image quality parameter characterizing spatial resolution as a function of contrast and local noise. TTF plays an important role in describing the spatial resolution of CT systems in non-linear and shift-variant iterative reconstruction. TTF is analogous to MTF. However, when reporting TTF, contrast and local noise are also reported [26]. To measure TTF, circular disk-shaped inserts made of various materials are required. In the ACR phantom, 4 circular objects are available, namely bone, air, acrylic, and polyethylene. These four objects are automatically detected to identify their coordinates. A circular ROI is placed on each object coordinate and the object edge responses obtained radially. The ESF is calculated as the average of the edge response samples. The rest of the process is similar to those for edge MTF. Figure 7 shows an example of TTF measurement in IndoQCT.

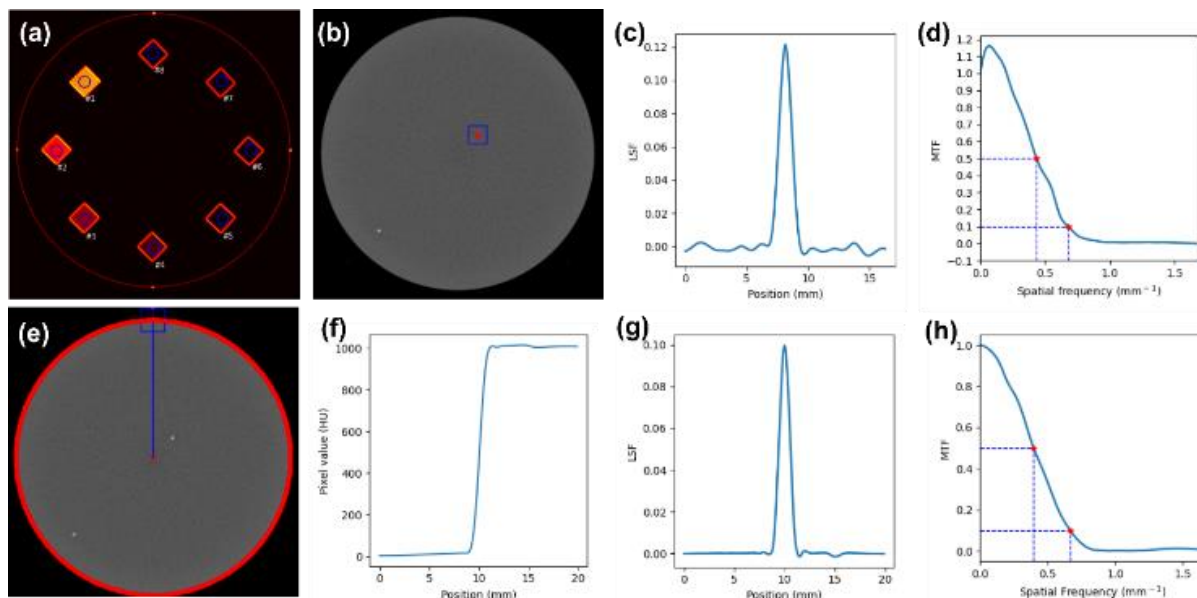


Fig. 6 Automatic measurements of spatial resolution on ACR phantom. (a) SD map with line pair annotated, (b) ROI placement on point object, (c) Example of zeroed and normalized PSF, (d) MTF curve derived from (c), (e) ROI placement on phantom's edge, (f) Example of ESF obtained, (g) LSF derived from (f), and (h) MTF curve derived from (g).

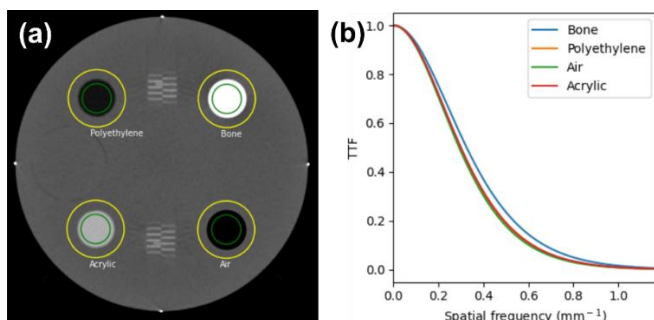


Fig. 7 Automatic measurements of TTF on ACR phantom. (a) ROI placement on 4 circular objects, (b) Example of TTF curves from various materials.

2.3.5 Low contrast detectability

In the tab of the low contrast, visual low contrast detectability and contrast-to-noise ratio (CNR) assessments are provided. Low contrast detectability can be visually observed by a human observer. In the ACR phantom, a low contrast module consisting of a series of cylinders with various diameters is provided. An automated low contrast detectability assessment workflow is available in IndoQCT. After opening a suitable image, the user can set the window width and window level to 100 and 100, as recommended by ACR, using a button provided. By doing so, the appearance of low contrast objects will become clearer for identification. Using an automated method, IndoQCT identifies the coordinates of each target object through a reference object (a 25 mm diameter cylinder) to place a ROI on each target, in addition to placing a ROI in the center of the phantom for the background. The CNR of each object against the

background at the center of the phantom is calculated using equation (4). Using the set CNR threshold, the CNR of the object series that is not less than the threshold is considered resolvable against the background. The smallest object series that is still resolvable indicates low contrast detectability of the image [27]. Figure 8a shows the detection result of the low contrast object series on the ACR phantom.

In addition to visual observation, CNR is also widely considered to describe the ability of a CT system to emphasize low contrast lesions. IndoQCT provides an automated tool for CNR measurement on a phantom. In CNR measurement, two ROIs are drawn on the object (25 mm diameter cylinder) and background (Figure 8b)., Segmentation of the phantom and the low contrast object is performed to obtain the center coordinates of both. CNR is then calculated using equation (4).

$$CNR = \frac{|I_{object} - I_{background}|}{\sigma} \quad (4)$$

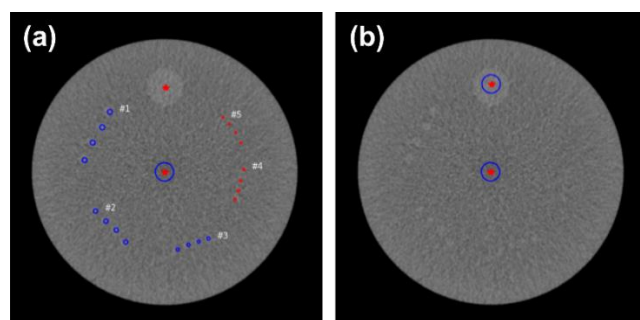


Fig. 8 Automatic measurements of low contrast detectability on ACR phantom. (a) Visual observation of series of objects (blue circles indicate

resolvable objects, and red circles indicate non-resolvable objects), (b) CNR measurements.

2.3.6 Slice thickness

On the tab of the slice thickness, slice thickness can be automatically measured. In the ACR phantom, a pair of wire ramps with a spacing of 0.5 mm each is provided. Slice thickness measurement is performed by enumerating the number of wires visible on the axial image. To minimize the subjectivity of manual observation, IndoQCT provides an automated method [28]. Two profile lines are drawn on the left and right sides so that they crossed both ramps. The pixel profiles from both sides are then normalized. The number of peaks is calculated as a representation of the number of enumerated objects. Slice thickness in mm is measured by multiplying the object count by the distance between them (0.5 mm). Figure 9 displays the ROI placement of the automatic slice thickness measurement on the ACR phantom.

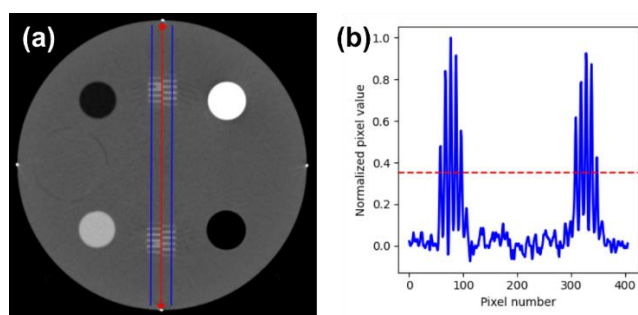


Fig. 9 Automatic slice thickness on ACR phantom. (a) Two profile lines placed on wire ramps, (b) Example of object counting from their normalized pixel profile. Red line indicates the threshold value and it can be set by user.

2.3.7 Laser alignment

Laser alignment is the mechanical aspect test of CT. Laser alignment as a tool helping to locate the phantom on the iso-center. The accuracy of the phantom placement at the iso-center directly influences the image quality and the dose distribution within it. In the ACR phantom, several markers (at 3, 6, 9, 12 o'clock) to evaluate alignment are provided. These marker objects exist in modules #1 and #4, shown in Figure 1a and 1d. Through laser alignment measurement, the accuracy of phantom positioning in the X, Y, and rotational axis directions in degrees can be determined. IndoQCT segments the alignment marker objects and measures their precision against the image's central axis [29]. Figure 10 shows the automatic detection of the alignment measurement.

2.3.8 Distance accuracy

ACR phantom provides a module for distance accuracy measurement, in the form of two point objects at a distance of 100 mm in module #3 (Figure 1c). This parameter

evaluates the accuracy of CT reconstruction, especially in terms of geometry in XY coordinates. IndoQCT provides a feature for automatic measurement of distance accuracy in the distance tab. An example of the detection results of the two point objects measuring distance accuracy on the ACR phantom is shown in Figure 11.

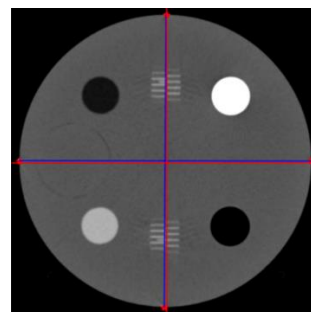


Fig. 10 Automatic phantom alignment measurements on ACR phantom module #1. The red lines indicate the lines through the center of the image, and the blue lines connect four markers.

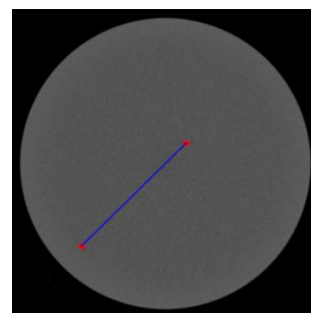


Fig. 11 Automatic measurements of distance accuracy on the ACR phantom.

2.3.9 Gantry tilt

Gantry tilt measurements can be easily and automatically done on the axial image using IndoQCT. By segmenting the phantom object, the lateral (LAT) and anterior-posterior (AP) diameters can be obtained. The tilt angle (θ) is calculated using equation (5) [30]. The measurement results are compared with the gantry tilt information that can be accessed from the DICOM tags, using the (0018,1120) Gantry/Detector Tilt tag. Figure 12 shows the detection of LAT and AP diameters on the ACR phantom.

$$\theta = \cos^{-1} \left(\frac{LAT}{AP} \right) \quad (5)$$

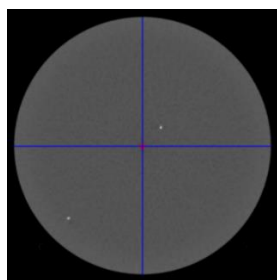


Fig. 12 Automatic gantry tilt measurement on ACR phantom.

2.4 Initial assessment

As an initial study, various parameters of image quality of ACR phantom scanned from 3 scanners were measured. The acquisition parameters for the 3 scanners are shown in Table 2. Measurement of image quality parameters was performed using the default configuration of IndoQCT.

Table 2 Acquisition parameters of ACR phantom image from 3 different scanners

Parameter	Scanner #1	Scanner #2	Scanner #3
Scanner type	GE Discovery LS	GE Revolution ACTs	GE Revolution EVO
Scan mode	Axial	Axial	Axial
Tube current (mA)	250	200	120
Tube voltage (kV)	120	120	120
Slice thickness (mm)	5	10	5
Field of view (mm)	240	250	233
Filter type	Body	Head	Head

VI. RESULTS

Table 3 shows a summary of the results of the ACR phantom image quality assessment from the 3 scanners automatically using IndoQCT. In some measurements, the results were evaluated automatically using the standards set by ACR. Of the various measurement parameters, laser alignment showed results that did not meet the standard, especially in scanner #1, where the delta x and y exceeded the 2 mm tolerance limit. This indicates an off-center phantom position up and to the right. In the measurement of CT number of multiple objects, IndoQCT can detect the target objects correctly and obtain the desired measurement results. The CT numbers for the bone insert were above the upper recommended range for scanners #2 and #3. The NPS measurement describes the noise distribution at different frequencies, indicating a difference in texture between the 3 scanners despite them having similar noise levels. In the spatial resolution measurement using several methods, the measurement results showed close agreement between line pair assessment, point, and edge MTF.

VII. DISCUSSION

As a tool in carrying out QC procedures in productive healthcare facilities, IndoQCT is reliable and provides a simple workflow to run. This is demonstrated from the measurements in the Results section, where all parameters in every dataset were comprehensively evaluated in only about 5 minutes.

Table 3 Summary of image quality assessment for ACR phantom image from 3 different scanners

Main parameter	Sub parameter	Scanner #1	Scanner #2	Scanner #3	Standard
CT number of water	Accuracy (HU)	-1.0	-2.2	-2.0	-7 to +7
	Uniformity (HU)	3.3	0.8	1.6	≤ 5
CT number of multiple object	Accuracy (HU)				
	• Air	• -998.8	• -978.0	• -993.5	• -970 to -1005
	• Polyethylene	• -91.8	• -99.5	• -97.2	• -107 to -84
	• Solid water	• -1.0	• -1.7	• -1.3	• -7 to +7
	• Acrylic	• 120.9	• 118.3	• 119.8	• 110 to 135
	• Bone	• 916.7	• 1052.4	• 980.0	• 850 to 970
Noise image	Linearity (R ²)	0.9984	0.9906	0.9958	-
	Noise level (HU)	5.3	2.47	3.16	-
	Uniformity (HU)	1.0	0.4	0.3	-
	NPS: Peak frequency (mm ⁻¹)	0.29	0.06	0.23	-
Spatial resolution	NPS: Average frequency (mm ⁻¹)	0.33	0.26	0.29	-
	Automatic assessment on line pair object (mm ⁻¹)	0.70	0.60	0.70	0.50
	Point MTF: 10% MTF (mm ⁻¹)	0.68	0.63	0.70	0.50
	Edge MTF: 10% MTF (mm ⁻¹)	0.62	0.58	0.78	0.50
	10% TTF (mm ⁻¹)				
	• Air	• 0.69	• 0.60	• 0.76	-
	• Polyethylene	• 0.67	• 0.62	• 0.73	-
	• Acrylic	• 0.73	• 0.60	• 0.74	-
	• Bone	• 0.69	• 0.57	• 0.90	-
Low contrast detectability	Automatic assessment with various size (mm)	4	3	5	≤ 6
	CNR	1.3	2.6	1.7	≥ 1
Slice thickness	Slice thickness (mm) / Difference (mm)	5.2 / 0.2	9.8 / 0.2	4.8 / 0.2	Difference ≤ 1.5

Laser alignment	<ul style="list-style-type: none"> • x-axis (mm) • y-axis (mm) 	<ul style="list-style-type: none"> • 4.9 • 8.4 	<ul style="list-style-type: none"> • -0.5 • 0.8 	<ul style="list-style-type: none"> • 1.8 • 0.4 	<ul style="list-style-type: none"> • ≤ 2 • ≤ 2
Distance accuracy	Distance accuracy (mm) / Difference (mm)	100.1 / 0.1	100.1 / 0.1	100.1 / 0.1	Difference ≤ 1
Gantry tilt	Gantry tilt ($^{\circ}$)	0.0	0.0	0.0	-

*Bold shows FAILED values.

VIII. DISCUSSION

As a tool in carrying out QC procedures in productive healthcare facilities, IndoQCT is reliable and provides a simple workflow to run. This is demonstrated from the measurements in the Results section, where all parameters in every dataset were comprehensively evaluated in only about 5 minutes.

This study only showed the measurement of various parameters on the ACR phantom using IndoQCT. IndoQCT itself can measure various parameters from many other phantoms, such as Catphan, AAPM CT performance, GE, Siemens, Toshiba, Philips, Hitachi, and Neusoft. With the many phantom options in IndoQCT, it helps healthcare facilities having different phantoms. The automated method in IndoQCT improved efficiency for the evaluation of a set of image quality parameters. Moreover, automatic detection reduces manual user interventions and leads to more objective results. IndoQCT can also save the image quality evaluation in the database. This is very useful for observing shifts in quality trends over time, leading to its potential for research and monitoring.

Using IndoQCT, medical personnel can develop a report in a pdf file from the results of QC tests conducted periodically. This feature helps medical personnel to report QC results to related parties and to physically archive data. It is noted that the image quality parameters discussed in this report were also limited to the most commonly evaluated parameters. This report did not include advanced parameters such as CT number homogeneity, noise homogeneity, z-MTF, and so on.

One of the challenges for automation software such as IndoQCT is its robustness to various image conditions. Object detection algorithms that use thresholding techniques or other image processing operations may suffer when applied to images with extreme conditions, i.e. high noise or prominent artefacts. Suboptimal object detection may result in mis-positioning of the ROI, leading to measurement inaccuracies. Therefore, in addition to the automatic method, the option of a manual method is also provided. The workflow of the manual method depends on the type of phantom and the image quality parameters to be measured. For example, in Figure 2, in the parameter input section, a measurement method option was provided for each parameter. When the manual option is activated, the user can manually place the ROI on the desired object, and proceed to the calculation as usual. Another example is the slice thickness measurement on the ACR phantom, where the manual method only requires the user to enumerate the wire

objects and select the number in the user interface (UI) provided. IndoQCT is still at the development stage. Improvements are needed to assess new types of phantoms, as well as new methods for CT image evaluation.

IX. CONCLUSIONS

IndoQCT was used to automatically evaluate the image quality of the ACR phantom. The image quality parameters were CT number (water), CT number of multiple objects, noise, spatial resolution, low contrast, slice thickness, laser alignment, and distance accuracy. Due to its simple workflow displayed on an intuitive GUI, IndoQCT has the potential to increase the work efficiency of medical personnel for QC procedure.

ACKNOWLEDGMENT

This work was funded by the Riset Publikasi Internasional Bereputasi Tinggi (RPIBT), Diponegoro University (No. 569-187/UN7.D2/PP/IV/2023).

REFERENCES

- [1] Roa AM, Andersen HK, Martinsen AC. CT image quality over time: comparison of image quality for six different CT scanners over a six-year period. *J Appl Clin Med Phys.* 2015;16(2):4972. Published 2015 Mar 8. doi:10.1120/jacmp.v16i2.4972
- [2] Karius A, Bert C. QAMaster: A new software framework for phantom-based computed tomography quality assurance. *J Appl Clin Med Phys.* 2022;23(4):e13588. doi:10.1002/acm2.13588
- [3] Greffier J, Barbotteau Y, Gardavaud F. iQMetrix-CT: New software for task-based image quality assessment of phantom CT images. *Diagn Interv Imaging.* 2022;103(11):555-562. doi:10.1016/j.diii.2022.05.007
- [4] Medical Physics Perth. CT quality inspector (<https://medicalphysicsperth.com/ct-quality-inspector-ctqi>)
- [5] QA Benchmark. AutoQA Plus CT (<http://qabenchmark.com/ct/>)
- [6] Hobson MA, Soisson ET, Davis SD, Parker W. Using the ACR CT accreditation phantom for routine image quality assurance on both CT and CBCT imaging systems in a radiotherapy environment. *J Appl Clin Med Phys.* 2014;15(4):4835. Published 2014 Jul 8. doi:10.1120/jacmp.v15i4.4835
- [7] Mason D. SU-E-T-33: Pydicom: An Open Source DICOM Library. *Med Phys.* 2011;38(Issue6Part10): 3493-3493. doi:10.1118/1.3611983
- [8] Harris CR, Millman KJ, van der Walt SJ, et al. Array programming with NumPy. *Nature.* 2020;585:357-362. doi: 10.1038/s41586-020-2649-2
- [9] van der Walt S, Schönberger JL, Nunez-Iglesias J, et al. scikit-image: Image processing in Python. *PeerJ.* 2014;2:e453. doi:10.7717/peerj.453
- [10] Virtanen P, Gommers R, Oliphant TE, et al. SciPy 1.0: fundamental algorithms for scientific computing in Python. *Nat Methods.* 2020;17(3):261-272. doi:10.1038/s41592-019-0686-2

- [11] Badan Pengawas Tenaga Nuklir. Peraturan Badan pengawas Tenaga Nuklir Nomor 2 Tahun 2018 tentang Uji Kesesuaian Pesawat Sinar-X Radiologi Diagnosik dan Intervensial. Bapeten: Jakarta, Indonesia. 2018.
- [12] INTERNATIONAL ATOMIC ENERGY AGENCY. Quality Assurance Programme for Computed Tomography: Diagnostic and Therapy Applications, IAEA Human Health Series No. 19. IAEA: Vienna. 2012.
- [13] Anam C, Amilia R, Naufal A, Budi WS, Maya AT, Dougherty G. Automated measurement of CT number linearity using an ACR accreditation phantom. *Biomed Phys Eng Express*. 2023;9(1):017002. doi:10.1088/2057-1976/aca9d5
- [14] Anam C, Amilia R, Naufal A, Sutanto H, Dwihapsari Y, Fujibuchi T, Dougherty G. Impact of Noise Level on the Accuracy of Automated Measurement of CT Number Linearity on ACR CT and Computational Phantoms. *J Biomed Phys Eng*. 2023;13(4):353-362. doi:10.31661/jbpe.v0i0.2302-1599
- [15] Anam C, Amilia R, Naufal A, Ali MH. Automatic measurement of CT number in the ACR CT phantom and its implementation to investigate the impact of tube voltage on the measured CT number. *Rad Phys Chem*. 2024;216:111434. doi:10.1016/j.radphyschem.2023.111434
- [16] Anam C, Triadyaksa P, Naufal A, Arifin Z, Muhlisin Z, Setiawati E, Budi WS. Impact of ROI size on the accuracy of noise measurement in CT on computational and ACR phantoms. *J Biomed Phys Eng*. 2022;12(4):359-368. doi:10.31661/jbpe.v0i0.2202-1457
- [17] Anam C, Naufal A, Sutanto H, Adi K, Dougherty G. Impact of iterative bilateral filtering on the noise power spectrum of computed tomography images. *Algorithms*. 2022;15(10):374. doi:10.3390/a15100374
- [18] Setiawan AMB, Anam C, Hidayanto E, Sutanto H, Naufal A, Dougherty G. Comparison of noise-power spectrum and modulation-transfer function for CT images reconstructed with iterative and deep learning image reconstructions: An initial experience study. *Pol J Med Phys Eng*. 2023;29(2):104-112. doi:10.2478/pjmpe-2023-0012
- [19] Greffier J, Si-Mohamed S, Frandon J, et al. Impact of an artificial intelligence deep-learning reconstruction algorithm for CT on image quality and potential dose reduction: A phantom study. *Med Phys*. 2022;49(8):5052-5063. doi:10.1002/mp.15807
- [20] Li Y, Jiang Y, Liu H, et al. A phantom study comparing low-dose CT physical image quality from five different CT scanners. *Quant Imaging Med Surg*. 2022;12(1):766-780. doi:10.21037/qims-21-245
- [21] Anam C, Fujibuchi T, Budi WS, Haryanto F, Dougherty G. An algorithm for automated modulation transfer function measurement using an edge of a PMMA phantom: Impact of field of view on spatial resolution of CT images. *J Appl Clin Med Phys*. 2018;19(6):244-252. doi:10.1002/acm2.12476
- [22] Anam C, Fujibuchi T, Haryanto F, Budi WS, Sutanto H, Adi K, Muhlisin Z, Dougherty G. Automated MTF measurement in CT images with a simple wire phantom. *Pol J Med Phys Eng*. 2019;25(3):179-187. doi:10.2478/pjmpe-2019-0024
- [23] Anam C, Haryanto F, Widita R, Arif I, Dougherty G. An investigation of spatial resolution and noise in reconstructed CT images using iterative reconstruction (IR) and filtered back-projection (FBP). *J Phys: Conf Ser*. 2019;1127:012016. doi:10.1088/1742-6596/1127/1/012016
- [24] Anam C, Ainurrofik N, Sutanto H, Naufal A, Haekal M. Rectangular and radial region of interests on the edge of cylindrical phantom for spatial resolution measurement. *Indonesian J Elec Eng Comp Sci*. 2023;31(2):747-754. doi:10.11591/ijeecs.v31.i2.pp747-754
- [25] Hak EZ, Anam C, Budi WS, Dougherty G. An improvement in automatic MTF measurement in CT images using an edge of the PMMA phantom. *J Phys: Conf Ser*. 2020;1505(1):012039. doi:10.1088/1742-6596/1505/1/012039
- [26] Samei E, Bakalyar D, Boedeker KL, et al. Performance evaluation of computed tomography systems: Summary of AAPM Task Group 233. *Med Phys*. 2019;46(11):e735-e756. doi:10.1002/mp.13763
- [27] Setiawati E, Anam C, Widayarsi W, Dougherty G. The quantitative effect of noise and object diameter on low-contrast detectability of AAPM CT performance phantom images. *Atom Indonesia*. 2023;49(1):61-66. doi:10.55981/aij.2023.1228
- [28] Insiano DA, Anam C, Hidayanto E, Naufal A, Maya AT. Optimal Threshold for Automatic Slice Thickness Measurement using Images of the American College of Radiology (ACR) CT Accreditation Phantom. *Int J Sci Res Sci Tech*. 2022;9(6):437-444. doi:10.32628/IJSRST229651
- [29] Anam C, Amilia R, Naufal A, Dougherty G. Algorithm development for automatic laser alignment assessment on an ACR CT phantom and its evaluation of sixteen CT scanners. *Biomed Phys Eng Express*. 2023;9:067002. doi:10.1088/2057-1976/acff76
- [30] Noviliawati R, Anam C, Sutanto H, Dougherty G, Mak'ruf MR. Automatic validation of the gantry tilt in a computed tomography scanner using a head polymethyl methacrylate phantom. *Pol J Med Phys Eng*. 2021;27(1):57-62. doi:10.2478/pjmpe-2021-0008

Contacts of the corresponding author:

Author: Choirul Anam
 Institute: Diponegoro University
 Street: Jl. Prof. Soedarto SH, Tembalang
 City: Semarang, Central Java
 Country: Indonesia
 Email: anam@fisika.fsm.undip.ac.id

BOOK REVIEW

TRUE TALES OF MEDICAL PHYSICS: INSIGHTS INTO A LIFE-SAVING SPECIALTY

By JACOB VAN DYK

Geoffrey S. Ibbott ^{1,2}

¹ Professor and Chair Emeritus, UT MD Anderson Cancer Center, Houston, Texas, USA.

² Associate Executive Director, American Board of Radiology, Tucson, Arizona, USA.

I. BOOK DETAILS

True Tales of Medical Physics: Insights into a Life-Saving Specialty

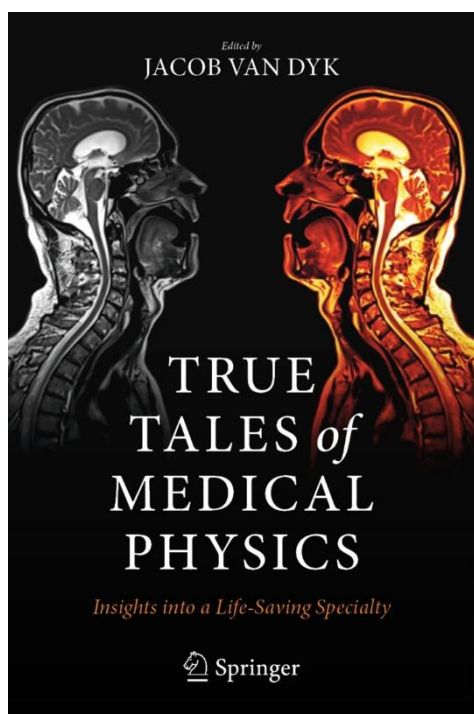
Author/Editor: Jacob Van Dyk

Publisher: Springer Nature, Switzerland

Soft cover or eBook: 575 pages

ISBN: 978-3-030-91723-4

978-3-030-91724-1 (eBook)



But in fact, the first person whose job title was “medical physicist” was none of these admittedly legendary pioneers, but a French physician called Jean-Noel Hallé (1754-1822). He was appointed the first Professor of Medical Physics and Hygiene at the Paris École de Santé (School of Health) in 1794, more than 100 years before Roentgen’s report of his discovery. The term “medical physics” itself had been coined long before that, in 1719, and appeared in print as the title of a journal: *Les Mémoires de Médecine et de Physique Médicale*, in 1779. The journal published accounts of general physics in medicine, including reports of the use of electricity and magnetism. The founder of the journal, Félix Vicq d’Azyr, was instrumental in reforming French medical education, including the teaching of general physics and medical physics as one of the important basic sciences. The reform, and Hallé’s appointment, led to the recruitment of physicists to teach in medical schools, and the publication in the early 1800s of textbooks containing “medical physics” in the titles. Hallé developed a curriculum that included general physics with applications in medicine, including temperature, light, electricity, and magnetism.

I learned this fascinating history of our profession from one of the first chapters in this new book by Professor Jacob van Dyke of Western University in London, Ontario, Canada. The chapter was written by Professor David Thwaites and is spellbinding in its description of the applications of physics in medicine, going back to the earliest recorded history of medicine itself. This chapter is representative of the remainder of the book. Each chapter is written by a medical physicist of note who, in one way or another, answers the question we’ve all been asked: “what is a medical physicist?”

II. REVIEW

Many of us equate the origins of medical physics with the discovery of x rays by Wilhelm Conrad Roentgen in 1895. Indeed, we might think of Roentgen as the first medical physicist, as Juan del Regato clearly did in his book *Radiological Physicists*. [1] Roentgen is the subject of the first chapter, with Marie Curie, Max Planck and Ernest Rutherford following in the second through fourth chapters, respectively.

Professor van Dyk tells us that the contributors to the book are all award-winning medical physicists whose recollections will give the reader an unusual insight into the field. As such, the book, while educational and entertaining for practicing medical physicists, also will be of value to people who have a passing acquaintance with the field, such as the friends and relatives of medical physicists. It also will be enlightening for members of the public, particularly those who anticipate undergoing a medical procedure such as diagnostic imaging or radiation

therapy, or perhaps have recently done so. By reading about the work of the medical physicist, as told by those physicists themselves, they will gain an appreciation and a personalization of the field, rendering it far less opaque than it probably seems to many of them.

Some of the contributors used this opportunity to describe their own entry into the field. For example, I learned that while in high school, Marcel van Herk built a working computer based on a recycled Intel 8080 chip and programmed it to solve chess problems. He would have entered a computer science program in college, had it been available in Amsterdam, but instead studied physics because, as he explains “physics is such a wide field ... it teaches problem solving more than specific topics”. At an early point in graduate school, van Herk investigated research options and chose to work with a medical physicist at the Netherlands Cancer Institute who was building an electronic x-ray imager. The project allowed van Herk to combine his interests in physics and computer science and clearly led to the work in imaging and treatment planning for which he is known. By the way, van Herk’s high-school computer is still functional, having been upgraded numerous times with parts acquired from flea markets and cast-offs from various sources.

Other contributors take a different approach, such as Arthur Boyer, who described a typical day in life, his life, as a medical physicist. He relates a representative day early in his career, driving to work in San Antonio, reviewing the class he would be teaching to the radiology residents later that day. After arriving at work, he finalized some shielding calculations he had prepared for a proposed addition to the cancer center, requiring occupied space to be constructed over the linac vaults. He attended his regular weekly meeting with the medical director of the cancer center, who was Boyer’s boss, to discuss minor staffing issues and also a new project; the replacement of one of the institute’s cobalt units with a linear accelerator. This presented another shielding problem. He also spent part of that day with a colleague, refining their development of the superposition convolution algorithm in dose calculations. Boyer credits his introduction to, and consequent familiarity with this algorithm to his education in fast Fourier transforms while a graduate student at Rice University in Houston.

Cari Borrás recalls a day in her professional life that was anything but typical and describes it as “the scariest day of my life.” She explains how, in 1989, early in her career with the Pan American Health Organization, she was assigned to travel to El Salvador as part of a PAHO mission to investigate a radiation accident at an industrial irradiator. The fact that the unfamiliar device was not a medical irradiator was just the beginning of a series of rather terrifying events; amplified by the uncertainty arising from a decrepit and unsafe facility, and the lack of

security associated to a visit to a country in the 10th year of a bloody civil war. Her investigation of the accident involved interviewing several of the operators who had received high doses and had been evacuated to a hospital in Mexico. She describes driving through San Salvador in a taxi whose driver had to change directions frequently to avoid the sounds of gunfire. She arrived at the airport early in the morning, as advised by the airline, only to find the doors locked and to hear the sounds of approaching troops. Scary indeed!

It might be interesting to determine how many medical physicists have performed some sort of public service, as medical physics, like all of medicine, is a “giving” profession. Stephen Thomas is certainly an example, having served in the Peace Corps while taking a sabbatical from graduate school. Dr. Thomas writes that he spent two years in Ghana, Africa, teaching physics in one of the secondary schools in the capital, Accra. A section of Thomas’s chapter is devoted to his volunteer experiences, which were mostly very positive, and his time immersed in a country embroiled in unrest leading to a military coup, from which he emerged unscathed but educated to life in a country far from his home.

In his own chapter, van Dyk describes a laundry cart that played a critical role in the construction of the first cobalt unit to deliver patient treatments, and another laundry cart that was employed to measure tissue-air ratios in large field sizes from one of the subsequent clinical cobalt units. These measurements were needed for calculations of dose to patients receiving hemi-body or total-body therapy. Once completed, the measurements were used to extend the TAR data in tables published in supplements of the British Journal of Radiology. The BJR supplements were relied upon widely by medical physicists for treatment planning calculations as, at the time, scanning water phantoms were expensive and uncommon. While all of this seems improbable, I leave it to the reader to learn just how a lowly piece of hospital hardware could have figured so significantly in the early days of megavoltage radiation therapy.

The book is loosely organized by topic, with chapters covering similar aspects appearing in appropriately-named sections, although there is naturally some overlap and random assortment of discussions. For example, the chapters by both Thwaites and van Dyk appear in a section called “Medical Physics: More than History”. The chapter by Boyer is grouped with several others in a section called “Medical Physics: More than Clinical Service, while those by Thomas and van Herk are grouped under “Medical Physics: More than Research” and Borrás’s chapter is one of several in “Medical Physics: More than Protection of the Public”.

The remaining sections are called “More than Teaching” and “More than Commercial Developments”. The authors not mentioned above include Peter R. Almond, Gary T. Barnes, James A. Purdy, John W. Wong, Paul L. Carson, C. Clifton Ling, Terry M. Peters, Carlos E. de Almeida, Arun Chougule, Jerry J Bastista, Thomas Kron, Martin Yaffe, Aaron Fenster, Maryellen L. Geiger, Thomas “Rock” Mackie, and Radhe Mohan.

The book can be read cover-to-cover, but of course one can jump from one author to another, as each chapter stands on its own. Each contributor describes both the scientific aspects of note that defined his or her career, the principles that guided their work, and the seemingly random and often surprising events that led to their entry into the field. This glimpse into the personal lives of some of our senior

colleagues is fascinating, and learning how they navigated the events, sometimes challenges, of their early careers offers a window into their personalities that most of us might never experience otherwise. This book is highly entertaining and recommended reading for those interested in learning a little about medical physics and what medical physicists do, as well as for those who have spent their careers in the field.

III. REFERENCE

Radiological Physicists, by Juan A. del Regato, MD. American Institute of Physics, New York, NY. 1985.

INFORMATION FOR AUTHORS



PUBLICATION OF DOCTORAL THESIS AND DISSERTATION ABSTRACTS

A special feature of Medical Physics International (online at www.mpijournal.org) is the publication of thesis and dissertation abstracts for recent graduates, specifically those receiving doctoral degrees in medical physics or closely related fields in 2010 or later. This is an opportunity for recent graduates to inform the global medical physics community about their research and special interests.

Abstracts should be submitted by the author along with a letter/message requesting and giving permission for

publication, stating the field of study, the degree that was received, and the date of graduation. The abstracts must be in English and no longer than 2 pages (using the MPI manuscript template) and can include color images and illustrations. The abstract document should contain the thesis title, author's name, and the institution granting the degree.

Complete information on manuscript preparation is available in the INSTRUCTIONS FOR AUTHORS section of the online journal: www.mpijournal.org.

INSTRUCTIONS FOR AUTHORS

The goal of the new IOMP Journal Medical Physics International (<http://mpijournal.org>) is to publish manuscripts that will enhance medical physics education and professional development on a global basis. There is a special emphasis on general review articles, reports on specific educational methods, programs, and resources. In general, this will be limited to resources that are available at no cost to medical physicists and related professionals in all countries of the world. Information on commercial educational products and services can be published as paid advertisements. Research reports are not published unless the subject is educational methodology or activities relating to professional development. High-quality review articles that are comprehensive and describe significant developments in medical physics and related technology are encouraged. These will become part of a series providing a record of the history and heritage of the medical physics profession.

A special feature of the IOMP MPI Journal will be the publication of thesis and dissertation abstracts for will be the publication of thesis and dissertation abstracts for recent doctoral graduates, specifically those receiving their doctoral degrees in medical physics (or closely related fields) in 2010 or later.

MANUSCRIPT STYLE

Manuscripts shall be in English and submitted in WORD. Either American or British spelling can be used but it must be the same throughout the manuscript. Authors for whom English is not their first language are encouraged to have their manuscripts edited and checked for appropriate grammar and spelling. Manuscripts can be up to 10 journal pages (approximately 8000 words reduced by the space occupied by tables and illustrations) and should include an unstructured abstract of no more than 100 words.

The style should follow the template that can be downloaded from the website at:

http://mpijournal.org/authors_submitpaper.aspx

ILLUSTRATIONS SPECIAL REQUIREMENTS

Illustrations can be inserted into the manuscript for the review process but must be submitted as individual files when a manuscript is accepted for publication.

The use of high-quality color visuals is encouraged. Any published visuals will be available to readers to use in their educational activities without additional approvals.

REFERENCE WEBSITES

Websites that relate to the manuscript topic and are sources for additional supporting information should be included and linked from within the article or as references.

EDITORIAL POLICIES, PERMISSIONS AND APPROVALS

AUTHORSHIP

Only persons who have made substantial contributions to the manuscript or the work described in the manuscript shall be listed as authors. All persons who have contributed to the preparation of the manuscript or the work through technical assistance, writing assistance, financial support shall be listed in an acknowledgements section.

CONFLICT OF INTEREST

When they submit a manuscript, whether an article or a letter, authors are responsible for recognizing and disclosing financial and other conflicts of interest that might bias their work. They should acknowledge in the manuscript all financial support for the work and other financial or personal connections to the work.

All submitted manuscripts must be supported by a document (form provided by MPI) that:

- Is signed by all co-authors verifying that they have participated in the project and approve the manuscript as submitted.
- Stating where the manuscript, or a substantially similar manuscript has been presented, published, or is being submitted for publication. Note: presentation of a paper at a conference or meeting does not prevent it from being published in MPI and where it was presented can be indicated in the published manuscript.
- Permission to publish any copyrighted material, or material created by other than the co-authors, has been obtained.
- Permission is granted to MPI to copyright, or use with permission copyrighted materials, the manuscripts to be published.
- Permission is granted for the free use of any published materials for non-commercial educational purposes.

**MEDICAL PHYSICS INTERNATIONAL
INSTRUCTION FOR AUTHORS**

A. FamilyName¹, B.C. CoauthorFamilyName², D. CoauthorFamilyName¹

¹ Institution/Department, Affiliation, City, Country
² Institution/Department, Affiliation, City, Country

Abstract— Paper abstract should not exceed 300 words. Detailed instructions for preparing the papers are available to guide the authors during the submission process. The official language is English.

Keywords— List maximum 5 keywords, separated by commas.

I. INTRODUCTION

These are the instructions for preparing papers for the Medical Physics International Journal. English is the official language of the Journal. Read the instructions in this template paper carefully before proceeding with your paper.

II. DETAILED INSTRUCTIONS

Paper Size: A4

Length: The maximum document size is usually 8 pages. For longer papers please contact the Editor(s).

Margins: The page margins to be set to: "mirror margins", top margin 4 cm, bottom margin 2,5 cm, inside margin 1.9 cm and outside margin 1.4 cm.

Page Layout: 2 columns layout.

Alignment: Justified.

Fonts: Times New Roman with single line spacing throughout the paper.

Title: Maximum length - 2 lines. Avoid unusual abbreviations. Font size - 14 point bold, uppercase. Authors' names and affiliations (Institution/Department, City, Country) shall span the entire page.

Indentation: 8 point after the title, 10 point after the authors' names and affiliations, 20 point between author's info and the beginning of the paper.

Abstract: Font - 9 point bold. Maximum length - 300 words.

Style: Use separate sections for introduction, materials and methods, results, discussion, conclusions, acknowledgments and references.

Headings: Enumerate Chapter Headings by Roman numbers (I, II, etc.). For Chapter Headings use ALL CAPS. First letter of Chapter Heading is font size 12, regular and other letters are font 8 regular style. Indents - 20 point before and 10 point after each Chapter Heading. **Subchapter Headings** are font 10, italic. Enumerate Subchapter Headings by capital letters (A., B., etc.). Indents

- 15 point before and 7,5 point after each Subchapter Heading.

Body Text: Use Roman typeface (10 point regular) throughout. Only if you want to emphasize special parts of the text use *Italics*. Start a new paragraph by indenting it from the left margin by 4 mm (and not by inserting a blank line). Font sizes and styles to be used in the paper are summarized in Table 1.

Tables: Insert tables as close as possible to where they are mentioned in the text. If necessary, span them over both columns. Enumerate them consecutively using Arabic numbers and provide a caption for each table (e.g. Table 1, Table 2, ...). Use font 10 regular for Table caption, 1st letter, and font 8 regular for the rest of table caption and table legend. Place table captions and table legend above the table. Indents - 15 point before and 5 point after the captions.

Table 1 Font sizes and styles

Item	Font Size, pt	Font Style	Indent, points
Title	14	Bold	Aft: 5
Author	12	Regular	Aft: 10
Authors' info	9	Regular	Aft: 20
Abstract	9	Bold	
Keywords	9	Bold	
Chapters			
Heading - 1 st letter	12	Regular	Before: 20
Heading - other letters	8	Regular	Aft: 10
Subchapter heading	10	Italic	Before: 15, Aft: 7,5
Body text	10	Regular	First line left: 4mm
Acknowledgment	8	Regular	First line left: 4mm
References	8	Regular	First line left: 4mm
Author's address	8	Regular	
Tables			
Caption, 1 st letter	10	Regular	Before: 15
Caption - other letters	8	Regular	Aft: 5
Legend	8	Regular	
Column titles	8	Regular	
Data	8	Regular	
Figures			
Caption - 1 st letter	10	Regular	Before: 15
Caption - other letters	8	Regular	Aft: 5
Legend	8	Regular	

MANUSCRIPT PROPOSALS

Authors considering the development of a manuscript for a Review Article can first submit a brief proposal to the editors. This should include the title, list of authors, an abstract, and other supporting information that is appropriate. After review of the proposal the editors will consider issuing an invitation for a manuscript. When the manuscript is received it will go through the usual peer-review process.

Figures: Insert figures where appropriate as close as possible to where they are mentioned in the text. If necessary, span them over both columns. Enumerate them consecutively using Arabic numbers and provide a caption for each figure (e.g. Fig. 1, Fig. 2, ...). Use font 10 regular for Figure caption, 1st letter, and font 8 regular for the rest of figure caption and figure legend. Place figure legend beneath figures. Indents - 15 point before and 5 point after the captions. Figures are going to be reproduced in color in the electronic versions of the Journal, but may be printed in grayscale or black & white.

'REFERENCES': Examples of citations for Journal articles [1], books [2], the Digital Object Identifier (DOI) of the cited literature [3], Proceedings papers [4] and electronic publications [5].

III. CONCLUSIONS

Send your papers only in electronic form. Papers to be submitted prior the deadline. Check the on-line Editorial Process section for more information on Paper Submission and Review process.

ACKNOWLEDGMENT

Format the Acknowledgment headlines without numbering.

REFERENCES

The list of References should only include papers that are cited in the text and that have been published or accepted for publication. Citations in the text should be identified by numbers in square brackets and the list of references at the end of the paper should be numbered according to the order of appearance in the text.

Cited papers that have been accepted for publication should be included in the list of references with the name of the journal and marked as "in press". The author is responsible for the accuracy of the references. Journal titles should be abbreviated according to Engineering Index Inc. References with correct punctuation.

Equations: Write the equation in equation editor. Enumerate equations consecutively using Arabic numbers

$$A + B = C \quad (1)$$

$$X = A \times e^t + 2lkt \quad (2)$$

Items/Bullets: In case you need to itemize parts of your text, use either bullets or numbers, as shown below:

- First item
- Second item

1. Numbered first item
2. Numbered second item

References: Use Arabic numbers in square brackets to number references in such order as they appear in the text. List them in numerical order as presented under the heading

Contacts of the corresponding author:

Author:
Institute:
Street:
City:
Country:
Email:

SUBMISSION OF MANUSCRIPTS

Manuscripts to be considered for publication should be submitted as a WORD document to:

Francis Hasford, Co-editor: haspee@yahoo.co.uk

Sameer Tipnis, Co-editor: tipnis@musc.edu

BOOK OF ABSTRACTS

The MPI (Vol. 11 No. 2, 2023) features two books of abstracts:

Book of Abstracts of the 26th International Conference on Medical Physics (ICMP 2023)
held in Mumbai, India, from 06 – 09 December 2023

&

Book of Abstracts from the International Centre for theoretical Physics (ICTP)
Master of Medical Physics (MMP) programme

ANNEX 1

BOOK OF ABSTRACTS
of the
INTERNATIONAL CONFERENCE ON
MEDICAL PHYSICS
(ICMP-2023)
Mumbai, India
December 06 – 09, 2023



International Organization for Medical Physics



26th International Conference on Medical Physics



AMPICON 2023 **AOCMP 2023** **ISEACOMP 2023**

Theme: Innovations in Radiation Technology & Medical Physics for Better Healthcare

December 6th - 9th 2023, DAE Convention Centre, Anushaktinagar, Mumbai, India

BOOK OF ABSTRACTS



Conference Organizing Committee

Chairs

Dr. Dinesh Kumar Aswal
Director, HS&EG, BARC, Mumbai

Dr. John Damilakis
President, IOMP

Co-chairs

Dr. B. K. Sapra
Head, RP&AD, BARC

Dr. Sunil Dutt Sharma
President, AMPI

Dr. Eva Bezak
President, AFOMP

Dr. Chai Hong Yeong
President, SEAFOMP

Members

Dr. Magdalena Stoeva
Secretary General, IOMP

Dr. Vellaiyan Subramani
Secretary, AMPI

International Advisory Committee

Chair: Dr. Eva Bezak, President, AFOMP, Australia

Dr. Ehsan Samei, USA	Dr. Singaravelu Ganesan, India	Dr. Jatinder R. Palta, USA
Dr. Arun Chougule, India	Dr. Stephanie A. Parker, USA	Dr. Loredana Marcu, Romania
Dr. Beckham Wayne, Canada	Dr. Mohamed Metwaly, UK	Dr. Hasin Anupama Azhari, Bangladesh
Dr. Annalisa Trianni, Italy	Dr. Youngyih Han, South Korea	Dr. Annemari Groenewald, South Africa
Dr. Naoki Hayashi, Japan	Dr. Francis Hasford, Ghana	Dr. Erick Hernandez, Guatemala
Dr. Samuel Inyang, Nigeria	Dr. Renato Dimenstein, Brazil	Dr. Meshari Alnuaimi, Kuwait
Dr. Jose Luis Rodriguez, Chile	Dr. Hassan Kharita, Qatar	Dr. Patricia Mora, Costa Rica
Dr. Ng Kwan Hoong, Malaysia	Dr. Deepak Dattatray Deshpande, India	Dr. Anchali Krisanachinda, Thailand
Dr. Kulandaivel Muthuvelu, India	Dr. Freddy Haryanto, Indonesia	Dr. B. Paul Ravindran, India
Dr Ram Kishan Munjal, Delhi		



Scientific Program Committee

Co-chairs: Dr. M. Mahesh, USA, Dr. Sunil Dutt Sharma, India, Dr. Shigekazu Fukuda, Japan

Coordinators: Dr. Rajesh Kumar, India, Dr. Sudesh Deshpande, India

Members

Dr. Kalpana M. Kanal, USA	Dr. Delmar Arzabal, Philippines	Dr. Renato Dimenstein, Brazil
Dr. Nhu Tuyen Pham, Vietnam	Dr. Meshari Al Nuaimi, Kuwait	Dr. Melvin Chew Ming Long, Singapore
Dr. Lorenzo Brualla, Germany	Dr. Ashok Kumar Bakshi, India	Dr. Chris Trauernicht, South Africa
Dr. Biplab Sarkar, India	Dr. Stephanie A. Parker, USA	Dr. Sai Subramanyam, India
Dr. Taku Inaniwa, Japan	Dr. N. V. N. Madhusudanan Sresty, India	Dr. Vanessa Panettieri, Australia
Dr. Raghavendra Holla, India	Dr. Yoonsun Chung, South Korea	Dr. Pratik Kumar, India
Dr. Tsi Chian Chao, Taiwa	Dr. K. M. Ganesh, India	Dr. Chris Boyd, Australia
Dr. Nagesh Bhat, India	Dr. Yong Yin, China	Dr. Henry Finlay, India
Dr. Hui-Yu Tsai, Taiwan	Dr. Abhijit Mondal, India	Dr. Taweap Sanghanthum, Thailand
Dr. Ghanshyam Sahani, India	Dr. Supriyanto Ardjo Pawiro, Indonesia	Dr. Saju Bhasi, India
Dr. Aik Hao Ng, Malaysia	Dr. Lakshmi Santanam, USA	

Publication Committee

Chair: Dr. A. S. Pradhan, India

Members:

Dr. T. Ganesh, India	Mr. Lalit Chaudhary, India	Dr. Francis Hasford, Ghana
Dr. Subhalakshmi Mishra, India	Dr. Mohammed Hassan Kharita, Qatar	Dr. Nobuyuki Kanematsu, Japan
Dr. Satish Pelagade, India	Dr. Md. Akhtaruzzaman, Bangladesh	Mr. P. Shaju, India
Dr. Emily Simpson-Page, Australia	Mr. Yogesh Ghadi, India	Dr. Hafiz Zin, Malaysia
Ms. Melanie Marquez, Philippines	Dr. Jeannie Wong, Malaysia	



International Organization for Medical Physics



Finance Committee

Co-chairs: Dr. Ibrahim Duhaini, Treasurer, IOMP and Dr. Sridhar Sahoo, Treasurer, AMPI

Members:

Dr. Shigekazu Fukuda, Japan	Mr. Suresh Chaudhari, India	Dr. Byungchul Cho, South Korea
Dr. Mahendra More, India	Dr. Kitiwat Khamwan, Thailand	Dr. Sudhir Kumar, India
Dr. A. Pichandi, India	Mr. Anand Jadhav, India	Dr. Pramod Kumar Sharma, India
Mr. Anand Pinjarkar, India		

Exhibition Committee

Co-chairs: Ms. Kalpana Thakur, India, Dr. Lukmanda Evan Lubis, Indonesia

Members:

Dr. Siva Sarasandarajah, Australia	Mr. Rahul Kumar Chaudhary, India	Mr. Md Jobairul Islam, Bangladesh
Dr. Hideyuki Mizuno, Japan	Mr. Ath Vanyat, Cambodia	Dr. Laurentcia Arlany, Singapore
Dr. Narender Singh Rawat, India	Mr. Changadev Tahakik, India	

LOCAL ORGANIZING COMMITTEE

Organising Secretary: Dr. Rajesh Kumar (BARC) and Dr. Shobha Jayaprakash (AMPI)

Treasurer: Dr. Nitin Kakade, RPAD, BARC

Jt. Treasurer: Mr. Ankit Srivastava, RPAD, BARC

Members:

Dr. Jayanta Pal, Kolkata	Dr. Raj Kishor Bisht, New Delhi	Dr. T. Anil Kumar, Hyderabad
Dr. P. Senthilmanikandan, Bangalore	Dr. G. Bharanidharan, Chennai	Mr. Rahul Phansekar, Rajkot
Mrs. Usha Nair, Mumbai	Mr. Heigrujam Malhotra, Delhi	

National Advisory Committee

Dr. K. N. Govinda Rajan, Coimbatore	Dr. P. G. G. Kurup, Thiruvanthapuram	Mr. S. P. Agarwal, Mumbai
Dr. B. S. Rao, Mumbai	Dr. Jitendra Kumar Singh, Patna	Dr. J. P. Agarwal, Mumbai
Dr. K. Raghuram Nair, Thiruvanthapuram	Dr. S. P. Mishra, Lucknow	Dr. A. K. Shukla, Lucknow
Dr. Ramesh Desai, Gurgaon	Dr. Kamlesh Passi, Ludhiana	Mr. Deepak Arora, New Delhi
Dr. K. Krishna Reddy, Hyderabad	Dr. M. Ravi Kumar, Bengaluru	Dr. D. C. Kar, Mumbai
Dr. Apurba Kabassi, Kolkata	Dr. Arabinda Kumar Rath, Bhubaneswar	Dr. Bedangadas Mohanty, Bhubaneswar
Dr. M. M. Musthafa, Kozhikode	Dr. Manoj Kumar Semwal, New Delhi	Dr. Pradeep Kumar Hota, Cuttack

National Organizing Committee

Dr. M. S. Kulakarni, Mumbai	Dr. Anil Kumar Bansal, New Delhi	Mr. Probal Chaudhury, Mumbai
Dr. Satish Uniyal, Dehradun	Dr. A. Vinod Kumar A, Mumbai	Dr. Oinam Arun Singh, Chandigarh
Dr. P. K. Dash Sharma, Mumbai	Dr. Rituraj Upreti, Mumbai	Mr. Alok Srivastava, Mumbai
Dr. N. Vijayaprabhu, Puducherry	Dr. T. Palani Selvam, India	Dr. Suwendu Kumar Sahoo, Cuttack
Dr. P. Tandon, Mumbai	Dr. D. R. Mishra, Mumbai	Dr. Ajay Kumar Srivastava, Meerut
Mr. Arshad T. Khan, Mumbai	Dr. P. Kaliyappan, Chennai	Mr. E. Rajadurai, Bangalore
Dr. L. M. Agarwal, Varanasi	Dr. C. P. Bhatt, New Delhi	Dr. S. S. Sanaye, Mumbai
Dr. A. Sathish Kumar, Vellore	Dr. P. Aruna, Chennai	Dr. Niyas Puzhakkal, Kozhikode
Dr. J. Velmurugan, Chennai	Dr. S. Karthikeyan, Bangalore	Dr. Vinod Kumar Dangwal, Patiala
Dr. Arvind Shukla, Udaipur	Dr. K. J. Maria Das, Lucknow	Dr. Anuj Tyagi, Agra
Dr. Challapalli Srinivas, Mangalore	Dr. Hemant Ghare, Nagpur	Dr. Sanjeev Vashisht, Bhopal
Dr. Anil Kumar Maurya, Prayagraj	Dr. K. Chithra, Noida	Dr. Navin Singh, Lucknow
Dr. Jibon Sharma, Guwahati	Dr. Vinod Pandey, Haldwani	Dr. Raghu Kumar, Thiruvananthapuram
Dr. Malik Mohib-ul-Haq, Srinagar	Dr. Alok Kumar, Kolkata	Dr. Sathiyam Swaminathan, Bangalore
Dr. Dilip Kumar Ray, Kolkata	Mr. Parimal Patwe, Nagpur	Dr. Dayanand Sharma, Chennai
Dr. Gopi Shankar, New Delhi	Dr. E. Varadharajan, Chennai	Ms. Debolina Mukherjee, Mumbai
Dr. C. Sureka, Coimbatore	Dr. Santosh Kumar, Patna	Dr. K. R. Muralidhar, Hyderabad
Mr. Raghubansh Kumar, Patna		



Accommodation and Transport Committee

Mr. S. M. Pradhan, Mumbai – **Coordinator**

Dr. Bhushan Dhabekar, Mumbai – **Co-coordinator**

Dr. Anuj Soni, Mumbai	Dr. Sandeep Kanse, Mumbai	Mr. R. S. Vishwakarma, Mumbai
Mr. Ravi Chilkulwar, Mumbai	Mr. Munir Pathan, Mumbai	Mr. S. Jalaluddin, Mumbai
Mr. Mukesh Uke, Mumbai	Dr Rajib Lochan Sha	Dr Bibekananda Mishra
Shri Pramod Kumar Dixit		

Registration Committee

Ms. Philomina Akhilesh, Mumbai – **Coordinator**

Dr. Kirti Tyagi, Mumbai	Dr. Usha Yadav, Mumbai	Mr. Kishore Joshi, Mumbai
Ms. Susain Kasturi Samuel, Mumbai	Ms. Arpana Siwach, Mumbai	Ms. Shatabdi Chakraborty, Mumbai
Ms. Madhumita Bhattacharya, Mumbai	Ms. Rama Prajapati, Mumbai	

Catering Committee

Mr. Sanjeev N. Menon, Mumbai – **Coordinator**

Dr. Sridhar Sahoo, Mumbai – **Co-coordinator**

Ms. Kshama Srivastava, Mumbai	Dr. Rajesh Kumar Chaurasiya, Mumbai	Mr. Sandipan Dawn, Mumbai
Mr. Neeraj Dixit, Mumbai	Mr. Arghya Chattaraj, Mumbai	Dr. Reena Sharma, Mumbai

Hall Management Committee

Ms. Rupali Pal, Mumbai – **Coordinator**

Ms. Vandana Srivastava, Mumbai – **Co-coordinator**

Dr. Manish Joshi, Mumbai	Dr. Rosaline Mishra, Mumbai	Ms. Reena Ph, Mumbai
Mr. Ankit Srivastava, Mumbai	Mr. G. G. Gaware, Mumbai	Ms. Mariyam, Mumbai
Ms. Sonal Kadam, Mumbai		



**ABSTRACTS OF
INTERNATIONAL CONFERENCE ON MEDICAL PHYSICS 2023**

**HELD AT
DAE CONVENTION CENTRE, ANUSHAKTINAGAR
MUMBAI 400094, INDIA**

DECEMBER 6 - 9, 2023

ABSTRACTS OF ORAL PRESENTATIONS

DOSIMETRIC COMPARISON OF GATED VERSUS FREE BREATHING TECHNIQUES FOR LUNG STEREOTACTIC BODY RADIOTHERAPY

Amalu Hanna Alex, ZheniaGopalakrishnan, SajuBhasi, P. Raghukumar

¹Division of Radiation Physics, Regional Cancer Centre, Thiruvananthapuram

Email: amaluhanna.rcc@gmail.com

BACKGROUND/PURPOSE: Respiratory gating has shown increasing evidence of reducing volumes of irradiated normal lung tissue during Stereotactic Body Radiotherapy (SBRT). The technique involves the delivery of radiation only during a pre-determined portion (gating window) of the breathing cycle. The aim of this study was to compare the dosimetric differences between non-gated (free breathing) versus gated treatments in SBRT lung treatments.

MATERIALS/METHODS: Treatment plans of twenty lung SBRT cases treated using ITV generated in free breathing condition with dose prescription 48Gy/4 for 15 cases and 50Gy/5 for 5 cases were used for the study. These cases were re-planned with the same dose prescription in 4DCT images with ITV generated from Maximum Intensity Projection (MIP) images generated by selecting all phases (RA_MIP_ALL) and that generated by selecting 30% (mid-exhale) - 70% (mid-inhale) phases (RA_MIP_30-70) of the patient's breathing cycle. PTV was generated by adding a 5mm margin to ITV. Dose to critical organs involved was assessed and compared based on RTOG 0915/0813 Protocols.

RESULTS: There was a significant reduction in ITV and PTV volume, which was decreased from 30.98±26.24cc to 17.46±17.72cc and 65.97±44.57cc to 44.29±32.33cc respectively (p-value: <0.001) in gated plans. PTV coverage and mean dose to PTV in both the cases were same. D_{2%}(Gy), D_{95%}(Gy) and D_{50%}(Gy) of the PTV and conformity and homogeneity index of the plans were comparable while gradient measure and R_{50%} showed a significant difference between the RA_MIP_ALL and RA_MIP_30-70 plans (p-value: <0.001). For gated plans, mean lung dose has been reduced by 1.11Gy (p-value <0.001) and volume of normal lung receiving 20Gy, 10Gy and 5Gy in percentage were found to be reduced significantly. All the gated plans were characterized by a reduction in dose for heart, esophagus, bronchus and ribs (p-value: <0.05) except for spine, skin and great vessels. The Monitor Units (MU) calculated in both plans were found to have no significant difference.

CONCLUSION: Phase selection for gated SBRT treatments allows a significant reduction in ITV and PTV, while maintaining similar PTV coverage, and lower doses to critical organs. Thus gated treatment is a useful method to account for respiratory motion in lung SBRT.

KEYWORDS: Stereotactic Body Radiotherapy, Respiratory Gating.

ACCURACY OF EXTERNAL TUMOUR MOTION MONITORING IN LIVER SABR: RESULTS FROM THE TROG 17.03 LARK TRIAL

Chandrima Sengupta¹, Doan T Nguyen¹, Trevor Moodie², Alicja Kaczynska¹, Daniel Mason³, Trent Causer³, Sau F Liu⁴, Tim Wang², Yoo Y Lee⁴, Kirsten V Gysen³, R O' Brien⁵, Paul J Keall¹

¹Image X Institute, University of Sydney, Australia, ²Crown Princess Mary Cancer Centre, Australia, ³Nepean Cancer Care Centre, Australia, ⁴Princess Alexandra Hospital, Australia, ⁵RMIT University, Australia.

Email: Chandrima.Sengupta@sydney.edu.au

BACKGROUND: Image guidance in liver SABR utilises several motion management strategies including external surface markers or spirometry-based systems to try to achieve accurate treatment delivery. However, external surrogates may not be well correlated with the internal liver tumour motion. The aim of this work was to investigate the accuracy of the external motion monitoring for liver radiotherapy compared to an intrafraction internal tumour motion monitoring technology.

MATERIALS AND METHODS: A real-time image-guided tumour motion monitoring technology named Kilovoltage Intrafraction Monitoring (KIM) was commissioned for tumour motion monitoring for 14 liver cancer patients in the multi-institutional TROG LARK trial on standard Varian TrueBeam (9 patients) and Elekta linear accelerators (5 patients). Patients received treatments in one of four treatment schedules: 3×17Gy, 5×10Gy, 5×8Gy, 5×6.5Gy either in breath-hold or using free-breathing techniques. During treatment, if the patient motion was outside a set threshold in KIM (3mm/5mm for 5 secs), a couch shift was performed to correct for the motion. External surface position monitoring (Varian RPM) or spirometry (Elekta ABC) was simultaneously used to measure the patients' motion. To evaluate gating accuracy of the external surrogate, the percentage of the treatment the tumour motion would have been outside the KIM threshold but within the RPM/ABC threshold was evaluated. Pearson's correlation coefficients between KIM and RPM signals for every treatment fraction were then evaluated.

RESULTS: For breath-hold treatments, motion greater than 10 mm was detected by KIM in 14% of treatment fractions, however, this was not detected by standard-of-care external surrogates. The proportion of the treatment when the tumour was out of the KIM threshold but within the RPM/ABC threshold varied across patients and fractions ranging from 0% to 92% for the RPM system (mean±std=34±33%) and 0% to 100% for the ABC system (mean±std=45±35%). There was a high variability in the correlation coefficients between KIM and RPM across different fractions with mean±std=-0.1±0.3 for breath-hold patients and =-0.1±0.6 for free-breathing patients.

CONCLUSIONS: This work indicates the potential false assurance of using traditional external surrogate to assess tumour motion in liver SABR patients demonstrating the importance of real-time internal motion monitoring in liver radiotherapy.

KEYWORDS: intrafraction liver tumour motion monitoring, motion management

Presentation ID: O-003

Abstract ID: Y5016

CARDIAC ABLATIVE SBRT FOR TREATING VENTRICULAR TACHYCARDIA - A CASE STUDY

Sambasivaselli R¹, KarthikeyanN¹, SenniandavarV², SaurabhaKumar¹, Naveen VigneshJ¹

¹Narayana Health Ltd, Bangalore, India,

²Sri Mata Vaishno Devi NarayanaSuperspeciality HospitalKatra, Jammu

Email: Sellismash@Gmail.Com

BACKGROUND: Ventricular Tachycardia (VT) refers to a type of abnormal heart rhythm that originates from ventricles and is difficult to manage or control with standard treatments, such as medications or repeated catheter ablation. Cardiac Stereotactic body radiation therapy (SBRT) is a novel technique with capability of delivering high doses of radiation to the target with sub-millimeter accuracy for the treatment of refractory VT patients. This has demonstrated decrease in arrhythmia episodes with favourable short term safety profile. This study discusses the feasibility of cardiac SBRT as a treatment option with our initial experience

MATERIALS: A 44 years old male patient presented with a history of refractory VT with implantable cardioverter defibrillator (ICD). After failure of standard treatment, in view of large left ventricular thrombus, hemodynamically unstable VT, SBRT was considered. Patient was immobilized with vacuum bags with the assistance of respiratory gating. A CT scan of 2mm slice thickness was acquired for the planning purpose. The target volume was delineated with the help of cardiac MRI fused with planning CT images and approved by electrophysiologist. A margin of 5mm was given to target volume to grow PTV and a VMAT plan was generated using 6FFF beam in Monaco V5.5.1 TPS.

RESULTS/DISCUSSION: A dose of 25Gy in single fraction was prescribed. The dose distribution with 95% of prescribed dose coverage to 95% of the target volume was achieved. By using TG 101 dose constraints for single fraction, dose to the heart was restricted to prevent grade 3+ pericarditis. The D15cc to Heart-PTV was <21Gy. Patient specific QA performed to ensure the 95% gamma passing rate with 2% 3mm criteria. Post CBCT verification and correction using Hexapod 6D couch, the treatment was delivered in 15 minutes with total of 11115.4 MU's.

CONCLUSION: Non-Invasive cardiac radioablation has proven to be a valid new therapeutic options for the refractory VT patients. In the modern treatment era, with the help of advanced imaging modalities, treatment modalities and sophisticated software along with high definition cardiac imaging, Cardiac SBRT can be considered as a front line alternative therapy for refractory VT patients

KEYWORDS: SBRT, Cardiac radioablation, Ventricular Tachycardia, Quality assurance, treatment planning.

A RETROSPECTIVE DOSIMETRIC COMPARISON OF TG-43 BASED ALGORITHM AND COMMERCIALY AVAILABLE ADVANCED COLLAPSED CONE ENGINE (ACE) BASED ON TG-186 FOR PATIENTS UNDERGOING APBI USING Co-60 HDR BRACHYTHERAPY

AlkaKataria, ArindamPujari, Sanju, Sanjay Barman, VinaySaini, Narender Kumar,
Ashutosh Mukherjee, SatyajitPradhan

Department of Radiation Oncology, Mahamana PanditMadan Mohan Malaviya. Cancer Centre &Homi Bhabha Cancer Hospital, (Units of Tata Memorial Centre, Mumbai), Varanasi, UP, India

Email: alka@mpmmcc.tmc.gov.in

AIM/BACKGROUND: Currently used Task Group-43 based calculation algorithm does not account for (a) Tissue heterogeneity, (b) Skin/Body surface, and (c) Scattered photon dose deposition, which leads to inaccuracies in resultant dose distribution. The commercially available ACE (Collapsed Cone Calculation) algorithm accounts for above mentioned factors and provides a dose distribution closer to the actual dose distribution. The present study aims to determine how clinically significant the differences in the results, of these two algorithms, are for APBI patients.

MATERIALS AND METHODS: This study involves the treatment plans of 20 patients planned on OncentraBrachy (v4.6). Plans were calculated using two algorithms, (a) TG-43 based Algorithm and (b) ACE by Elekta, based on TG-186. Contours (Body, Lungs, Ribs, CTV, Skin, Heart, etc.) were drawn on the planning CTs, and mass density, type of material, and priority was also assigned to all the contours. All plans originally calculated with TG-43, were recalculated using 'Standard' accuracy with TG-186 based CCC algorithm (MBDCA) with the Oncentra TPS integrated with Graphics Processing Unit (GPU). Differences in the result were evaluated based on PTV coverage (V90, V100), Volume of high dose (V150, V200), and Dose Volume Histogram(DVH) for different Organs at Risk (OARs) such as Heart, Rib, Lungs, Skin, etc. Wilcoxon signed-rank test was used to determine the median differences in the clinical indices V90, V100, V150, V200, and highest-dosed 0.1 cm³ and 1.0 cm³ of rib, heart, and lung, while comparing the two algorithms.

RESULTS: Statistically significant ($p < 0.05$) differences were observed in the values of clinically relevant DVH parameters of PTV and OAR, except for the volume of high doses. Differences of PTV were relatively small with a slight overestimation of dose by the TG-43 algorithm. The average dose difference for PTV, V100, and V90 were 1.7%±0.8 and 2.1%±0.7, respectively, and for OARs i.e., Lung, Ribs, Heart, and Skin were of the order of 1.2%, 2.3%, and 1.8%, and 2.13% respectively.

CONCLUSIONS: ACE calculates the dose with better accuracy than TG-43, especially for regions with significant tissue heterogeneity. Significant differences in the isodoses were seen at the larger distances from the source, i.e. dose deposited by scattered components of photons. Currently, TG-186 dose calculation should be reported along with TG-43 until we obtain studies with larger cohorts to realize the potential of MBDCA dosimetry fully.

KEYWORDS: Oncentra, Collapsed Cone calculation algorithm, TG-43, TG-186, APBI, Advanced Collapsed Cone Engine.

VALIDATION OF SIGMOID POINTS FOR SIGMOID DOSE ACCUMULATION AND REPORTING FOR MULTIFRACTIONATED BRACHYTHERAPY FOR CERVICAL CANCER

Kamalnath J¹, Anjana A K¹, Kunal Prajapati², Prachi Mittal¹, Ankita Gupta¹, Nisarga Vontikoppal Manjunath¹, Jeevanshu Jain², Subhajit Panda², Supriya Chopra²

¹Department of Radiation Oncology and Medical Physics, Tata Memorial Hospital, Tata Memorial Centre, HomiBhabha National Institute, Mumbai, Maharashtra, India,

²Department of Radiation Oncology, Advanced Centre for Treatment Research and Education in Cancer, Tata Memorial Centre, HomiBhabha National Institute, Mumbai, Maharashtra, India

Email: kamalnathmphy@gmail.com

OBJECTIVE: Consistent localization of high-dose regions in sigmoid during multi-fractionated brachytherapy (BT) for locally advanced cervical cancer (LACC) is challenging. This work aims to validate effective sigmoid points (SP1 and SP2) which have been previously described in literature¹ and are proposed surrogates for reporting sigmoid D_{2cc} doses.

MATERIALS AND METHODS: Consecutive patients who were previously treated for LACC with (chemo)radiation and multifractionated HDR brachytherapy in clinical trials from 2018 to 2022 were evaluated. Sigmoid points¹ 1 (SP1) and 2 (SP2) (SP1=0.5cm right, 1.5cm posterior, and 2.5cm cranial to cervical os along the body axis; SP2=0.5cm anterior and 4.5cm cranial to cervical os along the body axis) were assigned on the treated BT plans. The correlation between SP1 and SP2 with sigmoid $D_{0.1cc}$ and D_{2cc} doses was analyzed, and the effect of type of applications (ICA and ISBT) was also studied.

RESULTS: One hundred and sixteen CT/MR data sets of intracavitary (ICA) and interstitial BT (ISBT) applications from 62 patients were analysed. Different applicators used were tandem-ovoid (n=49), tandem-ring (n=22), Vienna with needles (n=18), and Venezia (n=27) applicators. On visual inspection, in 64% of applications the proposed SP1 points lied inside or in vicinity of sigmoid as compared to SP2 points, that were within or in close vicinity of sigmoid structures only 18% of times. Since SP2 did not lie in sigmoid, the point was discarded and only calculation with SP1 was done. For the entire cohort, the median difference between D_{2cc} and SP1 was 1.33 Gy (95% CI [1.29Gy-1.71Gy]) and between $D_{0.1cc}$ and SP1 was 1.43Gy (95%CI [1.41 Gy-1.84Gy]). For the subset of ICA applications, the median difference between D_{2cc} and SP1 was 1.11 Gy (95% CI [1.06 Gy-1.47 Gy]) and for $D_{0.1cc}$ with SP1, the median difference was 1.38 Gy (95% CI [1.28Gy-1.74Gy]). Similarly, for ISBT application, the median difference from D_{2cc} was 1.67 Gy (95% CI [1.47 Gy-2.39 Gy]) and for $D_{0.1cc}$ 1.59 Gy (95% CI [1.39Gy-2.27Gy]). It was observed that SP1 positively correlates with D_{2cc} ($p=0.014$) and $D_{0.1cc}$ ($p=0.023$) and acts surrogate for D_{2cc} and $D_{0.1cc}$ sigmoid doses statistically.

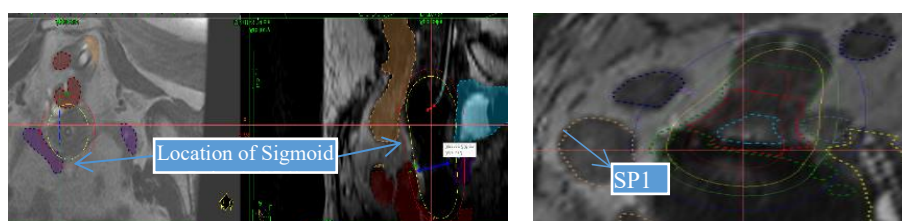


Figure 1: The Figure indicates the positions of SP1 point in two different patients

CONCLUSION: Our result shows, that SP1 point shows a correlation with D_{2cc} and $D_{0.1cc}$ of sigmoid doses and can be considered as an anatomically reproducible surrogate and may possibly be of utility to correlate sigmoid doses and clinical outcomes in future studies.

KEYWORDS: Sigmoid reference point, gynecological brachytherapy, cervical cancer

REFERENCE:1. Bindal A, Mittal P, Shinghal A, Scaria L, Prajapati K, Swamidas J, Gurram L, Berger D, Sturdza A, Chopra S. Sigmoid dose accumulation and reporting for multifractionated brachytherapy for cervical cancer: Methodological development of sigmoid points through virtual endoscopic method. *Brachytherapy*. 2023 May-Jun;22(3):325-333. doi: 10.1016/j.brachy.2023.01.003. Epub 2023 Mar 5. PMID: 36882345.

A DOSIMETRIC COMPARISON OF CT/MR MULTICHANNEL APPLICATOR VERSUS SINGLE CHANNEL CYLINDER FOR THE TREATMENT OF GYNAECOLOGICAL CANCERS WITH HIGH DOSE RATE BRACHYTHERAPY

Anjana A K¹, Kamalnath J¹, Ankita Gupta¹, Jeevanshu Jain², Prachi Mittal¹, Supriya Chopra²

¹Department of Radiation Oncology and Medical Physics, Tata Memorial Hospital, Tata Memorial Centre, Homi Bhabha National Institute, Mumbai, Maharashtra, India,

²Department of Radiation Oncology, Advanced Centre for Treatment Research and Education in Cancer, Tata Memorial Centre, Homi Bhabha National Institute, Mumbai, Maharashtra, India

Email: anjanaanil0070@gmail.com

AIM: This study was conducted to analyse and compare the dosimetric characteristics of the vaginal CT/MR multichannel applicator (Elekta/Nucletron) with the conventional single channel cylindrical applicator (CVS) used for gynaecological brachytherapy.

MATERIALS AND METHODS: Brachytherapy plans of patients with gynaecological cancers treated at our centre with CT/MR multichannel applicator were retrieved from the database. For each patient, an in-silico plan was created on the same dataset, simulating the effect of the conventional single channel cylindrical applicator by keeping active dwell positions only in the intravaginal cylinder, while removing all dwell positions in the surface channels. Brachytherapy planning was done on the ONCENTRA v4.6.2 treatment planning system. Dose optimization was performed by keeping CTV D90% same between both plans to appreciate the possible dose variation in the organs at risk (OARs). Total equivalent dose in 2 Gy fractions (EQD2) was calculated for the rectum (D_{2cc}), bladder (D_{2cc}), sigmoid (D_{2cc}) and bowel (D_{2cc}) and compared between the two plans using student t test. Pvalue < 0.05 was considered as statistically significant.

RESULT: Twenty-one patients with cervical (14), vaginal (7) and endometrial (4) cancer were treated using the multichannel applicator between June 2021 and July 2023. Seventeen patients with history of prior hysterectomy were treated using the intravaginal cylinder with surface channels, while 4 patients with intact uterus were treated using an additional intrauterine tube. All patients received EBRT to a dose of 45-50.4 Gy in 1.8-2 Gy per fraction. Brachytherapy dose prescription ranged from 4-7 Gy per fraction for 4-5 fractions. Mean D_{2cc} (EQD_{2,3Gy}) for bladder, rectum, sigmoid and bowel were 73.3 Gy, 71.2 Gy, 57 Gy and 54.7 Gy, respectively with the multichannel applicator, and 74 Gy, 75.3 Gy, 58 Gy and 55.4 Gy, respectively with single channel. For the same target dose, consistently lower doses were obtained for all OARs with the multichannel applicator, with statistically significant reduction in doses to the rectum (P=0.00).

CONCLUSION: Utilization of multichannel applicator for gynaecological brachytherapy gives a dosimetric advantage over conventional single channel cylinder by giving freedom of optimization and hence sparing the OARs, with significant reduction in rectal dose.

KEYWORDS: Vaginal brachytherapy, CT/MR Multichannel applicator, Single Channel Cylinder, Cervical Cancer, vaginal cancer, endometrial cancer.

Presentation ID: O-007

Abstract ID: B7540

ESTABLISHMENT OF LOCAL DIAGNOSTIC REFERENCE LEVELS FOR ADULT 18-F FDG-WHOLE-BODY PET/CT EXAMINATION AT SQCCRC, MUSCAT, OMAN

Noura Al Makhmari¹, Zakyia Awlad Thani², Naema Al Maymani¹, Subhash Kheruka¹, Huoda Al Saidi¹, Sana Al Rashdi¹, Khulood AL Riyami¹

¹Radiology and Nuclear Medicine Department, Sultan Qaboos Comprehensive Cancer Care and Research Centre, ²College of Science, Sultan Qaboos University

Email: nmakhmari90@gmail.com

BACKGROUND: The optimization of radiation exposure and patient safety is paramount in the field of nuclear medicine. Diagnostic Reference Levels (DRLs) serve as crucial benchmarks for evaluating and optimizing radiation doses in nuclear medicine imaging. By establishing local DRLs, institutions can enhance radiological protection practices and provide essential guidance for new departments to adhere to these standardized levels.

OBJECTIVE: This study aimed to establish DRLs for adult 18-F FDG-Whole-Body PET/CT Examination using a digital PET/CT (Vision 600 Siemens) at the Sultan Qaboos Comprehensive Cancer Care and Research Center (SQCCRC) in Muscat, Oman.

METHODS: Data were collected from a representative sample of 130 patients undergoing 18-F FDG-Whole-Body PET/CT examinations. The administered activity of radiopharmaceuticals, CT index dose (CTDI) and scan length product (DLP) were carefully recorded. The DRLs were set at 75th percentile of the radiopharmaceutical administered activity, CTDI and DLP of the collected examinations. Additionally, the effective dose per examination was calculated following the recommendations of the International Commission on Radiological Protection (ICRP).

RESULTS: The survey successfully established the DRLs for commonly performed PET/CT procedures at SQCCRC. The determined DRL values are 18-F FDG Activity :217.79 MBq, CTDI: 8.11 mGy and DLP : 756.4 for the administered activity and CT radiation dose respectively. The average effective dose was 15.83 ± 2.72 mSv for PET/CT examination. comparable to Korea, Japan, and Kuwait.

CONCLUSION: The determined DRL values for 18-F FDG activity and effective dose at SQCCRC provide essential benchmarks for evaluating and optimizing radiation doses during PET/CT examinations, ensuring patient safety.

KEYWORDS: Diagnostic reference levels, PET/CT, patient safety, Vision 600 Siemens, whole body PET/CT

Presentation ID: O-008

Abstract ID: H3381

^{99m}Tc-MDP BONE SCAN IMAGE DENOISING USING TRIMMED MEAN FILTER

Abhishek Kumar Karn, Anil Kumar Pandey, Chetan Patel, Rakesh Kumar

Department of Nuclear Medicine, All India Institute of Medical Sciences, New Delhi, India

Email: abhishekkumarkarn1230@gmail.com

BACKGROUND/OBJECTIVE: In routine nuclear medicine practice, ^{99m}Tc-MDP images are noisy. The amount of random noise varies from image to image depending on the photon statistics. In the presence of random noise, the detectability of the lesions may be compromised. We hypothesize that denoising ^{99m}Tc-MDP bone scan image using trimmed mean filter can improve the detectability of the lesion. Trimmed mean is calculated by dropping a fixed number of sorted values from each end and then taking an average of the remaining values.

MATERIALS AND METHODS: Forty-Nine ^{99m}Tc-MDP images were processed using trimmed mean filter of size 3 × 3, 5 × 5 and 7 × 7 pixels; and dropping the four sorted values (irrespective of the filter size) from both the ends, and then taking the average of the remaining values. The denoised images with 3 × 3 and 5 × 5 and 7 × 7 pixels trimmed mean filter were visually compared to its corresponding input images.

The image which was (very smooth leading least sharpened lesion and very poor differences between inter-costal ribs space and inter vertebral space), (moderate smooth and moderate sharpened lesion and moderate differences between inter-costal ribs space and inter vertebral space) and (least smooth, sharpened lesions and better difference between inter-costal ribs space and inter vertebral space) compared with input images were labeled as **good**, **better** and **best**.

RESULTS: The result of visual assessment is summarized in the Table-1. 45 out of 49 denoised images with 3 × 3 trimmed mean filter were labelled as **best**, and 4 out of 49 were labelled as **better**. 41 out of 49 denoised images with 5 × 5 trimmed mean filter were labelled as **better**, and 8 out of 49 were labelled as **best**. 49 out of 49 denoised images with 7 × 7 trimmed mean filter were labelled as **good**.

Table 1: result of visual assessment of 3 × 3, 5 × 5 and 7 × 7 trimmed mean filtered image

	3 × 3	5 × 5	7 × 7	TOTAL
GOOD	0	0	49	49
BETTER	4	41	0	49
BEST	45	8	0	53
Total	49	49	49	147

CONCLUSIONS: Denoising ^{99m}Tc-MDP bone scan image using 3 × 3 trimmed mean filter improves the detectability of the lesion.

KEYWORDS: Trimmed mean filter, denoising, ^{99m}Tc-MDP bone scan

Presentation ID: O-009

Abstract ID: N4020

AI METHODS TO IMPROVE PERFORMANCE OF A PORTABLE HYBRID GAMMA-OPTICAL CAMERA (HGC) FOR NUCLEAR MEDICINE

Yangfan Jiang¹, Sarah Bugby¹, Georgina Cosma²

¹Department of Physics, Loughborough University, UK,

²Department of Computer Science, Loughborough University, UK

Email: Y.Jiang@lboro.ac.uk

BACKGROUND/OBJECTIVE: Portable small-field-of-view gamma cameras offer advantages in clinical flexibility, patient comfort, and intraoperative imaging capabilities (Farnworth&Bugby, 2023). Real-time image reconstruction is crucial for intraoperative imaging, while automatic feature detection can enhance surgical assistance and enable functionality such as stereoscopic depth estimation (Bugby et al., 2021). Although AI is commonly used in medical imaging, applying pre-trained models directly to real-time gamma images with low signal-to-noise and spatial resolution is not appropriate. This talk will describe the application of AI methods in this challenging scenario.

MATERIALS AND METHODS: The HGC is a handheld scintillator-based hybrid gamma-optical camera (Bugby, 2015). An intelligent light splash detector, named DeepSplashSpotter (DSS) (Jianget al., 2022) was derived by transfer learning a Faster-Region-Based Conventional Neural Network to localize scintillation light splashes. A Monte Carlo model was developed and validated to simulate gamma photon detection in the HGC, generating a sizable dataset of gamma images. This dataset was used to train a deep learning model for automatic localization of gamma sources.

RESULTS: DSS achieves accurate localization of scintillation light splashes (precision: 0.906) and size determination (correlation coefficient: 0.984) at a consistent speed of 21 frames per second. For gamma images, the proposed deep learning model exhibits a source localization accuracy of 0.96 for features (including incomplete features) of various sizes within 4pixels of the ground truth. This implies that in a practical stereoscopic imaging scenario, the maximum distance uncertainty is about 3.5mm and 10mm at imaging distances of 50mm and 120mm, respectively.

CONCLUSIONS: AI deep learning methods have enhanced the performance of the HGC and enabled automatic distance estimation. The techniques presented in this study illustrate the broader application of these methods to low-count gamma imaging.

KEYWORDS: Advance in Emission imaging, Artificial Intelligence and Medical Physics, Modelling and Simulation, Quantitative and Synthetic imaging.

REFERENCES:

1. Farnworth, A. L., & Bugby, S. L. (2023). Intraoperative Gamma Cameras: A review of development in the last decade and Future Outlook. *Journal of Imaging*, 9(5), 102. doi:10.3390/jimaging9050102
2. Bugby, S L, Lees, J. E., McKnight, W. K., & Dawood, N. S. (2021). Stereoscopic portable hybrid gamma imaging for source depth estimation. *Physics in Medicine & Biology*, 66(4), 045031. doi:10.1088/1361-6560/abd955
3. Bugby, S. L. (2015). Development of a hybrid portable medical gamma camera. PhD thesis University of Leicester.

Presentation ID: O-010

Abstract ID: N1530

IMPACT OF PHYSICAL CHARACTERISTICS OF PHOTON-COUNTING DETECTORS ON CT IMAGE QUALITY: A COMPARATIVE STUDY BETWEEN IN-HOUSE CDTE- AND CZT-BASED VIRTUAL PHOTON-COUNTING CT SCANNERS

Mridul Bhattarai^{1,2,3}, Nicholas Felice^{1,2,3}, Raj Kumar Panta^{2,3}, Darin Clark^{2,3}, W. Paul Segars^{1,2,3},
Ehsan Abadi^{1,2,3}, Ehsan Samei^{1,2,3}

Medical Physics Graduate Program, Duke University, USA
Center for Virtual Imaging Trials (CVIT), Duke University, USA
Department of Radiology, Duke University School of Medicine, USA

Email: mridul.bhattarai@duke.edu

BACKGROUND/OBJECTIVE: Photon-counting CT (PCCT) is a spectral CT technology that uses photon-counting detectors (PCDs) made of semiconductor materials such as Cadmium Telluride (CdTe) and Cadmium Zinc Telluride (CZT) to count the number of photons across multiple energy thresholds. Clinically approved CdTe- and prototype CZT-based PCCT scanners are available; however, their comparative evaluation is not cost and time efficient, and they may possess distinct geometrical configurations and image processing mechanisms (proprietary information). An effective approach to assess the effects of detector material on image quality is through virtual imaging, utilizing computational phantom models and scanner simulators to generate scanner-specific images. The purpose of this study was to design CdTe- and CZT-based virtual PCCT systems (DukeCounter) with identical scanner components and compare their task-generic image quality.

METHODS: A Monte-Carlo simulation developed in Geant4 was used to model the interactions between x-ray photons and the detector in 10-140 keV range. Furthermore, charge sharing was applied forming a Gaussian charge cloud at each interaction point and assuming the energy shared between detector elements was proportional to the area of charge cloud projection on those elements. Thus, detector-specific spatio-energetic covariance correlation matrices for 3-mm thick CdTe and CZT were generated. Identical scanner parameters such as projections per rotation, focal spot size, anode angle, detector shape, source-to-isocenter and source-to-detector distances, number of detector rows and channels, and size of a detector element were defined. The computed-matrices and defined-scanner components, including source spectrum, bowtie filter, and anti-scatter grid were integrated with DukeSim, a validated CT simulation platform, to develop virtual CdTe- and CZT-based DukeCounter scanners that generated CT sinograms. The sinograms were reconstructed using an in-house Multi-Channel Reconstruction toolkit. The performance evaluation was done by “scanning” an ACR phantom using both scanners at 150 and 300 mAs.

RESULTS: The average differences (CdTe-CZT) for 150 and 300 mAs acquisitions were the following: noise magnitude -1.96 HU and -0.57 HU, CT number for bone insert -5.94 HU and -6.56 HU, and CT number for acrylic insert 3.92 HU and 1.04 HU.

CONCLUSIONS: CdTe- and CZT-based PCCT with identical scanner components did not have substantial difference in task-generic image quality.

KEYWORDS: photon counting CT, Cadmium Telluride, Cadmium Zinc Telluride, virtual imaging, in silico clinical trails

TOWARDS DOSIMETRY FORMALISM FOR THREE-DIMENSIONAL ROTATIONAL ANGIOGRAPHY (3DRA): MONTE CARLO SIMULATION AND DIRECT MEASUREMENTS

Akbar Azzi¹, Ani Sulistyani¹, Novrizki Daryl Rachman¹, Michael Christian Satrio², HanendyaDisha Randy Raharja³, Lukmanda Evan Lubis^{1,4}

¹Department of Physics, Faculty of Mathematics and Natural Sciences, Universitas Indonesia, Kampus UI Depok 16424, Indonesia,

²Center for Medical Physics and Biophysics, Institute for Applied Sciences, Faculty of Mathematics and Natural Sciences, Universitas Indonesia, Depok 16424, Indonesia,

³Department of Radiology, MRCCC Siloam Hospitals Semanggi, South Jakarta, Jakarta 12930, Indonesia,

⁴Radiology Unit, Universitas Indonesia Hospital, Kampus UI Depok 16424, Indonesia.

Email: akbar.azzi@sci.ui.ac.id

BACKGROUND/OBJECTIVE: This study aims to formulate and validate a dosimetry method for Three-Dimensional Rotational Angiography (3DRA) procedures.

MATERIALS AND METHODS: The study is conducted in two parallel stages, involving Monte Carlo (MC) simulation and direct measurement of dose distribution using relative dosimeters. BEAMnrc was employed to simulate the X-ray tube. Furthermore, five virtual Computed Tomography Dose Index (CTDI) phantoms with various dosimeter positions (center, 3, 6, 9, and 12 o'clock), which irradiated from 200° X-ray tube rotation, were simulated by using DOSXYZnrc user code. For direct measurement, the calibrated dosimeters (thermoluminescence dosimeter (TLD), Gafchromic® XR-QA2 Film, and Gafchromic® XR-RV3 Film) were placed within a cylindrical in-house phantom and irradiated by using a Philips AlluraXper FD20 angiography system in three preset modes. The verified measurement was performed using an ionization chamber (IC) to formulate a dose index for 3DRA, which can serve as a dose metric.

RESULTS: Both simulation and direct measurements showed that the most exposed area to radiation in all three preset modes of 3DRA were located at 3, 6, and 9 o'clock of the phantom. The highest accuracy value was obtained in MC simulation at center position of the Xper CT Cerebral HD mode with a dose different to IC of 0.9%. In contrast, the lowest accuracy was obtained in the Xper CT Cerebral LD mode at the 6 o'clock position with a discrepancy of 647.3%. Among the relative dosimeters used in this study, Gafchromic® XR-RV3 was found to be the most accurate dose distribution with average discrepancy of 33.82% compared to IC.

CONCLUSIONS: MC and measurement based with several detectors showed a different dose distribution of the peripheral positions of CTDI phantom from 3DRA procedures. 3DRA gave a U-shape dose distribution to the CTDI phantom with the highest dose values were observed at the 3, 6, and 9 o'clock positions, while the lowest dose values were recorded at the 12 o'clock position.

KEYWORDS: 3DRA, dose distribution, ionization chamber, Monte Carlo, TLD, radiochromic

Presentation ID: O-012

Abstract ID: X9688

DISPLAY OF BLOOD FLOW DIRECTION AND BLOOD FLOW VELOCITY BY FLOW CT IMAGE

Katsumi Tsujioka

School of Medical Sciences, Fujita Health University, Toyoake-city, Aichi, Japan

Email: tsujioka@fujita-hu.ac.jp

BACKGROUND/OBJECTIVE:It is possible to perform a dynamic volume scan with current CT. However, its display method has not yet been developed, and four-dimensional image diagnosis is difficult. To solve this problem, we developed flow CT imaging. Furthermore, with the latest CT, it has become difficult to display the entire blood vessel due to improved temporal resolution. We solved that problem too with Time MIP and Time Averaging.

MATERIALS AND METHODS:We have developed two types of phantoms. One is a time density curve phantom and the other is a spiral tube phantom. Dynamic volume CT scans were performed on these phantoms. Sequential subtraction was performed on the resulting volumetric dynamic CT dataset. Then color coding was applied. In addition, the CT images were displayed in Time MIP, Time averaging and Time MIP and Time averaging composite display.

RESULTS:With conventional live images, the presence of the contrast agent could be confirmed, but the inflow and outflow of the contrast agent could not be confirmed. The direction of blood flow was easily observed in the sequential subtraction images. When the sequential subtraction image is color-coded, the red area indicates the inflow of the contrast agent, and the blue area indicates the outflow of the contrast agent. The direction of blood flow has become easier to understand by displaying sequential subtraction images with color codes. It performed same as the color doppler in ultrasound. By performing Time MIP and Time averaging display, we were able to observe the entire blood vessel even with a CT device with excellent time resolution.

CONCLUSIONS:Sequential subtraction images enabled us to grasp the direction of blood flow on a single still image. In addition, it can determine which blood vessels are arteries and which are veins. In addition, the direction of blood flow has become easier to understand by displaying sequential subtraction images with color codes. By making full use of Time MIP and Time Averaging, it has become possible to observe the entire blood vessel. Flow CT imaging is a useful technique for clinical diagnosis.

KEYWORDS: X-ray CT, Flow CT image, sequential subtraction, color code display, Time MIP, Time averaging

FEASIBILITY OF IN VIVO DOSIMETRY FOR ADAPTIVE RADIOTHERAPY ASSESSMENT IN HEAD AND NECK CANCER PATIENTS

Parimal Patwe¹, SudeshDeshpande², Gajanan Mahajan³

¹School of Physical Sciences, Swami Ramanand Marathwada University, Nanded, India

²Department of Radiation Oncology, P. D. Hinduja National Hospital, Mumbai, India

³Department of Physics, Shri Datta Arts, Commerce & Science College, Nanded, India

Email: parimal19@gmail.com

BACKGROUND/OBJECTIVE: ART is a promising approach in the treatment of H&N cancer, to account for anatomical changes. This study aims to assess the feasibility of using in vivo dosimetry to quantify the need for ART.

MATERIALS AND METHODS: Retrospectively, 20 post-operative H&N cancer patients treated with VMAT were selected. CBCT images from fractions 1, 5, 10, 15, 20, and 25 were included in this study. The SmartAdapt DIR (Eclipse TPS) software was utilized to register the planning CT (pCT) with these CBCT scans. The contours from the pCT were deformed and propagated to all registered CBCT scans. The original plan (OP) from the pCT was copied and pasted on CBCT. The dose was recalculated for each CBCT scan, and the resulting plans were designated as TP1, TP5, TP10, TP15, TP20, and TP25, respectively. To establish TP1 as the reference plan (RP), it was compared to the OP using the 3DVH in-vivo dosimetry software. A plan matching rate (PMR) of over 90% was considered acceptable. Subsequently, TP5, TP10, TP15, TP20, and TP25 were compared with RP using 3DVH to assess the necessity for ART.

RESULTS: In 3DVH, global gamma analysis was carried out to compare plans, with PMR above 90% for TP5, TP10, and TP15, and below 90% for TP20 and TP25. We also conducted a DVH comparison between RP and other plans, using a paired two-sample Student's t-test to determine statistical significance. The percentage increase in maximum doses for PTV54-1.98% (p- 0.0038) & 2.71% (p-0.0036), spinalcord- 3.67%(p-0.0047) & 4.48%(p-0.0026), brainstem-3.18%(p-0.002) & 3.6%(p-0.0031) and mandible-2.01%(p-0.0022) & 2.79%(p-0.0102) for TP20 and TP25 respectively. The percentage increase in mean doses for PTV60-1.18%(P-0.0031) & 1.78%(p-0.0024), PTV54-1.83%(p-0.0031) & 2.39%(0.0006), Lt Parotid-3.4%(p-0.0006) & 4.31%(p-0.0016), Rt Parotid-2.86%(p-0.0037) & 3.9%(p-0.0003) and larynx-2.21%(p-0.003) & 3.55%(p-0.0035) for TP20 and TP25 respectively.

CONCLUSIONS: PMR results can be correlated with changes in PTV & OAR doses during the course of RT. This study demonstrates the feasibility of using 3DVH software, to assess the need for ART in H&N cancer patients.

ABSTRACT KEYWORDS: Adaptive radiotherapy, CBCT, Gamma Analysis, In-vivo dosimetry

ROLE OF EXIT FLUENCE ACQUIRING AND ANALYSIS IN HALCYON

Pooja Moundekar, V. K.Sathiyarayanan, Raghavendra Holla, Sajini Kurup

Ruby Hall Clinic, Pune, Maharashtra, India

Email: pooja27790@gmail.com

OBJECTIVE: Treatment delivery verification has always been a topic of interest in radiation therapy resulting in some commercial products which can be externally fitted to the conventional C-arm therapy machine and monitor the planned and exit fluence through gantry. Since Halcyon has ring gantry it demands a different approach. Halcyon is equipped with an in-built EPID system which is in line with the beam and continuously acquires exit fluence with full field coverage during patient treatment without user interaction. These images can be retrieved and analyzed to monitor the delivery of planned treatment throughout and can be used as a decision making criteria for adaptive planning or rescan and replan as per the department protocol for the changed anatomy.

METHODS: 10 head and neck patients treated with simultaneous integrated boost technique with doses of 60Gy and 54Gy in 30 fractions were selected retrospectively for this study. For each patient daily treatment transmission, EPID images are automatically updated in the system under the portal dosimetry module. These images were used to create a composite image for plans with two or more arcs. The resulting image was then compared to the reference composite image which is first or second day's treatment transmission image in the portal dosimetry module using gamma index. The criteria for gamma passing is 3%/3mm with threshold of 5% and "field" as an option for region of interest. The images for first three fraction for all the patients were analyzed after which alternate fractions were considered up to 21st fraction for analysis.

RESULTS: 10 head and neck patients with a total of 110 fractions were analyzed for local and global gamma with gamma passing criteria of 3%/3mm. The average local and global gamma were 96.82, SD=4.14 and 97.84, SD=3.38 respectively. 4 of the 10 cases showed gradual drop in the gamma value beyond 15th fraction i.e. three weeks of treatment. The trend was observed both in local and global gamma value. The average local gamma value dropped from 98.82 to 88.4 for the 21st fraction for this set of patients.

Investigating the fractions with the lowest gamma value for the above 4 cases revealed that the setup error for these patients were within acceptable limits hence indicating changes in the patient's anatomy which was also evident in KVCBCT images acquired during treatment.

CONCLUSIONS: Halcyon being equipped with EPID fixed in line with the exit beam and imaging as mandatory criteria for treatment, provides a unique scope for inter-fraction treatment monitoring. By visually monitoring the expected and acquired fluence on that day, we will be able to identify any significant treatment error brought on by the patient's non-cooperation or technical disruptions before conducting any analysis. Analysis of automatically acquired exit fluence images can be utilized to monitor the actual delivery of the treatment course through all the fractions for every patient. This analysis helps in completing the loop of treatment verification giving significant degree of confidence that the planned treatment is delivered within acceptable tolerances. This will help us to detect and address any mid treatment changes attributing to patient's anatomy change such as weight loss or edema in the region of interest or any setup related issues which can be site or diagnosis specific. After 15 fractions, or three weeks of treatment, 40% of the patients showed a significant drop in their gamma passing rate. For this group of patients, the average local gamma value decreased from 98.82 to 88.4 for the 21st fraction, which demanded intervention. All the four cases had noticeable weight loss and were rescanned and replanned for remaining fractions. To obtain the threshold gamma values and other characteristics, however, more research with a larger data set is being undertaken. These factors will aid in the development of better clinical judgements.

KEYWORDS: Halcyon, exit fluence, inter-fraction treatment monitoring.

Presentation ID: O-015

Abstract ID: A5741

THE EVALUATION OF CONTOUR DOSE AND POSITION OF HEART IN THORAX REGION FOR CANCER RADIATION THERAPY

Yeenang Nuttawut¹, Sumanaphan Wanwanat¹, Manila Wannita¹, Homkaenjan Sopa², Pungpeng Bundit²

¹Medical Physics Division, Department of Radiation Oncology, Lampang Cancer Hospital, Thailand.

²Radiation Therapy Division, Department of Radiation Oncology, Lampang Cancer Hospital, Thailand.

Email: nattayee@gmail.com

BACKGROUND/OBJECTIVE: Thorax radiation is a region where organs such as the lung and heart move constantly. Hearts consist of plenty of blood vessels. A miscalculated amount of radiation could yield side effects. Knowing the proper contours and positions of a heart is, therefore, necessary to prevent it from receiving overdosed radiation while evaluating the right amount. The objectives of this study are to evaluate the contour, dose, and positions of the heart as well as an appropriate heart dose evaluation and protection.

MATERIALS AND METHODS: In total, 189 non-contrast media (Non-CM), 4D-CT, and CBCT images of 21 thorax region patients were collected. Non-CM, 4D-CT images were reconstructed from 3D-CT images to obtain the Maximum Intensity Projection (MIP) and Average Intensity Projection (AIP). Then, a radiotherapy was designed for AIP images, and the contour, dose, and position transplanted to all images were calculated using Raystation 11B. The dose on the CT image was obtained by deformable registration of the dose; the mean dose (D_{mean}), V_5 , V_{10} , V_{20} , V_{30} , and V_{40} for the heart dose in AIP, MIP, and Non-CM were compared. For the heart contour in AIP, MIP, Non-CM, and CBCT, and the heart position of inter-fraction in AIP and CBCT.

RESULTS: The size of the heart contour shows that all image sets have statistically significant different sizes from an AIP set (p-value 0.05), from big to small: MIP, AIP, Non-CM, and CBCT, respectively. Dose evaluations of V_5 and V_{40} between the AIP and MIP reveal statistically different results (p-value 0.05). The heart positions show that the changes in heart positions are fewer than 0.2 cm.

CONCLUSIONS: The MIP image suitable for heart contouring for heart dose evaluation has more accuracy. The inter-fraction heart position is stable as the planning contour has coverage.

KEYWORDS: heart contour, thorax region cancer, 4D-CT, radiation therapy, CBCT

Presentation ID: O-016

Abstract ID: D2617

DOSIMETRIC COMPARISON OF GLIOBLASTOMA BRAIN VOLUMETRIC MODULATED ARC THERAPY PATIENTS WITH DIFFERENT CALCULATION GRID SIZES IN ECLIPSE TREATMENT PLANNING SYSTEM

Krishna Chandrasekar¹, Karthik Kumar², Kavya³, Sinchana⁴

¹Department of Radiation Oncology, Mangalore institute of Oncology, Mangalore, India.

Email: krcolinac@gmail.com

BACKGROUND/OBJECTIVE: Volumetric Modulated Radiation therapy (VMAT) has been employed to increase the local tumor control in cancer treatments. Various techniques related to the treatment planning, the beam delivery and the imaging have been developed to achieve a more accurate and conformal dose distribution. To investigate feasible treatment planning parameters, we aimed to evaluate the dosimetric impact of the calculation grid size in the Volumetric Modulated arc therapy (VMAT) plan for Glioblastoma brain patients.

MATERIALS AND METHODS: Twenty patients with Glioblastoma were selected and the treatment plans were initially generated with anisotropic analytical algorithm (AAA) with 2.5 mm grid size and recalculated with 1 mm and 5 mm grid sizes. The later 2 grid sizes plans (1mm and 5 mm) optimisations were run with the same priorities. Dosimetric parameters such as homogeneity index (HI) and conformity index (CI), D95 and doses to OARs such as Lens, Optic Nerve and Brainstem were calculated.

RESULTS: Significant differences were observed in the planning target volume (PTV) coverage between three grid sizes (1mm, 2.5 mm and 5 mm) and the V95%, HI, and CI of the plans were significantly affected by grid. On 1 mm grid, the mean dose of brainstem, optic nerve and lens dose differences were less compared to other 2 grid sizes (2.5 mm and 5 mm) The PTV coverage is less in 5 mm grid size plans compared to other 2 grid sizes (1 mm and 2.5 mm) Compared to 1 mm grid size, the 2.5 mm grid size showed comparable dose calculation accuracy with short calculation time.

CONCLUSIONS: Considering the dose calculation performance for heterogeneous area, we recommend AAA with 2.5 mm grid size for improving treatment efficiency of Glioblastoma brain patients.

KEYWORDS: Treatment planning, Calculation grid size, Glioblastoma VMAT.

Presentation ID: O-017

Abstract ID: F9163

IMPACT OF HIPPOCAMPUS DOSIMETRY PARAMETERS ON NEUROCOGNITIVE FUNCTION IN PROPHYLACTIC CRANIAL IRRADIATION

Suryakanta Acharya^{1,2}

¹Assam Cancer Care Foundation, Lakhimpur Cancer Centre, Lakhimpur, India

²PAY-W Clinic, Nayagarh, India

Email: suryaoncology@gmail.com

BACKGROUND: Small-cell lung cancer (SCLC) is an aggressive type of cancer associated with poor prognosis. Several studies have shown prophylactic cranial irradiation (PCI) to be an independent prognostic factor. Hippocampal sparing (HS) PCI 25 Gy/10 fractions has minimum impact on neuro-cognitive function while Whole Brain RT (WBRT) 30Gy/10 fractions has maximum impact.

METHODS: In this cohort study 10 LS-SCLC patients were administered HS-PCI with IMRT, and same number of patients received WBRT from January 2019 to April 2020. Baseline neuro-cognitive function was measured before administering radiation and final neuro-cognitive function was measured after median follow up of 18 months. Neuro-cognitive function was assessed by Montreal Cognitive Assessment (MoCA) and compared with hippocampus dose in both groups.

RESULTS: Mean hippocampus dose in HS-PCI and WBRT groups are 9.5 Gy and 30.9 Gy respectively. HS-PCI and WBRT group mean pre-treatment MoCA score are 27/30 and 26/30. At the end of 18 months, mean post-treatment MoCA score for the groups are 25/30 and 21/30 respectively.

CONCLUSIONS: WBRT affects neuro-cognitive function more than HS-PCI. Hippocampal sparing as well as lower radiation dose in HS-PCI could be the major factors for this outcome.

KEYWORDS: hippocampus sparing, cognitive function, prophyl

PLANNING LAYOUT AND EQUIVALENT UNIFORM DOSE MEASURES IN HIGH DOSE LATTICE THERAPY TO LARGE AND LOCALLY ADVANCED BLADDER CANCER

Bhagyalakshmi AT^{1,2}, Velayudham Ramasubramanian¹

¹Vellore Institute of Technology, Vellore campus, Katpadi, Tamil Nadu, India

²American Oncology Institute at Baby Memorial Hospital, Indira Gandhi Road, Kozhikode, Kerala, India
Email: bhagyalakshmiat@gmail.com

PURPOSE/BACKGROUND: This study aimed to assess the effects of systematic and random placement patterns of lattices and the effect of the number of lattices on equivalent uniform dose (EUD) in bladder cancer radiotherapy and to determine optimal planning techniques for lattice therapy.

MATERIALS AND METHODS: Seventy treatment plans were generated for 5 bladder cancer patients with extensive disease. Three sets of plans (for PTV and HD-lattices) were created using Rapid Arc (RA) and Intensity Modulated Radiation Therapy (IMRT) techniques, nine and seven field arrangements. EUD was calculated using the Niemierko equation for plans with systematic and random lattice placement patterns and different numbers of lattices. The relationship between EUD and the number of lattices, as well as the effect of placement pattern on EUD change, were analyzed using composite RA plans.

RESULTS: Comparable dose distributions were observed among the techniques, with the PTV receiving the full prescription dose as follows: RA plans, 96.2%; 7-field IMRT plans, 94.6%; and 9-field IMRT plans, 95.7%. The conformity index values were 0.88, 0.86, and 0.87, for RA, 7-field IMRT, and 9-field IMRT, respectively. The HD-lattice plans had conformity index of 0.72. The RA plans demonstrated superior dose fall-off compared to the IMRT plans. The introduction of lattices resulted in a linear increase in the EUD, with no significant difference between systematic and random lattice placement ($p = 0.151$).

CONCLUSION: All three techniques- RA, 7-field IMRT, and 9-field IMRT-yielded comparable dose distributions in terms of PTV coverage; however, in the context of organ sparing 9 field IMRT gave better results. Both systematic and random lattice placement strategies improve the EUD, with random placement showing a slightly higher EUD. Random placement of lattices also helped to reduce the dose to normal structures, as lattices can be placed while avoiding Organ at Risks (OARS). These results will contribute to optimizing treatment plans and enhancing the effectiveness of lattice therapy in bladder cancer radiotherapy.

KEYWORDS: Lattice therapy, EUD, dose fall off, high dose, placement pattern

Presentation ID: O-019

Abstract ID: D9811

RADIOBIOLOGY FOR PERSONALIZED RADIOTHERAPY OF EARLY AND INTERMEDIATE PROSTATE CANCER

Narimane Dahdouh¹, Zine El Abidine Chaoui^{1,*}, Ismail Zergoug²

¹Laboratory of optoelectronics and devices, ²Clinique Oncopolel'espoir, Oran, Algeria

Email: zchaoui@univ-setif.dz

BACKGROUND/OBJECTIVE: Radiobiological evaluation remains one of the development paths to further optimize and personalize radiotherapy treatments. The aim of this study is to predict in a precise and personalized way the early and late effects caused by high energy photon beams in healthy tissues for early and intermediate prostate cancer cases treated with VMAT. Furthermore, to suggest alternate fractionation schedules to reduce the period of treatment.

MATERIALS AND METHODS: We have modelled a robust and fast inhouse program to compute radiobiological models; namely the RS (Relative Seriality), LKB (Lyman-Kutcher-Burman), LM (Logit Model), SP (Simple Poisson) and MP (modified Poisson) to calculate NTCP (normal tissue complication probability), TCP (tumour control probability)^{1,2}, UTCP (uncomplicated tumour control probability) and an effective optimized tool for isotoxic plans ³. Several endpoints of the major dose-limiting organ are evaluated to predict early and late effects. Included are comparison Radbiomode and Biosuite¹ software.

RESULTS: NTCP perfectly model the difference between the dose constraints for the three models RS, LKB and LM. The RS models the late and early effects better. The TCP values calculated with the three models MP, SP and LM showed good local control of the tumour after planification (greater than 90%). Our optimization tool, based on alternate fractionation and isotoxic plans, has been applied and reduced effectively the late effects.

CONCLUSIONS: Present radiobiological calculations show exactly which organ is very sensitive and critical in the treatment plan validation unlike the dosimetric indices. Our optimization tool for isotoxic plans revealed to be powerful and possible to be applied as a personalized radiotherapy tool to predict alternate fractionation and reducing the fraction number.

KEYWORDS: radiobiological models; NTCP; UTCP; TCP; Fractionation

REFERENCES:

1. Chang JH et al. RADBIOMOD: A simple program for utilising biological modelling in radiotherapy plan evaluation. *Physica Medica*. 2016 ; 32 : 248- 254. doi: 10.1016/j.ejmp.2015.10.091
2. Shuryak I et al. Optimized Hypofractionation Can Markedly Improve Tumor Control and Decrease Late Effects for Head and Neck Cancer. *Int J Radiation Oncol Biol Phys*. 2019 ; 105 : 231-232. doi: 10.1016/j.ijrobp.2019.02.025
3. Semenenko V A et al. Lyman–Kutcher–Burman NTCP model parameters for radiation pneumonitis and xerostomia based on combined analysis of published clinical data. *Phys. Med. Biol*. 2008 ; 53 : 737- 755. doi: 10.1088/0031-9155/53/3/014

Presentation ID: O-020

Abstract ID: D1032

DEVELOPMENT OF COLLAPSED CONE DOSE CALCULATION ALGORITHM FOR BHABHATRON-II TELECOBALT MACHINE

SaiSirisha Nadiminti¹, Munir S Pathan², Mahesh Punna¹, S Padmini¹,
T. Palani Selvam^{2,3}, Rajesh Kumar^{2,3}

¹Electronics Division, Bhabha Atomic Research Centre, Mumbai

²Radiological Physics & Advisory Division, Bhabha Atomic Research Centre, Mumbai

³Homi Bhabha National Institute, Anushaktinagar, Mumbai

Email: nsirisha@barc.gov.in

BACKGROUND/OBJECTIVE: Bhabhatron-II is a telecobalt radiotherapy machine developed by BARC. Radiotherapy is facilitated using the software called Treatment Planning System (TPS), in which the dose calculation algorithms form an integral part. The model-based dose calculation algorithms provide a balance between performance and accuracy, in which the Total Energy Released per Unit Mass (TERMA) is convolved with the dose deposition kernel. The model-based dose calculation algorithm, namely, Collapsed Cone Convolution (CCC) approximates the kernel in the form of cones from the point of interaction, reducing the time taken to calculate dose without compromising on accuracy. Algorithm was augmented with features to support the development of TPS for Bhabhatron-II.

MATERIALS AND METHODS: In the developed algorithm, fluence is calculated based on the three-source model approach, which considers point source, annular source, and exponential source to account for primary photons, scatter from the primary collimator and leakage through collimation system. A binary block plane is modelled to account for the field size which is smoothed using a gaussian filter considering the finite size of the ⁶⁰Co source. The source strength and the Gaussian filter were fitted according to the field size. The curvature correction in the fluence is done to account for the increase in isodose curvature for large field sizes which is unique to telecobalt radiotherapy. TERMA is calculated by considering energy lines for ⁶⁰Co source and is convolved with Monte Carlo-based pre-calculated energy deposition kernels to calculate dose. The calculated dose profiles are in good agreement with the measured dose profiles in the test phantoms.

RESULTS: The clinically relevant parameters such as field size, left and right penumbra width, flatness and maximum deviation derived from the calculated dose profiles are within the acceptable limits.

CONCLUSIONS: The results indicate that the CCC algorithm is well suited for implementation in the TPS for Bhabhatron-II telecobalt machine.

KEYWORDS: Treatment Planning System, telecobalt radiotherapy, dose calculation, collapsed cone convolution

ASSESSMENT OF TREATMENT PLANNING AND DOSIMETRIC UNCERTAINTIES IN HIP PROSTHESIS CASES ON TOMOTHERAPY

Pawan Kumar Singh^{1,6}, Rohit Verma¹, Deepak Tripathi⁵, Sukhvirsingh³, Manindra Bhushan²,
Lalit Kumar⁴, Soumitra Barik²

¹Department of Physics, Amity Institute of Applied Sciences, Amity University (AUUP), Noida, India.

²Division of Medical Physics & Department of Radiation Oncology, Rajiv Gandhi Cancer Institute and
Research Centre, New Delhi (India).

³Radiological Physics & Internal Dosimetry Group, Institute of Nuclear Medicine & Allied Sciences, Defence
Research & Development Organisation Timarpur, Delhi.

⁴Department of radiation oncology, Max super speciality hospital, Saket, New Delhi-India.

⁵Department of Physics, USAR, Guru Govind Singh University, Suraj mal Vihar, New Delhi

⁶Medical Physics, Department of Radiation Oncology, Vardhman Mahavir Medical College and Safdarjang
Hospital Delhi, India

Email:pawansingh786125@gmail.com

BACKGROUND: The metal prosthesis creates errors in treatment planning and delivery due to artifacts created by the high Z materials. Therefore, the dosimetric variations must be studied for hip prosthesis cases.

MATERIALS & METHODS: 10 Patients with a hip prosthesis suffering from cervix carcinoma were simulated, in the head-first supine position, on a Sensation Open CT simulator with a 5 mm slice thickness and thermoplastic masks. The PTV, CTV, femur, implanted femur, bladder, posterior bladder wall, rectum, rectum wall and bowel structures were drawn. The Accuray Precise TPS generated two Helical IMRT treatment plans for 45Gy in 25 fractions for delivery on the Tomotherapy machine. Plan1 had no beam restriction, and Plan2 was the plan with restricted beam entry through the metallic implant. The cylindrical phantom (length = 21cm, diameter = 20 cm) of Perspex, with implants of two stainless steel metal rods, was used. The phantom was scanned on the CT simulator. The chamber volume was contoured as a target. 20 OSLD chips were staged at different positions in the phantom to read the delivered doses after treatment. The contours drawn on the phantom were similar to the patient's anatomy marking the target and organs. The phantom plans were delivered under the guidance of MVCT.

RESULTS: No significant variations in the dosimetric parameters were evaluated for Plan1 and Plan 2. The treatment time increases significantly from Plan1 417.6 ± 89.3 sec to Plan2 433.4 ± 108.4 sec (P value = 0.03). The TPS doses compared with OSLD measured doses for the phantom, the TPS underestimated the bladder doses by 3.5% in Plan1 and 5.4% in Plan2, bladder wall doses were overestimated by -6.3% in Plan1 and underestimated by Plan2 by 7.4%, rectum wall doses were underestimated by 4.3%, 4.3% by Plan1 and Plan2 respectively. The rectum doses were overestimated by Plan1 -1.6% and underestimated by Plan2 3.4%.

CONCLUSION: The dosimetric analysis of two different planning methods did not affect the plan quality in TPS. However, a significant variation in the planned and measured doses in the phantom suggests the careful handling of patients with implants.

Keywords: Metallic implant, Tomotherapy, Helical IMRT, OSLD

INVESTIGATING THE EFFECT OF CONTRAST AGENTS ON DOSE CALCULATION OF INTENSITY MODULATED RADIOTHERAPY PLANS FOR HEAD AND NECK CANCER

Vikram Mittal^{1,2}, Nidhi Jain³, A. Manikandan¹, Meenakshi Mittal¹

¹Department of Radiation Oncology, Ivy Hospital, Mohali, Punjab, 160071; ²Department of Physics, GLA University, Mathura, Uttar Pradesh, 281406; ³Department of Radiation Oncology, Paras Hospitals, Panchkula, Haryana, 134109

Email: vicky.mittal2609@gmail.com

BACKGROUND/OBJECTIVE: Accurate CT imaging is crucial for precise radiotherapy dose calculations. Contrast agents are often used to enhance tissue delineation in CT scans, and acquiring both contrast-enhanced and non-contrast CT sets is a standard practice in radiotherapy planning. This study aims to investigate the impact of contrast agents on dose calculations for IMRT plans in head and neck cancer patients.

MATERIAL AND METHOD: In this research, a cohort of fifteen patients diagnosed with head and neck cancer underwent both planning CT scans with contrast (CCT) and without contrast (NCCT). Subsequently, the treatment plans were recalculated using the NCCT data and then compared to the original CCT plans. The analysis focused on evaluating the variations in Hounsfield Units (HU) and dose distributions for critical structures and target volumes. Various metrics such as mean HU, mean and maximum relative dose values, D2%, D98% and 3D gamma analysis were employed to assess the difference, and statistical significance was determined using the Wilcoxon signed rank test.

RESULT: Statistically significant Hounsfield unit (HU) variations were observed for most structures ($p < 0.05$). However, these differences were not considered clinically significant since the mean HU values remained within 30HU for soft tissue. The variations in D2% and D98% values for target volumes were found to be insignificant ($p > 0.05$). Moreover, the dose maximum differences were less than 2% for all critical structures and target volumes. Notably, the 3D gamma analysis results indicated that all treatment plans met the criteria of 3% dose difference and 3mm distance to agreement.

CONCLUSION: For the radiotherapy planning purposes, it is recommended to acquire CCT instead of NCCT, as there is no clinically significant difference in dose calculations based on image set.

KEYWORDS: Contrast CT, NCCT, CECT, IMRT, Head and Neck Cancer

RADIATION DOSE ENHANCEMENT EFFECTS ON PANCREATIC CANCER CELLS BY ULTRASOUND-STIMULATED MICROBUBBLES

Masao Nakayama^{1,2,3}, Ayaha Noda^{2,4}, Hiroaki Akasaka^{1,5}, Takahiro Tominaga⁴, Giulia McCorkell², Moshi Geso², Ryohei Sasaki¹

¹Division of Radiation Oncology, Kobe University Graduate School of Medicine, ²Discipline of Medical Radiations, School of Health and Biomedical Sciences, RMIT University, ³Division of Radiation Therapy, Kita-Harima Medical Center, ⁴Department of Clinical Radiology, Faculty of Health Sciences, Hiroshima International University, ⁵Department of Chemical Engineering, The University of Melbourne

Email: naka2008@med.kobe-u.ac.jp

BACKGROUND/OBJECTIVE: Microbubbles (MB) have been used clinically as contrast agents in ultrasound imaging. Recently, there has been interest in using ultrasound-stimulated MB (USMB) as dose enhancers for radiation therapy. Here, we investigated the cell-killing effects of commercially available USMB with X-rays on pancreatic cancer cells in vitro.

MATERIALS AND METHODS: Sonazoid MB (GE Healthcare Japan) and LOGIQ e portable ultrasound unit (GE Healthcare) were used for USMB treatment. The size and morphology of MB and the number of burst MB after ultrasound exposure with different mechanical parameters were evaluated microscopically. Two different pancreatic cancer cell lines, MIAPaCa-2 and PANC-1, were treated with the different concentrations of MB at a 4-MHz frequency and a mechanical index of 1.0 ultrasound. After 3 minutes of ultrasound sonication, the cells were exposed to 150 kVp X-rays. WST-1 and clonogenic assays were performed to assess cell viability. Intracellular reactive oxygen species (ROS) were determined using carboxy-2',7'-dichlorofluorescein.

RESULTS: The mean size of the MB was confirmed to be 2.0 μm in diameter. They could be burst after ultrasound sonication and the number of burst MB increased with higher mechanical index and exposure time. Three minutes of exposure to US at a frequency of 4 MHz and a mechanical index of 1.0 caused 97% of the MB to burst. Cellular cytotoxicity was significantly increased by USMB treatment even in the absence of X-ray irradiation. Cell survival rates for cells treated with 0.01% and 0.4% USMB were 88% and 34% for MIAPaCa-2 and 81% and 16% for PANC-1 cells, respectively. The ROS levels in cells treated with the combination of 0.01% USMB and 6 Gy of X-rays were significantly higher than those in cells treated X-rays alone. The significant radiation dose enhancement effect was found in MIAPaCa-2 treated with 0.01% USMB, but was not significant in PANC-1. For the 0.4% USMB, there were no dose enhancement effects in either cell line.

CONCLUSIONS: Our results suggest that USMB treatment can additively enhance the therapeutic efficacy of radiation therapy on pancreatic cancer cells. However, their synergistic dose-enhancing effects are likely to be cell type and MB concentration dependent.

KEYWORDS: Microbubbles, Ultrasound, Radiation Therapy, Radiosensitiser

Presentation ID: O-024

Abstract ID: M9190

INVESTIGATING THE EFFECT OF RADIOTHERAPY AND SONODYNAMIC THERAPY IN THE PRESENCE OF APIGENIN-COATED GOLD NANOPARTICLE ON BREAST CANCER CELLS

Ali Neshastehriz^{1,2}, Zeinab Hormozi-Moghaddam^{1,2}, Seyed Mohammad Amini², Seyedeh Mona Taheri¹, Zahra Abedi^{3,4}

¹Radiation sciences department, Iran University of Medical Sciences (IUMS), Tehran, Iran, ²Radiation Biology Research center, Iran University of Medical Sciences (IUMS), Tehran, Iran, ³Department of Genetics, Faculty of biological Sciences, TarbiatModares University, Tehran, Iran, ⁴Institute for Cardiovascular prevention (IPEK), Ludwig-Maximilians University Munich, Germany.

Email: Hormozimoghadam.z@iums.ac.ir

BACKGROUND/OBJECTIVE: Sonodynamic therapy and nanoparticles with green compounds, along with radiotherapy, can reduce complications and improve the treatment of cancer. This study aimed to investigate the efficacy of low-dose radiotherapy and sonodynamic therapy in the presence of apigenin-coated gold nanoparticles on the breast cancer cell.

MATERIALS AND METHODS: The synthesized apigenin-coated gold nanoparticles were confirmed by UV-visible, HR-TEM, DLS, zeta-potential, and FTIR. Ultrasound parameters were estimated at the acoustic cavitation threshold by mechanical index modeling. The toxicity of the nanoparticles and cell viability were measured by MTT. The concentration of apigenin-coated gold nanoparticles was measured, and they were then irradiated by ultrasound and 2 Gy x-ray radiation.

RESULTS: Ultrasound with a mechanical index of 0.40 was estimated at a distance of 1 cm from the 1-MHz transducer with 2 W/cm² in the continuous mode. The MTT assay indicated that sonodynamic therapy combined with radiation therapy at the concentration of 8 µg/ml nanoparticles significantly affected cell death (0.26± 0.02).

CONCLUSIONS: Using sonodynamic therapy as a non-invasive and non-ionizing treatment with novel sensitizers based on optimum physical parameters can increase cell death in low-dose radiation therapy. Moreover, this study used green nanoparticles versus chemical sensitizers to gain insights into the elimination of cancer treatment side effects.

KEYWORDS: Sonodynamic therapy, Radiation therapy, Apigenin-coated gold nanoparticles

TO ASSESS THE DOSIMETRY PROPERTIES OF N-ISOPROPYL ACRYLAMIDE (NIPAM) GEL WITH X-RAY CT READOUT MODALITY FOR THREE DIMENSION RELATIVE DOSE MEASUREMENT IN RADIOTHERAPY

D N Singh¹, D K Ray²

¹Department of Radiation Oncology, Command Hospital, Kolkata-700027

²Department of Radiotherapy, Chittaranjan National Cancer Institute, Kolkata-700026

Email: dnsdrdo@gmail.com

BACKGROUND: Radiation dosimetry plays an important role in treatment planning and precise dose delivery to various types of malignant tumour. Polymer gel dosimeters have shown potential for three-dimensional relative dose measurement in radiotherapy. They are tissue equivalent radiosensitive chemicals. They act as phantom as well as dosimeter so there is no need of any dose perturbation correction. Other advantages include their ability to determine integrated three-dimensional relative dose distributions, as well as their ability to fabricate in different shapes and sizes.

OBJECTIVE: To assess the dosimetry properties of N-isopropyl acrylamide (NIPAM) gel with X-ray CT readout modality for three-dimensional relative dose measurement in radiotherapy

METHODS: The NIPAM gel dosimeter was prepared on the bench-top of radiotherapy department. The calibration of gel dosimeter was performed on a Telecobalt machine. An anthropomorphic cylindrical gel phantom was designed in-house for the study of central axis depth dose and dose profile at d_{max} . The axial cuts of images were acquired on a dedicated X-ray CT scanner. The MATLAB software was used for readout analysis of NIPAM gel.

RESULTS: The effects of kV and mA were evaluated to optimize the X-ray CT protocol for readout of NIPAM gel. The effect of slice thickness on dose sensitivity, CT-Dose response was evaluated. The response of the gel was linear up to 15 Gy ($p < 0.01$). The pre and post-irradiation stability, energy independence, relative depth dose along the central axis and cross beam profile at d_{max} were measured. The PDD of NIPAM gel was measured and compared with ion-chamber results for high energy photon beam. Up to 5 cm depth, the NIPAM gel PDD varies from $\pm 1.3\%$ to $\pm 3.7\%$ ($p < 0.05$) with the ion chamber PDD. Beyond 5 cm depth, the PDD of NIPAM gel varies from $\pm 2.5\%$ to $\pm 8.5\%$ ($p = 0.21$). The cross beam profile of NIPAM gel at d_{max} shows a variation of ± 3 to $\pm 5\%$ with ion-chamber which is in close agreement with similar study on PAGAT gel dosimeter with X-ray CT imaging.

CONCLUSIONS: NIPAM gel dosimeter with X-ray CT imaging as readout modality is suitable for three-dimensional relative dose measurement in radiotherapy.

Presentation ID: O-026

Abstract ID: S6166

DEVELOPMENT OF THIN $\text{CaSO}_4:\text{Dy}$ EMBEDDED TEFLON DISCS BASED TLD SYSTEM FOR PERSONNEL MONITORING

S. M Pradhan^{1,2}, Munir S Pathan^{1,2}, T. Palani Selvam^{1,2}¹Radiological Physics & Advisory Division, Bhabha Atomic Research Centre, Mumbai, India²Homi Bhabha National Institute, Mumbai.

Email: smppms@barc.gov.in

PURPOSE / BACKGROUND: A high throughput monitoring system is one of the requisites to reduce the dose reporting time and optimise the resources at monitoring laboratories. With the reduction in mass, dosimeter discs of lesser thickness can be heated faster requiring less time to complete the readout. Thin disc elements are advantageous for dosimetry of weakly penetrating radiation. In the past thin tape (0.4 mm thick), of $\text{CaSO}_4:\text{Dy}$ Teflon with anti-buckling device was studied with contact heating. However, such dosimeters had limited success possibly due to the use of the anti-buckling device and contact heating. The present study describes the development of a thin disc based TLD card and compatible gas heating based TLD badge reader for personnel monitoring

MATERIALS AND METHODS: $\text{CaSO}_4:\text{Dy}$ embedded Teflon discs of different thicknesses (0.2 - 0.8 mm) and phosphor proportions (25 - 50%) were prepared using the technique as standardized for 0.8 mm discs. Based on these discs, thickness, and phosphor proportion were optimized. Further, a new design of the TLD card was evolved to securely hold the thin discs. A modified TLD badge reader with a facility of variable readout time and temperature profile was developed to read the cards. The readout parameters including the gas clamping temperature, N_2 flow rate, and readout duration per disc were optimized based on experimental readouts and simulations of readouts. Subsequently initial characterization of the system for precision, MDL, sensitivity variation with repeated use was studied.

RESULTS: The thickness of the thin disc was optimised to 0.4 mm based on the variation of sensitivity and fabrication considerations. The phosphor proportion was finalized to 40% by analyzing the variation of optical density and the sensitivity with the proportion. The new design of the card is found to protect the discs and is compatible with the existing cassettes. The results on sensitivity, precision, MDL, and sensitivity variation with repeated use are quite encouraging.

CONCLUSION: TLD cards based on 0.4 mm discs and compatible reader developed in the study lead to a reduction in readout time with consistent dosimetric properties and the TLD system is suitable for personnel monitoring.

Presentation ID: O-027

Abstract ID: R6866

RADIOLUMINESCENT DOSIMETER WITH TIME-DIVISION MULTIPLEXING FOR RADIOTHERAPY APPLICATION

JanatulMadinah Wahabi^{1,2}, Ngie Min Ung³, Ghafour A. Mahdiraji⁴, WuYi Chong⁵, Jeannie Hsiu
Ding Wong¹

¹Department of Biomedical Imaging, Faculty of Medicine, Universiti Malaya, Malaysia ²Ministry of Health,
Malaysia

³Clinical Oncology Unit, Faculty of Medicine, Universiti Malaya, Malaysia

⁴Flexilicate Sdn. Bhd., Universiti Malaya, Malaysia

⁵Photonics Research Centre, Universiti Malaya, Malaysia

Email: janatul9@gmail.com

BACKGROUND/OBJECTIVE: Ionising radiation plays a critical role in patient care, serving as a screening tool for trauma and accidents, diagnosing illnesses, and delivering cancer treatment. To ensure accuracy, a radiation dosimeter is used. This study aimed to develop and prototype a radioluminescent (RL) dosimetry system that integrates the time-division multiplexing (TDM) concept, characterising and applying it in clinical settings.

MATERIALS AND METHODS: The system was developed using an SP101 plastic scintillator coupled to an optical fibre as a light guide. The optical fibres were connected to a 2-by-1 optical switch, and the switch's output was connected to the photodetector. The photodetector converted the detected light into an electrical pulse, which a pulse counting unit counted. The measured signal was recorded and converted into a dose using an in-house computer script. The acquisition duration, switching time, dead time, crosstalk and SNR were characterised. Then the system was applied to measure the surface dose for conformal radiotherapy.

RESULTS:In evaluating the acquisition duration for each channel, channel-1 was accurate compared to channel-2. The switching time was 3 ms, and the dead time was 0.04 mGy. The system exhibit 15 % crosstalk, and the SNR was 344.62. Surface dose measurement showed that the accuracy of the dosimeter ranged between -6.13 % to 3.19 % for conformal radiotherapy.

CONCLUSIONS:The study evaluates the capability of the RL dosimeter in adapting the TDM concept. The developed prototype showed a promising solution for multi-sensor measurement that can be used for in vivo dosimetry.

KEYWORDS: fibre optic dosimetry, radioluminescence dosimetry, radiotherapy, time-division multiplexing

Presentation ID: O-028

Abstract ID:G8735

ANALYSE THE PERFORMANCE OF THE UPGRADED POSITIVE ION DETECTOR AS A GAS SENSOR

S.Dharshini¹, G.Sowmiya¹, R. Hemapriya¹, C. S. Sureka¹, R. Mohandoss¹, Amol Bhagawat², Alok J.Verma²

¹ Department of Medical Physics, Bharathiar University, Coimbatore-641 046, Tamil Nadu, India

²SAMEER, IIT Campus, Powai, Mumbai-400 076, Maharashtra, India

Email: leelasiva03@gmail.com

BACKGROUND:Breath Analysis is a non-invasive technique that can be used to diagnose cancer at an early stage. It can be performed with a 3D positive ion detector that operates on the principle of ion-induced impact ionization. This study focused on evaluating the effectiveness of an upgraded version of the positive ion detector as a gas sensor.

MATERIALS AND METHOD: A high voltage of -490V is applied to the oxygen-free high conductivity copper cathode and +120V is applied to the aluminium anode of the 3D positive ion detector. This study is performed in nitrogen and atmospheric air at a pressure range from 5 to 25 mbar using an Am-241 source. To capture the output signal, a 2 series four-channel Multiple Signal Oscilloscope (MSO) was used.

RESULTS: In nitrogen medium at 20 mbar pressure, the total number of pulses are 165 ± 10 where 53%, 28%, and 5% pulses are in the voltage range of -0.5V to -1.5V, -1.5V to -2.5V, and -2.5V to -3.5V respectively. Similarly, in an atmospheric medium, the total number of pulses are 180 ± 10 where 35%, 20%, 7.8%, and 6.2% in the voltage range of -0.5V to -0.8V, -0.8V to -1.0V, -1.0V to -1.3V, and -1.3V to -1.5V respectively. From this result, it is observed that signal amplitude under nitrogen environment was 4.5 times higher than atm air and the rise time, fall time, and negative pulse width are higher in nitrogen. For both gases, as the pressure increases from 5 to 25 mbar the frequency is decreased from 6 kHz to 25 Hz.

CONCLUSION: Nitrogen can be used as a reference working medium of the positive ion detector. By comparing the differences in amplitude, rise time, fall time, number of pulses, and frequency between nitrogen and atmospheric air, it is concluded that the positive ion detector's response is heavily influenced by the type of gas being used. Therefore, it can be used as a gas sensor and so it has the potential to function as a detector for diagnosing cancer by exhaled breath.

KEYWORDS: Breath Analysis, Positive ion detector, Gas sensor

ACKNOWLEDGEMENT:The authors acknowledge the Department of Science and Technology (DST), New Delhi, Government of India for financial assistance under the Biomedical Device and Technology Development Programme (BDTD).

CHARACTERIZATION AND DOSIMETRIC EVALUATION OF A LIQUID-FILLED ARRAY DETECTOR FOR FLUENCE VERIFICATION: COMPARISON WITH AIR-FILLED ARRAY DETECTOR

BeneetaSukumar, PariBooshna, RetnaPonmalar, Abel Juhan Thomas, Timothy Peace Henry Finlay Godson.

Department of Radiotherapy Oncology, Christian Medical College, Vellore

Email: beneeta1203@gmail.com

BACKGROUND/OBJECTIVE:To evaluate the dosimetric parameters of the recently introduced OCTAVIUS 1600 SRS array detector (OD1600) with 1521 liquid-filled ionization chambers for fluence verification and to compare with the OCTAVIUS 1500 detector array (OD1500) with 1405 air-filled ionization chambers.

MATERIALS AND METHODS:In this study, the dosimetric characteristics such as MU linearity, relative dose per MU, reproducibility, MU stability, sensitivity as well as dependence on dose rate, field size, energy and SSD were performed in TrueBeam linear accelerator for 6MV, 10MV, 15MV, 6MV-FFF and 15MV-FFF photon beams. Both Wedge field and Open field dose profiles were acquired with these 2D-array detectors for two different field sizes and the dosimetric parameters were investigated. Also, the response of the detectors in 2D were analyzed for different standard fluence patterns.

RESULTS:Both array detectors showed a linear response with MU ranging from 1 to 500 MU and the reproducibility was within $\pm 1\%$. For dose rate dependence, a deviation of -2.07%, -1.93% and -4.63% was observed with 15MV, 6MV-FFF and 10MV-FFF beams with OD1600. The energy dependence was found to have a maximum deviation of 1.9% for OD1600 and a maximum deviation of 0.4% for OD1500. The output factors measured for OD1600 showed a maximum deviation of 18.5% for flattened beams and a maximum deviation of 20.7% for unflattened (FFF) beams with the Semiflex ionization chamber measurements for the field size of $1 \times 1 \text{cm}^2$. The profile measurements showed that the penumbra width was doubled in OD1500 as compared to OD1600. Gamma analysis carried out for the two detectors showed values of 84.6% for 1mm 1% criteria, 97.3% for 2mm 2% criteria for 6MV Wedged fields and values of 82.9% for 1mm 1% criteria, 100% for 2mm 2% criteria for 10MV Wedged fields.

CONCLUSIONS: The extensive tests performed in this investigation for the dosimetric properties of both the detectors showed that they can be used as reliable 2D detectors. However, care should be taken for the over-response of OD1600 and under-response of OD1500 in small fields due to the presence of iso-octane liquid and air in the detectors respectively.

KEYWORDS:Octavius 1600SRS, Octavius 1500, Dosimetric characteristics.

SECOND CANCER RISK TO CONTRA-LATERAL BREAST AFTER SINGLE-SIDED BREAST IMRT

Shatabdi Chakrabarty¹, Amanjot Kaur², T. Palani Selvam^{1,3}

¹Radiological Physics & Advisory Division, Bhabha Atomic Research Centre, Mumbai, India

²Department of Radiotherapy, Mahatma Phule Charitable Trust Hospital, Navi Mumbai, India

^{1,3}Homi Bhabha National Institute, Mumbai, India

Email: shatabdic@barc.gov.in

BACKGROUND/OBJECTIVE: Presently, breast cancer is the most common malignancy among Indian women. Cancer-specific survival is on rise. However, patients of age-group 30-40 years are up-surg-ing. Furthermore, increase in use of complex radiotherapy techniques like intensity-modulated-radiotherapy (IMRT) is associated with higher low-dose exposure to organs-at-risk (OAR). All these aspects might result in risk of developing post-radiotherapy secondary-cancer. In this study, risk of secondary-cancer in contralateral-breast (CLB) post IMRT is estimated using BEIR VII risk model.

MATERIALS AND METHODS: Computed tomography (CT) data of 30 females who underwent whole-breast radiotherapy (15 left-sided, 15 right-sided) with lymph-nodes involved were selected randomly. Target volume (TV) and OAR were delineated. 7-beam IMRT plans generated to deliver 40 Gy in 15 fractions. Differential dose-volume-histograms (dDVHs) were retrieved from Treatment Planning System (TPS). Organ-equivalent dose (OED) of CLB was calculated on the basis of linear (mean), linear-exponential, plateau and mechanistic dose-response models. Secondary-cancer risk for CLB was estimated in terms of Excess Absolute Risks (EAR) and Lifetime Attributable Risk (LAR) as reported in BEIR VII Report.

RESULTS: Mean dose to CLB varies from 59.2-301.7 cGy for TV-to-CLB distances 3.84 and 1.55 cm, respectively. Linear-exponential, plateau and mechanistic OED values are 153.6, 146.7 and 152.2 cGy respectively. The EAR per 10,000 persons per year per Gy at age of 70 after undergoing radiotherapy at age of 30 are 20±7, 17±5, 16±5 and 17±5, respectively. These EAR values upon undergoing radiotherapy at 50-year age are 7±2, 6±2, 6±2 and 6±2 respectively, at the age of 70. LAR values per 10,000 women undergoing radiotherapy at 30-year age and survival till 70 year of age are 269±92, 230±67, 220±62 and 228±66.

CONCLUSIONS: Except linear, the above-mentioned three OED models lead to similar risk estimation. CLB receives up to 7.5% of prescribed dose in IMRT which is not negligible. Risk of secondary-cancer to CLB is found high. Lesser the age during radiotherapy and more the attained age, greater is the risk of secondary-malignancy. In light of these observations, other radiosensitive OARs (most importantly lung) and other treatment modalities (e.g. Volumetric-modulated-arc-therapy) need to be further investigated.

KEYWORDS: Organ Equivalent Dose, Excess Absolute Risk, Lifetime Attributable Risk, Breast Cancer, Secondary Cancer Risk

EVALUATION OF DOSIMETRIC CHARACTERISTICS OF 10MV FLATTENED AND UNFLATTENED PHOTON BEAM IN TRUEBEAM STX LINEAR ACCELERATOR

Rajadurai E², Govindarajan KN², Saravana Kumar A² Karthikeyan¹

² PSG Institute of Medical Sciences, Department of Medical Physics Coimbatore Tamil Nadu India

¹Aster CMI hospital Benagloru Karnataka

Email: duraisr@gmail.com

INTRODUCTION: Removing the filter to obtain FFF beams changes the natural peak shape of the beam profile compared to the conventional FF photon beam. Given the development of computational techniques in this field, more sophisticated treatment planning systems, and treatment techniques, homogeneous dose distribution is not required. FFF beams have increased substantially because the dose rate is much higher in FFF beams than in FF beams. Consequently, the exposure time may be shorter and the probability of patient movements between fractions may be reduced.

AIM: This work compares and evaluates the dosimetric properties of 10MV flattening filter (FF) and flattening filter-free (FFF) photon beams generated from a Varian TrueBeamSTx medical Linear accelerator. These properties include dosimetric parameters such as percentage depth dose, dose rate, beam profile, out-of-field, energy spectra, head scatter factor, total scatter correction factor, field size, penumbra, and surface dose. This study has also been implemented with the case study of physical parameters including dose distributions, histograms, and treatment time to compare with the effect of 10MV FF and FFF beams.

MATERIALS AND METHODS: The measurements were carried out on a Varian TruebeamStx Linear accelerator using high energy photon beam 10MV FF & FFF beams. A Radiation Field Analyzer (RFA) from IBA called Blue Phantom 2 was used for measurements.

RESULTS: The removal of the flattening filter enhanced the accelerator's properties in terms of smaller penumbras and reduced MLC leakage. It was discovered that removing the filter increases the dosage rate by 3.4 times for 10MV on the beam's central axis. These values demonstrate the ratio of radiation produced in the accelerator to that remaining in the usable beam after interactions with the filter. Clearly, removing the filter reduces the number of head scatter photons and hence dosages to normal tissues and organs dramatically, especially for deep-seated tumors.

KEYWORDS: Flattening filter-free beams, dosimetry of unflattened beam, PDD, head scatter factor

IMPLEMENTATION THE TOTAL BODY IRRADIATION (TBI) BASE VOLUMETRIC MODULATED ARC THERAPY (VMAT): THE EXPERIENCE AND PROCEDURE AT FV HOSPITAL – VIETNAM

Tran Anh Duong^{1*}, VoThi Tran Nhat Linh¹, Le Thanh Xuan¹, Dr. Basma Mbarek², Dr. Nguyen Huynh Ha Thu³, PhangDuc Tin⁴.

¹Physicist, HyVong Cancer Care Centre – FV Hospital – VietNam.

²Head of HyVong Cancer Care Centre – FV Hospital – VietNam.

³Radiation Oncologist, HyVong Cancer Care Centre – FV Hospital – VietNam.

⁴Therapeutic radiographer, HyVong Cancer Care Centre – FV Hospital – VietNam.

Email: duong2.tran@fvhospital.com

Purpose: Total body irradiation (TBI) is an important part of the conditioning regimens frequently used to prepare patients for stem cell transplantation. Compared with Conventional extended SSD TBI techniques, VMAT allows to more accurate and precise dose calculation, OAR protection, and homogenous dose distributions. In this work, we introduce the experience and procedure of total body radiotherapy based volume-modulated arc technique (TBI-VMAT) at FV Hospital – Vietnam.

Materials and methods: Patient was treated in 6 fractions of 2Gy, two fractions per day over 3 days as part of the conditioning protocol established by the Blood transfusion bone marrow transplantation team. Two CT study sets was acquired on the GE DiscoveryRT CT scanner, with a slice thickness of 5 mm. One head-first supine (HFS) from vertex to lower thigh and one feet-first supine (FFS) from toe to pelvic. Simulation devices including: a thermoplastic mask and OrfitRaycast base plate for head support, Elekta Bluebag for whole body support. PTV consisted of whole body, cropped 3 mm inside the body, kidneys PRV and 5 mm overlap margins with lungs. The OARs including: lens, eyes, kidneys, lungs. Planning was performed using Monaco version 5.11.03 with the Monte Carlo dose calculation algorithm. The planning aims were to deliver 12 Gy to at least 90% of the PTV ($V_{100\%} \geq 90\%$) and 11.4 Gy to at least 95% of the PTV ($V_{95\%} \geq 95\%$). Mean doses to lungs and kidneys were restricted less than 10 Gy, and maximum dose to lens were restricted less than 6 Gy. The dose homogeneity index (HI) of PTV < 1.2 . Quality assurance were performed by using Octavius 4D-PTW and In vivo dosimetry were performed with Gafchromic EBT3 film. Patient setup was verified using XVI 5.0 kV cone-beam CT (CBCT) image guidance and MV portal images for all isocenters before each fraction delivery.

Results: The VMAT-TBI plan were achieved all of planning aims: The average mean lung dose was 9.97 ± 0.21 Gy, mean kidney dose 9.5 ± 0.11 Gy, maximum lens dose 3.9 ± 0.33 Gy, $V_{100\%} = 94.02 \pm 0.92\%$, $V_{95\%} = 97.80 \pm 0.36\%$, mean dose = 13.2 ± 0.1 Gy, $D_{2cc} = 15.33 \pm 0.22$ Gy, $D_{5cc} = 15.21 \pm 0.21$ Gy, $D_{10cc} = 15.12 \pm 0.21$ Gy, conformity and heterogeneity index of PTV was 0.93 ± 0.01 and 1.19 ± 0.02 . The positioning of the patient needed on couch 7 Cone Beam CTs and 4 portals and a mean duration of 90 minutes for each session.

Conclusion: Total Body Irradiation (TBI) using Volumetric Modulated Arc Therapy (VMAT) has the potential to homogenize dose distribution to target, and to reduce dose on specified organs. TBI-VMAT has been successfully performed and is now the standard procedure at FV-Vietnam hospital. Although TBI-VMAT is a complex and multi-step procedure, it can be implemented in radiotherapy centers where VMAT is already a standard treatment technique. Longer follow-up time is necessary to evaluate our method and long-term toxicity.

Keywords: TBI, VMAT; Total body irradiation; VMAT-TBI.

ENHANCING DOSE MEASUREMENT ACCURACY IN SINGLE ISOCENTRE MULTIPLE TARGETS SBRT: AN ANALYSIS OF IN-PHANTOM ROTATION MEASUREMENTS WITH MYQA SRS

Dinesan C¹, Gopinath Mudhan², RavikumarM¹

¹Sri Shankara Cancer Hospital & Research Centre Bangalore, India

²Vellore Institute of Technology, Vandalur - Kelambakkam Road, Chennai

Email: dinesanchinnaiya@gmail.com

PURPOSE: Single isocentre multiple targets (SIMT) SBRT revolutionizes treatment by delivering radiation to multiple tumour sites from a single isocentre. However, accurately measuring radiation dose is challenging due to target variability in position and the need for higher dose capture, resulting in a time-consuming process. Limited detector orientations further complicate capturing higher doses in multiple targets. This study investigates in-phantom rotation measurement with myQA SRS for verifying SIMT SBRT plans, aiming to develop an advanced approach for precise capture of higher doses in a single setup.

MATERIALS AND METHODS: The myQA SRS device, consisting of 105,000 complementary metal-oxide-semiconductor (CMOS) arrays with an active area of 12x14 cm² and a resolution of 0.4 mm, was evaluated. The myQA SRS software is capable of extracting dose planes for specific detector angles from the TPS 3D dose distribution. QA plans were generated for 10 SIMT SBRT cases, and the dose files were exported to the myQA SRS software. The planner viewer tool (PVT) was employed to determine the optimal detector angle for capturing multiple high-dose regions in a single setup. Each QA plan was delivered with in-phantom rotation using the desired detector angle found in PVT and without in-phantom rotation (detector angle 0°). The phantom-based QA measurements were acquired and analysed using a gamma criterion of 3%/1 mm with 10% threshold.

RESULTS: The study demonstrated a significant increase in the average gamma passing rate with in-phantom rotation using myQA SRS. The average gamma passing rates increased from 96.1 to 98.7 with in-phantom rotation for a gamma criterion of 3%/1mm, 10% Threshold. Additionally, in-phantom rotation measurements substantially increased the number of pixels above 50% dose, with a 14-fold rise and 51.3 times increase in the maximum intensity. The improved detector positioning within high-dose regions resulted in higher accuracy and precision in dose measurement.

CONCLUSION: In-phantom rotation with myQA SRS accurately captures higher doses in SIMT SBRT, eliminating the need for multiple measurements. This instills confidence in delivering high doses to multiple targets from a single isocentre. Combining high-resolution array dosimetry and rotational detectors offers an efficient patient-specific QA method for treatments with multiple targets.

SIMULATION OF STEREOTACTIC CRANIAL RADIOSURGERY GUIDED BY FUNCTIONAL MAGNETIC RESONANCE

Luis Alfredo Ancari Iniguez, Guillermo Alvarez, Abril Vergne, Rodrigo Alcala, Federico Gonzalez, Roberto Isoardi, Daniel Fino

Fundación Escuela Medicina Nuclear FUESMEN, Garibaldi 405, Mendoza, 5500, Argentina

Email: luis.ancari@ib.edu.ar

INTRODUCTION: Stereotactic cranial radiosurgery (SRS) is a non-invasive technique that delivers high doses to the target in 1-5 fractions, generally used to treat lesions located in deep and eloquent regions of the brain. It is possible that functional regions of the brain near the lesion receive a dose higher than the tolerable limit (Sun et al, 2017); these areas can be detected through resting-state functional magnetic resonance imaging (rs-fMRI) studies. This technique is used to examine intrinsic networks in the brain while the patient is not performing a specific task. The set of regions with a high degree of correlation in the blood oxygenation level dependent signal (BOLD) are called resting state networks (RSNs) (Fröhlich, 2016). Doses received by near-target RSNs can be reduced by incorporating these regions as functional OARs (fOARs) into the treatment planning systems (TPS). The aim of this project is to recognize and incorporate the RSNs into the SRS planning process to minimize doses in those areas of the brain.

MATERIALS AND METHODS: An MRI protocol was performed using a 3T PET-MR scanner in 7 pathological cases. This acquisition included: rs-fMRI and 3D-GRE-T1. The RSNs were detected by independent component analysis (ICA) with MELODIC/FSL; followed by a semi-automated classification process that combines an AI multi-level classifier algorithm (FIX) and manual labeling. The boundaries of the RSNs were established with an empirical z-score value. Clinical visualizations and segmentation parameters were defined with 3D-Slicer (Fig. 1). A Python code was developed to convert image volumes from NIFTI to DICOM format, this is required to introduce them into the Treatment Planning System (TPS). Organs at risk (OAR) -including RSNs- were segmented by radio-oncologist and medical physicists. Two VMAT plans (with and without RSNs) were designed in Eclipse TPS for each subject. Dose reduction was evaluated through dose-volume histogram (DVH), homogeneity index (HI), and conformity index (CI).

RESULTS: The implementation of FIX reduced the classification time by approximately 25% compared to manual labeling. Z-score values between 3 and 5 showed a good compromise between RSNs delineation and noise reduction. The following RSNs were found: visual 1-3, somatosensory, motor, default mode network (DMN), language, orbitofrontal, right and left frontoparietal. Only RSNs close to the target were considered as fOAR in the SRS planning. Additionally, the spatial resolution of the selected RSNs was improved using the FLIRT/FSL tool, without modifying the limits or the intensity of the activation zones (Fig. 2). Two VMAT treatment plans were performed in VARIAN TPS Eclipse: Plan-SRS and Plan-SRSIF (with dose reduction to fOAR). It was possible to reduce the average dose in fOAR between 15 and 18% and the maximum dose between 14 and 15%; without generating significant changes in the dose of conventional OARs or in the coverage of PTVs (Fig. 3).

CONCLUSIONS: In this study we showed that it is possible to incorporate rs-fMRI studies into the radiotherapy planning process in order to protect functional areas of the brain. The proposed method allows the detection of multiple RSNs from a single rs-fMRI study, achieving comparable results to other previous studies as mentioned in Sours et al. at their study from 2019. However, it is necessary to form an interdisciplinary group to protocolize the identification of the RSNs and the dose limits in those regions.

Presentation ID: O-035

Abstract ID: C5864

CLINICAL EVALUATION OF DEEP LEARNING-ASSISTED AUTOMATIC RADIOTHERAPY TREATMENT PLANNING FOR LUNG CANCER

Ningyu Wang¹, ZhiqiangLiu, Jianrong Dai

National Cancer Center/National Clinical Research Center for Cancer/Cancer Hospital,
Chinese Academy of Medical Sciences and Peking Union Medical College, Beijing, China.

Email: wny820588019@163.com

BACKGROUND/OBJECTIVE: The purpose of this study is to investigate the clinical assessment of deep learning-based automatic radiotherapy treatment planning for lung cancer patients.

MATERIALS AND METHODS: We developed a deep learning model for predicting patient-specific dose that was trained and validated on a dataset of 235 lung cancer patients, and the model was integrated into the clinical workflow to assist planners in generating treatment plans. We retrospectively selected 50 clinically treated lung cancer patients' manual volumetric modulated arc therapy (VMAT) treatment plans with different target volumes and different treatment patterns, and the deep learning-assisted automatic VMAT treatment plans were created for each patient. Both manual and automatic plans were then compared in terms of overall plan quality metric (PQM), targets coverage and homogeneity, organs at risk (OARs) sparing, monitor units (MUs), and planning time.

RESULTS: The average PQM score was 40.67 ± 13.12 for manual plans and 40.77 ± 13.46 for deep learning-assisted automatic plans, and they had equivalent overall plan quality. The targets coverage and homogeneity of the automatic plans were considered equivalent or superior when compared to manual plans. Both plans have their own advantages in OAR sparing, such as better sparing of lung for manual plans and better sparing of heart for automatic plans. It is worth to note that the average planning time of automatic plans was reduced from 103.06 ± 18.48 minutes to 32.64 ± 5.33 minutes ($P < 0.001$) and the MUs were reduced from 789.86 ± 234.28 to 692.50 ± 210.68 ($P < 0.001$).

CONCLUSIONS: The deep learning-assisted plans for lung cancer patients achieved comparable or improved plan quality compared to the manual plans, and showed enhanced planning and treatment efficiency, reduced the planning time and MUs significantly. It has the potential to maintain plan quality and enhance the workflow of radiation oncology departments, ultimately benefit lung cancer patients undergoing radiotherapy.

KEYWORDS: Lung cancer; Automatic planning; Deep learning; VMAT

DOSIMETRIC COMPARISON OF BARC AND BEBIG ROUND TYPE RU-106 EYE PLAQUE SOURCE USED IN TREATMENT OF OCULAR CANCER

Rajesh Kumar^{1,2} Ankit Srivastava¹, NitinR. Kakade^{1,2}, S.D. Sharma^{1,2} and B.K. Sapra^{1,2}

¹Radiological Physics & Advisory Division, Bhabha Atomic Research Centre, Mumbai, India

²Homi Bhabha National Institute, Mumbai

Email: rajeshr@barc.gov.in

BACKGROUND/OBJECTIVE: 106Ru/106Rh based eye plaques are very popular for treatment of tumour with apical height upto 5 mm due to its number of advantages. Recently, BARC has also developed 106Ru/106Rh eye plaque for the treatment of eye cancer. 106Ru/106Rh eye plaque manufactured by BEBIG was available and used worldwide. The present work describes the dosimetric comparison of these two sources used in treatment of ocular cancer.

MATERIALS AND METHODS: Dosimetric parameters of CCA plaque manufacturer by BEBIG and round type plaque manufactured by BARC were compared. Both plaques are shaped like spherical caps and have inner radius of 12 mm along the symmetry axis. The outer diameters of the caps across the rim are 15.5 mm for the CCA model and 15.8 mm for the BARC developed plaque. For both plaques, the cap is 1 mm thick and is divided into 3 layers. The thicknesses of these layers from the inner to the outer surface of the cap are 0.1, 0.2, and 0.7 mm. All layers are made of silver, with the middle layer containing the 106Ru. Uniformity of activity distribution of sources was estimated using small dimension diode dosimeter. The depth doses along the central axis for both sources were measured using EBT3 films and diode dosimeter with dedicated phantoms. The finally the depth dose rates were obtained using a regression function. Using the function the dose rates were determined at 0 mm, 1mm, 2 mm, 4 mm and 8mm and compared.

RESULTS: Uniformity of activity distribution of sources were found to be 6.8% and 12 % for BEBIG and BARC source respectively. These values are well within the acceptance limit of 20%. Measured relative percentage depth dose at zero mm, 1mm, 2mm, 4 mm and 8 mm from the inner surface of the plaque were found to be 163.0 & 160.6; 130.0 & 130.2; 100 & 100; 53.6 & 51.5; 9.2 & 9.4 for BEBIG and BARC source respectively.

CONCLUSIONS: The dosimetric parameters of both plaques were measured and found to be comparable with each other.

ABSTRACT KEYWORDS: Brachytherapy, eye plaque, Ru-106

DESIGN, DEVELOPMENT AND CHARACTERIZATION OF HOMOGENEOUS SPHERICAL GRAPHITE CAVITY IONIZATION CHAMBER AS IONOMETRIC REFERENCE STANDARD FOR STRENGTH DETERMINATION OF HIGH DOSE RATE BRACHYTHERAPY SOURCES

Sudhir Kumar, Rahul K Chaudhary, S D Sharma, B K Sapra

Radiological Physics and Advisory Division, Bhabha Atomic Research Centre, CT&CRS Building, Anushaktinagar, Mumbai, India.

Email: sudhirku@barc.gov.in

BACKGROUND/OBJECTIVE: Source strength measurement is considered a fundamental part of a quality assurance programme for brachytherapy treatment delivery, in order to keep the dose delivered to an adequate level. Therefore, strength of high dose rate (HDR) brachytherapy source reported by manufacturer/supplier must be verified independently before using for treatment of cancer patients. Having the uniform response, spherical ionization chamber is always a preferred choice for strength determination of HDR brachytherapy sources. This paper describes the design and characteristics of the homogeneous spherical graphite cavity ionization chamber (HSGCIC) which was developed as ionometric reference standard for standardization of HDR brachytherapy sources.

MATERIALS AND METHODS: The main components of the HSGCIC are the wall and central electrode made up of graphite ($\rho = 1.76 \text{ g cm}^{-3}$), insulating material, ventilating hole at the right side of the bottom, the electrical connections to the wall and central electrode. The chamber has nominal inner diameter of 7.6 cm. The nominal estimated volume is around 228 cm^3 . The chamber has 0.3 cm graphite wall thickness to achieve the charged particle equilibrium. The central electrode height and diameter are equal to 0.8 cm and 3.8 cm respectively. The chamber has been tested at hospital having HDR unit loaded with Ir-192 source. The basic characteristics such as charge leakage, precision, linearity, stability, charge collection efficiency (f) and inverse square law (ISL) validity were evaluated experimentally. The chamber was operated at an applied potential of 400 V.

RESULTS: The charge leakage, precision (n=10), linearity, stability (24 hrs) and ISL validity of the HSGCIC were found equal to 0.02%, 0.03%, 0.02% and 0.05% and $\pm 0.5\%$ respectively. The experimentally determined 'f' of HSGCIC in the radiation field (of Ir-192 source having reference air kerma rate = 15.44 mGy/hr) was found to be 0.9988. The theoretically estimated value of 'f' was 0.9991. These two values of 'f' are in excellent agreement to each other within 0.03% variation.

CONCLUSIONS: The measured dosimetric characteristics of the HSGCIC indicate that the chamber fulfills the requirement of Reference Air Kerma Standard for standardization of HDR brachytherapy sources.

KEYWORDS: Source strength, high dose rate, dosimetry, ionization chamber

A NOVEL MATHEMATICAL EXPRESSION FOR ESTIMATING IR-192 SOURCE DWELL TIMES BY UTILISING CO-60 SOURCE DWELL TIMES IN OPTIMISED BRACHYTHERAPY PLANS

Devaraju Sampathirao¹, Shekhar Dwivedi¹, Avtar singh¹, Gurvinder singh¹, Nagarjun B², Tapas Dora²

¹Department of Medical Physics, Homi Bhabha Cancer Hospital and Research Centre, A unit of Tata Memorial Centre, Punjab, India ²Department of Radiation Oncology, Homi Bhabha Cancer Hospital and Research Centre, A unit Tata Memorial Centre, Punjab, India

Email:devaraju.sr@gmail.com

BACKGROUND/AIM: The aim of this study was to make the comparison study simpler, yet accurate, introduced a novel method for computing Ir-192 source dwell times using Co-60 source dwell times in the Oncentra treatment planning system (TPS). This formula was validated and found to be accurate.

MATERIALS AND METHODS:The Oncentra TPS (version 4.6.0) is configured with Flexi Co-60 source for brachytherapy treatment. The minimum source step size is 1 mm. The TPS is additionally configured with a Microselectron Ir-192 source for the purpose of conducting the comparative study and the minimum source step size is 2.5 mm. In this study, a total of five optimised Co-60 intracavitary plans (ICA) were selected. The catheters were copied from the Co-60 ICA plan to the Study Ir-192 ICA plan. The date and time of the Ir-192 plan were modified to align with the Co-60 ICA plan. The plans are initially normalized at point A in order to determine the dynamic correction factor (D.C.F) using the formula: $D.C.F = (U_{Co-60} \times DT_{Co-60}) / (U_{Ir-192} \times DT_{Ir-192})$, where U, is the air kerma strength and DT, is the dwell time. After obtaining the D.C.F. value, we proceeded to determine the optimised dwell time for Ir-192 corresponding to optimised Co-60 ICA plan dwell times, employing the formula. $DT_{Ir-192} = (U_{Co-60} \times \text{optimised } DT_{Co-60}) / (U_{Ir-192} \times D.C.F.)$ The calculated dwell times for Ir-192 were manually inputted into the 'Study_Ir-192' plan, corresponding to their respective dwell positions to get the optimised ICA plan.

CONCLUSION: Using this formula, we found that the estimated dwell time and TPS dwell time precisely matched with validation method-I. With confirmation method-II, OAR and HRCTV dose variations were minimal. This formula can be used for comparative studies to calculate Ir-192 source dwell time by substituting the Co-60 source dwell time in optimised brachytherapy plans.

LEARNING AND PREDICTING THE RADIONUCLIDE COMPOSITION FROM SIMULATED PLASTIC SCINTILLATOR GAMMA SPECTRA USING AN ARTIFICIAL NEURAL NETWORK

Pratip Mitra¹, Amit Silswal^{2, 4}, Biswajit Sadhu^{3, 4}, S. Anand^{3, 4}

¹Environmental Monitoring and Assessment Division, Bhabha Atomic Research Centre,

²Radiation Safety Systems Division, Bhabha Atomic Research Centre,

³Health Physics Division, Bhabha Atomic Research Centre, ⁴Homi Bhabha National Institute, Mumbai, India

Email: pratipm@barc.gov.in

BACKGROUND/OBJECTIVE: Plastic scintillators, owing to low effective atomic numbers, primarily produce gamma spectra that are devoid of full-energy-peaks and contain only Compton continua. Therefore, analysis of such spectra for identification and quantification of individual radionuclides is difficult. Spectrum deconvolution, which requires knowledge about the detector response matrix, is generally used for this purpose. In this paper, we propose an alternative ANN based approach for determination of composition of six radionuclides present simultaneously in simulated plastic scintillator spectra.

MATERIALS AND METHODS: A dataset containing 1000 crude gamma spectra (1024 channels each) was generated using simplified Monte Carlo calculations by mixing six important radionuclides (⁶⁰Co, ¹³⁷Cs, ⁴¹Ar, ¹³¹I, ⁴⁰K, ²⁰⁸Tl) in random proportions (restricting their sum to unity). The set of these six proportions for each spectrum was used as the corresponding label. The dataset was split into training and test datasets with a ratio of 80:20. The input linear layer, having 1024 features (neurons), was sequentially squeezed down through four intermediate linear layers having 500, 100, 50, and 6 neurons, respectively. Nonlinearity was introduced after each layer except the last one by using the ReLU activation function. Softmax activation function was used after the last intermediate layer to produce the output layer having six probabilities corresponding to the relative intensities of the six radionuclides. The model was trained with Adam optimizer for 100 epochs with a batch size of 32 on the training dataset. The mean squared error (MSE) loss function was used during training.

RESULTS: Performance of the trained model was evaluated on the test dataset. Mean of the 200 MSE-values between predicted and true relative intensities was 0.01. The small error-margin for majority of the spectra on predicting the radionuclide composition suggests that the trained model has learnt the underlying radionuclide signatures within the spectra well for better characterization of plastic scintillator spectra (see Figure 1).

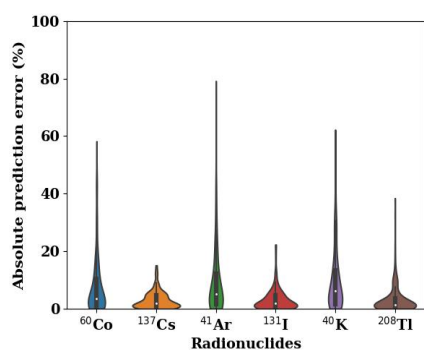


Figure 1: Absolute error in prediction (%) vs. radionuclides. The distribution density of errors for each radionuclides in test dataset are presented as a violin plot. The higher distribution density with lower prediction errors indicates the good accuracy of the model on characterizing the composition of radionuclides present in the spectra.

CONCLUSIONS: The trained ANN model shows promising results on predicting the radionuclide composition from crude plastic scintillator gamma spectra, despite the absence of full-energy-peaks. Studies on hyper-parameter optimization for further improvement of the ANN are under progress.

KEYWORDS: ANN, plastic scintillator, spectrum deconvolution

EVALUATING THE POTENTIAL DOSIMETRIC BENEFITS OF AN ARTIFICIAL INTELLIGENCE BASED ONLINE ADAPTIVE WORKFLOW UTILIZING ETHOS TREATMENT SYSTEM FOR PELVIC CARCINOMAS

Bijina TK, Pichandi A, Muthuselvi CA, Jerrin A, Ramkumar K, Yuvrajan S, Sam Skennet Das

Department of Radiotherapy, Healthcare Global Enterprises, Bangalore, India

Email: tkbijina@gmail.com

BACKGROUND: Adaptive radiotherapy emerged in order to account for inter-fraction variability by modifying the treatment plan during treatment. Online adaptive radiotherapy (oART) though has shown potential in improving treatment outcomes; its routine implementation has been hindered by resource-intensive approaches. This study aims to evaluate the potential dosimetric benefits of an Artificial Intelligence based online adaptive workflow utilizing the Ethos Treatment System for pelvic carcinomas.

MATERIALS AND METHODS: Three patients with prostate cancer and two with rectum cancer were among the five patients evaluated with the AI based oART Ethos system. 101 treatment delivery sessions for these patients were evaluated in terms of treatment duration for each process (Image acquisition, Patient Model, Plan Selection, Technical Review, Position Verification, and Treatment Completion), primary planning target volume PTV volume changes, OAR volume changes and dose constraint fulfillment for PTV and influencer structures.

RESULTS: The average duration of the oART, consisting of image acquisition to treatment delivery was $29:57 \pm 4:30$ min. The PTV volume were slightly reduced (average \pm SD: $3.85\% \pm 1.2\%$) in the adapted plans than in the reference plans. $PTVD_{95\%}$ exhibited no significant changes when considering all plans, but $PTVD_{2\%}$ increased by $1.08\% \pm 0.2\%$ on average. The average bladder and rectum volumes increased by 33.9cc and 15cc respectively among the sessions analyzed. There was a reduction in the mean dose to the bladder, (average \pm SD: $2.55\% \pm 1\%$) on average and the mean dose to bowel bag, femoral heads were similar to the planned dose. The AI segmentation and auto-planning processes demonstrated clinically acceptable results, allowing for adaptation within reasonable timeframes.

CONCLUSION: The results of this study contribute to the growing body of evidence supporting the use of oART in clinical practice. The findings suggest that the implementation of an AI-driven adaptive workflow can enhance treatment planning and delivery in pelvic carcinomas.

KEYWORDS: Online Adaptive Radiotherapy, Ethos, Artificial Intelligence

AI ENABLED PHOSPHOR IMAGING SYSTEM FOR BIOMEDICAL APPLICATIONS

Ratnesh S Sengar¹, A K Upadhyay¹, Y S Rajpurohit², D C Kar¹

¹Division of Remote Handling & Robotics, and ²Molecular Biology Division, Bhabha Atomic Research Centre Mumbai, India.

Email: rssengar@barc.gov.in

BACKGROUND: The phosphor imaging system (see Fig.1) is an advanced computed digital radiography, designed in-house for precise quantitative measurements of radio-isotopic labelled biological specimens. Its applications include fragment analysis, genetic typing, and DNA scanning. The system features variable mode laser scanning for rapid, high-resolution imaging, enabling accurate quantification of proteins, nucleic acids, and other bio-molecules. Utilizing filmless autoradiography with storage phosphor screens, it can detect a broad range of isotopes, such as 3H, 14C, 32P, 33P, and 35S, allowing both target localization and quantification. This capability offers valuable insights into biomedical applications.

MATERIALS AND METHODS: Phosphor imaging employs a technique that identifies and quantifies its target by measuring the light emitted when excited electrons return to their ground state, they release photons. A sensitive photo multiplier tube (PMT) captures these photons, even from very low signal-to-noise ratio (SNR) emissions. To ensure optimal performance, precise calibration and filtering techniques are applied to the PMT to establish the minimum voltage threshold and gain required for detecting weak signals effectively. However, PMT is susceptible to various sources of noise and crosstalk, which can lead to noisy images with reduced contrast, especially when dealing with low SNR signals. To address this, a novel deep learning approach has been developed, combining wavelet and transformer attention mechanisms to restore noiseless PMT signals.

RESULTS: The testing and qualification of the system has been successfully concluded, employing ³²P radioisotope labelled biological samples. The results outperform conventional gel images in evaluating mutants in single-strand DNA analysis. Table-1 presents a comprehensive assessment of the DprA protein's single-strand DNA binding characteristics, including its wild-type form and various point mutants.



TABLE I: RESULT	
	<ol style="list-style-type: none"> 1. C - Control lane with no protein, 2. WT - Wild type <i>DprA</i>, 3. Point mutants affecting DNA binding (R334D, R137D, and F249R), 4. Point mutants affecting <i>RecA</i> interaction (G249R and D277A), 5. Oligomerization mutant (L293A).
<p>Assessment of the single-strand DNA binding characteristics of the <i>DprA</i> protein in its wild type form and various point mutants visualized by developed imaging system</p>	

CONCLUSION: Phosphor imaging is a highly sensitive and efficient technique, surpassing X-ray film in rapid image development and a broader dynamic range. Widely adopted in molecular biology, medical research, and nuclear studies, it incorporates AI-based algorithms for precise quantification and visualization of radio-labelled samples. This intelligent system enhances data analysis, providing valuable insights into molecular interactions for diverse research applications.

KEYWORDS: Phosphor imaging, deep learning, wavelet, radio-labelled samples

ON-SITE SOURCE STRENGTH VERIFICATION OF HDR BRACHYTHERAPY SOURCES

S.D. Sharma, Rajesh Kumar, Ankit Srivastava, Philomina Akhilesh, NitinKakade, B.K. Sapra

Radiological Physics & Advisory Division, Bhabha Atomic Research Centre, Mumbai

Email: simpleyankit@gmail.com

Background/Objective: High dose rate(HDR)brachytherapy is one of the important treatment modalities for managing different types of malignancies. It has the ability to deliver locally high dose to the tumour and relatively less dose to surrounding normal tissues. However, any misadministration in high dose rate brachytherapy may lead to unacceptable consequences. Source strength plays a vital role in patient dose calculation. Thus, accurate measurement of source strength at the hospitals needs to be verified for the adequacy and safety of brachytherapy treatment. Measurements of strengthsof HDR brachytherapy sources were conducted by on-site using a carried a calibrated well type ionisation chamber. The results of this on-site audit of source strength verification of HDR brachytherapy systems are presented in this abstract.

Materials and methods: Strengths of HDR brachytherapy sources in terms of Reference Air Kerma Rate (RAKR) were measured using a recently calibrated BDS1000 well type ionisation chamber (Rosalina, Instruments, Mumbai, India) and Dose1 electrometer (IBA Dosimetry GmbH, Schwarzenbruck, Germany). The dosimetry systems were taken to eight hospitals chosen to include different makes and models of HDR brachytherapy sources for independent measurement of the RAKR. Seven hospital were using Ir-192 and one hospital was using Co-60. Further, ^{192}Ir HDR sources under investigation were of different makes and models which include two Microselectronsources, two Flexitronsources, two Gammamed sources and one Varisource. ^{60}Co HDR source included in this study was Bebig'sSaginova. The measured source strength of each source was compared with the source strength measured by hospitals and provided in the source certificate.

Results: The maximum percentage variations between the measured RAKR and certificate quoted RAKR was found to be 1.91% while the maximum percentage variations between themeasured RAKR and hospital's measured RAKR was found to be 1.61%.

Conclusions: The on-site HDR source strength verification has shown good agreement between the measured, certificate quoted and hospital measured RAKR values. The independent verification of source strength may be considered as a one of the important component of dosimetry audit program in HDR brachytherapy.

Keywords: Brachytherapy, RAKR measurement, dosimetry audit

DOSIMETRIC ANALYSIS OF INDIGENOUSLY DEVELOPED SENFLAP TISSUE EQUIVALENT BOLUS WITH IMPORTED BOLUS AND WAX BOLUS

Senthilkumar Shanmugam¹, Aruna Ganesh², Nandhini Muruges²

¹Regional Cancer Center (RCC), Madurai Medical College & Govt. Rajaji Hospital, Madurai, India.

²Anna universitycollege of engineering, Kotturpuram, Chennai, India

Email:nandhumadaa@gmail.com

BACKGROUND/OBJECTIVE : This dosimetric analysis aims to compare the performance of an indigenously developed SENFLAP tissue equivalent bolus with commercially imported bolus and traditional wax bolus materials in radiation therapy. Tissue equivalent bolus materials are frequently used in radiation therapy to modify the dose distribution and improve treatment accuracy for superficial tumors.

MATERIALS AND METHODS: The SENFLAP tissue equivalent bolus was designed and fabricated using locally available materials to achieve properties similar to human tissue. To assess its dosimetric equivalence, the material was characterized in terms of its mass density, electron density, and photon attenuation coefficient. The imported bolus, a well-established and commonly used commercial product, and the wax bolus, a traditional material, were also characterized for comparison. A series of treatment plans were created for various clinical scenarios using a treatment planning system. The plans included superficial tumor targets at different depths within a water-equivalent phantom. For each scenario, three sets of treatment plans were generated: one using the SENFLAP tissue equivalent bolus, another using the imported bolus, and the third using the wax bolus.

RESULTS: Dose measurements were conducted using ionization chambers and radiochromic film to validate the accuracy of the treatment plans. The measured dose distributions were compared among the three types of bolus materials to evaluate their dosimetric performance. The results of this study indicated that the SENFLAP tissue equivalent bolus exhibited radiological properties similar to the imported bolus, showing its potential as an effective dose-modifying material. The dose distributions obtained using the SENFLAP bolus closely matched those achieved with the imported bolus, demonstrating its dosimetric equivalency. Moreover, compared to the traditional wax bolus, both the SENFLAP and imported bolus materials showed improved dose conformity to the target volume, as evidenced by steeper dose gradients and reduced hotspots.

CONCLUSION: The use of locally developed bolus materials like SENFLAP offers a cost-effective and accessible solution for radiation therapy treatments, especially in regions with limited access to imported products. In conclusion, the results of this study support the implementation of the indigenously developed SENFLAP tissue equivalent bolus in radiation therapy treatments. Further clinical studies and verification with patient treatments are warranted to validate its performance in real-world applications and to explore its potential benefits in diverse clinical scenarios.

KEYWORDS: indigenously developed, SENFLAP tissue equivalent bolus, imported bolus, wax bolus, radiation therapy.

A CLINICAL EVALUATION OF A CUTTING-EDGE SURFACE- GUIDED RADIATION TREATMENT (SGRT) SYSTEM

AdhimoolamSaravana Kumar¹, Varshini Raju¹, SowmiyaSampath Rajan², VeluthattilAswin Chandran², K N Govindharajan¹, Dinesh Babu¹, Manimaran Perumal¹, Amal Jose¹, T Balaji³

¹Department of Medical Physics, PSG Hospitals, Coimbatore, Tamil Nadu

²Department of Radiation Oncology, PSG Hospitals, Coimbatore, Tamil Nadu

³Institute of Oncology, PSG Hospitals, Coimbatore, Tamil Nadu

Email: sarava87@gmail.com

OBJECTIVE: In radiation therapy for safe delivery, reproducible and accurate techniques for patient positioning are essential to reduce the risk of error and ensure optimal delivery of radiation to cure the cancer. Surface imaging is a rapidly growing technique which is applied for positioning and motion management during the course of treatment. Herein, we report our practices of the SGRT (C RAD, Uppsala, Sweden) system installed with Varian True beam linear accelerator for treatment accuracy, positioning and motion management.

MATERIALS AND METHODS: This prospective single-centre study included a series of patients treated on Varian True beam between Jan 2023 to April 2023. The accuracy of patient setup using SGRT was investigated by comparing kV CBCT images for all patients who were treated using SGRT for their entire treatment course. In addition, the auto beam hold technique was analysed throughout the treatment sessions. Further setup, imaging, and beam delivery times were also recorded and compared against standard sessions without SGRT.

RESULTS: 14 patients were successfully treated in the Varian true beam linac with the help of the C-Rad SGRT and Varian kV CBCT systems, and the maximum differences between the SGRT and kV CBCT images were recorded at -1.1 mm, -2.4 mm, and 2.6 mm for lateral, longitudinal, and vertical, respectively. Additionally, the patient is greatly protected during delivery by the tattoo-free auto-beam hold technology.

CONCLUSIONS The adoption of SGRT in our department was an evolutionary procedure from the beginning. A decision was taken after an evaluation of the SGRT systems by a group of clinicians, physicists and RTTs. SGRT was quickly and readily unified into our clinical workflow, and it improves setup accuracy, normal tissue sparing, and patient comfort to aid optimise clinical treatment.

KEYWORDS: optical surface imaging (OSI), surface-guided radiotherapy (SGRT), tattoo-less patient setup, patient motion monitoring, image-guided radiotherapy (IGRT)

QUALITY CONTROL TOOL FOR PATIENT FLOW OPTIMIZATION AT MAYO CLINIC FLORIDA

Sridhar Yaddanapudi, Keith Furutani, Jun Tan, Justin Park, Bo Lu, Xiaoying Liang, Chris Beltran

Department of Radiation Oncology, Mayo Clinic, Jacksonville, Florida, USA

Email: Yaddanapudi.Sridhar@mayo.edu

BACKGROUND/OBJECTIVE: The objective of this work is to present a quality control tool that simulates patient waiting times at the first in America combined Proton-Carbon Therapy Center at Mayo Clinic Florida. Cost control requires that a single synchrotron provide a beam for up to five treatment rooms which therefore adds additional complexity in scheduling optimization using a finite resource. The tool is designed to optimize the scheduling of a representative mixture of patient appointments to achieve the Carnot efficiency of the patient experience.

MATERIALS AND METHODS: Using the electronic health record system data, a process-based discrete event simulation framework based on Python, SimPy, was used to model the patient flow through the facility. The model considers the probability distribution function for factors including patient arrival, localization, gantry rotation, irradiation times, and finite resource availability. The simulation model can be used to test and predict different scenarios and therefore identify robustness in patient appointment schedule. For example, it can determine the optimal time of day for scheduling adaptive planning for a particular patient on a given treatment day, identify the impact of an unanticipated hardware failure, and provide an immediate optimal rescheduling solution for the remaining patients. The tool can also be used to identify areas where technological and process improvements should be made to achieve a higher Carnot efficiency.

RESULTS: Our results show that the tool effectively identifies areas for improvement and reduces patient wait times. By accurately modeling patient flow through the facility, just-in-time bottlenecks contributing to unnecessarily long wait times can be identified and mitigated. We believe that other facilities can use this tool to improve the quality of care provided to patients.

Conclusions: In conclusion, this quality control tool is designed to help healthcare providers optimize the scheduling of a representative mixture of patient appointments to achieve the Carnot efficiency of the patient experience.

KEYWORDS: Quality control, patient wait time, simulation, charged particle facility

DEVELOPMENT OF TISSUE EQUIVALENT MATERIALS FOR APPLICATIONS IN MEDICAL PHYSICS

Reena Sharma¹, S K Suman², A K Dubey², Sunil Dutt Sharma¹, B K Sapra¹

¹Radiological Physics & Advisory Division, Bhabha Atomic Research Centre, India,

²Radiation Technology Development Division, BARC Mumbai

Email: reenas@barc.gov.in

BACKGROUND/OBJECTIVE: In India, the simulation of biological tissues for medical imaging relies on expensive imported materials. To address this issue and create more affordable alternatives, we investigated the melt compounding of polymers.

MATERIALS AND METHODS: EVA+CaCO₃ (Ethylene Vinyl Acetate + Calcium Carbonate) based composites were prepared, and their physico-mechanical properties were analyzed through tensile strength measurements. Dumbbell-shaped specimens were cut from nanocomposite sheets using a standard steel die. Tensile strength and elongation at break were measured using a universal testing machine. The densities of the samples were determined following ASTM D792-08. Thermo-gravimetric analysis and Fourier transform infrared (FTIR) spectroscopy were conducted to evaluate the thermal stability and chemical characteristics of the developed materials.

RESULTS: The developed tissue equivalent composites demonstrated excellent mechanical properties, with tensile strength exceeding 5 MPa and elongation at break surpassing 500% in all composites. These results indicate remarkable mechanical durability and flexibility compared to typical oligomer-based processes used for synthesizing tissue equivalent polymer phantoms. Thermal analysis revealed that the composites exhibited single-step decomposition, and the peak decomposition temperature remained consistent at 777 °C, irrespective of filler loading. Furthermore, the FTIR spectra of composites with different loadings showed no significant shifts in peak positions or peak ratios, suggesting that the chemical characteristics were unaffected after composite formation. The novel tissue equivalent composites successfully provided computed tomography (CT) contrast in the range of biological tissues with measured Hounsfield units in the range of - 100 to + 116 at 120 kVp.

CONCLUSION: With their superior mechanical flexibility and processing characteristics, EVA+CaCO₃ composites offer promising alternatives to the conventional methods for synthesizing tissue equivalent polymer phantoms. Further research is underway to develop composites tailored for specific tissues, which could have significant implications for medical imaging and diagnostic applications.

KEYWORDS: Polymer, Tissue equivalent, CT, FTIR spectroscopy

REGIONAL VARIATION OF CANCER INCIDENCE IN NEPAL

Rudra Prasad Khanal¹, Ishwar Koirala¹, Kanchan P. Adhikari²

¹Central Department of Physics, Tribhuvan University, Nepal

²NAMS, Bir Hospital, Tribhuvan University, Nepal

Email: kxanlrp14@gmail.com

INTRODUCTION: Non-communicable disease, such as cancer has spread all over the world for some last decades. Even though the advancement of technology, it has been a burden for every country. In the context of Nepal, 10 to 15 thousand new cancer incidences are being registered in different hospitals for treatment. Since the date of starting nuclear medicine at Bir Hospital in 1998, cancer patients are getting treatment regularly. According to the data of the population-based cancer registry, approximately 60% of the population having a middle-class income is being affected by cancer in Nepal.

METHODS AND MATERIALS: The study is aimed to find out the particular place where the population density of new cancer incidence is highest in Nepal and to inform the concerned regulatory body that is working for cancer screening and early detection for the proper treatment from the beginning. For this purpose, all the data of cancer patients were collected from five different renowned hospitals and also from the population-based cancer registry center and then analyzed the data. The history of cancer patients was studied from 2003 to 2020, but here the data are analyzed from 2015 to 2020 only, to find the latest trend of cancer incidence.

RESULTS: In the five major hospitals in Nepal, the total new cancer incidence was 61783 from 2015 to 2020. Out of those 34617 were female and 27176 were male. This research shows that female cancer patients were more every year. In the male, lung cancer patients were more than cancer of other organs, but in females, the number of breast cancer patients was greatest. The age-adjusted mortality rate for males in Kathmandu valley was 36.3 and for females was 27.0 per 100,000 populations. The cancer incidence and mortality rate were slightly lesser in other districts of Nepal. This rate increased with the increase in the age of people. Over 60 years, cancer incidence and mortality rates have been found to increase rapidly.

CONCLUSION: This research supports conducting the program of cancer screening and early detection at Kathmandu valley with high priority and then Morang, Rukum, SSDM, etc. to control cancer.

KEYWORDS: new cancer incidence, cancer screening program, lung cancer patients, female.

OPTIMAL BEAM CHOICE OF MONO-ISOCENTRIC STEREOTACTIC RADIOTHERAPY FOR MULTIPLE BRAIN METASTASIS: A DOSIMETRY COMPARISON BETWEEN 6X-SRS AND 6XFFF BEAM

Priyanka Agarwal, NinadPatil, Vishal Gangwar, SwapnaGayen, AshutoshMukherji, SatyajitPradhan

Department of Radiation Oncology, Homi Bhabha Cancer Hospital, (Tata Memorial Center), Varanasi, India

Email pr.agarwaljan@gmail.com

BACKGROUND / OBJECTIVE:The multiple brain metastasis is always a complex and challenging case due to many PTVs and proximal OARs. Optimal beam choice is necessary for SRT planning for sharp dose gradient and optimum OAR doses. However, there are many photon beams in advanced linear accelerators with various dose rates for SRT planning. The aim is to optimize with 6X-SRS and 6XFFF beam selection for multiple brain metastasis generated with mono-isocentric hyper arc planning.

MATERIALS & METHODS:A total of 10 multiple brain metastasis patients were chosen randomly from the institution database. The treatment re-planning was generated for Truebeam STX linear accelerator (Varian Medical System) using high-definition MLC. Each plan was generated on Eclipse TPS (ver15.5.51) for 6X-SRS (FF beam, 1000 MU/min dose rate) and 6XFFF beam (FFF beam, 1400 MU/min dose rate). The prescribed dose was 30 Gy in 5 fractions & planned with hyper arcs (one full arc and two non-coplanar arcs). The optimization was performed with a photon optimizer and dose was calculated using Acuros Algorithm. The optimization parameters and dose constraints were kept the same in both planning. For plan evaluation, coverage index, conformity index (CI) of PTV, and gradient index (GI) were compared. Both plans were analyzed qualitatively and quantitatively for PTV and OARs doses. For the statistical analysis, Wilcoxon signed rank test were used using SPSS software, and p -value <0.05 was considered statistically significant.

RESULTS:The mean volume of GTV and PTV were 2.52(\pm 1.7)cc and 7.58(\pm 3.7)cc, respectively. GTV received 100% of the prescription dose in both cases, however, PTV mean doses were 26.8(\pm 0.43) and 26.12(\pm 0.25) for 6X-SRS & 6XFFF respectively. The CI was 1.002 same for both the plans. The MU was 1.11 ($p<0.05$) times more for 6XFFF compared to 6X-SRS, however, treatment time (TT) was 0.98 ($p>0.05$) less for 6XFFF compared to 6X-SRS. GI was 0.99 times less for 6X-SRS. OARs were comparable in both the cases (Table1).

OARs Name	Parameters	6XSRS	6XFFF	p-value
Brain	Mean (Gy)	4.8	4.92	0.06
Eyes Lt	Mean (Gy)	1.4	1.45	0.39
Eyes Rt	Mean (Gy)	1.57	1.55	0.41
Eye Lens Lt	Max (Gy)	1.4	1.7	0.26
Eye Lens Rt	Max (Gy)	1.4	1.52	0.23
Optic Nerve Lt	Max (Gy)	2.51	2.45	0.09
Optic Nerve Rt	Max (Gy)	2.45	2.31	0.09
Cochlea Lt	Mean (Gy)	0.67	0.73	0.01
Cochlea Rt	Mean (Gy)	0.61	0.74	0.25
Brain -PTV	Mean (Gy)	4.43	4.44	0.42
Brain -PTV	V50% (cc)	35.5	37.9	0.08
Optic Chiasm	Max (Gy)	3.4	3.6	0.14
Body	Mean (Gy)	1.52	1.6	0.045

Table 1: Organs at risk dose comparison between 6X-SRS and 6XFFF.

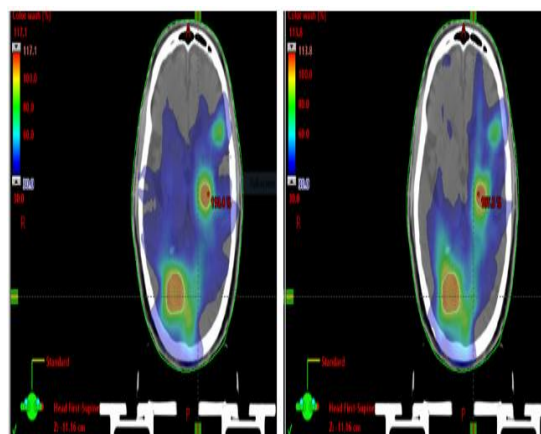


Fig 1: Dose color wash of 30% of the prescription dose showing spillage using beam 6XFFF (Left) and 6X-SRS (Right) for Hyper arc planning.

CONCLUSION:Both the plans were comparable w.r.t. PTV coverage and OARs doses. However, GI is better for 6X-SRS and TT is less for 6XFFF beam. More data and clinical outcomes is required.

KEYWORDS: Hyper arc planning, multiple brain metastasis, stereotactic beam, flattening filter free beam.

THE IMPACT OF CRANIOPLASTY IMPLANTS IN STEREOTACTIC RADIOTHERAPY: A COMPARISON OF COMMERCIAL TREATMENT PLANNING SYSTEM VERSUS MONTE CARLO CALCULATIONS

Sumeesh S^{1,2}, Shaiju V S², Sarin B², Raghukumar P², V.K. Sathiya Narayanan¹,
Raghavendra Holla¹

¹Ruby hall clinic, Pune, Maharashtra, India

²Regional Cancer Centre Thiruvananthapuram, Kerala, India

Email: sumeesh88.s@gmail.com

BACKGROUND/OBJECTIVE: To evaluate the dosimetric impact of cranioplasty implant artifacts on dose calculations of the Commercial treatment planning system (TPS) versus Monte Carlo (MC) calculations in Stereotactic Radiotherapy Planning.

MATERIALS AND METHODS: An indigenously fabricated Polymethyl methacrylate (PMMA) head phantom was used for this study. To quantify the effect of cranioplasty artifacts in the dose calculations of the AAA, AXB algorithms, and the PRIMO MC code. Two types of cranioplasty implants were modeled, the first one is made with titanium alloy, and the second one is with stainless steel alloy having a thickness of 2mm. The implant was fixed on the right Parietal bone region to mimic the patients, who performed craniectomy for traumatic injuries on the parietal region of the head. To mimic the scalp a 5mm wax coating is also done on the outer layer of the implant.

In the first phase of this study, the AAA, AXB algorithms, and the PRIMO MC model were compared against point dosimetry in an indigenously fabricated head phantom with and without a cranioplasty implant. The intention of this phase is to assess the accuracy of the AAA, AXB algorithms, and MC model in the presence of high-Z materials. In the second phase, A planning target volume (PTV) is drawn on the right side of the head phantom, which mimics a target volume on the cerebral hemisphere of the brain, and Two separate plans for AAA and AXB are created in 2 CT sets with two different cranioplasty implants of Titanium and Stainless steel alloys. The treatment verification plans are generated and the effect of the CT artifacts on the dose calculation accuracy of the AAA, AXB algorithm, and the MC model was compared using the gamma index evaluation tool provided by the PRIMO MC code.

RESULTS: The Dose variations for two cranioplasty implants were calculated and compared between two CT sets. The dose deviations found significant difference between the Titanium and Stainless implants. The deviation between measured and PRIMO is less than 1%. The mean dose deviations to the PTV are higher for AAA, when compared to Acuros XB and PRIMO MC. The gamma analysis (2%, 2 mm) of Acuros XB shows a good agreement between simulation and measurements. It was observed that, there is a reduction in the dose for the Stainless steel implant as compared to the Titanium implant.

CONCLUSION: In this work, we assessed the impact of the cranioplasty implant materials on dose calculations of the AAA and Acuros XB Algorithm against PRIMO MC Dose calculations. This study aids the users in selecting the appropriate dose calculation algorithm, where the artifact generated heterogeneity is prominent during stereotactic radiosurgery/radiotherapy planning.

DOSIMETRIC IMPACT OF GRID SIZE AND STATISTICAL UNCERTAINTY ON MONTE CARLO ALGORITHM IN VMAT PLANNING WITH MONACO TPS FOR SINGLE LESION BRAIN STEREOTACTIC RADIOTHERAPY

M. Akhtaruzzaman^{1,2}, KM Rafic¹, T. Ahmed¹, M.A. Ebert^{2,3}

¹Evercare Hospital Chattogram, Chattogram, Bangladesh, ²The University of Western Australia, Perth, Australia,

³Sir Charles Gairdner Hospital, Perth, Australia

Email: akhzam@gmail.com

BACKGROUND AND OBJECTIVE: Calculation grid size (CGS) and statistical uncertainty (SU) are important parameters in a Monte Carlo (MC) based treatment planning system (TPS), which determine the dose calculation accuracy and time. This study aimed to investigate the dosimetric impact of CGS and SU by varying beam energies and number of arcs in stereotactic radiotherapy of brain metastasis using Monaco TPS.

MATERIALS AND METHODS: Ten single lesion brain metastasis patients with tumour volume ranging from 2.47 cc to 4.64 cc were included in this study. The VMAT plans were generated using Monaco v6.0 TPS with a reference calculation using a CGS of 0.2 cm and SU of 1.0% for dual partial arcs with a 6FFF photon beam. Each plan was recalculated with CGS and SU values range from 0.1 to 0.3 cm and 0.25% to 2.0% respectively. For each CGS and SU combination, the variation from the ground truth calculation was determined for a range of dose volume metrics and plan quality indices as well as plan optimization time. The ground truth calculation was also evaluated using different beam energies and number of arcs.

RESULTS: Varying beam energies and number of arcs have no significant impact on dose volume metrics. However, such variations affect the conformity, homogeneity and gradient indices (CI, HI and GI) and total monitor unit (MU) up-to 4% and 7% respectively. Moreover, variable grid size calculation results in up to 4.5% difference in plan quality indices and 11.0% in MU. On the other hand, SU variations showed no influence on CI, GI and HI (<2.0%) and 6.4% variation in MU. However, increasing the SU results in reduced calculation time while increasing the maximum dose to the PTV.

CONCLUSION: The CGS has more impact on the dose distribution than SU. Further investigation is required to explore all suitable dose calculation parameters for small field SRT plans.

KEYWORDS: Stereotactic radiotherapy, Monte Carlo, Treatment planning

SYNCHROTRON RADIATION BASED X-RAY IMAGING FOR MEDICAL RESEARCH

Yogesh Kashyap^{1,2}, Balwant Singh^{1,2}, Ashish Agrawal^{1,2}, and Mayank Shukla^{1,2}

¹Neutron and Synchrotron Radiation Physics Section, Technical Physics Division, Bhabha Atomic Research Centre, Mumbai, India

²Homi Bhabha National Institute, Anushaktinagar, Mumbai, India

Email: yskashyap@barc.gov.in

Over the past 100 years, x-rays have been utilized for diagnostic medical imaging; nevertheless, despite the development of new methods like computed tomography, little has changed in the process of manufacturing x-rays. Synchrotron radiation sources offer numerous, incredibly powerful, and tuneable photon beams with energies ranging from infrared to hard x-rays. Their introduction improved a number of experimental methods, and synchrotron radiation is now used in a variety of domains, from molecular dynamics to imaging. It has led to the development of a number of techniques for analyzing live and moist tissue samples, providing details on both structure and content at all length scales, down to the atomic level. Such methods have been helpful in the advancement of molecular biology and the treatment of protein problems. The use of synchrotron radiation in radiography is currently growing, and it is established that very significant improvements in image quality and patient dose are possible.

Synchrotron radiation has a wide range of medical applications. The primary use of x-rays in medicine is diagnostic imaging, although this is only one of several procedures currently made possible by synchrotron radiation. Some of the approaches currently utilized in medicine could be significantly improved with the use of synchrotron radiation sources. Some of these techniques can be applied in vivo whilst others are more suited to in vitro studies which are potential constituents of the pathologist's tool kit.

An x-ray imaging beamline is currently operational at the Indus-2 synchrotron radiation source, RRCAT, Indore. The beamline covers energy range from 6-35keV in monochromatic mode and upto 50keV in white beam mode. Other than conventional x-ray radiography and tomography, new techniques such as grating interferometry, analyser based phase contrast imaging and fly-scan imaging mode have been implemented.

This paper presents overview of synchrotron radiation's generation and characteristics followed by a look at some of the ways in which this unique technology has previously been used for medical research, as well as some possible medical and diagnostic research applications.

KEYWORDS: synchrotron radiation, x-ray imaging, x-ray radiography, x-ray phase contrast imaging

CT-BASED DELTA-RADIOMIC IN DISCRIMINATION OF BENIGN AND MALIGNANT PULMONARY NODULES

Wenlong Li,¹Xiance Jin, Ph.D^{1,2}

¹Radiotherapy Center, First Affiliated Hospital of Wenzhou Medical University, Wenzhou, China, 325000,

²School of Basic Medical Science, Wenzhou Medical University, Wenzhou, China, 325000

Email: 1410024357@qq.com.

PURPOSE: To investigate the feasibility and accuracy of a preoperative CT-based delta-radiomic in discrimination benign and malignant pulmonary nodules.

METHODS: CT images 6 and 3 months before operation for a total of 177 patients with pulmonary nodules (72 benign and 105 malignant) in authors' hospital were retrospective enrolled and trained at a ratio of 7:3. Additional 34 patients (16 benign and 18 malignant) from second hospital enrolled for external validation. Target volumes were contoured by two professional radiologists with over 15-years of experience. Then the target volumes were expanded uniformly by 3mm to obtain the intratumoral and peritumoral volumes. Radiomics features were extracted from these regions and selected through Manney Whitt U test and LASSO to develop final radiomics models using support vector machine (SVM), Logistic regression (LR), and decision tree (DT).

RESULTS: The area under curve (AUC) achieved by SVM, LR and DT models with delta, tumor target, intra- and peri-tumoralradiomics features in the validation sets were 0.86, 0.80, 0.64; 0.84, 0.83, 0.71; 0.84, 0.83, 0.76; and 0.78, 0.83, 0.61, respectively. The models were further improved by integrating clinical factor with an AUC of 0.86, 0.85 and 0.87 in the differentiating of malignant and benign nodes for SVM, LR and DT, respectively. In the external validation, the combined models achieved an AUC of 0.80, 0.80 and 0.91 for SVM, LR and DT, respectively.

CONCLUSIONS:Preoperative CT based delta radiomics integrating with clinical factors achieved a high diagnostic rate for predicting benign and malignant pulmonary nodules.

KEYWORDS : Delta-radiomics, Radiomics, Intratumoral, Peritumoral.Pulmonary nodules

ARE DUAL- AND SINGLE-ENERGY CT ACQUISITION PROTOCOLS FOR PEDIATRIC THORAX IMAGING EQUIVALENT REGARDING RADIATION EXPOSURE?

Kostas Perisinakis, Nikos Ntoufas, John Damilakis,

University of Crete Medical School, Voutes, Heraklion Crete, Heraklion, 71003, Greece

Email: nickntoufas@gmail.com

PURPOSE-BACKGROUND: There is an ongoing debate regarding dose equivalency between dual-energy computed tomography (DECT) and conventional single-energy computed tomography (SECT) imaging. The purpose of this study was to quantitatively compare the dose to pediatric patients undergoing fast kV switching dual-energy computed tomography (DECT) against conventional single-energy computed tomography (SECT) thorax examinations when resulting efficiency to discriminate lesions is similar.

MATERIALS AND METHODS: A pediatric anthropomorphic phantom that simulates the body of an average 10-year-old individual, was used. Solutions of normal saline and iodine contrast agent with concentrations of 0.5% w/v, 0.3%w/v, and 0.1% w/v were employed to replicate high, medium, and low contrast lesions, respectively.

A CT scanner system capable of acquiring SECT and fast kV switching DECT protocols was used. Seven SECT image series were acquired by utilizing a SECT thorax acquisition protocol optimized for pediatric patients weighing between 30 and 50 kg with various levels of image noise. Additionally, a DECT thorax imaging acquisition was performed with the lowest dose selectable DECT imaging protocol. The CTDIvol was recorded after each scan. Contrast – to – Noise Ratio (CNR) of each lesion was calculated as an indication of resulting image quality. SECT and DECT acquisitions resulting in similar CNR values for the considered lesions were compared regarding associated radiation exposure.

RESULTS:The CNR values of the SECT images acquired with CTDIvol = 4.13 mGy were found not to differ significantly from DECT imaging acquired with CTDIvol = 10.3mGy for high-contrast lesions ($p=.27$), medium-contrast lesions ($p=.96$), and low-contrast lesions ($p=.14$). DECT imaging was found to be associated with 2.5 times higher radiation of exposure of SECT acquisition when resulting image series provide the same diagnostic efficiency of considered lesions.

CONCLUSION:Our results indicate that the fast kV switching DECT technique cannot replace SECT in clinical routine for thorax imaging in children and should only be used in cases where the diagnostic task is such that cannot be achieved with conventional SECT imaging.

INTEGRATING MODELS WITH RADIOMIC FEATURES, CLINICAL FACTORS, AND SERUM MARKERS IN THE DIFFERENTIATION BENIGN AND MALIGNANT PULMONARY NODULES

Heng Li, Huan Liu, Xiance Jin,

Department of Radiotherapy Center, 1st Affiliated Hospital of Wenzhou Medical University, Department of Radiotherapy Center, 1st Affiliated Hospital of Wenzhou Medical University, Wenzhou-325000, China

Email: 2296781476@qq.com

PURPOSE:To investigate the feasibility and accuracy of combined models integrating radiomic features, clinical factors, and serum markers in the classification of benign and malignant pulmonary nodules, so as to improve the accuracy of early diagnosis of lung cancer (LC) patients.

MATERIALS AND METHODS:A total of 316 patients with confirmed benign and malignant pulmonary nodules (174 benign and 142 malignant nodules) between July 2019 and July 2021 were retrospectively enrolled and reviewed from authors' hospital. Five serum markers including carcinoembryonic antigen (CEA), carbohydrate antigen 125 (CA125), squamous cell carcinoma antigen (SCC), neuron specific enolase (NSE), and cytokeratin 19 fragment antigen 21 -1 (CYFRA21-1) were included in the study. The CEA, CA125 and CYFRA21-1 level were determined using the immunoradiometric assay, and the NSE and SCC level were determined using electrochemiluminescence. Clinical factors associated with benign and malignant pulmonary nodules were selected using a univariate and multivariate regression. Radiomics features were extracted from the target volumes in the preoperative CT images and selected through Mann-Whitney U test and least absolute shrinkage and selection operator (LASSO). The radiomics features, clinical features, and serum markers were integrated across scales to establish support vector machines (SVM) and logistic regression models.

RESULTS:Based on univariate and multivariate analysis, anamnesis and size were the clinical factors that are associated with pulmonary nodules. After adjusting the parameters of the regression model, 13 features were screened from the 1288 radiomic features after Mann-Whitney U test using the elastic mesh method. The area under the curve (AUC) value achieved by the SVM and logistic model with integrated radiomic features, clinical features and serum markers was 0.931 and 0.888, respectively. With was 0.11 and 0.061 higher than models with radiomics and clinical factors alone, respectively. Finally, the classification ability of the model was verified in patients with negative serum markers.

CONCLUSIONS: The above results showed that the combined model integrating the advantages of the radiomic features, clinical features, and serum markers to distinguish pulmonary nodules effectively and made up for the disadvantages of their application alone.

KEY WORDS:Lung cancer; Radiomics; Serum markers; Node classification

MRI IMAGING FOR METASTATIC LESIONS USING MR SPECTROSCOPY-BASED METABOLITE RATIO ANALYSIS

Alamgir Hossain¹, Shahed Hossain²

¹Department of Physics, University of Rajshahi, Rajshahi-6205, Bangladesh,

²Popular Diagnostic Centre Limited, Laxipur, Rajshahi-6000.

Email: hossain447a@gmail.com

BACKGROUND/OBJECTIVE:The goal of MRS (magnetic resonance spectroscopy) is to obtain metabolic biochemical information from normal and pathological brain parenchyma in a non-invasive and quick manner. It is one of the methods for obtaining metabolic data by determining the molecular structures of viable brain tissues. For a small cohort, we wanted to see how accurate magnetic resonance spectroscopy (MRS) was at predicting Metastatic lesions.

MATERIALS AND METHODS:A Popular Diagnostic Centre Limited enrolled patients with neuroepithelial tumors. Using the ¹H CSI MRS of the brain, we can detect changes in the concentration of specific metabolites caused by metastatic lesions. These metabolites include N-acetyl-aspartate (NAA), creatine (Cr), and choline (Cho). The metabolic ratio was calculated using the division method for Cho, NAA, Cr, and Cr₂.

RESULTS: The NAA for tumor cells was 0.63 and 5.65, 1.86 and 5.66 for normal cells 1, 1.84 and 10.6, 1.86 and 5.66 for normal cells 2. In the tumor cell, Cho was as low as 0.8 and 10.53, compared to 1.12 and 2.7 for normal cell 1 and 1.24 and 6.36 for normal cell 2, respectively. Cho/Cr₂ was only marginally more significant than the other ratios. Tumor cells had significance for Cho/NAA, Cho/Cr₂, NAA/Cho, and NAA/Cr₂ ratios. For normal cell 1, the ratios of Cho/NAA, Cho/Cr, NAA/Cho, and NAA/Cr were all significant.

CONCLUSION: ¹H-MRSI can help improve the clinical outcome of metastatic lesions by guiding the extent of resection. Despite its noninvasive nature and lack of procedural difficulties, MRS has been shown to predict the detection of metastatic lesions.

KEYWORDS:Metabolite Ratio, MRI images, Metastatic lesion, MR Spectroscopy, Chemical Shift Imaging

AN ARDUINO-BASED DISTANCE SENSOR FOR REMOTE DEEP INHALE BREATH HOLD TRAINING

Rohit Inippully, Jishan Jaladharan, Rajesh K R, Iqbal Al Amri

Sultan Qaboos Comprehensive Cancer Care and Research Center, Muscat, Oman.

Email: rohitinippully@gmail.com

Deep inhale breath hold (DIBH) techniques are vital in radiation therapy for accurate treatment of thoracic and upper abdominal regions, especially for left breast to reduce radiation dose to the heart. However, training patients for consistent DIBH is challenging, especially for those unable to attend frequent hospital visits. This study presents the development of an affordable and portable Arduino-based distance sensor system to facilitate remote DIBH training from home. The system utilizes the VL53L0X Time-of-Flight (ToF) laser-ranging module connected to an Arduino microcontroller, interfaced with a custom graphical user interface (GUI) on the Nextion display for real-time feedback. The system was mounted on a phone holder that allows the sensor to be positioned above the patient's sternum and the display above the patient's head. The GUI displays the chest's vertical position during breath holds, allowing patients to visualize and maintain the desired depth. Initial testing with DIBH patients demonstrated the reliability and usability of the sensor system. Patients reported increased confidence in maintaining consistent breath hold depths due to the visual feedback provided by the device. The remote training approach reduced the burden of hospital visits, making DIBH training more accessible and convenient. The Arduino-based sensor system using the VL53L0X ToF laser-ranging module and Nextion display offers a promising solution for remote DIBH training, empowering patients to actively participate in their treatment planning and improve treatment accuracy. Further optimization and validation studies are necessary to evaluate the system's efficacy in a larger patient population and its impact on treatment outcomes. This cost-effective and portable solution has the potential to enhance DIBH training and benefit patients undergoing radiation therapy targeting thoracic and upper abdominal regions.

CSS ALERT -AN IN-HOUSE DEVICE DESIGNED FOR THE PROPER POSITIONING OF CSS THE IN CATH-LAB ROOM.

Sajeesh S Nair^{1,2}, Saral Kumar Gupta¹, Shine N S¹, K T Thomas², Bijumon P R³, Paul Thomas³,
Vijo George³, Gopakumar³

¹.Department of Physical Science, Banasthali Vidyapith, ²Department of Radiation & Oncology, General Hospital Ernakulam, ³Department of Cardiology, General Hospital Ernakulam, Kerala, India

Email:pgphb19268_sajeesh@banasthli.in

PURPOSE:The Ceiling suspension shield (CSS) is a simple lead equivalent transparent sheet used in the Cath lab to reduce scattered doses to the staff. According to IAEA data, CSS can give 90% protection to the staff from the scattered dose. It is important to change the position of the CSS according to the position of the X-ray tube and detector, the failure leads to loss of protection. The busy schedule of the Cath-lab procedures will lead to neglecting the proper usage of this crucial protective device. This study aims to design an alert system to increase the safety level of staff by prompting them to use CCS when it was not in the proper position during the procedure.

MATERIAL AND METHODS: The main components used in this device are the Ultrasonic Sensor module, IC 555, IC 7404, 10 K and 1 K resistors, 100 μ F and 10 μ F capacitors, Piezo buzzer, LEDs and power supply. IC 555 is wired as an astablemultivibrator for producing continuous square pulses to trigger the ultrasonic transmitter to produce Ultrasonic sound (USS) signals. The reflected USS signal was detected by the receiver in the sensor module to produce an output signal. The whole circuit is enclosed in a small box and attached to the side of the flat-panel detector (FD) of the cath lab machine. When switching on the device, it will continuously emit USS signals, and these signals are reflected by CSS. The receiver in the device identifies the signals and confirms the CSS presence, the contrary situation leads to the production of alert signals

RESULT: When the CSS is not positioned in between FD and the operator (Cardiologist), the device produces an alert signal in the form of red lights and alarms. The range of detection was 40 cm.

CONCLUSION:These types of alert mechanisms and interlocks are significant in interventional radiological procedures. We suggest incorporating a similar circuit with these machines helps to increase the radiation safety level in these procedure rooms resulting in the reduction of staff dose.

KEYWORDS:Interventional Radiology, Radiation Protection, Cath-lab

RADIOMIC SIGNATURES FOR DIAGNOSING BENIGN AND MALIGNANT ABNORMALITIES IN X-RAY MAMMOGRAMS

AritaHalder, Manjunatha Mahadevappa

School of Medical Science and Technology, Indian Institute of Technology, Kharagpur, India

Email: aritahalder@gmail.com

PURPOSE/BACKGROUND: Breast cancer is one of the leading causes of mortality among women. Early detection of breast cancer is of utmost importance for women's well-being. Radiomics, an emerging field in medical research, leverages quantitative features to characterize regions of interest in radiological images. This abstract presents the findings of a radiomic analysis conducted on a recently published public dataset to diagnose benign vs malignant breast cancer.

MATERIALS/METHODS: The CDD-CESM data set obtained from The Cancer Imaging Archive was used in this study [*Journal of Digital Imaging*. 2013 Dec;26(6):1045-57. DOI: 10.1007/s10278-013-9622-7]. Contrast enhanced digital mammography (DM) images of the medio lateral oblique (MLO) view from 255 female patients were utilized for this study. From a total of 822 abnormalities (474 Malignant, 348 benign) identified by radiologists, 102 radiomic features, including texture, shape and first-order intensity-based features, were extracted using the pyRadiomics package in python. The dataset was divided into a 70:30 ratio for training and testing purposes. To reduce the dimensionality of the feature space and focus on the most relevant features, a wrapper-based feature selection method called recursive feature elimination (RFE) was employed. Five machine learning models were trained: Support Vector Machine (SVM) with radial basis function, SVM with linear kernel, Random Forest, Logistic Regression and XGBoost. Performance metrics and receiver operating characteristic (ROC) curves were assessed to evaluate the effectiveness of the models. Moreover, the feature importance of the best-performing model was determined to provide additional insights into the classification capabilities.

RESULTS: Feature selection using RFE resulted in a reduced feature dimension of just 36 features. The XGBoost classifier outperformed other models with an accuracy of 0.80 and Area Under the ROC Curve (AUC) of 0.87. Feature importance analysis revealed that texture and shape features played a crucial role in classifying benign and malignant abnormalities. The top 10 features consisted of 5 texture features, 3 shape features and 2 first-order features.

CONCLUSIONS: The findings of this study contribute to the understanding and development of radiomic-based approaches for early detection and accurate diagnosis of breast cancer. Radiomic signatures thus provide information beyond human perception and help radiologists in the decision-making process.

KEYWORDS: radiomics, machine learning, breast cancer diagnosis, X-ray mammograms

IMAGING HARMONIZATION WITH DEEP LEARNING FOR ULTRASOUND IMAGES BASED RADIOMICS

Zeshuo Zhao¹, Juebin Jin², Xiance Jin^{1,3}

¹Department of Radiotherapy Center, 1st Affiliated Hospital of Wenzhou Medical University, Wenzhou, China, ²Department of Medical Engineering, 1st Affiliated Hospital of Wenzhou Medical University, Wenzhou, China, ³School of Basic Medical Science, Wenzhou Medical University, Wenzhou, China

Email:jinx1979@hotmail.com

BACKGROUND: Ultrasound (US) based radiomics is susceptible to variations in scanners, sonographers.

OBJECTIVE: To investigate the feasibility an adapted cycle generative adversarial networks (cycle-GAN) in the style transfer for US based radiomics in the prediction of lymph node metastasis (LNM) with images from multiple scanners for patients with cervical cancer (CC).

METHODS: The cycle-GAN was firstly trained to transfer paired US phantom images from one US device to another one; the model was then further trained and tested with clinical US images of CC by transferring images from four US devices to one specific device; finally, the adapted model was tested with its effects on the accuracy of LNM prediction in US based radiomics for CC patients.

RESULTS: Phantom study demonstrated an increased image quality using Cycle-GAN with 934 paired phantom images. The average Pearson correlation coefficients were 0.604 and 0.813 for radiomics features extracted from original and generated images in correlation with the target phantom images, respectively. Clinical US images of 169 CC patients were enrolled for style transfer model training and validation. The area under curve (AUC) of LNM prediction radiomics models with features extracted from generated images of different style transfer models ranged from 0.732 to 0.850. The AUC was improved from 0.784 with features extracted from original images to 0.850 with style transferred images.

CONCLUSIONS: The adapted cycle-GAN network was feasible and accurate to convert US images from different US devices into images of one specific device to improve the image quality and radiomics studies performance.

KEYWORDS: Harmonization; Generative adversarial networks; Ultrasound; Radiomics; Lymph node metastasis

PREDICTION AND CORRELATION OF GAMMA PASSING RATES WITH COMPLEXITY METRICS USING MACHINE LEARNING TECHNIQUES FOR INTENSITY-MODULATED RADIATION THERAPY

Dinesh Saroj, Suresh Yadav, Neetu Paliwal, Ravindra Shende, Subhas Haldar, Gaurav Gupta

Department of Radiotherapy, Balco Medical Center, A Unit of Vedanta Medical Research foundation, Sector 36, Upparwara, New Raipur, Raipur, 493661, India

Email: dinesh.saroj@ymail.com

BACKGROUND/OBJECTIVE: Intensity-modulated Radiation Therapy (IMRT) allows for more precise dose painting of tumor targets, however, it can lead to increased beam modulation, longer treatment times, and higher dosimetric uncertainty. As a crucial step in modern radiation therapy, patient-specific quality assurance (PSQA) aims to ensure treatment accuracy and safety by identifying any discrepancies between planned and delivered radiation fluence. Variability in PSQA results can contribute to differences in measured or calculated dose distributions. Complexity metrics are essential in characterizing IMRT plans based on various factors like fluence, MLC positions, and aperture shape providing valuable insights into the treatment plan complexity and modulation. Excessive complexity in IMRT plans can increase dose uncertainty, prolong treatment times, and raise susceptibility to changes in patient or target geometry. This study aims to identify the best regression model to predict the gamma passing rates (GPR) for IMRT treatment plans and find its correlation with various treatment plan complexity metrics.

MATERIALS &METHODS: We have selected 30 patients of Head & Neck Cancer, treated with 6MV photon beam with IMRT technique for retrospective study. Five machine-learning models were explored to identify the best-performing regression model for predicting GPR. Predictors used in these models consist of monitor units (MU), control points (CPs), beam area (BA), and modulation complexity score (MCS). Model performance was evaluated in terms of Mean Squared Error (MSE), Root Mean squared Error (RMSE), and R2 score.

RESULTS: Gamma index analysis was performed using portal dosimetry with 3% and 3mm and 10% threshold criteria. The linear regression model has an MSE of 0.689 % and R2 of 0.88, Ridge regression has an MSE of 1.70% and R2 of 0.71, Decision Tree regression has an MSE of 2.41% and R2 of 0.58, Random Forest regression has an MSE of 1.54% and R2 of 0.74. XGBoost regression has an MSE of 1.31% and R2 of 0.77. MCS shows a strong positive correlation with MU (65%) and CPs (79%).

CONCLUSION: Using complexity metrics, linear regression shows the best fit to predict the GPR of portal dosimetry. This model can potentially be applied to predict the GPR before performing the PSQA.

KEYWORDS: Intensity-modulated Radiation Therapy, Complexity Metrics, Machine Learning, Gamma Passing Rate, Patient-specific Quality Assurance

DEVELOPMENT OF A 3D-PRINTED HETEROGENEITY PHANTOM FOR ENHANCED PATIENT-SPECIFIC DOSIMETRY FOR HYPOFRACTIONATED RADIOTHERAPY

Ashish Binjola^{1,2}, V. Subramani¹, N. Gopishankar¹, Sukhvir Singh³, R. K. Bisht², D. N. Sharma¹, Pratik Kumar²

¹Department of Radiation Oncology, Dr. B. R. A. Institute Rotary Cancer Hospital, All India Institute of Medical Sciences, New Delhi – 110029,

²Department of Medical Physics Unit, Dr. B. R. A. Institute Rotary Cancer Hospital, All India Institute of Medical Sciences, New Delhi – 110029,

³Institute of Nuclear Medicine & Allied Sciences, DRDO, New Delhi-110054

Email: ashishbinjola2002@yahoo.com

BACKGROUND: For patient-specific radiation dosimetry, water-equivalent homogeneous phantoms are generally utilized. However, this limits the evaluation of the effects of a patient's anatomical heterogeneity on the dose calculation accuracy. To provide an economical solution to this problem, a Polylactic Acid (PLA) phantom was printed with varying infill percentages. This phantom was used to perform measurements related to hypofractionated (VMAT-based SRS/SBRT) treatments.

MATERIALS AND METHODS: Five slabs of 100 mm X 100 mm X 10 mm dimensions with infill percentages of 20, 30, 40, 80, and 100 (with grid pattern) were printed using PLA filament using material extrusion Creality Ender 3 S1 Pro 3D printer. To print a 3D printed object, first, a model of the object is prepared in 3D designing software then this model is processed in slicer software to generate the Gcode. Gcode is sent to a 3D printer to print the object. CT of the phantom with an IBA-I'matrix Array detector was taken at 120 KV using a Philips CT simulator. CT was imported to the Monaco TPS version 5.11.03. QA plans were generated for 5 patients (two prostates, two lungs, and one brain) and the required dose planes were exported to IBA My QA-patient software. All calculations in TPS were performed using X-ray Volume Monte Carlo (XVMC) algorithm with 1% uncertainty and 0.3 mm grid resolution. QA Plans were delivered on the phantom and TPS calculated and measured doses were compared.

RESULTS: Comparison of calculated and measured doses show a gamma passing rate of 96.7 % and 97.3 % for prostate SBRT cases, 97.6% and 97.8% for lung SBRT cases and 98.9 % for Brain SRS with a gamma passing criteria of dose difference of 3% and distance to travel agreement of 2 mm (3%, 2mm).

CONCLUSION: This 3D-Printed phantom is a simple, lightweight, and economical tool that offers valuable insights into the accuracy of dose calculation algorithms for heterogeneous media. It represents anatomical diversity in a better manner compared to water-equivalent commercial phantoms.

KEYWORDS: 3D-Printed Phantom, Patient-Specific Dosimetry, SRS, SBRT

SPLIT JAW TECHNIQUES IN VMAT: DOSIMETRIC IMPACT OF JAW TRACKING METHOD FOR EXTENDED TARGET VOLUMES OF HEAD AND NECK CANCERS

Boopathi M^{1,2*}, D Khanna¹, P Mohandass³, P Venkatraman⁴, K Venkatesan⁵

¹Karunya Institute of Technology and Sciences, Coimbatore, ²Dharan Cancer Speciality Centre, Salem, ³Fortis Cancer Institute, Mohali, ⁴Department of Medical Physics, Bharathidasan University, ⁵Medanta The Medicity, Gurugram, India

Email: pathi_05@yahoo.com

OBJECTIVE: Purpose of this study is to investigate dosimetric impact of Jaw Tracking (JT) method in the treatment of extended target volumes of head and neck cancer using Volumetric modulated arc therapy (VMAT).

MATERIALS AND METHODS: For this study, a total of twenty-one head and neck patients retrospectively were selected from clinical data base. Two sets of VMAT plans were generated using Jaw tracking and fixed Jaw (FJ) method. All the VMAT plans were generated with 6MV photon beam using Eclipse™ treatment planning system (TPS) for Varian TrueBeam™ STx machine. The reference FJ-VMAT plan was compared with JT-VMAT plan using various dosimetric indices. For comparison, homogeneity index (HI), conformity index (CI), mean dose, max dose and dose received by planning target volume (PTV) were analysed. The dose received by organ at risk volumes (OAR) such as spinal cord, brain stem, left parotid, right parotid were compared. In addition, total monitor units (MU), dose volume received by healthy tissues, gamma index of dose to distance agreement of 3%/3mm, 2%/2mm, and 1%/1mm were compared between FJ-VMAT and JT-VMAT plans.

RESULTS: The results of mean dose, max dose and dose volume received by PTV volume (D98%) did not show any significant dose different between FJ-VMAT and JT-VMAT plans ($p>0.05$). The CI and HI results were 0.967 ± 0.01 , 0.969 ± 0.01 ; 1.105 ± 0.01 , 1.111 ± 0.02 between FJ-VMAT and JT-VMAT plans and no significant difference were observed ($p>0.05$). Similarly, mean dose, max dose and dose volume received by spinal cord, brain stem, left parotid, right parotid showed insignificant difference in JT-VMAT as compared to FJ-VMAT ($p>0.05$). A slight increase of gamma index and dose received by healthy tissues in FJ-VMAT than JT-VMAT plans ($p>0.05$). Moreover, total MU of JT-VMAT was higher as compared to FJ-VMAT ($p<0.05$).

CONCLUSION: From the above results, for head neck plans, the dosimetric impact of JT-VMAT was almost similar to FJ-VMAT in terms of PTV coverage, OAR dose. However, a significant increase of MU was found in JT-VMAT as compared to FJ-VMAT.

KEYWORDS: Jaw tracking, Split jaw techniques, VMAT

REFERENCES:

1. A Dosimetric Study Using Split X-Jaw Planning Technique for Treatment of Endometrial Carcinoma, Jeanette Keil, MS, CMD, RT(R)(T), AAMD 44th Annual Meeting, June 16 – 20, 2019.
2. A Dosimetric study using split x-jaw planning technique for the treatment of endometrial carcinoma by Jeanette Keil, MS, CMD, RT(R)(T) a, *, Joanne Carda, MS, CMD, RT(R)(T) b, Jade Reihart, MS, CMD, RT(T) c, Marjorie Seidel, CMD, RT(R)(T) a, Nishele Lenards, PhD, CMD, RT(R)(T), FAAMD d, Ashley Hunzeker, MS, CMD d. Medical Dosimetry, AAMD, April 2020.
3. Impact of split X-jaw technique on target volume coverage and organ at risk sparing in prostate cancer: a comparative dosimetric study by Gautam sarma, Jyotiman Nath, Shachindra Goswami, Pranial Goswami, Shashi Bhushan Sharma, Apurba Kumar Kalita. Published online by Cambridge University Press: 13 May 2022.
4. Dosimetric Importance of Implementing Jaw Tracking Technique in Radiotherapy Treatment Plan Execution. Hridya V T, Khanna D, Raj A, Padmanabhan S, P M. Asian Pac J Cancer Prev. 2022 Apr 1;23(4):1397-1403. doi: 10.31557/APJCP.2022.23.4.1397. PMID: 35485702; PMCID: PMC9375617.

CLINICAL IMPLEMENTATION OF HYBRID SOLITARY DYNAMIC PORTAL PLANNING TECHNIQUE FOR POST-MASTECTOMY RADIOTHERAPY WITH VERSA HD LINEAR ACCELERATOR

¹K Mohamathu Rafic, ²M Akhtaruzzaman, ²Tanvir Ahmed, ²Hasnina Akter, ²Sajjad Mohammad Yusuff

¹Govt Medical College and Hospital, Department of Radiation Oncology, Pudukkottai, 622004, India

²Evercare Hospital, Department of Radiation Oncology, Chattogram, 4337, Bangladesh

Email: drkmrafic@gmail.com

BACKGROUND AND OBJECTIVE: A monocentric hybrid solitary dynamic portal radiotherapy (h-SDPRT) planning technique for postmastectomy chest-wall and regional lymph node irradiation was formerly developed using Eclipse Treatment Planning System (TPS) to overcome the limitations imposed by conventional and conformal techniques (Rafic et al., 2020). This study focuses on the clinical implementation of h-SDPRT for postmastectomy radiotherapy (PMRT) using Monaco TPS to complement the results published previously.

MATERIALS AND METHODS: Twenty patients who underwent surgical mastectomy followed by PMRT were included in this study. The h-SDPRT plans were computed to deliver about 80-85% of prescribed dose using static open fields and 15-20% of dose using less complex solitary dynamic field (created from medical tangent) that consists of 10 to 15 field-in-fields (4-5% per segment). It can be computed with minor amendments to the global normalization method using Monaco TPS. Dosimetric analysis for the treatment plans and fluence verification for the solitary dynamic portals were performed.

RESULTS: The h-SDPRT planning technique showed excellent dose coverage ($V_{95\%} > 95\%$), higher degree of tumor dose conformity (≤ 1.3) and homogeneity (≤ 0.13) without compromising the organ-at-risk (OAR) sparing in PMRT chest-wall and regional lymph node irradiation. The h-SDPRT considerably reduced the dose to ipsilateral lung and heart, and completely spared contralateral OARs ($V_5 < 3.5\%$) and healthy normal tissues without affecting the dose homogeneity. The Monaco TPS results are in good agreement with previously published data using Eclipse TPS. The gamma evaluation of dynamic portals showed more than 97% pixel pass rate for standard 3%/3 mm dose difference and distance-to-agreement criteria. Moreover, h-SDPRT plan offers less probability of “geometrical miss” and better compromise on delivery uncertainty associated with highly irregular chest-wall with regional nodes.

CONCLUSION: It is feasible to compute h-SDPRT plan using Monaco TPS. The h-SDPRT technique is an effective method to achieve homogenous dose distribution across the chest-wall and regional nodes. Static portals with adequate relaxation margins for breathing, along with less complex solitary dynamic portal offer promising treatment option for PMRT. The future scope of this study is to adapt the Active Breathing Coordinator to h-SDPRT technique.

KEYWORDS: Hybrid Planning, Post-mastectomy Radiotherapy, Breast Cancer

Presentation ID: O-064

CONTRAST-CALIBRATED PHOTON-COUNTING X-RAY COMPUTED TOMOGRAPHY USING A CADMIUM TELLURIDE FLAT PANEL DETECTOR WITH HIGH SPATIAL RESOLUTIONS

Jiro Sato¹, Eiichi Sato², Kazuki Ito¹, Hodaka Moriyama¹, Osahiko Hagiwar¹, Toshiyuki Enomoto¹, Manabu Watanabe¹, Sohei Yoshida³, Kunihiro Yoshioka³, Hiroyuki Nitta⁴

¹Department of Surgery, Toho University Ohashi Medical Center, 2-22-36 Ohashi, Meguro, Tokyo 153-8515, Japan

²Honorary Professor of Physics, Iwate Medical University, 2-14-6 Kawaramachi, Wakabayashi, Sendai, Miyagi 984-0816, Japan

³Department of Radiology, School of Medicine, Iwate Medical University, 2-1-1 Idaidori, Yahaba, Iwate 028-3694, Japan

⁴Department of Surgery, School of Medicine, Iwate Medical University, 2-1-1 Idaidori, Yahaba, Iwate 028-3694, Japan

Email: jiro.sato@med.toho-u.ac.jp

Background/Objective: Cadmium telluride (CdTe) detectors are useful for measuring photon energy, and the energy resolution has been improved to 1% at 59.5 keV. Therefore, we developed several first-generation photon-counting X-ray computed tomography (PCCT) scanners to perform K-edge CT using iodine (I) and gadolinium (Gd) contrast media. Using these scanners, the spatial resolution was improved to 0.25 mm, and fine blood vessels were observed at a high contrast. Subsequently, we developed a cone-beam PCCT scanner using a CdTe flat panel detector (FPD) to reduce the scanning time and to improve the spatial resolution. However, the contrast variations were slightly different from those obtained using a first-generation PCCT with a high energy resolution. In this regard, we performed contrast-calibrated cone-beam PCCT using the FPD.

Materials and methods: The cone-beam PCCT scanner mainly consists of a 0.1-mm-focus X-ray generator, an FPD, a turntable, and a personal computer (PC). The object is irradiated by the X-ray generator, the penetrating photons are detected using the CdTe FPD, and 720 radiograms from the FPD are sent to the PC to reconstruct tomograms. The standard image contrast as a density difference between two different-concentration Gd media was measured using a first-generation PCCT with a CdTe detector and a high energy resolution. The image density difference between the two media was shifted to one obtained using the first-generation CT utilizing photon-energy shifting. In this case, the effective photon energy increases with increasing digital amplification factor utilizing beam hardening.

Results: In the cone-beam PCCT, we carried out Gd-K-edge CT using Gd media and photons ranging from 50 to 100 keV. The tube voltage was 100 kV, and the threshold energies were 20 and 50 keV. Thus, we used two energy ranges of 20-100 and 50-100 keV, and the image contrast of the media improved according to increases in the threshold energy. The effective energy of the 50-100 keV tomograms was lower than that of the first-generation tomograms, the energy was slightly shifted to higher energies using the digital amplifier. Utilizing the image-contrast calibration, fine blood vessels in a rabbit head were visible.

Conclusions: We constructed a cone-beam PCCT using a CdTe FPD and a 0.1-mm-focus X-ray tube, and Gd-K-edge CT was performed. The image contrast was calibrated using a first-generation PCCT, and the effective energy of tomogram increased with increasing digital amplification factor. The spatial resolution was improved below 0.1 mm, and fine blood vessels were observed at a high contrast.

Keywords: photon-counting CT, cone-beam, CdTe FPD, contrast calibration, Gd-K-edge CT

SKIN REACTIONS ASSOCIATED WITH FLUOROSCOPIC INTERVENTIONAL PROCEDURES IN RELATION WITH EQUIPMENT DISPLAYED DOSE PARAMETERS

Dharuman Vadivel, Susama Rani Mandal, Sanal Narayanan, Visvanathan N, Thamarai Selvi P, Raj Kishor Bisht, Pratik Kumar

Medical Physics, AIIMS, Dr. Bra. Irch, AIIMS, Ansari Nagar, New Delhi, India

Email: dharumanphy@gmail.com

BACKGROUND/ OBJECTIVE: Interventional procedures like, Interventional Radiology (IR), Interventional Cardiology (IC) and Interventional Neurology (IN), generally guided by fluoroscopy procedures are much appreciated and popular practice among the radiologist fraternity in recent years. Interventional procedures are economical, minimally invasive, and favor patient health in lowering the post-operative clinical risk. In addition to the cited benefits, prolonged exposure during procedures causes an increased but significant ionizing radiation dose (direct to indirect) to the patients and operating staff. In view of reasonably increased levels of radiation exposure to the skin of the patient, the presented study was performed to evaluate the health effects of the patient using supportive dose parameters, physics protocol, and acceptance.

MATERIALS AND METHODS: The data of the prospective patients scheduled for x-ray fluoroscopic interventions in 6 modern fluoroscopic machines of the institute belonging to cardiology, radiology, cardiac-radiology and neuro-radiology were collected and analyzed for various dose-parameters. A modest data sheet that includes the values of Dose Area Product (DAP), total Air- KERMA ($K_{a,r}$), and the total fluoroscopy time (minutes) was prepared for selected machines. The data was collected for a period of 6-months and recorded. The trigger value of this study was kept as per IAEA protocol, which was DAP value of 500 Gy-cm², Air-KERMA of 5 Gy, and a fluoroscopic-time of 60 minutes. The parameters exceeded the triggered values were recorded and the systematic health check was conducted during planned follow-ups.

RESULTS: The datasheet of 1300 distinct patients undergoing fluoroscopy guided intervention was prepared for this study. The parameters of 43 (3.3%) patients exceeded on various trigger values. The mean of DAP, $K_{a,r}$ and exposure time of these 43 patients who exceeded any of the three trigger values was 290.841 Gy-cm², 14.51 Gy and 76.92 minutes. A systematic follow-up was done. Though no patients reported adverse health effect to the physician/radiologist on their own, the systematic follow-up and pointed and structured enquiry revealed that 2 patients (0.15%) were presented with skin reactions in the form of erythema over a period of one week after fluoroscopic examinations.

CONCLUSION: In this study, we can conclude with the use of indirect patient dose parameters such as total air kerma, total fluoroscopy time, and DAP; the health effects of the patients undergoing interventional procedure can be assessed with systematic follow up.

REFERENCES:

International Atomic Energy Agency (2010). Patient Dose Optimization in Fluoroscopically Guided Interventional Procedures Final Report of a Coordinated Research Project (IAEA-TECDOC--1641). International Atomic Energy Agency (IAEA).Bjelac, O.C., Dabin, J., Farah, J., Järvinen, H., Malchair, F., Siiskonen, T. and Knežević, Ž., 2019. Patient maximum skin dose in interventional procedures in radiology and cardiology: summary of WG 12 activities.

KEYWORDS: Interventional procedure, Skin reaction, indirect patient dose parameters

QUICK QUALITY ASSURANCE PROGRAM IN AN ENGAGED DIAGNOSTIC RADIOLOGY DEPARTMENT: AN INTRODUCTION TO THE FREQUENT BUT SHORT TESTS

Sanal Narayanan, Susama Rani Mandal, Dharuman Vadivel, , Visvanathan N, Thamarai Selvi P, Ram Karan, Raj Kishor Bisht, Pratik Kumar

Medical Physics, AIIMS, Dr. Bra. Irch, AIIMS, Ansari Nagar, New Delhi, India

Email: sanalnnn@gmail.com

BACKGROUND/OBJECTIVE: Foremost performance of elementary to modern radiation-generating equipment has implications for the safety of the patient, staff, and machine. The optimal performance of radio-diagnostic machines for agreeable imaging, analysis & regulatory compliance needs frequent quality-assurance (QA) tests. In India, these QA tests must be reported to the regulatory authority biennially. In view of the expected variation in various machine parameters through these two years, the study was designed to check the intermittent quality of machines in an engaged radiology department.

MATERIALS AND METHODS: A modest data sheet for quick-quality-assurance (QQA), was prepared for various X-ray, CT, and fluoroscopic machines. Congruence between optical and radiation field, central axis analysis, tube voltage (kVp) accuracy, current-time investigation (mAs), radiation output, and dose rate measurements in addition to a radiation survey of installations was done for 30 equipment in a month's interval for a period of 5 years.

RESULT: The maximum variation in the field congruence was 3.6% (mean-2.2 %), the central beam alignment varies within 1.5°, and the variation in kVp was found to be ± 3.44 kVp (max-4.70kVp) when the tests performed per "the tool on couch" arrangement. However, the optical-to-radiation field concurrency exceeds the tolerance of 2cm in the interval of 6 months for 60% of fixed X-ray & fluoroscopic machines. There was no significant variation in timer (max-0.8%) and radiation output (with a coefficient of variation-0.048) was observed. Mechanical and electrical checks exhibited substantial disparity and appeared of most challenging. The warning lights, controlled area signs, couch movement/console switch functions, and undesirable mechanical movement of the machine are a few inconsistencies observed during QQA. The radiation survey of the installation showed higher radiation leakage at the control console and patient entrance door when compared with the readings from six months before. The lead lining of the door was found frayed in most of the installation due to ragged use.

CONCLUSIONS: All the discrepancies were found despite the equipment having undergone monthly QQA-tests. The periodic nature of the proposed QQA-test promotes continued excellence in patient care, and machine performance in addition to improvement of the general standard of radiological services.

KEYWORDS: diagnostic radiology, quick quality assurance, patient care

REFERENCES: 1. Atomic, Energy Regulatory Board. *Radiation safety in manufacture, supply and use of medical diagnostic X-ray equipment*. No. AERB/RF-MED/SC--3 (REV. 2). Atomic Energy Regulatory Board, 2016. 2. INTERNATIONAL ATOMIC ENERGY AGENCY, Handbook of Basic Quality Control Tests for Diagnostic Radiology, IAEA Human Health Series No. 47, IAEA, Vienna (2023)

IN-HOUSE FABRICATION OF AN ERGONOMIC PRONE BREAST BOARD AS AN INNOVATION IN MEDICAL PHYSICS FOR BETTER DELIVERY OF RADIATION THERAPY IN EARLY STAGE BREAST CARCINOMA

Misba Hamid Baba^{1,2}, Benoy Kumar Singh¹

¹Department of Physics, Institute of Applied Sciences & Humanities, GLA University, Mathura- 281406, Uttar Pradesh, India; ²Department of Radiological Physics & B.E, Sher I Kashmir Institute of Medical Sciences, Soura, Srinagar, J & K India-190011

Email: misba8@gmail.com

BACKGROUND AND PURPOSE: The ergonomic prone breast board fabricated in-house is an innovation in medical physics, specifically in the field of breast cancer treatment, aimed at enhancing treatment outcomes at the clinic itself. The device is engineered with a deep understanding of human anatomy and ergonomics, ensuring that patients are positioned in a manner that promotes both comfort and accurate treatment delivery. The ergonomic features of the prone breast board allow for the natural distribution of breast tissue, reducing strain on the patient and minimizing the potential for discomfort during prolonged treatment sessions. Furthermore, the ergonomic design of the prone breast board contributes to enhanced treatment precision and efficacy. By optimizing patient positioning and immobilization, the device enables precise targeting of the breast tissue while minimizing radiation exposure to surrounding healthy structures.

MATERIALS AND METHODS: Ergonomic prone breast board was customized using the Styrofoam blocks (density 0.075g/cc). It is fabricated in three parts to support three areas of the patient's body viz- head, the lower wedge abdo-pelvic part to hold abdomen and pelvis and the central breast bridge placed in between the head and abdo-pelvic assembly to hold the contralateral breast away from the beam path and position the involved breast hanging in the cavity that it forms when positioned between the head and the abdo-pelvic assembly. The dosimetric transmission factors through various parts were measured using ionization chambers.

RESULTS: The Ergonomic breast board fabricated showed a mean transmittance of 95.70%. The transmittance values for perpendicular incidence were 95.76% for head part, 95.78% for breast bridge, and 95.58% for the abdo-pelvic wedge. The oblique transmittance value through the head was 95.76%, 95.72% for the breast bridge, and 95.57% for the abdo-pelvic wedge.

CONCLUSIONS: The transmittance values measured depicts that radio transparent nature of our innovation thereby confirming the suitability of the ergonomic prone breast board to be used in clinics with ease and in a cost effective manner. In conclusion, the ergonomic prone breast board represents a significant advancement in medical physics and breast cancer treatment.

KEYWORDS: Ergonomic, Prone Breast Board, Cost effective

ASSESSMENT OF SAFETY CULTURE IN RADIOTHERAPY FACILITIES USING SAFETY PERFORMANCE INDICATOR (SPI): THE INDIAN EXPERIENCE

Smriti Sharma^{1,2}, S. Mahalakshmi¹, Arti Tripathi¹, Namitha Krishnakumar¹, P.K. Dixit¹, G. Sahani¹, P. K. Dash Sharma¹, J. P. Agarwal³, R. A. Kinkhikar^{2,3}

¹Radiological Safety Division, Atomic Energy Regulatory Board, Anushaktinagar, Mumbai-400094, India.

²Homi Bhabha National Institute, Anushaktinagar, Mumbai-400094, India.

³Tata Memorial Centre, Mumbai, India.

Email: sharmasmriti.24@gmail.com

PURPOSE/BACKGROUND: The International Atomic Energy Agency defines safety culture as “The assembly of characteristics and attitudes in the organizations, its managers and workers which assures that, as an overriding priority, safety issues receive the attention warranted by their significance.”

It is well acknowledged fact that lack of safety culture is one of the main contributory factors to incident/accident in radiotherapy. Considering the necessity towards enhancement of safety culture in radiotherapy, pilot study for its independent assessment was planned and developed Safety Performance Indicator(SPI) checklist. This paper describes the methodology of development of SPI, its execution process and reports the finding of the safety culture assessment of radiotherapy facilities in India.

MATERIAL AND METHODS: SPI checklist was prepared based on the regulatory requirements, international standards and good work practices. The Checklist was broadly classified in eight major sections such as management involvement towards regulatory compliance, allocation of resources, availability of security/emergency plan, reporting of unusual occurrences and compliance of earlier & current regulatory inspection. For quantitative assessment, scoring criteria was decided on the scale of 0 to 2 of each section. Intermediate scores with reason/justification (in steps of 0.5) were assigned by assessor. The total maximum score was 46. The facility was considered to meet high levels of regulatory compliance and safety culture if it scores >80%. Institute with scores<50%, additional measures such as specific training and guidance was planned to advise institute to enhance culture.

Safety culture assessment using checklist along with planned regulatory inspection was carried out at Seventeen radiotherapy institutes. Advisory letters were sent to all the institutes indicating the SPI score, areas of strength and areas of improvement.

RESULTS: SPI score of seven institutes found to be more than 80% while for remaining ten institutes SPI score was in the range of 67.4% to 80%.

CONCLUSION: Developed SPI checklist found to be good tool for safety culture assessment. Score indicates that good safety culture is in place in majority of radiotherapy institutes. Though, AERB is planning to assess safety culture of radiotherapy institutes, in future, the checklist may be utilized by Radiological Safety Officer for self-assessment in order to identify the areas of improvement.

OPTIMIZATION OF TARGET, BEAM, AND DEGRADER FOIL PARAMETERS FOR ^{64}Cu PRODUCTION USING SOLID TARGETARY SYSTEM OF A MEDICAL CYCLOTRON

Sukhvir Singh, Jayshree Dadheech, Kirti Dhingra, Puja Panwar Hazari

Division of Cyclotron and Radiopharmaceutical Sciences (DCRS)
Institute of Nuclear Medicine and Allied Sciences, DRDO, Timarpur, Delhi-110054

Email: puja.inmas@gov.in

BACKGROUND/OBJECTIVE: ^{64}Cu has emerged as versatile and important theranostic radioisotope and finding its way in routine clinics after FDA approval. Unique decay scheme of ^{64}Cu , featuring β^- , β^+ decay and electron capture makes it ideal agent of theranostic. However, limited availability of ^{64}Cu at affordable costs restricts its use in India. INMAS has taken up a task to produce high purity novel radioisotopes including ^{64}Cu . Present study discusses the optimization of ^{64}Cu production yield using ^{64}Ni (p,n) ^{64}Cu nuclear reaction with respect to beam, target, foil parameters, and contaminant radioisotopes. GEANT4 Monte Carlo simulations were utilised to model medical cyclotron (PETtrace) beam transport system and interaction of proton beam with the target material.

MATERIALS AND METHODS: GEANT4 (ver.11.0.2) Monte Carlo simulation toolkit was utilized to simulate the production yield of Cu-64 and other contaminant radioisotopes for various nuclear reactions on two different enrichments (95% & 99.29%) of Ni-64 target of specified geometry. All-particle high-precision physics model QGSP_BIC_AllHP and TALYS-based Evaluated Nuclear Data (TENDL-2019) libraries of nuclear cross sections were utilised. $^{64}\text{Ni}(p,n)^{64}\text{Cu}$ reaction cross sections were calculated for the simulated MC model and were compared with the TENDL-19 library, IAEA recommended cross sections, and various experimental results, for energies from 2MeV to 18MeV. Multiple aluminum degrader foil thicknesses ranging from 0.01mm to 1mm at various beam currents (20 μA to 35 μA), were simulated to study the proton energy degradation across the foil and heat generated in the foil. Different enrichments of Ni-64 target, thickness ranging from 0.01mm to 0.5mm, were irradiated using proton beam of 16.5 MeV, 20 μA for 4 hours.

RESULTS: The simulated cross-section values align well with the experimental results and follow the IAEA's recommended reaction cross section with the maximum deviation of $\pm 4.2\%$. The optimised Al foil thickness in the present study is 0.32 mm for a current time factor of 80 μAh to prevent the risk of melting and rupturing the degrader foil. The thick target yield of Cu-64 increases with the target thickness and reaches at saturation yield of 8.5-9 mCi/ μAh after 0.35mm thickness. Relative contaminant yield remain $<5\%$.

CONCLUSIONS: The results obtained from this study are quite instrumental in guiding the design and optimization of targets, degrader foil, and beam parameters for solid target irradiation system.

EVALUATING THE FEASIBILITY OF USING UTILIZED AQUAPLAST/THERMOPLASTIC MASKS AS A CUSTOM MADE IN-HOUSE BOLUS

Lavanya Murugan, Gopiraj Annamalai, Ananthi Muthuramalingam,
Narmatha Mariyappan, Satheesh Kumar Anbazhagan

Department of Medical Physics, Rajiv Gandhi Government General Hospital and Madras Medical College,
Chennai, India

Email: lavanive04@gmail.com

OBJECTIVE: A bolus is used to compensate for tissue irregularities or increase the skin dose during radiotherapy treatment with Mega Voltage photon beams. Various types of bolus are available, and the choice of material and shape can be debated in terms of cost-effectiveness. This study aims to evaluate the potential of utilizing utilized thermoplastic masks as custom-made bolus for individual patients.

MATERIALS AND METHODS: Thermoplastic/aquaplast masks are used as immobilization materials in radiotherapy for precise treatment delivery. The utilized masks, which have surpassed their shelf-life or reusability, are no longer suitable for immobilization and are disposed of according to institutional protocols. These masks were collected and used in this study. These thermoplastic/aquaplast mold with a thickness of 3.2mm was cut into pieces measuring 10x10 cm². The cut pieces were divided into three batches for dosimetric analysis as custom bolus:

- i) One sheet of thermoplastic (1 layer)
- ii) Two sheets of thermoplastic superimposed on each other (2 layers)
- iii) Three sheets of thermoplastic superimposed on each other (3 layers)

Dosimetric measurements were performed on RW3 slab phantoms using various detectors at different depths and field sizes. The results were then compared with the TPS. Additionally, the utilized thermoplastic masks were used on a few patients to assess their advantages as bolus material.

RESULTS: The measured values are less than $\pm 2\%$ with TPS calculated values. The transmission factor was compared with a standard gel bolus. The transmission factors of the 1-layer and 2-layer masks closely matched those of a 5mm gel bolus, indicating an increase in 6MV photon dose of up to 40-60% at the surface and 12-16% at a depth of 5mm. The masks effectively compensated for body curvature and tissue irregularities without any air gaps.

CONCLUSIONS: The thermoplastic masks has revolutionized the use of bolus. Their customization, adaptability, stability, reproducibility, patient comfort, ease of use, cost-effectiveness, and reusability make utilized thermoplastic mask an ideal choice for providing a uniform dose distribution and compensating for irregularities in the patient's body surface.

KEYWORDS: bolus, aquaplast, thermoplast, mould, immobilization masks

AN INTEGRATED MONTE CARLO DECISION TREE MODEL FOR PREDICTING LIFE EXPECTANCY BASED ON DOSIMETRY QUALITY IN RADIOTHERAPEUTIC TREATMENT OF GLIOBLASTOMA MULTIFORME

Praveen Kumar C¹, Neeraj Sharma²

¹School of Biomedical Engineering, Indian Institute of Technology-BHU, Varanasi, India ²School of
Biomedical Engineering, Indian Institute of Technology-BHU, Varanasi, India

Email: praveenkumarc1980@gmail.com

BACKGROUND/OBJECTIVE: In the present research, we have developed a lucid dosimetry quality audit methodology for radiation oncologists in the treatment of Glioblastoma multiforme (GBM) based on the Integrated Monte Carlo Decision Tree Model (IMCDT). Dose computations accomplished through water phantom, tissue-equivalent head phantoms are neither cost-effective, patient-specific non-customized and less accurate.

MATERIALS AND METHODS: IMCDT strategy recreates visualization of thirty-eight GBM treatment environments on Computational Anthropomorphic Brain (CAB) phantom. A decision tree architecture is formulated for predicting the life expectancy of patients by computing energy deposition which governs radiation-induced cancer cell death and laceration to healthy cells encircling tumors. IMCDT architecture is an amalgamation of novel proposed Lotka-Volterra competition Radiotherapy Quality Assurance (LVCRQA) bio-mathematical model, linear Boltzmann radiation transport model, Talarach-Tournoux image coordinate system for positioning GBM and a binary classifier-based decision tree formulation for predicting life expectancy after RT of GBM.

Treatment plan visualizations for GBM RT were mathematically recreated on CAB phantom with density variations of each tissue commencing from scalp, skull, periosteal dura mater, arachnoid tissue, subarachnoid trabeculae with CSF, pia mater, grey-white matter healthy tissue and tumor tissue. Brain biopsy reports, biochemical compositional open data of GBM and healthy brain layers/tissues from cadaveric and animal tissue in vivo and in vitro experiments, CT scan data, peptide atlas protein sequences and National Institute of Standards & Technology's atomic and molecular data for radiotherapy were assessed and compiled to recreate the phantom. Radiation transport within the phantom were analyzed and computed using Electron Gamma Shower (EGSnrc) open-source software by creating EGS, BEAMnrc input files using MORTAN and C languages. Binary classification of computed dose values was implemented using MATLAB programs.

RESULTS: Binary classifier uncertainty index μ depicting the quality of dose deposition were assigned grading values - 1 for marginal and +1 for a substantial amount perceived by the GBM locus.

CONCLUSIONS: 75% of the total thirty-eight treatment environments were able to deliver substantial dose to GBM locus on the contrary 74% and 65% of treatment environs deposited substantial dose to healthy tissues encircling tumor tissue such as Pia mater and Subarachnoid trabeculae.

KEYWORDS: IMCDT, CAB Phantom, EGSnrc, thirty-eight

DEVELOPMENT AND VALIDATION OF MACHINE LEARNING APPROACH FOR PREDICTING PROTON THERAPY BEAM SPOT CHARACTERISTICS

Ranjith C P^{1,2}, Mayakannan Krishnan¹, Vysakh R², Lalit Chaudhari², Siddhartha Laskar³

1. D. Y. Patil Education Society Deemed to be University, Kolhapur, Maharashtra, India

2. Department of Radiation Oncology, Advanced Centre for Treatment Research and Education in Cancer, Homi Bhabha National Institute, Mumbai, Maharashtra

3. Department of Radiation Oncology, Tata Memorial Centre, Homi Bhabha National Institute, Mumbai, Maharashtra, India

Email: ranjithcp007@gmail.com

PURPOSE/BACKGROUND: Machine learning (ML) approaches have evolved as a promising method for enhancing and automating quality control and machine performance evaluation in advanced radiotherapy techniques such as Proton beam therapy. Verifying the proton spot characteristics is a crucial quality assurance (QA) test in Pencil Beam Scanning (PBS) proton therapy. These tests can be performed virtually using the irradiation log file information rather than physical measurements. By employing ML techniques on log file information, more robust and efficient QA procedures can be developed, reducing the time and human resources required. This work focuses on developing and validating an Artificial Neural Network (ANN) model for predicting spot dosimetric characteristics.

MATERIALS/METHODS: Dosimetric measurements of proton spots were conducted in the energy range of 70.2 MeV to 226 MeV using a scintillation-based detector in the IBA (Ion Beam Applications, Louvain-la-Neuve, Belgium) proteus plus proton therapy machine. The corresponding irradiation log files were obtained and compared with the measurement data, revealing certain inconsistencies. An ANN model was developed using both measured and log file information to address this issue and to improve the accuracy of spot dosimetric characteristic prediction. The ANN model was fine-tuned by determining the optimal number of neurons and hidden layers, and the activation function and optimiser were selected through trial and error. Separate ANN models were created to predict spot size and position. The accuracy of the model's predictions was evaluated using various statistical tools.

RESULTS : The model's prediction accuracy was evaluated using different statistical metrics such as root mean squared error, mean squared error, R-Square etc. All the spot size prediction model's RMSE was less than 0.05 mm with R square values greater than 99%. The different normality tests and residual plots show that the model prediction is unbiased to the input data. The k-fold cross-validation R-square values are greater than 98% for all the models.

CONCLUSION : A novel ANN-ML model was developed and validated for predicting the spot characteristics based on log file data. This tool can be used in the clinical setting as a potential solution for automating the PBS QA.

KEYWORDS: Proton therapy, Machine learning, Quality assurance, Log file analysis.

MODELING AND COMPARATIVE ANALYSIS OF FLASH RADIOTHERAPY FOR HEAD AND NECK CANCER AND LUNG CANCER: PROTON THERAPY AND HEAVY PARTICLE BEAMS

Erato Stylianou Markidou¹, Costantinos Koumenis², Amir Abdullahi³ Andrea Mairani⁴

¹ Department of Physics, University of Cyprus,

²Department of Radiation Oncology, Perelman School of Medicine, University of Pennsylvania

³Department of Radiation Oncology, Heidelberg Therapy Ion Center

⁴Department of Biophysics, Heidelberg Therapy Ion Center.

Email: eratostylmark@gmail.com

BACKGROUND/OBJECTIVE: This study aims to develop a mathematical/biophysical model to predict the impact of oxygen depletion, chemical recombination, and vascular effects on cell and tissue survival in FLASH radiotherapy. The model considers various parameters such as dose, mean dose rate, environmental oxygen level, radiation quality, DNA damage repair kinetics, and cell-line characteristics. The research is conducted in collaboration with the University of Heidelberg and the University of Pennsylvania, utilizing their expertise in Radiobiology and Medical Physics Research. Experimental validation will be performed on animal models at both institutions to refine the model.

MATERIALS AND METHODS: This study focuses on comparing the specificities of irradiating two different types of cancer, Head and Neck Cancer and Lung Cancer, using proton therapy (both standard and FLASH) at the University of Heidelberg and the University of Pennsylvania. The comparison involves utilizing an anthropomorphic phantom irradiated with different quality proton beams, and the results are analyzed and presented. Additionally, the research includes irradiation with heavy particles such as Carbon and Helium beams, optimizing the fractionation scheme and doses to achieve the best treatment outcomes in terms of organ-at-risk (OAR) sparing and tumor control.

RESULTS: The Monte Carlo algorithm and in-house software system owned by HIT is used for analysis of the results, with the use of Ray Station as the treatment planning system. The optimization of treatment conditions is performed remotely from the University of Cyprus.

CONCLUSIONS: This study contributes to an improved understanding of the interplay between various parameters in FLASH radiotherapy, facilitating the optimization of clinical applications and the development of suitable modalities based on FLASH therapy.

KEYWORDS: FLASH radiotherapy, Head and Neck Cancer, Lung Cancer, Monte Carlo algorithm, mathematical/biophysical model

DOSIMETRIC STUDY OF A HIGH ENERGY PROTON THERAPY SYSTEM

A. Zeghari¹, Rajaa Cherkaoui El Moursli¹, Karim Bahhous¹, Nourdine Slassi¹

¹Laboratory of Nuclear Physics (ESMAR), Faculty of Sciences, Mohammed V University, Rabat, Morocco

Email: a.zeghari@um5s.net.ma

BACKGROUND/OBJECTIVE: Recently, many worldwide leader societies try to develop proton therapy technology. It strives to make proton therapy available to all cancer patients who could benefit from it to improve their quality of life. This is a shared purpose with radiation oncologists, medical physicists, radiotherapists, and hospital directors around the world. The introduction of proton therapy systems with the adjustments of the momentum analysis system, might have clinical consequences.

MATERIALS AND METHODS: The momentum analysis system alters typically the energy of the clinical proton beam, and hence the shape and position of the Bragg peak. FLUKA, a Monte Carlo-based software was used to simulate different beam setups by dropping the proton beam in a water phantom. The Bragg peak was read out and compared to the Bragg peak with different setup simulations. The results have shown that the Bragg peak is changed for a proton therapy system with and without a modulator for all the possible tumor depths.

RESULTS: The results obtained showed that the position of the Bragg peak can be changed from $z = 31.4$ cm for deep tumors such as prostate to $z = 2.6$ cm for spinal axis tumors by just changing the depth of modulator from $\Delta Z_{\text{modulator, PMMA}} = 5$ cm to $\Delta Z_{\text{modulator, PMMA}} = 30$ cm for energy 250 MeV.

CONCLUSIONS: It is recommended that this potential dosimetric consequence is investigated further for clinics that are interested in obtaining such a proton therapy system.

KEYWORDS: Proton therapy, FLUKA, Dose Distribution, Bragg-Peak, Modulator

AUTOMATION IN EBRT FOR CERVICAL CANCER USING KNOWLEDGE BASED PLANNING: MULTI-CENTRIC VALIDATION AND GLOBAL APPLICABILITY

¹Jeevanshu Jain, ²Marianne Assenholt, ³Monica Serban, ¹Varsha Hande, ¹Jamema Swamidas,
⁴Yvette Seppenwoolde, ⁵Joanna Alifieri, ²Kari Tanderup, ¹Supriya Chopra

¹ACTREC, TMC, Kharghar, Navi Mumbai, 410210, India

²Aarhus University Hospital, Entrance D, Level 2, Junction D403, Pallet Juul-Jensens Boulevard, Aarhus, 8200,
Denmark, ³Princess Margaret Cancer Centre, 610 University Ave, Toronto, Canada

⁴ErasmusMC Cancer Centre, Dr. Molewaterplein 40, Rotterdam, 3015, Netherlands

⁵McGill University Health Centre, 1001, Decarie Blvd, Montreal, Canada

Email: jeevs.jn@gmail.com

BACKGROUND: Intensity Modulated Radiotherapy (IMRT) is increasingly being used for treatment of cervical cancer and has the potential to improve the therapeutic ratio. However, it is a time-consuming and planner dependent process. This study describes the development, validation and cross-validation of two automated planning models at three institutions using a commercially available software. The performance of these models has also been compared with multi-institutional plans created by 67 centers participating in EMBRACE-II clinical study.

MATERIALS & METHODS: Two Knowledge-based planning (KBP) models were created and validated at the Tata Memorial Centre (TMC) – India (RapidPlan v13.5.23, Varian Medical Systems) and Aarhus University Hospital (AUH) – Denmark (RapidPlan, v16.1) using their respective patient plans optimized according to the EMBRACE-II protocol. The KBP models were exchanged between three institutions (TMC, AUH and McGill University Health Centre (MUHC), Canada) and validated on 20 node positive (N+) and 20 node negative (N-) datasets: 20 from TMC and 10 from each AUH and MUHC. Manually optimized, Tata and Aarhus KBP-based plans were created for each data set and dosimetrically compared with the manual plans using Wilcoxon signed-rank test. A p value of <0.05 was considered statistically significant. One patient case was also planned by 67 different centres as a part of EMBRACE-II trial accreditation and 14 OAR dose parameters were compared with KBP plans.

RESULTS: For all the N+ & N- validation sets, the KBP plans yielded similar coverage for the targets as compared to the manual plan. Statistically significant improvement was observed in OAR sparing with either one or both the KBP models in 7/8 and 6/8 EMBRACE-II OAR soft constraints for N+ and N- cohorts respectively. The multi-institutional comparison showed that in Aarhus and Tata KBP plans, the OAR doses were lower than the respective median values of the 67 submitted plans in 14/14 and 12/14 OAR parameters, respectively.

CONCLUSION: Knowledge-based IMRT planning has the potential to deliver high-quality plans in a time-efficient manner. KBP models can be utilized as a quality check for plans and also contribute to the harmonization of planning eliminating variations that depend on individual planners.

KEYWORDS: Automation in EBRT; Cervical Cancer; Knowledge Based Planning; EMBRACE-II.

COMBINED RADIOMICS AND DOSIOMICS IN THE PREDICTION OF TREATMENT RESPONSE FOR PATIENTS OF BRAIN METASTASES TREATED BY STEREOTACTIC RADIOTHERAPY

Ji Zhang, Chengyu Li, Xiance Jin

Wenzhou Medical University, Radiotherapy Center, First Affiliated Hospital of Wenzhou Medical University, Wenzhou, China, 325000

Email: 1157556618@qq.com

BACKGROUND: Although, the median survival time for patients with brain metastases (BMs) has been improved, about 20% of patients still developed local progression after stereotactic radiotherapy (SRT). The purpose of this study is to combine computed tomography (CT)-based radiomics and dosiomics to predict the treatment response of patients with BMs after SRT in one hospital and validate models with external data from another two hospitals.

MATERIALS AND METHODS: A total of 99 lesions from 78 patients and 20 lesions from 18 patients were enrolled with a number of response and non-response lesions of 59 vs. 40 and 13 vs. 7 in the training cohort and external validation cohort, respectively. The posttreatment response of BMs after SRT were assessed according to RECIST 1.1 based on magnetic resonance images (MRI). The Mann–Whitney U tests and the least absolute shrinkage and selection operator (LASSO) were used to select features. A nomogram was developed by integrating radiomics signature, dosiomics signature and clinical factors. The performance of nomogram was assessed by the areas under curve (AUCs) in both the training and external validation cohorts.

RESULTS: Based on the Mann–Whitney U test and the LASSO logistic analysis with the tuning of λ , a final number of 16, 11 and 9 features were screened out of the selected gross tumor target volume (GTV) radiomics features, GTV dosiomics features and plan target volume (PTV) dosiomics features to classify lesions in the training cohort, respectively. The AUCs of GTV radiomics features, GTV dosiomics features and PTV dosiomics features was 0.806 vs. 0.808 vs. 0.714 and 0.802 vs. 0.780 vs. 0.527 in the training cohort and validation cohort, respectively. A nomogram was constructed by integrating radiomics signature and dosiomics signature to predict the response after treatment for patients with BMs. An AUC of 0.899 and 0.879 was achieved in the training cohort and validation cohort, respectively.

CONCLUSIONS: Radiomics features extracted from brain contrast-enhanced computed tomography (CECT) images were feasible to predict the response of BM to SRT. The addition of dosiomics features is helpful to improve the performance of the models.

KEY WORDSBrain metastases; SRT; Response prediction; Radiomics; Dosiomics

A SELF-SUPERVISED 3D U-NET BASED AUTO-CONTOURING TOOL FOR OAR SEGMENTATION ON HEAD AND NECK CT IMAGES

Niyas Puzhakkal¹, Seenia Francis², Jayaraj P.B²

¹Department of Medical Physics, MVR Cancer Centre& Research Institute, Kerala, India.

²Department of Computer Science and Engineering, National Institute of Technology, Kerala, India

Email address: pniyas@gmail.com

BACKGROUND/OBJECTIVE: The accurate and fast delineation of Organs At Risk (OAR) has great significance in modern radiation treatment planning. Manual contouring is the time-tested method, however it demands more time and expertise for accuracy. Automatic contouring is a better alternative, with least contouring time and lesser inter and intra-user variation. There are many techniques for auto contouring and their performance is largely depends on various factors employed in it. In this paper, a 3D Residual UNet architecture based deep learning model is proposed to automatically delineate OARs in Head and Neck (HN) CT images.

MATERIALS AND METHODS: This model works in self-supervised learning method by using unlabeled data, obtains general features from CT images and utilizes it for segmentation. It consists of self-supervision and segmentation blocks (fig1). The Model genesis and Image context restoration techniques are the self-supervision methods. A 3D U-Net with attention blocks is used for segmentation. The OARs in this study are Brainstem, Mandible, Optic chiasm, Optic nerves and Parotids. The Convolution Block Attention Mechanism (CBAM) is used for better accuracy in smaller OARs (ex: Optic chiasm). A new loss function is implemented by integrating Focal loss, Tversky loss and Cross-entropy loss. The model is implemented in PyTorch framework and training is done on NVIDIA DGX station. Out of the total 232 CT image data, 212 were used for training and 20 were used for testing.

RESULTS: The proposed model outperformed in various quantitative matrices such as DSC, HD95, MSD, Sensitivity and PPV; the results are shown in Table1. The results are also compared with the state-of-the-art AnatomyNet model and it has been found that the CBAM and Self-supervision improved the model's performance. A noticeable 4% increase in the DSC of Optic chiasm is observed. The visualization of segmentation results are depicted in figure2.

CONCLUSIONS: The proposed self-supervised deep learning model can perform auto segmentation for seven OARs in HN CT images with better efficiency. Most of the existing solutions for auto contouring are quiet expensive. This model is made available as open source tool, which can be used to perform auto contouring in radiation treatment planning.

COLLABORATION WITH AMERICAN ASSOCIATION OF PHYSICISTS IN MEDICINE THROUGH THE NETWORK OF GLOBAL REPRESENTATIVES

Eugene Lief¹, Wilfred Ngwa²

¹Department of Radiation Oncology, VA Medical Center, Bronx, New York, USA, ²Department of Radiation Oncology & Molecular Radiation Sciences, Johns Hopkins Medicine, Baltimore, MD, USA, ³Rutgers Global Health Institute, Rutgers University, Newark, NJ, USA

Email: eugenelief@hotmail.com

Background/Objective: American Association of Physicists in Medicine (AAPM) actively collaborates with foreign sister societies and colleagues from Low and Middle Income Countries (LMIC). Some initiatives of a newly formed International Council (IC) of AAPM include determining and prioritizing immediate needs of our colleagues overseas.

Materials and methods: IC includes a newly formed Global Needs Assessment Committee (GNAC) and its Global Representative Subcommittee (GRSC). The purpose of the latter is to create a network of regional representatives to better communicate the local needs. Members of the Subcommittee attended several regional conferences, such as 19th SEACOMP in 2021, and in 2022: ALFIM in Brazil, Greater Horns of Africa Oncology Summit (GHOS) in Tanzania, and 1st Regional Conference of the Federation of African Medical Physics Organizations (FAMPO) in Morocco. AAPM sponsored our Consultant, President of FAMPO, Christopher Trauernicht to speak at the 64th Annual Meeting in Washington DC.

Results: As of this moment, GRSC has recruited 5 representatives from major geographical regions (North and South Africa, South America, Europe and Australia) to serve as Consultants. 3 of them gave virtual presentations at the parent Committee meeting (GNAC) on the regional needs, with few more in preparation. Communications at the meetings and afterwards allow us to build a comprehensive Global Representatives Network (GRN).

Conclusions: The most effective help to LMIC should be based on adequate assessment and prioritizing of the local needs. The AAPM Committee and GRN structures allow proper two-way communication by the AAPM with the sister societies and individual physicists. We encourage all our colleagues from LMIC to get in touch with GRSC represented by the speaker or your local Consultant to our Subcommittee.

Keywords: American Association of Physicists in Medicine, Low and Middle Income Countries, International Council, Global Representatives Subcommittee

WORLD OF MEDICAL PHYSICS: A WEBSITE OF OPEN RESOURCES FOR LEARNING AND DEVELOPMENT OF MEDICAL PHYSICISTS FOR RADIATION ONCOLOGY MEDICAL PHYSICS RESIDENTS

Parminder S. Basran^{1,8}, Jacob Van Dyk^{2,8}, Yakov Pipman⁸, Anna Rodrigues^{3,8}, Cortney Buckey^{4,8},
Jenny Bertholet^{5,8}, Shannon O'Reilly^{6,8}, Radim Barta^{7,8}

¹Cornell University, Ithaca, NY, USA, ²Western University, London, ON, Canada, ³Duke University Medical Center, Durham NC, USA, ⁴Mayo Clinic Arizona, Phoenix AZ, USA, ⁵Inselspita, University Hospital, Bern, Switzerland, ⁶University of Pennsylvania, Philadelphia PA, USA, ⁷Alberta Health Services, Red Deer, AB, Canada, ⁸Medical Physics for World Benefit, USA/Canada

Email: psb92@cornell.edu

BACKGROUND/OBJECTIVE: A significant challenge for medical physics trainees in low and middle-income countries is access to quality educational content and resources. Achieving competency in medical physics practice must include exposure and mastery of medical physics standards of practice, most of which are encapsulated in curricula defined by bodies such as the Commission on Accreditation of Medical Physics Education Programs and the IAEA. While there is a wealth of freely accessible educational content, no generalized hierarchical syllabus directly links core medical physics competencies with online content. This work aims to share and demonstrate a new resource, *WORLD of Medical Physics*, developed by Medical Physics for World Benefit volunteers, based on the IAEA TC-37 report *Clinical Training of Medical Physicists Specializing in Radiation Oncology*, designed to meet this challenge.

MATERIALS AND METHODS: Over five years, a team of volunteers has generated a compendium of medical physics resources. The learning objectives, core competencies, and training topics for each of the eight major learning modules (Clinical Introduction, Radiation Safety and Protection, Radiation Dosimetry, Radiation Therapy, External Beam Treatment Planning, Brachytherapy, and Professional Studies/Quality Management/Research/Teaching and Development) in the IAEA TC-37 report were compiled in a master spreadsheet. Training topics were then linked to freely accessible resources, which include digital documents (PDFs), presentations, websites, videos, podcasts, and web pages. Contributions from medical physics educators can license their work through the Creative Commons and have content hosted on local MPWB servers.

RESULTS: The TC-37 report resulted in approximately 780 unique training topics, of which approximately 492 links to open access external resources (hosted on the world wide web) and 104 links to internal resources (accessible via local server) were matched. All training topics, links to the resources, and associated meta-data is managed through a single, editable, and living spreadsheet.

CONCLUSIONS: The Website of Open Resources for Learning and Development of Medical Physics (WORLD of MP) platform is still in its early stages but has immense potential to improve access to critical educational content for trainees, particularly given its organizational simplicity and reference to the IAEA TC-37 training document.

KEYWORDS: residency, training, radiation oncology, education, open access

Presentation ID: O-080

Abstract ID: J2197

Determining and Prioritizing Needs of LMI Countries by American Association of Physicists in Medicine

Eugene Lief¹, Wilfred Ngwa^{2,3}

¹Department of Radiation Oncology, VA Medical Center, Bronx, New York, USA, ²Department of Radiation Oncology & Molecular Radiation Sciences, Johns Hopkins Medicine, Baltimore, MD, USA, ³Rutgers Global Health Institute, Rutgers University, Newark, NJ, USA.

Email: eugenelief@hotmail.com

Background/Objective: International collaboration of American Association of Physicists in Medicine (AAPM) is centered around helping colleagues from Low- and Middle-Income Countries (LMIC). International Council (IC) of AAPM formed Global Needs Assessment Committee (GNAC) to define main needs of LMIC

Materials and methods: GNAC started with a systematic way of developing the questionnaires for LMIC. The first survey was intended for the institutional and departmental leaders in radiation oncology and radiology, second - for clinical medical physicists and the third - for industrial partners. Another way to address day-to-day needs is through Equipment Donation Program (EDP). The program uses equipment donated by institutions and private parties, utilizes volunteer efforts of Accredited Calibration Laboratories for free calibration and uses its small budget to ship the equipment to LMIC, in collaboration with a similar program of International Organization for Medical Physics.

Results: The survey was distributed using email correspondence, website placement and conference presentations. Results of the surveys have shown the most important needs of the local clinics in LMIC. For some of the developments, GNAC awarded microgrants – seed amounts of money for exploring and developing certain programs. EDP sent some medical physics tools to our LMIC colleagues based on their needs. Some other needs revealed by the survey, such as educational courses and clinical training are being addressed in collaboration with our colleagues from other Committees of AAPM IC.

Conclusions: Determining the most important needs of LMIC Medical Physics is the key to fruitful collaboration. While working in this direction, we are soliciting input of all colleagues from LMIC. We encourage all Medical Physicists from LMIC to address GNAC to express your needs.

Keywords: American Association of Physicists in Medicine, Low and Middle Income Countries, Global Needs Assessment Committee, Equipment Donation.

Presentation ID: O-081

CANCER VISUALIZATION USING GADOBUTROL-GLUCOSE SOLUTION AND 7.0T MAGNETIC RESONANCE IMAGING

Eiichi Sato¹, Manabu Watanabe², Jiro Sato², Kazuki Ito², Hodaka Moriyama², Osahiko Hagiwara², Toshiyuki Enomoto², Yuichi Sato³, Sohei Yoshida⁴, Kunihiro Yoshioka⁴, Hiroyuki Nitta⁵

¹*Honorary Professor of Physics, Iwate Medical University, 2-14-6 Kawaramachi, Wakabayashi, Sendai, Miyagi 984-0816, Japan*

²*Department of Surgery, Toho University Ohashi Medical Center, 2-22-36 Ohashi, Meguro, Tokyo 153-8515, Japan*

³*Central Radiation Department, Iwate Medical University Hospital, 2-1-1 Idaidori, Yahaba, Iwate 028-3694, Japan*

⁴*Department of Radiology, School of Medicine, Iwate Medical University, 2-1-1 Idaidori, Yahaba, Iwate 028-3694, Japan*

⁵*Department of Surgery, School of Medicine, Iwate Medical University, 2-1-1 Idaidori, Yahaba, Iwate 028-3694, Japan*

Email: dresato@iwate-med.ac.jp

Background/Objective: Cancer tissue absorbs 3 to 8 times more glucose than normal tissue. In this regard, 18F-fluorodeoxyglucose (FDG), which resembles glucose, is used in positron emission tomography (PET). However, it is not easy to improve the spatial resolutions, and there is radiation exposure to the patient. Therefore, we developed a gadobutrol-glucose solution for 7.0 T magnetic resonance imaging (7T-MRI) to visualize whole cancerous regions at a high contrast without radiation exposing.

Materials and methods: The contrast medium consists of gadobutrol and glucose solutions, and these solutions are mixed before the vein drip infusion. We used readily available solutions, and the concentrations of the gadobutrol and glucose solutions were 60 and 5.0%, respectively. To visualize cancerous region, we used a 3.3 kg rabbit with a VX7 thigh cancer. First, the vein injection was carried out using 10.0 ml gadobutrol-saline solution containing 0.3 mL gadobutrol, and T1WI was performed. 24 hours after the first experiment, we performed T1WI of the VX7-cancer region using a 50.3 mL gadobutrol-glucose solution including 0.3 mL gadobutrol.

Results: In the T1WI using gadobutrol saline, although it was easy to image the cancer-growth tissue with new blood vessels, hypoxic cancer was not visualized clearly. Using the gadobutrol-glucose solution, the signal intensity of the hypoxic-cancer region substantially increased. The visualizing duration for the gadobutrol-glucose solution was beyond 90 min, and the rabbit survived after the infusion.

Conclusions: We confirmed significant signal-intensity increases in the whole VX7-cancer region of a rabbit thigh utilizing vein infusion of gadobutrol-glucose solution, since the gadobutrol molecules were absorbed into entire cancer region along with glucose molecules.

Keywords: gadobutrol glucose, 7T-MRI, T1WI, hypoxic cancer, angiographic effect

APPLICATION OF FAILURE MODE AND EFFECT ANALYSIS TO MEDICAL EMERGENCY MANAGEMENT IN HIGH DOSE IODINE THERAPY

Jayadevan P.M.¹, Somasundaram V. H¹, Jaicob Varghese¹, Julius James G.¹, Gopinath Mamballikalam²

¹Rajagiri Hospital, Aluva, Kerala, India, ²HAMAD Medical Corporation, Doha, Qatar.
Email of presenting author: jayadevanpm@gmail.com

BACKGROUND/OBJECTIVE: Failure Mode and Effect Analysis (FMEA) is a systematic approach to analyse process risks, evaluate failure effects, and develop corrective actions. The absence of protocols for management of medical emergencies in shielded isolation rooms during high dose iodine therapy challenges radiation safety and patient care. The aim of the study is to analyse the risks in patient care and radiation hazard to healthcare personnel during medical emergency management in high dose iodine therapy and take initiatives in mitigating them thereby enhancing patient care and radiation safety of staff.

MATERIALS AND METHODS: The process of FMEA includes several key steps. These steps encompass the review of processes, brainstorming potential failures, establishing a Risk Priority Number (RPN) scale, listing the effects of each failure mode, assigning ratings for severity, occurrence, and detection, calculating the RPN for each effect, prioritizing failure modes for action, recommending appropriate actions, and continuously monitoring the resulting RPNs as failure modes are addressed and eliminated.

RESULTS: In the process mapping, a total of 11 processes and 43 sub-processes were identified. The FMEA focused on managing and improving efficiency in patient care and reducing unwanted radiation exposure to staff. To decrease the risk priority number (RPN), several measures were implemented. These included developing policies and protocols for medical emergency management, conducting training to increase awareness, and implementing a checklist to reduce human errors. As a result, the overall RPN score decreased from 5104 to 2682. For patient care, mitigation plans targeted processes with RPN scores over 100, resulting in a decrease from 3620 to 1998. Similarly, plans for reducing unwanted radiation exposure to staff focused on processes with RPN scores over 60, leading to a decrease from 1484 to 684 in the RPN score.

CONCLUSIONS: FMEA is a highly effective tool in evaluating system failures, improving patient care, and reducing radiation exposure for healthcare workers. It enables targeted interventions, optimising care delivery, mitigating risks, and prioritizing safety. FMEA ensures improved outcomes for high dose iodine therapy patients and healthcare professionals.

KEYWORDS: Failure mode and effect analysis, radiation protection, radiation safety, high dose therapy

MEDICAL CYCLOTRON FACILITY: BEST PRACTICES AND LESSONS LEARNED

Dilshad Kottuparamban, Anees Muhammed, Raviteja Nanabala,
M.R.A. Pillai, K.N.S. Nair, Ajith Joy

Molecular Cyclotrons Pvt. Ltd., Molecular Multispeciality Hospital Campus, Belbo-LNG Road, Puthuvype,
Kochi, Kerala, India.

Email: dilshadkottuparamban@gmail.com

PURPOSE/BACKGROUND: The increasing prevalence of cancer, neurological disorders, and cardiovascular diseases, has surged the demand of diagnostic radiopharmaceuticals in nuclear medicine. It has necessitated the widespread use of medical cyclotron facilities in modern healthcare. However, managing such facilities efficiently while maintaining adherence to the principles of radiation safety and stringent quality requirements of radiopharmaceuticals remain a challenge. This paper presents result-driven approaches and best practices implemented in a leading medical cyclotron facility to optimize operations and enhance the delivery of radiation technology for better healthcare outcomes.

MATERIALS/METHODS: The study encompasses a retrospective analysis of the operational processes and protocols employed at a commercial medical cyclotron facility over a period of six years. The facility is equipped with Siemens Eclipse HP 11 MeV self-shielded cyclotron capable of accelerating proton beam with maximum current of 120 μA , Von Gahlen Hot Cells for synthesis and dispensing of radiopharmaceuticals installed in a Class C clean room, international standard Type A packages, and other associated equipment and instruments. Key aspects such as facility design, radiation shielding, personnel training, cyclotron performance optimization, and radiopharmaceutical production were evaluated. Furthermore, radiation safety in unexpected equipment failures, radiation dose received by the operational staff, and management of radioactive waste were also investigated.

RESULTS: The findings reveal that a well-designed medical cyclotron facility, complemented by robust radiation safety protocols and strict adherence to quality assurance, significantly contributes to improved efficiency and safety. The implementation of standard operating procedures for all the facility operations resulted in a reduction in manual errors. Maintaining regular records of relevant parameters of equipment enhanced overall productivity. Periodic staff training helped to minimize the personnel exposure to radiation. Moreover, optimized cyclotron configurations, strict maintenance of clean room environment, and periodic services of the hot cells and other auxiliary instruments resulted in improved uptime of cyclotron and higher yields and purity of radiopharmaceuticals.

CONCLUSIONS: By incorporating failure-safe and trial-error approaches, while upholding the highest standards of radiation safety and quality control, medical cyclotron facilities can achieve optimal performance. These best practices can contribute to the advancement of radiation technology in radiopharmaceutical production and thereby improved patient care.

KEYWORDS: medical cyclotron, particle accelerator, nuclear medicine, radiopharmaceuticals, radiation safety.

ABS CUBOID PHANTOM FOR DOSIMETRY AUDIT OF ADVANCED RADIOTHERAPY

Nitin R. Kakade, Rajesh Kumar, S.D. Sharma, B. K. Sapra

Radiological Physics and Advisory Division, Bhabha Atomic Research Centre, Mumbai-400094, India

Email: ni3kakade@gmail.com

OBJECTIVE: Independent external dosimetry audit plays a crucial role in ensuring the quality and accuracy of radiotherapy treatments of individual institution. An ABS cuboid phantom was designed, fabricated and used for conducting dosimetry audit of advanced radiotherapy.

MATERIAL AND METHODS: A specialized cuboid audit phantom made of Acrylene Butadiene Styrene (ABS) was designed and fabricated. This phantom has dimensions of 16x16x16 cm³ with removable insert (size: 10x10x10 cm³) containing a C-shaped structure mimicking planning target volume (PTV) and a cylindrical structure representing an organ at risk (OAR). The PTV was designed to accommodate thermoluminescent dosimeters (TLDs) disc of size 3.8 mm diameter, 0.8 mm thickness at 12 different locations and film at the sagittal plane to record the delivered dose. Additionally, the OAR was equipped with TLDs and film to measure the delivered dose.

Computed tomography images of the phantom were acquired, and the treatment plan was generated for intensity modulated radiation therapy (IMRT) and volumetric modulated arc therapy (VMAT) according to dose volume criteria recommended in the TG-119 protocol using a radiotherapy treatment planning system (TPS). The planned treatment was delivered on the phantom using a 6 MV medical linear accelerator. The TPS-calculated dose at various locations in the PTV and OARs were compared with the measured dose.

RESULTS: The relative percentage difference between TPS calculated and measured dose with respect to prescribed dose for IMRT and VMAT ranged from -2.90% to 4.27% and -4.23% to 4.85%, respectively which is less than the IAEA acceptance limit of $\pm 5\%$. For both IMRT and VMAT, the relative percentage differences were found to be less than $\pm 3.5\%$ for most of the studied points. However, some higher relative percentage difference may be attributed to position of dosimeters in high dose gradient regions.

CONCLUSION: ABS cuboid phantom proved to be useful for dosimetry audit in advanced radiotherapy techniques. The phantom can facilitate end-to-end verification of radiotherapy, encompassing imaging, planning, and delivery processes. Moreover, developed phantom and methodology may also be useful for establishing a national dosimetry audit network in India.

KEYWORDS: Quality Audit, Cuboid phantom, IMRT, VMAT

ADVANCING RADIATION THERAPY: 3D PRINTING FOR PRE-TREATMENT SBRT PLAN VERIFICATION AND BRACHYTHERAPY APPLICATOR INNOVATION

Arun Krishnan M P, Sreelakshmi K, Niyas Puzhakkal, Mohammed Afsal, Saveri J.S, Nithish M David, Seby George, KS Vijaygopal

MVR Cancer Center and Research Institute, Calicut, Kerala

Email: arunkrishnanmp@gmail.com

BACKGROUND/OBJECTIVE: This study aimed to verify the system-generated point dose in stereotactic body radiation therapy (SBRT) for liver treatment using a hybrid 3D printed phantom and verify the same using a Dolphin detector array. Additionally, this study aimed to evaluate the viability of a novel 3D-printed cylindrical vaginal surface (3DCVS) applicator with peripheral loading for targeting the medial one-third of the parametrial tissue.

MATERIALS AND METHODS: An Institutionally developed hybrid 3D printed phantom was used to verify the point dose from the treatment planning system (TPS) in a simulated treatment scenario of 35 clinically acceptable SBRT liver plans, selected retrospectively. The results were cross-verified using the Dolphin detector array and Compass software by gamma analysis (3% and 2 mm) and DVH comparisons.

To evaluate the novel 3DCVS applicator, a dosimetric comparison was made against pre-existing CVS applicator. Patient geometry was established by fusing CT image of 3DCVS with a patient CT which had been treated using a conventional CVS applicator. Two sets of graphically optimized plans with twenty high-risk clinical target volumes (HR-CTV) were created in Oncentra TPS, and dosimetric parameters were analyzed according to the GYN GEC ESTRO guidelines.

RESULTS: The 3D printed phantom measured point dose showed good agreement with a deviation of less than $\pm 3\%$ for all SBRT plans. The gamma criteria analysis demonstrated excellent agreement between the planned TPS and Dolphin-reconstructed doses for the 10% isodose line and PTV volumes. The DVH comparison of planned and reconstructed doses showed negligible variation within $\pm 3\%$.

The evaluation of the novel 3DCVS applicator revealed significantly lower mean doses in the specific bladder, rectum, and sigmoid volumes than the CVS applicator ($p < 0.01$). The mean $D_{98\%}$ values were comparable between the two applicators, and the total reference air kerma was significantly lower in the 3DCVS applicator.

Conclusions: The study confirmed the accuracy and reliability of the hybrid 3D printed phantom for SBRT liver pre-treatment verification. The results of the 3DCVS applicator reveal that it is feasible to treat vaginal cancers with parametrial invasion while lowering the dose to nearby normal structures.

Keywords: 3D printed phantom, SBRT, Pre-treatment verification, Gamma, CVS

ASSESSMENT OF STATISTICAL PROCESS CONTROL TO SET TOLERANCE AND ACTION LIMITS FOR PORTAL IMAGE BASED PATIENT-SPECIFIC QUALITY ASSURANCE

Sumanta Manna^{1,2}, Benoy Kumar Singh¹, K J Maria Das³

¹Departemnt of Physics, GLA University, Physics, Mathura, Uttar Pradesh India; ²Medical Physics, Kalyan Singh Super Specialty Cancer Institute, Lucknow, India, ³Department of Radiotherapy, Sanjay Gandhi Postgraduate Institute of Medical Sciences, Lucknow, India

Email: Sumanta7915@gmail.com

BACKGROUND/OBJECTIVE: Statistical process control (SPC) is a popular analytical decision-making tool to monitor process behaviour through statistical analysis based on the process itself. This study aims to investigate the application of SPC to evaluate tolerance and actions limits of patient-specific quality assurance (PSQA) for different gamma criteria in Head and Neck Sites.

MATERIALS AND METHODS: To study the baseline performance of the control charts, first, we have included thirty patients to establish the lower control limit (LCL), which is most important for the PSQA. Further various gamma criteria (3%/3mm, 3%/2mm, 2%/3mm and 2%/2mm) for both local and global gamma were applied. All head and neck patients were planned using RapidArc in the eclipse planning system and delivered in TrueBeam SVC integrated with TrueBeam PortalVision imager (aS1200 amorphous silicon) was used. The first ten patient's data was used to calculate the I-MR chart to set the tolerance and action limits. Then, the Exponentially Weighted Moving Average (EWMA) and Cumulative Sum (CUSUM) chart were used to study small drift in the control chart. Finally, after reviewing the baseline, 350 head and neck patients were used to study to assess the action and tolerance limits for a large population

RESULTS: The lower control limits evaluated from the I-MR chart were (96.82, 95.99, 94.05 and 89.42) & (91.40, 88.54, 88.03 and 83.06) for 3mm/3%, 2mm/3%, 3mm/2% and 2mm/2% criteria with global and local gamma respectively. The EWMA and CUSUM chart found that the control charts were within the tolerance limit except for stringent global gamma 2mm/2% and local gamma. The action limits obtained after the above tests are (96.35, 94.34, 91.88 and 86.60) & (87.37, 82.33, 79.93 and 70.73) for 3mm/3%, 2mm/3%, 3mm/2% and 2mm/2% criteria with global & local gamma respectively.

CONCLUSIONS: Statistical process control is an effective tool for studying processes like PSQA in IMRT. In the current study, we establish the tolerance and action limits for head and neck patients undergoing PSQA before treatment. As a result, all our tolerance and action limits are well under control and satisfy the recommended values of the AAPM TG-218 report.

KEYWORDS: SPC, PSQA, Radiotherapy, Gamma, IMRT QA, Tolerance limits, Action Limits

EFFECT OF MODULATION FACTOR ON PASS RATES OF AAA AND MONTE CARLO CALCULATED SRT VMAT DOSE DISTRIBUTIONS EVALUATED WITH IN-HOUSE 3D PORTAL IMAGING DOSIMETRY

Elena Timakova¹, Isabelle Gagne¹, Lesley Baldwin¹ and Sergei Zavgorodni¹

¹Department of Medical Physics, Vancouver Island Centre, BC Cancer Agency, Canada

Email: szavgorodni@bccancer.bc.ca

BACKGROUND/OBJECTIVE: In our institution, the electronic portal imaging device (EPID) is routinely employed for SRT patient-specific quality assurance (PSQA), using the in-house 3D Portal Dosimetry (3DPD) method developed by Ansbacher (2006). In this work, 3DPD was used to evaluate the effect of modulation factor (MF), defined as delivered monitor units divided by the dose at the center of treatment volume, on passing rates for SRT VMAT plans calculated using Eclipse AAA and Monte Carlo algorithms.

MATERIALS AND METHODS: Twenty-three SRT VMAT plans, designed to cover 2cm diameter PTV, with MFs of 1.6 to 14.0 MU/cGy, were delivered to EPID on Varian TrueBeam STx on-axis, and thirteen plans were delivered 6cm off-axis. 3D dose distributions for these plans were reconstructed into a 20cm diameter water cylinder phantom using 3DPD, and were also calculated using Eclipse AAA and Vancouver Island Monte Carlo (VIMC) system utilizing VMC++ code. Calculated and 3DPD-reconstructed doses were compared using chi-factor analysis with criteria of 3% dose difference, 1mm distance-to-agreement, and 80% low dose threshold. Percentage of voxels within these criteria was reported as passing rate, with acceptance criteria set at 90%.

RESULTS: For on-axis AAA or VIMC calculated dose distributions, mean chi-factor pass rates reported by 3DPD were 87% and 94%, respectively; 87% of VIMC-calculated plans met 90% acceptance criteria, while this was 35% for AAA plans. Plot of passing rates against MFs showed downward trend with linear coefficient of -0.6 for both AAA and VIMC. The trend line for VIMC was higher, offset by 6.4%; therefore, most VIMC calculated plans passed, while most AAA plans failed. Off-axis, 3DPD reported mean chi-factor pass rates were 86% and 94% when compared to AAA or VIMC, respectively; 92% of VIMC-calculated plans met the 90% acceptance criteria, while this was only 31% for AAA plans. Passing rates against MFs also showed downward trend with linear coefficient of -0.16, and off-set of 7.8% between VIMC and AAA.

CONCLUSIONS: Decreasing 3DPD passing rates with MFs were seen for both AAA and VIMC calculated dose. Better agreement was demonstrated between 3DPD and VIMC dose distributions compared to those calculated by AAA.

KEYWORDS: Patient specific quality assurance, portal dosimetry, AAA, Monte Carlo

MONTE CARLO VALIDATION AND BEAM DATA COMPARISON BETWEEN EXPERIMENTAL, RAYSTATION TPS, AND TOPAS SIMULATION FOR PROTON SPOT SCANNING.

Umesh Bharat Gayake¹, Bhushankumar J Patil², S. D. Dhole³, Kantaram Darekar¹, Lalit Chaudhary¹

¹ Department of Radiation Oncology, Advanced Centre for Treatment, Research, and Education in Cancer (ACTREC), Tata Memorial Centre, Homi Bhabha National Institute, Mumbai, India.

² Department of Physics, Abasaheb Garware College, Savitribai Phule Pune University, Pune.

³ Department of Physics, Savitribai Phule, Pune University, Pune, India

Email: ugayake@gmail.com

BACKGROUND/OBJECTIVE: This study aims to validate the TOPAS monte carlo simulation with the recently installed scanning proton beam. Also, to model an accurate monte carlo engine for a further research study in proton therapy. The study evaluates the thorough comparison of measured beam data required to model the treatment planning system (TPS) with Geant4-based TOPAS (TOol for Particle Simulation) simulation.

MATERIALS AND METHODS: The Measurements such as Integrated depth dose (IDD), Spot size, and Absolute dose were performed depending on the requirement of the treatment planning system (TPS). The IDD and absolute dose were measured in the water phantom with a stingray chamber and Parallel plate chamber (PPC05). The spot size was measured in the air with a plastic scintillation-based lynx detector for 33 energies ranging from 70 to 226.2 MeV. Similarly, the TOPAS Geant4-based simulation was performed to validate measured IDD, absolute dose, and spot size for 11 proton energies from 70.18 to 226.2 MeV. The simulation result is compared with the measured and Raystation TPS model.

RESULTS: THE range of pristine Bragg peak R90 and R80 was compared for 11 energies, and it is well within 0.5mm. The Bragg peak widths M80 and M90 were found within 1mm. The TPS and TOPAS simulation calculated that the surface dose was higher for 70.18 MeV, 1.66% in the TPS, but all others are within 0.7%. The surface dose was slightly uncertain for the TPS model. The distal dose fall was found within 0.6mm for TPS and TOPAS comparison with measured data. The spot size was also accepted within 0.11 mm. The energy beam spread is plotted for energy is plotted for all the energy, and it decreases for the actual energy. The absolute dose was matched exactly in the simulation. The variation between the calibrated ions per MU for TPS computed and the TOPAS simulated was within 2.6%.

CONCLUSIONS: The Monte Carlo simulation was accurately modeled and validated through the scanning proton beam commissioning data. The comparison of measured, TPS, and TOPAS demonstrated good agreement to use the simulation for clinical validation in the future.

KEYWORDS: Monte Carlo simulation, commissioning, proton therapy, pencil beam scan, and validation.

AN INTEGRATED MONTE CARLO DECISION TREE MODEL FOR PREDICTING LIFE EXPECTANCY BASED ON DOSIMETRY QUALITY IN RADIOTHERAPEUTIC TREATMENT OF GLIOBLASTOMA MULTIFORME

Praveen Kumar C¹, Neeraj Sharma²

¹School of Biomedical Engineering, Indian Institute of Technology-BHU, Varanasi, India ²School of
Biomedical Engineering, Indian Institute of Technology-BHU, Varanasi, India

Email: praveenkumarc1980@gmail.com

BACKGROUND/OBJECTIVE: In the present research, we have developed a lucid dosimetry quality audit methodology for radiation oncologists in the treatment of Glioblastoma multiforme (GBM) based on the Integrated Monte Carlo Decision Tree Model (IMCDT). Dose computations accomplished through water phantom, tissue-equivalent head phantoms are neither cost-effective, patient-specific non-customized and less accurate.

MATERIALS AND METHODS: IMCDT strategy recreates visualization of thirty-eight GBM treatment environments on Computational Anthropomorphic Brain (CAB) phantom. A decision tree architecture is formulated for predicting the life expectancy of patients by computing energy deposition which governs radiation-induced cancer cell death and laceration to healthy cells encircling tumors. IMCDT architecture is an amalgamation of novel proposed Lotka-Volterra competition Radiotherapy Quality Assurance (LVCRQA) bio-mathematical model, linear Boltzmann radiation transport model, Talarach-Tournoux image coordinate system for positioning GBM and a binary classifier-based decision tree formulation for predicting life expectancy after RT of GBM.

Treatment plan visualizations for GBM RT were mathematically recreated on CAB phantom with density variations of each tissue commencing from scalp, skull, periosteal dura mater, arachnoid tissue, subarachnoid trabeculae with CSF, pia mater, grey-white matter healthy tissue and tumor tissue. Brain biopsy reports, biochemical compositional open data of GBM and healthy brain layers/tissues from cadaveric and animal tissue in vivo and in vitro experiments, CT scan data, peptide atlas protein sequences and National Institute of Standards & Technology's atomic and molecular data for radiotherapy were assessed and compiled to recreate the phantom. Radiation transport within the phantom were analyzed and computed using Electron Gamma Shower (EGSnrc) open-source software by creating EGS, BEAMnrc input files using MORTAN and C languages. Binary classification of computed dose values was implemented using MATLAB programs.

RESULTS: Binary classifier uncertainty index μ depicting the quality of dose deposition were assigned grading values - 1 for marginal and +1 for a substantial amount perceived by the GBM locus.

CONCLUSIONS: 75% of the total thirty-eight treatment environments were able to deliver substantial dose to GBM locus on the contrary 74% and 65% of treatment environs deposited substantial dose to healthy tissues encircling tumor tissue such as Pia mater and Subarachnoid trabeculae.

KEYWORDS: IMCDT, CAB Phantom, EGSnrc, thirty-eight

EGSnrc BASED MONTE CARLO SIMULATION OF Ir-192 HDR FLEXISOURCE IN WATER AND DIFFERENT PHANTOM MATERIALS

Jerema Persis Reaiah, Henry Finlay Godson, Silas Ebenezar and Retna Ponmalar

Department of Radiation Oncology, Christian Medical College, Vellore, india

Email: jeremajohn13@gmail.com

BACKGROUND/OBJECTIVE: The accuracy of dose measurements in brachytherapy is reliant on the precise measurement of source-to-detector distance. The source-detector distance can be precisely determined in solid phantoms, leading to more reliable and consistent dose measurements. Hence, a Monte Carlo simulation was carried out to investigate the effect of different phantom materials on the dosimetric parameters of the ^{192}Ir Flexisource.

MATERIALS AND METHODS: The EGSnrc code was employed to simulate the behavior of ^{192}Ir Flexisource in water and several phantom materials. The research focused on obtaining two crucial dosimetric parameters, the radial dose function and the anisotropy function. These parameters were calculated for different phantoms such as Water, RW3, Solid water, PMMA and Polystyrene and the reference media was kept as water.

RESULTS: The radial dose function values and anisotropy function values showed the dose fall-off around the ^{192}Ir Flexisource at different distances and for different phantoms. Below 0.8cm a deviation of -0.6% and above that +4.8% deviation was found for PMMA. Up to 10cm Polystyrene showed a deviation of +2.4% and RW3, a deviation of +4.8% and Solid water showed a deviation of +1.3% up to 1cm and -7% above 1cm up to 10cm from the centre of the source. The anisotropy function values showed that at (1cm, 0°) PMMA showed a deviation of -12% and at (2cm, 170°) +2.5%. Polystyrene showed a deviation of 14.8% (1cm, 180°) and +4.5% (5cm, 60°). RW3 showed a deviation of +3.7% (5cm, 60°) and -15.9% at (2cm, 0°). Solid water showed a deviation of -3% at (5cm, 100°).

CONCLUSIONS: The results of the radial dose function and anisotropy function obtained in RW3, Solid water, PMMA and Polystyrene phantoms for ^{192}Ir Flexisource demonstrated a small difference from corresponding data obtained in a liquid water phantom. These differences were attributed to the change in the density of the different phantoms. These water equivalent phantoms were found to be suitable for dosimetric measurements around ^{192}Ir sources as, despite these small deviations, the results were found to correlate well with each other.

KEYWORDS: Brachytherapy, Ir-192, high-dose-rate, Monte-Carlo simulation, Solid phantom

IDENTIFICATION OF CS-137 BEAM QUALITY CORRECTION FACTOR USING DIFFERENT METHODS

Ahmed Mohamed Maghraby¹, Ahmed Soltan Monem², and Hoda Mohamed Eissa¹

¹National Institute of Standards (NIS) –Ionizing Radiation Metrology Laboratory, Giza, Egypt.

²Cairo university – Faculty of science – Biophysics department, Giza, Egypt.

Email: maghrabism@yahoo.com

BACKGROUND AND OBJECTIVES: The specification of the quality of a photon beam has been the subject of numerous studies due to its relevance to radiation dosimetry especially for radiation therapy. However, no beam quality specifier has been found that satisfies all possible requirements of being a unique specifier for the entire energy range of photon energies used in radiotherapy and standards laboratories.

METHODS: In this work, three specifiers for the photon beam quality were used and compared to each other. The three methods for the determination of the beam quality correction factor (K_{Q,Q_0}) are the tissue-phantom ratio, $TPR_{20,10}$, the percentage depth dose ratio, D_{20}/D_{10} , and the calculated K_{Q,Q_0} .

RESULTS: It was found that the three estimated value for the beam quality correction factor of the cs-137 beam are in accordance with each other; 1.00384, 1.00585, and 1.00485 respectively.

KEYWORDS: Radiation dosimetry, Beam Quality, Cs-137, Tissue-Phantom ratio, Depth-Dose Ratio.

RADIOPROTECTIVE EFFECT OF HESPERIDIN/DIOSMIN COMPOUND AGAINST ^{99m}Tc-MIBI-INDUCED CARDIOTOXICITY

Fereshteh Koosha

Department of radiology technology, School of Allied Medical Sciences, Shahid Beheshti University of Medical Sciences, Tehran, Iran
Email: frshkkoosha@yahoo.com

BACKGROUND/OBJECTIVE: Patients with coronary artery disease around the world may be exposed to Tc-^{99m} for SPECT myocardial perfusion imaging (MPI) several times during their life. MPI is a major contributor to the collective population radiation dose for patients. This study was designed to evaluate radioprotective effect of hesperidin/diosmin compound (HDC) against the cardiotoxicity indicate due to ^{99m}Tc-MIBI injection in myocardial perfusion imaging in wistar Rats.

MATERIALS AND METHODS: Twenty five male rats were randomly divided into five groups. The rats in Group 1 (control) only received PBS. For Group 2 (HDC only) the rats treated with only HDC , orally administered. The rats in Group 3 (radiation) received PBS before injection and exposure to 1 mCi ^{99m}Tc-MIBI. The rats in Group 4 (HDC + radiation) treated with HDC before exposure. For Group 5 (radiation + HDC) the rats were exposed and thereafter administered HDC. Then, the rats were sacrificed and afterwards their heart tissues were carefully extracted for biochemical and histopathological evaluations.

RESULTS: According to our results in the radiation group, the rate of rupture of cardiomyocyte fibers was higher than other groups, and in some fibers, the presence of lymphocytes was observed. Relative improvement was observed in radiation + HDC group compared to the radiation group and also a small number of cardiomyocyte fibers were torn and in some fibers, the presence of lymphocytes was observed, which was less than the model group. Collagen deposition significantly increased in radiation group compared to control group ($P < 0.05$). It can be seen that the percentage of collagen deposition decreased substantially in the group treated with HDC before or after radiation compared to radiation group ($P < 0.05$). The MDA activities significantly reduced ($P < 0.05$) in both (HDC + radiation) and (radiation + HDC) groups. SOD activity significantly increased in both (radiation + HDC) and (HDC + radiation) groups compared to that of radiation group ($P < 0.05$)

CONCLUSIONS: It could be concluded that the HDC is safe and promising useful therapeutic agent in radiation induced cardiotoxicity for patients undergoing nuclear medicine procedures

KEYWORDS: radiation protection, Hesperdin/Diosmin, cardiotoxicity

END TO END TESTING USING ANTHROPOMORPHIC PHANTOM IN CYBER KNIFE

Sangaiah Ashok Kumar, Subramani Vendhan, Marudaiyah Kalaiselvi, Sarswathi Chitra, Mari Vel
Department Of Radiation Oncology, Apollo Speciality Hospitals, Teynampet, Chennai, India

Email: ashok_sangaiah@apollohospitals.com

AIM: Aim of this study is to perform E2E for the CK S7 system equipped with Fixed, Iris and MLC collimators using anthropomorphic phantom.

MATERIALS AND METHODS: CK treatment delivery systems capabilities include precise target tracking and correcting for target movements. The target is monitored throughout the treatment and any motion immediately modifies the delivery. Target tracking and motion compensation are achieved through the use of the imaging system integrated with the treatment delivery system. Different target tracking methods available are 6D skull tracking, fiducial tracking, XsightSpine Tracking and Xsight Lung Tracking system. The Synchrony Respiratory Tracking System and the InTempoAdaptive Imaging System are motion compensation technologies and are used in conjunction with applicable tracking method.

End-to-end (E2E) testing is a unique part of the periodic quality assurances performed in CK. E2E for the CK system is the quantitative measure of the overall system's targeting accuracy. It involves all the essential steps of a routine patient treatment workflow starting from patient setup, CT acquisition accuracy, treatment planning, DRR image processing, setup imaging, robot movement, beam alignment and treatment delivery.

The E2E QA test uses an anthropomorphic phantom containing a target to simulate an actual patient. Orthogonal radiochromic films are placed within the phantom for measurement and analysis of delivered dose. Spatial distribution of delivered dose is compared to the planned dose at the 70% isodose line and verified using E2E QA software. The main purpose of this study is to verify the accuracy of spatial delivery of planned dose for different collimator systems using individual tracking systems.

RESULTS: The E2E testing is done for different types of collimators in various tracking methods that is skull tracking, fiducial tracking and spine tracking with their suitable aperture size. The obtained results are within the tolerance limit of <0.95mm as per the recommendations from AAPM TG135.

KEYWORDS: CYBER KNIFE, S7,E2E, SKULL PHANTOM,6FFF,anthropomorphic phantom.

EVALUATION OF THE EFFICACY OF AUTOMATED PLAN GENERATION USING VARIAN ETHOS INTELLIGENT OPTIMIZATION ENGINE AND A COMPARATIVE ANALYSIS WITH ECLIPSE TREATMENT PLANNING SYSTEM (TPS) PLAN

Anand Jadhav

Sir HN Reliance Foundation Hospital, 407/B, Mumbai, 400603, India

Email: anandraojadhav45@gmail.com

BACKGROUND/OBJECTIVE: Historically, treatment plans were manually created by planners using tools in the treatment planning system (TPS). However, plan quality varied based on individual skills and institutional protocols. One technique of automatic plan generation is Knowledge-based planning (KBP). Recently, Varian introduced Ethos, an adaptive treatment planning and delivery system that uses an intelligent optimization engine (IOE) to automate the plan generation process. The study's primary focus is to evaluate the quality of treatment plans generated by each TPS. Dosimetric parameters like target coverage, dose conformity, and organ-at-risk sparing will be compared. Additionally, the planning process efficiency, time for plan creation and optimization, will be assessed.

MATERIALS AND METHODS: 10 retrospective patients, 5 diagnosed with prostate cancer and 5 diagnosed with Head and Neck cancer were selected. Previously approved plan in ECLIPSE with AAA algorithm recalculated and reoptimized with same objective function was then exported to ETHOS TPS through Citrix. ETHOS TPS is a template-based planning system which uses Intelligent Optimization Algorithm to generate 7, 9, 12 Field IMRT plans and 2, 3 arc VMAT plans with fixed beam geometry. The plan imported from eclipse to ETHOS will be used to generate two plans, one which will have all the parameters the same from eclipse and only perform the calculation, and second plan which will perform re-optimization and then be calculated.

RESULTS: After checking the normality of the data using the Shapiro-Wilk test, paired t-test was used to find the difference in the mean readings between ETHOS and ECLIPSE. There was a significant difference in the mean for CI, HI, and Hotspot (p -value=0.000). ICC two-way mixed model was used to find the consistency between the two readings. The single measure ICC rating was 59 percent for CI, 79 percent for HI, 83 percent for Hotspot, and 87 percent for Total MU.

CONCLUSION: Based on initial results, Eclipse plan outdoes the auto-generated plans on the Ethos system on the basis of HI, CI & Hot Spot. However, being a novel system, better understanding of the Ethos system, greater sample size and evaluation of more dosimetric parameters will help deduce a satisfactory comparison.

KEYWORDS: TPS, Ethos, Eclipse, Intelligent Optimization Engine

A NOVEL DOSE-VOLUME HISTOGRAM (DVH) SCORING ALGORITHM FOR AUTOMATIC DVH-BASED PATIENT-SPECIFIC QUALITY ASSURANCE FOR VOLUMETRIC MODULATED ARC THERAPY

Boda Ning, Zhixi Lin, Ji Zhang, Xiance Jin

Radiotherapy Center, 1st Affiliated Hospital of Wenzhou Medical University, Wenzhou, China

Email: 1007547054@qq.com

OBJECTIVE: To develop a novel dose-volume histogram (DVH) scoring algorithm to define the importance of different DVH metrics automatically, then to classify patient specific quality assurance (PSQA) results efficiently.

MATERIALS AND METHODS: Total of 200 cervical cancer (CC) patients underwent volumetric modulated arc therapy (VMAT) from 2019 to 2022 were enrolled in this study. VMAT plans treated by Infinity (109 cases) and Synergy (91 cases) linear accelerators were used as technical testing (TT) and technical validation (TV) datasets, respectively, which was then randomly divided into training, validation and testing set at a ratio of 7:1:2. U-net-like network with skip-connection modules (called T-Net) was adapted to predict PSQA dose distribution. A novel weight-based DVH scoring (WDS) algorithm was developed and trained to classify “pass” or “fail” (PoF) of PSQA results based on the dose errors (DEs) and volumetric errors (VEs) calculated between predicted and planned DVHs.

RESULTS: T-Net achieved a best performance in predicting PSQA dose distribution in comparison with other deep learning models. The WDS method achieved a sensitivity, specificity and accuracy of 100.00%, 50.00%, 0.955, and 100.00% ,33.33%, 0.890 in TT and TV, respectively, which was better than models of random forest (RF) and support vector machines (SVM) with an accuracy of 0.909, 0.833 and 0.864, 0.722 in TT and TV. The threshold DVH score for 22 and 18 validation patients were 49.62 and 57.62 in the TT and TV with a precision, recall rate and F1 score of 0.952, 1, 0.976 and 0.882, 1, 0.938, respectively.

CONCLUSIONS: The suggested novel WDS algorithm was able to classify the PoF of PSQA objectively and automatically and improve the accuracy and efficiency of DVH-based PSQA for patients underwent VMAT.

KEYWORDS: Deep learning, Patient-specific quality assurance, Volumetric modulated arc therapy, Classification, Dose-volume histogram

NORWEGIAN PARTNERSHIP PROGRAMME FOR GLOBAL ACADEMIC COOPERATION (NORPART) ON GHANA-NORWAY COLLABORATION IN MEDICAL PHYSICS AND RADIOGRAPHY EDUCATION

Stephen Inkoom^{1,4}, John J. Fletcher^{2,4}, Pål E. Goa³, Mercy Afadzi³, Catharina de Lange Davies³,
Francis Hasford^{4,5}, Samuel Y. Opoku⁶, Samuel B. Dampare⁴ Y. Serfor-Armah⁴ J.R. Fianko⁴,
E.K. Sosu⁴

¹Radiation Protection Institute, Ghana Atomic Energy Commission. P.O. Box LG 80, Accra, Ghana.

²Department of Applied Physics, Faculty of Applied Sciences, University for Development Studies, Navrongo, Ghana.

³Department of Physics, Norwegian University of Science and Technology, Trondheim, Norway.

⁴Graduate School of Nuclear and Allied Science, University of Ghana, Atomic Campus. P.O. Box, AE 1, Accra, Ghana.

⁵Radiological and Medical Science Research Institute, Ghana Atomic Energy Commission.
P.O. Box LG 80, Accra, Ghana.

⁶Department of Radiography, School of Biomedical and Allied Health Sciences, College of Health Sciences, University of Ghana, Accra, Ghana.

Email: sinkoom@hotmail.com

BACKGROUND/OBJECTIVE: Norwegian University of Science and Technology (NTNU) and Universities in Ghana have had a long time collaboration regarding quota students from Ghana at NTNU. The School of Nuclear and Allied Sciences of the University of Ghana and the Norwegian University of Science and Technology (NTNU), and other partner Institutions have been involved in a Norwegian Partnership Programme for Global Academic Cooperation (NORPART) project since 2017. NORPART Project was funded by the Norwegian Ministry of Education and Research and Norwegian Ministry of Foreign Affairs with a grant of NOK 4,950, 000 (US\$ 600,000.00). The main goal of this project was to establish a partnership for education and research between institutions in Ghana and Norway within the fields of Medical Physics, Radiation Protection and Radiography. Under the project, two main activities were proposed, namely; (i) Annual Summer School in Ghana and (ii) A student exchange program at master and PhD levels. This paper highlights the experiences of the project after 7 years of implementation.

MATERIALS AND METHODS: The Ghana Norway Summer School in Diagnostic Imaging and Radiotherapy was held at different locations in Ghana for students and practitioners of Medical Physics, Radiation Protection and Radiography. It included theoretical presentations and practical sessions at the hospital. Under the students exchange, students from Ghana undertook part of their thesis research in Norway under joint supervision from experienced researchers from the partner institutions.

RESULTS: There have been 5 successful editions (2016-2020) of the Summer School with 362 students and Lecturers/Facilitators from Ghana and Norway taking part. 22 exchange students (17 Masters and 5 Phds) from Ghana to Norway have benefited from the project. A digital mobile X-ray equipment and Quality Assurance kit was donated to GAEC.

CONCLUSIONS: It is anticipated that at the end of the project cycle, there would be increased mobility, contact, quality and internationalization between staff and students among the partner institutions.

KEYWORDS: NORPART project, Medical physics, radiography

EDUCATION AND TRAINING OF PERSONNEL WORKING IN SECONDARY STANDARDS DOSIMETRY LABORATORIES

Zakithi Msimang, Mauro Carrara

Dosimetry and Medical Radiation Physics Section, Division of Human Health, Department of Nuclear Sciences and Applications, International Atomic Energy Agency, Vienna International Centre, PO Box 100, 1400 Vienna, Austria.

Email: m.carrara@iaea.org

BACKGROUND/OBJECTIVE: Dosimetry is fundamental to every technique using ionizing radiation whether it is for treatment e.g. radiation therapy or diagnosis e.g. nuclear medicine and diagnostic radiology. The foundation for dosimetry is the standards used for providing measurement traceability to international standards and the persons operating these standards. This could be personnel working in radiation dosimetry laboratories, referred to as radiation metrologists or medical physicists. The training of medical physicists has been standardized and harmonized in most regions and the IAEA publications on clinical and academic programme have assisted with this. However, this has not been the case for radiation metrologists. Until recently, there were no guidelines on the training nor was there a standardized definition of role of radiation metrologists.

MATERIALS AND METHODS: In February 2023 the International Atomic Energy Agency, IAEA, published a guidance document that provides information on the training needed and the competences required for persons working as radiation metrologists. The presentation aims to highlight the framework for the education, practical training, and competencies of radiation metrologists responsible for secondary standards dosimetry laboratories (SSDL). The presentation will also highlight how the academic training may be linked to the medical physics academic training programme.

CONCLUSIONS: When these guidelines are implemented, they will contribute in harmonizing the education of radiation metrologists. This training programme may be adapted by personnel working in other laboratories such as those for personnel dosimetry, radioactivity measurements and even primary standards dosimetry laboratories.

KEYWORDS: dosimetry, SSDL, calibration, training, radiation metrologist, medical physics

OPTICAL COHERENCE ELASTOGRAPHY: ADVANCING NON-IONIZING RADIATION DIAGNOSTICS FOR TISSUE MICROSTRUCTURE BIOMECHANICS USING MICROSTRAIN MAPPING

Sweta Satpathy, Raju Poddar

Biophotonics Lab, Department of Bioengineering and Biotechnology
Birla Institute of Technology, Mesra, Ranchi, Jharkhand, India.

Email:phdbe10007.22@bitmesra.ac.in

BACKGROUND/OBJECTIVE: Optical Coherence Elastography (OCE) systems provide a non-invasive tissue biomechanical assessment. This technology enables early disease detection, personalized treatment planning, and therapy monitoring. An external mechanical palpation is induced in the tissue, and a 100 kHz A-line rate, swept-source optical coherence tomography (SSOCT) detects phase shifts using a 1064 nm-based infrared laser. Its ability to probe tissue biomechanics is demonstrated using strain maps showing the varying elastic responses of different sample features.

MATERIALS AND METHODS: Quasi-static excitation is generated from a 4-ohm speaker, and OCE measurements were performed on two samples. One sample is composed of an agar matrix with 5 % concentration, consisting of 3% agar inclusion. This sample was designed to mimic the diseased softer regions inside a tissue, while another sample was obtained from freshly excised chicken, constituting a muscle-tendon intersection. A 5 Hz square wave-based palpation was executed on the sample, and 1000 B-Scans were acquired with 2000 x1000 pixels over a 4x4 mm field of view with 100 kHz A-line rate. A mathematical model has been developed to unwrap phase and calculate strain with pixel by pixel error correction using Discrete Cosine Transform (DCT). It efficiently handles phase wrapping issues, such as phase ambiguity, branch cuts, noise sensitivity and discontinuities, reducing computational complexity and enabling faster processing.

RESULTS: The strain maps are directly obtained from phase data reducing the elastic measurement complexity and computational time. A phase sensitivity of 3.4 radians at 11 dB strain sensitivity is observed for our experiments. Microstrain elastograms have been obtained for both biological and tissue mimicking sample. A strain shift of 25 $\mu\epsilon$ takes place between muscle and tendon while that of 7 $\mu\epsilon$ is observed between agar matrix and inclusion. The elastograms have been spatially correlated with B-Scans for spatial feature detection.

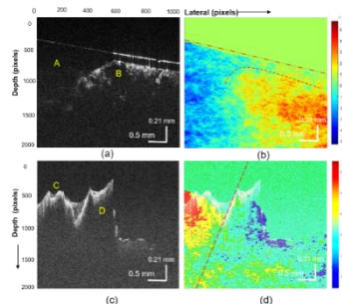


Figure 1. (a) OCT B-Scan of 5% agar phantom [A] matrix with 3% agar inclusion [B]; (b) Elastogram showing low strain region in blue being a stiffer phantom and higher strain region in red being soft due to lower concentration; (c) OCT B- Scan of muscle[C] with connecting tendon [D]; (d) Elastogram showing tendon experiencing lower strain than muscle

CONCLUSIONS: Hence, the combination of external mechanical palpation and high-speed SSOCT imaging enables efficient characterization of tissue biomechanics, providing valuable measurements into the elastic response of different tissue features using DCT. OCE holds promise for enhancing clinical diagnostics and improving patient care.

KEYWORDS: optical coherence tomography, elasticity imaging, tissue biomechanics, non-ionizing radiation, discrete cosine transform

DESIGN AND DEVELOPMENT OF AN ULTRASOUND PHANTOM TO EVALUATE GREYSCALE CONTRAST IN ULTRASOUND IMAGING

Abjasree S., Debjani Phani, P Raghukumar

Division of Radiation Physics, Regional Cancer Center, Thiruvananthapuram
Email: abjasrees.rcc@gmail.com

OBJECTIVE: The purpose of this study is to develop an ultrasound (US) phantom containing targets with varying echogenicities embedded in gel-wax and evaluate the different grey-scale contrasts images using diagnostic ultrasound scanners.

MATERIALS AND METHODS: Five targets with different densities were prepared by modifying the acoustic properties of gel-wax material with glass spheres, paraffin wax, carnauba wax, graphite and chalk powder as additives. Table-1 lists the compositions of the additives added to obtain the targets

Table-1

Target	Additives	Weight W_0 (g)
Sample A	Glass sphere	2 w/w%
	Paraffin wax	5 w/w%
Sample B	Glass sphere	0.5 w/w%
	Paraffin wax	2 w/w%
Sample C	Carnauba wax	17 w/w%
Sample D	Graphite	20.8 g/L
Sample E	Chalk powder	2.5 w/w%

Targets were created by melting gel-wax, mixing the additives and pouring the mixture into a cylindrical nylon mold (height 8cm, inner diameter 4cm). The gel-wax (20g) was melted, and the targets were carefully placed to prepare the phantom and allowed it to settle overnight. A 16-slice CT (Optima CT580W, GE Healthcare) was used for Computed Tomography (CT) imaging. The US scans were performed using SuperLinear™ Model SL10-2 with a linear probe.

RESULTS: The image contrast of each target was analysed using CT and US imaging.

CT Imaging Results

Against the contrast of the gel-wax background

- target A was hypodense, while C, D, and E were hyperdense.
- target B could not be resolved, although its composition varied from gel-wax.

US Imaging Results

Against the contrast of the gel-wax background

- targets A and B, with same additives in different concentrations, exhibited different echogenicities.
- the contrast of target C was similar thus, the resolution was limited by the transducer. The target surface could be identified from impedance mismatch.
- despite having different additives targets B and D, appeared identical in the US image.

The US images clearly showed Target B, which was not visible during CT imaging, illustrating the limitations of CT.

CONCLUSIONS: A gel-wax based phantom with different echogenic targets was designed and developed in this study. It is found that present phantom with embedded targets is suitable for grey-scale evaluation in diagnostic US scanners.

KEYWORDS: Ultrasound, Acoustic property, Quality Assurance, grey-scale contrast, Tissue Mimicking Materials

CONTRAST ENHANCED ULTRASOUND IMAGING USING MICROBUBBLES FOR VISUALIZATION OF MICROVASCULATURE IN A TISSUE MIMICKING PHANTOM

Sumana Halder^{1,2}, Koel Chaudhury¹, Subhamoy Mandal²

¹Clinical Biomarkers Research Laboratory, School of Medical Science and Technology, Indian Institute of Technology, Kharagpur, ²Medical Imaging and Theranostics Laboratory, School of Medical Science and Technology, Indian Institute of Technology, Kharagpur, India

Email: sumanahalder006@gmail.com

BACKGROUND/OBJECTIVE: Non-ionizing diagnostic imaging techniques using ultrasound (US) based microbubbles (MBs) have emerged as a promising tool in medical imaging due to its safety, cost-effectiveness, and real-time imaging capabilities. MBs are micro-sized gas-filled spheres. B-mode US images provide only anatomical information but these MBs enhance the reflection or backscatter of the US signal, thus allowing increased reflection for improved detection and visualization of blood flow, tissue perfusion, and vascular structures. This abstract presents the diagnostic potential of in-house synthesized protein shelled MBs in a tissue mimicking phantom with vessel mimicking structures.

MATERIALS/METHODS: The method of sonication was opted for the synthesis of MBs. The vials containing protein were at first subjected to vacuum and purged with oxygen gas. Then a steady flow of oxygen gas was maintained and the protein solution was sonicated at the gas-solution interface. Subsequently, the vials containing sonicated samples containing were stored in a chilled environment. Optical microscopy images of freshly sonicated MBs were obtained immediately. To mimic the US properties of biologic tissues a phantom was prepared. Agar was chosen as the tissue mimicking material because of its well characterized performance and ease of fabrication. Following a standard operating procedure, the components for the phantom were mixed homogeneously under constant heating. While casting the mixture into a mould, straws were embedded to mimic the vessels present in the tissue bed. The MBs were then flown through the phantom and imaged using a portable US.

RESULTS: The microscopy results obtained suggest successful synthesis of micron sized MBs. It was observed that there was an increase in signal intensity in the vessel mimicking structures when the MBs flow through the phantom. Thus we can infer that the MBs do not perfuse all throughout the phantom but enter only through the vessels which can provide important insights of the microvasculature.

CONCLUSIONS: Tumors are characterized by an abundance of blood vessels within their structures. Our results indicate that contrast enhanced ultrasound using microbubbles has the potential in early detection of tumors by enhancing the visualization of tissue microvasculature which is not possible using normal US images.

KEYWORDS: diagnostic imaging, ultrasound, non-ionizing radiation, microbubbles

DOSIMETRIC EVALUATION OF DUAL LAYER MLC FOR AN O-RING GANTRY SYSTEM

Arvind Kumar^{1,2*}, Kiran Sharma¹, C P Bhatt³, Swati Verma², Sougata Basu², Pooja Dhaundiya², Deepak Kaushik²,

¹Graphic Era Deemed to be University, Dehradun, Uttarakhand, India 248002

²All India Institute of Medical Sciences (AIIMS), Rishikesh, Uttarakhand, India 249203

³Sarvodaya Hospital and Medical Research Center, Faridabad, Haryana (Delhi NCR), India 121006

Email: arvindiundi7@gmail.com

BACKGROUND/OBJECTIVE: An O-ring gantry system Halcyon™ comes with a 6MV flattening filter-free (FFF) beam with a jawless design that features a new dual-layer stacked and staggered multileaf collimator (MLC) system. It is having proximal and distal banks with faster speed (5.0 cm/s). It has 114 leaves (29/bank on proximal, 28/bank on distal). The leaf width is 1 cm projected at the isocenter. Leaves of proximal and distal banks have 0.5 cm offset in the direction perpendicular to the travel. It is capable of producing a maximum 28*28 cm² field size for clinical use. The purpose of this study is to evaluate various dosimetric characteristics of new design MLCs.

MATERIALS AND METHODS: New designed stacked and staggered dual-layer MLC is used for this study. MLC leakage measurement is performed for proximal and distal banks and combined setup. A dosimetric leaf gap (DLG) measurement is also performed. Picket fence test without and with error performed. Penumbra measurements are performed for various field sizes. MLC leaf position accuracy and reproducibility are evaluated from machine performance check (MPC), as Li et al. reported on the appropriateness of MPC for Halcyon™.

RESULTS: Maximum photon leakage radiation through MLCs is measured at D_{max} and 10 cm depth for the proximal bank, distal bank, and combined setting and its maximum value is 0.44 % for the proximal bank. Picket fence test performed without and with error and value found within tolerance. All other MLC QAs performed as per AAPM TG-142 & TG-50 guidelines.

CONCLUSIONS: Dosimetric characteristics of newly designed stacked and staggered MLC for O-ring gantry system evaluated. All the tests are well in agreement with the tolerance value. Measurements show accuracy with TPS data.

KEYWORDS: O-ring system, Halcyon, commissioning, validation

PERFORMANCE COMPARISON BETWEEN DIFFERENT PATIENT SPECIFIC QA SYSTEMS FOR VMAT AND IMRT PLANS ON VARIAN TRUEBEAM

Farheen Kagdi¹, Satish Pelagade¹, Anagha Pachat¹, Ankita Parikh²

¹Department of Medical Physics, ²Department of Radiation Oncology, The Gujarat Cancer and Research Institute, Ahmedabad, India.

Email: farmk.60@gmail.com

PURPOSE: The purpose of this work is to review a prompt and efficient patient specific quality assurance (QA) for pre-treatment verification of intensity modulated radiation therapy (IMRT) treatments at our institute, showing analytical performance across different treatment verification systems; ion chamber & slab phantom, Portal dosimetry (EPID), Matrix Detector array and Delta⁴ phantom.

MATERIALS AND METHODS: Twenty test cases were selected for each study, that were grouped according to the anatomical site: Head & Neck, Thoracic and Pelvic regions. All these plans were created and recomputed using Varian Eclipse treatment planning system. The evaluation of these dosimetric systems was performed for VMAT and IMRT deliveries using a Varian TrueBeam linear accelerator. Dose Distributions were compared using the gamma index criteria of 3% dose difference and 3 mm distance-to-agreement.

RESULTS: Our results showed that all the verification devices gave similar results. All patient plan verification passed our Gamma passing criteria. Across the 20 patient plans, the percent dose difference for the ion chamber ranged from 0% to 4.01%. The average gamma percentage for Head & Neck, Thoracic and Pelvic regions obtained by EPID was 99.2%, 99.1% and 98.9%; by Matrix detector array 97.32%, 97.28% and 96.95% and by Delta⁴ phantom 98.52%, 98.73% and 97.42% respectively.

CONCLUSION: Our review of patient-specific IMRT QA plans highlights a number of major and minor issues. The statistical analysis performed showed that all the measurement methods can be used interchangeably. Various Dosimetric device and software combinations show varied levels of agreement with expected analysis for the same pass-rate criterion. This can be further seen by the fact that setup contributes more variation than the readout analysis for all of the methods. Thus one should carefully develop its QA procedure by determining the value of gamma index criteria and dosimetric tools for pre-treatment verification of system planned dose distributions.

KEYWORDS: Varian TrueBeam, Intensity modulated Radiation Therapy, Patient specific quality assurance, Gamma index

ABSTRACTS OF POSTER PRESENTATIONS

INVESTIGATION OF EFFECTIVE POINT OF MEASUREMENT (EPOM) FOR PERCENTAGE DEPTH DOSE (PDD) WITH DIFFERENT DETECTOR BY INTRODUCING NEW POLYNOMIAL CORRECTION FACTOR FOR EBT3 FILM

Yuvarajan Sankaran

HCG Hospital, Bengaluru, India

Email: yuvarajsnsankaran29@gmail.com

BACKGROUND/OBJECTIVE: Percentage Depth Dose measurement, the average dose deposition in air at depth (ZR) will typically be different from the absorbed dose at the same point (ZM). A displacement correction factor (Pdis) is needed to convert ZR into ZM shifting the chamber geometric center with respect to the EPOM of the respective detector. In this work, EBT 3 radio chromic film was taken as references, which have thin enough thickness to almost completely eliminate the displacement effect. Biggest challenge using EBT 3 radio chromic film for PDD measurement is overestimation of dose due to energy spectra which will change at larger depth due to beam hardening. The most precise method for measuring and analyzing the effects of Gafchromic EBT3 on percentage depth dose (PDD) curves is Monte Carlo (MC) computations. Unfortunately MC simulations are limited and most institutes do not have them available. Concerning all above we introduced polynomial correction factor (PCF). By incorporating PCF, we are attempting to resolve the Gaf chromic overestimation. EPOM shift at various detectors of different sizes were investigated, including E-type silicon diode that have not been studied previously.

MATERIALS AND METHODS: We Examined Semiflex(31010), Pinpoint(31016), Markus (23343) and silicon diode(60017) by measuring PDD for 6 MV beam depending on the respective chambers recommended field size and compared those curves with corrected EBT 3 film.

RESULTS: The shift difference between PDD_{gaf} and PDD_{IC}, Markus, Diode E was represented as EPOM shift. To account for EPOM shift after depth of D_{max} we have taken baseline as DTA: 1.0 mm, DD: 1.0%, Ref: Local. PDD values neither breached nor exceeded the baseline value. Semiflex chamber showed an upstream shift of -0.5 rcav for Field Size (FS) above 10x10 cm² and -0.3 rcav for FS below 10x10 cm². Pinpoint chamber showed no EPOM for FS below 8x8 cm². We were unable to predict EOM shift above 10x10 cm² due to polarity dependency. Markus chamber showed no EPOM shift above 5x5 cm² and it showed downstream shift of +0.8 for FS below 5x5 cm². Diode no EPOM shift upto 10x10 cm²

CONCLUSIONS: The detector-individual EPOMs need to be considered for measurements of PDD curve

ABSTRACT KEYWORDS: Gafchromic EBT3, Effective Point of Measurement, polynomial correction factor, Dosimetry

DESIGN AND DEVELOPMENT OF A PHANTOM FOR PRESCRIPTION RADIATION DOSAGE VERIFICATION WITH RADIOCHROMIC FILM (EBT3) IN A SINGLE-CHANNEL HDR VAGINAL CYLINDER BRACHYTHERAPY APPLICATION

Challapalli Srinivas, Dilson Lobo, Athiyamaan M S, Sourjya Banerjee, John Sunny,
Abhishek Krishna

Department of Radiation Oncology, Kasturba Medical College (An associate hospital of Manipal Academy of
Higher Education: MAHE, Manipal), Mangalore, India

Email: challapalli.srinivas@manipal.edu

BACKGROUND/OBJECTIVE: High Dose Rate (HDR) brachytherapy is carried out in majority of endometrial carcinoma patients using vaginal cylinders with the prescription dose given either on to the surface or at 5mm from the surface of cylinder with a treatment length depending upon the vaginal cuff in order to reduce the possibilities of recurrence along the vaginal wall. A phantom is built and developed to validate the prescription dose computed by the treatment planning system using radio chromic film (EBT3) in these applications.

MATERIALS AND METHODS: An acrylic box is intended to contain 10cm×10cm acrylic plates in six slots separated by 20mm. Concentric arc type slots with widths of 25, 35, and 45mm on plate-A and 20, 30, and 40mm on plate-B were designed to fit a calibrated EBT3 film as well as a 5.0mm circular opening for placement of an intrauterine tube at center. The diameters of these arcs were chosen based on the available vaginal cylinders (25, 30, and 35mm) and the distance of dose prescription (on or 5mm from the surface). A plan is generated in TPS (SagiPlan®), with the prescribed dosage mimicking with 3mm and 5mm dwell positions along the prescription length. Irradiations are performed in water phantom using Co-60 based HDR brachytherapy unit (Eckert & Ziegler BEBIG GmbH MultiSource®). The scanned films were compared for gamma assessment and dose estimation calculated by TPS to guarantee that the dosage was distributed uniformly around the film as required in vaginal cuff irradiation.

RESULTS: The test findings show that the estimated vs measured dosages differ by 5%. The 3% to 3mm gamma passing threshold is preferable for 3mm over 5mm dwell positions.

CONCLUSIONS: This phantom will help ensure prescribed dose delivery as well as dose homogeneity in single channel HDR vaginal cuff irradiations with varying dwell locations.

KEYWORDS: Vaginal cuff irradiation, EBT3 film, Quality assurance

REFERENCES

1. Sabater S., Andres I., Lopez-Honrubia V., Berenguer R., Sevillano M., *et al.* Vaginal cuff brachytherapy in endometrial cancer – a technically easy treatment? *Cancer Management and Research* 2017;9: 351–362.doi: 10.2147/CMAR.S119125.
2. Sureka C S, Sunny C S, Subbaiah K V, Aruna P and Ganesan S. Dose distribution for endovascular brachytherapy using Ir-192 sources: comparison of Monte Carlo calculations with radiochromic film measurements. *Phys.Med.Biol* 2007; 52:525–37.
3. Aldelaijan S, Mohammed H, Tomic N, Liang L H, DeBlois F., *et al.* Radiochromic film dosimetry of HDR ¹⁹²Ir source radiation fields *Med. Phys* 2011;38: 6074–83.

ESTIMATION OF RADIATION DOSE AT DIFFERENT LOCATIONS INSIDE BUNKER OF REMOTE AFTER LOADING HDR BRACHYTHERAPY MACHINE

Ranjna Agarwal, Sushovan Bairagya, Sooraj K.M.

Lions Cancer Detection Centre Trust, Surat, Gujarat, India

Email:agarwalranjna8@gmail.com

BACKGROUND/OBJECTIVE: Co-60 source is being used in HDR brachytherapy machine for delivering highly conformal dose to the tumor in very short time. High energy Co-60 source may pose high radiation risk to the staff in accidental exposure. Although there are many inbuilt safety features and last man out switch, quality assurance tests and preventive maintenance services are done to prevent any kind of malfunction and radiation accidents. This abstract present the estimated radiation dose level at different positions inside cobalt-60 HDR brachytherapy room.

MATERIAL AND METHODS: HDR brachytherapy machine having Co-60 source of present activity 1.517 Ci and exposure rate constant 1.3 roentgen per hour at 1 meter was used in this study. This HDR UNIT is installed in room of inner size 5.8×7.8 m² including maze area. A treatment plan was made for applicator length 1400 mm with source dwell position at tip of the applicator. This plan was delivered in QA mode and radiation survey was done at chest level inside machine room at various locations. All the dose levels were measured by using calibrated survey meter in freeze mode

RESULT: Radiation level was found to be 0.44 R/hr near hand crank when source remain outside machine. When hand crank is used to retract source it moves very fast inside machine and dose level increases to 2.9 R/hr. As the transit time is 8 sec. for source to return inside machine, the exposed person will get exposure rate from 0.44 R/hr to 2.9 R/hr. If maximum dose level is considered for safety point of view for 5 minute of duration, then dose will be 0.24 R which is approximately 2.4 mSv. If this is calculated for 2 Ci (highest activity) source then it will be 3.16 mSv. The dose from other positions will be added in it as person moves from console to machine for handling emergency. Dose levels at other locations are mentioned in full paper.

CONCLUSION: Dose estimation inside brachytherapy room is useful to estimate dose received by staff in radiation accidents. It also helps in time management to handle actual accidental conditions.

KEY WORDS: HDR brachytherapy, radiation dose level, radiation accident, radiation survey

ANALYSIS OF RELATION OF RMM VALUE OF CO-60 SOURCE AND OUTPUT OF CO-60 TELETHERAPY MACHINE

Ranjna Agarwal, Sushovan Bairagya, Sooraj K.M.

Lions Cancer Detection Centre Trust, Surat, Gujarat, India

Email:agarwalranjna8@gmail.com

BACKGROUND/ OBJECTIVE: In India, Co-60 sources for teletherapy machines are supplied by Board of Radiation and Isotope Technology (BRIT). As its activity decays exponentially with time, the output of machine also decreases. As per AERB recommendation source has to be replaced by new source on output < 50 cGy/min. The activity of source, mentioned in RMM by BRIT is verified by using calibrated dosimeter after it is loaded in teletherapy machine. Now a days dosimetry is done in water using ionization chamber having calibration factor $N_{D,w}$. This study has been carried out to calculate RMM (Roentgen per minute at one meter) value of cobalt-60 source and its relation with output of teletherapy machine.

MATERIAL AND METHODS: Two telecobalt machines viz. Th-780C and Th-Phoenix (Theratronix Pvt Ltd, Canada) having Co-60 source were used in this study in which sources have been replaced five times after their useful life. Activity of the sources in RMM was measured in air by using calibrated FC65-G Farmer type ionization chamber and Dose-1 Electrometer (IBA Dosimetry Systems, Germany). Chamber was set in air with buildup cap, source to chamber center distance was 80 cm and field size was set to 35×35 cm². Charge per minute was noted after irradiation. N_x (R/C) was calculated using SSDL provided $N_{D,w}$ (Gy/C) by using formulae. RMM was calculated using N_x (R/C). Output (cGy/min.) of machine was measured in water for 10×10 cm² field size at 80 cm SSD.

RESULTS: Measured RMM was within accuracy of $\pm 2\%$ of the supplied activity. RMM of the source quoted is based on the measurement carried out in BRIT hot cell. The structure of BRIT hot cell and telecobalt machines in hospitals are entirely different hence it requires measurement of activity within $\pm 10\%$. Mean ratio of output (cGy/min) to RMM was found to be 1.51 (SD: 0.03).

CONCLUSION: Supplier and user method of activity measurement are different. The conversion of $N_{D,w}$ to N_x for RMM measurement requires many physical quantities. Knowledge of relation between output of machine (cGy/min) and RMM is useful for verifying initial output measurement after source loading.

KEYWORDS: Cobalt-60, output, roentgen per minute at one meter, teletherapy unit

HUGE USE OF X-RAYS IN MEDICAL SCIENCE

Rajesh Kumar Rajput

Apex University, Jaipur, Rajasthan, India

Email: barrodrajesh707@gmail.com

Rontgen in 1895 discovered the x-rays, when was studying the phenomenon of discharge of electricity through rarefied gases. He found that when the pressure in the discharge tube is reduced to 0.001 mm of mercury and electric discharge is passed between cathode and anode, the glass wall behind cathode begins to glow with greenish yellow color. During his experiment he also observed that fluorescent screen placed close to discharge tube continued to fluoresce close to the discharge tube continued to fluoresce even if the discharge tube was completely covered with a black paper. Although the intensity of fluorescence was reduced by interposing various thickness of different substance between screen and tube but it could not be cut off entirely. When plate of iron was placed it casts a shadow on the screen showing that certain radiation are coming out from the discharge tube. After performing a series of experiment Rontgen concluded that when a beam of fast moving electrons strikes a solid target, invisible high penetrating radiation is produced. Because of their unknown nature Rontgen called these radiation as X-Ray.

A COMPARATIVE STUDY ON EFFECTIVENESS OF AUTOFLASH MARGIN IN MONACO TREATMENT PLANNING SYSTEM

Vikash K. Pathak, Anchal Sharma, Pranjali Shrivastava

All India Society for Health Aid Education and Research, Venkateshwar Hospital, New Delhi, India

Email: vikashaimsphysics@gmail.com

BACKGROUND/OBJECTIVE: To obtain surface dose, usual practice is to put bolus on the skin of the patient, where megavoltage beam used for photon irradiation. Few treatment planning systems (TPS) based on Monte Carlo simulation and fluence based optimisation (e.g., Monaco) possess auto flash margin function to obtain surface dose, where it is required for example, in chest wall irradiation and for the tumor proliferated to the skin surface.

Objective of this study is to compare efficacy of auto flash margin of the treatment planning system for surface dose with third party dosimetry system.

MATERIALS AND METHODS: Materials used for the purpose were optically stimulated dosimeter (OSLD) with Quasar body phantom for surface dose measurement and Monaco treatment planning system with XVMC code for dose calculation.

A treatment planning was performed on the CT image of quasar body phantom simulating the chest wall irradiation. VMAT inverse planning on the CT image using fluence based optimisation and MC based dose calculation was done using auto flash margin to obtain surface dose. Prior to imaging Beryllium oxide chips were pasted on the surface of body phantom. In linear accelerator the surface dose was measured using the OSLD system.

RESULTS: This comparative study found that deviation between TPS calculated and OSLD system measured surface dose was within $\pm 1\%$.

CONCLUSIONS: The test result suggests that auto flash margin for surface dose can be used instead of physical bolus.

KEYWORDS: MC, TPS, OSLD, Auto flash margin

UNRAVELING THE GENOMIC PROFILES OF RADIORESISTANT HNSCC TO IDENTIFY PREDICTIVE BIOMARKERS FOR THERAPY RESPONSE

K R Muralidhar¹, R Venkataramanan², Moni Kuriakose², Prashant Kumar²

¹Karkinos Healthcare private Limited, Hyderabad, India, ²Karkinos healthcare private limited, Mumbai, India

Email: muralidhar.kr@karkinos.in

BACKGROUND: Radiation therapy is the mainstay treatment for head and neck squamous carcinoma (HNSCC), one of the most prevalent cancers among Indian population. Nonetheless, in majority of patients, HNSCC tumors display radioresistance resulting in poor survival of these patients. Thus, understanding the mechanisms of radioresistance and identifying predictive biomarkers of radiotherapy response will significantly improve treatment outcomes. Our aim is to investigate the genomic alterations associated with radioresistance in HNSCC patients to identify potential biomarkers of radiotherapy response.

MATERIALS AND METHODS: Whole genome sequencing will be performed on pre-treatment biopsies of 50 HNSCC eligible for receiving post operative radiotherapy. Based on the response, patients will be classified into radiosensitive and radioresistant group. Using an in-house developed pipeline, the WGS data will be analyzed for studying the underlying genomic alterations including single nucleotide variations, copy number alterations and structural variations. Based on comparative analysis of genetic variations in radiosensitive and radioresistant groups, potential biomarkers of radioresistance will be identified. The candidate biomarkers will be functionally validated using *invitro* assays of radioresistance.

RESULTS: Our study will reveal the comprehensive analysis of genetic alterations or mutational signatures associated with radioresistance in HNSCC patients. These biomarkers could serve as predictive indicators for treatment response and pave way for initiation of personalized radiotherapy in these cancers. Additionally, the findings may shed light on potential strategies to overcome radioresistance and enhance the efficacy of radiotherapy in HNSCC.

CONCLUSIONS: Our study will provide crucial insights into the molecular basis of radioresistance in HNSCC patients. The identification of biomarkers may help in better selection of patients for radiotherapeutic regimens, ultimately leading to enhanced treatment outcomes and quality of life.

BONE PALLIATION USING THERAPEUTIC ¹⁵³Sm RADIOPHARMACEUTICAL: OUR EXPERIENCE IN RADIATION SAFETY MEASURES

Deboleena Mukherjee¹, Kirti Tyagi¹, A G Pandit³, Hari Mukundan¹, Vigneshwaran M²

¹Nuclear Medicine Department, INHS Asvini, Mumbai, India,
²Radiation Oncology Centre, INHS Asvini, Mumbai, India

Email: deboleena.rso@gmail.com

BACKGROUND/OBJECTIVE: Radiopharmaceutical (RP) Samarium available as ¹⁵³Sm-Ethylene Diamine Tetra Methylene Phosphonate (EDTMP) injection is used nowadays to palliate bone pain due to metastases. As a rule, all reasonably acceptable measures should be taken to decrease radiation exposure “ALARA” criteria. At our centre we administered ¹⁵³Sm to 20 patients (12 males & 8 females). Our experience in radiation safety measures is discussed.

MATERIALS AND METHODS: RP was administered intravenously as per patient’s body weight range (40-85Kg), dose range (40-105 mCi) in Nuclear Medicine (NM) ward. Before injection an informed consent taken and proper advice regarding radiation safety was given by RSO in a prescribed format. After injecting patients were monitored by GM survey meter (audio alarm facility). Staff handling took proper measures like wearing hand gloves, TLD (chest/wrist) badges and checked for any contamination. Patients underwent whole body scan at 48 hrs after administration using a Dual head Gamma Camera (Siemens) for confirmation of uptake in metastatic areas (Fig.1). Follow up was done at 4 weeks interval. Special advice was given to observe proper toilet practices at home & in case of Emergency to reach hospital immediately.

RESULTS: 20 patients were palliated with ¹⁵³Sm following Surgery/Radiotherapy & Chemotherapy with age range (50-85) years. 01 patient (Ca Prostate) received repeated dose of 60mCi at 5 months interval & 02 male and 03 female patients were incontinent needed catheterization and after therapy the urine bags were kept in lead shields in radioactive storage area of NM ward & after decay (10 half-lives) were disposed. At exposure rate 5mR/hr at one meter distance patient were discharged. (Table 1).

CONCLUSIONS: Advantages of ¹⁵³Sm are low beta & gamma energy and suitable for imaging for its biological distribution, short physical half- life (46.3hrs) reducing long period of stay in isolation to facilitate the disposal of urine and other body fluids with less radiation hazards, and treat bone pain at multiple sites. Urinary excretion of unbound material in 48 hours following administration is the main issue concern especially for incontinent patients. All these patients tolerated well. Proper counseling about radiation hazards is necessary before therapy.

KEY WORDS: Bone palliation, Samarium, Radiation safety

Fig. (1) shows WB Scan of ¹⁵³Sm confirmation of uptake in metastatic areas.

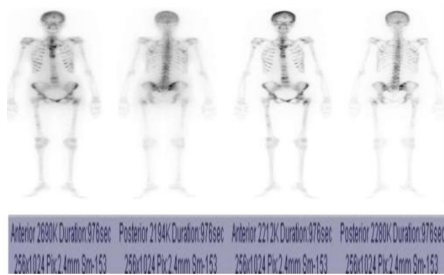


Table (1) shows isotope dose range, age range, sex, weight range, and diagnosis and exposure rate at 1 meter for all patients.

Isotope & Dose injected	Age range (yrs)	Sex (M/F)	Weight (Kg)	Diagnosis	Exposure rate at 1 meter
¹⁵³ Sm 40-105mCi	50-85	12 M 08 F	50-85 40-75	6- Ca Prostate (M) 6-Ca Thyroid with bone mets (M) 1-Spindle cell Sarcoma (F) 1-Rectum (F) 6-Breast (F)	5mR/hr

QUALITY ASSURANCE PROGRAM OF PET/CT SCANNER FOR RADIATION THERAPY

Deboleena Mukherjee¹, Kirti Tyagi¹, Hari Mukundan¹, A G Pandit², Vigneshwaran M²

¹Radiation Oncology Centre, INHS Asvini, Near R.C.Church, Colaba, Mumbai, India,

² Nuclear Medicine Department, INHS Asvini, Mumbai, India

Email: deboleena.rso@gmail.com

BACKGROUND/OBJECTIVE: PET/CT scanners are widely used for radiotherapy (RT) applications. Several studies incorporating PET/CT imaging into treatment planning system (TPS) for (RT) have been reported¹⁻⁴. To identify/minimize the sources of uncertainties/errors, a rigorous quality assurance (QA) protocol is mandatory for proper functioning and effective image integration for RT. Our experience in QA program of PET/CT scanner is discussed.

MATERIALS AND METHOD: A PET/CT scanner (M/s Wipro GE) was installed (Apr 2014). Till date more than 2000 patients (40-90Kg body weight) underwent WB ¹⁸F-FDG-PET (Dosage 0.1mCi/Kg) scans successfully. QA tests as per AERB /NEMA protocols^{5,6} were carried out using 200 mCi (¹⁸F-FDG), Ge-68 VQC and other phantoms, and Ge-68 pin source (0.5mCi) used for daily transmission scanning. As per institutional protocol, RT patients underwent CT imaging with fiducial radiopaque lead markers on thermoplastic mould aligned with lasers in region of interests (ROIs) in flat couch and are reconstructed (between 0.625mm-3.75mm) slice thickness⁷. Various image registration techniques (Manual, Identity, Landmark approach, Surface matching and Mutual information) in TPS (Oncentra™) are available.

RESULTS: Daily QA, monitors the image quality over a time period. Here single events, coincidence, dead time, peak energy spectrum of the detectors are measured. Weekly QA, all detectors are irradiated and corrections are made for the detector outputs. Quarterly and Annual QA provides the system with a benchmark for counting variations and overall system performance. Measurements included position of single events, update gain, energy, detector coincidence timing characterization, 2D normalization, 3D geometric and well counter calibrations. Vendor performed QA of image acquisition and data transfer and developed a Standard disease specific image acquisition protocol, optimized, confirmed and were used by routine inspection of clinical procedures^{8,9}. Standard uptake values (SUV) forms the basis for quantitative use of imaging data and automated segmentation. Delineation of target volumes (GTV, CTV, PTV) for RT is done by Visual interpretation, Threshold SUV, Thresholding percentage (e.g., 40%) of the maximum uptake and source-to-background ratio (Fig.1).

Fig(1) shows various phantoms used in QA program and Ge-68 pin source for daily calibration & fusion of CT and PET images in TPS for Lung Cancer.



CONCLUSIONS: PET/CT imaging plays an important role in patient staging, RT planning and therapeutic assessment. A comprehensive QA program is followed for success in treatment planning and therapy.

KEYWORDS: PET/CT imaging, Quality Assurance, Treatment planning.

ARTIFICIAL INTELLIGENCE AND MEDICAL PHYSICS

Sahar Heidary

Faculty of health science, Yeditepe University, Istanbul, Turkey

Email: sahar.heidary@std.yeditepe.edu.tr

ABSTRACT: Artificial intelligence (AI) is a rapidly evolving field with vast potential to revolutionize various industries, including medical physics. This paper provides an overview of the intersection between AI and medical physics, highlighting the significant impact and promising applications of AI techniques within this domain. Medical physics utilizes physics principles and techniques in healthcare, encompassing areas such as diagnostic imaging, radiation therapy, and nuclear medicine. By integrating AI into medical physics, we can enhance accuracy, efficiency, and patient outcomes. AI algorithms have the capability to analyze complex medical data, including radiological images and patient records, thereby aiding in diagnosis, treatment planning, and prognosis assessment. Machine learning and deep learning techniques allow AI systems to extract valuable insights from large datasets, resulting in improved disease detection, treatment optimization, and personalized medicine. One notable area where AI has shown promise in medical physics is image analysis. AI algorithms can automatically detect abnormalities in medical images, such as tumors or lesions, with an accuracy that often rivals or exceeds human experts. This facilitates early disease detection and assists in treatment planning by providing precise anatomical and functional information. Moreover, AI algorithms can track tumor response during radiation therapy, enabling adaptive treatment strategies that enhance therapeutic outcomes. Furthermore, AI has the potential to facilitate the integration of multiple imaging modalities and data sources, providing a comprehensive understanding of patient conditions. By fusing information from diverse sources, AI algorithms generate multimodal images and quantitative measurements, allowing clinicians to obtain a more holistic view of the patient's health status. In conclusion, the integration of AI into medical physics has the potential to revolutionize healthcare by improving diagnosis, treatment planning, and patient outcomes. Through advanced image analysis, data fusion, and decision support systems, AI can assist medical physicists and clinicians in providing more accurate, efficient, and personalized care. However, careful consideration must be given to ethical, legal, and technical aspects to ensure the responsible and effective implementation of AI in medical physics practice.

KEYWORDS: Artificial intelligence, medical physics, healthcare, AI techniques, transformative technology, diagnostic imaging, radiation therapy.

TO STUDY THE IMPACT OF MINIMUM SEGMENT WIDTH ON THE QUALITY OF VMAT PLANS USING MONACO TPS FOR ENDOMETRIUM CANCER

Avtar Singh¹, Amit Saini¹, Gurvinder Singh², Rahul Kalita¹,

¹Department of Medical Physics, Homi Bhabha Cancer Hospital, Sangrur, Punjab, A unit of TMC Mumbai, ²Department of Medical Physics, Homi Bhabha Cancer Hospital & Research Centre, Mullanpur, Mohali, Punjab, India, A unit of TMC Mumbai

Email: avtar.medphy@gmail.com

OBJECTIVE: Volumetric Arc Therapy (VMAT) is an advance radiotherapy treatment technique in which the radiation dose rate, gantry speed and motion of the multi-leaf collimators (MLC) and jaws can be modulated while the radiation beam is on. Monitoring Units (MUs), control points and minimum segment width (MSW) are important VMAT planning parameters to assess the plan quality. The goal of this study was to investigate the impact of the MSW on the quality and deliverability of VMAT plans for endometrial cancer.

MATERIALS AND METHODS: In this study, retrospectively pretreated ten patients were randomly selected for re-planning and evaluation. The VMAT plans were generated in Monaco (version 5.11) Treatment Planning System (TPS) by changing the MSW in steps of 0.5cm (0.5cm-2.0cm) and keeping other parameters unchanged. A total dose of 50Gy in 25 fractions was delivered to Planning Target Volume (PTV) using two full arcs of 360°.

For four VMAT plans with different MSW, the Conformity Index (CI), Homogeneity Index (HI), maximum dose to target volume, MUs, control points and the Dose Volume Histogram (DVH) parameters of organs at risk (OARs) were compared. Paired t-test was used to check the statistically significant difference (if $p < 0.05$) in the intergroup comparison of dosimetric parameters of PTV and OARs.

RESULTS: For VMAT plans with different MSW, no statistically significant variation was observed in the dosimetric parameters of PTV and OARs. The MSW of 0.5cm which is generally used for planning was considered as baseline for comparison. The mean reductions in total MUs for MSWs of 1.0cm, 1.5cm and 2.0cm were $17.8 \pm 6.8\%$, $34.6 \pm 11\%$ and $40.1 \pm 13.4\%$ respectively, when compared to the 0.5 cm MSW. Similarly, the reductions in control points were $10.4 \pm 5.5\%$, $18.1 \pm 7.6\%$ and $21.6 \pm 7.2\%$ for 1.0cm, 1.5cm and 2.0cm MSWs, respectively. With increased MSWs, the plan delivery time decreased significantly ($p < 0.05$).

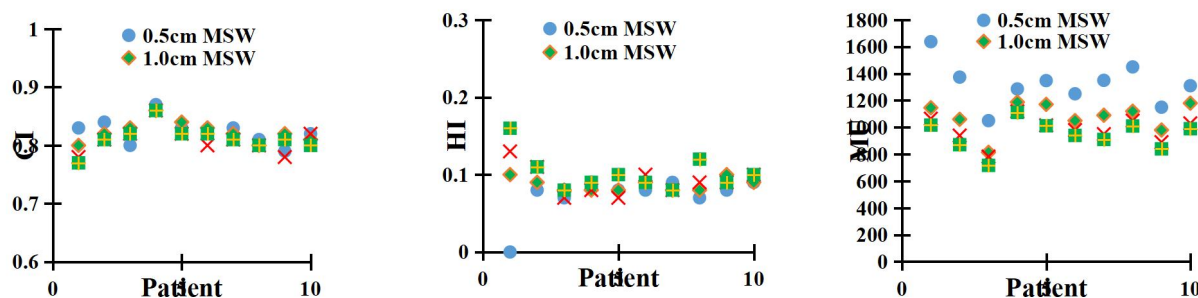


Figure: The figure (a) and (b) showing the conformity index (CI) and homogeneity index (HI) of PTV for 10 endometrium VMAT plans, the figure (c) showing the variation of MUs with different MSWs settings.

CONCLUSION: Without significantly impacting the quality of VMAT plan, increasing the MSW enables better efficiency in plan delivery by decreasing MUs, control points and treatment delivery time. The quality of the plan, delivery and effectiveness of endometrium VMAT radiation therapy were enhanced by MSWs of 1.0 cm, 1.5 cm and 2.0 cm.

KEYWORDS: VMAT planning, Monaco TPS, Minimum segment width

IMPROVED PLAN STUDY FOR HIPPOCAMPUS SPARING IN WHOLE BRAIN RADIATION THERAPY: DOSIMETRIC COMPARISON OF NON-COPLANAR ARC PARTIAL FIELD TECHNIQUE VMAT WITH DUAL-ARC AND SPLIT-ARC PARTIAL FIELD TECHNIQUE.

Biju P Thomas ¹, Naiby Joseph ¹, Dona Shaji ¹, Dr.Jenny Joseph ¹, Judith Aaron ¹, Elice M Paul²,
Meera S Nair ³

¹Department of Radiation Oncology, Caritas Hospital&Institute of Health Sciences, Kerala, India,

²Department of Medical Physics,JSS Academy of Higher Education &Research, Mysuru, Karnataka, India,

³Department of Physics, University of Calicut, Thenhipalam, Kerala, India

Email: meerasnair.meera@gmail.com

BACKGROUND: Whole brain radiotherapy is a palliative option for patients with brain metastases. In dual-arc (dac-VMAT), the large irradiation field for whole brain planned target volume (PTV) requires a wide jaw opening in which substantial low dose volume to hippocampus. In co-planar VMAT the radiation beam delivered will share same geometric plane in accordance with patient. In non co-planar VMAT radiation beam don't share same geometric plane, as a result beam overlapping will be reduced. Hence it reduces the radiation dose. The present study investigates the potential of a radiation therapy technique with Non co-planar, reduced field size to spare the hippocampus along with eyes during WBRT.

MATERIALS AND METHODS: Five patients, who had been previously treated with WBRT were randomly selected and enrolled in the present study. All patients had a previous primary cancer diagnosis that had metastasized and infiltrated the brain. Hippocampus, eyes, lens were considered. The selected treatment was done using Varian UNIQUE performance. It works integrately with ARIA Oncology information system and Eclipse treatment planning system version 13.6. The treatment planning system is equipped with photon optimization and use analytical anisotropic algorithm (AAA algorithm). The hippocampus was manually delineated by following the Radiation Therapy Oncology Group (RTOG) 0933 protocol. Plans delivering a specified dose were generated for each patient using dual-arc (dac), split-arc-partial-field (sapf) and Non co-planar VMAT.

RESULTS: Hippocampus of Non-coplanar -VMAT (8.69Gy, $p < 0.001$) had a significantly lower average $D_{100\%}$ compared to Sapf (9.61Gy). At the same time it is statistically comparable to Co-planar (8.56 Gy). A decrease in hippocampus D_{max} using non-coplanar (14.63Gy, $p < 0.001$) was statistically significant compared to sapf (15.85Gy) and Co-planar (14.73Gy). The resulting mean dose to the hippocampus were 10.81Gy for non-coplanar VMAT and mean dose to hippocampus were 10.13Gy for Co-planar VMAT. The mean dose of non-coplanar VMAT was significantly lower than sapf (11.61Gy, $p < 0.001$). For eye lens, non coplanar shows a significant lowered doses of 5.69Gy compared to sapf VMAT of 10.69Gy and co-planar VMAT of 20.42Gy.

CONCLUSION: Over sapf and co-planar VMAT, sparing of hippocampus and OARs such eyes and eye lenses is the primary advantage of applying non-co-planar VMAT in WBRT.

KEYWORDS: Hippocampus, Whole brain radiotherapy, Non co-planar VMAT.

ESTIMATION OF RADIATION EXPOSURE TO THE CAREGIVERS OF PATIENTS UNDERGOING F-18 FDG PET SCAN

Kirti Tyagi¹, Deboleena Mukherjee¹, Sreejith S Nair¹, A G Pandit¹, Vigneshwaran M¹, Hari Mukundan²

¹Nuclear Department, INHS Asvini, Mumbai, India,

²Head, Radiation Oncology Centre, INHS Asvini, Mumbai, India

Email: callkirti@yahoo.com

BACKGROUND/OBJECTIVE: Positron Emission Tomography (PET) has been playing a key role in important clinical decision making in many areas ever since its inception in the field of medical imaging. The purpose of this study is to measure the radiation dose received by the caregiver person accompanying the patients during Positron Emission Tomography (PET)/Computed Tomography (CT) scan.

MATERIALS AND METHODS: A prospective study was carried out comprising of 20 male caregivers of planned patients for PET/ CT (M/s Wipro GE – Discovery PET CT 690 Elite) scan at Nuclear Medicine department of INHS Asvini (Fig 1, Fig 2). These caregivers were provided calibrated digital pocket dosimeters (Aloka-PDM 122-RH) for monitoring on their arrival till they left the department (Fig. 3). The patients were in the age group of 37yrs to 72 yrs and caregivers were in the age group of 26 yrs - 44 yrs. Patient preparation and imaging were done as a routine protocol. For whole body PET/CT imaging around 260 MBq - 300 MBq F-18 FDG injection administered to the patient and image were acquired after 45 min to 1hr after intravenous injection. Caregivers were needed to give support during injection time and during scan time, otherwise instructed to avoid close contact with patients. The readings of pocket dosimeters were noted and doses received by each caregiver were recorded.

RESULTS: The doses received by the caregivers from a PET/CT patient were found to be in the range of 0.02 μ Sv to 10 μ Sv (Table 1). The dose recommended by AERB/ICRP for general public is 5 mSv over a span of 5 years.



Fig 1

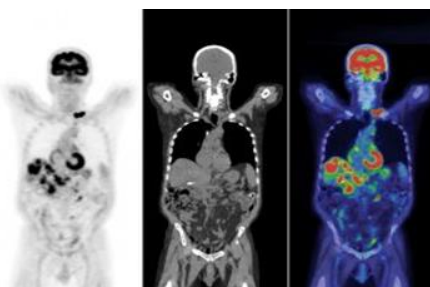


Fig 2 a,b,c



Fig 3

Fig 1: GE Healthcare Discovery PET/CT Scan Machine
Figure 2: (a) PET image (b) CT image (c) PET/CT fused image
Fig 3: Personal radiation monitors worn by accompanying person

CONCLUSIONS: Irrespective of the age group of the injected patients, the caregivers of non-ambulatory patients received higher radiation dose due to more time spent near the radiation source i.e. the injected patient. The highest dose received was well below the dose limits recommended by AERB and ICRP for general public. Thus, the radiation risks of the caregivers found to be very low and almost insignificant when compared to the radiation received by natural background (3-4 mSv) per person over a year.

KEYWORDS: PET-CT scan, Radiation exposure, Pocket dosimeter

QUALITY ASSURANCE TESTS AND INSTALLATION OF 3D MAMMOGRAPHY UNIT AT A TERTIARY CARE CENTRE

Kirti Tyagi ¹, Deboleena Mukherjee ¹, Eesha Rajput ³, T C Bhatt ⁴, Hari Mukundan ⁵

¹Radiation Oncology Centre, INHS Asvini, Mumbai, India,

²Radiodiagnosis & Imaging, INHS Asvini, Mumbai, India

Email: callkirti@yahoo.com

BACKGROUND/OBJECTIVE: Mammography is an accepted tool of diagnosis for early detection of breast cancers. There are two types of mammography – Full Field Digital Mammography (FFDM) and Digital Breast Tomosynthesis (DBT). Digital Breast Tomosynthesis (DBT) is an advanced form of breast imaging where multiple images of the breast from different angles are captured and reconstructed into a 3D image set. DBT uses the same amount of radiation and time as FFDM. The advantage is that it provides significant clarity of the images reducing the chances of raising false alarms and early detection of cancer. Acceptance tests and commissioning is an integral part of installation of any radiation generating equipment. This paper discusses the commissioning of DBT mammography unit and results of the quality assurance tests carried out at the hospital.

MATERIAL AND METHODS: A mammography unit (Selenia Dimensions AWS, M/s Hologic) was installed in May 2023 at INHS Asvini, a tertiary care hospital. The lay out diagram of the room for installation of mammography unit was submitted to Atomic Energy Regulatory Board (AERB) through its electronic portal (electronic Licensing of Radiation Application - eLORA) for obtaining procurement permission of the mammography unit. During commissioning of the unit Quality Assurance (QA) tests were carried out using tools like kVp meter, Mammography image quality phantom, half value layer attenuator set, photo timer consistency test tool, digital x-ray timer and radiation survey meter. QA tests pertaining to accuracy of operating potential and timer, linearity of current, reproducibility of output, performance of imaging phantom and radiation leakage levels from X-ray tube housing were performed.

RESULTS: The measurements related to accuracy of operating potential, timer, linearity of tube current, reproducibility of radiation output, total filtration and aluminium equivalence of compression, performance of imaging phantom, radiation leakage levels and radiation protection survey of the installation were found within specified tolerance limits.

CONCLUSION: All measurements were found to be well within the limit as recommended by the regulatory body. The registration of the unit obtained from AERB through eLORA portal. The mammography unit was installed, commissioned and made operational for medical use.

KEY WORDS: Mammography, Quality Assurance tests, Digital Breast Tomosynthesis

REFERENCES:

1. AERB safety code for medical diagnostic equipment & installations AERB/SC/MED-2(Rev. 1).
2. Quality assurance and quality control in mammography: a review of available guidance worldwide - Cláudia Reis & Ana Pascoal & Taxiarchis Sakellaris & Manthos Koutalonis – Insights Imaging, published online: 4 August 2013, DOI 10.1007/s13244-013-0269-1.
3. Digital Breast Tomosynthesis with Hologic 3D mammography Selenia Dimensions System for use in breast cancer screening – A Report 2017

VOLUMETRIC MODULATED ARC THERAPY FOR CA-OESOPHAGUS ; OUT- OF- FIELD AND IN -FIELD DOSIMETRIC COMPARISON BETWEEN FFF AND FF BEAM

Hemalatha.A¹, Athiyaman.M¹, Gokul Raj.M¹, Bhagisma¹, Neethi Sharma², Arun Chougule³

¹Dept of Radiological Physics, SP Medical College, Bikaner, Rajasthan, India

²Dept of Radiotherapy, SP Medical College, Bikaner, Rajasthan, India

³Swasthya Kalyan group of Institutions, Jaipur, Rajasthan, India

Email: mailtohemathi@gmail.com

BACKGROUND: Due to the rapid development of radiotherapy technology, Volumetric Intensity-Modulated Radiotherapy (VMAT) is now often utilised to treat oesophageal cancer. In clinical practise, the use of flattening filter free (FFF) beams generated by standard linear accelerators is increasing. The goal of this research is to discover any dosimetric benefits of FFF beam in VMAT treatment over FF beam.

MATERIAL AND METHODS: Thirty patients with Ca-Middle oesophagus treated with VMAT were chosen for this study. The FF beam plan was reoptimized in the Eclipse Treatment Planning system (V15.6.06) using the same criteria for FFF beam. The dose Homogeneity Index (HI) and Conformity Index (CI) in PTV were used to analyse the in-field dose distribution, and the dose to OAR was also considered. Furthermore, the peripheral dose was measured in the linear accelerator (True Beam, Varian Medical Systems, Palo Alto, US) using a MOSFET detector from the field edge for both FF and FFF plans.

RESULTS: The calculated HI (p-0.42) and CI (p-0.49) show insignificant difference between both the plans. In addition, the plan comparison revealed an insignificant difference in lung dose of volume receiving 5, 10, 15, 20, 25, 30 Gy. The dose to the heart indicates that the volume receiving 10 (p-0.02) and 15 (p-0.01) Gy was significantly greater with a FF beam than with an unflattened beam. The FFF plan was found to have a lower mean dose to the lungs and heart. Furthermore, the volume of the heart receiving 5, 20, 25, and 30 Gy differs insignificantly. The maximum dose to the spinal cord also shows no discernible difference (p-0.77). The MU of 30 patients was examined, and it was discovered that FFF plans were associated with significantly higher MU (p-0.02). The peripheral dose measurement shows that up to 12 cm from the field edge, the FFF beam delivers a higher dose, and then the FF beam delivers a higher out of field dose.

CONCLUSION: This study compared treatment planning for VMAT –Oesophageal cases and found that FF and FFF treatment plans were of comparable quality in general.

EFFECTS OF CT PROTOCOL VARIATION ON EFFECTIVE DOSE AND RISK FOR CT CHEST-ABDOMEN-PELVIC (CAP) EXAMINATION

Tadelech Sisay Mekonin

Addis Ababa university, Ethiopia.

Email: tadelech.sisay@aau.edu.e

OBJECTIVE:- To propose a method for estimating the effective life time risk of radiation –induced cancer from different abdomen-chest-pelvis (ACP) scan protocol in both pediatrics and adults and to develop a prospective method for estimating the number of cancer case for patients undergoing CT (ACP) scans when using different scanning parameter.

MATERIAL AND METHODS: - a series of CT dosimeter experiments will be conducted at Addis Ababa the capital city of Ethiopia. Both adult and pediatric ATOM phantoms will be imaged using a standard CT ACP protocol across wide range of protocol variation. Dose measurement will made using MOSFETs. Effective dose and lifetime a attributable cancer risks will be calculated from MOSFETs organ and tissue absorbed dose measurement in both phantom.

CONCLUSION:-The CT chest-abdomen-pelvis examination is generally used for the diagnosis of chronic and acute disease, as well as cancer staging.

KEYWORDS: Radiation dose, CT scanner, CT protocol, dosimeter.

BREAST CANCER SUBTYPE PREDICTION MODEL EMPLOYING ARTIFICIAL NEURAL NETWORKS AND ^{18}F -FDG PET/CT

Alamgir Hossain¹, Shariful Islam Chowdhury²

¹Department of Physics, University of Rajshahi, Rajshahi-6205, Bangladesh, ²Institute of Nuclear Medicine and Allied Sciences, Rajshahi-6000, Bangladesh Atomic Energy Commission, Bangladesh

Email: hossain447a@gmail.com

BACKGROUND/OBJECTIVE: PET/CT is a routine procedure for the measurement of breast cancer, but it does not classify subtypes automatically. Therefore, this research aims to evaluate the clinical subtypes of breast cancer based on the value of tumor marker using an artificial neural network.

MATERIALS AND METHODS: One hundred forty-two breast cancer patients (Training, Testing) who underwent ^{18}F -FDG PET/CT to diagnose the subtypes of breast cancer in our nuclear medical center. Before the scanning procedure, the patients were given ^{18}F -FDG-18 injections. We followed the routine procedure for the scan. The softmax function with cross-entropy loss is used in the output layer of the artificial neural network to diagnose subtypes of breast cancer based on the value of the tumor marker.

RESULTS: The result demonstrates the ANN model for k-fold cross validation including an accuracy of 95.77%. The average sensitivity and specificity were 0.958 and 0.955 respectively. The average AUC was 0.985.

CONCLUSION: The proposed model can classify breast cancer subtypes. Following the clinical implementation of the proposed model, the PET/CT may be upgraded to diagnose breast cancer subtypes using the appropriate tumor marker value.

KEYWORDS: Artificial neural network, Prediction model, histological subtypes, breast cancer, ^{18}F -FDG PET/CT

ASSESSING THE ADVERSE IMPACTS OF BIODEGRADABLE PLASTIC BAGS: HEAVY METALS AND RADIONUCLIDES CONSIDERATIONS

M. Mohery, A. Mindil

Department of Physics, College of Science, University of Jeddah, Jeddah 23890, Saudi Arabia

Email: mmohery@uj.edu.sa

ABSTRACT: Biodegradable plastic (BP) products are considered potential substitutes for conventional plastics and are increasingly used in various fields and applications. However, concerns remain regarding their safety and potential impact on the environment, humans, and ecosystems. This research examined biodegradable shopping plastic bags for their elemental content, including radioactive elements, using the neutron activation analysis (NAA) technique. Naturally occurring radioactive elements/radionuclides such as ^{40}K , Th, and U were also investigated in the specimens. The results obtained revealed that BP shopping bags contain higher concentrations of heavy elements (e.g., Cr, Co, Ba, Zn, Mn, V, Cd, Mo), halogens (Br and Cl), and radioactive elements (Th and U) compared to shopping bags made from conventional plastic materials. To assess the potential human health risks associated with BP shopping bags, the radiological and elemental hazards were evaluated by calculating the relevant hazard indices. For non-carcinogenic risks, the average daily intake of each element through different exposure pathways, as well as the hazard quotient, hazard index, and total exposure hazard index, were estimated. For carcinogenic risks, the incremental lifetime cancer risk was calculated. Possible hazards arising from radiological exposure were assessed by determining the excess lifetime cancer risk and other indices. Overall, the results showed that BP shopping bags do not pose a significant radiological or elemental threat to human health. However, attention should be given to controlling and monitoring the Cr content in BP bags.

KEYWORDS: Biodegradable plastic; shopping bags; toxic elements; radionuclides; neutron activation

FUTURE TRENDS AND DEMONSTRATIVE APPLICATIONS OF ARTIFICIAL INTELLIGENCE IN NUCLEAR MEDICINE

A K Shukla ,Satyawati Deswal , Manisha Pradhan And Devesh Bhatt

Department of Nuclear Medicine, Dr Ram Manohar Lohia Institute of Medical Sciences, Lucknow, Uttar Pradesh, India

Email: ajaikumarshukla@yahoo.com

INTRODUCTION: In the era of precision medicine, the application of artificial intelligence has emerged as transformative technology in medical imaging and also one of the most promising health innovation. In nuclear medicine artificial intelligence finds its application in image acquisition, processing, clinical reporting, data storage and mining etc..

This paper presents an overview of the application of AI in nuclear medicine particularly highlighting its utility in imaging, dosimetry and treatment scheduling etc.The use of AI can be extended to planning, scanning, reading and image interpretation/reporting.

PLANNING: For optimal preparation and planning of a particular investigation gathering patient related information often requires navigating through set of unstructured text documents. An AI algorithm extracting patient information in formatted form might render enormous assistance to clinicians and instantly check for certain contraindications or reduce unnecessary duplication of investigations by analyzing past examinations/investigations.

IMAGE ACQUISITION:In SPECT and PET imaging attenuation and scatter correction is primarily needed to optimize the images and help in improving the clinical decision making.Such image based attenuation and scatter corrections can be effectively applied using AI. Denoising of the images can also be explored using convolutional neural network (CNN) particularly in PET images.

IMAGE INTERPRETATION AND REPORTING: Automatic segmentation and quantification of PET CT images is often required for precision radiotherapy and AI algorithm can be successfully used although for fully automated tumor segmentation logistically feasible AI algorithms are still in the pipeline. Polar maps can be used for F-18 FDG PET scans using deep learning. Similarly training data set can be applied to reveal diagnosis with appreciable accuracy in SPECT images. Using radiomics features from F18 FDG PET CT one can also demonstrate therapy response.

Clinical dosimetry being essential aspect of nuclear medicine can also be benefitted by AI enabling optimization of patient specific radiation dose calculations based on individual anatomic variations, tumor characteristics and kinetics of radiopharmaceutical used.Machine learning algorithms can also be used optimizing therapy protocols, minimizing radiation doses to normal tissue and maximizing therapeutic efficacy.

CONCLUSION: Despite these promising applications, the integration of AI along with its widespread applications in every compartment of activities shall continue to be a challenge due to factors like data privacy, inter-variability of various models etc.

EFFICACY OF MULTICRITERIAL COST FUNCTION ON PLAN OBJECTIVE WITH MONTE CARLO DOSE CALCULATION ALGORITHM FOR VMAT TECHNIQUE IN HEAD AND NECK CANCER

Mukesh Meshram¹, Apoorv Vashishth², Pardip Deshmukh³

¹Department of Radiation Oncology, NCI, Nagpur, ²Department of Radiation Oncology, CIMS Hospital Pvt.Ltd., Ahmedabad, ³Department of Radiotherapy, Aditya Birla Memorial Hospital, Pune, India

Email: physics_med@rediffmail.com

BACKGROUND/OBJECTIVE: The purpose of this study is to compare the results and evaluate the benefits of multicriterial parameter with monte carlo dose calculation algorithm for VMAT technique in head and neck cancer.

MATERIALS AND METHODS: Study group consists of 15 head and neck cancer patients with VMAT delivery technique. All the plans were optimized on Monaco TPS with monte carlo dose calculation algorithm. Two different optimization protocols were used for each patient plan. The plans were optimized with and without use of multicriterial parameter for spinal cord and brainstem along with both biological cost function as well as physical cost function. Both the optimized plans were evaluated in terms of max dose and mean dose of OARs. Also we analyzed the monitor units, dose conformity, dose heterogeneity of calculated plans.

RESULTS: The average reduction of max dose with the use of multicriterial parameter were found to be 63.54% and 62.49% for spinal cord and brainstem respectively. No significant changes to the mean dose of other OAR were observed. Use of multicriterial result in higher MU per plan. It also result in slightly decrease plan conformity index as well as uniformity index.

CONCLUSIONS: The multicriterial based optimization protocol yielded less max dose to the serial organ and were found to be superior in better OARs sparing. Multicriterial parameter along with biological inputs can be suitable for patients in which OAR sparing is more important like patient with Re-irradiation plan.

A SYSTEMATIC REVIEW OF LET-OPTIMIZATION IN PROTON THERAPY: IDENTIFYING THE CURRENT STATE AND FUTURE NEEDS

Melissa McIntyre¹, Puthenparampil Wilson^{2,3}, Peter Gorayski^{1,2,4}, Eva Bezak^{1,5}

¹Allied Health & Human Performance, University of South Australia, Adelaide, SA 5001, Australia,

²Department of Radiation Oncology, Royal Adelaide Hospital, Adelaide, Australia,

³UniSA STEM, University of South Australia, Adelaide, Australia,

⁴Australian Bragg Centre for Proton Therapy & Research, Adelaide, SA 5000, Australia.

⁵Department of Physics, University of Adelaide, Adelaide, SA 5001, Australia

Email: melissa.mcintyre@mymail.unisa.edu.au

BACKGROUND/OBJECTIVE: The clinical benefits of proton therapy for cancer are well understood. Its capability to deliver a highly conformal target dose with significant normal tissue sparing makes it an ideal candidate for challenging cases and paediatric patients. A major contribution to the uncertainty encountered in treatment planning is the biological effect. Attempts to mitigate this uncertainty using a variable-RBE approach are not currently accurate enough to implement into clinical treatment planning because it is dependent on tissue-specific parameters that have large uncertainty. As such, LET-optimization has been proposed as a surrogate for RBE-optimization. This abstract presents the outcomes of a systematic review of LET-optimization in proton therapy to identify its current state and knowledge gaps.

MATERIALS AND METHODS: The systematic review is performed in-line with the PRISMA 2020 guidelines. A keyword search of the MEDLINE and Scopus databases gathered 51 relevant articles to be included in the review after removing duplicates. Our exclusion criteria included conference abstracts, literature published prior to 2000 and on heavy-ion therapy. Due to highly diverse patient-cohorts, plan objectives and evaluation metrics, a meta-analysis could not be performed. Instead, the capability of each optimization method to meet its objectives was assessed including the method's advantages and drawbacks.

RESULTS: The review identifies 3 study categories associated with LET-optimization; retrospective studies that investigate LET and adverse-effect correlations, LET-optimization methods through delivery techniques or by inclusion of objectives in the optimization function. Clinical evidence of LET-adverse-effect correlations is not unanimous due to high dependence on the endpoint. The LET contribution to long-term adverse-effects is often diluted by the patient's biological-response to the treatment, while a stronger correlation was observed for early-effects. Generally, LET-optimization methods achieve the objectives they pursue, however effectiveness is patient-dependent. Patients with tumours proximal to critical structures see the most benefit and hence are primary candidates.

CONCLUSIONS: LET-optimization methods generally achieve the objectives they pursue, allowing consideration of clinical feasibility regarding computation time and compatibility with current protocol. Clinical data with more frequent follow-up times will clarify the clinical benefit of LET-optimization to inform patient-selection protocol and quantification of LET-based objectives.

KEYWORDS: proton therapy, treatment planning, linear energy transfer, optimization

ESTABLISHMENT OF DIAGNOSTIC REFERENCE LEVELS FOR PREDOMINANT NUCLEAR MEDICINE IMAGING PROCEDURES USING TC^{99M} RADIOISOTOPE – MULTI-CENTRE STUDY

M. Senthilkumar¹, C. Senthil Kumar¹, J. Velmurugan²

¹Southern Regional Regulatory Centre, Atomic Energy Regulatory Board, Chennai,

²Department of Medical Physics, Anna University, Chennai, India

Email: senthil@aerb.gov.in

BACKGROUND/OBJECTIVE: The need for optimizing radiation dose delivered to patients undergoing nuclear medicine imaging is absolutely necessary to minimize avoidable radiation exposure. Towards achieving this, Diagnostic Reference Levels (DRLs) play a vital role to ensure that patients receive only the needed radiation dose. DRLs serve as guidelines for optimizing imaging protocols in nuclear medicine. They help healthcare providers achieve the desired diagnostic quality while keeping radiation doses as low as reasonably achievable (ALARA). By comparing the radiation doses received by patients with the established reference levels, healthcare facilities can identify potential areas for improvement in terms of equipment calibration, imaging protocols and in overall procedure optimization. DRLs also promote standardization and consistency across different healthcare facilities. However, in India, specific DRLs have not been established for imaging studies.

The concept of DRLs was initially introduced in the International Commission on Radiation Protection (ICRP) Publication 73. DRLs serve as investigation levels and typically focus on easily measurable quantities, such as the administered activity (measured in MBq) in nuclear medicine imaging studies. It is important to note that while DRLs aim to prevent excessive radiation exposure to patients while maintaining adequate image quality, they should not be used as dose constraints or limits. Optimization, on the other hand, refers to managing the radiation dose to the patient in accordance with the medical purpose. Many regulatory authorities and professional organizations incorporate DRLs into their guidelines and regulations.

MATERIALS AND METHODS: In this investigation, a survey was conducted at 11 Nuclear Medicine (NM) centers in Tamil Nadu to establish DRLs for NM imaging in adult patients. The study involved collecting data on the administered activity (measured in Mega Becquerel, MBq) from nuclear medicine departments for commonly performed imaging procedures. A minimum of 20 patients, with an average body size of 65 ± 10 kg, were included in the analysis for each procedure. By utilizing expert discussions and statistical analyses, the 75th quartile value (Q3) was identified as the preliminary DRL for each procedure.

RESULTS: For the Bone scan using Tc-99m MDP, the established DRL value is 740 MBq. The range for administered activity varies from 370 MBq to 925 MBq. Among the eleven centres analyzed, three centers have set their DRL at 925 MBq, two centres at 851 MBq and 786 MBq respectively, five centers at 740 MBq, and one centre at 647 MBq.

CONCLUSIONS: The finding indicates that there is good scope to optimize NM imaging procedures in the future. The predefined DRL values derived from the actual operating experience can serve as a valuable resource for optimization purposes. Collaborating with Nuclear Medicine personnel in such real-life data analyses may offer opportunities to decrease the elevated levels of administered activities. By implementing the DRLs, radiation protection in nuclear medicine imaging field can be effectively optimized. Compliance with these guidelines ensures that healthcare facilities adhere to recognized standards and best practices in radiation protection.

KEYWORDS: nuclear medicine, diagnostic reference level, administered activity, patient dose optimization

SIGNIFICANCE OF TANGENTIAL IMRT TREATMENT PLANNING TECHNIQUE IN REDUCING LOW DOSE SPILLAGE OF LUNGS IN SYNCHRONOUS BILATERAL BREAST CARCINOMA (SBBC)

Dona Shaji¹, Biju P Thomas¹, Naiby Joseph¹, Dr.Jenny Joseph¹, Dr. Judith Aaron ¹, Meera S Nair²

¹Department Of Radiation Oncology Caritas Hospital and Institute of health Sciences, Kottayam, Kerala,

²Department Of Physics, Calicut University, Kerala, India

Email: donashaji01@gmail.com

BACKGROUND/OBJECTIVE: To compare the dosimetric parameters of 3 Dimensional Conformal Radiation Therapy (3DCRT), Rapid Arc(RA) and Intensity Modulated Radiation Therapy. (IMRT) planning techniques for Synchronous Bilateral Breast Cancer(SBBC) using hypofractionation regimen. The patients are treated with non DIBH technique and planning was done on Eclipse (Version 13.6) TPS.

MATERIALS AND METHODS: We analyzed the different SBBC planning techniques with dual isocenter while using hypofractionation regimen(40Gy/15). All 5 patients had undergone bilateral modified radical mastectomy(MRM). The free breathing CT images were taken with 3mm slice thickness on Siemens Somatom Emotion CT Scanner after immobilizing patients on breast board. The images were exported to Varian Eclipse treatment planning system, which is incorporated with Analytical Anisotropic algorithm (AAA) for the dose calculation of photon beams and Photon Optimization (PO) algorithm to improve the Volumetric Modulated Arc Therapy (VMAT) optimization.

The anatomic regions of interest such as planning targets, organs at risk etc, were delineated slice by slice by the Radiation Oncologist. Different techniques of planning such as 3DCRT with tangential fields, Rapid Arc with half arcs and tangential IMRT with 16 beams were analyzed in this study using various dose constraints.

RESULTS: From the different planning techniques, the mean cardiac dose was 6.37 ± 2.33 , 11.39 ± 6.84 , 6.83 ± 2.85 and V25 was 8.63%, 9.98%, 5.97% for 3DCRT, RA and IMRT respectively. There is significant dose variation in low dose spillage of the lungs in IMRT plans with V5 of 56.03% where as it is 57.62 % in 3DCRT and 80.74% in RA. The mean lung doses were 15.43 ± 2.33 , 15.14 ± 4.93 , 13.09 ± 2.38 and V20 of lungs is 33.12%, 29.89% and 28.73% for 3DCRT, RA and IMRT respectively. Although 3DCRT technique met with all the target dose constraints, it failed to avoid the junction doses.

CONCLUSIONS: For radiation treatment delivery in Synchronous Bilateral Breast Cancer patients (post MRM) using hypofractionated regimen, IMRT technique with dual isocenter stands out in reducing the low dose spillage of lungs(V5) without compromising on the target coverage.

KEYWORDS: bilateral breast cancer, 3DCRT, Rapid Arc, IMRT, Hypofractionated Radiotherapy

EVALUATION OF PRE- AND POST-THERAPY RADIOIODINE AVIDITY INDEX (RAI) IN THYROID CANCER PATIENTS

A K Shukla, Satyawati Deswal, Astha Upadhyay, Shashwat Verma, Devesh Bhatt

Department Of Nuclear Medicine, Dr Ram Manohar Lohia Institute Of Medical Sciences, Lucknow, Uttar Pradesh, India

Email: ajaikumarshukla@yahoo.com

INTRODUCTION: In order to achieve optimal therapeutic efficacy in patients treated with high doses of radioactive iodine, it is essential to have quantification of the I-131 concentration either in thyroid remnant or distant metastatic lesions. In the present study we have attempted to use a parameter radioiodine avidity index (RAI) depicting ratio of the quantitative value of accumulated I-131 concentration subsequent to oral administration of the I-131 activity both in pre and post therapy whole body scan.

The parameter was defined as:

$$\text{RAI} = 1000 * \text{CPP}(\text{remnant/met}) / \text{activity administered in MBq}$$

Where CPP is the counts per pixel of the delineated lesion or thyroid remnant either in pre therapy or post therapy scan.

MATERIAL AND METHODS: A total number of 08 thyroid cancer patients having histo-pathological findings as papillary and/ or follicular thyroid carcinoma were included in the present study. Consequent to administration of low dose for pre therapy scan or high dose radioactive iodine for treatment of thyroid cancer patients (post thyroidectomy), whole-body imaging was performed on a dual head gamma camera Discovery NM/CT670 using HEGP collimators. After image acquisition ROIs (Region of Interest) were drawn over remnant/ metastatic lesions to compute number of counts per pixel. Thereafter Radioiodine Avidity index (RAI) was calculated for all lesions visualized on the whole body pre or post therapy scan including thyroid remnant.

In pre-therapy whole body scan RAI values were found to be ranging from 46.48 to 4674 with reference to same administered activity of 74 MBq I-131 in each case. However in post therapy whole body scan, RAI values were found to be ranging from 4.35 to 666.9 against the variable activities of I-131 administered ranging from 1850 MBq to 7400 MBq. Serum thyroglobulin (Tg) levels in these patients were found to be ranging from <0.2 to 32,400 ng /ml.

CONCLUSION: Despite similar activity of I-131 administered, the values of RAI had wide variation in pre therapy scan whereas in post therapy scan values of RAI depicted extremely significant and larger variation. RAI thus represents the quantification of I-131 accumulated after I-131 administration and can be considered as one of the indicators for prognostic outcome

ASSESSING VARIABILITY IN EXPERT CONTOURING OF CAROTID PATHOLOGY: ESTABLISHING MINIMUM CLINICAL STANDARDS FOR MACHINE LEARNING PERFORMANCE

Chris Boyd^{1,2} Timothy J. Kleinig^{3,4} Joseph Dawson^{5,6} Sandy Patel⁷ Gregory Brown¹ Wolfgang Mayer⁸ Mark Jenkinson^{9,10,11} Eva Bezak^{1,12}

¹Allied Health and Human Performance, University of South Australia, Australia; ²Medical Physics & Radiation Safety, South Australia Medical Imaging, Adelaide, Australia; ³Department of Neurology, Royal Adelaide Hospital, Adelaide, Australia; ⁴Adelaide Medical School, The University of Adelaide, Adelaide, Australia; ⁵Discipline of Surgery, University of Adelaide, Adelaide, Australia; ⁶Department of Vascular & Endovascular Surgery, Royal Adelaide Hospital, Adelaide, Australia; ⁷Department of Medical Imaging, Royal Adelaide Hospital, Adelaide, Australia; ⁸Industrial AI Research Centre, UniSA STEM, University of South Australia, Australia; ⁹Australian Institute for Machine Learning (AIML), School of Computer and Mathematical Sciences, University of Adelaide, Adelaide, Australia; ¹⁰South Australian Health and Medical Research Institute (SAHMRI), Adelaide, Australia; ¹¹Wellcome Trust Centre for Integrative Neuroimaging (WIN), Nuffield Department of Clinical Neurosciences (FMRIB), University of Oxford, Oxford, UK; ¹²Department of Physics, University of Adelaide, Adelaide, Australia

Email: eva.bezak@unisa.edu.au

PURPOSE/BACKGROUND: Carotid atherosclerosis is a common cause of ischemic stroke; internal carotid artery (ICA) percentage stenosis guides medical and surgical intervention [1], although plaque area and thickness may also predict recurrence risk. Such measurements currently require medical specialists to hand-measure imaging. This work seeks to quantify measurement variability to establish expert performance levels, against which machine learning (ML) models can be compared.

MATERIALS/METHOD: Forty-eight carotid vessel CT Angiography (CTA) series were collected, evenly distributed in stenosis severity (none, mild, moderate, and severe). Images were hand-segmented by a medical physicist, radiographer, vascular surgeon, vascular neurologist and neuroradiologist, using 3D SlicerTM[2]. To reduce contouring time requirements, 50 mm centred on the ICA origin, were linearly re-sampled from 0.5 to 2.5 mm slice thickness. Several months later, vessel contouring was repeated by the vascular surgeon, neurologist, and medical physicist for one patient from each category. The medical specialists' contours, and one generated "synthetic" contour set, were ranked from best to worst for six patients with the highest variability. Descriptive statistics investigated ranking variability and, if possible, sought to identify a preferred contour.

RESULTS: Dice Similarity Coefficient (DSC) was lower for pathology than lumen, with mean lumen DSC (0.88 ± 0.03) highest, followed by Calcific Plaque (0.66 ± 0.09) and Soft Plaque (0.28 ± 0.11). HD was smallest (best) for Calcific Plaque, likely due to the high subject contrast, (0.27 ± 0.06 mm), with Soft Plaque (0.83 ± 0.33 mm) and Lumen (1.05 ± 0.17 mm) much worse. Values obtained for intra-observer analysis were similar, with only Soft Plaque (0.45 ± 0.23) DSC showing improvement. Fleiss Kappa of contour rankings were negative, indicating that clinician decisions had a probability less than chance, and without consensus. This was supported by low Kendall's W values, between 0.26 ± 0.14 and 0.69 ± 0.34 .

CONCLUSION: For segmentation of carotid pathology from CTA, expert clinician performance is a DSC for lumen, calcific plaque, and soft plaque of 0.85, 0.60 and 0.30 respectively, with a mean HD of 1.0 mm. Any machine learning tool developed should be expected to perform equivalent to this standard.

REFERENCES:

- [1] G. G. Ferguson *et al.*, "The North American Symptomatic Carotid Endarterectomy Trial : surgical results in 1415 patients," *Stroke*, vol. 30, no. 9, pp. 1751-8, Sep 1999, doi: 10.1161/01.str.30.9.1751.
- [2] A. Fedorov *et al.*, "3D Slicer as an image computing platform for the Quantitative Imaging Network," *Magn Reson Imaging*, vol. 30, no. 9, pp. 1323-41, Nov 2012, doi: 10.1016/j.mri.2012.05.001.

Presentation ID: P-026

Abstract ID: S7226

EVALUATION OF LOCAL DIAGNOSTIC REFERENCE LEVELS IN DIGITAL BREAST TOMOSYNTHESIS (DBT) MAMMOGRAPHY IN INDIA

Adhimoolam Saravana Kumar¹, T. Manojkumar¹, Manimaran Perumal¹, Dinesh Babu¹, Varshini Raju¹, B. Devanand², T Balaji³, Sudhir Kumar⁴

¹Department of Medical Physics, PSG Hospitals, Coimbatore, Tamil Nadu, ²Department of Radiation, PSG Hospitals, Coimbatore, Tamil Nadu, ³Institute of Oncology, PSG Hospitals, Coimbatore, Tamil Nadu,

⁴Radiological Physics & Advisory Division, BARC, Mumbai, India

Email: sarava87@gmail.com

PURPOSE: The purpose of this study was to assess local diagnostic reference levels (LDRLs) for digital breast tomosynthesis in India.

METHODS: Data from 500 women were collected from five different digital tomosynthesis facilities in Tamil Nadu, India. The assessed LDRLs were defined as the 75th percentile of the mean average glandular dose (MGD) distribution.

RESULTS: The median MGD recorded in this study included prime and tomo for both breasts and was 1.60 mGy for all centers. The recorded mean MGDs are 1.53 mGy, 1.81 mGy, 1.41 mGy, and 1.72 mGy for the RCC, RMLO, LCC, and LMLO projections, respectively. The mean compressed breast thickness (CBT) values recorded in this current study were 60 mm, and the LDRLs reported for all centres were 1.77 mGy, 2.39 mGy, 1.73 mGy, and 2.28 mGy for RCC, RMLO, LCC, and LMLO projections, respectively. The LDRLs found in the current study were also compared with those from earlier studies conducted in other nations, such as the European Commission, United States, the United Kingdom, Japan, Morocco, Sri Lanka and Ghana.

CONCLUSION: The present study is the first of its kind to determine the LDRL for the DBT scanners operating in the Tamil Nadu region, India, and is suggested as a starting point that will allow professionals to evaluate and optimise their practice. Furthermore, Similar studies in other regions of India are necessary in order to establish a National DRLs.

KEYWORDS: diagnostic radiology, digital breast tomosynthesis (DBT) and radiation risk, DRLs

RAPID ARC BASED TOTAL MARROW AND LYMPHOID IRRADIATION(TMLI) – AN ALTERNATIVE TO TOTAL BODY IRRADIATION(TBI)

Naiby Joseph¹, Biju P Thomas¹, Judith Aaron², Dona Shaji¹, Jenny Joseph², Shabnam Abdul Kader², Vidya Gopalan², Meera S Nair¹

¹Department of Radiation Physics, Caritas Hospital and Institute of Health Sciences, Kottayam, Kerala, India

²Department of Radiation Oncology, Caritas Hospital and Institute of Health Sciences, Kottayam, Kerala, India

Email: naibyjosephnjv@gmail.com

BACKGROUND/OBJECTIVE:Total Body Irradiation (TBI) has remained the standard for conditioning prior to Allogenic Stem cell transplantation. But the difficulties in execution and setup along with limitation of dose escalation have given way to a more targeted marrow and lymphoid radiation called TMLI. Here we aim to implement the TMLI technique instead of the historical TBI technique.

MATERIALS AND METHODS:Three Aplastic anemia patients with ages ranging from 4 to 7 years, irradiated with doses of 2-6 Gy were considered for this study. Vac-lok indexed to All In One (AIO) board and thermoplastic brain mask were used for immobilization. Five sets of three fiducial markers were placed on the skull, chest, abdomen, pelvis and thigh respectively during Computed Tomography(CT) simulation. Patients were positioned in head first, supine with arms by side and moved inferiorly in cranio-caudal direction for imaging of the upper body. They were then positioned foot first supine to acquire CT images of lower extremities. CTs were acquired with 3 mm slice thickness. Target volumes and Organs at risk were contoured. Treatment planning was done with seven isocenters. All planning isocenters were placed in the same coronal and sagittal planes. Treatment planning for brain and neck were done with two isocenters and two full rotations each. Chest, Abdomen and pelvis plans were done with three isocentres and five full arc rotations. Chest plan had three full arcs including two partially blocked collimated arcs that reduced lung dose. Ramp-down structures, rings and avoidances were used to reduce dose to encased structures. Lower extremities were treated with 3DCRT using AP-PA fields. Treatment was delivered using Varian unique performance machine having 120 millennium MLC. Each isocenter was broken into a singular plan and portal images were taken to verify accurate positioning during the treatment.

RESULTS: We could deliver Rapid arc based TMLI with more dose homogeneity and comfortable setup position. RA based TMLI reduced doses to critical organs considerably thus allowing for future dose escalations as well.

CONCLUSIONS: RA based TMLI can be implemented in institutions facing technical difficulties for planning and executing TBI.

KEYWORDS:TMLI, TBI, RA based TMLI, Aplastic anemia

Presentation ID: P-028

Abstract ID: J4804

EFFECT OF VARIOUS FILTERS ON IMAGE QUALITY AND OTHER PARAMETERS IN ^{99m}Tc- SESTAMIBI MYOCARDIAL PERFUSION SPECT IMAGING

Satyawati Deswal, Manisha Pradhan , A.K. Shukla, Shashwat Verma, Devesh Bhatt

Department Of Nuclear Medicine, Dr. Ram Manohar Lohia Institute Of Medical Sciences, Lucknow,
Uttar Pradesh, India

Email: satyadeswal@rediffmail.com

INTRODUCTION: In order to reduce the statistical noise and produce optimum images of clinically acceptable qualities, filters are used in nuclear medicine imaging. Myocardial perfusion imaging using ^{99m}Tc sestamibi in SPECT/CT is used to ascertain viability of myocardial cells by assessing its physiological functioning. A variety of filters including Hann, Butterworth, Gauss, Metz, Wiener and Hamming both in FBP (Filtered Back Projection) and iterative reconstruction (Ordered Subset Expected Maximization) mode of image reconstruction are deployed. The present study was conducted to study the effect of various filters on image quality and associated parameters in cardiac SPECT, CT, MPI studies.

MATERIALS AND METHODS: Cardiac SPECT studies using ^{99m}Tc sestamibi (740-925) MBq were performed on 8 patients. Consequent to acquisition of image data the reconstruction was undertaken on xeleris workstation with ECT toolbox. Various filters as described were used both in FBP and OSEM reconstruction mode by selecting appropriate critical frequencies.

RESULTS: The cut-off frequency of 0.45 Nq and order 11 revealed best image quality and size accuracy with ejection fraction. Whereas the cut-off frequency of 1.14Nq and point spread of 2.5 with order 1.81 gave best result for Hann and Metz filters respectively. The cut-off frequency of Gaussian filter with FWHM (X, Y) 1.13 and FWHM Z 1.55 gave the optimum image quality. The cut-off frequency of Wiener (point spread :2.5-4, Pn/PF: 0.10-0.19) and Hamming (cut-off frequency:0.62-1.09, alpha: 0.44-0.50) gave moderate image quality. The value of Ejection Fraction (EF) was almost similar in case of all types of filters used as well the method of image reconstruction OSEM / FBP. However when ROI was uncharged other parameters like Summed Rest Score (SRS), Summed Stress Score (SSS) and Summed Difference score (SDS= SSS-SRS) gave variable values with reference to various types of filters used.

CONCLUSION: The overall review of results reveals that the Butterworth filter can be used to provide an optimal compromise between signal to noise ratio and clinically acceptable image quality in myocardial perfusion studies. The findings of present study also suggest that Butterworth filter provides adequate qualitative and quantitative assessment in MPI ^{99m}Tc cardiac SPECT/CT studies.

MEASUREMENT OF EXTERNAL RADIATION LEVELS IN PATIENTS UNDERGOING 18FDG-PET CT PROCEDURES

Naincy Golus, Satyawati Deswal, A K Shukla, Devesh Bhatt

Department Of Nuclear Medicine, Dr. Ram Manohar Lohia Institute Of Medical Sciences, Lucknow, Uttar Pradesh, India

Email: satyadeswal@rediffmail.com

INTRODUCTION: The number of PET CT procedures involving use of 18FDG have registered a geometric growth particularly in oncology applications causing concerns in terms of increased occupational exposures to those handling these patients. These procedures are usually performed several times in a patient to enable identification of disease stage and thereafter monitoring of therapy response. It is therefore necessary to measure the radiation levels around the patient and also at the time of release of the patient so as to minimize them to the extent of as low as reasonably achievable.

MATERIALS AND METHODS: In the present study 15 patients with age ranging from 05-75 years and mean weight of 53.8 Kg (range 16-83 Kg) reporting to dept of nuclear medicine of this institute were included. The injected dose of F18-FDG ranged from 148 MBq to 370 MBq with an average injected dose of 263 ± 75 MBq. Radiation levels in terms of micro sievert were measured using calibrated survey meter in patients immediately and 2 hrs after injection and thereafter at release of the patients. Measurement location was the point in front of the patient recording maximum and all measurements were repeated at 0cm, 30cm, 100cm, 150cm and 200 cm distance from the patient to ascertain the effect of time and distance on measured radiation levels.

RESULTS: Measurements indicated that the average radiation levels respectively at 0cm, 30cm, 100cm, 150cm, 200cm and at time of release were observed to be 60.7 μ Sv/hr, 12.5 μ Sv/hr, 3.5 μ Sv/hr, 1.5 μ Sv/hr and 1.1 μ Sv/hr. Average radiation levels at 0 distance from the patient and at 0 min, 2 hrs after injection and at the time of release of the patient were respectively observed to be 268.9 μ Sv/hr, 105.0 μ Sv/hr and 60.7 μ Sv/hr.

CONCLUSIONS: The radiation levels measured at various locations around the patients administered with F18- FDG and undergoing PET CT investigations can be safely released at 2 hrs after injection and completion of the study though phased urination of the injected patients would help in further reducing the radiation levels. It would also be necessary to observe minimal proximity with injected patients so as to ensure minimal radiation exposure to those involved in handling of the patients.

Presentation ID: P-030

Abstract ID: L4769

COMPARISON AND PERIODICAL MONITORING OF QC PARAMETERS IN DUAL HEAD SPECT/CT USING NEMA PROTOCOLS

Maitri Bharadwaj, A K Shukla, Satyawati Deswal, Devesh Bhatt And Anoop Srivastava

Department Of Nuclear Medicine, Dr. Ram Manohar Lohia Institute Of Medical Sciences, Lucknow, Uttar Pradesh, India

Email: deveshbhatt1993@gmail.com

INTRODUCTION: Quality assurance of SPECT/CT is required as per NEMA Standards Publications NUI-2001 and NUI-2007. Consequent to acceptance QC and installation of SPECT/CT, it is essential to have periodical monitoring and comparative assessment of performance status to ensure sustained image quality. The Performance characteristics of GE Discovery 670 NM SPECT/CT system installed in the department of Nuclear Medicine, have been compared with QA results found at various intervals.

MATERIALS AND METHODS: Study periodical monitoring and comparison of QC parameters including intrinsic and extrinsic flood-field uniformity, intrinsic and extrinsic resolution (FWHM and FWTM) at 0,10,20 cm distance from detector surface, system spatial linearity, system planar sensitivity at 10 cm from detector surface, collimator hole angulation, dead time with and without scatter medium (two source/manufacturer's method), multiple window spatial registration, detector head shielding leakage etc. were performed using NEMA protocols.

RESULTS: Intrinsic integral and intrinsic differential uniformity for detector 1 was observed to be 0.7588 (UFOV) and 0.624 (UFOV) in 2016 and changed to 2.0 (UFOV) for intrinsic integral uniformity and 1.6105 for intrinsic differential UFOV. Thereafter in 2023 results were 2.16 for intrinsic integral uniformity and 1.55 for intrinsic UFOV differential uniformity. For detector 2, intrinsic integral and intrinsic differential was observed to be 0.9987 (UFOV) and 0.673 (UFOV) in 2016. The values changed to 1.762 (UFOV) for intrinsic integral uniformity and 1.3155 for intrinsic differential UFOV. Thereafter in 2023, values were 0.7 for intrinsic integral uniformity and 1.12 for intrinsic differential UFOV uniformity. Energy resolution both for detector 1 and 2 was also delineated. Several other parameters related to periodical QC as per NEMA standards were performed and ascertained to give acceptable QC results.

CONCLUSIONS: The periodical monitoring and comparison of QC parameters in any SPECT/CT system is essential to ensure acceptable functioning or identification of any deficiencies to have timely corrective action. QC monitoring has revealed consistent performance of SPECT/CT system over a period of five years indicating the significance of QC in SPECT/CT systems.

Presentation ID: P-031

Abstract ID: X2541

EXPERIENCE WITH VARIAN HALCYON V3 LINEAR ACCELERATOR: DUAL-ISOCENTER VMAT PLANNING AND DELIVERY WITH PORTAL DOSIMETRY FOR DIFFERENT CANCER SITE TREATMENTS

Hanuman Bajirao Doke, Vaibhav Patil, Dinesh Badakh

Department of Radiation Oncology, Prerana Hospital Ltd (Aster Aadhar hospital), Kolhapur, Maharashtra, India

Email: hbdoke321@gmail.com

OBJECTIVE: The aim of this study was to report our experience with Halcyon 3.1 for a dualisocentre Volumetricmodulated ARC therapy (VMAT) planning and delivery for variable site of cancer patients and analyse portal dosimetry.

MATERIAL & METHODS: Variable type of cancer site patients were treated with extendedfield VMAT technique using two isocentres on medical linear accelerator Varian Halcyon 3.1 to treat pelvis and pelvic/or para-aortic nodes region, Breast, palliative spine, Oesophagus, Stomach, Lung bath, CSI etc. The contouring was drawn by clinician according to site and stage. All treatment plans, pre-treatment patientspecific QA and treatment delivery records including daily in vivo portal dosimetry were retrospectively reviewed.

RESULTS: For in vivo daily portal dosimetry analysis, each fraction was compared to the reference baseline (1st fraction) using gamma analysis criteria of 3 %/3 mm. For variable site of cancer patients as Stomach, Prostate, cervix, lung bath, Spine, axillary node, shoulder, breast, CSI, oesophagus, 85%, 99.3% 99.45%,98.85%, 99.94%, 94.5%, 98.26%, 93.5%, 96.15% respectively, of total pixels in the portal image planar dose.All extended-field VMAT plans met the planning criteria and delivered as planned. Treatment delivery time was from 5.0 to 6.5 min.

CONCLUSION: Halcyon 3.1 is effective to create complex extended field VMAT plans using dual isocentres with efficient and fast delivery. Some interfractional changes were detected in random pattern depending upon on internal organ motion and SSD changes. Also, Halcyon in vivo dosimetry is feasible for daily treatment monitoring for organ motion, internal or external anatomy, and body weight which could further lead to adaptive radiation therapy.

KEYWORDS: dual isocenter, extended- field VMAT, Halcyon 3.1, In vivo portal dosimetry

DIAGNOSIS OF PNEUMOTHORAX USING MACHINE LEARNING ALGORITHMS AND RADIOMICS: INVESTIGATING THE POSSIBILITY OF REPLACING SIMPLE CHEST RADIOGRAPHY INSTEAD OF CT SCAN TO REDUCE THE RADIATION DOSE

Hanieh Alimiri Dehbaghi¹, Karim Khoshgard², Hamid Sharini³, Samira Jafari⁴, Farhad Naleini⁵

¹Department of Medical Physics, ²Department of Medical Physics, ³Department of Biomedical Engineering, School of Medicine, ⁴Student Research Committee, School of Health, ⁵Department of Radiology, School of Medicine, University of Medical Science, Kermanshah, Iran

Email: hapnm@yahoo.com

BACKGROUND/OBJECTIVE: The use of artificial intelligence algorithms to help accurate diagnosis in medical images is one of the most important applications of this technology in the field of medical imaging. In this research, the possibility of replacing simple chest radiography instead of CT scan using machine learning models to identify pneumothorax was investigated in cases where CT is usually requested.

MATERIALS AND METHODS: The data used in this research was extracted from the files of 350 patients suspected of pneumothorax. The collected images were pre-processed in MatLab software. Then, three machine learning algorithms, including Logistic Elastic Net Regression (LENR), Logistic Lasso Regression (LLR), and Adaptive Boosting (AdaBoost) were used. To evaluate the performance of these models, the criteria of precision, accuracy, sensitivity, specificity, area under the receiver operating characteristic curve, F1 score, and misclassification were used.

RESULTS: In the AdaBoost model, the accuracy value in radiographic and CT images was calculated as 98.89% and 98.63%, respectively, and the precision value was calculated as 99.17% and 98.27%, respectively. These findings indicate that by implementing machine learning algorithms in radiographic images, diagnostic performance equivalent to CT can be achieved, and in this way, the radiation dose received by the patient can be reduced.

CONCLUSIONS: According to the criteria evaluated in the present study, two LLR and AdaBoost models have similar performance in radiographic and CT images in terms of pneumothorax detecting ability; so this complication can also be diagnosed with high precision level using machine learning techniques on the radiographic images and thus receiving higher levels of radiation doses due to CT scan can be avoided in these patients.

KEYWORDS: pneumothorax, radiomics, artificial intelligence, machine learning, radiation dose reduction

OPTIMIZATION OF IMAGE RECONSTRUCTION FOR 68GA-PSMA ON A DIGITAL PET/CT SCANNER: A COMPARISON OF TOF AND PSF RECONSTRUCTION FOR IMPROVED CONTRAST-TO-NOISE RATIO (CNR)

Subhash Kheruka, Sharjeel Usmani, Naema Al Maymani, NouraMohammed, SanaAl Rashdi, KhuloodAl Riyami, Rashid Alsukaiti

Sultan Qaboos Comprehensive Cancer Care and Research Centre, Muscat, Oman

Email: skheruka@gmail.com

AIM/INTRODUCTION:The advancement of PET/CT technology has significantly improved the detection of lesions with greater precision and efficiency. This study aimed to optimize the reconstruction techniques for 68Ga-PSMA PET/CT in prostate cancer patients using a newly installed PET/CT system. Additionally, the impact of different reconstruction methods on image quality, lesion detection rate, and noise level was evaluated.

MATERIALS AND METHODS:A total of 20 patients were included in the study, with 10 patients having a body mass index (BMI) of less than 30 kg/m² and 10 patients with a BMI greater than 30 kg/m². Images were acquired following the intravenous injection of a 2.2 MBq/kg (0.06 mCi/kg) dose of 68Ga-PSMA. The data were acquired using a Biograph Vision 600 scanner and reconstructed using two different methods: Time-of-Flight (TOF) reconstruction and TOF combined with Point Spread Function (PSF) reconstruction. The scans were visually analyzed by two observers, who ranked the images based on overall image quality (IQ), noise level, background soft tissue, and lesion detectability. Additionally, the contrast-to-noise ratio (CNR) was calculated.

RESULTS:The visual analysis of the individual IQ parameters consistently ranked PSF reconstruction highest for overall image quality, noise level, and background soft tissue. Lesion delineation was excellent and independent of the reconstruction method employed, as all relevant lesions were identified using both techniques. On quantitative analysis, the mean CNR for TOF+PSF was found to be 15% higher compared to TOF alone. Specifically, the CNR SUV_{mean} and CNR SUV_{max} for TOF+PSF were measured at 134.35 and 229.02, respectively, while for TOF alone, they were 116.85 and 199.69, respectively.

CONCLUSION:The utilization of 68Ga-PSMA on a digital PET/CT system enables the acquisition of high contrast-resolution images, facilitating accurate detection and localization of prostate cancer lesions. The implementation of PSF reconstruction further enhances overall image quality, improves image resolution, and reduces partial volume effects.

TOXICITY AND SECOND CANCER ESTIMATE FOR HYPO-AND-CONVENTIONAL FRACTIONATION FOR VMAT RADIOTHERAPY OF PROSTATE CARCINOMA

Assya Boughalia¹, Yasmine. Chaouchi ², Nour El Imane Kebaily²

¹Atomic and Radiologic Physics Department, Physics Division, Nuclear Research Centre of Algiers-Algeria,

²Physics Faculty, University Houari Boumedienne-Algiers Algeria

Email: a.boughalia@crna.dz

BACKGROUND/OBJECTIVE: The Toxicity and the second cancer induction probability following hypofractionated and conventionally fractionated radiotherapy has been estimated for a cohort of prostate cancer patients treated with volumetric arc therapy (VMAT).

MATERIALS AND METHODS: twenty prostate cancer patients, median age 71 years, various stages, were assessed for toxicity and second cancer in the rectum, bladder and small bowel. This was done according to Lyman-Kutcher-Burman model and excess absolute risk based on the Organ Equivalent Dose “OED” model developed by Uwe Schneider.

For each patient three treatment plans were created for conventional (38 fractions of 2 Gy) and hypofractionated (20-28 fractions of 2.5-3 Gy) radiotherapy, toxicity and second cancer risk were computed for each of these three schedules using various models.

RESULTS: In case of rectum, the NTCP (rectal bleeding) = 9.5% for 2Gy fractions, 10.24% and 7.6% in case of hypofractionated total doses of 70Gy and 60Gy respectively. Negligible toxicity for bladder was estimated: 0.05%, 0,07% and 0.01% for 76Gy, 70Gy and 60 Gy respectively.

A linear relationship between 2nd cancer risk and “OED” for the linear exponential model was obtained for the bladder. For small bowel and bladder, the estimated excess risk, EAR, was quantified as 2.10 and 1.96 respectively at 60Gy; 2.04 and 2.73 at 70Gy; 6.30 and 2.18 at 76Gy. For doses greater than 70Gy, our study yields increased values for the linear exponential and mechanistic models but a constant value for the plateau model.

CONCLUSIONS: For prostate carcinoma treated with VMAT, hypofractionated schedules decreases the toxicity of OARs and the corresponding estimated risk of a second cancer compared to conventional fractionation.

KEYWORDS:second cancer, mechanistic model, linear exponential model, plateau model, rectum, prostate cancer, conventional fractionations, hypofractionation.

ASSESSMENT OF HEALTHY TISSUES DOSES AND ASSOCIATED SECOND CANCER RISK AFTER INVOLVED SITE RADIATION THERAPY (ISRT) IN HODGKIN LYMPHOMA: A COMPARISON OF 3D-ISRT AND HELICAL TOMOTHERAPY

Assya Boughalia

Atomic and Radiologic Physics Department, Physics Division, Nuclear Research Centre of Algiers-Algeria

Email: a.boughalia@crna.dz

BACKGROUND/OBJECTIVE: Modern radiation therapy treatment techniques provide accurate dose distribution maps and better gain in tumor control, although in some cases large volume of healthy tissues is irradiated. The aim of this study is to assess and compare doses delivered to healthy tissues using 3D Involved Site Radiation Therapy (3D-ISRT) and helical Tomotherapy (HT) and estimate the associated cancer risk in the case of Hodgkin Lymphoma.

MATERIALS AND METHODS: Ten radiotherapy plans (mean age 29 years within a range of (17-37 years) from patients treated previously with Involved Site Radiation Therapy (ISRT), the prescribed dose was 30 Gy delivered in 15x2 Gy fractions. For each patient two plans were computed (3D-CRT and HT) and compared dosimetrically (Homogeneity index (HI), conformity index (CI) and mean dose) and biologically. Tumor control (TCP) and normal tissue complication probability (NTCP) were computed for 3D-ISRT and HT using Poisson /LKB model respectively. Cancer induction was estimated and compared for 3D-CRT and HT using mechanistic model based on organ equivalent Uwe Schneider dose concept.

RESULTS: HT treatment achieved better CI and HI compared to 3D-CRT: $97.18 \pm 1.8\%$ vs $95.72 \pm 2\%$ and $6.71 \pm 0.5\%$ vs $14.51 \pm 0.9\%$ respectively. Maximum TCP was obtained with HT treatment (96.3% vs 93.44 % for 3D-CRT. The toxicity of the different organs at risk was in favour of HT and was found to be 0.43% vs 0.71% for breast, 0.18% vs 0.25% for lung. These values are similar to those calculated by Vitaliana et Bolzan for these two organs at risk. NTCP calculations for breast, lung (Lt and Rt), and thyroid provided maximum values of complications for 3D-ISRT in comparison with HT. The associated excess absolute risk "EAR/10000 PY" calculated were 16.32 vs 11.89 and 20.21 vs 18.07 for breast and lung, respectively. These results were similar to those obtained by Uwe Schneider (11.7 and 18.4 for breast and lung /10000PY) for HT vs 3D-CRT.

CONCLUSIONS: This study shows the potential impact of 3D-ISRT technique in which achieved better HI, CI, TCP and protection of OARs using HT treatment. The EAR was higher while using HT compared to 3D-ISRT.

KEYWORDS: Hodgkin cancer, Involved Site Radiation Therapy "ISRT", Excess absolute risk, Helical Tomotherapy.

COMMISSIONING GUIDELINES AND VALIDATION OF MRT DOSIMETRY FOR ^{177}Lu -BASED RADIOPHARMACEUTICAL THERAPY

Siju C. George¹, E. James J. Samuel²

¹Department of Radiation Oncology, Miami Cancer Institute Baptist Health, Miami, FL,

²Department of Physics, Vellore Institute of Technology, Vellore, Tamilnadu, India

Email: sijug@baptisthealth.net

BACKGROUND/OBJECTIVE: Radiopharmaceutical therapies take a significant role in cancer treatment. As a result of its convenient half-life of 6.647 days, its +3-oxidation state for easy radiolabeling, and its high energy, ^{177}Lu has become a popular radionuclide in recent years. Numerous studies and investigations are being conducted to identify and deliver ^{177}Lu to various cancer using different tagging mechanisms and physiological processes following the approval of two newly developed radiopharmaceuticals, LUTATHERA® (2018) and PLUVICTO® (2022). To accurately assess radiopharmaceutical doses delivered with radiopharmaceutical therapy based on Lu-177, a practical framework should be developed for evaluating radiopharmaceutical dosimetry protocols. Dosimetry tools should be evaluated and commissioned methodically to avoid errors and generate acceptable results.

MATERIALS AND METHODS: Using MIM sure plan MRT recommendations, image registration was not optimal for dosimetry on our first set of scans. After appropriate intervention on the image registration issues, we re-acquired the Jaszczak Phantom and the NEMA Phantom scans for characterizing the Lutathera. The NEMA Phantom with the background dose and the spheres filled from the previous scan repeated the SPECT protocol, which generated three data sets for our research. These data sets were later evaluated and analyzed to characterize ^{177}Lu RPT agents. They confirmed the MIM sure plans' adequacy to generate valuable dosimetry output.

A rigorous quality assurance system is required to confirm registration accuracy in a hybrid imaging system. Aligning CT and SPECT images on a GE SPECT scanner involves iterative adjustments until a satisfactory match is achieved. In principle, image-based dosimetry based on voxel-based models can provide the foundation for calculating the absorbed dose distribution. It is possible to produce a dose-volume histogram based on this information to show how targets and OARs absorb doses. However, when using 3D SPECT images as input, one has to be aware that many parts of the imaging process and the reconstruction methods significantly impact the distribution of voxel values of the radiation absorbed dose. It is, therefore, possible that the variations in dose amounts within individual voxels can be explained by factors other than the actual variations in the physically absorbed dose. Proper understanding and mitigation of these issues should be addressed before the software is clinically used to generate patient-specific dosimetry reports.

CONCLUSIONS: During the characterization of the ^{177}Lu radiopharmaceutical with the MIM Sureplan MRT (MIM Software Inc. 25800 Science Park Drive - Suite 180 Cleveland, OH 44122), some of the findings we encountered are clinically very significant and will affect the quantitative results if ignored during commissioning. Therefore, they should be considered when the system is configured. Also, these tools and recommendations help medical physics practitioners prepare for the clinical implementation of radiopharmaceutical quantification software like MIM Sureplan MRT.

KEYWORDS: ^{177}Lu , Absorbed Dose, Patient-specific Dosimetry, Dose Calculations, Imaging, characterization, commissioning.

AN AUDIT ON RADIATION DOSES ON PATIENTS UNDERGOING HEAD, CHEST, ABDOMINAL, AND PELVIS CT EXAMINATIONS USING 640 SLICE CT SCANNER AT A PRIVATE HOSPITAL IN KANDY

L. P. De Silva¹, V. Sivakumar¹, and T. Amalaraj²

¹Faculty of Science, University of Peradeniya, Peradeniya, Sri Lanka, ²Faculty of Science, University of Colombo, Colombo, Sri Lanka. Email: limeshad@sci.pdn.ac.lk

Background / Objective: Dose auditing is extremely important in order to optimize the radiation dose imparted on patients, especially in Computed Tomography (CT) as it delivers larger amount of dose compared to normal projection type x-rays. Moreover, the number of patients undergoing CT examinations increased over the past decades around the world. We sought to audit radiation doses on patients undergoing CT examinations at a chosen private hospital in Kandy.

Materials and Methods: This study includes single-phase head, neck, chest and abdominal CT scans of 75 adult patients using the latest generation of 640-slice CT utilizing the hospital's image archiving and communication system. The radiation dose parameters such as dose length product (DLP), volumetric CT dose index (CTDIvol) and Effective Dose (ED) were calculated from the above data.

Results: Median CTDIvol values were calculated to be; 64.40 mGy for the head, 28.30 mGy for the neck, 12.45 mGy for the chest, and 19.00 mGy for the abdomen and pelvis. Median DLP values obtained were 1450.90 mGy.cm for the head, 911.10 mGy.cm for the neck, 537.60 mGy.cm for the chest and 922.60 mGy.cm for the abdomen and pelvis. Median ED values obtained were 3.05 mSv for the head, 5.38 mSv for the neck, 7.53 mSv for the chest, and 13.84 mSv for the abdomen and pelvis. Compared to published dose reference levels, median CTDIvol values of head and neck were low, whereas median DLP and ED values of head, neck, chest, abdominal and pelvis remained within acceptable limits.

Conclusions: The majority of the calculated dose reference levels (DRLs) in this study were found to be well within acceptable ranges and align with international standards. It is advisable to implement strategies aimed at mitigating elevated radiation doses during after-hours examinations.

Keywords: Computed Tomography; Effective dose; Dose length product; Volumetric CT dose index

LESSONS FROM PUTTING UP A CLINICAL PET/CT CENTER IN THE PHILIPPINES DURING THE COVID-19 PANDEMIC

Jae L. Inamarga, Jackson U. Dy, MD

Radiology Department, Makati Medical Center, Makati City, Philippines

Email: jaenamarga@yahoo.com

BACKGROUND/OBJECTIVE: As of 2021, the Philippines is home to more than 100 million Filipinos and is comprised of more than 7,000 islands. PET/CT is an imaging modality that uses short-lived radionuclides to measure metabolic activity of cells for imaging. A PET/CT scan may detect the early onset of a disease before it is evident on other imaging tests due to its ability to observe changes on a cellular level. As of June 2023, the Philippines has four (4) cyclotron centers and less than twenty (20) PET/CT facilities. This abstract presents the learnings and experiences in terms of radiation protection, finances, patient workflow, and administrative tasks when putting up and operating a PET/CT facility during the COVID-19 pandemic.

MATERIALS AND METHODS: The PET/CT facility was established by a core team composed of nuclear medicine physicians, radiologists, medical physicist, radiologic technologists, nurses, and administrative staff. For the shielding requirements, the AAPM Task Group 108 formalism was used to assess the thickness of the walls of the facility. Certain assumptions were made on the number of patients, occupancy factors, maximum activity at any given time, operating days, imaging time and uptake time, and sources of radiation for the computation. Moreover, adjustments in the patient flow, room usage, and scanning protocols were made to minimize the impact and spread of COVID-19.

RESULTS: The results of the shielding verification were found to be acceptable and below the regulatory limits except for the doors of the uptake rooms. Moreover, the summary of annual effective dose reports since the start of the center's operations have not exceeded limits set by the regulatory body.

CONCLUSIONS: A good framework of radiation protection should serve as the foundation of planning a clinical PET/CT center. Moreover, judicious planning of patient flow and clinical protocols can augment the radiation protection practices for all stakeholders. It is imperative that review of clinical protocols and radiation protection guidelines be done regularly to ensure the safety of everyone.

KEYWORDS: PET/CT, shielding, radiation protection, COVID-19

INVESTIGATING THE EFFECT OF DIFFERENT IMAGING PARAMETERS IN THE SEGMENTATION OF BRAIN MRI USING DEEP NEURAL NETWORK

Iman Azinkhah

Department of Medical Physics, School of Medicine, Iran University of Medical Sciences, Iran

Email: imanazinkhah@gmail.com

Background/Objective: Automatic segmentation of brain MR images has always been one of the challenges in the field of neuroimaging. With the entry of machine learning into the field of medical imaging, we are witnessing new segmentation methods. The use of 3D U-Net network is one of these cases. One of the advantages of this method is that there is no need for conventional pre-processing. Also, performing this segmentation in different MRI contrasts is a strength of this method. In this study, the pre-trained 3D U-Net Network method was investigated in different imaging conditions, including different weight contrast and resolution.

Materials and methods: In this study, brain MR images of 20 patients in healthy conditions were selected. In all these patients, three different weighted contrasts T1, T2, and FLAIR with thicknesses of 1, 2, 3, 5, and 7 mm were taken. Pre-processing including resampling, alignment, cropping, and normalization was performed on all data. All processing was done in a MATLAB environment, so a pre-trained TensorFlow-Keras convolutional neural network was used. All the images were segmented using pre-trained 3D U-Net network method in the MATLAB environment. To improve the predicted final segmented images, post-processing steps, smoothing, and morphological filtering were also performed. All the final images were compared using the DICE method.

Results: In all three weighted contrasts T1, T2, and FLAIR, with the increase in image resolution, the decrease in DICE value is quite evident, so that the highest and lowest DICE correspond to resolutions of 1 mm and 7 mm are 0.92 and 0.68, respectively. The highest amount of DICE in all three weighted contrasts in a similar resolution is related to T1, T2, and FLAIR, respectively. The amount of DICE for T1, T2, and FLAIR weighted contrasts at 1 mm resolution was respectively equal to 0.92, 0.81, and 0.73.

Conclusions: The results show that all the segmentations in all three weighted contrasts T1, T2, and FLAIR were done optimally by the Pre-trained 3D U-Net Network method and it seems that this method can be very effective in the field of deep learning in the segmentation of medical images.

Keywords: Segmentation, Brain MRI, Deep Neural Network, Medical Image Processing

APPLICATION OF TG-119 PROTOCOL FOR VMAT TREATMENT PLANS CALCULATED WITH AAA AND ACUROS XB ALGORITHM USING RUBY MODULAR QA PHANTOM UNDER TRUEBEAM LINEAR ACCELERATOR

Srimanta Pramanik¹, Babai Pal¹, Sayan Das¹, Dilip Kumar Ray²

¹Medica Superspecialty Hospital, Mukundapur, Kolkata, India, ²Chattaranjan National Cancer Hospital, Rajarhat, Kolkata, India
Email: skpramanik20@gmail.com

OBJECTIVES: The objective of study was to evaluate the end to end commissioning accuracy of volumetric modulated arc therapy (VMAT) treatment plans calculated with AAA and Acuros XB dose calculation algorithm of TrueBeam linear accelerator using RUBY Modular QA phantom.

MATERIALS AND METHODS: As per the test cases of TG-119 protocol the VMAT plans were created on RUBY modular QA phantom on Eclipse treatment planning systems of TrueBEAM linear accelerator. The plan doses had been calculated with AAA and Acuros XB algorithm. Planning goals and the dose prescription were set as per TG-119 protocol. The point dose measurements at high and low dose gradient regions were carried out with Semiflex 3D (0.07cc) ion chamber with RUBY phantom. The calculated and measured planner dose distribution were compared using gamma index criteria of 3% dose difference (DD) and 3mm distance to agreement (DTA) with Octavius 4D and Portal Dosimetry.

RESULTS: All planning goals had been achieved as per AAPM, TG-119 report. At high dose point measurement mean dose differences averaged over all test cases calculated by AAA and Acuros XB algorithm for 6MV photon beams were 0.010 ± 0.017 and 0.032 ± 0.022 respectively and the corresponding confidence limit were 0.044 and 0.076 respectively. At low dose point measurement mean dose averaged over all test cases calculated by AAA and Acuros XB algorithm for 6MV photon beams were 0.0004 ± 0.014 and 0.027 ± 0.016 respectively and the corresponding confidence limit were 0.014 and 0.058 respectively. The gamma passing rate averaged over all test cases calculated with AAA and Acuros XB algorithm were $99.30\% \pm 0.64$ and $99.62\% \pm 0.53$ respectively for 3mm/3% criteria. The overall confidence limit for composite planar dose measurement for AAA and Acuros algorithm were 1.936 (i.e., 98.064% passing) and 1.412 (i.e., 98.588 % passing) for 3%/3mm criteria.

CONCLUSION: Planning and delivery of VMAT treatment plans had been validated using published TG119 report results. Mean point dose differences for high and low dose region for Acuros XB algorithm showed higher value compared to AAA algorithm due to mass density effect of medium. Whereas the gamma passing rate for both algorithm's plans were indistinguishable.

KEYWORDS: VMAT- Volumetric Modulated Arc Therapy, AAA-Anisotropic Analytical Algorithm, TG-Task Group, AAPM-The American Association of Physicists in Medicine, Acuros XB algorithm

ACCURACY OF RADIATION OUTPUTS OF CALIBRATED AND UN-CALIBRATED ION CHAMBER FOR COMPUTED TOMOGRAPHY AND X-RAY

Joanne Hang, Jessen How, Koon Liang Chia

National University Hospital, Singapore

Email: oanne_ZY_HANG@nuhs.edu.sg

Medical imaging scanners, which are ubiquitous in every tertiary healthcare center, make use of ionising and non-ionising radiation to carry out non-invasive imaging. To ensure the accuracy of the indicated radiation outputs, annual quality control tests should be carried out. The International Atomic Energy Agency (IAEA) recommends that radiation measuring instruments be routinely calibrated to a primary or secondary standards laboratory to ensure the reliability of its measurements. However, such calibrations may on occasion be intentionally skipped for operational or costing reasons.

We investigated the impact of omitting routine calibration by comparing the readings of three separate ion chambers (henceforth referred to as A, B, and C) when measuring the radiation output of a CT, general x-ray, and mammography scanner. Ion chambers A and B were calibrated within one year of the experiment, while ion chamber C was not calibrated for approximately five years. The three different scanners were chosen to reflect the range of tube potentials used in the clinic. The measured dose metrics were $CTDI_{100, \text{air}}$ and incident air kerma.

Results indicate that the deviation between the calibrated and uncalibrated ion chambers was approximately 0.6% when measuring $CTDI_{100, \text{air}}$. For incident air kerma, the deviation was approximately 2.2% for the general x-ray. The results are not expected based on the calibration frequency as recommended by the manufacturer and international publications. The adoption of a modified calibration scheme that takes advantage of the excellent agreement between the calibrated and non-calibrated ion chambers can result in cost savings.

However, the importance of instrument calibration should also not be taken lightly as radiation instruments are important operational tools used to fulfill radiation safety requirement and quality check. Therefore, one of the ion chambers still need to be sent for calibration annually to meet the required accuracy and ensures traceability to the international measurement system.

DOSIMETRIC COMPARISON BETWEEN 6MV FF AND 6MV FFF FOR HEAD AND NECK, PELVIC AND STEREOTACTIC RADIOSURGERY (SRS) PLANS USING VMAT TECHNIQUE

Srinu Aketi¹, Sangeetha K¹, Venkata Krishna Reddy P², Vishwa M³

¹Department of Medical Physics, ²Department of Radiation Oncology, Mahatma Gandhi Cancer Hospital and Research Institute, Visakhapatnam, India, ³Department of Medical Physics, Anna University, Chennai, India

Email: asrinu.srinu@gmail.com

OBJECTIVE: To compare the treatment plan quality between 6MV FF (with flattening filter) and 6MV FFF (free from flattening filter) for SRS, head and neck and pelvic plans using the VMAT technique.

MATERIALS AND METHODS: Ten head and neck and 10 pelvic plans were planned on Ray Station 12A TPS and 10 SRS plans were planned on MONACO 6.01 with 6MV FF and 6MV FFF by keeping the same planning and dose calculation parameters. Target coverage (GTV, CTV, PTV), organs at risk (OAR) doses, conformity and homogeneity indices (CI & HI), monitor units (MUs), different dose volumes (V50%, V40%, V30%, V10% and V5%), integral dose and treatment delivery time were compared using Wilcoxon Signed Rank Test.

RESULTS AND DISCUSSION: Integral Dose by 4%, treatment delivery time by 39% and different dose volumes by 2 to 5% were statistically lower with FFF in all the three sites ($p < 0.05$). Monitor Units were statistically higher by 23% with FFF in head and neck and pelvic plans ($p < 0.05$). SRS plan had no difference in MUs likely due to smaller volumes. Eye and optic nerve doses were statistically lower in FFF plans but might not be clinically significant due very minimal dose variation of less than 1Gy. There was no significant difference observed in PTV coverage, remaining OAR doses, CI, HI, and maximum doses between the FF and FFF plans.

CONCLUSION: FFF plans can significantly reduce integral dose, spillage of dose and treatment delivery time at all sites. Higher MUs in FFF does not translate to higher integral dose or higher treatment time. Target coverage and OAR doses were similar in both FF and FFF plans.

KEYWORDS: Dosimetry, Head and neck, Pelvis, SRS, VMAT, flattening filter

ANGULAR DISTRIBUTION OF X-RAYS AND Γ -RAYS EMANATING FROM A BODY DUE TO ATTENUATION AND SCATTERING IN THE CONTEXT OF CT AND NUCLEAR MEDICINE

Rezvan Ravanfar Haghighi¹, Vyas Akondi², Sabyasachi Chatterjee³, Vani V. C⁴

¹Medical Imaging Research Centre, Shiraz University of Medical Sciences, Shiraz Iran,

²Department of Physical Sciences, Indian Institute of Science Education and Research (IISER) Berhampur, Berhampur, Odisha, India,

³Retired Scientist from Indian Institute of Astrophysics, Present Affiliation: Ongile, 79 D3, Sivaya Nagar, Reddiyur Alagapuram, Salem, India.

⁴Department of Instrumentation and Applied Physics, Indian Institute of Sciences, Bangalore, India

Email: sravanfarr@gmail.com

BACKGROUND/OBJECTIVE: In medical imaging e.g., Computed Tomography (CT) and Nuclear Medicine (NM), x-ray and γ -rays emerging out of the patient's body are the source of radiation for diagnostic imaging and also of hazards for medical staff and the patient's carer. The present study aims to estimate the angular distribution of photons that emanate from a patient's body on propagation and scattering.

MATERIALS AND METHODS: The photon flux from the body results from propagation, attenuation and scattering in the object, by the material inside it. For NM, the γ -ray source is localized in the body e.g. in the heart, and it radiates in all directions. For CT, the source of x-rays is external to the body but is unidirectional. The emergent photon distribution is calculated by numerically solving the corresponding radiative transfer equation, using inputs like, photoelectric absorption coefficient, cross-sections for coherent and incoherent scattering which add together to give the photon attenuation coefficient (μ). Medium of propagation is assumed to be a cylinder of 32 cm diameter and length \gg attenuation length ($1/\mu$) photon in the object. The object is considered to be uniform medium. In addition, the photon source is considered to be monochromatic, which is true for the γ -ray case, while for the x-ray case, we have made the estimates by using an approximation which considers the photon flux to be of single energy, being at the equivalent energy of the source.

RESULTS: For water, the emergent photon flux gets confined to a lateral distance $(2/\sqrt{\pi})(r/\mu)$ from the point of entry, owing to attenuation due to propagation, i.e. lies within a cone of angle $2/\sqrt{\pi\mu r}$. For the case mentioned above, this angle is close to 15° . Beyond this angle, the flux falls off rapidly.

CONCLUSIONS: For CT imaging and for radiation protecting in NM protective shields in an angle of 15° around the initial flux direction has to be provided.

KEYWORDS: radiation protection, attenuation coefficient, Computed Tomography, nuclear medicine

COMPARATIVE ANALYZING OF THE SETUP MARGIN IN CARCINOMA BREAST USING DIFFERENT IMMOBILISATION DEVICES AND IMAGE REGISTRATION METHODS

Sarath S Nair¹, Jyothi Nagesh¹, Shambhavi K², Dr Shirley L Salins¹

¹Department of Radiotherapy and Oncology Kasturba Medical College Manipal Academy of Higher Education Manipal, ²Department of Medical physics program Manipal college of Health Profession Manipal Academy of Higher Education Manipal, India

Email:sarathshyam007@gmail.com

BACKGROUND: To quantify the difference in setup margin in Carcinoma breast using XVI setup imaging for three different breast immobilisation devices and with two different image registration methods.

MATERIAL AND METHODS: 33 breast cancer patients participated in the trial. They were immobilized using three various immobilisation techniques, including breast boards, blue bags, and mould. They then received a Canadian dose fraction of 42.5 Gy over the course of 16 fractions. During patient setup, 198 CBCT images were taken and examined for setup margin. The patient's positional inaccuracy in three translational directions, including the medial lateral, crania-caudal, and anterior-posterior directions, was noted using a clip box region of interest between the reference and CBCT images. This was done using the patient-based coordinate system from the XVI imaging and verification system. The setup margin was determined using the van Herk ptv method, and the shift errors were assessed for both the Boney Landmark and Soft Tissue matching.

RESULT: Regardless of the immobilisation devices and registration techniques employed, it was reported that random mistakes were found to be high. With a value of 6mm in the Y direction for the mould device, the random error of bone registration is discovered to be slightly higher. The systematic errors for vacloc, mould, and wing boards were (2.9,1.8,2.2), (1.8,2.3,3.2), (2.8,3.2,2.5) mm, with random errors for bone registration (3.6,2.9,4.1), (3.0,6.0,3.0), (3.7,2.9,3.4), and soft tissue registration (3.9,2.6,3.6), (2.7,6.0,2.6), (3.7,2.5,4.3) mm following, respectively. Van Herk's PTV margin was found to have a maximum of 10 mm for cranial-caudal orientation and a minimum of 6.0 mm for Medio-lateral orientation for both registration methods.

CONCLUSION: Neither registration method, regardless of the immobilisation devices used, shows any discernible change. Additionally, it was noticed that regardless of the devices utilized, the maximum shift is seen in the Y direction. When compared to other devices used, vacuum immobilisation exhibits marginally improved ptv margins, although this difference is not determined to be particularly significant.

KEYWORDS: Carcinoma, Cone beam CT, X-ray Volumetric Imaging, soft tissue, planning target volume, vac-bag

Presentation ID: P-045

Abstract ID: F1511

A FEASIBLE VMAT BASED PLANNING TECHNIQUE FOR CRANIOSPINAL IRRADIATION & ITS IMPLEMENTATION: OUR EXPERIENCE AT CNCI, KOLKATA

Rajib Das, Bijan Ku. Mohanta, Atanu Kumar, Dillip Ku. Misra, Dilip Ku.Ray, Debarshi Lahiri,
Palas De, Tapas Maji

Chittaranjan National cancer Institute, Kolkata, India

Email: rdas.cnci@gmail.com

PURPOSE: Cranio-spinal irradiation (CSI) involves many technical challenges due to its involvement of large irregular treatment volume, the radio sensitivity of the spinal cord and close proximity of the other critical structures. VMAT can deliver a relatively homogeneous dose distribution to the spinal cord and reduce the high doses outside the target volume. The objective of this study was to develop a practically possible VMAT technique for supine CSI and to discuss its advantage in improving the target volume coverage and the OAR sparing along with reducing the uncertainties of beam setup and intrafraction patient motion.

MATERIALS AND METHODS: 5 male patients were included in our study. For all patients CT datasets were acquired using 16 slice (G.E, Optima CT 580W) CT-simulator in supine position. The head and shoulders of the patients were immobilized with five clamp thermoplastic mask and a full body Vac-Loc bag. Scans were performed with 3mm slice thickness. The CT images were transferred to Monaco treatment planning system (Elekta, version 5.11.03) for contouring and subsequent treatment planning. Planning CT images were fused with Post-op MRI images of brain and spine for accurate target delineation. Contouring was done following SIOPE guideline. The Cranial part of CTV includes the entire brain, cranial nerves and meninges. The spinal part of CTV contained the spinal canal as observed in the fused images including the cerebro spinal fluid extension to the spinal ganglia. The inferior limit of the spinal CTV was at the caudal extension of thecal sac. The PTV was created by giving a uniform 5mm volumetric margin to the CTV. For the pediatric patient PTV spine includes entire vertebral bodies. OARs include B/L lenses, heart, B/L lungs, Liver, small bowel, B/L Kidneys, esophagus, B/L parotids and thyroids. In addition D4, D7, D10 and L2 vertebra were contoured for daily setup verification. All the patients were planned for 6 MV photon beam with VMAT technique. Four high risk Medulloblastoma adult patients received 36Gy in 20 fractions followed by tumor bed boost for 18Gy/10#s whereas Low risk patient was received 23.4Gy in 13 fractions with concurrent chemotherapy (Vincristine) followed by tumor bed boost for 30.6Gy /17#s. All the VMAT plans were created with 3 isocenters, with on an average 22-25 cm of separation from each isocenters. Two co-planner full arcs for the brain and upper spine region and two co-planner partial arcs for the inferiorly two spine isocenters. All the arcs were optimized together at the same time. Daily setup verification was performed using cone beam CT (XVI imaging).

RESULTS: The VMAT plans provided a comparatively homogeneous dose to the entire PTV. V95% for the target volume was increased from 96.7 % to 98.89 %. V107% was significantly reduced for VMAT plans from 7.4% to 0.65%. Mean dose to the heart reduced to 7.95Gy for VMAT compared to 14.5 Gy for 3DCRT, Mean dose to the lungs were increased for VMAT plans as compared to 3DCRT however V20Gy was reduced in VMAT plans.

CONCLUSION: Irradiation of the Cranio-spinal axis of the patients in the supine position is reproducible and can be easily maintained. VMAT for Cranio-spinal irradiation may reduce late toxicities in particular cardiotoxicity. With our experience, we conclude VMAT for CSI with daily imaging is an efficient technique and is feasible in a busy radiotherapy department with a dedicated team.

EVALUATION OF BETWEEN PLANNED AND DELIVERED DOSES DIFFERENCE USING DEFORMABLE IMAGE REGISTRATION AND DOSE ACCUMULATION FOR PROSTATE SBRT PATIENTS WITH DOMINANT INTRA-PROSTATIC NODULE (DIL)

Reena Phurailatpam, Mahima Choudhari, Divya Patil, Maneesh Singh, Vedang Murthy

Department of Radiation Oncology, ACTREC, Tata Memorial Centre, Mumbai, India

Email: reena.ph@gmail.com

BACKGROUND/OBJECTIVE: To quantify the difference between the planned and the delivered dose using deformable image registration (DIR) and deformable dose accumulation (DDA) for patients treated with Stereotactic Body Radiotherapy (SBRT) for prostate cancer with dominant intra-prostatic nodule (DIL).

MATERIAL AND METHOD: Five prostate cancer patients previously treated with SBRT were retrospectively analysed for this study. The prescribed dose for Prostate was 36.25 Gy in 5 fractions, while the prescribed dose for DIL was (40-42.5) Gy in 5 fractions. Patients underwent SBRT according to the institutional protocol, which includes imaging, contouring, treatment planning, dose delivery and IGRT. All patients were treated with Rapid Arc (RA) using 10MV FFF beams (Varian Eclipse TPS 16.1, True Beam v2.1, Varian Medical Systems, Palo Alto). Daily cone beam CT (CBCT) as per the institutional protocol, which includes a strict full bladder (volume range 200-350 cc), empty rectal and a bowel protocol which reproduces the anatomy on the treatment day as compared to the simulation day. Using a novel adaptive dose accumulation workflow, synthetic CTs were created and the daily delivered dose was recalculated. The daily dose distributions were accumulated and target coverage and organ dose were assessed using (Velocity v 4.1). Target coverage was estimated by comparing the differences between the planned and accumulated doses of PTV, CTV and DIL in terms of volumes receiving 98% and 95% of the prescribed dose ($V_{98\%}$ & $V_{95\%}$) and doses D_{mean} (Gy) and D_{max} (Gy). For bladder and rectum, dosimetric parameters viz D_{max} (Gy), D_{mean} (Gy), volumes receiving various doses (14Gy, 17.5Gy, 31.5Gy and 35Gy) were also evaluated. For femoral heads, volume receiving 14 Gy was evaluated. Statistical analysis of the two groups was done using the standard two-tailed paired t-test or Wilcoxon signed rank test, and $p < 0.05$ was considered significant.

RESULT: There is no statistically significant difference between the planned dose and the delivered dose in both target and organs at risk (OARs).

CONCLUSIONS: We have established a dose accumulation workflow using daily CBCT images and found that our clinical treatment margins and strict protocols for OAR fillings resulted in adequate doses for PTV, CTV and DIL while sparing OARs.

KEYWORDS: Adaptive radiotherapy; Deformable image registration; Dominant intraprostatic lesion; Dose accumulation;

COMPREHENSIVE METHOD TO ANALYZE 50% SPILLAGE DOSE IN HEAD AND NECK VMAT TREATMENT PLANS

¹Basil George, ¹Manoj S Kumar, ³Jincy C D, ⁴Aslam Pa, ⁵Vineeth C, ⁶Ratheesh K E, Deepali
⁷Bhaskar Patil, ⁷Mukesh Zope

¹Starlit Cancer Center, Ahmedabad, India; ²Varian Medical System, Chennai; ³GCRI Ahmedabad; ⁴Medanta Hospital, Lucknow; ⁵BMCHRC, Jaipur; ⁶HCG Cancer Center, Borivali, Mumbai; ⁷IGIMS, Patna, India

Email: basilpgeorge92@yahoo.in

OBJECTIVE: The goal of radiotherapy is to deliver the prescribed dose to the target while minimizing dose spillage outside the target volume. While there are indices available to assess conformity to the target, little data is available on how to quantify spillage dose. This abstract present a new method to quantify and evaluate the spillage dose in head and neck VMAT treatment plans.

MATERIALS AND METHODS: Based on the target shape and the geometry of the arcs used VMAT Head and Neck cases which includes SIB cases were divided in to 4 sets. All treatment plans were evaluated and approved by the respective consultant based on RTOG guidelines. The patient body created were restricted to 5cm above and 5cm below the target volume. Spillage Dose (D_{SP}) was calculated using the following formula:

$D_{SP} = ((D_{PTV1} * V_{PTV1} + D_{PTV2} * V_{PTV2} + D_{PTV3} * V_{PTV3} + \dots + D_{PTVn} * V_{PTVn}) / (V_{C.PTV})) / 2$ where D_{PTV} (Dose prescribed to the PTV) and V_{PTV} (Volume of the PTV)

The spillage index is thus calculated using the formula

$SI = (V_{SP} / V_{BODY-PTV}) * (V_{BODY} / (V_{C.PTV} + V_{SP}))$ where

V_{SP} (Volume of Spillage Dose in BODY volume excluding PTV)

$V_{BODY-PTV}$ (Volume of BODY – PTV)

V_{BODY} (volume of total Body contour)

$V_{C.PTV}$ (volume of the Combined PTV's)

The value of SI ranges from 0 to 1.

- When $V_{SP} = 0$, $SI = 0$ ideal scenario without any dose spillage outside the PTV.
- When $V_{SP} = V_{BODY-PTV}$, $SI = 1$ representing the case where there is dose spillage over entire Body volume.

Median values of the spillage indices of these different treatment sites were considered as a representative value for that particular site.

RESULTS: SI values shows a common trend for each set of cases from each institute but considerable difference were found in values among different institutes. Also found considerable difference in SI values for inter institute comparison with Old plans of same institute which were planned without taking the SI value in to consideration..

CONCLUSION: The Results shows that the spillage index is an effective tool for quantifying and evaluating spillage dose outside the PTV volume. By considering the spillage dose, treatment plans can be optimized to minimize dose spillage and enhance treatment quality.

THE IMPACT OF FLATTENING FILTER FREE (FFF) AND FLATTENING FILTER (FF) ON DOSIMETRIC OUTCOMES IN SBRT LUNG TREATMENT PLANS

Md. Jobairul Islam¹, Sadia Afrin Sarah²

¹Department of Radiation Oncology, Labaid Cancer and Super Speciality Centre, Bangladesh, ²Department of Radiation Oncology, Delta Hospital Limited, Bangladesh

Email: jobairul@gmail.com

BACKGROUND/OBJECTIVE: Radiation therapy plays a crucial role in the treatment of tumors by effectively targeting the diseased area while minimizing the impact on surrounding healthy tissues. In this study, we aimed to compare the dosimetry of 6MV FFF (Flattening Filter Free) beams and 6MV FF (Flattening Filter) beams in Volumetric Modulated Arc Therapy (VMAT) for the treatment of medically inoperable primary lung cancer using Stereotactic Body Radiation Therapy (SBRT).

MATERIALS AND METHODS: Treatment plans were prepared for lung SBRT patients using identical fields and physical parameters for both 6FFF and 6FF energies. The prescribed dose ranged from 36-60Gy in 3-5 fractions for lung cases, following the RTOG 0813/0915 protocols. Highly conformal coplanar VMAT plans were utilized, and various parameters, including total lung doses, planning target volume doses, and quality metrics (GI, HIICRU, HI, CI, MU), were compared between the two plans.

RESULT: Both 6FFF and 6FF plans adhered to the RTOG 0915, 0813 protocols for lung cases, respectively. Notably, the comparison of monitor units (MUs) revealed lower values for 6FF energy compared to 6FFF. While several dosimetric parameters such as GI, CI, HIICRU, max dose, min dose, V107, V95, D2%, and D98% were similar between the two energies, a significant difference was observed in the HI value, with the HI value of the 6FF energy being higher than that of the 6FFF energy.

DISCUSSION: It highlights that both 6FFF and 6FF energies are suitable for lung SBRT, with no notable dosimetric differences. The variation in MUs can be attributed to the dose rate of the 6FFF energy. Based on the findings, the 6FFF energy is deemed more suitable for SBRT treatment due to reduced treatment time, decreased intrafraction errors, and enhanced patient comfort facilitated by the use of FFF beams.

CONCLUSION: This study provides valuable insights into the dosimetric comparison between 6MV FF and 6MV FFF beams for lung SBRT treatment. The results indicate that while both energies yield similar dosimetric outcomes, the 6FFF energy offers advantages in terms of treatment efficiency and patient comfort.

KEYWORDS: SBRT, Lung, Dosimetric, VMAT

DOSIMETRIC VERIFICATION BETWEEN 6 MV FF & 6 MV FFF BEAM FOR SBRT SPINE TREATMENT PLAN

Sadia Afrin Sarah¹, Md. Jobairul Islam², Suresh Das³, Hasin Anupama Azhari⁴, Golam A. Zakaria⁵

¹Department of Radiation Oncology, Delta Hospital Limited, Bangladesh, ²Department of Radiation Oncology, Labaid Cancer and Superspeciality Center, Bangladesh, ³Department of Radiotherapy, Narayana Superspeciality Hospital, India, ⁴Centre for Biomedical Science and Engineering, United International University, Bangladesh ⁵Department of Medical Radiation Physics, Gummersbach Hospital, University Cologne, Germany

Email: sadiasarah55@gmail.com

BACKGROUND/OBJECTIVE: When using radiation to treat tumors, it is important not only to cover the target area, but also to minimize the dose to surrounding normal tissues. The aim of the study is the dosimetric comparison of 6MV FFF beams and 6MV FF beams in VMAT for the Spinal Oligometastases in SBRT plan.

MATERIALS AND METHODS: Treatment plans of Spine SBRT patients were prepared using the same fields and physical parameters for 6FFF and 6FF energies. Total prescribed dose was 21-24Gy in 2-3 fractions for Spine cases. Highly conformal coplanar VMAT plans are used. Total spine doses, planning target volume doses, quality of plans GI, HI_{ICRU}, HI, CI, MU values had been compared between the two plans. All parameters were followed to RTOG 0631 protocols.

RESULT: Both plans were agreed to RTOG-0631 protocols compliance respectively for spine cases. Significant changes were shown in the MU comparison, lower MU values were obtained with 6FF energy compared to 6FFF. 6FFF plan was almost similar to 6FF plan in terms of GI, CI, HI_{ICRU} and max dose, min dose, V₁₀₇, V₉₅, D_{2%}, D_{98%} but significant change was found in HI value, the HI value of 6FF energy was higher than the 6FFF energy.

DISCUSSION: The 6FFF and 6FF both are suitable for Spine SBRT. There are no dosimetric differences between the 6FF and 6FFF energy. Only the differences can be found in MU comparison due to the dose rate of 6FFF energy.

CONCLUSIONS: The 6FFF energy is more suitable for SBRT treatment because the treatment time & intrafraction error can be reduced and also patient comfortable treatments by using the FFF beam.

KEYWORDS: SBRT, Spine, Dosimetric, VMAT

DOSIMETRIC COMPARISON OF 6XFFF AND 6XFF PHOTON BEAMS FOR VMAT-BASED STEREOTACTIC BODY RADIOTHERAPY (SBRT) PLAN FOR SPINAL OLIGOMETASTASES: A SINGLE-INSTITUTIONAL STUDY

Sadia Afrin Sarah¹, Md. Jobairul Islam², Suresh Das³, Hasin Anupama Azhari⁴, Golam A. Zakaria⁵

¹Department of Radiation Oncology, Delta Hospital Limited, Bangladesh, ²Department of Radiation Oncology, Labaid Cancer and Superspeciality Center, Bangladesh, ³Department of Radiotherapy, Narayana Superspeciality Hospital, Howrah, India, ⁴Centre for Biomedical Science and Engineering, United International University, Bangladesh, ⁵Department of Clinical Engineering, Anhalt University of Applied Sciences, Germany

Email: sadiasarah55@gmail.com

BACKGROUND/OBJECTIVE: When using radiation to treat tumors, it is important not only to cover the target area, but also to minimize the dose to surrounding normal tissues. The aim of the study is the dosimetric comparison of 6MV FFF beams and 6MV FF beams in VMAT for the Spinal Oligometastases in SBRT plan.

MATERIALS AND METHODS: Treatment plans of Spine SBRT patients were prepared using the same fields and physical parameters for 6XFFF and 6XFF energies. Total prescribed dose was 21-24Gy in 2-3 fractions for Spine cases. Highly conformal coplanar VMAT plans are used. Total spine doses, planning target volume doses, quality of plans GI, HI_{ICRU}, HI, CI, MU values had been compared between the two plans. All parameters were followed to RTOG 0631 protocols.

RESULT: Both plans were agreed to RTOG-0631 protocols compliance respectively for spine cases. Significant changes were shown in the MU comparison, lower MU values were obtained with 6FF energy compared to 6XFFF. 6XFFF plan was almost similar to 6XFF plan in terms of GI, CI, HI_{ICRU} and max dose, min dose, V₁₀₇, V₉₅, D_{2%}, D_{98%} but significant change was found in HI value, the HI value of 6XFF energy was higher than the 6XFFF energy.

DISCUSSION: The 6XFFF and 6XFF both are suitable for Spine SBRT. There are no dosimetric differences between the 6XFF and 6XFFF energy. Only the differences can be found in MU comparison due to the dose rate of 6XFFF energy.

CONCLUSIONS: The 6XFFF energy is more suitable for SBRT treatment because the treatment time & intrafraction error can be reduced and also patient comfortable treatments by using the FFF beam.

KEYWORDS: SBRT, Spine, Dosimetric, VMAT

THE ROLE OF DOSE RATE AND GANTRY SPEED VARIATIONS IN PROGRESSIVE RESOLUTION OPTIMIZER (PRO) AND PHOTON OPTIMIZER (PO) ALGORITHMS FOR RAPIDARC™ VOLUMETRIC MODULATED ARC THERAPY DELIVERY

S. Venugopal^{1,2}, D. Khanna¹, P. Mohandass³, Titiksha vasudeva²

¹Department of Applied Physics, Karunya Institute of Technology and Sciences, Coimbatore, Tamilnadu, India,

²Meherbai Tata Memorial Hospital, Jamshedpur, Jharkhand, India, ³Department of Radiation Oncology, Fortis Hospital, Mohali, Punjab, India

Email: venuonco@gmail.com

INTRODUCTION: The study was performed to assess and compare the performance of two different RapidArc™ optimization algorithms such as PRO and PO by changing the Gantry speed and Dose Rate technical parameters. Additionally, the study aimed to assess the plan quality, agreement between plan delivery and TPS calculation, technical delivery performance using with trajectory log files.

MATERIAL AND METHODS: Total five patients selected for this study from each site: Brain, Head and Neck, Hodgkin's Lymphoma, Advanced Right Lung, Ca cervix. The RapidArc™ plans were generated using Varian Eclipse TPS v15.6 PRO and PO algorithms with maximum range of Dose Rates (DR) from 100 to 600 MU/min, minimum 0.5 and maximum Gantry Speed (GS) fixed at 6.0 deg/sec. The reference plans were created for all patients by PO algorithm with GS 6.0 deg/sec and DR 600 MU/min, other plans were re-optimized using same dose constraints and objectives, for each patient 24 plans were generated and total 120 plans were created.

RESULTS: The result of the study shows: (i) Plan quality values both algorithms achieved similar results and no significant differences were observed; (ii) Closely similar results of dynamic range MU/deg is achieved across all dose rates with both gantry speed modulation and the values range from 2.244 ± 0.38 and 2.027 ± 0.35 (iii) Total mean Monitor Units (MU) for PO maximum is 14 % higher than the PRO; (iv) Reduced total beam on time is a major benefit of high DR and GS compare to constant DR and GS; (v) DR has higher priority over GS modulation and compensation mechanism adjustment between both algorithms are different for higher DRs.

CONCLUSION: These results show that new PO algorithm is either clinically beneficial or neutral in terms of plan quality and efficiency in comparison to PRO. The parameters GS and DR in optimization engine might be undeviating for those variables and capable of generating plans unaided from the limits chosen. The pattern of DR variation between adjacent Control Points in PO was significantly different than PRO.

OPTIMIZING HIGH SPECIFIC ACTIVITY (HSA) COBALT-60 UTILIZATION: EXPLORING MEDICAL APPLICATIONS AND EXPANDING GLOBAL REACH IN RADIOTHERAPY

T. M Ashraf¹, S. A Tariq¹, R. Sahu², P. Mukherjee²

¹Regional Centre (RAPPCOF), Board of Radiation and Isotope Technology, RR Site, India, ²Board of Radiation and Isotope Technology, Navi Mumbai, India

Email: ashraf.t@britatom.gov.in

BACKGROUND/OBJECTIVE: High Specific Activity (HSA) Cobalt-60 has widespread use in Radiotherapy for cancer treatment. Achieving a Specific Activity exceeding 200 Ci/g from Indian Pressurized Heavy Water Reactors (PHWR) proved challenging, leading the Board of Radiation and Isotope Technology (BRIT) to import HSA Co-60 for teletherapy sources to meet the significant demand until 2010. Currently, over 20% of the indigenously produced Co-60 activity comprises HSA Co-60. However, the demand for Cobalt-60 Teletherapy Sources (CTS) has decreased due to the availability of medical linear accelerators (Linacs) and the earlier scarcity of indigenous CTS. This paper explores BRIT's opportunity to effectively utilize HSA Co-60 for cost-effective teletherapy treatment in developing countries and advanced medical gamma machines.

MATERIALS AND METHODS: Cobalt-60 is produced as a byproduct in Indian Nuclear Reactors through the neutron activation of natural Cobalt-59. The specific activity of Cobalt-60 is strongly dependent on the thermal neutron flux inside the reactor core. Until 2010, the specific activity obtained from Indian PHWRs was less than 180Ci/g and it was impossible to fabricate CTS with indigenous activity alone.

RESULTS AND DISCUSSIONS: The Indo-US Civil Nuclear Agreement (123 agreement) ensured the availability of nuclear fuel for power generation in India, leading to an increase in the production of indigenous HSA Co-60. However, only a small portion (>10%) of the produced HSA Co-60 is utilized for teletherapy sources and the majority being used for Multi-Purpose Gamma Irradiator Sources, which do not necessarily require a high specific activity. This underutilization of HSA Co-60 presents an opportunity for India to explore its potential applications for providing cost effective radiotherapy treatment to underdeveloped countries, where still lack of access to radiotherapy. The potential utilisation of HSA Co-60 in advanced gamma therapy applications such as Tele gamma Tomotherapy, Gamma knife, Gamma Pod, HDR Brachytherapy, etc. needs to be explored.

CONCLUSIONS: Utilizing HSA Co-60 in the above applications will be a judicious utilization of the same, a way to grab the domestic and global market, helping the needy country in turn generating foreign exchange revenue to this country.

KEYWORDS: High Specific Activity Cobalt-60, Cobalt Teletherapy Source, Co-60 Production, Radiotherapy access.

IRON OVERLOAD EVALUATION IN BETA-THALASSEMIA MAJOR: HEPATIC AND CARDIAC ASSESSMENT USING MRI T2* AND SERUM FERRITIN LEVELS IN SISTAN AND BALUCHISTAN PROVINCE

Zeynab Yazdi Sotoodeh¹, Amir Hossein Heydari², Aghile Hosseini³

¹M SC of Medical Imaging, Department of Radiology, faculty member of paramedicine, Zahedan University of Medical Science, Zahedan, Iran, ²Students Research Committee, Zahedan University of Medical Sciences, Zahedan, Iran ³Students Research Committee, Zahedan University of Medical Sciences, Zahedan, Iran

Email: AmirHHeydari.Academic@gmail.com

BACKGROUND AND PURPOSE: Thalassemia major, a genetic blood disorder causing chronic anemia, often requires blood transfusions that lead to iron overload and organ damage. To assess iron overload levels, doctors typically rely on serum ferritin levels and MRI T2* measurements. This study aimed to investigate the correlation between iron overload in the liver and heart among patients with the beta-thalassemia major from Sistan and Baluchistan province, Iran.

MATERIALS AND METHODS: This retrospective cohort study involves 115 beta-thalassemia patients. Using specialized software called "CMR Tools," we analyzed the data extracted from serum ferritin and MRI T2* measurements. Our statistical analysis helped determine the extent of iron overload in these patients. All statistical analyses were conducted in SPSS V27.0.

RESULTS: Our findings revealed that 92.1% of our patients exhibited liver iron overload, with the average liver iron content measuring 15.91 ± 7.94 mg/g. Meanwhile, the cardiac T2* measurements indicated varying degrees of iron overload in the heart. We observed a strong correlation between liver iron overload and serum ferritin levels ($r=0.275$, $P<0.003$). On the other hand, the correlation between cardiac T2* and serum ferritin was weak and inverse ($r=-0.385$, $P<0.001$). We did not find a significant correlation between cardiac T2* and liver iron overload ($r=-0.150$, $P<0.001$).

CONCLUSION: Our study highlights the valuable role of MRI T2* in assessing iron overload in the heart and liver of beta-thalassemia major patients. We confirmed a strong association between liver iron overload and serum ferritin levels. To obtain a comprehensive evaluation of iron status, we recommend including both cardiac and hepatic T2* MRI in conjunction with serum ferritin measurements. The use of MRI T2* provides a rapid and reliable assessment, enabling long-term monitoring of iron levels. Ultimately, it stands as the current gold standard for evaluating hemosiderosis in thalassemia patients.

KEYWORDS: MRI, Thalassemia major, Hemosiderosis

INVESTIGATION OF EPID UNIFORMITY AS A PREDICTIVE FACTOR OF γ -PASS RATE IN O-RING LINIAC

Masakazu Otsuka¹, Kenji Matsumoto¹, Kazuki Kubo², Takahiro Sakamoto¹, Naohiro Nishigaito¹, Takahiro Saika¹, Hiroyuki Kosaka¹, Miyuki Araki¹, Hidekazu Nambu¹, Hajime Monzen², Yukinori Matsuo²

¹ Radiology Center, Kindai University Hospital, ²Department of Radiation Oncology, Kindai University Faculty of Medicine, Bangaluru, India

Email:m-otsuka@med.kindai.ac.jp

BACKGROUND/OBJECTIVE: Halcyon (Varian Medical Systems Inc, CA, USA), an O-ring linear accelerator, performs machine performance check (MPC) as a part of its daily quality assurance (QA). The uniformity of the electronic portal imaging device (EPID) is measured as one of the QA items. We hypothesize that γ -pass rate degradation on portal dosimetry (PD), which is induced by irradiation damage to the semiconductor, can be detected by checking the EPID uniformity. The aim of this study was to evaluate the predictive value of the EPID uniformity for γ -pass rate degradation.

MATERIALS AND METHODS: The EPID uniformity, γ -pass rates for the two benchmark VMAT plans, and cumulative monitoring units (MU) were obtained daily by Halcyon from January 4 to April 1, 2023. To evaluate the EPID degradation due to irradiation, the cumulative MU and EPID uniformity were compared. The daily measurement of γ -pass rate (criteria 1%/1mm) was conducted using two benchmark VMAT plans with different field sizes (long: X=16.0 cm, Y=25.4 cm, and short: X=6.4 cm, Y=5.8 cm). The changes in the EPID uniformity and the γ -pass rate due to the calibration of the EPID were evaluated, and the EPID uniformity and the γ -pass rate of two benchmark VMAT plans were also compared.

RESULTS: The EPID uniformity decreased linearly with the cumulative MU (linear regression, $r^2 = 0.82$). Before the calibration, the EPID uniformity and the γ -pass rates of two benchmark VMAT plans (long and short irradiation ranges) were 1.39%, 88.0%, and 87.1%, respectively. After calibration, these values improved to 0.59%, 95.3%, and 96.3%, respectively. The γ -pass rate tended to decrease as EPID uniformity decreased. Furthermore, there were the correlation between EPID uniformity and the γ -pass rate of two benchmark VMAT plans with different field sizes (linear regression, $r^2 = 0.571$ and $r^2 = 0.725$).

CONCLUSION: EPID uniformity is useful for predicting γ -pass rate degradation. Periodic calibration of the EPID is necessary for accurate PD implementation.

KEYWORDS: EPID, quality assurance, dosimetry, MPC

GREEN SYNTHESIS OF CDS AND CDS/RGO NANOCOMPOSITE: EVALUATION OF ELECTROCHEMICAL ANTI-MICROBIAL AND PHOTOCATALYTIC PROPERTIES

Arpana Parihar^{1*}, Palak Sharma², Nishant Kumar Choudhary², Raju Khan^{1,3}

¹CSIR-Advanced Materials and Processes Research Institute (AMPRI), Hoshangabad Road, Bhopal, MP, India,

²NIMS Institute of Allied Medical Sciences and Technology, NIMS University, Jaipur, Rajasthan, India,

³Academy of Scientific and Innovative Research (AcSIR), Ghaziabad, India

Email: arpana_parihar@yahoo.com

BACKGROUND/OBJECTIVE: The green approach has been employed for the synthesis of various types of nanomaterials, including metal nanoparticles, metal oxides, and carbon-based nanomaterials. These processes involve natural sources that contain bioactive compounds that can act as reducing agents, stabilizing agents, and capping agents for the formation and stabilization of nanomaterials. This study reports the green synthesis of CdS and CdS/rGO nanocomposites, their characterization, and evaluation of antimicrobial, electrochemical, and photocatalytic properties.

MATERIALS AND METHODS: The CdS and CdS/rGO nanocomposites were synthesized via green synthesis approach using *Lactobacillus* bacteria. The UV-visible spectrophotometer, FESEM, TEM, EDX, Raman spectroscopy, and FTIR were used for the characterization of the nanocomposite. The electrochemical characterization was done via CV, DPV, and EIS using the electrochemical analyzer. The photocatalytic activity of the nanocomposite was assessed using a methylene blue degradation assay. The antimicrobial activity of synthesized nanocomposite was determined by disc diffusion assay in gram-positive and gram-negative bacteria.

RESULTS: The UV-visible spectrophotometer, FESEM, TEM, EDX, Raman spectroscopy, and FTIR confirms the synthesis of the nanocomposite. The electrochemical characterization using CV, DPV, and EIS revealed that the CdS/rGO nanocomposites showed a higher electron transfer rate compared to CdS nanoparticles, indicating the potential of the nanocomposites for biosensing applications. The zone of inhibition revealed significant antimicrobial activity against *E. coli* and *S. aureus* for both CdS nanoparticles and CdS/rGO nanocomposites. Moreover, CdS-rGO nanoparticles exhibited high photocatalytic activity for the degradation of methylene blue Dye when compared to CdS.

CONCLUSIONS: Overall, this study demonstrates that the synthesized CdS and CdS/rGO nanocomposites have good photocatalytic, and electrochemical, and antimicrobial properties, therefore can be employed for various applications such as biosensing, photocatalysis, and antimicrobial activity.

KEYWORDS: Cadmium sulfide (CdS) nanoparticles, CdS/rGO nanocomposites, *Lactobacillus*, antimicrobial activity, Electrochemical properties, and photocatalysis.

EVALUATION OF DOSE METRICES FOR STEREOTACTIC RADIOTHERAPY PLANS (SRT) FOR BRAINS METS PATIENTS USING VOLUMATIC ARC THERAPY TECHNIQUE

Rahul Phansekar, Divya S, Hemendra Mod

Aaruni Hospital Pvt.Ltd , Jaimal Parnar Mag Rajkot, Gujarat, India

Email : rahulphansekar21@gmail.com

BACKGROUND/OBJECTIVE: Aim of this study is evaluation of dose metrics for the assessment of Plan quality of SRT treatment for patients with brain metastasis.

MATERIALS AND METHODS: Seven cases of patients with brain metastasis treated with SRT are selected for this study. The target volume ranges from 12.8cc to 51.42cc. All the patients are planned on Elekta Monaco 5.11 treatment planning systems and treated on Elekta Synergy Linear Accelerator with Agility Head. Plan dose calculation was done using Monte Carlo algorithm with grid size of 2 mm. The parameters used for dose metrics evaluation are Total Volume of PTV (TV), TV(100) volume of the PTV covered by 100% of prescribed dose, Volume of the PTV covered by 95% isodose line (TVRI (95%)) which is our reference isodose line, Volume of Reference Isodose line (VRI), D2, D5, D50 (median dose), D95 and D98. For all the cases; plans were evaluated using following indices: Conformity Index (CI100) = $TV(100)/TV$ and $CI95 = TVRI(95)/TV$, Uniformity Index (UI) = $D5(Gy)/D95(Gy)$, Homogeneity Index (HI) = $(D2(Gy) - D98(Gy))/D50(Gy)$, Conformity Number = $(TVRI)^2/(TV \times VRI)$ and Gradient Index = $V50\%RI/VRI$ where VRI is volume of reference isodose line and VRI(50%) is volume of 50% of reference isodose line.

RESULTS: The maximum dose to the brain stem ranges from 1.459 Gy to 14.83 Gy depending on location of PTV with respect to brain stem. The Uniformity Index (UI) varies from 1.048 to 1.1023 and average is 1.0657. The Homogeneity Index (HI) varies from 0.1601 to 0.0605 and average is 0.0900. The Conformity Index (CI) varies from 0.9765 to 0.9988 and average is 0.9856 whereas Conformity Number varies from 0.5879 to 0.8616 and average value for both indices are 0.9856 and 0.7496 respectively. Conformity index of the PTV for 100% isodose line varies from 0.9499 to 0.9704 and average value is 0.9539. Gradient Index which is a measure of dose fall off outside the PTV varies from 2.4187 to 3.1048 and mean value is 2.7297.

CONCLUSIONS: The evaluation of dose metrics provides good tool and insight for the assessment of Stereotactic radiotherapy plan quality and encourages planner for improvements in future.

KEYWORDS: SRT, Conformity, Homogeneity, Gradient Index.

DOSIMETRIC EVALUATION OF VOLUMETRIC ARC THERAPY (VMAT) PLANS FOR HEAD AND NECK PATIENTS

Rahul Phansekar, Surya J, Hemendra Mod

Aaruni Hospital Pvt.Ltd , Jaimal Parnar Mag Rajkot, Gujarat, India

Email : rahulphansekar21@gmail.com

BACKGROUND/OBJECTIVE: Aim of this study is dosimetric evaluation of Volumetric Arc therapy (VMAT) plans for head and neck patients with bilateral target volume.

MATERIALS AND METHODS: Eleven head and neck cases of with bilateral target volume are selected for this study. All the patients are planned with 2 full VMAT arcs on Elekta Monaco 5.11 treatment planning systems and treated on Elekta Synergy Linear Accelerator with Agility MLC with 160 leaves. For all plans dose calculation was done using Montecarlo algorithm with grid size of 3 mm. Multicriterial optimization is used for OARs.

For all cases doses for spinal cord, left and right parotids, thyroid and DARS were evaluated. The parameters used for dose matrices evaluation are Total Volume of PTV (TV), Volume of the PTV covered by 95% isodose line (TVRI (95%)) which is our reference isodose line, Volume of Reference Isodose line (VRI), D2, D5, D50 (median dose), D95 and D98. For all the cases, plans were evaluated using following indices: Conformity Index $CI_{95} = TVRI(95)/TV$, Uniformity Index $(UI) = D5(Gy)/D95(Gy)$, Homogeneity Index $(HI) = (D2(Gy) - D98(Gy))/D50(Gy)$, Conformity Number = $(TVRI)^2/(TV \times VRI)$ and Quality of coverage QRTOG = (I_{min}/RI) .

RESULTS: The maximum dose to the spinal cord varies from 30.71 Gy to 37.45Gy. Mean dose to the left parotoid varies from 18.54Gy to 25.52 Gy, and the average mean dose is 22.29 Gy. Mean dose to the right parotoid varies from 14.75Gy to 24.75 Gy, and the average mean dose is 21.99 Gy. Mean dose to the thyroid varies from 21.52Gy to 37.06 Gy and average is 27.02 Gy and the mean DARS dose varies form 15.27Gy to 34.89Gy. we archived Uniformity Index (UI) for all patients from 1.0408 to 1.0686. The Homogeneity Index (HI) varies from 0.0584 to 0.09359. The Conformity Index (CI) ranges from 0.9831 to 0.9985; whereas the Conformity Number varies from 0.6252 to 0.8482. Quality of coverage (QRTOG) achieved was from 0.9384 to 0.9684.

CONCLUSIONS: VMAT technique can produce quality plans with good PTV coverage and better OAR sparing with multicriterial optimization for head and neck cases.

KEYWORDS: VMAT, Head and Neck, Spine, Conformity, Homogeneity Uniformity Index.

ASSESSMENT OF RADIOTHERAPY TREATMENT ACCURACY AND THE EFFECTIVE IMPACT OF CARBON BASE PLATE ATTENUATION IN MEGAVOLTAGE HIGH ENERGY X-RAYS

¹R. Narayanan, ²Amy Sharon Janet V, ³B. Preethi

¹Radiotherapy and Radiography RST cancer hospital regional cancer centre & research institute, Department of radiation oncology Nagpur, Maharashtra

²Medical Imaging Technology Jain deemed to be university Bangalore, Bangluru

³SRM Medical College Hospital & Research centre, SRMIST Kanchipuram, Tamilnadu, India

Email: narayananmedphy@gmail.com

BACKGROUND/OBJECTIVE: The aim of radiotherapy is to deliver the maximum radiation dose to the target and the minimum dose to the critical normal tissues. Entire radiotherapy treatment, the carbon couch and base plate attenuate the X-ray beam. In this study is to focus on assessing the treatment accuracy of radiotherapy and the impact level of carbon base plate attenuation in radiotherapy treatment.

MATERIALS AND METHODS: The materials are a Linac (Elekta Versa HD), base plates, electrometer, PTW farmer ion chamber of 0.6 cm³. The method is couch and gantry angles set at 90⁰ and 270⁰, for an in-air setup with an independent SSD. Other measurements carried in a medium, such as couch and gantry angle, both set at 0⁰, SSD-100 cm, and different thicknesses base plate metre reading obtained in nC for in air, Dmax & 10cm depths. Constant field size (10X10cm) and 200 MU for all measurements.

RESULTS: Without the base plate, the average metre reading was 3.378 nC for independent distance; for various thicknesses, the attenuation factor gradually drops to 0.999, 0.971, and 0.954. The average metre reading without the base plate for the Depth of Dmax in Solid Phantom was 35.66 nC, and the attenuation factor for different thicknesses, gradually declined to 0.991, 0.979, and 0.966. Average metre readings for depths of 10 cm in solid phantom were 24.73 nC and the attenuation factor rapidly decreased to 0.983, 0.969 and 0.954 for various thicknesses. Differences in attenuation factor noted and the % deviation for in-air setup are 1.62%, 0.2%, 0% for Dmax, 0.8%, 1.03%, and 1.25% respectively.

CONCLUSIONS: My conclusion is both the treatment couch and the base plate are made of carbon. In the future, the couch itself can be created as a patient fixation device in place of adding a base plate. We can simply prevent the attenuations caused by the over-thickness of carbon materials underneath the patients (or) for improved radiation treatment accuracy, I strongly advise that the attenuation factors (treatment couch and baseplate) be taken into account.

KEYWORDS: carbon base plate, treatment table, Megavoltage X-rays, Immobilizing device, ion chamber, PTV.

QUALITY ASSURANCE OF PET/CT AND SPECT/CT IN THE PHILIPPINES: FROM ACCEPTANCE TESTING TO CLINICAL OPERATIONS

Jae L. Inamarga

Radiology Department, Makati Medical Center, Makati City, Philippines

Email: jaeinamarga@yahoo.com

BACKGROUND/OBJECTIVE: The Philippines has more than 70 nuclear medicine facilities. These facilities generally offer diagnostic and therapeutic services such as imaging, radioimmunoassay, and I-131 therapy, among others. Most of these facilities have SPECT, SPECT/CT and/or PET/CT imaging equipment. As far as installation is concerned, these imaging equipment need to undergo proper tests in order to establish good performance. The aim of this paper is to present the findings and experience in conducting the acceptance/performance testing and establishing a quality control and quality assurance program for SPECT/CT and PET/CT in the Philippines. Moreover, the prevailing local regulations will be briefly discussed as well.

MATERIALS AND METHODS: The PET/CT and SPECT/CT were both installed in 2020. The PET and SPECT component were tested following the manufacturer's recommendations and the NEMA NU 2 standards. On the other hand, the CT component of both imaging modalities was tested following ACR guidelines. Appropriate phantoms such as ACR phantom, Jaszczak phantom, NEMA IEC PET Body phantom, NEMA PET Scatter phantom, and NEMA PET Sensitivity phantom were used in the performance tests of the said equipment.

RESULTS: For the PET/CT, six tests were performed for the PET component. For the SPECT/CT, a total of 13 tests were done for the SPECT component. However, intrinsic spatial resolution and intrinsic spatial linearity were not tested due to system limitations of the SPECT/CT equipment. For the CT component in both equipment, a total of seven tests were performed to evaluate the image quality test.

CONCLUSIONS: The performance tests of both equipment were found to be satisfactory. The test tools, essential in the conduct of acceptance test, can be packaged in the purchase of the new imaging equipment. Routine conduct of these tests should form part of the quality assurance and quality control of the equipment to ensure proper performance. Moreover, thorough planning during acquisition must be done to maximize the resources that come with a new equipment.

KEYWORDS: NEMA test, acceptance testing, PET/CT, SPECT/CT

ACCEPTANCE TESTING, COMMISSIONING AND QUALITY ASSURANCE FOR A FLEXITRON ^{192}Ir HDR BRACHYTHERAPY AFTERLOADER AT AIMS, KOCHI

Doddi Divakar Babu, Soumya N M, Dr. Annex E.H, Debnarayan Dutta

Department of Radiation Oncology, Amrita institute of Medical Sciences, Ponekkara P. O Kochi, Kerala

Email: d.divakarbabu@gmail.com

BACKGROUND/OBJECTIVE: In High Dose Rate (HDR) Brachytherapy facility, a sealed radioactive source (^{192}Ir) is placed in and around the tumor volume to treat variety of cancer cases. It has application in Intracavitary, Interstitial, Surface mould, Intraluminal, Intraoperative, and Intravascular techniques. Structural design is necessary for brachytherapy treatment room for protecting the staff and public from radiation exposure. Initial source installation tests, acceptance test and quality assurance prescribed by Atomic Energy Regulatory Board (AERB) were performed for the acceptance and commissioning of HDR brachytherapy unit for clinical use.

MATERIALS AND METHODS: In this study, we evaluated the shielding design by manual calculation. At a predefined position of the source, the shielding thickness of wall is calculated in all directions as mentioned in the layout design, taking the maximum workload at different occupancy factor of the facility. A Calibrated Radiation survey meter RAYSAFE 452 is used to assess radiation levels at different locations as per the layout and to measure HDR unit leakage at 5cm and 1m positions. Source position check is performed by using the transfer tube and fixed source position indicator with the help of source monitoring camera. The sweet spot measurement is carried out by using calibrated well type ionization chamber and electrometer, from that air-kerma strength of the ^{192}Ir source is determined. In addition, Timer Linearity, End Error and Timer Error are also determined. Various QC and QA measurement required for the commissioning of HDR machine has been performed i.e., contamination check, safety and Treatment planning system checks (TPS) etc.

RESULTS: The constructed wall thickness is more than the required (calculated) thickness. Radiation survey around the layout is within tolerance, the maximum reading found at the door interlock, which is less than 1mR/hr. Maximum leakage at the unit surface is within the tolerance limit. Source position accuracy and reproducibility is less than 1mm. Source strength verification deviation observed is 0.628%. Timer linearity, timer accuracy and Timer Error are within the tolerance limit.

CONCLUSIONS: The test results for the Treatment unit, TPS and safety aspects and Acceptance tests are satisfactory. The flexitron machine is successfully installed and commissioned.

KEYWORDS: brachytherapy, quality assurance, quality control, radiation protection, radiation safety, commissioning, flexitron

EVALUATING THE IMPACT OF PLASTIC DETECTOR MATERIALS ON THE OUTPUT MEASUREMENTS FOR VERY SMALL PHOTON FIELDS

Eyad Alhakeem¹ and Sergei Zavgorodni²

¹Medical Physics Department, Taif Military Hospitals-Alhada, ²Department of Medical Physics, British Columbia Cancer Agency–Vancouver Island

Email: eyadali404@gmail.com

OBJECTIVE: The purpose of this work was to investigate the impact of possible variations in a plastic scintillator detector (PSD) material on the output factors (OFs) of 6 MV photon beam collimated by small and very small circular cones.

MATERIALS AND METHODS: EGSnrc/egs_chamber Monte Carlo (MC) code was used to model a 1mm diameter, 1mm length PSD. Previously generated and verified TrueBeam Phase-space files (PSFs) of 6 MV photon beam collimated by circular fields of 1.41, 2.41, 3.59, 10, 12.5, 15 and 40mm diameter were used. OFs were calculated using a PSD model with polystyrene and polyvinyltoluene sensitive volume and different housing materials: resin, RW3, and PMMA. OFs were calculated from the dose scored in the detector's sensitive volume for the aforementioned fields relative to the 40 mm cone. OFs were calculated with detectors placed isocentrically in a 20x20x40 cm³ water phantom at 1.5 cm depth. The output correction factors ($k_{Q_{clin}, Q_{msr}}^{f_{clin}, f_{msr}}$) were derived from MC calculations in a water volume of 0.008 mm³ using formalism by Alfonso *et al.* Additionally, contributions due to other perturbation factors were calculated separately to quantify the impact of investigated materials.

RESULTS: Contribution to $k_{Q_{clin}, Q_{msr}}^{f_{clin}, f_{msr}}$ due to housing materials was 1.7%-3.9% and <0.6% for 1.41-3.59 mm and 10-40 mm cones, respectively. However, the total correction factors (including the effect of volume averaging) for all the investigated materials were -8.9%–2.4% for 1.41-10 mm cones and 0.7–1.7% for 12.5-40 mm cones. The OFs calculated for polystyrene and polyvinyltoluene scintillator volume materials were within 0.5%.

CONCLUSIONS: The findings of this work show that the investigated materials have up to 3.9% impact on the calculated OFs of PSDs for very small fields. The volume averaging effect is the dominant factor in $k_{Q_{clin}, Q_{msr}}^{f_{clin}, f_{msr}}$ calculation, reaching up to 8.8% for the smallest field. There was no significant difference between polyvinyltoluene and polystyrene when used as scintillating materials.

KEYWORDS: MC calculations, small field, dosimetry, Output factors, correction factor, plastic detectors.

PREOPERATIVE PREDICTION OF CLINICAL AND PATHOLOGICAL STAGES FOR PATIENTS WITH ESOPHAGEAL CANCER USING PET/CT RADIOMICS

¹Xiyao Lei, ²Yao Ai, ²Xiance Jin

¹Department of Radiation Oncology, Lishui Centre Hospital, Lishui, China, ²Department of Radiotherapy Center, 1st Affiliated Hospital of Wenzhou Medical University, Wenzhou 325000, China

Email:1246864634@qq.com

PURPOSE: To investigate the feasibility and accuracy of PET/CT based radiomics in preoperative prediction of clinical and pathological stages for patients with Esophageal cancer (EC).

METHODS: Histologically confirmed 100 EC patients with preoperative PET/CT images were enrolled retrospective and randomly divided into training and validation cohorts at a ratio of 7:3. The Maximum Relevance Minimum Redundancy (mRMR) was applied to select optimal radiomics features from PET, CT, and fused PET/CT images, respectively. Logistic regression (LR) was applied to classify the T stage (T_{1,2} vs. T_{3,4}), lymph node metastasis (LNM) (LNM₍₋₎ vs. LNM₍₊₎), and pathological state (pstage) (I-II vs. III-IV) with features from CT (CT_LR_Score), PET (PET_LR_Score), fused PET/CT (Fused_LR_Score), combined CT and PET features (CT+PET_LR_Score), respectively.

RESULTS: 7, 10 and 7 CT features, 7, 8 and 7 PET features, and 3, 6 and 3 fused PET/CT features were selected using mRMR for the prediction of T stage, LNM and pstage, respectively. The area under curves (AUCs) for T stage, LNM, and pstage prediction in the validation cohorts were 0.846, 0.756, 0.665, 0.815; 0.769, 0.760, 0.665, 0.824; and 0.727, 0.785, 0.689, 0.837 for models of CT_LR_Score, PET_LR_Score, Fused_LR_Score, and CT+PET_LR_Score, respectively.

CONCLUSION: Accurate prediction ability was observed with combined PET and CT radiomics in the prediction of T stage, LNM, and pstage for EC patients.

KEY WORDS: Esophageal Neoplasms; PET/CT; Lymphatic Metastasis; Neoplasm Staging

ESTABLISHMENT OF NATIONAL DIAGNOSTIC REFERENCE LEVELS FOR DIGITAL MAMMOGRAPHY IN NEPAL

RN Yadav^{1,3}, BR Shah², N. Sharma³, K. Devkota⁴, NJ. Ansari⁵, HA Azhari⁶, J. Jeyasugithan¹

¹Department of Nuclear Science, University of Colombo, Sri Lanka,

²Nepal academy of science and technology, Lalitpur, Nepal

³BP Koirala memorial cancer hospital, Bharatpur, Chitwan, Nepal,

⁴Department of radiology, BP Koirala institute of health sciences, Dharan, Nepal,

⁵Department of radiology, National Medical College, Birganj, Nepal,

⁶Centre of Biomedical Science and Engineering, United International University, Bangladesh

Email: rnyadav99@yahoo.com

BACKGROUND/OBJECTIVE: Mammography is widely used for detecting breast pathology and cancer. Due to the high sensitivity of breast to radiation, repeated mammography scans for screening purpose can potentially increase the risk of radiation-induced cancer. Therefore, it is imperative to minimize the radiation dose to the breast. Dose optimization strategies are implemented to adhere to the ALARA principle, which aims to minimize radiation exposure. This study aims to establish National Diagnostic Reference Levels (NDRLs) specifically for digital mammography to enhance dose optimization efforts. Setting these reference levels can ensure that radiation doses during digital mammography procedures remain within safe limits while maintaining the image quality.

MATERIALS AND METHODS: In this retrospective study, mean glandular dose (MGD) and entrance skin dose (ESD) were extracted from DICOM files of mammograms in cranial-caudal (CC) and mediolateral oblique (MLO) views of both breasts. The study included 786 patients from six out of seven which have digital mammography. A minimum of 50 patients was included in the analysis for each mammogram. Additionally, technical parameters such as tube voltage (kVp), tube current (mAs), compressed force (CF), and compressed breast thickness (BCT) were also documented for further analysis.

RESULTS: The established NDRLs for digital mammography are 1.03 mGy, 1.02 mGy, 1.18 mGy and 1.15 mGy for RCC, LCC, RMLO and LMLO views respectively. The mean compression breast thickness (CBT) and compression force (CF) are 56 ± 13 mm and 122 ± 29 N, respectively. The established NDRL values CC: 1.03 mGy and MLO: 1.17 mGy were higher than those reported in a Nigerian study (CC: 0.63 mGy and MLO: 1.04 mGy) but lower than those found in a UK study (CC: 2 mGy and MLO: 2.1 mGy), Ireland (CC: 1.28 mGy and MLO: 1.37 mGy), Malaysia (CC: 1.54 mGy and MLO: 1.82 mGy), Norway (CC: 1.18 mGy and MLO: 1.32 mGy), Spain (CC: 1.80 mGy and MLO: 1.95 mGy), and Sri Lanka (CC: 1.47 mGy and MLO: 1.95 mGy).

CONCLUSIONS: The comparisons with other countries emphasize the potential for dose optimization to achieve lower yet diagnostically adequate levels. By implementing dose optimization strategies, it is possible to further reduce patient radiation exposure during digital mammography without compromising diagnostic capabilities.

KEYWORDS: Digital mammography, DRLs, MGD, ESD.

COMPARISON OF TREATMENT PLANNING FOR STEREOTACTIC RADIOSURGERY(SRS) AND STEREOTACTIC BODY RADIATION THERAPY(SBRT) TECHNIQUES WITH 2.5MM AND 5MM MULTILEAF COLLIMATOR(MLC)

¹Rechal Nisha Dsouza, ²Krishna Sharan, ³Suresh Sugumar, ²Srinidhi G C, ¹Shreekripa Rao, Shirley Lewis Salins⁴, Umesh V⁴, Senthil Manikandan⁵

¹Medical Radiation Physics Program, MCHP, MAHE, Manipal.

²Department of Radiotherapy and Oncology, Justice K S Hegde Charitable Hospital, Mangalore.

³Department of Medical Imaging Technology, MCHP, MAHE, Manipal.

⁴Department of Radiotherapy and Oncology, KMC, Manipal.

⁵Department of Radiation Physics, Kidwai Memorial Institute of Oncology, Bengaluru, India

Email: rechal.nisha@manipal.edu

BACKGROUND: The APEX micro-MLC(mMLC) for planning SRS/SBRT gives excellent dose distribution, but it offers disadvantages such as prolonged treatment duration and technical errors in terms of mMLC and gantry calibration which adds to the total treatment duration. Hence, we aim to compare the treatment planning performed with 2.5mm APEX mMLC and 5mm MLC (Agility) for brain and lung targets treated with SRS and SBRT in Elekta Versa HD.

MATERIALS AND METHODS: The study included 10 patients, five each with brain and lung targets. Two treatment plans were performed for each case using, MONACO(5.11.03) treatment planning system(TPS) with 2.5mm and 5mm MLC. The x-ray photon beam of energy 6FFF was used for the planning purpose with various gantry, couch, and collimator combinations. The comparison of these two plans was performed using target coverage(TC), conformity index(CI), homogeneity index(HI), gradient index(GI), and organ at risk (OAR) doses.

RESULTS: There was no significant difference found in the target coverage, CI, HI, and OAR doses in both MLC designs. VMAT with 5mm MLC gave equivalent tumor coverage with an additional number of monitor units(MUs). OAR doses were comparable in both MLC widths for brain targets whereas, for the lung targets, OAR doses were slightly lower with 2.5mm mMLC($p=0.048341$). GI was superior in 2.5mm mMLC compared to 5mm MLC giving a steep falloff in the dose distributions($p=0.21821$).

CONCLUSION: The TC, CI, HI and OAR doses were similar with both 2.5 and 5mm based VMAT plans. The gradient index was better in the 2.5mm mMLC resulting in steep dose gradients which further reduces the lower isodose volumes. Therefore, 5mm MLC(agility) can also be used for the SRS/SBRT treatment planning with a further reduction in the gradient index. However, the study has to be extended further with more samples and with multiple comparing parameters.

KEYWORDS: Stereotactic Radiotherapy, Stereotactic Body Radiotherapy, micro multileaf collimator(mMLC), Multi leaf collimator (MLC), Treatment planning, Volumetric Modulated Arc Therapy, Dynamic Conformal Arc Therapy

ESTABLISHMENT OF DIAGNOSTIC REFERENCE LEVEL AND RADIATION DOSE VARIATION IN HEAD & NECK AND PELVIS TREATMENT PLANNING IN RADIATION THERAPY COMPUTED TOMOGRAPHY

Shreekripa Rao¹, Rajagopal Kadavigere², Krishna Sharan¹, Suresh Sukumar², Shirley Lewis Salins, Srinidhi GC¹, Rechal Nisha Dsouza¹

¹Department of Radiotherapy and Oncology,

²Department of Radiodiagnosis and Imaging, MCHP, KMC, MAHE, Manipal, India

Email: shreekripa.rao@manipal.edu

BACKGROUND/OBJECTIVE: The objective of the present study is to establish a Diagnostic Reference Level (DRL) for radiotherapy planning CT scans and to optimize the radiation dose for cancer patients undergoing Head & Neck and Pelvic Computed Tomography scans. By determining the DRL, the study aims to provide guidelines for the appropriate radiation dose in these specific cases, ensuring safe and effective imaging while minimizing potential risks to the patients.

MATERIALS AND METHODS: In this prospective study we have taken CT scans in Philips 16 slice big bore CT machine, commonly employed for radiotherapy simulation in our department. A total of 120 patients with head and neck cancers and 90 patients with pelvic cancers were included. The study recorded information on patient gender, region of interest, field-of-view (FOV), type of cancer, dose length product, and computed tomography dose index (CTDIvol). The examination protocol and exposure parameters for the scans were documented. All data collected were fully anonymized, and the study exclusively included patients aged 18 years or older. In this study we have included and analysed CT procedures of Head & Neck and Pelvis.

RESULTS: Significant variation was found in the DLP, CTDIvol and effective dose when compared with other diagnostic and Radiotherapy CT scans studies. Head and Neck DRL of our institution was significantly low but Pelvic DRL of our institution is slightly high when compared with some other radiotherapy studies.

CONCLUSIONS: The first regional RT CT simulation DRLs have been proposed and provide a platform for dose comparison and optimization. Due to the lack of literature on RT CT DRLs, the present study is compared with only a few studies. Comparison with previously published RT CT DRLs showed some variation in radiation doses so exposure parameters should be reviewed and optimized.

KEYWORDS: Radiotherapy, Diagnostic reference level, Dose length product, Computed tomography, effective dose

DOSIMETRIC COMPARISON OF DIFFERENT DOSE PRESCRIPTION POINT EFFECT WITH DIFFERENT DOSE CALCULATION ALGORITHMS IN CARCINOMA BUCCAL MUCOSA TUMORS

^{1,2}Bharath Pandu, ¹Khanna D, ³Mohandass Palanisamy, ²Rajadurai Elavarasan, ²Saro Jacob

¹Karunya institute of technology and sciences, Bangalore, India, ²Bangalore Baptist Hospital, Hebbal, Bangalore

³Fortis Hospital, Mohali, Punjab, India

Email: bharathmphy@gmail.com

AIM: Objective of the present study is to analyse the accuracy of different dose calculation algorithms at dose prescription points placed on tissue, Bone, and tissue-bone interface using 3D-Conformal radiotherapy (3DCRT) in carcinoma buccal mucosa patients.

METHODS AND MATERIALS: Twenty-one patients with carcinoma of the buccal mucosa were retrospectively selected for this study. The reference 3DCRT treatment plan for 60Gy/30# was generated using the Monaco™ Version 5.51 treatment planning system(TPS) using 6MV photon beam energy. The dose prescription point was kept on the central axis(CAX) of the beam in the tissue and a reference plan(RP) was generated with the Monte Carlo(MC) algorithms. The RP was modified with the dose prescription point into the bone, tissue-bone interface along with the CAX of the beam using MC algorithm. Similarly, the dose prescription point and dose calculation algorithms were changed to tissue, bone, and bone-tissue interface for Collapsed Cone(CC) and Pencil Beam(PB) algorithms. A total of 189 3DCRT plans were generated with different dose calculation algorithms for comparison. The dose received by the target volume and other organ at risk volumes(OAR) were compared for all dose calculation algorithms.

RESULTS: The study results showed that the mean dose, total MU, V95%, and homogeneity index were $<\pm 2\%$ of the deviation between different dose prescription points for all the treatment algorithms as compared reference plan. Conformity index results showed that the deviation was $<\pm 2\%$, except for the CC treatment plan at tissue-bone interface. The MC plan with different dose prescriptions showed that all target parameters and OAR results were within $\pm 3\%$ deviation. However, prescription point at bone with MC and CC algorithms showed overdose(V107%) to tumour such as 6.5% and 3.6% as compared with reference plan. The dose received by the OAR volume such as spinalcord, Ipsilateral parotid, Ipsilateral parotid 50% volume, brain stem was higher with CC and PB for all three interface treatment plans.

CONCLUSION: The MC treatment planning using different interfaces showed that all target parameters and OAR results were within $\pm 3\%$ deviations. The dose received by the OAR was higher for plan calculated with CC and PB algorithm with all interfaces than reference plan.

KEYWORDS: Dose prescription point, Dose calculation algorithms, Bone-Tissue interface

METHOD TO ENHANCE THE SENSITIVITY OF RADIOCHROMIC FERROUS AMMONIUM SULFATE-BENZOIC ACID-XYELNOL ORANGE (FBX) SOLUTION

Sakshi Singhal¹, Aruna Kaushik¹, Maria D'Souza¹, Manoj K. Semwal²

¹Department of Radiological Nuclear and Imaging Sciences, Institute of Nuclear Medicine and Allied Sciences, Delhi, India, ²Department of Radiation Oncology, Army Hospital Research and Referral, Delhi, India

Email: sakshisinghal534@gmail.com

BACKGROUND/OBJECTIVE: FBX solution is a known dosimeter in the dose range applicable in radiation oncology. Several attempts at improving its dose sensitivity have been reported in literature. These methods include varying the concentration of different components in the solution or selecting the wavelength exhibiting the highest sensitivity. The current work explores a method to enhance the sensitivity of the dosimeter in the range 0-10Gy using the originally proposed standard composition of the solution.

MATERIALS AND METHODS: FBX solution was fabricated using the standard composition. Solution was irradiated to radiation doses in the range 0-10Gy at a dose rate 0.647Gy/min in Telecobalt radiation facility. UV-Visible spectrometer (Double Beam Optical System with Automatic 8-Cell Changer- Model 3200, LABINDIA) was used to record the absorption spectra of the irradiated samples on the same day of irradiation. Dose response of the solution was obtained at different wavelengths ranging from 520-620nm. Also, whole spectrum was divided into several wavelength bands: 500-540nm, 540-580nm, 580-620nm, 570-650nm and 500-570nm. Integrated absorbance values were plotted against the radiation doses for each wavelength band. Curves exhibiting the linear dose response were fitted using linear equation employing least square fitting method. Values of slope and Pearson's correlation coefficient were noted and compared for each fitted curve. Reproducibility of the results was also assessed.

RESULTS: When dose response curve was plotted at discrete wavelengths, highest sensitivity with linearity of the response was observed at 540nm with sensitivity being 0.0643/Gy ($r=0.998$). When dose response curve was plotted with wavelength bands, maximum sensitivity was observed in the wavelength band 500-570nm with sensitivity being 4.39/Gy ($r=0.998$). This is 68 times higher than the sensitivity obtained at wavelength 540nm. Results were found to be reproducible with an error of 0.7%.

CONCLUSIONS: The test results indicate that integrated absorbance in the 500-570nm wavelength band can be used for radiation dosimetry using FBX solution.

KEYWORDS: Radiation dosimetry, FBX solution, UV-Visible spectrophotometer

OPTIMIZATION OF X-RAY TUBE PARAMETERS TO MINIMIZE RADIATION EXPOSURE IN DIAGNOSTIC CT SCANS WHILE MAINTAINING DOSES WITHIN DIAGNOSTIC REFERENCE LEVELS

Mallikarjuna Adavala ¹, K. Chandrasekhar Reddy ², Sashidhar Kaza ³, Shakambari Sadangi ⁴

¹Department of Physics, Rayalaseema University, Kurnool, AP, India & AIG Hospitals, Hyderabad, India,

²Department of Physics, Govt Degree College, Uravakonda, AP, India,

³Department of Radiology, AIG Hospitals, Gachibowli, Hyderabad, India,

⁴Department of Radiation oncology, AIG Hospitals, Gachibowli, Hyderabad, India

Email: amallikarjuna@gmail.com

OBJECTIVE: Diagnostic computed tomography (CT) scans are widely used in clinical practice for accurate and detailed imaging of various anatomical sites. However, the associated ionizing radiation poses potential risks to patients. This study aims to optimize X-ray tube parameters to minimize radiation exposure in CT scans while maintaining the dose within the range of diagnostic reference levels (DRLs). The optimization process considers CT dose index (CTDI), dose-length product (DLP), and other relevant parameters.

MATERIALS METHODS: A retrospective analysis of patient data was conducted, encompassing various anatomical sites scanned using CT. The data included CTDI and DLP values from previous scans, along with patient characteristics. Initial X-ray tube parameters, such as tube current, tube voltage, and rotation time, were recorded for each scan. A comprehensive optimization framework was developed to determine the optimal combination of X-ray tube parameters that minimizes radiation exposure while adhering to DRLs.

RESULTS: By systematically adjusting the X-ray tube parameters, radiation exposure was reduced by an average of 20% across all anatomical sites studied. The optimized parameters resulted in a decrease in both CTDI and DLP values, ensuring that the doses remained within the range of established DRLs. The optimization process effectively balanced the need for image quality and diagnostic accuracy with the objective of reducing patient radiation exposure.

CONCLUSION: This study demonstrates the feasibility and effectiveness of optimizing X-ray tube parameters to minimize radiation exposure in diagnostic CT scans. By implementing the proposed optimization framework, clinicians can reduce patient radiation doses while maintaining image quality and diagnostic accuracy within acceptable limits. These findings have significant implications for improving patient safety in diagnostic CT imaging and contribute to the ongoing efforts to optimize radiation exposure in medical imaging.

KEYWORDS: optimization, X-ray tube parameters, radiation exposure, diagnostic CT scans, CTDI, DLP, DRLs.

CONFORMAL CEREBRO-SPINAL IRRADIATION USING VOLUMETRIC MODULATED ARC THERAPY

Gleetus Timothy¹, Sonu Goyal¹, Adarsh P P¹, Anet Abraham¹, Mary Joan²

¹Department of Radiation Oncology, Apex Hospital, Jaipur,

²Department of Radiation Oncology, Christian Medical College and Hospital Ludhiana, India

Email: gleetus@gmail.com

BACKGROUND: Medulloblastoma is one of the most sensitive childhood brain tumors to radiation. Postoperative radiotherapy has a significant impact on local control and overall survival. The goal of radiation therapy is to administer a precise radiation dose to a well-defined tumor volume with minimal possible dose healthy tissues, resulting in tumor eradication, optimum quality of life and increased survival with reasonable side effects.

MATERIALS AND METHODS: Post-operative intracranial medulloblastoma patients treated with VMAT-CSI on Elekta Synergy with MLC i2 linear accelerator from January 2019 to March 2023 were retrospectively reviewed for this study. A dose of 36Gy/20 fractions to the whole craniospinal axis and boost with conformal therapy restricted to the tumor bed to a total dose of 54Gy was prescribed.

Whole body VacLoc and thermoplastic head mask is used for immobilization in prone position and Computed tomography (CT) simulation was done as per the departmental protocol. A 6 MV photon beam was used for the VMAT treatment planning in Monaco TPS version 5.11.03 with Monte Carlo isodose calculation. The plan required three isocenters, and the isocentric shifts from reference CT markers were calculated from the TPS. The plans were evaluated for dose coverage, organs at risk (OARs) sparing and number of monitor units.

RESULTS: VMAT CSI plans provided more uniform dose distribution specifically around the vertebral column and hence will cause reduced incidence of uneven bone growth in children receiving CSI. There was a lower mean dose to vital organs such as heart, thyroid, and esophagus of at least <4 Gy with VMAT. This significant reduction in dose to OAR meant reduced late side effects and overall increased quality of life. Another important advantage of VMAT compared to IMRT is the relative ease of implementing the therapy. The time required to deliver treatment in VMAT is 10 to 15 min lesser than IMRT.

CONCLUSIONS: VMAT CSI plans created greater conformity and homogeneity with better uniform dose distribution and improved dose sparing of OAR's. Daily image-guidance improves accuracy and reduces the risk of spinal cord overdose without increasing treatment time.

KEYWORDS: craniospinal irradiation, medulloblastoma, VMAT, conformity, homogeneity

RADIATION DOSIMETRY OF RU-106 EYE PLAQUE USING EGS_BRACHY MONTE CARLO CODE

Harishchandra Gupta¹, Ashok Kumar², Aruna Kaushik¹, Manoj K. Semwal²

¹Department of Radiological Nuclear and Imaging Sciences, Institute of Nuclear Medicine and Allied Sciences, Delhi, ²Department of Radiation Oncology, Army Hospital Research and Referral, Delhi, India

Email: harishchandra.gupta.du@gmail.com

BACKGROUND AND OBJECTIVES: Ru-106 beta source is being employed for the treatment of ocular tumors using eye plaque. Accurate radiation dosimetry is a pre-requisite for effective treatment of the cancer. Radiation dosimetry studies have been reported using various physical dosimeters and Monte Carlo simulation techniques. In this study, our aim was to determine the dose distribution of a BARC-make Ru-106 eye plaque using the EGS_Brachy code.

MATERIAL AND METHOD: EGS_Brachy is a recently developed EGSnrc-based Monte Carlo code specially designed for brachytherapy applications. The code is written in a script file and uses the given libraries of EGSnrc. A water phantom was modelled at the origin to place the eye plaque and dose-scoring objects. The eye plaque was modelled as three layers of spherical sheets with thicknesses of 0.9 mm (Ag), 0.1 μm (Ru-106), and 0.1 mm (Ag) as described by the manufacturer. Forty cuboidal detectors were modelled with dimensions 0.53 x 0.53 x 0.44 mm³ for dose scoring. The simulation results were saved in a file that contained the data as region versus dose/particle. Region and dose/particle were converted to spatial coordinates and dose rate (mGy/min) respectively. The depth versus dose rate curve was plotted and compared with the certificate.

RESULTS AND CONCLUSION: The dose rates at a reference depth of 2 mm were 58.99 mGy/min in the simulation and 60.49 mGy/min in the certificate. The results differed from the certificate by 2.47% at a reference depth of 2 mm. The notch has no significant influence on the depth dose at the center.

KEYWORDS: Brachytherapy, Monte Carlo simulation, EGSnrc, EGS_Brachy, BARC-Ru-106 eye plaque

GEUD BASED OPTIMIZATION: A STRONG TOOL TO REDUCE HEART AND LUNG DOSE IN VMAT BREAST PLANS WHEN USED IN CONJUNCTION WITH VOLUME OBJECTIVE CONSTRAINTS IN ECLIPSE PHOTON OPTIMIZER

Thushant T Nair, Rugmini B

Department of Radiation Oncology, Paras Hospitals, Gurgaon, Delhi- NCR, India

Email: thushant.phy@gmail.com

BACKGROUND/OBJECTIVE: Breast cancer is the most common cancer in the world with almost 12.5% accounting from rest of the cancers in the year 2020 according to WHO. The most important OAR in treatment of breast is lung and heart. Even though the advancement in the treatment techniques have grown exponentially well in many cancers but till date many consider 2D and 3D FiF as the golden standard in treatment of malignant breast tumors. This abstract presents how gEUD objective in conjunction with a specific 'a' value works as a strong tool in VMAT planning when used along with the volume objective constraints to spare lung and heart. This tool produces a VMAT plan that is comparable to tangential IMRT and 3D FiF technique. VMAT plans are not usually implemented for breast planning as they have higher low dose spillage. This tool can be used as a curb in overcoming the low dose spill effectively. VMAT plans have lesser MU to Dose ratio and hence lesser delivery time and better dose conformity. This study keeps 3DFiF as the golden standard for comparison.

MATERIALS AND METHODS: 30 Breast patients were selected with either side malignant breast tumor and they were divided equally in two sections as left and right sided breast. The sample included BCS and MRM patients. Treatment planning for all the patients was done using Eclipse 16.1 version and the treatment delivery system was Truebeam STx with High Definition MLC. gEUD objective optimization was used along with the volume objective constraints. Patients whose tumor size extending beyond 22 cm was rejected as there is a requirement of either rotating the collimator or by keeping at least two isocenters. Each patient was planned in all the three techniques. Here we have compared the lung dose of V5, V10, V15, V20 and V30 and heart dose of V5, V10, V15, V20, V30 and also mean dose. The remaining OAR doses were also evaluated and analyzed. Homogeneity index, Conformity index and Integral Dose was also evaluated for all the patients.

RESULTS: The dosimetric analysis of VMAT plans with 3DFiF and IMRT showed that VMAT plan has better conformity index and homogeneity index than 3DFiF. HI and CI was comparable and didn't have much significant difference for VMAT and IMRT. Low dose spill is better in 3DFiF than IMRT or VMAT technique. Low dose spill of VMAT and IMRT didn't have significant difference for ipsilateral lung. High dose spill is lesser in VMAT and IMRT plans compared to 3DFiF. Mean dose to the contralateral lung was least in 3DFiF followed by IMRT and VMAT. Heart mean dose was less in 3DFiF and no significant difference was observed in IMRT and VMAT. Integral dose was almost same in all the three plans. Monitor Unit was 2.8 times more in IMRT than in VMAT. Coverage to the PTV was better in VMAT and IMRT than 3DFiF.

CONCLUSIONS: The test result indicate that VMAT plans with the use of gEUD along with volume objective constraints in optimization can reduce the dose to lung and heart significantly and it is comparable to IMRT tangential technique. VMAT has lesser ratio in terms of monitor unit to dose compared to IMRT reaching around 3:1. Since the MU is less, the time spent by the patient in the treatment room is also less. This reduces the intrafraction movement. Suitable technique for DIBH as the delivery is faster.

IMPLEMENTATION OF ECLIPSE SCRIPTING APPLICATION PROGRAMMING INTERFACE (ESAPI) TO EASE THE WORKFLOW OF CREATING REST/CROPPED STRUCTURES FOR VARIOUS TREATMENT SITES

Deepak Mahor, Vinay Saini, Narender Kumar, Sanju, Alka Kataria, Sanjay Barman, Ashutosh Mukherjee, Satyajit Pradhan

Department of Radiation Oncology, Mahamana Pandit Madan Mohan Malaviya Cancer Center & Homi Bhabha Cancer Center, A Unit of Tata Memorial Center, Varanasi, India

Email: deepak24mahor@gmail.com

BACKGROUND: Varian's ESAPI was released in the year 2012, with the first version providing read-only access to planning data. In subsequent releases, a number of functionalities such as optimization support and write-enabled capabilities were introduced. However, the process of cropping and creating duplicated structures manually with number of tools on the contouring station remained time-consuming and prone to errors sometimes. To address this issue, we developed an in-house script utilizing Varian's ESAPI and a dedicated Graphical User Interface (GUI) to enhance efficiency, streamline the workflow, and minimize errors in treatment planning.

MATERIALS AND METHODS: The script was developed using Varian's research box (T-BOX), ESAPI v15.5, Microsoft's Visual Studio 2019, and Varian's TPS. We employed Windows Presentation Framework (WPF) technology to provide users with a GUI for selecting desired structures. The main ESAPI script was written in C# code. The development and testing of the script were conducted on the T-BOX with Visual Studio, and its implementation in the planning workflow was subsequently performed on the TPS.

RESULTS: Our script significantly reduced the cropping time to just a few seconds. It eliminated the risk of errors such as cropping or overwriting other structures. By selecting all the structures, the script automatically cropped only the overlapping regions, eliminating the need for manual identification. The streamlined workflow was achieved through a single GUI window, ensuring a smooth and error-free process.

CONCLUSIONS: The in-house developed script proved to be highly effective when integrated into the TPS workflow. It successfully enhanced efficiency, reduced cropping time, and minimized errors in the planning process. The implementation of this script holds great potential for reducing the overall planning time, especially along with rapid planning scenarios.

KEYWORDS: ESAPI, Research BOX, T-BOX, WPF, Visual Studio IDE, C#.

HOW TO ARCHIVE ADEQUATE DOSE AND IMAGE QUALITY IN PEDIATRIC CHEST CT ?

Renato Dimenstein¹, Douglas Carli Silva², Pamela Bertolazzi² Gabriel Lubke¹ Liza Suzuki³

¹Medical Physicist RAD, ² B.Sc of Siemens Healthineers, ³ Radiologist Fleury

Email: renato.dimenstein@gmail.com

BACKGROUND/OBJECTIVE: CT for pediatric presents challenges when it comes to selecting acquisition protocols that strike a balance between achieving satisfactory image quality and minimizing radiation dose. However, achieving this equilibrium remains a complex task, partly due to equipment technologies. Consequently, it is imperative to establish a methodology for parameter acquisition and image reconstruction. In line with the ALARA principle, we conducted a study employing an anthropomorphic phantom to establish a protocol that achieves a satisfactory trade-off between dose and image quality in pediatric chest CT.

MATERIALS AND METHODS: The methodology involved the use of an anthropomorphic phantom equivalent to a five-year-old child (CIRS model ATOM), without subjecting actual patients to radiation exposure. The study utilized a Dual Source CT scanner (Siemens model Force). The simulations were done with different types of modulation techniques that involved adjustments in tube current (mAs) and tube voltage (kVp). Subsequently, the acquired images were reconstructed using an iterative algorithm (ADMIRE). The image quality analysis was obtained by the measure the contrast-noise-ratio (CNR), with the region of interest (ROI) for parenchyma and mediastinum. The values of dose length product (DLP) were obtained from the DICOM report of the scanner. The image simulations were analysed by pediatric radiologist to establish a routine protocol for chest CT.

RESULTS: The best balance between dose and image quality for chest CT of the phantom was obtained using 70 kVp and 32 mAs with average force modulation and semi kVp settings. The CNR values were 32.44 (parenchyma) and 33.96 (mediastinum). The DLP value was 8.06 mGy.min .



CONCLUSIONS: The experimental methodology it was useful to establish a routine protocol for 5 years old chest CT examinations, with a balance between adequate dose and image quality.

KEYWORDS: pediatric chest tomography, image quality, contrast-to-noise ratio (CNR), radiation dose.

A DOSIMETRICAL STUDY OF CA LARYNGES GRADE-IV USING DOUBLE ARC RAPIDARC (RA) WITH CONVENTIONAL IMRT (7 FIELDS) TECHNIQUE

Santosh Kumar¹, Satya Kumar¹, Alok Kumar², Rajesh Kumar Singh³

¹Department of Medical Physics, State Cancer Institute, IGIMS, Patna, Bihar, India, ²Department of Radiation Oncology, Netaji Subhas Chandra Bose Cancer Hospital, New Garia, Kolkata, West Bengal, India, ³Department of Radiation Oncology, State Cancer Institute, IGIMS, Patna, Bihar, India

Email: igimsdrsantoshkumar@gmail.com

BACKGROUND/OBJECTIVE:The aim of this study was to dosimetrically evaluate and compare double arc RapidArc (RA) with conventional IMRT (7 fields) plans for irradiation of locally advanced CA larynges (CAL), focusing on target coverage and doses received by organs at risk (OAR).

MATERIALS AND METHODS:Computed tomography scans of 10 patients with CAL were obtained. Contouring of the target volumes and OAR was done. Two plans were made for each patient one using 7 fields IMRT and the other double arc RA, and calculated doses to planning target volume (PTV) and OAR were compared. Monitor units for each technique were also calculated.

RESULTS: PTV coverage was similar in all two techniques. The homogeneity index (HI) was higher for the IMRT plans with a value of 0.108 ± 0.021 compared to 0.0975 ± 0.017 for double arc RA plans (p-value of 0.540). The double arc RA plans achieved better conformity with a CI 95% = 1.01 ± 0.021 compared to 1.05 ± 0.057 achieved with the IMRT plans (p-value of 0.036). The average monitor units (MU) \pm SD were 930.5 ± 142.42 for the IMRT plans as opposed to 484.25 ± 69.47 for the double arc RA plans (P-value of 0.002). Double arc plans provided better OAR sparing with a significant p-value of 0.002 and 0.004 for the esophagus and trachea, respectively.

CONCLUSIONS: RA is a rapid and accurate technique that uses lower MUs than conventional IMRT. Double arc plans provide better dose conformity, OAR sparing, and a more homogeneous target coverage compared to IMRT.

KEYWORDS:Larynx, Rapid Arc, VMAT, IMRT, Planning Study

DOSIMETRIC IMPACT OF AUTOMATICALLY CONVERTED RADIOTHERAPY PLANS BETWEEN TWO TOMOTHERAPY MACHINES

Vidhi Soni¹, Vipul Vishal², Vidhan Soni³

¹Medical Physicist, Paras Hospitals Panchkula, Haryana,

²Research scholar, Indian Institute of Technology, kharagpur, India

Email: vsstar365506@gmail.com

OBJECTIVE: In radiation therapy, the continuity of a plan is an important thing. But due to continuous machine breakdowns, it is not possible. If there are two linear accelerators available at the same center then continuity of treatment can be possible. This study aims to evaluate the dosimetric parameters, plan quality, accuracy, and effectiveness of transferred plans between two tomotherapy machines.

MATERIALS AND METHOD: A Total number of 25 patients have been taken for cervical cancer who received radiation treatment originally in Hi-Art. The prescription dose of the target volume (PTV) was 45 Gy in 25 fractions. We transferred all the patients from Hi-Art to Radixact by using the automatically converted plan transfer tool. There are two ways of dosimetric analysis: first, with a dose volume histogram (DVH), and second, with patient-specific quality assurance. In DVH analysis, we evaluate and compare Planning target volume (PTV) coverage, Homogeneity index (HI), conformity index (CI), and sparing of organs at risk (OARs) for both plans. In patient-specific quality assurance, we compared the absolute dose for all plans by using a cheese phantom with an Ion chamber EXRADIN A1SL. Maximum differences and p-values were also calculated by using t-test and checking whether it is significant or not.

RESULTS: The maximum difference (%) of PTV coverage volume at 95% prescribed dose was 0.32 percent and it is statistically insignificant. For the homogeneity and conformity index, the value of maximum Differences were 0.22% & 0.76%. For all Organs at Risk, the maximum difference was 0.50%. The average of maximum difference for absolute dose measurement was 1.22%.

CONCLUSION: In this study, we can conclude that automatically radiation therapy plan conversion is a reliable and suitable process. And it will reduce stress among both hospital staff and patient to improve treatment result.

KEYWORDS: machine breakdown, homogeneity index, conformity index, EXRADIN A1SL ionization chamber.

A DOSIMETRIC COMPARISON OF DIFFERENT PLANNING TECHNIQUE FOR HEAD AND NECK CANCER TREATMENT

Vidhi Soni¹, Vipul Vishal², Nidhi Jain³, Parneet Singh⁴

¹Medical Physicist, Paras Hospitals Panchkula, Haryana,

²Research scholar, Indian Institute of Technology, kharagpur,

³Radiation Safety Officer, Paras Hospitals Panchkula, Haryana,

⁴Radiation Oncologist, Paras Hospitals Panchkula, Haryana, India

Email: vsstar365506@gmail.com

OBJECTIVE: Head and Neck Cancers are a major public health problem in India. Intensity modulated radiation therapy (IMRT) and Volumetric arc therapy (VMAT) over conventional 3DCRT are the best way to achieve full Planning target volume (PTV) coverage and minimal dose to Organs at risk (OARs). Aim of this study was to evaluate and compare of dosimetric parameters for VMAT and IMRT in Head & Neck cancers with Elekta synergy linear accelerator.

MATERIALS AND METHODS: A total sample of 30 patients has been taken for Head and Neck cancer. Two plans VMAT and IMRT were generated by using the Monaco Planning system for each patient. VMAT plan with two full Arc and IMRT plan with seven coplanar dynamic MLC beams (0°,51°,102°,153°,204°,255°,306°) were created. Remaining all parameters were standard and same for both plans. The prescription dose of PTV was 60Gy in 30 fractions. To evaluate and compare all parameters(like MUs, overall treatment time, PTV coverage, homogeneity and conformity index of PTV and sparing of OARs), p-values were calculated by using t- test and checked whether it is significant or not.

RESULT: Result shows that this study was comparable as expected; the mean \pm standard deviation and p-value were calculated for all parameters. The PTV coverage at 95% volume is slightly higher in VMAT (96.5646 \pm 1.199) % than IMRT (96.427 \pm 1.214) %, and it is statistically insignificant. For OARs sparing especially for mean parotids, IMRT doses [(23.758 \pm 3.0295) Gy] is less than VMAT doses [(26.022 \pm 3.5188) Gy]. Total numbers of MUs are less in IMRT but overall treatment time is more.

CONCLUSION: In this study we are able to say that in terms of plan quality, IMRT is a suitable technique. In terms of treatment delivery time, patient comfort and institutional patient load, VMAT is a better technique than IMRT. But consideration of optimum plan quality and machine utility, VMAT technique is more suitable.

KEYWORDS: Volumetric arc therapy, Intensity modulated radiation therapy, homogeneity index and conformity index.

TREATMENT RESPONSE ASSESSMENT USING PHOTOACOUSTIC IMAGING IN RADIOTHERAPY: A REVIEW

Vipul Vishal¹, Sumana Halder¹, Vidhi Soni²

¹SMST, Indian Institute of Technology, Kharagpur, West Bengal, India,

²Paras Hospital Panchkula, Haryana, India

Email: vipulkgp@kgpian.iitkgp.ac.in

BACKGROUND/OBJECTIVE: Radiotherapy is one of the most practised treatment methods to cure solid tumour and is vitally important for palliative treatment. Conventional imaging takes more than a week to evaluate the radiological response, while Image guided real time radiological response monitoring can be potentially perform by emerging Photoacoustic imaging (PAI). Different constituents present in the tissue have distinguished optical absorption based on that total blood haemoglobin, blood oxygen saturation and vascular changes measured in cancerous and normal tissue. Laurie J. Rich et al. were compared oxygen saturation using Photoacoustic Imaging and oxygen enhanced MRI and observed the utility of PAI in detecting tumour and normal tissue hemodynamic response to radiation in head and neck cancers.

MATERIALS AND METHODS: Photoacoustic imaging is a non-invasive and non ionising imaging technique where biological samples illuminated by the pulsed laser light, induced ultrasound wave detected by a US transducer. A typical PAI system includes pulsed (<10 ns) laser source, US transducer, signal processing and image acquisition system. For specific cancer type Photoacoustic contrast agent developed and introduced.

RESULTS: Li et al., Oraevsky et al., Dean-Ben et al., and Diot et al., Ermilov et al., Dean-Ben et al. introduced photoacoustic imaging which shows comparative better accuracy than the mammography in breast cancer. Combined Transrectal ultrasound and photoacoustic imaging system developed for accurate diagnosis of prostate cancer. Wang et al developed a handheld PAI with high spatial resolution, high imaging speed and rich contrast for melanoma detection on mouse models. Volumetric melanoma growth rate analysis is useful for diagnosis, staging and treatment evaluation.

CONCLUSIONS: This paper summarises the potential of state-of-the-art Photoacoustic imaging systems for providing predictive treatment response of radiotherapy treatment. Integrating multi-scale PAI in radiotherapy with existing imaging modalities, for treatment guidance to early tumour response assessment and radiation toxicity, could therefore open new paradigm in the future of radiation oncology.

KEYWORDS: Photoacoustic Imaging (PAI), Transducer

CHROMATIC ABERRATION ANALYSIS BY SELECTIVE PLANE ILLUMINATION MICROSCOPY: FAST, LABOUR LESS AND 3D ANALYTICAL PROCEDURE

Vipul Vishal¹, Sumana Halder², Vidhi Soni³

¹SMST, Indian Institute of Technology, Kharagpur, West Bengal, India,

²Paras Hospital Panchkula, Haryana, India

Email: vipulkgp@kgpian.iitkgp.ac.in

BACKGROUND/OBJECTIVE: Chromosomal aberration analysis (CAA) is used as biological dosimeters for dose estimation in radiation accident and therapy. Peripheral blood sample were collected from the radiation exposed personnel and were used for the chromosome aberration and micronucleus assays. Light microscope were used to determine the frequencies of dicentric chromosomes and rings and CBMN in the first mitotic division in in-vitro culture of lymphocytes to estimate radiation dosimetry. Optical Microscopes used 2D cell culture for microscopic analysis which required slide preparation, a time consuming, labour intensive and expert personnel. While Selective plane Illumination Microscopy (SPIM) an emerging microscopic system having ability to perform 3D imaging with high spatial and temporal resolution can be used for CAA. 3D cell cultures are more physiological relevant, predictive and provide better simulation of condition in a living organism. This abstract presents an alternative 3D culture based SPIM system for CAA and micronucleus assay analysis in place of 2D optical microscopy.

MATERIALS AND METHODS: Blood samples from 10 patients treated for head and neck cancer at cancer hospital were collected and cultured in non-scaffold based microfluidic channels (3D culture). Dose estimation calibration curve was established in vitro by exposing blood samples from healthy donors to γ -radiation from Cs-137/Co-60 source. Blood sample collection followed the method devised by M.S. Sasaki. Dicentric chromosome (dic) and rings (r) were scored under SPIM and then in light microscopy for dose estimation and co-validation of their outcomes.

RESULTS: The study is in the progression, but the primary result shows that the estimation of radiation dose based on dic + r analysis of exposed blood sample using SPIM system were comparable to the actual dose delivered and dose estimated by slide based light microscopy.

CONCLUSIONS: In summary, the results from the present study indicate that CAA and micronucleus assay analysis made by the SPIM system provide a reliable estimation of radiation exposure.

KEYWORDS: Chromosomal aberration analysis, Selective plane illumination microscopy, Microfluidic channel

BLADDER SEGMENTATION IN MRI FOR HIGH DOSE RATE BRACHYTHERAPY USING DEEP CONVOLUTIONAL NETWORK

Suresh Das¹, Subhayan Mondal¹, Saumik Bhattacharya², Sayantari Ghosh³

¹Department of Radiation Oncology, Narayana Superspeciality Hospital,

²Department of E&ECE, IIT Kharagpur, ³Department of Physics, NIT, Durgapur, West Bengal, India

Email: dassureshster@gmail.com

BACKGROUND/OBJECTIVE: Delineation of organ-at-risk (OAR) such as bladder which affects the delivered dose to the target volume, is an important part in high dose rate brachytherapy, owing to the steep dose gradient. In this work we propose U-net based deep network architecture for fast and reproducible auto contouring.

MATERIALS AND METHODS: MRI images of 50 patients with locally advanced cervical cancer were considered in this study. We used a deep convolution neural network, which uses long and short skip connections to improve feature extraction procedure and accuracy of segmentation. 30 patients were randomly used for training, 10 patients for validation and 10 patients for testing. Well established quantitative metrics such as 'Accuracy' and 'Intersection Over Union' (IoU) were used for evaluation.

RESULTS: The performance of the U-net based deep auto segmentation network was validated using manual annotations by expert radiologists. The validation loss was well within acceptable limit resulting in a good Mean IoU value. We also analyzed the performance of different state of the art algorithms and open-source softwares reported in the literature and observed that proposed network demonstrates performance at par, or better for the mentioned task.

CONCLUSIONS: The proposed model achieved a very good agreement between the predicted and manually defined contour of bladder, thus improving the reproducibility of contouring in brachytherapy workflow.

KEYWORDS: deep learning, autosegmentation, brachytherapy, cervical cancer

DOSIMETRIC IMPACT OF AIR POCKETS IN THE VAGINAL CUFF BRACHYTHERAPY USING MODEL-BASED DOSE CALCULATION ALGORITHM

Lakshmi VenkataramanaPuriparthi, Anil Kumar Talluri, Akkineni NagaPrasanthi, Venkatappa RaoTumu, NVN MadhusudhanaSresty, Krishnam Raju Alluri

Basavatarakam Indoamerican caner Hospital & RI, Hyderabad, India

Email: lakshmianil.puriparthi@gmail.com

INTRODUCTION: Endometrial cancer is the 6th most common cancer in women worldwide and is the most common cancer of the female reproductive system in the West. However, vaginal cuff brachytherapy (VCB) has intrinsic advantages compared to External beam radiation therapy (EBRT) due to the close contact between radioactive sources and volume to treat, and the movement of the vagina [1]. The presence of air pockets between the vaginal mucosa and the applicator results in an underdose of the target that could potentially lead to relapse. Newly developed model-based dose calculation algorithms (MBDCA) significantly improved dose calculation accuracy compared with TG-43 [2]. The present study aims to assess the dosimetric effect of air pockets on vaginal mucosal dose using the Acruos BV algorithm and compare the results with that of TG-43.

MATERIALS AND METHODS: This is a retrospective study with a population consisting of 23 patients. Majority of patients were treated with a cylinder diameter of 3.0 cm (range 2 to 3.5cm). Each patient was imaged after insertion of the cylinder on computed tomography (CT) scanner with a slice thickness of 2.5 mm. The axial CT images were transferred to the Brachy vision TPS for the generation of a treatment plan with a dose calculation grid size of 2.5 mm. For each patient, two plans were created. The first plan with TG-43 dose calculation and the second plan by dose distribution recalculation using the Acruos BV maintaining the same dwell positions and dwell times. Air pockets that were present between the cylinder and the vaginal mucosa were contoured on axial CT slices enabling TPS to measure its volume. A total of 33 air pockets were found in the selected patient's CT scans. The change in the mucosal dose due to the air pocket was assessed by taking ratios of point doses from the TPS at the surface of the cylinder and mucosa on the same axial slice where maximum separation was presented. The correlation between the dose ratio and separation of the vaginal mucosa due to air pocket was calculated using the Pearson correlation test.

RESULTS: Among 23 patients, two patients had three air pockets, six had two air pockets, and the remaining had only one air pocket. The average volume of air pockets was 0.08 cc. Among 33 air pockets, 84% of air pockets displaced the vaginal mucosa by ≥ 0.2 cm. When the TG-43 algorithm was used to calculate doses, the ratio of doses of the maximum displaced mucosa by air to the dose at the cylinder surface was calculated and it is in the order of 0.53 to 0.89. The average ratio was 0.77 ± 0.09 (1 SD). The mucosa received a reduced dose as compared to the cylinder surface by an average of 22.72% (range of 47.3%–10.65%) due to the presence of an air pocket. The ratio of doses of the maximum displaced mucosa by air to that of the dose at the cylinder surface was in the order of 0.51 to 0.88 when doses were re-calculated using the Acruos BV with the same dwell positions and dwell times obtained with TG-43. The average ratio was 0.78 ± 0.09 (1SD). Due to the presence of air, the Acruos BV showed that the mucosa received a reduced dose by an average of 23.29% (range of 49.00%–11.82%). When TG-43 and Acruos BV dose ratios are examined, we found that there was no appreciable distinction with a p-value of 0.39.

DISCUSSION: Air gaps between vaginal mucosa and cylinder could be considered as one of the possible reasons for vaginal recurrence. Onal C *et al.* [3] observed that the occurrence of air pockets is more predominant in post-menopausal patients and patients treated with brachytherapy alone than in pre-menopausal patients or patients treated with EBRT and brachytherapy. The occurrence of air pockets around the vaginal cylinder was observed in 43% of patients, while 57% of patients had no air pockets. Cameron *et al.* [4] reported that 75% (18 out of 25) of patients had an average of one air pocket. Richardson *et al.* [5] reported that 80% of patients had one or greater than one air pocket in at least 1 out of 6 treatment fractions. In this study, we included patients with air pockets around the cylinder, as we aimed to study the dose prediction using the Acruos BV algorithm and compared it to the TG-43 algorithm. The maximum volume of air pockets was 0.3 cc and the average volume was 0.08 cc, which is lower than that reported by Richardson *et al.* (0.34 cc). In Richardson *et al.* study, the majority of patients were treated with a 2.5-cm diameter cylinder and only one was treated with a 3.0-cm diameter cylinder. In our study, the majority of patients were treated with a 3cm diameter vaginal cylinder which could be the reason for the formation of small volume air pockets.

CONCLUSION: Both algorithms demonstrated dose reductions at the mucosal surface due to the presence of air pockets, with an average of 22.7% and 23.9%, respectively. Hence the usage of the TG-43 algorithm for VCB dose calculation is reasonable even in the presence of air pockets.

ESTIMATION OF VOLUMETRIC BREAST DENSITY FOR THE EARLY DETECTION OF BREAST CANCER: A STUDY IN GHANA

Caroline Kachana Pwamang¹, Mary Boadu², Edem Sosu³

¹Radiological and Non-Ionizing Installations Directorate, Nuclear Regulatory Authority, School of Nuclear and Allied Sciences, University of Ghana,

²Radiological and Medical Science Research Institute, Ghana Atomic Energy Commission, School of Nuclear and Allied Sciences, University of Ghana,

³School of Nuclear and Allied Sciences, University of Ghana, Radiological and Medical Science Research Institute, Ghana Atomic Energy Commission.

Email of presenting author: pwamangc@yahoo.com

INTRODUCTION/OBJECTIVE: Studies have shown that the incidence of breast cancer is high among women with high BD and vice versa, high BD also reduces mammographic sensitivity. There is a dearth of research on mammographic BD in Ghana, and BD patterns among Ghanaian women are yet to be established. A preliminary study revealed that radiologists in Ghana categorizes mammographic breast densities of women by visual inspection of images, which is qualitative and subjective. There is currently no quantitative method of breast density estimation in Ghana. The objective of this study is to quantitatively estimate the VBD of the average Ghanaian woman and to establish their breast density patterns for the early detection of breast cancer. The specific objectives are to undertake a study on the visual BD estimation by radiologists in Ghana, to estimate the VBD of screened women in Ghana using an already existing commercial software, VOLPARA, to develop a model for the quantitative estimation of VBD, and to evaluate the performance of the developed model using clinical data and compare it with existing models.

MATERIALS AND METHOD: Purposive sampling technique was used in extracting unprocessed mammograms of 900 pre and post-menopausal women from a digital mammography equipment (HelianthusC) at Ghana's national referral hospital – the Korle-Bu Teaching hospital. Volpara software is currently being used to generate volumetric breast densities from the extracted images.

RESULTS: Study is ongoing.

CONCLUSION: It is expected that at the end of the study, VBD of the average Ghanaian woman will be successfully estimated. It is also expected that breast density patterns within the study population will be identified and characterized. Visual BD estimation by radiologists will be done, as well as an assessment of its accuracy and reliability. Additionally, a model for quantitative VBD estimation will be developed and assessed for its effectiveness. Finally, it is expected that the results of this study would be a significant contribution to the understanding of breast density patterns among Ghanaian women, serve as a baseline data upon which further research can be done, and possibly influence clinical practices related to breast cancer screening and diagnosis in Ghana.

KEYWORDS: Breast, Density, Mammography, Ghana, Women, Cancer.

DOSIMETRIC COMPARISON OF FLATTENED AND UN FLATTENED BEAM FOR HYPOFRACTIONATED VOLUMETRIC ARC RADIOTHERAPY

Ratheesh K. E¹; Sherin J. Maxwell², Sunil N²

¹D. Y. Patil Education Society, Kolhapur, ²HCG Apex Cancer Centre, Mumbai, India.

Email: kmayakannan.phy@gmail.com

AIM/BACKGROUND: The objective of this study was to examine the effects of using flattened (FF) and unflattened (FFF) radiation beams in hypofractionated volumetric Arc radiotherapy (VMAT). The main aim was to explore the characteristics of FFF beams, which exhibit low-dose regions when transitioning from the center to the edges, and to identify the advantages of using FFF beams over FF beams.

MATERIALS & METHODS: We evaluated a group of twenty-two patients who had previously completed treatment with FF VMAT. The prescribed doses were 60 Gy/20#s (N0:8) and 55 Gy/20#s (N0:14), with the intention of delivering 95% of the target volumes (D95%) at the prescribed dose and achieving a dose homogeneity of 95-107%. The dose rate was set at 600 MU/min for FF plans and 1400 MU/min for FFF plans. The optimization goals and iteration numbers remained the same for both types of plans. The evaluation of treatment volumes focused on the near-maximum dose (D2%), average dose (D50%), and near-minimum dose (D98%) as defined in the protocol outlined in the ICRU 83 Report. The homogeneity index (HI), conformity index (CI) and Gradient Index (GI) were analysed. Also to compare the two types of plans, we assessed the total MU and treatment duration by delivering the plans under phantom conditions.

RESULT: There were no significant disparities observed between the two approaches when examining the D2% (Gy), D98% (Gy), D50% (Gy), HI, and CI. The doses to the OAR were comparable in both plan types. However, FFF plans exhibited a favourable gradient index compared to FF plans. Notably, FFF plans required higher MU than FF plans, demonstrating a significant difference. On the other hand, the utilization of FFF plans led to a substantial reduction in treatment time.

CONCLUSION: Our studies revealed a notable decrease in treatment duration when utilizing the FFF beam compared to the FF beam. This reduction in time is particularly advantageous, considering the high relative biological effectiveness (RBE) of FFF beams, especially in the context of hypofractionated radiotherapy. Additionally, the use of FFF beams can contribute to minimizing errors caused by intra-fractional motion. It is essential to conduct further investigations into the effects of higher monitor units (MU) in VMAT treatment delivery to assess its implications on the prognosis and quality of life of cancer patients.

KEYWORDS: VMAT, Hypo fractionated RT, FFF, FF, Gradient Index

CREATING A CT TEMPLATE-BASED ATTENUATION CORRECTION METHOD FOR PELVIC PET/MR IMAGING

Kalpana Parajuli¹, Karuna Raya Chhetri², Usha Poudel Lamgade³, Surendra Maharjan⁴, Jarmo Teuhon⁵, Mika Teras⁵

¹Department of Biosciences, Abo Akademi University,

²Department of Radiology & Imaging, Sharda University, Greater Noida, India,

³Department of Radiology & Imaging, Chitwan Medical College, Bharatpur, Nepal,

⁴Department of Radiology & Imaging Sciences, Indiana University School of Medicine,

⁵Turku PET Center, University of Turku, Turku, Finland.

Email: karunaraya7@gmail.com

BACKGROUND/OBJECTIVE: Three-class MR-based attenuation correction (3C MRAC) in Philips Ingenuity TF PET/MR ignores attenuation by bone. The omission of bone in the attenuation map has been shown to cause clinically significant bias of over 10% in PET quantification. In this study, a new method of attenuation correction in pelvic PET/MR that uses a CT template and accounts for attenuation by bone is proposed.

MATERIALS AND METHODS: Out of 21 CT datasets that were previously acquired during PET/CT examination of prostate cancer patients at Turku PET center, one CT image was chosen as a reference and the remaining datasets were brought to the same anatomical space using B-spline deformable registration. Simple averaging of aligned CT images resulted in a CT template of the pelvis region, which was warped onto the target MRI space to generate a patient-specific pseudo-CT (pCT) using multi-modal registration. The pCT was used for attenuation correction and for each patient, three different PET images were generated, two of them with continuous (PET_{continuous}) and discrete attenuation coefficient for bone (PET_{discrete}) respectively, and the other one without bone information (PET_{no bone}). These images were compared to a PET image corrected by the CT-based attenuation map (PET_{CT}). Linear regression analysis (LRA) was performed for 7 volumes of interest (VOI), namely rectum, urinary bladder, iliacus muscle, prostate gland, vertebra, femur and gluteus maximus muscle. Correlation and Bland Altman plot were conducted and Standardized Uptake Values (SUVs) were compared.

RESULTS: Visual inspection of the relative difference image revealed a spatially varying bias for all three methods. PET_{continuous} showed least SUV bias compared to PET_{discrete} and PET_{no bone}. Bland Altman plot of PET_{continuous} showed least SUV bias for bony vertebra and femur VOIs, whereas excellent correlation was measured between SUV of PET_{CT} and all three different PET images.

CONCLUSIONS: A template-based pCT from MRI images could be used for attenuation correction in pelvic PET/MRI.

KEYWORDS: attenuation correction, PET/MRI, quantification, segmentation, atlas

DIRECTION MODULATED BRACHYTHERAPY TANDEM APPLICATORS FOR TREATMENT PLANNING COMPARISON WITH THE AARHUS[®] HYBRID APPLICATOR

Dylan Richeson¹, Suresh Chaudhari², Vibhor Gupta², Binod Manandhar¹, Sushil Beriwal^{2,3}, William Y Song¹

¹Department of Radiation Oncology, Virginia Commonwealth University, Richmond, VA, USA

²American Oncology Institute, India, ³Varian, Palo Alto, CA, USA

Email: sureshc1@americanoncology.com

BACKGROUND/OBJECTIVE: The rise of image guided adaptive brachytherapy (IGABT) in combination with advances in inverse optimization has led to a growing investigation into the use of anisotropic dose distributions for improving plan quality. The MR-compatible Direction Modulation Brachytherapy (DMBT) six-groove tandem applicator accomplishes this by using a novel six-peripheral-source-channel design. The authors sought to quantify the improvement in plan quality when compared against a state-of-the-art intracavitary-interstitial (IC-IS) hybrid applicator (Aarhus[®]).

MATERIALS AND METHODS: A cohort of three retrospective clinically delivered HDR cases using Varian's new Aarhus[®] hybrid applicator was re-planned within the BrachyVision[®] (v16.1) treatment planning system (BV-TPS), using the latest VEGO[®] inverse optimization algorithm, with dose heterogeneity accounted for through the AcuroSBV[®] model-based dose calculation algorithm. Two DMBT tandem models (5.4 & 8 mm thick) designed with a MR-compatible tungsten alloy were used for re-planning each of the three clinical cases under two scenarios: 1) with needles and 2) removing needles, resulting in total of 12 plans. A two-step inverse optimization technique was performed such that the lowest possible OAR D2cc doses could be achieved while 1) keeping equivalent target coverage ($\Delta\text{CTV}_{\text{HR-D90}}$ to within $\pm 0.5\%$) and, at the same time, 2) maintaining the general dose distribution of the original plan.

RESULTS: The 8 mm DMBT tandem model improved OAR sparing in both the with& removed interstitial needles cases, whereas the 5.4 mm model improved OAR sparing in the with interstitial needles cases. Hence, both models produced notable plan quality improvements over the Aarhus[®] hybrid applicator plans.

CONCLUSIONS: The DMBT tandem models were successfully incorporated into a commercial TPS and were each able to generate notable D2cc reductions to OARs, without compromising target coverage, compared against the latest Aarhus[®] IC-IS hybrid applicator. In addition, the 8 mm DMBT tandem allowed removal of all needles while still achieving better plans. Larger study is necessary to validate this early finding.

KEYWORDS: Brachytherapy, image guided adaptive brachytherapy, intracavitaryapplicator

LINEAR ACCELERATOR RADIATION BUNKER SHIELDING INADEQUACY CONSTRUCTION ANOMALY – A REPORT

¹Ramamoorthy Ravichandran, ¹Tarani Mondal, ²Rajesh Kinhikar, ²Shrikant.N.Kale, ¹Ravi Kannan

¹Cachar Cancer Hospital and Research Centre, Silchar-788 015, Assam, India

²Tata Memorial Centre, Mumbai, Maharashtra-400012 India.

Email: ravichandranrama@rediffmail.com

BACKGROUND/OBJECTIVE: In a True Beam© Varian linear accelerator installation site, 2.4m concrete barrier with $\rho=2358\text{Kg/M}^3$ in two primary walls and roof were constructed. During preliminary radiation survey excess radiation levels were encountered. Further corrective actions are outlined. Investigations related to all aspects of concrete shielding, including planning, patterns of radiation leaks, reasons for shielding inadequacy and cost benefit from risk perspective.

MATERIALS AND METHODS: The Linac was energized in in October 2022. The maximum radiation levels for 15 MV (600MU/min) were 46 $\mu\text{Sv/h}$ (4.6mR/h), 29 $\mu\text{Sv/h}$ (2.9mR/h) and 76 $\mu\text{Sv/h}$ (7.6mR/h) (at gantry orientations 90°/180° 270°). Emitted photon energy was confirmed. Regulatory Body (AERB)) objected higher radiation level for 270° orientation, outer facing wall, with occupancy for public T=1. Accredited Lab reports of concrete were all above 2500Kg/M³ (n=75), but transmission calculations yielded $\rho=1.9\text{-}2.0$ g/cc. Matrix Survey revealed three different patterns; normal pattern for 180° beam(towards roof) , uniform higher transmission in inner wall (90°) and patchy type hot spots in the outer wall (270°). Regulatory authority permitted primary 4.6mR/h, as the Annual time averaged dose rate (TADR) 15MV 0.80 mSv/y (with occupancy for radiation workers). They recommended 1 HVT of additional shielding to reduce the Annual TADR from 1.395 mSv to < 1.00 mSv, for general public. Steel plate 3.30m x3.30mx40mm (1HVT for 15MV) is fixed in primary beam area. After adding shielding (40mm Steel), the annual TADR (15MV) reduced from 1.395mSv/y to 0.59 mSv/y.

RESULTS: We confirmed application of vibrators and adequate supervision during concreting. Our clarifications on all other factors appears to be in order. We feel that the utilization of river bed rubles crushed stone fragments (aggregates) instead of correct type machine crushed granite stones, and labor issues around Covid prevailing period would have caused construction issues.

CONCLUSION:It is strongly recommended that correct type of stone aggregates should be used for such intricate shielding civil executions.

KEY WORDS: Linear Accelerator, Radiation Bunker, radiation levels, RCC aggregates

REFERENCES:

1. Ravichandran R, Bandana Barman, Tarani Mondal, Shrikant.N.Kale, Rajesh A. Kinhikar, Ravi Kannan. Shielding Conformity issues in a concrete bunker of a high energy linear accelerator. J Med Phys. Under Print. 2023.

EVALUATION OF SET-UP ERRORS USING DELIVERY ANALYSIS AND ARC-CHECK IN RADIXACT X9

Unnimaya V.S, Sreedevi E, Debnarayan Dutta

Department of Radiation Oncology, Amrita Institute of Medical Sciences, Kochi, India

Email : unnimayasudhi98@gmail.com

BACKGROUND/OBJECTIVE: Radixact is the latest generation of tomotherapy delivery system with a shorter irradiation time than Hi-Art & Tomo-HD. Delivery analysis(DA) is a stand-alone platform that compares the pre-treatment and measured in-treatment data and quantifies the consistency of post-patient detector signals during treatment. ArcCHECK is a pre-treatment verification tool that utilizes a 3D array of detectors to monitor the dose delivered.

MATERIALS AND METHODS: Radixact, DA, cheese phantom, density plugs, ArcCHECK.

A cheese phantom to mimic pelvic anatomy, was moved in X, Y and Z directions (1mm, 3mm, 5mm, 10mm) to simulate set-up errors. The corresponding sinograms were acquired by a 1D array of in-built detectors. DA's ability to detect the motion was evaluated by comparing the sinogram obtained by moving the phantom with a reference sinogram obtained without movement.

The above shifts were delivered to ArcCHECK and passing rates were noted using a in-built gamma analysis software.

RESULTS: As observed from the gamma analysis in DA, the tolerance did not change significantly upto 2mm/2%.When the tolerance values were lowered, the results were affected. For 0.3mm/0.3% the average gamma pass rates in X,Y & Z directions were 93.227%, 86.66% and 85.427%. The pass rate decreases in proportion to the magnitude of shift amount & no significant difference was found with the direction of movement.

The pass percentage of 5mm shifts in X,Y and Z directions, observed from ArcCHECK measurements are 83.5%, 72.7% and 90.5%.

CONCLUSIONS: ArcCHECK serves as an efficient tool for pre-treatment dose analysis with high detection sensitivity to assess the setup errors that can happen during treatments. On the other hand, DA enables in-treatment assessment of setup errors, automatically by using exit detector sinogram data.

KEYWORDS: Delivery Analysis, Tomotherapy, sinogram, ArcCHECK, gamma analysis.

THE RADIATION-INDUCED CHARACTERISTIC SHIFT ON CONTROL-SEMICONDUCTORS USED IN LINAC HEAD

Shyamprasad S¹, Christopher Varghese¹, Rijin NT², Mithun Mohan¹, Navin Singh³, Shraddha Srivastava³, Teerthraj Verma³, M. L. B. Bhatt³ and M.M Musthafa¹

¹ Nuclear and Radiation Physics Group, Department of Physics, University of Calicut, Kerala² Jain University, Department of Physics, Bangalore³ Department of Radiotherapy, King George's Medical University, Lucknow

Email: shyamprasad151@gmail.com

BACKGROUND/OBJECTIVE: Ionizing radiation can alter the properties of semiconductor devices for desirable or undesirable amounts depending on the dose imparted. Radiotherapy equipment has components made of semiconductors. When these devices are operated, these semiconductors are exposed to radiation fields. The purpose of this study is to analyse the radiation-induced I-V Characteristics shift of Semiconductor devices used in Linac using expEYES-17. These abstract analyses the characteristics of the non-irradiated device compared with the lifetime irradiated device.

MATERIALS AND METHODS: ExpEYES-17-which functions as a low-frequency oscilloscope, function generator, programmable voltage source, frequency counter and data logger was used to study the variation in output characteristics of the semiconductor devices. MOSFETs and DIODEs used for this purpose were taken from: one of the components of the Gantry Head of Linac (Elekta Synergy) functioning for the 9 years; another one which is newly purchased and irradiated manually for 30 minutes by placing it on dmax for 15MV energy photon, and a non-irradiated one of the same model. The variation in the output characteristics (I-V Characteristics) for all the devices was analysed using expEYES-17.

RESULTS: Radiation effects are making a prominent change in the output characteristics of the devices. Variations were observed in the I-V Characteristics and this variation shows that the doping is changed and the depletion layer is narrowing. These shifts in the characteristics significantly affect the device's performance.

CONCLUSIONS: The results show that lifetime exposure from the medical linear accelerators **significantly changes** the output characteristics of electronic devices, especially MOSFET, Diode etc. The formation of dark current and the tunnelling effects impact the characteristic behaviour of the device dosimetrically. However, proper shielding is sufficient for safety and the MLC's accuracy, affecting treatments like SRS and SBRT. Therefore, the performance of these devices should be monitored periodically to ensure the quality and accuracy of the treatment delivered.

KEYWORDS: Linear Accelerator, Control Semiconductors, Dosimetry, Radiation Safety.

STANDARDISATION OF SURFACE GUIDED RADIATION THERAPY PHYSICS COMMISSIONING IN A MULTI-CAMPUS ORGANISATION

Deepak Basaula¹, Jenny Lydon¹ Keith Offer¹, Sisira Herath¹, Rachitha Anthony¹, Joby Matthew¹, Deloar Hussain¹, Adam Yeo¹, Derrick Wanigaratne¹, Jidi Sun¹, Vanessa Panettieri^{1,4,5}, Tomas Kron^{1,2,3}

¹Department of Physical Sciences, Peter MacCallum Cancer Centre, Melbourne, Australia

²Sir Peter MacCallum Department of Oncology, University of Melbourne, Australia

³Centre of Medical Radiation Physics, University of Wollongong, Australia

⁴Central Clinical School, Monash University, Melbourne, VIC, Australia

⁵Department of Medical Imaging and Radiation Sciences, Monash University, Clayton, VIC Australia

Email: Deepak.Basaula@petermac.org

BACKGROUND/OBJECTIVE: Surface Guided Radiation Therapy (SGRT) is a technique increasingly adopted in Radiation Therapy for daily setup and intra-fraction monitoring of patients treatments. SGRT uses non-ionising structured light to acquire 3D surface images of the patient on the treatment couch that can be matched to the reference surface acquired during CT simulation. Our organisation installed a total of 10 AlignRT systems (Vision RT, London, UK) system since 2021 across five campuses. Here we report our approach of commissioning of these systems and key results and challenges encountered during the commissioning process in multi-campus environment.

MATERIALS AND METHODS: A physics working group consisting of at least a representative from each campus was formed and a standardised comprehensive commissioning plan was developed through relevant literature. A equipment roster to schedule for certain phantoms and equipment that are only available in limited quantity at our organisation was made to ensure the smooth commissioning process at each campus. Additional test objects were 3D printed in advanced and dispatched to each relevant campuses. Appropriate vendor and in-house training were organised prior the system installation for staff to familiarize themselves with the system and specific tests.

RESULTS AND DISCUSSION: Commissioning included all tests recommended by AAPM TG 302 and ESTRO-ACROP guideline. End-to-end workflow-testing for intended treatment sites allowed for smooth collaboration with other professionals. AlignRT real time deltas (RTDs) at the couch extreme position of 90° for both translational and rotation axis were found within 0.3mm/0.1° of expected shifts. However, it was noted that the accuracy of positioning was strongly dependent on the choice of Region of Interest (ROI), which needs to be appropriate in size and have variation in topography. The standardisation approach taken was proven to be effective in commissioning and developing the treatment guidelines and QA procedures. Interruption of clinical operation was minimized by performing the 4 day commissioning program mostly on weekends and after hours.

CONCLUSIONS: Commissioning of ten SGRT systems in 5 campuses was completed in a timely manner through a comprehensive planning and standardisation allowing minimal interruption to treatment machines workload.

KEYWORDS: Surface-guided radiation therapy, Patient Setup, treatment monitoring

STUDY OF CAPABILITY OF DELIVERY ANALYSIS SYSTEM TO DETECT THE INTRAFRACTIONAL CHANGES DUE TO MOTION, INTERRUPTION AND THE PRESENCE OF GAS/AIR CAVITY IN RADIXACT DELIVERY SYSTEM

Sreedevi E¹, Unnimaya V S², Debnarayan Dutta³

Department of Radiation Oncology, Amrita Institute of Medical Sciences & Research Center, Kochi, Kerala, India.

Email: krishnansreedevi@yahoo.com

BACKGROUND/OBJECTIVE: Radixact is the latest generation of Tomotherapy Delivery Systems which enables continuous delivery from 360 degrees with a shorter irradiation time than Hi-Art & Tomo-HD. Delivery Analysis (DA) is a stand-alone platform that compares pretreatment and measured in-treatment data with information describing planned treatment delivery. It is intended to compare quantitatively measured detector sinogram and planned MLC sinogram. The purpose of this study is to evaluate the capability of DA to detect the intrafractional changes during Image Guided Radiotherapy in tomotherapy mode.

MATERIALS AND METHODS: The study was performed in Radixact X9 Delivery system and used the DA software for evaluation. A Cheese phantom with different density plugs was used to replicate the pelvic anatomy. To study the intrafractional changes due to motion, the phantom was moved in X,Y& Z directions with 1,3,5 &10mm shifts and corresponding sinograms were acquired. The ability of DA to detect the motion was evaluated by comparing the sinogram obtained by moving the phantom with a reference sinogram obtained without movement. To assess the sensitivity of Gamma analysis tolerances, the values were changed to 3mm/3%,2mm/2%,1mm/1%,0.5mm/0.5% and 0.3mm/0.3%.Treatment interruptions were made and studied. Also various air cavities were introduced in different positions of the phantom, which is analogues to the residual gas present in the abdomen.

RESULTS: It was observed from the gamma analysis that the tolerance did not change significantly up to 2mm/2%.When the tolerance was lowered, significant changes were noticed. Pass rate decreases in proportion to the magnitude of the shift and no significant difference was found with the direction of movement. Treatment interruption showed no significant change. The pass rates remained almost same for different air cavities in different parts of phantom.

CONCLUSIONS: In-treatment assessment of DA provides high detection sensitivity and is an efficient tool that can detect the intrafractional changes.

KEYWORDS: Delivery Analysis, Radixact, sinogram, gamma analysis.

DOSIMETRIC COMPARISON AND EVALUATION OF SINGLE ARC AND DOUBLE ARC VMAT PLANNING TECHNIQUES FOR PROSTATE CANCER

Roshini V¹, Prabhu R², Sasipriya P², Shrividhya A², Manju K¹, Alex John Peter D²

¹School of Medical Physics, Bharathidasan University, Tiruchirappalli, India

²Department of Radiation Oncology, Harshamitra Oncology Private Limited, Tiruchirappalli, India,

Email: prabhumedphy@gmail.com

BACKGROUND/OBJECTIVE: This paper aims to compare dosimetry differences based on of radiotherapy plans using single arc and double arc VMAT plan for the carcinoma of prostate. VMAT were planned for 10 patients with the prescription of 80 Gy in 40 fractions.

MATERIALS AND METHODS: All patients were in supine position and the legs and pelvis were fixed using a belly-board. Then Computedtomography (CT) was performed from the top of the iliac crests to the perineum with 3 mm CT slices. Before the CT scan, each patient's rectum was empty. The bladder was filled to a degree that was sustainable and reproducible for daily treatment. All of the patients were planned with single-arc (SA) and double-arc (DA) VMAT techniques in Varian Eclipse v13.7.39 (Varian Medical Systems, USA) planning system was used for RT contouring and RT planning. The first arc was created with 181°-179° degrees clockwise by rotation 15° degrees of collimator. The second arc clockwise was created with 179°-181° degrees opposite clockwise by rotation 345° degrees of collimator. All of them had same dose-rate which was 600 MU/min and 6MV photon energy. Radiation Oncologist contoured gross tumour volume (GTV) to include all known diseases with elective pelvic node irradiation including obturator, internal, external iliac and presacral lymph nodes in the RT field. A dose volume histogram (DVH) is used to analyse each evaluation index of planning target volumes (PTV) Conformity index and homogeneity index. Organs at risk (OAR) such as the bowel, rectum, bladder, left and right femur heads compared with SA and DA VMAT plans.

RESULTS: The SA and DA plan to provide a reasonable balance of delivery time and enhanced plan efficiency. The Double arc VMAT revealed a statistically significant improvement in PTV (D99) coverage and OAR sparing; specifically, the rectum and bladder wall (D50), in addition to the penile bulb. VMAT double arc plans expressed superior conformity with fewer monitor units and shorter treatment time.

CONCLUSIONS: This study demonstrates double arc VMAT plan has better control of the organ at risk, lesser MU and protects the normal tissue irradiation and is recommended for patient's benefit.

KEYWORDS: Prostate Cancer, VMAT, Single Arc, Double Arc, Dose Volume Histogram, Dosimetry

DOSIMETRIC EVALUATION OF CRANIOSPINAL IRRADIATION PLANNED WITH VMAT AND 3DCRT

Ahamed Basith¹, Reshma Bhaskaran¹, Sushama P¹, Ajayakumar T¹

¹Department of Radiotherapy, Government Medical College, Kozhikode

Email: ahamedbasith04@gmail.com

BACKGROUND/OBJECTIVE: Three dimensional conformal radiotherapy (3DCRT) with daily feathering is widely accepted technique for Craniospinal Irradiation (CSI). The treatment results in longer treatment times due to the beam preparation time and couch kicks. Volumetric Modulated Arc Therapy (VMAT) is another method to treat CSI in which treatment time is significantly reduced in our initial observation. This is a desirable achievement for a busy centre with limited staff strength, like ours. However detailed dosimetric and clinical evaluation should be done prior to putting the technique in use for all patients. This is an attempt to compare the dosimetric parameters of 3DCRT and VMAT to arrive at a department protocol at our hospital.

MATERIALS AND METHODS: This study included treatment plans of 23 CSI cases from 2014 to 2022 at Government Medical College, Calicut. 3DCRT and VMAT plans were done for each case using Eclipse version 15.5.1 (Varian Medical Systems, Palo Alto, CA). The plans were compared using various dosimetric indices and dose to organs at risk (OAR) were analysed using DVH. Average treatment execution time was retrieved from the treatment summary available in the ARIA system.

RESULTS: VMAT plans show better mean CI of 0.91 ± 0.05 and mean HI 0.09 ± 0.01 in comparison to 3DCRT. Better normal tissue sparing is also achieved in VMAT. 3DCRT has the advantage of lesser mean dose for laterally spaced critical organs, like Larynx, Lungs, and Kidneys. VMAT is more useful for sparing of all the other organs in the study, such as Eyes, Parotid, Thyroid, Esophagus and Heart. The average maximum dose of ovary/testis is only 61 ± 87.22 cGy in VMAT in comparison to 3DCRT (126.66 ± 287.62 cGy). The average time taken to treat one fraction of VMAT is 25.9 minutes compared to 42.33 minutes for 3DCRT.

CONCLUSIONS: VMAT shows better organ sparing for medially located organs at risk and is easier to setup. The treatment time required is also relatively less for VMAT in comparison to 3DCRT. However the relatively higher dose received by the laterally placed organs warrants further studies in terms for Secondary cancer complications probability and clinical correlation with the results, prior to its implementation.

EVALUATION OF EFFECTIVENESS OF VIRTUAL BOLUS AND SKIN DOSE FOR TOTAL SKULL IRRADIATION TREATED WITH HELICAL TOMOTHERAPY.

Ashitha M K, Alma Peter, Amala N Kumar, Annex E H. Debnarayan Dutta

Department of Radiation Oncology, Amrita institute of Medical Sciences, Ponekkara P. O Kochi, Kerala, India.

Email: ashitha20945@aims.amrita.edu

BACKGROUND/OBJECTIVE: The huge, shallow, and curved treatment volume presents technical and dosimetric issues in scalp radiation. The multiple matched electron fields and electron photon combination of traditional treatments in the Linear Accelerator causes complications with dose homogeneity, considerable exposure to the brain, and the potential overdose or underdose at the field junctions. The ability to deliver tangential beamlets to the scalp at all points, helical tomotherapy gives more advantage over Linac based IMRT delivery of total scalp. The tomotherapy plan gives the best target coverage and conformity, with low doses to the brain and organs at risk. Since the inverse planning is involved, the potentiality of over fluence peak generated at the skin to ensure dose homogeneity is an important concern, dosimetrically and clinically. Virtual bolus is introduced to avoid overdose on the skin surface. This study evaluates the performance of the virtual bolus and the evaluation of skin dose in the treatment delivery.

MATERIALS AND METHODS: The target is delineated on the whole scalp during complete scalp irradiation, from the surface of the scalp skin to the depth of the skull. To simulate the same, Planning Target Volume (PTV) scalp is contoured in arcCHECK phantom. The phantom plans are created in Precision Planning system (Accuracy Inc). To avoid the shared voxels of PTV with air, virtual bolus is used during optimization, by adding the virtual bolus thicknesses of 0 to 10mm in the steps of 1mm. The same plans are delivered in the phantom, the gamma analysis was carried out using SNC arcCHECK software. In the delivery, the bolus was absent. To evaluate the surface dose, the EBT3 gafchromic film is placed on the phantom during the delivery.

RESULTS: When the virtual bolus thickness is increased from 0 to 10mm in steps of 1mm, the gamma pass percentage (3%,2mm criterion) falls. And up to 5mm virtual bolus thickness, the gamma pass rates are in acceptable limits. Gamma pass rates for the plan decreased to 50% for 10mm virtual bolus thickness. In the film analysis, the higher skin dose is observed in the plan where the PTV is with zero margin and no bolus is used for optimization. In the plan where the virtual bolus of optimal thickness is present for optimization, there is a considerable reduction in skin dose.

CONCLUSIONS: The optimal virtual bolus thickness is found by avoiding the over fluence peak while maintaining adequate dose delivery precision.

KEYWORDS: Skull Irradiation, Tomotherapy, Virtual Bolus, arcCHECK

DETERMINATION OF PATIENT SET-UP ERROR FOR PELVIC RADIOTHERAPY: IS COMBINED-IMMOBILIZATION TECHNIQUE BETTER THAN CONVENTIONAL IMMOBILIZATION?

G.Kesavan¹

¹Department. of Radiotherapy, Vadamalayan Hospitals, Madurai.

Email: k7_mp@yahoo.co.in

BACKGROUND/OBJECTIVE: Radiotherapy plays a vital role in the treatment of pelvic malignancies such as the uterine cervix, endometrium, rectum, and prostate. In conformal external beam radiation therapy, accurate daily patient positioning is essential to reduce the likelihood of a geographical miss. The preference for immobilization must minimize mobility throughout the treatment session while keeping the patient's body in a reproducible position. The primary objective was to assess set-up errors and secondary objective was to determine optimal immobilization with highly reproducible method for pelvic radiotherapy.

MATERIALS AND METHODS: A total of 60 patients received pelvic external beam radiotherapy (50 Gy in 25 fractions). Among them, 20 patients were immobilized using a whole-body vacuum bag cushion (VBC), 20 patients were immobilized using a six-point thermoplastic immobilization system, and 20 patients were immobilized using a combined-immobilization technique (CIT) both VBC and the four-point thermoplastic immobilization system. Two orthogonal digitally reconstructed radiographs (DRR) were constructed as reference images. Similarly during set up two orthogonal [Anterior-Posterior and Right Lateral] images were taken in the portal image. The reference DRR and portal images were compared for shifts, and SE was calculated in the X-axis, Y-axis, and Z-axis directions. Furthermore, the planning target volume margin was calculated using the Van Herk equation for all three techniques and statistically analyzed.

RESULTS: A total of 840 images were assessed using portal images. The systematic errors and random errors were the highest in the VBC and six-point thermoplastic compared with CIT. 3D Systematic error (Σ) was 1.2, 2.0, and 1.8 mm for CIT respectively in the x, y, and z axes. 3D random error (σ) was 2.4, 2.5, and 2.1 mm for CIT respectively in the x, y, and z axes. The calculated PTV margins were the smallest for the CIT with 4.68, 6.75, and 5.97 mm, respectively, in the x, y, and z axes.

CONCLUSIONS: Based on our results we can conclude that among the three techniques, the combined-immobilization technique (CIT) was the most reproducible technique with the smallest PTV margins.

KEYWORDS: Set-up error, PTV margin, portal image

TIME TO QUESTION ON USING GENERIC CALIBRATION COEFFICIENT (N_{DW}) FOR NON-STANDARD FIELDS (IMRT) CLINICAL REFERENCE DOSIMETRY: A PRELIMINARY STUDY

Sathiyaraj¹ Gowtham Raj¹, Sampath kumar¹, Sandeep kumar¹ Kadirampatti Ganesh¹

¹ Deapartment of Radiation Physics, Kidwai Memorial Institute of Oncology, Bengaluru, Karnataka, India

Email: sathiarajmedphy@gmail.com

BACKGROUND: In reference dosimetry protocols such as IAEA TRS 398 and AAPM TG51, the absorbed dose-to-water calibration coefficient (N_{DW}) incorporates all perturbation correction factors. These correction factors were derived from standard reference conditions. However, in the clinical situation the modulated beams produce different beam fluences and create nonstandard conditions where the standard condition-based correction factors are expected to breakdown. This study aimed to investigate the reliability of adapting standard calibration coefficient for non-standard field reference dosimetry in IMRT patient specific quality assurance.

MATERIALS AND METHODS: The field chamber was cross calibrated against SSDL calibrated chamber for different clinical situations such as variable field sizes, dose rates, off axis conditions and for modulated beam conditions. For modulated conditions, a plan class specific reference (PCSR) field was created and used as one of the calibration reference fields. A total of nine non-standard calibration coefficients (N_{DW-ns}) were determined. IMRT clinical reference dosimetry (point dose) was performed for 70 (n=70) patients using these nine N_{DW-ns} and the results were compared with the TPS calculated dose.

RESULTS: For all patients the delivered IMRT plan dose calculated using each N_{DW-ns} individually. The measured dose was compared with TPS dose. The maximum measured dose deviation was observed up to 10% from TPS calculated dose. P value ($p < 0.001$) shows statistical significance between different non-standard conditions. The surprise results noticed that the variations in the measured dose for different non-standard conditions. PCSR and 6x6 fields based N_{DW-ns} were closer to the TPS calculated dose.

CONCLUSION: In radiation dosimetry there is an inherent assumption that the standard condition based N_{DW} valid for non-standard condition dosimetry like IMRT clinical reference dosimetry. In our study it is evident that this assumption is not correct since the measured dose varies as a function of different nonstandard condition based N_{DW-ns} . For IMRT clinical reference dosimetry we need plan specific correction factor rather than using generic N_{DW} which is derived from the standard reference conditions.

KEYWORDS: Reference dosimetry, IMRT, Patient specific qa, Treatment planning system and Plan class specific reference fields

EVALUATION OF OPTIMAL MINIMUM SEGMENT WIDTH IN VOLUMETRIC MODULATED ARC THERAPY FOR PROSTATE CANCER-AN INSTITUTIONAL STUDY

Gleetus Timothy¹, Sonu Goyal¹, Adarsh P P¹, Anet Abraham¹, Mary Joan²

¹Department of Radiation Oncology, Apex Hospital Jaipur, ²Department of Radiation Oncology, Christian Medical College and Hospital Ludhiana

Email: gleetus@gmail.com

BACKGROUND/OBJECTIVE: For radiotherapy treatment plans, the minimum segment width (MSW) plays a significant role in shaping optimized apertures and creation of segments of varying sizes and shapes. The effect of MSW on dose distribution in patients planned with VMAT for prostate cancer was evaluated using dose volume histogram (DVH) analysis in this study.

MATERIALS AND METHODS: Various penalties on minimum segment widths of 0.5, 1.0 and 1.5 cm was used to generate VMAT plans while other parameters kept constant for each of the 10 prostate patients selected for the study. The plans were done using 6MV photons in Monaco treatment planning system. The prescribed dose was 74Gy/37F to the PTV high dose and 56Gy/37F to the PTV low dose. The conformity index (CI) and homogeneity index (HI) of the planning target volumes (PTV), Dose to organs at risk (OARs), control points (CP), monitor units (MU), plan execution time (ET), and gamma passing rates (GPR) were compared between the three MSW groups. The treatment delivery accuracy was quantitatively analyzed for the influence of varying MSW using 2D array of 729 detectors along with Octavius phantom. GPR with a 3%DD, 3mm DTA were compared among three groups.

RESULTS: Comparison between plans of three different MSW's showed that treatment plan quality using MSW of 0.5cm and 1cm was found to be superior to 1.5cm. PTV coverage D95 reduced significantly when the MSW is increased to 1.5cm. In terms of plan deliverability, VMAT plans produced with MSW of 0.5cm had significantly higher MU's, CP's and plan execution time. Dose to OAR's showed smaller deviations regardless of MSW's. It is observed that as the MSW increases the total MU decreases and the GPR also fare better.

CONCLUSIONS: The 0.5cm and 1cm MSW groups had better VMAT plan quality than 1.5cm MSW. However plans with 0.5cm MSW had poor delivery efficiency than the other two groups. So in order to make ideal, we can choose 1cm MSW as an optimal choice to ensure good delivery plan quality and treatment efficiency for prostate VMAT plans

KEYWORDS: minimum segment width, dose volume histogram, VMAT, prostate cancer

A RADIOTHERAPY TREATMENT PLANNING EVALUATION FOR BILATERAL BREAST CANCER USING SINGLE ISOCENTER VOLUMETRIC MODULATED ARC THERAPY

Karthik S¹, Prabhu R², Shrividhya A²

¹Department of Radiation Oncology, Kauvery hospital, Trichy., India.

²Department of Radiation Oncology, Harshamitra Oncology Private Limited, Trichy., India.

Email: karthikmphy@gmail.com

BACKGROUND/OBJECTIVE: Delivery of irradiation in women with bilateral breast conserving surgery (BCS) represents a technical challenge. To evaluate plans using single isocenter volumetric modulated arc therapy techniques specifically for synchronous bilateral breast cancer patients undergoing right-sided lumpectomy, left-sided mastectomy and regional lymph node dissection (level I, II axillary lymph nodes).

MATERIALS AND METHODS: Five bilateral breast cancer patients underwent right-side lumpectomy, left-sided mastectomy, and regional lymph node dissection. All Patients immobilized using vacuum bag in a supine position with both the arms above the head. CT scans were done with a slice thickness of 3 mm during normal breathing. The PTV (right and left breast) was delineated in accordance with standard guidelines. Organs at risk (OARs) contoured were both lungs and heart. VMAT plan were generated with a prescription dose of 50 Gy in 25 fractions. Eclipse V13.7.39, (Varian Medical Systems, USA) treatment planning system (TPS) was used for all planning purposes. VMAT plan was done using three continuous arcs (arc length: 150°–210°) with 6 MV photon beams on Unique Performance linear accelerator (Varian Medical Systems, USA). A single isocenter placed medially under the sternum was used for optimization. The collimator angle was set to a value of +10°.

RESULTS: VMAT provided sufficient dose coverage and a high dose conformity index for all right breast, left chest wall and lymph node targets. The dose distribution was almost homogenous. The correlation between the monitor units and the conformity indices was significant for both the right and the left breast. In the VMAT plan, the PTV 95% dose covered 48.85 ± 0.76 Gy, the results of Dmean and V20Gy of lungs using VMAT (17.6%). The mean V5Gy in VMAT plans (46.16%) Also, VMAT resulted in Dmean to heart (8.23Gy).

CONCLUSION: Single Isocenter VMAT is an effective treatment technique for bilateral breast cancer patients, providing a highly conformal dose and a good dose distribution. The correlation between the MU and the dose conformity serves as a useful evaluation tool for this technique. Overall, the results indicate a better sparing of lung and heart at low doses with VMAT.

KEYWORDS: Bilateral Breast Cancer, Breast Conserving Surgery (BCS), VMAT, Single Arc, Double Arc, Dose Volume Histogram.

REAL TIME PATIENT IDENTIFICATION AI TOOL TO PREVENT PATIENT MISIDENTIFICATION IN RADIOTHERAPY

Teerthraj Verma^{1*}, Shriram Rajurkar¹, SP Mishra², MLB Bhatt¹

¹Department of Radiotherapy, King George's Medical University, UP Lucknow

²Dr ram Manohar Lohia Institute of Medical Sciences, Lucknow

Email: teerth05kashi@gmail.com

BACKGROUND & OBJECTIVES: The care of cancer has improved to an advanced level with ease and rapidity in the last few decades. However, one of the radiological events in radiation therapy facilities is mistakes in correctly identifying the patients. The administration of the incorrect dose at the incorrect site, to the incorrect patient, during radiopharmaceutical administration, radiological scans, etc may be caused by an error in correctly identifying the true patients. This may results in an immutable radiation exposure effect. The purpose of this work is to develop a real-time patient identification programme based on deep learning in Python that will help in reduction of errors in correctly identifying the patients.

METHODS: To develop and implement a python deep learning based real-time patient identification program, we have created an artificial intelligence (AI) Python programme to prevent such unwanted events, taking into account the radiological and medication administration instance of the wrong patient receiving treatment due to patient misidentification. This programme was created in three steps and has two distinct user interface versions, version 1.0 and version 2.0. This program can be run in any OS having python environment. Additionally, an external camera embedded with the OS for the purpose of face detection was installed at the end of maze wall so that patient can be verified just before their radiotherapy. The display of the camera may be placed at the console area for the convenience and confirmation of the correct patient by operator of the radiotherapy unit.

RESULT: This programme provides real-time patient identification information together with the other pre-set parameter such as disease site etc. The programme facilitate output "Unknown" if a patient's relative or an unknown person is found in a restricted region. The results of this Python-based programme allow patient identification which has already registered in the programme.

INTERPRETATION & CONCLUSIONS: This Python-based programme is useful for verifying the patient's identity before beginning therapy, giving medications, and beginning other medical procedures, among other things, to avoid unintended medical and health-related complications that may arise as a result of mis-identification.

KEYWORD: AI tools, Patient Identification, Incidence in radiotherapy, Misidentification in Healthcare, Python

ENHANCING BRACHYTHERAPY PRECISION: EXPLORING THE DOSIMETRIC IMPACT OF VARIABLE POLYLACTIC ACID INFILL RATIOS IN 3D PRINTED PATIENT-SPECIFIC VAGINAL APPLICATORS

Narender Kumar¹, Nithin P¹, Ninad Patil, Vinay Saini, Abhishek Singhal, Sanju, Alka Kataria, Sanjay Barman, Ashutosh Mukherji, Satyajit Pradhan

¹Department of Radiation Oncology, MPMCC, TMC, Varanasi, India

Email: narenderkumar816@yahoo.com

BACKGROUND: Brachytherapy is a widely used technique for precise radiation therapy delivery in cancer treatment. The emergence of 3D printing technology has opened up new possibilities for customized brachytherapy applicators. This study investigates the fabrication of brachytherapy applicators using a Fuse Deposition Modeling(FDM) 3D printer and polylactic acid (PLA) and Polyethylene Terephthalate+Glycol(PET-G) filament with varying infill percentage ratios. The goal is to dosimetrically compare these affordable applicators with the commercially available ELEKTA CVS applicator.

METHODS: The study employed a well-type ionization chamber, Flexitron brachytherapy unit housing 2 Ci CO⁶⁰ source, 3D printed vaginal cylinder applicators of different materials (PLA and PET-G) and different infill ratios, a 3D printed water-filled reference cylinder with 1.2mm outer wall thickness with matching geometry to the applicators, and the ELEKTA CVS applicator. The same dosimetric plans were created for each applicator and water-filled reference applicator, with consistent dwell positions relative to the bottom of the well-type ionization chamber. The experimental setup ensured each applicator was positioned precisely at the chamber's center. The charge collected by the chamber was recorded for all applicators and the water-filled reference applicator after executing the plan with the Flexitron brachytherapy unit. Results from each 3D-printed applicator and the CVS applicator were compared to those of the water-filled reference applicator.

RESULTS: The percentage variation in charge collected by the ionization chamber for each 3D printed applicator material compared to the water-filled reference applicator was within 3%. The CVS applicator exhibited a charge collection variation of 2.15% compared to the water-filled reference applicator.

CONCLUSIONS: The study demonstrates that 3D-printed applicators hold promise for patient-specific HDR brachytherapy treatment. However, further assessment of 3D printing techniques and material approval is necessary before clinical implementation.

KEYWORDS: Brachytherapy, 3D printing, polylactic acid, applicators, ionization chamber, ELEKTA CVS applicator.

DOSIMETRIC SENSITIVITY TO VARIOUS COMMISSIONING MEASUREMENT ERRORS FOR A LIAC INTRAOPERATIVE ELECTRON-BEAM RADIOTHERAPY UNIT

Mohammad Amin Mosleh-Shirazi^{1,2*}, Raziieh Rashidfar^{1,3}, Sareh Karbasi², Mazyar Mahdavi^{1,3}

¹Ionizing and Non-Ionizing Radiation Protection Research Center, School of Paramedical Sciences, Shiraz University of Medical Sciences, Shiraz, Iran, ²Physics Unit, Department of Radio-oncology, School of Medicine, Shiraz University of Medical Sciences, Shiraz, Iran, ³Department of Radiology, School of Paramedical Sciences, Shiraz University of Medical Sciences, Shiraz, Iran.

Email: mosleh_amin@hotmail.com

BACKGROUND/OBJECTIVE: *SWL-LIAC* is a commissioning-data-generation software that simulates the relative dosimetric characteristics of the *LIAC* intraoperative electron-beam radiotherapy unit, using only measured percentage depth-doses (PDDs) of four fields as inputs. The sensitivity of the generated dosimetric characteristics (used in patient dose calculations) to measurement errors of these crucial input PDDs is little reported. We aimed to study this for all generated outputs (4–12 MeV energies, flat-ended and 0°–45° beveled applicators of 3–10 cm diameters) for a ‘*LIAC-12MeV*’ unit. The findings can have practical and clinical accuracy consequences.

MATERIALS AND METHODS: The required *SWL-LIAC* inputs were measured with each beam intentionally misaligned on a water phantom. Intentional errors included 1° rotation or lateral (2 mm) or vertical (± 2 mm) displacements. Also, inaccurate water surface definition for the detector was simulated by ± 2 mm-shifted PDDs. To identify the most influential of six possible errors, measured PDDs, off-axis dose profiles and relative output factors resulting from misaligned measurements and inaccurate water surface definition scenarios were compared to the corresponding ‘error-free’ ones.

RESULTS: All the resulting errors in R90, R50, flatness, symmetry and penumbra were within 3.9 mm, 2.8 mm, 4.3%, 4.6% and 3.5 mm, respectively. The overall averages of the absolute differences in these indices from the ‘error-free’ fields were 0.8 mm, 0.8 mm, 0.6%, 0.4% and 0.5 mm, respectively. Errors in water surface definition for the detector had 4.4 to 22 times greater influence on PDDs than the other errors. The corresponding dose-profile values were 1.3 to 5.8 times. R90 and R50 were less affected by the errors in the small (3 and 4 cm diameter) and 45° beveled applicators.

CONCLUSIONS: On average, the studied errors caused relatively small changes in beam characteristics, although the maximum magnitudes of the observed errors were substantial. Among the investigated errors, defining the water surface inaccurately has the largest impact on the studied dosimetric characteristics. Overall, sensitivity to the investigated errors was found to be greatest with large-diameter flat applicators and/or lower electron energies. Given that these errors may occur simultaneously, special attention should be paid to ensuring correct dosimetric setup at commissioning.

KEYWORDS: intraoperative radiotherapy, IOERT, measurement setup uncertainty, dosimetry

ASSESSMENT OF THE USE OF SYNTHETIC CT PRODUCED BY DEFORMABLE IMAGE REGISTRATION OF PLANNING CT AND ON BOARD CBCT IN ADAPTIVE RADIOTHERAPY TREATMENTS OF HEAD AND NECK CANCERS

Sanju Sanju, Alka Kataria

Mahamana Pt Madanmohan Malviya Cancer Centre(MPMCC),TMC, Varanasi, Varanasi, India

Email: sanju@mpmcc.tmc.gov.in

BACKGROUND: Today imaging has an inevitable role in radiotherapy. Images of different modalities are used for diagnosis, treatment simulation, treatment planning, and treatment delivery. Deformable image registration (DIR) can also be used in various applications of radiotherapy including Atlas based segmentation, Multi modal image fusion, MRI based dose calculation, Contour propagation and adaptive radiotherapy. This study uses Velocity 4.0 (Varian Medical Systems, Palo Alto, CA) to perform deformable image registration. The new synthetic CT images generated by this software combine the anatomy of CBCT with calibrated voxel values from the CT Simulator images. Thus, there is a scope that the treatment plan, considered for adaptive radiotherapy can be replanned on these synthetic CT images. This will help save time and resources and reduce imaging doses for the patient.

MATERIALS AND METHODS: Type of study- Prospective observational pilot study (2 arms matched cohort study for dosimetric purposes). Both the original planning CT (Day 1) and acquired CBCT (as per inclusion criteria) were imported in Velocity software and a new synthetic CT was created. The newly generated synthetic CT image along with the new structure sets contoured on it were sent to TPS for Replanning and dose calculation. The new treatment plan made on re-simulation CT for treatment delivery was executed on synthetic CT to compare the geometric differences in structures and dosimetric differences in treatment plans between the two images.

RESULTS: Comparison of synthetic CT vs resimulation CT was done for all OARs and PTV volumes ($p < 0.01$): Geometric Evaluation: 1. Mean distance to agreement $< 0.2\text{mm}$. 2. Dice similarity coefficient $= 0.88 \pm 0.093$. Evaluation of differences in HU Values: 1. Difference in Mean HU value $< 2\%$. 2. Difference in the standard deviation of HU value in the two images $< 1.2\%$. Dosimetric evaluation: 1. Gamma analysis for global $\gamma < 1, 3\%/3\text{mm}$, was $> 95\%$. 2. Doses to OARs $< 2\%$ and PTV were found to be $< 2.8\%$ in all cases.

CONCLUSION: In this preliminary study, the Velocity generated synthetic CT was found to give acceptable results when compared with actual Simulation CT images. In order to implement it clinically further investigation with a large sample size is required.

KEYWORDS: Deformable image registration, synthetic CT images, Mean distance to agreement, Dice similarity coefficient

ETHOS - IMRT COMMISSIONING (TPS VALIDATION) BY USING MOBIUS 3D PHANTOM BASED ON TG-119

Naveen M, Suresh Chaudhari, Rampally Kumar

Department of Radiation Oncology, American Oncology Institute, Hyderabad, Telangana, India

Email: naveenm@americanoncology.com

BACKGROUND/OBJECTIVE: The purpose of this study was commissioning the Photon beam Intensity Modulated Radiation Therapy (TPS Validation) using TG 119 protocol and to define standard IMRT planning “problems” that physicists can use to test the accuracy of their IMRT planning and delivery systems. Differences between measurement and prediction may be caused by measurement uncertainty, limitations in the accuracy of dose calculations, and limitations in the dose delivery mechanisms. These tests will not serve to distinguish between these sources, but will serve to test the overall accuracy of the IMRT system.

MATERIALS AND METHODS: Ethos Machine and Ethos TPS, The American Association of Physicists in Medicine (AAPM) Task Group 119 prescribed a protocol to evaluate overall accuracy of IMRT system rather than independent uncertainty in dose calculation, dose delivery and measurement system. FF beam Open field (10cmx10cm), FFF beam Open field (10cmx10cm & 25cmx25cm) and four clinical test cases contouring has done by the institution based on the phantom Limitations and also the plans were created with different dose prescriptions (SIB) and planning objectives by institution (Hard Plans) and also created as per the TG-119 dose prescription and plan objectives. Then all the verification plans were created in a MOBIUS3D (Varian Medical Systems) phantom which contains 7 different location of measurement points (1 central axis point, 4 Off axis points, 1 Anterior point & 1 Posterior point) and aSi1200 electronic portal imaging device (EPID). High dose gradient and low dose gradient points (7 points) were measured using CC13 (Sensitive Volume-0.13CC) ionization chamber in Varian Medical Systems ETHOS Ring Gantry Linear Accelerator.

RESULTS: All the measurement points in off axis, anterior and posterior with ion chamber measured and planned doses were compared and % deviation calculated based on the TG-119 formulas and The gamma analysis was carried out by EPID, and the results were analysis with the acceptance criteria of 3% DD (dose difference) and 3 mm DTA (distance to agreement).

CONCLUSIONS: Our results were well within the limit given by AAPM TG119 report and this study providing us adequate confidence in delivering IMRT treatment and based on this report we are going to start the regular IMRT treatments

KEYWORDS: Ethos Machine & TPS, Mobius 3D Phantom, TG-119, Dosimetry

DOSIMETRIC COMPARISON OF HELICAL TOMOTHERAPY® IMRT (HT-IMRT) AND VOLUMETRIC MODULATED ARC THERAPY (VMAT) FOR BILATERAL BREAST CARCINOMA.

Megharaj V.Borade, Supriya M. Borade

HCG Manavata Cancer Centre, Nashik, 422002, Maharashtra, India

Email: mbmegharaj11@gmail.com

BACKGROUND/OBJECTIVE: Bilateral breast cancer is a rare disease found among women. Bilateral breast irradiation with conventional techniques could not achieve all the clinical and dosimetric goals. Whereas modern techniques like volumetric modulated arc therapy (VMAT) and helical TomoTherapy® (HT) can overcome those difficulties over conventional techniques. However, a comparative study of both of these techniques is needed to choose the suitable technique that can produce the best results.

In this study, the dosimetric comparison of HT-IMRT and VMAT for bilateral breast carcinoma with and without lymph nodes is performed. These two delivery techniques have been evaluated in terms of dosimetric matrices such as conformity index, homogeneity index, OAR doses, treatment time, monitors units and delivered and planned fluence compared and analyzed.

MATERIALS AND METHODS: Five cases of bilateral carcinoma of breast retrospectively selected which were already treated on TomoTherapy® with helical IMRT technique. Two cases out of five were chest walls plus supra clavicle nodes (MRM). One was only right breast (BCS) and left chest wall including sc nodes (MRM), one was right breast with right sc nodes (BCS) with left chest wall (MRM) and the last one was with both breast without lymph nodes (BCS). The prescribed dose was 40 Gy in 15 fractions for all cases except one case.

All treated cases were re-planned with VMAT on Eclipse™ version 13.7 and 16 treatment planning system with four full arcs. Plans were optimized to get the best possible results. Calculated VMAT plans were compared with HT plans in terms of CI, HI, OAR doses, MUs, and total treatment time.

RESULT: The mean conformity Index (CI) for HT was 0.9894 ± 0.009 and for VMAT was 0.9626 ± 0.014 . The significant difference found in Homogeneity Index (HI), HI for HT was 0.0845 ± 0.02 , and for VMAT it was 0.1152 ± 0.016 . The lung doses V20, V10, V5 and mean doses (19.79 ± 2.69 , 36.998 ± 6.32 , 53.4 ± 16.12 , 1138.1 ± 140.17) were significantly reduced with HT than VMAT (28.7 ± 4.73 , 76.43 ± 14.79 , 99.02 ± 1.13 , 1692.7 ± 195.61). The heart doses were significantly reduced with HT (662.8 ± 103.78) compared to VMAT (1144.4 ± 231.32). HT generates greater number of monitor units (MUs) and hence the treatment delivery time is more (8839.4 ± 3189.4 MUs, 10.34 ± 3.65 min) than VMAT (819.6 ± 69.77 , 1.37 ± 0.12).

CONCLUSION: This study found that the helical TomoTherapy® plans could provide superior target coverage and excellent OAR sparing than VMAT plans.

KEYWORDS: Helical Tomotherapy IMRT and VMAT

LONGTERM EVALUATION OF CORRELATION BETWEEN DISEASE FREE SURVIVAL (DFS) VERSUS QUALITY ASSURANCE RESULT AND OTHER PERFORMANCE INDICATORS FOR THE BRAIN METASTASIS PATIENTS TREATED WITH STEREOTACTIC RADIOSURGERY.

Biplab Sarkar¹

¹Apollo Multispeciality Hospitals, Kolkata, India

Email: biplabphy@gmail.com

BACKGROUND/OBJECTIVE: To evaluate the correlation between disease free survival (DFS) with the quality assurance result and standard performance indicators for brain metastasis patients treated by stereotactic radiosurgery (SRS).

MATERIALS AND METHODS: Total 81 patients with brain metastasis who received SRS in 1 to 3 fractions using volumetric modulated arc therapy techniques between 2019-2022 march were evaluated in this study. Depending upon the geometrical position and histopathology of disease, two kinds of prescription (RxD) are prescribed. RxD-1: Target coverage is 100% with centre (core) $\leq 110\%$ dose (homogeneous). RxD-2: Target coverage 100% with centre (core) $\approx 120\%$ dose (heterogeneous). Plans were created according to RxD-1 or RxD-2; point dose measurement (dose to MU agreement) in solid water phantom with 0.01cc ion chamber and gamma analysis in EPID dosimetry were done. DFS were analysed for the following factors: QA result, primary disease, Karnofsky Performance Status (KPS), target volume, and number of metastases.

RESULTS: Number of patients in RxD-1 and RxD-2 groups was 37 and 42, respectively. For RxD-1, Dose/MU agreement $2.7 \pm 1.5\%$ and Gamma passing rate (1%DD-1mmDTA)= $94.3 \pm 1.4\%$, 2%-2mm= $97.8 \pm 1.6\%$. For RxD-2 Dose/MU agreement, $5.1 \pm 3.1\%$; and Gamma passing (1%DD-1mmDTA)= $92.3 \pm 6.1\%$, and 2%DD-2mmDTA= $94.1 \pm 3.1\%$. Patients followed-up done with MRI imaging at 4-6 months intervals. Average DFS for RxD-1 and RxD-2 is 7.4 ± 6.9 , and 7.8 ± 6.0 months, respectively. Univariate analysis shows that dose to MU and gamma index have very a low correlation of 34.4% and 28.6% with DFS, respectively. RxD-2 shows a slightly better DFS but statistically not significant ($p=0.13$). Breast as primary disease site shows highest DFS 8.1 months, while lung shows the least DFS (6.7 months). DFS is highly correlated to KPS ($p=0.003$) and loosely correlated with number of metastases and volume of target ($p=0.045$ and $p=0.047$).

CONCLUSIONS: For SRS of Brain metastasis, heterogeneous dose plans offer a lower passing rate of QA results than homogeneous dose plans. Nevertheless, heterogeneous plans offer a better DFS than homogeneous plans, but this is statistically not significant. Other prognostic factors, KPS score, primary disease, number of metastases, have more influence on DFS, whereas QA results have no or insignificant correlation with DFS.

KEYWORDS: Brain Metastasis, Disease free Survival, SRS, Dose heterogeneity.

DOSIMETRIC ANALYSES OF CRITICAL ORGANS (KIDNEY,LIVER AND SPLEEN) OF PATIENTS WITH NEUROENDOCRINE TUMOURS TREATED WITH ¹⁷⁷LU-DOTATATE

Santosh Kumar Gupta¹, Jay prakash Kumar², Manojkumar Chauhan, Ravi Kumar Chauhan¹

¹Department of Nuclear Medicine and PET, Mahamana Pandit Madanmohan Malaviya Cancer Centre, ²HBCH (a Unit of TMC),Varanasi, UP 22105

Email: drsantoshgupta13@gmail.com

BACKGROUND: ¹⁷⁷Lu labelled with DOTATATE is widely acceptable to treat Neuroendocrine Tumour (NET) disease and it better improvement of quality of patients' life since few years ago. However, the radionuclide toxicity becomes the main limitation of the (NET) treatment.

OBJECTIVES: The aim of this work was to calculate the radiation absorbed dose to kidneys, liver and spleen of Patients with diagnosed neuroendocrine tumours (NETs) treated with ¹⁷⁷Lu-DOTATATE.

METHODS: We enrolled 81 patients (male/female patients, 60/21) with mean age of 48.1±15.3 years affected by different types of NETs diagnosed with ⁶⁸Ga-DOTANOC PET-CT and biochemical markers. For radiation protection of kidneys, amino acid mixture (lysine and arginine) was co-infused; 3.7 to 7.4 GBq (100-200 mCi) of ¹⁷⁷Lu-DOTATATE was infused to each patient over 30 minutes. Each patient underwent a series of 9 whole-body scans at 30 minutes (pre-void) and 4, 24, 48, 96, 144, and 168 h. The organs included in dosimetric calculation were kidney, liver, spleen, pituitary gland, and NETs. All dosimetric calculations were done using the OLINDA/EXM 1.0 software.

RESULTS: Physiological uptake of ¹⁷⁷Lu-DOTATATE was seen in all patients in kidneys, liver, spleen, and pituitary gland. Radiation absorbed doses were calculated: 0.54 ±0.1 mGy/MBq for kidneys, 0.23 T 0.05 mGy/MBq for liver and 1.27 ± 0.14 mGy/MBq for spleen.

CONCLUSIONS: The maximum cumulative activity of ¹⁷⁷Lu-DOTATATE that can be safely administered to a patient within permissible renal threshold in our study was found to be 40 GBq (1100 mCi). However, there are considerable interpatient differences in absorbed doses of all organs requiring individualized dosimetry for optimizing tumour dose.

KEYWORDS: Radiopharmaceutical Dosimetry; ¹⁷⁷Lu-DOTATATE and Neuroendocrine Tumors

DEVELOPING A REMOTE OPERABLE SMART EMERGENCY CONTAINER TO HANDLE POST EMERGENCY HDR BRACHYTHERAPY (COBALT – 60) SOURCE TRANSFER

Arup ratan Nandi¹, Bulbul Hossain¹, Sukriti Das¹, Partha Sarathi Lakshman²

¹Department of Radiotherapy, Burdwan Medical College & Hospital, Burdwan, West Bengal,

²Partha Sarathi Lakshman, Department of Mechanical Engineering, Dr. B.C. Roy Engineering College, Durgapur, West Bengal, India.

Email: arupratan007@gmail.com

BACKGROUND/OBJECTIVE: HDR Brachytherapy Cobalt – 60 (1 Ci) source stuck emergency occurred in our Institute. Due to mechanical stuck the source wire was damaged. The source was retrieved in the Emergency Lead Container following emergency protocols. We devised a new mechanical tool, designed our own procedure and transferred such high activity source manually to transport container successfully. This is first of its kind as there is no such incident reported earlier in literature. Hence the chances of radiation emergency resulting over exposure to occupational workers were high during this newly invented procedure. To avoid such situation we are developing a design of smart emergency container which can transport such highly radioactive Brachytherapy Cobalt – 60 source to its transport container safely by remote operation. This abstract presents the electro-mechanical design of the same and its feasibility to replace the manual vulnerable technology comprising all radiation safety aspects.

MATERIALS AND METHODS: Standard Mechanical, Electromechanical and Electronics designing software were used for simulation of a smart emergency container which can handle the minute Brachytherapy source precisely and transfer it to the transport container using a remotely controlled motor drive. The electromechanical implementation of motor drive at the surface of the container with a proper shielded interface to prevent radiation leakage is simulated. The dummy source could be used for trial runs on actual device.

RESULTS: The project is in a developmental stage. The simulation shows all feasibility of successful working of this smart device. Actual result could be shown after test run using dummy source.

CONCLUSIONS: This smart device with new innovative cutting edge technology will immensely reduce exposure to occupational radiation workers and will also reduce chances of emergency during such source transfer operation.

KEYWORDS: HDR Brachytherapy, Cobalt - 60 source, radiation emergency, radiation exposure, radiation safety, Technology development, designing a device.

IMPACT OF FLUENCE SMOOTHING ON STEP-N-SHOOT INTENSITY MODULATED RADIOTHERAPY PLANNING AND DELIVERY

Megharaj V. Borade, Supriya M. Borade

HCG Manavata Cancer Centre, Nashik, 422002, Maharashtra, India

Email: mbmegharaj11@gmail.com

BACKGROUND/OBJECTIVE: Commercially available Eclipse™ treatment planning system (TPS) incorporated with X-Y smoothing factor within the objective function which permits a user to play during optimization to vary delivery fluence complexity. This paper studies the impact of varying smoothing factors on inverse IMRT planning and step-n-shoot delivery mode.

MATERIALS AND METHODS: We selected four disease sites for this study treated with IMRT at our institute: tongue carcinoma (Ca. Tongue), buccal mucosa carcinoma (Ca. BM), glioblastoma (GBM), and prostate carcinoma (Ca. Prostate). Total 300 treatment plans were designed on Varian Eclipse TPS version 13.5 for Siemens Primus medical LINAC equipped with 6MV photon beam and 84 leaves MLCs which is capable to deliver step-n-shoot IMRT. Base plan optimized with vendor recommended default X-Y smoothing values. Other experimental plans were then re-optimized and recalculated with varying discrete smoothing values ranging from 0-0 to 100-100. Plans have been analyzed in terms of dosimetric matrices like Paddick Conformity Index (CI_{Paddick}), ICRU Homogeneity Index (HI_{ICRU}), OAR, and PTV min, max, mean and median doses, and delivery parameters like MUs, segments, MU factor, Delivery complexity (DC).

RESULTS: It was anticipated that smoothing is inversely related to delivery complexity, conformity was found to be better at "no smoothing" and get worsen with an increase in smoothing. Homogeneity improved with increasing smoothing. OAR sparing not greatly improving with an increase in smoothing. Monitor units showed a reducing trend with increased smoothing, which can lead to a decreased potential risk of low doses due to head leakage. The total number of segments in a plan was observed to be increasing with smoothing.

CONCLUSION: Our observation showed that plan would be less complex and every other dosimetric parameter is acceptable nearer to 40-30 X-Y smooth values. However, the complexity of the RT plan depends on the planer strategy, the complexity of PTV and location of OAR near to PTV, and relative priority assigned to PTV and OARs during optimization.

KEY WORDS: Step-n.-shoot IMRT, Optimization, Fluence smoothing

IN-FIELD PLANAR DOSE STUDY IN CRANIAL RADIOTHERAPY TREATMENT PLANS USING OPTICALLY STIMULATED LUMINESCENCE DOSIMETER

Amal Jose, Shaiju V.S., Raghukumar P

Division of Radiation Physics, Regional Cancer Centre, Thiruvananthapuram, Kerala
Email: amaljose.rcc@gmail.com

BACKGROUND/OBJECTIVE: Point dose measurements, planar dose measurements, and three dimensional (3D) volumetric dose measurements are commonly used to verify the discrepancy between treatment planning system (TPS) calculated and the machine delivered dose as a part of patient specific quality assurance (PSQA). Optically Stimulated Luminescence Dosimeter (OSLDs) is rarely used for PSQA. Therefore, our study aims to measure the in-field planar dose (at multiple points in a plane) in cranial volumetric modulated arc therapy (VMAT) plans using OSLDs in an indigenously fabricated Polymethyl methacrylate (PMMA) head phantom and compare it with the TPS dose values.

MATERIALS AND METHODS: In this study, nanoDot OSLDs and MicroStar reader (Landauer, Inc., Glenwood, IL) were used. Initially, 60 OSLD nanoDots were calibrated against the reference cylindrical farmer type chamber FC65G (IBA Dosimetry), and calibration factors for each in units of 'cGy per count' were obtained. This was done using PMMA slab phantom for 6 MV beams. An indigenously fabricated PMMA head phantom used in this study has provisions for placing five OSLDs either in a horizontal or vertical plane containing isocenter. Computed tomography (CT) imaging of the head phantom with OSLDs in place was taken for dose calculation in TPS. The angular dependency of OSLDs in head phantom was also verified for different gantry angles and compared with the calculated dose. In this study, VMAT plans of twenty five patients were selected retrospectively. Pre-treatment verification plans for the selected patients were created using Eclipse v15.6.05 TPS. The average dose to each calibrated OSLDs were calculated in TPS and was then compared with the measured dose value. Statistical analysis was done using Paired t-test and Wilcoxon signed rank test.

RESULTS: The OSLD shows no significant angular dependency ($p = 0.176$) within the head phantom. Also, there is no statistically significant difference between measured and TPS calculated dose ($p = 0.271$) for planar dose verification.

CONCLUSION: This study concludes that the OSLDs can be used as a suitable dosimeter for planar dose verification as a part of PSQA.

KEYWORDS: OSLD, Patient Specific QA, Head phantom

AI TOOL FOR PREDICTION OF HEART DOSE IN LEFT BREAST CANCER RADIOTHERAPY BASED ON ANATOMICAL DIMENSION

Shriram Rajurkar^{1*}, Teerthraj Verma¹, SP Mishra², MLB Bhatt¹

¹Department of Radiotherapy, King George's Medical University, UP Lucknow

²Dr ram ManoharLohia Institute of Medical Sciences, Lucknow

Emai: shriram.ashok.rajurkar@kgmcindia.edu

BACKGROUND/OBJECTIVE: The aim of this study was to develop a novel artificial intelligence (AI) tool for predicting heart dose before radiotherapy treatment planning. The objective was to create a tool for the accurate heart dose estimation received during radiotherapy and providing recommendations for the suitability of Deep Inspiration Breath Hold (DIBH) technique in the left breast cancer radiotherapy.

METHOD AND MATERIAL: The retrospective data of eighty seven patients has been used to design this AI tool which was trained on a large dataset of patient images, associate heart doses, etc. The transverse diameter of the chest was divided by the anterior-posterior distance derived from the chest CT scan of the patient. These two distances were recorded from the axial slice exhibiting the smallest distance between the anterior surface of the vertebral body and the posterior surface of the sternum for the purpose of calculation of Haller index using the developed programme.

RESULT: The AI tool demonstrated high accuracy in predicting heart dose very close to the corresponding value calculated by TPS, with a difference of as low as 30 cGy providing valuable information for treatment planning. Additionally, the tool offered recommendations for suitability of DIBH Implementation based on patient-specific factors such as breathing pattern, tumor location type of treatment site such as MRM or Intact breast etc.

CONCLUSION: The developed AI tool for predicting heart dose in radiotherapy treatment planning showed promising results. It provided accurate estimations of heart dose and offered recommendations for DIBH, thereby assisting clinicians in minimizing radiation-induced cardiac complications. The integration of this AI tool into clinical practice has the potential to improve treatment planning accuracy and enhance patient outcomes. Furthermore, the tool's ability to provide recommendations for DIBH allows for personalized approaches during radiotherapy.

KEYWORDS: AI in Medicine, DIBH, Cardiac Toxicity, Left Breast Cancer Radiotherapy, Python Programming.

DOSIMETRIC COMPARISON OF DYNAMIC CONFORMAL ARC THERAPY STEREOTACTIC RADIOSURGERY AND VOLUMETRIC MODULATED ARC STEREOTACTIC RADIOTHERAPY FOR CARCINOMA BRAIN

Suhani Pinto¹, Shree Kripa Rao¹, Krishna sharan³, Shirley Salins², Srinidhi G.C²

¹Manipal College of Health Professions, Manipal, India

²Kasturba Medical College, Manipal, India

³ K S Hegde Memorial Academy, Mangalore, India

Email: shrinidhi.gc@manpal.edu;shrinidhigc@gmail.com

BACKGROUND/OBJECTIVE: Stereotactic radiosurgery (SRS) is commonly delivered using dynamic conformal arc therapy (DCAT) however, volumetric modulated arc therapy (VMAT) simulating SRS has the potential to enhance target conformity and reduce organ-at-risk doses through inversed planning methods. Limited studies have directly compared DCAT and VMAT, in patients with single-brain carcinoma using four-fraction VMAT SRT. To address this gap, we conducted a planning study comparing DCAT and VMAT simulating SRS with DCAT for treating single brain tumor carcinoma.

MATERIALS AND METHODS: In this study, a retrospective selection was made of a total of 20 patients who underwent treatment for single brain tumors. For each patient, the same CT images with corresponding structures were utilized for both VMAT SRT and DCAT planning. Both VMAT SRT and DCAT plans were generated, each utilizing a single isocentre. The comparison included target conformity, doses to the brainstem, optic chiasma, and cochlea as well as monitor units (MUs). All these plans were carried out using Monaco TPS 5.11.

RESULTS: The VMAT SRT plans demonstrated significantly improved conformity indices (IP-CI) compared to the DCAT SRS plans. Moreover, the VMAT SRT plans exhibited smaller V15Gy, V12Gy, V10Gy, and V5Gy values for brainstem and optic chiasma compared to the other modality. The MUs were higher in the VMAT SRT compared to the DCAT SRS plans.

CONCLUSIONS: VMAT SRT demonstrates superiority over DCAT SRS in multi-fraction brain SRS for patients with single-brain carcinoma, particularly in terms of target conformity and the risk of brain radiation necrosis. However, DCAT SRS may be considered in selected cases where patients have a poor performance status or low tolerance to lengthy radiotherapy sessions due to their shorter treatment duration.

KEYWORDS: Dynamic conformal Arc therapy; Volumetric Arc Therapy; Stereotactic Radiosurgery; Stereotactic Radiotherapy

EVALUATION OF JUNCTION DOSE OF BIPHASE IRRADIATION OF ARTERIOVENOUS MALFORMATION (AVM)

Arun Adhikari, Ashitha MK, Annex EH, Debnarayan Dutta

Department of Radiation Oncology, Amrita institute of Medical Sciences, Ponekkara P. O Kochi, Kerala India.

Email: arunadhik26@gmail.com

BACKGROUND/OBJECTIVE: To assess the junction dosage of AVM patients that were irradiated in two sessions separated by six months. Because of the large volume and therapeutic dosage constraints, stereotactic radiosurgery (SRS) treatment is biphasic. To achieve better results, adequate spacing between two phases is essential.

MATERIALS AND METHODS: SRS/SRT is preferred for AVM treatment reason being minimally invasive, less trauma, faster recovery, minimal hospitalization, and fewer complications. SRS/SRT can be provided with LINAC-based X-ray knife, Gamma knife or Cyberknife (AccurayInc). It is a frameless approach that detects patient movement and adapts to positional changes to provide high precision treatment delivery. AVM are treated in biphasic with a gap of six months. The separation between the targets in the two phases is crucial during the treatment planning to avoid the overdose and underdose in the target volume. Two plans are created in the simulation CTs for both phases (six month gap) using Precision treatment planning system (AccurayInc) with the separation at the junction. For each study the PTV separation of phase I and phase II is given as 0.625mm, 1.25mm, 1.87mm, 2.5mm and 3.125mm and the composite plan of Phase I and II with above mentioned separation is evaluated using MIM software (AccurayInc). To quantify the dose overlap evaluate the dose volumes of 50% to 200% of the prescribed dose. The parameters like volume of PTV, prescription and other planning parameters are evaluated. The dose delivery at the junction is measured with EBT3 gafchromic films using SNC Patient ArcCHECK software.

RESULT: The composite plan with lesser separation the overlapping dose volumes are high and decreases with increasing separation. In the composite plan the junction dose is function of parameters like PTV volume, PTV cross sectional area at the junction, prescription isodose percentage, prescription dose, collimator selection, achieved conformality in both phases and dose constraints achieved for critical structures nearby.

CONCLUSIONS: The appropriate gap at the junction between the slices depends on the volumetric distribution of PTV and will differ for each patient.

KEYWORDS: AVM, SRS, Cyberknife, EBT3 Film.

DEVELOPMENT OF AN ANTHROPOMORPHIC HETEROGENEOUS FEMALE PELVIC (AHFP) PHANTOM FOR DOSIMETRIC VERIFICATION OF ADVANCED RADIOTHERAPY TECHNIQUES

Neha Yadav^{1,3}, Manisha Singh¹, S.P. Mishra²

¹Department of Applied Physics, Amity School of Engineering & Technology, Amity University Madhya Pradesh, Maharajpura Dang, Gwalior, India.

²Department of Radiation Oncology, Dr. RMLIMS, Lucknow, India.

³Department of Medical Physics, Apollo Hospitals Bilaspur, Chhattisgarh, India.

Email: nehadav51990@gmail.com

BACKGROUND/OBJECTIVE: Accurate dosimetric verification is essential in advanced radiotherapy techniques to optimize treatment planning and ensure adequate tumor coverage while minimizing the dose to surrounding healthy tissues. The use of anthropomorphic phantoms can provide realistic representations of human anatomy and tissue heterogeneity, facilitating precise dosimetric measurements. This paper presents a systematic approach to the construction of the AHFP phantom, considering anatomical accuracy, tissue heterogeneity, and dosimetric measurements.

MATERIALS AND METHODS: An anthropomorphic heterogeneous female pelvic phantom was constructed using materials including paraffin wax, a female pelvic bone, water, gauge, polyvinyl chloride (PVC), and polymerized siloxanes. To assess the resemblance of the finished phantom to a real patient, the AHFP phantom underwent computed tomography (CT) scanning at 120 kilovolt peak (kVp) and 250 mAs, with a slice thickness of 2 millimeters (mm). The acquired CT images were subsequently transferred to the Eclipse (Varian Medical System, Palo Alto, USA) treatment planning system (TPS) for further analysis and evaluation.

RESULTS: The CT numbers and relative electron densities, with respect to water, of the uterus, bladder, rectum, muscles, fat, bones, and cavities in the AHFP phantom closely approximated those observed in real patients. The mean percentage variations between the planned and measured doses of all rapid arc quality assurance (QA) plans were determined to be 2.14, with a standard deviation of 0.633, for the slab phantom. In contrast, for the AHFP phantom, the mean percentage variation was 8.31, with a standard deviation of 2.77.

CONCLUSIONS: The use of the AHFP phantom can enhance the efficiency and safety of dosimetric verification, ultimately improving the quality of care for cervical cancer patients undergoing advanced radiotherapy treatments.

KEYWORDS: homogeneous phantom, heterogeneous phantom, radiation dosimetry, anatomical accuracy, tissue heterogeneity, advanced radiotherapy techniques

OCCUPATIONAL RADIATION EXPOSURES TO THE EYES, THYROID AND EXTREMITIES IN INTERVENTIONAL CARDIOLOGY PROCEDURES: EXPERIENCE IN A TERTIARY REFERRAL CENTRE

Satish Chandra Uniyal¹, Vikram Singh¹, Anurag Rawat²

¹Department of Radiology, ²Department of Cardiology, Himalayan Institute of Medical Sciences, Swami Rama Himalayan University, Jolly Grant, Dehradun, Uttarakhand, India.

Email: dr.suniyal@gmail.com

BACKGROUND/OBJECTIVE: The occupational exposures during cardiac interventions have become a cause of concern owing to the increasing workload, potentially high radiation levels and lack of radiation safety culture in many centres. The present study was aimed to estimate the radiation exposure to the eye lens, thyroid and extremities of the operator, and to demonstrate the effect of lead protection on operator's doses during interventional procedures.

MATERIALS AND METHODS: The study was performed in a dedicated cardiac catheterization laboratory with an average workload of 20 patients per day. Radiation doses to eyes, thyroid and fingers of two physicians were measured by applying discs of thermoluminescent dosimeter (TLD) material (LiF: Mg,Cu,P) on appropriate locations on physician's organs of interest during 20 coronary angiography (CA) and 25 percutaneous transluminal coronary angioplasty (PTCA) procedures. During the procedures, it was ensured that the physicians used the adequate personal protective means. In order to quantitate the effect of lead protection, a sets of TLDs was applied both inside and outside the lead barrier over eyes and thyroid regions. Dose to fingers were measured by applying one TLD to the index finger and another to the wrist of each hand without any lead protection. Before measurement of dose, TLDs were annealed and calibrated according to the standard methods available in the literature. The irradiated TLDs were read using a commercial TLD reader (Rexon UL-320, US).

RESULTS: With the use of lead protection, the measured doses to right eye, left eye, and thyroid were found to be lower by 76.8%, 80.9% and 74.2% for PTCA and by 74%, 73% and 72.9% for CA procedures, as compared to the corresponding unprotected dose values. The average finger doses (without lead protection) of 283 μ Sv and 149 μ Sv were measured for PTCA and CA respectively.

CONCLUSIONS: The study demonstrates that the occupational doses to eyes and thyroid during interventional procedures can be effectively optimized by the use of lead eyewear and thyroid shield respectively. The dose to the unprotected organ may approach or even exceed the maximum permissible organ dose limits, particularly in centres with high workload per operator.

KEYWORDS: Occupational dose, cardiac intervention, coronary angiography, TLD

AN INVESTIGATION ON THE DEPENDENCE OF EBT³GAFCHROMIC FILM ON ENERGY, DOSE, AND POST EXPOSURE SCANNING TIME

Jibon Sharma, Banashree Kalita

Department of Radiation Oncology, State Cancer Institute, Gauhati Medical College, Guwahati, Assam, India.

Email: sharma5jibon@gmail.com

BACKGROUND/OBJECTIVE:The Gafchromic EBT³film is widely used in radiation oncology to measure dose distribution and absolute doses for various energies. EBT³ films are exposed to radiation over a wide energy range and doses in order to provide a complete picture of energy and dose dependency. Additionally, we also examined the evolution of optical density as a function of time after irradiation.

MATERIALS AND METHODS:The study used of ⁶⁰Co gamma (1.17-1.33) Mev and megavoltage X-rays (6,10 and 15MV) to measure the film's response to energy. The Gafchromic EBT³film's response to each of the above energies were measured over the dose range of (0.1-10Gy). The optical densities of irradiated films were read 24,48 and 72 hours after irradiation to evaluate the fluctuation of optical density with post exposure scanning time. The study used an Epson Expression12000 XL flatbed scanner and Image-J software to assess the optical densities. Each film strip was placed on the scanner bed with care in the same orientation at the same location.

RESULTS: When compared⁶⁰Co, the optical density of the EBT³film noticeably different for the three energies 6,10 and 15 MV. For 15MV higher differences are seen at lower doses and gradually decrease with increase of doses, with 18.2% at 10cGy and 6.5% at 100cGy. The dose above 100cGy, no statistical difference was observed between 6 and 15 MV beam. We observed significant changes of optical density at low doses (<100 cGy) due to post irradiation time.

CONCLUSIONS: According to the findings of our study indicate that Gafchromic EBT³film is a reliable dosimeter with insignificant energy independent responses across a wide range of beam energies and modalities used in Radiation Oncology.

KEYWORDS:Gafchromic films, Dose response curve, energy dependence, post exposure scanning time.

AN INSTITUTIONAL EXPERIENCE OF PATIENT SPECIFIC QUALITY ASSURANCE OF TOMOTHERAPY CRANIOSPINAL IRRADIATION USING ARCCHECK

Mayura S¹, Soumya N M², Annex E H³, Debnarayan Dutta⁴

Department of Radiation Oncology, Amrita Institute of Medical Sciences, Ponnakara P.O,
Kochi, Kerala, India.

Email: mayurashedigumme@gmail.com

BACKGROUND/OBJECTIVE: Craniospinal irradiation (CSI) is a treatment option for cancers of the central nervous system. The therapy covers the whole brain and spinal cord, providing complete dose coverage. The topic at hand focuses on patient-specific quality assurance (QA) of CSI in Helical Tomotherapy.

MATERIALS AND METHODS: In the CT images of ten patients, the critical target volume (CTV), gross tumor volume (GTV), planning treatment volume (PTV), and critical structures were all contoured. Plans were created in Tomotherapy treatment system with a dynamic jaw width of 5 cm and a prescribed dosage of 36Gy in 20 fractions. The dose coverage for planning target volume was 95% of the prescribed dose. The doses received by Organs at Risk (OAR) are within the tolerance limit. The ArcCHECK 1220 model, which consists of a cylindrical array of 1386 diode detectors that assess entrance and exit dosages, was utilized for patient-specific quality assurance. A cumulative dosage is shown on a 2D matrix as the measured result. SNC software was used to evaluate the TPS (Treatment Planning System) estimated dosage and the ArcCHECK measured dose, and the gamma passage rate was validated.

RESULTS: The plan quality assurance check was done using ArcCHECK and results were analysed using two gamma passing criteria: 3% dose difference and 3mm distance (3% 3mm) as well as 3% dose difference and 2mm distance (3% 2mm). In both cases, an average passing rate above 90% was achieved.

CONCLUSIONS: Conformal dose coverage is achieved in Helical Tomotherapy. The result showed a good agreement between the measured dose and pretreatment planned dose. Additionally, all these CSI Tomotherapy plans are yet to compare with the Volumetric Modulated Arc Therapy in LINAC.

KEYWORDS: ArcCHECK, Helical Tomotherapy, Patient-specific Quality Assurance

A COMPARATIVE STUDY USING DIFFERENT FIELD WIDTHS IN HELICAL TOMOTHERAPY FOR HEAD AND NECK CANCERS AND PRE-TREATMENT QUALITY ASSURANCE OF THE SAME USING ARC CHECK

Soumya N M¹, Mayura S², Anoop R³, Debnarayan Dutta⁴

Department of Radiation Oncology, Amrita Institute of Medical Sciences, Ponnakara P.O,
Kochi, Kerala, India.

Email: soumyamazhooor@gmail.com

BACKGROUND/OBJECTIVE: The objective of this study is to analyze the effect of changing the field widths during optimization in helical Tomotherapy for Head and Neck cancers and the pre-treatment patient-specific quality assurance of the same using ArcCHECK. The Tomotherapy machine has fixed and dynamic jaw widths. This study aims to compare the target coverage, critical organ doses, dose conformity, total treatment time, and patient-specific quality assurance of the same.

MATERIALS AND METHODS: In Tomotherapy, treatment plans can be generated using fixed jaw mode and dynamic jaw mode. The fixed field sizes for treatment are 1cm, 2.5 cm, and 5 cm at isocentre and the dynamic jaws have the ability for the jaws to open to 2.5 cm and 5 cm field widths. The field width in the X-direction is determined by MLC.

For this study, 10 Nasopharynx cases were selected. The prescribed dose was 70Gy in 33 fractions. For each case, five plans were generated for all fixed and dynamic jaws. PTV coverage and critical organ doses were compared. ArcCHECK 1220 model was used for patient-specific quality assurance, consisting of a cylindrical array of 1386 diode detectors. SNC software was used to compare the TPS-calculated dose and the ArcCHECK measured dose, and the gamma passing criteria were validated.

RESULTS: In all cases, 95 % of the prescribed dose was received by the PTV. For each case, the plans were compared for fixed and dynamic jaws and the results were within acceptable limits. There was a small difference in the conformity index and homogeneity index for the target according to jaw mode for each field width. And an average gamma passing rate of 90 % was achieved.

CONCLUSIONS: With 5 cm the BeamOnTime was less compared to 2.5 cm or 1 cm with satisfactory dose distribution. With fixed jaws spill in the inferior-superior slices was more compared to dynamic jaws. The result was in good agreement between the measured dose and the pre-treatment planned dose.

KEYWORDS: Dynamic and Fixed Jaw, Nasopharynx, ArcCHECK.

FABRICATION OF UVC PORTABLE CHAMBER FOR CELL IRRADIATION

Nishasri S¹, Sureka CS¹, Venkatraman P².

¹Department of Medical Physics, Bharathiar University, Coimbatore, India.

²Department of Medical Physics, Bharathidasan University, Trichirapalli, India.

E-mail: nishanishasri23@gmail.com

BACKGROUND/OBJECTIVE: Normally, ionizing radiation or high-energy particles like x-rays, gamma rays, electron beams, and protons are used to irradiate cancer cells. The use of ultraviolet C (UVC) irradiation is described as an alternative to current techniques for killing cancer cells in the process of proliferating. The purpose of this study is to examine the UVC Light Emitting Diode (LED) work as an irradiation system. Optically Stimulated Luminescence Dosimeter (OSLD) is used to assess the setup's effectiveness and optimize dosage.

MATERIALS AND METHODS: Sterilization light emitting diode LED, a PCB solder-able component that is robust, impact resistant, and appropriate for applications in a variety of sectors, is used in Ultraviolet C (UVC) irradiation system. The UVC LED is utilized as the irradiation light source. The UVC area has several applications in the realm of radiobiology, and its doses are highly effective in profoundly irradiating in the 200–280 nm range. UVC renders viruses inactive and causes cancer cells to undergo apoptosis. After optimizing and validating the overall setup's dose with OSLD, the cancer cells are exposed to radiation, the UVC LED exposure dose is determined, and the viability of the exposed cancer cells is shown as a graph. Irradiation with UVC LEDs is strongly advised for radio sensitizer and radioprotection. UVC LED setup is also suitable for blood irradiation in hospitals.

RESULTS: In this fabrication we are analyzing the UVC light system, lamp characteristic and irradiation system. Low cytotoxicity and high cell death are the effects of UVC LED irradiation, and irradiated cancer cells proliferate less than unirradiated cancer cells do. The effectiveness of the UVC LED irradiation setup is demonstrated by a graph that plots the viability of treated cancer cells.

CONCLUSIONS: According to the test findings, the UVC LED irradiation setup is operating in accordance with specifications and may be turned into a suitable UVC irradiator, or portable device.

KEYWORDS: Radiation dosimetry, UVC irradiation, OSLD, Cancer cell irradiator.

A NOVEL PRACTICAL METHOD TO RETRIEVE DOSE LOST DURING HIGH DOSE RATE BRACHYTHERAPY: A MONTE CARLO STUDY

Mandar S Bhagwat

Massachusetts General Hospital, Harvard Medical School, Boston, USA.

Email: mbhagwat@mgh.harvard.edu

BACKGROUND/OBJECTIVE: The brachytherapy calculation algorithm recommended by AAPM's Task Group-43 used in all brachytherapy treatment planning systems (TPS) assumes full scatter conditions. The report from Task Group-186 provides guidance on implementing heterogeneity correction algorithms (HCA) in the clinic, but not all TPS provide HCA for clinical use. Thus, alternatives that replicate full scatter conditions during dose delivery need to be explored. One such option for treatment of superficial lesions with HDR brachytherapy is evaluated in this work.

MATERIALS AND METHODS: The geometry of skin lesions treated with Freiburg applicators was simulated by enclosing coplanar 3cmX3cm and 9cmX9cm grids of Ir192 dwell locations in 0.5cm of water on one side of the plane and 10cm of water on the other side. Radiation dose was calculated using MCNP6 at 1cm along the axis perpendicular to the plane of the applicators on the 10cm side of water. Calculations were performed by adding layers of water (0.5cm, 1.5cm, 2.5cm, 3.5cm, 5.5cm, 9.5cm) to the 0.5cm side. Calculations were also repeated by adding layers of copper (0.01cm, 0.05cm, 0.1cm, 0.15cm, 0.2cm, 0.25cm) to the 0.5cm side of water. The increase in dose from water layers was compared to that from copper layers. A grid size dependent model to calculate optimal copper thickness was developed.

RESULTS: The 9.5cm water layer increased the dose by 1.4% for the 3x3 grid and 3.9% for the 9x9 grid. To achieve similar dose enhancement a 0.2cm layer of copper for the 3x3 grid and 0.25cm layer for the 9x9 grid was needed. The equation $y = a*(1-\exp(-b*x))$ was found to correlate thickness of copper required to reproduce full scatter conditions in water for all grid sizes.

CONCLUSIONS: The retrieval of loss of delivered dose from lack of backscatter during superficial treatment of skin lesions with HDR brachytherapy would require almost 10cm of water to be added on top of the surface Freiburg applicator. This is obviously impractical. Instead, a practical, easily implemented solution would be to place a few mm of copper (depending on the size of the lesion) on the surface applicator.

KEYWORDS: Freiburg applicator, Monte Carlo

ESTIMATION OF DOSE DIFFERENCE IN THE TREATMENT PLAN OF ARTERIOVENOUS MALFORMATIONS (AVM) STEREOTACTIC RADIOSURGERY(SRS) DUE TO ELECTRON DENSITY OF EMBOLIZATION MATERIAL ONYX-18

Irfad MP, AmithMohan,Muhsin P, Suraj, Sathyam, Puneet Pareek, SonalVarshney

All India India institute of Medical Science Jodhpur

Email: mpirfad@gmail.com

BACKGROUND/OBJECTIVE: Embolization of arteries and veins using non-adhesive embolizing agents like Onyx 18, followed by stereotactic radiosurgery(SRS), is a standardized treatment for arteriovenous malformations (AVM). Onyx-18, a liquid embolic agent, is used prior to SRS to reduce AVM size and vascularization. The study investigates potential dose differences in the SRS treatment plan caused by variations in the electron density of the embolization material. Onyx-18 consists of ethylene-vinyl alcohol copolymer mixed with tantalum powder, providing radio-opacity for imaging. The presence of tantalum powder has high electron density, which potentially affecting treatment planning accuracy. Most planning systems (TPS) estimate relative electron density (RED) up to 2. Onyx-18 has an estimated RED of approximately 2.7-2.9. Our case has a maximum electron density value of 1.73 corresponding to HU value 1205. TPS considers RED as 1.73 for all HU values beyond 1205HU, this is underestimating the RED value and leading to dose calculation discrepancies.

MATERIALS/METHODS: Five clinically approved AVM SRS plans created using Monaco planning system. Onyx embolized areas were contoured, and 3 different RED values were assigned to estimate dose distortion. First, RED was set at 2.7 (recommended for Onyx). Second, RED was set at 1 (pre-embolization treatment plan). Finally, maximum ED value of 1.73 in our TPS. All plans (PL_ED_2.7, PL_ED_1.7, and PL_ED_1) were recalculated for these RED values. Dosimetric quantities (TV, TVRI, VRI, Dmax, V150, V130, V120, V100, V90, V80) were estimated. Data underwent correlation and graphical analysis using in-house scripted Python.

RESULTS: Comparing Dmax of PL_ED_2.7 and PL_ED_1.7 with PL_ED_1, mean dose differences were 0.86 ± 0.7 Gy and 0.69 ± 0.47 Gy, respectively. The maximum dose difference in Dmax was 2Gy for the plan with RED 2.7. Dose differences for V120 were 0.79 ± 0.65 (PL_ED_2.7) and 0.47 ± 0.37 (PL_ED_1.7). Other parameters (V150, V130, V100, V90, V80) showed dose differences less than 0.6. All plans exhibited similar conformality index (CI).

CONCLUSIONS: This study investigates the dose difference when RED is not assigned for Onyx embolization material. Although not assigning any RED value does not cause clinically relevant dose differences.

FLATTENING FILTER-FREE TECHNIQUE IN VOLUMETRIC MODULATED ARC THERAPY-BASED RADIOSURGERY FOR BRAIN METASTASIS: A DOSIMETRIC COMPARISON WITH THE FLATTENING FILTER TECHNIQUE

Aravind S.¹

¹Division of Radiation Physics, Regional Cancer Centre, Thiruvananthapuram

Email: aravinds.rcc@gmail.com

BACKGROUND AND OBJECTIVES: Brain metastases can be treated with stereotactic radiosurgery (SRS) in which highly localized and hypo fractionated dose is delivered. The long delivery time involved in SRS may reduce patient comfort and compromise immobilization. The removal of the flattening filter (FF) of the linear accelerator can produce unflattened beams that can be delivered at higher dose rates which can drastically reduce the treatment time in hypo-fractionated treatments. This study presents the outcome of a comparison between the FF technique and with flattening filter-free (FFF) technique in Volumetric modulated arc therapy-based SRS for brain metastases. The difference in plan quality indices and beam on time between FF and FFF techniques were studied.

MATERIALS AND METHODS: Thirty consecutive patients with solitary brain metastasis who were treated using SRS (20 Gy in single fraction) in our institution from January 2017 to December 2021 were selected for this study. All patients were immobilized using BrainLAB® thermoplastic patient mask and CT scans were taken with a slice thickness of 1.25mm. The VMAT plans with planar as well as non-coplanar arcs were generated for Varian TrueBeam™ linear accelerator in the Eclipse treatment planning system. A maximum dose rate of 600 MU/min and 1400 MU/min were used for FF plans and FFF beams respectively. The AcurosXB algorithm was used for dose calculation. The beam arrangements and optimization criteria were the same for FF and FFF plans. Treatment plans were generated for four-photon energies namely 6FF, 6FFF, 10FF, and 10FFF.

RESULT & DISCUSSION: The results of our study show no significant difference in plan quality for 6 MV and 10 MV VMAT plans. The comparison between FFF VMAT plans with FF VMAT plans showed a significant difference in GIPaddick. The use of FFF resulted in a significant reduction in brain volumes receiving lower doses and a significant reduction in beam-on-time.

CONCLUSION: FFF technique resulted in a significant reduction in Beam-On-time and better sparing of the Brain compared to the FF technique. The FFF is an efficient technique for VMAT-based SRS for Brain metastasis that improves patient comfort and reduces resource utilization.

KEYWORDS:SRS, FF, FFF, VMAT, IMRT, Dosimetric Comparison, Beam-on-time

OBSERVATION STUDY TO ANALYSE DOSES RECEIVED BY PATIENT DURING CONE BEAM COMPUTED TOMOGRAPHY (CBCT) OF PELVIC REGION

Jyoti Bisht¹, Ravi Kant¹, Meenu Gupta¹, Vipul Nautiyal¹, Viney Kumar¹, Rishabh Dobhal¹,
Mushtaq Ahmad¹, Sunil Saini²

¹Radiation Oncology & ²Surgical Oncology
Himalayan Institute of Medical Sciences, Swami Rama Himalayan University, Dehradun, Uttarakhand

Email: jyoti797bisht@gmail.com

BACKGROUND AND OBJECTIVES: Cone beam computed tomography (CBCT) is the golden standard for patient positioning in IGRT treatment. CBCT imaging doses are not taken into account with treatment planning dose although the CBCT doses are measured while calibration of CBCT. This study is to measure the CBCT dose with the Octavius II phantom setup for pelvic patients and compare it with measured CBCT doses.

METHOD AND MATERIAL: Total 108 patients of pelvic region were included in this study. CBCT imaging of ca cervix, ca rectum, ca urinary bladder and ca prostate patients were taken with Varian True Beam 2.7 Linear accelerator. CBCT protocols were defined for pelvic region i.e. 125 KV, 1080mAs trajectory full and fan type half for ca cervix, ca rectum, ca urinary bladder patients and for ca prostate 140 KV, 1687.5 mAs fan type half and trajectory full was selected. Information was extracted from each patient for scanning protocol, CTDI_{vol}, DLP and total kV dose. Octavius II phantom was exposed for each scanning protocol for selected patients of different sites.

RESULTS: SPSS 16.0 and MS excel software was used for statistical analysis. CTDI_{vol} (p=0.027) and Octavius II observed doses (p=0.025) were significant in one sample t-test. Paired t-test was also performed for CTDI_{vol} and Octavius II observed doses and it was statistically significant (p=0.012). Doses for CTDI_{vol} and Octavius II are tabulated below.

Case	CTDI _{vol} (mGy)	Observed Octavius II dose (mGy)	Difference between CTDI _{vol} (mGy) dose and Octavius II observed doses (mGy)
Ca Cervix	15.98	17.9	-1.92
Ca Rectum	15.98	18.2	-2.22
Ca Urinary Bladder	15.98	18.2	-2.22
Ca Prostate	36.78	40.8	-4.02

DISCUSSION AND CONCLUSION: This study provided an information regarding CBCT doses delivered in pelvis cases and encourage to use the other dosimetry tool for it's verification. CBCT has become an essential tool for IGRT treatment and for pelvis region i.e. ca urinary bladder and ca prostate daily CBCT is necessary therefore for the total dose received by CBCT should be analyzed and monitored for future reference.

DOSIMETRIC COMPARISON OF SCHWANNOMA FOR ROBOTIC RADIOSURGERY: COMPARISON WITH C-ARM LINEAR ACCELERATOR

Deepak .P¹, Bhavya.P², Shridhar.P³, Shyam.S³, Pichandi.A³, Suhas.R³, Bhavin.V³, Unmesh.M³

Department of Radiation Oncology, Hcg-Ics Khubchandani Cancer Centre. Colaba Mumbai

BACKGROUND/OBJECTIVE: Schwannomas are benign tumors that originate from Schwann cells which are responsible for insulating and supporting nerve fibers in the peripheral nervous system. In recent years advancements in radiation therapy techniques specifically robotic radiosurgery and C-arm linear accelerators have shown promising results in the treatment of Schwannomas. Robotic radiosurgery such as the CyberKnife system utilizes a robotic arm to deliver highly precise radiation to the tumor while minimizing damage to surrounding healthy tissues. The aim of the Study is to compare the dose evaluation and distribution of Robotic radiosurgery for the target as well as OARs for Schwannoma with C-arm Linear Acceleration based plans. C-arm Linac-based plans included VMAT and non-coplanar VMAT with 1, 2, and 3 non-Coplanar arcs.

MATERIAL/METHODS: The dosimetric comparison of Schwannoma treatment between robotic radiosurgery and C-arm linear accelerators focuses on evaluating the radiation dose distribution and its impact on tumor control and normal tissue toxicity. 40 patients were selected for this study, with a dose of 27 Gy in three fractions planned. For each patient, 5 plans were made i.e. one for Cyberknife and 4 with C-arm Linac. Dose Coverage (100%), Conformity index (CI), Gradient index (GI), GTV Volume (cc), 10 Gy Volume (cc), 5 Gy Volume (cc), 2.5 Gy Volume (cc), 50% Spill (cc), 30% Spill (cc), Maximum dose (D_{max}) of OAR, Monitor Unit (MU) and Beam ON Time (BOT) were evaluated.

RESULTS: The Gradient index of Cyberknife plans are found to be lower than the C-arm Linac. The Dose Coverage of Cyberknife plans was found better and in-between 92%-95%. MU and BOT are less in C-arm linac. OARs dose can be controlled effectively with Cyberknife Plan.

CONCLUSION: Comparative studies have demonstrated that robotic radiosurgery offers several advantages in Schwannoma treatment. The high degree of accuracy provided by robotic systems allows for precise target localization and tracking enabling the delivery of high radiation doses to the tumor while sparing nearby critical structures.

KEYWORDS: CyberKnife, C-arm Linear Acceleration, Schwannoma, Gradient index, Conformity index.

EMPOWERING THE NEXT GENERATION: TEN YEARS' EXPERIENCE OF THE UK SCIENTIST TRAINING PROGRAMME

Claire-Louise Chapple¹, Jemimah Eve²

¹Newcastle upon Tyne Hospitals NHS Foundation Trust, ²Institute of Physics and Engineering in Medicine

Email: claire-louise.chapple@nhs.net

BACKGROUND/OBJECTIVE: Statutory registration is required to practice as a Clinical Scientist in the UK and currently there are at least 2,000 Clinical Scientists working in Medical Physics and Engineering in the UK. A national initiative in 2010 led to a new programme of training and registration for Clinical Scientists, including both medical physicists and clinical engineers. The programme was developed in consultation with a wide range of stakeholders comprising governmental and professional bodies, including IPeM, staff groups and the public.

PROGRAMME OUTLINE: The Scientist Training Programme (STP) is a three-year programme of work-based learning, supported by a university accredited master's degree. Trainees are employed by an NHS hospital for the duration of the programme and spend time in a range of departments in the first year, before specialising in one area. An endpoint assessment is carried out and trainees have to pass this in addition to completing all competencies and passing the MSc course in order to become registered as a Clinical Scientist. The annual intake for Medical Physicists has risen from 70 in the first year (2011 enrolment, completing 2013) to 99 in 2023. A separate certification scheme, at a higher level, has been developed more recently for Medical Physics Experts.

EVALUATION: The STP has generally been well received by both employers and aspiring medical physicists. Feedback from the early years, along with changing workforce demands, were considered in a full curriculum review in 2020. The programme is funded by government and so places are limited and are currently insufficient to fully meet recruitment needs within the Medical Physics workforce. Alternative routes to registration include practical on-the-job training, and assessment by portfolio, and are supported by IPeM, for those with the necessary academic qualifications and an equivalence route for those with international qualifications and training.

CONCLUSIONS: The UK STP has proved to be a valuable and effective method for training and registration of the next generation of high-quality Medical Physics and Engineering workforce. The close involvement of stakeholders and an active system of review has enabled improvements to be identified and implemented as required.

KEYWORDS: education; training; registration; medical physics expert

SMALL FIELD DOSIMETRY USING 0.01 CC CHAMBER AND DIODE DETECTOR

Hetvi Usadadiya¹, Satish Pelagade¹, Jincy CD¹, Ankita Parikh²

¹Department of Medical Physics, ²Department of Radiation Oncology, The Gujarat Cancer & Research Institute, Ahmedabad, India

Email: hetviusadadiya34@gmail.com

BACKGROUND/OBJECTIVE: The scope of this work is to investigate the variation in efficiency of 0.01 cc ion chamber and diode detector in small fields of TrueBeam linear accelerator. Rather it be dynamic IMRT, VMAT or stereotactic treatments, the small fields play a role in ensuring dose conformity and minimizing normal tissue toxicity. This abstract presents the outcome of the tests conducted on an advanced multi-energy TrueBeam linear accelerator.

MATERIALS AND METHODS: The linear accelerator (Varian, TrueBeam) was used in the experiments of the present study. All the experimental measurements were made with 0.01 cc Razor chamber and Photon Field Detector (PFD) detectors in Blue Phantom² (IBA – Dosimetry), controlled by MyQA Accept software. The dosimetric parameters, including the percentage depth dose, percentage surface dose, beam profiles, field width and output factors at the 1×1, 2×2, 3×3, 4×4 and 10×10 cm² field sizes were evaluated for both dosimeters. The beam profiles were taken in step-by-step mode at 10 cm depth and the PDD was measured for depth 30 to -0.05 cm.

RESULTS: The empirical and statistical analyses of the present study showed that some differences could be observed between the dosimetric performances of the ion chamber, compared to that reported for the diode detector in small field. Penumbra width measured with razor chamber was approximately 1.35 times wider than obtained with the diode detector. The measured PDD curves for all detectors are almost similar. Percentage surface dose result from razor chamber is around 7% less than that of diode detector. Field width measured with both detectors shows no significance difference. Output factors vary by 8% for 1×1 cm² field size but, in larger field size differences was around 5%.

CONCLUSION: The dosimetric characteristics of the razor chamber and diode detector illustrated with some differences, especially in terms of beam profiles for the small field. Based on the results, we consider the diode detector as an appropriate small field detector, while 0.01cc Razor can lead to some errors when used in small field under 4×4 cm².

KEYWORDS: Small field dosimetry, diode detector, ionization chamber.

VERIFICATION OF BEAM QUALITY INDEX USING PERCENTAGE DEPTH DOSE MEASUREMENTS WITH RADIATION FIELD ANALYZER IN CLINICAL RADIOTHERAPY

Warang Sagar Yashwant, Susanjita Biswal, Senthil Kumar P, Suresh Chaudhari

Department of Radiation Oncology, American Oncology Institute, Hyderabad, Telangana, India

Email: warangsagar73@gmail.com

BACKGROUND/OBJECTIVE: The aim of this scientific investigation was to validate the Beam Quality Index ($TPR_{20/10}$) of photon beams by employing Percentage Depth Dose (PDD) measurements at depths of 20 cm and 10 cm, facilitated by the Radiation Field Analyzer (RFA). As per Technical Report Series 398 (TRS-398) guidelines, the Tissue Phantom Ratio (TPR) at depths of 20 cm and 10 cm has been designated as the indicator of beam quality for clinical accelerators and study investigates the use of alternatives in routine clinical practice.

MATERIALS AND METHODS: The study employed the Varian True-beam LINAC system and followed the prescribed protocol outlined in TRS-398. The RFA was used for measuring $PDD_{20/10}$ values. These values were measured at depths of 20cm and 10cm for a field size of 10cm x 10cm. The $TPR_{20/10}$ values were obtained using the RFA measurements and the relationships provided in TRS-398 were utilized for verification. The following relationships were employed:

$$TPR_{20/10} = 1.2661PDD_{20/10} - 0.0595$$

Where $PDD_{20/10}$ represents the ratio of percentage depth dose at depths of 20 cm and 10 cm for a field size of 10cm x 10cm. additionally, the relationship for percentage depth doses at a depth of 10 cm, measured for a field size of 10 cm x 10 cm at a Source-to-Surface Distance (SSD) of 100 cm, was used:

$$TPR_{20/10} = -0.7898 + 0.0329PDD(10) - 0.000166PDD(10)^2$$

RESULTS: The experimental values of $TPR_{20/10}$ obtained using the RFA were compared with the $TPR_{20/10}$ values derived from the $PDD_{20/10}$ measurements using the relationships provided in TRS-398.

CONCLUSIONS: The results of this scientific study demonstrated that the experimental values of $TPR_{20/10}$ obtained using the RFA were in agreement with the $TPR_{20/10}$ values derived from the $PDD_{20/10}$ and $PDD(10)$ measurement. These findings provide strong evidence to support the use of $PDD_{20/10}$ or $PDD(10)$ as an alternative method to determine beam quality in routine clinical practice.

KEYWORDS: medical accelerator, TRS-398, dosimetry, PDD, $TPR_{20/10}$

DOSIMETRIC COMPARISON OF LUNG PATIENTS TREATED WITH IMRT & RAPIDARC USING AAA AND AXB ALGORITHMS

Alpa Langhanoda¹, Satish Pelagade¹, Suchitra Laishram¹, Ankita Parikh²

¹Department of Medical Physics, ²Department of Radiation Oncology, Gujarat Cancer & Research Institute, Ahmedabad, India

Email: ap898684@gmail.com

BACKGROUND/OBJECTIVE: This study aimed to investigate the dosimetric difference between Acuros XB (Acuros External Beam) and AAA (Anisotropic Analytical Algorithm) algorithms in IMRT & RapidArc plans for lung cancer. Treatment planning for lung cancer is challenging because the combination of low density (air) medium, bone, soft tissue cause charge particle disequilibrium near air and tissue interface. The treatment outcome and accuracy of the dose delivered to cancer patients highly depend on the dose calculation algorithm.

MATERIALS AND METHODS: We selected total of ten lung cancer patients whose prescription dose was 60Gy in 30 fractions. For each patient, two plans were generated by eclipse software using the AAA and AXB algorithms, in which beam angles and beam geometries were decided according to target location and varied from patient to patient and were kept same for both AAA and AXB plans for a patient. The dosimetric parameters, such as conformity index (CI), gradient index (GI), homogeneity index (HI), Dmean, Dmax dose to the OAR, and volume of lung receiving 5% and 20% of the prescribed dose, are recorded for comparison. The PTV coverage was defined by V95%.

RESULTS: The average HI in the AXB (0.1139) algorithm was more than AAA (0.1036). The average CI in the AXB (0.80) algorithm was better than the AAA (0.75). The average GI of AXB (2.605) algorithm is lower value than AAA (2.748). We observed no significant difference in the Dmax, Dmean dose received by the OAR, dose received ipsilateral and contralateral lung V5%, V20% when compared across the two algorithms. The maximum and minimum dose delivered to heart (2991.2cGy, 26.1 cGy for AAA and 2852.8cGy, 28.7cGy for AXB), Esophagus (3653.2cGy, 1046.2 cGy for AAA and 3628.2cGy, 1054.2cGy for AXB) from overall Dmean dose in patients, similar maximum and minimum dose delivered to spinal cord (4268.6cGy, 1859.5cGy for AAA and 4397.4cGy, 1882.6cGy for AXB) from overall Dmax dose in patients.

CONCLUSIONS: The study demonstrated that both algorithms were reliable in lung cancer planning, but the AXB algorithm showed superior performance in maintaining dose conformity and dose fall-off.

KEYWORDS: AAA, AXB, IMRT, RapidArc

EFFECT OF DETECTOR VOLUME AND INTERMEDIATE FIELD SIZE IN DETERMINATION OF FIELD OUTPUT FACTORS USING THE DAISY CHAIN CORRECTION METHOD

Srayas Prasannakumar¹, Annex Edappattu Haridas¹, Ashitha M K¹

¹Department of Medical Physics & Radiation Safety, Amrita Institute of Medical Science and Research Centre

Email: srayas.thathuamasi@gmail.com

BACKGROUND/OBJECTIVE: Dosimetry of a small field ($< 3 \times 3 \text{ cm}^2$) has been great challenges in radiotherapy because of (a) a lack of lateral electronic equilibrium, (b) steep dose gradients, and (c) partial blocking of the source. The aim of this study is to investigate the effect of different normalization conditions and choice of intermediate field f_{int} and detector volume on accurate measurement of the output factors ($OF_{det}^{f_{clin}}$) of the small fields formed by the fixed collimator system of a CyberKnife (CK) robotic radiosurgery system, and determine the $k_{Q_{clin}, Q_{msr}}^{f_{clin}, f_{msr}}$ correction factors for EDGE and Semiflex detectors.

MATERIALS AND METHODS: Three active high resolution diode detector including (EDGE, Diode E and Semiflex detector) and one passive detector (Gafchromic EBT3 Film) were used for Output factors measurement of small circular collimator of diameter range from 5mm to 60mm of a CyberKnifeusing SNC 3D Scanner and slab phantom at 1.5cm d_{max} and at SAD=80cm.

RESULTS: All the active detectors used in the study underestimated the output factor for the 5 mm, 7.5 mm, and 10 mm collimators by more than 2% compared to Accuray's multiuser data. The SNC EDGE diode detector demonstrated excellent agreement and the highest response across all collimator sizes and Semiflex detector exhibited the highest variation, especially for small fields. EBT3 film measurements was found to be most efficient method for small fields ($< 15 \text{ mm}$) with variation of only 0.4%. The selection of intermediate field sizes f_{int} exhibited a strong impact on the daisy chaining method of output factor determination with a 30mm intermediate field size giving the least variation of -5.8%. The correction factor $k_{Q_{clin}, Q_{msr}}^{f_{clin}, f_{msr}}$ obtained using the unshielded Diode E detector was found to be more accurate than one using EBT3 films.

CONCLUSIONS: The study corroborated that the normalization condition will have critical effect on the output factor determination of small field and a minimum of 30mm field size is suggested in daisy chaining method. The detectors volume will also have severe effect on field output factor and correction factor determination.

KEYWORDS: Small field dosimetry, CyberKnife, Output factor, EDGE, Semiflex, Diode E, EBT3

EVALUATING THE CORRELATION BETWEEN THE GAMMA PASSING RATE AND THE GRADIENT DOSE SEGMENTED ANALYSIS FOR VMAT TREATMENT PLANS

Simoné Wiid¹, Christoffel van Reenen², Christoph Trauernicht²

¹Division of Medical Physics, Tygerberg Hospital ²Department of Medical Physics, Tygerberg Hospital and Stellenbosch University, South Africa

Email: cjt@sun.ac.za

BACKGROUND/OBJECTIVE:The gamma index evaluation identifies and quantifies the differences between two dose fluence maps. The gradient dose segmented analysis (GDSA) segments the dose regions based on dose gradients to calculate the change in the planning target volume (PTV) mean dose for the reference and comparison dose distributions. The objective of the study is to determine the correlation between the gamma analysis and the GDSA for VMAT treatment plans.

MATERIALS AND METHODS:This retrospective study entailed the collection and analysis of the transmission fluence maps of 10 anonymised prostate cancer patients treated on the Varian Halcyon Linear Accelerator in the Radiation Oncology Department of Tygerberg Hospital. The transmission fluence map of the first fraction of treatment was used as the reference dataset. A composite map was created for multiple arcs. The composite transmission fluence maps of all subsequent fractions was then compared to the reference map by means of the gamma passing rate and the GDSA analysis. A total of 220 treatment fractions were analysed. The results of the gamma passing rate and the GDSA were evaluated to determine a possible correlation.

RESULTS: 14% of the fractions failed the 95% gamma pass rate using the 2%/2 mm criteria, while only 5.5% of the fractions failed the 95% gamma pass rate for the 3%/2mm criteria. A weak positive correlation was obtained between the area $\gamma < 1$ with a 95% gamma pass rate and the mean of the GDSA for all the gamma criteria considered. A moderate positive correlation coefficient of 0.62 was obtained between the average gamma of the gamma analysis (using 2%/2 mm) and the standard deviation of the GDSA.

CONCLUSIONS: The mean GDSA correlates to changes in the PTV mean dose. However, the standard deviation of the GDSA correlates better with the gamma passing rate than the mean GDSA. This corresponds to findings in literature that suggest the gamma passing rate alone does not correspond to clinically useful dosimetric values. It also indicates that a high variability in the PTV mean dose, indicated by a higher standard deviation of the GDSA, can lead to lower gamma passing rates.

KEYWORDS:GDSA analysis, gamma index evaluation, VMAT, EPID

CORRELATION SEARCH BETWEEN "RADIOMIC FEATURES" AND LUNG TUMORS: STAGE, THERAPEUTIC SUCCESS&SURVIVAL TIME

Hasin Anupama Azhari¹, Md. Ridwanur Rahman², Golam Abu Zakaria³, Thomas Schrader⁴

¹Centre for Biomedical Science & Engineering, United International University, Bangladesh,

²Department of Computer Science & Engineering, United International University, Bangladesh

³Faculty of EMW, Anhalt University of Applied Sciences, Germany,

⁴Department of Informatics & Media, Technische Hochschule Brandenburg, Germany

Email: ahanupama@uiu.ac.bd

BACKGROUND/OBJECTIVE: Radiomics is a method that extracts a large number of features using data-characterization algorithms. These features, called “radiomic features”, have the potential to uncover disease characteristics that fail to be appreciated by the naked eye. The correlation between radiomic features and lung tumors has gained significant attention in recent years as a potential means of predicting important clinical outcomes. This study aims to explore the relationship between radiomic features extracted from computed tomography (CT) images of lung tumors and three key clinical parameters: stage, therapeutic success, and survival time to help in deciding better treatment plan & strategy for lung tumor patients.

MATERIALS AND METHODS: Pyradiomics, a python-based library was used to extract relevant features from segmented portion of the lung which is in this case the tumor from the 48 patients, The features are categorized in three major parts: 1st order, 2nd order & higher order. The features that are mostly go with lung tumors were clustered to match with the clinical data and gene expression data later on to validate whether radiomics based features can actually be trusted to determine stage (among 4 stages) of the tumor. After that, based on the data to predict stage of the tumor we focused on whether the particular treatment plan assigned by experts could be beneficial for the patients. The validated features would tell us what kind of treatment plan should be incorporated in order to shrink tumor to lengthen patients’ life span if the stage falls in higher stage, which is quite hard to recover from. We trusted these features because they were matched with original clinical data and reoriented when necessary. Based on this level of data our model could predict the survival time of the tumor affected patients using deep learning techniques.

RESULTS: Preliminary findings revealed promising correlations between specific radiomic features and tumor stage, therapeutic success and survival time. Some features also provide vital information related with therapeutic success and survival time.

CONCLUSIONS: Above mentioned preliminary results support the notion that radiomic analysis can provide valuable insights into lung tumor characteristics and clinical outcomes.

KEYWORDS: radiomics, pyradiomics, feature extraction, segmentation, deep learning

DOSE PREDICTION OF EBT3 GAFCHROMIC FILM USING SUPERVISED MACHINE LEARNING MODEL

Saravjeet Kaur¹, Gaganpreet Singh², Arun S Oinam², Vivek Kumar¹

¹Centre for Medical Physics, Panjab University Chandigarh, India

²Department of Radiotherapy, PGIMER, Chandigarh, India

Email:saravrathour@gmail.com

BACKGROUND/OBJECTIVE: The use of EBT3 Gafchromic film in radiotherapy gains popularity due to its easy processing and quick use. Machine QA, Invivo dosimetry, and patient specific quality assurance (PSQA) test for special procedures like SRS requires the use of GafChromoic films. The calibration, processing and interpretation are mostly affected by user handling and discrepancies in the operating procedures. In this study, to mitigate/minimize such types of errors, ML based approaches is used to perform the analysis and interpretation of the gafchromic films for PSQA.

MATERIALS AND METHODS: Dose response curve was generated using 6MV flattening filter beam (available with the Versa HD linear accelerator) using EBT3 films for a wide range of doses which varies from 10 cGy to 2400 cGy. All the films were scanned using Epson XL11000 scanner with 48 bit scan mode and 600 dpi resolution without any color corrections. Python was used to process the scanned film data in tiff format and Sklearn library was used to create the ML based logistic regression model. Supervised ML technique was used to train the model to fit the pixels values obtained from tiff images with respect to dose. Each pixel of the image was treated as an input feature and its corresponding labels was assigned to known dose values. The entire data was split into training and testing dataset. The models was developed for different color channels. Further, the fitted model was used to predict the composite doses on the gafchromic films.

RESULTS: The accuracy of fitted ML regression model for red, green and blue color channel was obtained as 94.75%, 93.85% and 83.39% respectively shown in Figure 1, 2 and 3 respectively. The model was able to predict the composite doses from the pixel values within $\pm 15\%$ uncertainty.

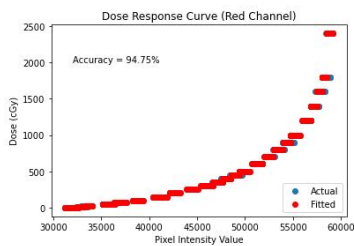


Figure 1: Actual and fitted dose response curve for red channel.

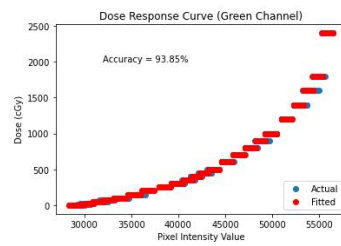


Figure 2: Actual and fitted dose response curve for green channel.

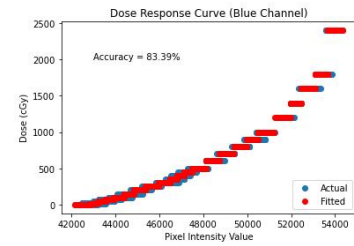


Figure 3: Actual and fitted dose response curve for blue channel.

CONCLUSION: ML models can be used as an alternative and easy to use tool for prediction of the doses from the gafchromic film scanned images, This limitation of this study is simple assumptions to fit the model without taking into account complex procedure. This study can be further utilized for the patient specific quality assurance tests for special procedures.

KEYWORDS: Machine Learning, Automation, Dose prediction

EFFECT OF VARIOUS PARAMETERS ON DOSIMETRY LEAF GAP MEASUREMENT FOR ROUNDED LEAF END MLC SYSTEM

Raviraj Patel¹, Satish Pelagade¹, Ansu Sara Mani¹, Ankita Parikh²

¹Department of Medical Physics,²Department of Radiation Oncology, Gujarat Cancer and Research Institute, Ahmedabad, India.

Email: patelraviraj7296@gmail.com

BACKGROUND/OBJECTIVE: Dosimetry leaf gap (DLG) parameter attempts to model the physical difference between the radiation and light field and accounts for inherent leakage between adjoining leaves. This parameter to model the round-leaf-end effect of multi-leaf collimators (MLC). Correct value of DLG inside Treatment Planning System (TPS) is significant for precise dose calculation especially when applied to small target with the DMMLC delivery technique in IMRT, IGRT, SRS and SBRT. In this study we investigated on the relationship between the DLG values and affecting parameters on DLG measurement.

MATERIALS AND METHODS: A linac (Varian True Beam) with 6 FF MV, 10 FF MV, 15 MV FF photon beams and equipped with the 120 Millennium MLC and the Eclipse™ TPS was used in this study. Using Integral sliding fields doses with different gap widths (2 mm, 4 mm, 6mm, 10 mm, 14 mm, 16 mm and 20 mm) for linear extrapolation to zero dose and intercepting at the gap width axis with an 0.13 cc ionization chamber, Dose-1 electrometer, water equivalent slab phantom. The DLG was measured at various measurement depths, photon beam energy, SSD, chamber orientation, dose rate.

RESULTS: The DLG characterization has been shown insensitive to measurement orientation from the sweeping beam direction, (for perpendicular and parallel orientation of chamber from the sweeping beam direction it is 1.15844 mm and 1.14537 mm respectively). Variations in source to surface distance (SSD) (for 90 cm and 100 cm SSD it is 1.14537 mm, 1.05803 mm respectively), depth of measurement (for 5 cm and 10 cm depth it is 1.06343 mm, 1.14537 mm), dose rate (for 400 MU/MIN and 500 MU/MIN dose rate it is 1.14537 mm, 1.29329 mm) affected to DLG value. While it increases with photon beam energy increases like 1.14537mm, 1.27057mm, 1.30293mm for 6 FF MV, 10 FF MV, 10 FF MV respectively.

CONCLUSIONS: Variation in TPS DLG value and the measured DLG value results in underdose or overdose to the target volume in small field irradiation. Accurate DLG values are necessary for accurate dose delivery.

KEYWORDS: dosimetry leaf gap, treatment planning system, leaf transmission, DMMLC

LEFT CHEST WALL IRRADIATION: COMPARISON OF DIFFERENT DOSIMETRIC INDICES OF O-RING LINEAR ACCELERATOR WITH DIFFERENT C-ARM LINEAR ACCELERATOR

Palanivelu D^{1,2}, D.Khanna¹, P.Mohandass², M.Thirumal³, R.J.Raghul⁴, Narendra Kumar Bhalla², Muhammed Ashik.M², Abhishek Puri²

¹Department of Physical Sciences, School of Sciences, Arts and Media, Karunya Institute of Technology and Sciences, Coimbatore, Tamilnadu, India.

²Department of Radiation Oncology, Fortis Cancer Institute, Fortis Hospital, Mohali, Punjab, India.

³Department of Radiation Oncology, Yashoda Superspeciality hospital and Cancer Institute, Ghaziabad, Uttar Pradesh, India.

⁴Department of Radiation Oncology, Jaypee Hospital, Noida, Uttar pradesh, India.

Email: palani.nathan92@gmail.com

BACKGROUND/OBJECTIVE: Objective of this study is to compare different dosimetric indices of O-ring linear accelerator (Linac) with different C-arm Linacs for left chest wall irradiation.

MATERIALS AND METHODS: Five left breast cancer patients with prescription dose of 50Gy in 25 fractions retrospectively selected for this study. Plans were generated using volumetric modulated arc therapy (VMAT) for two different C-arm linac such as Elekta Synergy® (ES) and Varian trueBeam™ STx (VTB) and O-ring Varian Halcyon® Linac (VH). The reference VMAT plan was generated on simulation CT data set using Monaco™ treatment planning system (TPS) for ES. The same CT data sets were transferred to Eclipse™ TPS and generated Rapid Arc plan for VTB and VH for comparison. The dosimetric indices such as V95 (volume receiving 95% of prescribed dose), mean dose, maximum dose, conformity index (CI), homogeneity index (HI) for tumour volume were analysed. In addition, the dose received by organ at risk volume (OAR) such as ipsilateral lung, heart, contralateral lung, contralateral breast, spinal cord, oesophagus, liver and Monitor Unit (MU), Modulation index (MI), Integral dose were compared.

RESULTS: The results of V95, mean dose, maximum dose, CI and HI of target volume did not show any significant dose difference between ES, VTB and VH plans. Similarly, no significant difference was found in MU and MI. A slight increase of dose for contralateral lung, contralateral breast, oesophagus, liver and decrease of integral dose were observed in ES VMAT plan as compared to VTB and VH plans. However, significantly less dose difference was found in heart and ipsilateral lung for VH plan than ES and VTB plans.

CONCLUSION: For left breast irradiation, both O-ring and C-Arm Linacs were able to generate clinically acceptable VMAT plans. However, dose volume received by heart and lung was significantly less in VH as compared to VTB and ES.

KEYWORDS: Left Breast, Volumetric Modulated Arc therapy, Linear Accelerator

DOSIMETRIC COMPARISON OF MAXIMUM SPINAL CORD DOSE WITH DIFFERENT VERSIONS OF ECLIPSE TREATMENT PLANNING SYSTEM SOFTWARE DOSE CALCULATION ALGORITHM (AAA) FOR DIFFERENT TYPES OF HEAD AND NECK CANCERS

S. Suvalakshmi^{1,2}, Dr. Biplab Sarkar², Mahasin Gazi², SubhraSnigdha Biswal², Kirubha George², Sandipan Roy Chowdhury², Prosenjit Soren², Supratip Kapat².

¹Department of Medical physics, Bharathiar University, Coimbatore, Tamilnadu.

²Department of Radiation oncology, Apollo Multi-Specialty Hospitals, Kolkata, India.

Email: suvasubu2223@gmail.com

BACKGROUND/OBJECTIVE: Spinal cord toxicity can be dreaded complication while treating head and neck cancers by conventional radiotherapy. So, reducing the spinal cord dose is very much important Intensity Modulated Radiotherapy (IMRT) and Volumetric Modulated Arc Therapy (VMAT) are playing an important role in reducing spinal cord dose by using different optimization and dose calculation algorithm with different versions. This abstract presents the comparison of maximum spinal cord dose with different versions of Eclipse Treatment planning System software for different types of Head and Neck cancers.

MATERIALS AND METHODS: In this study, 50 Head and Neck Carcinoma patients each from Tongue, Oropharynx, Buccal Mucosa, Larynx and Nasopharynx. The total administered radiation doses are 60Gy in 30# and 66Gy in 33#. For each patient two plans were created by VMAT technique with 3&2 full opens arcs. In AAA versions 11.031 and 15.6.03 the created plans were optimized by using Progressive Resolution optimization (PRO) and Photon Optimizer (PO) respectively in Eclipse TPS software.

RESULTS: The obtained overall Mean and SD for maximum spinal cord dose, CI and relative dose which is covered by 95% of the target volume in version 11.031 and 15.6.03 for tongue, oropharynx, buccal mucosa, larynx, Nasopharynx cases are 39.42±1.7, 39.7±1.8, 37.14±3.3, 39.43±2.3, 41.58±3.2 and 31.32±3.3, 30.95±2.9, 31.52±4.8, 33.08±5.5 respectively, 0.66±0.12, 0.67±0.14, 0.66±0.13, 0.66±0.13, 0.67±0.14 and 0.85±0.06, 0.84±0.08, 0.85±0.06, 0.85±0.06, 0.83±0.08 respectively. 96.08±2.2, 96.05±3.1, 95.9±3.1, 96.48±1.6, 95.8±2.5 and 98.33±0.8, 98.17±0.9, 98.35±0.8, 98.5±0.8, 98.34±0.8 respectively.

CONCLUSIONS: The study results shows that AAA algorithm version 15.6.03 has significantly reduced the spinal cord dose as well as target volume(PTV) coverage is more conformal than AAA algorithm version 11.031 for all type of head and neck cancers.

KEYWORDS: AAA algorithm, spinal cord, VMAT, PRO and PO.

ASSESSMENT OF VARIAN TRUE BEAM REAL-TIME POSITION MANAGEMENT (RPM) GATING SYSTEM FOR GATED IMRT DELIVERY IN BREAST CANCER PATIENTS: EVALUATION OF DOSIMETRIC IMPACT

Laya vinod k¹, Vetrivel D¹, Sabari kumar P¹, Suresh Chaudhari²

¹Department of Radiation Oncology, American Oncology Institute, Vijayawada, Andhra Pradesh

²Department of Radiation Oncology, American Oncology Institute, Hyderabad, Telangana, India

Email: layavinod21@gmail.com

BACKGROUND/OBJECTIVE:The aim of this study was to assess the performance of the Varian True Beam Real-time Position Management (RPM) gating system in the delivery of gated intensity-modulated radiation therapy (IMRT).

MATERIALS AND METHODS:A total of 10 patients diagnosed with breast cancer were included in this study. The Varian True Beam machine, in conjunction with the RPM system, was used to investigate the dosimetric impact of gating during IMRT delivery. The accuracy of the gated IMRT radiotherapy delivered using the Varian True Beam Linear accelerator and RPM system was evaluated by measuring absolute dose in a slab phantom for all patients.

RESULTS:The delivery time for gated IMRT was found to be longer compared to non-gated IMRT. The data collected indicated that dosimetric errors were higher in the gated IMRT delivery as compared to continuous IMRT. The Varian portal dosimetry software calculated and compared the predicted dose and measured relative portal dose distributions for both gated and non-gated treatments and found variations which are acceptable within clinical limits.

CONCLUSION:This study highlights the role of a stable respiratory pattern in ensuring accurate gated intensity-modulated radiation therapy (IMRT) treatment. It emphasizes the importance of maximizing the gating window time, which determines the number of start-and-stop motions during treatment. The results confirm that the combination of the Varian True Beam Linear accelerator and the real-time position management system effectively delivers gated rapid arc radiotherapy with clinically acceptable dose differences in gated IMRT treatment in breast cancer patients.

COMPARISON OF DOSE DISTRIBUTION TO THE TARGET VOLUME AND ORGANS AT RISK IN CARCINOMA CERVIX: A STUDY ON TWO INTRACAVITARY APPLICATORS FOR HDR BRACHYTHERAPY

Vidhya Ramalingam¹, Kotiyala Venkata Jagannadh Rao Naidu¹, Manikumar singamsetty¹, Raghavendrarao V kolleru¹, Singamala subbarayudu¹Sharma¹, Suresh Chaudhari²

¹Radiation Oncology Department, American Oncology Institute, NRI branch, Guntur, Andhra Pradesh

²Department of Radiation Oncology, American Oncology Institute, Hyderabad, Telangana

Email: vidhyakasthuri98@gmail.com

BACKGROUND/OBJECTIVE: The purpose of this study was to compare the dose distribution to the target volume (HR-CTV) and organs at risk (OARs) between two intracavitary applicators commonly used in high-dose-rate (HDR) brachytherapy for carcinoma cervix.

METHODS AND MATERIALS: Patients diagnosed with carcinoma cervix and treated at our center were included in this study. A total of 20 patients with FIGO stage III and stage IV disease were randomly allocated to receive treatment with either the Fletcher Suit or Ring applicator. All patients underwent external beam radiation therapy (EBRT) with a total dose of 45Gy delivered in 1.8Gy fractions. Brachytherapy was administered using CT-based planning, and all patients received a total dose of 7Gy in 4 fractions using Ir-192 HDR remote after-loading technique.

RESULTS: Analysis of the dose to the HR-CTV and OARs revealed that patients treated with the Fletcher Suit applicator received significantly higher mean doses compared to those treated with the Ring applicator.

CONCLUSION: In Intracavitary brachytherapy for carcinoma cervix, the Fletcher Suit applicator was found to deliver higher doses to the OARs compared to the Ring and Tandem applicators. The choice of applicator should be based on factors such as the presence of residual disease at the time of brachytherapy and patient anatomy and considering the potential impact on dose distribution to the OARs.

KEYWORDS: intracavitary brachytherapy, ring and tandem, ovoids, HR-CTV

DETECTION ACCURACY OF A LIGHT-SECTION METHOD-BASED 3D BODY SURFACE DETECTION SYSTEM INSTALLED IN A TREATMENT PLANNING CT ROOM

Naoki Hayashi¹, Tatsunori Satito², Kazuki Onishi²

¹School of Medical Sciences, Fujita Health University, Japan

²Department of Radiology, Seirei Hamamatsu General Hospital, Japan

Email: hayashi@fujita-hu.ac.jp

BACKGROUND/OBJECTIVE: We installed a light-section method-based 3D body surface detection system (VOXELAN) in our treatment planning CT room, which is the same type as in the radiation therapy room. However, unlike the treatment system, there is a problem with the clearance of the CT system, which may cause noise in detection data. Because the object is moved on the bed during helical CT imaging, it is necessary to perform post-processing on the data detected by the VOXELAN. In this study, the detection accuracy of VOXELAN in a treatment planning CT room was evaluated and compared with that of VOXELAN in a treatment room.

MATERIALS AND METHODS: To evaluate the detection accuracy of VOXELAN, the following contents were conducted: 1. Evaluation of detection performance of stationary objects. The object was moved by an arbitrary amount (± 5 cm in the longitudinal direction and ± 2 cm in the vertical direction) at 1 cm intervals and scanned by VOXELAN for 10 seconds. The mean value of multiple points of interest was evaluated for accuracy and the standard deviation was evaluated for stability. 2. evaluation of detection performance during CT imaging of a stationary object. The object was scanned with VOXELAN during helical CT imaging, and the data were post-processed using specially developed software to compare CT imaging data with VOXELAN data.

RESULTS: As a result of the detection performance evaluation of a stationary object, the accuracy was within 1 mm for any movement within the evaluated range; however, the larger the movement, the lower the detection stability. In the evaluation of detection performance during CT imaging of a stationary object, the higher the bed speed, the more noise was detected in the body surface data, and the lower the stability.

CONCLUSIONS: The VOXELAN installed in the treatment planning CT room showed good detection accuracy, comparable to that in the treatment room, and object detection during helical CT imaging was possible using post-processing software. By linking VOXELAN in the radiotherapy treatment planning CT room with VOXELAN in the radiotherapy room, it may be possible to address respiratory movement measures as well as patient position detection.

KEYWORDS: detection accuracy, light-section method, surface guided radiation therapy

REPRODUCIBILITY EVALUATION OF THE MONACO OPTIMIZATION ALGORITHM IN EXTERNAL BEAM RADIOTHERAPY PLANNING SOFTWARE: A STUDY ON HEAD AND NECK CANCER PATIENTS

Vidhya Ramalingam¹, Sathyaraj P², Ganesan Bharanidharan³

¹American Oncology Institute, NRI Branch, Guntur, Andhra Pradesh, India

²Department of Radiation Physics, KIDWAI Memorial institute of Oncology, Bangalore, India

³Department of Medical Physics, Anna University, Chennai, India

Email: vidhyakasthuri98@gmail.com

BACKGROUND/OBJECTIVE: The Monaco Optimization Algorithm, also known as the Monte Carlo Algorithm, is widely used in External Beam Radiotherapy planning software on the Elekta Platform. This study aimed to assess the reproducibility of the algorithm in optimizing treatment plans for patients with Head and Neck cancer.

MATERIALS AND METHODS: Fifteen patients diagnosed with Head and Neck cancer were enrolled in this study. Seven patients were planned using intensity-modulated radiation therapy, while eight patients were planned using volumetric-modulated arc therapy. Each patient's treatment plan was optimized ten times, keeping the structures and volumes unchanged. Dose coverage was evaluated using DVH statistics, including parameters such as the volume of the planning target volume (PTV) receiving 100% and 95% of the prescribed dose, monitor units, global maximum dose, and doses to organs at risk.

RESULTS: The obtained data were compared with those of the reference plan, and the mean and standard deviation for each optimized plan were calculated and tabulated. The results indicated variations in the optimized plans compared to the reference plan.

CONCLUSION: Based on this study, the reproducibility of the Monaco Software, when applied to optimize treatment plans for Head and Neck cancer patients, was found to be very feasible with negligible differences. The stability of the software's reproducibility was demonstrated across multiple optimization iterations, as long as the structures and constraints remained unchanged. These findings highlight the reliability of the Monaco Optimization Algorithm in External Beam Radiotherapy planning software for the Elekta Platform.

KEYWORDS: Optimization, algorithm, monaco, head and neck cancer

IN RAPID ARC THERAPY FOR PROSTATE CANCER, A COMPARISON OF DOSE STATISTICS FOR THE BLADDER WALL AND THE RECTUM WALL VERSUS THE ENTIRE ORGAN YIELDS ENCOURAGING RESULTS

Soumya Roy^{1,2}, Anusheel Munshi¹, Biplab Sarkar^{2,3}, Anirudh Pradhan², Maria Asha¹

¹Manipal Hospital Dwarka, New Delhi, ²GLA University, Mathura, India, ²Apollo Multispecialty Hospital, Kolkata, India

Email: soumyaroy91@gmail.com

BACKGROUND/OBJECTIVE: The goal of this research is to perform a statistical comparison of dose statistics for walled and solid structure contours for both the bladder and the rectum in the context of the treatment of prostate cancer with volumetric arc therapy (VMAT) for intermediate risk patients. Since the dose supplied to the inside of a hollow organ would be unrelated to the level of radiation damage, dose-wall histograms (DWHs) have been utilised as alternatives to dose-volume histograms (DVHs) for hollow organs. This is on the basis of the reasoning that dose-wall histograms (DWHs) are more appropriate for hollow organs.

MATERIALS AND METHODS: For the purpose of a pilot research analysing DVH and DWH data, ten patients who had previously been treated as were chosen. The inner and outer walls of the bladder were contoured over a distance of 18 mm beyond the most inferior and superior contoured CTV slices, respectively, during the contouring process. A thickness of three millimetres, with the contouring done by manually on each transverse slice. The inner and exterior walls of the rectum were contoured over a distance of 18 mm beyond the most inferior and superior CTV slices, respectively. A thickness of three millimetres, accomplished by hand on each transverse slice. Utilisation of a 3D automatic tool was used during the creation of the wall-based structures. The following is the radiation prescription that was used for the planning stage. 66.25 Gy/25#(Prostate + Seminal Vesicle); 58.7 Gy per 25 # (P+SV+6mm margin); 45Gy/25#(Pelvic LN). All of the designs were created with a 0.25 cm dose calculation grid size, 2 full arcs, 6 MV beam energy, AAA 15.6 algorithm Eclipse treatment planning system (V15.6, Varian Medical Systems, Palo Alto, California), and used in order to maintain uniformity. The nonparametric Spearman statistic correlation test was applied to the significant pair of histogram points in order to investigate the degree to which the DVH curve and the DWH curve correspond with one another. This statistical method is quite comparable to the one utilised by Garcia-Vicente et al.

RESULTS: After looking at the data from the different situations, it was found that the rectum and the wall of the rectum have a strong connection in all of them. There was a strong link between the bladder and the bladder wall as well. If the relationship is linear, we can predict the wall constraint with the formula $y = mx + b$, where m and b are the slope and intercept of the line that best fits the scatterplot. According to our result the ' m ' value is the slope, the ' b ' value is the intercept, the ' y ' value is the wall tolerance, and the ' x ' value is the solid tolerance.

CONCLUSIONS: The dose statistics of the rectum wall and solid rectum were consistently correlated. Similar results for bladder and bladder wall. We computed identical constraints for the rectum/bladder wall using our original solid constraint values. The maximum dose received was the same, showing that the bladder/rectum maximum dose was in the bladder wall/rectum wall, which contradicts the literature.

KEYWORDS: Dose volume histogram, Tubular structure, dose wall histogram, Rapid Arc

COMMISSIONING, EVALUATION AND QA ANALYTICS USING QATRACK+: AN OPENSOURCE COMPREHENSIVE RADIOTHERAPY QA SOFTWARE

¹Amit Kumar, ²Gaganpreet Singh, ²Arun S Oinam

¹Centre for Medical Physics, Panjab University, Chandigarh, India

²Department of Radiotherapy, PGIMER, Chandigarh, India

Email: atrao6366@gmail.com

BACKGROUND/OBJECTIVE: QATrack+ is a quality assurance management web-based application to streamline and automate quality control processes. QATrack+ provides comprehensive tracking and analysis of quality control data over time. QATrack+ software uses SQL database and Python framework to provide an interactive web-based user interface. In this study, the QATrack+ software was commissioned for various customized radiotherapy quality assurance procedures and their calculations were performed using pylinac module integrated with the software. Further, data analytics of tracking and trend analysis of these QA procedures was also demonstrated.

MATERIALS/METHODS: Customized tests related to mechanical, dosimetric, and imaging QA were developed using customized fields and functions using pylinac module and Python. Mechanical tests involve field size, laser, SSD, physical iso-center of the couch, collimator and gantry, etc; Dosimetric tests involve output measurement, TPR(20,10), MLC tests, CBCT QA using CATPhan, Isocenter verification using the Winston-Lutz tool for radiation and Physical isocenter verification; Imaging QA involves CATPhan CBCT analysis, Planar imaging using the LEEDS TOR phantom and EPID images. The frequency and record of these tests were assigned as per standard protocols. The framework involves different types of input data, directly from the users or in the form of DICOM files. These tests were created for different machine configurations.

RESULTS: QATrack+ Software was commissioned as per the user guidelines and found to be fully functional and successfully integrated with pylinac module of Python language. Over the period of 4 months, we observed the variation of output constancy of a single machine within $\pm 0.5\%$ and found it to be within tolerance limits. MLC and imaging QA were also performed and found to be within tolerance.

CONCLUSIONS: In this study, it is found that QATrack+ (open-source and freeware) software has the potential to optimize the equipment management, calibration, and quality assurance processes. Further, this software can be utilized for tracking records, auditing, and as a tool for investigation of the failure modes over a long duration of time. This study recommends to use the QATrack+ software as an alternative to commercial software solutions for machine QA and QA analytics.

KEYWORD: Automation, QA, Pylinac, MLC, CBCT, QATrack+

VERIFICATION OF INTENSITY MODULATED RADIATION THERAPY (IMRT) PLAN DELIVERY USING GAMMA ANALYSIS WITH EPID AND POINT DOSE MEASUREMENT

Susanjita Biswal, Warang Sagar Yashwant, Senthil Kumar P, Suresh Chaudhari

Department of Radiation Oncology, American Oncology Institute, Hyderabad, Telangana

Email: biswalsusanjita23@gmail.com

BACKGROUND/OBJECTIVE: The purpose of this study was to verify the accuracy of intensity modulated radiation therapy (IMRT) plan delivery by employing gamma analysis with Electronic Portal Imaging Device (EPID) and point dose measurement. The objective was to gain more confidence in the IMRT treatment delivery system due to its complex nature.

MATERIALS AND METHODS: This study employed TrueBeam linear accelerator equipped with aSi-1000 EPID, small volume chamber (0.125cc), electrometer (Dose 1), and slab phantoms for the verification of intensity modulated radiation therapy (IMRT) plan delivery. A total of twenty patients were selected for the study. IMRT plan delivery was performed using the EPID system. For the assessment of plan accuracy, gamma analysis was conducted using the PDIP algorithm in Eclipse system (v16.1) in accordance with the prescribed protocol TG-218. The gamma analysis utilized a 2%/2mm gamma criteria. To further validate the treatment delivery, point dose measurements were acquired at the central axis, corresponding to the treatment plans. The obtained values from the PDIP analysis, as well as the measurements from the point dose analysis, were compared for further analysis and evaluation.

RESULTS: The IMRT plans in this study successfully met the clinical acceptance criteria of 2% and 2mm for gamma analysis, with an average gamma value of 95.57% among the cohort of patients. A slight deviation in the central axis dose was observed between portal dosimetry and small volume chamber point dose measurements, with a maximum deviation of 6%. The treatment planning system (TPS) calculated central axis dose exhibited better agreement with the small volume chamber point dose measurements than with the electronic portal imaging device (EPID) measurements.

CONCLUSION: Based on the results of this scientific study, it was concluded that the measured values of point dose obtained from the experiments and the PDIP analysis were well within the 2% limit specified by TG-218. This study provided sufficient confidence in the accurate delivery of IMRT treatment using the evaluated system.

KEYWORDS: Linear accelerator, Electronic Portal Imaging Device (EPID), Portal Dose Image Prediction (PDIP), TG-218, Point Dose Measurement.

PERSPECTIVE ON AUTOMATED IMAGE SEGMENTATION OF THE BRAIN FOR RADIOTHERAPY WITH DIFFERENT T1 AND T2, MRI SEQUENCES

Akash T.G., Niya Mariya Baby, Sreedevi E, Annex EH, Debnarayana Datta

Department of radiation oncology, Amrita Institute of Medical Science, Ponnakara P.O, Kochi, Kerala, India.

Email: akashtg677@gmail.com

BACKGROUND/OBJECTIVE: A quick and accurate segmentation of medical images is a crucial component of treatment delivery due to the rapid advancements in radiation therapy (RT), particularly image guidance and treatment adaptation. Despite being time-consuming and subject to intra- and inter-observer variability, manual delineation of target volumes and organs at risk remains the norm for most clinics. Automated segmentation techniques aim to simplify the establishment of organ boundaries and reduce workload associated with contouring. This study compares the current auto-segmentation sequences, CT with T2 FLAIR and CT with T1+CONTRAST and examines pre-treatment auto-segmented images of patients who underwent WBRT. It also reviews the variations in various critical structure volumes, which could lead to wider acceptance of a particular sequence in routine clinical practice.

MATERIALS AND METHODS: The volumetric data were analysed using the Accuray precision 2.0.0.1 [5] software (Accuray Inc.). 10 patients were considered for comparative study, for each patient two sequences should be auto-segmented (T2flair and T1+contrast) and generated an auto-segmented contours in the image. Using an auto-suggestion tool within the Accuray precision software for the automated segmentation of CT and MR images. A series of images can be auto segment using the auto segmentation wizard, we focus on the white matter volume, considering it as the largest volume, along with the whole brain volume. This enables us to explore volume dissimilarities and assess their significance in the context of radiotherapy planning. Each brain volume is averaged over 10 patients, and the resulting volume differences are calculated.

RESULTS: In each patient's auto-segmented images, the volumetric analysis of the total brain and the white matter shows a substantial difference between T2 flair and T1+contrast images. The average difference in whole brain volume observed is 22.415 cm³, with white matter exhibiting a difference of 2.32 cm³.

CONCLUSIONS: Our study analyzes the vital significance of carefully choosing the best MRI sequences to obtain an accurate and exact auto-segmented volume for medical imaging and therapeutic dose assessment.

KEYWORDS: Auto segmentation, WBRT, MRI, CT

DOSE-RESPONSE RELATIONSHIP OF ¹⁷⁷LU-DOTATATE(LUTATE) ON NEUROENDOCRINE TUMOUR (NET) PATIENTS TREATED WITH PEPTIDE RECEPTOR RADIONUCLIDE THERAPY (PRRT): RETROSPECTIVE STUDY

Madhulika Mehrotra, Sanjana Ballal, Prashant Mishra, Chandrasekhar Bal

Department of Nuclear Medicine, All India Institute of Medical Sciences (AIIMS), New Delhi, India.

Email: madhulikamehrotra@gmail.com

BACKGROUND/OBJECTIVE: The study aims to perform a retrospective study to analyze the tumour radiation dose-response relationship on NET patients treated with PRRT, ¹⁷⁷Lu-DOTATATE (LuTate) therapy. We sought to assess the activity uptake for lesions and physiological organs on post-therapy quantitative SPECT/CT molecular imaging tool scans, after each cycle of treatment.

MATERIALS AND METHODS: Patients with Neuroendocrine Tumour (NET) who received PRRT with LuTate from 2019 to 2022, followed by quantitative SPECT/CT scans were retrospectively reviewed. The scans of four post-PRRT treatment cycles administered to three patients are assessed. Firstly, to know the activity uptake response at five time-points for lesions, liver, kidney (left & right), spleen and bone marrow, to study the dosimetry workflow in the first cycle. Secondly, to estimate the radiation absorbed dose response to the target lesions for four PRRT cycles of LuTate.

RESULTS: The SPECT/CT scan data of three patients are been analyzed with respect to activity response for five time-points study in the first cycle with LuTate. The dose-response relationship for the targeted lesions is also been investigated for the standard administered activity of 8GBq per cycle, in comparison to the patient-specific dosimetry of PRRT with LuTate therapy. *(The study is in progress and the final result analysis will be presented during the conference)*

CONCLUSIONS: The radiation dose to the targeted lesion during ¹⁷⁷Lu-DOTATATE PRRT with a standard activity per cycle study, indicates that the development of a personalized perspective in dosimetry can improve the overall outcome. *(This work is part of an ongoing project of the Department of Nuclear Medicine, AIIMS, New Delhi; funded by the Department of Science & Technology (DST), Ministry of Science & Technology, Government of India; Grant Reference No. - SR/WOS-A/PM-14/2019)*

KEYWORDS: Peptide Receptor Radionuclide Therapy (PRRT), Neuroendocrine Tumour (NET), ¹⁷⁷Lu-DOTATATE (LuTate) therapy, SPECT/CT

ASSESSMENT OF THE USE OF ELECTRONIC PORTAL IMAGING DEVICE FOR PATIENT-SPECIFIC QUALITY ASSURANCE IN VOLUMETRIC MODULATED ARC THERAPY

Aswani Janardhanan¹, Anna George¹, Arunkumar Kesavan¹, Suresh Chaudhari²

¹Department of Radiation Oncology, American Oncology Institute, Nagpur, Maharashtra

²Department of Radiation Oncology, American Oncology Institute, Hyderabad, Telangana

Email: aswanijs99@gmail.com

BACKGROUND/OBJECTIVE: The objective of this study is to investigate the feasibility and effectiveness of utilizing the Electronic Portal Imaging Device (EPID) for Patient Specific Quality Assurance (PSQA) in Volumetric Modulated Arc Therapy (VMAT).

MATERIALS AND METHODS: A total of 20 patients were selected for this study. Verification plans for each patient were generated for portal dosimetry and subsequently executed on the EPID system to measure the spatial distribution of radiation dose. The calculated and measured dose distributions were compared to evaluate the Gamma Index (GI) passing criteria, including a Dose Difference (DD) of 3% and a Distance-to-Agreement (DTA) of 3 mm. Additional criteria considered were an Area Gamma (γ_{\leq}) value greater than 95%, an Average Gamma (Ave) less than 0.5%, and a Maximum Gamma (Max) less than 3.5%. The central axis dose in the measured dose in portal dosimetry workspace were compared with point dose measurements using small volume chamber.

RESULTS: The analysis of clinical cases involving VMAT plans demonstrated an average pass rate of 98.92% for the 3%/2 mm criteria and 99.58% for the 3%/3 mm criteria when using the EPID system. The central axis dose and point dose measurements in the selected patient cohort exhibited average deviations of less than 5%, indicating a high level of agreement between the two methods.

CONCLUSION: This study demonstrates that the use of Electronic Portal Imaging Device (EPID) for Patient Specific Quality Assurance (PSQA) in Volumetric Modulated Arc Therapy (VMAT) shows promising results. The analysis of clinical cases revealed high pass rates, meeting the defined criteria for dose difference, distance-to-agreement, area gamma, average gamma, and maximum gamma. These findings suggest that EPID-based portal dosimetry can be effectively integrated into routine clinical practice for VMAT treatment verification.

KEYWORDS: Portal dosimetry, EPID, VMAT, Patient-specific quality assurance, Gamma index

DOSIMETRIC ASSESSMENT OF HEART AND LUNG IN CANCER ESOPHAGUS PATIENTS TREATED BY CHEMORADIATION

Jyothi N¹, Shambhavi², Sarath S Nair¹, Krishna Sharan³

¹Department of Radiotherapy and Oncology, Kasturba Medical College, Manipal Academy of Higher Education, Manipal, Karnataka, ²Medical Radiation Physics programme, Manipal college of Allied Health professionals MAHE, Manipal, Karnataka, ³Department of Radiotherapy Justice KS Hegde Medical College, Deralakatte, Nitte, Mangalore, Karnataka, India

Email: jyothi.nagesh@manipal.edu

BACKGROUND/OBJECTIVE: Cardiopulmonary complications are common late toxicities of thoracic Radiotherapy (RT) and are associated with significant morbidity. There is a need for better understanding of the radiation dose effects on the heart and lung sub-structures which may predict the cardiopulmonary complication. This study was designed to compare the dosimetric parameters of Heart and Lung in patients with carcinoma esophagus planned by Volumetric modulated arc therapy (VMAT) and Three-dimensional conformal (3DCRT) technique.

MATERIALS AND METHODS: 12 patients with carcinoma esophagus treated with VMAT Technique to a dose of 41.40 Gy in 23 fractions were retrospectively taken for this study and corresponding 3DCRT plans are generated for the study purpose. Total of 24 plans were generated. The dosimetric parameters of the resulting plans were compared for planning target volume (PTV) and organs at risk for Heart, Heart sub-structures (left, right ventricle and right, left atrium) both lungs, lung sub-structures (left upper and lower lobe, right upper, lower, middle lobe) and spinal cord.

RESULTS: A significant improvement was observed in Homogeneity (HI), Conformity (CI) Index with VMAT technique. A significant reduction in heart substructure and various volumes of the Heart (V25, V10, V20, V30, V40) and mean dose was seen. Also, a significant reduction in right lung and left lung (V30, V40) was found. Both lungs V20, mean dose was comparable.

CONCLUSIONS: VMAT is better than 3DCRT in terms of comparison with Homogeneity and conformity. Also VMAT enables reduction in Dose to heart and lungs, better sparing of heart and lung substructure which may contribute to decreased incidence of radiation induced long term cardiopulmonary complications.

KEYWORDS: Volumetric modulated arc therapy (VMAT), Three-dimensional conformal radiotherapy (3DCRT), Heart, Lung, Dosimetric parameters.

DESIGNING A BEAM SHAPING ASSEMBLY FOR ACCELERATOR DRIVEN BORON NEUTRON CAPTURE THERAPY (AD-BNCT)

Dimpal Saikia^{1*}, Mridula Baro², Sandeep S Ghugre³, Abhijit Barthakur², Kalyanee Baruah⁴, Jiban Jyoti Das², Moon Moon Devi⁵, Sachindra Goswami⁶, Betylda Jyrwa⁷, Anup K. Nath², Mahadev Patgiri², Rajarshi Raut³, Prakash Chandra Rout⁸, S. Santra⁸, Jibon Sharma¹, Shashi Sharma, Ganesh Chandra Wary²

¹Department of Radiation Oncology, State Cancer Institute, Gauhati Medical and Hospital, ²Department of Physics, Cotton University, Guwahati, Assam, ³UGC-DAE CSR, Kolkata Centre, WB ⁴Department of Physics, Gauhati University, Guwahati, Assam, ⁵Department of Physics, Tezpur University, Assam, ⁶BBCI, Guwahati, Assam, ⁷Department of Physics, North Eastern Hill University, Shillong, Meghalaya, ⁸Nuclear Physics Division, Bhabha Atomic Research Centre, Mumbai, India

Email: dimsaikia.22@gmail.com

BACKGROUND/OBJECTIVE: BNCT has a unique property of tumour-cell-selective particle irradiation. BNCT can form large dose gradients between cancer cells and normal cells, even if the two types of cells are mingled at the tumour margin. The IAEA has provided recommendation of different beam parameters for BNCT to get the desired clinical neutron beam. To meet the required energy spectrum, the Beam Shaping Assembly (BSA) is required.

MATERIALS AND METHODS: The neutron energy depends on the energy of the incident particle and nuclear reaction. Therefore, the BSA should be designed considering the neutron energy dependency. It is mainly composed of the following parts: a) Target, b) Moderator/ Filter, c) Reflector and d) shielding. Target is either a Lithium or Be target in which neutrons will be produced after 5 MeV Proton beam is bombarded. Here, LiF, TiF are materials which act as fast neutron moderator. Ni absorbs the thermal neutrons and increases the intensity of epithermal neutrons. Bi absorbs the gamma that is produced in the former layers. 0.5 mm Cd is used to absorb the thermal neutron. The purpose of reflector is to increase the neutron flux in the beam and to reduce the neutron leakage out of the system. Lead as reflector surrounds the Moderator of BSA. A shielding of lead surrounds the moderator and the reflector.

RESULTS: Preliminary design is made and detailed simulations using GEANT4 is in progress. The characteristics of the resulting epithermal neutron beam will be compared with the IAEA reference spectrum to validate our GEANT4 simulations. The recommended parameters are $f_{\text{epithermal}} > 10^9$ (n cm⁻² s⁻¹), $f_{\text{epithermal}}/f_{\text{fast}} > 20$, $f_{\text{epithermal}}/f_{\text{thermal}} > 100$, Dose rate $f_{\text{fast}}/f_{\text{epithermal}} < 2 \times 10^{-13}$ (Gy cm²), Dose Rate $\gamma/f_{\text{epithermal}} < 2 \times 10^{-13}$ (Gy cm²). Some hardware modifications may be required if gross discrepancies are found.

CONCLUSIONS: This study would lead to study of more clinical trials using therapeutic BNCT epithermal neutron beam in India. Also, it would help in better understanding of neutron in the field of Physics as well as Medicine.

KEYWORDS: BNCT, BSA, tumor, GEANT4 simulation.

ACKNOWLEDGEMENTS: This work is supported by the grant Ref: CRS/2021-22/02/526 from UGC DAE CSR Kolkata Centre.

OPTIMAL LIBRARY SIZE DETERMINATION FOR RAPID PLAN KNOWLEDGE-BASED PLANNING SYSTEM

Subhra S. Biswal^{1,2}, Biplab Sarkar^{1,2}, Monika Goyal²

¹Department of Radiation Oncology, Apollo Multispeciality Hospitals, Kolkata, West Bengal, ²Department of Physics, GLA University, Mathura, Uttar Pradesh, India

Email:subhrabswl@gmail.com

OBJECTIVE: This study aims to find out the optimal number of library plans for the Rapid Plan knowledge based planning system.

MATERIAL AND METHOD: This study evaluates two types of cancer: tongue (H&N) and cervix (Ca Cx). cervical (Cx) patients stage IIB-IVA treated with VMAT between 2017 -2020 and postoperative tongue (head and neck:HN) patients with group staging IIIa-IIIb planned and treated VMAT between 2019-2021 were extracted from the institutional data base.All the plans were created using the Eclipse planning system (Varian Medical Systems, Palo Alto, CA, USA) version 15.6 using three full arcs .The Rapid Plan (RP) library was created and validated using 100 patients for each site. All 100 patients have a clinically delivered plan,Library set was divided into 20, 40, 60, 80, and 100 plans and five different RP modules were created. 20 patients from each site were run through five libraries and dosimetrically compared with human generated plan know as Validation plan(VP) along with statistical analysis using Person correlation and Greenhouse-Geisser analysis.

RESULT : For VP and 5 KBP plans PTV D95% varies $97.6\pm 0.7\%$ - $98.1\pm 0.6\%$ and $98.8\pm 0.3\%$ - $99.0\pm 0.4\%$ H&N and cervix cases,respectively.All organs at risk in both sites, except D0.1cc spinal cord, showed a statistically insignificant variation between all six plans. All OAR shows a lesser dose for KBP plans than VP plans except for rectum V40(%), rectum V30(%), bowel V40Gy(cc) and bowel V30Gy(cc).

CONCLUSION: There is very minimal variation in the dosimetric parameters as a function of the library size. This is because all plans chosen for library was done by experienced physicist and there is only one target in both the cases it may not work for multiple targets. reducing the possibility of dosimetric improvement. The preferred number of library plans is around 30 (excluding outliers) for single PTV.

KEY WORD: Knowledge based planning, Rapid Plan, library size,Dosimertric

COMPARISON OF PRE-TREATMENT QUALITY ASSURANCE OF RAPID ARC PLANS WITH DIFFERENT DOSE GRID SIZES USING ARC CHECK AND PORTAL DOSIMETRY

Srinu Aketi¹, Parasa Prasad³, Venkata Krishna Reddy P², Palanikkannu M⁴

¹Department of Medical Physics, ²Department of Radiation Oncology, Mahatma Gandhi Cancer Hospital and Research Institute, Visakhapatnam, India, ³Department of Radiation Oncology, Delta Hospital, Rajahmundry, India, ⁴Department of Radiation Oncology, GSL Trust Cancer Hospital and Research Center, Rajahmundry, India.

Email: asrinu.srinu@gmail.com

OBJECTIVE: To evaluate the effect of dose calculation grid size on results of patient specific quality assurance for Rapid Arc delivery using Arc Check and Portal dosimetry.

MATERIALS AND METHODS: RapidArc plans for 15 head and neck cases were done with Eclipse v15.6 and verification plans were generated on SNC Arc Check and EPID aS1200 using grid sizes of 1, 2 and 3mm. The respective verification plans were executed on Arc Check and EPID using True Beam linear accelerator. The measured dose distributions of Arc Check and EPID were matched with the TPS calculated doses using gamma evaluation method in absolute mode and with threshold value of 10% in SNC patient software v8.4 and Portal Dose Image Prediction (PDIP) software respectively. The global and local gamma passing rates and maximum gammas were noted for the gamma criteria of 3%/3mm, 3%/2mm, 2%/2mm, 1%/1mm and the results were compared using Paired T test analysis in SPSS software.

RESULTS AND DISCUSSION: This study showed that 3%/3mm had significantly better match between calculated and measured dose distributions compared with other gamma criteria ($p=0.005$). The gamma passing rate and maximum gamma were significantly better with 1 mm grid size. The 3%/3mm gamma criteria with 1mm grid size showed global and local gamma passing rates and maximum gammas of 99.92%, 97.26%, 1.12 and 1.84 for Arc Check and 95.71%, 93.15%, 1.84 and 2.15 for EPID respectively. This study showed that clinically acceptable results with Arc Check up to 2%/2mm and 2mm grid size, while EPID showed with only 3%/3mm and 1mm grid size.

CONCLUSION: Arc Check gave better acceptable results compared with EPID. Higher grid sizes with variable gamma criteria can still be used with Arc Check. Global gamma passing rates and maximum gamma are preferred over local.

KEYWORDS: Gamma evaluation, Arc Check, EPID, portal dosimetry, dose grid.

DOSIMETRIC EVALUATION OF THE COLLAPSED CONE ALGORITHM CALCULATED RADIOTHERAPY PLANS IN IMRT AND VMAT FOR THORACIC TUMORS

Atul Mishra¹, Kailash Kumar Mittal¹, Anoop Kumar Srivastava², Surendra Prasad Mishra²,
Surendrakumar Dayashankar Maurya³

¹Department of Radiation Oncology, Uttar Pradesh University of Medical Sciences, Saifai, Etawah (U.P.)

²Department of Radiation Oncology, Dr. Ram Manohar Lohia Institute of Medical Sciences, Lucknow (U.P.)

³Department of Radiation Oncology, Shalby Hospitals, Indore

E-mail: meetatulmishra@gmail.com

BACKGROUND/OBJECTIVE: This study aimed to assess the effectiveness of using the Collapsed Cone Algorithm to generate treatment plans for thoracic esophageal cancer using Intensity-Modulated Radiation Therapy (IMRT) and Volumetric Modulated Arc Therapy (VMAT). The primary objective was to evaluate the efficacy of these treatment approaches in delivering radiation therapy to patients with thoracic esophageal cancer.

MATERIALS AND METHODS: We assessed a group of ten patients who had previously undergone VMAT treatment. The planning parameters were analyzed, focusing on maximum dose, mean dose, homogeneity index, conformity index for the planning target volume, and doses to organs at risk. Additionally, we recorded the total number of monitor units, treatment time, and the gamma passing index as part of our evaluation.

RESULTS: All ten patients in this evaluation successfully met the clinical dosimetry criteria for target dose distribution in both VMAT and IMRT plans. When comparing plans with equivalent target coverage, the VMAT plan exhibited superior performance in terms of conformity index, monitor unit, treatment time, and gamma passing index rate compared to the IMRT plan. These differences were statistically significant, highlighting the advantageous attributes of the VMAT approach.

CONCLUSIONS: The employment of the collapsed cone algorithm in VMAT has shown promise as a potentially superior and more effective approach for treating esophageal cancer compared to IMRT.

KEY WORDS: Dosimetry, Intensity Modulated, Radiotherapy Planning, Homogeneity Index, Conformity Index

EVALUATION OF SURFACE DOSE FOR FLATTENING FILTER AND FLATTENING FILTER FREE PHOTON BEAMS IN VARIAN TRUE BEAM MEDICAL LINEAR ACCELERATOR: A COMPARATIVE STUDY

Ankit Yadav¹, Kulbir Singh¹, ManGobinda Chowdhary¹, Munish Kumar¹, Gaurav Choudhary¹, Suresh Chaudhari²

¹Department of Radiation Oncology, American Oncology Institute, Ludhiana, Punjab

²Department of Radiation Oncology, American Oncology Institute, Hyderabad, Telangana

Email: ankityadav1008@gmail.com

BACKGROUND/OBJECTIVE: This study aimed to assess the surface dose delivered by 6MV and 10MV flattening filter (FF) beams and flattening filter free (FFF) beams of various square field sizes on a Varian True Beam medical linear accelerator using a parallel plate ionization chamber.

MATERIALS AND METHODS: The experimental setup involved a phantom composed of solid water slabs measuring 30x30 cm² with varying thicknesses. Additional solid water sheets were added to capture readings in the build-up region for both source-to-surface distance (SSD) and source-axis distance (SAD) techniques. Surface dose measurements were obtained using a parallel plate chamber (PPC) and MAX 4000 plus chamber electrometer at 1 mm intervals, with all results normalized to the dose measured at the depth of maximum dose (D_{max}) for different field sizes. Surface dose readings were reported as relative surface dose.

RESULTS: The surface dose exhibited a linear increase with increasing field size for both FF and FFF photon beams in linear accelerators, regardless of the SSD or SAD setup. The FFF beams consistently delivered higher surface doses compared to the FF beams across all field sizes. The surface dose difference between FF and FFF beams was more prominent for larger field sizes compared to the reference 10x10 cm² field size of 6FF. For the 6FF and 6FFF beams, the surface dose difference was -5.27% for a 5x5 cm² field and 12.91% for a 30x30 cm² field. The measured surface dose difference between the SSD and SAD setups showed no statistically significant difference ($P > 0.740$).

CONCLUSION: The difference in surface dose between the SSD and SAD setups was found to be negligible. Furthermore, the surface dose difference between FF and FFF beams was not statistically significant. Therefore, FFF beams can be considered as an alternative to FF beams, particularly when delivering higher dose fractions.

KEYWORDS: flattening filter free beam, surface dose, solid water, treatment time

USEFULNESS OF LOCALLY CONSTRUCTED PHANTOMS FOR THE VALIDATION OF PLANNED RADIATION FOR BREAST CANCER RADIOTHERAPY TREATMENT

Theresa Bebaaku Dery¹, Adolf Kofi Adolf¹, Samuel Nii Tagoe², Joseph Amoako³, Paul Kingsley Buah-Bassuah⁴

¹Radiological and Medical Sciences Research Institute, Ghana Atomic Energy Commission,

²National Centre for Radiotherapy and Nuclear Medicine Department,

³Department of Health Physics, School of Nuclear and Allied Sciences,

⁴Department of Physics, University of Cape Coast

Email: theresadery2000@gmail.com

BACKGROUND/OBJECTIVE: GLOBOCAN estimates, indicate that 4645 new cases were diagnosed and 1871 death occurred due to breast cancer in Ghana in 2018; making it the commonest female cancer and a major public health problem. To ensure the facilities in Ghana implement quality control measures, this study was designed to determine and compare planned with actual doses delivered to the breast during treatment. This is to achieve this, the major limitation of the non-availability of phantoms was addressed by the construction of phantoms, using perspex and locally available materials that mimic organs of the female thoracic cavity.

MATERIALS AND METHODS: Based on scanned images, two phantoms were constructed. Balloons, mango seed, cassava stick and candle were radiologically assessed and used as surrogates for the lung, heart, spinal cord and glandular tissue of the breast respectively. Higher photon energies from a ⁶⁰Co and LINAC machine were targeted at the left breast of a standard and the two constructed phantoms. EBT3 film dosimeter was used to measure absorbed doses to the breast and non-target organs.

RESULTS: The deviations of delivered doses from planned doses when the standard anthropomorphic phantom, constructed phantoms A and B were used, ranged as follows, -0.05 – 0.03 Gy; -0.08 – 0.01 Gy; -0.14 – 0.01 Gy respectively, when the radiation was delivered by a Cobalt-60 machine. When the radiation was delivered by a linear accelerator systems, the deviations were -0.05 – 0.03 Gy; -0.06 – 0.07 Gy; -0.06 – 0.04 Gy respectively. The left lung and spinal cord received the highest and lowest unintended dose, 0.74 ± 0.04 Gy (Co-60) and 0.78 ± 0.01 Gy (LINAC), and 0.03 ± 0.02 Gy and 0.05 ± 0.01 Gy respectively.

CONCLUSIONS: The study has demonstrated that local materials are potentially useful for the construction of phantoms, which can be good substitutes for standard commercial phantoms in ensuring the safety of patients under-going radiotherapy treatment for breast cancer.

KEYWORDS: radiation dose, phantoms, cobalt-60, linear accelerator

DOSIMETRIC EVALUATION OF VOLUMETRIC ARC THERAPY (VMAT) AND DYNAMIC INTENSITY MODULATED RADIOTHERAPY (IMRT) IN GLIOBLASTOMA

Anoop Kumar Srivastava, Farhana Khatoon, Anupam P B, Abu Musha Shah, S P Mishra, Rohini Khurana, Madhup Rastogi

Department of Radiation Oncology, Dr Ram Manohar Lohia Institute of Medical Sciences, Lucknow, India

Email: dranooprmlims@gmail.com

BACKGROUND/OBJECTIVE: Radiotherapy treatment plan of brain tumours poses multiple and complex challenges in attaining dose homogeneity in target volume without exceeding the dose constraints of vital brain structures. This evaluation attempts to analyse the efficacy of IMRT Vs VMAT in terms of integral dose, constraint to vital structures (brainstem, optic chiasm, optic nerve) and intensification of dose in target volume.

MATERIALS AND METHODS: Ten patients of glioblastoma were selected for the comparative analysis. The dose constraints and the target doses were brainstem- 60 Gy volume, Optic chiasm – 54 Gy Dmax, Optic nerve- 54 Gy Dmax, Target 60 Gy prescription with 95 % of volume covered with 95 % of prescribed dose. The doses escalation upto 60 Gy were planned in single phase and delivered by VMAT. Similar target dose and dose constraints were attempted to achieve using 5-7 field IMRT and both were compared. CT simulation slices of 3mm were generated for target volume delineation, OAR and RVR_brain using RTOG (0525) and planning using ICRU 83 recommendations. The doses were delivered with 6 MV photon after patients specific QA protocols were verified and recommended specifications were attained.

RESULTS: It was observed that both the techniques achieved the target dose escalation upto 60 Gy with a heterogeneity index of 1.04-1.06 and conformity index 0.8-0.9. The VMAT plans consumed higher MU (~1500) compared to IMRT (~700). The Integral doses to the remaining volume of brain for IMRT ranged from 13.8-23.6 Gy-Lt in comparison VMAT 11.1-21.2 Gy-Lt. Both the plans obtained the similar OAR constraints. Statistically it was found that it was not significant in terms of ability to achieve dose constraints in both the plans. It was noted that the target coverage in VMAT plans for 98 % of the volume was superior to IMRT but 95 % target coverage was achieved for both the techniques.

CONCLUSION: Clinical input suggested that VMAT is preferred mode of treatment plan in complex geometry posed by glioblastoma however Radiobiological evaluation and comparison may provide better clinical interpretations.

INTRA FRACTION MOTION AND POSITIONING UNCERTAINTIES IN STEREOTACTIC GAMMA KNIFE IMAGE-GUIDED RADIOSURGERY USING CONE BEAM CT

Nandakarthik, Ponnusamy, Banumathy, Dhaval Shukla

Department of Neurosurgery, National Institute of Mental Health & Neurosciences, Bengaluru, India

Email: sg.nanda@gmail.com

BACKGROUND/OBJECTIVE: Gamma Knife Radio Surgery (GKRS) can deliver highly conformal precise radiation to the intracranial brain disorders. Fine beams of gamma rays from multiple Co-60 radioactive sources (upto 192 sources) are focused on the tumor area with extreme accuracy. GKRS treatments deliver high radiations >10 Gy in a single or in minimal fractionations and demands conformal delivery and precise localization. Traditional frame based fixations been used for the immobilization of the head during the treatment. With advent of new Gamma knife (ICON) frameless surgery using non invasive thermoplastic mask is getting more popular due to minimal discomfort, especially during fractionated radiosurgery treatments. Reproducibility of immobilized head with high precision is mandatory for safe delivery of high dose of radiations. In the frame-based gamma knife treatment, indicator box localization has been utilized using fiducial markers to set the coordinate system whereas in ICON CBCT has been introduced, to facilitate fractionated treatments to verify the stability of head fixation from the beginning of imaging till the end of treatment and also to verify the setup error during the head mounted on the machine.

MATERIALS AND METHODS: This study is to investigate the consistency of the frame fixation and setup errors by using CBCT image guidance to quantify the inter and intra fraction movement for the patients undergoing gamma knife radiosurgery with rigid frame and thermoplastic mask based treatments. Dosimetric study with motion and Lucy 3D phantoms are performed to verify the image fusion, intrafraction motion and setup accuracy for Gamma Knife ICON equipped with CBCT on-board imaging and couch mounted with infrared camera with motion control to estimate the displacement error with adults and paediatric patients

RESULTS: The dosimetric deviation with setup and for various factors such as head rotation, chin movement and multiple treatment interruptions are considered in this study and deviations are estimated to be within 3%.

CONCLUSIONS: The integration of Imaging and treatment in stereotactic radiosurgery underscoring the importance of continuous evaluation of dose delivery, patient comfort and reproducibility. The finding of this study indicates the geometric uncertainties and the dosimetric impact of this intrafraction motion with longer fractions.

KEYWORDS: Gamma knife ICON, CBCT, Intrafraction motion

DEVELOPMENT AND CHARACTERIZATION OF A NOVEL BOLUS FOR PHOTON AND ELECTRON THERAPY

Kazuki Kubo¹, Hajime Monzen¹, Kenji Nakamura^{1,2}, Hiroshi Doi³, Takuya Uehara³, Masakazu Otsuka¹, Kenji Matsumoto¹

¹Department of Medical Physics, Graduate School of Medical Sciences, Kindai University, ²Department of Radiotherapy, Takarazuka City Hospital, ³Department of Radiation Oncology, Faculty of Medicine, Kindai University, Osakasayama, Japan

Email: panda.kazu1002@gmail.com

BACKGROUND/OBJECTIVE: The purpose of this study was to develop a new bolus (HM bolus) that had tissue equivalence, transparency, reusability, and free shaping at approximately 40°C for excellent adhesion, and to evaluate its features for clinical use.

MATERIALS AND METHODS: The HM bolus was controlled to prevent phase separation by adjusting the contents of ethylene propylene rubber, styrene, butadiene rubber, thermoplastic resin, temperature-sensitive adjuster, and silica. The density was adjusted to 0.96 gcm⁻³. A vinyl gel sheet bolus (Gel bolus) and HM bolus placed on a water-equivalent phantom were used to obtain the percent depth dose (PDD) of electron (6 and 9 MeV) and photon (4 and 6 MV) beams. The average difference of the PDDs between the HM bolus and Gel bolus was calculated. The Gel bolus, a soft rubber bolus (SR bolus), and HM bolus were placed in adherence to a pelvic phantom. CT images were taken after shaping and 1, 2, and 3 weeks after shaping, and the adhesion and reproducibility were evaluated on CT images using air gap and dice similarity coefficient (DSC) metrics.

RESULTS: The average difference of the PDDs for electron beams was 0.16% ± 0.79%, and for photon beams was 0.06% ± 0.34%, within 1% of the PDD results. The HM bolus showed the same build-up effect and dose characteristics as the Gel bolus. The mean air gap values for the Gel bolus, SR bolus, and HM bolus were 96.02 ± 43.77 cm³, 34.93 ± 21.44 cm³, and 4.40 ± 1.50 cm³, respectively. The mean DSC values for the Gel bolus, SR bolus, and HM bolus were 0.36 ± 0.04, 0.56 ± 0.04, and 0.84 ± 0.02. The HM bolus showed the smallest air gap at all time points and the DSC closest to 1. Excellent adhesion was observed in the CT simulation and during the treatment period.

CONCLUSIONS: We succeeded in developing a novel bolus with unique characteristics for clinical use. The HM bolus had the same build-up effect and dose characteristics as a Gel bolus and excellent adhesion, which could satisfy the conditions of an ideal bolus.

KEYWORDS: bolus, free shaping, adhesion

POTENTIAL OF EXPLAINABLE ARTIFICIAL INTELLIGENCE (XAI) IN RADIOTHERAPY

Sumana Halder, Arita Halder

School of Medical Science and Technology, Indian Institute of Technology, Kharagpur, India.

Email: sumanahalder006@gmail.com

BACKGROUND/OBJECTIVE: Artificial Intelligence (AI) has recently gained momentum in healthcare but its use has been marred with controversy. So, developers have turned to explainability techniques to assist users in comprehending the effectiveness and limitations of AI algorithms. These techniques shed light on the prediction process, making the "black-box" more transparent. In the field of radiotherapy, explainable AI offer transparent and interpretable insights regarding the decision-making processes of radiotherapy treatment planning and delivery. While XAI is widely used in medical imaging, it remains underexplored in radiotherapy. This abstract presents a short review of XAI in the field of radiotherapy.

MATERIALS/METHODS: The XAI process involves data pre-processing, methodology design, explanation of decisions and actions, and re-evaluation through user feedback for each decision to enhance the system's performance and acceptance. Various explainability methods, such as Grad-CAM, Layer-Wise Relevance Propagation (LRP), statistical functions, SHapley Additive exPlanations (SHAP), attention maps, and Local Interpretable Model-Agnostic Explanations (LIME), are utilized in the medical domain to provide justifications for model predictions. These methods enable better understanding in scenarios involving changing disease conditions and changes in data volume. Recently, CENTAI, a part of the PRE-ACT (Prediction of Radiotherapy side Effects using explainable AI for patient Communication and Treatment modification) project, is developing an AI-driven platform for breast cancer radiotherapy, predicting side effects and ensuring fairness. By modelling cancer treatment outcome metrics, X-CART platform leverages explainable AI to analyze associations between local social determinants of health and radiation therapy interruptions. In a study by the City of Hope group, XAI identified the patient subgroups benefitting from adjuvant radiotherapy for stage III-N2 non-small cell lung cancer. Another group created a survival prediction system for locoregionally advanced nasopharyngeal carcinoma (NPC) patients, forecasting distant metastasis using XAI.

RESULTS: It is seen that the robust XAI methods developed can predict treatment outcomes, disease progression, etc. efficiently giving us valuable insights into the decision-making processes of the algorithms. These models can prove to be beneficial to the clinicians.

CONCLUSIONS: XAI in radiotherapy has the potential to improve treatment planning, increase transparency, enhance patient safety, and facilitate the adoption of AI systems in clinical practice.

KEYWORDS: radiotherapy, artificial intelligence, explainable AI

MATHEMATICAL RELATIONSHIP BETWEEN LEFT CORONARY ARTERY AND HEART DOSE AND ITS CORELATION WITH LONG TERM ISCHEMIC HEART DISEASE.

Sudipta Santra¹, Biplab Sarkar², Suresh Yadav³, Suryanshu Choudhary⁴

¹ Ruby General Hospital, Kolkata, West Bengal, India

² Apollo Multispeciality Hospital, Kolkata, West Bengal, India

³ Gandhi Medical College, Bhopal, India

⁴ SAM Global University, Bhopal, India

Email: sudiptasnr5@gmail.com

BACKGROUND/OBJECTIVE: The landmark trial (2013) by Sarah Durby et al. established the relationship between long term cardiac toxicity (myocardial infraction: MI) and dose to heart. It was found that the rate of MI increases 7.4% per Gy. Later, it was found left coronary artery (LCA) is more responsible for MI than the heart's mean dose.

This study tries to find the mathematical relationship and other characteristic correlations between the dose to heart, LCA, and rate of MI for left sided breast radiotherapy using 3DCRT and tangential IMRT techniques.

MATERIAL AND METHOD: Total 100 patients planned for 40Gy in 15 fractions included in this study. All patients were planned with FiF and 5 field t-IMRT plan and doses to OARs were captured. Correlation coefficient (ccf) and statistical significance difference (defined at $p \leq 0.05$) were calculated using a paired sample t-test. For 3DCRT and IMRT, Heart vs. LCA doses were $ccf=50.5\%$ ($p=0.000$) and $ccf=65.1\%$ ($p=0.04$) respectively. Mean heart dose (IMRT vs. 3DCRT) $ccf=80.7\%$ ($p=0.000$). Mean LCA dose (IMRT Vs 3DCRT) $ccf=92.5\%$ ($p=0.000$). The mathematical relationship between heart and LCA dose for 3DCRT and IMRT is $y = 3.6456x + 737.82$ ($R^2 = 0.2555$) and $y = 5.0293x - 227.73$ ($R^2 = 0.4232$). Mean percentage increased risk of MI for 3DCRT and IMRT were $36.2 \pm 11.4\%$ and $25.210.6\%$. Mean LCA volume is 5.3% of heart volume.

CONCLUSION: Mean dose LCA statistically significantly different (poorly corelated) with heart dose, for 3DCRT and IMRT correlations were 50.5% and 65.1% respectively. Although anatomical position of the LCA is apparently fixed within the heart volume, the smallness of the LAC contributes a non-corelated variation between heart and LCA dose. Most important factor is heart position with curvature of the chest wall, and volume and position of the breast tissue. Tangential radiotherapy creates a triangular-shaped dose cloud, and heart falls in a high dose gradient region, where left upper quadrant is receiving prescription dose with a sharp dose fall off in other part. Therefore, it is difficult to create a robust mathematical model between the LCA dose and increased MI risk based on the early study data.

KEY WORD: ischemic heart disease, myocardial infraction, left coronary artery, Heart, dose.

ADAPTIVE PLANNING FOR INTER FRACTIONAL CHANGES IN TOMOTHERAPY MACHINE

Amala N Kumar, Soumya N M , Annop R , Debnarayan Dutta

Department of Medical Physics and Radiation Oncology, Amrita Institute of Medical Science, Cochin, Kerala, India

Email: amalank41@gmail.com

BACKGROUND/OBJECTIVE: The study aims to determine to what extent and how interfractional changes due to anatomical changes can be corrected using adaptive planning - Precise ART Adaptive Radiotherapy Software.

MATERIALS AND METHODS: Precise ART Adaptive Radiotherapy Software (Accuray precision treatment planning with MIM Module) was utilized for adaptive monitoring. Adaptive monitoring included merging the MVCT's acquired for each fraction of radiation therapy on to the planning CT (to identify the apparent anatomical changes), calculation of daily dose on the merged image, deform or rigidly transfer daily dose on to planning CT and summing the accumulated doses. Projected DVH was reviewed daily to ensure doses to critical OAR's is within the limits. Adaptive replanning was deemed necessary when the projected dose exceeded the cutoff dose constraints and PTV coverage.

RESULTS: Adaptive radiotherapy treatment is superior to non adaptive treatment. The advantages include minimum doses in the target structure and reduction in cumulative maximum doses of OAR's.

CONCLUSIONS: Daily adaptive planning helps to pick up the difference at the earliest time, leading to better OAR protection by strictly adhering to planned dose constraints. The most common cause of change in PTV coverage was weight loss. In patients who had adaptive replan, the time of replan is most probably between 10th and 20th fraction.

KEYWORDS: Precise ART adaptive radiotherapy software, tomotherapy machine, MVCT, DVH.

RADIATION FROM RADON INDOOR AND BUILDING MATERIALS. RISK ASSESSMENT AND MANAGEMENT.

Luca Gentile, Marco Simone Ravera, Diego Chiapale, Massimiliano Porzio, Camilla Lion
Daniela Rembado

SSD Environment, Physical Agents and Radiation Protection of the Department of Prevention of the ASLCN1
Cuneo, Italy

Email: omarkayam@alice.it

BACKGROUND/OBJECTIVE: Natural radiations accompanied the evolution of life, including that of man, even at higher levels than today; in the 20th century, after having represented economic opportunities. G. in the field of wellness, they are today in our area a radiation protection problem. The purpose of this work is a synthesis of radon risk assessment and management in our company and in its territory according to international and national standards for over 20 years.

MATERIALS AND METHODS: The measuring has been planned before 2003 considering underground rooms (E.G. bunkers, magnetic resonance sites, archives...) and ground floor rooms in risk areas. The definition of "Underground" is radon risk specific. The risk areas were firstly identified as those of the uranium rush from 50s or with silica lithotypes, then from 2003 on the official publications and from 2020 on specific laws. The measures were performed by passive systems during a solar year while active tools were used to design radon reductions. Specific radiation protection statements have been issued, also valid for new structural acquisitions included the building materials.

RESULT: All workplaces of the company were evaluated. In 2020, for the new law, the documentation in the records of the competent corporate Structures were examined. Out of 151 buildings, 53 were identified and, after site inspection, the measurements were carried out in 13 locations and in one case the concentration exceeded the reference limit and the mitigations were compulsory. By sniffing and active measurements also a radon reservoir over 10,000 Bq/m³ is found under the floor. An initial reduction must be updated with new remediation following new fire prevention measures. Education and training seems appreciated by workers.

CONCLUSION: To assess the risk could contribute to the knowledge of the real conditions for health promotion strategies and also for informing patients and population about the degree of radiological risk in nuclear medicine and diagnostics and, hopefully never needed, during a radiological/nuclear emergency. The MP-RPE with physicians and the staff of the our SSD have nowadays a task of risk assessment at their facilities and of information and vigilance on their territory.

KEYWORDS: radiation protection, radon, reduction, training

VALIDATION OF UNFLATTENED PHOTON BEAM DOSIMETRY ON A HYPERARC TRUEBEAM™ ACCELERATOR WITH AN SNC125C THIMBLE IONIZATION CHAMBER USING A CYLINDRICAL WATER SCANNING SYSTEM

Saravana Kumar A, Govindarajan KN, Rajadurai E

PSG Institute of Medical Sciences, Department of Medical Physics, Bangalore Baptist Hospital
Bengaluru, India

Email: Sarava87@gmail.com

ABSTRACT: With the aid of advanced high-end linear accelerators and the availability of various imaging methods, the practice of radiation therapy has been examined from broader margin fields to smaller volume precise field therapy. These methods include stereotactic radiosurgery (SRS), volumetric modulated arc treatment (VMAT), intensity modulated radiation therapy (IMRT), and stereotactic body radiotherapy (SBRT). This study aims to report small dosimetric aspects fields with a HyperArc high-definition radiotherapy linear accelerator. The measurements were performed at PSG Medical College & Hospital in Coimbatore. This study aimed to investigate small field dosimetric parameters with a semi-flux detector and evaluate the consistency of response with small field to reference field for 6MV and 10MV Flattening Filter Free (FFF) beams. In this work, we report the feasibility of a thimble ionization chamber and cylindrical RFA system with FFF beams and evaluate the commissioning data measurements.

METHOD & MATERIALS: The study included data for the profile, the percent depth dose (PDDs), output factor matrix and it tested how they responded to reduced field sizes. Measurement field sizes ranged from 0.5x0.5 cm² to 10x10 cm² for profile and PDD and OPF matrix measurements up to 40 x 40 cm², these data were normalized to AERB Protocol. The latest generation TruebeamSTx (Varian Medical System, Palo, Alto, CA) with HyperArc has recently demonstrated a linear accelerator and has many features including Stereotactic Radiosurgery (SRS) for single or multiple brain metastasis. The measurements were carried out in the SNC125c thimble ionization chamber using Sun Nuclear's recently released SunScan TM 3D cylindrical water scanning equipment.

RESULT: Relative and output factor measurements with a thimble ionization chamber were pertinent to initial beam data measurements, which were performed on flattening-filter-free (FFF) beams. The viability of a thimble chamber in small field measurements was also assessed. The thimble chamber responds well when the field size is 3 x 3 cm², but when the field size is smaller, the chamber's performance is not up to the mark. The measurements were carried out in the SNC125c thimble ionization chamber using Sun Nuclear's recently released SunScan TM 3D cylindrical water scanning equipment. The measurements were carried out in the SNC125c thimble ionization chamber using Sun Nuclear's recently released SunScan TM 3D cylindrical water scanning equipment. The study's recommendation is to utilize additional detectors like micro or nano chamber and stereotactic diode to measure the magnitude of the stereotactic field.

KEYWORDS: small field dosimetry, Hyper Arc, Thimble chamber, flattening-filter-free (FFF), cylindrical water scanning system

PLANNING DOSE EVALUATION AND OPTIMIZATION FOR HEART AND LUNG DOSE BY DIBH AND FREE BREATHING FOR LEFT SIDE BREAST CANCER

Md. Mokhlesur Rahman¹, Md. Abdul Mazed¹, Md. Zulkarnaen¹, Md. Khairul Islam³, Md. Anwarul Islam², Md. Khairul Islam⁴

¹Department of Medical Physics and Biomedical Engineering (MPBME), Gono University, Savar, Dhaka, Bangladesh, ²Department of Radiotherapy, Square Hospital Limited, Dhaka, Bangladesh, ³Institute of Nuclear Medical Physics, AERE, BAEC, Bangladesh, ⁴Cancer Center, CMH, Dhaka.

Email: hsmaklesur553@gmail.com

BACKGROUND/OBJECTIVE: Deep inspiration breath hold (DIBH) is a common method used worldwide for reducing the radiation dose to the heart. The aim of this study is to compare the reductions of heart dose and volume using DIBH with the dose/volume of free breathing (FB) for patients with left-side breast cancer and to analyse the patient-specific dose reduction parameters.

MATERIALS AND METHODS: In this study we were considered clinical dose plans for 40 left side breast cancer patients were evaluated: 20 patients treated with DIBH technique, 14th patients were received radiation in IMRT planning technique & 6th patients were undergoing in 3DCRT) and 20 free-breathing (FB) patients (10 patients were received radiation in IMRT planning technique & 10 patients were in 3DCRT). All patients received whole breast irradiation (WBI) with supraclavicular (SC) by tangential fields. Respiratory gating system (RGS) was used in this research to tracking chest wall movement. CT simulation and treatment were performed with the patient in the head first supine position. The planning CT scans consisted of 5 mm spaced slices of the whole chest, acquired during DIBH and FB. The prescribed dose was 40.05Gy in 15 fractions, 2.67Gy per fraction on the PTV breast.

RESULTS: The heart mean dose 4.1 ± 0.62 Gy and 6.378 ± 1.14 Gy, in DIBH and FB respectively for IMRT, heart mean dose 5.69 ± 3.53 Gy and 8.49 ± 2.70 Gy, in DIBH and FB respectively for 3DCRT planning. Heart dose at V25 4.56 ± 0.795 Gy and 7.572 ± 1.89 Gy, in DIBH and FB respectively for IMRT. Heart dose at V25 4.57 ± 3.92 Gy and 6.99 ± 3.86 Gy in DIBH and FB respectively for 3DCRT planning. Lung mean dose 13.39 ± 1.83 Gy and 17.46 ± 1.85 Gy, in DIBH and FB respectively for IMRT. Lung mean dose 13.28 ± 2.91 Gy and 15.325 ± 1.4 Gy in DIBH and FB respectively for 3DCRT planning. Lung dose at V20, 20.91 ± 2.52 Gy and 25.358 ± 1.784 Gy in DIBH and FB respectively for IMRT. Lung dose at V20, 30.97 ± 5.49 Gy and 36.30 ± 1.59 Gy in DIBH and FB respectively for 3DCRT planning.

CONCLUSIONS: DIBH is one of the best techniques to reduce heart and lung mean doses in left side breast cancer RT. DIBH with IMRT can be better than other techniques for conformity and homogeneity.

KEYWORDS: DIBH, 3DCRT and IMRT planning

EVALUATION OF WORKFLOW IN PELVIC PATIENTS USING SURFACE GUIDED RADIOTHERAPY WITH INTER-FRACTIONAL SIX-DIMENSIONAL SETUP

Sumanta Manna¹, Sharad Singh², Pramod Kumar Gupta², Ragul T¹

¹Medical Physics,²Radiation Oncology, Kalyan Singh Super Specialty Cancer Institute, Lucknow, Uttar Pradesh, India

Email:Sumanta7915@gmail.com

BACKGROUND/OBJECTIVE: Surface Guided Radiation Therapy (SGRT) is a non-invasive technique that utilizes real-time imaging of the patient's body surface to ensure accurate and precise delivery of radiation therapy. This study aims to evaluate the workflow efficiency of SGRT using the inter-fractional setup in pelvic patients and to assess setup time, accuracy, and reproducibility.

MATERIALS AND METHODS: In total, 44 patients from the pelvis cohort were included in this study and divided equally into two different workflows for initial patient positioning, one with skin marks and the other with the AlignRTSGRT system. The initial 8 to 10 treatment fractions of each patient were assessed, and subsequently. To minimize the overall treatment time and burden on patients, the workflow for SGRT was conducted 2 to 3 times a week instead of daily. The following parameters were analyzed: the translational (lateral, longitudinal and vertical) and rotational (pitch, yaw and roll) residual shifts of patient position based on cone beam computed tomography (kVCBCT) image matching. The average (μ) and the standard deviation (SD) were calculated for all studied treatment fractions. The resulting cohort residual setup imaging correction vectors were divided into two kinds of setup errors: systematic setup errors (Σ) and cohort residual random setup errors (σ). The time spent on patient positioning and kV image matching was recorded. The statistical differences two workflows were evaluated using the paired Wilcoxon signed-rank test, and $p < 0.05$ was considered significant.

RESULTS: SGRT decreased the translational magnitude shifts significantly ($P < .05$) by 0.7 ± 1.6 mm; further, a significant reduction was observed in both lateral and vertical directions. Rotational corrections were predominantly lowered with SGRT with significant differences in pitch and yaw direction ($p = .002$). The patient positioning time decreased significantly compared to skin marks ($p = 0.032$).

CONCLUSIONS: The SGRT system demonstrated improved efficiency with reduced setup time and enhanced accuracy compared to traditional methods. So, by implementing SGRT with an inter-fractional six-dimensional setup in the pelvis, patients can optimize workflow and contribute to improved treatment outcomes. The quality of patient positioning before treatment has been optimized using SGRT without additional imaging doses.

KEY WORDS: Inter-fractional 6D setup; kV-CBCT; SGRT, Systematic Error, Random Error

STUDYING THE IMPACT OF FINITE SIZED IONISATION CHAMBER ON GAMMA ANALYSIS (PATIENT SPECIFIC QA) DUE TO BEAM PROFILE PENUMBRA BROADENING

Hitesh Bisht¹, Anurupa Mahata², Samar Mandal³

¹Department of Radiation Oncology TMC Kolkata & School of Medical Science and Technology, IIT Kharagpur, ^{2,3}Department of Radiation Oncology TMC Kolkata, India

Email: hitesh13bisht@gmail.com

BACKGROUND/OBJECTIVE: ICRU 24 recommended that the Dose delivered to the patient should be within 5% of the Prescription. This requires the total error from all the sources- calibration, commissioning, dose calculation, patient setup, margins, and dose delivery. Beam data commissioning has the potential to impact the treatment delivery of every patient- every fraction. There has been a long debate on the use of the 3% 3mm criterion for gamma analysis when the contemporary LINACs MLCs have an accuracy of 1mm. Switching to more stringent criteria of 2% 2mm would help us detect finer errors in beam delivery and will help us reduce the chance of giving a max dose to serial organs as acceptable changes in the MLC pattern can change my max doses. For this, we need are commission to be extremely accurate and one of the parameter that can be improved is Beam Profile Penumbra estimation. The standard practice for beam profile measurement during commissioning uses a 0.125 cc Ionisation Chamber which causes the broadening of the beam penumbra and subsequently, our data has some inherent error built in. We aim to reduce this error by employing film dosimetry.

MATERIAL AND METHODS: We are using Truebeam Stx S No. 3191, iba Dose 2 RFA and iba cc13 0.125cc ionisation chamber. The true profile is obtained from film dosimetry while the convolved profile is obtained from the ionization chamber. This is used to derive the convolution kernel defining volume averaging effect for my ionisation chamber. This kernel will help us get the true profile at different depths and field sizes required for commissioning by deconvolution of the ionisation chamber measured profile. Eclipse TPS is commissioned with this new waveform and the portal images would be calculated for the plans again and would be compared with the EPID portal dose distribution.

RESULTS / OBSERVATION: We expect to get a gamma passing rate of more than 90% for 95% of our cases with 2% 2mm as achieved by earlier studies.

CONCLUSION: The work is in the data collection stage.

FAN BEAM (TOMOTHERAPY) VS CONE BEAM (NOVALIS TX) BASED TREATMENT PLANNING DOSIMETRY FOR CERVICAL CARCINOMA PATIENTS WITH PARA-AORTIC NODAL INVOLVEMENT

¹Lakshmi Venkataramana Puriparthi, ¹Anil Kumar Talluri, ¹Akkineni Naga Prasanthi,
²Venkatappa Rao Tumu, ¹NVN Madhusudhana Sresty, ¹Krishnam Raju Alluri

¹Basavatarakam Indoamerican cancer Hospital & RI, Hyderabad

²Department of Radiation Oncology, National Institute of Technology, Warangal

Email: lakshmianil.puriparthi@gmail.com

INTRODUCTION: Cervical cancer accounted for 9.4% of all malignancies and 18.3% (123,907) of new cases in India in 2020. About 90% of the new cases and deaths worldwide in 2020 occurred in low- and middle-income countries [1]. Extended field irradiation is the standard management in cervical carcinoma patients with para-aortic nodal involvement. Extended-field radiotherapy with cisplatin chemotherapy for patients with para-aortic nodal metastasis from cervical cancer is associated with significant acute and late toxicities. For cervical cancer patients undergoing pelvic and para-aortic radiation, intensity-modulated radiation therapy (IMRT) lowers the doses to the small bowel, rectum, and bladder [2]. Rapid arc IMRT (R-IMRT) and helical tomotherapy (HT) are the latest advanced techniques available for IGRT treatment. The current study aims to evaluate the dosimetric results of R-IMRT and HT for the treatment of carcinoma cervix along with para-aortic nodal irradiation.

MATERIALS AND METHODS: A total of 25 carcinoma cervix patients with para-aortic nodal involvement were selected for this retrospective study. Patients were instructed to empty their rectum and to follow institutional bladder protocol before CT simulation and daily treatment. For all patients, plain and contrast-enhanced computed tomography (CT) images were acquired with a 5mm slice thickness using the Brilliance CT Big Bore. The CT images were exported to the Eclipse treatment planning system (TPS). For each patient, 2 plans were generated. The first plan was created (R-IMRT) with Eclipse planning system version 15.6.8. (Noavlis Tx machine). The R-IMRT plans were optimized using a photon optimizer and the dose was calculated using the anisotropic analytical algorithm (AAA). The second plan (HT) was generated with the Tomo planning station, version 5.1.1.6 (Tomotherapy machine). collapsed-cone convolution is used for the dose calculation. For each patient, both plans were compared using a dose-volume histogram (DVH). The parameters considered for the comparison of PTVs are the conformity index (CI) and the homogeneity index (HI). For the bladder and rectum, the volumes receiving 30 Gy, and 40 Gy (V30, and V40, respectively), as well as the mean dose (Dmean), max dose (Dmax), and dose received by 2cc volume were compared. For bowel volume receiving 45Gy (V45) and mean dose were considered. For femoral heads mean dose (Dmean), max dose (Dmax) and volumes receiving 30 Gy (V30) were taken. For kidneys, the volumes receiving 12Gy, and 20 Gy (V12 and V20 respectively) and the mean dose were chosen. For the spinal cord max dose and dose received by 1% volume were included. For bone marrow volumes receiving 10 Gy, 20Gy, 30 Gy, and 40 Gy (V10, V20, V30, and V40, respectively), mean doses were compared. For patient volumes receiving 5Gy, 10Gy, 20 Gy, and 30 Gy (V5, V10, V20, and V30, respectively) were considered for lower doses.

RESULTS: RIMRT plans were compared with respect to TH plans dosimetrically using DVH for the PTV as well as OAR doses. For the rectum, a statistically significant difference was observed for mean V40, with 61.41 ± 7.45 and 53.11 ± 12.11 , mean Dmax with 51.6 ± 0.84 and 52.85 ± 0.76 , and mean D2cc with 50.11 ± 0.89 and 51.25 ± 0.86 for RIMRT and TH plans respectively. For bladder mean V30, with 89.09 ± 6.62 and 71.74 ± 13.56 , mean Dmax with 52.03 ± 0.85 and 53.53 ± 1.04 and mean D2cc with 50.96 ± 1.04 and 52 ± 0.58 for RIMRT and TH plans respectively. For the target, the CI values are 0.88 ± 0.03 and 0.84 ± 0.03 for RIMRT and HT respectively. The HI values are 0.87 ± 0.03 and 0.11 ± 0.18 for RIMRT and HT respectively

DISCUSSION: The results of the current study are in good agreement with chenJl [3].

CONCLUSION: Even though both techniques were a good option to treat cervical carcinoma patients with para-aortic nodal involvement, Tomo is better when compared to OAR doses and lower doses by the patient, which may lead to secondary carcinogenic.

VARIATIONS IN PATIENT DOSE AND EXPOSURE PARAMETERS IN ABDOMINAL RADIOGRAPHY: A COMPARATIVE ANALYSIS

Sachith Welarathna^{1,2}, Sivakumar Velautham², Sivananthan Sarasanandarajah³

^{1,2}Department of Physics, University of Peradeniya, Peradeniya, Sri Lanka, ²Postgraduate Institute of Science, University of Peradeniya, Peradeniya, Sri Lanka, ³Peter MacCallum Cancer Institute and RMIT University, Melbourne, Australia

Email: sachith.welarathna@sci.pdn.ac.lk

BACKGROUND: Abdominal radiography, routinely performed to diagnose patients with acute abdominal pain, is associated with higher patient doses than most other projection radiography examinations. Consequently, it is necessary to keep patient doses within the framework of as low as reasonably achievable (ALARA) and as low as diagnostically acceptable (ALADA) principles to promote good practice. The aim of this study was to investigate the variations in patient doses and exposure parameters during abdominal X-ray examinations.

METHODS: Body weight, body mass index (BMI), tube voltage (kVp), and tube current-exposure time (mAs) were collected for 90 adult patients referred for supine abdominal X-ray examinations from six major government hospitals in Sri Lanka. The kerma-area product (KAP) was measured using a KAP meter mounted on the collimator of the X-ray tube. Descriptive statistics were computed to investigate the variation in KAP, kVp, and mAs distributions. The Kruskal-Wallis H test was used to compare the differences in KAP, kVp, and mAs values among hospitals ($p < 0.05$).

RESULTS: Eighty patients were included in the analysis (age: 18-84 years, weight: 38-78 kg). As indicated by the median BMI, the patients' sizes were comparable among hospitals (BMI: 21.2-22.8 kg/m²). The median (range) KAP values for six hospitals varied broadly, with values of 1.42 (0.423-52), 1.78 (1.41-2.97), 1.79 (1.29-3.04), 1.84 (1.69-2.93), 2.37 (1.40-3.96), and 2.42 (1.31-3.74) Gy·cm². The median kVp used ranged from 66 to 74, while the median mAs varied from 32.0 to 40.0 among hospitals. There were statistically significant differences in the median KAP ($p = 0.003817$) and kVp ($p = 0.0003912$) among the hospitals but not in the mAs values ($p = 0.06379$). This highlights the importance of maintaining kVp at certain levels to minimize variation in KAP values. The third quartile value of the median KAP distributions among hospitals was 2.28 Gy·cm², comparable with the recently published values.

CONCLUSIONS: The wide variations in kVp, and mAs among and within hospitals revealed that further optimization of patient dose would be possible without compromising the diagnostic information of the examination. Comparisons with hospitals reinforce the need for further radiation dose optimization, appropriate use of exposure parameters and collimation in current radiographic practice.

KEYWORDS: abdominal radiography, kerma-area product, exposure parameters, patient dosimetry, radiation protection

THE EFFECT OF DWELL TIME GRADIENT RESTRICTION ON TREATMENT PLAN USING HYBRID INVERSE PLAN AND OPTIMIZATION IN MANAGEMENT OF CERVICAL CANCER WITH INTERSTITIAL HDR BRACHYTHERAPY

Chandrasekar G

Archarya Tulsi Regional Cancer Institute, Annangar 3rd Street, Tiruvannamalai, 606601 India

Email: chandrishi05@gmail.com

PURPOSE: To determine the ideal Dwell Time Gradient Restriction (DTGR) value for hybrid inverse planning and optimization in high dose rate interstitial cervix brachytherapy.

MATERIAL METHOD: This is a Dosimetric study of 30 patients planned with CT images using Nucletron Oncentra treatment planning system. The patients were treated with CT image-based high dose brachytherapy using MUPIT applicator. Using hybrid inverse planning and optimization of the plans had been optimized for every patient with different DTGR (Dwell Time gradient restriction) Value from 0.0 to 1.0, in the increasing order of 0.2. The analysis of physical dose parameters such as Total Dwell time, Conformity index (COIN), Coverage index (CI), Dose Homogeneity Index (DHI), Dose Non – Uniformity Ratio (DNR), Over Dose Volume Index (ODI), External Volume Index (EI), Plan Quality Index1 (PQI1), Plan Quality Index2 (PQI2), Plan Quality Score (PQS) were performed. Dose to the OAR, such as Bladder (B0.1cc, B1CC, B10CC, B2CC), Rectum (R0.1CC, R1CC, R10CC, R2CC) and Sigmoid (S0.1CC, S1CC, S10CC, S2CC) surrounding the HR CTV has been noted. The Gain factor of bladder (GFB), Rectum (GFR), Sigmoid (GFS) and the Total Gain factor (GF) has been calculated. Dose Volume indices for HRCTV (D90, D100) and high dose volume parameters (V150, V200, V300) were taken in to consideration. The quality of various DTGR values were compared using Plan Quality Score and Plan Modulation Index. The Dosimetric Parameters were compared and analysed for the range of DTGR values, from 0.0 to 1.0. One sample T-test in the SPSS software was used for the statistical analysis.

RESULT: There is a decline in gain factor of bladder, and rectum. There is rise in the Gain Factor of the Sigmoid. The gradual decline in the Readings of B0.1cc, B1CC, B10CC, B2CC, R 0.1CC, S0.1CC, S1CC, S10CC, and S2CC has been noted. The D90% HR CTV steadily rises from 0.2 to 1.0 while its D100% gradually declines from 0.2 to 1.0. DNR, ODI, and EI steadily rise as CI, COIN, and DHI decrease from 0.2 to 1.0. The Plan Quality Score (PQS) is calculated and analyzed; the PQS is high at 0.0 and gradually declines at the DTGR value till 1.0. Similarly, according to the plan modulation index the optimization decrease from the DTGR value 0.0 to 0.6 and then stagnates. At 0.0, the Treatment Time is minimal and rises as the DTGR value increases. This data is statistically significant.

CONCLUSION: Dwell time gradient restriction in HIPO optimization of HDR Cervix interstitial brachytherapy plans may be used to optimize the Dwell Time. The recommended value for the DTGR parameter is 0.6 or higher. The Plan Quality Index was only reduced by an average of 2.83 to 3.26% as a result, but in comparison, there was better Modulation factor until 0.6 compared to 0.0 of 30% and then became constant. The PQS is at an acceptable level and the Plan Modulation Index value is good at the DTGR value of 0.6. Hence, 0.6 is the optimal DTGR value for the optimization. We may also use 0.8 and 1.0.

ROLE OF MR IMAGING IN THE EVALUATION OF PITUITARY LESIONS

Mehrdad Baranzehi, Zeynab Yazdi Sotoodeh, Mahdiyeh Zarei

Iran-Zahedan-Sistan V Balouchestan-Zahedan-Zums Zahedan, 123321, Islamic Republic of Iran

Email: mehrdad.baranzehi.bff@gmail.com

INTRODUCTION: Pituitary gland plays a central role in body growth, metabolism, and reproductive function. Pituitary lesions, albeit relatively infrequent, can significantly alter the quality of life. Recent advances in neuroimaging helps the radiologists and endocrinologists to study the pituitary region in greater detail. Magnetic resonance imaging (MRI) is the imaging modality of choice for evaluating hypothalamic-pituitary-related endocrine diseases. Magnetic resonance imaging (MRI) is the examination of choice for evaluating hypothalamic pituitary-related endocrine diseases. Pituitary masses are diagnosed with increased frequency with magnetic resonance imaging (MRI) advancements and availability, but indications and diagnostic outcomes of MRI screening for sellar lesions are not defined. Although pituitary adenomas are the most frequently encountered sellar mass lesions, other etiologies should be considered in the differential diagnosis of a sellar mass.

IMAGING MODALITIES: Pituitary imaging is important not only in confirming the diagnosis of pituitary lesions but also in determining the differential diagnosis of other sellar lesions. Plain skull radiographs are poor at delineating soft tissues, and infrequently requested these days for diagnosing sellar and parasellar pathologies. The radiographic size of sella is not a sensitive indicator of pituitary gland abnormality, as the empty sella may itself lead to enlargement of size. Thus the plain radiographs have been replaced by cross-sectional imaging techniques such as CT scanning and MRI. MRI is the examination of choice for sellar and parasellar pathologies due to its superior soft tissue contrast, multiplanar capability and lack of ionizing radiation. In addition, MRI also provides useful information about the relationship of the gland with adjacent anatomical structures and helps to plan medical or surgical strategy. MRI techniques in diagnosing pituitary lesions have witnessed a rapid evolution, ranging from noncontrast MRI in late 1980s to contrast-enhanced MRI in mid-1990s. Introduction of dynamic contrast-enhanced MRI has further refined this technique in diagnosing pituitary microadenomas. Recently, a variety of advanced MR techniques have been evolved which are particularly helpful in evaluating specific cases. These include 3D volumetric analysis of pituitary volume, high-resolution MR imaging at 3 Tesla (T) for evaluating pituitary stalk, diffusion-weighted imaging, MR spectroscopy, magnetization transfer ratio, and intraoperative MRI. The aim of MR imaging is to obtain a high-spatial-resolution image with a reasonable signal to noise ratio. Pituitary MRI identifies sellar tumors and pituitary masses and offers high contrast and multiplanar, thin pituitary cuts enabling evaluation of small soft tissue changes. MRI also allows accurate visualization of mass effects on neighboring soft tissues. Although most adenomas are detected on nonenhanced MRI, microadenomas may become visible only after contrast injection.

CONCLUSION: Pituitary adenomas are among the most common central nervous system tumors. Extension of pituitary adenomas can occur in a suprasellar, retrosellar, or lateral fashion. Suprasellar extension of macroadenomas is the most common direction of extension and can result in penetration of the floor of the third ventricle and hypothalamus. Headache is a common clinical indication for imaging leading to discovery of incidental pituitary masses. Pituitary tumor-related headaches may improve in up to 70% of patients after adenoma resection. Furthermore, the presence of headaches does not necessarily correlate with the mass size. Several mechanisms have been proposed for the cause of headaches in patients harboring pituitary masses, although these have not been uniformly substantiated. Regardless, the higher rate of headache occurrence observed for nonadenomatous lesions vs. both nonfunctioning and functioning adenomas suggests that nonadenomatous lesions are more likely to cause headache ($P < 0.001$). Headache (57%) was the most common presenting symptom in patients with nonadenomatous masses identified by MRI. Dedicated pituitary MRI is the preferred diagnostic imaging modality for evaluation of sellar and parasellar tumors, including adenomas. In particular, when functioning adenomas are suspected, a dynamic pituitary MRI, which obtains images within seconds after gadolinium contrast injection, may be more useful because it has higher sensitivity than other imaging modalities for detecting small microadenomas. Overall, given the compelling list of possible diagnoses, when a nonsecreting pituitary mass is observed by MRI, a high clinical suspicion and thorough endocrine and possible pathological assessment is required to exclude the presence of a nonfunctioning pituitary adenoma.

VOLUMETRIC MODULATED ARC THERAPY (VMAT) CRANIOSPINAL IMAGE-GUIDED RADIOTHERAPY EXPERIENCE USING AN ADVANCED RING GANTRY LINAC IN A LOWER- INCOME COUNTRY

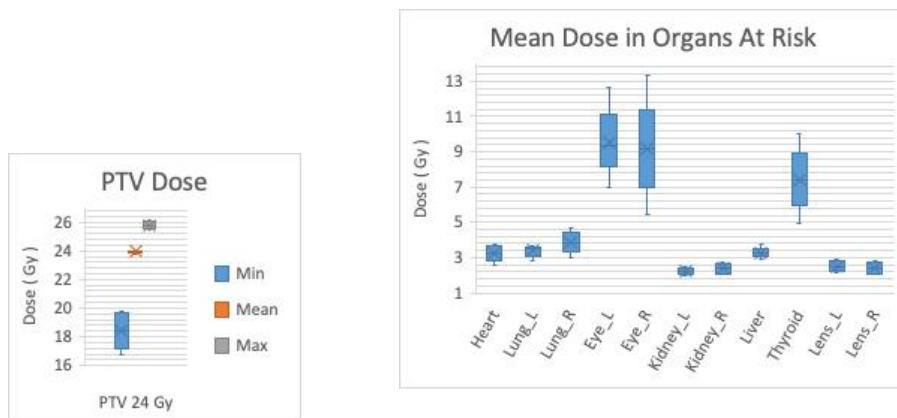
Milton Ixquiác¹, Erick Montenegro¹, Edgar Ruiz¹, Vicky de Falla¹, Osmar Hernandez¹, Franky Reyes¹
¹Liga Nacional Contra elCáncer – INCAN, Department of Radiation Oncology, ²Department of Radiotherapy, Guatemala

Email: miltonestuardo@gmail.com

BACKGROUND/OBJECTIVE: Implementation of a modern radiotherapy techniques require a lot experience and some cases require a little more than just modulated beams. This is the case of the craniospinal radiotherapy treatments using an advanced-ring-gantry linac. In 2019 a modern linac was installed and commissioned in Guatemala City for a more precise treatment with high quality. This work describes the experience about the VMAT treatments delivered to craniospinal cases using an advanced ring gantry linac in lower-income country.

MATERIALS AND METHODS: For the skull region, each plan is created using two opposite fields with the irregular surface compensator option. This fields avoid completely the lenses. Manually the fluence is edited to create a gradient in the caudal direction. A second plan, the thoracic region, is created with full arcs using an option for muti-isocenter option with the specific software for this device. A set of muti-isocenter to cover the thoracic area and one to the lumbar area. Every field has a good amount of overlap with the following to avoid hot or cold spots on delivery. These plansareoptimized using the cranial plan as base plan and using avoidance sectors on both sides to reduce dose to shoulders and arms. Finally, it is separated in three different plans deliver ready each with image guidance setup. Each plan must be verified trough the Patient Specific Quality Control (PSQA) using Portal Dosimetry and Matrix quality control process.

RESULTS: The values achieved for the organs at risk are acceptable is we compare the data with others reports about creaniospinal (IMRT Zheng Wan et all 2013, VMAT Yun Zhan 2023,Kenji Matsumoto 2023, EnricaSeravalli 2018), our plans are similar in almost all organs and in some cases we achieve better protection for the OARs.



CONCLUSIONS: This study reports a practical and effective treatment plan for craniospinal treatment using an advanced-ring-grantry achieving good dosimetric values, making it safer the patient and using less time than the C-arm linacs. We still planning in this way to increase the statistic and try to feed a knowledge-based plan software to optimize the time of planning.

KEYWORDS: ring based linac, craniospinal, planning

MULTISCALE DIGITAL TWINS FOR PRECISION DOSIMETRY AND CELL SURVIVAL OUTCOMES IN RADIATION TREATMENTS

Anuj J. Kapadia¹, Paul Inman¹, Ashok Tiwari¹, Debsindhu Bhowmik¹, Matthew Andriotty², Zakaria Aboulbanine¹, and Greeshma A. Agasthya¹

¹Oak Ridge National Laboratory, USA, ²Georgia Tech University, USA

Email: kapadiaaj@ornl.gov

BACKGROUND/OBJECTIVE: Digital twins have the potential to revolutionize radiation treatment in oncology by creating virtual replicas of patients, enabling personalized treatment planning, predicting outcomes, and facilitating real-time monitoring. However, limitations exist. Accurate modeling of patient anatomy and complex biological systems requires precision and may introduce inaccuracies. Computational demands and time constraints pose challenges to real-time applicability. Variations in treatment response among patient populations and disease types limit generalizability. Integration into existing workflows and interoperability with systems require careful coordination. We aim to overcome these challenges, refining and expanding digital twin capabilities to enhance radiation treatment and improve patient care.

MATERIALS AND METHODS: We have developed a multiscale computational framework that utilizes digital twins for precision dosimetry and outcome prediction in radiation treatments. Using a combination of GEANT4, TOPAS-nBIO, CompuCell3D and XCAT phantoms, we track radiation effects at multiple scales ranging from the whole body to the DNA level and use these measurements to estimate cell survival in both tumors and surrounding tissue. We evaluated the utility of our computational framework in both external beam and radiopharmaceutical therapy in adult and pediatric XCAT phantoms. External beam treatments modeled gamma and proton beams at dose fractions ranging from 4-40Gy. Radiopharmaceutical treatments modeled ¹⁸F and ²²⁵Ac at multiple activities. In all cases, DNA damage, subsequent repair, and cell survival outcomes were tracked for the XCAT digital twin.

RESULTS: Our framework accurately predicted cell survival and treatment response in radiation treatment, aligning with expected estimates and published literature. The automated pipeline between CC3D and GEANT4 seamlessly estimated dose maps and tumor response at different time points. Dose maps were generated for the tumor and surrounding regions as well as for other vital organs in the body. Each irradiation resulted in dose-dependent decreases in the corresponding tumor cell volume.

CONCLUSIONS: Our multiscale computational framework, utilizing CC3D, GEANT4, TOPAS-nBIO and XCAT phantoms, successfully assessed radiation effects on cell survival in multicellular human digital twins. We now aim to validate and expand this framework to predict cell survival and treatment outcomes in various cancer types and in multiple oncology applications including external beam, brachytherapy, and radiopharmaceutical treatments.

KEYWORDS: Modeling, Simulation, Dosimetry, Cell survival, Treatment, High-performance computing, Monte Carlo, XCAT, GEANT4, TOPAS-nBIO, CompuCell3D

ACCESS TO STEREOTACTIC RADIOSURGERY TREATMENT IN AFRICA: PRACTICAL GUIDELINES FOR IMPLEMENTATION

Emmanuel Fiagbedzi

Department of Medical Physics, University of Ghana Accra, 233, Ghana

Email: emmanuel2g4@gmail.com

PURPOSE: Radiosurgery with the Gamma Knife is the golden standard for the treatment of brain metastasis cases but its accessibility however in many countries in Africa is limited. Modern radiotherapy has made this treatment possible using other equipment such as linear accelerator and cyberknife. The objective of this work was to explore the distribution of radiotherapy equipments for the treatment of brain metastasis in Africa and provide practical guidelines to the establishment of a SRS Program.

MATERIAL AND METHODS: Data was gotten from the Directory for Radiotherapy Centres (DIRAC), an electronic, centralized, and continuously updated database of radiotherapy centres created and maintained by the Division of Human Health of the IAEA. Data on modern radiotherapy equipment for the 54 Africa countries were extracted from this database. Cancer incidence and brain metastasis predictions were made using data from the GLOBOCAN 2020 database of the International Agency for Research on Cancer and country's income was assessed on the worldeconomics database. Further literature search was also carried out on the availability of dedicated equipments for brain metastasis management in Africa in PubMed. All these searches were done in December,2022.

RESULTS: There is increase in the number of brain metastasis cases. There is 1 only Gamma Knife machine in Africa located in South Africa. Three Cyberknives, two in Egypt and one in kenya and 381 linacs distributed across the continent. The cost of a Gamma Knife machine could be up to US\$7 million compared to that of linac between \$2.4 to \$2.8 million and cyberknife between \$3 to \$5 million. A country's (GDP)income was an important predictor of the availability of these machines: in countries without any machines versus in countries with at least one machine.

CONCLUSION: Access to radiosurgery treatment for brain metastasis with the Gamma Knife or Cyberknife is limited due to the low number of these equipment. With the increase in radiotherapy expansion with linear accelerators, it is likely that the continent will be able to increase its stereotactic radiosurgery treatment centers by implementing linac-based SRS following suitable guidelines. This will help provide comprehensive care to patients and promote quality of life.

KEYWORD: Stereotactic radiosurgery, Gamma knife, Cyberknife, Linac, brain metastasis

RADIATION PROTECTION EFFICIENCY OF HIGH DENSITY CONCRETES: A COMPARATIVE STUDY

Amandeep Sharma

Department of Physics, Akal University Talwandi Sabo (Bathinda), Punjab, India

Email: adsphy@gmail.com

BACKGROUND/OBJECTIVE: Nowadays, radiation technology is extensively used in radiology departments of hospitals, nuclear power plants, agriculture and industrial sectors. Since X-/ Gamma-ray emitting sources are mainly involved in these places therefore it is of crucial importance to guard the humans in close vicinity of these areas from the hazardous penetrating radiations. As composition of any shielding material is one of the important considerations to protect against dangerous effects of penetrating radiations. Thereby, determination of various parameters concerned on the transportation of ionizing radiations through any shielding composition is of critical interest.

MATERIALS AND METHODS: The theoretical computations have been made by employing the Phy-X/PSD (Photon Shielding and Dosimetry) and XCOM database at useful X-/Gamma energies of 0.04, 0.05, 0.06, 0.08, 0.1, 0.15, 0.2, 0.3, 0.4, 0.5, 0.6, 0.8 and 1.0 MeV for selected heavy density concretes. The data tables have been presented on important shielding parameters (transmission factor, radiation protection efficiency and half value layer) of selected concretes.

RESULTS: The study estimated and compared various shielding parameters for three high-density concrete samples with that of normal concrete material through two software programs. It has been concluded that shielding parameters obtained from XCOM and Phy-X/PSD are in good harmony, with maximum relative difference of 0.3%. The shielding parameters reported here support the concrete sample having higher value of density (3.365 g/cm^3) as the 'best shielding composition' among the investigated samples.

CONCLUSIONS: The shielding parameters for different high density concrete materials have been computed and compared at X-/Gamma-ray energy range of 0.04 - 1.0 MeV. Concrete sample with the maximum weight fraction of higher atomic numbered elements shows the highest values of radiation protection efficiency.

KEYWORDS: X-/Gamma-rays, Radiation shielding, Transmission factor, Protection efficiency

STATISTICAL ANALYSIS OF EXPOSURE LEVELS FOR MEDICAL RADIATION WORKERS DURING 2011-2021

Seethal Johnson, Arshad Khan and B K Sapra

Radiological Physics and Advisory Division, Bhabha Atomic Research Centre, Mumbai, India

Email: seethal@barc.gov.in

INTRODUCTION: Personnel monitoring of radiation workers is of great significance to ensure adequate safety in various radiological applications of ionizing radiation, and reduce subsequent health risks. The evolution of advanced techniques in medical physics like diagnostic radiology, nuclear medicine and radiation therapy are considered as essential tools in various branches of medicine which has increased the use of radiation in last few decades. Personnel monitoring helps to reduce the potential harm caused by the radiation by proper assessment of the dose data of workers and keep the radiation exposure to individuals well below the specified limits as prescribed by AERB. Occupational exposure data of radiation workers in various medical practices. Diagnostic Radiology (DR), Dental, Radiotherapy, and Nuclear Medicine (NM) and other uses were collected and analyzed from 2011 to 2021.

METHODOLOGY: National Occupational Dose Registry System (NODRS) of Radiological Physics and Advisory Division, BARC is the national registry for dose data records of radiation workers (RW) since 1953. $CaSO_4:Dy$ based TL dosimeter is used to monitor doses to exposed workers by external radiations like X-ray, gamma ray and beta radiations with quarterly service. The trend analysis of the data was conducted using non-parametric tests, namely the Mann-Kendall and Sen's slope test in medical sector.

RESULTS AND DISCUSSION: The total number of RW as well as the workers exposed to radiation in medical practices has consistently increased over aforementioned period (Fig 1). However, there is a deviation in the trend, due to reduction of radiation activities during Covid-19 pandemic in 2020. The observed growth rate is 201.46% in number of medical RW during the reported period compared to 118.8% growth rate of total RW in India. The percentage of RW receiving measurable annual dose (\geq detection limit, i.e. 0.05 mSv) has come down from 45.5% to 28.7% over the years (Fig 1). There is an overall downward trend observed in average annual dose ranging from 0.42 - 0.23 mSv reflecting improvement of safety standards as well as better regulatory control (Fig 2). The Mann-Kendall test has been applied to this dose data for trend analysis. There is evidence to support an increasing trend in collective dose data in medical at the 99% confidence level ($Z=2.82$, $p=0.0048$) and a decreasing trend in average annual effective dose data in medical at the 99% confidence level ($Z=-3.4$, $p=0.0006$). Furthermore, it is found that the decreasing rate of average annual effective dose is 0.018 mSv/year calculated using Sen's slope indicator which also agrees with linear regression fit for the data (Fig 3). The major contribution to total collective dose is predominantly due to Diagnostic radiography which is 86%. The average annual effective dose during the period was estimated to be 0.3 mSv which is well below the worldwide average annual effective dose of 0.5 mSv for Medical sector during the period 2010-2014 (UNSCEAR 2020/21). However, the average annual effective dose of nuclear medicine is 0.59 mSv which is higher than the worldwide average of 0.4 mSv for nuclear medicine given in the period 2010-2014 (UNSCEAR 2020/21). This is due to the use of unsealed radiation sources in nuclear medicine which causes higher external and internal exposure to the staff. The control of occupational exposure in nuclear medicine can be effectively carried out by design of facilities, designation of workplaces in control and supervised areas, area monitoring, monitoring for contamination, use of appropriate personal protective devices etc.

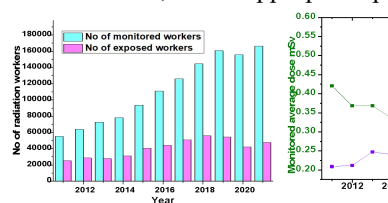


Fig 1: Number of Monitored RW and RW Receiving Measurable Dose (2011-2021)

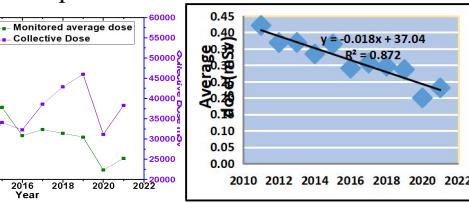


Fig 2: Monitored Average Annual Effective Dose of RW and Collective Dose of RW (2011-2021)

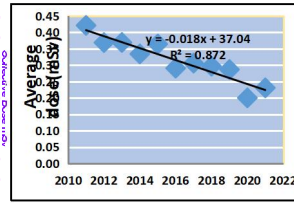


Fig 3: Comparison of Monitored Data and Linear Fitted Data for Average Annual Effective Dose Received by Radiation Workers (2011-2021)

CONCLUSIONS: The number of radiation workers availing personnel monitoring is significantly on a rise in medical sector. The trend analysis using statistical non parametric tests shows increasing trend in collective dose due to increase in number of radiation facilities. However, there is a declining trend in average effective dose of monitored radiation workers due to the improvement of safety standards as well as better regulatory control. The average dose is highest in nuclear medicine practices which is due the handling of unsealed sources. Although radiation safety practices followed in medical sector are at par with international safety standards, still additional measures are required for achieving better compliance of safety standards.

IMPACT OF SPOT PARAMETER SELECTION ON LINEAR ENERGY TRANSFER DISTRIBUTION IN HEAD AND NECK INTENSITY-MODULATED PROTON THERAPY

Vysakh Raveendran,¹Prakash Shinde,¹ Shwetabh Sinha,¹Ranjith C P,¹Lalit Chaudhari,¹Anuj Kumar,¹Samarpita Mohanty,¹Sarbani Ghosh Laskar,²Siddhartha Laskar²

¹ Department of Radiation oncology, Advanced Centre for Treatment Research and Education in Cancer (ACTREC), Homi Bhabha National Institute, Mumbai, Maharashtra, India

²Department of Radiation Oncology, Tata Memorial Centre, Homi Bhabha National Institute, Mumbai, Maharashtra, India

Email:vraveendran@actrec.gov.in

PURPOSE/BACKGROUND: Evaluating the Linear Energy Transfer (LET) distribution could provide crucial insights into the biological effects of Intensity-Modulated Proton therapy (IMPT). While it has been proven that the quality and robustness of IMPT plans depend on spot and energy layer (EL) selection, the impact of these factors on LET distribution remains unexplored in the existing literature. This study investigates the influence of spot and EL selection on the LET distribution and plan quality for head and neck (HN) IMPT plans.

MATERIALS AND METHODS:IMPT plans were retrospectively generated for five HN patients in the Ray Station Treatment Planning System. For each case, 21 treatment plans were generated by systematically varying parameters, including the distance between EL, spots and the number of proximal and distal EL. The LVH (LET Volume Histogram) was evaluated for different structures and LVH parameters such as volume of the high LET region (volume above 6 keV/ μ m ($V_{>6LET}$)), LET in 1% volume (LET_{1%}) was evaluated. The Plan robustness, target and Organ at Risk (OAR) doses, target homogeneity index (HI) and conformity index (CI) were assessed for each case. Multilinear Regression analysis examined correlations between variables.

RESULTS:The increase in ELs due to reduced EL separation led to higher $V_{>6LET}$ ($p = 0.00015$, $r = 0.74$) and LET_{1%} ($p = 0.0032$, $r = 0.71$). However, increasing the number of spots by reducing the spot separation does not correlate with the LET distribution ($p = 0.3$, $r = -0.05$).The target CI and HI positively correlated with the number of spots ($p = 0.01$, $r = 0.52$) rather than ELs ($p = 0.83$, $r = 0.23$). More spots increased treatment time and plan complexity. The OAR doses negatively correlated with the number of spots and ELs. The plan robustness reduced as the distance between EL and spots increased. Adding extra distal ELs has increased plan robustness with reduced $V_{>6LET}$.

CONCLUSIONS:EL selection affects LET distribution and plan quality in PBS treatment planning. Even if the spot separation doesn't correlate with the LET distribution, it is crucial in deciding the plan's quality and complexity.

KEYWORDS: Proton Beam Therapy, Linear Energy Transfer, IMPT, Radiobiology

MATERIAL DECOMPOSITION USING IODINE QUANTIFICATION ON SPECTRAL CT FOR CHARACTERIZING NODULES IN THE CIRRHOTIC LIVER

Subhash Chand Kheruka, Ravi Balaji, Rashid Al Sukati, Naema Almaymani,
Noura Al Makhmari

Department of Radiology & Nuclear Medicine, Sultan Qaboos Comprehensive Cancer Care and Research Center, Muscat, OMAN.

Email: skheruka@gmail.com

OBJECTIVE: The objective of this study is to investigate the utility of material decomposition using iodine quantification on spectral computed tomography (CT) for the characterization of nodules in the cirrhotic liver. By separating iodine from other materials within the liver, this technique aims to provide quantitative measures and functional information to enhance diagnostic accuracy and guide treatment decisions. This would help in distinguishing regenerative and dysplastic nodules from hepatocellular carcinomas.

INTRODUCTION: Liver cirrhosis is a progressive condition associated with the development of nodules within the liver parenchyma. Accurate characterization of these nodules is crucial for appropriate patient management and determining treatment strategies. Conventional CT imaging has limitations in differentiating between benign and malignant nodules. Spectral CT, which exploits the energy-dependent attenuation properties of different materials, offers a promising approach to overcome these limitations. Material decomposition techniques based on iodine quantification enable the assessment of iodine content within nodules, providing valuable functional information for characterization.

MATERIALS AND METHODS: This study utilized spectral CT imaging techniques for material decomposition and iodine quantification. Dual-energy acquisition and image reconstruction algorithms were employed to quantify iodine within cirrhotic nodules. The study included patients with liver cirrhosis who underwent spectral CT scans were performed. Quantitative analysis of iodine content was conducted using specific regions of interest within the liver nodules.

RESULTS: The results of this study demonstrate the potential clinical utility of material decomposition using iodine quantification on spectral CT for characterizing nodules in the cirrhotic liver. The technique allows for direct measurement of contrast enhancement within nodules, aiding in the assessment of perfusion characteristics and angiogenesis. The differentiation between intensely accumulating iodine lesions, such as hepatocellular carcinoma (HCC), dysplastic and regenerative nodules facilitates accurate diagnosis and treatment planning. Additionally, the technique enables the detection of subtle iodine enhancements within indistinct or small nodules that may be missed on conventional CT scans.

CONCLUSION: Material decomposition using iodine quantification on spectral CT shows promise in the characterization of nodules in cirrhosis. The technique provides quantitative measures, such as iodine concentration, wash-in/wash-out rates, and iodine maps, offering valuable functional information for differentiating benign and malignant lesions. This approach has the potential to improve diagnostic accuracy, guide treatment decisions, and ultimately contribute to personalized patient management. Further research and clinical validation are necessary to establish its clinical utility, optimize imaging protocols, and evaluate its impact on patient outcomes.

KEYWORDS: cirrhotic liver, nodules, spectral computed tomography, material decomposition, iodine quantification, contrast enhancement, hepatocellular carcinoma, functional imaging, diagnostic accuracy.

ESTIMATION OF THE THERMAL AND HUMIDITY-DEPENDENT DOSE RESPONSE FOR THE GAFCHROMIC EBT3 FILM AND ITS CLINICAL RELEVANCE

Gaurav Trivedi^{1,2}, Pushendra P. Singh², Arun S. Oinam¹

¹Post Graduate Institute of Medical Education and Research, Chandigarh, India

² Indian Institute of Technology, Ropar, India

Email: gauravtrivedi25@gmail.com

BACKGROUND/OBJECTIVES: The higher spatial resolution, large range of dose measurement makes Radiochromic films (RCF) more useful in-vivo dosimeter for hypo-fraction or Stereotactic Radiosurgery. This study aimed to find the thermal and humidity-dependent behavior of EBT3 films. The changes in the film sensitivity, Net Optical density as well as the dosimetric region of interest of small-size films due to their storage and setup condition were evaluated.

MATERIAL AND METHODS: Three sets of films were kept at three different thermal storage conditions. 15 films from each set were kept at 0°C, 20°C, and 40°C storage conditions for 24 hrs. Similarly, 15 films of each set were kept for a period of 48 hrs. One film from each thermal environment was irradiated with the doses of 10cGy to 2000cGy by a 6MV X-Ray beam produced from the Trilogy Linear Accelerator. Seven films were kept under water for seven different time periods i.e. 0.5 hrs., 1.0 hrs., 2.0 hrs., 4 hrs., 6 hrs., 12 hrs., and 24 hrs. to estimate the humidity effect on the film.

RESULTS: The film sensitivity was found 1.035 for the films stored at 40°C whereas 0.976 for the films kept at 0°C with respect to the sensitivity of the films kept at 20°C for 48 hrs. The measured mean dose difference from the delivered dose was overestimated by the films stored at 40°C for 48 hrs. by 12.15 %, whereas it was underestimated by -5.09% for the films stored at 0°C for 48 hours. The water diffusion rate at the corner of the EBT3 films due to humid storage was found < 0.4 mm/hr. An increment of 6.8% in the optical density at the central region of the film was observed for the film kept under water for a period of 24 hrs. as compared to the films that were outside the water medium.

CONCLUSION: The correction factors for the changes in the net optical density due to the thermal effect and the humidity effect must be incorporated into the current protocols of film dosimetry.

KEYWORDS: Film calibration, In-vivo dosimetry, ImageJ software, GafChromic EBT3 film, TG 235

THE INFLUENCE MATERIAL ASSIGNMENT UNCERTAINTY ON AcurosXB DOSE CALCULATION ACCURACY

Perumal Murugan, Ravikumar Manickam, Tamilarasan Rajamanickam, Sivakumar Muthu,
Dineasan C, Karthik Appunu, Abishake Murali

Sri Shankara cancer hospital and research centre, 1st cross shankarapuram, Basavanagudi, Bengaluru

Email: perumal.medphy@gmail.com

PURPOSE: Particle tracking based dose calculations engines like Monte Carlo and AcurosXB requires elemental composition information of voxels for accurate interaction cross section calculations. The primary objective of this study is to investigate the effects of uncertainties in elemental composition and mass density assignments on the accuracy of AcurosXB dose calculations.

METHODS: Three conditions were examined to investigate the effects of overlapping mass density boundaries between two material types and the uncertainty in HU-mass density calibration on the accuracy of AcurosXB dose calculations; 1) Dose variation due to incorrect material assignment 2) Dose variation due to incorrect mass density 3) Dose variation due to incorrect material and mass density assignment. In Eclipse TPS v16.1, a 30 cm cubic phantom with a 4 cm thick insert (10 cm in width and length) was created. Dose calculations were performed with various materials (biological and non-biological) and mass densities assigned to the insert. Impact of using the auto material assignment process for high density materials in CT scans acquired with 12-bit depth CT scanners on the accuracy of AcurosXB dose calculations was also evaluated.

RESULTS: Condition one exhibited significant dose variations for air-lung (12.1%) and cartilage-bone (2.8%) misassignments, while for other misassignments differences were less than 2%. Condition two showed notable dose differences of 5.5% for air and lung, 2% for bone, and less than 1% for other materials. Condition three resulted in the highest dose errors, reaching 16.1% for air as lung assignment with 1% HU uncertainty and 3% for cartilage as bone with 20% HU uncertainty. Incorrect assignment of non-biological materials led to dose discrepancies ranging from 1% to 4% for phantom and immobilization materials. The combination of HU saturation in 12-bit CT scanners and the auto assignment feature resulted in incorrect material and mass density assignment to high density prosthesis materials leading to dose errors even exceeding 20% depending on the material type and thickness.

CONCLUSION: Proper HU-to-mass-density calibration and accurate material assignment are crucial for precise AcurosXB dose calculations. Errors in material assignments, particularly for air, lung, cartilage, bone, and implants, significantly impact dose calculation accuracy of AcurosXB.

KEYWORDS: AcurosXB, Interaction cross section, Mass density misassignment, Material misassignment.

CLINICAL IMPLEMENTATION OF DYNAMIC BEAM FLATTENING (DBF) MLC PATTERN ON HALCYON FOR 3DCRT

Ben Johnson Varghese, Mohan Raj Uthiran, Siva Kumar Radhakrishnan, Lakshmana Perumal S, Saran Raj V, Raja Babu CH, Jagan C

Department of radiation Oncology, Omega Hospitals, Hyderabad, India

Email: benjohnson262@gmail.com

OBJECTIVE: To evaluate the dosimetric parameters and implementation of 3DCRT in the Halcyon linear accelerator's using dynamic beam flattening MLC pattern.

MATERIALS AND METHODS: The Halcyon used to flatten the 6MV flattening filter free (FFF) beam using a pre-defined multi-leaf collimator (MLC) pattern. Investigations were conducted into the flattened beams' dosimetric parameters such as beam flatness, beam symmetry, beam quality (TPR20/10), output factors, MU linearity and Open beam MU tests. All the Measurements were done using radio chromic films, Electronic Portal Imaging Device (EPID), water phantom equipped with a 0.07 cm³ PTW Semi flex 3D Ion Chamber and 0.6 cm³PTW Farmer® Ionization Chamber. The MLC position accuracy was acquired from EPID images. Additionally, DBF plans for a Bilateral field Brain and a 4-field box rectum were created in order to assess the impact of the DBF sequence on the quality of 3DCRT plans in Eclipse (Ver 16.1). These 3DCRT plans were regenerated with True Beam 6MV FF and compared dosimetrically. On these DBF plans, patient-specific QA was carried outwith PTW OCTAVIUS® 4D.

RESULTS: The flatness was observed < 106 % in the radial and transverse profiles for the field size ≤ 14X14 cm². The flatness shown a propensity to rise with field size for both larger and smaller fields respectively. The symmetry was 1% or less across all the field sizes. All measured output factors and MU test were within 1% of the TPS prediction. For all measurements, MU linearity and reproducibility were < 1%. The Beam Quality of 6MV DBF exceeded 6 MV FFF by 0.32%. The MLC positions accuracy were within the vendor-specified tolerance. On both treatment plans, it was determined that the Halcyon plans that were established without using DBF were not therapeutically adequate. However, the Halcyon plan with the DBF sequence and the True Beam plan were both regarded as being clinically appropriate. **CONCLUSION:** The DBF sequence and its parameter on the Halcyon were investigated. According to the results of the investigation, the DBF sequence can be employed on the Halcyon to develop clinically acceptable 3DCRT plan for patients' treatments.

KEYWORDS: Halcyon, DBF sequence, True beam, 6MV FFF

ARTIFICIAL INTELLIGENCE IN NUCLEAR MEDICINE IMAGING: REVOLUTIONIZING DIAGNOSIS AND TREATMENT

Pankaj Tandon

Radiological Safety Division, Atomic Energy Regulatory Board, Mumbai, India

Email: drpankaj@aerb.gov.in

BACKGROUND: Artificial Intelligence (AI) has emerged as a disruptive technology in various fields, and its potential in revolutionizing healthcare is becoming increasingly evident. In the realm of nuclear medicine imaging, AI holds great promise in enhancing diagnostic accuracy, improving treatment planning, and optimizing patient outcomes. This paper explores the applications of AI in NM imaging and its impact on the field.

MATERIALS AND METHODS:

- a) *AI-enhanced Image Analysis:* AI algorithms have demonstrated remarkable capabilities in analyzing and interpreting images obtained through Nuclear Medicine (NM) techniques. By leveraging machine-learning and deep-learning techniques, AI can assist in improving the accuracy and efficiency of image interpretation. AI algorithms can automatically detect and quantify abnormalities, such as tumors or metastases, leading to faster and more accurate diagnoses.
- b) *Image Reconstruction and Enhancement:* By utilizing AI-based reconstruction techniques, NM images can provide higher spatial and temporal resolution, leading to more precise localization and quantification of disease activity that will give the accuracy of diagnoses and guide treatment decisions.
- c) *Personalized Treatment Planning:* AI algorithms have the potential to revolutionize treatment planning in NM imaging. By integrating patient-specific data, such as medical history, genetic information, and imaging findings, AI can assist in predicting treatment response and identifying optimal therapeutic strategies. This will provide the most effective treatment options by optimizing radiation dose delivery and minimizing potential side effects.
- d) *Prognostic and Predictive Modeling:* AI algorithms can analyze imaging data, clinical variables, and genomic information to generate personalized prognostic models that predict disease progression, treatment response, and overall survival.
- e) *Quality Assurance and Workflow Optimization:* By monitoring and analyzing image acquisition protocols, AI algorithms can provide real-time feedback to technologists, enabling them to optimize image quality and minimize errors.

CONCLUSION: AI has the potential to revolutionize NM imaging by enhancing diagnostic accuracy, treatment planning, and patient outcomes. AI algorithms can improve image analysis, reconstruct images, personalize treatment plans, develop prognostic models, and optimize workflow. As AI continues to advance, it is crucial to ensure ethical implementation, validation, and integration into clinical practice. AI in NM imaging holds immense promise for improving patient care and advancing the field.

COMPARISON OF DOSIMETRIC PARAMETERS OF MONO VERSUS MULTI-ISOCENTRIC TECHNIQUE FOR MULTIPLE BRAIN METASTASIS: A SINGLE INSTITUTIONAL EXPERIENCE

Swapna Gayen¹, Priyanka Agarwal, Ninad Patil, Vishal Gangwar, Dandpani Epili, Ajay Krishnan, Ajay Choubey, Sambit Nanda, Ashutosh Mukherji, Satyajit Pradhan

¹Department of Radiation Oncology, Homi Bhabha Cancer Hospital (TMC), Varanasi, India

Email: swapnasnagar@gmail.com

BACKGROUND / PURPOSE: Brain metastases (BM) are the most common intracranial tumors in adults. SRT of multiple metastases needs dosimetric appropriateness and fast delivery. Linear accelerator based SRT assures this by multiple non-coplanar arcs with a single isocenter. The aim of this study is to compare the dosimetric parameters of mono versus multi-isocentric techniques for multiple metastases.

MATERIALS & METHODS: In this analysis, a total 10 previously treated patients were chosen randomly, with approximate five BM targets. All patients were planned for a configured Truebeam STX (Varian Medical System) linear accelerator with high-definition MLC. The patients planning was generated on Eclipse TPS (Ver. 15.5.51), using 6XFFF beam having dose rate of 1400 MU/min. The total dose for SRT planning was prescribed 30Gy in 6 fractions. The treatment planning was performed in two ways. First, a mono-isocentric hyper arc plan (Plan_A) was generated for all PTVs considered as one target and evaluated, and second ways, each PTV was planned separately with partial co-planar or non-coplanar arcs (total 5 plans) and the sum plan (Plan_B) was evaluated. Each plan was optimized with photon optimizer algorithms and dose was calculated with Acuros algorithm. Both planning evaluation and comparison was performed qualitatively and quantitatively. For quantitative evaluation of PTV, Coverage, conformity, gradient index was compared. For sharp dose gradient, reference isodose was considered 90%. For statistical analysis of PTV and OARs, Wilcoxon signed rank test was performed and $p < 0.05$ was considered statistically significant.

RESULTS: The mean volume of GTV and PTV were $2.78(\pm 2.06)$ and $7.45(\pm 3.38)$, respectively. The coverage ($p < 0.05$) for Plan_A and Plan_B was $28.9(\pm 0.41)$ and $29.4(\pm 0.64)$, respectively. Similarly, the conformity ($p < 0.05$) was $1.5(\pm 0.12)$ and $1.7(\pm 0.15)$, respectively. Similarly, homogeneity index ($p < 0.05$) was observed $12.5(\pm 1.6)$ and $15.9(\pm 4.65)$. Gradient index was observed 0.93% for Plan_B rather than Plan_A. However, MU variation ($p < 0.05$) was observed 40% more in Plan_B compared to Plan_A. OAR doses were observed less in Plan_B.

CONCLUSION: As per observations, both plans were acceptable w.r.t. PTV evaluation. The MU & treatment time were more in Plan_B, however, OAR doses are less in Plan_B. More data & Clinical outcomes are required.

RETROSPECTIVE ANALYSIS OF PORTAL DOSIMETRY WITH EPID: PRE-TREATMENT QA OF VARIOUS CLINICAL SITES USING 4 LINEAR ACCELERATORS

¹Tanya Bahl, ²Udita Upreti, ²Priyadarshini Sahoo, ²R.A.Kinhikar

¹Varian Medical Systems, 246 Guru Nanak Nagar, Ram Bagh Road, Ambala Cantt, Haryana

²Tata Memorial Hospital, Parel, Mumbai, India

Email: tanyabahl5991@gmail.com

AIM AND OBJECTIVE: To compare results from quality assurance of same plans (similar fluence) of various clinical sites across 4 Linear accelerators using Electronic Portal Imaging Device and to validate Electronic Portal Imaging Device (EPID) as a reliable patient QA as a hassle free QA tool in a busy centre like Tata Memorial Hospital, Parel, Mumbai and compare

MATERIALS AND METHODS: Same quality plans for 25 patients from 5 disease management groups were optimised for 4 Linear Accelerators taking one machine as reference. The optimisation parameters were kept the same and the plan quality for all the plans was compared with the help of Dose Volume Histogram (DVH) for the PTV. QA plans were then made using the Portal Dose Image Prediction Algorithm (PDIP) and the calculated image was then obtained. The portals of all 4 machines were then calibrated. Patient specific Quality Assurance was performed for all the plans on all the machines using EPID and gamma was evaluated using relative normalisation.

RESULTS: The gamma values obtained for the QA plans were analyzed using gamma evaluation criteria in which the relative gamma was obtained normalizing to “maximum of predicted dose” and to “minimise difference”. The patient specific QA plans for the same patient on all the machines yield comparable results. Initially, the relative gamma was evaluated using normalization to “maximum of predicted dose”. But, it was found that some patient plans did not pass well within 95% for 3%, 3mm passing criteria. On analysing it was found that the normalization mode used i.e. relative to maximum of predicted dose did not aptly satisfy the criteria for evaluation as the dose maxima lay in the periphery or gradient region. After changing the normalization mode to minimize difference, the Gamma passed well within 95% for 3%, 3mm evaluation criteria.

CONCLUSION: Advantages of using an EPID is that the QA images are immediately available without the cost and time needed for developing a film. Also, the images obtained from an EPID are digital which facilitates image processing and image matching and allows easy access over a network computer and so portal and predicted doses can be easily compared.

EPIDs of all 4 machines yield comparable results across all machines on execution of same plans (similar fluence). We can rely on EPID for routine patient QA as a hassle free and accurate QA tool. In a busy centre like Tata Memorial Hospital, Mumbai, EPID can be used as an efficient QA tool for routine QA purpose.

DOSIMETRIC COMPARISON OF TWO-ARC VS THREE-ARC VOLUMETRIC MODULATED ARC THERAPY (VMAT) FOR HEAD AND NECK PATIENTS WITH A SIMULTANEOUS INTEGRATED BOOST (SIB) TECHNIQUE

Rajkumar Chauhan, Suresh Chaudhari, Sushree Chaudhari, Jui Deb

American Oncology Institute 1-100/1/CCH Near Aparna Sarovar, Nallagandla Serilingampally, Hyderabad
Telangana – 500019, India

Email:raj.rc.chauhan@gmail.com

BACKGROUND/OBJECTIVE: Aim of this study is to quantify plan quality improvement of 3 arc VMAT plan over on 2 arc VMAT plan for Head and Neck patients treated with a simultaneous integrated boost (SIB) technique.

MATERIALS AND METHODS: 10 head and neck (H&N) patients treated previously with SIB doses of 60Gy/30# and 54Gy30# were selected for this study. Plans were generated for Truebeam machine with HD MLC having jaw tracking capability. Un-flattened 6MV beam was used for planning. Both plans were created with similar dose constraints and optimization parameters. The two-full arc plan utilizes asymmetric jaws that are adjusted to a maximum field size of 15x15 cm² with complimentary collimator angles of 30 degrees. The 3 ARC plan contains utilizes asymmetric jaws that are adjusted to a maximum field size of 15x15 cm² with collimator angles of 10°,350°and90°. Both plans were optimised with PO optimiser and dose was calculated with AAA. Both plans were compared for PTV coverage as per ICRU83, OAR constrains as per RTOG protocol and 50% dose spillage. Treatment delivery time and MU per plan was also documented.

RESULTS: Both plans resulted in similar PTV coverage with no significant difference for normal organ doses. Monitor Units for 2 Arc plan were consistently higher ranging from 30MU to 165MU. 50% dose spillagewas also similar for both plans. Delivery time for 3 arc was longer by on an avg 1min.

CONCLUSIONS: No significant dosimetric difference was found between 2 arc vs 3 arc plans. The 3ARC plan may be more efficient in terms of fewer MU's, however with longer treatment time. The choice between the 2 arc and 3 arc plans involves a trade-off between treatment delivery time and the desired dose distribution.

KEYWORDS: dosimetry, plan comparison. VMAT

Presentation ID: P-179

Abstract ID: K6433

EVALUATION OF PLANNED AND DELIVERED DOSES IN OVERLAP REGION DURING TOTAL BODY IRRADIATION (TBI) USING OPTICALLY STIMULATED LUMINESCENCE DOSIMETERS (OSLDS) IN PATIENTS TREATED ON TOMOTHERAPY

Abhay Kumar Singh¹, Manindra Bhushan ¹, Sandeep Singh¹, Dipesh¹, Jaskaran Singh Sethi¹, Varghese Antony¹, Munish Gairola¹

Department of Radiation Oncology, Division of Medical Physics, Rajiv Gandhi Cancer Institute and Research Center, New Delhi, India

Email: singh.abhay15aug@gmail.com

OBJECTIVE: Patients for bone marrow transplant require whole body radiation, the height of the patient is a limiting factor in delivering the doses to the desired target. This study investigated the dose received in the overlap region during TBI using OSLDs treated with Helical Tomotherapy.

METHODS AND MATERIALS: A total of 20 patients with a height greater than 125cm and a prescription dose of 2Gy per fraction were evaluated. Scans were performed using Siemens sensation in two orientations: Head-First Supine (HFS) and Feet-First Supine (FFS). Planning target volumes (PTVs) were delineated for both scans, for dose gradient regions PTV_UPPER, PTV95%, PTV90%, PTV75%, PTV50%, PTV25%, and PTV5% delineated to achieve 100% dose coverage in the overlapping region, using 2cm margins. Similarly, PTV_LOWER and other complementary PTVs were contoured in FFS. Two treatment plans, Plan Upper and Plan Lower, were generated and optimized using the Accuray treatment planning system (TPS) for HFS and FFS scans, respectively. Evaluation of PTVs in plan sum were conducted using metrics $D_{95\%}$, $D_{50\%}$, D_{mean} , and D_{max} obtained from the dose volume histograms of both Plan_UPPER and Plan_Lower in plan sum to get 100% dose in overlap region. Patient doses were measured using OSLDs from Radpro Freiberg Instruments GmbH.

RESULTS: The study revealed that the average $D_{95\%}$ measured dose from the TPS, after summation of the complementary PTVs in junction region was 1.96Gy. Similarly, D_{mean} and $D_{50\%}$ were at 2.19Gy and 2.15Gy, respectively, and the D_{max} was 2.39Gy. The average dose measured by OSLDs on the patient's surface was 2.2Gy in junction region. Therefore, the $D_{50\%}$ and the D_{mean} parameters were comparable with the measured OSLD doses.

CONCLUSION: The close agreement between the measured dose (OSLDs) and calculated dose (TPS) suggests that the gradient PTVs in both the plans helped in controlling over or under exposure in overlap region. Moreover OSLDs provide prominent results for Planned and delivered dose.

KEYWORDS: OSLDs, TBI, Junction doses Gradient PTVs, Tomotherapy

DETERMINATION OF REFERENCE AIR KERMA RATE FOR HIGH DOSE RATE BRACHYTHERAPY COBALT - 60 SOURCE THROUGH GEOMETRIC SEQUENCE NUMERICAL METHOD AND COMPARISON WITH THE TPS & MEASURED VALUE.

Athiyaman M, Hemalatha A, Gokulraj A

S.P.Medical college, Radiological Physics department, Bikaner, Rajasthan, India

Email: athiyaman.bikaner@gmail.com

INTRODUCTION: Geometric sequences are generally characterized by a common ratio between successive terms. This type of series is used throughout mathematics, important applications in physics, engineering, biology, economics, computer science, queuing theory, and finance. The purpose of this study was to compare the accuracy of Reference Air kerma rate (RAKR) for Co-60 HDR Brachytherapy source between theoretically estimated value using geometric sequence numerical approach, measurement value, and Treatment Planning System value.

MATERIAL AND METHODS: The RAKR was theoretically computed using Numerical method (decay factor) at a specific time for a period of 10 days. The common sequence ratio was estimated by considering the half life value 1925.20 days as recommended by National Institute of Standards and Technology. Geometric series was framed based on the above. Measurement part was performed at the same predefined time for 10 days in HDR Brachytherapy machine (Make: Eckert & Ziegler Bebig GmbH, Model: Multisource, Sr. No: 542,) and with well type Ion chamber. The observation part was performed in the Treatment Planning System and the series of AKS was framed for three methods. For each of the three series, the sequence ratio was calculated and compared to the other series. The ANOVA test was used to determine statistical significance, and the p value was calculated.

RESULTS: The geometric series was tabulated for all the three methods. The average, maximum and minimum common sequence ratios were estimated. Statistical significance was estimated based on ANOVA method (p value >0.05) and no significant difference was found.

CONCLUSION: The purpose of this research was to explore whether Numerical Analysis could be utilized to estimate the RAKR value for Brachytherapy sources. The predicted common sequence ratios from all three techniques are comparable. The AKS series was further evaluated, and found that it is a convergence series.

KEYWORDS: Brachytherapy, Radiation Dosimetry, Radioisotope

DEEP INSPIRATION BREATH-HOLD (DIBH) AND FREE BREATHING (FB) RADIATION THERAPY IN LEFT-SIDED BREAST CANCER PATIENTS: A SINGLE-INSTITUTION RETROSPECTIVE DOSIMETRIC ANALYSIS

Md. Jobairul Islam¹, Md. Abdul Mannan¹, Md. Mahfujur Rahman², A. Al. Mamun¹, AFM Kamal Uddin¹, Mostafa Aziz Sumon¹, Parvin Akhter Banu¹, Ehteshamul Hoque¹

¹Department of Radiation Oncology, Labaid Cancer and Super Speciality Centre, Bangladesh.

²Department of Radiation & Clinical Oncology, Evercare Hospital Dhaka, Bangladesh

Email: jobairul55@gmail.com

BACKGROUND/OBJECTIVE: Radiotherapy for left-sided breast cancer can potentially lead to cardiac injury. Deep inspiration breath-hold (DIBH) technique has emerged as a cardiac-sparing approach, offering dose reduction to vulnerable cardiac structures compared to free breathing (FB) during treatment. This study aims to evaluate and compare the dosimetric differences between DIBH and FB techniques in a single-institution setting.

MATERIALS AND METHODS: A total of 20 patients with left-sided breast cancer, who underwent breast-conserving surgery (BCS) or mastectomy (ME) along with axillary lymph node staging, received adjuvant radiation therapy. The Real-time Position Management™ (RPM) system (Varian Medical Systems, Palo Alto, CA) was used to monitor breathing during both FB and DIBH scans via a reflective marker box placed at the level of the xiphoid process. All patients were able to hold their breath for greater than twenty seconds to accommodate the scan during DIBH. In 3DCRT, IMRT, VMAT plans heart, left anterior descending coronary artery (LAD), ipsilateral lung and contralateral breast doses, patient anatomical factors, location of tumors and physical factors were analyzed.

RESULTS: All dosimetric parameters for cardiac structures showed significant reduction in the DIBH group compared to the FB group except five patients. The mean heart dose (Dmean) in the DIBH group was 3.42 Gy (range 1.8-5.13) and 5.00 Gy (range 2.1-7.0) in the FB group. The average V20 for the ipsilateral lung in DIBH was 17.82Gy (range 7.80-29.7) versus 17.15 Gy (range 4.00-33.0) in FB. The Dmean for the left anterior descending artery (LAD) was 9.34 Gy (range 4.64-20.6) in DIBH compared to 13.41 Gy (range 4.05-27.89) in FB. Increased left lung volume in the DIBH position correlated with dose sparing of cardiac structures.

CONCLUSIONS: This retrospective dosimetric analysis demonstrates that the DIBH technique provides a significant dose reduction to cardiac structures in left-sided breast cancer patients undergoing radiation therapy but a few of the patients do not significant benefit from DIBH technique due to their anatomical position. The findings of this study are important for resource allocation, as DIBH may be unnecessarily recommended for some patients with little dosimetric benefit.

KEYWORDS: Deep inspiration breath-hold (DIBH), Free-breathing (FB), Cardiac-sparing, left anterior descending coronary artery (LAD), Breast cancer

TO STUDY THE POLYMERIZATION REACTION IN GAFCHROMIC FILM DOSIMETRY AND THE PARABOLA EFFECT IN DOSE DETERMINATION BY FLATBED SCANNER.

Ranjit Singh, Parsee Tomar, Ngangom Robert

Department of Radiotherapy, PGIMER, Chandigarh, India

Email: ranjit783@gmail.com

PURPOSE/BACKGROUND: The mechanism of polymerization reactions with radiochromic film is proposed in the current work. The di-acetylene monomer unit in radiochromic films undergoes a 1-4 addition polymerization reaction when exposed to ionising radiation. Three basic steps—chain initiation, chain propagation, and chain termination—make up the entire polymerization reaction and are each explained with a mechanism. Additionally, the flatbed scanner's scan area's EBT3 response is not consistent due to the parabola effect, and its relative value depends on how much radiation is received.

METHOD AND MATERIAL: Films exposed to a 15 MeV electron beam are examined for changes in scanning position over the scan area of flatbed scanners for dosages ranging from 10 cGy to 500 cGy, and the read-out data for two distinct scanners, namely the Epson 11000XL and Epson 12000XL, are contrasted. The flatbed scanner's entire scan area is divided into nine quadrants, each with three rows and three columns, depending on how the film is positioned within it.

RESULTS: In the centre quadrant, the highest differences for the blue, green, and red channels in the Epson 11000XL and Epson 12000XL printers are 74.6%, 76.9%, and 89.5%, and 74.5%, 22.1%, and 34.7%, respectively. While the largest difference for doses of 500 cGy in Epson 11000XL and Epson 12000XL for the blue, green, and red channels is 4.1% & 4%, 2.5% & 10.1% and 2.5% & 6.7%, respectively.

CONCLUSION: Over the whole scan region, the film readout is not uniform, and this non-uniformity is particularly obvious at low radiation doses. As a result, it is advised to scan all films in the same position and orientation as was used to scan the calibrated film. This will result in less uncertainty and higher dose estimation accuracy, particularly for radiation doses less than 100 cGy.

KEYWORDS: Radiochromic film, Polymerisation, flatbed scanner, parabola effect

PAROTID GLANDS DOSES IN PALLIATIVE WHOLE BRAIN RADIOTHERAPY: A RETROSPECTIVE EVALUATION

Prashantkumar Shinde, Maheshkumar Upasani, Parimal Patwe, Mukesh Meshram, Hemant Ghare, Manish Mathankar, Sameer Chandorkar

Department of Radiation Oncology, National Cancer Institute, Nagpur, Maharashtra, India

Email: pk.shinde16@gmail.com

BACKGROUND/OBJECTIVE: Palliative whole-brain radiation therapy (WBRT) is an effective therapeutic option for patients with brain metastasis. There have been little efforts to preserve normal tissues while delivering palliative WBRT. Parotid glands are prominent organs at risk in the head and neck. The assessment of parotid gland dosages in WBRT becomes essential to further limit the doses for better quality of life. The purpose of this abstract is a retrospective review of parotid gland dosages in short-course palliative WBRT.

MATERIALS AND METHODS: This study included 46 palliative WBRT patients treated with 20 Gy in 5 fractions of 3DCRT. Twenty-three patients had a lower border of PTV up to C1 vertebra (Group-I) and twenty-three patients had PTV up to or below C2 vertebra (Group-II). The patient's planning data was retrieved, and parotid glands were contoured retrospectively on the original treatment planning computed tomography images. The parotid gland doses were evaluated using biologically equivalent doses of conventional dose-limiting parameters. Single parotid $D_{\text{mean}} < 12.9$ Gy (BED_3 of 20Gy) and Total parotid $D_{\text{mean}} < 15.32$ Gy (BED_3 of 25Gy) of RTOG. Single parotid $D_{\text{mean}} < 15.8$ Gy (BED_3 of 26Gy) and $V_{17.7\text{Gy}}$ (BED_3 of 30Gy) $< 50\%$, and Total Parotid $V_{12.9\text{Gy}}$ (BED_3 of 20Gy) $< 20\text{cc}$ of QUANTEC. The patients were further divided into two groups depending on the lower border of the PTV, and a comparative evaluation of the parotid dose indexes was performed using two sample student t tests.

RESULTS: The means of all dose indexes for all patients were within the limits of QUANTEC and RTOG for single parotid and total parotid. However, Single parotid $D_{\text{mean}} < 12.9$ Gy (BED_3 of 20Gy) and Total Parotid $V_{12.9\text{Gy}}$ (BED_3 of 20Gy) $< 20\text{cc}$ exceeded in patients with lower borders of the PTV up to or below C2 vertebra. The means of all dose indexes for Group-II were significantly ($p < 0.05$) higher than for Group-I patients.

Conclusions: Limiting the PTV border to C1 vertebra may further reduce parotid dosage. Assessment of parotid dosages will aid in the development of strategies for reduced parotid doses, offering greater comfort and quality of life for patients.

KEYWORDS: WBRT, Parotid, Palliative Radiation Therapy, Brain metastasis.

A STUDY ON VMAT PLAN OPTIMIZATION STRATEGIES -EFFECT OF MULTI RESOLUTION (MR) LEVELS IN TREATMENT PLAN OPTIMIZATION WITH PHOTON OPTIMIZER (PO) IN THE ECLIPSE TREATMENT PLANNING SYSTEM

Avdhoot Sutar¹, Sushant Raniwala¹, Yogesh Ghadi¹, Shrikant kale¹, Rituraj Upreti¹, Rajesh Kinhikar¹, Sarbani Ghosh-Laskar², J. P. Agarwal²

¹Dept of Medical Physics, Tata Memorial Hospital,

²Dept of Radiation Oncology, Tata Memorial Hospital, Mumbai, India

Email: sutarab@gmail.com

BACKGROUND/OBJECTIVE: VMAT (Volumetric Modulated Arc Treatment) is treatment delivery technique used for conformal dose delivery and to reduce the dose to OARs. The Eclipse treatment planning System (Varian Medical Systems) optimizes VMAT plan as per clinical requirement. It has four Optimization levels (MR levels) through which plans are optimized and user can interplay with plan optimization parameters at any stage. In this study we have analyzed the effect where constraints given to the system at different MR levels and the impact on plan Quality is evaluated.

MATERIALS AND METHODS: Five Head & Neck Patients were retrospectively selected for this study. The plans were optimized on Eclipse Treatment Planning System (Eclipse v16.1.0) with the Photon optimizer. Each Plan planned with two full Arcs. Four types of plans were generated for the each of the patients where all the constraints and priorities are defined in optimization at pre-decided MR level. Plans in which all constraints and priorities defined in MR level 1 are labeled as P1, then these plans were allowed to optimize without any interruption till final dose calculation. Similarly in P2 & P3 plans, priorities and dose constraints are defined (Expect for PTVs which is given in MR1 to start the optimization) in MR2 and MR 3 levels respectively. In P6 Plans Dose constraints defined after plan has run through all levels and final dose calculation and these plans are again run for the optimization and optimization parameters defined at MR2. All four types of these plans evaluated with different parameters No. of MUs, OAR doses, Conformity index (CI), Homogeneity index (HI), PTV coverage etc and compared.

RESULTS: All Plans were comparable with nearly same plan Quality. In P3 plans MU were lesser compare to other groups. Plan P6 shown Better OAR sparing with still lesser MU's with respect to P1 & P2.

CONCLUSIONS: Treatment plans group P6 shown better OAR control with comparatively lesser MU's. Before defining OAR constrains if user runs the plan through all MR levels then quality of plans can be improved. Adding constraints at MR1 (P1 Plans) can increase significant no of MU's.

KEYWORDS: Plan Optimization, Multi-Resolution levels, VMAT

THE IMPACT OF STATE RECOGNITION TO JOB POSITION OF THE MEDICAL PHYSICIST IN INDONESIA: SURVEY STUDY FROM 2015 – 2021

Supriyanto Ardjo Pawiro^{1,2}, Lukmanda Evan Lubis^{1,2}, Ika Hariyati², Indah Lestariningsih²,
Djarwani Soeharso Soejoko¹

¹Departement of Physics, Faculty of Mathematics and Natural Sciences, Universitas Indonesia, Depok, 16424 Indonesia, ²Aliansi Fisikawan Medik Indonesia, Jakarta, Indonesia.

Email: supriyanto.p@sci.ui.ac.id

BACKGROUND/OBJECTIVE: State recognition of the medical physicist profession in Indonesia was started by the Ministry of Health Decree in 2007 and followed by Nuclear Regulatory Agency regulation (BAPETEN) in 2011.

MATERIALS AND METHODS: The seven-year survey was conducted to see the impact of the recognition by the government to the new job position of the medical physicist in Indonesia. The data were divided into two groups of medical physicists' positions in the government and private sector for three specialists in radiation oncology, diagnostic radiology, and nuclear medicine.

RESULTS: The result shows the delayed impact of recognition to new job position of medical physicist and increasing rapidly after four years and eight years for BAPETEN regulation and Ministry of Health Decree, respectively. The ratio between the number of medical physicists to radiotherapy centres increased from 1.7 to be 2.7 and 2 for government and private hospitals, respectively. However, the ratio between medical physics to nuclear medicine facilities is not much changes around 1. In addition, the big impact the recognition medical physics is in diagnostic radiology facility. We start with few physicists to be 391 medical physicists

CONCLUSIONS: The study found the big impact of the recognition to a new job position in diagnostic radiology and the radiotherapy department.

KEYWORDS: medical physics, recognition, job, placement

A PRELIMINARY STUDY OF CW-OSL AND TL OF LiCaAlF₆: Eu PHOSPHOR

Pooja Seth¹, Anuj Soni², Shruti Aggarwal¹

¹University School of Basics & Applied Sciences, Guru Gobind Singh Indraprastha University, Dwarka, New Delhi, 110075 India.

²Radiological Physics and Advisory Division, Bhabha Atomic Research Centre, Mumbai, India.

Email: drpoojaseth@gmail.com

BACKGROUND/OBJECTIVES: The demand for OSL (optically stimulated luminescence) based dosimeters in the field of medical dosimetry is increasing worldwide. OSL has become a well-known technique to measure the radiation dose absorbed due to its advantages such as fast to read, easy to handle and require no heating. Therefore, it is indispensable to develop highly sensitive efficient OSL dosimetry material. LiCaAlF₆ is emerged as a potential OSL material due to its wide band gap, great storage efficiency, non-toxicity and high thermal durability. The present study is focused on the synthesis of Eu- doped LiCaAlF₆ phosphor using melting method with better OSL dosimetric properties.

MATERIALS AND METHODS: Undoped and Eu doped LiCaAlF₆ phosphor was prepared using salts of the constituent metals and rare earth salt Eu in the form of Eu₂O₃ (Europium Oxide) in the stoichiometric ratios in a graphite crucible and heated in the resistive heating furnace at ~ 950°C in argon gas atmosphere. The samples were annealed at 400°C for 1 h before use. The CW-OSL and TL was recorded on Risø TL/OSL reader after irradiation with a beta dose of 500 mGy.

RESULTS AND DISCUSSION: The photoluminescence studies confirm the incorporation of Eu in LiCaAlF₆ host by showing strong emission at 590 nm with excitation from 340nm. The OSL sensitivity of beta irradiated LiCaAlF₆: Eu phosphor is found to be ~30 times higher than undoped LiCaAlF₆ and ~3 times higher to that of commercially available Al₂O₃: C (BARC) as shown in Fig. 1. TL glow curve structure has shown a broad TL peak positioned around 169°C which is mainly composed of overlapping peaks. Further, TL and CW-OSL correlation has been studied by preheating of samples at different temperatures. This helps in understanding the contribution of different TL traps on respective OSL intensity. A histogram of the fractional OSL signal of the sample at different preheating temperature suggest that intense OSL signal emerges from shallow trap levels.

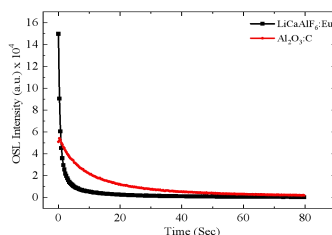


Fig. 1. CW-OSL decay curve of LiCaAlF₆: Eu and Al₂O₃:C (BARC) after irradiation with 500mGy beta dose

CONCLUSION: Undoped and Eu doped LiCaAlF₆ phosphor has been synthesised using melting method in argon gas atmosphere and their CW-OSL decay curve has been investigated. The OSL intensity of LiCaAlF₆: Eu is 30 times higher than undoped LiCaAlF₆ whereas three times as compared with commercially available Al₂O₃: C (BARC). The enhanced sensitivity may be attributed to the additional defect centers created by Eu doping. Further, the phosphor has shown a broad TL glow curve with overlapping peaks. The correlation between TL peaks and CW-OSL response has been established.

KEYWORDS: Optically Stimulated Luminescence, Thermoluminescence, radiation Dosimetry, phosphor

WATER PHANTOM FOR PATIENT SPECIFIC QA OF IMRT AND VMAT

Sunilkanth Mishra

Apex Wellness Hospital Nashik (M.S.), India

Email: msunilkanth@gmail.com

BACKGROUND/OBJECTIVE: Initially, a cylindrical acrylic water phantom which can hold a Farmer Ionisation Chamber at the centre of the phantom was fabricated for the IMRT/VMAT patient-specific QA. This phantom can be used for measuring radiation dose at the isocentre only. The clinical utility of such water phantom can be enhanced by providing option for measurement of doses at off-centre and off-axis points. For the purpose, a water phantom which can hold three ionisation chambers (ICs), one at the centre and two on either side of the central chamber at 5 cm is fabricated.

MATERIALS AND METHODS: Water is an ideal medium for dosimetry. This water phantom is made of an acrylic cylinder of length 30 cm and diameter of 30 cm for providing scatter saturated conditions. The phantom can hold three ICs available in the RT department. One IC at the centre and two on the either side of this at 5 cm. The marks on the chamber holders match with the effective point of measurement and the central axis of the respective ICs. The central holder is to hold a 0.6 cc Farmer chamber and the other two holder are for 0.125 cc ICs. The thickness of the caps of the chamber holders are as per suggested in the TRS-398. The 0.125 cc ICs can be cross calibrated to measure the doses. A sturdy base of acrylic rings to hold the water filled cylinder and a heavy foundation which is supported by swivel levelling screws have been fabricated. The water filling and draining point is given on the top to avoid any water leakage.

RESULTS: The centres of the IC holders are in one plane and the effective points of measurement of ICs are at the centre of the phantom (within 1 mm) for the dose measurement accurately and reproducibly. The phantom can be levelled accurately for the purpose with the help of swivel levelling screws.

CONCLUSIONS: The fabricated cylindrical water phantom can be used for the clinical dosimetry of patient specific QA for IMRT and VMAT. This phantom is affordable for RT department with limited financial resources.

KEYWORDS: IMRT and VMAT, quality assurance, dosimetry

VALIDATION OF BEAM MODEL IN RAYSTATION TREATMENT PLANNING SYSTEM FOR PENCIL BEAM SCANNING PROTON BEAM THERAPY

Rohidas Punde¹, Ranjith C P¹, Prakash Shinde¹, Lalit Chaudhari¹, Siddharth Laskar²

¹Department of Radiation Oncology, Advanced Centre For Treatment Research and Education in Cancer, Tata Memorial Centre, Homi Bhabha National Institute, Mumbai, India

²Department of Radiation Oncology, Tata Memorial Hospital, Parel, Mumbai, India

Email: rohidas75@gmail.com

BACKGROUND/OBJECTIVE: Beam model data acquisition and its validation is one of the crucial phase of the commissioning of a Pencil Beam Scanning (PBS) proton system. The purpose of this study is to demonstrate the beam data requirement for the Raystation treatment planning system (TPS) and its validation,

MATERIALS AND METHODS: The beam data measurement for Raystation TPS (RaySearch Laboratories, Sweden) was done as per the recommendation of Raystation. Proton spot profiles, Pristine Bragg peaks, absolute dose measurements, and Source-to-axis distance(SAD) were measured using various IBA dosimeters, and beam modeling was done. Range calculation accuracy of TPS was verified using a meat slab and the head of a goat. Cubes of different field sizes were created and optimised for uniform dose for different modulation, with and without range shifters, and different beam computational settings for validation of the beam model. Dose measurement was carried out in Bluephantom2 using a PPC05 ionization chamber at different depths. Spread-out Bragg peak (SOBP) was measured using MultiLayer Ionization Chamber. 25 spot pattern was created in TPS and measurement was done using a Lynx detector. Spot size, symmetry, and position were analyzed.

RESULT: In the beam model the beam divergence was positive, and all the pristine Bragg peak intensities were around the nominal energies. The maximum difference between nominal energy and R80 was -0.42 MeV. The maximum difference between the TPS and the measured range was -1.08%, 0.38%, and -0.08% for muscle, fat, and bone tissue respectively. The maximum dose difference for various cubes was 1.84%. The maximum longitudinal and lateral uniformity was 1.65% and 1.53% respectively. The maximum difference in SOBP width was -1.58%. The maximum variation in spot size was 0.27 mm at a gantry angle of 0°. The maximum positional error observed was 0.34 mm. The average spot symmetry observed was 8.28%. Gamma analysis showed good agreement between calculated and measured dose distribution.

CONCLUSIONS: The Beam model and its validation done successfully. All the results are within acceptable limits.

KEYWORDS: Pencil beam scanning, treatment planning system, Validation, Proton beam therapy

DOSIMETRIC ANALYSIS FOR ENERGY SELECTION OF FLATTENING FILTER FREEBEAM IN SINGLE TARGET INTRACRANIAL STEREOTACTIC RADIO SURGERY TREATMENTS.

Pawan Kumar Yadav, Supratik Sen

Department of Radiation Oncology, HCG Cancer Centre, Ahmedabad, Gujarat, India

Email: supratiksen494@gmail.com

BACKGROUND: The aim of this study was to conduct a comprehensive dosimetric analysis comparing the plan quality of 10FFF beams versus 6FFF beams in intracranial SRS treatments. The dosimetric evaluation focused on assessing radiation therapy oncology group (RTOG) dose conformity and gradient indices, as well as the volume of normal brain tissue exposed to irradiation.

MATERIALS AND METHODS: A total of 30 SRS patients were included in the study, and treatment plans were developed using both 6FFF and 10FFF. The plans were optimised with 3-4 arcs including non-coplanar arcs depending upon the target location. The prescribed doses ranged from 8-30 Gy, depending on the target volume ranging from 1-43cc, and were delivered in 1-5 fractions, considering the proximity of the target to critical organs. Both the plans were optimized with similar constraints to achieve the same dose criteria and maintain plan uniformity. The analysis involved the evaluation of Conformity Index, Gradient Index and low dose spillage. The statistical analysis was conducted using the Paired t-test with a significance level set at $p < 0.05$.

RESULTS: Preliminary results indicated that the dose conformity of both 10FFF and 6FFF were identical ($p = 0.6093$). The volume of tissue receiving 50% and 30% of the prescribed dose was observed to be statistically lower in 6FFF as compared to 10FFF ($p = 0.0005$ and $p = 0.0267$) respectively. The Gradient Index of 10FFF beams were observed to be marginally higher than 6FFF, reinforcing the dosimetric advantages of 6FFF beams in intracranial SRS treatments. The total MU were observed to be lower in 10FFF compared to 6FFF ($p = 0.0003$), which can be delivered with a higher dose rate thus reducing the beam on time.

CONCLUSIONS: This dosimetric analysis highlighted the importance of energy selection in intracranial SRS treatments. The use of 6FFF beams showed superior plan quality in terms of low dose spillage providing valuable insights for radiation oncologists and treatment planners. The results support the optimization of treatment techniques in order to maximize tumour control and minimize the risk of normal brain tissue toxicity. However larger studies are needed to validate these findings and guide clinical decisions.

KEYWORDS: medical accelerator, quality assurance, dosimetry, radiation safety

INFLUENCE OF THE HYSTERESIS OF THE COLLIMATOR IN SMALL FIELD OUTPUT FACTORS

Nithyashree, Sathiya Raj, Shwetha B, Kadirampatti Ganesh

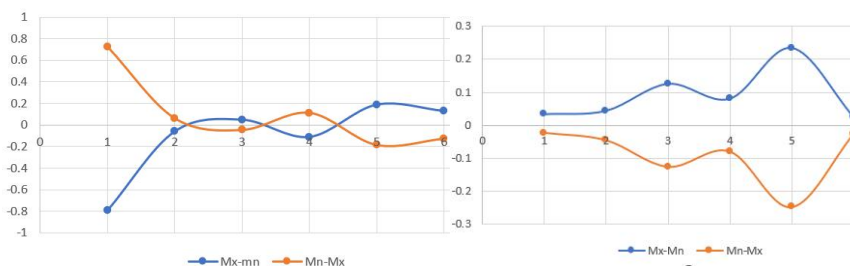
Department of Radiation Physics, Kidwai Memorial Institute of Oncology, Bengaluru, Karnataka, India

Email: nithyashreehs.s1814121@gmail.com

BACKGROUND: Intensity modulated radiotherapy (IMRT) may have different treatment delivery sequences of the collimator setting. One way is that the sequence starts from smaller segment and another way is the sequence starts from larger segment. Due to these different sequences of beam delivery the output factor may vary particularly for small segments/fields. This study aimed to determine this effect in case of small fields.

MATERIALS AND METHODS: Small field output factors were obtained using CC01 ion chamber and EFD unshielded diode detectors for 6 MV photon beam. All measurements were carried out in a Radiation field analyser with SSD set to 90 cm and depth 10 cm. The output factors were obtained by opening the collimator to large field size and reduce to actual field size (Mx-Mn), similarly opening the collimator from smallest field size to actual field size (Mn-Mx). Meter readings of the chamber were averaged. The average meter readings were corrected for all influence quantities along with chamber dependent correction factors (from TRS 483).

RESULTS: The corrected output factors for CC01 were 0.6580, 0.8167, 0.8583, 0.887, 0.9145, 0.9388 for 1x1, 2x2, 3x3, 4x4, 5x5 and 6x6 cm² respectively. Similarly, for EFD the output factors were 0.6725, 0.7933, 0.8386, 0.8723, 0.8989 and 0.9239 for the same field sizes. The average deviation was -1.23% between CC01 and EFD over the range of field sizes. The calculated P- values shows no significance ($P > 0.05$) in output factors between Mx-Mn and Mn-Mx. For both detectors the difference in the output factors of Mx-Mn and Mn-Mx with respect to average output factors complement each other and hence it is proved that by taking average output factors of Mx-Mn and Mn-Mx one can eliminate the hysteresis of collimator. The complementing effects of CC01(left) and EFD (right) detectors are shown in the figures below.



CONCLUSION: Influence of the hysteresis of the collimator in small field output factors was studied successfully using CC01 and EFD detectors. Both detectors show that the variations in the output factors of Mx-Mn and Mn-Mx complement each other, hence it is advised that taking average of output factors for these two collimator settings will minimize the error.

KEYWORDS: Output factor, small field dosimetry, diode and ion chamber.

QUALITY ASSURANCE TESTS PERFORMED ON THE LEKSELL GAMMA KNIFE ICON TREATMENT UNIT.

N. Ponnusamy^{1,3}, Senthil Manikandan², M. Muthuvinyagam³, S. Asath bahadur^{3*},
Dwarakanath Srinivas¹, Bhanumathy¹

¹National Institute of mental health and neurosciences, Bengaluru, Karnataka, India.

²Kidwai memorial institute of oncology, Bengaluru, Karnataka, India

³Department of Physics, School of Advanced Sciences, Kalasalingam academy of research and education,
Tamilnadu, India.

Email: ponnusamyp@gmail.com

BACKGROUND/OBJECTIVE: The Leksell Gamma Knife ICON system from Elekta AB to effectively treat brain diseases. With its 192 Cobalt-60 sources, this system allows us to precisely target specific areas for treatment. Additionally, the CBCT image guidance system provides paralleled accuracy. We conducted thorough testing of the installation and radio physical aspects, and successfully commissioned Gamma Knife, CBCT and IFMM systems.

MATERIALS AND METHODS: This study included measuring the beam alignment precision, Gamma Knife accuracy, Center Position measurements, Off Center Position Measurements, height of absorbed dose rate, and Relative Output factor measurement. We used high-resolution EBT3 Gafchromic film and small-volume ion chambers (Exradin A16 0.007cc and PTW 0.125cc) to conduct the study. Our results confirmed the unit was suitable for source confirmation tests and absorbed dose rate measurement. We measured the dose rate with a 16mm collimator for each sector with all other sectors blocked, using a Solid Water phantom. To confirm the proper installation of all 192 sources in all eight sectors, the dose rate was measured in each sector while other sectors were blocked. We found the sum of all the sector's dose rates to be 3.4371 Gy/min. The absorbed dose rate measured with the same setup while keeping all the sectors (1 to 8) opened was 3.433Gy/min. The percentage difference between the sums of dos rates of all individual sectors and the dose rate at the isocenter was 0.11%

RESULTS: In order to verify that all 192 sources in the eight sectors were properly installed. The total dose rate for all sectors was found to be 3.4371 Gy/min. The dose rate was also measured while all sectors were open and the absorbed dose rate was 3.433 Gy/min. This resulted in a difference of only 0.11% between the sum of the individual sector dose rates and the machine output

CONCLUSIONS: Our study found that Exradin A16 ion chambers were found suitable for the source conformation test and absorbed dose rate measurement as well. All our results are comparable with earlier literature values and within the tolerance of international guidelines within the acceptable limits

KEYWORDS: Gamma Knife, AAPM TG report, Position measurement, EBT3 Gafchromic film, Output factor measurement.

ESTABLISHING LOCAL DIAGNOSTIC REFERENCE LEVELS FOR IMAGE-GUIDED INTERVENTIONAL PROCEDURES: A STUDY AT SULTAN QABOOS COMPREHENSIVE CANCER CARE AND RESEARCH CENTRE

Naema Al Maymani¹, Zakyia Awlad Thani², Subhash Kheruka¹, Noura Al Makhmari¹, Huoda Al Saidi¹, Sana Al Rashdi¹, Rashid Al Sukaiti¹

¹Department of Radiology, Sultan Qaboos Comprehensive Cancer Care and Research Centre

² College of Science, Sultan Qaboos University

Email: naemaalmaymani@gmail.com

BACKGROUND: Fluoroscopy in medical applications can lead to high radiation doses for patients and operators. Local Diagnostic Reference Levels (DRLs) have been implemented in interventional radiology to minimize radiation exposure while optimizing imaging quality and patient safety.

PURPOSE: This study aimed to establish DRLs for Image-Guided Interventional Procedures (IGIPs) at Sultan Qaboos Comprehensive Cancer Care and Research Centre (SQCCCRC). The objective was to enhance radiological practice by setting specific benchmarks for radiation doses, optimizing patient safety, imaging quality, and therapeutic outcomes.

MATERIALS AND METHODS: The study focused on various IGIPs, collecting data such as dose area product (DAP), air kerma at the reference point (AK_{Ref}), fluoroscopy time (FT), frames, kilovoltage (kV), and milliampere-seconds (mAs). The data pertained to adult patients weighing 60kg to 80kg. DRLs were set as the 3rd quartile of DAP values and fluoroscopy time.

RESULTS: Determined DRLs for DAP and fluoroscopy time in the studied procedures were as follows: Catheter Insertion: DAP: 0.73 Gy*cm², FT: 0.52 min, Stent Insertion: DAP: 63.73 Gy*cm², FT: 12.42 min, Nephrostomy: DAP: 2.21 Gy*cm², FT: 1.6 min, Embolization: DAP: 136.28 Gy*cm², FT: 23.65 min, Chemoembolization: DAP: 155.35 Gy*cm², FT: 22.51 min, Cholangiogram: DAP: 4.31 Gy*cm², FT: 2.62min, and Biliary Drainage: DAP: 10.09 Gy*cm², FT: 9.31 min.

CONCLUSION: The established DRLs align with international studies, ensuring radiation doses in IGIPs at SQCCCRC are within acceptable limits and global best practices. The study contributes to radiation safety knowledge, providing guidance for healthcare professionals and patient safety.

KEYWORDS: Diagnostic Reference Levels, Image-Guided Interventional Procedures, Radiation Doses

REFERENCES:

- [1] Hart D, Wall BF. UK population dose from medical X-ray examinations. *Eur J Radiol.* 2004 Jun;50(3):285-91.
- [2] Padovani R, Vano E, Trianni A. Reference levels at European level for cardiac interventional procedures. *Radiat Prot Dosimetry.* 2008; 129(1-3):104-7.
- [3] Marshall NW, Chapple CL, Kotre CJ. Diagnostic reference levels in interventional radiology. *Phys Med Biol.* 2000 Dec; 45(12):3833-46.

EVALUATION OF DIRECT DENSITY ®ALGORITHMFOR RADIOTHERAPY PLANNING AND UNDERSTANDING DOSIMETRY DIFFERENCES COMPARED TO STANDARD PRACTICE.

Vishram Naik, Amit Nirhali, Sharad Gadhave, Dr.Sanjay MH

Department of Radiation Oncology, Sahyadri Super Speciality Hospital(Unit-HDP), Pune, India.

Email: ashunaik7200@gmail.com

BACKGROUND/OBJECTIVE: The objective of this study is to evaluate the reliability and applicability of the Direct Density ® algorithm, recently introduced by Siemens Healthineers, for radiotherapy planning. The algorithm aims to optimize the radiotherapy treatment process by enabling customized kilovoltage (kV) settings during patient CT scans.

MATERIALS AND METHODS: To investigate the algorithm's performance, we utilized the scan of Catphan® 503 phantom to plot a comprehensive graph of electron density vs. Hounsfield Units (HU) for different energy levels, including 80kV, 110kV, and 130kV. The CT to ED curves were then analyzed, revealing minimal discrepancies between HU values for all energy levels compared to the standard HU values, with deviations within the range of ± 40 HU. Subsequently, we performed treatment planning on these CT images using Monaco 5.51.10 Treatment Planning System (TPS) by Elekta® and compared the results with conventional planning typically conducted at 120kV or 130kV energy level.

RESULTS: The analysis of the Catphan® 503 data demonstrated remarkable consistency in electron density across the different energy levels. These findings led to the establishment of an average CT to ED conversion file, encompassing 80kV, 110kV, and 130kV, ensuring the feasibility of using customized kV settings for patient scans. Dosimetry comparisons between the Direct Density ® algorithm-based plans and the standard 120kV or 130kV plans showcased minimal variation, with a mean dose difference of less than 0.8%.

CONCLUSIONS: The successful implementation of the Direct Density ® algorithm for radiotherapy planning offers several advantages, including the ability to individualize patient scans with customized kilovoltage settings. This adaptability can potentially lead to reduced patient doses during CT simulation, enhancing radiation safety and precision in medical accelerator treatments. Moreover, the algorithm's accuracy in CT to ED conversion makes it a reliable tool for improving the overall quality assurance and dosimetry in radiation oncology.

KEYWORDS: medical accelerator, quality assurance, dosimetry, radiation safety, CT simulation, CT to ED

Commissioning and Validation of SmartAdapt® and Velocity™ Deformable Image Registration Systems: A Comparative Study

Raghavendra Hazare, Bhakti Dev Nath, Sreelakshmi K K, Umesh Mahantshetty

Homi Bhabha Cancer Hospital & Research Centre, NH 16, Aganampudi Village, Visakhapatnam, India

Email: rhajare13@gmail.com

AIM: To commission and validate commercial deformable image registration systems (SmartAdapt® and Velocity™) using TG-132 digital phantom datasets. Additionally, the study compares the deformable image registration (DIR) algorithms of the two systems.

METHODS & MATERIAL: Commissioning & Validation of two DIR systems in our institution. Downloaded and imported TG-132 Digital phantoms from AAPM website. Geometric phantom with 5 modalities (CT, T1/T2-MR, PET, CBCT) with known shifts- translation and rotation. Anatomic pelvis phantom with 4 modalities with known shifts/deformation (CT, T1/T2-MR, PET, CBCT). Commissioning & Validation performed using rigid registration and results compared to known shifts (Translational and Rotational). Additional sources: Clinical data: 10 H&N patients CBCTs from our institution. Manual contours considered gold standard. Accuracy evaluated by computing Dice Similarity Coefficient (DSC), Mean Distance Agreement (MDA) and Jacobian metrics between deformed contours and manual contours in CBCT. Compare the obtained metrics/indices between SmartAdapt® and Velocity™.

RESULTS: Commissioning and Validation TG -132 recommended criteria is error < 0.5 * voxel dimension (vd)¹. Translation only: Table 1 shows commissioning results of Velocity and SmartAdapt for rigid registration in translational axes alone, both systems met TG-132 recommendations except CT- PET registration in velocity (1.1 * vd). PET images could not be imported into SmartAdapt (technical issues). Translational and rotational: Table 2 shows commissioning results of Velocity and SmartAdapt for rigid registration in both translational and rotational axes, both systems failed the criteria for all modalities (For Velocity, error ranged from 0.6*vd (CT-CT registration) to 3.4*vd (CT-CBCT registration). For SmartAdapt® it was 0.6*vd (CT-CBCT) to 3.6*vd (CT-CT)).

DIR comparison of 10 H&N patients between SmartAdapt® and Velocity™: Tolerance values for assessing the DSC, MDA and Jacobian metrics of the image registration as per TG-132 report. And table 4 shows Mean ± SD for DSC, MDA and Jacobian.

CONCLUSION: The DIR algorithms of SmartAdapt® and Velocity™ were commissioned and their deformation results were compared. The study involved a comparison between SmartAdapt® and Velocity™ for head and neck clinical cases. While there were only minimal differences between the two systems, Velocity™ provided lower values for parotids (soft tissue) compared to SmartAdapt. However, for mandible, spinal cord, and femoral heads (rigid structures), both systems showed nearly identical results.

REFERENCES: Brock KK, Mutic S, McNutt TR, Li H, Kessler ML. Use of image registration and fusion algorithms and techniques in radiotherapy: report of the AAPM Radiation Therapy Committee Task Group No. 132. Med Phys. 2017; 44: e43–e76. Kujtim Latifi | Jimmy Caudell | Geoffrey Zhang | Dylan Hunt | Eduardo G. Moros | Vladimir Feygelman. Practical quantification of image registration accuracy following the AAPM TG-132 report framework. J Appl Clin Med Phys 2018; 1–9

IMPACT OF NUCLEAR REACTIONS ON GAN -HEMT 2D DOSIMETER USED IN PROTON AND CARBON THERAPY

Rijin NT¹, Dinesh Kumar Sharma¹, MM Musthafa², Midhun CV²,
JS Das Gupta³, J Datta³

¹Jain University, Department of Physics, Bangalore-560069, India,

²Department of Physics, University of Calicut, Calicut, Kerala-673635, India,

³Analytical Chemistry Division, BARC-VECC, Kolkata-700064, India

Email: rijin@jainuniversity.ac.in

BACKGROUND/OBJECTIVE: Nuclear reaction transmutation doping in GaN - 2D layer-based MOSFETs, crucial for precise dose measurements in heavy ion radiotherapy machines, poses potential long-term radiation damage. These MOSFETs are optimal for satisfying restricted stopping power conditions and delta-ray equilibrium across various charged particles in proton and heavy ion therapy. Yet, producing new reaction residues during their use can significantly alter dosimeter calibration, warranting thorough research. Hence, this study delves into the impact of nuclear reaction transmutation doping on dosimetry, as its effect remains unexplored despite being a significant concern.

MATERIALS AND METHODS: The study estimated an average energy equivalent of 38 MeV for the cross-section-weighted charged particle spectrum. Using a 45 MeV α beam from a VECC K-130 cyclotron, the GaN-HEMT was irradiated in activation analysis mode. Isotopes formed were detected by counting the irradiated GaN-HEMT with a 100cc HPGe and employing a ¹⁵²Eu-based calibration for HPGe's intrinsic efficiency determination, reproduced with a quadratic fit. Candle data analysis framework identified and quantified peaks corresponding to produced isotopes. Counts were converted to yield using the standard activation equation. The energy degradation of α in each GaN HEMT layer was determined using SRIM-based calculations. Experimental yields were reproduced with Talys-1.96 nuclear reaction calculations, Optimizing reaction model parameterization for natGa(α ,*) and natSi(α ,*) cross-sections from EXFOR. Thick target yields for each reaction residue and their corresponding Z yields were calculated. Finally, the study analyzed the impact of nuclear reactions on doping levels. By combining experimental data and nuclear reaction calculations, this research sheds light on the behaviour of GaN-HEMT under α irradiation, which is crucial for understanding dosimetry and potential radiation damage in this context.

RESULTS: Radiation-induced elemental transmutation effects on GaN devices were quantified using activation analysis, analyzing the yield of formed dopants. Residues with Z>Ga were predominantly produced, resulting in increased n-type doping. This change in differential doping level significantly modified the Dose-Drain current calibration.

CONCLUSIONS: Studied the α impact on GaN MOSFET for Dose-Drain current calibration shifts. Nuclear transmutation doping in GaN 2D layers had a significant influence on calibrations.

KEYWORDS: Heavy ion Dosimetry, 2D Layer Dosimeters, MOSFET, Quality Assurance, Radiation Damage, Radiation Safety

Presentation ID: P-196

Abstract ID: X7468

EFFICIENCY ANALYSIS OF HYPERARC PLANS AND COMPARISON WITH CONVENTIONAL VMAT FOR SINGLE AND MULTIPLE INTRACRANIAL STEREOTACTIC TREATMENTS

Siva Kumar, Gopinath Mudhana, Ravi Kumar, Tamilarasan R, Perumal Murugan, Dinesan C, Abishake M, Karthik A

Sri Shankara Cancer Hospital & Research Centre, 1st Cross, Shankarapuram, Basavanagudi, Bengaluru
Vellore Institute of Technology, Chennai, India

Email: Sivam1985@Gmail.Com

AIM: This study aimed to evaluate and compare the efficiency of Hyperarc (HA) plans with and without Automatic Lower Dose Objective (ALDO) and to compare these plans with non-coplanar conventional volumetric-modulated arc therapy (C-VMAT) for both single and multiple brain metastases.

METHODS: A total of 34 patients with single and multiple brain metastases, ranging from 1 to 15 lesions with volumes from 0.6cc to 18cc, were included. Three treatment plans were generated: HA with ALDO (HA-ALDO), HA without ALDO (HA-NOALDO), and non-coplanar C-VMAT (C-VMAT). All plans were created using a TrueBeam with HDMLC and a 6MV flattening filter-free (FFF) beam. Dosimetric parameters, including conformity index (CI), homogeneity index (HI), high-dose spillage 120% (HDS), gradient index (GI), intermediate dose spillage 50% (IDS), and volumes of brain tissue receiving doses from 18Gy to 4Gy, were evaluated. Maximum doses to critical structures (brainstem, chiasma, optic nerve, eyes, lens, and cochlea) were also assessed. The physical characteristics of the plans, such as the number of monitor units (MUs) required, were also considered.

RESULTS: The HA-ALDO plans showed significant improvements in all evaluated dosimetric parameters. HA-ALDO achieved better CI, GI, and IDS 50% (0.82 ± 0.07 , 3.87 ± 1.0 & 22.75 ± 27.54) compared to HA-NOALDO (0.77 ± 0.09 , 4.52 ± 1.59 & 26.27 ± 27.45) and C-VMAT (0.76 ± 0.09 , 5.19 ± 2.17 & 34.18 ± 52.18). The HI and HDS 120% were more with HA-ALDO (0.36 ± 0.07 & 2.0 ± 1.52) compared to NOALDO (0.16 ± 0.03 & 0.18 ± 0.31) and C-VMAT (0.13 ± 0.02 & 0.09 ± 0.17) as upper dose objective is not supported in HA-ALDO. HA-ALDO plans significantly reduced doses to normal brain tissue (V18Gy, V15Gy, V12Gy, V8Gy & V4Gy: 8.42 ± 8.66 , 11.89 ± 13.17 , 17.05 ± 20.34 , 31.22 ± 40.31 & 101.19 ± 153.4) compared to HA-NOALDO (9.27 ± 8.42 , 13.35 ± 12.79 , 19.42 ± 20.01 , 35.81 ± 39.88 & 113.6 ± 151.31) and C-VMAT (9.98 ± 10.41 , 14.93 ± 18.34 , 23.44 ± 33.09 , 53.25 ± 83.53 & 171 ± 199.48). Moreover, HA-ALDO plans significantly reduced the dose to other critical structures as well. However, the MU with HA-ALDO plans was significantly higher compared to HA-NOALDO and C-VMAT.

CONCLUSIONS: HA-ALDO plans demonstrated better conformity, rapid dose falloff, and improved sparing of organs at risk (OAR) when compared to HA-NOALDO and C-VMAT plans. However, the increased number of monitor units required for HA-ALDO plans should be considered when evaluating treatment efficiency.

KEYWORDS: HyperArc, ALDO, VMAT, Planning

VALIDATION AS PER TG-306 REPORT FOR QA AND QC OF RADIXACT MACHINE: AN INSTITUTIONAL EXPERIENCE

Deepak Thaper, Rose Kamal, Manigandan Durai, Rishabh Kumar, Bhaskar Vishwanathan,

Department of Radiation Oncology, School of Medicine, Amrita Vishwavidyapeetham, Panjab University
Faridabad, India

Email: deepak.thaper33@gmail.com

BACKGROUND: After the publication of Task Group (TG) 148, so many advancements occurred in dose calculation, processes, and hardware of tomotherapy and able to do the delivering with advanced dynamic jaw. This TG 306 aims to provide updated guidelines for tomotherapy hardware, imaging, treatment planning, and patient QA.

MATERIALS AND METHODS: The various test has been performed as suggested in TG 306. The dynamic jaw delivery performs a sliding- window open-and-close jaw movement at the superior and inferior edges of the treatment target during irradiation. Three specific QA tests performed for dynamic jaws which is field width, jaw sweep, and jaw timing. In field width dynamic jaw test, an additional seven beam profiles were measured including asymmetric field size. In jaw sweep dynamic jaw test, an accurate timing of the jaw movement calculated to ensure gantry and couch movement synchronization. For jaw timing Accuracy and jaw speed consistency, both jaws are allowed to move at their planned speeds during dynamic jaw delivery. Jaw speed continuous and discrete consistency test also performed with a fixed jaw size. In MLC QA non-linear leaf behavior test MLC leaves do not move instantaneously when command is issued. Initially, a linear fit was performed between actual and commanded LOT. The slope and offset obtained at each projection time was tabulated and correction factors based on the latency table were applied at the end. In synchrony motion QA, the target motion computed from the continuously acquired external marker positions and corrected using MLC and jaw adjustments.

RESULTS: The results of all the tests found within the tolerance as mentioned in the TG 306.

CONCLUSIONS: TG 306 report can be utilized to validate the testing and to enhance the confidence for accurate and precise treatment delivery of the beam using advanced Radixact machine with dynamic jaws.

DOSIMETRIC ANALYSIS OF RADIOTHERAPY TECHNIQUES IN THE TREATMENT OF CARCINOMA RECTUM

Leena Dutta¹, Dimpal Saikia¹, Dr. Smriti Goswami¹, Shabnam Biswas², Dr. Fahim Arman Hassan¹, Dr. Bibhas Chandra Goswami¹, Mr. Jibon Sharma¹

¹Department of Radiation Oncology, State Cancer Institute, Gauhati Medical College, Guwahati,

²Assam Cancer Care Foundation, Guwahati, India

Email: leenadutta111@gmail.com

AIMS & OBJECTIVES: Dosimetric analysis on Radiotherapy Planning techniques in Carcinoma Rectum.

MATERIALS & METHODS: For our study, we analysed fifteen patients of Carcinoma Rectum. The patients were planned in prone decubitus. CT simulation was carried out with 5mm slice thickness and then images were transferred to Monaco 3.0 Treatment Planning System. The External body, GTV, CTV and OARs viz, Bladder, Bowel bag, Femoral Heads and Penile Bulb were contoured. The PTV was then created. Then planning was carried out using four techniques viz., Parallel Opposing AP-PA technique, Three field technique, Four Field Box technique and 3 Dimensional Conformal Radiotherapy (3-DCRT). Dose to PTV was ensured to be as per 3-DCRT guidelines. The data were collected for the following parameters- V95% of PTV, Global Max dose, Mean dose of OARs from the Dose- Volume Histogram Statistics of Monaco TPS. One-way ANOVA test and Mann-Whitney test were performed for the statistical analysis considering Three-field technique as the reference one. P-value < 0.05 was considered as significant.

RESULTS & DISCUSSIONS: In our data, PTV coverage was found superior in 3-DCRT (p-value < 0.00001) in comparison to other techniques. Global Max dose was found highest in 3 field technique (10/15 patients). Mean dose to Femoral heads was significantly found highest in 3 field technique (p-value < 0.00001) and least in AP-PA technique. Mean dose to Bladder and Penile Bulb was found highest in AP-PA technique. Mean dose to Penile bulb was found almost similar in other three techniques. Mean dose to Bowel bag was found similar in all techniques. Details of data analysis will be illustrated in the presentation.

CONCLUSION: 3DCRT was found superior in terms of PTV coverage and OAR sparing. If 3DCRT is not feasible, then we suggest to go for four field technique.

THE CLINICAL IMPLEMENTATION, VALIDATION AND ADVANTAGE OF VOLUMETRIC MODULATED ARC THERAPY (VMAT) TOTAL MARROW AND LYMPH NODE IRRADIATION (TMLI)

C.P. Bhatt, Ajai Kumar Yadav

Sarvodaya Hospital and Research center, Sector 8, Faridabad, Haryana, Delhi NCR, India

Email: cpbhatt.phy@gmail.com

OBJECTIVE: Total Marrow and Lymph Node Irradiation (TMLI) is a modern radiotherapy technique that selectively targets the bone marrow and lymph nodes. The aim of this study is to evaluate the clinical Implementation and validation of VMAT TMLI.

MATERIALS AND METHODS: Patient simulation was done with Elekta BlueBAG™ with a brain thermoplastic mask. CT simulation was done in 2 CT data sets with Headfirst supine (HFS) and Feet first supine (FFS). Contouring and planning were done with Monaco TPS (Elekta Medical system). CTV included all the Bone marrows and Lymph nodes with a 5 mm margin to create PTV. The OARs contoured are optical structure, oral cavity, lungs, liver, kidneys, bowel loops, bladder and rectum. A 3-5 isocenters and 5-9 VMAT arc of 6 MV photon beam plan was generated and optimized to deliver a uniform dose of 12 Gy in 6 Fractions over three days. The planning aim was to deliver 12 Gy to at least 90% of the PTV ($V_{100\%} \geq 90\%$) and 11.4 Gy to at least 95% of the PTV ($V_{95\%} \geq 95\%$). 1-2 Isocenters AP-PA plan was created in FFS and the patient was treated twice daily with a minimum inter-fraction gap of 6 hours.

RESULTS: For the PTV, $V_{12\text{ Gy}}=92\%$ and $V_{11.4\text{ Gy}}=96\%$ achieved. For OARs Lungs and Kidneys, the Mean doses were 7.8 & 8.1 Gy and 7.2 & 6.9 Gy, respectively, for LT & RT lung and Kidney; Oral cavity, Heart, Liver & Bowel bag, the mean dose of 7.5 Gy, 8.6 Gy, 8.2 Gy & 8.1 Gy and Lens and parotid mean doses of 5.1 & 5.8 Gy and 8.8 & 8.4 Gy to LT & RT Lens and Parotid were achieved. QA for VMAT TMLI plans was performed using an Octavius 4D phantom (PTW, Germany). The 3D dose fluence of the VMAT plan is measured for individual isocenters; Point dose measurements for all isocenters and junctions are also performed.

CONCLUSIONS: Clinical implementation of TMLI represents a significant advancement in radiotherapy for patients with reduced toxicities, improved disease control, and personalized treatment opportunities, making TMLI a promising option in modern oncology.

KEYWORDS: TMLI, TBI, Total Marrow and Lymph Node irradiation; Volumetric Modulated Arc Therapy, BMT, ALL; AML

ANALYSIS OF SMALL VOLUME TARGETS BY POINT DOSE METHOD WITH 0.13CC & 0.01CC IONIZATION CHAMBER

Subhrendu Ghosh, A David Perianayagam, Suman Mitra

Desun Hospital, Department of Medical Physics, Kolkata-107

Email: subhrendu.g@gmail.com

PURPOSE: The point dose measurement method is a renowned technique for the verification of the treatment plan. It is a very reliable method when the target size is small, moreover the role of fluence measurement is limited and uncertainty arises. In IMRS, done through VMAT treatment technique the dose delivered is very high compared to the conventional dose protocols. So, the verification becomes a very important step. However, it is seen that when the target size is very small, the selection of ionization chamber becomes a very difficult process as the smaller the target more the uncertainty in measurement. This study aims at finding the smallest possible volume of the target where point dose measurement can be carried out and comparing the same with two different ionization chambers namely 0.01cc and ionization chamber of 0.13cc and thus concluding the best possible combination of ionization chamber for a given volume.

MATERIALS & METHODS: Materials used in this study are as followed-PMMA Slab phantom – Water equivalent.-Linear Accelerator – Elekta Infinity with (6FFF).-Ionization Chamber – IBA ionization chamber (0.13cc) & IBA micro chamber(0.01cc).-Electrometer – IBA electrometer Dose 1-TPS – Monaco 6.0.1. Temperature and pressure are taken from calibrated instruments. The treatment plans are generated on Monaco 6.0.1 TPS and Quality Assurance plans are made on the PMMA slab. In the QA phantom, the treatment plans are superimposed and the dose is calculated using Monte Carlo. Two different types of measurement are done.-With zero Gantry angle.-With real gantry angle. The results are then matched with the measured dose and error percentage is calculated.

RESULTS: The measured dose for the CC13 chamber shows that the deviation is more with the TPS calculated dose and it should not be used for the lower size targets. On the other hand, 0.01CC chamber provides a very good agreement with the TPS calculated dose and the measured dose, even in very small targets (≈ 1 CC). The fixed notation suggesting that the plans (IMRS VMAT) were calculated on QA phantom by keeping the gantry fixed at zero degree and the measurements were done likewise. It is also important to note that even in CC13 as the volume increases, the deviation between the TPS calculated dose and the measured dose shows a decreasing trend. The results show that both Real and Fixed Gantry angle provides good agreement with the TPS calculated value for 0.01CC. However, if it can be looked a bit closely, it can be seen that on one to one marking the Real Gantry angle has a little edge over the Fixed Gantry angle results. Just like the previous case, it can be seen that the results are inclined towards the Real Gantry angle by a good amount. Unlike 0.01CC, the agreement between TPS calculated dose and measured dose increases considerably with an increase in target volume.

CONCLUSION: The measurements were completed and as expected the results were inclined towards the use of micro chamber in smaller volume. However, it can be suggested that for better results the use of Real Gantry angles or simply both the measurements can be done and analyzed accordingly. The deviation in smaller targets ≈ 1 CC, uncertainty in measurement increases highly due to the effects of small field. The mean % deviation for 0.01CC chamber was calculated, with standard deviation of 2.67 under 95% confidence interval, was found out to be -1.6575 ± 1.66 . It is also observed that CC13 chamber is not suitable for the measurement of dose up to 25CC target volume & it is probably due to lateral CPE failure. But as the trend suggested and extrapolated, the data sets were studied found to be accurate in an exponential plot with regression value of 0.8. It can be seen from that curve, the measurements achieving the passing criteria near 60cc target volume. The same has been verified by measuring.

DESIGN AND DOSIMETRY OF A PROTOTYPE BI-RADIONUCLIDE HYBRID OCULAR BRACHYTHERAPY PLAQUE: A FEASIBILITY STUDY

¹Sanjay Saxena, ¹Yogendra Kumar, ²Shubhalaxmi Mishra, ²Sridhar Sahoo, ²T. Palani Selvam

¹Bhabha Atomic Research Centre, Therapeutic & Reference Sources Section, Radiopharmaceuticals, Division, Bhabha Atomic Research Centre, Mumbai, India

²Bhabha Atomic Research Centre, Radiological Physics & Advisory Division, Mumbai

Email: sksaxena@barc.gov.in

OBJECTIVE: The objective of this study is to investigate suitability of prototype hybrid plaque designs consisting of ¹⁰⁶Ru/¹⁰⁶Rh and ¹²⁵I for ocular brachytherapy. Two different designs are conceptualised and investigated using Monte Carlo method.

MATERIALS AND METHODS: The plaque is in the form of a spherical shell with radius of curvature 12.5 mm. A thin layer of ¹⁰⁶Ru/¹⁰⁶Rh is supposed to be electrochemically deposited on the concave surface of a 0.2 mm-thick high purity silver. This layer is encapsulated between the concave surface of a 1.2 mm thick base plate of silver and the convex surface of a 0.1 mm-thick layer of silver (exit window). Figure 1 presents Design I consisting of 3 elements: (1) 1.2 mm thick silver base plate, (2) about 20 µm thick ¹⁰⁶Ru deposited on a 0.2 mm silver disk, and (3) water equivalent gel consisting of twelve ¹²⁵I-LDR OcuProsta seeds. In Design II, order of the plaque elements are 2, 1, 3 from the top. Dose distributions are calculated in a spherical water phantom of 30 cm diameter using the brachy_code of the Monte Carlo-based EGSnrc code system. For comparison purpose, plaques with either ¹⁰⁶Ru/¹⁰⁶Rh or ¹²⁵I are also included in the study.

RESULTS: Figs. 2 and 3 present the depth doses for Design I and Design II, respectively along with standard ¹²⁵I and ¹⁰⁶Ru/¹⁰⁶Rh, applicators. Dose differences are significant for distances less than 6 mm between Designs I and II. The gradient of the depth dose profiles can be adjusted by varying the activity ratio between ¹²⁵I and ¹⁰⁶Ru/¹⁰⁶Rh for different tumour thicknesses. The bi-radionuclide plaque ¹²⁵I-50%+¹⁰⁶Ru-50% means both radionuclides contribute the same amount of the dose to the sclera. Similarly, ¹²⁵I-25%+¹⁰⁶Ru-75% and ¹²⁵I-10%+¹⁰⁶Ru-90% plaques imply dose contributions to sclera from ¹⁰⁶Ru/¹⁰⁶Rh are 3 and 9 times higher than the contribution of ¹²⁵I, respectively. The values are normalized to 1000 Gy to illustrate the typical range of dosage for eye plaque therapy.

CONCLUSION: The bi-radionuclide plaque offers better tumour coverage, dose uniformity and significant dose reduction laterally as compared to standard plaques with single radionuclide.

KEYWORDS: ¹²⁵I, ¹⁰⁶Ru/¹⁰⁶Rh, bi-radionuclide plaque, ocular brachytherapy, Monte Carlo

IMPLEMENTATION OF COUCH STRUCTURE IN MONACO TPS AND ITS DOSIMETRIC IMPACT ON BREAST SBRT PLAN

Sandeep Kumar B.S, Sathiyaraj P, Sampath kumar, Shashai N, Ganesh KM

Department of Radiation Physics, Kidwai Memorial Institute of Oncology, Bengaluru, Karnataka, 560029, India

Email: kumarasandeep685@gmail.com

BACKGROUND: There are many factors involved in the treatment planning of radiotherapy that affects the dose delivery, such as the intervention of treatment couch system that supports the patient. This study aimed to investigate the dosimetric effect of carbon fiber couch on treatment plan and its delivery.

MATERIALS AND METHODS: Carbon fiber couch of three linear accelerators (all Elekta-Versa HD) were scanned with sufficient buildup and scattering condition. The obtained electron density (ED) values were applied during treatment planning. Simple square field plans were done for different gantry angles, one set of plans with couch (assigned ED values) and another set of plans without couch (not assigned ED values). Two clinical plans of prone position breast cases (SBRT-15Gy/1#) were also selected from TPS. Along with point dose measurements (only square fields) gamma analysis was also performed with passing criteria set to 2%1mm, global normalization. All volumetric gamma values were compared.

RESULTS: An average ED of 0.63 for carbon fiber and 0.18 for foam core was obtained. The percentage difference in measured and TPS calculated point dose with couch was -1% at 180°, 3.2% at 240°. Without couch the point dose differed by -4.64% at 180° and -6.3% at 240°. The average dose difference for without couch measurements from 180° to 90° / 180°-270° was -4.76% and 0.52% for with couch measurements. For clinical SBRT plan the gamma passing rate was improved from 64.6% to 87.1% after accounting couch ED values. For the second patient the gamma passing rate improved from 79.8% to 85.8%. The calculated P – value (is less than 0.001) shows very significant difference between adding and removing couch during treatment planning. The significance was noticed both in the square field and clinical plans/measurements.

CONCLUSION: From the statistical analysis it was evident that the couch impact in dose distribution was considerable. We found that ignoring the couch in the dose calculation can change patient's target doses significantly (underdose). It is advised to always include a couch during planning particularly for tangential VMAT/IMRT plans.

PARAMETER ESTIMATION OF LYMAN-KUTCHER-BURMAN NTCP MODEL FOR RADIATION INDUCED DYSPHAGIA IN HEAD & NECK CANCER PATIENTS OF INDIAN DEMOGRAPHICS

Ganeshkumar Patel, Abhijit Mandal

¹Department of Radiotherapy & Radiation Medicine, Institute of Medical Sciences, BHU, Varanasi, India

Email: ganeshgravity@gmail.com

AIM & BACKGROUND: To validate the LKB NTCP model based on patient reported questionnaire at the institutional level and to derive biological parameters of the LKB model for dysphagia toxicity of head & neck cancer patients.

MATERIAL AND METHODS: The present study has two parts, in first part LKB model validation is performed and in second part LKB model parameters estimated. There are 70 patients of head & neck cancer treated at RTRM department, IMS, BHU from April 2019 to December 2021. Out of 70 patients, 44 patients were treated by RT alone which includes post-operative and radical treatment. Acute and late dysphagia evaluated according to the guidelines established by the Radiation Therapy Oncology Group and the European Organization for Research and Treatment of Cancer (*RTOG/EORTC*). NTCP is calculated by in-house developed programme in MATLAB (2016b) version using LKB model for larynx and pharyngeal constrictor muscle. This program accepts DVH file of organ at risk in .txt format. The calculated value of NTCP more than 60% by LKB model for larynx assumed for grade 2 toxicity as an endpoint. It means if predicted NTCP is more than 60% of an organ and there is associated grade 2 toxicity observed in an organ otherwise if it is less than 60% and there is no grade 2 toxicity, this condition is applied for checking the performance of the model. In later part, assuming $n = 1$, the m and TD50 biological parameters of the LKB model were estimated by the maximum likelihood method from plots of complication rate as a function of mean organ dose. Ninety five percent confidence intervals for parameter estimates were obtained by the profile likelihood method.

RESULT: The following parameter estimates were obtained for the endpoint dysphagia: $m = 0.16$ (95% CI 0.15, 0.20) and TD50 = 43.6 Gy (95% CI 42.5, 45.8).

CONCLUSION: LKB model can be used as a reliable radiobiological model for plan evaluation.

THE IPEM MASTERS-LEVEL COURSE ACCREDITATION FRAMEWORK FOR MEDICAL PHYSICS AND ENGINEERING COURSES

Mark McJury, Liz Parvin, Jemimah Eve and Philip Riches

On behalf of the Course Accreditation Committee, Institute of Physics and Engineering in Medicine, York UK

Email: jemimah@ipem.ac.uk

BACKGROUND/OBJECTIVE: Most training programmes for Medical Physicists and Engineers, include an essential educational component – typically a Masters degree programme. To ensure that the course is of appropriate quality and relevance for training needs, it is beneficial to obtain some form of accreditation by the national body for Medical Physicists and Engineers. In the UK, that national body is the Institute of Physics and Engineering in Medicine. Following restructuring of national training for physicists and engineers, IPEM revised their Masters level accreditation framework (MLAF), which accredits both national, and international courses for medical physicists and engineers.

MATERIALS AND METHODS: In consultation with higher education institutions, the IPEM MLAF was revised to meet the needs of changing trends in student background, prior experience, and recruitment. The framework has maintained its core components, involving assessment of site-based, and distance programmes; assessment of courses aimed at those going forward to academic, industrial and healthcare roles; and institution visit but also accommodates a virtual/distance accreditation process. A key aspect of the assessment process remains the sharing of educational best practice across institutions. IPEM is also developing undergraduate course accreditation framework (ULAF).

RESULTS: The MLAF was relaunched, and currently accredits twelve UK MSc programmes, and one international MSc programme. There are currently two further UK programmes awaiting their first accreditation.

CONCLUSIONS: IPEM accreditation framework for Masters level medical physics and engineering programmes has been revised in consultation with UK higher education institutions. The framework remains a rigorous assessment of educational quality, and continues to represent a sought-after certification of high-quality education relevant to training for those progressing to roles as professional medical physicists and engineers.

KEYWORDS: education and training, quality assurance, programme accreditation

DETERMINATION OF PLANNING TARGET VOLUME MARGIN FOR RADIOTHERAPY OF HEAD AND NECK CANCERS AT A TERTIARY CANCER CARE CENTRE

Krishna Prasad P, Reshma Bhaskaran, Sushama P, Ahamed Basith, AjayaKumar T

Government Medical College Kozhikode, India

Email: krishnaprasad870@gmail.com

INTRODUCTION: Cancers of the oral cavity and pharynx form around 14 percent of all cancer incidence in India. These cancers show very good prognosis, if diagnosed early and treated accurately. Precision radiotherapy (RT) plays a very crucial role in the disease outcome. Planning Target Volume (PTV) accounts for the systematic and random errors encountered during the course of RT. Hence adequate margin for PTV is imperative for the success of RT. Modern linear accelerator was introduced at Government Medical College Kozhikode (GMC KKD) in 2014 and since then 3000 patients are treated annually, on an average, with RT. Since the technologist and other clinical staff have gained an experience of nearly 10 years, the aim of this work was to analyse the adequacy of the PTV margins with regard to the setup errors and bring changes if required.

METHODOLOGY: 60 patients treated for Carcinoma Hypopharynx (Ca Hpx) and 40 patients treated for Carcinoma Nasopharynx (Ca Npx) were selected for the retrospective study. 5 planar images were analysed per patient. For Ca Npx three regions were identified for offline image matching and shifts were noted in all the three regions. The complete data was analysed to find the systematic and random error as per the Van Herk formula. The PTV margin was calculated for Ca Hpx and Ca Npx accordingly using the formula.

RESULT :The patients for head and neck carcinomas are generally planned with uniform PTV margin of 5 to 7mm. The treatment is executed with Volumetric Modulated Arc Therapy (VMAT). The PTV margin for Hpx was found to be the maximum of 5 mm in Hypx in the medio lateral direction. The remaining two directions required margins less than 3.5mm. In Ca Npx the maximum PTV margin was found for the C2 vertebral region in the medio lateral direction. Remaining two regions required margin less than 5mm.

CONCLUSION: For Ca Hpx the existing margin of 5mm may be continued. For Ca Npx differential PTV margins may be considered with higher margin in the c2 Vertebral region. This will be very effective in sparing the optical structures.

DOSIMETRIC EVALUATION OF CRANIOSPINAL IRRADIATION (CSI) IN VOLUMETRIC MODULATED ARC THERAPY (VMAT) & THREE-DIMENSIONAL CONFORMAL THERAPY (3DCRT) AND SPILLAGE OF DOSE TO VARIOUS CRITICAL STRUCTURE: A NEW PERSPECTIVE

Farhana Khatoon, Anoop Kumar Srivastava, Anupam P B, Abu Musha Shah, Diviya kukraja, S P Mishra, Rohini Khurana, Madhup Rastogi

Department of Radiation Oncology, Dr Ram Manohar Lohia Institute of Medical Sciences, Lucknow, India

Email: dranooprmlims@gmail.com

BACKGROUND: Craniospinal irradiation (CSI) poses a complex dosimetric challenge in radiation therapy planning due to structural gradient and critical structure in close proximity. This presentation attempts to dosimetrically evaluate the patients treated with multi-arc VMAT and comparatively evaluate the same plans with 3DCRT for analysis of Doses to OAR. Dosage reduction in rigorously optimised VMAT plan for OAR in comparison to 3DCRT has been analysed.

METHODS: 10 patients of various age groups both adult and paediatric were planned by VMAT with 36 Gy in 18 fractions. CT simulation slice of 3mm in supine were taken from head to mid of pelvic and Target volume and OAR were delineated. 6MV photons and a mixture of 6MV and 10 MV photons were utilized for VMAT and 3DCRT plans respectively from Elekta Infinity LINAC. Organ at Risk considered for dose constraints were brainstem, eye balls, eye lens, optic nerves and, optic chiasm, thyroid, larynx, oesophagus, heart, lungs, bladder, rectum, kidney, spleen, liver, bowel bag, rectum and bladder. Judicious combination of full and partial arc was used to achieve the maximum PTV coverage and minimum dose spillage to all the OAR's. These dosimetric values obtained were compared with 3DCRT for analysis.

RESULTS: It was found that the integral dose to the patient was 2.5 times higher in 3DCRT. Mean doses to thyroid, oesophagus, heart, right lung, left lung, spleen, bowel bag, bladder, rectum, right kidney and left kidney were reduced by 1.34, 1.37, 2.45, 2.5, 2.1, 2.3, 1.45, 2.25, 1.09, 1.5 and 1.6 times in comparison to 3DCRT while maintaining the $\geq 95\%$ of the prescribed dose received by $\geq 95\%$ of the PTV. The doses to the brainstem, eyeball, optic nerve, optic chiasma were also reduced. MU consumed were higher by 4 times in VMAT. Average CI of PTV was 1.1 in VMAT and 1.7 in 3DCRT but heterogeneity indexes of PTV were comparable in both cases.

CONCLUSION: A new perspective in dose reduction to various critical organs with high conformity index could be achieved thus reducing the toxicity. VMAT offers superior dosimetry results in CRANIOSPINAL IRRADIATION, especially in the vulnerable paediatric groups.

KEYWORDS: Craniospinal Irradiation, VMAT, 3DCRT, Dose Reduction.

TRAINING AND EDUCATION ON THE PATH OF M.ME CURIE

Luca Gentile¹, Maria Grazia Alberico², Alberto Baratti³, Alessandro Rapa³ Diego Chiapale¹
 Massimiliano Porzio¹ Alessandra Peirona¹ Daniela Rembado¹ Ivo Riccardi⁴

¹ SSD Environment, Physical Agents and Radiation Protection of the Department of Prevention of the ASLCN1 Cuneo Italy

² SC Occupational Medicine of the ASLCN1 Cuneo Italy

³ SS Skills development and continuous quality improvement of the ASLCN1 Cuneo Italy

⁴ Arpa Piemonte Italy

Email: luca.gentile@aslcn1.it

BACKGROUND/OBJECTIVE: The identification of Uranium minerals in the area of Lurisia (Piedmont – Italy) is attributed to Pia Bassi in 1913, a geology student, near a quarry for building materials. That site was made famous in 1918 by the visit of M.me Curie, in search for new radium deposits. Nowadays, the site host courses, conferences and intercomparison exercises for medical doctors and physicists, managers, workers and stakeholders. The aim is to develop a synoptic culture regarding ionizing radiation (radiodiagnostic, radioactivity, radiological emergencies, authorization regime, surveillance and patient radiation protection).

MATERIALS AND METHODS: The curriculum of the courses includes a theoretical part and experimental experiences, along with a symposium and a learning test. The theoretical part changes from year to year and deals with the main technical and regulatory innovations in the field of medical physics and radiation protection; the practical exercise part consists in identifying mineralization, measuring beta and gamma counts, radon concentration and environmental dose and doing comparisons in the Galleria Curie a mine tunnel. At the end there is a discussion and finally a multiple-choices test and the exercise: "calculate your annual absorbed radiation dose". The symposium, usually is an integral part of the course. The teachers regularly change seats at the tables during brunch with the participants so that questions can be asked in a convivial way. The tunnel represents a severe place where it is mandatory to wear PPE as and to follow behaviour rules as there are also mining wells.

RESULTS: In the past editions there were lectures and/or measurements from the Italian and international medical physics eminences like professors M Toossi, A. Chougule, FMilano. The Symposium course in detail has now been held for more than 5 years with two editions per year. An international intercomparison has been organized there during 2014 with a final conference in 2015

CONCLUSION: The measurements and intercomparison under field conditions less controlled (drops, humidity,..) are much more challenging for participants. The events are very appreciated by those who have to attend radiation protection training but do not like traditional education and favor professional human interactions among different roles.

KEYWORDS: radiation protection, education, training, cross-disciplinary,

WOBBLING NATURE OF GAMMA PASSING RATE IN PATIENT SPECIFIC QA AS A FUNCTION OF CALIBRATION FIELD SIZES

P. Sathiyaraj

Department of Radiation Physics, Kidwai Memorial Institute of Oncology, Bengaluru, 560029, Karnataka

Email: sathiarajmedphy@gmail.com

BACKGROUND: Conventionally 10x10 cm² field size was used to calibrate patient specific quality assurance (PSQA) detectors. In reality the IMRT plans are having multiple segments with different field dimensions mostly lesser than 10x10cm². In this study we aimed to demonstrate the influence of calibration field size on gamma passing rate (GPR) in PSQA.

MATERIALS AND METHODS: To analyze the impact of calibration field size on GPR we used two independent detectors PTW OCTAVIUS 4D detectors (4DOCT) and Arc check (Arc check). VMAT plans were done for 26 patients (14 for arc check and 12 for 4DOCT). Plans were delivered by Varian unique machine (with 4DOCT) and Varian true beam (with Arc check). Each plan was delivered with different calibration factors like 4x4, 6x6, 8x8 10x10, 12x12 and 15x15 cm² field sizes. Gamma analysis was performed using 2%2mm , 2%3mm and 3%3mm gamma criteria.

RESULTS: GPR varies for the different calibration factors used. Below 10x10 cm² calibration factors GPR was increasing in good approximation, above 10x10 cm² it was in reducing trend. Both detectors show similar results on GPR for range of calibration factors. The correlation between 4DOCT and Arc check In tighter criteria 2%2mm the R² value was 0.9957, in moderate criteria (2%3mm) the R² value was 0.9868 and for liberal criteria (3%3mm) the R² value was reduced to 0.4226.

CONCLUSION: We demonstrated that the calibration field sizes significantly affect the GPR in PSQA. Since the GPR is not same for all calibration fields size the results of PSQA may not reliable for give calibration field size. We are suggesting that the plan specific calibration may require obtaining accurate results of PSQA.

COMPARISON BETWEEN DEFORMABLE AND RIGID IMAGE REGISTRATION FOR CRANIAL STEREOTACTIC RADIOSURGERY

Venkatesan K, Shyam Bisht, Tamilselvan S, Susovan Banerjee, Deepak Gupta, Dayanithi K, Susan Abraham, Tejinder Kataria

Medanta The Medicity, Sector 38, Gurgaon, Haryana, 122001, India

Email: venkphysics@gmail.com

BACKGROUND: Target delineation is of paramount importance for cranial stereotactic radiosurgery (SRS). Multi-modality imaging is required for identifying the natural extension of the tumor. The image fusion between modalities is crucial for evaluating the target delineation. An accurate image fusion can provide proper tumor assessment which leads to an increase of tumor control probability (TCP) and reduces the normal tissue complication probability (NTCP). Image registration (IR) has been broadly divided into rigid (RIR) and deformable (DIR) based on its morphological parameters. The aim of this study to compare the rigid and deformable image registration accuracy and its dosimetry effect on cranial stereotactic radiosurgery.

MATERIALS AND METHODS: Sixteen patients (10- Benign and 6- brain metastases) who underwent robotic SRS were taken for the study. All the patients were immobilized with thermoplastic cast and computed tomography scan (CT) was performed with 1mm slice thickness. A non-contrast CT (NCCT) followed by a contrast-enhanced CT was carried out. The planning T1 weighted contrast enhanced Magnetic resonance imaging (T1C-MRI) was performed with 1mm slice thickness and images (NCCT, CECT, and T1MRI) were exported to treatment planning system (TPS). For treatment planning, the NCCT was taken as the primary imaging modality and the images were fused with CECT and T1C- MRI using RIR. Once the accuracy of fusion was verified anatomically, the DIR was performed between NCCT and T1C-MRI. During the fusion, the volume of interest (VOI) chosen closer to target region to get proper image fusion in DIR. The target delineation was performed in both the image sets (RIR and DIR) and named as gross tumor volume rigid (GTV_{rigid}) and deformed ($GTV_{deformed}$). SRS dose planning was done based on RIR and DIR target volumes in robotic SRS system using cones (CyberKnife®, Accuray incorporated). The dosimetric parameters were compared between these two plans for all the patients using IBM SPSS®. Consequently, the images and contours sets were exported to 3DSLICER® for comparison of GTV using segment comparison morphology (SCM) module. Using SCM, the Hausdorff distance (HD) and dice similarity metrics (DCM) were evaluated between GTV_{rigid} and $GTV_{deformed}$. The dosimetric parameters like Radiation Therapy Oncology Group and Paddick conformity index (CI_{RTOG} and $CI_{Paddick}$), target coverage and normal brain doses were compared using paired sample students t-test.

RESULTS: In GTV_{rigid} target plan, the mean deviation found in CI_{RTOG} was 24.45 ($P=0.00$) and $CI_{Paddick}$, it was 22.5% ($P=0.00$) when comparing GTV_{rigid} and $GTV_{deformed}$ targets. The mean difference in target was 7.1 % and the mean difference in mean dose to the target was statistically insignificant ($P=0.213$). In $GTV_{deformed}$ plan, the mean deviation CI_{RTOG} was 6% ($P=0.016$) and in $CI_{Paddick}$, it was 16.7% ($P=0.005$). The mean difference in target coverage between these two plans was 13.025 ($P=0.05$). There was no significant ($P=0.348$) deviation found in target in deformed fusion plan. For normal brain dose, the mean difference between rigid and deformed plan was 5.53 % ($P=0.007$) and 17.86% ($P=0.017$) for 1 cc and 10 cc volume respectively. In brainstem, there was no statistically significant deviation. The mean volume was 0.95cc ($SD=0.76cc$) and 0.86cc ($SD=0.72cc$) for RIR and DIR based target delineation respectively. The mean HD between these two-imaging data set was 2.46 mm ($SD=0.92mm$) and in 95% conformity, the mean HD was 1.44mm ($SD=0.49mm$). The mean dice coefficient between these two data sets was 83% ($SD=8\%$) and the true positive value was 18.7%. The false positive and false negative was 2.14 % and 4.89%.

CONCLUSION: Image fusion is an important aspect in SRS/SRT. In our study, the DIR was covered with CECT to account for variation in periphery which is not truly accounted in RIR. The cumulative volume which includes the RIR and DIR along with CECT could provide the target volume which eliminates the missing gross disease

EXPERIMENTAL DETERMINATION OF INTERBEAM QUALITY CONVERSION FACTOR FOR BEAM MATCHED LINEAR ACCELERATORS:

Gowtham Raj D, Sathiyaraj P, Sampath kumar Ganesh Kadirampatti

Department of Radiation Physics, Kidwai Memorial Institute of Oncology, Bengaluru, Karnataka, India.

Email: rajgowtham44@gmail.com

BACKGROUND: In recent times linac based calibration for reference dosimetry is evolving gradually. Leading reference dosimetry protocols such as TRS 398 and AAPM TG51 also suggesting linac based calibration will be more appropriate. In the present study, the utilization of linac based chamber calibration coefficient for the beam matched linacs were performed.

MATERIALS AND METHODS: Our field chamber (FC) FC65-G was cross calibrated against reference chamber (FC65-G) in one of the linac-LA4 (reference beam quality machine), then calibration coefficient has been obtained. Similarly for other linacs named as LA2 and LA3 calibration coefficients were obtained. The cross calibration was performed in slab phantom for field size of 10x10 cm² and SSD=95 cm for the reference beam quality (6 MV x-ray –LA4). Beam quality conversion factors were derived in two methods: 1. Normalized calibration coefficient (NCC) method ($^{LA2}Nd_{w(LA2/LA4)}$, & $^{LA1}Nd_{w(LA1/LA4)}$) and 2. Normalized beam quality conversion (NBQC) method ($K_{QL2,QLA4}$ & $K_{QL1,QLA4}$). In addition, the conventional beam quality conversion factor ($K_{Q,Q0}$) also used to compare the results. The reliability of this method was tested by performing IMRT patient specific QA for 105 patients (n=105). Reference dosimetry was also performed using conventional beam quality conversion factors and linac based conversion factors

RESULTS: Measured dose was compared with TPS and found to be NCC method slightly superior over NBQC and conventional method. The average percentage difference between TPS & measured dose was 0.75% (NBQC), 0.1% (NCC) and 1.06% (conventional) for LA1 machine. Similarly the results were 1.2% (NBQC), 1.02% (NCC) and 1.5% (conventional) for LA2 machine. Reference dosimetry performed and results were 0.75% (conventional), 0.34% (NBQC) and 0.11% (NCC) for LA1 machine. Similarly, the results were 1.5% (conventional) 1.2% (NBQC) and 0.98% (NCC) for LA2 machine.

CONCLUSION: The difference in beam quality conversion factors in three beam matched linacs were appreciable and reflected in IMRT point dose measurements & reference dosimetry. For beam matched linac also there is a considerable variation in beam quality conversion factor even though the chamber calibrated at same user beam quality (6 MV).

MONTE CARLO SIMULATIONS OF ELECTRON INTERACTIONS IN DRY AND HYDRATED DNA

Aouina Nabila Yasmina¹, Zine el Abidine Chaoui^{1,2}

¹Laboratory of Optoelectronic and devices;UFAS1

²Physics department, faculty of sciences, UFAS1

Email: zchaoui@univ-setif.dz

BACKGROUND/OBJECTIVE: electron distribution of energy losses, the most probable energy loss and average energy loss of electrons in living cells are efficiently simulated by Monte Carlo (MC) codes where huge data tables are needed. We modeled the transport of electrons in a 2 nm and 4 nm DNA segments including the influence of water content. The number of water molecules in the DNA molecule varies with environmental conditions in a living cell. To be able to assess the influence of the water content, simulations with 6.28, 8, 12.5 and 20 molecules of water per nucleotide are carried out.

MATERIALS & METHODS: Electron elastic and inelastic cross sections, mean free paths have been calculated in DNA and liquid water using quantum mechanics formalism from 10 eV to 100 KeV. For elastic interactions, partial wave analysis is used for atomic case with scar additivity rule for DNA as macromolecule. Inelastic cross sections are calculated using dielectric formalism by means of full Penn modelling.

RESULTS: Important differences in the electron energy loss distribution, electron average energy loss and most probable electron energy deposited have been found when including the influence of water content in dry DNA.

CONCLUSIONS: We highly recommend to consider hydrated DNA, at least with 20 molecules as layers of hydration, in further studies of interaction of electrons in living cells. The modelling and the cross sections presented in present study can be adopted as a model.

KEYWORDS: Mean free path, cross sections, dry DNA, hydrated DNA, energy loss;

DETERMINATION OF SET-UP ERRORS AND PLANNING TARGET VOLUME (PTV) MARGIN IN CANCER PATIENTS OF HEAD & NECK, BREAST, AND BRAIN

Shraddha Srivastava¹, Shyamprasad S¹, Christopher Varghese¹, Nara Moirangthem Singh²

¹Department of Radiotherapy, King George's Medical University, Lucknow, India

²Department of Radiation Oncology, Dr. Bhubaneswar Borooah Cancer Institute, Guwahati, India

Email: shraddha686@gmail.com

PURPOSE: To investigate the set-up errors and estimate the planning target volume (PTV) margin in cancer patients of head & neck, breast and brain using an electronic portal imaging device (EPID).

MATERIALS AND METHODS: 20 patients of three different cancer sites (head-and-neck, breast and brain) treated with external radiotherapy were retrospectively studied. For each patient, pretreatment anterior-posterior and lateral images were acquired with EPID. Reference images from Xio TPS (Elekta) were compared with the portal images. Set-up error corrections were made before treatment for the translational set-up error greater than 3 mm. Mean displacements (MDs), population systematic (Σ) and random errors (σ) were calculated. PTV margins were calculated using International Commission on Radiation Units and Measurements (ICRU) Report 62, Stroom's and van Herk's formulae.

RESULTS: MDs for head and neck patients were 1.2mm, 1.9mm and 1.8mm; for breast, MDs were 1.6mm, 1.3mm and 2.4mm; for brain, MDs were 1.4mm, 1.9mm and 1.3mm, in x, y and z directions respectively. In head and neck patients, $\Sigma \pm \sigma$ was 1.5 \pm 1.4mm, 2.3 \pm 2.2mm and 1.8 \pm 1.7mm; in breast, $\Sigma \pm \sigma$ was 2.0 \pm 2.0mm, 1.7 \pm 1.7mm and 1.5 \pm 1.4mm; in brain, $\Sigma \pm \sigma$ was 1.3 \pm 1.4mm, 1.3 \pm 1.4mm and 1.6 \pm 1.7mm in x, y and z directions respectively.

For head and neck, PTV margins using ICRU 62, were 2.1mm, 3.2mm and 2.5mm in x, y and z directions, respectively; with Stroom's formula and van Herk's formulae margins were 4.0mm, 6.1mm and 4.8mm and 4.7mm, 7.2mm and 5.7 mm in x, y and z directions, respectively. For breast, PTV margins calculated from ICRU 62 formula were 2.8mm, 2.4mm and 2.0mm, while from Stroom's and van Herk's formulae, were 5.4mm, 4.6mm, 4.0mm and 6.4mm, 5.4mm and 4.7mm in x, y and z directions, respectively. For brain, ICRU 62 calculated margins were 1.8mm, 1.8mm, and 2.2mm while from Stroom's and van Herk's formulae were 3.5mm, 3.5mm, 4.4 mm and 4.2mm, 4.2mm and 5.1mm in x, y and z directions, respectively.

CONCLUSION: The set-up error was less than 5mm in all directions for all three sites. Set-up error impacts the PTV margin. Therefore, it should be considered before using a published margin recipe.

KEYWORDS: Portal imaging, set-up error, radiotherapy, head and neck cancer

UNCERTAINTY ANALYSIS AND ITS IMPACT ON DVH ANALYSIS FOR MULTIPLE BRAIN-METASTASIS CASES

Priyanka Agarwal, Ninad Patil, Swapna Gayen, Vishal Gangwar, Ashutosh Mukherji, Satyajit Pradhan.

Department of Radiation Oncology, Homi Bhabha Cancer Hospital, (Tata Memorial Center), Varanasi, India.

Email: pr.agarwaljan@gmail.com

BACKGROUND/OBJECTIVE: Stereotactic radiation therapy of multiple brain meta-stasis(BM) presents complexity in treatment planning as well as in dose delivery. Even 1mm uncertainty in dose delivery may generate large deviations in dose-volume histogram(DVH) of PTV. In this study, we propose to incorporate uncertainty analysis on DVH calculations for multiple BM cases.

MATERIALS & METHODS: A total of five multiple BM patients were chosen, randomly. Stereotactic volumetric modulated arc therapy plan of patients was generated using Varian Eclipse TPS, v15.5, with 6XFFF photon energy by two techniques, mono-isocentric (Plan_A) and multi-isocentric (Plan_B). Planning was performed for Truebeam-STX with HD-MLC with a total dose prescription of 30 Gy at 5 Gy per fraction. To evaluate the impact of uncertainty on DVH, the first plan was considered as baseline for each patient and technique. An uncertainty of ± 1 mm was incorporated in $\pm X$, $\pm Y$, and $\pm Z$ directions and compared w.r.t. base plan. In total, 70 plans were evaluated for both techniques. The DVH analysis was performed by two ways: for Plan_A (which is combination of multiple PTV), each separated PTV was evaluated and compared with original PTV and for Plan_B, total PTV analysis was done. DVH and statistical analysis was performed by R software (ver4.3.1).

RESULTS: Compared to base plans, mean PTV coverage ($p < 0.05$) was reduced by 0.96% for Plan_A and 0.95% for Plan_B. Maximum dose (Dmax) variation was not observed for Plan_A. However, the average Dmax ($p < 0.05$) was increased 1.01 times compared to base plan for Plan_B. These are average quantitative parameters in all six directions. The uncertainty DVH for PTV has been presented in Fig1 for Plan_A and Plan_B.

CONCLUSION: The effects of intra-fractional motions and residual errors could have highly undesirable effects on the DVH of PTV for both planning techniques. By incorporating an uncertainty analysis in the DVH calculation, the resultant changes in the DVHs will help physicians to make better informed decisions in plan selection or margin adjustment to reduce the likelihood of geographical miss of PTV.

KEYWORDS: Uncertainty analysis, PTV uncertainty, multiple brain-metastasis dosimetry

EXPERIMENTAL EDUCATION PROGRAM TO OBTAIN ADEQUATE RELATION BETWEEN DOSE AND IMAGE QUALITY IN CHEST TOMOGRAPHY

Renato Dimenstein¹, Claudia Maria de Figueiredo², Gabriel Lubke Gaviraghi³, Lisa Suzuki²

¹ Medical Physicist RAD, ² Radiologists Fleury Group, ³ Undergraduate Physicist RAD

Email: renato.dimenstein@gmail.com

BACKGROUND/OBJECTIVE: The challenges in tomography are related to select the acquisition protocols to obtain the satisfactory image quality and low dose. However, the paradigm image quality with low dose it is not easy to archive. These inconsistencies were partly related to technological diversity and heterogeneity in the qualification of operators. To minimize these differences, a continuing education program was carried out. The purpose of the training was to enable operators to identify the factors that affect the quality and dose of radiation. In this way, it would be possible for operators to expand the potential use of the technological resources made available by the different manufacturers of tomography equipment.

MATERIALS AND METHODS: To support the training, simulations were performed with an anthropomorphic adult phantom (CIRS mod Atom), so as not to irradiate the patients. The phantom simulations were performed with different scanners (GE Revolution Evo, Philips Brilliance and Siemens Somatom Edge). Image chest acquisitions were obtained by selecting different technical parameters, table positions, modulators, and reconstruction algorithms. After the acquisition of the simulations, the analysis of image quality and radiation dose values was performed, by the operators.

RESULTS: The application of experimental models in the education process contributed to the development of knowledge and skills of professionals, in obtaining low doses of radiation in exams. The practical methodology with phantom allowed to the operators associate the physical aspects of image acquisition and the impact of the patients' doses.



CONCLUSIONS: The transformation of knowledge in establishment of skills is a continuous task, due to the diversity of equipment and rapid technological evolution, according to ethical principles as ALARA. The practical approach allowed to harmonize the knowledge of the professionals regarding the equipment of different manufacturers so, in the end, the relation between dose and image can maintaining.

KEYWORDS: chest tomography, image quality, radiation dose.

SAFETY REVIEW AND PERFORMANCE EVALUATION OF INDIGENOUSLY MANUFACTURED SIDDHARTHA-II ICONIC MEDICAL ACCELERATOR

Rajib Lochan Sha, Smriti Sharma, P.K. Dixit, G. Sahani, P.K. Dash Sharma

Radiological Safety Division, Atomic Energy Regulatory Board, Mumbai

Email: rajibsha@gmail.com

BACKGROUND/OBJECTIVE: Atomic Energy Regulatory Board (AERB), Mumbai carries out the safety review and type approval test to ensure the performance of any new model of medical accelerators before its clinical use in India. During safety review, all relevant standards, customer acceptance protocol (CAP) provided by vendor and AERB acceptance test criteria/QA protocol are referred. With rapid advancements in technology aimed at faster & accurate treatment delivery, new features are regularly incorporated in medical accelerator units. In some instances, standards/QA protocol are not available for testing the new features for acceptance. In such cases, it is required to arrive at a value which is practical, achievable and in-line with the manufacturer's protocol without compromising the radiological safety. This abstract presents the safety review and acceptance test criteria of several new features of the indigenously manufactured medical accelerator model Siddharth-II Iconic.

MATERIALS AND METHODS: Recently, Panacea Medical Technologies Pvt. Ltd., India approached AERB for obtaining the requisite regulatory clearances of Siddharth-II Iconic unit. AERB has carried out the safety review of documents pertaining to performance of the Siddharth-II Iconic unit and its type approval testing. The major difference that were observed compared to the other approved models of medical accelerator are (i) dual flattening filters for same 6MV energy (one is useful for field size maximum up to 16cmx16cm and other is useful for maximum field size up to 30cmx30cm) (ii) mobile app based hand pendent to control the movement of unit (iii) patient positioning by laser alignment (iv) field size defined by MLC only (v) absence of optical field light & optical distance indicators (ODI), (vii) restricted field size (maximum 30 cm x30 cm) etc. As no ODI was available, the SSD for the radiation field analyzer (RFA) was set using the laser alignment and kV imaging. The complete acceptance tests using AERB QA protocol were carried out.

RESULT AND DISCUSSION: It was observed that beam quality index and percentage of depth dose (PDD) of both 6MV small filter (6MV SF) and 6MV large filter (6MV LF) exceeds the limit prescribed by relevant standards and AERB QA protocol. These differences are due to use of dual flattening filters which have specific design in order to use the limited beam current to achieve adequate dose rate. As standard values are not available for beam quality index and PDD for 6 MV SF and 6MV LF, those measured values were accepted after judicious discussion in-line with the manufacturer's protocol. Due to absent of optical field light, imaging for each patient is compulsory prior to treatment delivery. In order to avoid unlikely situation of use of mobile app based hand pendent, it has been interlocked for operation only inside the treatment room.

CONCLUSION: Safety review of the radiotherapy equipment is essential in order to ensure the safety in radiotherapy. It is essential to ensure that advanced features available with the radiotherapy units are checked and accepted as per the applicable protocols and standards. New features of the Siddharth-II Iconic unit were tested as per applicable standards and manufacturers protocols were found acceptable. However, being developed by the manufacturer first time, consistency of the performance of the equipment needs to be verified.

KEYWORDS: medical accelerator, quality assurance, dosimetry, radiation safety

STUDY ON THE CHARACTERISTICS OF ^{60}Co SOURCE STRENGTH MEASUREMENT USING A WELL-TYPE DOSIMETER.

Shinji Kawamura¹, Natsuki Sakamoto², Tooru Kojima³, Mikio Nemoto²

¹Division of Radiological Sciences, Graduate School of Health Sciences, Teikyo University, ²Department of Radiation Oncology, Jichi Medical University Hospital Shimotsuke-shi, Tochigi-ken, Japan, ³Department of Radiation Oncology, Saitama prefectural hospital, Saitama, Japan

Email: kawamura@fmt.teikyo-u.ac.jp

BACKGROUND/OBJECTIVE: Measurements for ^{60}Co sources in medical facilities have traditionally been conducted using farmer-type dosimeters and solid phantoms. However, this method has been known to present measurement issues, such as the requirement for a cobalt calibration constant (N_c). In 2022, the Japan Radio Isotope Association (JRIA) introduced a calibration service for well-type dosimeters used in ^{60}Co source measurements. This study aims to evaluate source strength measurements using well-type dosimeters at three facilities and compare their characteristics with those of conventional farmer-type dosimeters.

MATERIALS AND METHODS: We conducted source strength measurements using a well-type dosimeter (SOURCE CHECK 4Pi) at three facilities equipped with ^{60}Co sources (GK60M21, Co0.A86). The results of the reference air kerma rate obtained from this measurement were compared with those obtained using farmer-type dosimeters and solid phantoms in other facilities, as well as with the source certificates provided by the source suppliers. Monte Carlo simulations (Phits) were adapted to evaluate the source location and sensitivity characteristics of the well-type dosimeter in comparison with those of the ^{60}Co (Co0.A86) and ^{192}Ir (v2r) sources.

RESULTS: The differences in the reference air kerma rates between the farmer-type dosimeter and the source certificate for this measurement method were $1.4\pm 0.9\%$ and $1.6\pm 0.4\%$, respectively. Measurements with well-type dosimeters were found to offer advantages such as a larger ionization volume and the ability to directly assess ionization values. Monte Carlo simulation results revealed that the maximum sensitivity point of the ^{60}Co source was 4.78 cm from the bottom of the ionization volume, which is equivalent to that of ^{192}Ir . The absorbed dose in the ionization volume of the ^{60}Co source was 1.99 times higher than that of ^{192}Ir .

CONCLUSIONS: The characteristics of the ^{60}Co source strength measurement using a well-type dosimeter were evaluated, and the advantages of this method were confirmed.

KEYWORDS: ^{60}Co source, well-type dosimeter, source strength, reference air kerma rate

RENEWABLE ENERGY PRODUCE FROM SCATTER RADIATION THROUGH ACTIVATED CARBON

P. Venkatraman¹, Lalit M Aggarwal²

¹Department of Medical Physics, Bharathidasan University, Trichy, Tamil Nadu, India.

²Department of Radiotherapy & Radiation Medicine, Institute of Medical Sciences, Banaras Hindu University, Varanasi (UP), India

Email: venkat00108@gmail.com

INTRODUCTION: Activated carbon from jujube hull is refined by physical method using imported jujube hull as raw material. It has the characteristics of good wear resistance, high adsorbent and long service time. This method is based on the analysis of electro chemical method. It has excellent effect on the manufacture of pure water and high purity water. It is an ideal material for thermoelectric, beer, beverage and high purity water equipment. Activated carbon from jujube hull is a porous carbon-containing material with highly developed pore structure and excellent adsorbent. The adsorptive area of activated carbon from jujube hull is more than eight tennis fields per gram. Its adsorptive effect is achieved by physical adsorptive force and chemical adsorptive force. In addition to carbon, its constituents contain a small amount of hydrogen, nitrogen, oxygen and ash. The structure is formed by the accumulation of hexacycles formed by carbon. Due to the irregular arrangement of hexacyclic carbon, the characteristics of multi-microporous volume and high surface area of jujube hull activated carbon are caused. It is irradiated in the LINAC at 6MV energy for 100 MU.

PURPOSE: By studying the biocompatibility and adsorption characteristics of the activated carbon from coconut shell nut it can be used as a radiation sensor.

MATERIALS AND METHODS: Activated carbon coconut shell nut is an appropriate radiation shielding material due to its biocompatibility and adsorption characteristics. That the material is irradiated in 6 MV LINAC with 100 monitor units, The influence of gamma radiation as a sterilization process on the adsorption and mechanical properties of activated carbon coconut shell nut was investigated. The specific surface area, micropore volume, pore size distribution, surface chemistry as well as the breaking load of activated carbon coconut shell nut before and after gamma radiation were examined. The quantity absorbing property of coconut shell nut is $670 \text{ cm}^3/\text{g}$. Characterization by nitrogen adsorption showed that the activated carbon coconut shell nut was a microporous material with a high specific surface area and micropores smaller than 1 nm. Gamma radiation decreased the specific surface area and micropore volume but increased the pore width. The sterilization process changed the surface chemistry quantitatively, but not qualitatively. In addition, the breaking load decreased but without any influence considering the further application of this material.

RESULTS AND DISCUSSION: It is irradiated in 6MV LINAC photon beam at 100 monitor units. By the charge collecting characteristics of the quantity of activated carbon coconut shell nut is $670 \text{ cm}^3/\text{g}$, so it can collect more no. of positive ions and it can be used as a radiation sensor material. This property is considered to be used as a radiation sensor.

CONCLUSION: Based on the Analysis of Electrochemical method, X-ray diffraction and Raman spectral studies also by surface functional groups, surface morphology, pore diameter and specific surface area have been identified through FT-IR, SEM and N₂ Adsorption/ desorption isotherm methods properties of activated carbon is studied. According to this study, the material is perfectly suitable for radiation sensor properties.

KEYWORDS: Activated carbon, N₂ Adsorption/desorption, LINAC, FT-IR, SEM.

MECHANICAL AND DOSIMETRIC VALIDATION OF BRASS BLOCK AND STATIC APERTURES USED IN PENCIL BEAM SCANNING PROTON THERAPY

Kantaram Darekar^{1,2,3}, Umesh Gayake^{1,2,3}, Lalit Chaudhari¹, Siddhartha Laskar¹, S. D. Dhole⁴, Bhushankumar J. Patil³.

¹Department of Radiation Oncology, Advanced Centre for Treatment, Research, and Education in Cancer, Tata Memorial Centre, Navi Mumbai, India.

²Homi Bhabha National Institute, Mumbai, India.

³Department of Physics, Abasaheb Garware College, Pune, India.

⁴Department of Physics, Savitribai Phule Pune University, Pune, India.

Email: kantaramdarekar@gmail.com

BACKGROUND/OBJECTIVES: Achieving sharper lateral penumbra in pencil beam scanning (PBS) proton therapy is challenging due to the properties of proton beams. Metallic apertures of high atomic number materials, such as brass blocks, can be utilized to achieve sharper penumbra. So, it is important to perform its mechanical and dosimetric properties checks before clinical use. This study aims to validate some of the mechanical and dosimetric properties of brass blocks and static apertures used in the PBS proton therapy.

MATERIALS AND METHODS: The standard block and static aperture used in this study are of the dimension 4 cm thick, an outer diameter of 180 mm, and an aperture opening diameter of 6.35 mm. This can be used with a dedicated PBS scanning nozzle (Proteus Plus 235, IBA, Belgium). The water equivalent thickness (WET) of the brass block was measured using proton beam energies 226, 190, 185, and 180 MeV along the beam central axis. Measurements were conducted using Giraffe Multi-Layer Ionization Chamber (MLIC) with 180 large area plane-parallel ionization chambers and OmniPRO Incline Analysis Software (IBA Dosimetry, Germany). The Lynx 2D scintillation detector (Fimel, Paris, France) and MyQA analysis software (IBA Dosimetry, Germany) was used for the radiation isocentre accuracy verification for 100 MeV proton beam at 0°, 90° and 270° gantry angles and three different snout positions ranging from 5 to 30 cm air gap.

RESULTS: The measured WET of the brass block was 22.72, 22.52, and 22.41 gm/cm² for 226, 190, and 185 MeV proton beam energies, respectively, with average WET is 22.55 gm/cm². The brass block aperture can be utilized for clinical proton beams up to the 20 gm/cm² range considering enough safety margin after the practical range. The maximum deviation in isocenter accuracy for snout movement with the brass aperture along the beam axis up to 30 cm was 0.9 mm, which is within the allowed tolerance of 1 mm.

CONCLUSION: The mechanical and dosimetric validation of brass block and static apertures was performed. This aperture may be used clinically upon further thorough validations for beam data commissioning and TPS dose calculations as per the standard recommendations.

KEYWORDS: pencil beam scanning proton therapy, water equivalent thickness, static apertures, brass block

GREEN SYNTHESIS AND EVALUATION OF HYPERICIN FROM HYPERICUM PERFORATUM AS AN PHOTOSENSITIZING AGENT FOR PHOTODYNAMIC THERAPY

Monosha Priyadarshini¹, Kanishka S², Vidhya S², Arunai Nambi Raj N¹

¹Department of Physics, School of Advanced Sciences, Vellore Institute of Technology (VIT) Vellore, India, ²Department of Sensor and Biomedical Technology, School of Electronics Engineering, Vellore Institute of Technology (VIT), Vellore, India.

Email: monoshapradhan@gmail.com

BACKGROUND/OBJECTIVE: Anthraquinone derivative naphthodianthrone, also known as hypericin, is a naturally occurring photosensitizer that has received a lot of interest recently owing to its possible application in photodynamic therapy for the treatment of cancer. In herbal therapy, hypericin has also been utilised for centuries due to its antiviral and antidepressive effects. Photodynamic therapy is a non-invasive treatment that employs a particular drug known as a photosensitizing agent, as well as light as an activator, to treat skin infections, bacterial, fungal infections and also cancer. Traditional techniques of hypericin production, on the other hand, necessitate the use of toxic solvents and chemicals that are hazardous to the environment and human health. To circumvent these constraints, researchers have increasingly concentrated on creating green synthesis techniques for hypericin. In this article, we isolated and evaluated hypericin, a key photosensitizer, from leaves of a natural source, *Hypericum perforatum*.

MATERIALS AND METHODS: In our current effort, we used *Hypericum perforatum* (St. John's-wort), ultrasonicator, centrifuge, and column chromatography to extract hypericin, a green synthesis technique to employ chemicals and solvents with little environmental effect, hence enhancing process safety.

RESULTS: NMR, HPTLC confirmed the formation of hypericin. UV results showed the corresponding wavelength to which the drug would respond. The depletion of 1,2-Dibenzoylbenzene (DPBF) was tracked using UV-Vis spectral shifts. There were no changes in Q band intensities during the singlet oxygen quantum yield determinations, demonstrating that complexes are not destroyed during singlet oxygen generation. The cell viability and anti-microbial results also showed positive results.

CONCLUSIONS: The test results indicate that the hypericin is a prominent photosensitizer for photodynamic therapy.

KEYWORDS: hypericin, photodynamic therapy, singlet oxygen, anti-microbial.

POINT DOSE-BASED PATIENT SPECIFIC QUALITY ASSURANCE WITH INDIGENOUS THORAX PHANTOM

Putha Suman Kumar¹, Challapalli Srinivas², Dilson Lobo², Ruthra T¹, Dakshna Moorthy¹, Thara M Nair¹

¹Department of Radiation Oncology, MGM Cancer Institute, Chennai India, ²Department of Radiation Oncology, Kasturba Medical College Hospital, Attavar, Mangalore, India.

Email: radiationsafetyofficer@mgmcanerinsitute.in

BACKGROUND: The patient specific quality assurance (QA) is the significant tool to ensure the advanced dose delivery techniques such as IMRT, VMAT etc. though the machine QA is being performed routinely. Many methods are available to warrant the planned dose delivery to the patient viz. MU calculation, point dose, film dosimetry, fluence measurements etc. However, ionization chamber point dose measurements are considered to be one of the standard parameter in patient specific QA.

MATERIALS AND METHODS: An in-house developed anthropomorphic phantom was used to carry out this the point dose measurements in this study. 10 cases of right post mastectomy were selected for the patient specific QA measurements. The selected cases were planned with IMRT or VMAT techniques. All treatment plans were generated by means of Monte Carlo algorithm available in Monaco (Make: Elekta Solutions, AB, Version: 6.00.01) treatment planning system. The planned doses were delivered on the phantom, whereas a miniature ionization chamber (Make: PTW Dosimetry, Germany. Model: Semiflex 3D) was in place as a detector.

RESULTS: Positively the point doses deviation among the calculated and measured was varied from 0.04% to 3.46%. The average and standard deviation were confirmed as 1.244 and 1.463 respectively.

CONCLUSIONS: The point dose measurement based patient specific QA could serve as a basic evidence in case of unavailability of array detectors or film dosimetry. Utilizing anthropomorphic phantom could be an added advantage since the inhomogeneous structures are present.

KEYWORDS: patient specific QA, point dose, IMRT

PREDICTION AND CORRELATION OF GAMMA PASSING RATES WITH COMPLEXITY METRICS USING MACHINE LEARNING TECHNIQUES FOR INTENSITY-MODULATED RADIATION THERAPY

Dinesh Kumar Saroj^{1,3}; Suresh Yadav²; Neetu Paliwal³; Ravindra Shende¹; Subhas Haldar⁴; Gaurav Gupta¹

¹Department of Radiotherapy, BALCO Medical Center, A Unit of Vedanta Medical Research Foundation, New Raipur, Chhattisgarh, India, ²Department of Radiotherapy, Gandhi Medical College, Bhopal, India, ³Department of Physics, Rabindranath Tagore University, Raisen, Madhya Pradesh, India, ⁴Department of Radiotherapy, Saroj Gupta Cancer Centre and Research Institute, Kolkata, India

Email: dinesh.saroj@ymail.com

BACKGROUND/OBJECTIVE: Intensity-modulated Radiation Therapy (IMRT) allows for more precise dose painting of tumor target, however, it can lead to increased beam modulation, longer treatment times and higher dosimetric uncertainty. As a crucial step in modern radiation therapy, patient-specific quality assurance (PSQA) aims to ensure treatment accuracy and safety by identifying any discrepancies between planned and delivered radiation fluence. Variability in PSQA results can contribute to differences in measured or calculated dose distributions. Complexity metrics are essential in characterizing IMRT plans based on various factors like fluence, MLC positions and aperture shape providing valuable insights into treatment plan complexity and modulation. Excessive complexity in IMRT plans can increase dose uncertainty, prolong treatment times, and raise susceptibility to changes in patient or target geometry. This study aims to identify best regression model to predict the gamma passing rates (GPR) for IMRT treatment plan and find its correlation with various treatment plan complexity metrics.

MATERIALS & METHODS: We have selected 30 patients of Head & Neck Cancer, treated with 6MV photon beam with IMRT technique for retrospective study. Five machine learning models were explored to identify the best performing regression model for predicting GPR. Predictor used in these models consist of monitor units (MU), controls points (CPs), beam area (BA), and modulation complexity score (MCS). Model performance was evaluated in terms of Mean Squared Error (MSE), Root Mean squared Error (RMSE), and R2 score.

RESULTS: Gamma index analysis was performed using portal dosimetry with 3% and 3mm and 10% threshold criteria. Linear regression model has MSE of 0.689 % and R2 of 0.88, Ridge regression has an MSE of 1.70% and R2 of 0.71, Decision Tree regression has MSE of 2.41% and R2 of 0.58, Random Forest regression has MSE of 1.54% and R2 of 0.74. XGBoost regression has an MSE of 1.31% and R2 of 0.77. MCS shows a strong positive correlation with MU (65%) and CPs (79%).

CONCLUSION: Using complexity metrics, linear regression shows the best fit to predict the GPR of portal dosimetry. This model can potentially be applied to predict the GPR before performing the PSQA.

KEYWORDS: Intensity-modulated Radiation Therapy, Complexity Metrics, Machine Learning, Gamma Passing Rate, Patient-specific Quality Assurance

PLANNING AND DESIGNING OF STRUCTURAL SHIELDING LAYOUT OF TELETHERAPY ROOM TO HOUSE A HIGH ENERGY LINEAR ACCELERATOR- OUR EXPERIENCE:

N. Balasubramanian, Ashok Chauhan, Rajeev Atri, Rakesh Dhankhar, Narayan P Patel, Sunder Singh, Diptajit Paul.

Department of Radiation Oncology, PGIMS, Rohtak, India

Email: baluwda@yahoo.com

INTRODUCTION: Cancer incidence in India is steadily increasing. While planning radiation installation, it is important to ensure the radiation safety of Radiation worker and general public. Structural shielding thickness of primary, secondary barriers for a 15 MV medical linear accelerator (Linac) are calculated as reported in the National Council on Radiation Protection (NCRP) Report No. 151, Atomic Energy Regulatory Board (AERB) Safety code and International Atomic Energy Agency (IAEA) SRS No.47.

OBJECTIVE: The aim of this study is designing structural shielding layout plan to house a High Energy Linear Accelerator.

MATERIALS AND METHODS: A committee has been framed as per IAEA SRS No.47 to set up a Linear Accelerator treatment facility to cancer patients. The Memorandum of Understanding (MoU) has been signed by HLL Infra Tech Services Limited (HITES) and Institutional authority for the construction of Linear Accelerator Complex. Site selection is free from all encumbrances and building layout plan has been prepared as per AERB requirements incorporating structural shielding thickness suggested by physicist. The figure 1 shows the layout plan of radiotherapy Linac bunker, cross sectional drawings with shielding thickness. The shielding thickness of primary, secondary barrier, maze thickness has been calculated using empirical formulae after duly considering all parameters, which includes workload (W), use factor (U), occupancy factor (T), distance from the X-ray target (d), and permissible dose limit (P) as prescribed by the competent authority of India. The design goal limit is 400 μ Sv/week and 20 μ Sv/week for radiation workers and general public, respectively.

RESULTS AND DISCUSSION: The shielding thickness calculated was in line with various investigators. The final site and layout drawings are prepared as per the guidelines stated in the e-Licensing of Radiation Applications System (eLORA) and submitted. After scrutiny, the layout plan has been approved by competent authority of India.

CONCLUSION: From this study, the layout plan has adequate shielding thickness to ensure radiation safety of staff and public. The dose levels in and around the Linac bunker is well within the dose limit recommended by competent authority. It is safe to install a High Energy Accelerator in the premises.

KEYWORDS: Linear Accelerator, bunker, Radiation protection, concrete shielding

COMPARATIVE ANALYSIS OF FOUR DIFFERENT HYBRID VOLUMETRIC MODULATED ARC THERAPY WITH RAPID ARC (H-ARC) TECHNIQUES FOR ESOPHAGEAL CANCER PATIENT: A TREATMENT PLANNING STUDY

¹Deepali Patil, ¹Mukesh Kumar Zope, ²Dinesh Saroj, ¹Dinesh Sinha, Seema Devi, ¹Swati P

¹Department of Medical Physics, State Cancer Institute, Indira Gandhi Institute Of Medical Sciences, Patna, Bihar, ²Department of Radiation oncology. Balco Medical Center, New Raipur Chhatishgarh, India

Email:mpdeepali23@gmail.com

PURPOSE::The purpose of this study was to identify the most suitable planning techniques and dose weighting for hybrid volumetric modulated arc therapy with Rapid arc (H-Arc) in patients with esophageal cancer.

MATERIALS/METHODS::Fourteen patients with esophageal cancer, who had previously received radiotherapy using Rapid Arc (RA) techniques at our department, were included in the study. Retrospective analysis was performed, and four different radiation treatment plans were designed for each patient. These plans combined two different conformal fields techniques with two different dose proportions of 3DCRT and Rapid Arc plans, including: H-Arc1 (33% AP-PA conformal/67%Arc), H-Arc-2 (33% AP, RPO, LPO conformal/67% Arc), H-Arc 3 (60% AP-PA conformal/40% Arc), H-arc 4 (60% AP, RPO, LPO conformal/40% Arc), The prescription dose for all plans was 50.4 Gy/ 28# delivering using a 6 MV flattening filter beam. Planning Target Volume and Organ at Risk was evaluated using Dose Volume histogram.

RESULT::The study found no statistically significant difference among the four techniques regarding the Planning Target Volume doses of Dmax, D95% (dose received by 95% of the target volume), conformity index, and homogeneity index. However, a significant difference was observed in the Monitor Unit of three techniques, except for H-Arc 1 (P-value 0.358). Regarding Lung mean dose and V20Gy (volume receiving 20 Gy), H-Arc-3 plan showed slightly lower values (14.5±3.97, 21.09±9.02) compared to the other three H-Arc plans. No statistically significant difference was observed between H-Arc 2 and H-Arc 4 plans (p-value 0.358, p-value 0.217) observed in both lung mean and V20Gy. Additionally, no statistically significant difference in Heart mean doses was found among H-Arc 1 and H-Arc 2, H-Arc 3 and H-Arc 4 plans (p-value 0.462, p-value 0.542). However, a statistically significant difference in Dmax of the spinal cord was observed only for H-Arc 1 (p-value 0.024).

CONCLUSION::The hybrid H-Arc technique can be applied effectively in the treatment of esophageal cancer patients, with slightly different outcomes depending on the specific combination of conformal fields and dose proportions used. The H-Arc techniques offer viable option for the treatment of esophageal cancer providing potential benefits in dose delivery to the lung and spinal cord.

KEYWORDS:Esophageal cancer, Hybrid Volumetric modulated arc therapy with Rapid Arc and Conformal therapy.

DOSIMETRIC EVALUATION OF NON-COPLANAR VERSUS COPLANAR VOLUMETRIC MODULATED ARC THERAPY WITH RAPID ARC TECHNIQUE FOR ESOPHAGEAL CANCER PATIENTS

Deepali Patil¹, Mukesh Kumar Zope¹, Swati P¹, Dinesh Sinha¹, Seema Devi¹, Dinesh Saroj², Rajesh Singh¹

¹Department of Medical Physics, State Cancer Institute, Indira Gandhi Institute Of Medical Sciences, Patna, Bihar, ²Department of Radiation oncology. Balco Medical Center, New Raipur Chhatishgarh, India

Email: mpdeepali23@gmail.com

PURPOSE/OBJECTIVE: The purpose of this study was to compare the dosimetric variations between two radiotherapy techniques, optimized non-coplanar (ncRapid Arc) beams, and coplanar (cRapid Arc) beams using volumetric modulated arc therapy in esophageal cancer patients.

MATERIALS AND METHODS: Fourteen patients with esophageal cancer who had previously received radiotherapy using cRapid Arc (RA) techniques at our department were included in this retrospective study. Each patient's treatment plan was recalculated and optimized using ncRapid Arc plans, with a prescription dose of 50.4Gy delivered in 28 fractions. Dose volume histograms were used to analyze and compare treatment plans based on the Planning Target Volume (PTV), Conformity Index (CI), Homogeneity Index (HI), Conformation number (CN), doses to the organs at risk (OARs), and monitor units (MU).

RESULTS: There was no statistically significant difference observed PTV doses of Dmax (54.2Gy, 54.79Gy, p Value 0.182); D95% (dose received by 95% target volume) (96.58%, 96.28%, p value 0.245), HI (0.082, 0.087, p value 0.118), CI (0.979, 0.976, p value 0.454), CN (0.857, 0.921, p value 0.335) among cRA and ncRA treatment plans. However, ncRA plans were observed significantly lower both lung mean doses, V5Gy (volume receiving 5Gy), and V20Gy (volume receiving 20Gy) compared to cRA plans (p Values of 0.004, 0.028, and 0.015, respectively). The mean lung doses were 16.14Gy and 15.24Gy, the V5Gy doses were 89.15% and 86.76%, and the V20Gy doses were 25.51% and 23.75% for cRA and ncRA plans, respectively. There were no statistically significant differences in heart mean doses (p Value 0.863), V30Gy doses (p Value 0.447), and spinal cord maximum doses (p Value 0.171) between cRA and ncRA plans. Additionally, no significant difference in monitor units (MU) was observed between cRA and ncRA plans (517.47, 566.0 respectively (p Value 0.078)).

CONCLUSION: In the treatment of esophageal cancer, ncRapid Arc plans demonstrated dosimetric advantages over cRapid Arc plans, particularly in reducing lung doses while maintaining comparable target coverage and sparing other critical organs at risk.

KEYWORDS: Esophageal cancer, Non coplanar, Volumetric modulated arc therapy with Rapid Arc

EXPLORING THE APPROPRIATENESS OF CONVENTIONAL AND UNCONVENTIONAL METHODS OF SETUP MARGIN ESTIMATION IN EXTERNAL BEAM RADIOTHERAPY

Kalyan Mondal^{1,2}, Muskaan¹, Himanshu Mishra¹, Suresh Yadav³, Anuj Vijay², Ritusha Mishra¹, Lalit Mohan Aggarwal¹, Shajid Syed Mohamed¹, Navin Singh⁴, Abhijit Mandal¹

¹Department of Radiotherapy and Radiation Medicine, Institute of Medical Sciences, Varanasi, India,

²Department of Physics, GLA University, Mathura, Uttar Pradesh, India, ³Department of Radiation Oncology, Gandhi Medical College, Bhopal, Madhya Pradesh, India, ⁴Department of Radiotherapy, King George Medical University, Lucknow, Uttar Pradesh, India

Email: kmphysics123@gmail.com

BACKGROUND/OBJECTIVE: Setup margin (SM) in radiotherapy is important as it may influence the treatment outcome. Setup errors or margins estimated by using various available conventional methods may be overestimated or underestimated if set-up error data is not normally distributed. In that case, an unconventional method that does not depend on the normality condition may be more useful & practical to estimate SM comparatively. Purpose of this study is to evaluate the appropriateness of setup margin estimation using the widely accepted conventional methods and the unconventional method for various treatment sites.

MATERIALS AD METHODS: Population-based setup errors and margins for all translational directions were calculated using the conventional method & margin recipes for a total of eighty patients with cancer in the brain, head & neck (H&N), thorax, and pelvis region. A total of 800 registered electronic portal images acquired for online setup verification were used to analyze the setup uncertainty. Setup errors or setup margins are directly calculated from histograms of daily setup errors by a statistic-geometrical approach as the unconventional method.

RESULTS: Setup data sets were not necessarily normally distributed and setup errors or SMs were underestimated for conventional methods compared to the unconventional method. Estimated SMs by these two types of method approximately differed by 2 mm for brain or H&N, 4 mm for thorax, and 3 mm for pelvis case.

CONCLUSIONS: Unconventional method may be useful & more appropriate when small number of patients considered. However, more rigorous and careful review is needed in comparison to existing conventional methods before implementing them in clinics.

KEYWORDS: Cancer, Setup margin, Electronic portal imaging, Image-guided radiotherapy

A TOOL TO PREVENT GENERATION AND RECURRENCE OF NON-COMPLIANCES IN ELORA SYSTEM OF AERB

Aruna Kaushik¹, Manoj K. Semwal², Maria D'Souza¹

¹Department of PET Imaging, Institute of Nuclear Medicine and Allied Sciences, Delhi, India

²Department of Radiation Oncology, Army Hospital Research and Referral, Delhi, India

Email: kaushik_aruna@rediffmail.com

BACKGROUND/OBJECTIVE: Atomic Energy Regulatory Board (AERB) has automated the regulatory processes associated with the applications of ionizing radiation in India by implementing a state-of-the-art e-Governance system, e-LORA (e-Licensing of Radiation Applications). For any deviation from regulatory requirements, 'Non-compliance'(NC) is raised in e-LORA and the notification is sent to employer/licensee. Similarly, the non-compliances observed during regulatory inspections are also communicated to the institution through e-LORA. These NCs need to be resolved within a defined time period failing which the value of electronic Safety Performance Indicator (eSPI) falls and may invite regulatory sanctions by the competent authority. It is thus imperative on the user to take timely action to prevent generation and recurrence of NCs. Manual maintenance and updating of the data on e-LORA and keeping track of validity of permissions is a challenging task especially in the institutes that possess many equipment. It is, therefore, required that a software be developed that could notify the user before the expiry of the due date of regulatory permission. The objective of the present work was to develop a tool to prevent generation and recurrence of NCs at the user end.

MATERIALS AND METHODS: The data on license, no objection certificates, calibration of instruments, quality assurance tests, safety status reports, operational status, transport permission pertaining to various profiles in the institute was entered as separate worksheets in the excel software. Date of issuance of permission and validity were also entered in the sheets. Report was generated by excel Visual Basic for Applications (VBA) macro programs and the action items were displayed on the dashboard. A provision to notify the user through email from dashboard was made for ensuring timely action before the expiry of validity of permission.

RESULTS: The action items could be pulled on the dashboard from respective sheets and displayed in different colours based on the urgency of the desired action.

CONCLUSIONS: The developed tool would be useful in establishing a mechanism for ensuring regulatory compliance and thus enhancing safety culture by preventing generation and recurrence of NCs.

KEYWORDS: e-LORA, non-compliance, eSPI, dashboard

DOSE EVALUATION OF THE CAREGIVER OF COMPUTED TOMOGRAPHY

Hiroki Ohtani, Akari Hirata, Aimi Ishikawa

Teikyo University, Tokyo, Japan

Email: ohtani@med.teikyo-u.ac.jp

BACKGROUND/OBJECTIVE:X-ray computed tomography is carried out also in emergency care, and a patient to be cared for exists at the time of photography. In this case, although a radiological technologist may care for at an X-ray CT room, the exposure management as a caregiver other than occupation exposure is needed. However, there are few reports of dose evaluation of the caregiver at the time of X-ray CT. The purpose of this research is to perform dose evaluation of a caregiver by the experiment which used the human body phantom.

MATERIALS AND METHODS:X-ray CT equipment is ECLOS by a Hitachi medical company. The human body phantom as a caregiver was installed near the gantry and the photography bed. The fluor glass dosimeter was stuck on the surface of a caregiver phantom. A fluor glass dosimeter is Dose Ace GD-301 by an Asahi techno glass company. Measurement parts are a crystalline lens, fingers, a chest, and a genital gland. Head X-ray CT and body part X-ray CT were performed using the human body phantom as a patient.

RESULTS: A caregiver's position is 1 m from the center of CT gantry. The biggest value at body CT is 43 mGy. This is because those fingers of caregiver are in a gantry. The dose of chest and gonad are larger than the eye lens. Because of position to gantry, Chest and gonad is near center of gantry and eye lens is far of gantry. About Head CT, it was a single scan, and since Body CT was a helical scan, in the dose, a helical scan became high.

CONCLUSIONS: The caregiver's dose in X-ray CT was calculated in the human body phantom experiment. The dose changed with parts of a caregiver's body and the position at the time of care and the influence of a way to support were great. Moreover, it was suggested by devising the method of protecting to each part that a dose decreases.

KEYWORDS:caregiver dose, X ray CT, glass dosimeter

DOSIMETRIC COMPARISON OF ICR AND ISBT FOR CA CERVIX CASES USING VAGINAL CONSTRAINTS

Juliyet K Joy¹, Srinidhi Chandraguthi²

¹Maniapal Academy of Higher Education, Manipal College of Health Professions, Manipal, Karnataka, India,

²Department of Radiotherapy & Oncology, Kasturba Medical College, Karnataka, India,

Email: juliyetmaryjoy@gmail.com

BACKGROUND/OBJECTIVE: Vaginal toxicity is a major problem following radiation therapy for cervical cancer. At present, the vagina is not considered an organ at risk (OAR) for ca cervix. The vaginal dose of ca cervix cases treated with EBRT (external beam radiotherapy) followed by ICR (intracavitary brachytherapy) or ISBT (interstitial brachytherapy) was evaluated and compared since the vagina is anatomically proximal to the cervix.

MATERIALS AND METHODS: A two-dimensional methodology is used to calculate the vaginal dose by providing vaginal reference points at PIBS, and plus two points of ± 2 cm. Extra points for BT (brachytherapy) were carefully selected for the upper vagina. This retrospective population enrolled 32 patients who had been treated for cervical cancer.

RESULTS: At PIBS (Posterior Inferior Border of Symphysis) and 2 cm, the combined EQD2 doses were 56.62(42.6-112.83), 92.22(64.85- 193.61), 42.52(0.30-73.3), respectively. On CT, the average VRL was 5.005cm (3.02–6.8).

CONCLUSIONS: The current study found significant dose variations amongst patients treated with different types of BT (ISBT/ICR), as well as in all regions of the vaginal wall, due to EBRT and BT contributions.

KEYWORDS: brachytherapy, external beam therapy, intracavitary brachytherapy, interstitial brachytherapy, posterior inferior border of symphysis.

CHARACTERIZATION AND CORRECTION OF ELEMENT SENSITIVITY FACTORS AND ENERGY DEPENDENCE IN $\text{Al}_2\text{O}_3:\text{C}$ -BASED OSLDs FOR DIAGNOSTIC X-RAY BEAM APPLICATIONS

Jeannie Hsiu Ding Wong^{1,2} and Wan Hazlinda Ismail²

¹ Department of Biomedical Imaging, Faculty of Medicine, Universiti Malaya, 50603 Kuala Lumpur, Malaysia

² Medical Physics Laboratory, Malaysian Nuclear Agency, Bangi, 43000 Kajang, Selangor, Malaysia

Email: jeannie_wong80@um.edu.my

BACKGROUND/OBJECTIVE: $\text{Al}_2\text{O}_3:\text{C}$ -based optically stimulated luminescent dosimeters (OSLDs) hold promise for radiation dose measurements in diagnostic X-ray beam applications. However, challenges arise due to their energy dependence (ED) and variable element sensitivity factors (ESFs), especially at low doses and energies. This study aimed to develop a methodology for determining ESFs and ED of Landauer nanoDot™ OSLDs using clinical diagnostic X-ray beams while investigating associated uncertainties.

MATERIALS AND METHODS: The methodology involved assessing the radiation field uniformity of a diagnostic X-ray unit, establishing ESFs at the central axis of the X-ray field ($2 \times 2 \text{ cm}^2$). A comprehensive investigation utilized 97 OSLDs, including "controlled" and "less controlled" samples, with ESFs determined using an 80 kVp X-ray beam in free air geometry. Cross-calibration with an ion chamber was performed to establish average calibration coefficient and ESF for accurate measurements. OSLD linearity was examined, followed by irradiation at tube potentials ranging from 50 to 150 kVp to determine ED. Uncertainty analysis evaluated measurement reliability.

RESULTS: ESFs varied between controlled and less controlled OSLDs, with batch homogeneity percentages of 2.4% and 8.7%, respectively. ED of the OSLDs ranged from 1.125 to 0.812 for tube potentials from 50 to 150 kVp. An empirical model describing ED as a function of the half-value layer (HVL) was established. Direct doses calculated from the MicroStar reader did not account for ESF and ED inaccuracies in diagnostic X-ray beams. However, applying ESF and ED corrections significantly reduced total uncertainty to 6.3% and 11.6% for controlled and less controlled OSLDs, respectively, from a potential high of 16%.

CONCLUSIONS: The study demonstrates the feasibility and importance of determining OSLD's ESFs using clinical diagnostic X-ray beams to improve dosimetric accuracy. Correcting OSLDs with user-defined ESFs and ED substantially reduces uncertainty, particularly for managing batches of less controlled OSLDs. These findings have the potential to enhance dose measurements in diagnostic X-ray beam applications, promoting safer and more reliable radiological practices.

KEYWORDS: OSLDs, energy dependence, element sensitivity factor, diagnostic X-ray beams, dose measurements.

SMALL FIELD DOSIMETRY OF 6 FFF BEAM WITH DIFFERENT DETECTORS AND IMPLEMENTATION IN ECLIPSE TPS

Pooja Patwari, Aparna Tomar, Shrikant kale, Rituraj Upreti, Rajesh Kinshikar

¹Department of Medical Physics, Tata Memorial Hospital Parel, Mumbai

Email: poojapatwari8@gmail.com

BACKGROUND/OBJECTIVE: The dosimetry of small fields requires a more scientific approach as described in IAEA TRS-483. The aim of this study is to compare output factors generated from configuring TPS using measured small field data (up to $0.6 \times 0.6 \text{ cm}^2$) to existing clinical data (which extrapolates beyond $3 \times 3 \text{ cm}^2$) (Varian Eclipse Version 16.1) for 6 Flattening Filter Free photon beam.

MATERIALS AND METHODS: The beam profiles, depth dose profiles and output factors were measured for field sizes ranging from $0.6 \times 0.6 \text{ cm}^2$ to $6 \times 6 \text{ cm}^2$ using three different detectors i.e PTW31006-pinpoint (0.015cc), IBA-CC01 (0.01cc) and PTW-Diode-E for Varian Truebeam linear accelerator in SSD condition using the Sun Nuclear 3D Scanner RFA. The field output factors were generated using daisy chaining method. The Eclipse TPS is capable of configuring profiles for field size up to $2 \times 2 \text{ cm}^2$ and output factors up to $1 \times 1 \text{ cm}^2$. The separate configuration was performed up to $10 \times 10 \text{ cm}^2$ using measured data.

Output factors were calculated and omega factors corresponding to the field sizes and detectors from TRS-483 were multiplied. This corrected field output factors were compared with the Monte Carlo simulated values from literature.

The validation plans were prepared in TPS to deliver 100 cGy dose at 10 cm depth on $30 \times 30 \times 30 \text{ cm}^3$ phantom using the AAA algorithm of Eclipse TPS with a grid resolution of 0.125 cm for different field sizes in SSD setup for small fields.

RESULTS: The discrepancy between the calculated MUs obtained from existing clinical data and the small field data was found to be within 3% for field sizes upto $2 \times 2 \text{ cm}^2$ and within 5% for field sizes upto $0.6 \times 0.6 \text{ cm}^2$. The field output factors was compared with the Monte Carlo simulated values and was found to be within 3% for all field sizes for the clinical model and within 4% for the small field data.

CONCLUSIONS: The existing clinical model is found to be in close agreement with the measured small field data as well as the Monte Carlo simulated values and be used clinically for field sizes beyond $3 \times 3 \text{ cm}^2$ after validation with the measured values.

KEYWORDS: Small field dosimetry, field output factors, Eclipse TPS commissioning

IMMOBILIZATION EXPERIENCE WITH FRAXION SYSTEM (ELEKTA) FOR SRT/SRS TREATMENT IN A LINEAR ACCELERATOR ENVIRONMENT (DEPARTMENTAL EXPERIENCE)

Laishram Amarjit Singh, Ajay K.V., Vineeta Goel

Radiation Oncology Department, Fortis Hospital Shalimar Bagh Delhi,

Email: hansamar08@gmail.com

BACKGROUND/OBJECTIVE: Stereotactic Radiosurgery is an advanced radiotherapy technique used to treat many neurological and other disease conditions like Brain Tumor, AVM, Trigeminal Neuralgia, Lung Cancer, Liver Cancer and Spine etc. This treatment procedure involves multiple steps which require extreme care and accuracy to get a quality therapy.

MATERIALS AND METHODS: Fraxion system does not come as a single equipment. It comprises of many other accessories. It has components like Fraxion Vacuum Pump, Vacuum Cushion, Head Support, Thermoplastic Mask or Mask Nose, Stereotactic Frame and Marking sheets. It also comes with adapters for CT imaging or for attaching to tabletops. The Fraxion Stereotactic Frame may be used for two purposes: the target localization and target positioning. In the target localization, the purpose of the frame is to impose fiducials on images of the patients acquired during CT scanning. The fiducials are used for determining target coordinates and slice alignment using the treatment planning software. In the target positioning, the stereotactic frame may be used to determine the location of the treatment target in the coordinate system. We may attach patient-specific prepared Fraxion Marking sheets on each side of the stereotactic frame to support this setup procedure. The Fraxion workflow consists of mounting the stereotactic frame to head support module and aligning the stereotactic frame to lasers. Then, we align the treatment target to isocenter and remove the stereotactic frame. The position is confirmed by imaging and treatment is performed.

RESULTS: There is significant improvement with position accuracy seen in the treatment delivery with Fraxion system. With this Fraxion system, translational and rotational shift error is very less with respect to non-frame treatment delivery. Moreover, the artifact (if any) with fiducials is avoided since it does not involve any fiducial. The quality of treatment delivery is much better.

CONCLUSION: This Fraxion system is quite a technique to increase our treatment accuracy. This frame gives you confidence in treating the most advanced technique especially in brain site.

KEYWORDS: Stereotactic Surgery, Fraxion System, Accelerator, Imaging, Positioning, Target Coordinates.

COMMISSIONING AND VALIDATION OF TOTAL BODY IRRADIATION (TBI) IN A STANDARD LINEAR ACCELERATOR (LINAC) BUNKER

Dandpani Epili^{1,2}, Vishal Gangwar¹, Swapna Gayen¹, Satyajit Pradhan¹, Kamal Kaushik¹, Nitish Kumar¹, Priyanka Agarwal¹, Sambit Nanda¹, Ninad Patil¹, Ashutosh Mukherji¹.

¹Department of Radiation Oncology, Homi Bhabha Cancer Hospital- Varanasi

²Department of Physics, GLA University, Mathura

Email: dandpani@gmail.com

AIM: Reporting the results of commissioning and validation of Total Body Irradiation (TBI) in a standard LINAC bunker.

METHODOLOGY: The commissioning employed a Truebeam linac from Varian Medical Systems in Palo Alto, CA, USA, along with a specialized TBI stand for extended field size delivery in Total Body Irradiation (TBI). Parameters at the isocenter were 6MV photon energy, 90° gantry angle, 45° collimator angle, and 40 × 40 cm² nominal field size. Maximum treatment distance in the bunker was 313 cm, with a 297 cm target-to-surface distance to the 1 cm thick acrylic beam spoiler.

Flatness and symmetry were measured for the maximum field size using a Farmer-type ionization chamber and Radiochromic-films, with a 200 MU/min dose rate. Beam output, linearity, and dose rate stability were measured with a Farmer-type ionization chamber (SNC 600C) from Sun Nuclear Corporation, USA. Absolute calibration was performed in a 30 × 30 cm² Solid water phantom till 30 cm depth, with corrections based on AAPM Report no 17.

Beam output was analyzed for distance from the source and position in the plane perpendicular to the beam axis. Percentage depth dose (PDD) measurements were conducted using Farmer-type ionization chamber (SNC 600C) and Parallel plate chamber (SNC 350P). External dose verification and validation involved measurements in the CIRS body phantom (30 cm long x 30 cm wide x 20 cm thick) and Solid water slabs, using Ionization chamber, OSLD, and Radiochromic films.

RESULTS: The output of the Linac at the treatment distance was 0.11029 cGy/MU. The flatness and symmetry in the horizontal and vertical planes with maximum possible treatment field size were 2.188% and 2.071% (Flatness), 100.3% and 100.1% (Symmetry) respectively. The PDD showed a maximum dose at 2mm with values of 88.61%, 75.21% and 51.82% at depth of 5cm, 10cm and 20cm, respectively. The verification and validation measurements showed a deviation of 0.3% using an ionization chamber at various locations in the field, The OSLD & gafchromic film measurements showed a deviation 2.4% & 0.5%.

CONCLUSION: TBI was commissioned and validated successfully in Varian True beam Linear accelerator as per recommendations of AAPM Report no.17.

ASSESSMENT OF PLAN ROBUSTNESS WITH PATIENT SETUP UNCERTAINTY

Arvind Kumar^{1,2}, Kiran Sharma¹, C P Bhatt³, Amit Sharma²

¹Graphic Era Deemed to be University, Dehradun, Uttarakhand, India 248002

²All India Institute of Medical Sciences (AIIMS), Rishikesh, Uttarakhand, India 249203

³Sarvodaya Hospital and Medical Research Center, Faridabad, Haryana (Delhi NCR), India 121006

Email: arvinddiundi7@gmail.com

BACKGROUND/OBJECTIVE: The accuracy of dose delivery is of paramount importance in radiotherapy, but on the other hand, many uncertainties are associated with it. These arising uncertainties may cause differences between the actual planned and delivered dose. In the present study, we have investigated the impact of uncertainties associated with patient setup errors, if these are not corrected how it would impact the dose delivery?

MATERIALS AND METHODS: A total of 130 plans (10 clinically delivered and 120 uncertainty plans) of patients treated on Halcyon™ medical linear accelerator with VMAT of different HNC have been selected. On-line and off-line shifts are calculated from megavoltage cone beam computed tomography (MV-CBCT) for consecutive first-five fractions, and an average of these shifts is calculated. These shifts are introduced in the original clinical plan to evaluate the impact of uncertainties. Dosimetric verification is performed on EPID-generated fluence maps by editing the drawing exchange format (.dxf) file and Octavius 4D phantom by introducing the uncertainties.

RESULTS: The uncertainty-perturbed plans have a mean dose of $D_{95\%}$ for low-risk, intermediate-risk, and high-risk planning target volumes are 95.42%, 94.52 %, and 95%, respectively. The dose-volume histogram (DVH) analysis shows that with higher setup uncertainty there is more deviation in organ at risk doses. EPID-generated (2D) transit fluence maps show good agreement between gamma (γ) of points passing by >95 % for 3% and 3mm criteria, whereas Octavius 4D data shows in some of the uncertainty generated plans average γ is <95%.

CONCLUSIONS: To reduce uncertainties, it is essential to follow recommended quality assurance measures, clinical protocols, imaging protocols, and other clinical standard operating protocols (SOPs). Independent dosimetry audits should be performed to assess the treatment dose delivery accuracy.

KEYWORDS: uncertainty, robustness, VMAT, HNC

COMPARISON OF LINEAR QUADRATIC(LQ), LINEAR QUADRATIC LINEAR(LQ-L) AND UNIVERSAL SURVIVAL CURVE (USC) MODELS TO PREDICT THE HIGH DOSE FRACTIONATION RESPONSE IN LUNG CANCER.

Hartanya Bhamra^{1,2}, Ranjit Singh², Manpreet Kaur^{3,2}, Arvind Shukla¹

¹RNT Medical College & Associated Gr. Of Hospitals, Udaipur, ²Post Graduate Institute of Medical Education & Research, Chandigarh, India, ³Max super-speciality hospital, Bathinda, India

Email: hartanyakaur@gmail.com

OBJECTIVE: To compare Linear Quadratic(LQ), Linear Quadratic Linear(LQ-L) and Universal Survival Curve (USC) Models to predict the High Dose Fractionation Response in Lung Cancer using cell survival curves.

MATERIALS AND METHODS: The cell survival curves of James Carmichael et al and Desmond N Carney et al for *small cell* NCI H69, *Adenocarcinoma* NCI H358, *Squamous* NCI H520, *Large cell* NCI H157, NCI H82, NCI H146, and NCI H249 were exported to WebPlot Digitizer and digitized. The data was extracted and exported to *OriginPro* software for analysis. Manual iterations were carried out on these data sets, and values of α and β were obtained. These data were additionally entered into the USC and LQ-L model's BED parameters to calculate the dose per fraction. This dosage per fraction value was compared to the LQ model's calculated dose per fraction and the RTOG 0813 limits.

RESULTS: Beyond the LQ model dose fractionation domain, i.e. high dose fraction domain, an exponential fit to the radiation cell survival data of most cell lines, and parameters D_0 and n , The LQ and radiation survival parameters lacked the same precision as the original study. The LQ-L model and the USC model proved to be a better fit for the experimental data. These models eliminate the dose range ambiguity of α/β by requiring the model to fit the entire experimental range of dose. This enforces a dose range independent approximation for α/β which in turn allows for dose range independent inter-comparison of fractionation regimens using BED. Each cell line is different and has its own α/β value which cannot be grouped in a single category and is required to be viewed as an individual SC.

CONCLUSIONS: The fitting of the experimental data in the high-dose region yielded the LQ-L model being the best solution. The LQ-L model uses biological parameters which are well characterized and have few unknowns which is not the case for the USC model where the number of unknowns for the BED_{USC} is greater which makes it a challenging task to incorporate into daily clinical practice.

MODELING AND VALIDATION OF THE TOPAS MONTE CARLO SIMULATION DOSE ENGINE USING COMMISSIONING BEAM DATA OF PENCIL BEAM SCANNING PROTON THERAPY DELIVERY SYSTEM FOR CLINICAL RESEARCH PURPOSES.

Umesh Bharat Gayake^{1,2,3}, Kantaram Darekar^{1,2,3}, Lalit Chaudhary¹, S. D. Dhole⁴, Bhushankumar J Patil¹, Sidhartha Laskar⁵

¹Department of Physics, Abasaheb Garware College, Pune, Maharashtra, India.

²Department of Radiation Oncology, Advanced Centre for Treatment, Research, and Education in Cancer, Tata Memorial Centre, Navi Mumbai, India

³Homi Bhabha National Institute, Mumbai, India.

⁴Department of Physics, Savitribai Phule Pune University, Pune, Maharashtra, India.

⁵Department of Radiation Oncology, Tata Memorial Hospital, Homi Bhabha National Institute, Mumbai, Maharashtra, India.

Email: ugayake@gmail.com

BACKGROUND/OBJECTIVE: The study aims to model and validate the TOPAS monte carlo simulation dose engine using the recently installed Pencil Beam Scanning (PBS) proton therapy delivery system. The study evaluates a thorough comparison of measured beam data such as Integrated Dose Depth (IDD), spot size, and absolute dose with Geant4-based TOPAS (TOol for Particle Simulation) simulation.

MATERIALS AND METHODS: IDD, spot size, and absolute dose measurements were performed as per the requirements of the commercially available treatment planning system (TPS) (Raystation, RaySearch Labs, Sweden). The water phantom measurements were done for IDD and absolute dose using a stingray chamber and Parallel plate chamber (PPC05) (IBA Dosimetry, Germany), respectively. The spot size was measured in the air with a plastic scintillation-based lynx detector for 70 to 226.2 MeV energies with the step of 5 MeV. The TOPAS model input files for IDD, spot size, and absolute dose simulation included the exact dimensions, material, and geometry of dosimeters and beam-specific parameters used during the commissioning. The TOPAS Geant4-based simulation was validated by comparing modeled results of IDD, spot size, and absolute dose for 11 proton energies from 70.18 to 226.2 MeV with the measured beam data.

RESULTS: The pristine Bragg peak R90 and R80 range was compared for 11 energies and is well within 0.5 mm. The Bragg peak width M80 and M90 were found within 1 mm. The TOPAS simulation computed surface dose was evaluated but could not be compared with the current measurements due to the limitations of the dosimeter. The TOPAS computed distal dose fall was found within 0.6 mm with measured data. The spot size variation was within 0.11 mm. The measured and TOPAS-computed absolute doses were matched to calibrate the ions per MU for future dose evaluation in clinical scenarios.

CONCLUSIONS: The monte carlo simulation was accurately modeled and validated through the beam data of the PBS proton delivery system. The comparison of measured beam data with the TOPAS simulated data demonstrated good agreement to use the simulation for clinical research in future studies.

KEYWORDS: Monte Carlo simulation, commissioning, proton therapy, pencil beam scan, and validation.

KNOWLEDGE BASED PLANNING OF LUNG SBRT(AN APPROACH OF AUTOMATED PLAN USING ARTIFICIAL INTELLIGENCE)

Man Gobinda Chowdhury¹, Shrikant Kale², Lilawati Meena³

¹Department of Radiation Oncology, American Oncology Institute (Jalandhar Unit), ²Department of Medical Physics, Tata Memorial Hospital, Mumbai,

³Department of Radiation Oncology, Proton Therapy Centre, Navi, Mumbai,

Email: manngovind_ind@outlook.com

PURPOSE: To develop a robust and adaptable knowledge-based planning (KBP) model with commercially available RapidPlan™(Varian Eclipse v16.1) for early stage, peripherally located non-small-cell lung tumors (NSCLC) treated with stereotactic body radiotherapy (SBRT) and improve a patient's "simulation to treatment" time.

METHODS: The KBP model was trained using 52 clinically accepted high-quality coplanar volumetric modulated arc therapy (n-VMAT) lung SBRT plans with delivered prescriptions of 60Gy in 5 or 8 fractions. Another 12 independent clinical n-VMAT plans were used for validation of the model. KBP and n-VMAT plans were compared via Radiation Therapy Oncology Group (RTOG)-0236 protocol compliance criteria for conformity (CI), gradient index (GI), maximal dose 2 cm away from the target in any direction (D2cm), dose to organs-at-risk (OAR), treatment delivery efficiency, and accuracy.

RESULTS: Knowledge-based plans were similar or better than n-VMAT plans based on a range of target coverage and OAR metrics. Planning target volume (PTV) for training cases was range 8.21–261.69 cc. KBPs provided an average CI of 0.978 ± 0.01 vs. n-VMAT plan's average CI of 1.05 ± 0.463 for 95% coverage and for 90% coverage n-VMAT archives 0.997 ± 0.003 which is improved little bit using KBP as 0.998 ± 0.002 . D2cm is improved havoc between the KBPs and n-VMAT plans. KBPs provided lower lung V10Gy, V20Gy, and mean lung dose. KBPs had overall better sparing of OAR at the minimal increased of average total monitor units.

CONCLUSION: The RTOG-compliant adaptable RapidPlan model for early stage SBRT treatment of peripherally located lung tumors was developed. All plans met RTOG dosimetric requirements in less than 30 min of planning time, potentially offering shorter "simulation to treatment" times. OAR sparing via KBPs may permit tumoricidal dose escalation with minimal penalties.

KEYWORDS: FFF beam, knowledge based planning, lung SBRT,

VALIDATION AND OPTIMISATION OF AN INDIVIDUALIZED, LOCALLY DESIGNED BRACHYTHERAPY SURFACE MOLD FOR SKIN CANCER TREATMENT

Mahendra More, Sanja George

Apollo Hospitals, Navi Mumbai, India
Email: drmahendra_m@apollohospitals.com

BACKGROUND: The customized mold using Gel Bolus and flexible implant tubes is prepared for treatment of skin lesions. The study was carried out to validate this surface mold and its effectiveness in brachytherapy with various optimization possibilities and dose distribution at surface and at various depths.

MATERIALS AND METHODS: Surface mold were constructed in gel bolus of 5mm thickness with insertion of nine implant tubes used for 70×70 mm² area. The catheter spacing was kept to be 7mm and inserted in gel bolus with one direction to achieve uniform spacing and avoid overlap. The high dose rate (HDR) brachytherapy treatment planning system (Oncentra TPS - Version 4.5.4, Elekta – Nucletron) and Microselectron 18 channel with 192-Iridium source was used. Solid phantom, Brain Lab Cranial Phantom and TLD dosimeters were used for dosimetry. The plans were generated with various spacing between catheters (from 7mm to 50mm) within customized surface mold. Skin dose and dose at 10mm depths were evaluated with continuous and alternate dwell position loading and at various catheter spacing. Optimised and non-optimised plans were evaluated for uniform dose to surface and at depth of 10mm.

RESULT: Newly designed surface mold with appropriate catheter spacing and optimization can deliver uniform dose. The TPS overestimated the calculated dose to the surface while skin dose can be reduced from 250% to 150% of the prescription dose by increasing catheter spacing and differential loading. There was 7.7% difference in the calculated dose by TPS and the measured dose with good agreement between film dosimetry and TPS results in lesser depths.

CONCLUSION: Each BT department should validate any individualized material chosen to construct the customized surface BT mold. Increasing the catheter spacing and with differential loading pattern one can treat lesions without overexposing the skin surface. Newly designed superficial BT mould can be recommended as an appropriate treatment option for some skin lesions and suitable for various shape like Nose, Ear etc. with pre-planning considerations employing appropriate catheter spacing.

KEY WORDS: Brachytherapy; mold; skin cancer

FRAMEWORK FOR COLLECTION AND MONITORING OF DOSE TO THE PATIENTS UNDERGOING COMPUTED TOMOGRAPHY EXAMINATIONS

Anand Pinjarkar¹, Parimal Patwe²

¹Directorate of Regulatory Affairs and Communication, Atomic Energy Regulatory Board, Mumbai, India,

²School of Physical Sciences, SRTM University, Latur, India

Email: anand.ngp@gmail.com

BACKGROUND/OBJECTIVE: As per latest UNSCEAR report [2022], total annual number of examinations worldwide is assessed as 2.6 billion for conventional radiography, 1.1 billion for dental radiography and 400 million for CT. Although, the contribution of CT in diagnostic radiology examinations is 9.6%, it makes the largest contribution to the overall collective dose from medical exposure with the frequency-weighted effective dose estimated as 6.4 mSv per examination against 0.37 mSv for conventional radiology and 0.01 mSv for dental radiography. CT is widely utilized medical imaging modality and its examinations is an increase of 82% from the 220 million examinations per annum estimated in the previous UNSCEAR assessment [2008]. Radiation dose monitoring programmes were developed in various parts of the world to address the growing concerns regarding radiation risk from CT. This abstract summarizes framework for collection and monitoring of CT radiation exposures to patients with an aim of optimization and providing aid towards enhancing quality control.

MATERIALS AND METHODS: DICOM is a standard for handling, storing, and transmitting information in medical imaging. DICOM Tag is one of the data elements that identifies attributes e.g. Patient's ID, Study description, etc. Data dictionary of DICOM Tag also includes patient dose related parameter such as CTDI Vol. Framework for radiation dose collection and monitoring involves following: (i) capturing scan and dose related data using commercially available products or API, (ii) centralized accumulation of data in server or cloud storage (iii) application software providing controlled access to data for analysis. The framework provides capabilities to tag the data with patient's Aadhar no. and track patient's radiation exposure history.

RESULT: The framework has capability to compare variation in CT doses for same examination/procedure for similar patient group across CT equipment connected in the framework network. This will indicate the need for standardization of dose and reduction in variation in dose without compromising the clinical purpose of each examination.

CONCLUSIONS: The framework has potential for its implementation at larger geographical region and establishment of DRLs. Examination-specific DRLs for various patient groups can be established and provide the stimulus to promote improvements in patient protection.

KEYWORDS: computed tomography, information technology, radiation dose monitoring, DRL, radiation protection of patients.

ESTIMATION OF DEPTH VS BIOLOGICAL DOSE PROFILE OF CLINICAL PROTON BEAMS: A MONTE CARLO STUDY

Arghya Chattaraj^{1,2} and T Palani Selvam^{1,2}

¹Radiological Physics & Advisory Division, Bhabha Atomic Research Centre, Mumbai, India

²Homi Bhabha National Institute, Anushaktinagar, Mumbai, India

Email: arghyac@barc.gov.in

BACKGROUND/OBJECTIVE: The advantage of proton therapy is its inherent tissue-sparing capabilities and lower integral dose as compared to modern photon-based therapies. Based on the clinical requirements, the Spread-out Bragg peak (SOBP) can be created to deliver uniform dose to the target region. The current practice is to employ a generic RBE of 1.1 independent of dose and depths. The present study is aimed at calculating biological dose of SOBP proton beams based on depth and dose specific Relative Biological Effectiveness (RBE) using TOPAS Monte Carlo code.

MATERIALS AND METHODS: 50 and 250 MeV SOBP proton beams were created using TOPAS time features. A plane parallel proton beam (radius 5 cm) was incident on a $40 \times 40 \times 40 \text{ cm}^3$ water phantom which was voxelized along the central axis. Absorbed dose to water (D) and dose average Linear Energy Transfer (LET_d) were scored at each voxel of dimension $4 \times 4 \times 2 \text{ mm}^3$. These quantities were combined on a voxel by voxel basis to get Biological Dose (BD) as a function of depth. Present study considered the model by Chen and Ahmad (Chen and Ahmad 2012) to calculate BD of V79 cells. As per this model:

$$BD_{Ch}(D_p) = D \times \frac{\sqrt{\alpha_x^2 + 4D_p\beta_x(\alpha + \beta_x D_p)} - \alpha_x}{2D_p\beta_x}$$

where $\alpha = 0.1 + \frac{(1-e^{-0.0013})LET_d^2}{0.045LET_d}$ and $\beta = \beta_x$.

α and β are cell specific parameter. Suffix 'x' is for reference radiation (^{60}Co).

RESULTS: Values of BD are calculated using $RBE_{ch}(2 \text{ Gy})$, $RBE_{ch}(4 \text{ Gy})$ and constant RBE of 1.1. $BD_{ch}(2 \text{ Gy})$, $BD_{ch}(4 \text{ Gy})$ and $BD_{1.1}$ are comparable at the entrance region whereas they differ significantly within the SOBP region and exhibits a peak close to the distal dose fall-off region. At the SOBP region, $BD_{ch}(2 \text{ Gy})$ is systematically higher than the corresponding $BD_{ch}(4 \text{ Gy})$.

CONCLUSIONS: Use of $RBE = 1.1$ produces uniform BD in the SOBP region. However, when depth-specific RBE value is used, a uniform physical dose in the SOBP region does not deliver a uniform BD. There is a sharp increase in BD at the distal end of the SOBP. The biological dose is higher at lower delivered dose.

KEYWORDS: SOBP, Monte Carlo, RBE, LET

PRIMARY TPS COMMISSIONING AND DOSIMETRIC VALIDATION OF EXTENDED TOTAL BODY IRRADIATION (TBI) FOR MONACO TREATMENT PLANNING SYSTEM.

C. P. Bhatt, Ajai Kumar Yadav

Sarvodaya Hospital and Research center, Sector 8, Faridabad, Haryana, Delhi NCR
Email: cpbhatt.phy@gmail.com

OBJECTIVE: This study aims to investigate the primary suitability of the Monaco Treatment Planning System (TPS) for Extended Total Body Irradiation (TBI) without a spoiler, taking advantage of its enhanced dose calculation capabilities and accuracy.

MATERIAL AND METHOD: For 6 MV & 10 MV, the PDD, profile and output measurements are taken from 2x2 to 40x40 cm² field size with BEAMSCAN® RFA (PTW Dosimetry) at 100 SSD as per the requirements of Collapsed Cone (CC) beam commissioning algorithm. The extended TBI patient treatment is planned at 400cm SSD, so output measurements are done for 10x10 field size at 400 SSD with slab phantom. For further validation of commissioning, we also measured the output at 300, 350 and 450 cm for both energies. With 100 SSD beam data (PDD, profile and output) and output at 400cm, the CC algorithm is commissioned in TPS as a new LINAC for only extended SSD calculations. In TPS the point dose measurements were calculated for 300, 350, 400 and 450 SSD at 10cm depth with solid water phantom and verified with the point dose measurements with slab phantom.

RESULTS: All the measured PDD, profile and output measurements are within the prescribed limit for 6 and 10 MV beams. The measured output factor for 400 cm at 10 cm depth was 5.095cGy/100MU and 5.324cGy/100MU for 6 and 10 MV respectively. The TPS calculated point dose at 400 SSD at 10 cm depth was 50.40 cGy and 52.80cGy while the measured dose was 50.3cGy and 53.07cGy for 6MV and 10MV respectively. So point dose variation between the TPS and estimated dose for extended SSD calculations are within 1% and also for other SSD 300, 350 and 450cm, the variation between the results of TPS calculated VS measured is within 1%.

CONCLUSION: This research contributes to the growing body of knowledge, without spoiler Extended TBI planning with the Monaco Treatment Planning System. The successful commissioning and dosimetric validation demonstrate the reliability and safety of this advanced technique, supporting its integration into clinical workflows for enhanced patient care and treatment outcomes.

KEYWORDS: Total Body Irradiation, TBI, Extended TBI, Monaco TPS

IMPACT OF GAS FLOW RATE IN POSITIVE ION DETECTOR USED FOR BREATH ANALYSIS

A. K. Siva¹, V. Naveen Prasath¹, R. Hemapriya¹, C. S. Sureka¹, P. V. Paramaguru¹, Amol Bhagawat², Alok J.Verma²

¹ Department of Medical Physics, Bharathiar University, Coimbatore-641 046, Tamil Nadu

²SAMEER, IIT Campus, Powai, Mumbai-400 076, Maharashtra

Email: sivaashok0316@gmail.com

BACKGROUND: Breath analysis is the most efficient non-invasive way to diagnose the cancer at the earliest stage. Breath analysis can be done using the indigenously developed multilayer PCB technology-based 3D positive ion detector. The air flow rate is considered to be one of the factors to affects the results of Breath analysis. Based on this, this study is focused to analyze the detector response at different flow rates using nitrogen gas as working medium.

MATERIALS AND METHODS: 3D positive ion detector system consists of a vacuum chamber with OFC cathode and Al anode assembly was used. The voltage applied to anode and cathode is +120 V and -490 V respectively. Flow rate valve was used to control the flow rate of nitrogen gas. The detector response is studied at different flow rates of nitrogen gas using a cobalt-60 source for three trails. The output signal is read out using the MSO system.

RESULTS: In this study, we have observed that the number of pulses for different ranges of amplitudes of (-0.5 to -0.7 V), (-0.7 to -0.9 V) and greater than -1 V and tends to fall in the range of 56 to 94 for normal flow rate at different pressures of 5 mbar, 10 mbar, 15 mbar and 20 mbar while the number of pulses ranging from 35 to 40 at low flow rate of nitrogen gas. The amplitude of the pulse tends to be in the range of -1 to -8 V at a normal flow rate when we maintain the pressure at 15 mbar and 20 mbar and the amplitude of the pulses was lower than -1 V at a lower flow rate. When the flow rate is very high, it results in vacuum arcing from 7 mbar onwards.

CONCLUSION: It is concluded that the output signal of the positive ion detector used for breath analysis is highly dependent on the flow rate of the input gas. It also affects the reproducibility of the result. Therefore, it is recommended to optimize the flow rate of exhaled breath samples.

KEYWORDS: Breath analysis, Positive ion detector, Gas sensor

ACKNOWLEDGEMENT: The authors acknowledge the Department of Science and Technology (DST), New Delhi, Government of India for financial assistance under Biomedical Device and Technology Development programme (BDTD).

ANALYSIS OF OUTPUT CONSISTENCY IN POSITIVE ION DETECTOR USED FOR BREATH ANALYSIS

C R Harshavardani¹, K. Udhaya¹, R. Hemapriya¹, C. S. Sureka¹, P. Venkatraman², Amol Bhagawat³, Alok J.Verma³

¹ Department of Medical Physics, Bharathiar University, Coimbatore- 641 046, Tamil Nadu

² Department of Medical Physics, Bharathidasan University, Trichy -620 024, Tamil Nadu

³SAMEER, IIT Campus, Powai, Mumbai-400 076, Maharashtra

Email:harshasekar9@gmail.com

BACKGROUND: Disease diagnosis by breath analysis is an emerging field in medical diagnosis and research, by knowing the importance of breath analysis for early detection of diseases, we have developed a multilayer technology-based 3D positive ion detector and published its suitability for various applications. Towards the process of its clinical prototype development, this study is focused on the measurement of the duration of signal that can be captured from the positive ion detector.

MATERIALS AND METHOD: This study uses the indigenously developed positive ion detector that works under the principle of ion-induced impact ionization with modification in the cathode material as Oxygen Free Copper. Channels 1 and 2 collect cathode and anode signals while channels 3 and 4 collect signals from the X and Y layers of the detector respectively. The applied voltages are -490V and +120V through 10 MΩ resistance to the cathode and anode. The ionizing radiation Am²⁴¹ ionizes the gas molecules. In this study, various data were collected for 3 trials for various ranges of amplitude such as 0.5- 1, 1- 1.5, 1.5- 2, and 2- 2.5V for every four minutes for a period of 20 minutes at 20 mbar pressure in N₂.

RESULTS AND DISCUSSION: It is recorded that the number of pulses is in the range of 110 to 150. When the signal collection time increases, the percentage of low voltage pulses (0.5V-1V) increases from 65% to 98.2%, the pulses with a voltage of (1-1.5V) and (1.5-2 V) decrease with the percentage of 17% to 1.76% and 15% to 0% while the percentage of high voltage pulses (2-2.5V) decreases from 0.7% to 0%, amplitude, rise and fall time of the signal decrease from 3.4 to 0.39V, 231.9ms to 17.2μs and 924.8ms to 17.3μs respectively, frequency of the signal increases from 13.3Hz to 6.3 kHz, Similarly, the period of the signal decreases from 159.8ms to 350.4μs. The delay time between channels 3 and 4 is recorded as 208.5ns ± 10ns.

CONCLUSION: Based on this study, it is concluded that the output signal is consistent for 4 minutes. When the present positive ion detector is used clinically, it is recommended to capture the signal within 4 minutes.

KEYWORDS: Breath Analysis, Positive ion detector, Gas sensor.

ACKNOWLEDGEMENT: The authors acknowledge the Department of Science and Technology (DST), New Delhi, Government of India for financial assistance under Biomedical Device and Technology Development and Programme (BDTD).

ESTIMATING ^{99m}Tc-METHYLENE DIPHOSPHONATE IMAGE FROM ITS NOISY VERSION USING HARMONIC MEAN FILTER

Beauty Rani, Anil Kumar Pandey, Chetan Patel, Rakesh Kumar

All india institute of medical sciences, New Delhi

Email: ranibeauty541998@gmail.com

BACKGROUND/OBJECTIVE: ^{99m}Tc-MDP bone scan Images are noisy. In the presence of noise, the ability of observer to detect lesions may be impaired/compromised. The observed ^{99m}Tc-MDP image can be modeled as an image degraded with additive noise only i.e. $g(x, y) = f(x, y) + n(x, y)$. In the case of unknown noise term {i.e., $n(x, y)$ }, $f(x, y)$ is estimated using spatial filtering when only additive random noise is present. Let S_{xy} represents the set of coordinates in a rectangular sub image window (neighborhood) of size maximum, centered on point (x, y) . The harmonic filtering operation is given by the expression

$$f(x, y) = \frac{mn}{\sum_{(r,c) \in S_{xy}} \frac{1}{g(r,c)}} \quad (1)$$

Here each restored pixel is given by the product of all the pixel in the sub-image area, raised to the power $1/mn$, m and n are number in the x and y direction of sub-image area. In this study, we have estimated the ^{99m}Tc-MDP image {i.e., $f(x, y)$ } from its noisy version (observed ^{99m}Tc-MDP image; $g(x, y)$) using the harmonic mean filter defined by equation (1).

MATERIALS AND METHODS: Fifty-one Tc-^{99m} MDP whole-body bone scan studies ($51 \times 2 = 102$ images; one study has two images: one anterior and another posterior image) were included in this experiment. ^{99m}Tc-MDP image was estimated from its noisy version using the size of filter having 3×3 , 5×5 , and 7×7 pixel. The estimated images were compared visually with its input image. The estimated image which had minimum noise, least distortion in edges, and better signal (metastatic lesion) to noise (i.e., background) ratio was selected as the best estimated image. A MATLAB script was written for processing images; and entire experiment was performed on personal computer.

RESULTS: 89 out of 102 estimated images obtained with 3×3 harmonic mean filter were selected as the best image. The estimated image with 3×3 harmonic mean filter was least smooth, and have better lesion to background ratio and also the difference between inter-costal ribs space and inter vertebral space were better visualized compared to input image and other two estimated obtained with 5×5 , and 7×7 filter.

CONCLUSION: The estimated ^{99m}Tc-MDP image from its noisy version using harmonic mean filter of size 3×3 filter was found to have better signal to noise ratio, and better contrast between inter-costal ribs space and inter vertebral space, compared to its input image.

KEYWORDS: Harmonic mean filter, ^{99m}Tc-MDP bone scan.

ADVANCING COLORECTAL CANCER RESPONSE ASSESSMENT: A STUDY ON ARTIFICIAL INTELLIGENCE IN FDG-PET/CT ANALYSIS

Subhash Kheruka, Anjali Jain, Sharjeel Usmani, Khulood Al Riyami, Naema Almaymani, Noura Almakhamari, Rashid Alsukaiti

Department of Radiology and Nuclear Medicine, SQCCRC, Department of Radiology and Nuclear Medicine Sultan Qaboos Comprehensive for Cancer Care and Research Centre, Al-Khoud, Muscat-566, Oman Muscat

Email: s.kheruka@cccrc.gov.com

BACKGROUND: Colorectal cancer is a global health issue and accurate response evaluation is essential for treatment choices. Response evaluation using systems like SyngoVia is inaccurate. Recently, AI has shown promise in addressing these issues.

MATERIALS AND METHODS: This research used pre and post-treatment FDG-PET scans from 9 colorectal cancer patients. SyngoVia and AI calculated SUVmax, SUVmean, MTV, and TLG values for primary tumour. To compare SyngoVia with AI, each patient's percentage and mean differences were calculated.

RESULTS: The results reveal notable differences between SyngoVia and AI methods for SUVmax, SUVmean, TLG, and MTV. The mean difference between SyngoVia and AI SUVmax is 8.81, with a percentage difference of 24.59%. Similarly, the mean difference between SyngoVia and AI SUVmean is 19.49, with a percentage difference of 39.79%.

For MTV, the mean difference between AI and SyngoVia MTV is 25.58, with a percentage difference of 84.46%. While the mean difference between AI and SyngoVia TLG is 25.89, with an average percentage difference of 31.56%.

DISCUSSION: The observed differences between SyngoVia and AI demonstrate the impact of the choice of method on colorectal cancer response assessment. The mean differences indicate consistent tendencies for one method to yield higher or lower values compared to the other, while the percentage differences quantify the magnitude of these variations.

The higher percentage differences in SUVmean, TLG, and MTV highlight the potential of AI to produce higher values compared to SyngoVia. These differences may arise from algorithmic variances and measurement accuracy inherent in the AI system.

CONCLUSION: AI role in colorectal cancer response evaluation is highlighted in this research. It emphasizes the necessity of method selection for accurate and trustworthy clinical interpretations. Integrating AI may improve colorectal cancer response evaluation and therapy choices over other methods which requires further research and validation.

EVALUATION OF IMPACT ON DOSE CALCULATION USING CT NUMBER TO ELECTRON DENSITY CURVES OBTAINED FROM TWO COMPUTED TOMOGRAPHY(COMMISSIONED AND NON-COMMISSIONED)

Rajesh Kumar

Netaji Subhas Chandra Bose Cancer Hospital, 3081, Nayabad, Kolkata, India

Email: rajeshmedphy106@gmail.com

BACKGROUND/OBJECTIVE: Dose calculation is based on Computed Tomography(CT) numbers to electron density curves . CT numbers depends on energies and in turn tube voltages of x-ray tube in CT machine. CT is a standard modality used for dose calculation purposes in Radiation Oncology. In a busy department there may be more than one CT which could be installed later and so it may not be included in commissioning of treatment planning system(TPS). This abstract presents the difference in outcome in terms of dose calculation using data of commissioned and non-commissioned computed tomography.

MATERIALS AND METHODS: Two Computed Tomography-one commissioned and other non-commissioned, appropriate gadgets, Phantom (CATPHAN), treatment planning system etc. CT images contain informations of relative electron density (RED) of tissues in terms of CT numbers which has been utilized in radiotherapy dose calculations. In this study, images were acquired at different tube voltages from 80 kV to 140 kV and at optimum tube currents. CT numbers of different materials in CATPHAN (Phantom) has been determined. Further, dose calculations in 3DCRT, IMRT and VMAT treatment plans were performed. All above methods were applied in both (commissioned and non-commissioned) in a similar manner. CT number to electron density curves were obtained on both scanned images. Finally, calculated dose using CATPHAN images were compared.

RESULTS: Collection of data in this study have been just completed. Analysis is in the process. Therefore it is not being possible to present results. But, it would definitely be presented during presentation.

CONCLUSION: Since analysis of data is in the process it is too early to conclude at this moment.

DESIGN AND STUDY OF INDIGENOUSLY DEVELOPED PRESSURE SENSOR-BASED DEEP BREATH HOLD DEVICE FOR LEFT-SIDE BREAST CANCER PATIENTS

Senthilkumar Shanmugam

Regional Cancer Center, Madurai Medical College & Govt. Rajaji Hospital, Madurai, India.

Email: senthildir21@gmail.com

BACKGROUND/OBJECTIVE: The main aim of this study was to design, develop, and conduct a comprehensive evaluation of an indigenously developed Pressure Sensor-based Deep Breath Hold Device (PS-DBHD) for left-side breast cancer patients undergoing radiotherapy. The PS-DBHD is intended to improve treatment precision by ensuring consistent breath-hold positions and reducing radiation exposure to critical organs, specifically the heart.

MATERIALS AND METHODS: PS-DBHD consists of indigenously developed software, Mouth piece, Nasal Air closer, viewing goggles, Presser sensor, Laptop, digital video camera and Mouth Piece holding device. The indigenously developed PS-DBHD was designed to be non-invasive, user-friendly, and affordable for wider accessibility. It was equipped with pressure sensors strategically placed on the patient's mouth to accurately measure the inhalation, Exhalation of lung movements during breath-hold sessions. The indigenously developed PS-DBHD successfully integrated pressure sensors and demonstrated real-time feedback capabilities during breath-hold sessions. Individual patient's breath holding threshold can be fixed in the software and exceed the level audio alarm and video display will alert, If connected with Radiotherapy machine will stop the radiation beam.

RESULTS: A preliminary feasibility study involving left-side breast cancer patients showed promising outcomes, with the device effectively promoting treatment precision by reducing variations in breath-hold levels and minimizing radiation exposure to critical organs. Real-time feedback was delivered to the patient through a user-friendly interface, helping them achieve and maintain consistent breath-hold positions. The PS-DBHD significantly improved treatment accuracy by minimizing variations in breath-hold levels and reducing radiation exposure to critical structures like the heart.

CONCLUSION: The design and study of an indigenously developed PS-DBHD present a promising innovation in the radiotherapy treatment of left-side breast cancer patients. This in-house developed solution offers an affordable and accessible option to optimize treatment accuracy and reduce critical organ radiation exposure. If proven successful, this indigenously developed device has the potential to significantly improve radiotherapy outcomes for left-side breast cancer patients, particularly in resource-limited settings, ultimately enhancing patient care and treatment accessibility. It can offer several advantages, Cost-Effectiveness, Enhanced Treatment Precision, Reduced Dependence on Imports, Patient Comfort and Compliance, Reduced Radiation Exposure and easy to implement in any radiotherapy machine.

KEYWORDS: indigenously developed, Pressure Sensor-based, Deep Breath Hold Device, Left-Side Breast Cancer Patients.

SECONDARY PARTICLE PRODUCTION ON INTERACTION OF THERAPEUTIC PROTON UP TO 200 MEV

Farhana Thesni M P, Midhun.C.V, M.M.Musthafa,Vafiya Thaslim TT

Nuclear and Radiation Physics Group, Department of Physics, University of Calicut, Calicut, India
Email: farhanathesnimp@gmail.com

BACKGROUND/OBJECTIVE: Proton therapy for cancer treatment gained significant attention due to its high conformity towards dose deposition, described by the Bragg peak. Proton therapy is performed by utilizing high energy proton beams up to 250 MeV. The current dosimetry of proton therapy is based on water phantom which is considered as tissue equivalent, which is correct only in terms of electronic interactions. The human tissue is having more elements and their isotopes. This contributes to additional dose deposition, due to Rutherford scattering and nuclear interactions that produce high LET charged particles, with momentum direction other than the primary beam. Current study is focused on the nuclear reactions induced by therapeutic proton on constituents of human tissue and estimates the impact of nuclear reactions on dose distribution.

MATERIALS AND METHODS: The ejectile spectra corresponding to each element on $p\text{-}^{nat}\text{C}$, $p\text{-}^{nat}\text{O}$, $p\text{-}^{nat}\text{N}$, $p\text{-}^{nat}\text{Ca}$ and $p\text{-}^{19}\text{F}$ are generated using Talys statistical model calculations. The available residue cross sections for proton induced reactions, from IAEA-EXFOR compilation, were used to optimize the Talys-1.96 model parameters corresponding to each projectile target combination. The residual cross section available in the energy range of 0-120 MeV has been used. Optical potential by Koning and Delaroche has been used for the calculations. The microscopic level densities based on HFB model calculation were used for the compound nuclear part. Pre-equilibrium is accounted by the exciton model with optical model based collision probabilities. The direct reaction has been optimized to reproduce the experimental data by adjusting the scaling parameter for knockout reactions. The ejectile particle spectra in lab frame, corresponding to proton induced reactions on ICRU-A150, is calculated for proton energies of 100, 150 and 200 MeV, in $d\sigma/dE$ units. This is then converted into yield per particle energy bin accounting the elemental weight fraction in ICRU-A150 tissue, number density and beam current.

CONCLUSIONS: The secondary particles p , n , d , α and γ produced by the interaction of 100, 150 and 200 MeV proton on ICRU-A150 are having significant energy and cross section. From the secondary particle cross section, it is clear that there is unavoidable contribution of dose by the nuclear reactions.

KEYWORDS: proton therapy, nuclear reaction, Talys, secondary particles

ASSESSING THE EFFECTIVENESS OF ALUMINUM SHIELDING AGAINST GALACTIC COSMIC RAYS (GCR) USING FLUKA

Rohit¹, A.K. Bakshi^{1,2}, B.K. Sapra^{1,2}

¹Radiological Physics & Advisory Division, Bhabha Atomic Research Centre

²Homi Bhabha National Institute, Anushaktinagar, Mumbai, India

Email: rohityadav@barc.gov.in

BACKGROUND/OBJECTIVE: Galactic Cosmic Radiation (GCR) represents a complex and hazardous radiation environment prevalent in deep space beyond the protective magnetic shield of our planet. It is characterized by high-energy particles originating from remote astrophysical sources, such as distant stars and supernovae. The deleterious effects of GCR pose significant health risks to astronauts, space travelers, and space missions, necessitating advanced shielding strategies to mitigate exposure. Aluminum, due to its favorable properties like high cross-section for nuclear reactions, corrosion resistance, and excellent thermal conductivity, has emerged as a promising material for spacecraft construction to safeguard against GCR-induced damage. This study sought to assess the efficacy of aluminum shielding in mitigating the impact of GCR using Monte Carlo simulations.

MATERIALS AND METHODS: Monte Carlo code FLUKA (FLUktuierende Kaskade), equipped with the Dual Parton Model (DPM) and the Quark-Gluon String Model (QGS), enables detailed simulations of particle transport and interactions in complex environments. The GCR spectrum considered in this investigation includes a broad range of charged particles with atomic numbers (z) ranging from 1 to 28 with solar modulation parameter (Φ) of 465 MV corresponding to solar minimum conditions. The energy spectrum ranged from 1MeV/amu to 103 GeV/amu was considered as it mainly contributes to the overall radiation dose. An International Commission on Radiation Units and Measurements (ICRU) sphere was used as the detector, and it was housed with aluminum shielding of varying thickness, ranging from 0 g/cm² (no shielding) to 50 g/cm². To replicate realistic conditions, the particles were transported isotropically from a spherical source towards the Al housing with ICRU sphere positioned at the center as the target. Within the ICRU sphere, essential radiation dosimetric quantities, such as the absorbed dose, dose equivalent, and average quality factor ($\langle Q \rangle$), were evaluated using the FLUKA's USRBIN card. The uniform cutoff energy of 100 keV was imposed on all simulated particles to maintain consistency and accuracy across the simulations. To ensure statistical robustness, each simulation tracked up to 107 particle histories, with the statistical uncertainty constrained to less than 2%.

RESULTS: Simulated values shows a slight increase in the absorbed dose with respect to thickness from 0.40 mGy/day without shielding to 0.48 mGy/day at 50 g/cm² shielding. Increase in the absorbed dose is mainly attributed to increase in the number of secondary particles due to shielding. Dose equivalent decrease from 1.47 mSv/day without shielding to 0.98 mSv/day at 20 g/cm² due to breaking down of high LET particles to low LET secondaries. Beyond 20 g/cm², dose equivalent started increasing with respect to the shielding thickness and become 1.06 mSv/day at 50 g/cm², due to neutron buildup and more secondary protons produced from neutron-hydrogen elastic collisions and proton-nucleus nonelastic collisions. Average Quality factor ($\langle Q \rangle$) also follows the same trend as that of dose equivalent.

CONCLUSIONS: Simulated study show that there is slight increase in the absorbed dose values due to increasing the shielding thickness, however, dose equivalent values are found to be less than that without shielding. A local minima of dose equivalent was found at 20 g/cm² which match with previous published studies. Average quality factor ($\langle Q \rangle$) decreased from 3.71 to 2.21 at 50 g/cm².

KEYWORDS: Aluminum shielding, Galactic Cosmic Rays (GCR), Monte Carlo simulation, GCR dose

OPTIMIZATION OF CATHODE VOLTAGE OF 3D POSITIVE ION DETECTOR FOR BREATH ANALYSIS

B. Abinaya¹, M. Hajima¹, S. Swetha¹, R. Hemapriya¹, C.S. Sureka^{1,*}, Alok J. Verma², Amol Bhagwat²

¹ Department of Medical Physics, Bharathiar University, Coimbatore, Tamil Nadu

²SAMEER, IIT Campus, Powai, Mumbai, Maharashtra

Email: ayaniba.b@gmail.com

BACKGROUND: The usage of 3D positive ion detectors for breath analysis is under development. As it requires optimization of various parameters in order to develop it suitable for the clinical environment, this study is focused to analyze the output signal at different cathode voltages.

MATERIALS AND METHODS: This indigenously fabricated 3D positive ion detector with optimized Oxygen Free Copper Cathode is used. The applied cathode voltages are -450V, -470V, and -490V under Nitrogen medium at various pressures viz., 5, 10, 15, 20, 25, and 50 with a constant anode voltage of +120V. The gaseous molecules are ionized using Am-241 source and signals are observed through a four-channel MSO. The data for various parameters viz., the number of pulses, amplitude, frequency, rise time, fall time, and RMS are compared.

RESULTS AND DISCUSSION: At -450V, the number of pulses is 480 where 97.5% and 2.5% of pulses are in the range of (0.5-1V) and (1-1.5V) respectively. The frequency and RMS values obtained were averaged to 4.915kHz and 73.382mV. The fall time and rise time decrease by 5% with an increase in pressure. At -470V, the number of pulses is 1074 where 69.5%, 27.5%, and 2.6% are in the range of (0.5-1V), (1-1.5V), and (1.5-2V) respectively. At 20mbar pressure, 0.4% of pulses were obtained in the range of (2-2.5V). The mean frequency and RMS values obtained are 37.474kHz and 99.934mV increasing with pressure. The fall time and rise time increased with pressure until 15mbar and non-linearity was observed for 20 and 25mbar respectively. At -490V, the number of pulses is 760 where 83.6% and 14.9% are in the range of (0.5-1V), and (1-1.5V) respectively. At 20 and 50mbar pressure, about 1.5% of pulses were obtained in a range of (1.5-2V). The frequency and RMS values increased with pressure averaged to 60.999kHz and 88.5663mV. The fall time and rise time increased linearly with pressure until 15mbar and decreased drastically above it.

CONCLUSION: Applied cathode voltage of -490V is appropriate to operate the present positive ion detector and the same can be chosen to develop the clinical prototype for Breath analysis.

KEYWORDS: Breath analysis, Positive ion detector

ACKNOWLEDGMENT: The authors acknowledge the Department of Science and Technology (DST), New Delhi, Government of India for financial assistance under Biomedical Device and Technology Development programme (BDTD).

ESTIMATING 99MTC-METHYLENE DIPHOSPHONATE IMAGE FROM ITS NOISY VERSION USING GEOMETRIC MEAN FILTER

Sharad kumar¹, Anil Kumar Pandey¹, Chetan Patel¹, Rakesh Kumar¹

Department of Nuclear Medicine, All India Institute of Medical Science, New Delhi India.

Email: sharadmbbs15@gmail.com

BACKGROUND/OBJECTIVE: 99mTc-MDP bone scan Images are noisy. In the presence of noise, the ability of observer to detect lesions may be impaired/compromised. The observed 99mTc-MDP image can be modeled as an image degraded with additive noise only i.e. $g(x, y) = f(x, y) + n(x, y)$. In the case of unknown noise term {i.e., $n(x, y)$ }, $f(x, y)$ is estimated using spatial filtering when only additive random noise is present. Let S_{xy} represents the set of coordinates in a rectangular sub image window (neighborhood) of size maximum, centered on point (x, y) . An image restored using a geometric mean filter is given by the equation (1).

$$f(x, y) = \left[\prod_{(r,c) \in S_{x,y}} g(x,y) \right]^{\frac{1}{mn}} - (1)$$

Here each restored pixel is given by the product of all the pixels in the sub-image area, raise to the power $1/mn$, m and n are number pixels in the x and y direction of sub-image area.

MATERIALS AND METHODS: Fifty Tc-99m MDP whole-body bone scan studies (50 = 100 images; one study has two images: one anterior and another posterior image) were included in this experiment. 99mTc-MDP image was estimated from its noisy version using the size of filter having (3×3) , (5×5) , and (7×7) pixel. The estimated images were compared visually with its input image. The estimated image which had minimum noise, least distortion in edges, and better signal (metastatic lesion) to noise (i.e., background) ratio was selected as the best estimated image. A matlab script was written for processing images; and entire experiment was performed on personal computer.

RESULTS: 84 out of 100 estimated images obtained with (3×3) geometric mean filter were selected as the best image. 3 out of 100 estimated images obtained with (5×5) geometric mean filter were selected as the best image. The estimated image with (3×3) geometric mean filter was least smooth, and have better lesion to background ratio and also the difference between inter-costal ribs space and inter vertebral space, pelvic lesions were better visualized compared to input image.

CONCLUSION: The estimated 99mTc-MDP image from its noisy version using geometric mean filter of size 3×3 filter was found to have better signal to noise ratio, and better contrast between inter-costal ribs space and inter vertebral space, and pelvic lesions compared to its input image.

Keywords: geometric mean filter, 99mTc-MDP bone scan.

VERIFICATION OF HIPO ALGORITHM VIA MOSFET DOSIMETRY

Ajit Ansuman Moharana

Deenanath Mangeshkar Hospital & Research Center, Erandawane, Pune

Email: ajitansumanm@gmail.com

INTRODUCTION: In our current practice in radiotherapy, we just try to minimize the dose to organ at risks (OARs), at the same time we also considered about dose conformity to targeted region. So we need better optimization techniques that to give a target delineation dose distribution in an optimum time. So our main motive is to verify the point dose that given by the optimization techniques via availability dosimetry instrument. Point dosimetry, relative dosimetry, in vivo dosimetry may be a good option for the validation of the optimization techniques. If we analyzed properly then in vivo dosimetry is not a best option because initially we are not ensure about that optimization techniques. So we have a best option is relative dosimetry at a particular reference point or at the given reference points by any dosimeter.

MATERIALS AND METHODS: For that verification we make a mini cylindrical phantom of wax materials (Dia-9cm and height-8.5cm) .To make a proper dosimetry we make 7 holes .Out of 7 holes, 6 holes for the plastic tubes and another hole just cross the sweet point of the phantom where we set our Mosfet. After that we reconstruct our catheters on the basis of ct imaging, and try to make a plan for calibration of Mosfet with respect to wax phantom and also generate a calibration factor of Mosfet for Ir-192 source only. .By help of that factor we try to justify our TPS dose data is accurate or not.

DESTINATION: Try to justify the HIPO optimization techniques working properly or not.

RESULT: From our experimental result, it confirmed that data collected by Mosfet of proper calibration with respect to specific phantom was varying 10 percentages with respect to the TPS giving data and data variation with respect to manual calculation within 12 percentages.

CONCLUSION: At the time of experiment positioning of Mosfet plays a significant role. Because at the time of experiment if Mosfet position are varying 1mm with respect to current position that introduced 3 percentages setup error in our measurement process. When we performing a setup approximately 2 to 5 mm positioning error were found .so from our previous data we confirmed that data variation within 6 to 15 percentages due to positioning error. Hence we can say that our data collections are comparatively good if we performing a quality assurance with respect to a specific phantom.

IMPACT OF HEAT ON INDEGENEOUSLY DEVELOPED 3D POSITIVE ION DETECTOR USED FOR BREATH ANALYSIS

Aishwarya KN¹, Krishna Nataraj VV¹, R.Hemapriya¹, C. S.Sureka^{1,*}, P.V.Paramaguru¹, Amol Bhagawat², Alok J.Verma²

¹ Department of Medical Physics, Bharathiar University, Coimbatore-641 046, Tamil Nadu,India

²SAMEER, IIT Campus, Powai, Mumbai-400 076, Maharashtra,India

Email: knaishu19@gmail.com

BACKGROUND: A 3D positive ion detector based on the ion-induced impact ionization principle can detect disease from human's breath samples in a non-invasive manner. The output of the detector is significantly affected by physical conditions such as pressure and temperature and it is presented in this study.

MATERIALS AND METHODS: The 3D positive ion detector consists of a cathode and anode assembly, Am-241 source, a vacuum system, high-voltage power supplies, meters to measure temperature and pressure, and a mixed-signal oscilloscope (MSO). The anode and cathode were supplied with voltages of +120V and -490V, respectively and are recorded in the channels 1 and 2. The remaining two channels were connected with the X and Y layers of the detector, which gives the output signal. Signals were collected immediately and 20 minutes after the first measurement.

RESULT AND DISCUSSION: Under normal condition at 10 mbar pressure, the amplitude of the signal was from -0.5V to 1.26V, the number of pulses were from 64 to 74, frequency was 36Hz - 20.231kHz, the rise time and fall time were from 4.1290 μ s to 712.65 μ s and 5.5652 μ s to 940.18 μ s. When the temperature rose, the amplitude was from -0.7V to -2.14V, frequency was 70Hz to 21.33kHz, the rise time and fall time were from 11.940 μ s to 4.0391ms and 9.8813 μ s to 3.9402ms correspondingly. After 20 minutes time gap, the amplitude was 0.5V to -1.38V, the number of pulses were 60 to 78, frequency was 142.05Hz to 22.575kHz, the rise time and fall time were 6.1625 μ s to 1.0201ms and 5.3408 μ s to 920.07 μ s when the signal was taken without any time gap between the previous measurement, the amplitude, frequency, rise time, fall time and the number of pulses were gradually increased due to increase in temperature but if the signal is taken after some time gap, it behaves normally.

CONCLUSION: Temperature and pressure have an impact on the performance of the detector. In order to obtain accurate, and reproducible, increase in temperature inside the chamber should be avoided. Therefore, the clinical prototype of the positive ion detector should use an appropriate cooling system in order to increase the effectiveness of breath analysis.

KEYWORDS: Breath analysis, positive ion detector, gas sensor.

ACKNOWLEDGEMENT: The authors acknowledge the Department of Science and Technology (DST), New Delhi, Government of India for financial assistance under Biomedical Device and Technology Development programme (BDTD).

URETHRAL SPARING IN HYPOFRACTIONATED RADIOTHERAPY – A DUAL MALIGNANCY CASE STUDY

Asma Javid¹, Senni Andavar², Rajpal Singh³

^{1,2,3}Shri Mata Vaishno Devi Narayana Superspeciality Hospital, Jammu, India

Email: asmajavid611@gmail.com

BACKGROUND/OBJECTIVE: High dose of radiation to the Urethra has been shown to lead to an increase in the urethral strictures and urinary obstruction. Hence, to avoid these radiation related toxifies, urethral sparing was done in the case of a Dual Malignancy with a Hypo fractionated dose prescription.

MATERIALS AND METHODS: A 58-year-old male patient presented with Dual malignancy of Metastatic Urinary Bladder and Castration Sensitive Prostate Carcinoma was prescribed Radiation Therapy at our centre. For the simulation procedure, a pelvis vac-lok was made followed by a Contrast Enhanced- CT scan acquired for the planning purpose. The CT was fused with the MRI and PET for better visualization. The PTVs as well as the OARs like bladder, rectum, bowel, and penile bulb were drawn. The proximal, as well as distal parts of the urethra, were also delineated. A hypo-fractionated dose in a Simultaneously Integrated Boost (SIB) pattern was prescribed. The bladder PTV was prescribed a dose of 55Gy in 20# whereas the prostate PTV was prescribed a dose of 60Gy in 20# with an additional 45Gy in 20# to the nodes. A VMAT plan was generated using 6MV Photon Beam on MONACO TPS V5.11.03. The PTV coverage was noted and the dose received by the Urethra and other OARs were evaluated.

RESULTS: The Prostate and Bladder PTV coverage was such that 95% of the PTV received 57.42 Gy and 54.11 Gy respectively. Dose-effect relations were observed for Urethra. D0.1cm³, D5%, and the mean dose were 59.53Gy, 59.80%, 53.77 Gy respectively. Daily kV CBCT was taken during the entire course of treatment to check for any positional errors in the delivery.

CONCLUSIONS: This study may help in paving the way for further research on similar cases where urethra sparing may prove beneficial and help improve the quality of life for the patients.

KEYWORDS: Dual Malignancy, Hypo fractionation, Urethra, Carcinoma

DENOISING F-18ML-104 TAU PET IMAGES USING DISCRETE COSINE TRANSFORM

Jyoti Yadav, Anil KumarPandey, Madhavi Tripathi

All India Institute Of Medical Science, New Delhi

Email: yjyoti1108@gmail.com

INTRODUCTION: F-18ML-104 TAU is a novel tracer used for diagnosis of cognitive impairments. The PET images obtained in routine practice are noisy. The random noise present in the image interfere during the process of making diagnosis. In this study, we have tried to improve the signal to noise ratio in the F-18-Tau image by utilizing the property of Discrete cosine transformation (DCT).

MATERIAL AND METHOD: The application of DCT on F-18ML-104 TAU PET image results in an image of the size equal to the input image in which pixel value is now called DCT coefficients. Higher value of DCT coefficients represents the signal while lower value of DCT coefficients represents insignificant contribution towards the image (usually noise). Thus, lower DCT coefficients can be discarded, and the inverse DCT can be applied to get denoised image. The image was divided into 8×8 blocks and then DCT was applied and at different thresholds (namely: 15, 25, 35, and 45) DCT coefficients were discarded and then inverse DCT was applied to get the denoised image. The process was repeated for 16×16 blocks. The denoised images were compared with its input image. A total of 206 F-18ML-104 TAU PET images were included in this study. Images that were smooth and having better contrast difference with no loss of sharpness (details in the brighter region) were labelled the best.

RESULT: The denoised image with threshold: 15, and block size: 8×8 were labelled as the best image; these images were better than the input image in terms of perceived signal to noise ratio. At the threshold: 45, the denoised images were found to be highly smoothed leading to merging of two closely spaced small uptake region into one.

CONCLUSION: The improved signal-to-noise was observed when F-18ML-104 TAU PET image was denoised with threshold: 15 and block size: 8×8 using DCT

RELATIVE DOSIMETRY IN ROBOTIC RADIOSURGERY USING SYNTHETIC MICRODIAMOND DETECTOR FOR DIFFERENT COLLIMATOR SYSTEMS

Sangaiah Ashokkumar, Subramani Vendhan, Rajasekaran Mariyappan, Sarswathi Chitra,
Mari Vel

Department Of Radiation Oncology, Apollo Speciality Hospitals, Teynampet, Chennai-600035

Email: ashok_sangaiah@apollohospitals.com

OBJECTIVE: The aim of this study is to validate the performance of commercially available PTW-60019 Synthetic microdiamond for relative dosimetric measurements in the commissioning of a clinical Cyberknife S7 system equipped with Fixed, Iris and MLC collimators.

MATERIALS AND METHODS: The CyberKnife S7™ system allows submillimetre positional accuracy for SRS, SBRT and hypofractionated radiotherapy treatments with true robotic precision and real-time motion synchronization. The radiation beam is collimated using 12 circular collimators with sizes defined at SAD = 800 mm ranging from 5 mm to 60 mm. As an alternative, auto-adjustable Iris Variable aperture collimator defining dodecahedronic apertures i.e., 2 stacked hexagonal banks of tungsten segments that together produce a 12-sided aperture. In addition, InCise2 Multileaf Collimator using 2 banks of 26 tungsten leaves to rapidly adjust the aperture size and create clinical shapes. Each leaf is 3.85 mm wide at 800mm SAD. Small field dosimetry concerns are heightened in stereotactic treatments and requires suitable detector for beam data acquisition. A PTW synthetic microdiamond detector is used to measure TPRs, Profiles and Output factors for all collimators and compared against composite reference data.

RESULTS: The relative dosimetric measurements are carried out for the three different collimator systems available. Small fields correction factors were applied to measured output factors. It was found that the relative dosimetric parameters like Tissue Phantom Ratio, Off - Center Ratio and Output Factors for 6MV unflattened beam measured using Synthetic microdiamond detector for Fixed Collimator, Iris Collimator and Multi-leaf Collimator are in good agreement with reference data. The standard reference data provided by Cyberknife manufacturer – Accuray is a composite of data measured using variety of detectors. The accuracy and performance of Synthetic micro Diamond detector in small field relative dosimetric measurements is evaluated.

Presentation ID: P-256

Abstract ID: O2935

DESIGN AND STUDY OF INDIGENOUSLY FABRICATED X-RAY SHIELDING BLOCKS USING DAMAGED OLD RADIATION PROTECTIVE LEAD APRONS

Senthilkumar Shanmugam

Regional Cancer Center (RCC), Madurai Medical College & Govt. Rajaji Hospital, Madurai, India.

Email: senthildr21@gmail.com

BACKGROUND/OBJECTIVE : This study presents the design and investigation of indigenously fabricated X-ray shielding blocks using damaged old radiation protective lead aprons. Radiation shielding is essential in medical facilities to safeguard healthcare professionals and patients from the harmful effects of ionizing radiation during X-ray procedures. By repurposing damaged lead aprons, this research aims to provide a sustainable and cost-effective, economical and environmentally friendly solution for radiation protection.

MATERIALS AND METHODS: The fabrication process involves collecting discarded and damaged radiation protective lead aprons, extracting the lead core, and processing it to obtain suitable shielding material. The lead core is then combined with other recycled materials to form shielding blocks with appropriate dimensions and radiation attenuation properties. A comprehensive study is conducted to evaluate the structural integrity, radiation shielding efficiency, and mechanical properties of the indigenously fabricated X-ray shielding blocks. The study evaluates various design configurations to optimize the shielding effectiveness while ensuring ease of integration into existing radiation protection infrastructure. The study also considers various design configurations to optimize shielding effectiveness and ease of use. Cost-effectiveness analysis and environmental impact assessments are conducted to highlight the sustainability benefits of using recycled materials.

RESULTS: Preliminary results indicate that the indigenously fabricated X-ray shielding blocks effectively attenuate ionizing radiation and meet safety standards when appropriately implemented. The use of damaged lead aprons for recycling not only minimizes waste but also reduces the need for new raw materials. The study concludes that this novel approach offers a promising solution for radiation shielding in medical facilities while promoting resource conservation and environmental responsibility.

CONCLUSION: The findings of this study have significant implications for healthcare institutions seeking to adopt environmentally responsible and economically viable radiation protection measures. The fabrication of X-ray shielding blocks using damaged old lead aprons offers multiple advantages, including cost-effectiveness, promote waste reduction, resource conservation, and improve their overall environmental footprint without compromising on radiation safety. This eco-friendly approach aligns with the principles of sustainability while maintaining the highest standards of safety and regulatory compliance in medical facilities.

KEYWORDS: X-ray shielding blocks, radiation protection, ionizing radiation, damaged lead aprons, recycling, medical facilities.

Presentation ID: P-257

Abstract ID: E7578

VALIDATION OF NEW TG 119 PHANTOM FOR INTENSITY MODULATED ARC THERAPY (IMRT) AND VOLUMETRIC ARC THERAPY (VMAT)

Mahendra More, Sanja George

Apollo Hospitals, Navi Mumbai, India

Email: drmahendra_m@apollohospitals.com

ABSTRACT: The purpose of this study was to validate newly designed TG 119 phantom with single target and organ at risk (OAR) for Intensity Modulated Radiotherapy (IMRT) and Volumetric modulated arc therapy (VMAT) and to compare VMAT plans with IMRT plan data on True Beam Stx Linear Accelerator with High-Definition MLCs.

MATERIAL AND METHOD: A newly designed TG119 phantom with 'C' shaped planning target volume (PTV) target and circular core as OAR was planned for testing the accuracy of IMRT / VMAT planning and delivery system. We generated two treatment plans, the first plan using 9 dMLC IMRT fields and a second plan utilizing two-arc VMAT technique. Dose optimization and calculations performed using 6 MV flattened and Flattening Filter Free (FFF) photons and Eclipse treatment planning system. Dose prescription and planning objectives were set according to the TG 119 goals.

RESULT: Plans were scored based on TG 119 planning objectives and Treatment plans were compared using conformity index (CI) for reference dose and homogeneity index (HI). C-shape target prescription dose 50Gy (95% of volume to receive at least 50Gy dose & 10% of volume to receive no more than 55Gy). The 5% volume of core to receive no more than 25Gy. VMAT dose distributions were comparable to dMLC IMRT plans. The studied treatment plans have Paddick conformity indices ranged from 0.90 - 0.92 (IMRT) and 0.92 - 0.95 (VMAT). VMAT plans using FFF beam shows higher conformity than FF beam plan. The Gradient Indices (GI) varies from 1.10 to 1.05 and homogeneity indices ranged from 9.0%–11.0% in both IMRT and VMAT techniques. The ratio of total monitor units necessary for dMLC IMRT to that of VMAT was in the range of 1.66 - 2.34. The results of Portal dosimetry and point dosimetry are within acceptable limit.

CONCLUSION: Our planning results are comparable to TG 119 planning results. Newly designed TG 119 phantom test phantom with single PTV and OAR is useful to generate IMRT / VMAT baseline plans. At preclinical implementation stage, plan comparison of VMAT and IMRT plans allowed us to validate and understand basic capabilities of IMRT and VMAT technique with FFF photon beam.

STUDY OF THE DEPENDENCY OF LATERAL PENUMBRA ON AIR GAP FOR PENCIL BEAM SCANNING PROTON THERAPY

Subhajit Panda¹, Lilawati Meena¹, Ranjith CP¹, Manimala K¹, Lalit Chaudhari¹,
Siddharth Laskar²

¹Department of Radiation Oncology, Advanced Centre for Treatment Research and Education in Cancer, Homi Bhabha National Institute, Mumbai, Maharashtra

²Department of Radiation Oncology, Tata Memorial Centre, Homi Bhabha National Institute, Mumbai, Maharashtra.

Email: pandasubhajit21@gmail.com

OBJECTIVE/BACKGROUND: Lateral Penumbra (LP) is one of the critical beam parameters influencing the treatment accuracy of pencil beam scanning (PBS) proton therapy. Though the LP depends upon multiple factors, such as nozzle design, beam energy, and spot size; the air gap, defined as the distance between the patient's surface and the nozzle exit, can affect the LP significantly due to multiple scattering and energy loss. Thus, it is crucial to understand the dependency of LP on air gap for different field sizes for each PBS facility prior to going clinical, this study reports the dependency of LP with air gap.

MATERIALS AND METHODS: Inversely optimized PBS treatment plans of varying field widths which include 5x5cm², 10x10 cm², 15x15 cm² and 20x20 cm² were generated in the Raystation Treatment Planning System v12A on a virtual water phantom for IBA Proteus 235 Proton Therapy machine. The modulation and maximum range of the plans were kept the same (10 cm) for each plan. A range shifter of water equivalent thickness (WET) of 4 cm is used for each plan. For each field size, different plans were generated with similar optimization criteria for different air gaps that is 5cm, 10cm, 15 cm, 20 cm, and 25 cm. Left and right LP for each plan was evaluated at 5 cm depth for both inline and crossline profiles using myQA software (IBA Dosimetry). TPS data was validated by measurement using solid water phantom and Gafchromic EBT films.

RESULTS: LP increased linearly with the air gap for all the field widths (average Pearson correlation coefficient, $r = 0.997$). For 10x10 cm² field width, the LP increased from 7.5 to 11.4 mm as the air gap increased from 5 cm to 25 cm. TPS calculated and the measured data were found to be well within the recommended tolerance.

CONCLUSION: The increase in LP with air gap can decrease the dose conformity in PBS treatment planning. Therefore, it is important to select the optimum air gap taking into consideration the LP as well as patient clearance.

KEYWORDS: Proton therapy, pencil beam scanning (PBS), Lateral Penumbra (LP), Air gap

DESIGN AND DEVELOPMENT OF A PHANTOM FOR PRESCRIPTION RADIATION DOSAGE VERIFICATION WITH RADIOCHROMIC FILM (EBT3) IN A SINGLE-CHANNEL HDR VAGINAL CYLINDER BRACHYTHERAPY APPLICATION

Challapalli Srinivas, Dilson Lobo, Athiyamaan M S, Sourjya Banerjee, John Sunny, Abhishek
Krishna

Department of Radiation Oncology, Kasturba Medical College (An associate hospital of Manipal Academy of
Higher Education: MAHE, Manipal), Mangalore, India.

Email: challapalli.srinivas@manipal.edu

BACKGROUND/OBJECTIVE: High Dose Rate (HDR) brachytherapy is carried out in majority of endometrial carcinoma patients using vaginal cylinders with the prescription dose given either on to the surface or at 5mm from the surface of cylinder with a treatment length depending upon the vaginal cuff in order to reduce the possibilities of recurrence along the vaginal wall. A phantom is built and developed to validate the prescription dose computed by the treatment planning system using radio chromic film (EBT3) in these applications.

MATERIALS AND METHODS: An acrylic box is intended to contain 10cm×10cm acrylic plates in six slots separated by 20mm. Concentric arc type slots with widths of 25, 35, and 45mm on plate-A and 20, 30, and 40mm on plate-B were designed to fit a calibrated EBT3 film as well as a 5.0mm circular opening for placement of an intrauterine tube at center. The diameters of these arcs were chosen based on the available vaginal cylinders (25, 30, and 35mm) and the distance of dose prescription (on or 5mm from the surface). A plan is generated in TPS (SagiPlan®), with the prescribed dosage mimicking with 3mm and 5mm dwell positions along the prescription length. Irradiations are performed in water phantom using Co-60 based HDR brachytherapy unit (Eckert & Ziegler BEBIG GmbH MultiSource®). The scanned films were compared for gamma assessment and dose estimation calculated by TPS to guarantee that the dosage was distributed uniformly around the film as required in vaginal cuff irradiation.

RESULTS: The test findings show that the estimated vs measured dosages differ by 5%. The 3% to 3mm gamma passing threshold is preferable for 3mm over 5mm dwell positions.

CONCLUSIONS: This phantom will help ensure prescribed dose delivery as well as dose homogeneity in single channel HDR vaginal cuff irradiations with varying dwell locations.

KEYWORDS: Vaginal cuff irradiation, EBT3 film, Quality assurance

REFERENCES

1. Sabater S., Andres I., Lopez-Honrubia V., Berenguer R., Sevillano M., *et al.* Vaginal cuff brachytherapy in endometrial cancer – a technically easy treatment? *Cancer Management and Research* 2017;9: 351–362. doi: 10.2147/CMAR.S119125.
2. Sureka C S, Sunny C S, Subbaiah K V, Aruna P and Ganesan S. Dose distribution for endovascular brachytherapy using Ir-192 sources: comparison of Monte Carlo calculations with radiochromic film measurements. *Phys.Med.Biol* 2007; 52:525–37.
3. Aldelaijan S, Mohammed H, Tomic N, Liang L H, DeBlois F., *et al.* Radiochromic film dosimetry of HDR ¹⁹²Ir source radiation fields *Med. Phys* 2011;38: 6074–83.

A COMPARATIVE STUDY OF PATIENT-SPECIFIC QUALITY ASSURANCE RESULTS FOR SPINE SBRT USING PORTAL DOSIMETRY AND OCTAVIUS 4D WITH 2D ARRAY SYSTEMS

Mallikarjuna Adavala ¹, K. Chandrasekhar Reddy ², Shakambari Sadangi ³

1 Department of Physics, Rayalaseema University, Kurnool, AP, India & AIG Hospitals, Gachibowli, Hyderabad, India

2 Department of Physics, Govt Degree College, Uravakonda, AP, India

3 Department of Radiation oncology, AIG Hospitals, Gachibowli, Hyderabad, India

Email: amallikarjuna@gmail.com

OBJECTIVE: Stereotactic body radiotherapy (SBRT) has become a standard treatment option for spinal lesions due to its high precision and excellent tumor control. Patient-specific quality assurance (PSQA) is critical in ensuring the accuracy and safety of SBRT delivery. This study aimed to compare the PSQA results of Spine SBRT treatments using two different QA systems: Portal Dosimetry and Octavius 4D with 2D Array.

METHODS: A retrospective analysis was performed on 20 patients who underwent Spine SBRT treatment at our institution. For each patient, two independent PSQA evaluations were conducted: one using Portal Dosimetry and the other using Octavius 4D with 2D Array. The measured dose distributions were compared to the calculated treatment plans for both systems.

RESULTS: The PSQA results obtained from both Portal Dosimetry and Octavius 4D with 2D Array systems demonstrated excellent agreement. The average gamma passing rates for the two systems were well within clinically acceptable limits, with mean gamma passing rates exceeding 95% (3%/3mm) for both systems. The analysis of passing rates across all patients indicated no statistically significant difference between the two QA techniques, reaffirming the robustness and consistency of the treatment planning and delivery processes.

CONCLUSION: This study provides compelling evidence of the high level of concordance in patient-specific quality assurance results for Spine SBRT between Portal Dosimetry and Octavius 4D with 2D Array systems. Both QA techniques have proven to be reliable and effective in verifying the accuracy of treatment plans and radiation delivery for this complex treatment modality. The selection of either QA system can be based on institutional preferences, available resources, and user familiarity. These findings reinforce the confidence in the accuracy and precision of Spine SBRT treatments at our institution and suggest that either QA system can be confidently utilized in clinical practice.

KEYWORDS: Stereotactic body radiotherapy, Spine SBRT, Patient-specific quality assurance, Portal Dosimetry, Octavius 4D with 2D Array, Gamma passing rate.

PERFORMANCE EVALUATION OF 3D POSITIVE ION DETECTOR IN TERMS OF ACTIVITY OF SOURCES

A. Sathiyarayanan¹, A.S. Ajay¹, R. Hemapriya¹, C. S. Sureka^{1,*}, R. Mohandoss¹, Amol Bhagawat², Alok J. Verma²

¹Department of Medical Physics, Bharathiar University, Coimbatore, Tamil Nadu

²SAMEER, IIT Campus, Powai, Mumbai, Maharashtra, India

Email: sathyaanbarasu222@gmail.com

BACKGROUND: This analysis, examines the response of ionization in the range of pulses in high activity and low activity of the reference cobalt-60 source with the emission of Beta and Gamma radiation. This gamma-ray emission provides utility for the isotope in medical applications.

MATERIALS AND METHOD: This study used two reference cobalt-60 sources, one of which has high activity (0.33 μ ci) and the other has low activity (0.08 μ ci). The source was sealed in aluminium foil and implanted in the evacuated chamber with working gas (N₂) at various pressures, like 10 mbar, 15 mbar, and 20 mbar. The 3D positive ion detector induces impact ionization and creates an avalanche of electrons. The pulses were recorded from MSO (multiple signal oscilloscope) at the applied voltage and analysed for high and low activity sources. The study was done for three trials.

RESULT: When using a high-activity source, 113, 135, and 97 are the number of pulses collected at 10, 15 and 20 mbar, respectively. At 15 mbar, all the pulses are recorded in the amplitude range of 0.5 to 1.0V where 62.92%, 25.92%, 8.88%, 1.48% and 0.74% of the pulses are in the range of 0.5 to 0.6V, 0.6 to 0.7V, 0.7 to 0.8V, 0.8 to 0.9V and 0.9 to 1.0V respectively. With a low-activity source, 93, 106, and 102 are the number of pulses collected at 10, 15, and 20 mbar, respectively. At 15 mbar, 66.98%, 16.98%, 8.49%, 6.60%, and 0.94% of pulses are in the amplitude ranges of 0.5 to 0.6V, 0.6 to 0.7V, 0.7 to 0.8V, 0.8 to 0.9V, and 0.9 to 1.0V, respectively. From this result, it is observed that the high-activity source has more pulses than the low-activity source, as it has higher disintegration than the other.

CONCLUSION: This research concluded that a 3D positive ion detector would be an efficient way to distinguish radioactive sources in terms of the activity. Therefore, the detector can be used in the field of radiation protection.

KEYWORDS: Breath analysis, positive ion detector, gas sensor.

ACKNOWLEDGEMENT: The authors acknowledge the Department of Science and Technology (DST), New Delhi, Government of India for financial assistance under Biomedical Device and Technology Development programme (BDTD).

OPTICALLY STIMULATED LUMINESCENCE STUDIES IN TOUCH SCREEN GLASS OF MOBILE PHONES FOR ACCIDENT DOSIMETRY

Sonal Kadam^{1,2}, S. N. Menon¹, Bhushan Dhabekar^{1,2}

¹Radiological Physics & Advisory Division, Bhabha Atomic Research Centre, ²Homi Bhabha National Institute, Mumbai, India
Email:kadamsonal25@gmail.com

BACKGROUND/OBJECTIVE: There is a growing concern about radiation exposures in public domain due to radiological or nuclear accidents/incidents. Non-availability of conventional radiation dosimeters in public domain increases the difficulties in dose estimation. In such scenarios, retrospective dosimetry provides a very important dosimetric tool, in which, commonly available materials can be used as a radiation dosimeter. Mobile phone is nowadays, ubiquitously used common material carried with person. This abstract presents the Optically Stimulated Luminescence (OSL) studies carried out in touch screen glass of mobile phone, to check its feasibility as a dosimeter in case of radiological/ nuclear accidents.

MATERIALS AND METHODS: Touch screen glasses of three different brands of mobile phones (Nokia (N), Samsung (S) and Red MI (M)) were removed and cut into 4 mm x 4 mm pieces for recording OSL signal. All OSL reading were recorded on RISO TL/OSL reader DA-20 under dark conditions. In-built source of Sr⁹⁰-Y⁹⁰ with dose rate of 20mGy/s was used for irradiation. All experiments were carried out on pre-bleached samples for assuring the absence of residual OSL signal. Various dosimetric characteristics such as, dose response, reusability, fading, MDD etc. were studied for all three types of touch screen glasses. Based on the results appropriate dose estimation methodology was developed.

RESULTS: From the OSL studies it was found that sensitivity of S is maximum, whereas sensitivity of N and M are 73 and 84% of S respectively. For all samples dose response is linear up to 2 Gy beyond which response is sub linear. At room temperature OSL signal of N and S fades up to ~40% of its initial value within 5 days after exposure, thereafter OSL signal gets stabilized. In case of M, there is continuous fading in OSL signal for the studied period of 16 days. Results obtained from dose estimation study shows that OSL signal of touch screen glasses can be used to estimate doses > 1Gy within an acceptable error.

CONCLUSIONS: OSL signal from touch screen glasses of mobile phone can be used for dose estimation in case of radiological/nuclear emergency.

KEYWORDS: Retrospective dosimetry, Mobile phone, touch screen glass, OSL

ASSESSMENT OF TREATMENT DELIVERY ACCURACY OF TWO BEAM MATCHED ELEKTA SYNERGY LINEAR ACCELERATORS: A STUDY OF EXTENSIVE TPS DOSE VERIFICATION

Hari Prashaath R¹, Sambasivaselli R¹, Naveen Vignesh J¹, Shanmathi V¹, Karthikeyan N¹

¹Department of Radiation Oncology, Mazumdar Shah Medical Center, Narayana Health Ltd, Bangalore, Karnataka, India
Email: harirgm4971@gmail.com

OBJECTIVE: The objective of this study is to evaluate the dose delivery accuracy of two beam matched linear accelerators and ensure their compliance through TPS dose verifications, 2D planar dose distribution and various beam matching parameters.

MATERIALS AND METHODS: Two beam matched Elekta Synergy linear accelerators (LINACs) equipped with Agility 160 leaves MLC were taken for this study. Beam data parameters such as PDD, Flatness, Symmetry and penumbra for photon and electron beams were measured and compared between both linacs. For the extensive investigation of beam matching accuracy, the TPS calculated dose were compared for photons of different field sizes and electrons of difference cones in both linacs. Patient specific quality assurance (PSQA) based on planar dose verification for 10 different plans were performed in both linacs to validate the similarity. The measurements were compared with TPS dose profile using gamma evaluation method.

RESULTS: The measured results of PDD₁₀ and D_{max} for photon beams shown a close correlation between two LINACs, with variation less than 0.6% and 0.14cm respectively, Similarly for electrons, R50 and R80 variations were within 0.3mm and 0.07mm, respectively. No significant variation was observed for measured flatness and symmetry between two LINACs. The maximum variation of TPS calculated dose for different field sizes were 3.79%, 1.28% and 3.03% for 4MV, 6MV and 15MV respectively and 0.71%, 1.21%, 1.77%, 1.08% and 1.09% for 4 MeV, 6 MeV, 8 MeV, 10 MeV and 12MeV electron beams respectively. The patient specific QA was performed for all the plan and found that all the plans were passing more than 95% with gamma criteria of 3%/3mm.

CONCLUSION: TPS dose verifications and 2D planar dose distribution verifications among two LINACs were analysed along with beam matching parameters and the results were within acceptable criteria. Therefore, it is possible to interchange accelerators for ongoing irradiated patients without re-planning.

KEYWORDS: Linear accelerator, Treatment Planning System, dose verification, beam matching

AUTOMATING TLD ELEMENT SCREENING USING CONVOLUTIONAL NEURAL NETWORKS FOR CaSO₄:Dy-PTFE-BASED THERMOLUMINESCENT DOSIMETERS

Munir S Pathan^{1,2}, S. M Pradhan^{1,2}, T. Palani Selvam^{1,2}, B. K Sapra^{1,2}

¹Radiological Physics & Advisory Division, Bhabha Atomic Research Centre, Mumbai, India

²Homi Bhabha National Institute, Mumbai.

Email: mspathan@barc.gov.in

BACKGROUND/OBJECTIVE: Thermoluminescent Dosimeters (TLDs) are used for personnel monitoring in various practices involving the use of radiation sources. The TLD badge being used in India comprises of three CaSO₄:Dy-PTFE elements (discs). During preparation for field use and readout, the TLD cards undergo different processing and handling, which may impair the disc. This impairment can be in the form of coloration, scratches, deposition of foreign particles etc., leading to variations in the disc's sensitivity. Hence, routine screening of the dosimeter before field use is required. However, the manual screening of lakhs of TLD discs can be time-consuming, subjective, and strain-inducing for the human eye. To address these challenges, an attempt is made to automate the screening process of TLD discs by developing a Convolutional Neural Network (CNN) model. The objective is to achieve a high classification accuracy for distinguishing between "good" and "bad" TLD discs, leveraging a dataset of ~150 images captured using a mobile phone camera.

MATERIAL AND METHODS: A dataset consisting of ~150 TLD disc images was obtained by capturing photographs using a mobile camera while placing the TLD cards against an X-ray illuminator. The images comprised both "good" and "bad" discs, and labeled by experts. The dataset was split into separate training and validation sets for training and evaluating the Convolutional Neural Network (CNN) model, respectively. The CNN architecture was optimized, and the hyper-parameters were tuned to ensure robustness and accuracy. By leveraging deep learning and pattern recognition, the CNN model effectively learned intricate features from the TLD disc images, facilitating accurate classification between "good" and "bad" discs.

RESULTS: The proposed CNN-based automated screening approach demonstrated remarkable performance. During the training phase, the model achieved a classification accuracy exceeding 98% on the training dataset, while achieving an accuracy of 96% on the validation dataset. This high accuracy showcases the capability of the CNN model to efficiently differentiate between "good" and "bad" TLD discs, substantially reducing the need for manual screening.

CONCLUSION: Automating the screening of TLD discs using a CNN model has proven to be a promising solution for quality control at personnel monitoring laboratory. By significantly reducing the manual screening effort, this automated system can alleviate eye strain and minimize human subjectivity in the screening process.

KEYWORDS: Thermoluminescent Dosimeters, Convolutional Neural Network, radiation safety.

VERIFICATION OF THE SIGNAL CAPTURED FROM THE 3D POSITIVE ION DETECTOR

G.T. Sarvesh¹, E. Padmanaban¹, R. Hemapriya¹, C. S. Sureka¹, P. Venkatraman¹,
Amol Bhagawat², Alok J. Verma²

¹ Department of Medical Physics, Bharathiar University, Coimbatore - 641 046, Tamil Nadu, India

²SAMEER, IIT Campus, Powai, Mumbai - 400 076, Maharashtra, India

Email: sarveshthirupathi26@gmail.com

BACKGROUND: The Printed Circuit Board (PCB) technology-based 3D positive ion detector has been identified as a device for breath analysis. Unlike invasive clinical studies, the Breath Analysis study is non-invasive and low-risk. The purpose of this study is to verify the signal captured from the upgraded version of the 3D positive ion detector to make it suitable for breath analysis.

MATERIALS AND METHOD: In this study, we utilized the 3D positive ion detector that works under the principle of ion-induced impact ionization as our principle. This process involves collecting ion pairs through electrodes. The polarity applied to the electrodes was -490V and 120V, respectively. To achieve ionization, we used Am-241 sources. The output signal is captured through Mixed Signal Oscilloscope (MSO) in the presence and absence of a source at various pressures from 5 to 25mbar and analyzed various parameters viz., number of pulses, amplitude, frequency, rise time, fall time, and RMS.

RESULTS AND DISCUSSION: Upto 10 mbar pressure, there was no signal in both the presence and absence of a source. In the absence of the source, pressures ranging between 15 and 25 mbar, and 1 or 2 pulses were detected in the negligible magnitude of parameters. However, in the presence of the source at 15 mbar, the number of pulses, amplitude, frequency, rise time, fall time, and RMS are 39, 40.360 mV, 7.7232 kHz, 18.259 μ s, 18.333 μ s & 83.761 mV respectively. At 20 mbar, the number of pulses, amplitude, frequency, rise time, fall time, and RMS are 70, 2.6400 V, 170.42 Hz, 445.56 ms 1.2908 s, and 109.03 mV respectively. At 25 mbar, the number of pulses, amplitude, frequency, rise time, fall time, and RMS are 83, 3.520 V, 57.524 Hz, 2.7085 s, 26.550 ms, and 107.55 mV respectively. Due to the presence of the source, ionization takes place, and ions are captured through the detector.

CONCLUSION: Based on the results, it is evident that the presence of a source leads to a significant output signal of the positive ion detector.

KEYWORDS: Breath analysis, Positive ion detector, Gas sensor

ACKNOWLEDGMENT: The authors acknowledge the Department of Science and Technology (DST), New Delhi, Government of India for financial assistance under the Biomedical Device and Technology Development Programme (BDTD).

DETERMINATION OF STATIC CHARACTERISTICS OF THE 3D POSITIVE ION DETECTOR

R. Hemapriya¹, C.S. Sureka¹, P.Venkatraman², Alok J. Verma³, Amol Bhagawat³

¹Department of Medical Physics, Bharathiar University, Coimbatore, Tamil Nadu

²Department of Medical Physics, Bharathidasan University, Trichy, Tamil Nadu

³SAMEER, IIT Campus, Powai, Mumbai, Maharashtra

Email: hemaram3199@gmail.com

BACKGROUND: Breath analysis, a non-invasive technique is now considered as an emerging tool or as an alternative analysis method for early screening of cancer or any disease which will impact society in a great manner. Exhaled Breath(EB) consists of more than hundreds of Volatile Organic Compounds(VOCs)and there are several techniques in which VOCs can be identified. Ion detectors for disease detection is still under development, 3D positive ion detector is one among them which can be used in this field of research. A detector analyzing human biomatrices should possess certain keycharacteristics. This abstract presents the static characteristics of the 3D positive ion detectorto make it suitable for Breath analysis.

MATERIALS & METHODS: High vacuum chamber setup consisting ofcathode as Oxygen Free High Conductivity and anode as aluminum , high voltage power supplies, gauges to read out the pressure and the sensitive part of the experiment is the multilayer PCB technology-based3D positive ion detector and the sensing performance of the detector for any gas is done by the active region, a microcurie radioactivity Am-241 source, different target gases and a Multiple Signal Oscilloscope (MSO) is used as the read-outsystem. Static parameters like sensitivity, limit of detection, working range, span, linearity, reproducibility, repeatability were studied.

RESULTS: The gas sensing static characteristicsfor atmospheric air such as sensitivityis found to be 0.41V/mbar, limit of detectionof 7mbar, working rangefrom 11-25mbar, Span of 14mbar and the detector also possessattributes of linearity (the linear coefficient is found to be 0.9), high degree of reproducibility, repeatability, and stability. The p-value of the output data is found to be 0.01 which is statistically significant. There is a gradual increase in the amplitude of the output signal when the pressure is increased from 10 to20mbar. There is a degradation of output pulse when the pressure reaches above 25mbar.

CONCLUSION: Based on the above results, it is concluded that the 3D positive ion detector has shown significant acceptable characteristics. Therefore, the present detector can be used for Breath analysis.

Keywords: 3D positive ion detector, Breath analysis, Gas sensor

ACKNOWLEDGEMENT: The authors acknowledge the Department of Science & Technology (DST), New Delhi, Government of India for financial assistance under the Biomedical Device and Technology Development (BDTD) programme .

RADIATION DOSE PROFILE USING PIRANHA MEDICAL DOSIMETRY IN DUAL ENERGY CT

Preethi Baskar¹, Vignesh Kannaiyan ², Dr. K. Muthuvelu ¹

¹Department of RadioDiagnosis, SRMIST, SRM medical college Hospital & RC, Chennai ,²Department Radiology , AVIT Chennai, Mumbai.

Email: preethibaskar2406@gmail.com

BACKGROUND/ OBJECTIVES:Quality Assurance is a management tool which, through the development of policies and establishment of review procedures, aims to ensure that every exam or treatment in a radiology department is necessary and appropriate to the medical problem and that it is performed. TG-66 give an extensive report on the QA tests to be carried out on a CT system and their significance.In this work the QA for the Somatom emotion duo CT unit is carried out as per TG-66 protocol.To carry out the mechanical and radiation dose verification QA tests for Siemens Emotion Due CT simulator as per AERB QA protocol and verify that their result are with in the acceptable tolerance limits.

MATERIALS / METHODS: The piranha can perform instant real time analysis during measurements. Table/ laptop acts as both an interactive display during the measurement and as a powerful analysis tool. It is really an all in-one multi- function meters connect with the computer wireless or Via USB . The Piranha uses solid state detector it is possible to measure HVL in one shot for mammography, Radiography, CT and dental. No need to compensate temperature and pressure and can measure on scanning beam optimized for X ray equipment from a large number of manufactures. Built- in energy compensation can be used together with ion chamber. Wide - range detection of total filtration, 100 meter Bluetooth range. Unique detector design to minimize position and rotation dependence. Automatic recognition of external probes.

RESULT:QA test of CT simulator Accuracy of kVp, mAs, reproducibility, dose test, resolution test, radiation leakage test are in tolerance limit.

CONCLUSION: Siemens Emotion Duo can be used clinically to obtain optimized images with minimum radiation dose to the patient. It is mandatory to carry out periodic CT QA as per the national and international QA protocols.

COMPARISON OF CONE ARC AND MLC –VMAT PLAN FOR STEREOTACTIC RADIOSURGERY OF SINGLE SMALL BRAIN METASTASIS BASED ON PLAN QUALITY INDICES

Shaju Pilakkal, Jennifer E P, Asmita Kawade, Afeefa P S, Dr.Sumit Basu,Dr.Pranav Chadha

Department of Radiation Oncology, Kokilaben Dhirubhai Ambani Hospital, Mumbai, India

Email:shajup2@gmail.com

OBJECTIVE: This study aims to compare Cone-based ARC (Cone-ARC) and MLC-based VMAT (MLC-VMAT) approaches for stereotactic radiosurgery (SRS) for a single small brain metastasis of volume less than 1.5 cc.

MATERIALS AND METHODS: Cone ARC and MLC VMAT plans were generated retrospectively using Eclipse (13.6) for 12 patients with single small brain mets of GTV volume ranging from 0.4cc to 1.5cc. The plans were created using HD MLC & Stereotactic Cones, with 6FFF energy in Varian Edge Linear Accelerator using AcurosXB and Cone Dose Calculation algorithm(CDC) respectively. The cones were selected as per Equivalent Sphere of Diameter of the lesion which varies from 0.9cm to 1.5cm. The numbers of ARC and gantry angles were similar in both the plans. The plans were prescribed to 80% isodose for MLC VMAT and cone arc. The parameters compared included Coverage, Paddick conformity index(CI), gradient index(GI), R50%, efficiency index(EI) and treatment time (MU). Since no OARs were in the close vicinity, doses to the OARs were not compared.

RESULTS: The Paddick CI was higher for MLC VMAT plans compared to Cone –ARC plans, owing to the shape of the target. The mean value of CI achieved with the MLC and cone based plans are 0.60 ± 0.052 and 0.68 ± 0.09 . The Cone ARC plans were scoring better mean GI (2.06 ± 0.16) compared to MLC plan (2.785 ± 0.46). Mean R50% values for Cone and MLC-VMAT plans are 3.18 ± 0.95 and 5.02 ± 1.28 . The Average EI of Cone ARC plans is 37.5% (varies from 32.3% to 44.65%) and that of MLC-VMAT plan is 30.2% (varies from 25.2% to 34.7%). These values are in the lower side due to small and complex targets. The Avg Beam On time/MU was less in Cone ARC plan. The mean target coverage in MLC plan (0.93 ± 0.11) is better compared Cone plan (0.83 ± 0.09).

CONCLUSIONS: For single small brain metastasis (volume <1.5cc), Cone –ARC plan is a good alternative to MLC-VMAT plans. MLC based plans were better in coverage but poor in CI, GI, R50% and EI. The centers may choose either of these method for SRS of small brain metastasis, but Cone will be a better option for small spherical target

KEY WORDS: VMAT, MLC, Arc, Stereotactic Cones, Edge, Brain metastasis, AcurosXB, CDC

TO STUDY THE IMPACT OF CALCULATION GRID SIZE ON THE PLAN QUALITY PARAMETERS OF STEREOTACTIC RADIOSURGERY PLAN

Shaju Pilakkal, Asmita Kawade, Jennifer E P, Pranav Chadha, Sumit Basu

Department of Radiation Oncology, Kokilaben Dhirubhai Ambani Hospital, Mumbai, India

Email: shajup2@gmail.com

PURPOSE: To evaluate the impact of dosimetric Grid size (GS) on the plan quality parameters of stereotactic radiosurgery treatment plans for single small brain metastasis.

MATERIALS AND METHODS: Stereotactic treatment plans were retrospectively generated for 14 patients with small brain metastasis, of target volume varying from 0.4cc to 4.5cc. The VMAT treatment plans were created using Varian HD MLC with 6FFF energy, to cover the target by 90% isodose in single fraction and calculated using AcurosXB (Ver.13.6) algorithm with grid size 1mm. The final plan was recalculated with different calculation grid size 1.5mm, 2mm and 2.5mm. These plans were compared using various quality parameters like Paddick conformity index (CI), gradient index (GI), efficiency index (EI), Calculation time, mean, minimum and maximum dose to the Target and maximum dose to the OAR (Brainstem D0.03cc).

RESULTS: The mean Paddick CI for GS 1mm is 0.757 ± 0.06 and that for GS 2.5 mm is 0.904 ± 0.11 . The GI also varies with GS, as the mean GI for GS 1mm is 4.56 ± 0.77 and that for GS 2.5mm is 7.18 ± 2.06 . The average variation in Max dose to the target (D0.03cc), with respect to GS 1 mm are 0.84% (1.5mm), 1.72% (2mm) and 1.65% (2.5mm). The average variation in mean dose to the target with respect to 1mm GS is 0.5% (1.5mm), 1.41% (2mm) and 2.78% (2.5mm). The variation in max dose to brain stem increases with increase in GS (1.26%, 2.66% and 4.11% for 1.5mm, 2mm & 2.5mm). The average time taken for calculation decreases with increase in GS. The average time taken for calculation of dose with 1mm GS and 2.5mm GS are 17.03 and 2.57 minutes respectively. The Avg. EI does not change much with change in GS but very slight edge is there for 1mm GS.

CONCLUSIONS: The finest (1mm) GS available is recommended if any serial OAR is in the close vicinity of the target. The finer GS leads to more heterogeneous dose distribution inside the target but help us to achieve sharp dose fall off. Depending on the volume of the target and proximity of OAR 1.5mm GS also can be used respecting the calculation time.

KEY WORDS: Grid size, VMAT, MLC, Stereotactic radiosurgery, Edge, Brain metastasis, AcurosXB.

ANALYSIS OF DYNAMIC CHARACTERISTICS OF THE 3D POSITIVE ION DETECTOR

K E Satheesh¹, M Guhan¹, R Hemapriya¹, C S Sureka¹, P V Paramaguru¹, Amol Bhagawat², Alok J Verma²

¹Department of Medical Physics, Bharathiar University, Coimbatore, Tamil Nadu, India

²SAMEER, IIT Campus, Powai, Mumbai, Maharashtra, India

Email: satheesheu@gmail.com

BACKGROUND: Cancer screening can be done in several ways and breath analysis is one of the effective methods that use volatile organic compounds (VOCs) as biomarkers. To do so, a multilayer printed circuit board (PCB) technology-based 3D positive ion detector with the principle of ion-induced impact ionization is very much helpful. This study analyses the time-dependent, so-called dynamic characteristics of the detector.

MATERIALS AND METHODS: The indigenously developed PCB-based 3D positive ion detector is placed inside the chamber setup with cathode material OFHC (Oxygen free high conductivity copper) and anode material Aluminium with a voltage of - 490V and + 120V respectively. The characteristics were studied under Nitrogen medium. For this study, the Y layer of the detector was used. A high Linear Energy Transfer (LET) Am-241 source was used to produce ionization inside the chamber. As the primary ionization induces multiple ionization, an avalanche of negatively charged electrons are collected by the detector under different pressure of 5, 10, 15, and 20 mbar. The output signals of the detector are analyzed with a mixed signal oscilloscope (MSO) in the form of pulses. The parameters analyzed were rise time, fall time, time constant, and response time of detector output.

RESULTS: This work investigates the fundamental dynamic characteristics of the detector such as the rise time which is in the range of 2 – 250 μ s, 2 - 260 μ s, 0.2 – 2 ms, 0.5 – 1.5 ms, 4 - 500 μ s, fall time in the range of 2 – 250 μ s, 2 – 260 μ s, 0.1 – 0.5 ms, 0.1 – 1.2 ms, 4 - 500 μ s at 5, 10, 15, 20, and 25 mbar respectively. The respective time constant is 1.49 minutes, response time is 7.4 minutes.

CONCLUSION: These dynamic characteristics of the positive ion detector conclude that it can effectively collect charges by the multiple ionization induced by positive ions. The stability of the detector holds good for the breath analysis.

KEYWORDS: Breath analysis, Positive ion detector, Gas sensor

ACKNOWLEDGMENT: The authors acknowledge the Department of Science and Technology (DST), New Delhi, Government of India for financial assistance under the Biomedical Device and Technology Development Programme (BDTD).

3D POSITIVE ION DETECTOR FOR ALPHA BETA AND GAMMA DETECTION

¹Arunkumar Gopikrishnan, ⁰Ganesh L, ¹Hemapriya R, ¹Sureka C .S., ¹Paramaguru P.V., ²Amol Bhagawat, ²Alok J. Verma

¹Bharathiar University, Department Of Medical Physics, Coimbatore, Tamil Nadu, India

²SAMEER, IIT Campus, Powai Mumbai

Email: arunprince25092001@gmail.com

BACKGROUND: We have developed a 3D positive ion detector that works under the principle of ion induced impact ionization. This work is focused on the usage of 3D positive ion detector to detect alpha, beta and gamma emitting isotopes.

MATERIALS AND METHODS: The 3D positive ion detector was used to detect radioactive sources such as Am-241 (Alpha+gamma source of activity 3.6 kBq), Co-60 (Beta+gamma source of activity 4.6 kBq) and Co-60 (Pure gamma with beta shielding). Aluminium and Oxygen-Free Copper (OFC) are used to make the anode and cathode respectively, and applied potential to anode is +120V through 10 M Ω resistance and -490V. In this study, output signal were captured for 3 times under nitrogen environment at 20mbar pressure.

RESULTS AND DISCUSSION: While using Am-241 source, the total number of pulses captured is 165 \pm 5 where 36.36%, 10.3%, 19.4%, 16.36%, 15.75%, 1.81% are in the voltage ranges of -0.5 to -1V, -1 to -1.5V, -1.5 to -2V, -2 to -2.5V, -2.5 to -3V and -3 to -3.5 V, respectively. For Co-60 (beta+gamma), the total number of pulses captured is 110 \pm 5 where 96.36%, 2.72%, 0.91% are in the voltage ranges of -0.5 to -1V, -2 to -2.5V and -2.5 to -3V, respectively. For Co-60 (with beta shielding), the total number of pulses captured is 224 \pm 5 where 98.6%, 0.45%, 0.9% are in the voltage ranges of -0.5 to -1V, -2.5 to -3V and -3 to -3.5V, respectively. Gamma's signal amplitude is 1.1 times larger than beta's and 1.2 times larger than alpha's. Alpha's frequency is 4 times larger than beta's and 57 times larger than gamma's. Gamma's rise time is 1.12 times larger than beta's and 1.54 times larger than alpha's. Alpha's fall time is 1.12 times larger than beta's and 3.13 times larger than gamma's. In contrast to beta and gamma, alpha has more high voltage pulses and less number of low voltage pulses.

CONCLUSION: Various radionuclides are discriminated based on the variation in output signal. Therefore, it is concluded that the 3D positive ion detector can be used in the field of radiation protection to detect alpha, beta and gamma emitting isotopes.

ABSTRACT KEYWORDS: Positive ion detector, Gas sensor, Breath analysis.

DOSIMETRIC ANALYSIS OF GLOBAL AND LOCAL GAMMA INDEX FOR STEREOTACTIC BODY RADIOTHERAPY PRETREATMENT VMAT QA BY FOUR DIFFERENT SYSTEMS

Shekhar Dwivedi^{1,4}, Devaraju Sampathirao¹, Jooli Shukla², Avinav Bharati³, Sandeep Kansal⁴, Vinod Kumar Dangwal⁵, and Tapas Dora¹

¹Departments of Radiation Oncology and Medical Physics, Tata Memorial Centre, Homi Bhabha Cancer Hospital and Research Centre, New Chandigarh, Punjab, India, ²Department of Physics, Dr. Bhimrao Ambedkar University, Agra, India, ³Department of Radiation Oncology, Dr. Ram Manohar Lohia Institute of Medical Sciences, Lucknow, India, ⁴Department of Physics, Maharaja Ranjit Singh Punjab Technical University, Bathinda, India, ⁵Department of Radiotherapy, Government Medical College, Patiala, India

Email: shekharbhul@gmail.com

BACKGROUND/OBJECTIVE: In the past, pretreatment quality assurance (QA) results are generally considered satisfactory when the gamma passing rate is over 95% and a tolerance of dose difference (DD) of 3% and a distance to agreement (DTA) of 3 mm is used as criteria. Today, after the AAPM-TG218 report, the criteria have been defined, i.e. 3%/2mm and 2%/1mm, respectively. However, the passing rates are dependent on the pretreatment verification tool used. It is therefore the responsibility of institutions to set an acceptance level for each tool rather than using a gamma of over 95% as the acceptance level for all tools. This study focuses on the analysis of the global and local gamma index for pretreatment QA of stereotactic body radiotherapy (SBRT) using volumetric modulated arc therapy (VMAT). The investigation involves the comparison of four distinct systems (MapCHECK 3, ArcCHECK, Portal Dose Image Prediction [PDIP], and PerFRACTION).

MATERIALS AND METHODS: Pretreatment verification was performed for fifty six SBRT plans, whose treatment regions corresponded to lung and spine cancer. These SBRT plans were generated on an anthropomorphic RANDO man phantom using FFF-based VMAT techniques. SBRT planning was carried out using 6-MV FFF photon beam from a True Beam linear accelerator (LINAC).

RESULTS: When it comes to global gamma passing rates that meet the 3%/3 mm criterion, only comparisons between PDIP and ArcCHECK or MapCHECK 3 were statistically different ($p < 0.05$). On the other hand, the results of the local gamma passing rate showed that all four pretreatment verification tools were statistically different from each other ($p < 0.05$) in most cases. However, PDIP and PerFRACTION yielded identical results for the 3%/3 mm criterion, and the same is true between ArcCHECK and MapCHECK 3. When the gamma criteria were reduced to 3%/2 mm, 2%/2 mm, 2%/1 mm and 1%/1 mm, the results showed that the four devices were statistically different ($p < 0.05$) in most cases.

CONCLUSIONS: The results of this study suggest that setting the same limit for all of these tools is less accurate than selecting an acceptable gamma passing rate based on the correlation between various pretreatment verification tools.

KEYWORDS: Pretreatment QA, MapCHECK 3, ArcCHECK, PDIP, PerFRACTION

SELECTION OF OPTIMAL FLATTENING FILTER-FREE ENERGY (FFF) FOR THE TREATMENT OF INTRACRANIAL HYPOFRACTIONATED STEREOTACTIC RADIOTHERAPY (HSRT)

Padmanaban V^{1,2}ArunaiNambiraj N²

¹ Department of Medical Physics, Government Arignar Anna Memorial Cancer Hospital, Karapettai, Kanchipuram, Tamil Nadu, India, ² Department of Physics, School of Advanced sciences, Vellore Institute of Technology, Vellore, India

Email: vpadmanaban88@gmail.com

Aim: The aim of this study was to select the optimal flattening filter-free (FFF) energy for volumetric-modulated arc therapy (VMAT) based hypofractionated stereotactic radiotherapy (HSRT) for intracranial lesions.

Methods & Materials: Twenty-one patients of different diagnoses were chosen with a mean PTV volume of $11.742 \pm 6.42 \text{ cm}^3$. 6MV-FFF plans were re-optimized by changing the beam quality to 10MV-FFF without altering other parameters and the optimizer was driven for 3 minutes with a single hold in each multi-resolution (MR) level. A dosimetric comparison of two plans including Monitor Unit (MU), Beam on Time (BoT), RTOG Gradient index (GI_{RTOG}), Conformity Index (CI_{RTOG}), and Paddick conformity Index (CI_{Paddick}) was studied. The dose gradient in the normal brain -PTV volume was analysed with low (GI_{Low}) and high gradient index (GI_{High}). The low dose volumes 2 Gy, and 5 Gy ($V_{2\text{Gy}}$ and $V_{5\text{Gy}}$) and the high dose volumes 10 Gy, and 12 Gy ($V_{10\text{Gy}}$ and $V_{12\text{Gy}}$) were compared for both energies.

Results: 10MV-FFF plans showed a 7% reduced MU, and 45.9% lesser BoT. CI_{RTOG} and CI_{Paddick} were comparable (1.046 ± 0.062 , 1.043 ± 0.058 and 1.246 ± 0.115 , 1.239 ± 0.110) between 6MV-FFF and 10MV-FFF. In 10MV-FFF, we observed a 5.691% reduction in GI_{Low} and a 4.04% and 3.65% reduction in $V_{2\text{Gy}}$ and $V_{5\text{Gy}}$ volumes respectively. An increase in GI_{High} of 2.693% and an increase of 2.5% and 2.76% were observed in the high dose volumes $V_{12\text{Gy}}$ and $V_{10\text{Gy}}$ respectively for 10MV-FFF. The increased lateral penumbra of 10MV-FFF leads to increased high-dose gradients.

Conclusion: The overall results showed that 10MV-FFF can be effectively used in HSRT with due importance to reduce the high dose region

Presentation ID: 274

Abstract ID: S8974

DOSIMETRIC COMPARISON OF ANISOTROPIC ANALYTICAL ALGORITHM (AAA) AND ACUROS XB (AXB) USING VOLUMETRIC MODULATED ARC THERAPY (VMAT) FOR OESOPHAGEAL CANCER

S. Sriram Prasath^{1,2}, Pallavi Mondal¹, Aarthi Pandi¹, L. Vinothini¹, C. Rajendran¹, Kiran Joshi¹, Catherine D' Souza¹, Satyam Arora¹, A. Prasheedha¹, Aranya Sarkar¹, Smita Jagdish Kalita¹, B. Arun¹, Moses ArunSingh¹, Tapesh Bhattacharya¹, Indranil Mallick¹, P. Ramesh Babu²

¹Department of Radiation Oncology, Tata Medical Center, Kolkata, India

²Department of Physics, Vellore Institute of Technology, Vellore, Tamilnadu, India

Email: sriramprasathss@yahoo.com

BACKGROUND/OBJECTIVE: To compare the dosimetric parameters of Volumetric Modulated Arc Therapy (VMAT) plans calculated using Anisotropic Analytical Algorithm (AAA) and to recalculate same plan using Acuros (AXB) for Oesophageal Cancer.

MATERIALS AND METHODS: Helical CT scan Image data sets of thirty Oesophagus cancer patients were selected for this retrospective Dosimetric study. VMAT plan using single Arc or dual Arc optimization was done in the Eclipse Treatment Planning systems (TPS) software (version15.1) Varian Medical Systems, Palo Alto, USA. For evaluation of PTV coverage, dosimetric comparison between AAA and AXB calculated VMAT plans was done using conformity index (CI) (Paddick et al) and Homogeneity Index (HI) (ICRU83). The Prescription doses were 41.4 Gy, 50 Gy, 55 Gy and 60 Gy to 15 patients, 13 patients, 1 patient and 1 patient respectively. The doses to organs at Risk (OAR) such as Maximum dose to Spinal Canal PRV, Total Lung (V20, V10, V5, were the relative Volume of Total Lung receiving 20 Gy, 10Gy, 5Gy respectively), mean dose to Total Lung, mean dose to Heart, were also compared between the AAA and AXB calculated VMAT plans. Statistical analysis was done using two sample t tests.

RESULTS: The mean difference in HI was 0.01,(p value=0.18),mean difference in CI was 0.22(p value=0.00048), the mean dose difference of 0.95 Gy, in Maximum dose to Spinal Canal PRV,(p value=0.50), the mean dose difference in mean dose to Total lung was 0.14 Gy (p-value=0.81), the mean difference in V20, V10, V5 of Total lung were 0.13(p-value = 0.94),2.03 (p-value = 0.83),3.11(p-value = 0.74),mean difference of 0.24 Gy (p-value = 0.90) in mean dose to Heart.

CONCLUSIONS: We observed from the results that the difference in HI, OAR doses were insignificant, but difference in the CI showed significant between AAA and AXB calculated VMAT plans. AAA overestimates the coverage in PTV when compared to AXB. This suggests that appropriate calculation algorithm to be chosen for sites having much heterogeneity in tissues surrounding the PTV.

KEYWORDS: AAA, Acuros, Algorithm, dose calculation

Presentation ID: 275

Abstract ID: E5112

STUDY ON THE OUTPUT SIGNAL OF 3D POSITIVE ION DETECTOR AT VARIOUS SAMPLING RATES

R. Velmani¹, A. Dhinesh¹, R. Hemapriya¹, C. S. Sureka^{1,*}, P. V. Paramaguru¹, Amol Bhagawat², Alok J.Verma²

¹Department of Medical Physics, Bharathiar University, Coimbatore, Tamil Nadu, India

²SAMEER, IIT Campus, Powai, Mumbai, Maharashtra, India

Email: rvelmani00002@gmail.com

BACKGROUND: A 3D positive ion detector aids in the field of breath analysis. Sampling rate (number of samples per second) is one of the important parameters used to design the clinical prototype of the positive ion detector. In the present study, we have analyzed the variation in its output signal at various sampling rates.

MATERIALS AND METHODS: This study used Am-241 source in the evacuated chamber with the working nitrogen gas as a medium. The 3D positive ion detector induces impact ionization and creates an avalanche of electrons. The output signals are analyzed at different sampling rates such as 25kS/s, 10kS/s, 5kS/s, 2.5kS/s, and 1kS/s at 20mbar in the Nitrogen medium. The signals are drawn from the detector output and displayed in the waveform through DSO (Digital Signal Oscilloscope).

RESULT AND DISCUSSION: At 25kS/s, 297 ± 5 number of pulses were captured where 74%, 6%, 12%, and 1% of pulses are in the amplitude range of 0.5 to 1V, 1 to 1.5V, 1.5 to 2V, and 2 to 2.5V, respectively. At 10kS/s, 133 ± 5 pulses were captured where 68%, 17%, and 15% of the pulses are in the range of 0.5 to 1V, 1 to 1.5V, and 1.5 to 2V respectively. At 5kS/s, 47 ± 5 pulses were captured where 28%, 55%, and 17% were in the range of 0.5 to 1V, 1 to 1.5V, and 1.5 to 2V respectively. At 2.5kS/s, 27 ± 5 pulses were captured where 26%, 55%, and 18% were in the range of 0.5 to 1V, 1 to 1.5V, and 1.5 to 2V respectively. At 1kS/s, 17 ± 5 pulses were captured where 41%, 52%, and 5% were in the voltage range of 0.5 to 1V, 1 to 1.5V, and 1.5 to 2V respectively. From these results, it is observed that when the sample rate decreases, the number of pulses is also decreased. High amplitude pulses would be missed when the sampling rate is not appropriate.

CONCLUSION: High sampling rate of 25kS/s is required to capture the signal from the positive ion detector when it is used for breath analysis.

KEYWORDS: Breath analysis, Positive ion detector, Gas sensor

ACKNOWLEDGEMENT: The authors acknowledge the Department of Science and Technology (DST), New Delhi, Government of India for Financial assistance under the Biomedical Device and Technology Development programme (BDTD).

CONSISTENCY IN QUALITY ASSURANCE OF HALCYON kV CBCT

Mahender Damera, P JyothiA Rekha

American Oncology Institute, Cancer Treatment Services Hyderabad Pvt Ltd Hyderabad, Bommidala cancer Institute Campus, Guntur, Andhra Pradesh, India

Email: mahender.damera@gmail.com

BACKGROUND: The field of radiation oncology is a middle period of rapid technological change. Advancements in imaging, treatment planning and delivery now enable unprecedented sophistication in the approach to radiation therapy (RT). Such advancements enhance the quality of treatment through better target delineation, dose delivery and normal tissue sparing, which collectively promise to improve the therapeutic ratio. The array of techniques implementing these modern imaging approaches has been termed image-guided RT (IGRT). A key feature of IGRT is the facilitation of four-dimensional (4D) target localization. For example, reproducible positioning the patient is an important element of fractionated RT delivery. However, both systematic and stochastic errors in patient setup contribute to variation in daily positioning. Reproducibility is also hindered by movement or changes occurring in target and normal tissues between (interfraction) or even during (intrafraction) treatment. Hence, imaging modality plays a very important role to encounter these problems. In order to get good image quality, the imaging systems require stringent QA in mechanical, geometrical and image quality in a regular interval.

MATERIALS AND METHODS: Our institute has Varian Halcyon linear accelerator with kV CBCT, The physical size is 43x43cm², 1280x1280 pixels, and it is 154cm from the kV source. The scintillator has been changed to Gd2O2S, and a 15:1 scatter grid is used. Behind the amorphous silicon photo-diodes, a 0.127mm thick sheet of tungsten provides a backscatter shield. The panel provides 16-bit images at 30 frames per second (fps). kV CBCT reconstruction produces a 512x512 pixel matrix and are fixed at a 2mm slice thickness. The kV system is mounted to the ring gantry, orthogonally to the MV beam axis. Note, there are no 2D kV imaging procedures. The kV imaging panel has a permanent lateral offset of 17.5cm, and all kV CBCTs will utilize a full gantry rotation. The kV source has a permanent half bow-tie filter, which compensates the beam for attenuation falloff at the edge of the patient.

The quality assurance of kV CBCT (i) CBCT isocenter check with Drum Phantom (via MPC) (ii) HU Linearity and Uniformity with Quart DVT Phantom (iii) Spatial linearity and Geometrical accuracy with Quart Phantom (iv) High Contrast resolution. The geometrical accuracy and the image quality checks are carried out at regular intervals (weekly) in our institute and the values are achieved within the tolerance limit.

RESULTS: The isocentre verification test are carried out using Drum phantom in Daily MPC and the values are in within the limit. The verification of kv mA and Ms were also in good agreement with the set value. kVCBCT images acquired it was showed good agreement for spatial resolution, spatial linearity and Hounsfield unit/CT (within the tolerance of ± 40)

CONCLUSIONS: The consistency of values achieved in the kV CBCT which have been performed in a regular basis shows that the kV CBCT system is working in a good geometrical condition and in good image quality.

SMALL-FIELD DOSIMETRY OF 10-MV UNFLAT AND FLAT PHOTON BEAM USING THREE DIFFERENT DETECTORS

Jooli Shukla^{1,*}, Shekhar Dwivedi², Vinod Kumar Dangwal³, and K P Tiwari¹

¹Department of Physics, Agra College, Agra (Dr. Bhimrao Ambedkar University, Agra, India), ²Department of Medical Physics, Tata Memorial Centre, Homi Bhabha Cancer Hospital and Research Centre, New Chandigarh, Punjab, India, ³Department of Radiotherapy, Government Medical College, Patiala, India

Email: julieshukla1@gmail.com

BACKGROUND/OBJECTIVE: The primary objective of this study was to measure and validate the small unflat beams using three different small-sized detectors. The purpose of this study was to expand the existing pool of dosimetric data pertaining to small unflat photon beams. Furthermore, a comparative analysis was conducted on the dosimetric parameters of small unflat and flat photon beams in order to increase the understanding of beam energy and spectrum. The study examined several dosimetric characteristics, including beam output, penumbra (d_{20-80}), percentage depth dose (PDD) at 10 cm (D_{10}) and percentage surface dose (D_s) for 10 MV small flattening filter-free (FFF) and flattening filter (FF) photon beams.

MATERIALS AND METHODS: The TrueBeam linear accelerator (LINAC, Varian Medical Systems) was employed in this study. The 10 MV FFF and FF photon beams were used to measure the output factor, depth dose, and beam profile of small-fields ranging in size from 1 cm × 1 cm to 6 cm × 6 cm. The PinPoint ionization chamber (PTW 31014) was employed to measure PDD at 10 cm and output factor, while the Gafchromic EBT3 films (Ashland Advanced Materials) and diode based EDGE detector (Sun Nuclear Corporation) were employed to measure beam profile and surface dose, respectively. The radiation field analyzer (RFA, Sun Nuclear Corporation) was used for measurement. All measurements were performed according to the TRS-483 protocols established by the International Atomic Energy Agency.

RESULTS: The output factors for FFF beams shown a notable increase compared to FF photon beams. The study found that the penumbras of FFF beams were marginally less in comparison to FF beams. This observation suggests the potential for improved conformity of tumor and a decrease in radiation doses to healthy organs. The FFF photon beams exhibited a larger surface dosage and a lower depth dose at a distance of 10 cm compared to the FF photon beams. This resulted in a significant degradation of beam energy for the unflat beams.

CONCLUSIONS: The results of this work are in line with data that has already been published, and they will be useful for future study and LINAC commissioning.

KEYWORDS: Small-field dosimetry, FFF beam, Output Factor, Penumbra, Surface dose

Presentation ID: 278

Abstract ID: M9570

COMPARISON OF OFFICIAL JOURNALS OF ASIA-OCEANIA FEDERATION OF ORGANIZATIONS FOR MEDIAL PHYSICS

Nobuyuki Kanematsu

Department of Accelerator and Medical Physics, Institute for Quantum Medical Science, National Institutes for Quantum Science and Technology, Chiba, Japan

Email: kanematsu.nobuyuki@qst.go.jp

BACKGROUND/OBJECTIVE: The Asia-Oceania Federation of Organization for Medical Physics (AFOMP) recognizes three medical physics journals as its official publications, which are Physical and Engineering Sciences in Medicine (PESM) from Australia, Radiological Physics and Technology (RPT) from Japan, and Journal of Medical Physics (JMP) from India. In Clarivate's Web of Science, while PESM is enlisted in the Science Citation Index Expanded (SCIE) database, RPT and JMP are in the Emerging Sources Citation Index (ESCI) database.

MATERIALS AND METHODS: We compared the three journals mainly using public information in their journal websites, and third-party services such as Journal Citation Report by Clarivate and Scimago Journal & Country Rank.

RESULTS: Their Journal Impact Factors for 2022 by Clarivate were 4.4 for PESM, 1.6 for RPT, and 0.9 for JMP. There are many distinctive features in these journals not evaluated in the citation metrics. PESM appears to be the most international. RPT encourages young inexperienced researchers in its editorial policy. JMP offers golden open access without any charge to authors.

CONCLUSIONS: The three AFOMP official journals are providing distinctive venues for research publication for their own domestic society members and other researchers in the world, and will contribute to the scientific progress in each country, the Asia-Oceania region, and the world.

KEYWORDS: medical physics, scientific publication, citation database

SYNTHESIS AND CHARACTERISATION OF TETRAGONAL BaTiO₃ NANOPARTICLES USING SOLVOTHERMAL METHOD FOR TISSUE ENGINEERING APPLICATIONS

Mariam G Varghese¹, Arunai Nambi Raj N¹

¹School of Advanced Sciences, Vellore Institute of Technology, Vellore, Tamil Nadu, India

Email: narunainambiraj@vit.ac.in

BACKGROUND/OBJECTIVE: In recent years, there has been a growing interest in the use of bioceramics in the biomedicine field. This is primarily due to their remarkable capability to interact with biological systems while providing desirable material properties. One such bioceramics that has gained considerable attention is Barium Titanate (BaTiO₃), known for its tetragonal perovskite structure. By incorporating BaTiO₃ into medical applications, researchers aim to enhance functionality and effectiveness of various medical structures and tools leading to overall patient well-being.

MATERIALS AND METHODS: The tetragonal BaTiO₃ nanoparticles were conveniently synthesized through solvothermal method, operating at low temperature for a period of 15 hours. The Ba to Ti molar ratio is taken as 1:1 with BaCO₃ serving as the Ba source and tetra butyl titanate as the precursor for Ti. The mineralizing agent, NaOH was dissolved in appropriate amount of ethanol for the preparation process.

RESULTS: XRD and FTIR results confirmed the tetragonal structure and molecular composition of the synthesized nanoparticles. The dielectric properties were investigated which indicated positive results that suggest its suitability in bone applications. Furthermore, the surface hydrophilicity demonstrated a robust inclination towards promoting interactions with biological fluids or facilitating the adherence of coatings or other materials. In addition, the nanostructured tetragonal BaTiO₃ exhibited good biocompatibility and antimicrobial effects.

CONCLUSIONS: Owing to their notable dielectric and biocompatibility, the prepared nanoparticles displayed great promise as a viable option for hard tissue repair.

KEYWORDS: BaTiO₃, tetragonal, dielectric properties, biocompatibility

MULTIFACETED CHARACTERIZATION AND THERAPEUTIC EVALUATION OF CO-PRECIPIATED COBALT FERRITE NANOPARTICLES FOR MAGNETIC HYPERTHERMIA CANCER THERAPY

Jafrin Reena R, Arunai Nambi Raj N

School of Advanced Sciences, Vellore Institute of Technology, Vellore, Tamil Nadu, India

Email: narunainambiraj@vit.ac.in

Background/Objective: Cancer has become the second major cause of death after cardiac arrest. So, there is a growing interest among scientists to develop nonconventional modalities of cancer therapy with increased efficacy. Magnetic-mediated Hyperthermia is a non-invasive technique for treating cancer in which the magnetic nanoparticles are incorporated in the cancer cells and an alternating magnetic field is generated to destroy them. Due to their favourable physical, chemical, and magnetic properties, such as their high anisotropy constant, high coercivity, moderate saturation magnetization, and ease of synthesis, cobalt ferrite nanoparticles have been recognized as one of the competitive contenders. The current study delves into the synthesis and characterization of cobalt ferrite magnetic nanoparticles (CF-MNPs) with a dual objective of augmenting magnetic properties and ensuring biocompatibility, without sacrificing the intrinsic benefits of ferrite nanoparticles like non-toxicity and their biodegradable nature.

Materials and methods: The Spinel ferrite, $\text{Co}_{1-x}\text{Zn}_x\text{Fe}_2\text{O}_4$ nanoparticles were synthesised at various compositions using the chemical coprecipitation method. The synthesized CF-MNPs underwent rigorous characterization using various techniques, including thermogravimetric analysis (TGA), X-ray diffraction (XRD), Fouriertransform infrared spectroscopy (FTIR), vibrating sample magnetometry (VSM), and dielectric studies. For assessing the biocompatibility and potential applications of CF-MNPs in biological systems, the samples were subjected to cell viability tests and in vitro studies for evaluating their cytotoxicity and cytocompatibility.

Results: Co-Zn ferrite nanoparticles were shown to have a single-phase cubic structure according to XRD research, which also revealed changes in structural parameters as Zn content increased. By examining FTIR spectra, it was possible to confirm that the ferrite phase was formed. Due to the different magnetic properties of the sample, the SEM images revealed the agglomeration of spherical grains.

Conclusions: Significant improvements were achieved in the magnetic properties of cobalt ferrite nanoparticles through substitution and doping, leading to increased efficacy for potential applications. Successful coating with the biocompatible layer ensures their safe use in biological systems.

Keywords: Magnetic Hyperthermia, $\text{Co}_{1-x}\text{Zn}_x\text{Fe}_2\text{O}_4$, Spinel ferrite, co-precipitation, cytotoxicity, biocompatibility,

COMPARISON OF DOSE PROFILE USING RADIOCHROMIC FILM AND ION CHAMBER IN HRCT

¹Vignesh Kannaiyan, ²Preethi Baskar, ²Dr. K. Muthuvelu

¹Department Radiology, SAHS, VMRF-DU Chennai, Tamilnadu, India

²Department of RadioDiagnosis, SRMIST, SRM medical college Hospital & RC, Chennai, Tamilnadu, India

Email: vigneshmphy9@gmail.com

BACKGROUND/OBJECTIVE: In chest CT Image acquisition protocols should be based on research to maintain or improve the image quality and reduce risks due to the use of ionizing radiation

For this reason, evaluation of the patient's mass and volume needs to be observed, the analysis of the optical density, the dose measurement and contrast are some factors to be considered to optimize the parameters for image acquisition with diagnostic quality. The Study to determine the low dose study using radio chromic film Low dose chest CT- dose chamber assessment by using CTDI head and body phantom with ionization chamber and radio chromic filmCTDI phantom will undergo CT acquisition with low dose protocols containing changes in:Kvp, mAs,Gantry rotationIn the study it was compared the dose index values obtained bythe pencil chamber measurement to the dose longitudinal profiles recorded by the film strips.

MATERIALS AND METHODS: Absorbed dose records by the radio chromic film strips for each position of measurement in the Head phantom were similar to the values obtained by the pencil ionization chamber.Film strips may be used as a reliable tool in the analysis of absorbed dose, in the search for optimizing the acquisition protocols for head CT scans.Based on CTDI100 values measured in the central and phantom peripheral openings, it was possible to calculate the weighted dose index (CTDI_w), and the volumetric dose index CTDI_{vol}.

RESULTS: Absorbed dose records by the radio chromic film strips for each position of measurement in thephantom were similar to the values obtained by the pencil ionization chamber.

Conclusions;Film strips may be used as a reliable tool in the analysis of absorbed dose, in the search for optimizing the acquisition protocols for HRCT scan

KEYWORDS: HRCT,Radiochromic Film, Ion Chamber, J image software

A PROSPECTIVE STUDY OF VMAT VERSUS IMRT FOR PREOPERATIVE RECTAL CANCER: A DOSIMETRIC ANALYSIS

Kazim Udin Olin, Md. Akhtarzaman, Md. MokhlesurRahman, Md. Jobairul Islam, Masum Chowdhury, Kazim UddinOlin

Gono Bishwabidyalay, Cumilla, Bangladesh,

Email: kazimddinolin050@gmail.com

INTRODUCTION: The study investigated a dosimetric comparison between intensity-modulated radiation therapy (IMRT) and volumetric-modulated arc therapy (VMAT) treatment plans in rectal cancer.

METHOD: Ten patients with rectal cancer previously treated with short course radiotherapy (25 Gy in 5 fractions) with X6 flattening filter free (FFF) beams using 9-Field IMRT and 2-Arcs VMAT were selected for this study. For each patient, plans were regenerated using 5-Field, 7-Field, 9-Field, 11-Field IMRT and 1A, 2A, 3A VMAT for X6, X10 and mixed X6 & X10 energies with the Eclipse TPS. Dose distributions to the target and the organs at risk (OARs) were compared for all techniques. Monitor units (MUs) were also assessed.

RESULTS: For both IMRT and VMAT plans, dose distribution to the target varied up to 2.6%. For X6, mean Homogeneity Index (HI) improved by 47.3% but MUs increased by 28.3% for 9F-IMRT compared to 5F-IMRT. Although MUs decreased by a mean 6.7% with X10 and mixed X6 & X10, HI fell by 6.0% for 9F-IMRT compared to X6. For X6, HI and MUs increased by 37.6% and 7.0% respectively for 2A-VMAT compared to 1A-VMAT. With 2A-VMAT for X6, HI was higher by 12.3% and MUs lower by 5.7% than X10 and mixed X6 & X10. The differences among 7F, 9F and 11F-IMRT and between 2A and 3A-VMAT were not significant. No considerable difference was observed for dose distribution to the target between 9F-IMRT and 2A-VMAT. However, a significant increase of MUs (72.7%) with 9F-IMRT was found. Regardless of techniques, energy, number of fields and arcs, OAR doses varied by no more than 10.0%.

CONCLUSION: Both 9F-IMRT and 2A-VMAT plans are recommended for short course treatment of rectal cancer. However, the improved delivery efficiency of VMAT, as revealed through significant reduction of MUs, makes it more practical for patient treatment in this context.

REFERENCES: Christopher Amaloo, Daryl P. Nazareth, Lalith K. Kumaraswamy, Comparison of hybrid volumetric modulated arc therapy (VMAT) technique and double arc VMAT technique in the treatment of prostate cancer, Radiation Oncology-2015, Page 291-298 , Takeshi Hira, Dosimetric Comparison between the Intensity Modulated Radiation Therapy and Volumetric Modulated arc Therapy for Prostate Cancer- A Case Study, American Journal of Medical Case Reports, 2014, Vol.2, No.1, 1-3 , N. Ozturk, N. Ozbek, B. Depboylu, Dosimetric comparison of IMRT, VMAT and HYBRID treatment methods in radical radiation therapy of prostate cancer, International Journal of Radiation Research, April 2022, Volume20, No-2 , Ramiz Abu-Hijlih, Shatha Afifi, Abdelatif Almous, Jamal Khader, Wafa Alhajal, Ibrahim AlRjoub, Sara Mheid et al, Volumetric-modulated arc therapy versus intensity-modulated radiotherapy for localized prostate cancer: a dosimetric comparative analysis of moderate hypofractionated radiation, Oncology and Radiotherapy, Vol.14, Iss.5:017-022 , Jun Shang, Wei Kong, Yan-yang Wang, Zhe Ding, Gang Yan and Hong Zhe, VMAT planning study in rectal cancer patients, Radiation Oncology 2014., Angelia Tran, Jingjing Zhang, Kaley Woods, Victoria Yu, Dan Nguyen, Gary Gustafson, Lane Rosen and Ke Sheng, Treatment planning comparison of IMPT, VMAT and 4 π radiotherapy for prostate cases, Radiation Oncology 2017, DOI 10.1186/s13014-016-0761-0 , Rapido protocol, Version 3.1, January 2016, NL36315.042.11, EudraCT number 2010-023957-12, CKS number 2011-7997, NCT01558921, NTR3230 , Huang, Yanxiao, Determination of effective point of measurement of cylindrical ionization chambers for high energy electron and photon beams in water phantom. June 2008; P. 7-9. , P. H. Charles, G. Cranmer-Sargison, D. I. Thwaites, S. B. Crowe, T. Kairn, R. T. Knight et al., A practical and theoretical definition of very small field size for radiotherapy output factor measurements. Medical Physics, Vol. 41, No. 4, April 2014.

COMPARISON OF DIFFERENT METHOD USED FOR TRANSIENT TIME MEASUREMENTS IN TELECOBALT AND HIGH DOSE RATE BRACHYTHERAPY UNIT

Parsee Tomar¹, Ranjit Singh¹, Ngangom Robert, Rakesh Kapoor¹, Arun Singh Oinam¹, J.S. Shahi²

¹Department of Radiotherapy, PGIMER Chandigarh, India

²Department of Physics, PANJAB University Chandigarh, India

Email: parsee.tomar923@gmail.com

AIM: The current study's objective is to compare various techniques used to detect transient times in radioactive sources used in radiotherapy units. The graphical method, two exposure method, single/double exposure, and Single/multiple exposure method were among these techniques.

METHODS AND MATERIAL: In the current study, Telecobalt machine unit e.g., Bhabhatron II TAW (Panacea Pvt. Ltd), and High dose rate Afterloading Brachytherapy Unit (Eckert & Ziegler BEBIG GmbH Multisource) are employed. The dosimetry on telecobalt unit is carried out with 0.6cc Cylindrical FC65 or PTW PPC05 Parallel plate chamber, 1-D water phantom or RW3 solid water phantom and unidosel electrometer. The measurement are carried out for different field sizes ranging from 5x5 to 35x35 cm² at 5cm depth in SSD (Source to Surface distance) 80 cm. For Brachytherapy unit, PTW well type Ionization chambers and UNIDOSE Electrometer are used.

RESULTS: The effect of transit time exposure time was analyzed for telecobalt machine and Brachytherapy machine whereas its dependence with field size was checked for TeleCobalt machine only. The average values of transit time (sec) evaluated by graphical method, two exposure method, single/double exposure, and Single/multiple exposure method are 0.554±0.084 & 0.874±0.034, 0.692±0.035 & 0.741±0.006, 0.642±0.145 & 1.867±0.171 and 0.684±0.167&1.883±0.117, respectively for telecobalt and multisource Brachytherapy unit. A average variation among single/double and single/multiple exposure is found to be 14% and 6% was observed for exposure time ≤120sec and >120sec, in telecobalt. The slightly significant variation was observed in transit time for field size variation in telecobalt unit.

CONCLUSION: The transit time calculation using different method shows a significant variation among them. The results for determination of transit time were comparable with two exposure and single/multiple exposure in telecobalt unit whereas the results of single/double and single/multiple exposure are comparable. In literature it was mentioned that the number of interruption increases the reliability and accuracy of transit time measurement and similar observation was also observed in current study.

KEYWORDS: Telecobalt, Brachytherapy, dosimetry, Transit time.

Presentation ID: 284

Abstract ID: X1121

DOSIMETRIC EVALUTION OF 1D WATERPHANTOM COMPARED WITH 3D RFA

¹Vignesh Kannaiyan, ²Preethi Baskar

¹Department Radiology, SAHS, VMRF-DU Chennai, ²Department of RadioDiagnosis, SRMIST, SRM medical college Hospital & RC, Chennai, Tamilnadu, India

BACKGROUND/OBJECTIVE: Radiation therapy is the treatment of malignant disease, using ionization radiations. Radiation can be used to kill cancer cells very effectively. Depending on the type and stage of cancer, radiotherapy is carried out by either curative treatment (to cure cancer and reduce the risk of it recurring) or by palliative treatment. Phantoms were used to measure the output of the Radiotherapy machines. The goal of the radiotherapy is to deliver maximum dose to the tumour and minimum dose to the surrounding normal tissues. The aim of this study was to compare and investigate between the 3D RFA and 1D Water Phantom by using the Ionization Chamber for the LINAC machine.

MATERIALS AND METHODS: The phantom measurements were carried out in a linac in 0° gantry angle and 0° collimator for 10×10 cm² field sizes. The 1D water phantom (30×30 x 30 cm³) is kept on the treatment couch and alignment done with laser light, such that the beam should normally incident on the phantom surface plane, also central axis of the beam should pass through the sensitive region of the chamber. Now the chamber is inserted into the water phantom measured. Farmer type chamber .6cc is used. and different size angle wedge using measured values. The Measurement is taken in the machine of LINACs.

RESULTS: 1D Water phantom to measure the 6 and 15 MV photon beams in LINAC machine. The accuracy of the 1D water phantom was measured mechanically using the standard scale with the counter meter of the 1D water phantom forward and backward movement of the counter. The counter meter readings were compared with standard scale reading. Both readings were found very close and accuracy of the 1D Water Phantom ± 1mm.

CONCLUSIONS: The 1D Water Phantom dosimetric measurement compared with imported 3-D RFA Phantom. Both the dosimetric & mechanical values compared and both values were good in agreement.

KEYWORDS: Radiotherapy, 1D Phantom, QA, 3DRFA

EFFECT OF DIFFERENT DELIVERY DOSE RATE ON DOSIMETRIC PARAMETERS AND PRETREATMENT QUALITY ASSURANCE: A PHANTOM STUDY

Moirangthem Nara Singh^{1,*}, Shantanu Kumar Mishra¹, Bimugdha Goswami¹,
Shraddha Srivastava²

¹Department of Radiation Oncology, Dr. B Borooah Cancer Institute, Guwahati, India,

²Department of Radiotherapy, King George's Medical University, Lucknow, India

Email: naraphysicist@gmail.com

BACKGROUND/OBJECTIVE: The aim of the work is to investigate how the different delivery dose rates in an intensity-modulated radiation therapy (IMRT) plan affect the precision and reliability of the prescribed dose to the anthropomorphic phantom.

MATERIALS AND METHODS: CT images of an anthropomorphic phantom was acquired in a Philips big-bore CT simulator with 1 mm slice thickness. Typical brain tumour targets and OARs (brainstem, right and left eye, right and left eye lens, right and left optic nerve, chiasm, mandible, and oral cavity) were contoured. Six IMRT plans were made in Varian Eclipse treatment planning systems (TPS), each plan with different delivery dose rates (100, 200, 300, 400, 500, and 600 MU/min). After fulfilment of the acceptability criteria of the plan, approved plans were delivered in Trilog Linear Accelerator. Dosimetric parameters such as homogeneity index (HI) and conformity index (CI), dose to the organs at risk, and monitor unit (MU) were analysed. On the delivery side, pretreatment plan verification was done using an electronic portal imaging device (EPID). The verification and delivered plans were analysed using quantitative evaluation parameters such as distance to agreement (DTA), maximum and average gamma, and the field area with a gamma value.

RESULTS: When the dose rate was decreased, the dosimetric outcomes, such as HI and CI of the target as well as dose sparing of organs at risk, are improved. It was found that increased dose rates gradually increased the delivered monitor unit. Moreover, the low dose rate resulted in a better gamma agreement between the calculated and measured portal doses. It observed that 400 MU/min was optimum, and lowering the dose rate gives better gamma agreement between the calculated and measured portal doses of complicated fields. It may be attributed to the less complex motion of MLC over time and the MU of the field/segment.

CONCLUSIONS: When comparing the dosimetric parameters of these six plans with varying delivery rates, the plans with lower delivery rates showed better results and required more treatment time. For minimal internal organ movement, however, a short treatment duration with a high dose rate plan works best practically.

KEYWORDS: Dose rate, Anthropomorphic Phantom, IMRT, Portal dosimetry

Evaluation of Aperture Based Complexity Metrics for Intensity-modulated Radiation Treatment Plan and its Correlation with Gamma Passing Rates

Suresh Yadav¹, Dinesh Kumar Saroj^{2,3}, Neetu Paliwal³, Ravindra Shende², Gaurav Gupta²

¹Department of Radiation Oncology, Gandhi Medical College, Bhopal-462001 (M.P.), India.

²Department of Radiotherapy, BALCO Medical Center, A Unit of Vedanta Medical Research Foundation, New Raipur, Chhattisgarh, India, ³Department of Physics, Rabindranath Tagore University, Madhya Pradesh, India

E-mail: syadav.gmc@gmail.com

BACKGROUND/OBJECTIVE: The complexity metric has been proposed as a viable and time-saving option in conjunction with existing quality control approaches. The complexity metric serves as a measuring tool within the quality assurance (QA) process, evaluating the level of challenge and the success of dose delivery by generating a complexity score based on the treatment planning results obtained from the treatment planning system. This study aims to find the correlation between plan complexity metrics and gamma index analysis in patient specific quality assurance (PSQA) of Intensity-modulated radiation therapy (IMRT) for carcinoma of oesophagus.

MATERIAL & METHOD: A Python-based script was used to compute the various complexity metrics. We used Beam Modulation (BM), Monitor Units (MU), Edge Metric (EM), and Modulation Complexity Score (MCS) to quantify the complexity of the IMRT treatment plan. Arc CHECK diode array detector was used to perform the PSQA to analyse the gamma passing rates (GPR) with commonly used criteria of 3% and 3mm and 2% and 2mm at 10% threshold.

RESULTS: The average reported value for BM, MU, MCS and EM were 0.734 ± 0.07 , 749.32 ± 231.10 , 0.313 ± 0.067 and 0.083 ± 0.022 respectively. The average gamma passing rates for the 3% 3mm and 2% 2mm were $98.93 \pm 1.6\%$ and $92.44 \pm 8.13\%$ respectively. For 3% and 3mm GPR criteria, the Pearson coefficient for BM vs GPR, BA vs GPR, EM vs GPR and MCS vs GPR were -0.477, -0.422, 0.313 and 0.095 respectively. For 2% and 2mm GPR criteria, Pearson coefficient for BM vs GPR, BA vs GPR, EM vs GPR and MCS vs GPR were -0.640, -0.740, 0.571 and 0.105 respectively.

CONCLUSION: Smaller value of BM, MCS, and EM indicates that the oesophagus IMRT plan are less complex in nature. MU shows the negative weak correlation with GPR. BM, MCS and EM are weakly correlated with GPR. The correlation between MCS, MU, and GPR is significant since it provides a straightforward measure of complexity and an indication of the plan's deliverability. This information can be valuable throughout the entire treatment planning and QA process.

KEYWORDS: Intensity-modulated Radiation Therapy, Modulation Complexity Score, Beam Modulation, Gamma Passing Rates, Carcinoma Oesophagus.

Presentation ID: 287

Abstract ID:M9886

Operational Experience of Internal Dosimetry Monitoring Using FAST-SCAN type WBC over a Decade at Kaiga Site

M. Uday Kishor¹, Sanyam Jain², R.M.Joshi², M.S.Vishnu²,G.K.Sunil¹, B.Vinod Kumar¹

¹ Kaiga Generating Station, Karnataka India,

²Environmental Monitoring and Assessment Division, BARC, Mumbai, India

Email: mukishor@npcil.co.in

BACKGROUND/OBJECTIVE: Whole-body counting is an indispensable tool in the Nuclear Industry where it plays a crucial role in the monitoring of internal exposure of high-energy gamma emitters in occupational radiation workers. Moreover, it can be utilised in assessing the radioactivity intake of the populace during significant nuclear accidents. This study highlights the benefits and operational experiences that can be derived from the implementation of a high throughput FAST SCAN type Whole Body Counting (WBC) System in a multi-unit Nuclear Power Plant Site.

MATERIALS AND METHODS: Internal contamination can be assessed by the use of various methods such as bioassay, whole-body counting, lung counting and thyroid counting. Shadow Shield Whole Body Counters with a small NaI (TI) scintillation detector are used for in-vivo monitoring high energy gamma emitters in Nuclear Power Plants (NPPs) in India, with a detection limit of approximately 300Bq for ¹³⁷Cs or ⁶⁰Co in 11 minutes. In 2007, a revolutionary FAST SCAN type Whole Body counter was introduced at ESL, Kaiga site, making it the first of its kind in India. FAST SCAN type WBC accurately measures ingested or inhaled radioactivity in subjects covering all their body size, using a linear geometry counter with two large NaI (TI) detectors. With a Minimum Detection limit of 150 Bq of ¹³⁷Cs or ⁶⁰Co in a 1-minute count, the device provides a reliable way to monitor internal exposure.

RESULTS: The multi-unit site of NPP has an average load of about 3000-5000 occupational workers yearly. The FAST SCAN type whole body counter has been utilized since 2007 and has counted over 46,000 occupational workers. The system was extremely useful to rule out internal exposure of gamma emitters in occupational workers during tritium uptake incidents at the Kaiga site.

CONCLUSION: The FAST SCAN type whole body counting system has proven to be an incredibly valuable tool for monitoring internal exposure at the Kaiga site during normal and emergency conditions.

Keywords: whole body counting, nuclear reactor, internal dosimetry.

Presentation ID: 288

Abstract ID: K8442

Establishing a link between practical and radiobiological consideration in cervical cancer: A single institution study

Asit panigrahy, Dr.kanan Jassal, Radhika V Kartaha, Chetan Verma, Dr.kiran Paul, Dr.Ravindra Mahajan

Department Of Radiation Oncology, Inlaks And Budhrani Hospital, Koregaon Park,Pune, Maharashtra, India

Email: asitsitu66@gmail.com

BACKGROUND/OBJECTIVE: The aim of this study is to analyze the radiobiological changes occurring due to the prolonged treatment duration and further adding the compensatory dose to obtain the desired TCP. External beam Radiotherapy in combination with brachytherapy is the line of treatment for curing cervical cancer and to ensure the overall tumor control probability (TCP). The overall treatment time may get increased due unavoidable factors. The prolonged treatment days must be taken into account. This can be achieved by evaluating the change in EQD2 and increasing the dose to achieve desired TCP.

MATERIALS AND METHODS: Seven patients were studied who underwent the external beam radiotherapy (EBRT) for 50.4 Gy / 28 # and brachytherapy for 7 Gy / 3 #. As per the international recommendations, the combined treatment of EBRT and brachytherapy in case of cervical cancer should be delivered within 8 weeks (56 days). Selected patients had prolonged treatment days as 58 to 81 days. Contouring of the HR-CTV, BLADDER and RECTUM were done by radiation oncologist as per ICRU 89. The parameters selected for the HR-CTV coverage was D98% (in Gy) and for the bladder and rectum D2cc (in Gy) were taken. EQD2, survival fraction and TCP were calculated using the formulas

$$EQD2 = \frac{\alpha/\beta}{2+\alpha/\beta} \left[D_{EBRT} \left(1 + \frac{d_{EBRT}}{\alpha/\beta} \right) + D_{BT} \left(1 + \frac{d_{BT}}{\alpha/\beta} \right) - \frac{\ln 2}{T_d} (T - T_k) \right], S = e^{\left(-\alpha d - \frac{\beta d^2}{n} - \frac{\ln 2}{T_d} (T - T_k) \right)}, TCP = e^{-(SK)}$$

RESULTS:

TCP OF DIFFERENT PATIENT WITH $\alpha/\beta=10\text{Gy}$, $T_d=4.5\text{days}$, $T_k=19\text{days}$, K (tumour clonogenic number) =965				
PATIENT NO.	TOTAL DAYS (EBRT+BT)	(EQD2) _{patient}	$\Delta EQD2 = (EQD2)_{reference} - (EQD2)_{patient}$	TCP
1	72	72.217	2.1626	0.99986
2	81	70.914	3.4657	0.99916
3	74	72.147	2.2334	0.99981
4	58	74.106	0.274	1
5	59	73.446	0.934	1
6	62	73.626	0.7539	1
7	59	73.882	0.4985	1
REFERENC E	56	74.38(EQD2) _{referenc e}		

CONCLUSIONS: Patients with prolonged treatment days greater than 70 show a reduction in TCP as well as change in EQD2. By adding 2.13 Gy, 2.13 Gy and 3.15 Gy for patient 1, patient 2, patient 3 respectively to the fractional dose in their last fraction of brachytherapy the desired TCP was achieved. After compensating for dose in brachytherapy the D2cc of bladder and rectum were under tolerance as per ICRU 89.

KEYWORDS: TCP,EQD2,Brachytherapy, EBRT

SMALL FIELD EXTERNAL BEAM DOSIMETRY AND DEVELOPMENT OF AN IN-HOUSE SOFTWARE USING PYTHON FOR THE ANALYSIS AND COMPARISON OF BEAM DATA PROFILES

Raja Kannan¹, Arul Pandiyan², Prabhakar Ramachandran³, Aruna Prakasa Rao³

¹Department of Medical physics, Anna University, Chennai, India,²Department of Medical Physics, Cancer Institute WIA Adyar, ³Department of Medical Physics, Anna University, Chennai, India

Email: rajakannan959@gmail.com

BACKGROUND/OBJECTIVE: This study showcases the collection of beam data for various beam energies in small fields and the development of an in-house software tool utilizing Python for the analysis of beam data profiles. The software's primary objectives are to provide a user-friendly platform to read and analyze both reference and measured profiles and to apply 1D gamma criteria for quantitative evaluation. Additionally, the software incorporates smoothing options to enhance accuracy and reproducibility of the analysis.

MATERIALS AND METHODS: Beam data profiles were acquired using a Varian Truebeam SVC linear accelerator, equipped with a high-definition multileaf collimator (HD MLC120). The dosimetric measurements were conducted using a computer-controlled radiation field analyzer, the PTW Beamscan water phantom. PTW Diode SRS and PTW Pinpoint cylindrical ion chambers were used as detectors for small field (2x2, 3x3, and 4x4) profile measurements. The project involved extensive data collection for 6 MV, 6 MV FFF, 10 MV, 10 MV FFF, and 15 MV x-rays, all within the realm of small field dosimetry. The software was developed using the Python programming language and open-source libraries, ensuring versatility and ease of access across various operating systems. It enables users to conveniently import reference and measured beam data profiles from different measurement devices. The software's 1D gamma criteria method allows for the calculation of gamma index values for each data point pair, thus quantifying the agreement between the two profiles. Additionally, it includes functionalities for computing symmetry, flatness, D20/D10, Dmax, surface dose, penumbra, and field size using the full-width at half-maximum method.

RESULTS & CONCLUSIONS: The developed in-house software presents a simple and accessible tool for beam data profile analysis of high-energy beams on linear accelerators. Ongoing efforts are focused on incorporating an optimization algorithm to identify the most effective smoothing technique for reducing noise present in the raw data, and developing a web-based interface for beam data analysis. The test results indicate that all the systems and sub-systems of this accelerator is performing as per specification and it may be commissioned for patient treatment.

KEYWORDS: Small field, beam data profile, python.

Presentation ID: 290

Abstract ID: T3950

PERFORMANCE EVALUATION OF PROTON THERAPY ACCELERATOR USING AERB ACCEPTANCE TEST/QA PROTOCOL

P. K. Dixit, G. Sahani, S. Mahalakshmi, Smriti Sharma, R. L. Sha, Kishore Joshi, P.K. Dash Sharma

Radiological Safety Division, Atomic Energy Regulatory Board, Mumbai, India

Email: dixit.pk@gmail.com

BACKGROUND/OBJECTIVE: Performance evaluation medical accelerators are carried out by Atomic Energy Regulatory Board (AERB) as an important part of safety review process before issuance of licence for its operation. As proton therapy accelerators were introduced in India, there was a requirement of comprehensive QA/Acceptance protocol. As no QA/Acceptance protocol was available for proton therapy accelerators, AERB prepared a comprehensive acceptance test/QA proton therapy accelerators. In the present paper, details of the QA/acceptance protocol and its usefulness while using it for performance evaluation proton therapy accelerators are discussed.

MATERIALS AND METHODS: The QA/acceptance protocol was used for proton therapy accelerators having maximum beam energy & beam current 230 MeV & 300 nA respectively. The QA/Acceptance protocol for proton therapy accelerator are divided into different parts. Initial part consists of general information about the proton therapy accelerator such as make, model, energies & current, ion source, details of nozzles & scanning, treatable field sizes. Second part provides performance of design safety features, tests related to mechanical accuracy & interlocks. Third part consist of dosimetric tests and other safety aspects such as availability of emergency preparedness plan and radiation monitoring/measuring instruments. The last part provides radiation protection survey in and around the installation. After preparation of the QA/Acceptance protocol it was used at the proton therapy facilities for ensuring its feasibility of testing/demonstration at the utility site.

RESULTS: The performance test results of the proton therapy accelerator using the QA/Acceptance protocol of AERB was found to be covering the required parameter for mechanical accuracy, electrical interlocks, dosimetric and radiation safety. All the parameters of the equipment are found to be satisfactory and found to be achievable within tolerance limit.

CONCLUSION: The comprehensive QA/Acceptance protocol of the proton therapy accelerator is found to be feasible for its implementation in the country and can be used by the institutions while carrying out commissioning tests of the proton therapy accelerator. Considering various recent publications from AAPM-TG and IEC, the QA/Acceptance protocol of AERB may be revisited.

Presentation ID:291

Abstract ID:X7490

STUDY OF BEAM PROFILE CHARACTERISTICS USING SNC RFA AND SNC IC PROFILER IN DIFFERENT DOSE RATE OF ELECTRON BEAMS

Jegatheeswaran.V,¹Dinesh.A,¹Dr Yogesh D Kale²

¹Department of Radiation Oncology, Sterling Hospitals, Vadodara, Gujarat, India

² Department of Physics,Parul University,Vadodara, Gujarat, India

Email: jegathees.physicist@gmail.com

BACKGROUND: The aim of this study is to evaluate beam profile characteristics verification in 6MeV and 6MeV HD electron beam with different dose rates and also performance of Sun Nuclear Corporation (SNC) IC profiler and Sun Nuclear Corporation (SNC) RFA

MATERIAL AND METHODS: Varian TrueBeam Stx machine here chosen for electron 6MeV and 6MeV HD electron beam with available applicators size 6x6, 10x6, 10x10, 15x15, 20x20 and 25x25 with depth of R80/2 used SNC RFA and SNC IC profiler with software.This study includes parameters such as Field Size, Flatness, Symmetry, Penumbra, Beam center with using IEC protocol.

RESULTS:(1)Low range dose rate 100-400MU/Min 6MeV(2)Medium range dose rate 500-1000 MU/Min 6MeV compared with High dose rate 2500 MU/Min 6MeV HD results are follows based on IEC using IC Profiler.(1-1)Characteristics are analyzed such as Field Size, Flatness, Symmetry, Penumbra, Beam center and differences are 0.7cm,±1.3%,±2.1%, ±0.25cm, ±0.2cm respectively in Inplane and ±0.6cm,±0.6%,±1.2%, ±0.28cm, ±0.02cm respectively in Cross plane. (2-1)Characteristics are analyzed such as Field Size, Flatness, Symmetry, Penumbra, Beam center and differences are ±0.6cm,±0.6%,±1.2%, ±0.28cm,±0.03cm respectively in Inplane and ±0.54cm,±1.52%,±1.92%, ±0.29cm, ±0.17cm respectively in Cross plane. (3)STD dose rate 600 MU/Min 6MeV (4) High dose rate 2500 MU/Min 6MeV HD using SNC IC profiler compared with SNC RFA results are follows based on IEC. (3-1)Characteristics are analyzed such as Field Size, Flatness, Symmetry Penumbra, Beam center and differences are±0.5cm,±0.4%,±0.4%,±0.15cm,±0.07cm respectively in Inplane and ±0.2cm,±0.6%,±0.02%, ±0.16cm, ±0.03cm respectively Cross plane.(4-1)Characteristic are analyzed such as Field Size, Flatness, Symmetry, Penumbra, Beam center and differences are ±0.4cm,±2.62%,±1.21%, ±0.08cm, ±0.61cm respectively in Inplane and ±0.41cm,±0.17%,±1.24%, ±0.114cm, ±0.021cm respectively Cross plane.

CONCLUSION: Over all differences observed in this study with in the limit, we noticed SNC IC profiler has some limitation, the ion collection efficiency of the profiler decreased as the dose per pulse increased. Flatness and Symmetry differences are more than ±2% in 6MeV HD electron but within the tolerance. In Profile, by using IC Profiler 6MeV HD electron flattened region are not smooth in comparison with RFA profile flattened region, it may be due to sensitivity of Ionization chamber in SNC IC profiler.

MONTE CARLO DOSIMETRIC STUDY IN WATER & BONE MEDIUM COMPARES WITH AAA AND ACUROS XB

Tanny Bepari¹, Md Mokhlesur Rahman¹, Md Anwarul Islam²

¹Department of Medical Physics and Biomedical Engineering (MPBME), Gono Bishwabidyalay, Savar, Dhaka, Bangladesh. ²Department of Radiotherapy, Square Hospital Limited, Dhaka, Bangladesh.

Email: attojatonny@gmail.com

BACKGROUND: The purpose of this study was to verify the Monte Carlo (MC) dose calculation for a Varian 2100CD linac and investigate the impact of MC simulation in water and bone media compared with other TPS algorithms. The Electron Gamma Shower (EGSnrc) Monte Carlo user codes had performed photon beam simulations. For 6MV photon energy, BEAMnrc software designed the geometry of the treatment head.

MATERIALS AND METHODS: The field size 10x10 cm² & 20x20 cm² has been used to characterize dose output, depth dose profiles, and photon spectrum. DOSXYZnrc created the virtual rectilinear voxel phantoms. In water medium for getting PDD, voxel size 01x01x.25 cm³ used along the z-axis & its phantom size was 40x40x30 cm³. At the same time, for the profile, voxel size 01x0.2x01 cm³ was used along the x and y axes & the phantom size was 40x40x30 cm³. In bone media, for getting PDD voxel size, 0.25x0.25x1 cm³ was used along the z-axis & its phantom size was 24.25x24.25x20 cm³.

RESULTS: The simulated PDD and beam profile ranges from 0.15 cm to 0.35 cm for full width half maximum (FWHM). The design of Varian 2100CD linac has been validated for a 6.4 MV spectrum beam with FWHM 0.35 cm. In water media, the average gamma pass rate of PDD for 3%/3mm, 2%/2mm, and 1%/1mm was 100%, and in the case of beam profile for 3%/3mm, 2%/2mm was 100%, and 95.2% respectively. In bone media, AAA calculation and simulated data showed good agreement, and the gamma pass rate was 100%. While in bone medium, Acuros XB calculation and simulated data showed a deviation of gamma pass rate 100%. There are no significant differences found in AAA, Acuros XB, and MC simulation for the 3%/3mm Gamma index.

CONCLUSIONS: The depth dose and beam profile were calculated using MC simulation code and found good agreement with measure data in both water and bone mediums. The MC dose calculation was more accurate than AAA in the presence of bone & more closely with Acuros XB results.

KEYWORDS: EGSnrc, Monte Carlo simulation, AAA, Acuros XB, TPS

INVESTIGATION ON INDIGENOUSLY DEVELOPED NON-METALLIC ARTIFACT FREE SENTHIL CT BREAST SCAR MARKER IN EXTERNAL BEAM RADIOTHERAPY

Senthilkumar Shanmugam¹, P.Arana², AnupriyaN²

¹Regional Cancer Center (RCC), Madurai Medical College & Govt. Rajaji Hospital, Madurai, Tamilnadu, India

²Anna University CEG CAMPUS Guindy, Chennai, Tamilnadu, India

Email:anuraj2331@gmail.com

BACKGROUND/OBJECTIVE: Breast cancer remains a significant global health concern, demanding precise and reliable diagnostic tools for early detection and treatment monitoring. This investigation explores the application of an indigenously developed non-metallic artifact-free Senthil CT breast scar marker in radiotherapy for breast cancer patients. Traditional metallic markers used for scar localization during radiotherapy can cause image artifact, shifting isodose and affecting treatment accuracy. The novel non-metallic marker aims to overcome this limitation and improve the precision of radiotherapy treatment planning.

MATERIALS AND METHODS: The marker is composed of a biocompatible, radiolucent material, which minimizes the potential for image distortions and artifacts, avoiding the interference that metallic markers commonly cause. Extensive phantom studies and simulations are conducted to evaluate the impact of the non-metallic CT marker on image quality and artifact reduction. Testing is performed using standardized phantoms and realistic breast tissue models to assess the performance of the non-metallic marker.

RESULTS: Preliminary results demonstrate that the indigenously developed non-metallic artifact-free Senthil CT breast scar marker provides clear and accurate visualization of breast scar tissue without introducing image artifacts. In phantom study the metallic markers shifting the isodose line under the marker but there is no such shift when using the non-metallic Senthil CT breast scar marker. The marker's non-metallic composition ensures it is well-suited for CT imaging applications, while also enhancing patient comfort during the examination.

CONCLUSION: This investigation demonstrates the potential of the non-metallic artifact-free Senthil CT breast scar marker to enhance the accuracy of radiotherapy for breast cancer patients. By eliminating image artifacts and improving treatment localization, the marker holds promise in optimizing radiotherapy outcomes and enhancing the quality of care in breast cancer management. The indigenously developed non-metallic artifact-free Senthil CT breast scar marker offers significant advantages in radiotherapy for breast cancer patients, including improved treatment accuracy, reduced image artifacts, enhanced patient safety, and cost-effectiveness.

KEYWORDS: non-metallic, artifact-free, Senthil CT breast scar marker, radiotherapy, breast cancer, image artifacts.

Presentation ID:294

Abstract ID: C9275

KVCBCT IMAGING OF HALCYON AND PTV MARGINS FOR HEAD AND NECK CASES

Sajini S Kurup, V.K.Sathiya Narayanan, Raghavendra Holla, Asmita Doiphode, Pooja Moundekar, Dince Francis, Surendra Pawar, Swapna Nakhale

Email: snjsk8@gmail.com

PURPOSE: The aim of the study is to assess CTV to PTV margin for Head and Neck Cancer cases based on daily KVCBCT imaging over the course of treatment in Halcyon machine and compare this with PTV margins obtained by MVCBCT of Oncor impression Plus machine.

MATERIAL AND METHODS: Radiotherapy for Head and Neck Cancer has been evolving greatly especially in terms of imaging while treatment. Hence, we have to ensure that the errors while patient positioning remains as low as possible. This can be achieved by having good imaging modality and calculating the systematic and random errors effectively. Forty Head and Neck Cancer were taken who were treated by Rapid Arc method between the periods of February 2021 to June 2021 in Halcyon machine. All the patients had CTV to PTV margin of 5 mm while treatment planning. Daily KVCBCT based matching was chosen as the reference method. Based on the shifts obtained, the systematic and random errors were calculated in the three directions X, Y and Z respectively using the Van Herk formula. These margins were then compared with the margins that were previously obtained with MVCBCT imaging.

RESULT: The study included forty patients with Head and Neck Cancer treated by Rapid Arc method. 400 CBCT images were obtained and taken for the study. The margins obtained were as given in the tabular column below.

Parameter	KVCBCT	KView(MVCBCT)
	Halcyon	Oncor
Systematic Error	3.08 mm	1.4 mm
Random Error	1.12 mm	2.2 mm
(PTV margin) AP=PA direction	3.7mm	4.9 mm
Medio-Lateral direction	4.35 mm	5.2 mm
Cranio-Caudal Direction	4.61 mm	5.1 mm

CONCLUSION: It is seen that as the image quality has improved from MVCBCT to KVCBCT, the PTV margins that has to be added has come down by a millimeter. This study is an on-going project in which more population and samples can be added so that the PTV margins can be calculated and taken as a standard margin value for Head and Neck Cancer cases which would be treated in Halcyon Machine

Presentation ID:295

Abstract ID:H6778

EMINENT ROLE OF OPERATIONS, AI AND BIG DATA ANALYTICS IN TRANSFORMING HEALTHCARE INDUSTRY

Pranjali Verma,PurnimaS. Sangle

¹National Institute of Industrial Engineering, Department of Analytics and Data Science, NITIE, Mumbai, India

Email: profpranjali@gmail.com

BACKGROUND/OBJECTIVE:AI and Big Data Analytics are the two emerging technologies influencing every field including healthcare. During pandemic with the help of these tools , algorithms and analytics we can analyze the affected areas and took preventive measures accordingly. For example: Deep Learning Algorithms and Markov Model are successful in detecting cancer cells at early stage. Healthcare industry is surrounded by lots of complex , unorganized, and unstructured data. Humans alone can't produce best insights out of this huge(peta and zettabytes) of data, so advanced AI Algorithms in combination with Big Data Analytics can be used to find hidden patterns and make a healthy world with predictive analytics for preventive healthcare. Confluence of AI , Big Data and Operations Management has a potential to revolutionize the healthcare industry.

MATERIALS AND METHODS:Reviewed existing journals, articles and research papers. A structured empirical study is done in order to foster the further advancements in this area.

RESULTS:Exploratory Data analysis of different AI/ML/DL algorithms and their success rates for different diseases. Management of Healthcare data and management Big Data technologies.

Conclusions: This research is based on critical literature analysis and outlines the recent propitious practices of AI and Big Data in Healthcare Industry with their future scope.

KEYWORDS:AI(Artificial Intelligence), Big Data Analytics, Deep Learning, Healthcare, Operations.

DOSIMETRIC COMPARISON OF VMAT AND IMRT PLANS FOR SBRT HEPATOCELLULAR CARCINOMA PATIENTS WITH AND WITHOUT FLATTENING FILTER

Anju K V, Hanuman PrasadYadav, Sreejesh M S, Deepti Sharma, Deepak Jagya, Subramani Vellaiyan

Email: anjurajankv@gmail.com

OBJECTIVE: Stereotactic Body Radiation Therapy (SBRT) is a potent and precise treatment for Hepatocellular Carcinoma (HCC). Volumetric Modulated Arc Therapy (VMAT) and Intensity-Modulated Radiation Therapy (IMRT) are commonly used in SBRT for HCC. The study aims to compare VMAT and IMRT plans for SBRT in HCC patients with and without a flattening filter, focusing on dosimetric parameters, target coverage, and organ-at-risk sparing.

MATERIAL & METHODS: In this retrospective study, fifteen HCC patients underwent SBRT, with treatment plans created using 10 MV in Monaco Treatment Planning System (TPS). Two treatment plans were compared: one using VMAT technique and the other using 7-field IMRT technique, both with and without the flattening filter, at a prescribed dose of 35 Gy in 5 fractions. Dosimetric parameters, including target coverage, conformity index (CI), homogeneity index (HI), and OARs doses were compared

RESULTS: VMAT-FFF exhibited improved conformity and homogeneity in these plans. VMAT consistently demonstrated reduced delivery time compared to IMRT plans, regardless of the flattening filter usage. IMRT FFF method generated a higher number of Monitor Units (MU) compared to all other techniques. Paired t tests showed highly significant differences in MU between VMAT with FF and FFF ($p=0.004$) and IMRT with FF and FFF ($p=0.0463$). In addition, VMAT with FF had significantly lower MU than other techniques, and FFF techniques resulted in lower OAR doses for both IMRT and VMAT compared to their respective FF counterparts. Analysis of the planned target volume (PTV) doses revealed that VMAT FFF techniques exhibited higher Dmean, Dmin and Dmax dose compared to VMAT FF techniques. Similarly, IMRT FFF techniques showed higher PTV doses than IMRT FF techniques. Despite the variations, no statistical significance was found.

CONCLUSION: The findings of this study suggest that VMAT offers improved dose conformity and homogeneity compared to IMRT for SBRT HCC patients, with or without the flattening filter. VMAT plans were not substantially influenced by the flattening filter's presence, whereas IMRT plans showed minor improvements with the filter. Further investigations with larger patient cohorts are warranted to validate these findings and assess long-term clinical outcomes.

Presentation ID:297

Abstract ID:R5701

OPTIMIZING INTENSITY MODULATED RADIATION TREATMENT PLANNING FOR ENHANCED CONSERVATION OF DARS

Chetanprakash Verma, Dr Kanan Jassal, Radhika Kartha, Asit Panigrahy, Dr. Kiran Paul, Dr Vaishali Shinde

Department of Radiation Oncology, Inlaks and Budhrani Hospital, Pune, India.

Email: chetanprakash16895@gmail.com

BACKGROUND/OBJECTIVE:The aim of this study is to investigate reduction in mean dose to DARS (Dysphagia Aspiration Risk Screen) without effecting the quality of the plan using Monte Carlo Algorithm. The variation in plan quality was determined using DHI (Dose Homogeneity Index) and C.I. (Conformity Index).

MATERIALS AND METHODS:

- 1. Patient Selection:** The study was conducted on 20 head and neck plans comprising diverse cases across different cancer types. These patients had dose prescription of 66Gy in 30 fractions and 60Gy in 30 fractions.
- 2. Treatment Planning System:** The Monaco 5.11.03 version was utilised as the primary treatment planning system for all patients.
- 3. Study Groups:** The selected cases were planned for both with constraints to DARS and without considering DARS in optimization. All other parameters were kept same in both study sets. 95% Isodose coverage to at least 95% of PTV volume was the primary checkpoint. Doses to the OARS was also verified using QUANTEC.
- 4. Dosimetric parameters:** Plan quality was evaluated using parameters such as C.I. (Conformity Index) and DHI (Dose Homogeneity Index). C.I. has been calculated in reference to 'Evaluation of Conformity and Homogeneity Indices Consistency Throughout the Course of Head and Neck Cancer Treatment With and Without Using Adaptive Volumetric Modulated Arc Radiation Therapy'

RESULTS: It was observed that average difference in percentage of plans without and with DARS optimization was $13.5\% \pm 4.034\%$. Average percent difference in Conformity Index calculated for without DARS optimization plans and with DARS optimization was $-1.1\% \pm 0.9\%$. Average percent difference in Dose Homogeneity Index calculated for without DARS optimization plans and with DARS optimization was $-1.34 \pm 0.2\%$

CONCLUSIONS: It can be concluded that plans with DARS optimization leads to better conservation of DARS and does not hamper the plan quality and improves the QoL (Quality of Life) of the patient.

KEYWORDS: DARS, Monte Carlo, DHI, CI

Presentation ID:298

Abstract ID: A1139

ANALYSIS OF VOCS USING GC-MS TECHNIQUE- A PILOT STUDY

N. Samta¹, R. Hemapriya¹, C.S. Sureka¹, P. Venkatraman², Alok J. Verma³, Amol Bhagawat³¹Department of Medical Physics, Bharathiar University, Coimbatore- 641 046, Tamil Nadu²Department of Medical Physics, Bharathidasan University, Trichy- 620 024, Tamil Nadu³SAMEER, IIT Campus, Powai, Mumbai-400 076, Maharashtra

Email: samtananju410@gmail.com.

Background : Gas Chromatography-Mass Spectroscopy (GC-MS) applications are becoming more common in field breath analysis across the world. VOC analysis has evolved as a viable noninvasive tool for the detection and monitoring of a variety of illnesses. Researchers used the GC-MS approach to identify a variety of volatile organic compounds, including alkane and aromatic chemicals, to identify a variety of disorders in human exhaled breath. Tedlar bag optimization was used to examine the GC-MS data.

Materials and Methods: Several samples were collected in tedlar bags for this experiment on the same day as the GCMS analysis. Nitrogen, acetone, formaldehyde, and ethanol were collected as a single compound, and the gases were combined at atmospheric temperature in the ratios of 1:2, 1:1, and 2:1 of acetone and formaldehyde. To analyze volatile chemicals, the trapping and purging process was utilized. The GCMS-TD (Thermal Desorption) detector was used in our experiment. The TD technique is used to heat solid or semisolid materials while they are surrounded by an inert gas flow. Water that cannot be injected into the capillary GC column is removed with the help of a sorbent housed in a second tube.

Results: The X-axis in GC-MS denotes retention time, while the Y-axis shows concentration or intensity counts. The time it takes for the analyzers to flow through the column and reach the mass spectrometer detector is shown on the x-axis of the gas chromatogram. The retention duration is affected by gas chromatography factors such as flow rate, injection temperature, oven temperature, and so on.. Nitrogen (G01) comprises n-Hexane, Benzene, and Dimethyl Disulfide as chemical molecules. Acetone (G02) comprises organic Halofantrine molecules. Formaldehyde (G03) comprises Nizatidine and Ethane 1,1 - diethoxy chemical molecules. The NIST library match factor mentioned above.

Conclusion: The most effective method for analyzing VOC biomarkers uses GC-MS for the high degree of sensitivity, easy metabolite identification, and multiple options for sample preparation. But there are a few limitations as sample preparation could be time-consuming, destructive analysis, system immobile, slow and expensive and not suitable for clinical use.

Acknowledgments: The authors acknowledge the Rashtriya Uchchattar Shiksha Abhiyan (RUSA) (BU/RUSA2.0/BCTRC/2020/BCTRC-CD09), for financial support and the Department of Science and Technology (DST-TDP-BDTD, (TDP/BDTD/02/2021/General and Capital)), India for knowledge up gradation.

PRAXIS OF PRINCIPLES OF OPERATIONS MANAGEMENT FOR FLAWLESS RADIATION THERAPY

Ajaykumar Arvind Deshmukh , Prashant Dhoke, Kartar Singh
R S T Regional Cancer Hospital Nagpur Maharashtra.

Email: ajayprecise@gmail.com

PURPOSE AND BACKGROUND: In present day context artificial intelligence entered into the modern radiotherapy setups. Technology SGRT,SRS,SRT, Tomotherapy. Particle therapy like Proton therapy where science and Technology are at its extreme to curb and eradicate cancer cell colony in body .Here it becomes essential to implement stringent standard operating procedures to maintain the accuracy and correctness of planned outcome. Medical Science and Technology culminates to achieve ideal result. Nonetheless, inadvertently induced error in process may augment manifold ,considerably deteriorating the expected results.

MATERIALS AND METHOD: While adopting modality like SGRT SRS SRT ,QA of Machine,TPS, patient plan and the QA of QA equipment like electrometer, chamber, RFA, 4D array, in Vivo probe becomes of vital importance. Machine ,beam, plan,mlc QA is very important . For those procedures, we have applied the principles of measurement system analysis(MSA) a tool of operations management.MSA is combined study of part to part variation and measurement variation. Source of variation in treatment process, machine, material ,method, planning and verification. Causes of variation(4M- man machine material method) applied TQM principles comprehension, commitment, competence, correction ,communication, continuance. Kizen and 5S seiri,seiton,seiso,seiketsu,shitsuke to organize internal department.Incorporated 7QC tools and lean sigma for process execution and improvement

RESULT:When measured, has two kinds of variation for part to part variation(true variation) and measurement variation which is due to operator. Using MSA we did comparative study of key parameters of measurement system. Accuracy(closeness to reference value)= Bias and Linearity Bias-Difference between observed average and true value. Bias=0 Then linear Stability- variation in average over a period of time. Precision(ability of system to repeat same readings)= Repeatability and Reproducibility. Repeatability-variation obtained by one equipment, one operator, for same identical part. Reproducibility-- variation obtained by one equipment, different operator, for same identical part.

CONCLUSION : Application of above QA and QC Principles and tools of operations management gives vivid insight of the whole process and workflow stream. Which directly facilitates to identify latent and systematic errors, mistakes and delusion. So as to rectify those shortcomings in a structured manner avoiding recurrence in future. Assuring the accuracy of expected results.

Key words : QA- quality assurance. QC- Quality Checks. MSA- Measurement System Analysis.

COMPREHENSIVE ASSESSMENT OF ORGAN DOSES AND EFFECTIVE DOSE ASSOCIATED WITH CHEST/THORAX COMPUTED TOMOGRAPHY (CT) SCANS

Yachika Chopal

Swami Vivekanand Multi Speciality Hospital, Yamunanagar, India

Email: yachikachopal@gmail.com

AIM: This research aims to perform a comprehensive assessment of organ doses and effective dose associated with Chest/Thorax computed tomography (CT) scans.

MATERIALS AND METHODS: The examinations were conducted in form of NCCT and/or CECT chest sequences. Effective dose (ED) was determined using two different approaches. The first method relied on the scanner-derived dose length product, whereas the second method involved utilizing specialized software that computed both organ and effective dose. This computation was based on the factors provided in Report 102 and 103 by the International Commission on Radiation Protection (ICRP).

RESULTS: In total 120 patients were studied. Males were having higher mean effective dose as compared to females (3.63 vs. 2.92 mSv).

CONCLUSION: By leveraging this comprehensive approach, we gained valuable insights into the distribution of radiation doses among different organs and tissues. The calculated data can serve as a basis for optimizing CT imaging protocols to minimize radiation exposure while preserving diagnostic image quality.

KEYWORDS: Organ Dose, Effective Dose, Chest, Thorax, CT scans, NCCT, CECT

IMPACT OF TOTAL TREATMENT TIME AND THE TIME INTERVAL BETWEEN SHOTS ON BIOLOGICAL EFFECTIVE DOSE (BED) FOR VESTIBULAR SCHWANNOMAS PATIENTS TREATED ON GAMMA KNIFE PERFEXION

Monika Duhan, Reena Sharma, ManjulTripathi

PGIMER Chandigrah, India

Email: reenapgi@gmail.com

BACKGROUND: The biological effect produced by tissue irradiation is usually described by the biologically effective dose (BED). The parameters considered in the calculation of the BED are the dose, the tissue radiosensitivity, the dose rate, the cell repair rate and the irradiation time. By using the bi-exponential repair model BED calculated for Tumor and organ at risk (OARs). The cochlea is the main OAR.

MATERIAL AND METHODS: 50 patients of Vestibular Schwannomas (VS) treated on LGK Perfexion taken for this retrospective dosimetric analysis. It is difficult to calculate BED manually per shots and also including repair rate between shots. Hence, an in-house C++ program was developed for BED calculation. The dose prescription ranges from 12-14 Gys, the dose rate was 1.517-2.819 Gy/min, the shot number/ ios-centers varies from 7-77 and the overall treatment time, including the gaps between shots was 36.4 minutes to 153.3 minutes. The used parameters for BED calculation were α/β -2.47Gy, fast and slow sub-lethal repair rates (hr^{-1}) 3.648 and 0.321 respectively for both TV and OARs. This model considers a two-component repair rate for tissues in which two repair half times are introduced.

RESULTS: Due to this reduction of the dose rate and the longer exposure times BED of the LGK treatment gets affected. The probability of sub-lethal damage repair increases both in TV and OARs. The calculated BED for TV including per shot repair is large and is approx 12.5% more in comparison to BED calculated for standard prescription dose range. Also, treatment plan in which certain shots are blocked completely or shaped dynamically in order to spare cochlea, the found difference between BED calculated for single total treatment time and BED calculated for each shot including repair rate is 27.8%. This calculated BED difference will be correlated with the observed complication data and is in the future scope of our study.

Conclusion: We found that BED is affected by the treatment time, dose rate, shot blocking and the number of shots along with the sub-lethal repair. It is also observed that BED is affected by the sequence of shots in the treatment plan.

Keyword: Biological Effective Dose (BED), Vestibular Schwannoma (VS)

WILL NANOPARTICLES ENHANCE THE DOSE-RESPONSE OF FRICKE GEL DOSIMETER

Ebenezer Suman Babu S, Prathibha Prasad, Elizabeth Gracelin Sarah J

Department of Radiation Oncology, Christian Medical College, Vellore, India

Email: emailstoebi@gmail.com

BACKGROUND/OBJECTIVE: Gel dosimeters are tissue equivalent dosimeters capable of recording three-dimensional (3D) dose information in a gelatin matrix. The restrictions on higher bloom (Type A) gelatin in India and its non-availability have led to the adaptation of lower bloom gelatin (Type B) for preparation of gel dosimeters, which affect the dose-response characteristics. Metal oxides being catalytic in their chemical nature, could be used as a tool for enhancing the low-dose response of gel dosimeters. This abstract presents the outcome of the dose-response characteristics of the FXG gel dosimeters incorporated with Magnesium Oxide nanoparticles (MgO NPs).

MATERIALS AND METHODS: Several batches of the diffusion controlled FXG-Glycine-EDTA gel dosimeter (taken as control), as well as the MgO NPs incorporated gels were prepared. Each batch of the gel dosimeter consisted of optimized concentrations of Sulphuric acid, Xylenol Orange, Ammonium Ferrous Sulphate, Glycine, EDTA and different concentrations of the nanoparticles. The gel solutions were poured into 4.5 ml cuvettes and kept in the refrigerator at 4 degrees centigrade for 12 hours prior to irradiation. The gel cuvettes were irradiated to doses ranging from 25-300 cGy from a telecobalt unit. The optical absorbance of all the gel cuvettes (control samples and irradiated samples) were measured at 585 nm with a UV-1800 double beam spectrophotometer. Dosimetric parameters such as the dose-response linearity, and short term dose stability after irradiation and optical characteristics such as background absorption and auto-oxidation were analyzed.

RESULTS: The dose response was found to be linear for the range investigated. There was a favourable increase in the low-dose response of the nanoparticle incorporated gel dosimeters. However, a further increase in the concentration of the MgO NPs resulted in a reduction of the overall optical clarity of the unirradiated gels compared to the control.

CONCLUSIONS: The results indicate that an optimal concentration of the nanoparticle incorporated in the FXG-Glycine-EDTA dosimeter would enhance the dose sensitivity with an acceptable optical clarity. This gel dosimeter recipe would enable the verification of 3D dose distributions where analysis of low-dose regions is imperative.

KEYWORDS: dosimetry, nanoparticle, Fricke gel, dose response

EVALUATION OF DOSIMETRIC CHARACTERISTICS BASED ON AAPM TG43 USING MOSFET AND ION CHAMBER

Sathish Kumar A, Rabi Raja Singh, Henry Finlay Godson, Timothy Peace

Department of Radiation Oncology, Christian Medical College Hospital, Vellore, Tamilnadu, India,
Email: sathishcmc@gmail.com

BACKGROUND/OBJECTIVE: To investigate dosimetric parameters recommended in AAPM TG43 with micro MOSFET dosimeter and to compare with ion chamber measurements for Ir-192 HDR Brachytherapy source.

MATERIALS AND METHODS: Dosimetric evaluation for Ir-192 brachytherapy source was carried out using micro MOSFET and 0.125 cc ion chamber. A jig was designed by keeping a catheter at center for source movement and separate provisions were made to keep MOSFET and ion chambers parallel to the source. To determine the maximum dwell position, both micro MOSFET and ion Chamber were kept parallel to each other at 3 cm from the source. Absorbed dose measurements were carried out with the same setup. Dose linearity was performed for the dose range from 50 to 800 cGy and timer linearity was performed for the variable time from 15 to 180 seconds. Reproducibility was carried out for the repeated irradiation of 50 cGy. Dosimetric measurements were carried out based on the AAPM TG 43 formalism. Air kerma strength, Dose rate constant, geometric factor of Ir-192 source were calculated for the radial distances from 0.5 cm to 5.0 cm. Radial dose function and Anisotropy function was calculated by measuring the dose from 1 to 5 cm from the source.

RESULTS: It was observed that the calibration curve was linear for both dose and time and the calibration factor obtained was 1.18 cGy/mV for microMOSFET. The dosimeter had a stable response of $\pm 1\%$ with repeated irradiations. The deviation for the measured absorbed dose to water with ion chamber was +2.05 %, and with MOSFET was -0.15% with reference to TG 43 values. . The calculated geometric factors were comparable with AAPM TG-43. Dose rate constant measured using microMOSFET and ion chamber was 1.114 cGy/h/U and 1.146 cGy/h/U. It was found that the radial dose function and anisotropy function measured using MOSFET dosimeter and Ion Chamber were in close agreement with AAPM TG-43 data.

CONCLUSIONS: The results indicated that MOSFET dosimeters can also be used to calculate the brachytherapy dosimetric functions described in AAPM TG-43. Though the dosimetric data were provided by manufacturer, but this study enable to validate the accuracy of the data.

KEYWORDS: Radiotherapy; dosimetric characteristics; micro MOSFET; Ion Chamber; AAPM TG43

EVALUATION OF DOSIMETRIC PROPERTIES OF SYNTHETIC SINGLE CRYSTAL MICRO-DIAMOND DETECTOR IN CLINICAL UNFLATTENED PHOTON BEAM

Mariyappan Rajasekaren, Madhurethaa S, VelM, AshokkumarSangaiah, Saraswathy Chitra S

Appollo Cancer Centre Teynampeth, Chennai, India

Email: madhurethaa@gmail.com

BACKGROUND: The study aims to evaluate the dosimetric properties of Synthetic Single Crystal Micro Diamond Detector (SCDD) in clinical un-flattened beams in small field dosimetry.

MATERIALS AND METHODS: For this study, the Single Crystal Diamond Detector (SCDD) is used for evaluating clinical dosimetry. Considering its unique design and material properties, the SCDD was used for assessing its unique characteristics in our newly installed Cyberknife S7™ Systems M/S Accuray Inc, making it a perfect choice for accurate small-field relative dosimetry. The analysis of parameters like Warmup/Stability, and Short term repeatability of the SCDD detector was evaluated along with the Dose-response Linearity, Dose Reproducibility, PDD, and Profiles were compared with different chambers as in the Photon Diode, Pin Point chamber, Semiflex 3D Chamber, and Semiflex Farmer chamber against the SCDD using Beamscan Therapy Beam Analyser.

RESULTS: Primarily during the Warmup/Stability test, the SCDD was irradiated ten times and the maximum deviation from the average reading was calculated. The SCDD system behavior was then evaluated using the Short-Term Repeatability method for high and low-dose responses showing the standard deviations of the measured dose for their corresponding mean values.

In the case of the detector response to Dose linearity, the Coefficient of Linearity is calculated for the different mentioned chambers against SCDD for the selected field sizes of 0.5×0.5 cm² and 6×6 cm², Fixed Cone collimator at 70 cm SSD and 10cm Depth. The coefficient of Variance was computed for the Dose reproducibility for all the above chambers and compared against SCDD. Furthermore, the Profiles and Pdd were analyzed for the mentioned chambers in counter to SCDD for the reference field size of 6×6 cm², Fixed Cone for the same setup.

CONCLUSION: Due to its excellent dosimetric characteristics, the SCDD represents an exceptionally alternate to other detectors. In addition, it has the advantage over the different chambers of being equivalent to water. Its response shows that SCDD is better in accuracy concerning dose prediction and an ideal chamber for small-field relative dosimetry.

COMPARATIVE STUDY ON COMET, GAMMA H2AX AND DICENTRIC CHROMOSOMAL ASSAY FOR DNA DAMAGE EVALUATION

Jose Solomon Raj L, Timothy Peace Balasingh, Rabi Raja Singh

Department Of Radiation Oncology, CMC, Vellore, India

Email: josesarc@gmail.com

AIM: To compare comet assay, gamma H2AX and dicentric chromosomal assay based on linearity, dose range, cost, time and their potential use as radiation biomarker was studied.

METHODS: Blood samples from five healthy individuals were collected under sterile condition in an ethylene diamine tetra acetic acid vacutainer. Prior to blood sample collection, informed consent was obtained from all the five individuals. The samples were irradiated in Equinox 80 telecobalt unit for the doses ranging 0 to 500 cGy in a temperature-maintained water bath (37°C) in order to simulate the human body temperature.

PERIPHERAL BLOOD MONONUCLEAR CELL (PBMC) ISOLATION: The irradiated whole blood was gently overlaid on a histopaque and were centrifuged at 1500 rpm for 30 minutes. The buffy coat of PBMCs which appears between plasma and histopaque were aspirated and processed for comet assay, gamma H2AX assay and dicentric chromosomal assay.

COMET ASSAY PROTOCOL: The PBMCs were suspended on a 0.75 % gel which were coated over a frosted slide and were processed for lysis (2.5 MNaCl, 100 mM Na₂ EDTA, 10 mM Tris-HCl, 1% Triton X-100; pH 10), electrophoresis (tri-acetateEDTA buffer; pH 8.5), fluorescent staining (2.5 ug/ml).

GAMMA H2AX ASSAY PROTOCOL: To activate the phosphorylation of histone proteins, the cells were treated with fetal bovine serum following which they were treated with primary and secondary antibody. The cells were stained with alexa fluor 488.

DICENTRIC CHROMOSOMAL ASSAY: The irradiated cells were cultured for 48 hours in a culture media followed by hypotonic and cell fixation procedure. The cells were later stained with giemsa stain.

RESULTS: Comet and gamma H2AX showed good correlation with radiation doses from 1 cGy to 500 cGy whereas, the dicentric chromosomal assay was sensitive above 10 cGy. Comet assay was found to be the most cost-effective method to evaluate DNA damage when compared with gamma H2AX assay and dicentric chromosomal assay. Gamma H2AX assay was found to be a rapid radiation biomarker for dose estimation.

CONCLUSION: It was found that comet assay and gamma H2AX assay has higher potential as radiation biomarkers when compared with dicentric chromosomal assay.

IMPACT OF CARBON FIBER COUCH ON BACK SCATTER RADIATION DOSE AT EXIT SURFACE

Suresh T.^{1,2}, SurekaC. S.¹, SasikaladeviT.¹

¹Department of Medical Physics, Bharathiar University, Coimbatore, India

²Aster CMI Hospital, Bangalore, India

Email: thasuresh@gmail.com

OBJECTIVE: Back-scattered radiation dose at the exit surface of the body has long been an area of concern where larger or multiple fields of high energy flattened and un-flattened beams are used. An attempt is made to study the effect of back-scatter from the couch, and dose enhancement under simulated treatment conditions by evaluating and comparing back-scattered photons and electrons at the exit surface by determining the ionization ratio (IR).

MATERIALS AND METHODS: This study is carried out in Varian True beams Tx (V2.7) linear accelerator carbon-fiber tabletop with its three different couch thickness branded with Exact IGRT couch (thin, medium, thick). Measurements are done at various depths from 8-23 cm with an interval of 3cm for various field sizes from 5x5 to 30x30 cm², with Polystyrene Phantom slabs on carbon-fibre table top with SSD 100 cm on the surface of the phantom using IBA parallel-plate chamber PPC40 placed at the exit portion with +300V polarizing voltage, with its thin mylar window facing away from radiation beam. The measurements are then carried out without carbon-fibre couch. The IR between the chamber readings with and without carbon-fibre are calculated for various energies. This study is carried out with and without AIO carbon-fibreboard and MOSFET also.

RESULTS: The analysis shows that back-scatter factor increases with increase in field-size. Minimal back-scatter is obtained for field sizes 5x5 cm² and it is found to be 1.001, 1.003, 1.005, 1.07, 1.10 for 6, 10, 15, 6FFF, 10FFF MV respectively. Similarly maximum IR is found for 30x30 cm² and it is 1.02, 1.05, 1.06, 1.30, 1.60 for 6, 10, 15 MV, 6FFF, 10FFF respectively. Due to the lack of charged particle equilibrium, the IR cannot be taken directly as the ratio of doses. However, the IR values for a particular field size decreases with increase in phantom thickness and this indicates the presence of less scatter radiation at larger phantom thickness due to absorption and scattering of the beam. The percentage of back-scatter is found to be 1.12% and 2.12% in case of thin couch.

CONCLUSION: The calculated IR indicate the value above 1, shows that there is an alteration in the dose distribution at exit plane due to x-ray photon back-scattering by the couch.

KEYWORDS: Carbon Fiber Couch, Back Scatter Radiation Dose, Exit Surface, Ionization ratio

A CORRELATION STUDY BETWEEN LOCAL AND GLOBAL GAMMA IN LARGE FIELD PLAN VERIFICATION USING PTW OCTAVIOUS PHANTOM

Reena Sharma, Rohit Kumar

Department of Radiotherapy and Oncology, PGIMER, Chandigarh, India

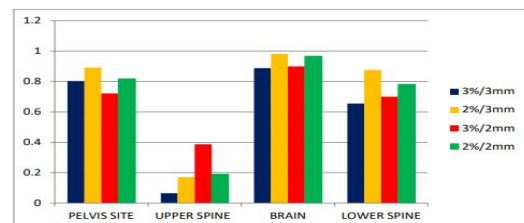
Email: reenapgi@gmail.com

OBJECTIVE::Non-uniform intensity delivered in IMRT aiming at achieving a high therapeutic ratio make the deviations between calculated and real dose distribution critical, even if they are very small, especially in regions close to organs at risk. The aim of PSQA is to check the agreement between dose distribution calculated by the TPS and the measured one. Gamma Index is proven to be an effective tool so as to compare the measured and calculated dose distributions. This study aims to find the correlation and reliability of gamma index for verifying large radiation field VMAT plans.

MATERIALS AND METHODS: A total of already treated 20 Patients (10 CSI &10 pelvis) were chosen for this study. Twenty clinically deliverable plans were generated on Varian Eclipse planning system version 11.0.47. Ten each, for CSI and pelvis. Octavius 4D 1500 device accommodating Octavius detector having 1405 ionization chambers arranged in checkerboard pattern was used to perform patient specific QA. To measure very long radiation field such as typically encountered in craniospinal treatments by combining two measurements, phantom was shifted in gun-target direction, rotated by 180 degrees and then measurement was repeated. For the TPS dose distribution, QA plans were generated on the extended Octavius 4D Phantom CT. Verisoft software was used to combine both measurements and compare them with the TPS dose distribution. The gamma (global and local gamma analysis) with four different criteria 3%/3mm, 3%/2mm, 2%/3mm and 2%/2mm all of them with a 10% threshold was evaluated and analysed for the correlation between Local and Global Gamma Index.

RESULTS: The global gamma analysis in case of large fields i.e. Pelvis and CSI (Upper spine) always resulted in higher passing rate than local gamma. Same results were found in brain and lower spine. While performing analysis using local gamma action, the confidence limits can be relaxed compared to global analysis. Results clearly indicated that applying stringent gamma criteria the difference between volumetric analysis for global and local gamma. The found average global gamma passing rates for 3%/3mm is above 95% regardless of site or technique. Also on independent analysis of pelvis and CSI even on applying stringent gamma criteria of 2%/2mm, Pelvis site plans gave higher global gamma passing rates compared to CSI. The Pearson correlation coefficients (r) between the global and local gamma passing rates are shown below in the table.

GAMMA CRITERIA	PELVIS r	CSI (BRAIN) r	CSI (Upper Spine) r	CSI (Lower Spine) r
5%/3mm	-	-	.894	-
3%/3mm	0.803	0.888	0.065	0.655
2%/3mm	0.891	0.982	0.171	0.876
3%/2mm	0.722	0.899	0.387	0.700
2%/2mm	0.818	0.967	0.190	0.782



For the pelvis, brain and lower spine a strong correlation was observed between global and local gamma passing rate. Regardless of criterion chosen. Also a strong correlation between the global and local gamma passing rates for the CSI (upper spine) was observed for 5%/3mm and a weak correlation for all other chosen criterion. This may be due to Inhomogeneous dose distribution along the long length of spine.

CONCLUSION :Based on evaluation results of local and global gamma, and Correlation between local and global gamma it is concluded that the Octavius-4D system is a suitable device for patient specific pretreatment verification QA for large field VMAT plan

PLANNING AND CLINICAL IMPLEMENTATION OF FAST FORWARDING BREAST RADIATION THERAPY-OUR INSTITUTIONAL STUDY

Kalaiselvi Marudaiah¹, Bharanidharan G², Subathira B¹, Pavithra V¹, Ashokkumar S¹, Vendhan Subramani¹, Saraswathi Chitra¹

¹Apollo Cancer Centre, 320 Padma Complexanna Salaitenampet, Chennai

²Anna University, College Of Engineering, Guindy

Email: selvi8609@gmail.com

OBJECTIVE:Our aim of this study is to emphasize the clinical implementation of the fast forward treatment modality for the left and right breast cases, with Deep Inspiration Breath Hold (DIBH).

MATERIALS AND METHODS:We had discussed 106 patients diagnosed with early-stage carcinoma breast who have undergone breast conserving surgery (BCS). Patients were acquired CT scan at 3mm interval. During CT scan, patients were supine positioned in the inclined breast board with arms above the head. CT scans with free breathing and Deep inspiration breath hold technique (DIBH) were acquired. After contouring process, the treatment planning is executed. The dose prescription 26Gy in 5 fraction scheduled for 1 week as used in the FAST Forward Protocol. An optimal PTV coverage should be between 95% and 107% of the prescribed dose. Dose constraints for ipsilateral lung i.e., $V_{30\%} \leq 17\%$ was considered mandatory but $V_{30\%} \leq 15\%$ was considered optimal and for heart was $V_{25\%} \leq 5\%$ and $V_{5\%} \leq 25\%$, respectively. By using photon 6MV plans were created. 10MV photons also used in few cases to increase the tumor homogeneity. Beam angle and collimator angle were chosen precisely to control dose to control ipsilateral lung, heart and contralateral breast. In all our breast planning we use field in field 3DCRT. Dose volume histograms were analyzed for Target and OAR. Volume of lung receiving 30% of the prescribed dose and volume of heart receiving 25% of the prescribed dose were analyzed in free breathing and DIBH method.

RESULTS:The dose constraints were effectively achieved in both right and left breast cases with the DIBH method. DIBH technique provides increase in the lung volume thus reducing the lung dose advantageous for the right and left breast cases. For comparable coverage and target dose homogeneity, the mean dose to heart is reduced in DIBH compared with FB the displacement of heart away from treatment fields reduces the heart doses and LAD dose. For right breast cases, the mean lung doses and mean liver dose is reduced comparing with FB.

CONCLUSION:Our study suggests that, the implementation of DIBH for Fast forward technique helps to achieve the dose constraints efficiently.

BALANCING EFFICIENCY AND EFFICACY: A COMPARISON OF HIPO AND IPSA INVERSE PLANNING METHODS IN ACCELERATED PARTIAL BREAST IRRADIATION HDRBRACHYTHERAPY

Sreejesh V. S., SubramaniVellaiyan, DayanandSharma, Gopishankar Natanasabapathi, SohamSanyal, Dhanabalan Rajasekaran

All India Institute of Medical Sciences, New Delhi

Email: sreejesh.ms@yahoo.com

PURPOSE: The purpose of this study was to conduct a comparative analysis of the IPSA and HIPO algorithm in the context of APBI.

MATERIALS AND METHODS: This retrospective study selected 15 patients who had undergone radiotherapy for breast cancer, specifically utilizing APBI through interstitial HDR brachytherapy. The Oncentra Brachy v. 4.3 software was employed for IPSA and HIPO planning. To ensure optimization, dose constraints were assigned in a manner such that both HIPO and IPSA plans should have deliver 100% prescribed dose to 90% of the target volume. As part of this study, 3HIPO plans and 3IPSA plans were developed for each patient, using 3 different settings for DTGR and DTDC - (0, 0.5, 1) respectively. This variation aimed to explore the most efficient setting for each patient. One-way ANOVA repeated measures statistical test was performed using R statistical software (v4.2.1).

RESULTS: The HIPO method generated plans with significantly lesser dwell times than the IPSA method. In terms of volume doses at V100, V150, and V200 for the PTV, HIPO demonstrated a statistically significant superiority over IPSA. The dose-volumetric parameters associated with the clinical target volume using IPSA were lower than those achieved with HIPO. Regarding the doses to the OARs such as the normal breast, skin, rib, heart, and lung, no statistically significant differences were found between IPSA and HIPO. Nonetheless, a slight percentage difference was noted, with HIPO being marginally better than IPSA. Furthermore, HIPO showed a statistically significant superiority over IPSA ($p < 0.0001$) in terms of Conformity Index (COIN) and excess dose coverage outside the PTV (normal breast). Conversely, in terms of the Dose Non-uniformity Ratio (DNR), IPSA demonstrated statistically significant superiority over HIPO. The Dwell Time Deviation Constraint (DTDC) and Dwell Time Gradient Restriction (DTGR) for both IPSA and HIPO exhibited optimal values at 0.5. This observation was made while considering the parameters of COIN and DNR.

CONCLUSION: Both the IPSA and HIPO dose optimization algorithms yield comparable dosimetric results. However, when considering dwell time and COIN values, HIPO presents advantageous results. An exception to this is the DNR, where IPSA exhibits superior performance.

STUDY OF DOSIMETRIC CHARACTERISTICS OF AN INDIGENOUS 3D PRINTED NECK REST ACCORDING TO THE AAPM REPORT NUMBER 176

Divya D. Patil, Reena Phurailatpam, Jeevanshu Jain, Mahima Tiwari, Shudhanshu S Rana, Umesh Gayke, Rajesh Bajbhuje, Akshay Bhavke

Advanced Centre for Treatment, Research and Education in Cancer, Tata Memorial Centre, Navi Mumbai.

Email: patildivya51@gmail.com

OBJECTIVE: In this study, an indigenously developed neck rest (INR) used for immobilising radiotherapy patients is compared with the commercially available neck rest (CNR). for material homogeneity, beam transmission, angular transmission and cost effectiveness.

MATERIAL AND METHOD: The INR was designed by reviewing CT datasets of 10 patients to be better suited for the Indian population and fabricated using polyurethane foam composition at the 3D printing laboratory at ACTREC. The INR mould's CAD model was designed using Fusion 360 and the file was sliced using slicing software. The mould was 3D printed using FDM 3D printer. The Polyurethane flexible foam kit from Smooth-On of density 0.16g/cm³ was cast in the 3D printed mould.

CT scans of 0.625 mm slice thickness were taken for both the neck rests with solid water slab phantom (30cmx30cmx10cm) and cylindrical phantom. The mean Hounsfield unit (HU) of the neck rests were compared. As per AAPM report no.176, a 0.6cc ionization chamber in solid water slabs was utilized to measure the transmission factors for 5x5, 10x10, 15x15, and 20x20 cm² field sizes for 6MV, 10MV & 15MV photon energy beams. The cylindrical tissue equivalent phantom with an A1SL chamber was used to study the angular response for 6 posterior oblique beam angles. The cost of both the neck rests was also compared.

RESULT: The mean HU of INR and CNR were found to be -830.34±5.34 and -979.34±2.66 respectively. For 6MV energy, with 10x10cm², the transmission factor for INR is 0.9796, whereas that for CNR is 0.9934. The INR and CNR transmission were similar for 10x10cm² field size for 10MV (0.9853, 0.9950) and 15MV (0.9858, 0.9969). The INR exhibits lower transmission than the CNR, the largest percentage difference between the two is 1.9% at 5x5 cm² at 6MV. Oblique incidence at 130° and 230° for INR and 150° and 170° for CNR results in the highest attenuation. The cost of constructing an INR was evaluated as approximately Rs. 1500 whereas that of a CNR is Rs. 15000 approximately.

CONCLUSION: When compared with the commercially available neck rest, the INR has provided satisfactory dosimetric properties of transmission and homogeneity and can be a more affordable option.

KEYWORDS: 3D printing, Immobilisation device, transmission factor measurements

SHINVA XHA600E DIGITAL PLATFORM LINAC WITH VMAT: ACCEPTANCE & COMMISSIONING TESTS

Jagadish R¹, NarsiLingampalli¹, Rashmi Puranik¹, DarshanaKawale¹, Anjali Uniyal¹
Sathiya Narayanan², Raghavendra Holla², Boopalan Balaji³, Pradip Deshmukh⁵,
BhooshanZade¹, Sanjay Deshmukh¹

¹Indrayani Hospital & Cancer Institute, Pune. ²Ruby hall clinic, Pune, ³KLES Belgaum Cancer Hospital, Belgaum. ⁵Aditya Birla Memorial Hospital, Pune, India
Email: jagadish.gasc@gmail.com

OBJECTIVE: The aim is to present results of acceptance & commissioning tests of the India's first Shinva XHA600E LINAC manufactured by M/S. Shinva Medical Instrument Co. Ltd., China which was installed by M/s. KTPL, Mumbai at Indrayani Hospital & Cancer Institute, Pune. Before we use the machine for clinical treatment, we performed acceptance tests as per manufacturer's CAT procedure followed by commissioning tests and guidelines laid down by AERB. In this study, the results of safety checks, mechanical tests & dosimetric measurements are presented.

MATERIALS & METHODS: The Shinva XHA600E equipped with digital platform and MV imaging capable to deliver 3D conformal, Dynamic-IMRT and VMAT technique with dose rate ranging from 0 to 600 MU/min and asymmetric jaws of maximum field size of 40x40cm² followed by 40 pairs of tertiary MLC & leaf speed of 3cm/sec. Dosimetric measurements were performed using 0.6cc Ionization Chamber for larger and semiflex chamber for smaller field sizes. The PDD & Profile measurements were performed with PTW MP3-M RFA water phantom with dimension 50x50x50 cm³. Radiochromic films were used for VMAT performance tests, field congruence test & spoke tests.

RESULTS: Acceptance test begins with safety checks to ensure safe environment for staff and public. The electrical tests and radiation safety tests are as per AERB recommendations with LASER based anti-collision interlock. All the mechanical test results are well within tolerance limits including VMAT technique. The beam quality index was 0.671. The PDD was 67.09% and D_{max} was 1.5cm. The beam penumbra at D_{max} is ≤ 6.00 mm for XY profiles. The photon beam reproducibility and MU linearity were 0.072 % and 0.45%. The flatness and symmetry for various static gantry and ARC mode field sizes at 10.0 cm depth in isocentric setup was well within the tolerance limits. For VMAT performance tests, the monitor chamber constancy during ARC mode was 0.120% and accuracy of dose with variation of dose rate and gantry speed was 1.067%.

CONCLUSION: Acceptance and Commissioning tests of Shinva Linac XHA600E were analyzed and were found satisfactory as per the AERB recommendations & IEC standards.

DOSIMETRIC VERIFICATION OF TWO-DIMENSIONAL EPID BASED MIDPLANE DOSIMETRY MODEL FOR CONFORMAL AND INTENSITY MODULATED BEAMS USING THE OCTAVIUS 1600 ARRAY

Aneesha Johny¹, S. Timothy Peace Balasingh¹, Henry Finlay Godson, Ebenezer Suman Babu¹, L. Jose Solomon Raj¹, Abel Juhan Thomas¹, Sheeba Ebenezer¹, Jenifer Sneha P¹, Rima Singhmahapatra¹

¹Department of Radiation Oncology, CMC Vellore, India

Email: aneeshamariajohny123@gmail.com

BACKGROUND/OBJECTIVE: With sophisticated treatment techniques such as intensity modulated radiotherapy (IMRT) becoming a fundamental part of radiotherapy, the requirement for precise delivery becomes crucial. With increasing complexities in the treatment planning and delivery chain, the probability of errors also increases. Hence, *in vivo* dosimetry has become vital to verify dose received by patients during treatment. The aim of this study was to dosimetrically verify a two-dimensional EPID-based mid plane *in vivo* dosimetry model for conformal and intensity modulated beams using Octavius 1600 array.

MATERIALS AND METHODS: This study was performed with the aS1200 EPID of the Varian True Beam STx linear accelerator. An EPID calibration model and software developed in-house was used to convert transit dose images to midplane dose maps using calibration curves that relate dose to EPID response. The EPID-based midplane dose maps of conformal and modulated plans were compared with that of TPS-calculated midplane doses and verified using the PTW Octavius 2D 1600 array. The gamma analysis was performed using PTW VeriSoft (v8.1).

RESULTS: The gamma passing rate (GPR) for standard criteria of 3mm DTA and 3% dose difference performed for 3 patient plans and a phantom plan was 100% for EPID vs Octavius 1600 midplane maps and 99.98% when compared to TPS. The TPS vs the 2D array was 97.67%. For the conformal 3D plan, the GPR was found to be 100% for EPID when compared with the 2D array and 99.21% when compared with the TPS calculated doses. The EPID-based midplane values were found to be very close to the high resolution 2D 1600 array and matched well with the TPS calculated values. The average variation found in point dose verification of IMRT fields was 1.35% and conformal fields was 1.96%.

CONCLUSIONS: This EPID-based *in vivo* dosimetry method, which requires no additional setup time, was found to be accurate when compared with the 'Gold standard' 2D array. It can be used on a routine basis for determining errors in the treatment delivery of 3D conformal radiotherapy and IMRT. Its applications can be expanded to verify VMAT and gated treatment in future.

KEYWORDS: EPID, IMRT, *in vivo* dosimetry

ANALYSIS OF GAMMA PASS RATE WITH DIFFERENT BEAM INTERRUPTIONS AND THRESHOLD DOSES IN DEEP INSPIRATION BREATH HOLD DELIVERY FOR LEFT BREAST CANCER

P. Mohandass¹, Mathew Abraham¹, D Palanivelu¹, C S Sureka², Narendra Kumar Bhalla¹,
R Sasikumar¹, Abhishek Puri¹

¹Department of Radiation Oncology, Fortis Cancer Institute, Fortis Hospital, Mohali, Punjab, India

²Department of Medical Physics, Bharathiar University, Coimbatore, India

Email: kpm303@gmail.com

AIM/BACKGROUND: The gamma passing rate is an important factor to ensure the deliverability of intensity modulated plan. This study analysed the variation in gamma pass rate for different beam interruptions (DBI) and without beam interruption (WBI) for deep inspiration breath hold (DIBH) technique. In addition, gamma pass results (GPR) analysed for different threshold doses for left side breast volumetric modulated arc therapy (VMAT).

MATERIALS AND METHODS: The measurements were performed using a PTW Octavius® II phantom with 1500 detector array. The setup arrangement was performed in Elekta™ Synergy® linear accelerator with 6MV photon beam using VMAT technique for DBI and WBI. Monaco™ 5.1 treatment planning system (TPS) was used for VMAT plan generation. The calculated TPS dose was compared with delivered dose to evaluate GPR. 2D and 3D dose gamma evaluation was performed by Verisoft® software for DBI like 20sec, 25sec, 30sec, 35sec and WBI. The GPR was analysed for three threshold doses like 5%, 10%, 15% for DBI. The percentage of GPR were evaluated for the criteria of 3mm/3%, 3mm/2%, 2mm/2%, 2mm/3% and results were analysed.

RESULT: The results revealed that gamma pass rate for DBI was almost similar with WBI and did not show any significant difference ($p>0.05$). The three different thresholds did not have any variation in the GPR for different interruptions and without interruption. From the values of standard deviation, the maximum standard deviation ± 0.9 was for 2mm/2% in 3D gamma for the three different threshold doses and the value of deviation was same. The minimum standard deviation ± 0.2 was for 3mm/3% in 2D gamma for the different threshold doses with the same value of deviation.

CONCLUSION: The results of 2D and 3D GPR did not make any significant difference and the variation observed was $< \pm 0.5\%$. When comparing interruptions and without beam interruptions the variation was $< \pm 0.8\%$ and no significant difference observed. The results of threshold dose 5%, 10%, 15% has no influence on the GPR for 2D and 3D. The study results ensured that different multiple interruption and threshold doses up to 15% did not affect DIBH technique for left side breast VMAT delivery.

KEYWORDS: Gamma pass rate, DIBH, VMAT, Threshold dose

RADIOLOGICAL SAFETY CONSIDERATIONS FOR THE SAFETY ASSESSMENT OF A COMMERCIAL RADIOPHARMACEUTICAL FACILITY (CRF)

Jolly Joseph K, G Sahani

Atomic Energy Regulatory Board, Anushaktinagar, Mumbai, 400094, India

Email: jollykj@gmail.com

AIM/BACKGROUND: Commercial radiopharmaceutical facility (CRF) is a centralised radiopharmaceutical facility which manufacture and supply ready to administer radiopharmaceuticals to the authorised nuclear medicine facilities for the diagnostic and therapeutic purposes. Since the commercial production of radiopharmaceuticals necessitates the handling of large amounts of radioactive materials, a thorough safety assessment is essential and the radiological safety considerations for the same is comprehended in this paper.

MATERIALS AND METHODS: The radiological safety assessment involves a systematic review and evaluation of potential radiological hazards related to various aspects such as handling, storage, transport and disposal of radioactive substances for ensuring the protection of workers, public, and the environment. The assessment follows established national and international guidelines and regulations concerning radiation protection and safety.

RESULT: Planning and design of the CRF may consider various requisites right from the site selection, layout design, radioactive materials receipt, storage, handling, radiopharmaceuticals production, quality control, packaging, storage and transport. Also, design should take in to consideration the radioactive waste (solid, liquid and gas) management, air handling, ventilation, radiation surveillance etc. Room arrangements should be according to the radiation field gradient such that the flow is from high activity area to low activity area. Rooms with adequate space should be available for ease of handling of radioactive materials.

All the radiopharmaceutical preparations are to be carried out in hot-cell with adequate shielding such that the dose rate at the operator position is well within the acceptable limit for the maximum radioactivity intended to be handled. The hot cells inside the production and handling area should be maintained at a lower pressure than the surroundings and the exhaust should be released through a stack after proper filtration. Appropriate arrangements with respect to access control and interlock need to be available to ensure safety and security. Radiological surveillance including area monitoring, personnel monitoring etc. also need to be provided.

CONCLUSION: The radiological safety considerations for safety assessment of a commercial radiopharmaceutical facility emphasizes the need for a comprehensive design, planning, shielding, containment, and surveillance measures to protect workers, public and the environment from potential hazards associated with handling large amounts of radioactive materials.

REFERENCE: AERB safety Guide on Radioisotope Handling facilities, AERB/RF-RS/SG-2, 2015.

A RETROSPECTIVE STUDY ON THE MECHANICAL ACCURACY, DOSIMETRIC CONSTANCY AND THE RELIABILITY ON TRACKING METHODS OF THE ROBOTIC RADIOSURGERY SYSTEM WITH 13 YEARS OF DATA

Kalaiselvi Marudaiyah¹, Bharanidharan G², Pavithra V¹, Ashokkumar S¹, Vendhan Subramani¹
Vel M¹, Mariyappan M R¹, Saraswathi Chitra¹

¹Apollo Cancer Centre, 320 Padma Complexanna Salaitenampet, Chennai, India

²Anna University, College Of Engineering, Guindy, Chennai, India

Email:selvi8609@gmail.com

OBJECTIVE:Our aim of this study is to investigate retrospective analysis of the mechanical accuracy and dosimetric constancy of the robotic radio surgery treatment system in long term period and also to determine the reliability and efficiency of using robotics in RT treatment delivery.

MATERIALS AND METHODS:AQA (Automated quality assurance) test, E2E (End to End) test and output measurement were acquired over a period from 2009-2022 with the Cyberknife™ (Accuray, Inc., Sunnyvale, CA) G4 treatment unit, at the Department of Radiation oncology, Apollo Cancer centre, Teynampet, Chennai. AQA is a targetting accuracy test, recommended by TG-135, which is similar to the Winston-Lutz test. It uses a AQA phantom with tungsten ball and 4 fiducials for tracking, with two radiochromic films placed inside it. A 1 path 2 node (horizontal and vertical beams) plan determines the targetting error from the offset evaluated through film analysis. The Output measurements were determined as per IAEA TRS 483 protocol. The End-to-End (E2E) test is a targetting test designed to demonstrate the geometric targetting accuracy of the CyberKnife System throughout all phases of treatment planning and treatment delivery. Targetting accuracy is quantified based on radiation delivered to a Ball-cube phantom. Dose distributions are recorded on films inserted into the Ball-cube and analyzed for available tracking systems .

RESULT:In this study, around 1588 AQA test were analyzed, among which 1519 test have radial error within 1mm from the baseline. Also, 98% of output measurements were within the tolerance limit. The E2E analysis for all tracking methods were evaluated, there analysis shows that they were within the given tolerance limit of less than 0.95mm.

CONCLUSION:Thus, our long term data analysis confers that the dosimetric and mechanical checks of the robotic radio surgery system are reliable and well within the tolerance limit, which ensures better achievement of sub millimeter accuracy treatment delivery.

IMPACT OF BEAMLET WIDTH VARIATIONS ON VMAT PLAN QUALITY IN LUNG CARCINOMA TREATMENT

Sreejesh M S, Gopishankar Natanasabapathi, Dhanabalan Rajasekaran, Vellaiyan Subramani,
Dayanand Sharma

Department of Radiation Oncology, Dr. B. R. A. Institute Rotary Cancer Hospital, All India Institute of Medical Sciences, New Delhi, India

Email: sreejesh.ms@yahoo.com

Background/Objective: The aim of this study is to ascertain the effects of beamlet width (BLW) on Volumetric Modulated Arc Therapy (VMAT) for Lung Carcinoma (Ca-Lung) and to establish the optimal parameters for an efficacious radiotherapy plan.

Materials and Methods: This study examined five patients with Ca-Lung, selected for VMAT delivery using 6 MV X-ray beam of Elekta Synergy Platform accelerator. Three arc plan with ARC1-100degree positioned anteriorly, ARC2-50degree and ARC3-50degree placed posteriorly were generated using Monaco TPS (Version 5.11.03) to achieve the best possible Dose Volume Histogram (DVH) parameters for sparing normal lung region. The BLW was the only parameter altered in the optimization process which was set to 1,2,3,4,6,8,10,15, and 20 mm (denoted as BLW1, BLW2, BLW3, etc., up to BLW20) respectively to study the influence on plan optimization for each patient. Further, parameters such as grid size, sequencing parameters, IMRT objectives and constraints kept constant. The DVH statistics were used to assess and rank the plans, and the dose results for the planning target volumes (PTVs) and organs at risk (OARs) were analyzed both objectively and comprehensively. Monitor unit values (MU) were also noted.

Results: In comparison of various DVH parameters for PTV, there was a minimal percentage variation with the increasing BLW. The OAR dose also showed a minimal increase with the increase in BLW. An intriguing observation was noted which showed TPS calculated planning parameter values remained constant from BLW8 to BLW20, warranting further investigation in this area. The MU increased up to BLW3, decreased at BLW4, later increased and remained constant up to BLW10. In BLW1, BLW2, BLW3, BLW4 and BLW6 plans <5MUs segments accounted for 74.86%, 70.11%, 74.62%, 79.02% and 74.62% of total segments, respectively with which lowest was in the BLW2 group.

Conclusion: In this study it was found that varying BLW influences the PTV coverage and OAR dose reduction minimally. However, beyond the BLW4, there is no influence of BLW on VMAT planning. Hence, we infer that for VMAT plans for Ca-Lung cases BLW3 and BLW4 is optimal. Further observation is required to investigate similar trend in other planning sites.

Keywords: Linear Accelerator, Beamlet Width, Monaco TPS, VMAT

CAN CT IMAGES BASED FEATURES BE USED FOR SURVIVAL PREDICTION OF PANCREATIC CANCER PATIENTS

Gaganpreet Singh¹, Divya Khosla², Arun S Oinam², Vandana Thakur²

¹Department of Medical Physics, Apollo Proton Cancer Centre, Chennai, ²Department of Radiotherapy and Oncology, Regional Cancer Centre, Postgraduate Institute of Medical Education and Research (PGIMER), Chandigarh, India

Email: gaganpreetsingh@live.com

BACKGROUND/OBJECTIVE: Extraction of useful information from medical images using advanced mathematics formulas and tools is commonly used nowadays and is also known as Radiomics. Correlating information of radiomics features with clinical outcomes is still a new and challenging area of concern. This pilot study attempted to analyze the association of CT-based radiomics features with overall survival (OS) in pancreatic cancer patients treated with SBRT.

MATERIALS AND METHODS: Ten patients of borderline resectable and locally advanced pancreatic cancer were included. All patients received neoadjuvant chemotherapy followed by SBRT 33 Gy to 42 Gy in 5-6 fractions followed by further chemotherapy and assessment for surgery. Using pyRadiomics, radiomic features of gross tumour volume were extracted using contrast-enhanced planning CT images acquired during SBRT planning. All the statistical analysis was performed using R software. Logistic and LASSO Cox regression analysis was performed to find the predictor of the survival based upon the radiomics features.

RESULTS: Three of the 10 patients were resected. Median follow-up was 15 months (range, 5-24 months), median OS was 25 months. A total of 851 radiomic features were extracted. Using Lasso Cox regression, six wavelet based features were found to influence the overall survival however, could not attain statistical significance due to limited sample size. Based on the radiomics score, patients were stratified into low and high risk categories. AUC value of 0.708 was obtained using ROC curves which shows radiomics score can be used as a predictor for OS.

CONCLUSIONS: This pilot study highlights the potential of CT-based radiomic features in predicting survival in patients with pancreatic cancer treated with chemotherapy followed by SBRT. The identified radiomic features, along with clinical parameters, offer valuable prognostic information that can aid in treatment decision-making and patient counseling. However, a larger number of patients are required to validate the results.

KEYWORDS: pancreatic cancer, radiomics, SBRT, survival

IMPACT OF DIFFERENT VOLUME CHAMBERS ON THE DOSIMETRIC CHARACTERISTICS OF SMALL FIELD

Sheenam Garg¹, Arun S. Oinam², Gaganpreet Singh²

¹Panjab University, Centre for Medical Physics ,Sector 25 , Panjab University ,Chandigarh, India

²PGIMER ,Sector 12 , Panjab University ,Chandigarh, India

Email: sheenamgarg786@gmail.com

BACKGROUND: Small field dosimetry plays crucial role in modern radiation therapy ,in advanced treatment techniques like stereotactic radiosurgery and intensity-modulated radiation therapy. Accurate dose measurements in small fields typically below 4*4 cm² present unique challenges due to increase influence of various factors such as electronic disequilibrium ,detector perturbations and output fluctuations.

PURPOSE: The study aims to evaluate and compare the effect of four detectors (Semiflex®3D,microdiamond,CC13 and FC65) on the dosimetric characteristics of small field .

MATERIAL/METHODS: In this experimental study, the effect of four different volume chambers on the dosimetric characteristics of small field were assessed under 6 MV Flattening Filter photon beam. Experimental data were acquired in water with IBA three-dimensional (3D) blue phantom. Square field sizes ranging from 0.5*0.5 – 5*5 cm² and 10*10 cm² were used for obtaining percentage depth dose curves (PDDs) at 20 cm and profiles at three different depths d_{max} (1.5 cm) ,5 cm and 10 cm with Source to Surface Distance(SSD) of 100 cm.

RESULTS: PDDs and profiles (inplane and crossplane) for all field sizes were compared .No significant difference was observed in comparing the dosimetric and geometrical field size except in FC65. However, significant difference was observed in the high dose gradient regions .

CONCLUSION: The results indicate the three detectors were well performed in small field relative dosimetry (except for FC65 having large volume)and for measuring penumbra, it is best to use microdiamond detector followed by Semiflex and then CC13 .

RHEOLOGICAL AND TENSILE PROPERTIES OF NOVEL RADIOTHERAPY GEL BOLUS – A PRELIMINARY STUDY

Ashish Binjola^{1,2}, Sukhvir Singh³, Raman Chawala³, Navneet Sharma³, V. Subramani¹, N. Gopishankar¹, R. K. Bisht², Ajay Gupta⁴, D. N. Sharma¹, Pratik Kumar²

¹Department of Radiation Oncology, Dr. B. R. A. Institute Rotary Cancer Hospital, All India Institute of Medical Sciences, New Delhi, ²Department of Medical Physics Unit, Dr. B. R. A. Institute Rotary Cancer Hospital, All India Institute of Medical Sciences, New Delhi, ³Institute of Nuclear Medicine & Allied Sciences, DRDO, New Delhi-110054, ⁴Gel Craft Healthcare Pvt Ltd, Ghaziabad

Email: ashishbinjola2002@yahoo.com

BACKGROUND: Bolus is an essential accessory for the treatment of superficial malignant lesions with megavoltage radiation. Commercial gel boluses are costly as these are imported from other countries. We have developed an environment-friendly plant oils-based polymer gel bolus with tissue-equivalent properties (specific gravity, electron density, effective atomic number, etc.) for radiation interactions. For assessing its physical and mechanical suitability for routine clinical use and storage we have conducted a series of tests (tensile, rheological, cold crack at $-30^{\circ}C$, fungus resistance, etc.).

MATERIALS AND METHODS: Gels can have solid as well as liquid-like behaviour, so it is essential to assess rheological as well as tensile properties. Rheological properties (storage modulus, loss modulus, viscosity, etc.) were measured using Anton Parr's twin-drive compact rotary rheometer. Flat steel plate geometry with a diameter of 30 mm and a height of 1.0 mm was used. Samples were prepared by cutting them as per geometric requirements. Amplitude and frequency sweep tests were performed for the gel bolus. Tensile properties were measured using Instron 3385 universal testing machine (UTM). Samples were prepared and fixed between the jaws of UTM then longitudinal stress was applied. Young modulus, elongation at break, tensile strength, etc. properties were measured for the developed and commercial bolus. Cyclic compression and extension tests were performed using Tinius Olsen UTM. Cold Crack tests and fungus resistance tests were performed as per respective ASTM standards.

RESULTS: The gel bolus has constant rheological properties over a range of strain rates and frequencies (large data). Young modulus is 0.01 KPa vs 2.8 KPa for commercial bolus, elongation at break is 4083% at 115 N vs 685% at 25 N load, and Energy at break is 35.852 J vs 1.046 J. It retains shape and elasticity after 1000 cycles of compressions and extensions. The gel bolus shows no cracks at low temperatures and no fungi growth at normal storage conditions.

CONCLUSION: The developed bolus is stronger and more flexible compared to the commercial bolus and demonstrates an improved ability to shape with patient contours and reduce air gaps between the patient skin and the bolus.

KEYWORDS: Novel Gel Bolus, Rheology, Tensile Testing,

DESIGN AND DEVELOPMENT OF PIN-HOLE COLLIMATOR FOR THE SPECTROMETRY OF DIAGNOSTIC X-RAY BEAMS

Rahul Kumar Chaudhary, Sudhir Kumar, S. D. Sharma, B. K. Sapra

Radiological Physics & Advisory Division, Bhabha Atomic Research Centre, Anushaktinagar,
Mumbai, India

Email: rahulkc@barc.gov.in

OBJECTIVE: Diagnostic x-ray beam (DXRB) can be fully characterized if the spectrum of beam is known accurately. Solid state detectors such as CdZnTe or CdTe are commonly used for the DXRB spectrum measurements, at high photon fluence rates (10^6 - 10^{10} photons/mm²sec) the detection system (detector and electronics) suffers from the problem of pulse pile-up (PPP) leading to the spectral distortion. Photon fluence rate can be reduced by increasing focus-detector distance, but in mammography distance cannot be increased beyond a limit due to the presence of cassette holder. Therefore, a pin-hole collimator (PHC) was designed and developed to reduce the photon fluence rate during the spectrum measurements.

MATERIALS AND METHODS: The PHC consists of a hollow open ended cylindrical tungsten (W) tube (density 19.3 gm/cc) of external and internal diameters 29 mm and 21 mm respectively and length 60 mm. The end of the tube facing the radiation source can be fitted with a circular W disc of 21 mm diameter and 4 mm thickness having a hole of 0.8 mm diameter at the centre. This disc is separated by 25 mm spacer from another similar inner concentric disc having a hole of diameter 0.5 mm at the centre.

The CdZnTe detector (crystal size 10 x 10 x 5 mm³) was kept at the distance of 1000 mm from the focal spot behind the inner disc inside the cylindrical tube, an exposure of 40 kVp, 400 mAs and 900 ms was given using the field size of 200 x 200 mm². ²⁴¹Am and ¹³³Ba gamma ray sources were used for the energy calibration of detection system. Mean energy of beam was determined from the measured spectrum and was compared with published values.

RESULTS: The mean energy of the x-ray beam determined from the measured spectrum and published values were 27.19±0.09 keV and 27.03±0.04 keV respectively, showing good agreement with each other.

CONCLUSION: The developed PHC was successfully used for the spectrum measurement of DXRB and hence is an effective solution to the problem of PPP at the detection system.

KEYWORDS: Pin-hole collimator, Mean energy, X-ray spectrum

DEEP LEARNING AI PROGRAM FOR LUNG CANCER DETECTION IN PATIENT CT SCAN IMAGE

JeevithaD¹, Senthilkumar Shanmugam², P.Aruna¹

¹Anna university, Chennai, India

²Regional Cancer Center, Madurai Medical College & Govt. Rajaji Hospital, Madurai, India

Email:jeevithadhinakaran2000@gmail.com

BACKGROUND/OBJECTIVE: This study presents the development and evaluation of a deep learning artificial intelligence program for lung cancer detection in patient CT scan images. Lung cancer is a prevalent and deadly disease, and early detection plays a crucial role in improving patient outcomes. Deep learning techniques, specifically Convolutional Neural Networks (CNN), have shown great promise in medical imaging analysis, including lung cancer detection.

MATERIALS AND METHODS: The program is trained on a large dataset of patient CT scan images, encompassing both cancerous and non-cancerous cases. Preprocessing techniques are applied to enhance the quality and consistency of the images. The CNN is then fine-tuned using transfer learning to optimize its performance in identifying lung cancer patterns. The program's performance is rigorously evaluated on a separate validation dataset, and its sensitivity, specificity, accuracy, and area under the receiver operating characteristic curve (AUC-ROC) are computed. Comparative analysis is conducted with other lung cancer detection methods, including radiologist interpretations.

RESULTS: To evaluate the program's performance, a separate dataset comprising CT scan images from a diverse group of patients was used for validation. The AI program was assessed based on sensitivity, specificity, accuracy, and the area under the receiver operating characteristic (ROC) curve. The results demonstrated that the deep learning AI program achieved high accuracy in lung cancer detection from CT scan images. The sensitivity and specificity of the program were comparable to or even surpassed the performance of experienced radiologists in detecting lung cancer. The AI program's ability to correctly identify lung cancer at an early stage holds the potential to significantly impact patient prognosis and treatment outcomes.

CONCLUSION: The study's findings suggest that the deep learning AI program has the potential to serve as a valuable tool for radiologists and clinicians in improving lung cancer detection accuracy. By aiding in early diagnosis, the program may facilitate timely and targeted interventions, leading to more personalized treatment strategies and ultimately contributing to better patient survival rates. Furthermore, the integration of such AI systems into clinical practice may streamline lung cancer screening and contribute to better population health outcomes.

KEYWORDS:: Deep learning, Artificial intelligence, Lung cancer detection, Patient CT scan, Image analysis, Medical imaging.

DETECTION OF LUNG CANCER USING CONVOLUTION NEURAL NETWORKS IN COMPUTED TOMOGRAPHYIMAGES

C. Senthamil Selvan¹, P. Manikandan², M. Rajesh Kumar¹, S. Amala Arpana²

¹ Department of Radio-Diagnosis, Mahatma Gandhi Medical College and Research Institute, Sri Balaji Vidyapeeth (Deemed to be University), Puducherry, India, ² Department of Data Science, Loyola College, Chennai, Tamil Nadu, India.

Email:senthamilselvan9108@gmail.com

BACKGROUND/OBJECTIVE:Deep learning aims to enhance the early identification, diagnosis, and categorization of lung cancer, which is responsible for the highest number of cancer-related deaths worldwide. Lung cancer occurs due to uncontrolled cell division in the lungs, leading to the formation of tumors that can obstruct breathing and metastasize to other body parts. The key objective of applying deep learning to lung cancer is to enhance precision and sensitivity in detection, facilitating prompt intervention, personalized treatment strategies, and ultimately, improved patient outcomes.

MATERIALS AND METHODS:Data were collected from the patient who is referred to our radio- diagnosis between January 2022 to May 2023. The data folder is organized into three subfolders: train, test, and valid, containing 613 patients, 315 patients, and 72 patients of CT image respectively. In this study, we explore the application of CNN in detecting lung cancer using CTscan image data. Our aim is to assess the CNN model's potential to accurately classify lung cancer images, enabling early diagnosis and personalized treatment strategies. To evaluate the model's performance, we utilize key metrics like accuracy, precision, recall, and F1-score.Through rigorous evaluation on a large dataset, the proposed CNN-based approach shows promising results, highlighting the potential of deep learning techniques in transforming lung cancer diagnostics and improving patient outcomes.

RESULTS: Out of these, train subfolder contains 195 patients of adenocarcinoma, 115 patients of large cell carcinoma, 155 patients of squamous cell carcinomaand 148 patient images are normal. In test subfolder, there are 120 patients of adenocarcinoma, 51 patients of large cell carcinoma, 90 patients of squamous cell carcinoma and 54 patient images are normal while validation subfolder has 23 patient of adenocarcinoma, 21 patients of large cell carcinoma, 15 patients of squamous cell carcinoma and 13 patient imagesare normal.In this analysis, it is observed that the CNN model is performed with an accuracy, precision, recall and f1-score of LR are 86%, 88%, 89%, 87%.

CONCLUSIONS: The results indicate that CNN model performed with the good accuracy value. Therefore, we conclude that this model is recommended for detection of lung cancer in future enhancement.

KEYWORDS:Lung Cancer, Early Detection, Prognosis Improvement, CT scan, Convolutional Neural Networks (CNN).

DOSIMETRIC CHARACTERISTICS OF WOMED IORT-50 INTRA OPERATIVE RADIATION THERAPY

Revathy P¹, Shanmukhappa B Kaginelli²

¹Department of Radiation Oncology, Ramaiah Medical College, Bangalore, ²Division of Medical Physics, School of Life Sciences, JSS Academy of Higher Education and Research, Mysuru, India

E-mail: revamsmedphy@gmail.com

BACKGROUND/OBJECTIVE:The aim of the study was to measure the dosimetric characteristics of surface and spherical applicators in Womed ioRT-50 kV intra operative low energy X-ray radiation therapy unit

MATERIALS AND METHODS:The low energy kV intraoperative radiotherapy unit (Womed ioRT-50) with five surface and five spherical applicators were taken for this study. An applicator covered the rod anode of the X-ray tube and the chamber was inserted at the surface of the slab phantom, which was set up on the table. The electrometer was connected to the chamber and the treatment duration was 60 seconds. Three readings were taken in nano Coloumb for each depth as it increases in 5mm increments. The average reading was taken and the same set up was repeated for all surface applicators. For spherical applicators, the same procedure repeated with water phantom kept above the slab phantom.

RESULTS: The percentage deviation varies from -0.1% to 2.7% for surface applicators and -3.1% to 2.4 % variation for spherical applicators respectively. Graphs show the percentage depth dose curves of applicators.

CONCLUSIONS: This is the first study to measure the dosimetric characteristics of Womed ioRT-50.

KEYWORDS: Intra operative radiotherapy, Womed ioRT-50, spherical applicator, surface applicator

ANALYSIS AND DOSIMETRY OF PATIENT SPECIFIC QA PERFORMED ON BEAM MATCHED LINEAR ACCELERATORS TO CHECK THEIR RELIABILITY AND DELIVERABILITY

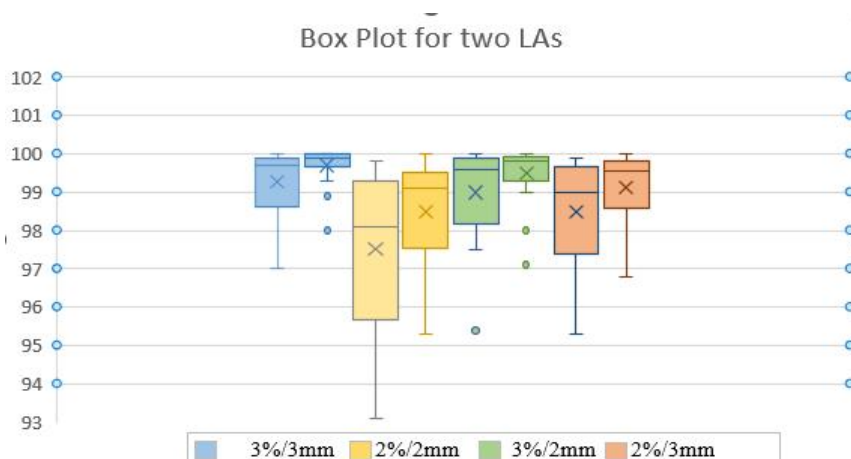
Gurvinder Singh, Ramandeep Singh, Shefali Pahwa, Devaraju Sampathirao, Shekhar Dwivedi, Avtar Singh, Amit Saini

Department of Radiation Oncology and Medical Physics, Homi Bhabha Cancer Hospital and Research Centre, Mullanpur, Punjab, India
Email: singhguru07@gmail.com

Background: Currently, HBCH & RC, Mullanpur has two identical linear accelerators (LINACs) with similar configuration and deliverable capabilities. To establish patient workload management in case of one machine failure or malfunctioning, an acceptable degree of beam matching needs to be determined.

Objectives: This study aimed to verify the dosimetric accuracy of beam-matching using Volumetric Modulated Arc Therapy (VMAT) patient plans of one machine, delivered on other machine and checked with two independent measurements using Portal Dose Imaging Prediction (PDIP) and Mapcheck.

Materials and methods: Randomly patient plans and their patient specific QA plans were generated for Linear Accelerator 1 (LA1) and delivered. Planar dose measurements of head and neck, thorax, and pelvis regions were collected from retrospective cancer patient's data. These VMAT plans were generated in the Eclipse Treatment Planning System (TPS) using a 6 MV photon beam and calculated with AcurosXB calculation algorithm. TPS doses calculated by LA1 were used as a reference for all measurements. The LA1's verification plans were irradiated in both LAs by doing the machine override option available in LA2 console. All of the VMAT plans were measured using the PDIP software and Mapcheck (by Sun Nuclear Corporation Ltd.) measurements. The data of PDIP and Mapcheck measurement were compared with the TPS calculated planar doses with gamma criteria of X% dose difference, and Y mm distance to agreement (X=3%, 2%/ Y= 3mm, 2mm). In addition, the statistically significant differences for gamma passing rates of PDIP and Mapcheck measurements between two LINACs were analyzed using a paired sample t-test at a 95% confidence interval (CI).



Results: For all cases, the gamma passing rates using PDIP measurements on two beam-matched LINACs were higher than 97% for all types (3%/3mm, 2%/2mm, 2%/3mm and 3%/2mm) of gamma criteria. The mean gamma passing rates of LA1 and LA2 were 99.3±0.8% and 99.7±0.5% for 3%/3mm, 97.5±2.2% and 98.5±1.4% for 2%/2mm, 99.0±1.3% and 99.5±0.8% for 3%/2mm and 98.5±1.5% and 99.1±0.9% for 2%/3mm respectively. Same will be analyzed for Mapcheck.

A STUDY ON SUSCEPTIBILITY WEIGHTED - PHASE IMAGING IN DIFFERENTIATING HEMOSIDERIN AND CALCIFICATION

R.Ragitha¹, S. Arunan Subbaiah², Senthil Kumar Aiyappan,³K.Muthuvelu⁴

¹Radiodiagnosis, SRM Medical college hospital and research centre, Kattankulathur Chengalpattu, Tamil Nadu,

²Department of Neurology, SRM Medical college hospital and research centre, Kattankulathur Chengalpattu,

Tamil Nadu , ³Department of Radiodiagnosis, SRM Medical college hospital and research centre,

Kattankulathur Chengalpattu, Tamil Nadu, ⁴Department of Radiation Physics, Division of Radiodiagnosis SRM

Medical college hospital and research centre, Kattankulathur Chengalpattu, Tamil Nadu

Objective: Our aim is to evaluate the role of SWI filter phase image in differentiating hemosiderin from Calcification.

Materials and Methods: Thirty-five patients were included in this study (17 calcifications and 18 hemosiderin). The age range (50-80 yrs) was selected without regard to sex to illustrate the application of the SWI and the validity of the technique. We performed a retrospective selection. In all cases, CT was used to validate the presence or absence of calcifications.

Results: Out of 17 Calcification 13 patients SWI filter Phase image shows a Positive signal change. Out of 18 patients 16 shows a positive signal change in SWI Phase image where the same patients CT doesn't reveal any changes. When comparing the size of the calcification, there was a significant correlation (0.01 level) between the phase image and the CT Image. For hemosiderin size, the filter-phase image did not show a significant correlation.

Conclusion: Filtered phase imaging is more effective in distinguishing between calcification and hemosiderin, perhaps eliminating the requirement for CT for correlation. It is possible to obtain additional information through the Susceptibility Phase image that cannot be approached by Susceptibility magnitude image alone.

Key words: SWI; susceptibility weighted imaging, CT computed tomography, Hemosiderin, calcification, Filter Phase imaging

ASSESSMENT OF CHRONIC KIDNEY DISEASE USING DIFFUSION-WEIGHTED MAGNETIC RESONANCE IMAGING AND ULTRASOUND DOPPLER

PunithaP.,Victor Rakesh Lazar,Senthil KumarA., Muthuvel K

SRM Medical College Hospital and Research centrepotheri,Chennai, India

Email:punithapk2910@gmail.com

PURPOSE/BACKGROUND:The purpose of this study is to assess CKD by analyzing ADC values and Doppler parameters.ADC values can be used to identify renal impairment and determine the various stages of CKD. Doppler measurements of RI and PI can also aid in the diagnosis of CKD. To assess the stages of CKD, imaging with DWI-MRI and Ultrasound Doppler can be utilized.

MATERIALS AND METHODS:A prospective study was performed on 120 patients with both normal and elevated renal parameters. Patients underwent DW- MRI (at b-values of 0, 250, and 500 s/mm²) and as well as renal Doppler examination.

Inclusion Criteria:

- Patients with elevated renal parameters Serum creatinine>1.5mg/dl, Blood urea>40mg/dl, and patients with normal renal function.
- Hypertension, diabetes, and primary renal disorders

Exclusion Criteria:

- Patient with Renal trauma,
- Pregnancy, and
- Claustrophobia

RESULTS:ADC values in patients with renal dysfunction were significantly lower than in patients with normal renal function. Average ADC value for both sides: 2.334×10^{-3} mm²/sec below, which indicates renal dysfunction.

CONCLUSIONS: The renal resistive index is not persistently elevated in all the patients with elevated renal parameters and couldn't be reliable in predicting CKD.ADC values may serve as an additional marker for assessing chronic kidney disease.

KEYWORDS: Chronic Kidney Disease, Diffusion-weighted Imaging, Ultrasound Doppler

SHIELDING PROPERTIES OF A NEWLY DEVELOPED HIGH-DENSITY CONCRETE MATERIAL FOR IR-192 BASED HDR BRACHYTHERAPY BUNKER

Amanjot Kaur¹, G. Sahani², R. K. Chouhan³, Manish Mudgal³, S D Sharma⁴, P. N. Pawaskar⁵

¹Department of Radiotherapy, Mahatma Phule Charitable Trust Hospital, Navi Mumbai, India

²Radiological Safety Division, Atomic Energy Regulatory Board (AERB), Mumbai, India

³Centre for Advanced Radiation Shielding and Geopolymeric Materials, Council of Scientific and Industrial Research - Advanced Materials and Processes Research Institute, Bhopal, Madhya Pradesh, India, ⁴Radiological Physics & Advisory Division, Bhabha Atomic Research Centre, Mumbai, ⁵Centre for Interdisciplinary Research, D. Y. Patil Education Society, Kolhapur, Maharashtra, India

Email: kaur.amanjot@live.com

PURPOSE/BACKGROUND: High-density concrete (HDC) are useful shielding materials for augmenting shielding thicknesses for retrofitting high-energy radiotherapy equipment in pre-existing low-energy radiotherapy bunker and for saving space for construction of a new radiotherapy vault. Council of Scientific and Industrial Research - Advanced Materials and Processes Research Institute (CSIR-AMPRI), Bhopal, Madhya Pradesh, India developed eco-friendly high-density concrete materials using red-mud, which is an industrial waste and disposal problem for the country. In this study, the reduction in tenth-value layer (TVL) are determined experimentally with reference to ordinary concrete for these newly developed shielding materials for their use in bunker for Iridium-192 (Ir-192) based high-dose-rate (HDR) brachytherapy.

MATERIALS AND METHODS: Two types of sample slabs i.e. cement based high-density concrete with red-mud based synthetic aggregate and fly-ash based high-density geopolymer concrete with red-med based synthetic aggregate, each of size 30cm(l)×30cm(w)×7.2cm(t), are prepared. Using Gammamed Plus iX remote-afterloader brachytherapy unit, the Ir-192 source was positioned behind the sample slab at a distance of 10 cm. The source, sample slab and detector were in the line-geometry. The detector is positioned 15 cm away from the material slab. PTW's 30cc Ionization Chamber with PTW's Unidos-E electrometer and low-impedance-tri-axial dosimetry cable was used for measurement of charge with/without slab. The charge measured was used to determine linear-attenuation-coefficient (LAC) for the newly developed HDC slabs. Similar measurements were carried out for the reference slab i.e. ordinary concrete for comparison with newly developed materials. The percentage reduction in TVLs for these materials with-respect-to ordinary concrete are calculated using measured LAC and are reported.

RESULTS: The cement based high-density concrete with red-mud based synthetic aggregate and fly-ash based high-density geopolymer concrete with red-med based synthetic aggregate provide 41.6% and 36.5% reduction in tenth-value layer with-respect-to the ordinary concrete material.

CONCLUSIONS: As the newly developed materials are high-density concrete developed from industrial waste and providing good preliminary shielding results; therefore, should be encouraged for vault construction. Furthermore, the results also indicate reduction in shielding requirements compared to the ordinary concrete.

KEYWORDS: tenth-value layer, high-dose-rate brachytherapy, shielding material, brachytherapy vault, high-density concrete

EXPLORING FEASIBILITY FOR INSTALLING HALCYON MEDICAL LINAC IN THE PRE-EXISTING TELECOBALT BUNKER

G. Sahani¹, Amanjot Kaur², S.D. Sharma³

¹Radiological Safety Division, Atomic Energy Regulatory Board, Mumbai, India, ²Department of Radiotherapy, Mahatma Phule Charitable Trust Hospital, Navi Mumbai, India, ³Radiological Physics and Advisory Division, Bhabha Atomic Research Centre, Mumbai, India

Email: gsahani@gmail.com

PURPOSE/BACKGROUND: Halcyon is a low energy (6 MV-flattening-filter-free(FFF)) advanced medical linear accelerator (linac) equipped with advanced dose delivery techniques such as volumetric-modulated-arc-therapy (VMAT)/RapidArc, intensity-modulated radiation therapy (IMRT), and three-dimensional conformal radiation therapy (3D-CRT). Several tele-cobalt users are desirous to replace their existing equipment with Halcyon medical linac due to its capability of delivering highly conformal dose. As X-ray photon energy of Halcyon linac is higher than that of a tele-cobalt machine; therefore, thicker wall shielding is needed for a Halcyon bunker for the same shielding design goal to protect radiation workers and the members of public posing challenge in augmenting shielding with the available existing space. This work presents to explore feasibility of installing Halcyon medical linac with minimum required changes in the pre-existing tele-cobalt bunker.

MATERIALS AND METHODS: Minimum room dimensions required for installing Halcyon medical linac are 5.9m(L) × 4.7m(W) × 2.8m(H) as recommended by manufacturer, whereas minimum room dimensions for tele-cobalt bunker is 6m(L)×5m(W)×3m(H). Based on the availability of space in tele-cobalt bunker, the orientation of Halcyon is suggested. Radiation shielding calculations were carried out for the augmentation of radiation shielding to the walls of pre-existing bunker by choosing appropriate workload, use factor, shielding design goal (permissible-dose-limit) for workers and general public, source-to-isocentre distance and isocentre-to-point of calculation distance.

RESULTS:Based on the shielding calculations, it is found that primary barrier thickness is adequate but additional shielding thickness is needed at the tapered corner of the wall (adjacent to primary) upto 65 cm of concrete (density=2.35 g/cc). Similarly, shielding of around 35 cm concrete required to augment the wall common between control console and bunker, whereas no additional concrete shielding is required to the wall opposite to this wall. No need to augment shielding to maze wall but one bend may be required for reducing radiation level at entrance door to use ordinary door. No additional shielding is required at primary barrier of the ceiling but needs to be provided for the secondary barrier region.

CONCLUSIONS:This work indicates that Halcyon unit can be installed in a pre-existing telecobalt bunker by augmenting minimum shielding.

KEYWORDS: Halcyon, tele-cobalt, bunker, shielding design goal

PERFORMANCE EVALUATION OF SOME MACHINE LEARNING MODELS IN THE ESTIMATING ORGANS AT RISK DOSES OF LEFT BREAST RADIOTHERAPY

Mostafa Robotjazi¹, Saba Ordibeheshti¹, Atefeh Rostami¹, Seyed Alireza Javadinia², Amir Alizadeh²

¹Department of Medical Physics and Radiological Sciences, Sabzevar University of Medical Sciences, Sabzevar, Iran, ²Department of Radiation Oncology, Sabzevar University of Medical Sciences, Sabzevar, Iran

Email: Robotjazim[a]medsab.ac.ir

BACKGROUND/OBJECTIVE: An optimal dose distribution in radiotherapy requires balancing the radiation dose in the target and the organs at risk (OARs). However, current optimization methods can be time-consuming and dependent on the user's expertise, hindering the development of streamlined and automated techniques. To address this issue, we evaluated the performance of several regression models in estimating OARs doses in left breast radiotherapy treatment planning. Our study results have the potential to pave the way for the development of more streamlined and automated techniques to generate optimal dose distributions.

MATERIALS AND METHODS: We analyzed 70 3D-conformal radiotherapy treatment plans for left breast cancer and extracted geometrical and dosimetric features, including field size, CLD, MLD, MHD, tangential fields angle, wedge angle, V_x, and D_x of the target and OARs. The OARs in the plans were the left lung and heart. We applied various regression models and optimized their hyperparameters. We selected the best model for each specific dosimetric parameter based on mean absolute error scores. We also performed feature selection to identify the most effective parameters for each OAR and model.

RESULTS: The KNN_regression model was the best for mean dose of the heart, lung, and V₂₀ of the lung. The SVR model was the best for the V₁₀ and V₅ of the lung. The AdaBoost model was the best for V₃₀ of the heart, and MLP_regression model was the best for V₅ of the heart. We identified the most important features for all models and OARs, which can be considered for accurate dose estimation.

CONCLUSIONS: Our study demonstrates the feasibility of using regression models to determine OARs dose in left breast radiotherapy treatment planning without relying on dose calculation algorithms. Our proposed method can potentially reduce the time required for plan optimization in 3D-CRT. We believe that our findings can lead to the development of more efficient and automated techniques for generating optimal dose distributions.

KEYWORDS: Machine Learning, Breast Cancer, Radiotherapy, Dosimetry, Organs at Risk

Presentation ID: P-330

Abstract ID: R5979

COMMISSIONING OF A WOMED T105 KILOVOLTAGE X-RAY UNIT: CHALLENGES, RESULTS, AND LONG-TERM PERFORMANCE

Tom Kupfer¹, Sherly Saju², Leah McDermott¹, Kym Rykers^{1,2}

¹Radiation Oncology Department, Austin Health, Victoria,²Ballarat-Austin Radiation Oncology Centre, Ballarat, Victoria

Email: Sherly.saju@gh.org.au

OBJECTIVE: Superficial x-ray radiotherapy (SXRT) plays an important role in skin cancer treatment in Australia. To improve public access to SXRT, a WoMed T105 unit was installed in a regional hospital in 2019 (Fig. 1). We present technical challenges encountered during its commissioning, beam measurement data and long-term performance data.



Fig. 1 WoMed T105 therapeutic x-ray unit

METHOD: Informed by SpekCalc® (commercial kV spectrum simulator), combinations of filtration and kVp were selected to obtain HVL of 0.7, 1.0, 2.0 and 4.0 mmAl. Commissioning followed ACPSEM guidelines. This included PDD measurements using a PTW Roos chamber in a scanning water tank, while surface dose was measured with a PTW thin-window plane parallel chamber in Solid Water phantom. Absolute dose-rate and timer error of the timer-based unit was measured according to the AAPM TG-61 protocol. Applicator factors and stand-off corrections were measured with a small-volume ionisation chamber in air. The inner-wall of the 4-cm diameter steel applicator was coated with nail varnish to reduce electron contamination. The performance of the unit's internal solid-state detector, which functions as an MU-counter and dose-rate monitor, was assessed. The drift of dose-rate and MU-counter was recorded over four years.

RESULTS: SpekCalc predicted the measured HVL to within 0.1 mmAl. The measured PDD differed by up to 13% from the BJR-25 reference data. Nail varnish reduced the surface dose by ~10%, without affecting the PDD or applicator factor. The output dose-rate showed no long-term drift and the timer error was negligible. However, the MU-counter was sensitive to pre-irradiation. Its maximum standard deviation and annual drift were 7.4% and -9.0%, respectively.

CONCLUSION: SpekCalc is useful for initial beam selection. The measured PDD agree within limits with PDDs tabulated in BJR-25. Nail varnish can significantly reduce surface dose present with a steel-walled applicator. The unit's output is stable, however, the variability of the MU-counter demands additional testing and ongoing monitoring.

KEYWORDS: SXRT, Skin cancer treatment

ACCEPTANCE, COMMISSIONING AND QUALITY ASSURANCE OF A 1.5T MRI MACHINE

M. Kumaresan, Ajay Chaubey, Surita Kantharia, Shubhra Gupta

Department of Radiology, Medical Division, BARC Hospital, Mumbai 400 094.

Email: kumaresa@barc.gov.in

BACKGROUND/OBJECTIVE: Magnetic Resonance Imaging (MRI) has become one of the most important imaging modalities in recent years. It is based on the principle of Nuclear Magnetic Resonance (NMR). MRI has the advantages of nonionizing radiation, superior soft-tissue contrast, and allowing quantitative analysis of functional images. Furthermore, in MRI, the desired level of imagecontrast among different tissues can often be precisely controlled with simpleadjustments to the acquisition timing parameters. A 1.5 T MRI machine (Model: Ingenia, Make: Philips) has been installed in our institute recently. A detailed acceptance tests were carried out prior to its clinical commissioning. This abstract presents outcome of the acceptance, commissioning and quality assurance this MRI machine.

MATERIALS AND METHODS: All the suitable tools and test equipment such as Torque wrench, magnetic field camera, magnetic shim kit etc. were used at the time of installation. Acceptance tests such as magnetic fringe field mapping, MR system inventory, mechanical system checks, emergency system checks, static magnetic field subsystem tests, RF subsystem tests were carried out. After the above tests, in order to put into clinical use, detailed quality assurance (QA) tests were also carried out. QA tests include Magnetic field homogeneity evaluation, Slice-position accuracy, Slice-thickness accuracy, table position accuracy, geometric accuracy measurements, high contrast resolution, low contrast detectability, and artifact analysis. All the above precommissioning mechanical, electrical and magnetic acceptance tests were carried out as per the ACR-MRI QC Manual 2015.

RESULTS: The acceptance tests and QA tests passed all the acceptance criteria as expected.

CONCLUSIONS: The test results indicate that all the systems and sub-systems of this MRI machine is performing as per specification and commissioned for patient treatment.

KEYWORDS: Magnetic Resonance Imaging, Quality Assurance, Acceptance tests

RADIOTHERAPY SETUP ERRORS IN IMRT AND VMAT TREATED HEAD AND NECK CANCER PATIENTS ON A RING BASED LINAC

Sridhar C. H., Donald J. F., Sandesh Rao, Krishna raj, Yashmitha K

Department of Radiotherapy Father Muller Medical College and Hospital Mangalore, India

Email: sridherch@gmail.com

OBJECTIVE: We assessed and determined to quantify the magnitude of setup errors in intensity-modulated radiotherapy (IMRT) and Volumetric Arc therapy treated Head and Neck cancer patients and recommend appropriate PTV margin.

METHODS: 65 patients with head and neck cancer required bilateral neck irradiation were planned and treated IMRT and VMAT technique either treated definitive or Adjuvant. Patients undergoing image-guided radiotherapy (IGRT) daily scheduled cone beam computed tomography (CBCT). The 3D displacements, systematic and random errors were calculated. The appropriate PTV expansion was determined using Van Herk's formula.

RESULTS: Mean 3D displacement was 0.2 cm in the vertical direction, 0.22 cm in the horizontal direction and 0.23 cm in the longitudinal direction.

CONCLUSION: Daily CBCT allows the planning target margin (PTV) expansion to be reduced according to our setup. The appropriate clinical target volume (CTV)-PTV margin for our institute is 0.30 cm, 0.25 cm, and 0.32 cm in the horizontal, vertical, and longitudinal directions.

KEY WORDS: IMRT, VMAT, Setup error, IGRT, CBCT

REVISITING REGULATORY FRAMEWORK FOR MONITORING OF QUALITY ASSURANCE IN DIAGNOSTIC RADIOLOGY IN INDIA: A SINGLE INSTITUTE EXPERIENCE

Gourav Kumar Jain¹, Rajni Verma¹, Arun Chougule²

¹Department of Radiological Physics, SMS Medical College and Hospital, Jaipur-302004 India,

²Swasthya Kalyan Group, Sitapura, Jaipur-302022, India

Email: gourav108@gmail.com

BACKGROUND/OBJECTIVE: According to UNSCEAR 2020/2021 report revealed that 4.2 billion of total annual number of medical radiological examinations were performed globally. Quality assurance (QA) of medical diagnostic X-ray equipment (MDXE) is one of the mandatory requirement as issued by national regulatory authority. The aim of present study was to analyze QA procedures and QA reports of medical diagnostic X-ray equipment.

MATERIALS AND METHODS: We have meticulously analyzed QA procedures and reports of 14 mobile X-ray units and 4 fixed X-ray units performed during October 2021 to June 2023 in several attached hospitals and reported results.

RESULTS: In order to facilitate QA tests of MDXE, it is a positive step that national regulatory authority has recognized QA agencies which are now accredited by NABL, to cater the need of huge and ever growing demand of MDXE in India. However, there is scope for improvements in regulatory framework provided by the AERB for the QA of MDXE. First, it has been observed that some of the QA agencies performing QA without having advanced automated tools and trained service engineer. For example, survey meters in manual mode were used during QA, however, wi-fi assisted and stand based solid state detectors can be used for strengthening radiation protection during procedure. The use of latest AI based QA toolkits may be encouraged. Second, QA test protocols lacks in comprehensive system based procedures for CR, DR and display monitor etc. related tests. AAPM and IAEA guidelines are useful to develop comprehensive system based QA procedures. Third, usually mobile X-ray QA reports has not been verified by approved radiation professionals. Any non radiation worker as institute representative may also sign QA reports without adequate knowledge of QA program. QA test report has to be verified by available radiation professional at the site. It is advisable to make provision that medical physicists may also verify the QA reports for other institutions. Importantly, medical physics should be developed stringently as speciality to adhere radiation safety norms in the country.

CONCLUSIONS: The present study provided useful insights by end user to regulators for strengthening QA in diagnostic radiology in India.

KEYWORDS: medical diagnostic X-ray equipment, quality assurance, diagnostic radiology, radiation protection

INSIGHTS ON SETTING UP A SUSTAINABLE INTERVENTIONAL RADIOLOGY RADIATION FACILITY IN INDIA: A SINGLE INSTITUTE EXPERIENCE

Gourav Kumar Jain¹, Rajni Verma¹, Arun Chougule²

¹Department of Radiological Physics, SMS Medical College and Hospital, Jaipur-302004 India,

²Swasthya Kalyan Group, Sitapura, Jaipur-302022, India

Email: gourav108@gmail.com

BACKGROUND/OBJECTIVE: UNSCEAR 2020/2021 report evaluated that 24 million of annual number of interventional radiology (IR) procedures performed worldwide. The aim of present study was to collect data and provide useful insights on setting up a sustainable interventional radiology facility.

MATERIALS AND METHODS: Our group was involved in the establishment of 4 new interventional radiology facilities including one cathlab, one neurosurgery digital subtraction angiography (DSA), two interventional units in interventional radiology department during October 2021 to June 2023.

RESULTS: We have observed that the placement of machine orientation/ X-ray tube away from patient waiting area was found appropriate in case feasible. This type of arrangement resulted in lowest radiation levels in patient waiting area. Trenches for cables were constructed on the ground, preferably over less occupied areas adjacent to walls moving towards control console optimizing overall length. An inspection was carried out during renovating the existing structure for installation of a DSA unit, we observed that the one of the physical wall thickness is not fulfilling the regulatory criteria according to approved layout of IR. Later, it was corrected. In installation of cathlab unit, few minor issues were observed such as door radiation beam indication light synchronization with machine, radiation symbol for awareness of pregnant women. Later, issues were rectified. In two IR units, we observed that the diagnostic image resolution test was failing in image processed mode. However, manufacturer claimed that the test will pass by using unprocessed image only. Later, the QA was found satisfactory. In order to achieve robustness in QA tests verification of IR, it is an excellent initiative that national regulatory authority has mandated to provide photograph of service engineer, concerned users along with QA toolkit on scheduled date for issuance of license. It is advised that the users and regulators need to stringently ensure equipment training is commenced after obtaining license and equipment training sheet may include license number issued by the national regulatory authority.

CONCLUSIONS: The present study provided a comprehensive overview for setting up a sustainable IR unit. The outcomes of present study is also useful for strengthening radiation protection in IR facility.

KEYWORDS: interventional radiology, quality assurance, license, radiation protection

ANALYSIS OF COMMON ISSUES OCCURRED DURING QUALITY ASSURANCE OF MEDICAL DIAGNOSTIC X-RAY EQUIPMENT

Rajni Verma ¹, Gourav Kumar Jain¹, Arun Chougule²

¹Department of Radiological Physics, SMS Medical College and Hospital, Jaipur, India,

²Swasthya Kalyan Group, Sitapura, Jaipur, India

Email: rajnigkj@gmail.com

BACKGROUND/OBJECTIVE: Medical diagnostic X-ray equipment are extensively used to perform medical radiological examinations. Quality assurance (QA) is an important aspect to ensure satisfactory performance of any of these equipment. The present study was aimed to analyze common issues occurred during QA of medical diagnostic X-ray equipment.

MATERIALS AND METHODS: In our institute, all the QA tests on medical diagnostic X-ray equipment has been done from the QA agencies approved by the national regulatory authority, after verification under the supervision of qualified medical physicist. Our group has analyzed QA of 14 mobile X-ray units and 4 fixed X-ray units performed during October 2021 to June 2023 in several attached hospitals. Among these, all the equipment were newly installed except 3 fixed X-ray units which are more than 3 years old equipment. These equipment were manufactured by various companies such as Epsilon, Allengers, Fuji, Konica Minolta etc.

RESULTS: During QA of medical diagnostic X-ray equipment, the common issues were observed that central beam alignment/ focal spot test, kVp accuracy and imaging tests were shown failing while performing QA tests. In one of the mobile X-ray unit, central beam alignment/ focal spot test was failing. The reason behind failing of test was observed that the collimator was not aligned properly and made parallel using spirit level tool. In another case, kVp accuracy test was failing. The probable reason was observed that this mobile X-ray unit was used occasionally as backup due to other available resources. Later, the kVp was recalibrated by the service engineer. In a another mobile X-ray unit, imaging test was failing since untrained service engineer has used over exposure parameter settings without optimization. These faults has been rectified and QA was found satisfactory for all the units.

CONCLUSIONS: The common issues observed during QA of medical diagnostic X-ray equipment were presented. They can be addressed by the probable solutions mentioned in the present study. The common faults and rectification methods has been reported for strengthening of radiation protection culture in a medical diagnostic X-ray facility.

KEYWORDS: medical diagnostic X-ray equipment, quality assurance, radiation protection

ESTIMATION OF SPECIFIC ABSORBED FRACTIONS FOR ¹⁸F

Minal Y. Nadar¹, D.K. Akar¹, H.K. Patni¹, S.K. Nandy² and P. D. Sawant¹

¹Radiation Safety Systems Division, ²RMC, Bhabha Atomic Research Centre, Mumbai, India.

Email: minalyn@barc.gov.in

BACKGROUND/OBJECTIVE: ¹⁸F based radiopharmaceuticals are used in nuclear medicine for diagnostic purpose. The estimation of dose to the patients as well as workers due to internal contamination is important from radiation protection point of view. Specific Absorbed Fractions (SAFs) are important dosimetric parameters for estimation of internal dose. In this study the SAFs are estimated for important source and target organs.

MATERIALS AND METHODS: To estimate the SAFs, ICRP reference male and female voxel phantoms are used as human surrogates in Monte Carlo code 'Fluka'. Source organs are selected based on the data obtained from literature and animal injection studies. The organs for which tissue weighting factors is given in ICRP 103 are chosen as target organs. Monte Carlo simulations were carried out in FLUKA by simulating ¹⁸F contamination in the selected organs of voxel phantom and scoring energy deposition in the target organs. Using Energy deposition in the target organs, SAFs are estimated for both, photon of 511 keV and beta spectrum of ¹⁸F using both the phantoms. SAF to the target organ is the ratio of energy absorbed in the target organ to the energy emitted in the source organ weighted by the mass of the target organ.

RESULTS: SAFs were evaluated for 511 keV photons for various source target combinations of male voxel phantoms are given in the following table. Similarly, SAFs were evaluated for beta spectrum and female voxel phantom. SAFs for the similar target organs in female voxel phantom are found to be higher than male voxel phantom due to lower organ weights. The SAFs for electrons are found to be higher than photons for both the phantoms. As beta spectrum of ¹⁸F has E_{avg} of 249.8 keV and E_{max} of 633.5 keV.

Table. SAFs for 511 keV photons using ICRP male voxel phantom for source organs given in row and target organs given in column.

Source organs	blood	bone	brain	gbcont	heart	kidney	liver	llicont	lungs	muscle	pancreas	sicont	spleen	stcont	ubcont	ulicont
Bladder	3.94E-15	4.78E-15	5.37E-18	9.36E-16	2.20E-16	1.23E-15	5.85E-16	1.69E-14	1.72E-16	4.25E-15	1.19E-15	5.51E-15	4.29E-16	6.04E-16	2.02E-13	2.23E-15
Bone-Marrow	7.93E-16	9.22E-16	3.96E-16	5.10E-16	6.14E-16	6.85E-16	5.69E-16	5.86E-16	7.37E-16	3.73E-16	6.72E-16	5.94E-16	6.32E-16	4.59E-16	7.99E-16	4.33E-16
Bone-Surface	7.25E-17	3.90E-16	6.88E-16	1.86E-16	5.31E-18	1.94E-17	2.04E-16	2.71E-16	5.87E-18	2.02E-16	9.64E-18	2.35E-16	1.84E-17	9.06E-18	4.40E-16	1.16E-17
Brain	2.19E-16	4.37E-15	9.22E-14	1.19E-16	3.42E-16	7.99E-17	1.85E-16	4.10E-17	5.76E-16	7.78E-16	8.48E-17	5.28E-17	1.82E-16	1.37E-16	4.93E-18	6.08E-17
Breast	7.67E-16	4.09E-16	9.41E-17	7.43E-16	5.65E-15	7.65E-16	1.04E-15	1.02E-15	2.90E-15	5.46E-16	1.33E-15	1.04E-15	2.33E-15	4.89E-15	5.35E-17	4.21E-16
Colon	3.58E-15	1.40E-15	2.07E-17	5.94E-15	1.11E-15	6.07E-15	3.59E-15	3.06E-14	7.32E-16	1.67E-15	7.67E-15	1.04E-14	1.67E-15	6.44E-15	5.84E-15	3.45E-14
Gonads	1.06E-15	6.54E-16	4.54E-19	6.23E-17	1.64E-17	8.20E-17	4.02E-17	6.35E-16	1.31E-17	2.07E-15	7.76E-17	2.12E-16	3.16E-17	4.27E-17	2.87E-15	1.36E-16
Liver	7.55E-15	2.63E-15	1.94E-16	5.93E-14	1.22E-14	1.70E-14	7.54E-14	3.95E-15	1.12E-14	2.23E-15	2.92E-14	9.04E-15	5.49E-15	1.53E-14	6.28E-16	1.88E-14
Lung	5.19E-15	1.77E-15	2.83E-16	2.15E-15	1.80E-14	1.79E-15	3.74E-15	1.06E-15	2.27E-14	1.34E-15	2.28E-15	1.46E-15	7.84E-15	5.88E-15	8.37E-17	8.66E-16
Oesophagus	2.92E-14	5.34E-15	1.17E-15	6.54E-15	3.79E-14	4.71E-15	1.15E-14	1.80E-15	2.14E-14	2.64E-15	7.71E-15	3.70E-15	1.05E-14	1.51E-14	1.78E-16	2.15E-15
RemainderTiss	8.41E-15	2.78E-15	3.01E-15	4.29E-14	1.29E-14	1.54E-14	9.89E-15	5.54E-15	6.80E-15	2.15E-15	4.42E-14	1.25E-14	3.85E-14	1.14E-14	8.21E-15	8.84E-15
Salivary-gland	5.38E-16	1.76E-15	5.93E-15	1.29E-16	6.87E-16	1.18E-16	2.11E-16	8.43E-17	1.01E-15	1.32E-15	1.27E-16	9.28E-17	3.82E-16	2.92E-16	6.96E-18	6.59E-17
Skin	4.79E-17	2.22E-16	1.33E-15	2.44E-17	7.76E-17	1.61E-17	3.68E-17	8.95E-18	1.24E-16	9.79E-17	1.93E-17	1.18E-17	3.65E-17	3.08E-17	1.10E-18	1.21E-17
Stomach	1.08E-14	2.13E-15	1.43E-16	1.46E-14	2.35E-14	1.25E-14	1.80E-14	2.12E-14	9.24E-15	2.09E-15	4.70E-14	2.39E-14	3.21E-14	1.35E-13	7.01E-16	9.14E-15
Thyroid	1.08E-14	4.02E-15	2.15E-15	1.14E-15	6.83E-15	7.92E-16	1.92E-15	3.85E-16	1.21E-14	3.26E-15	9.48E-16	5.60E-16	2.04E-15	1.69E-15	4.29E-17	5.11E-16

CONCLUSIONS: Using ICRP reference male and female voxel phantoms, SAFs are evaluated for 511 keV photons and beta spectrum of ¹⁸F. These results will be useful in assessment of internal dose coefficients after intake of ¹⁸F based radiopharmaceuticals.

KEYWORDS: ¹⁸F radiopharmaceutical, internal dosimetry, SAFs, voxel phantom

METHODOLOGY FOR ESTIMATION OF INTAKE AND COMMITTED EFFECTIVE DOSE IN REPEATED INTAKE SCENARIO

Sushanta Halder, Minal Y. Nadar and P. D. Sawant

Radiation Safety Systems Division, Bhabha Atomic Research Centre Mumbai 400085

Email: shalder@barc.gov.in

BACKGROUND/OBJECTIVE: While working in the nuclear facilities, radiation workers may be exposed to radionuclides due to unforeseen situations. These exposures can be acute, multiple, or chronic (lasting for extended periods). Estimating the retention fraction becomes essential in such scenarios. To address this issue, a Python program has been developed for calculating the retention fraction during repeated intake scenarios in the current study.

MATERIALS AND METHODS: This study involves the development of a Python program to handle scenarios of repeated intake. The computed fractions from this program serve as essential parameters for calculating intake or committed effective dose. Let R_n represents the acute retention fraction at the n^{th} day after intake. For cases of repeated intake spanning from day 1 to day m , the chronic retention fraction at any day 'n' can be determined using the formula $R^n = \sum_{i=1}^n R_i$ for $n \leq m$ and $R^n = \sum_{i=1}^m R_{i+n-m}$ for $n > m$. To facilitate this repeated intake scenario, the program requires information about the radionuclide, the duration of repeated intakes, the retention fractions due to acute intake and the days on which retention fractions due to repeated intakes are required. Using this information, the Program calculates retention fractions due to repeated intakes on the given days which then be employed to determine the intake using measurement data.

RESULTS: In the IDEAS/IAEA Intercomparison Exercise on Internal Dose Assessment (Case no-4), a repeated intake of ^{131}I was considered for validation. The guideline provided estimated intakes of 43.2 kBq for each of the three days. Using the above-mentioned program and the acute retention fractions from Mondal/Mondes, the retention fractions were calculated for repeated intakes, resulting in an intake of 43.22 kBq per day which validates the code. However, the program later incorporated thyroid retention data from the OIR data viewer. With this revised biokinetic model, the estimated intake and dose were found to be 11.2% and 23.9% lower, respectively, compared to the values provided by the IAEA.

CONCLUSIONS: The developed methodology can be used to find intake and dose in repeated intake scenarios for any radionuclide.

KEYWORDS: Repeated intakes, Internal dose assessment

ESTIMATION OF PU/AM RETENTION FRACTIONS IN AXILLARY LYMPH NODES

Lokpati Mishra, M. Y. Nadar, I. S. Singh, P. D. Sawant
Radiation Safety Systems Division, Bhabha Atomic Research Centre, Mumbai, India

Email: lokpati@barc.gov.in

BACKGROUND/OBJECTIVE: In case of wound injury on hand with insoluble Pu/²⁴¹Am, it shows tenuous retention at the wound site and then gets slowly transferred to axillary lymph nodes (LNs), blood and subsequently deposit in systemic organs (skeleton, liver etc.). Hence, it is essential to precisely estimate the ²⁴¹Am content in lymph nodes as it would interfere in ²⁴¹Am measurements in Lungs and Liver. Retention fractions for Pu/Am in axillary LNs are not provided by ICRP. These fractions are important for assessment of intake due to Pu/Am internal contamination in axillary lymph nodes after wound contamination.

MATERIALS AND METHODS: NCRP wound model in association with GI tract model and systemic biokinetic models is solved to study the temporal profile of retained activity in axillary LNs for five different wound categories viz. fragment, soluble, colloidal & intermediate state (CIS), particles, aggregates and bound states (PABS), and trapped particle and aggregates (TPA). Retention fractions, are shown in Figure 1 for Pu/Am compounds.

RESULTS AND DISCUSSION: Pu, and Am both the radionuclides show similar trends for retention fractions with minor variations. Transfer rates in wound and GI tract models are mostly the same, but differences arise due to systemic biokinetic variations for Pu and Am. PABS and CIS categories exhibit higher retention fractions in axillary LNs within the initial 100 days due to direct transfer from these compartments. CIS shows outward movement to three compartments (PABS, soluble, and LN), while PABS only moves towards soluble and LN compartments. The transfer rate from CIS to soluble is approximately 125 times greater than PABS to soluble transfer rate, leading to a more rapid reduction in CIS's retention fraction compared to PABS. Soluble (strong) and soluble (avid) categories exhibit similar trends in retention fractions, with slightly higher values in the avid category due to more inward transfer rates from CIS and PABS. Similarly, retention fractions for moderately soluble compounds are slightly higher than for weakly soluble compounds. Fragment category radionuclides have negligible outward transfer rates to the soluble compartment, leading to initial transfer to PABS and a subsequent rapid reduction and saturation around 1000 days. In this case, most of the radionuclides are trapped as TPA, with minimal transfer to axillary LNs in the initial few days after intake.

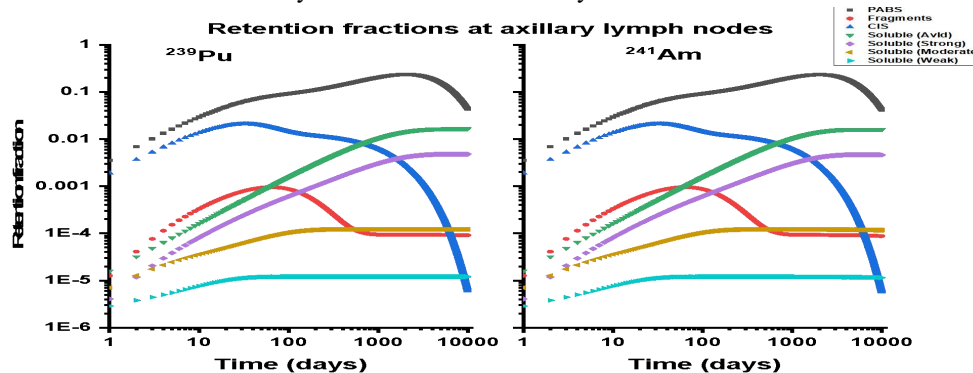


Figure 1: Pu/Am retention fractions in axillary lymph nodes for various categories of compounds after wound intake.

CONCLUSIONS: Pu and Am both exhibit similar retention in axillary LNs with minor variations which are mainly attributed to systemic biokinetic model variations for Pu and Am. These results will be useful in assessment of Pu/Am internal contamination after wound intake.

KEYWORDS: axillary lymph nodes, internal dosimetry, wound contamination

A DIGITAL PULSE SHAPE DISCRIMINATOR FOR SEPARATING LOW AND HIGH ENERGY PHOTON PULSES OF PHOSWICH DETECTOR

Deepak K. Akar^{1,2}, I. S. Singh², M. Y. Nadar², Lokpati Mishra², P. D. Sawant², R. G. Thomas^{1,3}

¹Homi Bhabha National Institute, Mumbai, India.

²Radiation Safety Systems Division, Bhabha Atomic Research Centre, Mumbai, India.

³Nuclear Physics Division, Bhabha Atomic Research Centre, Mumbai, India.

Email: akardeep@barc.gov.in

BACKGROUND/OBJECTIVE: Pulse shape discrimination (PSD) technique, distinguishes particles using pulses of different rise times by their interactions in detectors. In digital pulse processing (DPP), signals are digitized using fast analog to digital converters (FADC). Further mathematical algorithms are applied during acquisition or offline for any further mathematical analysis. This work presents its application to get both the low and high energy spectrum with phoswich detector simultaneously.

MATERIALS AND METHODS: A phoswich detector having 3 mm primary NaI(Tl) followed by 5 cm CsI(Tl) crystal and ¹³⁷Cs (662 keV) and ²⁴¹Am (59.5 keV) point sources kept at 10 cm from detector face have been used in this study. 60 keV photons are fully absorbed in the NaI(Tl) detector and 662 keV photons interact in Cs(Tl). The output pulses have rise time of 0.25 μs and 1.1 μs for NaI(Tl) and Cs(Tl) respectively. These pulses are recorded and analysed by DPP-PSD having 14-bit FADC, sampling at 250 MegaSamples/second, to get energy and PSD spectra. The PSD value is computed as $(Q_{long} - Q_{short}) / Q_{long}$, where Q is charge integrated from pulse in gate duration. In this study, long and short gates are kept as 2800 and 800 nsec to separate pulses coming from NaI(Tl).

RESULTS: The PSD and energy spectra for ¹³⁷Cs and ²⁴¹Am are shown in Figures. The unfiltered spectra are due to all pulses from phoswich detector. The lower PSD value is due to photon interactions in NaI(Tl) which gives filtered low energy photon spectrum.

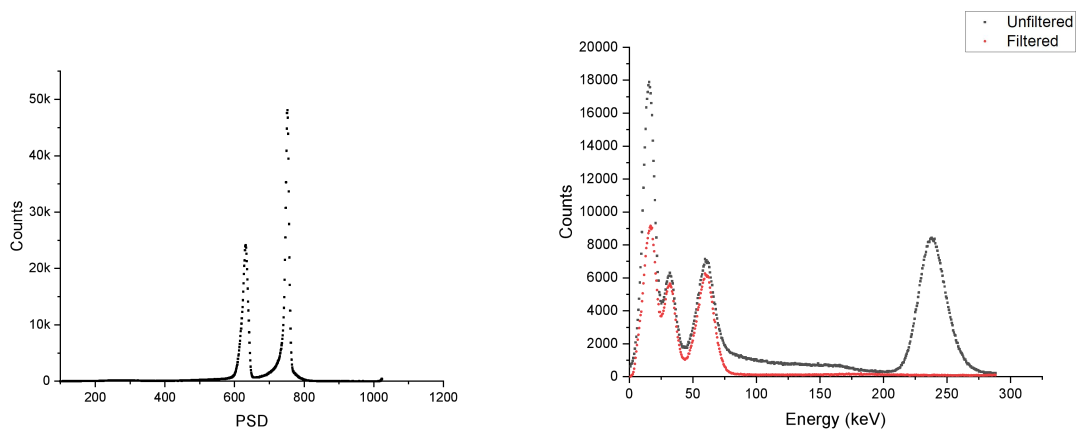


Fig: (a) Timing and (b) Energy spectrum of phoswich detector with ¹³⁷Cs and ²⁴¹Am.

Conclusions: This system will be useful for the in-vivo monitoring of low energy photos emitters in radiation workers in presence of high energy photon emitters.

Keywords: DPP-PSD, phoswich detector, pulse shape discrimination, in-vivo measurement.

RADIONUCLIDE TARGETED THERAPY WITH I-131 AND QUALITY AUDIT OF ITS ACTIVITY MEASUREMENTS WITH RADIONUCLIDES CALIBRATORS

Anuradha Ravindra, D.B.Kulkarni, Ritu Sharma, V.Sathian, Probal Chaudhury

Radiation Safety Systems Division, Bhabha Atomic Research Centre, Mumbai, India.

Email: anur@barc.gov.in

BACKGROUND/OBJECTIVE: Radionuclide targeted therapy is a form of treatment that delivers therapeutic radiation doses to destroy the cancerous cells and shrink the malignant tumors. It is a systematic and very specific form of treatment which delivers a localized dose to the specific organ, thus eliminating both the primary tumor site and cancer that has spread across the body. Several radionuclides like ^{131}I , ^{177}Lu , ^{153}Sm , ^{188}Re , ^{89}Sr , ^{204}Tl , ^{225}Ac , ^{211}At , ^{212}Bi are used for targeted therapy, but one of the most commonly used radionuclide in India is ^{131}I for treatment of thyroid ailments and other malignancies like myocardial and lymphomas. Prior to the dose delivery in the form of radioactivity to the patient, it is measured with the radionuclide calibrators (RC). Radiation dose delivered in external beam therapy, brachytherapy is precise and accurate while in nuclear medicine procedures dose delivered to the patient is difficult to measure directly. This is mainly due to the fact that the radiation source as radiopharmaceutical is situated internally in the patient's body and variation in the biological distribution of the radiopharmaceutical between patient to patient depends upon individual metabolism. Hence, it is essential to ensure that clinically prescribed activity is administered as accurately as possible. Thus, accurate activity measurements play a pivotal role in effective and successful treatment to the patient. BARC as designated institute (DI) of ionizing radiation ensures the traceability of radioactivity measurements in the field nuclear medicine by conducting nationwide quality audit programme (QAP) biannually. QAPs ensure the calibration and performance of radionuclide calibrators so that the activity measured before administering to patients for diagnostic/therapeutic applications is compliant within regulatory limits of $\pm 10\%$ of the prescribed activity.

MATERIALS AND METHODS: The audit protocol involves a test source in injection glass vial similar to the clinical geometry, calibrated by BARC against the national standard for activity measurements and then shipped to the participating hospitals/nuclear medicine centres. The sources are measured using RC by the participants as per protocols given and the results are reported to the DI (BARC) for further evaluation. This format of audit has an advantage of having a complete control of source preparation as well as calibration by the DI which ensures consistency, accuracy and harmonization of procedures at all stages. Detailed protocol for performing the measurements at the nuclear medicine centre (NMCs) and an excel spreadsheet was sent for maintaining uniformity in measurements as well as reporting of the measurement results.

RESULTS: The 20th national audit of ^{131}I activity measurements was organized during Nov 2022 – March 2023. 216 NMCs accepted to participate of the 450 registered with AERB. Most interestingly, a total of 437 results were reported from 216 NMCs which implies that many NMCs (62%) have more than one RC indicating an increasing demand for nuclear medicine procedures in India. The performance statistics of RCs were analysed using two methods: calculation by percentage difference and by z-scores. From both analyses, 93% of the results received from the NMCs have demonstrated compliance within the acceptable limits of $\pm 10\%$.

CONCLUSIONS: The audit results demonstrate effective therapeutic outcome to the patient. The rigorous efforts of BARC, as DI, to establish the measurement traceability, dissemination of ionising radiation standards to various NMCs in the country for safe and effective use of radiopharmaceuticals in the country is demonstrated by the QAP.

KEYWORDS: nuclear medicine, quality audit, targeted radionuclide therapy, radionuclide calibrators

DESIGN AND DEVELOPMENT OF AUTO-IRRADIATOR SYSTEM WITH EXISTING CS-137 SOURCE FOR CALIBRATION EXPOSURE OF TLD CARDS

M. K. Kamble, Deepika Dhamode, A. K. Bakshi and B. K. Sapra

TLD Unit, Radiological Physics & Advisory Division, Bhabha Atomic Research Centre, Tarapur, India

Email: mkkamble@barc.gov.in

BACKGROUND/OBJECTIVE: TLD Unit of Tarapur is responsible for TLD based personnel monitoring of radiation workers of BARC, Tarapur facilities on monthly basis. For calibration of TLD reader, it is required to irradiate TLD badges to ^{137}Cs source at a fixed distance with reproducible geometry and accurate output in terms of mR/h or mSV/h. The usual practice to irradiate TLD badges was to use a wooden plank based table and placing the source manually and using a manual timer for delivering required dose. The objective of the present study was to design and fabricate an automated irradiation system with existing source with proper source housing /storage and remote operation and reproducible geometry.

MATERIALS AND METHODS: Analytical method such as attenuation coefficient and inverse square law was used to calculate shielding thickness involving lead and mild steel for the source housing considering the present activity (283 mCi) of ^{137}Cs source. Input on design aspects namely (i) shielding thickness, (ii) radiation level outside the housing, (iii) height of the source in exposed position, (iv) diameter of the zig for irradiation of the TLD badge, (v) source dimension and weight, (vi) activity of source with date, (vi) source movement time, (vii) source movement mechanism, (viii) provisions in the operational software etc. were discussed with a private manufacturer for fabricating the automated irradiator.

RESULTS & DISCUSSION: Based on the inputs an Auto-irradiator system has been fabricated by M/s Noble Design Solutions, Navi Mumbai and installed at TLD Unit, Tarapur. It has two parts (a) Control panel and (b) source housing attached to Perspex Stage (50 cm radius) to hold TLDs. The control panel made with IP54 rated design, which contain all necessary electronics microcontroller, UPS and batteries, time can be set for required exposure and with commands and passwords from keypad, source is raised from storage using a actuator arm and expose TLDs placed on stage. Once time is over, source is lowered in housing and its door closes securing it. In any emergency or power failure, the source in ON position is safely returns to home position. The system has source transit time of 2.5 s. Control panel has two modes viz. dose mode or timer mode. Time for dose is calculated by the software. Control panel has alpha- numeric LCD display. Software has a provision to record all the details of the irradiation and store it in the memory which can be extracted or printed with a thermal printer for record keeping purpose. The system has door interlock as well as electro-mechanical lock in the housing as a necessary requirement to operate the system so that unwarranted exposure to other staff of the plant is ruled out as the source room is located at isolated place. Perspex ring is attached to the source housing in such a way that the TLD badges can be placed at height of 1.2 m from the floor and at 50 cm from the source with reproducible geometry. The source housing has 11 cm (lead +steel) shielding all around the source to keep radiation level < 1 mR/h outside source housing. After the system has been installed radiation survey with a gamma survey meter model RADOS, RDS- 31, MIRION Technology Makeabout 16 $\mu\text{R/h}$. Further, as the irradiation geometry has been changed, output of the source at 50 cm has been calibrated through Radiation Standards Section, RSSD, BARC. It is found to be 2.78 mSv/h. The same has been fed into the software for irradiation time calculation of the TLD badge using software taking care of the decay constant of the source.

CONCLUSION: A manually operated existing irradiation set up has been converted into an automated and remote controlled irradiation system with existing Cs-137 source. The radiation level outside the source housing with source off condition and output of the source at 50 cm have been measured. The system is working satisfactorily. It will enhance the reliability of the calibration irradiation of TLD badges. The in-built safety features of the system make the system more robust, free from manual error and safe to for staff to irradiate TLD badge without getting unnecessary dose due to manual handling of source.

MEFOMP VIEWS FOR EDUCATION AND TRAINING IMPROVEMENTS IN ITS MEMBER STATES

RiadShweikani¹, Mohammad Hassan Kharita², RabihWafiqHammoud², MeshariAlneaimi³

¹Department of protection and Safety, Atomic Energy Commission of Syria Damascus, P. O. Box 6091, Syria,

²Department of Radiation Safety, Hamad Medical Corporation, Qatar, ³Radiation Physics Department, Kuwait
Cancer Control Centre, Kuwait

Email:rshweikani@gmail.com

BACKGROUND/OBJECTIVE: Middle East Federation of Organizations of Medical Physics was established in 2009 with 12 participating countries. MEFOMP is part of IOMP efforts to further enhance and improve the status of medical physics in all regions across the Globe. One of MEFOMP mission is to enhance medical physics practice throughout Middle East by fostering the educational and professional development of medical physics.

MATERIALS AND METHODS: It is a challenge to acquire qualified medical physicists in MEFOMP MS due many reasons such as limited number of universities offering this specialty, limited awareness about the importance of this profession and absence of recognition of the profession by some of the local authorities. In addition Clinical training is also a big challenge due to: Lack of senior medical physicists for the training, Limited treatment, imaging and dosimetry equipment, the need for a comprehensive clinical training programme, lack of quality management systems and financial support.

RESULTS: Therefore, MEFOMP is working on collaborate with the international organizations to establish an accreditation system for educations and clinical trainings to be applied on the existed such programmes within MEFOMP MSs (Arabic & English), adopt a programme for certification of individuals to be medical physicists in the various specialties (diagnostic, therapy, nuclear medicine) in their countries, and establish cooperation programmes between MEFOMP MSs for clinical training for postgraduates students in medical physics. In addition MEFOMP encouraging its MS to recognize the medical physicists as a profession in their health systems, enforce the existence of MP in licensing medical practices and establish a clinical training programme for postgraduates or facilitate collaboration with other MEFOMP MSs.

CONCLUSIONS: MEFOMP is keen to establish an accreditation system for postgraduate education courses, clinical trainings and other training activities within MEFOMP member state, and a certification programme for individuals, under the supervision of MEFOMP, in collaboration with other international organizations.

KEYWORDS: clinical training, accreditation, certification, education and training

THE IMPACT OF TUMOR VOLUME ON DOSE TO PIBS POINTS IN BRACHYTHERAPY OF LOCALLY ADVANCED CERVICAL CANCER: A DOSIMETRIC STUDY

Lalit Mohan Aggarwal¹, Sunil Choudhary¹, AnkitaSingh¹, Ashish Verma² and AnkurMourya¹,

¹Department of Radiotherapy and Radiation medicine,²Department of Radiodiagnosis and Imaging Institute of Medical Sciences, Banaras Hindu University, Varanasi, India

Email: lalitm@bhu.ac.in

BACKGROUND/OBJECTIVE:To study the Variation in Dose to PIBS (Posterior Inferior Border of Symphysis) points with the change in Tumour volume in HDR (High Dose Rate) Brachytherapy of Locally Advanced Cervical cancer.

MATERIAL AND METHODS: A total of 45 untreated patients, with ECOG 0-2 registered from December 2019 to March 2021 with histopathologically proven carcinoma cervix from stage IIB to IVA were included in the study. All the patients received external beam radiation therapy (EBRT) on 6 MV Linear Accelerator with Volumetric modulated arc therapy (VMAT) to a dose of 45 Gy in 25 fractions to the pelvis and 55 Gy in 25 fractions to the positive nodal disease (Pelvic & Paraaortic) with simultaneous integrated boost (SIB) along with weekly concurrent cisplatin at 40 mg/m². Twenty-three patients were treated with Intracavitary Brachytherapy (ICRT) with a dose of 7 Gy per fraction for three weekly fractions. CT images of all the patients were obtained with 1 mm slice thickness & 3-D planning was done on the Oncentra treatment planning system. The contouring of targets and OARs (organs at risk) was done as per ICRU 89¹. Twenty-two patients were treated with interstitial brachytherapy (ISBT), with 6 Gy per fraction for four fractions. The dose was prescribed to HR CTV and point A for ISBT and ICRT respectively.

RESULTS: Out of 45 patients, 11 patients had a tumour volume of more than 100 cc. The dose at PIBS +2,0 (p=0.000; p=0.003) was significantly higher when the tumour volume was more than 100 cc. However, the dose at PIBS -2 (p=0.333) and rectovaginal point (p=0.992) were not significantly affected by the increase in tumour volume.

CONCLUSION: The dose at PIBS points should be reported along with rectal, bladder, sigmoid colon and other relevant organs at risk. in all patients of locally advanced cervical cancer. Efforts during brachytherapy planning should be taken to reduce the dose to PIBS points and hence vaginal toxicity².

KEYWORDS: MUPIT, HDR Brachytherapy, PIBS, Tumour Volume, Cervical cancer

AN OVERVIEW OF BARC DEVELOPED RUBY PLAQUES FOR EYE CANCER TREATMENT

Prithwish Sinharoy, Dayamoy Banerjee, Ramakant, Sumnesh Wadhwa, Sanjay Kumar,

Smitha Manohar

Nuclear Recycle Group, Bhabha Atomic Research Centre, Mumbai, India

Email: daya@barc.gov.in

Plaque brachytherapy is one of the most fruitful technologies used for treatment of intraocular melanoma which includes choroidal melanoma, uveal melanoma and retinoblastoma. Among all the brachytherapy sources, Ru plaques received significant advantages owing to its high beta energy (3.54 MeV) emanating from the decay of its daughter and higher radiological half-life (371 days). This paper summarizes development of an indigenous technology for the manufacturing of the RuBy plaques and its successful applications in eye cancer treatment in India over four years.

Till date, BARC has developed and deployed four types of configurations (Figure 1) for treatment of eye cancers located at different positions of eye while minimizing collateral effects to the healthy organs of the eye and these four configurations would treat almost 98% of Indian patients.



Figure 1: BARC developed RuBy Plaques for eye cancer treatment. MOC: Pure Silver (99.9%)

The successful journey of indigenous RuBy plaques deployment started on 21st September 2019 with A-type plaque to the patient having ocular surface squamous neoplasia with scleral invasion and presently it has crossed more than 150 treatments at ten hospitals of the country. All successful post treatment results coupled with low cost and easy to use, help RuBy plaque to earn trust of doctors and patients alike. More hospitals are progressively adopting RuBy Plaques for better and cost-effective treatment of eye cancers across the country. Indigenous development of RuBy Plaques is a major breakthrough in the area of AtmaNirbhar healthcare.

ACKNOWLEDGMENT: Authors sincerely thank scientists from RSSD, RPAD, and NRG, BARC for their contribution towards successful manufacturing and characterizations of RuBy Plaques. Authors whole heartedly thank BRIT officials for their help towards onward submission of plaques to hospitals.

REFERENCE: Prithwish Sinharoy, Dayamoy Banerjee, Rohit Gupta, Arvind Ananthanarayanan, Pawan D Maniyar Ramakant, Jayesh G Shah, Kailash Agarwal, Smitha Manohar, Development of ^{106}Ru bearing Sealed Source for Eye Cancer Treatment Applications, BARC Newsletter, July-August, 2018.

Presentation ID: P-345

Abstract ID: O4830

A COMPARISON OF MONTE CARLO SIMULATIONS AND MEASUREMENTS FOR PRE-TREATMENT POINT DOSE VERIFICATION FOR HEAD AND NECK VOLUMETRIC MODULATED ARC THERAPY

Sumeesh S,^{1,2} Mr. Sarin B,² Raghukumar P.,² Shaiju V. S.,² V.K.Sathiya Narayanan,¹
Raghavendra Holla¹

¹Ruby hall clinic, Pune, Maharashtra, India, ²Regional Cancer Centre, Thiruvananthapuram, Kerala, India

Email: sumeesh88.s@gmail.com

AIM: To investigate the feasibility of pre-treatment point dose measurements on an indigenously-fabricated head phantom for head and neck volumetric modulated arc therapy using Monte Carlo simulation.

MATERIALS AND METHODS: The treatment plans of twenty head and neck cancer patients were selected for this study retrospectively based on the prescribed dose. Pre-treatment verification plans for these twenty patients were generated on an indigenously-fabricated PMMA head phantom using Eclipse™ v15.6.05 planning system to perform the point dose measurements. The measurements were carried out using a True Beam™ (Varian Medical Systems®) linear accelerator. To verify the accuracy of Eclipse™ planning system the measured dose was compared with the Monte Carlo simulation and TPS calculated dose. Simulations were performed using PRIMO MC Code. Initially, validation of phase space for the 6MV photon beam for True Beam™ was done by comparing the simulated percentage depth dose (PDD) and transverse profiles against the measured curves, which were acquired during the commissioning. In addition, validation of the treatment planning system was also performed on an indigenously-fabricated PMMA head phantom using MC simulation in conjunction with point dose measurements.

RESULTS: Gamma analysis of measured and simulated PDD curves and profiles shows a minimum pass rate of 99% and 97.42%, utilizing 2 mm DTA and 2% percentage dose variations. A comparison of the mean dose to the detector volume obtained from PRIMO and TPS reveals that Acuros® XB Dw underestimates the TPS calculated dose by 1.79%. The mean % deviation between simulated and TPS calculated dose was much smaller for AAA and Acuros® XB Dm with -0.84% and -0.42%. The p value between the simulated dose and the dose calculated by Acuros® XB Dm was found to be 0.002. The % deviation between the measured and TPS calculated doses were studied, the maximum mean % dose variation was observed for Acuros® XB Dw (1.92%) and the minimum mean dose variation was observed for Acuros® XB Dm with -0.30%. The statistical analysis of the detector's mean dosage for both measured and MC was insignificant with a p value of 0.386.

CONCLUSION: In this study we evaluated the patient-specific dose estimations using MC simulation and point dose measurements. The comparison of measured data with other dose calculation methods, including MC, will help the users in selecting the optimal methodology for pre-treatment dose verification.

INVESTIGATING THE INFLUENCE OF MINIMUM SEGMENT WIDTH IN VOLUMETRIC MODULATED ARC PLANNING OF PROSTATE CANCER

Nidhi Jain, Alok Kumar, Ashok Kumar

Department of Physics, Amity institute of Applied Science, Amity University, Noida, UP
Department of Radiation Oncology, Netaji Subhas Chandra Bose Cancer Hospital & Research Institute, Kolkata

Email: jain.nidhi72@yahoo.com

INTRODUCTION: Prostate cancer is a prevalent form of cancer among men, and radiation therapy plays a crucial role in its treatment. Volumetric Modulated Arc Therapy (VMAT) is a precise radiation delivery technique that aims to target tumor volumes while minimizing the dose to surrounding healthy tissues. The planning process in VMAT involves various parameters, including the Minimum Segment Width (MSW), which determines the optimized apertures.

AIM: This study aims to investigate the impact of the minimum segment width on the planning outcomes of VMAT in patients with prostate cancer and find the optimum value(s) for this parameter.

MATERIAL AND METHOD: A retrospective analysis was conducted on 12 patients with prostate cancer who underwent VMAT treatment. For every patient, four treatment plans were created using different values of MSW (0.5cm, 1.0cm, 1.5cm, and 2.0cm). Other optimization parameters and objective constraints were kept the same across every case. Several dosimetric parameters were evaluated, including target coverage (Dmean - Mean dose to the planning target volumes (PTV), Dmax - Maximum dose to the PTV, conformity index (CI), homogeneity index (HI)), and dose to the organ at risk. Additionally, delivery efficiency metrics such as the number of control points (CP), Monitor units (MU), and treatment time were assessed. Statistical analyses were performed using Wilcoxon signed-rank test.

RESULT: Preliminary findings suggest that the choice of Minimum Segment Width significantly influences the quality of treatment plans and delivery efficiency in VMAT for prostate cancer. Narrower segments (MSW 0.5) yielded improved PTV coverage and conformity, while wider segments (MSW 2.0) led to faster treatment delivery but compromised dosimetric parameters. There was no statistically significant difference between MSW 0.5 and MSW 1.0 ($p > 0.05$) while the other MSW values showed statistically significant differences ($p < 0.05$).

CONCLUSION: Based on the analysis of the plan quality and delivery efficiency, both MSW values of 0.5cm and 1.0cm exhibit similar features in prostate cancer treatment plans. Further investigation with a larger number of patients and assessment of clinical outcomes is necessary to validate this conclusion.

KEYWORDS: Minimum Segment Width, Prostate Cancer, Volumetric Modulated Arc Planning, VMAT, MSW

ADVANCEMENTS IN DEEP LEARNING BASED SUPER-RESOLUTION ARCHITECTURES FOR MEDICAL IMAGES

Arita Halder¹, Sumana Halder¹

¹School of Medical Science and Technology, Indian Institute of Technology, Kharagpur, India.
Email of presenting author: aritahalder@gmail.com

BACKGROUND/OBJECTIVE: Image enhancement is crucial for improved medical image visualization and gaining valuable insights into systems biology. Super-resolution (SR) is a technique aimed at enhancing the spatial resolution of images beyond the inherent capabilities of the imaging system. In radiology, it has become a promising area of research as it holds the potential to improve image quality, aid in better diagnoses, and reduce the need for higher radiation doses. This abstract reviews current deep-learning (DL) based SR methods.

MATERIALS/METHODS: Traditionally, image enhancement relied on mathematical models. Super-resolution (SR) methods can be categorized into single-image SR (SISR) and multiple-image SR (MISR). In recent years, various DL architectures have been suggested for medical image super-resolution (SR). One such architecture, the SR convolutional neural network (SRCNN), can operate on high-resolution images like CT scans, Ultrasound images, or MRIs. It uses low-resolution (LR) images generated from the high-resolution (HR) images as input during training and aims to produce HR images as output through the training process. U-Net is a popular architecture in medical image SR. It includes a contracting path to capture context information and a symmetric expanding path for accurate localization. GANs are a type of deep learning model that consists of two networks: a generator and a discriminator. The generator network generates SR images from LR inputs, while the discriminator network tries to distinguish between real high-resolution images and the generated SR images. The two networks are trained adversarially, with the generator trying to produce more realistic SR images to fool the discriminator. GANs have been successful in producing high-quality SR results, although training can be challenging and requires careful tuning.

RESULTS: Super-resolution techniques are widely applied to improve medical image quality. Ultrasound SR aids in diagnostics by resolving echoes beyond the diffraction limit, especially for imaging microvasculature in organs and tumors. In CT, super-resolution enhances low-dose image quality, while neural network architectures enhance MRI for highly down-sampled images, enabling the display of diverse tissue properties in multi-contrast images.

CONCLUSIONS: Super-resolution techniques, particularly those leveraging deep learning architectures, hold great promise in enhancing medical image quality and aiding accurate diagnoses.

KEYWORDS: super-resolution, medical images, image enhancement, deep learning

MEASUREMENT OF EFFECTIVE VOXEL SIZE IN CT

Katsumi Tsujioka

School of Medical Sciences, Fujita Health University, Toyoake-city, Aichi, Japan

Email: tsujioka@fujita-hu.ac.jp

Background/Objective: Conventionally, evaluation of spatial resolution in CT has been performed using MTF. MTF does not perform a contrast comparison because normalization is performed in the middle of the calculation. However, in the assessment of small vessels, the contrast difference alters the visualization of the vessels. We propose an effective voxel size evaluation to solve this problem. The voxel size has a voxel size due to the structure of the CT device and an effective voxel size due to the image. We measured the effective voxel size of the CT machine from the experimental images.

Materials and methods: A spiral wire phantom was used for the experiment. The Spiral wire phantom is a 40mm diameter acrylic cylinder with a 0.1mm diameter metal wire wound spirally. The pitch of the spiral is 5mm per turn. Scans were performed with the long axis of the spiral wire phantom positioned along the Z axis of the CT machine. LSF and MTF in the X-Y plane were calculated from the CT images obtained by the experiment. LSF, MTF and slice thickness in the Z direction were calculated from the CT images obtained by the same experiment.

Results: The MTF of high-resolution CT was improved compared to conventional CT. The slice thickness of conventional CT was 0.625 mm, and the slice thickness of high-definition CT was 0.378 mm. The peak CT value of conventional CT was 579.2 HU, and the peak CT value of high-resolution CT was 1540 HU. The effective voxel size of high-resolution CT was 37.6% compared to that of conventional CT.

Conclusions: MTF alone cannot accurately assess small vessel visualization. Measurement of effective voxel size enabled evaluation of spatial resolution and vessel contrast. Measurement of effective voxel size will be a new evaluation method for small vessels by CT.

Keywords: X-ray CT, performance evaluation, small vessels, spatial resolution, voxel size

INTEGRATING PLAN COMPLEXITY AND DOSIOMICS FEATURES WITH DEEP LEARNING IN PATIENT-SPECIFIC QUALITY ASSURANCE FOR VOLUMETRIC MODULATED ARC THERAPY

Ce Han, Jinling Yi , Ji Zhang , Xiance Jin

Wenzhou Medical University, Shangcai Vallege, Wenzhou, 325000, China

Email: han_ce06@163.com

PURPOSE: To investigate the performance of deep learning (DL) models combined with plan complexity (PC) and dosiomics features in the patient-specific quality assurance (PSQA) for patients underwent volumetric modulated arc therapy (VMAT).

METHODS:Total of 201 VMAT plans with measured PSQA results were retrospectively enrolled and divided into training and testing sets randomly at 7:3. PC metrics were calculated using house-built algorithm based on Matlab. Dosiomics features were extracted and selected using Random Forest (RF) from planning target volume (PTV) and overlap regions with 3D dose distributions. Top 50 dosiomics and 5 PC features were selected based on feature importance screening. A deep learning (DL) DenseNet was adapted and trained for the PSQA prediction.

RESULTS:The measured average gamma passing rate (GPR) these VMAT plans was $97.94\% \pm 1.87\%$, $94.33\% \pm 3.22\%$, and $87.27\% \pm 4.81\%$ at the criteria of 3%/3mm, 3%/2mm, and 2%/2mm, respectively. Models with PC features alone demonstrated the lowest area under curve (AUC). The AUC and sensitivity of PC and dosiomics combined model at 2%/2 mm were 0.915 and 0.833, respectively. The AUCs of DL models were improved from 0.943, 0.849, 0.841 to 0.948, 0.890, 0.942 in the combined models (PC+D+DL) at 3%/3mm, 3%/2mm and 2%/2mm, respectively. A best AUC of 0.942 with a sensitivity, specificity and accuracy of 100%, 81.8%, and 83.6% was achieved with combined model (PC+D+DL) at 2%/2 mm.

CONCLUSIONS:Integrating DL with dosiomics and PC metrics is promising in the prediction of GPRs in PSQA for patients underwent VMAT.

ABSTRACT KEYWORDS: Deep learning; Dosiomics feature; Plan complexity; Classification; Patient-specific quality assurance;

COLLABORATION WITH AMERICAN ASSOCIATION OF PHYSICISTS IN MEDICINE THROUGH THE NETWORK OF GLOBAL REPRESENTATIVES

Eugene Lief¹, Wilfred Ngwa^{2,3}

¹Department of Radiation Oncology, VA Medical Center, Bronx, New York, USA, ²Department of Radiation Oncology & Molecular Radiation Sciences, Johns Hopkins Medicine, Baltimore, MD, USA, ³Rutgers Global Health Institute, Rutgers University, Newark, NJ, USA.

Email: eugenelief@hotmail.com

BACKGROUND/OBJECTIVE: American Association of Physicists in Medicine (AAPM) actively collaborates with foreign sister societies and colleagues from Low and Middle Income Countries (LMIC). Some initiatives of a newly formed International Council (IC) of AAPM include determining and prioritizing immediate needs of our colleagues overseas.

MATERIALS AND METHODS: IC includes a newly formed Global Needs Assessment Committee (GNAC) and its Global Representative Subcommittee (GRSC). The purpose of the latter is to create a network of regional representatives to better communicate the local needs. Members of the Subcommittee attended several regional conferences, such as 19th SEACOMP in 2021, and in 2022: ALFIM in Brazil, Greater Horns of Africa Oncology Summit (GHOS) in Tanzania, and 1st Regional Conference of the Federation of African Medical Physics Organizations (FAMPO) in Morocco. AAPM sponsored our Consultant, President of FAMPO, Christopher Trauernicht to speak at the 64th Annual Meeting in Washington DC.

RESULTS: As of this moment, GRSC has recruited 5 representatives from major geographical regions (North and South Africa, South America, Europe and Australia) to serve as Consultants. 3 of them gave virtual presentations at the parent Committee meeting (GNAC) on the regional needs, with few more in preparation. Communications at the meetings and afterwards allow us to build a comprehensive Global Representatives Network (GRN).

CONCLUSIONS: The most effective help to LMIC should be based on adequate assessment and prioritizing of the local needs. The AAPM Committee and GRN structures allow proper two-way communication by the AAPM with the sister societies and individual physicists. We encourage all our colleagues from LMIC to get in touch with GRSC represented by the speaker or your local Consultant to our Subcommittee.

KEYWORDS: American Association of Physicists in Medicine, Low and Middle Income Countries, International Council, Global Representatives Subcommittee.

INTERCOMPARISON STUDY OF INFLUENCING FACTORS ON PERFORMANCE OF RADIATION SURVEY METERS IN DIAGNOSTIC X-RAY ENERGY RANGE

Philomina Akhilesh¹, Sunil Dutt Sharma^{1,2} and Balvinder Kaur Sapra^{1,2}

¹Radiological Physics & Advisory Division, Bhabha Atomic Research Centre, Mumbai, India

²Homi Bhabha National Institute, Mumbai, India.

Email: pmina@barc.gov.in

BACKGROUND/OBJECTIVE: Ionisation chambers are regarded as the preferred technology for radiation survey measurements in diagnostic x-ray facilities because they exhibit a uniform response over a broad energy spectrum. However, in recent years semiconductor based survey meters have become an alternate choice due to factors like compact size and ruggedness. This abstract presents the outcome of the performance tests conducted on a semiconductor based survey meter against pressurized ion chamber survey meter in a diagnostic x-ray facility.

MATERIALS AND METHODS: The response variation of semiconductor survey meter and pressurized ion chamber survey meter was studied with respect to exposure time and energy. The studies were performed in Siemens Polydoros X-ray Unit. The x-ray exposure time was varied from 500 to 1800 ms. The response of both the survey meters were normalized with respect to the measured output exposure rate. The energy dependence of semiconductor based radiation survey meter was studied in the kilovolt range used in diagnostic x-ray imaging (40 kV to 110 kV) and compared against the response of pressurized ion chamber survey meter.

RESULTS: The results show that the response of semiconductor based survey meter is relatively independent of exposure time whereas pressurized ion chamber survey meters showed significant variation with time. The energy dependence response pattern of both survey meters were found similar in the studied energy range. However, large variation was observed between the responses of the studied survey meters to the same radiation field.

CONCLUSIONS: Pressurized ion chambers may underestimate the dose rate significantly in diagnostic x-ray energy range and therefore should be interpreted with correction factors. Semiconductor survey meter showed a stable response relatively independent of exposure times and hence was found more suitable for use in applications where prolonged exposure times are not possible.

KEYWORDS: radiation survey meter, diagnostic x-ray, semiconductor, ion chamber

COULD TEXTURAL ANALYSIS OF MR IMAGES REDUCE OVERDIAGNOSIS AND OVERTREATMENT IN PROSTATE CANCER

Ioannis Seimenis¹, Constantinos Loukas¹, Dimitrios Thanasis¹, Athanasios Tsochatzis², Efstratios Karavasilis³

¹Medical Physics Lab, Medical School, National and Kapodistrian University of Athens, Athens, Greece,²Department of Radiology, Hygeia Hospital, Athens, Greece,³Medical Physics Lab, Medical School, Democritus University of Thrace, Alexandroupolis, Greece.

Email: iseimen@med.uoa.gr

BACKGROUND/OBJECTIVE: Exclusion of clinically significant prostate cancer is essential to reduce harm from overtreatment. An accurate, non-invasive method is therefore required for identifying benign prostatic disease and for the active surveillance of localised prostate cancer. This work explores if textural analysis of acquired MR images can serve these goals.

MATERIALS AND METHODS: 40 patients with increased prostate specific antigen (PSA) and prostatic hyperplasia or neoplasia were enrolled in this study granted with ethical approval. Patients were scanned at 3.0T using a multiparametric protocol according to the **Prostate Imaging-Reporting and Data System (PIRADSv2)**. All patients underwent transrectal ultrasound guided biopsy following MRI, whilst the Gleason score and the International Society of Urological Pathology (ISUP) grade group were recorded. Acquired T2-weighted and diffusion-weighted images were reviewed by an experienced radiologist and the dominant visible lesion was segmented. Histogram and gray-level co-occurrence matrix (GLCM) features were calculated and correlated to Gleason score. Low ISUP grades (1-2) were compared against high ones (3-5). Area under the receiver operating characteristic (AUROC) curve was used to quantify the predictive power of texture features.

RESULTS: Various features extracted from T2-weighted and particularly diffusion-weighted images correlated negatively with the Gleason score. T2-based GLCM features could discriminate between low and high ISUP grades with AUROC being 0.71. GLCM entropy on diffusion-weighted images proved to be a competent indicator with an AUROC of 0.81, while combining texture parameters can increase the diagnostic power to 0.84. This study suffers from several limitations. Standardization of segmentation is required, whilst extending the study to a larger sample with longitudinal MRI scans is warranted.

CONCLUSIONS: Current findings indicate that MRI-based textural features could play a beneficial role as imaging biomarkers in excluding clinically significant prostate cancer and/or in the active surveillance of localised prostate cancer.

ACKNOWLEDGEMENT: This work has been financed by the Horizon 2020 Framework Programme of the European Commission (project code: 952179).

KEYWORDS: texture analysis, magnetic resonance imaging, prostate cancer, active surveillance

DOSE ESTIMATION FOR RADIATION WORKER DURING TARGETED ALPHA THERAPY

Pankaj Tandon¹ and Parul Thakral²

¹Radiological Safety Division, Atomic Energy Regulatory Board, Mumbai, India

²Fortis Hospital & Research Centre, Gurugram, Delhi, India

Email: drpankaj@aerb.gov.in

BACKGROUND/OBJECTIVE: Targeted Alpha Therapy (TAT) has the potential to deliver radiation dose in a highly localized and toxic manner because of its high Linear Energy Transfer (LET). In our study, we propose to evaluate the radiation safety aspects associated with the use of an alpha emitter i.e. Bi-213 as a targeted radionuclide therapy for neuroendocrine and prostate cancer patients.

MATERIALS AND METHODS: Radiation safety aspects are evaluated in one of the prestigious institution of the country where the alpha therapy started first in the country. This study was carried out for the patients with Castration Resistant Prostate Cancer (CRPC) and Neuro-endocrine tumor (NET). In all, twelve patients with Neuroendocrine tumor or Prostate cancer were enrolled for ²¹³Bi-DOTATOC or ²¹³Bi-PSMA therapy. Each patient received 2-3 doses of ²¹³Bi-peptide intravenously in a single cycle at an interval of 2-3 days. Doses to nuclear medicine personnel are assessed during different tasks such as elution, dispensing, injecting, collection of blood samples etc. Dose rates are measured at the surface and at a distance of 1m from the patients post therapy just after the administration, 1hr, 2hr and 4hr respectively. Dose rate from an unshielded source of ²¹³Bi is measured at the surface and at 1 m, compared to the other radionuclides and the normalized dose rates ($\mu\text{Sv/hr/MBq}$) are obtained.

RESULTS: The mean doses received by the radiopharmacist during synthesis, by the physicians during injection, by the technologists during imaging and by the nurses during sample collection are measured using the pocket dosimeter and found to be in the range of 2-7 μSv . The normalized dose rate per injected activity from the patients at 1m - is in the range of 0.002-0.005 $\mu\text{Sv/hr/MBq}$ immediately after injection.

CONCLUSIONS: The study shows that the use of ²¹³Bi-PSMA/DOTATOC for the therapy of CRPC and NET respectively has been simple, safe and straightforward. The radiation absorbed doses to the occupational workers are below the dose limits prescribed by the National regulatory Authority. The dose rates from the treated patients poses no detrimental effect on the environment and thus the patients may be treated as out-patient.

KEYWORDS: Target Alpha Therapy, Dosimetry

Presentation ID: P-354

DEVELOPMENT OF ANTHROPOMORPHIC HETEROGENEOUS FEMALE PELVIS (AHFP) PHANTOM EQUIVALENT TO HUMAN ANATOMY TO DELIVER ACCURATE DOSE DISTRIBUTION USING DIFFERENT ALGORITHMS

Ajay Katak^{1,2}, Balbir Singh³, Kruti Haraniya⁴, Rajesh Vashistha⁵, Lalit Kumar⁶, Deepak Basandrai¹

¹Department of Physics, Lovely Professional University, Phagwara

²Department of Radiation Oncology, Samanvay Multispeciality Hospital PVT LTD, Junagadh

³Department of Radiation Oncology, SLBSGMC & H, Nerchowk, Mandi

⁴Department of Radiation Oncology, Sir Sayajirao General Hospital, Vadodara.

⁵Department of Radiation Oncology, Max SuperSpeciality Hospital, Bathinda

⁶Department of Radiation Oncology, Max Superspeciality Hospital, Saket

Email: akatake95@gmail.com

AIM: The aim of current research study is to develop Anthropomorphic Heterogeneous Female Pelvis (AHFP) phantom for Quality assurance (QA) and to evaluate an accuracy and precision of radiation in AHFP phantom using different computational algorithms

MATERIAL AND METHODS: To design AHFP phantom the material was used Epoxy, Hardener, Polyvinyl Chloride (PVC), water and Paraffin wax. The internal organs bladder was made of ball filled with water, rectum was made of paraffin wax, bones were made of PVC and normal tissues and muscles were made of Epoxy and hardener ratio of 1:0.5. Mould was prepared with POP then other structures place on their position in mould and mixture of epoxy and hardener poured into that mould. Cavity placed at the position of uterus area in the phantom for different types of dosimeters inserted into it. Phantom was scanned on CT simulator at 130KVp, 203mAs with slice thickness of 2mm. Doses were computed using Anisotropic Analytical Algorithm (AAA) and Acuros XB (AXB) Algorithms in Eclipse TPS for various combination of treatment fields of 3DCRT and IMRT techniques for 6FFF (flattening filter free) beam energy of Halcyon machine and 6MV, 10MV, and 15MV beam energy of Vital Beam LINAC. The doses were measured using a 0.6cc cylindrical ionization chamber in AHFP phantom.

RESULTS: The maximum mean of percentage (%) deviation and standard deviation (SD) for the TPS calculated data and measured data were compared using various methods. The results showed that the differences in these parameters were 0.80% and 0.57% for the AXB algorithm and 1.57% and 1.41% for the AAA algorithms respectively. The AHFP phantom and the actual patient's maximum depth dose (PDD) at various depths were very identical, with a maximum absolute mean of % variation and SD were 0.86% and 1.11% for AXB algorithm and 1.69% and 1.06% for AAA algorithm. The percentage of variation in doses within $\pm 3\%$ for both the algorithms.

CONCLUSION: The designed AHFP phantom was found to be more suitable for patient specific QA and has provisions to accommodate various dosimeters. The absolute mean of % variation and SD of AXB was quite comparable than that of AAA algorithm.

KEYWORDS: AXB, AAA, Algorithm, TPS, Phantom

Presentation ID: P-355

ASSESSMENT OF RADIATION EXPOSURE LEVELS AND ESTABLISHMENT OF SAFE EXIT TIME CRITERIA FOR PATIENTS UNDERGOING PET SCANS

Arun Adhikari¹, Shanmuga Sundaram P², Kuriakose TT², Annex E.H¹, Sreedevi E¹

¹Department of Radiation Oncology, ²Department of Nuclear Medicine, Amrita Institute of Medical Sciences, Ponekkara P. O Kochi, Kerala, India

Email: arunadhik26@gmail.com

BACKGROUND/OBJECTIVE: To assess and quantify the radiation exposure levels of patients undergoing PET scan and establish safe exit time criteria from department to ensure protection of public and environment. Study will help to review and set radiation protection standards in Nuclear Medicine Department.

MATERIALS AND METHODS: In vivo structural imaging provides valuable data in clinical and preclinical studies. They reveal true structures of physiological time varying processes that explains disease phenomena. One of the common imaging modalities is Positron emission tomography (PET). It generates images depicting the distribution of positron emitting nuclides in patients. Patients who are scheduled to undergo PET scans are injected with FDG (Fluorodeoxyglucose) radiopharmaceuticals. Activity of pharmaceuticals and radiation emitted by these patients is noted at different intervals of time: 0 minute, 40 minutes, 90 minutes, and 120 minutes using RaySafe 452 radiation survey meter at 1 meter distance. Consent from the patient is taken and study adhere to ethical guidelines and ensure patient privacy. Collected data is compiled and analyzed to determine the criteria for when a patient can be discharged from the department. This analysis involves assessing various factors including patient radiation level at different time points, their clinical condition and relevant medical parameter recorded in patient's sheet.

RESULT: The radiation levels of fifty patients of different sex, age group, weight, creatinine level and GFR value were measured at different duration of time: 0 minutes, 40 minutes, 90 minutes, 120 minutes. It was observed that, for all patients, the radiation levels decreased over time, following an exponential pattern. It is found that higher the GFR clearance value corresponds to a more decrease in a patient's radiation level. Additionally, it was observed that, on average, radiation levels after 2 hours of administration tend to be around 1 milli-Röntgen per hour (1mR/hour). Taking into consideration of various factors like patient's condition, socio-economic factors and medical condition parameter like GFR value, patient weight, administered activity, exit time could be standardized to 2 hours after the FDG administration.

CONCLUSIONS: On average, radiation levels around 1 milliroentgen per hour (1mR/hour) after 2 hours of administering the FDG. The observation suggests the possibility of establishing a radiation level standard at 1mR/hour, which guide a standard patient exit time of 2 hours post administration.

Presentation ID: P-356

LEAK DOSIMETER USING A HIGH-SENSITIVITY CURRENT TO VOLTAGE AMPLIFIER WITH A T-TYPE FEEDBACK RESISTANCE OF 35 G

Eiichi Sato¹, Jiro Sato², Kazuki Ito², Hodaka Moriyama², Osahiko Hagiwara², Toshiyuki Enomoto², Manabu Watanabe², Yuichi Sato³, Sohei Yoshida⁴, Kunihiro Yoshioka⁴, Hiroyuki Nitta⁵

¹Honorary Professor of Physics, Iwate Medical University, 2-14-6 Kawaramachi, Wakabayashi, Sendai, Miyagi 984-0816, Japan

²Department of Surgery, Toho University Ohashi Medical Center, 2-22-36 Ohashi, Meguro, Tokyo 153-8515, Japan

³Central Radiation Department, Iwate Medical University Hospital, 2-1-1 Idaidori, Yahaba, Iwate 028-3694, Japan

⁴Department of Radiology, School of Medicine, Iwate Medical University, 2-1-1 Idaidori, Yahaba, Iwate 028-3694, Japan

⁵Department of Surgery, School of Medicine, Iwate Medical University, 2-1-1 Idaidori, Yahaba, Iwate 028-3694, Japan

dresato@iwate-med.ac.jp

Background/Objective: Currently, since the rise time of a readily available leak dosimeter is beyond 1 s, it is difficult to measure low-dose-rate X-ray pulses. The sensitivity of the dosimeter is primarily determined by the feedback resistance in the current to voltage (I-V) amplifier, and the maximum resistance is approximately 1 G . Therefore, we developed a high-sensitivity leak dosimeter by improving an I-V amplifier. In our research, major objectives are as follows: to improve the time resolution, to construct a T-type feedback resistance, to improve the sensitivity of dose rate measurements, and to develop a compact semiconductor dosimeter. Therefore, we developed a 35 G Ω -V amplifier and measured extremely low dose rates.

Materials and methods: The semiconductor dosimeter consists of an I-V amplifier with an effective feedback resistance of 35 G Ω a voltage to voltage (V-V) amplifier, and a silicon photodiode (PD) with sensor dimensions of 10 \times 10 mm². X-ray photons are absorbed by the PD, and the photocurrent flowing through the PD is converted into voltage using the I-V amplifier. The I-V output is then amplified using the V-V amplifier with an amplification factor of 10.

Results: The output voltage from the V-V amplifier increased with increases in the tube voltage, and was proportional to the tube current. The absolute value of the dose rate was determined using a semiconductor dosimeter (RaySafe, X2). The minimum dose rate measured was below 10 pGy/s, and the rise time of the amplifier output was approximately 10 ms.

Conclusions: We developed a semiconductor dosimeter using a 35 G Ω -V amplifier. We improved the dose-rate and time resolutions, and a low-dose-rate X-ray pulsed was detected at a high time resolution.

Keywords: 35 G Ω -V amplifier, X-ray, low dose rate, high time resolution, T-type feedback

Presentation ID: P-357

QUANTIFICATION OF ^{99m}Tc -PERTECHNETATE IN THYROID PLANAR IMAGING

Riska Putri Fadila¹, Iffa Prisella Wulan Agustina¹, Maria Evalisa², Fadil Nazir², Yanurita Dwihapsari¹

¹*Department of Physics, Institut Teknologi Sepuluh Nopember (ITS), Surabaya, Indonesia 60111*

²*Department of Nuclear Medicine, National Research and Innovation Agency (formerly National Nuclear Energy Agency), Jakarta, Indonesia (retired)*

Email : yanuritadh@physics.its.ac.id

Background/Objective: ^{99m}Tc -pertechnetate is used in thyroid scintigraphy for its low cost and low dose. Accurate quantification of dose activity is essential in nuclear medicine to increasing effectiveness of therapy while eliminates radiation exposures to the healthy tissues. In quantitative nuclear medicine, several correction factors have been applied to give more accurate dose.

Materials and methods: In this study, quantification was performed to anterior and posterior images to better predict activity dose in thyroid scan using ^{99m}Tc -pertechnetate planar imaging. Images were acquired using dual-head gamma camera (Mediso, Hungary) with low-energy-high resolution collimator and 20% energy window centered at 140 keV. Measurement was performed in the head and neck area of eight subjects in the anterior and posterior views 25 and 30 minutes after ^{99m}Tc -pertechnetate intravenous injection after background radiation measurement in the anterior and posterior. After manual segmentation and counting of thyroid lobes of interest, organ activities were calculated using conjugate view method and the correction was performed for uptake obtained in the anterior and posterior images.

Results: Quantification in our study showed higher uptake in the anterior compared to posterior camera. ^{99m}Tc thyroid uptake obtained in this study without correction ranged between 0.01% - 0.06%, significantly lower than the uptake calculated with correction which ranged between 0.3% - 0.97%.

Conclusions: The result showed the difference in the anterior and posterior measurement and the correction method was applied to increase the accuracy of uptake measurement.

Keywords: nuclear medicine, quantification, ^{99m}Tc , pertechnetate, thyroid, gamma camera

Presentation ID: P-358

QUALITY ASSESSMENT OF IMAGES IN BRACHIAL PLEXUS MAGNETIC RESONANCE IMAGING

Mohammad Sidik Cahyana¹, Faridatul Khusna Siwi¹, Mohammad Agus Pribowo², Yanurita Dwihapsari¹

¹*Department of Physics, Institut Teknologi Sepuluh Nopember, Surabaya, Indonesia 60111*

²*Department of Radiology, Gatot Soebroto Army Hospital (RSPAD Gatot Soebroto), Jakarta Indonesia 10410*

Email : yanuritadh@physics.its.ac.id

Background/Objective: Imaging of brachial plexus using magnetic resonance imaging (MRI) is challenging due to strong signal interference from surrounding tissues and complex anatomical coverage. 3D magnetic resonance imaging produces high quality images with high signal to noise ratio (SNR) but leads to extensive acquisition time. Shorter acquisition time can be achieved by applying compressed sensing but the technique is limited due to under sampling of data and limited reduction factor.

Materials and methods: The study was conducted to ten subjects using MRI 3 Tesla (Vida, Siemens, Germany) with a 16-channel head and body coil. Images were acquired using T2-Weighted Imaging (T2WI) and T2 short time inversion recovery (STIR) sampling perfection with application optimized contrasts using different flip angle evolution (SPACE) sequences. In addition, compressed sensing was applied with sparse under sampling k-space data in Cartesian phase encoding to T2 STIR SPACE sequence. Images were processed and reconstructed using maximum intensity projection. Five region of interests were selected and processed to obtain SNR. Quality was assessed by analyzing and comparing SNR from images with and without compressed sensing.

Results: The increasing image quality was noted in images with compressed sensing. SNR of five ROIs were also higher in images with compressed sensing compared to images without compressed sensing.

Conclusions: Compressed sensing increases the quality and SNR of brachial plexus magnetic resonance images.

Keywords: brachial plexus, compressed sensing, signal-to-noise ratio, STIR, SPACE

Special SYMPOSIUM:

**THE CONTRIBUTION OF MEDICAL PHYSICS EDUCATION AND TRAINING
TO THE IMPROVEMENT OF CANCER CONTROL STRATEGIES:
DEVELOPING VS DEVELOPED COUNTRIES**

Eva Bezak^{1,2,3,4}, Arun Chougule^{3,4,5}, Francis Hasford^{3,6,7}, Christoph Trauernicht^{7,8}, Magdalena Stoeva^{3,9},
Nupur Karmaker¹⁰

¹Medical Radiations, University of South Australia, Adelaide, SA, Australia.

²School of Physical Sciences, University of Adelaide, Adelaide, SA 5001, Australia.

³International Organization for Medical Physics (IOMP), York, UK.

⁴Asia-Oceania Federation of Organizations for Medical Physics (AFOMP), Bangkok, Thailand.

⁵Swasthya Kalyan Group, Jaipur, India.

⁶Department of Medical Physics, University of Ghana, Accra, Ghana.

⁷Federation of African Medical Physics Organizations (FAMPO), Accra, Ghana.

⁸Division of Medical Physics, Tygerberg Hospital and Stellenbosch University, Cape Town, South Africa.

⁹Department of Diagnostic Imaging, Medical University of Plovdiv, Bulgaria.

¹⁰Department of Medical Physics and Biomedical Engineering, Gono Bishwabidyalyay, Bangladesh.

BACKGROUND: Medical physics education, research, and professional training contribute to medical imaging practice, policy development, and the implementation of guidelines towards safe and effective use of ionizing radiation. Over the years diagnostic and radiation treatment modalities using ionizing radiation increased enormously. Further radiation is a dual-edged source and inappropriate use will lead to health hazards including cancer induction so it must be used cautiously, safely by well-trained, qualified staff. Appropriate education, training, skills, and competencies are needed and would be possible only with a high-quality structured education curriculum. Lack of sufficient human resources, infrastructure, research facilities, and hands-on training is the major hurdle in establishment of effective and cutting-edge cancer treatment facilities in developing countries. These limitations can be resolved with effective cooperation and assistance from the developed world. Medical imaging and radiotherapy play important roles in cancer diagnosis and treatment. Medical physicists need structured academic and clinical training to practice their profession.

PURPOSE: The key goal of this symposium is to represent the current response, challenges, probable solutions, and impact of regional cancer control strategies through medical physics education, research, and training.

MATERIALS AND METHODS: This special symposium will be embellished based on attractive talks from the International Organization for Medical Physics (IOMP), the Asia-Oceania Federation of Organizations for Medical Physics (AFOMP), and the Federation of African Medical Physics Organizations (FAMPO), experts. On "IOMP Medical Physics Workforce Survey 2022," Dr. Eva Bezak will deliver a presentation. Dr. Arun Chougule will address "Medical Physics Education and Training across the Globe with Special Reference to the AFOMP Region." Dr. Hasford and Dr. Trauernicht will present "FAMPO's Role in Education, Training, and Recognition of Medical Physicists in Africa." Dr. Chougule will serve as the symposium moderator. Dr. Magdalena Stoeva and Dr. Nupur Karmaker organized are organizers of this symposium.

RESULTS AND DISCUSSION: This symposium will provide more insight into exploring cancer control strategies and bring significant success for radiation in medicine. Here, notable international policies for both developed and developing nations will be stated. Students, academics, researchers, industry, and other associated professionals will have the opportunity to benefit from scientific discussion.

CONCLUSION: Initiatives from individuals' regions can be taken through this program. This is the right place to present this information for the future development of medical physics through enhanced communication and regional collaboration to support improved cancer prevention and control.

KEYWORDS: Cancer, Control Strategy, Medical Imaging, Education, Research, Training.

SCIENTIFIC PROGRAM



**26th
International Conference on
Medical Physics**

IOMP 2023

AMPICON 2023 | AOCMP 2023 | ISEACOMP 2023

Theme: Innovations in Radiation Technology & Medical Physics for Better Healthcare
December 6th - 9th 2023, DAE Convention Centre, Anushaktinagar, Mumbai, India



Scientific Program: Day 1, Wednesday, 6th December 2023 **HALL A**

8.00 - 9.00	Registration		
9.00 - 10.00	Opening Ceremony		
10.00 - 10.15	High Tea		
Time	Presentation ID/ Abstract ID	Title of the talk	Chairperson/ Moderator/ Speaker
10.15 - 11.15	Plenary Session 1: Current Trends in X-ray Imaging and Radiation Oncology		John Damilakis, IOMP
10.15 - 10.30	P-1	Can AI predict patient doses from X-ray examinations accurately enough?	John Damilakis, Greece
10.30 - 10.45	P-2	Grid, Flash and other superheroes of radiation therapy,	Eva Bezak, Australia
10.45 - 11.00	P-3	Hot topics in Radiation Protection	Madan Rehani, India/USA
11.00 - 11.15	----	Discussion	All
11.15 - 13.15	Special Symposium 1: Hadron and Ion Beam Therapy		Rakesh Jalali, India
11.15 - 11.35	S-01	Evolution and future challenges of ion beam therapy	Masahiro Endo, Japan
11.35 - 11.55	S-02	Clinical commissioning of Spot scanning proton therapy	Sung Yong Park, Singapore
11.55 - 12.15	S-03	Particle therapy in paediatric solid tumours - Impact on clinical outcomes	Sidharth Laskar, India
12.15 - 12.35	S-04	Therapeutic gain with current practice of IMPT	Dayananda Sharma, India
12.35 - 12.55	S-05	Future developments in IMPT for higher therapeutic gain	Narayan Sahoo, USA
12.55 - 13.15	----	Panel Discussion: Challenges and opportunities of ion beam therapy (Panelist: Masahiro Endo, Sung Yong Park, Sidharth Laskar, Dayananda Sharma, Narayan Sahoo)	Rakesh Jalali, India (Moderator)

13.15 - 14.00	Lunch & Social Time		
14.00 - 15.00	Scientific Session 1: Motion Management		Sudesh Deshpande, India
14.00 - 14.20	I-01	Off line to On line tumour tracking	Raghavendra Holla, India
14.20 - 14.30	O-001/ I6226	Dosimetric Comparison of Gated versus Free Breathing Techniques for Lung Stereotactic Body Radiotherapy	Amalu Hanna Alex, India
14.30 - 14.40	O-002/ V8119	Accuracy of external tumour motion monitoring in liver SABR: Results from the TROG 17.03 LARK trial	Chandrima Sengupta, Australia
14.40 - 14.50	O-003/ Y5016	Cardiac ablative SBRT for treating ventricular tachycardia – A case study	Sambasivaselli R, India
15.00 - 16.00	Scientific Session 2: Clinical Brachytherapy		Kamlesh Passi, India
15.00 - 15.20	I-02	Gamma Tile: Newest brain brachytherapy device	Mathew Hall, USA
15.20 - 15.30	O-004/ W8330	A retrospective dosimetric comparison of TG-43 based algorithm and commercially available advanced collapsed cone engine (ace) based on TG-186 for patients undergoing APBI using Co-60 HDR brachytherapy	Alka Kataria, India
15.30 - 15.40	O-005/ P6233	Validation of sigmoid points for sigmoid dose accumulation and reporting for multifractionated brachytherapy for cervical cancer	Kamalnath J, India
15.40 - 15.50	O-006/ G8473	A Dosimetric Comparison of CT/MR Multichannel Applicator versus Single Channel Cylinder for the Treatment of Gynaecological Cancers with High Dose Rate Brachytherapy	Anjana AK, India
16.00 - 16.15	Tea Break		
16.15 - 17.45	Special Symposium 2: Good-catches (GC) in radiation therapy		Vibha Chaswal/Bruce Thomadsen/M Mahesh
16.15 - 16.35			
16.35 - 16.55	S-07	Value of GCs and positively reinforced environment to nurture GC opportunities	Vibha Chaswal, USA
16.55 - 17.10	S-08	Good Catch Encounter Scenario – CT Scanning	M Mahesh, USA
17.10 - 17.25	S-09	Good Catch Encounter Scenario – EBRT/EMR/Electrons	Daxa Patel, Canada
17.25 - 17.45	S-10	Reap full benefit from good-catch discovery: Approaches to analyze reported incidents	Bruce Thomadsen, USA
18.00 - 19.00	Cultural program: Theme - Our India Our Pride		
19.30 - 22.30	Dinner at CIDCO Exhibition Lawn & Convention Centre Lawn, Sector 30A, Vashi, Navi Mumbai 400703		

Scientific Program: Day 1, Wednesday, 6th December 2023 HALL B

Time	Presentation ID/ Abstract ID	Title of the talk	Chairperson/ Moderator/ Speaker
11:15 to 12:15		Scientific Session 3: Innovations in Nuclear Medicine Imaging	A. K. Shukla, India
11.15 - 11.35	I-03	First positronium imaging of humans using modular J-PET scanner	Pawel Moskal, Poland
11.35 - 11.45	O-007/ B7540	Establishment of Local Diagnostic Reference Levels for Adult 18-F FDG-Whole-Body PET/CT Examination at SQCCRC Muscat Oman	Noura A L Makhmari, Oman
11.45 - 12.05	O-008/ H3381	99mTc-MDP bone scan image denoising using trimmed mean filter.	Abhishek Kumar Karn, India
12.05 - 12.15	O-009/ N4020	AI methods to improve performance of a portable Hybrid Gamma-Optical Camera (HGC) for nuclear medicine	Yangfan Jiang, UK
12:15 to 13:15		Scientific Session 4: Radiation Protection in Medical Imaging	Lalit Agarwal, India
12.15 - 12.35	I-04	Estimation of Patient Skin Dose in Fluoroscopy (Joint TG Report - AAPM & EFOMP)	Kalpna Kanal, USA
12.35 - 12.55	O-010/ N1530	Impact of Physical Characteristics of Photon-Counting Detectors on CT Image Quality: A Comparative Study between in-House CdTe- and CZT-based Virtual Photon-Counting CT Scanners	Mridul Bhattarai, USA
12.55 - 13.05	O-011/ U9275	Towards Dosimetry Formalism for Three-Dimensional Rotational Angiography (3DRA): Monte Carlo Simulation and Direct Measurements	Akbar Azzi, Indonesia
13.05 - 13.15	O-012/ X9688	Display of blood flow direction and blood flow velocity by Flow CT image	Katsumi Tsujioka, Japan
13.15 - 14.00		Lunch & Social Time	
14.00 - 15.00		Scientific Session 5: Radiotherapy Dosimetry	Challapali Srinivas, India
14.00 - 14.20	I-05	Advantages and limitations of available dosimeters for radiotherapy	K M Ganesh, India
14.20 - 14.30	O-013/C 3702	Feasibility of In Vivo Dosimetry for Adaptive Radiotherapy Assessment in Head and Neck Cancer Patients.	Parimal Patwe, India
14.30 - 14.40	O-014/N7472	Role of exit fluence acquiring and analysis in Halcyon	Pooja Moundekar, India
14.40 - 14.50	O-015/A5741	The Evaluation of Contour, Dose and Position of Heart in Thorax Region for Cancer Radiation Therapy	Nuttawut Yeenang, Thailand
15.00 - 16.00		Scientific Session 6: Advances in Radiosurgery	Jibon Sharma, India
15.00 - 15.20	I-06	Clinical implementation of cardiac radiosurgery for ventricular tachycardia	V Subramani, India
15.20 - 15.30	O-016/ D2617	Dosimetric Comparison of Glioblastoma Brain Volumetric Modulated Arc Therapy patients with different calculation grid sizes in Eclipse Treatment Planning System.	Krishna Chandrasekar, India
15.30 - 15.40	O-017/ F9163	Impact of Hippocampus Dosimetry Parameters on Neurocognitive Function in Prophylactic Cranial Irradiation	Suryakanta Acharya, India
15.40 - 15.50	O-018/ B1208	Planning layout and Equivalent Uniform Dose measures in High Dose Lattice Therapy to large and locally advanced bladder cancer	Bhagyalakshmi AT, India

16.00-16.15	Tea Break		
16.15 - 17.10	Scientific Session 7: Radiotherapy and Radiobiology		Rajesh Vashishtha, India
16.15 - 16.35	I-07	Re-irradiation in Head & Neck Cancers: Radiobiological Considerations	Manoj Gupta, India
16.35 - 16.55	I-08	Personalized ultra high dose stereotactic adaptive radiotherapy: Immuno radiobiological aspects of unconventional radiotherapy treatment model	T. S. Kehwar, India/USA
16.55 - 17.05	O-019/D9811	Radiobiology for personalized radiotherapy of early and intermediate prostate cancer	Zine El Abidine Chaoui, Algeria
17.10 - 18.10	Special Symposium 3: Contribution of Medical Physics Education and Training to the Improvement of Cancer Control Strategies: Developing Vs Developed Countries		Eva Bezak/ Arun Chougale
17.10 - 17.30	S-11	IOMP Medical Physics Workforce Survey 2022	Eva Bezak, Australia
17.30 - 17.50	S-12	Medical Physics Education and Training Across the Globe with Special Reference to AFOMP Region	Arun Chougale, India
17.50 - 18.10	S-13	FAMPO's Role in Education, Training and Recognition of Medical Physicists in Africa	Francis Hasford, Ghana Chris T, South Africa

Scientific Program: Day 1, Wednesday, 6th December 2023 **HALL C**

Time	Presentation ID/ Abstract ID	Title of the talk	Chairperson/ Moderator/ Speaker
11.15 - 12.15	Scientific Session 8: Modelling & Simulation in Radiotherapy		T. Palani Selvam, India
11.15 - 11.35	I-09	TCP & NTCP modelling	Arun Oinam, India
11.35 - 11.45	O-020/ D1032	Development of Collapsed Cone Dose Calculation Algorithm for Bhabhatron-II Telecobalt Machine	Sai Sirisha Nadiminti, India
11.45 - 12.05	O-021/ H7164	Assessment of treatment planning and dosimetric uncertainties in hip prosthesis cases on Tomotherapy	Pawan Kumar Singh, India
12.05-12.15	O-022/ I1850	Investigating the effect of contrast agents on dose calculation of intensity-modulated radiotherapy plans for head and neck cancer	Nidhi Jain, India
12.15 to 13.15	Scientific Session 9: Radiation Biology		Apurba Kabasi/Rajadurai, India
12.15 - 12.35	I-10	Radiation-induced bystander effect	Amit Kumar, India
12.35 - 12.55	O-023/ E6313	Radiation Dose Enhancement Effects on Pancreatic Cancer Cells by Ultrasound-Stimulated Microbubbles	Masao Nakayama, Japan
12.55 - 13.05	O-024/ M9190	Investigating the effect of radiotherapy and sonodynamic therapy in the presence of apigenin-coated gold nanoparticle on breast cancer cells	Zeinab Hormozi Moghaddam, Iran
13.05 - 13.15	O-025/ R3849	To assess the dosimetry properties of N-isopropyl acrylamide (NIPAM) gel with X-ray CT readout modality for three dimension relative dose measurement in radiotherapy	D N Singh, India
13.15 - 14.00	Lunch & Social Time		
14.00 - 14.50	Scientific Session 10: Dosimeters for Radiation Protection and Radiotherapy		M. S. Kulkarni, India

14.00 - 14.10	O-026/ S6166	Development of thin CaSO ₄ : Dy embedded Teflon discs based TLD system for Personnel Monitoring	Suresh Pradhan, India
14.10 - 14.20	O-027/ R6866	Radioluminescent Dosimeter with Time-Division Multiplexing for Radiotherapy Application	Janatul Madinah Wahabi, Malaysia
14.20 - 14.30	O-028/ G8735	Analyse the performance of the upgraded positive ion detector as a gas sensor	Dharshini S, India
14.30 - 14.40	O-029/ O6970	Characterization and Dosimetric Evaluation of a Liquid-Filled Array Detector for Fluence Verification: Comparison with Air-Filled Array Detector	Beneeta Sukumar, India
14.50 - 15.45	Scientific Session 11: Radiation Sources and Radiotherapy		Deepak Arora, India
14.50 - 15.10	I-11	Production of Radiopharmaceuticals for Diagnostic and Therapeutic Application in India	Sudipta Chakraborty
15.10 - 15.20	O-030/ U6782	Second cancer risk to Contra-lateral Breast after single-sided Breast IMRT	Shatabdi Chakrabarty, India
15.20 - 15.30	O-031/ S4252	Evaluation of dosimetric characteristics of 10 MV flattened and unflattened photon beam in Truebeam STx Linear accelerator	Rajadurai E, India
15.30 - 15.40	O-032/ C2807	Implementation of the Volumetric Modulated Arc Therapy based TBI: The Experience and Procedure at FV Hospital, Vietnam	Tran Duong, Vietnam
15.45 - 16.10	Tea Break		
16.10 - 17.15	Scientific Session 12: Poster Rapporteur - I		Arvind Shukla, India
16.10 - 16.25	Rapporteur 1	Posters 001 to 025	R K Bhisht, India
16.25 - 16.40	Rapporteur 2	Poster 026 to 050	N Gopishankar, India
16.40 - 16.55	Rapporteur 3	Posters 051 to 075	Rajni Verma, India
16.55 - 17.10	Rapporteur 4	Posters 076 to 100	Mary Joan, India

Scientific Program: Day 2, Thursday, 7th December 2023 HALL A

6.15 - 7.00			Yoga Session (Lawn of DAE convention centre)
Time	Presentation ID/ Abstract ID	Title of the talk	Chairperson/ Moderator/ Speaker
8.00 - 8.55	IOMP-IAEA Joint Session: Artificial Intelligence (AI) in Medical Physics		John Damilakis & M. Carrara
8.00 - 8.25	J-1	AI in medical physics and radiation oncology	M Carrara, IAEA/Italy
8.25 - 8.50	J-2	AI in medical physics and imaging	John Damilakis, Greece
9.00 – 10.15	Special Symposium 4: Emergence of MR-Linac for Adaptive Radiation Therapy (RT)		Indra Das, USA
9.00 - 9.20	S-14	Emergence of MR-Linac for Adaptive Radiation Therapy	Indra Das, USA/India
9.20 - 9.40	S-15	Clinical workflows and impact of MR Linac in Adaptive RT	Poonam Yadav, India/USA
9.40 - 10.00	S-16	MR Linac Quality Assurance	Bhudatt Paliwal, USA
10.00 - 10.15	S-17	Adaptive Radiotherapy by MR-Linac: Indian Experience	Sai Shanmugam, India
10.15 - 10.30	Tea Break		
10.30 - 11.10	Plenary Session 2: AMPI Ramaiah Naidu Memorial Oration		Sunil Dutt Sharma/ V Subramani
10.30 - 10.35	Introduction about Ramiah Naidu Memorial Oration Award and Presentation of Award Certificate		Sunil Dutt Sharma, President, AMPI
10.35 - 11.05	P-4	Harnessing Radiotherapy Data for Quality Care and Outcome Research	Jatinder R Palta, USA
11.05 - 11.10	Presentation of silver plaque and vote of thanks		V Subramani, Secretary, AMPI
11:15 to 12:15	Scientific Session 12: Dosimetry Audits in Radiotherapy		R Ravichandran, India
11.15 - 11.50	I-12	IAEA on Dosimetry Audit in Radiotherapy	Mauro Carrara, IAEA/Italy
11.50- 12.15	I-13	Dosimetry Audit in Radiotherapy- Indian scenario	Sunil Dutt Sharma, India
12:15 to 13:15	Scientific Session 13: Advance photon beam therapy		K J Maria Das, India
12.15 - 12.35	I-14	AAPM TG 178 recommendations on Imaging dose in CT & CBCT in radiotherapy	George X Ding, USA
12.35 - 12.45	O-033/ R7610	Enhancing Dose Measurement Accuracy in Single Isocentre Multiple Targets SBRT: An Analysis of In-Phantom Rotation Measurements with myQA SRS	Dinesan C, India
12.45 - 12.55	O-034/	Simulation of stereotactic cranial radiosurgery guided by functional magnetic resonance	Luis Alfredo Ancari, Argentina
12.55 - 13.05	O-035/ C5864	Clinical evaluation of deep learning-assisted automatic radiotherapy treatment planning for lung cancer	Ningyu Wan, China
13.15 - 14.00	Lunch & social time		
14.00 to 15.00	Technical Session - 1		Vegraj Singh, India
14.00 - 14.15	T-1	Varian	
14.15 - 14.30	T-2	Elekta	
14.30 - 14.40	T-3	PTW	
14.40 - 14.50	T-4	Per Fraction Automatic In-Vivo Monitoring	Jesus Fernandez, Sun Nuclear Corp

14.50 - 15.00	T-5	Accuray	
15.00 - 16.00	Scientific Session 14: Brachytherapy Dosimetry		Shinji Kawamura, Japan
15.00 - 15.20	I-15	The need for implementing model-based dosimetry in Brachy: AAPM TG 186 recommendations	Mandar Bhagwat, USA/India
15.20 - 15.30	O-036/ Y2124	Dosimetric comparison of BARC and BEBIG round type Ru-106 eye plaque source used in treatment of ocular cancer	Rajesh Kumar, India
15.30 - 15.40	O-037/ A7003	Design, development and characterization of homogeneous spherical graphite cavity ionization chamber as ionometric reference standard for strength determination of high dose rate brachytherapy sources	Sudhir Kumar, India
15.40 - 15.50	O-038/ F1794	A novel mathematical expression for estimating Ir-192 source dwell times by utilizing Co-60 source dwell times in optimized brachytherapy plans	Devaraju Sampathirao, India
16.00 – 16.15	Tea Break		
16.15 - 17.10	Scientific Session 15: Artificial Intelligence and Automation Process		PBLD Prasad/ A Sathish Kumar, India
16.15 - 16.35	I-16	Automation in High Dose Rate Gynaecological Brachytherapy - The Tygerberg hospital experience	Chris T, South Africa
16.35 - 16.45	O-039/ R9357	Learning and Predicting the Radionuclide Composition from Simulated Plastic Scintillator Gamma Spectra using an Artificial Neural Network (ANN)	Pratip Mitra, India
16.45 - 16.55	O-040/ H3663	Evaluating the Potential Dosimetric Benefits of an Artificial Intelligence based Online Adaptive Workflow utilizing Ethos Treatment System for Pelvic Carcinomas	Bijina T K, India
16.55 - 17.05	O-041/ X6543	AI Enabled Phosphor Imaging System for Biomedical Applications	Ratnesh S Sengar, India
17.10 - 18.10	Special Symposium 5: The Next Generation Cancer Treatments - The role of genomics and Artificial Intelligence		A. K. Rath, India
17.10 - 17.30	S-18	Unraveling the genomic profiles of radioresistant tumors to identify predictive biomarkers for therapy response	K R Muralidhar, India
17.30 - 17.50	S-19	Harnessing the power of AI in radiotherapy with caution	Dinesh Tawatia, India/USA
17.50 - 18.10	S-20	Current practices in radiation oncology and its drawbacks and scope for future developments	N P Patel, India
18.15 - 18.45	Evening Lecture: Quantum Physics of Life		D. K. Aswal, India
19.30 - 22.30	Dinner at The ACRES Club Lawn, Hemu Kalani Marg, Chembur, Mumbai 400071		

Scientific Program: Day 2, Thursday, 7th December 2023 HALL B

6.15 - 7.00	Yoga Session (Lawn of DAE convention centre)		
Time	Presentation ID/ Abstract ID	Title of the talk	Chairperson/ Moderator/ Speaker
8.00 - 8.55	IOMP School: Advanced Imaging (DECT & Perfusion CT) utility in RT Treatments		M Mahesh, USA/Eva Bezak, Australia
9.00 - 10.00	Special Symposium 6: Advancements in Nuclear Medicine: Revolutionizing Therapy Diagnosis and Treatment		P Tandon /S Somanesan/S Kheruka
9.00 - 9.20	S-21	Targeted Alpha Therapy: A Revolutionary Approach to Cancer Treatment	Pankaj Tandon, India
9.20 - 9.40	S-22	Vital Role of Medical Physicists in Quantitative Analysis in Nuclear Medicine	Subhash Kheruka, Oman
9.40 - 10.00	S-23	Advancement in Detector Technology and Quality Management in Theragnostics Services Delivery	Somanesan, Singapore
10.00 - 10.15	Tea Break		
11.15 - 12.15	Scientific Session 16: Advances in Radiation Oncology		C. Ramakrishna Rao, India
11.15 - 11.35	I-17	Flash Radiotherapy Dosimetry – A review	Paul Ravindran, India
11.35 - 11.45	O-042/ T2042	On-site source strength verification of HDR brachytherapy sources	Ankit Srivastava, India
11.45 - 11.55	O-043/ R1544	Dosimetric analysis of indigenously developed SENFLAP tissue equivalent bolus with imported bolus and wax bolus	Nandhini Muruges, India
11.55 - 12.05	O-044	Surface-guided radiation treatment (SGRT) system	Debabrata Bhowmik, C-Rad
12:15 - 13:15	Scientific Session 17: Newer Approaches in Radiation Oncology		J. Velmurugan, India
12.15 - 12.35	I-18	Development of O-18 enriched water for Clinical application	A R Dusane, India
12.35 - 12.55	O-045/ D5004	Quality Control Tool for Patient Flow Optimization at Mayo Clinic Florida	Sridhar Yaddanapudi, USA
12.55 - 13.05	O-046/ I7895	Development of tissue equivalent materials for applications in Medical Physics	Reena Sharma, India
13.05 - 13.15	O-047/ N2071	Regional Variation of Cancer Incidence in Nepal	Rudra Prasad Khanal, Nepal
13.15 - 14.00	Lunch & Social time		
14.00 - 14.55	Scientific Session 18: Radiosurgery and 3D Radiotherapy		M Rajasekar, India
14.00 - 14.20	I-19	Photon target to patient target - A walk through on SRS/SRT QA	S. Chitra, India
14.20 - 14.30	O-048/ X1086	Optimal beam choice of mono-isocentric stereotactic radiotherapy for multiple brain metastasis: A dosimetry comparison between 6X-SRS and 6XFFF beam	Priyanka Agarwal, India
14.30 - 12.40	O-049/ T9353	The impact of cranioplasty implants in Stereotactic Radiotherapy: A comparison of Commercial treatment planning system versus Monte Carlo calculations	Sumeesh S, India

14.40 - 14.50	O-050/	Dosimetric impact of grid size and statistical uncertainty on Monte Carlo algorithm in VMAT planning with Monaco TPS for single lesion brain stereotactic radiotherapy	Akhtaruzzaman, Bangladesh
15.00 - 15.55	Scientific Session 19: Technological advances in Medical Imaging - 1		Ajai Srivastava, India
15.00 - 15.20	I-20	Radiation Protection in Nuclear Medicine Imaging & Therapy	Sameer Tipnis, USA/India
15.20 - 15.30	O-051/ Y9637	Synchrotron radiation based X-ray imaging for medical research	Yogesh Kashyap, India
15.30 - 15.40	O-052/ X8314	CT-based delta-radiomic in discrimination of benign and malignant pulmonary nodules	Wenlong Li, China
15.40 - 15.50	O-053/O7615	Are dual-and single-energy CT acquisition protocols for pediatric thorax imaging equivalent regarding radiation exposure?	Kostas Perisinakis, Greece
16.00 - 16.50	Special Symposium 7: Applications of Machine Learning and AI in Cancer Radiation Treatment		Indra Das, USA
16.00 - 16.25	S-24	Artificial Intelligence and Machine Learning in Treatment Planning and Quality Assurance	Indra Das, USA/India
16.25 - 16.45	S-25	Clinical Applications of Artificial Intelligence for Radiotherapy Quality Assurance	Xince Jin, China
16.45 - 17.45	IOMP School: Utility of DRLs in Dose Optimization and Clinical DRLs		Kalpna Kanal, Paddy Gillin and M Mahesh

Scientific Program: Day 2, Thursday, 7th December 2023 **HALL C**

6.15 - 7.00	Yoga Session (Lawn of DAE convention centre)		
Time	Presentation ID/ Abstract ID	Title of the talk	Chairperson/ Moderator/ Speaker
11.15 - 12.15	Scientific Session 20: Technological advances in Medical Imaging - 2		K Chithra
11.15 - 12.15	O-054/ A8148	Integrating Models with Radiomic Features Clinical Factors and Serum Markers in the Differentiation Benign and Malignant Pulmonary Nodules	Heng Li, China
11.15 - 11.35	O-055/ N2606	MRI imaging for Metastatic Lesions using MR Spectroscopy-based Metabolite Ratio Analysis	Alamgir Hossain, Bangladesh
11.35 - 11.45	O-056/ Q8467	An Arduino-Based Distance Sensor for Remote Deep Inhale Breath Hold Training	Rohit Inippully, Oman
11.45 - 12.05	O-057/ A5988	CSS Alert -an in-house device designed for the proper positioning of CSS in the Cath-lab room	Sajeesh S Nair, India
12:15 to 13:15	Scientific Session 21: Artificial Intelligence and Medical Imaging		S. K. Koul, India
12.15 - 12.35	I-21	A paradigm shift in medical diagnostics: The machine learning era	Anuj Tyagi, India
12.35 - 12.55	O-058/ X-6042	Radiomic Signatures for Diagnosing Benign and Malignant Abnormalities in X-ray Mammograms	Arita Halder, India
12.55 - 13.05	O-059/ D7655	Imaging harmonization with deep learning for ultrasound images based radiomics	Xiance Jin, China
13.05 - 13.15	O-060/ R7924	Prediction and Correlation of Gamma Passing Rates with Complexity Metrics Using Machine Learning Techniques for Intensity-modulated Radiation Therapy	Dinesh Saroj, India

13.15 - 14.00		Lunch & social time	
14.00 - 15.00		Scientific Session 22: SBRT and Innovations in RT	Henry Finlay, India
14.00 - 14.10	I-22	The technical hurdles and uncertainties encountered in SBRT for lung treatment-A systematic review	Antoa Vaz, India
14.10 - 14.20	O-061/ P2884	Development of a 3D-printed heterogeneity phantom for enhanced patient-specific dosimetry for hypo fractionated radiotherapy	Ashish Binjola, India
14.20 - 14.30	O-062/ K3671	Split Jaw techniques in VMAT: Dosimetric impact of Jaw tracking method for extended target volumes of head and neck cancers	Marimuthu Boopathi, India
14.30 - 14.40	O-063/ B5127	Clinical Implementation of Hybrid Solitary Dynamic Portal Planning technique for Post-mastectomy Radiotherapy with Versa HD Linear Accelerator	K Mohamathu Rafic, Bangladesh
15.00 - 16.00		Scientific Session 23: Quality Assurance and Dosimetry in Medical Imaging	Krishna Reddy, India
15.00 - 15.20	I-23	Mammo QC - Comparative Analysis of QC tests for Hologic and Siemens Mammography 3D systems	S. Guruprasad, USA/ India
15.20 - 15.30	O-064	Contrast-calibrated photon-counting X-ray computed tomography using a cadmium telluride flat panel detector with high spatial resolutions	Jiro Sato, Japan
15.30 - 15.40	O-065/ W1291	Skin reactions associated with fluoroscopic interventional procedures in relation with equipment displayed dose parameters	Dharuman Vadive, India
15.40 -15.50	O-066/ E5704	Quick Quality Assurance program in an engaged diagnostic radiology department: An introduction to the frequent but short	Sanal Narayanan, India
15.55 - 16.15		Tea Break	
17.15 - 18.15		Poster Rapporteur- Poster Nos. 101 to 200	Bharanidharan, India
17.15 - 17.30	Rapporteur 1	Posters 101 to 125	Ranjana Bansal, India
17.30 - 17.45	Rapporteur 2	Poster 126 to 150	Amanjot Kaur, India
17.45 - 18.00	Rapporteur 3	Posters 151 to 175	Kuldeep Jadhav, India
18.00 - 18.15	Rapporteur 4	Posters 176 to 200	Rahul Phansekar, India

Scientific Program: Day 3, Friday, 8th December 2023 HALL A

6.15 - 7.00	Yoga Session (Lawn of DAE convention centre)		
Time	Presentation ID/ Abstract ID	Title of the talk	Chairperson/ Moderator/ Speaker
8.00 - 8.55	IOMP-IRPA Joint Session on Radiation Safety Culture in Healthcare		John Damilakis, Greece; Claire-Luise Chapple, UK
8.00 - 8.20	J-3	Radiation Safety Culture in Healthcare: The IRPA's viewpoint	Bernard Le Guen, France
8.20 - 8.40	J-4	Radiation Safety Culture in Healthcare: IOMP's Viewpoint	Magdalena Stoeva, Bulgaria
8.40 - 8.55	----	Discussion	All
9.00 - 10.00	Special Symposium 8: Imaging Dose Optimization in Cancer Treatment		M Mahesh, USA
9.00 - 9.20	S-26	Overview of imaging procedures during cancer treatment	Mahesh, USA
9.20 - 9.40	S-27	Radiation dose assessments from imaging procedures	George Ding, USA
9.40 - 10.00	S-28	Imaging dose to paediatric patients in nuclear medicine, radiotherapy and diagnostic reference levels	Saravana Kumar, India
10.00 - 10.25	Tea Break		
10.25 - 11.15	Plenary Session 3: AFOMP Kiyonari Inamura Memorial Oration 2023		Eva Bezak, Australia and Shigekazu Fukuda, Japan
10.25 - 10.30		Introduction	Eva Bezak, Shigekazu Fukuda
10.30 - 11.00	P-5	The Role of the Medical Physicist in Health Technology Assessment	Agnette Peralta, Philippines
11.00 - 11.10		Discussion and certificate presentation	Eva Bezak, Shigekazu Fukuda
11:15 to 12:15	Scientific Session 24: AMPI Best Oral Paper		Suresh Chaudhary/ S. Karthikeyan, India
11.15 - 11.25	O-067/ W6738	In-House Fabrication of an Ergonomic Prone Breast Board as an Innovation In Medical Physics for better delivery of Radiation Therapy in Early stage Breast Carcinoma	Misba Hamid, India
11.25 - 11.35	O-068/ K2798	Assessment of safety culture in radiotherapy facilities using Safety Performance Indicator (SPI): The Indian experience	Smriti Sharma, India
11.35 - 11.45	O-069/ W8931	Optimization of target beam and degrader foil parameters for ⁶⁴ Cu production using solid targetary system of a medical cyclotron	Sukhvir Singh, India
11.45-11.55	O-070/ M4104	Evaluating the feasibility of using utilized Aquaplast/thermoplastic masks as a custom made in-house bolus	Lavanya Murugan, India
11.55- 12.05	O-071/ Q8940	An Integrated Monte Carlo Decision Tree Model for Predicting Life Expectancy Based on Dosimetry Quality in Radiotherapeutic Treatment of Glioblastoma Multiform	Praveen Kumar, India
12:15 to 13:15	Technical Session - 2		Ramesh Desai, India
12.15 - 12.25	T-6	OncoTech	
12.25 - 12.35	T-7	Panacea	

12.35 - 12.45	T-8	IBA	
12.45 - 12.55	T-9	Team Best	
12.55 - 13.05	T-10	Ray Dose/ Oregon Health	
13.05 - 13.15	T-11	RIT/Bergen	
13.15 - 14.00	Lunch & social time		
14.00 - 14.55		Debate: Will AI Replace Clinical Medical Physicists?	Moderators : Anil Sharma, USA/M Mahesh, USA
14.00 - 14.55	Panelists: A.K. Rath, Sai Subramanian, Biplap Sarkar, Suresh Chaudhary		
14.55 - 15.50		Debate : Harmonization in Certification of Medical Physicist is Required?	Moderators: Manju Sharma, USA/ Sunil Dutt Sharma, India
14.00 - 14.55	Panelists: Bruce Thomadsen, Paul Ravindran, Hasin Anupama Azhari, C. P. Bhatt		
15.50 -16.05	Tea Break		
16.05 -17.00	Special Symposium 9: United Nations Scientific Committee on Effects of Atomic Radiation (UNSCEAR)		Borislava / S K Jha
16.05 - 16.25	S-29	UNSCEAR - Role, mandate and programme of work	Borislava, UNSCEAR
16.25 - 16.40	S-30	India's contribution to the work of UNSCEAR	Sanjay Kumar Jha, India
16.40- 17.00	----	Panel Discussion	All
17.00-17.55	Special Symposium 10: Writing and reviewing the manuscripts for publication in a peer reviewed journal		T Ganesh/Manoj Semwal
17.00 - 17.20	S-31	The right way of preparing a manuscript	Nobuyuki Kanematsu, Japan
17.20 - 17.40	S-32	The right way of reviewing a manuscript	T Ganesh, India
17.40 - 17.55	----	Panel Discussion: How to increase the chance of publishing a manuscript? -	Nobuyuki Kanematsu, Sunil Dutt Sharma, T Ganesh, Manoj Semwal
18.00 - 19.00	AMPI General Body Meeting		
19.30 - 22.30	Dinner at Imperial Banquets, Raghuleela Mega Mall, Vashi, Navi Mumbai 400703		

Scientific Program: Day 3, Friday, 8th December 2023 HALL B

6.15 - 7.00	Yoga Session (Lawn of DAE convention centre)		
Time	Presentation ID/ Abstract ID	Title of the talk	Chairperson/ Moderator/ Speaker
8.00 - 8.55	CMPI Teaching Course		T Ganesh/ M Ravikumar
9.00 - 9.55	Special Symposium 11: Growing careers in medical physics		Jemimah Eve/ Claire-Louise Chapple, UK
9.00 - 9.20	S-33	Training, development and professionalism for medical physicists	Jemimah Eve, UK
9.20 - 9.40	S-34	Empowering Medical Physics Globally: Key Initiatives of AAPM's International Council (IC)	Manju Sharma, USA
9.40 - 9.55	----	Panel Discussion	All
10.00 - 10.15	Tea Break		
11.15 - 12.15	Scientific Session 25: Particle Therapy		Taweap S, Thailand
11.15 - 11.35	I-24	Current Status of Heavy Ion Therapy	Shigekazu Fukuda
11.35 - 11.45	O-072/ G4999	Development and validation of machine learning approach for predicting proton therapy beam spot characteristics	Ranjith C P, India
11.45 - 11.55	O-073/ C5272	Modeling and Comparative Analysis of FLASH Radiotherapy for Head and Neck Cancer and Lung Cancer: Proton Therapy and Heavy Particle Beams	Erato Stylianou Markidou, Cyprus
11.55-12.05	O-074/ R2310	Dosimetric Study of a High-Energy Proton Therapy System	Abdelkrim Zeghari, Morocco
12:15 to 13:15	Scientific Session 26: Artificial Intelligence and Automation Processes		Probal Chaudhury, India
12.15 - 12.35	I-25	AI algorithm for auto segmentation of OAR based on deep image-image network	Suresh Chaudhary
12.35 - 12.55	O-075/ B8418	Automation in EBRT for Cervical Cancer using Knowledge Based Planning: Multi-Centric Validation and Global Applicability	Jeevanshu Jai, India
12.55 - 13.05	O-076/ S1906	Combined radiomics and dosiomics in the prediction of treatment response for patients of brain metastases treated by stereotactic radiotherapy	Ji Zhang, China
13.05 - 13.15	O-077/ A8320	A self-supervised 3D U-Net based auto-contouring tool for OAR segmentation on head and neck CT images	Niyas Puzhakkal, India
13.15 - 14.00	Lunch & social time		
14.00 - 14.45	Scientific Session 27: Sustainable Healthcare implementation and support in health services of LMI countries		B. K. Sapra, India
14.00 - 14.15	O-078/ R5048	Collaboration with AAAPM through the Network of Global Representatives	Eugene Lief, USA
14.15 - 14.30	O-079/ E9290	WORLD of Medical Physics: A Website of Open Resources for Learning and Development of Medical Physicists for Radiation Oncology Medical Physics Residents	Parminder Basran, Canada
14.30 - 14.45	O-080/J2197	Determining and Prioritizing Needs of LMI Countries by AAAPM	Eugene Lief, USA

14.50 - 15.50	Scientific Session 28: Innovations in Biomarkers and Radiopharmaceuticals		Siva Sarasanandarajah, Australia
14.50 - 15.10	I-26	Testing positronium biomarker in preclinical and clinical studies	Ewa Stepień
15.10 - 15.20	O-081	Cancer visualization using gadobutrol-glucose solution and 7.0T magnetic resonance imaging	Eiichi Sato, Japan
15.20 - 15.30	O-082/P3582	Application of Failure Mode and Effect Analysis to Medical Emergency Management in High-Dose Iodine Therapy	Jayadevan P M, India
15.30 - 15.40	O-083/ H7959	Medical Cyclotron Facility: Best Practices and Lessons Learned	Dilshad Kottuparamban, India
15.50 - 16.15	Tea Break		
16.15 - 17.05	IOMP School: Radiation Dose & Radiation Biology		Madan Rehani/M Mahesh, USA Nagesh Bhatt, India
17.10-18.10	Special Symposium 12: Insight into Current State and Challenges of MP Practice through International Surveys		Stephanie Parker/Simone Kodlulovich Renha/ M. Mahesh
17.10 - 17.30	S-06	Causes of radiotherapy incidents and what safety barriers to use – Analysis from the IAEA SAFRON system	Ola Holmberg, IAEA/Sweden
17.30 - 17.50	S-35	Insight into Medical Physics Practice in LMICs through a Survey of Departmental and Institutional Leaders-	Stephanie Parker, USA
17.50 - 18.10	S-37	Status of Medical Physicists in Diagnostic and Interventional Radiology in Europe	Paddy Gilligan, Ireland

Scientific Program: Day 3, Friday, 8th December 2023 HALL C

6.15 - 7.00	Yoga Session (Lawn of DAE convention centre)		
Time	Presentation ID/ Abstract ID	Title of the talk	Chairperson/ Moderator/ Speaker
9.00 - 10.00	Special Symposium 13: Total Body Irradiation using different techniques in current Radiotherapy practice		NVN Madhusudan Sresty/ T Anil Kumar
9.00 - 9.20	S-40	Total Body Irradiation with extended SSD and VMAT techniques	Biplab Sarkar, India
9.20 - 9.40	S-41	Total Body Irradiation with Tomotherapy	Madhusudhana Sresty, India
9.40 - 10.00	S-42	Planning, Dosimetry validation and clinical implementation of TMLI as a containing regimen using VMAT	Reena Ph, India
11.15 - 12.15	Scientific Session 29: Patient Specific QA and Dosimetry		Shobha Jayaprakash/ E. Vardharajan, India
11.15 - 11.35	I-27	Patient specific QA: Challenges & solution	Saju Bhasi, India
11.35 - 11.45	O-084/ W7193	ABS cuboid phantom for dosimetry audit of advanced radiotherapy	Nitin Kakade, India
11.45 - 11.55	O-085/ N8281	Advancing Radiation Therapy: 3D Printing for Pre-Treatment SBRT Plan Verification and Brachytherapy Applicator Innovation	Arun Krishnan MP, India
11.55 - 12.10	O-086/ E8810	Assessment of Statistical Process Control to set tolerance and action limits for Portal Image based Patient-Specific Quality Assurance	Sumanta Manna

12:15 to 13:15	Scientific Session 30: Regulation and Validation		Bychung Chul, South Korea/ Kalpana Thankur, India
12.15 - 12.35	I-28	Regulation of medical usage of ionizing radiation in India	Ghanshyam Sahani
12.35 - 12.55	O-087/A1929	Effect of modulation factor on pass rates of AAA and Monte Carlo calculated SRT VMAT dose distributions evaluated with in-house 3D portal imaging dosimetry	Sergei Zavgorodni, Canada
12.55 - 13.05	O-088/ U8760	Monte Carlo validation and beam data comparison between experimental Raystation TPS and TOPAS simulation for proton spot scanning	Umesh Gayake, India
13.05 - 13.15	O-089/ Q8940	An Integrated Monte Carlo Decision Tree Model for Predicting Life Expectancy Based on Dosimetry Quality in Radiotherapeutic Treatment of Glioblastoma Multiform	Praveen Kumar C, India
13.15 - 14.00	Lunch & social time		
14.00 - 16.00	Medical Physics Quiz		Quiz Masters:
			Ms Deboleena Mukherjee
			Ms Kalpana Thakur
			Ms Ranjana Agarwal
			Ms Reena Sharma
16.00 -16.15	Tea Break		
17.15-18.15	Poster Rapporteur - Poster Nos. 201 to 300		Vinod Pandey, India
17.15 - 17.30	Rapporteur 1	Posters 201 to 225	Kirti Tyagi, India
17.30 - 17.45	Rapporteur 2	Poster 226 to 250	S Senthil Kumar, India
17.45 - 18.00	Rapporteur 3	Posters 251 to 275	Niyas P, India
18.00 - 18.15	Rapporteur 4	Posters 276 to 300	Teerthraj Verma, India

Scientific Program: Day 4, Saturday, 9th December 2023 HALL A

6.15 - 7.00			
Yoga Session (Lawn of DAE convention centre)			
Time	Presentation ID/ Abstract ID	Title of the talk	Chairperson/ Moderator/ Speaker
8.00 - 8.50	CMPI Teaching Course		M Ravikumar/ T Ganesh
9.00 - 9.55	Scientific Session 31: Unsealed Source Therapy and Dosimetry		V. K. Dangwal, India
9.00 - 9.20	I-29	Advancement in Unsealed Radioisotope based Therapy in India	Sandip Basu, India
9.20 - 9.30	O-090/ H5710	ESGnrc based Monte Carlo simulation of Ir-192 HDR Flexisource in water and different phantom materials	Jerema Persis Reaiah R, India
9.30 - 9.40	O-091/ B1046	Identification of Cs-137 Beam Quality Correction factor Using Different Methods	Ahmed Maghraby, Egypt
9.40 - 9.50	O-092/ U3427	Radioprotective Effect of Hesperidin/Diosmin Compound Against 99mTc-MIBI-Induced Cardiotoxicity	Fereshteh Koosha, Iran
10.00 - 10.20	Tea Break		
10.20 - 11.00	Plenary Session 4: AMPI Dr. P. S. Iyer Oration Lecture		K Muthuvelu and Sridhar Sahoo, India
10.20 - 10.25	Introduction about Dr P S Iyer Oration		K Muthuvelu
10.25 - 10.55	P-6	Ru-106 Ocular Brachytherapy General, dosimetry, clinical and Safety aspects	K N Govinda Rajan
10.55 - 11.00	Presentation of Silver Plaque and vote of thanks		Sridhar Sahoo
11.05 - 11.55	Scientific Session 32: Radiotherapy Treatment Planning and Dosimetry		D. D. Deshpande/ S. S. Sanaye, India
11.05 - 11.20	I-30	Enhancing Patient-specific QA in VMAT: Integrating plan complexity & dosimetry features with deep learning	Dr. A. Pichandi
11.20- 11.30	O-093/ A7403	End to end testing using anthropomorphic phantom in cyber knife	Sangaiah Ashok Kumar, India
11.30 - 11.40	O-094/A 9434	Evaluation of the efficacy of automated plan generation using Varian Ethos intelligent optimization engine and a comparative analysis with Eclipse Treatment Planning System (TPS) plan	Anand Jadhav, India
11.40 - 11.50	O-095/Y2492	A novel dose-volume histogram (DVH) scoring algorithm for automatic DVH-based patient-specific quality assurance for volumetric modulated arc therapy	Boda Ning, China
12:00 to 12:45	Scientific Session 33: Radiotherapy Dosimetry and QA		Rajib Das, India
12.00 - 12.20	I-32	Halcyon Radiation Therapy - Beyond the Conventions (day 3)	Arun Shiva
12.20 - 12.30	O-101/ I8922	Dosimetric Evaluation of Dual Layer MLC for an O-ring Gantry System	Arvind Kumar, India
12.30 - 12.40	O-102/ M3851	Performance Comparison between different Patient Specific QA systems for VMAT and IMRT plans on Varian TrueBeam	Farheen Kagdi, India
12.45 - 13.15	Valedictory & Closing Ceremony		
13.15 - 14.00	Lunch & social time		

Scientific Program: Day 4, Saturday, 9th December 2023 HALL B

6.15 - 7.00			
Yoga Session (Lawn of DAE convention centre)			
Time	Presentation ID/ Abstract ID	Title of the talk	Chairperson/ Moderator/ Speaker
8.00 - 8.55	IOMP School: Accreditation & Professional Development (ETC and PRC)		Eva Bezak, Magdalena Stoeva, Arun Chougule and Simone Kodlulovich Renha
9.00 - 10.00	Special Symposium 14: Importance of a unified medical physics syllabus in AFOMP		Hasin Anupama Azhari/ Mary Joan
9.00 - 9.15	S-43	Unified Medical Physics Syllabus for AFOMP	H A Azhari, Bangladesh
9.15 - 9.30	S-44	Review of Medical Physics Curriculum In Japan by JBMP	Hayashi Naoki, Japan
9.30 - 9.45	S-45	Review of Medical Physics Curriculum Malaysian Perspective	Chai Hong Yeong, Malaysia:
9.45 - 10.00	S-46	Medical Physics Curriculum - Indian Perspective	S. D. Sharma, India
10.00 - 10.20	Tea Break		
11.15 - 11.40	Scientific Session 34: Medical Physics Education		P. Raghukumar, India
11.15 - 11.35	O-096/ I6226	Norwegian Partnership Programme for Global Academic Cooperation (NORPART) on Ghana-Norway Collaboration in Medical Physics and Radiography Education	Stephen Inkoom, Ghana
11.35 - 11.45	O-097/ V8119	Education and training of personnel working in secondary standards dosimetry laboratories	Zakithi Msimang, Austria
11:40 - 12:45	Scientific Session 35: Presentations by AFOMP Awardees		Hasin Anupama Azhari, Bangladesh; Aik Hao Ng
11.40 - 11.50	AFOMP Awards		Hasin Anupama Azhari
11.50 - 12.05	AP-1	Lifetime Achievement Award 2023	Jianrong Dai, China
12.05 - 12.15	AP-2	PN Krishnamoorthy Memorial AFOMP Young Achiever Award 2023	Lukmanda Evan Lubis, Indonesia
12.15 - 12.25	AP-3	Golam Abu Zakaria AFOMP Best Young Leadership Award 2023	Noramaliza Mohd Noor, Malaysia
12.25 - 12.35	AP-4	Dr. Udipi Madhvanath Memorial AFOMP Best PhD Award in Radiobiology 2023	Raizulnasuha Binti Ab Rashid, Malaysia
12.35 - 12.45	AFOMP Travel Awards		Hasin Anupama Azhari/ Aik Hao Ng, Malaysia
12.45 - 13.15	Valedictory and closing Ceremony in Hall A		
13.15 - 14.00	Lunch & social time		

Scientific Program: Day 4, Saturday, 9th December 2023 HALL C

6.15 - 7.00	Yoga Session (Lawn of DAE convention centre)		
Time	Presentation ID/ Abstract ID	Title of the talk	Chairperson/ Moderator/ Speaker
11.00 - 11.50	Scientific Session 36: Diagnostic Imaging Using Non-Ionizing Radiation		Jayanta Pal, India
11.00- 11.20	I-31	Recent advances in magnetic resonance imaging	Ioannis Seimenis, Greece
11.20- 11.30	O-098/ N4636	Optical Coherence Elastography: Advancing Non-Ionizing Radiation Diagnostics for Tissue microstructure biomechanics using microstrain mapping	Sweta Satpathy, India
11.30 - 11.40	O-099/ F4959	Design and Development of an Ultrasound phantom to Evaluate Greyscale contrast in Ultrasound imaging	Abjasree S, India
11.40 - 11.50	O-100/ D4300	Contrast Enhanced Ultrasound Imaging using Microbubbles for Visualization of Microvasculature in a Tissue Mimicking Phantom	Sumana Halder, India
12.00 - 12.45	Poster Rapporteur - Poster Nos. 301 to 360		Sakthivel, India
12.00 - 12.15	Rapporteur 1	Posters 301 to 320	Jeevanshu Jain, India
12.15 - 12.30	Rapporteur 2	Posters 321 to 340	Satish Pelagade, India
12.30 - 12.45	Rapporteur 3	Posters 341 to 359	Suresh Pangam, India
12.45 - 13.15	Valedictory and closing Ceremony in Hall A		
13.15 - 14.00	Lunch & social time		



IUPESM 2025

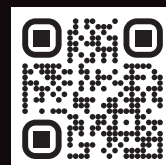
World Congress on Medical Physics
and Biomedical Engineering

29 September – 4 October 2025
Adelaide Convention Centre, Australia

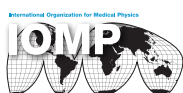


ACPSEM
Australasian College of Physical
Scientists & Engineers in Medicine

www.wc2025.org
#IUPESM2025



Host Organisations



Supported by



ANNEX 2

BOOK OF ABSTRACTS

of the

International Centre for Theoretical Physics (ICTP)

MASTER OF MEDICAL PHYSICS (MMP) THESES

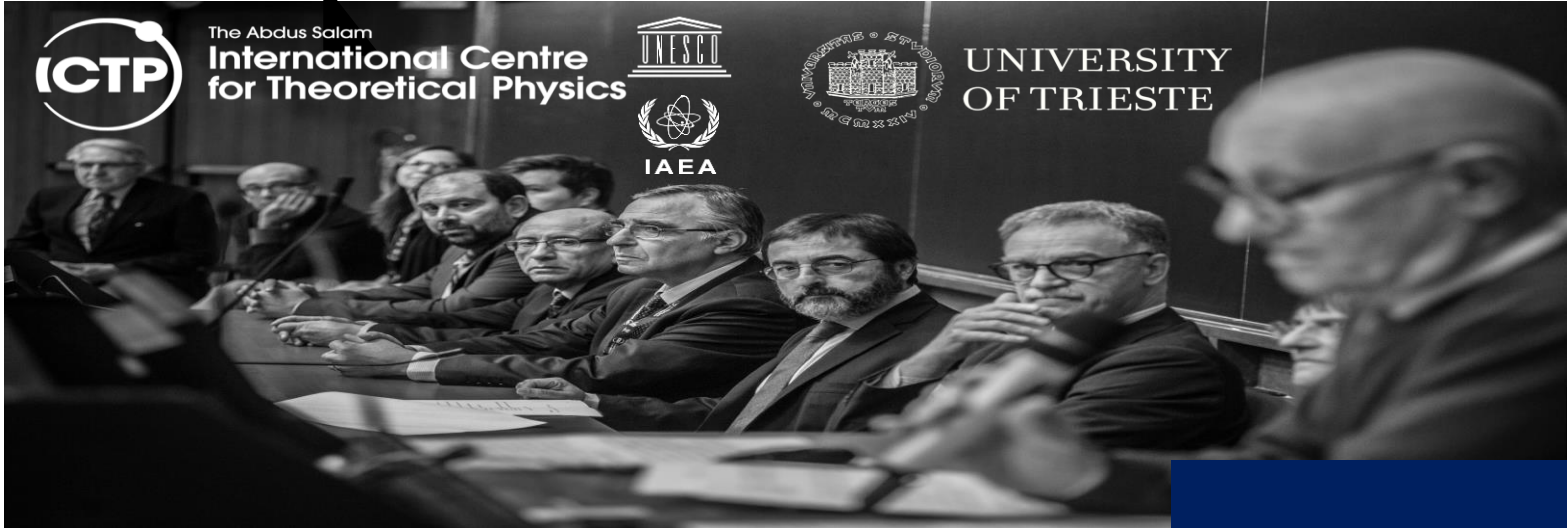
Trieste, Italy



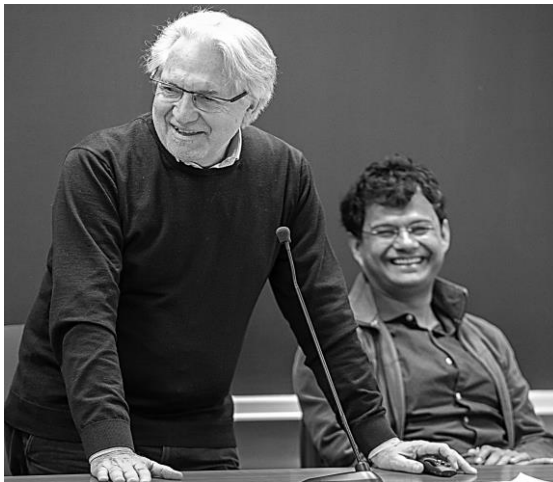
The Abdus Salam
International Centre
for Theoretical Physics



UNIVERSITY
OF TRIESTE



ICTP, December 2018



Abstracts Booklet of the MMP Thesis (8th & 9th cycles)

The programme is
accredited by The
International Organization
for Medical Physics (IOMP)



ICTP, December 2017





Board Members



Prof. Luciano Bertocchi (ICTP)
Coordinator of the ICTP Medical Physics Activities and board member
Email: bertocch@ictp.it
Office: ICTP-Leonardo Building- 2nd Floor- Room#227



Prof. Renata Longo (University of Trieste)
Director of the Master in Medical Physics
Email: renata.longo@ts.infn.it
Office: Via Alfonso Valerio, 2, Edificio F, Department of Physics, University of Trieste, 2nd Floor



Prof. Renato Padovani (ICTP)
Coordinator of the Master in Medical Physics
Email: padovani@ictp.it
Office: ICTP-Adriatico bulidng-1st Floor



Dr. Paola Bregant (University hospital of Trieste)
Board Memeber
Email: mario.dedenaro@asuits.sanita.fvg.it
Office: Via della Pietà, 4, Ospedale Maggiore, Fisica Sanitaria, 2nd Floor



Prof. Luigi Rigon (University of Trieste)
Board Member
Email: luigi.rigon@ts.infn.it



Prof. Edoardo Milotti (University of Trieste)
Board Member
Email: milotti@ts.infn.it



Prof. Slavik Tabakov (King's College London)
Scientific Adviser
Email: slavik.tabakov@emerald2.co.uk



Prof. Ahmed Meghzifene (IAEA)
Scientific Adviser
Email: a.meghzifene@iaea.org



Dr. Mauro Carrara (IAEA)
Scientific Adviser
Email: M.Carrara@iaea.org

MMP graduates 8th Cycle- 2020-2022



The Master is supported and sponsored by:



International Atomic Energy Agency



International Organization for Medical Physics



European Federation of Organisations for Medical Physics



Institute of Physics and Engineering in Medicine

Institute of Physics and Engineering in Medicine



Italian Association of Medical Physics



University Hospital of Trieste

Abstract booklet

Abstract booklet	#5 (8 th cycles)
Year	2023

Editorial team

- Renata Longo,**
University of Trieste, Italy
- Renato Padovani,**
International Centre for Theoretical Physics (ICTP), Trieste, Italy
- Hossein Aslian,**
Olivia Newton-John Cancer Wellness & Research Centre (ONJ), Melbourne, Australia



Hospitals in the Programme’s Training Network:

Az. Ospedaliero Universitaria Ospedali Riuniti	Ancona
IRCCS Centro di Riferimento Oncologico	Aviano
Az. Ospedaliera Papa Giovanni XXIII	Bergamo
Ospedale S. Orsola	Bologna
Spedali Civili	Brescia
Az. Ospedaliero Universitaria “Arcisp. Sant’Anna”	Ferrara
Az. USL Toscana Centro	Firenze
Ospedale Niguarda Ca' Granda	Milano
IRCCS Istituto nazionale tumori	Milano
Az. Ospedaliero-Universitaria di Modena	Modena
Az. Ospedaliera S. Gerardo	Monza
Az. Ospedaliero Universitaria Osp. Maggiore della Carità	Novara
Istituto Oncologico Veneto	Padova
Ospedale S. Matteo	Pavia
Az. Ospedaliero Universitaria Pisana	Pisa
Ist. Nazionale Tumori Regina Elena	Roma
Az. Ospedaliero Universitaria	Siena
Ospedale Mauriziano	Torino
A.O.U. Citta della Salute e della Scienza	Torino
Ospedale S. Chiara	Trento
Az. Ospedaiero Universitaria Ospedali Riuniti	Trieste
ASST dei Sette Laghi	Varese
Az. Ospedaliero Universitaria Integrata	Verona
ULSS 6 Vicenza, Ospedale San Bortolo	Vicenza





Small field Dosimetry with the new generation Exradin W2 scintillator detector

Prospective/Objective: The aim of this study is to evaluate the new generation of scintillator detector, Exradin W2, for commissioning measurements and routine check in small field dosimetry.

Materials and methods: Percentage dose depth, transverse profile and field output factors were measured in a 6 MV beams for small field sizes ranging between 1x1 cm² and 5x5 cm² in a PTW MP3 water phantom with four different detectors: PTW 31016 PinPoint3D, PTW 60023 microSilicon, PTW 60019 microDiamond and Exradin W2 scintillator detector. The parameters analyzed for PDD curves were relative surface dose (DS), depth of dose maximum (Dmax) and of 50% of dose (R50) and percentage dose at 100 mm (D100). In addition, maximum difference in distance (mm) and difference in Percentage Dose (%), within the 20-80% PDD region for all detectors (PinPoint, microSilicon, microDiamond), with respect to the Exradin W2 were evaluated. Penumbra width and field size were derived from transverse profiles both in cross and in-plane profile for each field size with all four detectors and were compared. OFs measurements were performed for each field size by the four detectors at 10-cm depth, 100-cm source–detector distance. The 5 × 5 cm² field size was used for the normalization of OFs. By adopting the methodology recommended in TRS4831 for small photon beam dosimetry, two orthogonal profiles were subsequently acquired with the smallest field size and each detector was positioned at the maximum detector signal point. The ratio of the readings in the clinical field and in the reference, field was evaluated for each detector. Then, the field output factor, was evaluated by applying the output correction factor for each detector and each effective field size. For the Exradin W2 no correction factors were applied. Relative Deviations between corrected measurements performed by each detector and the Exradin W2 were calculated.

Results: For PDD measurements, an agreement within $\pm 2\%$ was observed among the detector responses for all the field sizes over the whole PDD curve, except for the build up region. Penumbra width derived from in-plane and cross- plane profiles with the four detectors were within 1.5 mm for all field sizes. Field size differences evaluated for the four dosimeters were less than 1mm. For Field Output factors, differences between Exradin W2 and other detectors were less than 0.5% for field sizes larger than 1x1 cm². For 1x1 cm² field sizes we found a maximum difference of 2.9% between Exradin W2 and corrected PinPoint Ionization Chamber measurement. The combined uncertainties for the measurements were estimated to be within 1.5% for the all the dosimeters.

Conclusion: The new W2 Exradin detector proved to be a suitable detector for accelerator linear commissioning measurements and routine check in small field dosimetry. The problem related to the first commercial version of this kind of detectors, the Exradin W1, regarding the lack of possibility to perform scanning data measurements has been successfully overcome. The new electrometer MAX SD allows manipulation of baseline values like Cerenkov light ratio and collection of point measurements. In addition, the MAX SD can convert the Cerenkov corrected signal into analog output that can be read by an external single channel electrometer thereby making the W2 detectors useful for scanning dosimetry.



Xhulia Dosti

Xhulia-dosti@hotmail.com

Supervisor:

Dr. Serenella Russo

Santa Maria Annunziata
Hospital USCL, Toscana,
Italy





Rahnuma Shahrin

Rista

rahnumashahrin06@gmail.com

Supervisors:

Dr. Paola Chiovati
Dr. Michele Avanzo

Centro di Riferimento
Oncologico IRCCS, Aviano,
Italy



Novel Techniques of In Vivo Dosimetry in Low kV Intraoperative Radiotherapy

Prospective/Objective: Intraoperative Radio Therapy (IORT) is one of the most attractive radiotherapy techniques now-a-days with several positive sides. During IORT, a very important aspect is in vivo dosimetry. The purpose of this study was to calibrate two types of dosimeters, radiochromic films (RC) and MOSFETs, for in vivo measurements in IORT with low-kV x-rays delivered by Intrabeam system for breast cancer patients. We also wanted to make a comparison of the characteristics between both dosimeters and at the end choose the most suitable one to be used in our centre.

Materials and methods: The Intrabeam system is a miniature kV x-ray source manufactured by Zeiss and is designed especially for IORT applications. The calibration of both EBT-3 RC films and MOSFETs were done with Intrabeam which is the 50 kV source. EBT-3 films were calibrated using the red and green channels of the absorption spectrum in the 0–15 Gy dose range delivered by the low kV source. We also checked the effect of different self development time and orientation of scanning of EBT-3 films. The calibration of MOSFET was done for the same dose values. We used the calibrated films for in-vivo dosimetry during IORT of breasts for doing an independent QC of the treatment by placing one piece of RC film wrapped in sterile envelope on the skin of the patient after breast conserving surgery.

Results: We found from EBT-3 calibration that, in the low dose range the red channel shows better sensitivity, while starting from 5 Gy the green channel has better sensitivity. Then we built the calibration curve of RC film for both channels & these curves were used to measure skin dose during IORT. Moreover, dose to an implantable cardiac device was measured using films. Results from MOSFET calibration showed linear response in the dose range of interest. Results from in vivo measurements performed with RC films showed that, the technique is completely safe from side effects to the skin. The value of skin dose to each of the patient was within the threshold which is 5 Gy.

Conclusion: We were able to complete the task with clinical evidence which showed an excellent result for the RC films. In conclusion we can say that, IVD with EBT-3 films is a feasible procedure. Measured dose to the skin indicates that the technique is safe from side effects to the skin. As we calibrated MOSFETs also, we found that, MOSFET is also a strong dosimetry tool which can be used for IVD to the OAR such as skin.



S M Hasibul Hoque

hasibulshefat@gmail.com

Supervisors:

Dr. Paola Chiovati
Dr. Giovanni Pirrone

Centro di Riferimento
Oncologico IRCCS Aviano,
Italy



Geometric and Dosimetric Validation of An Artificial Intelligence Based Auto-Contouring System for Radiation Therapy Treatment Planning: A Clinical Feasibility Study.

Prospective/Objective: Geometric metrics are often used to evaluate automated contouring methods. A dosimetric parameter analysis may be more useful in clinical practice, although it is frequently absent in the literature. The purpose of this study was to look into the effect of state-of-the-art AI-generated anatomical delineations on dose optimization in radiation therapy (RT) for patients with prostate, breast, and H&N cancer.

Materials and methods: The auto-contouring system was evaluated using a database of 60 computed tomography images comprising prostate, breast, and H&N structures. Clinically accepted reference plans are directly copied for dose calculation of auto contoured structure sets. Dice similarity coefficient (DSC), Hausdorff distance (HD) and Relative Volume Difference (RVD) were used to assess geometric performance of contours. Dmax, Dmean, and D0.03cc indices were used to analyze OAR dose distributions with manual segmentation as a reference. For measuring overall plan acceptability, normalized plan quality metrics were evaluated. A Wilcoxon rank sum test was computed between dosimetric metrics. Inter-observer variability was also assessed for prostate cancer site.

Results: AI-based segmentation saved more than 57% contouring time and achieved an average DSC of 0.80 for prostate, 0.90 for breast and 0.75 for H&N with a few exceptions and the average HD (& RVD) were below 13mm (0.20), 25 mm (0.22) and 11mm (0.25), respectively. The dose parameters, Dmax, Dmean and D0.03cc for the prostate, breast and H&N patients, showed agreement between dose distributions within $\pm 8\%$, $\pm 5\%$ and $\pm 3\%$, respectively. In all situations, the difference in plan quality was less than 8%. The dose parameters changed slightly due to inter-observer variability. The comparison between geometric and dosimetric metrics showed no strong statistically significant correlation without a few exceptions.

Conclusion: Although auto-contouring system achieved state-of-the-art geometrical performance, human review is still unavoidable. Plans, based on auto-contouring, do not overdose nearby OARs. The auto-contouring system is recommended as a standard starting point with institutional geometric and dosimetric validation.



**Nkenang Nguefack
Sandra**

Sandranguenfack12@gmail.com

Supervisors:
Dr. Roberta
Matheoud

University Hospital
Maggiore della Carità
Novara, Italy



Characterization of a solid-state detector gamma camera dedicated to nuclear cardiology

Prospective/Objective: This study aims to characterize the solid-state detectors gamma camera DSPECT (Spectrum Dynamics Medical, Caesarea, Israel) by analyzing the quality of myocardial SPECT images through different figures of merit (spatial resolution, uniformity of perfusion, and contrast) over a wide range of counts statistics (1, 0.8, 0.6, 0.4, and 0.25 million counts) in the Left Ventricle (LV) wall while using an anthropomorphic phantom mimicking normal and pathologic LV perfusion conditions.

Materials and methods: The experimental part of the study was done in two sessions. Both sessions used an anthropomorphic phantom of the chest (Torso phantomTM and Cardiac InsertTM, Data Spectrum Corporation, Hillsborough, NC, USA) with lungs, liver, and dorsal spine insert included. Lung's insert is filled with Styrofoam beads and non-radioactive water to mimic the density of lung tissue attenuation. The first session consisted of the preparation of the anthropomorphic phantom by inserting a cold defect in the left ventricle (LV) wall simulating a transmural defect (TD) and the second one by mimicking a normal LV, i.e., without any cold insert. For the two preparations, the acquisition was made at different count statistics in the LV wall image area (1,0.8,0.6,0.4,0.25 million counts). Pathological phantom acquisitions were made twice for each count statistic and for each position (Ant, Lat, Post, and Sept) of the cold defect. The normal phantom was re-positioned three times and for each position, two acquisitions were performed for each level of count statistics. The quality of the reconstructed images was evaluated in terms of contrast of the internal cavity (C_{IC}), the thickness of the LV wall, and the sharpness index (SI). On the polar maps reconstructed from the short axis slices of the LV phantom, other parameters have been evaluated, including uniformity of segmental uptake for the uniform phantom and TD contrast and variation in the segmental uptake for the pathologic phantom.

Results: All the Images quality parameters (Thickness of the LV wall, Sharpness index, Contrast of the internal cavity, Uniformity of segmental uptake, contrast of the TD, and variation of the segmental uptake) showed no difference when moving from the reference level counts statistics (1 Mc) down to 0.25 Mc in the Left Ventricle wall. The segmental uptake of the uniform phantom showed a decrease in the perfusion in correspondence with the mid-basal infero-septal position, as already evidenced by the literature. Moreover, the TD contrast was significantly lower for the defect placed in the posterior wall, with respect to the other positions.

Conclusion: Our results demonstrate that in clinical circumstances and using the reconstruction parameters currently advised for the clinical routine there are no differences in the considered parameters along the range of counts statistics explored. This result allows to administer a lower activity to the patient or use reduced scan time, to enhance patient comfort and limit the radiation exposure of both patients and operators.



**Allangba Koffi
N'guessan Placide
Gabin**

pgallangba@gmail.com

Supervisors:

Dr. Traino Antonio

Claudio

Dr. Giuliano Alessia

Santa Chiara Hospital, Pisa,
Italy



Partial Volume Effect (PVE) correction in Single Photon Emission Computed Tomography (SPECT) imaging

Prospective/Objective: The purpose of this work was to implement a home-made post-reconstruction algorithm to correct the PVE in the SPECT image to improve its quality for better quantification in diagnosis and therapy

Materials and methods: The NEMA IEC phantom inserts the six spheres of different sizes to study the PVE of two activity concentration measurements of 4.6 and 12.19 mCi/L of ^{99m}Tc respectively filled with a 10:1 signal-to-background ratio. The scan was performed on the Discovery NMCT 670 GE using clinical protocol. The images were reconstructed by OSEM 2 iterations, 10 subsets, Butterworth filter 0.48, CT based attenuation and scatter correction was used. In addition, the non-filter image was studied. The system PSF was performed with the same protocol. Two methods were used to correct PVE. First, the post-reconstruction algorithm based on the mathematical theory implemented in MATLAB, was used to correct the PVE in SPECT images studied and the second method is the recovery coefficient (RC). The raw and corrected image quality of the IEC phantom has been studied in terms of RC and contrast. In clinical application, 10 Hepatocarcinoma patients treated with Yttrium 90 were studied. All data has been analyzed with MATLAB, image J, LIFE x v7.3.0 and Xeleris software.

Results: Results showed that at 4.6 mCi/L, a ratio of 10.26 was obtained for the filtered image only for the large sphere, while all other spheres, except the smallest of the non-filtered corrected image, achieved a ratio greater than 10. The mean recovery values measured at 12.19 mCi/L for the small spheres in the filtered image, were 38.18 % versus 0.8 % for the post-reconstruction method and the classical RC method respectively. PVE recovery in small spheres is more accurate for post reconstruction method. The mean recovery values for all spheres size, obtained by the post-reconstruction method for the filtered image were 45.16 % versus 47.45 % measured at 4.6 and 12.19 mCi/L respectively and for the non-filtered image 42.53 % versus 47.3 % measured at 4.6 and 12.19 mCi/L respectively. For the classical RC method, both image types gave 12.88 % versus 10.13 % measured at 4.6 and 12.19 mCi/L respectively. The quality of the image studied in terms of contrast showed that it increases as the size of the sphere increases. Clinical images of HCC patients treated with ^{90}Y microspheres were corrected for PVE. A significative improvement in contrast was demonstrated after this correction.

Conclusion: The post reconstruction method has proven more effective for clinical use. It is based on the mathematical theory of deconvolution to correct the PVE and depends on the sigma PSF system for its configuration. This is not an ideal tool as it is also limited by the scanning procedure such as phantom filling or patient injection and system spatial resolution.

aCommissioning and clinical implementation of the 1600 SRS Octavius detector



Zie Traore
traore857@gmail.com

Supervisor:
Dr. Alessandro
Scaggion

*Istituto Oncologico Veneto
(IOV), Italy*



Prospective/Objective: To commission a new device for pre-treatment patient specific verification of stereotactic treatments plans, which is capable of reconstructing 3D dose with high resolution (Octavius 1600SRS)

Materials and methods: Octavius 4D system (PTW) consists of an ion chamber array embedded in a cylindrical phantom which, assisted by an inclinometer, rotates synchronously with the gantry. It measures planar dose distributions as a function of gantry angle in order to compute the resulting 3D dose distribution. There are diverse options for the ion chamber array, we used the new Octavius 1600 SRS (small field size, high resolution). We have used one TrueBeam linac STx with MLC HD 120, the TPS has been Eclipse (v.15.5) and analysis have been performed with Verisoft (v.8.1). The commissioning measurements consisted of the following tests: (1) matrix calibration factors variation with dose rate and field size; (2) Dose rate dependence; (3) Field size dependence; (4) influence of geometry on PSQA results; (5) verification and analysis of typical SRS and SBRT plans, comparing TPS-calculated versus measured dose.

Results: We found the following results for Octavius 1600 SRS): (1) The matrix calibration factors has shown a maximal variations of 2.80% and 4.10%, respectively for 6FFF and 10FFF beams, within the range of field sizes and dose rates considered. (2) For dose rate dependence a maximal variations of 1.702% and 1.853% was recorded for 6FFF and 10FFF beams. (3) For what concern field size dependence a maximal variations, obtained at the smallest field of 1.498 % and 3.355% for 6FFF and 10 FFF beams was recorded with an energy dependence of 1.857%. (4) It has been shown that dose agreements can deteriorates when the main lesion is shifted from the center of the phantom and when PSQA are delivered in non-isocentric conditions. (5) Verification of SRS and SBRT plans showed that the 2%, 2 mm, cut-off 10% and mean local dose difference criterion could help to replicate the former PSQA outcome.

Conclusion: Octavius 4D system together with Octavius 1600 SRS is an adequate tool for patient specific QA of treatments requiring high spatial resolution, but the dependence of its response with field size and dose rate can hinder its clinical adoption if not properly tamed. The collected set of measurements suggests that PSQA results obtained with Octavius can approach those performed with IC or ArcCHECK if the following criteria are used for the analysis: -local 2%/2mm gamma with a cut-off of 10% of the dose and an action level of 95%; mean local dose difference with dose cut-off at 70% (to check the high dose regions) with an action level of 4%.



Mohammed Ahmed Shehu

Ma7512285@gmail.com

Supervisors:
Dr. D'Andrea Marco

*Istituto Nazionale Tumori
Regina Elena, Rome, Italy*



3D printed lung phantom design and applications in evaluating lung SBRT respiratory gating treatments with surface guided radiotherapy for positioning

Prospective/Objective: This study aims to develop a 3D printed lung phantom as an add-on to the QUASAR™ respiratory motion phantom and use it to evaluate lung SBRT respiratory gating treatments and testing surface guided radiotherapy for positioning. In particular TPS dose calculation accuracy on two different scans was tested against Gafchromic film measurement on a gated treatment.

Materials and methods: We evaluated the median diameter and volume of PTVs (spherical equivalent) for lung-SBRT using Eclipse (Varian Medical Systems) version 15.5 treatment planning system (TPS), taken from 41 patients who underwent lung SBRT with free breathing and 36 patients who underwent DIBH treatment. In total, 42 Lung SBRT PTVs have been selected based on 3-8 fractions of the lung SBRT treatment since 2021. The average planning volume (PTV diameter) was used to produce lung phantom using 3D printer technology. A patient-specific 3D-printed lung phantom was fabricated by using a 3-D printer (Original Prusa i3 MK3S+ 3D printer, Josef Prusa). Based on the QUASAR™ respiratory motion phantom geometry the phantom was printed with 8 cm diameter, 15 cm length. Besides the target is centered to the middle of the fabricated phantom with a mass density of 1.2 g/cm³ and Hounsfield Unit value of 68 HU. The surrounding tumor tissue is infill by PLA composite with a 30% infill density and -655 HU of surrounding tissue. The phantoms were splitted into half in order to measure 2-D dose delivery by inserting Gafchromic film dosimetry. Based 4-D CT construction ITV was delineated on 30%-70% of breathing phases. VMAT planning was used for treatment and selected 30%-70% of the breathing cycle as the gating window. As an application of the 3D printed lung phantom, the TPS plan was optimized with Base 30-70 % 10X-FFF and re-calculated with Av-IP (30-70%) 10X-FFF and finally compared with Gafchromic ETB-3 film measured dose.

Results: The measured passing rates of gamma analysis seen to over all 3%/3 mm, 3%/2 mm and 2%/2 criteria, (97,95 and 93 %), (95.6, 92.9 and 91.1 %) and (100,100 and 99.9 %) similar results between Gafchromic ETB-3 Vs Base 30-70 % 10X-FFF, Gafchromic ETB-3 Vs Av-IP: 30-70% 10X-FFF and Av-IP: 30-70% 10X-FFF Vs Base 30-70 % 10X-FFF respectively

Conclusion: It was found that the Dosimetry verification results were extremely similar for both calculated-TPS plan Vs Gafchromic ETB-3 film systems.



Commissioning of Elekta Unity MR-Linac and beam validation of Monaco Treatment planning System model: A single institution experience

Prospective/Objective: The purpose of this study was the commissioning of the Elekta unity MR-Linac installed at ASST Spedali Civili, Brescia and beam validation of Monaco treatment planning system model.

Materials and methods: Dosimetry measurements and Mechanical tests were performed on an MR-Linac using a different detectors. Dosimetry measurement consisted of comparison between measured and calculated PDDs and profiles, measuring beam quality, reference dosimetry and correlation between CT numbers Vs RED curve. Mechanical test included: MLC transmission, measurement of radiation isocentre diameter, Gantry angle accuracy and MR to MV Coincidence. Measurement devices included Semi flex 3D (PTW 31021), microdiamond (PTW 60019), and Farmer-type (PTW 30013) detectors in an Elekta PTW MP1 water phantom. PTW MP1 scanning water phantom was used to measure depth dose curves and profiles for various depths and for field sizes between 1 x 1 cm² and 57 x 22 cm² for an Elekta MR-linac beam with the perpendicular 1.5 T magnetic field. Gammex phantom was also used to correlate CT numbers Vs RED curve in the treatment planning system.

Results: Gantry angle accuracy was within $< 0.3^\circ$, the measured radiation isocentre was < 0.5 mm and the coincidence between MR and MV isocentre was $-0.14(x)$, $-0.61(y)$ and $-1.36(z)$ mm which is accounted for in the treatment planning system (TPS). The TPR_{20,10} was measured, as it is an adequate beam quality specifier for the MR-Linac beam. Gamma analysis is used to assess the agreement between calculation and measurement of dose distribution. Excellent agreements were obtained between calculated and measured dose distribution interims of percentage gamma passing rate criteria. The average gamma passing rate was 98% for profiles and 100% for PDD curves, considering 2% dose difference and 2mm distance to agreement as acceptance criteria. When we used 2 mm distance-to-agreement and 1% dose difference, the agreement between the TPS model and measured scan data showed a satisfactory level of agreement. 30.9% of profiles completely pass the chosen criteria, the analysis of remaining 69% of the profiles demonstrates that measurement error becomes a limiting factor in achieving a better score and 85.7% PDDs curves pass the chosen criteria.

Conclusion: As a result, Commissioning of Elekta Unity MR-Linac and beam validation of the Monaco treatment planning system model for the first time at AAST Spedali Civili of Brescia is suitable for clinical use.



Bruktawit Asnake Ewune

basnake34@gmail.com

Supervisor:
Dr.Barbara Ghedi

University Hospital of
Brescia, Italy

ASST DEGLI SPEDALI CIVILI
DI BRESCIA Italy





Implementation of quality assurance for a High Dose Rate brachytherapy system in the clinical environment

Prospective/Objective: This work focuses on the overall quality assurance of HDR brachytherapy system during: acceptance of the afterloader, source exchange and treatment, including HDR brachytherapy source strength determination and implementation of those quality assurance in the clinical environment.

Materials and methods: Safety quality control testing of HDR brachytherapy system were performed within and around the treatment room. Some selected frequency and tolerances of these safety and physical checks have been assessed. Five measurements were performed in order to ensure the accuracy of source dwell position by source position check ruler and the results were analyzed by imageJ software. To determine linearity of the timer, we collected charges on the electrometer at a fixed measurement position with varying dwell times, for 5, 10, 20, 40 and 80 seconds, the measurements were described graphically by plotting the reading versus dwell time graph. A sheet of Gafchromic film was used for assessment of the offset of some gynecological applicators. To determine the maximum sensitive point of the well-type ionization chamber, the source was moved from top of well chamber with a step size of 1 mm inside the source holder and a set of three measurements for each of the 21 selected dwell positions was taken. The reading (in nA) were tabulated and scattering contribution was assessed by placing the chamber in different scattering effect environment. Reference air kerma rate was determined by sending the source out to maximum sensitive position of the chamber and measurement value was compared with the expected value. During source exchange, a contamination test was also performed by wipe test. Finally, the relevant QA values are used within the treatment planning system.

Results: We found that the nominal and the measured source positions were accurately matched with a difference of less than 1 mm. Offset of applicators obtained in this work is the same with the values given by the vendor, with less than a half millimeter difference. Correlation between programmed times and acquired charges showed good linearity and the measurement was reproducible. The percentage of difference between reference air kerma rate measured with electrometer timer and machine timer is 0.1 % and 0.2 % which indicates the timer is accurate. Both measured values have 0.9% and 1.3% difference from the expected values, within 3% of tolerance in the determination of reference air kerma rate.

Conclusion: The results shows that the source is positioned accurately at expected dwell position. The offset for all the considered gynecological applicators matches the value given by the vendor, that is used in TPS. The timer has a good linearity and is also accurate. All other tests passed and were within acceptable tolerance levels. The performance of all these tests guarantees a proper and safe delivery of the radiation dose.

Geleta Desta Fekede

fekede_desta@yahoo.com

Supervisors:

Dr. Francesco Ziglio

Dr. Lino Nardin

Ospedale Santa Chiara di
Trento, Italy





Cristina Estefania

Ramirez Ramirez

cr.red7@gmail.com

Supervisors:

Dr. Carlo Alberto
Rodella

ASST Degli Spedali Civili di
Brescia, Italy

Sistema Socio Sanitario
 Regione
Lombardia
ASST Spedali Civili

Dosimetric Study of Fetal Dose during External Beam Radiotherapy using OSLD

Prospective/Objective: In the Nuclear Medicine department of the Spedali Civili di Brescia, therapy with Lutathera has been performed on 31 patients in the period between November 2019 and October 2022. Patients are released from hospital when their radiation exposure is below established radioprotection levels. The recommendations given to the patient are based on the principle that the radiation dose to people should be kept as low as reasonably achievable. The aim of this study is to evaluate if there is a correlation between the location of the different lesions of the patients and the exposure rate at 1 m.

Materials and methods: The recommended treatment regimen with Lutathera consists of four separate infusions of 7400 MBq each one. The Lutathera protocol requires SPECT-CT images taken at 24, 48 and 120 hours after the administration, always on the same gamma camera. The equipment used was Discovery 670 GE SPECT-CT system. The image correction is done using the algorithm IRACSC (iterative reconstruction attenuation and scatter correction and MIP (maximum intensity projection). For release the patient, dose rate measurements are taken at 1 m and 30 cm from the front of the mid-abdomen of the patients using a Geiger counter. Usually, when the average dose rate at 1 m is less than 5 $\mu\text{Sv/h}$, the patient is released from hospital. The internal dosimetry of OAR (organ at risk) and tumor lesions was performed with the MIRD (Medical Internal Radiation Dosimetry) average dose method, using the ImageJ, Pet-Ct Viewer and homemade plugins and the radiation dose assessment software OLINDA/EXM.

Results: It was found that there is a weak positive correlation between exposure rate at 1 m and anatomical localization of lesion when lesions are in the abdomen, a moderate positive correlation for lesions in the pelvis and a strong positive correlation with lesions present in the other regions (head, arms, and legs). While there is no correlation with the lesions located in thorax and column. Regarding the patient's response to therapy, according to the RECIST criteria, 88.89% of the patients present a stable disease, while 11.11% of the patients have a partial response. The average volume diminution of the lesions 17%. The mean dose to lesions was 89.25 Gy (min = 0.42 Gy, max = 905.56 Gy) and the mean dose to kidney was 3.62 Gy (min = 1.30 Gy, max = 4.73 Gy).

Conclusion: RPT with Lutathera results as a valid therapy, with a stable disease response to the therapy which is favorable for patients with an advanced state of cancer. On the other side, the anatomical localization of the lesions is not correlated with the exposure rate measured using external radiation detector.



**Valerie Argentina
Dominguez Rivera**

valerie1dominguez@gmail.com

Supervisor:
Dr. Gian Luca Poli

ASST Papa Giovanni XXIII
Hospital, Bergamo, Italy



Multicentre intercomparison of semi-quantification in neuro-imaging

Prospective/Objective: Brain imaging with DaTSCAN (Ioflupane I-123) is used to detect loss of functional dopaminergic neuron terminals in the striatum of patients with clinically uncertain parkinsonian syndromes. The uptake of this striatum is semi-quantitatively evaluated with VOI techniques. In this work, a standardization procedure of the acquisition and processing of DaTSCAN imaging between the different centers member of the Italian Neuroscience and Rehabilitation Network (Rete Italiana delle Neuroscienze edella Riabilitazione, RIN) was performed.

Materials and methods: The free software BasGanv2 was employed to assess the specific binding ratio (SBR) in the striatal sub-structures: caudate nucleus and putamen. This parameter was used to compute the recovery coefficient (RC), defined as the ratio of the true and the measured SBRs. Data were collected from 9 centers: 3 of them with SIEMENS and 6 with GE SPECT systems. In each center, images of a Striatal Phantom (with 4 different striatal to background ratios) were acquired following standard protocols. Two methods of tomographic reconstructions were studied: Filtered Back-Projection (FBP) and Ordered-Subsets Expectation-Maximization (OSEM). Analysis on the application of attenuation correction (AC) with the use of LEHR collimators was also performed with the acquisition of images of a cylindrical phantom.

Results: Differences in the processing software of these two vendors (SIEMENS and GE) were found. An optimization of the reconstruction parameters was performed for both systems: FBP with Butterworth filter with 0.45 Nyquist and order 10 for SIEMENS and its equivalent 0.68 cycles/cm and power 20 for GE; OSEM with 10 iterations and 10 sub-sets, using a Gaussian filter of 5 mm for SIEMENS and 1.42 pixel for GE. For both methods, attenuation correction and scatter correction were not applied. The results showed that, when using OSEM reconstruction, the RCs obtained for the SIEMENS SPECT systems are slightly higher than those obtained with the GE SPECT systems. When using FBP, the BasGanv2 software showed limitations in the image processing. Therefore, further investigations have to be carried out.

Conclusion: The presented standardization procedure was demonstrated to obtain comparable results between these RIN centers. o obtain comparable results between these RIN centers.



Geometric accuracy comparison between three different C-arm LINAC for Radiotherapy



Guram Shengelia

evillega@ictp.it

Supervisors:

Dr. Carlo Cavedon
Dr. Alessio Pierelli
Dr. Paolo Maria
Polloniato

Azienda Ospedaliera
Universitaria Integrata
Veneto, Italy



Prospective/Objective: Radiation therapy requires clinical linear accelerators to be mechanically and dosimetrically calibrated to a high standard. One important quality assurance test is the Winston-Lutz test which localizes the radiation isocentre of the linac. The delivery accuracy of highly conformal dose distributions generated using IMRT is strictly related to geometry accuracy of collimator, gantry, and that have many degrees of freedom is directly affected by the quality of the alignment between the radiation beam and the mechanical axes of a linear accelerator. For this purpose, quality control (QC) guidelines recommend a tolerance of ± 1 mm for the coincidence of the radiation and mechanical isocenters. Traditional QC methods for assessment of radiation and mechanical axes alignment (based on pointer alignment) are time consuming and complex tasks that provide limited accuracy. The purpose of this work is to evaluate and compare geometric accuracy for three different C-arm LINAC, analyzing the results of the Winston-Lutz test performed for each accelerator and also checking and comparing the isocenter accuracy of integrated imaging system.

Materials and methods: Study included two parts: one related to isocenter accuracy of integrated imaging systems (OBI and EPID: On Board Imaging System and External Portal Imaging System), and one related to radiation isocenter accuracy (Winston-Lutz test); both these parts are phantom based evaluation accomplished analyzing images realized in many different geometric conditions; for isocenter accuracy of integrated imaging systems, the Varian Marker Block Phantom, a plastic phantom has been used, this phantom contains one fiducial marker at the center and four other markers at known locations; for the Winston-Lutz test, the BrainLab Frameless SRS QA target pointer has been used. Both phantoms have been placed at LINACs isocenter according to the field light crosshair projections. Measurements were performed on three Varian machines: True Beam, DHX and C600 (in the last one there is only one imaging system: EPID). The images acquired were analyzed with the image-j free software or directly with the off-line review viewer included within the Treatment Planning System (TPS) in use (Aria/Eclipse vr-15.6 from Varian Medical System).

Results: We compare the mechanical performance between the LINACs and according with the international recommendation mostly from AAPM Reports 142 and 198, other than vendor specifications and tolerance, considering basic and stereotactic requirements, Obtained results were in the acceptable basic tolerance (2 mm) except for the oldest C600, currently used only for few palliative treatments a day; the newest True Beam LINAC showed the best mechanical performance according to both basic and stereotactic requirement (1 mm) and is currently used for this kind of treatment; the remaining DHX satisfied basic requirements but not strictly the stereotactic one, and is used mainly for standard fractionation treatments.

Conclusion: We have proposed an end-to-end IGRT test that accurately and rapidly meets the requirements of TG-142 and follows the workflow of clinical IGRT practice, analyzing separately imaging system and radiation isocenter accuracy. We propose these procedures like practical test with a recommendation to introduce this kind of quality evaluation especially for LINACs used for stereotactic treatments.



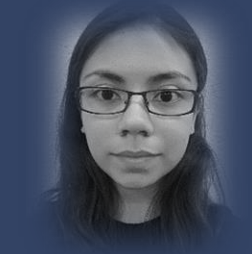
Commissioning of in vivo dosimetry using an Electronic Portal Imaging Device

Prospective/Objective: To leverage the verification system in radiation therapy by implementing in vivo dosimetry measurements using an EPID to prospectively analyze the transit images generated during treatment and estimate the dose delivered using point backprojection.

Materials and methods: An amorphous Silicon (a-Si) electronic portal imaging device (EPID) iViewGT was used for the commissioning of EPID in vivo dosimetry (EIVD). The dose is reconstructed using backprojection of the EPID signal. The signal collected by the EPID from the radiation passing through the patient (transit condition) is converted into an image, which is corrected for noise and non-homogeneous gains in the EPID's pixels. The dose is reconstructed using the point backprojection formalism: using conversion factors of EPID signal to absolute dose at EPID level, the dose for non transit conditions at EPID level is then calculated with finite tissue maximum ratios (FTMR), the maximum dose at SAD level is further calculated by using the inverse squared distance relationship, and finally, the dose at the point of interest is calculated using TMR factors. The conversion factors and FTMR factors were acquired by a combination of EPID and chamber measurements in non-transit conditions and in transit conditions, for various field sizes and phantom's thickness. The dose is calculated at a point in the planning tomography provided by the TPS, in this case Monaco's 6.0

Results: A model for dose reconstruction from EPID images of 6 MV photons was built, which is capable of calculating the dose to the isocenter of an homogeneous phantom with an accuracy under 0.55% for open fields. The dose reconstruction was evaluated along the central axis in a clinical relevant range of (3 - 20) cm, and found to be under a 2.5% of relative deviation from the dose calculated using. Additionally, the dose outside the central axis was assessed, in a radius of 9 cm and in a radius of 6 cm; the dose reconstruction relative deviation was under 5.8% and 2.84% respectively. The RMSE was evaluated for all off-axis measurements, with a maximum value of 6.62 for a dose range of (61-480), measured at different depths.

Conclusion: EIVD commissioning process and daily set-up is rather simple and little time consuming, furthermore, it provides an efficient and accurate assessment that can be implemented in the routinely practice to detect errors that otherwise would not be detected by pre-treatment quality assurance verifications.



Anayansi K. Ramirez

akrp.fisica@gmail.com

Supervisors:

Dr. Ziglio, Francesco

Dr. Menegotti Loris

Ospedale Santa Chiara di
Trento, Italy





Clinical validation of an automatic image segmentation system based on deep learning for its integration in the head and neck radiotherapy workflow

Prospective/Objective: Image segmentation of organs at risk (OAR) is a focal point of the radiotherapy planning (RT) workflow with implications on the overall quality of the radiotherapy process, including plan optimization/evaluation and dose delivery. Up to now, contouring requires large amount of human resources because it relies mainly on manual delineations which is time expensive and operator-dependent. Inter-intra-operator variability, lack of standardization are common issues of manual contouring. Automatic tools have the potential to address these flaws improving the efficiency of the procedure. The study aim was to validate the Raystation automatic image segmentation module based on Deep Learning (DL) via 3D-Convolutional Neural Network and U-Net architecture. The head and neck anatomical site (HN) was chosen for the purpose of validation with the following endpoints: a) to assess the quality of the automatic image segmentation through comparison with manual segmented ROIs from clinically delivered plans; b) to investigate the impact of the geometric uncertainties, originated from the mismatch between the automatic and manual contoured ROIs, on the overall plan quality in terms of target dose coverage and OARs

Materials and methods: CT planning datasets, including RT plans and RT structures, from a cohort of 24 HN patients, treated from 2018 until 2022 at the University Hospital of Novara, have been used. A total number of 496 manual segmented ROIs were available to generate the ground truth scenario used for the purpose of the DL auto-segmentation validation. The contours generated by the DL tool were compared to the reference ones by means of overlap metrics, the Dice Similarity Index (DSC), and distance metrics including Hausdorff Distance (HD), the 95th percentile of Hausdorff Distance (HD95) and Average Hausdorff Distance (AHD). The impact of OAR segmentation errors on dose distribution has been investigated evaluating the difference of the dose delivered to the targets and manually contoured OARs reoptimizing the original plan with the automatic contoured ROIs. Target coverage, maximum and mean dose differences have been computed for each structure. Linear generalized methods, logistic regression and ROC curves have been used to evaluate the relationship between the contour disagreement measured by AHD metrics and the dose increments to OARs.

Results: Good agreement was achieved for the majority of the segmented ROIs with DSC values higher than 0.75 and AHD comparable with the image voxel size (1x1x2 mm³). Moreover, our findings were in line with the literature benchmarks obtained from auto-segmentation challenges. HD95 highlighted significant discrepancies at the extremities of tubular organs due to low contrast images and failures depending from artifacts. AHD values > 2.5 mm were related to mean overdosages to OARs > 2.5 Gy. Target coverage was independent from the segmentation agreement.

Conclusion: The DL-based auto-segmentation was validated in the HN site: The agreement with the gold standard was within inter-operator variability. AHD was a valuable prognostic factor for plan dose distribution degradation originated by segmentation errors.

Muratbekova Ademi

amratbe@ictp.com

Supervisor:

Dr. Gianfranco Loi

Az. Ospedaliero
Universitaria Maggiore
della Carità di Novara, Italy



Azienda ospedaliero-universitaria
"Maggiore della Carità"
NOVARA



Garoson Albertine

Rasoatsaratanany

[raberygaroson@](mailto:raberygaroson@gmail.com)

[gmail.com](mailto:raberygaroson@gmail.com)

Supervisor:

Dr. Lidia Strigari

Az. Ospedaliero –
Universitaria S. Orsola
Bologna, Italy



Commissioning of modern Treatment Planning System (TPS) for nuclear medicine therapy using standardized virtual phantoms

Prospective/Objective: TPSs have been recently introduced to personalize the internal radiation therapy, unfortunately, there are no harmonization or guidelines on commissioning these tools. The aim of this study is to assess the discrepancies among three TPSs developed for radioembolization with ^{90}Y in terms of volumes of interest (VOIs) and dose metrics, i.e., mean absorbed dose and Dose Volume Histograms (DVHs).

Materials and methods: We used five (i.e., two experimental and three virtual) phantoms imported within three TPSs (Dosisoft, MIM, and Simplicity) used for ^{90}Y dosimetry. The experimental phantoms were acquired with SPECT/CT D670NM/CT (GE) and filled with $^{99\text{m}}\text{Tc}$ -pertechnetate. The virtual phantoms assuming to be filled with ^{90}Y were generated by MATLAB script and saved into DICOM format. NEMA homogeneous and kernel phantoms contained the following VOIs: body, body-1cm, target-2cm and target-1cm. The anthropomorphic phantom included the whole body, liver, and hot and cold spheres. Each TPS extracted the volumes of VOIs in ml. Three methods were used for voxel-based dosimetry calculations within the TPSs: the local deposition method (LDM), the LDM with scaling for known injected activity (LDMwS), and the dose kernel convolution (DKC) method. Simplicity used only the LDM approach, while MIM used the LDMwS one. LDM and DKC were applied to the Dosisoft software. The calculated volumes and dose metrics were exported using the TPSs or manually in a few cases. All the Bland-Altman plots and statistical results were calculated using RStudio software.

Results: There were no differences in volumes of VOIs for kernel and homogeneous virtual phantoms when evaluated within the same TPS. Differences up to 5% between homogeneous virtual phantom and experimental one and trivial differences between anthropomorphic virtual and experimental one were found. The difference of the mean absorbed dose for Kernel Phantom obtained from different TPSs for the same VOI was up to 50%, while the absorbed dose range varied between 0 Gy to 75000 Gy. The range of the mean absorbed dose for homogenous phantom was between 3 to 5.1 Gy. Concerning the two anthropomorphic phantoms, the dose difference was up to 10 times for the cold sphere, where the absorbed dose range of virtual phantom was shifted 100 Gy higher than the experimental one. The DVHs were different for homogeneous and anthropomorphic (virtual and experimental) phantoms due to the image noise and likely the low resolution of the experimental images. Besides the kernel phantoms, the DVH was generated, assuming that the administered activity was located inside a voxel. The Bland-Altman plots showed discrepancies for each VOI volume up to 25% and 10% for homogeneous and anthropomorphic phantom, respectively. In addition, the Bland-Altman plots comparing the mean absorbed doses of VOIs showed discrepancies up to 20% for the virtual phantoms and up to 10% for the experimental phantoms.

Conclusion: Significant discrepancies in calculated absorbed mean doses were found using the investigated TPSs. Further investigations are recommended using other radionuclides and TPSs.



Pratiksha Shahi

prati.mshahi@gmail.com

Supervisors:

Dr. Carlo Cavedon
Dr. Alessio Pierelli
Dr. Paolo Maria
Polloniato

Azienda Ospedaliera
Universitaria Integrata
Verona, Italy



Evaluating the effect on Hounsfield Units reproducibility with different algorithms in a dedicated radiation therapy CT scanner and its effect in detectability and dose.

Prospective/Objective: In a CT scan, Hounsfield Unit is proportional to the degree of x-ray attenuation and is allocated to each pixel to show the image representing the tissue's density. Currently, CT scanners provide several reconstruction algorithms to address specific issues during CT imaging. We aimed to assess the change of computerized tomography attenuation (Hounsfield unit-HU) for different materials of known electron density within a wide range, using these available post-processing algorithms. We considered different iterative algorithms for Metal Artifact Reduction (iMAR), used to reduce the metal artifact effect, and Direct Density algorithms used to perform the easy dose calculation from the HU values at one artificial-kV instead of many different original kV values. These algorithms are provided by the manufacturer at the installed Siemens Dual Energy Syngo CT.

Materials and methods: In this prospective study, the Gammex 467 phantom consists of a 33 cm diameter Solid Water disk approximating the size of an average pelvis (330 mm × 50mm ×H). The phantom was equipped with different tissue surrogate inserts and three different metal inserts of Aluminum, Titanium, and Steel. Image analysis was performed using Image J. Mean CT numbers and the standard deviation of the inserts were measured within the regions of interest (ROIs) in the inserts. The dose calculation was carried out in the Varian Treatment Planning System within the box plan with a cube digital phantom sized (20x20x20) and each field size 10x10.

Results: This study shows that for different iMAR algorithms (8 algorithms specific for 8 clinical situations metal implants), the HU variations have the same trend toward the electron density of different human tissue surrogates, but the amount of these differences is changing over the metal inserts used: in detail, it appears that the iMAR algorithms introduce an underestimation of the HU for low electron densities materials while an overestimation for high densities and also that these variations are more significant, in terms of CNR, as the density of the metal, that produces the artifact, is higher. In the scan without metal inserts, the iMAR algorithms don't bring any significant difference which instead is highlighted with the metal inserts, showing that the amount of HU change is dependent on the strength of these inserts. For the study of the Direct Density algorithm the calculated dose difference using the artificial 120 kV compared to the actual 120 kV scan, is almost negligible for soft tissue but for tissue with a higher density, like bone, there is a difference within 3%

Conclusion: Thus, from this study we concluded that although the algorithms described are of undoubted utility, their effect can lead to differences in the "output" which can produce errors, to be considered especially in processes based on an automated quantitative image evaluation or dose calculation based on tissue characterization.



**Monika Ndeshipanda
Ndahafa Sakaria**

ndakolomonika@gmail.com

Supervisor:
Dr. Lidia Strigari

Az. Ospedaliero –
Universitaria S. Orsola
Bologna, Italy



A systematic approach to identify the optimal input parameters of Personalized Planning.

Prospective/Objective: The main objective of the work is to evaluate the impact of different parameters in the new Pinnacle Evolution (version 16.4.3) by comparing it with their respective clinically accepted reference treatment plans. The plans were assessed according to the dosimetric parameters and monitor units.

Materials and methods: Two different clinical cases, i.e., prostate and head & neck, were treated with volumetric modulated arc therapy. Thirty-three plans were optimized for each clinical case: the clinically accepted reference plans were generated using specific plan parameters derived based on feasibility dose-volume histogram (FDVH) in PlanIQ. For each case, a reference plan was saved as a treatment technique, and before optimization, a single plan parameter was changed to determine its effect on the dose distribution and on the monitor unit amount. The plans were assessed according to the monitor units, dose metrics (i.e., dose volume criteria & DVHs) of both organs at risk (OARs) and Planning Target Volumes (PTVs). The evaluated OARs were the rectum and bladder for the prostate plan and the right parotid, lips and spinal cord for the head and neck plan.

Results: The conversion cycle adjusted to “10” and refinement cycles to “2” and “3” have produced a better plan quality with target coverage met and OARs sparing. Adjusting control MLC modulation to “Yes” spares OARs. Modulation amount parameter adjusted to “very high”, results in fewer monitor units (i.e., 681.2, 709, 743.9, and 699.5, MU for very high, high, medium, and low, respectively). “SRS/SBRT mode”, was effective for head and neck with both OARs sparing and target coverage met. For prostate, only the rectum and bladder mean dose was reduced with “standard fraction mode” compared to “SRS/SBRT mode”. Match target coverage adjusted to “No” showed a significant dose increase for targets and OARs mean dose and dose-volume criteria of both cases. For head and neck “weighting balance” parameter adjusted to “20” produced a better plan with OARs sparing and fewer monitor units (708.9 MUs compared 681.2 MUs). For prostate, weighting balance adjusted to “-20” produced a better plan with target coverage met and fewer monitor units of 977.2 MUs. For prostate target transition falloff rate adjusted to “30” or “40” have produced a better plan with fewer monitor units of 997.2 and 977.6 MUs, respectively. For head and neck target transition set to “40” spared right parotid and with fewer monitor units of 681.2 MUs. Target edge weight adjusted to “2” demonstrated to be the best choice for prostate and head and neck for OARs sparing.

Conclusion: The results indicate that parameter selection in Personalized Planning plays a vital role in improving the quality of treatment plans. It is concluded from the results that the dose variations with the change of input parameters are significant. The impact is greatest on the rectum, and right parotid mean dose of prostate and head & neck, respectively.



**Jean Baptiste
Gahimano**

gahima1234@gmail.com

Supervisor:

Dr. Gutierrez Maria
Victoria
Dr. Gabriele Guidi,

University Hospital of
Modena, Italy



Implementation of Code of Practice for Quality Assurance Program in High Dose Rate Brachytherapy with Ir-192 source

Prospective/Objective: To develop and implement the code of practice for Quality Assurance (QA) program in Brachytherapy (BT) with Ir-192 source. Because of the existence of variable BT equipment, AAPM TG-56 recommended each clinic to develop a dedicated QA program that suites its brachytherapy machine. In this thesis work, the code of practice for QA was written and implemented at Modena University Hospital aiming to assure accurate operation of BT equipment with a major focus on security controls, geometrical and dosimetical measurements and to verify safety conditions for radiation protection purposes as required by national regulations. Multichannel applicators were commissioned to establish its baseline operating performance.

Materials and methods: Following the guidelines (IAEA TECDOC-1274, AAPM TG56, and GEC-ESTRO booklet-8), the code of practice for QA in BT was developed for microSelectron HDR-V3 unit and OnCentra treatment plan system (TPS). Transfer tubes, well type chamber, electrometer, Gafchromic films, check ruler, set of applicators and film scanner were used for source calibration and for commissioning of Multichannel applicator. For radiation protection purposes, a calibrated Automess (6150 Ad-B) was employed to verify the existing shielding and to check the leakage radiation. An end-to-end test was performed by using Gafchromic films that were placed within Multichannel applicator in a solid PMMA water equivalent phantom. By means of 2D-gamma analysis, films dose maps were compared to RTDoses from the OnCentra TPS after being loaded into PTW-Verisoft software.

Results: The results from the source calibration showed optimal agreement between the measured air kerma rate (source strength) and the value of source certificate with a difference of 1.82% and the measured source positions were within ± 0.2 mm on average from the expected positions. The radiation protection results were in agreement with recommended limits, and the highest annual equivalence dose rate evaluated was 0.154 mSv/year in controlled areas. Results of first source positions for all Multichannel transfer tubes and needles evaluated were in agreement with respect to declared values, with a maximum difference of ± 0.5 mm. Gamma passing rate calculated between film and RTDose maps was 100% for the intrauterine VT and was 91.8% for needle-10, with 3%/3mm criteria.

Conclusion: Results showed that the status of the machine and its components ensured an acceptable clinical outcome. The deviation in source activity was less than the recommended tolerance limit 5%, uncertainties in source positions are less than 1mm and agreed with the GEC ESTRO (2004) recommendations. The walls bunker shielding were still suitable according to national regulations. The end-to-end results guarantee the correct dose delivery to patient.



Samuel Bugingo

busamu3@gmail.com

Supervisor:

Dr. Maria Rosa Fornasier

University Hospital of Trieste, Italy



Impact of data-driven respiratory gating algorithm on small lesions in PET/CT imaging.

Prospective/Objective: Respiratory motion induces artifacts in PET/CT imaging that may introduce significant image distortion, and an important cause of diagnostic uncertainty, particularly for lesions located in the lung/diaphragm interface. Our primary objective was to assess the effects of a data-driven respiratory gating (DDG) algorithm on lesion maximum standardized uptake value (SUVmax) and volume for small lesions with low and moderately low target-to-background ratios.

Materials and methods: We used the QUASARTM Programmable Respiratory Motion Phantom, which is designed to move cylindrical inserts in the superior-inferior direction within a torso shaped acrylic oval varying both speed and amplitudes. We have built an insert compatible with Quasar phantom motion platform that allows the simulation of the background. The insert was filled with water to simulate the liver density ($\sim 1.07 \text{ g/cm}^3$) and with water and polystyrene beads to mimic lung density ($\sim 0.3 \text{ g/cm}^3$). We placed inside the insert a glass sphere with 13 mm inner diameter to represent a small tumor. Both insert and sphere were filled with ^{18}F -FDG solutions of different concentrations to attain different target-to-background ratios. For the acquisitions, we used the Whole Body PET/CT protocol that includes the Q.Static acquisition mode, in which an automated motion correction technique is integrated. DDG-PET data were derived from a portion of the total PET data ($\sim 50\%$) in the end-expiration (EE) phase at 30% offset from the end-inspiration (EI) phase of each respiratory cycle. We investigated effects of data-driven respiratory gating algorithm on lesion maximum standardized uptake value (SUVmax) and volume by comparing DDG-PET images and non-gated PET images, both reconstructed with two available algorithms: VUE Point FX (VP) and Q.Clear (QC).

Results: For the 3:1 target-to-background ratio (TBR), the motion correction with DDG PET increased the lesion SUVmax by the average of $25 \pm 13\%$ for VP and $26 \pm 17\%$ for QC. The lesion volume decreased by $35 \pm 15\%$ for VP and $31 \pm 36\%$ for QC. For 3:1 TBR lung case, the motion correction with DDG PET increased the lesion SUVmax by the average of $26 \pm 10\%$ for VP and $27 \pm 17\%$ for QC. The lesion volume decreased by $31 \pm 40\%$ for VP and $27 \pm 32\%$ for QC. In these cases, the average was done over 4, 6, 8 and 10 mm motion amplitudes. For the 4:1 TBR, the motion correction with DDG-PET increased the lesion SUVmax by the average of $28 \pm 12\%$ for VP and $33 \pm 12\%$ for QC. The lesion volume decreased by $39 \pm 13\%$ for VP and $39 \pm 10\%$ for QC. In this case the average was done over 4, 6, 8, 10, 12 and 15 mm motion amplitudes.

Conclusion: Application of DDG was found to significantly increase the lesion SUVmax and decrease its volume with respect to non-gated images, by mitigating the blurring effects of respiratory motion, and to give more accurate representations of uptake as well.

Image quantification and analysis of SPECT DaTscanTM examinations of patients with suspected Parkinson's disease through two 3-D automatic tools

Prospective/Objective: This work reports a head-to-head comparison on the quantification of two software, BasGanV2 and Datquant[®], of DaTscanTM radio-tracer uptake in brain striatum regions through the correlation between quantification metrics, and the decision of these metrics towards isolating patients with Parkinson's disease (PD) from the sample with visual reading by the physician (the gold standard, GS). The metrics include specific binding ratio (SBR), putamen-to-caudate ratio (PCR), caudate-to-putamen ratio (CPR) and asymmetry indices (AI).

Materials and methods: The study analyzed 112 patients who underwent brain DAT (Dopamine active Transporter) SPECT imaging with DaTscanTM for a suspected parkinsonism. The post-processing of brain DAT images was performed using the two software for quantification purpose. The Bland-Altman analysis was used to reveal the mean bias between the two methods, while for instance the areas under ROC (receiver operating characteristic) curves (AUCs) of SBR values were utilized to measure the diagnostic accuracy of the metrics.

Results: The study found a significant correlation between the two software for each semi-quantification parameter. The correlation coefficients, r , ranges from 0.684 to 0.962. Among others, a strong correlation was observed for SBR values with, $r = 0.962, 0.9477, 0.9474, 0.946$, respectively, for left putamen, left caudate, right caudate and right putamen SBRs. Furthermore, with BasGanV2 quantification, out of 112 patients, 74 (66.07 %) had PD and 38 (33.93 %) were normal, while with Datquant[®], 68 patients (60.7 %) were positive to PD and 44 (39.3 %) were healthy patients. The GS confirmed PD in 64 patients (57.14 %) and 48 patients (42.86 %) were found normal. The PD diagnostic agreements between BasGanV2 and Datquant[®] software and doctor's decision, were, respectively, 85.71 % and 83.92 %. In addition, AUCs showed that the two tools offer a PD diagnosis to about 95.20-99.99 %.

Conclusion: All semi-quantitative metrics showed a significant correlation between Datquant[®] and BasGanV2 and higher values of AUCs support the accurate PD diagnosis with these tools. Along with this, the mean bias observed between the two methods, hints out that none of them is preferred over the other.

Uwitonze Emmanuel

Uwitonze_emmanuel@yahoo.com

Supervisor:

Dr. Gutierrez Maria Victoria

Dr. Gabriele Guidi,

Azienda Ospedaliero-
Universitaria di Modena,
Italy

SERVIZIO SANITARIO REGIONALE
EMILIA-ROMAGNA
Azienda Ospedaliero - Universitaria di Modena



Dosimetric commissioning of VMAT treatment on a Linac after a major MLC upgrade



Kajol Sahibdin

kajol.sahibdin95@gmail.com

Supervisor:

Dr. Angelo F. Monti

ASST Grande Ospedale
Metropolitano Niguarda,
Milano, Italy



Prospective/Objective: The complex dose distributions of the VMAT technique increase the importance of accurate beam data measurements and review in the commissioning process. In this work, a Synergy linac, containing a beam modulator MLC collimator gets upgraded with an Agility MLC. The aim of the present study is focused on the dosimetric commissioning and validation of the updated linac for 6MV photon beams and VMAT treatments as well as describing general concepts, regarding beam modeling in the TPS and dose verification before clinical use.

Materials and methods: For the dosimetric measurements of acquiring beam data of a Monte Carlo based TPS, "Monaco", a watertank was used, which can measure the dose distribution in all directions to obtain PDDs and profiles accurately, with the advantage that water mimics the radiation properties of human tissue. Beam modeling was done with special test beams, analyzing different parameters of the MLC's that can be optimized inside the TPS. These test beams were measured on a cylindrical phantom, a Delta4 WiFi, offering the analysis of 3D dose distributions. VMAT plans were calculated and optimized following the AAPM TG119 for dose prescriptions, planning objectives and dose verification. AAPM TG119 report presents guidelines from a dosimetric study, to facilitate and ensure the accuracy after commissioning processes for modulated techniques, proposing mock test plans with dedicated phantoms. An on board Epid and two cylindrical phantoms; the Delta4- and Matrix phantom were used for comparison of 2D/3D dose distributions, the Matrix was used for 1D single point absolute dose verification. The comparison of measured and calculated dose was done by using a global gamma criteria of 3%/3mm as well as 2%/2mm (10% cut of). Confidence limits (CL) were generated and compared with the TG119. Lastly, 20 clinical plans were irradiated with the updated linac, using the Delta4 and Epid for comparison of dose distributions. The interchanging between this linac and two other linacs with the same dosimetry was also tested.

Results: Measurements for verification of the TPS dosimetric model received from the manufacturer concluded that it was necessary to modify the Leaf Groove Width from 0 to 1mm, to obtain an acceptable match between calculated and measured dose distribution. The overall passing rate for the TG119 mock plans, using the 3%/3mm gamma criteria for the Delta4 and Epid were $99.8\% \pm 0.12$ (CL 0.47) and $97.4\% \pm 0.24$ (CL 3.1), respectively, and with the 2%/2mm gamma, they were $97.5\% \pm 1.3$ and $95.6\% \pm 0.49$. While measuring the 20 clinical plans with the Delta4 and Epid, at the reference QA criterion of 3%/3mm, the gamma passing rates were all above 97.7% and 94.7%, respectively. When the tolerances became stricter with 2%/2mm, the gamma passing rates were all above 90 % for the Delta4 and 85.1% for the Epid, which is still considered acceptable. The absolute dose measurements with the Matrix resulted in a mean difference of 1.3% with a standard deviation of 1.23. The interchanging between linacs showed differences in gamma passing rates $\leq 0.3\%$.

Conclusion: TG119 methodology and recommendations have successfully been used to evaluate commissioning accuracy of VMAT plans and the obtained data were found within the limits of TG119. After completing all the measurements described in this work and being satisfied with the results, this upgraded linac was ready to be used clinically.

Dosimetric Comparison of 3-Dimensional Conformal Radio-Therapy (3D-CRT), Volumetric Modulated Arc Therapy (VMAT), and Hybrid Volumetric Modulated Arc Therapy (H-VMAT) Techniques for Left Breast Cancer

Prospective/Objective: The aim of this study was to evaluate 3D-CRT, VMAT and Hybrid Volumetric Modulated Arc Therapy (H-VMAT) techniques for left breast cancer treatments. Dose homogeneity and conformity of the Planning Target Volume (PTV) and organs at risk (OAR) sparing were evaluated, as well as the plan's robustness against rigid patient shifts. The study was conducted in Azienda Ospedaliero Universitaria delle Marche (Ancona, Italy).

Materials and methods: We considered patients who underwent left-breast after-surgery radiation therapy with a dose of 40.05 Gy in 15 fractions prescribed to the whole breast, with no boost to the surgical bed. Seven patients treated with 3D-CRT plans were selected with the following criteria: $D2\% < 107\%$ and $D98\% > 90\%$ for PTV, $V16Gy < 20\%$ for left lung, $V8Gy < 20\%$ for heart and $Dmean < 20Gy$ for the Left Anterior Descending artery (LAD). Concurrent VMAT plans (Eclipse RapidArc®) were optimized imposing OARs constraints equal to the 3D outcomes. We used three different treatment techniques, Two tangential opposing open fields were used for 3D-CRT with field in field, three half arcs were used for VMAT, and for the H-VMAT (H-VMAT1a and H-VMAT2a), two tangential opposing open fields were used for the 3D-CRT part 80% of prescription, and one and two half arcs were used for the VMAT part with 20% of prescription. This should be finished for future clinical implementation of Breast cancer treatment. Moreover, only setup uncertainties in the ± 5 LL direction were included for evaluating the plan's robustness.

Results: Homogeneity Index (HI) mean value for H-VMAT 2a (0.07 ± 0.01) was improved respect to H-VMAT 1a (0.10 ± 0.02), VMAT (0.10 ± 0.02) and 3D-CRT (0.12 ± 0.01) with a p-value $p < 0.03$ among all techniques. No statistical difference was found between H-VMAT 1a and VMAT ($p = 0.8$). As expected, VMAT provided the highest conformity to target, with a Conformal Number (CN) mean value of 0.89 ± 0.01 for the isodose 95%. Conformity for both H-VMAT solutions was characterized by a mean value of 0.86 ± 0.04 , which was very close to VMAT outcome. No statistical difference was found between H-VMAT with one and two arcs ($p = 0.8$). CN of 3D-CRT was 0.75 ± 0.04 . Left Lung V16Gy for VMAT ($10.1 \pm 4.1\%$), H-VMAT 1a ($12.3 \pm 5.7\%$) and H-VMAT 2a ($12.0 \pm 5.7\%$) showed a negligible difference with 3D-CRT outcome ($0.09 < p < 0.22$). In the low dose region of the DVH, a decrease of the irradiated volume V4Gy was observed for H-VMAT 1a ($34.9 \pm 5.9\%$) and H-VMAT 2a ($33.4 \pm 5.2\%$) respect to VMAT ($39.7 \pm 7.0\%$). Contralateral lung and breast received an evident dosimetric advantage with the use of Hybrid techniques respect to VMAT plans. We found a mean dose value of 298 ± 22 , 49 ± 13 and 87 ± 13 cGy for right lung and 358 ± 35 , 80 ± 25 and 143 ± 23 cGy for right breast, using VMAT, HVMAT 1a and HVMAT 2a, respectively. Right lung low dose bath was characterised with V5Gy values never exceeding 1.2% for all H-VMAT plans, against a mean value of $16.2 \pm 5.2\%$ for VMAT. Compared to 3D-CRT dosimetry, H-VMAT outcomes for contralateral lung and breast should be a negligible source of clinical concern, especially if one arc is used. Mean dose value of heart in 3D-CRT technique was (124.93 ± 34.25 cGy), in VMAT technique (292.89 ± 55.58 cGy), H-VMAT 1a (185.14 ± 48.60 cGy) and H-VMAT 2a (182.99 ± 45.28 cGy) techniques. No statistical difference was found between H-VMAT 1a and H-VMAT 2a ($p = 0.7$). LAD mean dose did not show an appreciable difference among all techniques, with an overall mean value of 540 ± 328 cGy. In order to evaluate robustness against setup errors, a shift of ± 5 mm (IEC1217) in Latero-



**Bekzodbek
Abdurayimov
Jamolidin Ugli**

bekzod923113@gmail.com

**Supervisors:
Dr. Marco Parisotto**

Lateral direction was applied to isocenter. The CTV volumes covered by near minimum and near maximum dose, D98% and D2% respectively, were used for dosimetric evaluation. D2% and D98% values did not change significantly for shifted plans among all techniques ($0.33 < p < 0.64$).

Conclusion: Basing on our patient selection, we demonstrated that H-VMAT technique was a good trade-off between “pure” VMAT and 3D-CRT plans for left breast treatment. HVMAT provided good homogeneity and conformity to target while preserving heart, contralateral breast and lung. Furthermore, it had a limited impact on planning activity since it did not required any “skin flash” management to ensure robustness against moderate patient shifts.

AZIENDA OSPEDALIERO
UNIVERSITARIA delle
MARCHE, Ancona, Italy



MMP graduates

9th Cycle- 2021-2023



The Master is supported and sponsored by:



International Atomic Energy Agency



International Organization for Medical Physics



European Federation of Organisations for Medical Physics



IPEM Institute of Physics and Engineering in Medicine

Institute of Physics and Engineering in Medicine



Italian Association of Medical Physics



University Hospital of Trieste

Abstract booklet

Abstract booklet	#6 (9 th cycles)
Year	2023

Editorial team

- Renata Longo,**
University of Trieste, Italy
- Renato Padovani,**
International Centre for Theoretical Physics (ICTP), Trieste, Italy
- Hossein Aslian,**
Olivia Newton-John Cancer Wellness & Research Centre (ONJ), Melbourne, Australia




Joel Eduardo Epile.
jepile@ictp.it

Supervisor:
 Dr. Edoardo Mastella

Azienda Ospedaliero-
 Universitaria di Ferrara,
 Italy



SBRT for localized prostate cancer using single arc VMAT: plan quality, complexity, dose delivery accuracy, and efficiency

Prospective/Objective: Plan quality, complexity, dose delivery accuracy and efficiency were compared for low- and intermediate-risk prostate stereotactic body radiation therapy (SBRT) on a C-arm LINAC. Three different volumetric modulated arc therapy (VMAT) arrangements were investigated in order to minimize the treatment time, therefore reducing the intrafraction prostate motion uncertainties, while meeting the clinical objectives.

Materials and methods: A retrospective dataset of 11 patients was used. All plans were designed to deliver 40 Gy in 5 fractions to the prostate planning target volume (PTV) using a VersaHD C-arm linac (Elekta AB, Stockholm, Sweden). Two full arcs 6 MV flattening filter free (FFF) plans were compared to single full arcs using both 6 MV FFF and 10MV FFF. A plan quality index (PQI) was calculated to compare the achievement of treatment goals after optimization. Plan complexity was evaluated with the modulation factor. The dose delivery accuracy and efficiency were investigated with patient-specific quality assurance (PSQA) of all VMAT plans using the Octavius 4D phantom and the 1500 Detector (PTW, Freiburg, Germany).

Results All treatment plans met the planned dose constraints. No statistical differences were found in the PQIs and MUs comparison among the three techniques. The PSQA plans of all three techniques passed the γ criteria of 2%/2 mm with mean γ passing rates $> 96.5\%$. As expected, the techniques using single arcs showed a statistically significant decrease in the delivery time. The mean delivery times were 1.6 min (corresponding to a reduction of -46%) and 1.3 min (with a reduction of -56.2%) for 6 MV FFF and 10 MV FFF respectively.

Conclusion: High-quality plans have been achieved with reasonable complexity using single arcs VMAT for prostate SBRT. The reduction in treatment time, the accuracy and the reproducibility of the dose delivery of single-arc FFF treatments demonstrated that the proposed strategy is feasible for low- and intermediate-risk patients. In particular, the lowest delivery time required for 10MV FFF clearly demonstrated the advantage of this strategy in reducing intrafraction prostate uncertainties.

Evaluation of feasibility of using RayStation treatment planning system as an independent dose calculation system for the Unity MR-linac

Prospective/Objective: MR-guided radiotherapy (MRgRT) offers advantages over traditional x-ray methods, including enhanced soft-tissue contrast, real-time capabilities, and the ability to adapt treatment plans based on daily MR imaging. While measurement-based patient-specific QA methods are suitable for the Elekta Unity MR-linac, the impracticality of verifying adaptive plans with phantom measurements before treatment calls for a more efficient solution. However, for MR-linacs the dose calculation tends to become complicated with the existence of magnetic field. Therefore, only a few dose/MU check programs for Unity MR-linac were commercially available so far. The primary goal of this thesis is to examine the resemblance of dose distributions, generated by RayStation and Monaco, and to evaluate the feasibility of using RayStation TPS as a secondary dose calculation software for the purposes of MR Unity PSQA. Additionally, the second goal is to evaluate the feasibility of using RayStation as a basis for a measurement-less PSQA approach.

Materials and methods: Since RayStation does not simulate the influence of the magnetic field and has differences in dose calculation algorithms compared to the native Unity TPS (Monaco), two correction approaches were proposed and tested to enhance similarity between these TPS. Twenty clinical cases each for the brain and head & neck were exported to RayStation, and corrections were applied. Subsequently, the corrected dose distributions were compared to the original Monaco plans using gamma analysis, and the results were assessed against AAPM TG 219 recommendations. The correlation and agreement between RayStation and Monaco datasets were evaluated using Pearson Correlation Coefficient calculations and the Bland-Altman plot method. Finally, ten verification plans for both the brain and head & neck were recalculated in RayStation, and the results were compared with ArcCheck measurements to assess theoretical dose distribution similarity with real machine performance.

Results: An optimal 0.13 isocenter shift, both perpendicular to the magnetic field and along the central beam axis, was established to simulate the magnetic field's influence. Four different MU correction methods were proposed to address differences in dose calculation algorithms. The gamma comparison of all 40 plans (RayStation vs Monaco) revealed a passing rate exceeding 90% of points with gamma values ≤ 1 (3%/2 mm, 10% dose threshold). However, only a limited number of RayStation plans achieved a 90% passing rate in gamma comparison with ArcCheck measurements (RayStation vs ArcCheck). Only negligible correlation was observed between RayStation-related datasets and measurement results. Despite this, RayStation-related datasets demonstrated agreement with the measurements.

Conclusion: While the Bland-Altman plot method demonstrated agreement between RayStation-related datasets and measurements, the lack of correlation with ArcCheck measurements prevents the use of PSQA values of RayStation plans to predict specific measurement results. Despite the established agreement by the Bland-Altman plot method, the relatively high deviation in gamma analysis results (RayStation vs Monaco) widens the predicted range of differences (95% confidence limit), making it impractical for use. Nevertheless, the theoretical dose distributions' similarity between the two TPSs, meeting AAPM TG 219 criteria, supports the introduction of RayStation as an independent dose calculation system for the Unity MR-linac.



Yauheni Holdman

e.holdman9@gmail.com

Supervisors:

Dr. Luigi Spiazzi

Dr. Alfredo Fiume

Spedali Civili di Brescia,
Italy





GUISSOU K. Theophile

kguissou@ictp.it

Supervisors:

Dr. Carlo Cavedon
Dr. Paolo Polloniato
Dr. Emanuele Zivelonghi

Ospedale Borgo Trento-
Verona, Italy



End to end verification in gated-treatment delivery: a comparison between motion phantom devices

Prospective/Objective: to evaluate the impact of gated treatment and non-gated treatment from imaging to delivery and to quantify the impact of gating amplitude on the treatment delivery by means of phantom simulation and measurements.

Materials and methods: To achieve our goals, a CIRS Model 008A Dynamic Thorax Phantom and quasar programmable respiratory motion management phantom (QPRMP) was used. Standard and custom inserts with films were employed to mimic lung motion for end-to-end test measurements within the phantom. Using a Toshiba 16-slice CT scanner, we simulated phantoms and acquired 4DCT datasets by binning respiratory cycles triggered by the Varian RPM system into ten phases. Two plans were created in the Varian Eclipse Treatment Planning System for delivery: one delivered using the gated system (gated plan) and one without it (non-gated plan). The gated treatment plan delineates the target within a single breathing cycle phase, whereas the non-gated plan represents an average of ten static phases for targeting. The treatment plans were compared to evaluate the benefits of gated versus non-gated approaches in managing tumor motion. Radiochromic films EBT3 irradiated inside the moving phantom were used to assess the accuracy and the reproducibility of the treatment.

Results: In both for gating at 10% of the amplitude and 50%, we have a significant dose reduction compared to the non-gated as expected. The gated treatment by reducing the volume of the target spares high-dose spillage to non-target structures and enhancing dose distribution conformity compared to the non-gated. Film measurements showed optimal agreement between the calculated dose and measured dose distribution for gating at 10% of the amplitude with gamma passing ratio of 99, 4%. This value demonstrates the optimal quality for the end-to-end test. Yet, it decreased to 82.1% (failing the gamma test) when the gating amplitude was adjusted to 50%, highlighting the significant impact of gating amplitude on treatment efficacy.

Conclusion: Gated treatment outperforms non-gated approaches in managing tumor motion. However, finding the optimal amplitude is crucial. Smaller amplitudes improve treatment quality but prolong time. Striking a balance is key, ensuring an effective treatment while optimizing time efficiency.



**Miquette F
NGOUANFO NG**

nmiguett@ictp.it

**Supervisors:
Dr. STRIGARI Lidia
Dr. ZAGNI Federico**

*IRCC Azienda Ospedaliero-
Universitaria di Bologna,
Italy*

Commissioning And Quality Assurance Of A New PET/CT

Prospective/Objective: The PET/CT performance has a direct clinical impact. This study evaluated the physical performance of a new SiPM-integrated digital PET/CT scanner, uMI Vista from United Imaging Healthcare, installed in our Institute, comparing the Vendor tool results and free available software.

Materials and methods: Following the NEMA NU-2 2007 standards, and using the specific phantoms, spatial resolution, sensitivity, scatter fraction, accuracy and image quality tests were evaluated on the PET system. Spatial resolution was assessed by imaging three radioactive point sources in the air. System sensitivity was measured by using a NEMA sensitivity phantom. As described in the standard, we used a solid polyethylene cylinder with a line source positioned parallel to the tomograph axis at a few radial distances to measure the scatter fraction, and image quality was assessed with PET NEMA IEC phantom filling the four smaller spheres with radioactive solution and the two big with non-radioactive water. We processed the NEMA images acquired during the various tests with ImageJ software and compared the results obtained with those given by the manufacturer's software. The image quality and radiation dose were examined as part of the CT acceptance test using CATphan 600, system phantom, and standard PMMA phantom. The tube voltage and the HVL of the X-ray tube were also evaluated using an Unfors multimeter. The CT data have been analysed with IQworks software and Microsoft Excel.

Results: With the Vendor tool, the radial/tangential/axial FWHM were 2.99/2.99/3.03 mm and 5.54/5.24/5.26 mm at 1 and 10 cm off-centre, respectively, while using ImageJ they were $2.96 \pm 0.04/ 3.10 \pm 0.05/ 3.15 \pm 0.05$ mm and $3.47 \pm 0.025/ 3.22 \pm 0.03/ 3.32 \pm 0.02$ mm. Sensitivity at centre and 10 cm FOV given by the Vendor tool were 8.998 and 9.001 cps/kBq, respectively, while they were very different using ImageJ. The results given by the Vendor tool showed that at a clinically relevant activity concentration of 19.78 kBq/cc of ^{18}F -FDG, a Peak NECR is 122.58 kcps and scatter fraction 38.79%, while the percent error below the peak NECR was 3.03 %. The contrast recovery of 10, 13, 17, 22, 28 and 37 mm sphere diameters given by Vendor tool were 59%, 81.4%, 86.8%, 94.7%, 82.1% and 85.5%, respectively, while the background variability were 4.5%, 3.7%, 2.8%, 2.1%, 1.6% and 1.3%, respectively. ImageJ analysis gave 48%, 66%, 73%, 85%, 84% and 90% for the contrast recovery, and 3.8%, 3.1%, 2.6%, 2.3%, 1.9% and 1.5% for background variability, respectively. The lung error residual mean was 2.8% and 2.9% using the Vendor tool and ImageJ. Finally, the CT image quality and CTDI values resulted in the hospital's acceptance range.

Conclusion:

All the performance tests carried out on our new PET/CT were in the acceptable range given by the manufacturer, and the results of CT scanner were also acceptable for clinical use. This new scanner meets the highest standards of precision and safety and it opens new possibilities for patient diagnostic and treatment in our hospital.



Cornelio I. Martínez S.

cmartine@ictp.it

Supervisors:

Dr. Carlo Cavedon

Dr. Paolo Maria

Polloniato

Dr. Emanuele Zivelonghi

Azienda Ospedaliera
Universitaria Integrata,
Verona, Italy



Analysis and validation of the TQA quality assurance system in tomotherapy

Prospective/Objective: Tomotherapy combines the precision of intensity-modulated radiation therapy (IMRT) with the geometric layout of a computed tomography (CT) scanner, proving highly effective for treating various oncological diseases. The success of Tomotherapy relies on precise treatment delivery, ensured by the Tomotherapy Quality Assurance (TQA) system. TQA is a comprehensive software that performs pre, during, and post-treatment checks, including equipment, output and energy control, and dosimetric checks. Though complex and requiring specialized knowledge, TQA's clear benefits lie in ensuring high-quality care while optimizing time and personnel resources.

Materials and methods: The checks provided for in this program can be carried out with the equipment supplied by the company together with the Tomotherapy equipment integrated with a few other instruments normally and easily available in a radiotherapy centre. In particular, the necessary equipment consists of: TomoPhantom cylindrical phantom supplied, Rectangular solid water phantom composed of several overlapping layers of different thicknesses supplied with the tomotherapy system, a phantom equipped with a mobile arm with automatic movement system supplied with the tomotherapy system, Pencil chamber type ionization chamber at least 17 cm long with constant response along the entire length, Software for the acquisition and analysis of transverse, longitudinal and in-depth dose profiles acquired with ionization chambers in solid water phantom or water phantom, Cylindrical ionization chambers of the "minichamber" type (collection volume 0.056 cm^3).

Results: Measurements made with ionization chamber in a solid water phantom (Cheese- Phantom and Slab-Phantom) have become the baseline values for the reference dose of a standard IMRT plan and for an energy control parameter (PDD20-10). Before starting the treatments, patient-specific checks are routinely carried out on a cylindrical diode array (ArcCheck – Sun Nuclear) and the results obtained on the patients demonstrates excellent agreement after the gamma analysis (3% - 3 mm). Simultaneously with the creation of a baseline for reference dose and PDD (Percentage Depth Dose), the baselines were acquired via direct measurement with the integrated array of detectors into the TQA (Tomo Quality Assurance) software. This method of measurement and processing dosimetric data has made possible obtain an estimation of numerous fundamental parameters of the system.

Conclusion: TQA platform has demonstrated to be reliable in monitoring the main parameters of Tomotherapy. The main advantage is the low time needed to acquire and analyze data against a Farmer chamber. The Acuros calculation algorithm in Eclipse greatly underestimates the out of field dose and can be used only for a rough estimation in points not so far from the central axis of the beam (less than 20 cm). Ultimately, the Tomotherapy system analyzed was consistent with the specifications provided by the manufacturer and international protocols and has remained so over time.



Maria Isabel Subia

msubia_p@ictp.it

Supervisors:

Dr. Maria Victoria Gutierrez

Azienda Ospedaliero-
Universitaria Policlinico di
Modena, Italy



Dosimetric Evaluation of Prostate Motion using Multimodal Imaging on Extreme Hypo-fractionated SBRT

Prospective/Objective: Evaluate the dosimetric effect of prostate intrafraction motion on extreme hypo-fractionated SBRT treatments performed in Modena University Hospital, where SBRT-VMAT 6 MV FFF treatments for PCs are delivered using an Elekta VERSA HD accelerator with on-board CBCT X-ray Volumetric Imager (XVI®, Elekta Oncology Systems), and the image guidance of a Clarity Autoscan Ultrasound Based System (Elekta, Stockholm, Sweden) with transperineal probe for prostate movement monitoring and management.

Materials and methods: The data used for the analysis corresponded to 10 prostate acinar adenocarcinoma cases. The prescription was 36.25 Gy total dose in 5 fractions delivered every other day. The information relative to the mean movement of the prostate during each delivered fraction of the treatment for each patient was retrieved through the Clarity Autoscan Ultrasound Based System, to calculate an approximation of the motion-inclusive dose distributions and evaluate the dose difference between the planned and motion-inclusive dose considering the fulfillment and variation of the dose values related to the clinical constraints. Moreover, a tendency of the prostate movement was found and correlated to the dosimetric impact of under coverage of target and overdosage of OARs.

Results: Prostate movement in posterior direction seems to be recurrent during delivery of the treatment. For the target, dose under coverage as large as 4% (124 cGy) respect to the constraint value ($D_{98\%} > 95\%$) has been observed in some individual motion-inclusive simulated fractions (16% of the total number). Only rectum and penis bulb showed a worsening in achieving the clinical constraints due to the prostate movement, yet only for a few fractions.

Conclusion: The mean shifts of the prostate during delivery of the radiation treatment don't generate a significant worsening in achievement of the dose constraints in the surrounding organs at risk. For target coverage, a violation of the $D_{98\%}$ dose value constraint was found in a little number of fractions, yet over the course of treatment this issue won't be relevant as the displacements large enough to generate an insufficient target coverage are infrequent.



Angel H. B. Zaldaña

abanos_z@ictp.it

Supervisor:

Dr. Angelo F. Monti

ASST Grande Ospedale
Metropolitano Niguarda,
Milano, Italy



Evaluation of a new secondary independent dose calculation tool in VMAT treatment planning.

Prospective/Objective: IMRT and VMAT have become the predominant radiotherapy techniques for a variety of treatment sites. The steep dose gradients generated by means of dynamical multileaf collimator motion, gantry rotation speed and dose rate can increase potential errors. Consequently, extensive pre-treatment quality assurance program is needed for the dosimetric verification of the plan, in order to ensure the accuracy and safety of the treatment. The purpose of this work is to perform pre-clinical evaluation of the Delta4 Insight (Scandidos, SWE) as a quality assurance system capable of three-dimensional dose calculations on patients Computed Tomography dataset and a model-based Monte Carlo algorithm comparing it with a reference TPS “Monaco”.

Materials and methods: 3 planning situations have been considered: 3D plans in a 30×30×30 cm³ cubic phantoms created by superimposing slabs of varying densities to test the dose calculations within homogeneous structures and inhomogeneities in order to compare PDDs and dose profiles in different depths for both Monaco and Delta4 Insight; VMAT plans in a phantom based on the Task Group 119 and finally, 18 real patient plans in different anatomical sites, to evaluate real clinical situations, using a VMAT technique too. Calculations have been performed for 6 MV and 6 MV FFF photon beams.

Results: For the homogeneous cubic phantom, the mean values of the PDDs confidence limit for 6MV and 6MV FFF forced were (0.50±0.08) and (2.40±0.22), for non-forced (1.19±0.29) and (1.66±0.26), and the mean values of the profiles were (0.84±0.53) and (0.88±0.46). The mean values without forcing the structure (0.79±0.42) 6 MV and (0.75±0.33) 6MV FFF. Cubic phantom with internal low-density the mean values for the PDDs 6MV and 6MV FFF with 5 cm Inhomogeneity were (1.45±0.55) and (1.19±0.19). And for 10 cm (1.75±0.39) and (1.95±0.38). Profiles mean values for 6MV and 6MV FFF with 5 cm of Inhomogeneity were (0.83±0.45) and (0.71±0.33). And with 10 cm (1.02±0.51) and (0.70±0.31). For the cubic phantom with 3 cm internal low- and high-density inhomogeneity the mean values of the x-axis confidence limit for 6 MV and 6 MV FFF were (0.81±0.59) and (0.82±0.47). Regarding to the TG 119 phantom plans, the mean values of the GPR for 6 MV with different criteria were (82.4±5.7) 1%-1mm, (97.4±2.0) 2%-2mm and (99.6±0.3) 3%-3mm. And for 6 MV FFF (85.8±4.4) 1%-1mm, (98.8±1.0) 2%-2mm and (99.9±0.1) 3%-3mm. Finally for the 18 Real patient plans the mean values of the GPR for H&N and different criteria were (79.9±7.3) 1%-1mm, (95.7±2.8) 2%-2mm and (98.5±1.1) 3%-3mm, for Thorax (75.9±10.6) 1%-1mm, (93.9±4.0) 2%-2mm and (97.9±1.6) 3%-3mm, finally, for Pelvis (72.1±3.3) 1%-1mm, (93.8±2.1) 2%-2mm and (97.9±1.0) 3%-3mm.

Conclusion: This study revealed differences in profiles and PDDs, indicating a deviation from the expected shape and calculated dose levels. The comparison made performing the gamma analysis showed no significant discrepancies in both TG 119 and real patient plans, but the DVH comparison showed that DI always delivers higher doses to target and organs at risk, due to the different volume that DI takes into account. These results could suggest to Scandidos some changes in the software before its clinical implementation.



Gebre Dereje Ayalew

dgebre@ictp.it

Supervisors:
Dr. Federica Guida

*Instituto Oncologico of
Veneto, Department of
Radiotherapy, Padova ,
Italy*



Quantification and Assessment of Skin Dose in VMAT and Tomotherapy: a Comparative Study using In vivo Dosimeter

Prospective/Objective: This study aimed to evaluate the precision and accuracy of the MOSFET dosimeter in determining skin dose during Volumetric Modulated Arc Therapy (VMAT) and Tomotherapy treatments by comparing them with Gafchromic EBT3 film and the Treatment Planning System (TPS). The research was conducted at the Instituto Oncologico de Veneto.

Materials and Methods: Thomson & Nielsen, Canada, produced the TN502RD MOSFET detectors. A set of tests was done on the mobile MOSFETs to see how accurate, repeatable, and angle-dependent they were. We were measuring the surface dose in a 6 MV beam on the TrueBeam machine and TomoTherapy. Measurements were performed on a RANDO antropomorphic model simulating head and neck cancer and breast cancer. Treatment plans were generated using the Eclipse treatment planning system for TrueBeam and Raystation for Tomotherapy, adhering to clinical protocols. VMAT plans included two arcs for the head and neck, and for breast cases, two half arcs were employed. For patient-specific quality assurance, portal vision images and arc checks are conducted before taking measurements. This ensures that the positioning and setup align with the treatment plan and verifies the accuracy of the delivery system before actual dose measurements are taken. MOSFETs, along with small 4x4 cm² pieces of EBT3 films, were positioned identically on the RANDO phantom to facilitate a comprehensive comparison between them.

Results: The study examined average percentage dose differences in both in-field and out-of-field measurements. When measuring Tomotherapy in-field, MOSFET always shows a higher percentage dose (7.50%) than Gafchromic film. This could be a sign of a systematic bias. The negative percentage difference between MOSFET and TPS in the in-field setting suggests a tendency for TPS to overestimate doses compared to MOSFET (-6.53%). Out-of-field measurements in Tomotherapy show that MOSFET gives more accurate readings than Gafchromic film (4.25%), while TPS significantly overestimates (-3.38%). When we look at TrueBeam, the in-field measurements show that MOSFET readings are consistently higher than Gafchromic readings (13.22%), which could mean that the dose estimates are different. The positive percentage difference between MOSFET and TPS in the in-field setting suggests relatively good agreement between the two measurements (9.78%). However, in out-of-field measurements, MOSFET again shows higher readings than Gafchromic film (6.425%), and TPS exhibits a slight underestimation (1.32%) compared to MOSFET. A study by Rajesh A. Kinikar [14] and ZHEN-YU QI [13] showed a difference of 20–12%.

Conclusion: After a comprehensive analysis of our data, it is clear that our MOSFET system demonstrates stability and reliability, signifying its robust performance. The consistently accurate measurements obtained through MOSFET play a crucial role in upholding the overall quality and safety of the radiation treatment process. This steadfastness emphasizes the suitability of the device for precise dose verification, further strengthening its integral role in preserving the integrity of radiotherapy treatments.



The use of Hyperthermia to Enhance Radiotherapy Treatments

Prospective/Objective: Surgery and Radiotherapy are treatment of choice for early stage localized tumor lesions. However, recurrences and/or metastases can occur after incomplete eradication of the primary tumor and lead to acquired radio-resistant tumors, e.g. Hypoxic tumors. Combined radiotherapy and hyperthermia offer great potential for the successful treatment of radio-resistant tumors through thermo-radio-sensitization. The aim of this study was to see the dose escalation effect of hyperthermia on six soft tissue sarcoma patients treated with a preoperative radiotherapy with 25 fraction (2Gy/fr) (for five weeks) and hyperthermia once in a week. In addition we also evaluated local response to hyperthermia and radiotherapy as a preoperative regimen for STS from the post treatment assessment.

Materials and methods: External beam radiotherapy planning was done on a prescription dose of 50Gy in 25fractions using Eclipse v.15.1 TPS. A VMAT technique was used for the six STS patients using 6MV photon beam and evaluated according to the internal protocol for OARs and limiting the hotspots to the targets. Then the hyperthermia treatment planning was done on Plan2heat software using temperature optimization method (T_{90} , T_{50} and T_{10}) limiting the hotspots to $< 45^{\circ}\text{C}$. The Linear Quadratic (LQ) model extended with temperature dependent LQ parameters $\alpha(T, t_{int})(\text{Gy}^{-1})$ and $\beta(T, t_{int})(\text{Gy}^{-2})$ was used to model the radio-sensitization by hyperthermia. For the LQ parameters of hypoxic volume Oxygen enhancement ratio was used to take in to account that it has a lower sensitivity than the GTV. MIM Maestro[®] was used to calculate the Equivalent Radiation Dose for the combined treatment and also used to evaluate the treatment outcome by comparing the pre and post K_{trans} maps extracted from Dynamic Contrast Enhanced(DCE) MRI.

Results: A model to quantify the effect of combined radiation therapy and hyperthermia in terms of equivalent dose distributions was presented. Then dose escalation effect of hyperthermia was evaluated by comparing the equivalent dose distribution (EQDRT) for radiotherapy treatment only with the EQDRHT for the combined treatment. From the comparisons it was found that the higher the achieved temperature is the higher its enhancement will be. For the GTV using T_{10} the enhancement ranges from 4.1Gy (with T_{10} -41.90C) to 6.8Gy (with T_{10} -43.60C) and for the hypoxic volume the enhancement was 5.3Gy to 6.5Gy. For the treatment outcome evaluation hypovascularized volume of the tumor is evaluated with the MIM software as a subvolume of the GTV, for the patient with pleomorphic liposarcoma it has seen an increase in volume (+27%-GTV, +114%-hypoxic, with 40% necrosis) after the treatment because of the histology of the tumor while for the other the GTV and hypoxic volume becomes reduced (-37% , -21%, with 90% necrosis).

Conclusion: Biological modelling provides relevant insight into the relationship between treatment parameters and expected EQD. It has been shown that for a higher enhancement effect temperatures higher than 41°C should be applied in order to get a significant amount of equivalent dose from HT. The volumetric maps of K_{trans} allowed us to observe important variations between pre- and post-treatment, and therefore the sequence of DCE-MRI was found to be a potentially useful tool in monitoring radio-hyperthermia treatment outcome.

Kalkidan B.Nurelign

Maryamawit109@gmail.com

Supervisors:

Dr. Marco D'andrea

Dr. Antonella Soriani

Instituto Nazionale tumori
Regina elena, Italy





Melaku Teklehawariyat

mtekleha@ictp.it

Supervisors:

Dr. Michele Bigotto

Dr. Stefania Cora

Ospedale San Bortolo di
Vicenza, Italy



Commissioning of An Elekta VersaHD Linear Accelerator in Pinnacle Treatment Planning System.

Prospective/Objective: The commissioning of Radiotherapy Treatment Planning System (RTPS) is the most crucial parts of the whole planning process. Indeed, a thorough commissioning is mandatory to ensure an accurate correspondence of the delivered dose to the planned one. The purpose of this thesis was to implement a physical photon beam model for PINNACLE TPS and the electron beam model for RayStation TPS and to create a single physical model able to match the dose output of the three Clinical Elekta Linacs VERSA HD installed at the Radiotherapy Unit of San Bortolo Hospital. Software tests and algorithm validations were performed in order to verify inter-linacs matching of absolute dose and beam flatness for energies of 6FF MV, 6FFF MV, and 10FF MV. The aim was also to define dose characterization procedure for inter-comparison purposes for the three linacs to contribute to a better understanding of the accuracy of single physical model, and to establish a reliable tolerance test report process-based tolerance and action limits of our Elekta VersaHD linear accelerators according to TG-218.

Materials and methods: An Elekta VersaHD (Elekta VersaHD, Stockholm, Sweden) was commissioned, and photon energies of 6FF MV, 6FFF MV, and 10FF MV (profiles, percentage depth doses, and output factor) were acquired for field sizes of $0.6 \times 0.6 \text{ cm}^2$ to $40 \times 40 \text{ cm}^2$, for wedge fields in various sizes, including $3 \times 3 \text{ cm}^2$ (without reference detector), $5 \times 5 \text{ cm}^2$, $10 \times 10 \text{ cm}^2$, $20 \times 20 \text{ cm}^2$, and $40 \times 30 \text{ cm}^2$. For electron beams the electron cones (applicators of) $6 \times 6 \text{ cm}^2$, $10 \times 10 \text{ cm}^2$, $14 \times 14 \text{ cm}^2$, and $20 \times 20 \text{ cm}^2$ were used. The data obtained for both electron and photon beams type using a three-dimensional water phantom at a 100 cm SSD, detectors of various types, including Microdiamonds (PTW 60019), Sun nuclear edge detectors, Farmer chambers (TM 30013), Semiflex chambers (TM 31010), pinpoint (PTW 31014), and Advanced Markus (TM-34045), were used, the Sun Nuclear ArcCHECK was used for gamma analysis.

Results: The PDD of 6FF MV was marginally lower than that of 6FFF MV beams at a depth of 10 cm. When compared to open fields, wedge filters considerably reduce machine output while increasing the percentage depth dose. The energy output factor with the flattening filter was higher than that of the flattened beams for field sizes greater than $10 \times 10 \text{ cm}^2$, but lower for field sizes less than $10 \times 10 \text{ cm}^2$. The pass-rate metrics of 2 mm/2%, 2 mm/3%, and 3 mm/3% with an acceptable threshold of 90% for a Seven VMAT plans simulated using the Unicum model were clinically acceptable for the VersaPOD and VersaHD machines.

Conclusion: The VersaHD linac commissioning data, including depth dose, beam profiles, output factor, and other dosimetric data, were measured, analyzed, and characterized systematically. Photon beam modelling has been done for Pinnacle TPS, whereas electron beam modeling has been done for RayStation.




Waza Sisay Milkias
swaza@ictp.it

Supervisors:
 Prof. Lidia Strigari

POLICLINICO DI SANT'ORSOLA, Bologna, Italy



Setup of a system for online in vivo Dosimetry in VMAT treatments

Prospective/Objective: To secure the patient treatment quality many tools can be used. In this study, the impact of setup of a system for VMAT treatment was analyzed. The analysis was done on 16 treatment plans using a PTW Verisoft and EPIgray of DosiSoft software. Errors arising during VMAT treatment could cause severe injury to patient due to high radiation dose per single fraction; therefore giving priority for setup of the system we can reduce the risk of errors that could compromise treatment outcome.

Materials and methods: In order to determine the impact of shifts in positioning on a patient-like phantom, we deliberately introduced the following errors. Shift in isocenter of 5 mm and 20 mm in the lateral direction (Plan_L05 and Plan_L2 respectively), a shift of 10 mm and 20 mm in posterior direction (Plan_P1 and Plan_P2 respectively), and 20 mm shift in anterior direction (Plan_A2).

Moreover, in order to examine the sensitivity of the system for the change in size/shape or weight of the patient-like phantom, we introduced a bolus (Plan_B) with thickness 1 cm and area 15 x 15 cm² and in order to simulate and evaluate the impact of air bubble within the tissue we introduced a dedicated a 3 cm thick rotation unit chamber plate Farmer 0.3 cm³ (Plan_Farmer) into the PTW OCTAVIUS 4D phantom

Results: From Plan_L2, Plan_P1, Plan_P2 and Plan_A2, the expected dose difference (from Pinnacle TPS) were higher compared with DosiSoft. On the other hand, the dose deviation predicted from EPIgray of the DosiSoft for Plan_L2 are lower than the one predicted from the Pinnacle TPS. On the contrary for Plan-Farmer all evaluated structures have a deviation greater than 10%. This shows that EPID based EPIgray of DosiSoft is very sensitive to the change in the density by Farmer Chamber plate which mimics the presence of air bubble within tissues. When examining the gamma index analysis for both 6 MV and 6 MV FFF energies, the gamma analysis via VeriSoft between the Pinnacle TPS and the measured dose maps through PTW729 detector all plans except Plan_Farmer showed a dramatic drop on gamma passing rate relative to Plan_0. Here we can notice that the VeriSoft is not sensitive to air bubble simulated as the Farmer chamber plate, which inserted into the PTW OCTAVIUS phantom.

Conclusion: By combining the EPID based EPIgray of the DosiSoft with the existing PTW VeriSoft gamma analysis technique we can boost the safety of patient and we can offer a comprehensive patient specific quality assurance that can detect errors due to anatomical change, or due to air bubbles between tissues or slight increase on weight of the patient as well as patient positioning errors introduced in the isocenter shift.

Dose Optimization Process for Full-Spine Digital Radiography in the Pediatric Population Using Exposure Index

Prospective/Objective: the study should cover in multiple beams radiogram the entire vertebral spine in AP and lateral projection. Often, the acquisition should be repeated during long-term evaluation. Patients are normally pediatric. The cumulative dose and radiation risk are higher in comparison with other radiographies. The aim was to create a dose optimization process based on a weight of the patient protocol that allows to reduce dose and at the same time keeping a good image quality.

Materials and methods: We analyzed 132 patients: 75 females and 56 males. The ages covered were 3 to 17 years old. Studies were obtained on a Ysio Max Siemens system in the pediatric hospital Regina Margherita of Turin. The equipment created the image stitching multiple beam radiograms. Radiology information were extracted using PACS and the dose tracking system. The exposure index was used for the optimization process; in addition, we needed the weight of the patient and the mAs registered. To study exposure index variations, we analyzed images obtained from a homogeneous and an anthropomorphic phantom. To assess the image quality, four radiologists ranked a group of 20 clinical images obtained pre and optimization and we measured the SNR and CNR using Image J. To simulate organ doses and radiation risk, we used PCXMC 2.0, simulating patients whose ages were 5, 10, and 15 years old and we used a GAF chormic film to obtain beam geometry information for the simulation.

Results: The optimized protocols were classified according to the number of beam radiograms stitched, projection, and weight of the patient. Before the optimization, the exposure index presented high variation between each beam radiogram; after the optimization, this variation was reduced. The DAP mean value was reduced differently according to the protocol and the dispersion of DAP values was reduced more than 70%. Our study showed that the Exposure Index may vary by more than 30% depending on the clinical protocol set in the console. The radiologist's evaluation showed that the new protocols had good image quality. SNR measurements suggest a slightly lower quality of the thoracic vertebrae in AP projection. Radiation dose and radiation risk were reduced by even more than 50% in most of the organs according for early ages.

Conclusion: The dose optimization process succeeded in reducing the dose organs and obtaining a good image quality in most of the anatomy components. Optimized protocol turned the Exposure Index and DAP into more predictable variables to be used in future dose optimization programs. We consider that the method of dose optimization presented in this research can be applied to any radiological examination performed with digital equipment. It is important to consider that the exposure index should not be the only indicator into; it is also essential to take into account DAP and the correct radiography technique.



Tito E. Padilla M.

tpadilla@ictp.it

Supervisors:

Dr. Veronica Rossetti

*città della salute e della
scienza di Torino, Italy*





Verification of Ethos CBCT-guided online adaptive radiotherapy for prostate cancer using Raystation hybrid DIR algorithm, ANACONDA

Prospective/Objective: Radiotherapy plays a crucial role in managing localized prostate cancer, where the planning process involves utilizing a snapshot dataset of the patient's anatomy during simulation. However, anatomical changes can occur between and within fractions, necessitating adaptation strategies. This study aims to comprehensively analyze the dynamics of dose accumulation during the treatment localized of prostate cancer, utilizing both scheduled plans (SPs) (reference treatment plan recalculated on the daily anatomy) and adapted plans (APs) (reference treatment plan reoptimized to match the clinical directive) within the Ethos system, employing the Raystation ANACONDA DIR algorithm.

Materials and methods: Eight patients treated with Ethos oART (60Gy/20 fractions) were retrospectively selected. The initial reference treatment plan was generated based on the planning CT (pCT) using Ethos. Before treatment, cone beam CT (CBCT) images were obtained, and the pCT data was mapped onto the CBCT image, thus creating the synthetic CT (sCT). An artificial intelligence algorithm then identified the influencer organs (prostate, bladder, rectum, and seminal vesicle). Ethos' deformation algorithm utilized these influencer organs to guide the deformation of the CTV and PTV from the pCT to the CBCT image. SPs and APs were subsequently generated on the sCT.

Daily CBCT images, SPs, APs, and reference treatment plans were transferred to Raystation TPS. Rigid image registrations (RIRs) were executed between pCTs and sCTs, followed by the deformable image registrations (DIRs) using the influencer organs as controlling regions of interest (ROIs) for each fraction. The dose corresponding to the DIR was then deformed to the pCT, and a dose accumulation analysis was conducted for both scheduled and adapted plans across all patients. Evaluation metrics included the Dice similarity coefficient (DSC), mean distance to agreement (MDA), and the Jacobian determinant (JD).

Results: Results indicated favorable DIR metrics, with influencer organs mean DSC ranging from 0.89 to 0.98, and the MDA from 0.03 cm to 0.09 cm. JD values for prostate, bladder, rectum, and seminal vesicle ranged from 0.77 to 1.11. notably, AP demonstrated improved PTV coverage compared to SP. For D98% > 95%, 25% of the patients achieved an adapted mean of 94.65%, compared to 12.5% achieving a mean of 88.05% for the SP. For D95% > 95%, AP displayed enhanced PTV coverage, with 100% of the cohort attaining a mean of 97.16%, whereas 25% achieved 92.25% for SP. CTV coverage remained high in both plans, with mean values of 98.03% and 99.13% for SP and AP, respectively.

Although OARs met clinical goals in both plans, AP exhibited increase volumetric dose to OARs. Patient-specific results unveiled target coverage coincidence in four cases, while the remaining four showed a deviation of PTV coverage between Raystation and Ethos delivered dose accumulations, signifying the impact of anatomical changes during adaptation.

Conclusion: Ethos oART emerges as an appealing modality for intact prostate cancer treatment, offering satisfactory CTV and PTV coverage while safeguarding OARs. Potential improvements in PTV coverage could be achieved with enhanced patient preparation and increased clinical staff efficiency.



Damion Gilpin.

dgilpin@ictp.it

Supervisors:

Dr. Sonia Sapignoli
Dr. Paolo Caricato

Istituto Oncologico Veneto,
Italy





**Jordan Rudolph
Berthan Isaacs**

jisaacs@ictp.it

Supervisors:

Dr. Raffaele Villa

Dr. Sabrina Morzenti

Acceptance and commissioning of a Philips Incisive CT

Prospective/Objective: Acceptance testing of a CT is done when a new device has been installed or there was an upgrade to existing equipment. The objective of this study is to evaluate a Philips Incisive CT system recently installed at Desio Hospital, evaluating if the device is as declared by the vendor, if up to standard with national and international guidelines and establishing benchmark data from acquisitions.

Materials and methods: The Philips Incisive CT system has a 72cm bore and 50 cm field of view detector array used for head, body, cardiac and vascular applications. RaySafe measurement system with two sensors were used: the CT sensor is a 100 mm pencil-ionization chamber which can calculate kV, mA and or mAs from the measured voltage and the survey sensor, which will be used for leakage measurements. Catphan 600 for performance characterization, PMMA head and body phantoms of 160 and 320 mm respectively used for CTDI measurements. Philips Head and Body system performance phantom has a head phantom 200 mm in diameter and the body phantom 300 mm in diameter. Physics layer is for slice thickness and impulse response. Head water layer for measuring noise, CT number and uniformity. The PE and LEXAN/Acrylic cylinders are used for measuring the CT number linearity. The body water layer is used to measure CT number, noise and uniformity. The values to be examined with CT sensor are CTDI in air, weighted CTDI, CTDI reproducibility and linearity vs mAs and CTDI accuracy. With the Philips phantom spatial resolution, noise, mean CT number and uniformity, and slice width were assessed. The survey sensor accounted for the leakage. Finally, tube modulation was evaluated with the use of a combination of head and body phantom.

Results: The values for CTDI in air, weighted CTDI, CTDI reproducibility and linearity vs mAs and CTDI accuracy were all in agreement with the established manufacturer reference values of less than 20%. The declared values on the console for CTDI and geometric efficiency reflected accurately what was measured and calculated by the medical physicist. The current modulation of the x-ray tube illustrates higher variation for the larger collimation. Average radiation dispersion was measured to be 0.1 mGy/h, below the established reference value of 1 mGy/h. The automatic systems check evaluated the mean CT number and uniformity, noise and spatial in which all parameters received a 'Passed' status showing the fell within the benchmark ranges stipulated by the International Electrotechnical Commission (IEC).

Conclusion: The Philips Incisive CT passing these examinations suggest that from a theoretical point of view the device is ready for clinical use. That there can be strong levels of diagnostic confidence and that images the device produces will be of minimal noise, which means high levels of spatial resolution allowing the practitioner to be able to better identify structures and pathologies. Resulting in safer and better-quality patient outcomes. The radiologists make the final decision on its efficacy in clinical practice.

Ospedale San Gerardo Monza,
Italy





Miras Svaikulov.

msvaikul@ictp.it

Supervisors:

Dr. Loris Menegotti

Dr. Stefano Lorentini

Ospedale S.Chiera, Trento,
Italy



Replanning of a proton therapy plan with photons: Analysis of a fast and effective method.

Prospective/Objective: The aim of this study is to evaluate photon plans created as a backup to the main proton plan in the event of a breakdown of the proton cyclotron for up to 2 weeks. Backup plans are created using the volumetric modulated arc therapy (VMAT) technique for various areas of interest: brain, head-neck, column.

Materials and methods: Nine brain, head and neck (H&N), column VMAT plans for nine patients (3 patients for each case) were created, starting from clinical proton plans. Two tools within RayStation (version 12A) treatment planning system (TPS) were used: Fallback (FB) and autoplanning (AP) by Guided Planning Solution (GPS), which is a Monte Carlo and Collapses Cone-based TPS. Plan quality was evaluated by using dose metrics: V95%, V105%, D95 and limit dose to organs at risk (OAR) from prescription plan. Patient specific quality assurance (QA) was performed for one patient from each group case with gamma analysis.

Results: V95 dose coverage was achieved for half of all plans. Due to the proximity of the tumor to the primary OARs, the minimum dose coverage in V95(%) could not be achieved and a decision was made on the most achievable coverage while sparing most of the OAR for 4 patients. On one of the brain patients an additional optimization was performed, as a test for further improvement of the automatic plan quality. A reduction in dose to the primary OAR was achieved, with a small decrease in dose coverage for both methods. All gamma analysis carried out for patients passed the acceptable treatment limit of 90% with tolerance 3%/3mm. For further verification, tolerance of 2%/2mm was successfully tested; only in one brain case patient the gamma passing rate was lower than the limit.

Conclusion: Both FB and AP methods were effective in order to create a backup plan starting from the clinical proton plan for our sample of nine patients. FB is faster than AP, therefore it is more suitable when time is an issue. AP leads to a higher coverage of the PTV, compared to FB, if the OARs are not near to the target. Additional optimization is recommended in order to improve plan quality for both FB and AP, when OAR are in close proximity to the target. This requires an extra work of about 30 to 40 minutes.



A practical approach to Stereotactic Radiation Therapy plan verification with matrix detectors

Prospective/Objective: The aim of this work was to evaluate the impact of dose rate and fields dimension on the Octavius 1500 (OD1500) and Octavius 1600SRS (OD1600) detectors' measurements and to define a calibration procedure for the two matrices, in order to verify SBRT and SRS VMAT plans (6MV FFF and 10MV FFF energies).

Materials and methods: This first part of the work evaluated the response of OD1500 and OD1600 detectors (ODs) to different fields and dose rates for 6 MV, 10 MV and 6 MV FFF, 10 MV FFF energies of an the Elekta™ Versa HD accelerator. Output factors (OF) were compared to the measurements performed during the linac's acceptance test and annual QA verifications, with the dosimeters of reference: ionization chambers (PTW Semiflex 3D, PTW PinPoint, PTW micriOLion) and solide state detector (PTW Microdiamond). The second part of the work was focus on the determination of matrices' calibration factors corrections for SBRT QA plan verifications. The matrices were cross-calibrated ionization chambers PTW Pinpoint and PTW Semiflex 3D, with a 5x5cm² field at 6MVFFF and 10MVFFF energies. Dose measurements were acquired for small fields varying dose rates to determine the matrix's calibration's correction factors (k_{fs}^{dr}), as a function of field dimension and dose rate. k_{fs}^{dr} values were also compared with the literature. The proper k_{fs}^{dr} was defined for 6 SBRT/SRS plans that were previously analyzed and characterized by their mean segments' dimension and dose rate. The gamma analysis were then performed to compare calculated dose maps and measured dose maps, for each plan (with dose and distance tolerances of 2%, 2mm), before and after the corrections.

Results: OF measured with the OD1500 detector are in good agreement with the reference dosimeters: at field 4x4cm² and 3x3cm², deviations were within -0.5% and -1.5%, at field 2x2cm² the discrepancy is higher, -3.8%. OF measured with the OD1600 in good agreement with the reference dosimeters: at field 4x4cm² and 3x3cm², deviations are within 0.3% and 0.8%, at field 2x2cm² the discrepancy is 2%. Estimated matrix correction factors for the OD1500 are: 1.013±0.003 (for field 3x3cm²) and 1.082±0.003 (for field 2x2cm²) for energy 10MV FFF; 1.014 (field 3x3cm²) and 1.038 (field 2x2cm²) for energy 6MV FFF. These results are in good agreement with the literature; the correction factors for the field 2x2cm². Matrix correction factors for OD1600 are 1.0 (5x5cm²), 0.97 (3x3cm²) and 0.95 – 0.93 (2x2cm²) for energy 10MV FFF depends on dose rate, 1.0 (5x5cm²), 0.99 (3x3cm²) and 0.98 (2x2cm²) for energy 6MV FFF at maximum dose rate.

Conclusion: Two matrix detectors with OCTAVIUS 2D were analyzed to perform routine QA measurements for treatments SRS/SBRT plans. Our practical approach to correct the matrices' dependence on field size and dose rate give good results in terms of gamma analysis for the SBRT/SRS plans evaluated, but further verifications should be performed to confirm our correction factors estimations.

**Kassymkhan
TURIKBAYEV**

turikbayevk@gmail.com

Supervisors:

Dr. Anna DELANA

Dr. Francesco ZIGLIO

*St. Chiara Hospital, Trento,
Italy*



**Azienda Provinciale
per i Servizi Sanitari**
Provincia Autonoma di Trento

Dosimetric optimization and evaluation of hepatocellular carcinoma treatment effect prediction in Y-90 transarterial radioembolization

Prospective/Objective: This study aimed to optimize and standardize the pre- and post- dosimetry protocols for ^{90}Y TARE at ASST Papa Giovanni XXIII Hospital (Bergamo, Italy) and assess the predictive value of voxel dosimetry for treatment outcomes, including radiological response, adverse events and patient overall survival in HCC patients.

Materials and methods: In this retrospective study 133 HCC patients treated with ^{90}Y microspheres from 2013 to 2021 were analysed. Of those 95 were treated with resin microspheres, 38 with glass microspheres. The pre- and post-dosimetry protocols were optimized based on EANM guidelines, utilizing the Planet Dose software. Pre-dosimetry was done for all the patients and the calculated doses were used for statistical analysis. Post-dosimetry was performed for patients treated after installation of the PET/CT system in 2019. Association between mean dose delivered to the lesion and complete radiological response (CR) was assessed by Wilcoxon-Mann-Whitney test, when the dose was considered as a continuous variable, and by chi-square test when the dose was dichotomized using the best cutoff identified by ROC curve. Univariate and multivariable Logistic Regression models were fitted to identify predictors of CR. Cox Proportional-Hazard Regression models were fitted to identify predictors of death. A comparison of doses calculated during pre- and post-dosimetry was performed before and after the optimisation of PET/CT acquisition protocol.

Results: The optimal reconstruction for pre-treatment dosimetry with $^{99\text{m}}\text{Tc}$ -MAA with Siemens 'Symbia' SPECT/CT was determined as Flash 3D, 8 subsets, 8 iterations, and no filtering. For resin microspheres from the ROC curve plotted for mean dose delivered to the lesion predicting CR, a cutoff dose was found to be 233.2 Gy (AUC = 0.6191). A significantly higher proportion of CR was found in the patients who received a dose ≥ 233.2 Gy (49.1% of CR with higher doses vs. 23.8% of CR with lower doses, $p=0.012$), as well as a reduction of risk of death by 42% (HR=0.58, 95% CI 0.34-1.01, $p=0.054$). The number of patients with complete radiological response treated with glass microspheres was too low to implement a statistical model. No lung toxicity was observed for any of the patients involved in this study. No correlation between the dose delivered to the normal liver and adverse events was found during the statistical analysis. Comparison of pre- and post-dosimetry was performed for 34 patients before the optimisation of PET/CT protocol. In 8 patients mean lesion dose discrepancies of $>40\%$ were found. After the optimisation all the lesion doses were within 40% when the pre- and post-dosimetry was compared.

Conclusion: Dose to the lesion is a significant predictor of CR for resin microspheres, the mean dose delivered to the lesion should be at least 233.2 Gy. In patients receiving at least this dose, a reduction of risk of death was observed. The absence of lung toxicity and the lack of correlation between normal liver absorbed dose and adverse events suggests potential under-treatment, advocating for increased delivered doses in future interventions.



Laura Grikke

lauragrikke@gmail.com

Supervisors:

Dr. Gian Luca Poli
Dr. Claudia Bianchi

ASST Papa Giovanni XXIII
Hospital (Bergamo, Italy)





Phantsi Tsolo D.

tphantasi@ictp.it

Supervisors:

Dr. Spiazzi Luigi

ASST Spedali Civili di
Brescia, Brescia Italy



Comprehensive Assessment of Breast Cancer Treatment: Monaco TPS IMRT/VMAT Templates and Positioning using XVI/ *Catalyst*TM

Prospective/Objective: The first part of the thesis focuses into the development and optimization of IMRT and VMAT templates on Monaco TPS for breast cancer treatment. The second objective involves a comprehensive analysis of positioning shifts in breast cancer treatments, specifically comparing patients treated using XVI+*Catalyst*TM positioning to those treated using XVI positioning alone. Additionally, a subgroup analysis compares XVI versus *Catalyst*TM shifts. The study aims to evaluate the efficacy and equivalence of these positioning approaches.

Materials and methods: The methodology begins with the transfer of patient data, including RT Plan, Prescription, RT Structure, RT Dose and DICOM Images from Pinnacle TPS to Monaco TPS for template creation. The testing methodology for template assessment involves a direct comparison of Monaco created templates with established reference treatment plans, allowing for an in depth assessment of dosimetric parameters and plan quality. Additionally, prior to the template and reference plan comparison, an in-depth analysis of the coherence and reliability of Dose-Volume Histogram (DVH) data generated by both Monaco and Pinnacle TPS was conducted. Independent Samples T-Tests were employed for DVH data analysis. The second part of the thesis is a comprehensive analysis of positioning shifts in breast cancer treatments from August to November 2023. It compares a group of patients of XVI+ *Catalyst*TM positioning and a group of XVI positioning alone. The study involved 45 patients, and the total valid sample size (N) across all patients was 260 (N: 115 XVI+CAT and N: 145 XVI Alone). The study used Independent samples T-Test to find the statistical differences in lateral (LAT), longitudinal (LON) and vertical (VER) positioning components. Further analysis were on XVI vs *Catalyst*TM shifts on a group of 15 patients, with a (N) sample size of 96 data points. Paired sample T- Test was used on this case.

Results: Using Independent samples T-Test for 48Gy, 40.05Gy and 26Gy protocols, the study found p-values of $p=0.992602$, $p=0.939864$ and $p=0.984541$ indicating the equivalence of Monaco and Pinnacle TPS in DVH calculations. Moreover, following comparisons of Monaco- created templates with Pinnacle reference plans, using Independent Samples T-Tests for 48Gy ($p=0.995776$), 40.05Gy ($p=0.99082564$) and 26Gy ($p=0.991866$) demonstrated large p values, suggesting the equivalence of Monaco templates and Pinnacle in meeting the specified constraints for breast cancer protocols. In the positioning analysis of XVI+*Catalyst*TM vs XVI alone, no statistically significant differences are observed in LAT($p=0.926$) and LON($p=0.631$) components. However, the vertical (VER) positioning results reveal a significant difference (p-value:0.030). For analysis of XVI vs *Catalyst*TM shifts, a significant difference is in longitudinal shifts (p-value: 0.007). Lateral (p-value: 0.450) and vertical shifts (p-value: 0.134) demonstrate comparability.

Conclusion: Statistical analysis across breast cancer protocols indicates high p-values, confirming equivalence between Monaco and Pinnacle plans. Monaco templates are deemed safe for treatment planning. XVI+*Catalyst*TM vs XVI alone reveals comparable lateral and longitudinal positioning but a significant difference in vertical positioning. XVI vs *Catalyst*TM suggest attention in replacing XVI with *Catalyst*TM especially in scenarios requiring precise longitudinal positioning.



Almijsari Raja Faraj

ralmijsa@ictp.it

Supervisors:

Dr. Gianfranco Loi

AOU Maggiore della Carità
Novara, Italy



Minimax robust optimization of VMAT in stage III lung cancer patients: a dosimetric comparison with the PTV-based approach

Prospective/Objective: to study the performances of the Minimax Robust Optimization (MRO) approach for Volumetric Modulated Arc Therapy (VMAT) planning compared to the standard (PTV-Based) strategy to treat stage III lung cancer patients. The research aims to quantify the advantages of MRO in lung cancer settings by robust evaluation of standard plan quality metrics like DVH points dose conformity and homogeneity indexes.

Materials and methods: Standard and robust VMAT plans were generated by the TPS Raystation v12b, selecting a cohort of ten patients from a Stage III-NSCLC publicly available archive. For both plans, a 6MV photon beam from a clinically commissioned Linac Varian Trilogy equipped with a Millennium MLC system was employed. Treatments were planned using a synthetic CT obtained from an average of 10 phases of a 4D-CT scan; the same 4D sequence was used to generate the ITV for the standard plan arm. Systematic and random positioning errors from baseline and motion-induced shifts were evaluated on 14 patients, coming from the same archive, with 5 consecutive verification 4D-CBCT scans. A single population-based margin yielding ± 5 mm, ± 8 mm, and ± 5 mm in the LL, SI, and AP directions was derived and used for PTV generation in the standard arm and to set the robust optimization parameters in the robust one. The dose distributions were analysed using the TPS robust evaluation tool, comparing the values obtained for all the selected dose metrics in all the simulated geometrical uncertainty scenarios. Isotropic shifts of ± 3 , ± 5 , and ± 8 mm magnitude were applied to evaluate the robustness of the two approaches against the geometrical uncertainties. Descriptive statistics and a non-parametric Wilcoxon sign test were carried out to assess if the differences were statistically significant.

Results: No significant differences were found in terms of CTV coverage for uncertainties up to 5 mm. A statistically significant difference was found ($p = 0.001$) in the worst-case scenarios, slightly exceeding the robustness parameters. In this case, the robust plans underperformed the standard ones, highlighting their sensitivity to errors exceeding the limits set in robust optimization. In terms of dose conformity, robust plans significantly outperformed the standard ones without affecting dose homogeneity. The dose of OARs was systematically lower in the robust arm, with clinically and statistically significant differences ($p < 0.0001$). To cite the closest OAR to CTVs, the reduction of mean and maximum dose to the oesophagus was respectively 1.41 ± 1.55 Gy and 5.79 ± 7.86 Gy. Finally, robust plans required less modulation as a result of a significant reduction in the Monitor Unit number ($p = 0.012$).

Conclusion: MRO led to improved target coverage and dose reduction to OARs with a lower complexity profile without compromising the treatment safety with potential clinical benefits in advanced lung cancer treatments.



RANDRIAMANANTENA

Steph Eric

randriamanantenasteph@gmail.com

Supervisors:

Dr. Paola Bregant

Dr. Michele Signoriello

Ospedale Maggiore Trieste,
Italy



Performance assessment of different reconstruction algorithms, performed with AAPM Task Group 233 CT task-based image quality metrics.

Prospective/Objective: In the past few years, Computed Tomography (CT) vendors introduced Artificial Intelligence Deep Learning Reconstruction (AI DLR) algorithm to overcome the limitation of Iterative Reconstruction (IR) algorithm. The purpose of this work is to provide a qualitative characterization of IR and AI DLR algorithms of different commercial vendors, focusing on image quality protocol optimization based on the qualitative metrics suggested by AAPM TG 233 protocol.

Materials and methods: A 128 slices GE Revolution System and 320 slices Canon Aquilion One Prism were used in this study to assess image quality of advanced reconstruction algorithms. Acquisition were carried out using Catphan phantom model 600. A clinical head protocol was selected on GE Revolution CT. Different acquisitions were performed with three slice thickness (1.25, 2.5 and 5 mm) and CTDIvol values equal to 18.82, 18.88 and 20.77 mGy respectively. Images were reconstructed using one level of iterative ASIR (ASIR50) and AI DLIR with three different strengths (LOW, MEDIUM and HIGH).

On Canon Aquilion One Prism, both head and body protocols were used. Data were acquired with CTDIvol values equal to 52.7 mGy for head and respectively 3.2 and 6.3 mGy for body, with three slice thickness (1, 3, 5 mm). Images were reconstructed using AIDR 3D as Adaptive Iterative Dose Reduction algorithm and Advanced intelligent Clear-IQ Engine (AiCE) based on deep learning reconstruction technique. Task-based Transfer Function (TTF) and Noise Power Spectrum (NPS) were computed. Detectability Index (d') was calculated using the nonprewhitening matched with eye filter (NPWE) model observer.

Results: Generally, for each slice thickness the ASIR-50 shows a slightly superior or comparable values of TTF50% and TTF10% for all the Catphan inserts evaluated, respect to AI DLIR and its different strengths. Starting from ASIR50 to DLIR of different levels, a substantial reduction in noise magnitude is confirmed for all the slice thickness. Considering the peak frequency, an evident shift towards lower frequencies have been found only for slice thickness of 1.25 mm and 2.5 mm. Higher detectability index was obtained for AI DLIR and the increment is more evident for high contrast inserts; it also increases varying the strength of the reconstruction algorithm. In Canon CT, using head protocol, AiCE_brain shows a shape reduction of NPS compare to AIDR 3D and AiCE_Innear Ear. TTF was higher for AiCE_Inner Ear followed by AIDR 3D and AiCE_brain while an opposite result was found for detectability index. For body protocol, TTF50% and TTF10% were greater with AiCE than AIDR 3D at high contrast insert with low and high radiation dose, while a comparable values were found for low contrast inserts except for acrylic and polystyrene. The NPS was lower for DLR than IR. Higher values of DI were obtained with AiCE than with AIDR 3D at low and high radiation dose and it followed the increment of the contrast insert levels.

Conclusion. The results in this study confirm that both AI deep learning reconstruction algorithms reduce the noise magnitude and improve noise texture and detectability index. Both DLIR and AiCE have a greater impact than IR on the metric results obtained.



**Chabanas D.
Randrianantenaina**

rdeley@ictp.it

Supervisors:

Dr. Agnes Chendi
Dr. Gabriele Guidi

Azienda Ospedaliero-
Universitaria di Modena

Brachytherapy Gynecological Cancer: Equivalent Dose Calculation in Treatment Planning System

Prospective/Objective: The aims of the thesis is evaluate the feasibility of the treatment planning system in calculating EQD2 total doses to organs at risk (OAR) and target in combined external radiotherapy and brachytherapy treatments of cervical gynecologic cancers.

Materials and methods: Thirty cervical cancer patients treated with external beam Radiation Therapy (EBRT) combined with Brachytherapy (BRT) were reviewed. The simulation CT images of EBRT and four images (CT or MRI) BRT were imported into TPS Raystation (RaySearch Laboratories, Stockholm, Sweden) to perform dose summation based on deformed images (DIR). The total doses to organ at Risk (OARs: bladder, rectum, sigmoid, bowel) and targets (HR-CTV) obtained by adding the equivalent doses in 2 Gy fraction (EQD2) from the EBRT and BRT plans were used for quantitative comparison between the three methods (TPS, Preadsheet of excel and TPS Prospective).

Results: A statistical analysis was carried out to compare the values obtained for the doses of interest using the TPS Raystation module, the values obtained for the doses of interest using the method commonly used in clinical practice (Spreadsheet of Excel) and Prospective. In combined EBRT and BRT, the mean EQD2 sum dose of bladder D2cc calculated by TPS, Spreadsheet and TPS Prospective (TPSprosp) method was (91.7 ± 14.3) Gy, (91.9 ± 9.8) Gy and (93.5 ± 16.0) Gy, respectively. The mean EQD2 sum dose of rectal D2cc calculated by TPS, Spreadsheet and TPSprosp method was (76.1 ± 15.3) Gy, (76.0 ± 11.7) Gy and (80.7 ± 17.3) Gy, respectively. For the target HR-CTV D90 calculated by TPS, Spreadsheet, and TPSprosp method was (88.1 ± 8.9) Gy, (89.13 ± 4.9) Gy and (88.8 ± 6.0) Gy, respectively. End then for HR-CTV D98 for the three method was (76.4 ± 7.9) Gy TPS, (77.5 ± 5.4) Gy Spreadsheet and (74.2 ± 15.1) Gy for TPSprosp method. In this study, all of the p-value was above to 0.05 is it no significant difference between the three method.

Conclusion: The results show that all the values for each method are in line with the dose recommended by the EMBRACE protocol. Comparisons of EQD2 dose values between TPS Raystation to spreadsheet, and TPS Raystation to Prospective do not differ greatly, and are almost similar. The values obtained by these three methods did not show any significant statistical differences. Which allows us to conclude that the module introduced by TPS Raystation could be useful in clinical practice.



Francis G. Benard

fbenard@ictp.it

Supervisor:

Dr. Sabina Strocchi

ASST Sette Laghi, Ospedale di
Circolo e Fondazione Macchi,
Polo Universitario



Comparing accuracy of SPICE-CT and CTQA_cp with IQWorks software in Catphan600 image analysis for X-ray computed tomography quality assessment

Prospective/Objective: The significance of software tools in evaluating CT image quality, during quality control assessments of CT scanners, is indisputable. Despite the longstanding use of IQWorks at Circolo Hospital Department of Medical Physics, recent compatibility issues have surfaced. This study aimed at investigating alternative freely available software; SPICE-CT and CTQA_cp, and evaluate their accuracy in comparison with IQWorks for the analysis of Catphan600 phantom images. The goal was to offer insights into the usefulness of these alternatives, addressing accuracy concerns and ensuring a consistent and reliable CT image quality analysis.

Materials and methods: Catphan600 images obtained from various CT scanners between January 2022 and June 2023 were utilized. Central images from three Catphan600 modules: CTP404 for evaluating slice thickness, geometry, and CT-number; CTP591 for modulation transfer assessment; and CTP486 for examining uniformity and noise were selected. Axial images acquired from Toshiba Aquilion Prime SP, Toshiba Astelion, GE Medical Systems Evolution EVO, and Philips Brilliance 16 were included in the study. For spiral image analysis, images acquired from Philips Iqon-Spectral CT, Philips Brilliance 16, Toshiba Aquilion Prime SP, Toshiba Astelion, GE Medical Systems Evolution EVO, and Siemens Sensation 64 were utilized. Selected images were analyzed using each software tool. The differences in mean and standard deviation between each software and IQWorks were computed and compared to tolerance levels. The differences between each software and IQWorks were tested using Wilcoxon Signed-rank paired data test.

Results: Comparing SPICE-CT with IQWorks in axial images showed no significant differences in slice thickness ($P = 0.655$), geometry ($p = 0.294$), uniformity ($p = 0.721$), noise ($p = 0.915$), average CT-number (0.12 ± 3.41) HU ($p = 1.000$) with no discrepancies for individual insert materials, except for Acrylic. Comparing CTQA_cp with IQWorks in axial images revealed no significant differences in slice thickness ($p = 0.295$), geometry ($p = 0.390$), uniformity ($p = 0.926$), noise ($p = 0.275$), average CT-number (0.65 ± 3.45) HU ($p = 0.880$) with no significant discrepancies for individual insert materials except for Acrylic. In spiral images, no significant differences were observed between SPICE-CT and IQWorks in slice thickness ($p = 0.320$), geometry ($p = 0.642$), uniformity ($p = 0.785$), noise ($p = 0.323$), average CT-number (0.58 ± 2.73) HU ($p = 0.336$) with no significant differences for individual insert materials except Delrin. Generally, MTFs exhibited significant differences ($p < 0.001$) in all cases. While SPICE-CT and CTQA_cp adhered to acceptable tolerances for most parameters, they fell short of meeting the tolerance levels for some MTFs in axial images. SPICE-CT and CTQA_cp were in agreement with IQWorks and measured most parameters within acceptable tolerance levels. However, CTQA_cp did not perform analysis for spiral images.

Conclusion: SPICE-CT and CTQA_cp were consistent with IQWorks and calculated almost all considered image quality parameters to within acceptable tolerances. However, CTQA_cp confined its analysis to axial images. Consequently, SPICE-CT emerged as a viable alternative to IQWorks for axial and spiral Catphan600 image analysis.



Edith S. EL GHASSAL

selghass@ictp.it

Supervisors:

Dr. Andrea Dassie

Dr. Paola Chiovati

Centro di Riferimento
Oncologico IRCCS Aviano.,
Italy



Dose estimation to cardiac implanted electronic device in low voltage intraoperative radiotherapy

Objective: Intraoperative radiotherapy is a specific technique for treating breast cancer that offers several benefits. One crucial aspect of IORT is in vivo dosimetry, which measures the dose at varying distances. Can be also used to estimate the dose to cardiac implanted electronic devices and in this study we aim to estimate the safe distance for CIED. To achieve this, we need to calibrate a type of dosimeter among available dosimeters, thermoluminescence has been used to detect low dose levels. We used a low-voltage machine in our study for the delivery of radiation and a comparison of dose in patients with a water phantom to ensure an accurate estimation of this distance.

Materials & Methods: The low voltage machine is a small machine with a kV x-ray source designed specifically for IORT applications. We used this clinical machine to cross-calibrate TLD dosimeters in the clinical energy spectrum and in dose range of 0-4 Gy. During the IORT of breasts, we utilized this calibrated TLD to measure the dose at varied distances. We placed one package of TLD wrapped in a sterile envelope on the patient's skin after breast-conserving surgery to collect the dose at several distances. The data obtained from actual patients via TLD were compared thoroughly with the data collected in a water phantom using an ionization chamber and TLD.

Results: We cross-calibrated TLDs and determined that they are linear and more sensitive in the low dose range of 0.1-1.5Gy, but need a correction at doses above 1.5Gy. Using this cross-calibration, we measured skin doses during IORT treatment and estimated the dose to pacemakers. Preliminary cross-calibration showed a linear response in the relevant dose range. In vivo measurements using TLD indicated that the technique is completely safe for CIED. The dose at the location more than a certain distance where CIEDs are typically placed in patients was found to be below the threshold of 2Gy.

Conclusion: Clinical evidence was utilized to successfully complete the task. To summarize, the use of TLD in IVD to collect dose data is a viable procedure. The dose and the distance to the CIED were estimated but needed more patients for more accuracy. TLD can be employed for future measurements to well estimate the dose and distance to the CIED.



Laban Festus

flaban@ictp.it

Supervisor:

Dr. Serenella Russo

Ospedale Santa Maria
Annunziata, Florence- Italy



Commissioning of Elekta Versa HD WFF photon beams and clinical validation into the pinnacle treatment planning System.

Prospective/Objective: Radiation therapy is a complex process which involves many steps prior to the clinical use of the linear accelerator, each of which requires complete and thorough commissioning and quality assurance in order to ensure accurate delivery of the prescribed radiation dose to the target. A crucial role in the radiotherapy treatment procedure is played by the Treatment planning system (TPS) because it provides the means to plan individualized dose distributions to the target volume and organs at risk sparing. The purpose of this study is the Commissioning of the Elekta Versa HD linac newly installed in the Radiotherapy Department, the beam fitting and the dosimetric clinical validation of the Philips Pinnacle 3D dose calculation algorithm for external photon beams with flattening filter (WFF).

Materials and methods: An Elekta Versa HD linear accelerator was installed by Elekta company in the radiotherapy department. Acceptance testing was performed by the Elekta specialist together with the medical physicists of the department to verify that the machine performance meets the requested specifications. Following acceptance testing was the beam data collection for commissioning, which was performed for field size ranging from 1cm x1cm to 40 cm x 40 cm by using a single device, the microdiamond synthetic detector, because of its suitable physical characteristics. Beam data were collected with the microdiamond detector in parallel configuration in the PTW MP3 water phantom, which permits to scan the detector in three orthogonal directions in the radiation field. All the measurements were in terms of relative dose, normalized to the point of maximum dose along the beam's central axis for the depth dose curves and normalized to the central axis dose for the dose profiles. For relative field measurements a reference detector (PTW semi-flex chamber) was used in order to obtain a reference signal. Pinnacle Philips TPS was used to perform the beam fitting modelling for the dose computation and also to validate the dose output of the machine for clinical use, by employing various verification methods such as tests in homogeneous phantom and patient specific QA (PSQA). Different statistical tools such Distance To Agreement (DTA), maximum percentage difference and standard deviations, were used to evaluate the discrepancies between measured and computed doses.

Results: All the acceptance tests performed after the Linac installation are within the specified tolerances. Regarding the TPS beam modelling, measured depth dose curves and profiles are in strong agreement with TPS calculations within 2% Dose Difference (DD) in low gradient regions and 2 mm DTA criteria in high gradient regions. Beam specific calculation checks in homogenous media are in strong agreement with the IAEA recommended tolerances. PSQA checks for conformal treatments on different anatomical sites gave optimal results confirming that the dose planned in realistic situations relating to the real treatment of patients corresponds to the one actually delivered.

Conclusion: The Elekta Versa HD linac and the Pinnacle Philips TPS were successfully commissioned for external photon beams with flattening filter and are ready for clinical use.



Ganesh Subedi

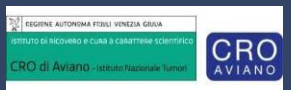
ganeshundkt@yahoo.com

Supervisors:

Dr. Paola Chiovati

Dr. Stefano Lorentini

Centro di Riferimento
Oncologico IRCCS Aviano,
Italy.



Feasibility study of robustly optimized intensity modulated plans with photon and proton beams in head and neck cancer.

Purpose: This study investigates the feasibility and potential of Multi Field Optimization (MFO) proton plans, Robustly Optimized Intensity Modulated Photon Therapy (RB IMXT) and Planning Target Volume (PTV) based IMXT. The study aims to compare the plan quality and evaluate the robustness.

Methodology: MFO proton plans, RB IMXT and PTV based IMXT plans were created for 3 oropharynx and 2 nasopharynx cancer patients. Plans were evaluated using dose statistics, homogeneity index, conformity number, integral dose and scoring method. Robustness of treatment plans were assessed by introducing residual uncertainties of ± 3 mm along the three translational axes. In protons, an additional range uncertainty of $\pm 3.5\%$ was introduced. Robustness of the plans was assessed according to worst scenarios. Statistical analysis includes paired-sample student's t-test and linear regression.

Results: Averaged scores “score is the sum of assigned score for each clinical goal that is achieved” for MFO IMPT was 23%, 13% higher than PTV based IMXT and RB IMXT plan respectively ($P < 0.05$). In MFO proton plan, dose to Organ At Risk (OAR) was reduced by 4% to 49% ($P < 0.05$) of their dose constraints, whereas for RB IMXT and PTV based IMXT, dose constraints could not be reached in parotids, oral cavity, and submandibular glands. The mean dose variation in Clinical Target Volume (CTV)s among planning techniques for D98% was less than 1.7 % of prescribed dose. The percentage of scenarios in which the clinical goals were achieved was higher for proton plans. Strong correlation was found between the worst scenario dose with nominal ($R^2 > 0.97$) and averaged scenario dose ($R^2 > 0.99$) for CTVs in all plans.

Conclusion: CTV to PTV margins are still used in photon planning. However, for comparable robustness of the plans and CTVs coverage, robustly optimized photon plans could be alternative to PTV based plans that improves conformity and in consequence reduces dose to OARs. MFO proton plans are most effective in decreasing OARs doses and enhancing target conformity keeping the reliability of the plan in terms of its robustness and coverage. It reduce integral dose to healthy tissue that decrease toxicities to patients.



Commissioning of a stereotactic radiosurgery (SRS) oriented treatment planning system (TPS)

Prospective/Objective: The purpose of this thesis is to commission and validate the Monte Carlo and Pencil Beam algorithms of a Brainlab Elements Treatment Planning System (TPS) for stereotactic radiosurgery (SRS) treatments delivered with a 6 MV flattening-filter free (FFF) beam of a Varian TrueBeam STx LINAC. Comparisons with other two clinically commissioned algorithms, AAA, and Acuros XB by Varian Eclipse, are also performed.

Materials and methods: As part of our commissioning and, quality assurance process, we tested different dose calculation algorithms PB with full beam data (Full PB), both Pencil Beam and Monte Carlo with reference beam data (RBM PB/RBM MC). We compared these algorithms with Acuros XB and AAA algorithms by Varian Eclipse, performing analysis to verify accuracy for SRS photon dose calculation. Validating beam and MLC models, we conducted measurements for depth dose curves, profiles, output factors, and Jaws Leakage. Parameters like offset, gain, leaf tip width, and transmission were determined for MLC. Small field profiles were verified using Gafchromic EBT3 Films, agreeing with water phantom measurements using the microDiamond detector with gamma analysis with DTA 2%/1mm. Clinical SRS plans were calculated with various algorithms at a 1 mm dose grid size and validated with SunNuclear EasyCube Phantom measurements for treatment verification.

Results: The 6 MV FFF beam characteristics aligned well with the literature. Validation confirmed our beam and MLC models for SRS treatments. Point dose measurements for larger field sizes ($1 \times 1 \text{ cm}^2$) had excellent agreement ($1\% \pm 0.5\%$) between the measured dose, pencil beam algorithm, and Monte Carlo algorithm. For smaller rectangular fields, Monte Carlo showed better accuracy and robustness (1% dose difference) due to its precise handling of heterogeneous materials. Acuros XB demonstrated similar accuracy to MC regarding differences from the measured dose.

Conclusion: The SRS EasyCube Phantom measurement agrees dosimetrically with the plans calculated by the Pencil Beam algorithm Full PB and both reference beam model Pencil Beam and Monte Carlo (RBM PB/RBM MC) by Brainlab, as well as the AAA, and Acuros XB dose calculation algorithm by Varian. Point dose calculation for small field dosimetry and differences using SRS EasyCube Phantom both showed that the Monte Carlo algorithm is more robust and is superior in regions of heterogeneous materials. The technical information and dosimetric data provided in this thesis will be a useful reference for other clinics/institutions that will commission the same machine energy in the BrainLab TPS.



**Mohammad Wael
ALMASRI**

waelalmasri1995@hotmail.com

Supervisors:

Dr. Marco Valenti
Dr. Marco Parisotto

University Hospital of
Marche, Ancona, Italy





Akouvi Odette SATSI

asatsi@ictp.it

Supervisors:

Dr. Stefania
LINSALATA

Dr. Patrizio BARCA

Dr. Claudio TRAINO

Comparison between two different devices for pre-treatment QA: Arc-check and EPID

Prospective/Objective: One of the most essential tasks of the medical physics workload is to ensure patient-specific quality assurance(PSQA). However, PSQA can be a time-consuming task. International regulations(such as the European Union 2013/59/EURATOM) still recommends it, especially for complex VMAT radiotherapy treatments. To achieve optimal quality assurance on patient plans while saving time, more efficient pre-treatment PSQA methods such as EPID-based measurements are preferred. However, the AAPM TG 218 discourages it because “using EPID to obtain an integrated image for VMAT is considered PC”(Perpendicular Composite). Recently, the AAPM TG 307 reported that few studies compare traditional methods of pre-treatment PSQA(based on ionization chambers or diode arrays) with EPID measurements. Furthermore, to the best of our knowledge, none of them reports results on the Sun-Nuclear Sun-Check Patient Software. This study aims to compare PSQA obtained with the Sun-Nuclear Sun-Check Patient Software against as well-established TC(True Composite) method for pre-treatment QA, such as the Sun-Nuclear Arc-check diode array. The primary objective is to investigate the possibility of replacing traditional pre-treatment PSQA methods with EPID measurements while maintaining the same level of quality assurance.

Materials and methods: During the study, thirty VMAT plans were subjected to repeated measurement using Arc-check in a composite way and with EPID per field. For each arc, an integrated EPID image was registered. It is worth noting that all of the VMAT plans were characterized by two or three arcs. Before every measurement session, linac output was carefully measured and found to be within 0.5% of the reference value. The process of pre-treatment verification of treatment plans is crucial in ensuring the accuracy and safety of radiation therapy. In this study, pre-treatment EPID images were acquired without couch and/or phantoms, and were processed using the Per-Fraction module of the Sun-Check Patient Software. The images were converted into planar dose in water slab at the EPID level and compared with calculated dose maps obtained by the embedded Sun-Nuclear Dose-Check algorithm. Moreover, Arc-check measurements were performed in absolute dose to water after calibrating the instrument, and were compared with the TPS calculations that utilized the Varian Acuros XB algorithm in dose-to-water. The Gamma Passing Rates(GPR) for both the comparisons in absolute doses were registered with different dose-DTA criteria, including 3%2mm, 3%1mm, 2%2mm, 2%1mm, 1%2mm and 1%1mm; all global and with threshold at 10%. The study also analyzed GPR distributions for each approach, and computed the main statistic descriptors such as median, inter-quartile range, maximum and minimum. Additionally, the correlation between each GPR distribution obtained with different detectors was also computed. For the EPID measurements, the per plan GPRs, which is the average of GPR values obtained for each plan arc, were considered. Finally, the study also calculated the action limits suggested by the AAPM TG 218 for each considered dose-DTA criterium. These findings provide valuable insights into the accuracy and reliability of pre-treatment verification methods in radiation therapy, which can ultimately improve patient safety and outcomes.

Results: The report provides descriptive statistics, including the median, inter-quartile range, maximum and minimum values, of the recorded GPRs(Gamma Passing Rate) in a table format. Additionally, the action limits were calculated based on the AAPM TG 218 recommendations. For the EPID(Electronic Portal Imaging Device) measurements, the average GPR values obtained for each plan

arc were reported. The data indicates a general overlap between all the reported GPR distributions, and no further statistical analyses were conducted to compare the groups. Pearson correlation coefficients were calculated for each combination of GPRs distributions with Arc-check and EPID. The coefficients ranged from -0.23 to 0.83, representing the relationship between the 1%1mm criterion for Arc-check and 1%2mm criterion for Per-Fraction Fraction0, and between the 3%2mm criterion for Arc-check and the 3%1mm criterion for Per-Fraction Fraction0. These results provide insight into the correlation between the two measurement methods and can be used to guide further analysis and interpretation of the data.

Conclusion: Based on our evaluation of the EPID pre-treatment PSQA system Sun-Check Per-Fraction and Arc-check, utilizing a sample of thirty VMAT plans, we have determined that there are no significant differences in GPRs distributions across various dose-DTA criteria. This indicates that the EPID pre-treatment dosimetry system could potentially be utilized as a less time-consuming substitute for traditional TC pre-treatment PSQA methods like Arc-check. However, it should be noted that further data obtained from multicentric contests would be necessary to validate this conclusion. Overall, our findings provide valuable insights into the effectiveness of the Sun-Check Per-Fraction system and its potential to improve the pre-treatment PSQA process for VMAT plans.



A data driven method for quality control of head and neck treatment planning

Prospective/Objective: The Head and Neck (HN) radiotherapy treatment requires complex planning, and the quality may vary greatly if the plans are manually generated. In fact, plan quality mainly depends on the planner's skills and experience, as well as the time available for optimization. Additionally, when the plans are calculated, there is a lack of consideration for geometric variability between patients. The overlap volume histogram (OVH) serves as an anatomical metric that acts as a tool to link dosimetric and geometric parameters between an organ at risk (OAR) and target volume when predicting expected dose-volumes in knowledge-based planning (KBP). This work investigates the OVH and dose-volume histogram (DVH) correlation as a quality control method for HN cases, in view of automatic planning optimization.

Materials and methods: The OVH curves were generated retrospectively for 19 patients for both left and right parotids using Oncentra V4.5 planning system. The quality control process is established using two distinct methods. The first method involves the expected mathematical relation between the OVH and the DVH for each parotid, to determine if a lower dose could have been achieved. The second method utilizes statistical analysis to establish further correlation between the dosimetric data and the geometric complexity of the parotids and PTVs, incorporating multiple key DVH and OVH metrics.

Results: The expected mathematical relation between OVH and DVH reveals that 13 of our 19 cases can benefit from a possible dose reduction. Out of these 13 patients, 5 of them may need optimization only on the right parotid, 2 patients need optimization only on the left parotid and 6 of them need optimization for both left and right parotids simultaneously. The correlation analysis suggests that the patients' data can be divided into two sets. The first set where dose reduction is difficult due to PTV-parotid proximity, these are high complexity plans. The second set, where the parotids are more far from the target, are plans of lower complexity, and dose reduction could be possible.

Conclusion: The OVH method proved to be an effective quality control tool that can be used to improve volumetric modulated arc therapy (VMAT) planning optimization and reduce user inter-variability.

**Farah BEN
HAMMOUDA**

fben_ham@ictp.it

Supervisors:

Dr. Arta Sulaj

Dr. Marco Esposito

Ospedale Maggiore Trieste,
Italy





Nyaradzo J. Murwira.

nmurwira@ictp.it

Supervisors:

Dr. Lidia Strigari

Dr. R. Padovani

Santa Orsola Ospedale
Bologna Italy



Robustness of lexicographic optimization based planning for cervical cancer according to different type of organ segmentation.

Prospective/Objective: In this study, according to literature auto-contouring is generally assessed by comparing with manual contouring, however the effect of the auto-contouring, manual contouring and auto-manual contouring is not known. The purpose of this study is to evaluate the robustness of auto-planning by creating a wish-list and using the same dosimetric constraints on the three types of contouring methods on the organ at risk.

Materials and methods: This study included a cohort of 10 cervical cancer patients treated with volumetric modulated arch therapy (VMAT) technique the prescription dose was of 50Gy in 25 fractions. Before the conduct of this research all the patient related information was anonymized deeply. A computed tomography simulation with 3mm slice thickness was used to acquire images for all the patients. The structure sets that were contoured by three different contouring type that is auto-contouring, auto-manual contouring and manual contouring. The auto-segmented contours were retrieved from the deep learning tool and were manually corrected by ROs where necessary. These contoured structure sets were then used in the auto-planning included the planning target volume PTV, bladder, bowel bag, femoral heads and rectum. The automatic planning was performed by mCycle implemented in the Monaco Elekta Solutions AB Monaco Research Version (v6.09.00), in which the lexicographic and the multi criterial-optimization are coupled with Monte Carlo calculation. Wish-list 1 was tuned according to the institutional clinical protocol to get wish-list 2 to obtain an optimal plan in a single optimization for all patient each with three different groups of contouring type. Data was exported from the TPS and imported in ProKnow. The impact of mCycle according to different contouring type were compared in terms of dose distribution and modulation complexity score. Their clinical acceptability was assessed by evaluating the plan quality index.

Results: The 120 automated planning task according to different contouring type using the wish-list 2 took 5 to 10 working days to complete clinically acceptable plans. The final dose calculation time can be estimated to 35 to 45 minutes to complete each plan. The dose comparison showed a comparable OAR spare. The PTV coverage were similar according to different contouring type auto, auto-manual and manual ($V_{95\%}$: 94.567, 94.539, 94.748, $p > 0.05$). The OAR bowel bag minus PTV no significant difference has been registered except for right femur head which registered significant differences as follows ($V_{45Gy}(cc)$: auto 200; auto-manual 342; manual 268, $p > 0.005$) and ($D_{5\%}(Gy)$: auto 0.544; auto-manual 0.767; manual 1.273, $p < 0.05$) respectively. The median plan quality index and MSC was (PQI: auto 36.99[2.87-52.53]; auto-manual 33.25[1.04-46.45]; manual 32.11[2.16-49.68], $p > 0.05$) and (auto 0.263[0.192-0.280]; auto-manual 0.239[0.195-0.271]; 0.234[0.199-0.276], $p > 0.05$) respectively, no significant difference has been registered.

Conclusion: mCycle plans according to auto, auto-manual and manual contouring of OAR were comparable to each other, with an exception of the OAR right femur head sparing which was not similar. More complex but clinically acceptable-like plans were registered similar.



ICTP- Strada Costiera, 11 I-34151 Trieste Italy
mmp@ictp.it



Via Alfonso Valerio, 2, Department of Physics,
University of Trieste, 34127 Trieste, Italy



Master in Medical Physics Alumni Association (MMPAA)



ICTP & UniTS's Medical Physics Graduates (IUMPG)